THE American Journal of ANATOMY

VOLUME 118
JANUARY, MARCH, MAY 1966

THE WISTAR INSTITUTE OF ANATOMY AND BIOLOGY
PHILADELPHIA PA

CONTENTS

No 1 JANUARY 1966

No 2 MARCH 1966

No 3 MAY 1966

Hypothalamic Neurosecretory System in the Normal and Partly or Completely Hypophysectomized Goldfish [1]

A G SATHYANESAN [2]
Department of Zoology University of Washington Seattle Washington

ABSTRACT The nucleus preopticus (NPO) of the normal goldfish examined at intervals of three hours for a complete day exhibits marked variation in their affinity for aldehyde fuchsin (AF) Some times in this nucleus the cells of the pars magnocellularis were deeply stained while those of the pars parvocellularis were lightly stained which suggests a functional difference Both NPO and the nucleus lateralis tuberis (NLT) are AF positive in the goldfish In the neurohypophysis three tinctorial types of Herring bodies were seen the AF positive bodies can be traced back to the NPO but the origin of the fast green and acid fuchsin bodies is uncertain In the hypophysectomized specimens without regenerating neurosecretory axons the NPO exhibited degenerative changes However if regeneration of the pituitary stalk occurred forming a neurohypophysis like organ the NPO was apparently normal Prominent AF positive granules were not obvious in the NLT of hypophysectomized specimens

Since the first report on the neurosecretory nature of some hypothalamic nuclear centers in fish (Scharrer 28 30 32a b 41) this subject has attracted the attention of many investigatiors Charlton (32) studied the nucleus preopticus (NPO) and nucleus lateralis tuberis (NLT) of about 125 species of teleosts Palay (45) described the hypothalamo-hyophysial pathway in fishes Special technique for demonstrating neurosecretory substance was initially introduced by Bargmann (49) which resulted in extensive study of the hypothalamic system (Hild 51 Bargmann 53 review Pickford and Atz 57 Diepen 54 Scharrer and Scharrer 54 63 Arvy et al 59 Dodd and Kerr 63) However the application of the newer techniques to study the NLT is restricted to a limited number of species (Bargmann 53 Brehm 58 Follenius 62 Stahl and Leray 62 Billenten 63) Even in a common experimental species such as goldfish the NLT has attracted little attention Effect of hypophysectomy on the eel hypothalamo-hypophysial system has been studied by Stutinsky (53) Kobayashi et al (59) described the neurosecretory system in the gobi *Lepidogobius lepidus* after interruption of the tract at various levels

In the present communication observations on the diurnal changes in the stainability of the hypothalamic nuclei in the normal goldfish are reported Changes occuring in this system after complete or partial hypophysectomy and during neurohypophysial regeneration are also described

MATERIALS AND METHODS

More than 150 adult goldfish were used in this study They were obtained from a fish farm and were kept 10 to 15 days in aerated aquaria at 70 F (± 3 F) under laboratory conditions prior to the experiments They were fed with powdered fish frozen brine shrimp or living tubificid worms Untreated fish were examined to determine the general pattern of the hypothalamo-hypophysial system In an experiment designed to determine the possible quantitative diurnal variations of the stainable neurosecretory substance groups of six normal fishes were killed at intervals of three hours beginning at 9 A M until 1 P M the next day (January 17 and 18

[1] Thi work was done while th thor held a post-doctor l fellow h p of the P pul t n C un il Rockefeller Found ti n in p rt at Columbia Univ ity and in part at th Uni ers ty of W hingt n M ter l upport for th rch wa recei d f om U S P H S grant N B 04887 (warded to D Go bm n) from the Instituti n l Can R e rch Fund of the Uni ers ty f W hington (Ameri n Canc Soci ty) as w ll from the Popul tion C unc l

[2] Perm nent address D p rtm nt of Zoology B n ar s Hindu Uni ersity Var nasi 5 Ind a

1963) This procedure was repeated on March 30 and 31, 1963 Another group of 19 specimens were partly and 20 were completely hypophysectomized and kept in 0 75% sea salt solution for two days to inhibit post operative infection These fish were decapitated at intervals from 5 to 75 days post operatively In routine studies appropriate regions were fixed in Bouin s fluid However Helly s fluid or mercuric chloride potassium chromium sulphate formol was also utilized Paraffin sections were cut 5 7 or 10 μ Gomori s aldehyde fuchsin (AF) Mallory s triple stain Foot s modification of Masson s trichrome Elftman s periodic acid Schiff (PAS) AF combination and chrome alum hematoxylin phloxin were used Palmgren s silver impregnation technique for nervous tissue was employed to study the neurosecretory pathways Since it is well known that the effectiveness of the differential stains varies with the age of the solution and their temperature care was taken to stain the experimental and control (sham operated) slides simultaneously in a single lot

RESULTS

The hypothalamo hypophysial system of the goldfish resembles that of other teleosts in its general pattern and topography The dorsal half of the NPO composed of large rounded or oval cells forms the pars magnocellularis smaller cells of the ventral half constitute the pars parvocellularis The neurosecretory cells of the NPO of an individual specimen often exhibit wide variations in their affinity for AF Even in the deeply stained NPO frequently lightly staining and chromophobic cells are present (fig 1) Vacuolated cells are also common (fig 2) In some AF positive globules and granules seem to occur inside the nucleus (figs 3 4) These may be cytoplasmic extensions into folds of the nuclear membrane The NPO is highly vascular some of the neurosecretory cells and axons are in close association with blood vessels (figs 5 6) Some others are directed anteriorly in the opposite direction of the main tract few may even terminate on the wall of the hypothalamus Occasionally AF positive dendrites and axons seem to enter the preoptic recess of the third ventricle (fig 7) It is often difficult to differentiate the finer axons from the AF positive ependymal lining of the recess Most of the beaded neurosecretory axons (fig 8) can be traced into the pituitary Small axons are seen in between the chromophils of the pars intermedia and proximal pars distalis Herring bodies accumulate in the neurohypophysis chiefly around blood vessels in the pars intermedia (fig 9) On the basis of tinctorial differences three types of Herring bodies may be identified in the main trunk of the neurohypophysis The first type stains with fast green or aniline blue the second type with acid fuchsin or Orange G and the third type is AF positive (fig 10) The AF positive Herring bodies can be traced back to the NPO along their axonal tract but the origin of the other two types is not clear Perhaps they represent different physiological states of the AF positive material

Colloid like globules staining with orange G or acid fuchsin are present in the pars intermedia and these also may occur in the neurohypophysis among the Herring bodies (fig 11) These globules appear to be derived from the pars intermedia and are not stained with AF They may be comparable to the colloid droplets of the toad pars intermedia (Iturriza and Koch 64)

Diurnal variation in the nucleus preopticus

Wide diurnal variation in the quantity of AF positive material in the NPO was obvious in normal animals The cells of the NPO were apparently stained deep during thhe photoperiod (figs 12 13) than at night Lightly stained cells seemed to be more abundant in the NPO of specimens examined in late evening and night (fig 14) In animals with a lightly stained NPO an abundant accumulation of Herring bodies in the neurohypophysis was often observed However some fish of the day group have a lightly stained NPO and some of the night group have deeply stained cells Thus three hourly examination of the NPO of normal fish for 24 hours reveals a considerable difference in their stainability Since these variations did not seem to be of a clear-cut sequence this may not be considered rhythmic

Often while the cells of magnocellularis were deeply stained those of pars parvocellularis were almost devoid of stain This may be significant since it suggests a possible functional difference between these two regions The difference in regional stainability of the NPO also has been reported in ammocoetes (Oztan and Gorbman 60)

Effect of partial or complete hypophysectomy upon the hypothalamo-hypophysial system

An abundant accumulation of neurosecretory substance was present at the proximal cut end of the pituitary stalk 5 to 7 days post hypophysectomy Occasionally such accumulation was also noticed at various levels along the hypopthalamo-hypophysial tract (fig 15) However the NPO appeared normal (fig 16) Two weeks after hypophysectomy an obvious increase in the number of deeply staining cells was seen in the NPO In fish examined 75 days post hypophysectomy these cells were heavily loaded with AF positive granules Some cells were clumped together and exhibited degenerative changes In these cases the pituitary stalk did not show signs of regeneration and there was little accumulation of AF positive material at the cut ends (fig 18) Prominent neurosecretory axons with AF material were absent along the hypothalamic tract The NPO of sham-operated controls were not obviously different from the normals (fig 19)

Some partially or fully hypophysectomized fish showed regeneration of the neurosecretory axons and infundibular stalk The regenerated axons developed a new relationship with the surrounding blood capillaries and seemed to function as a neurohypophysis like organ In some the axons grew into the underlying connective tissue (fig 21) This growth was not directed toward blood vessels for many blood capillaries and sinuses abundant near the cut end of the stalk were bypassed Such growing axons were found in some animals two or three weeks after hypophysectomy The NPO of the fish with regenerating and growing axons stained deep during the second or early third week (fig 20) they became almost normal during the fourth week or later These findings suggest that in the course of infundibular stalk regeneration at least some of the neurohypophysial function is maintained and thus the NPO does not show significant abnormal changes

Nucleus lateralis tuberis (NLT)

The NLT occurs above the pituitary gland in the lateral lateroventral and rostral aspect of the hypothalamus (fig 22) These cells are arranged continuously even though size variations are evident no size grouping of cells is present (fig 23) The cellular components of the NLT are also stained with AF as the NPO cells The cells of the NLT do not have distinctly elongated axons like those of the NPO However some are conical with attenuated tips and others have short axons (fig 24) Since the axonal pathway of the NPO lies along the anterior and anterolateral side of NLT accumulation of AF positive material belonging to the NPO is often seen in these regions of the NLT The neurosecretory products of both NPO and NLT are AF positive and cannot be differentiated on this basis Axonal pathways leading from the NLT into the pituitary could not be traced with certainty Even though axon like processes were seen lying between the NLT and the ependymal lining of the third ventricle a distinct tract leading into the third ventricle is not obvious Often specimens examined 15 or 30 days after hypophysectomy did not show visible AF positive granules in the cells of the NLT (fig 24) But in the control animals prominent granules are invariably present (fig 25)

DISCUSSION

The general structure of the hypothalamo-hypophysial system of the goldfish largely resembles that of other teleosts described by earlier investigators In *Fundulus* Scharrer (41) has observed that the large cells of the NPO are extremely variable and a study of 100 specimens did not fully exhaust the number of variations In the goldfish the quantitative variations in the AF positive material in the NPO is also large Even specimens examined at regular intervals of three hours during a

day, showed marked differences in the AF positive contents However the mechanism or factors producing such changes in this system is obscure

Some investigators have suggested an intranuclear origin of neurosecretory material (see Oztan 63) In the present study some AF positive globules superficially appear to be intranuclear However electron microscopical studies of the NPO indicate their extranuclear origin (Palay 60a b Follenius and Porte 62 Follenius 63) Nishioka and Bern (64) have reported that such seemingly intranuclear bodies present in the caudal neurosecretory cells of the teleost *Albula* are also cytoplasmic Occurrence of non hypophysial termination of neurosecretory axon was reported in several vertebrates (Oztan and Gorbman 60 Kobayashi et al 59 Legait and Legait 56 and Scharrer 51) In the goldfish some axons terminate on the wall of the hypothalamus or even into the third ventricle

The location of the NLT in the goldfish is similar to that of *Tinca vulgaris* (Brehm 58) Bargmann and Hild (49) Hild (51) and Brehm (58) have found that the cells of the NLT are not selectively stainable with Gomori s chrome alum hematoxylin In *Mugil Morone Scorpaena Diplodus Gadus* and *Hippocampus* Stahl and Leray (62) reported that the neurosecretory substance of the NLT did not stain with chrome alum hematoxylin AF or aldehyde thionine In *Salvelinus* the secretory material of the NLT did not show any affinity for AF or chrome alum hematoxylin (Billenstien 63) However in both the platyfish (Oztan 63) and the goldfish the NPO and NLT are stained with AF Thus the NLT of teleosts seems to exhibit a species specific variation in staining reaction Morphological observations suggest that the secretory products of NLT are released directly into the third ventricle (Hild 51 Brehm 58) Palay (45) and Bargmann (53) believe that the secretory material is distributed into the pituitary in the same manner as the NPO Stahl and Leray (62) reported the probable absence of an axonal pathway for the tuberal secretory material into the pituitary They have further suggested a tubero-ependymo-hypophysial pathway and vascular transport as two alternative methods for conduction of the neurosecretory material from the NLT Oztan (63) suggested that the secretory substance is conducted through the circulatory system of the hypothalamus Billenstien s (63) evidence supports the concept of axonal transport of the secretory material from the cells of the NLT to the hypophysis but does not exclude the possibility of secreting into the ventricular space In the goldfish some cells of the NLT have short axons but they could not be traced either into the third ventricle or into the pituitary with certainty Billenstien (63) has differentiated two types of secretory substances in *Salvelinus* AF positive and acid fuchsin or azocarmine stainable materials AF positive substance is believed to be of the NPO and the others belong to the NLT In the goldfish both nuclei are AF positive but the substances stained fast green or acid fuchsin present in the neurohypophysis could not be traced to these nuclei Further work with more selective staining techniques are required to demonstrate the secretory pathway of the NLT Since this nucleus is situated in a vascular bed the secretory material may have direct access to the blood vessels in the area of the nucleus

Stutinsky (53) has reported accumulation of neurosecretory material in the infundibulum and thickening of the neurosecretory axons in the hypophysectomized eel Kobayashi et al (59) observed accumulation of AF positive material at the proximal cut end of the neurosecretory tract in *Lepidogobius* In the hypophysectomized goldfish also accumulation of AF material was evident in the infundibulum and even along the hypothalamic axonal tract within a few days after the operation The cells of the NPO stained deep and exhibited degenerative changes two months post hypophysectomy if regeneration of the infundibular stalk did not occur Also there was no diurnal variations in the stainability of the NPO which is obvious in the normals In *Fundulus* hypophysectomy was followed by the degeneration of the NPO cells (Palay 53) The present study shows that in hypophysectomized fish the cut hypophysial stalk with its axons is capable of regenerating into a hypophysis

like organ as in mammals (Scharrer and Wittenstein 52 Billenstien and Leveque 55 and Moll 57)

ACKNOWLEDGMENTS

My thanks are due to the Population Council of the Rockefeller Institute New York for the award of a post doctoral fellowship during the tenure of which this investigation was carried out I am indebted to Dr Aubrey Gorbman Department of Zoology University of Washington for his encouragement and generous hospitality which I enjoyed in his laboratory I am grateful to Dr Ernst Scharrer Albert Einstein College of Medicine New York for critically reviewing the manuscript I am thankful to Dr Walter Chavin Department of Zoology Wayne State University for helping me to edit this paper in its present form

LITERATURE CITED

Arvy L M Fontaine and M Gabe 1959 La voie neurosecretrice hypothalamo-hypophysaire des Teleosteens J Physiologie *51* 1031–1085

Bargmann W 1949 Über das neurosekretorische Verknüpfung von Hypothalamus und Hypophyse Z Zellforsch *34* 610–634

——— 1953 Über das Zwischenhirn Hypophysen System von Fischen Z Zellforsch *38* 275–298

Bargmann W and W Hild 1949 Über die Morphologie der neurosekretorischen Verknüpfung von Hypothalamus und Neurohypophyse Acta Anat *8* 264–280

Billenstien D C 1963 Neurosecretory material from the nucleus lateralis tuberis in the hypophysis of the eastern brook trout *Salvelinus fontinalis* Z Zellforsch *59* 507–512

Billenstien D C and T S Leveque 1955 The reorganization of the neurohypophysial stalk following hypophysectomy in the rat Endocrinol *56* 704–717

Brehm H 1958 Über jahreszyklische Veranderungen im Nucleus lateralis tuberis der Schleie (*Tinca vulgaris*) Z Zellforsch *49* 105–124

Charlton H H 1932 Comparative studies on the nucleus preopticus pars magnocellularis and nucleus lateralis tuberis in fishes J Comp Neur *59* 237–275

Dodd J M and T Kerr 1963 Comparative morphology and histology of the hypothalamo-hypophysial system Sympo Zool Soc Lond *9* 5–27

Diepen R 1954 Über das Hypophysen Hypothalamussystem bei Knochenfischen (Eine vergleichend antomische Betrachtung) Ant Anz *100* 111–122

Follenius E 1962 Étude des neurones du noyau lateral du tuber de la Truite (*Salmo irideus* Gibb) au microscope électronique C R Soc Biol *156* 938

——— 1963 Étude comparative de la cytologie fine du noyau preoptique (NPO) et du tuber (NLT) chez la Truite (*Salmo irideus* Gibb) et chez la perche (*Perca fluviatilis*) Comparison des deux types de neurosecretion Gen Comp Endocrinol *3* 66–85

Follenius E and A Porte 1962 Étude du noyau preoptique de la Perche (*Perca fluviatilis* L) au microscope électronique C R Acad Sci *254* 930–932

Hild W 1951 Zur Frage der Neurosekretion im Zwischenhirn der Schleie und ihrer Beziehungen zur Neurohypophyse Z. Zellforsch *35* 33–46

Iturriza F C and O R. Koch 1964 Histochemical localization of some melanocyte stimulating hormone amino acid constituents in the pars intermedia of the toad pituitary J Histo Cytochem *12* 1

Kobayashi H S Ishii and A Gorbman 1959 The hypothalamic neurosecretory apparatus and the pituitary gland of the teleost *Lepidogobius lepidus* Gunma J Medical Sci *8* 301–321

Legait H E Legait 1956 Mise en evidence d voies neurosecretoiretoire extra hypothalamo-hypothysaires chez quelques batraciens et reptiles C R Soc Biol *150* 1429–1431

Moll J 1957 Regeneration of the supraoptico-hypophysial tract in the hypophysectomised rat Z Zellforsch *46* 686–709

Nishioka R S and H W Bern 1964 Secretion masses in the nuclei of the caudal neurosecretory cells of the teleost *Albula vulpes* Nature *203* 1191–1192

Oztan N 1963 The hypothalamic neurosecretory system of a poeciliid fish *Platypoecilus maculatus* and its sterile hybrid backcross with *Xyphophorus helleri* Gen Comp Endocrinol *3* 1–14

Oztan N and A Gorbman 1960 The hypophysis and hypothalamo-hypophysial neurosecretory system of larval lampreys and their response to light J Morph *106* 243–261

Pickford G E and J W Atz 1957 The Physiology of the Pituitary Gland of Fishes New York Zoological Society New York

Palay S L 1945 Neurosecretion VII The preoptico-hypophysial pathway in fishes J Comp Neur *82* 129–143

——— 1953 A note on the effects of hypophysectomy on the preoptico-hypophysial pathway in *Fundulus* Bull Bingham Oceanogr Coll *14* 42–45

——— 1960a The fine structure of the secretory neurons in the preoptic nucleus of the goldfish Anat Rec *138* 417–425

——— 1960 Fine structure of the neurosecretory cells in the preoptic nucleus of fishes Proc Europ Reg Conf Electron Micros 2 831–834

Scharrer E 1928 Die Lichtempfindlichkeit blinder Elritzen (Untersuchungen uber das Zwischenhirn der Fische I) Z vergl Physiol. *7* 1–38

——— 1930 Über sekretorische tatige Zellen im Thalamus von *Fundulus heteroclitus* L (Untersuchungen uber das Zwischenhirn der Fische II) Z vergl Physiol *11* 767–773

——— 1932a Die Sekretproduktion im Zwischen einiger Fische (Untersuchungen uber das Zwischenhirn der Fische III) Z vergl Physiol 17 491–509

——— 1932b Secretory cells in the midbrain of the European minnow (*Phoxinus laevis* L) J Comp Neur 55 573–576

——— 1941 Neurosecretion I The nucleus preopticus of *Fundulus heteroclitus* L J Comp Neur 74 81–92

——— 1951 Neurosecretion X A relationship between the paraphysis and paraventricular nucleus in the garter snake (*Thamnophis sp*)

Scharrer E and B Scharrer 1954 Neurosecretion In Handbuch der Mikroskopischen Anatomie des Menschen U Mollendorff und W Bargmann ed Springer Verlag Berlin 6 953–1066

——— 1963 Neuroendocrinology Columbia University Press New York

Scharrer E and G J Wittenstein 1952 The effect of interruption of hypothalamo-hypophysial neurosecretory pathway in dog Anat Rec *112 387 (abstract)*

Stahl A and C Leray 1962 The relationship between diencephalic neurosecretion and the adenohypophysis in teleost fishes In Neurosecretion Proc Third Intern Sympo Bristol Academic Press London pp 149–169

Stutinski F 1953 La neurosécrétion chez l *Anguille* normale et hypophysectomisée Z Zellforsch 39 276–297

Abbreviations (plates 1 2 and 3)

AF aldehyde fuchsin
BL blood vessel
CON connective tissue
EP ependymal lining
HR Herring body
INF infundibulum
NPO nucleus preopticus
NLT nucleus lateralis tuberis
NSA neurosecretory axon
PMC pars magnocellularis
PPC pars parvocellularis

PLATE 1

EXPLANATION OF FIGURES

1 Lightly and deeply stained chromophils and chromophobes in the NPO AF × 360

2 Arrow shows a vacuolated cell in the NPO AF × 360

3–4 Few NPO cells with simulating intranuclear AF positive globules Arrows show peripheral less dense regions in the cytoplasm AF × 360

5 AF positive cells of the NPO overlying blood vessels AF × 335

6 Small arrow shows axon overlying blood vessel Big arrows show AF positive bodies lying close to blood vessels in the NPO AF × 335

7 AF positive axons and dendrites of the NPO cells entering the third ventricle AF × 335

8 Arrows show the beaded axons in the region of the NPO AF × 335

9 Accumulation of Herring bodies around blood vessels in the pars intermedia Arrow shows finer axons lying in between cells AF × 200

10 Differentially colored Herring bodies in the neurohypophysis AF positive material is black in the figure AF × 335

11 Arrows show orange-G globules in the pars intermedia and neurohypophysis AF × 235

12 Deeply stained NPO of a specimen examined at 9 A M AF × 270

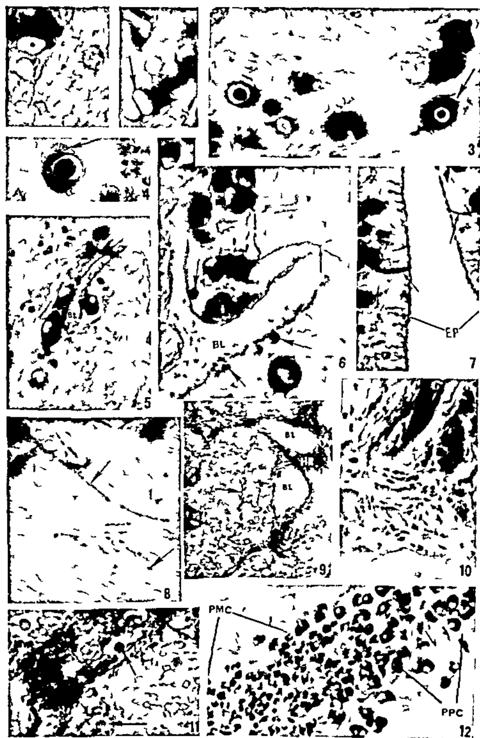

2
3
4
BL
5
BL
6
EP
7
8
BL
HR
BL
9
10
11
PMC
PPC
12

PLATE 2

EXPLANATION OF FIGURES

13 NPO showing deeply and lightly stained cells in a specimen examined at 3 P M AF × 270

14 NPO of a specimen examined at 12 P M showing fewer deeply stained cells Pars parvocellularis has very little stain AF × 270

15 Accumulation of AF positive material at different regions along the hypothalamic tract in a specimen seven days after hypophysectomy AF × 125

16 NPO of a specimen examined seven days after hypophysectomy showing almost the normal structure AF × 235

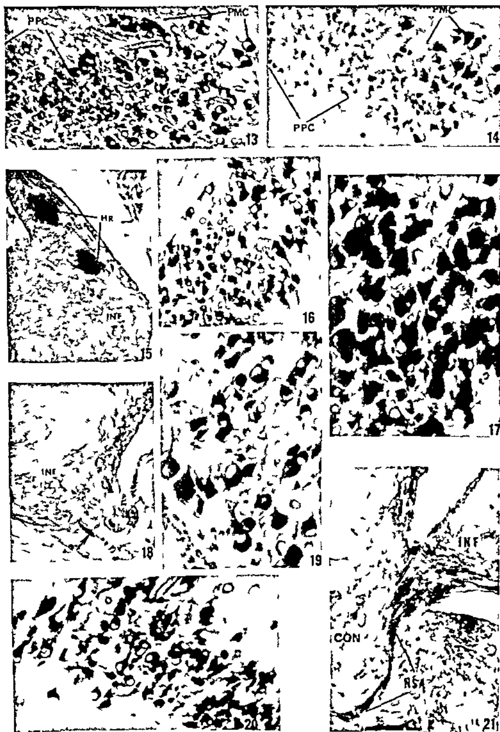
17 NPO of a specimen examined 78 days after hypophysectomy having no axonal regeneration Note the clumping up of intensely stained cells AF × 300

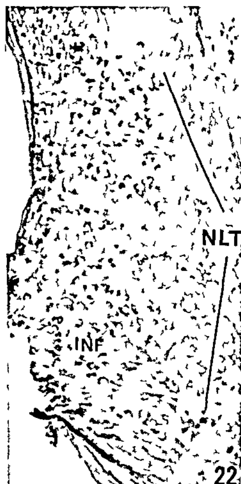
18 Non regenerated infundibular stalk of a specimen examined 78 days after hypophysectomy Arrow shows little accumulation of AF positive material at the cut end of the stalk AF × 115

19 NPO of a control specimen 78 days after sham operation showing normal condition AF × 300

20 NPO of a specimen 15 days after hypophysectomy having regenerated growing axons Note some cells are densely stained and grouped together AF × 235

21 Regenerated pituitary stalk 15 days after hypophysectomy showing neurosecretory axons growing into the connective tissue AF × 110


PPC
PMC
13
PMC
PPC
14
HR
INF
15
16
17
INF
18
19
INF
CON
RS
20
21









22 Nucleus lateralis tuberis AF × 200
23 NLT showing the scattered distribution of cells of varied size AF × 400
24 NLT of a specimen 32 days after hypophysectomy Note the absence of prominent AF positive granules in the cell bodies Arrows point cells with short axons AF × 450
25 Few cells of the NLT of a sham operated control having prominent cytoplasmic granules AF × 550

On Spirality in the Intestinal Wall

JOHN ELSEN AND LESLIE B AREY
Department of Anatomy Northwestern University

ABSTRACT Methods of stripping did not demonstrate a significant spiral course of fibers within longitudinal muscle coats of the jejuno-ileum of the dog cat hog or man Similar lack of spirality also characterized the large intestine of the dog The presence of taeniae in the hog and man and the extremely thin layer of muscle between them permitted only the demonstration of directly longitudinal muscle in taeniae

Bands of muscle stripped from circular coats of the small intestine of the dog and hog came off overwhelmingly in complete rings Stripping of the human intestine did not yield complete rings breakage at anastomoses with the adjoining muscle sheet may indicate oblique bands that link up a fiber system essentially circular into a functionally spiral system

Bands stripped from circular coats of the large intestine of the dog came off overwhelmingly as circles The taeniae of the hog and man prevent obtaining complete strips

Stripping of the submucosal stratum of the small intestine of the dog and man and of the large intestine of the dog revealed a latticed tube Its fibers intersect in double spirals coursing at angles of approximately 45 to the longitudinal axis of the intestine

HISTORICAL

The earliest testing of spirality in the circular muscle coat of the intestine was recorded by William Cole (1676) in a report to the Royal Society of London He boiled intestines of the ox and sheep and then stripped off bands of the circular muscle layer These were said to come off in a spiral manner — and apparently in a right handed helix (cf Lewis 22)

One hundred and forty five years later Carey (21) turned to this problem as a sequel to studies on the development of the epithelial lining of the intestine of the pig embryo Previously he had reported that mitotic figures pursue a left handed spiral when traced in successive serial sections that this spiral was closely wound during a rapid growth in diameter of the tube and that it was loosely wound during a rapid growth in length Such activities he believed should transmit tensions on the surrounding mesenchyme and produce a musculature arranged respectively as a close spiral in the inner layer and a loose spiral in the outer layer In 1921 to test the correctness of this hypothesis he everted the small intestine of the hog over a test tube and exposed the inner muscular coat A bundle of smooth muscle was then isolated and traced around the test tube through as many as 15 turns a complete turn occurred in every 0 5 to 1 mm or less of length In a similar way the outer muscular coat stripped in an uninverted intestine showed a spiral direction that made a complete left handed turn every 20 to 50 cm of length No mention was made of the number of animals used or of trials made These claims have gained wide acceptance by writers in journal articles and text books

Professor George F Sykes worked on this problem in the Harvard Anatomical Laboratory His findings of a clockwise spiral in the circular muscle remain unpublished except as cited by Lewis (22) In a private communication to the present senior author he wrote "As to Careys conclusions based on the distribution of mitotic cells I found that it was just as easy to link them up serially in right handed spirals as left handed ones Hence not trustworthy as evidence"

Alvarez (49) claimed to have confirmed Carey concerning the helicoidal arrangement of muscle in the intestine Also two sets of experimental observations might be interpreted as supporting a counterclockwise spirality as advanced by Carey Reid Ivy and Quigley (34) found that a bolus rotated a complete turn while passing a

distance of 23 to 35 cm in the dogs in testine Rotation was followed by wires attached to a bolus by a gyrometer used as a bolus and by a roentgenologic study of a radioopaque bolus Franklin and Maher Loughan (38) found that segments of intestine from the cat and rabbit suspended free by the proximal end twisted repeatedly in a clockwise direction which would correspond with a theoretically *counterclockwise spirality of the muscle*

Shortly after the publication of Carey s results Brandt (23) demonstrated macroscopic preparations of the muscular coats of the human intestine before the Anatomische Gesellschaft meeting at Heidelberg He did not find any discernible spiral in the longitudinal muscle The circular muscle was said to be primarily circular except that small twigs and sometimes stronger branches branched off the main bundles and rejoined neighboring bundles in an obliquely longitudinal clockwise direction *In this sense only could one speak* of a spiral course The concept advanced by Brandt was illustrated by Braus (24) in his textbooks of anatomy

The existence of connecting bundles as described by Brandt seems to have been observed many years ago by Boott (1733) from whose Latin dissertation a translation at point will suffice The inner layer whose dense and numerous fibers encircle the intestinal tube in true continuation in a circular manner — certain ones with drawing themselves in the midst of the *journey and neighboring ones connecting* Many authors deceived by this think that these fibers run down in a spiral manner

Goerttler (32) studied the structure of the human intestinal wall aided by polariscopic observations on the fibrous framework that contains and supports the muscle bundles The framework of the muscular coats was *found* to be a meshwork whose fibers slanted both cranio caudally and extero internally He did not observe spiralling in either layer *The circular mus*cle occurred in ring like bundles those of the small intestine being staggered in an overlapping manner The longitudinal muscle ran in courses paralleling the long axis of the *intestinal tube*

The arrangement of connective tissue fibers in the submucosa of the dog hog and man was studied by Mall (1896) by methods of drying and maceration He con*firmed the earlier findings of Clason (1872)* that there are two layers of connective tissue whose fibers cross at more or less acute angles (according to the tension exerted) and create a double spiral pattern *one clockwise and the other counterclock*wise This general arrangement was also asserted by Goerttler (32) who however emphasized the interwoven three dimensional aspect of the submucosa Carey (21) *mounted intestine on a test tube* removed the serosal and muscular layers and incubated the preparation at 37°C *Autolysis* occurred leaving the fibers of the submucosa intact As dessication proceeded *these fibers adhered to the test* tube in two spiral arrangements Both an inner close spiral and an outer loose spiral were said to course as counterclockwise helices

MATERIAL

Both the small and the large intestine together with their common mesentery were removed promptly after death from the dog cat *hog* and *man* After cleansing them externally and flushing out their contents dissections were done directly on the fresh untreated tubes Considerable experimentation with formalin preservation and with maceration and digestion procedures proved that these techniques are less satisfactory as a preliminary to ob*taining strips of muscle* Segments of convenient length for the particular work to be done were cut off consecutively as used For studies of muscle *direction* these segments were usually 12 inches in length When each segment of intestine was removed its cranial and caudal ends were marked to insure proper orientation during later handling

The intestines of the hog and man are similar in various ways Such features include *the diameter color texture thick*ness of the wall and the details of the muscle coats (including taeniae in the colon) They differ in that the mesocolon is free in the hog but is largely obliterated in man The intestines of the dog and cat are more similar to each other than to those of man or the hog

RESULTS ON THE LONGITUDINAL COAT

A Method

The serosal coat of all the animal types was difficult or impossible to remove Hence it was left in place since its presence or absence was found to make no demonstrable difference on the results obtained by stripping off of the bundles of muscle beneath Each cut off segment of the intestine was opened lengthwise along its mesenterial insertion When spread out serosa uppermost and pinned onto flat cardboard its shape was rectangular A small fine tooth tissue forceps was used to grasp a small portion of the longitudinal muscle layer that had been freed at its exposed end from the underlying circular layer A straight pull on the forceps then separated a strip progressively toward the far end of the pinned-down rectangle the torn edges following the grain of the muscle fiber arrangement The band usually included the entire length of the intestinal segment but it might leave some of its fibers behind attached to the circular layer and especially so toward the end of a strip The first strip was always made at the antimesenterial border of the intestine this was midway of the total rectangular specimen (fig 1) Here the muscle was thickest and the stripping most easily done Successive strips were then taken alternately until the two borders (representing the line of mesenterial attachment) were reached or until the strips became so thin (nearing the thinner layered mesenterial region) that they were difficult to obtain and uncertain to record In this manner 3 to 7 strips were obtained from each segment

The method of recording used was a simple plotting of the several dissected strips of a segment on a rectangle 12 inches long (the usual length of the segment) and arbitrarily 36 mm wide The beginning of each strip was recorded at the left hand end of the rectangle regardless of whether the dissection had proceeded in a caudal or cranial direction The location and width of each strip was plotted on the graph the positions of each end being indicated by dot marks In order to determine any direction and degree of spiralling the distance of each dot (representing the end of a torn edge) from the upper border of the rectangle

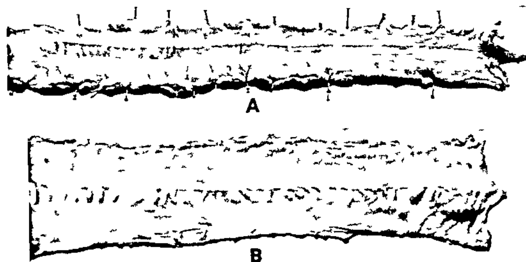


Fig 1 Exterior views of segments of the small intestine about 12 inches long Each segment has been opened along the mesenterial border and pinned flat A strip of longitudinal muscle has been torn away in a cranio-caudal direction × 50

A Dog showing tapering of the path of the approximately antimesometrial strip as the pull continued B Human showing the path of an antimesometrial strip essentially uniform in width

(representing the line of mesenterial attachment) was measured in millimeters If the sum of all the measurements of the distal set of plottings were numerically less than those at the proximal end, then this meant that, on a whole, the dissected strips of that intestinal segment were closer to the mesenterial border of the intestine at the distal end than at the proximal end In other words the preponderant tendency of all torn edges was counterclockwise (a left handed spiral) accordingly the sum total was recorded arbitrarily as a minus value In like manner if the sum of all distances measured were greater at the distal end then the preponderant edge deviation was clockwise (a righthanded spiral) and the sum was recorded arbitrarily as a plus value

In order to discover the degree of any general spiralling tendency in an intestine the average deviation from a direct line of a representative torn edge was computed by dividing the difference between the total plus and minus values by the average number of torn edges The degree of spiralling in relation to one full turn of 360 degrees could then be obtained by finding the ratio of this average deviation to the circumference of the intestine represented by 36 mm on the graph

B Small intestine

1 Dog The longitudinal muscle coat is well developed easily separable from the circular coat and favorable for stripping Twenty specimens of jejuno ileum were dissected and recorded in the manner already described A summary of results is assembled as table 1 In this tabulation the data from all the individual segments of each intestine are combined as totals The intestines of dogs nos 1 to 10 were dissected in a cranio caudal direction those of dogs 11 to 20 in the reverse direction

Inspection of the table shows at once that no intestine had a uniform tendency toward spiralling in any one direction Some divided the clockwise and counterclockwise deviations about equally among

TABLE 1

Records of stripping the longitudinal muscle coat in the jejunum ileum of 20 dogs

Intestine no	Length of jejunum ileum	Average clockwise deviation of edge lines	Average counter clockwise deviation of edge lines	Preponderant deviation of average edge line
		mm	mm	mm
1	10 6	+27 20	− 8 00	+19 20
2	10 8	+ 8 11	− 3 83	+ 4 28
3	9 6	+ 2 92	− 6 50	− 3 58
4	9 5	+11 70	− 8 33	+ 3 37
5	8 8	+ 9 13	− 3 73	+ 5 40
6	7 5	+ 6 58	− 5 10	+ 1 48
7	8 9	+20 00	− 2 70	+17 30
8	7 0	+ 5 75	− 6 00	− 0 25
9	12 8	+ 7 25	− 7 50	− 0 25
10	8 10	+ 5 00	−13 50	− 8 50
11	10 9	+12 16	−10 06	+ 2 10
12	11 0	+17 60	− 9 73	+ 7 87
13	14 0	+ 7 83	−10 70	− 2 87
14	8 10	+10 66	−10 43	+ 0 23
15	8 0	+13 00	− 8 75	+ 4 25
16	11 0"	+10 08	−12 37	− 2 29
17	8 0	+13 75	− 1 50	+12 25
18	10 8	+17 92	− 2 25	+15 67
19	10 6	+11 78	− 4 00	+ 7 78
20	8 0	+ 0 75	−11 75	−11 00
Totals	194 2	+219 17	−146 73	+72 44
Averages for single intestine	9 7"	+10 95	− 7 34	+ 3 62

the numerous strips made Others favored one direction or the other rather decisively Of the 20 intestines dissected 13 showed a preponderant deviation of the muscle strips favoring a clockwise spiral seven favored a counterclockwise spiral The actual measures of preponderance in terms of an average edge line are entered in the last column of the table The greatest deviation encountered in any one intestine (in terms of the average of the edge lines involved) was 27 20 mm (in dog no 1) or three fourths of a full turn in a clockwise direction over an intestinal length of 10 5 feet The smallest corresponding deviation in any single intestine was 0 75 mm (in dog no 20) also in a clockwise direction over a length of 8 0 feet this amounts to one fiftieth of a full turn In order to determine any dominant tendency toward a deviation in one direction or the other the numerical sum of all plus and minus values in the last column was obtained and reduced to an amount for a single intestine This calculation gives a clockwise deviation preference of 3 62 mm in relation to an average dissected intestine 9 6 feet in length At this rate it would require 93 feet of intestine to consummate one full turn It should be emphasized that the results in table 1 were based on about 1 000 edge line measurements It is obvious that a significant dominant spiralling tendency is not supported by these tests On the contrary the evidence obtained by permitting torn-off strips to follow any natural "grain" in muscle points to an essentially direct longitudinal arrangement of muscle fibers in the longitudinal muscular coat

Additional data from dog no 11 in table 1 will illustrate further details in relation to individual segments of the total jejuno-ileum Such information is representative of all intestines of all animal kinds used in this investigation Eleven successive intestinal segments were tested of these six showed preponderant clockwise deviations of an average edge line throughout the 12 inch segment ranging between 0 83 mm and 5 00 mm Similarly five gave preponderant counterclockwise departures ranging between 0 40 mm and 4 25 mm These opposite deviating tendencies occurred in random order throughout the 11 segments

As a further check the intestine of an additional dog was divided into 17 six inch segments and tested to see if shorter segments would change the results significantly On all points the findings were essentially as before

It was noticed that sometimes a muscle strip from the 12 inch segments recorded in table 1 would not be uniform in thickness throughout its width For example the central region might be of full thickness whereas the sides contained only the more superficial fibers In order to ascertain if any differences exist between such thick and thin layers (that is any stratification with different tendencies) nine well-developed intestines were dissected some cranio-caudally and others in the reverse direction All strips were plotted and where there were strips of mixed thickness both the thick and thin parts were recorded separately The results varied in different intestines but no constant tendencies were discovered that showed a significant difference in fiber direction in strips of full or partial thickness Hence there was no demonstrable difference in the orientation of muscle fibers that was related to depth in the longitudinal muscle coat

2 *Cat* The small intestine resembles a firm cord because the lumen is very small compared to the relatively robust wall Its muscular layers are well developed and the longitudinal coat is better represented than in any other of the animals studied It is easy to dissect and hence favorable for the purpose of this investigation The strips came off in full thickness and uniform widths throughout the entire length and breadth of the spread-out segments Eight specimens of the jejunum ileum were dissected in a cranio-caudal direction using six inch segments because of the shorter intestine of this animal

Omitting a detailed tabulation the essential results can be summarized Three intestines showed a preponderant tendency for an average edge line to take a clockwise deviation five intestines showed the opposite tendency The greatest deviation of an average edge line of any intes

tine was 5 75 mm (or nearly one seventh of a full turn) in a clockwise direction The least deviation was 1 0 mm (or one thirty sixth of a full turn) in a counter clockwise direction In order to determine the existence of any dominant tendency toward either clockwise or counter clock wise spiralling in all intestines studied the numerical sum of all plus and minus values for an average edge line in all in testines was obtained and then reduced to the average amount for a single intestine This value is 1 74 mm in a counter clock wise direction or one twentieth of one full turn — a figure of no significance with respect to functional spirality

3 *Hog* The small intestine is remark able for the thinness of its muscular wall It stands in sharp contrast to that of the cat which is several times thicker The longitudinal muscle layer of the hog is very thin more so than that of any of the other mammals studied and is not well defined grossly Slender bundles of fibers seem to produce small elevations of the serosa giving the appearance of fine lon gitudinal striations Even though the di rection of the muscle fibers could be dis cerned through the intact serosa the coat was difficult to dissect There was no clear separation of the two muscle layers and attempts at stripping produced a thin strip leaving behind a little of the longi tudinal muscle It was sometimes impos sible to obtain satisfactory strips except in the region of the antimesenterial bor der Although this mammal is not a choice one for the purpose at hand it was the one used by Carey (21) and for this reason 12 specimens were dissected all but one in a cranio-caudal direction Portions of the intestine distended with gas or chyme were not used because in dilated regions the muscular layers were thinned out and very difficult to dissect

The detailed data are presented as table 2 because it was solely from the hog that Carey (21) drew his conclusions on spirality in the longitudinal coat of mus cle The greatest departure of an average edge line from a direct course occurred in hog no 3 the amount was 50 83 mm (or 1 4 full turns) in a clockwise direction in a jejuno ileum nearly 40 feet long Sim ilarly the smallest divergence was in hog no 8 in which the departure was 1 75 mm (or one twentieth of a full turn) in a counter clockwise direction in usable por tions of an intestine totalling nearly 16 feet long Inspection of the last column of the table reveals that seven intestines show a preponderant tendency for an average strip edge to deviate in a clock wise direction five intestines show the reverse tendency As a whole the pre ponderant dominance in terms of an av erage edge line in an average intestine of 21 feet was 6 42 mm in a clockwise direc

TABLE 2

Records of stripping the longitudinal muscle coat in the jejunum ileum of 12 hogs

Intestine no	Intestinal length dissected	Average clockwise deviation of edge lines	Average counter clockwise deviation of edge lines	Preponderant deviation of average edge line
		mm	*mm*	*mm*
1	19 4	+25 00	−13 50	+11 50
2	22 0	+12 92	−20 83	− 7 91
3	39 6	+50 83	−29 00	+21 83
4	32 0″	+34 16	−20 83	+13 33
5	22 0	+13 42	−17 23	− 3 81
6	21 0	+31 75	−14 50	+17 25
7	18 5″	+11 25	−30 50	−19 25
8	15 10	+43 08	− 1 75	+41 33
9	14 0	+16 33	− 9 75	+ 6 58
10	15 0″	+ 8 33	−15 17	− 6 84
11	17 0″	+14 17	−28 42	−14 25
12	15 6″	+22 91	− 5 58	+17 33
Totals	251 7″	+284 15	−207 06	+77 09
Averages	20 11″	+23 68	−17 26	+ 6 42

tion At this rate of spiralling a full turn would be accomplished in 118 feet of intestine These results disagree flatly with Carey s contention of a consistent anticlockwise spiralling that completed a turn every foot or two of intestine

4 Man The human intestine and that of the hog were similar in size color texture and thickness of the wall In both gas and food material collected in certain portions whereas intervening portions were empty As in the hog strips taken even a little distance from the antimesenterial border were thin and frequently difficult to follow the full length of the segment Five specimens were dissected taken from all age groups but those from children and young adults were easiest to dissect and most reliable In such favorable specimens and especially at the antimesenterial border strips of full thickness came off with equal ease in both directions No strip showed thick and thin portions at the same level as did some of those from the dog

A summarization of results will be given without presenting a complete tabulation of data The greatest deviation encountered in any intestine in terms of an average edge line was in specimen no 2 the departure from a straight course was 14 75 mm (or two-fifths of a full turn) in a counterclockwise direction over an intestinal length of 15 feet Similarly the smallest deviation occurred in specimen no 5 the departure was 3 24 mm (or one eleventh of a full turn) in a counterclockwise direction over a distance of 11 feet Four intestines showed a preponderant tendency for an average edge line to deviate in a clockwise direction one intestine illustrated a tendency in the opposite direction The net preponderant deviation from a straight course in all five intestines was a 2 90 mm clockwise spiralling over an average intestinal length of 13 2 feet This is the equivalent of a full turn in 164 feet of intestine

C Large intestine

1 Dog The wall is somewhat thinner than that of the small intestine both actually and relative to the size of the lumen The rectum is easily distinguished from the colon by its markedly thicker layer of longitudinal muscle Seemingly weaker muscle bundles thinner muscle coats and increased connective tissue are factors that make separation of the muscle layers more difficult than in the small intestine

Omitting a detailed tabulation of results a summary of essential findings will be summarized as follows Twenty six intestines were dissected half of them in a cranio caudal direction and an equal number in the reverse direction Fourteen intestines showed a majority of the average edge lines taking a clockwise deviation Eleven intestines showed the opposite or counterclockwise tendency In one intestine the two sets of measurements balanced exactly producing no evidence of spiralling The greatest divergence of an average edge line from a straight course was 39 mm in a counterclockwise direction over 12 inches of intestine this equals 1 1 full turns The smallest deviation was 7 mm in a counterclockwise direction over eight inches of intestine this is the equivalent of one full turn in 3 4 feet These are tighter spiralling tendencies than was encountered in the small intestine but the following statements will show that the clockwise and counterclockwise tendencies largely offset each other in the entire set of experiments The net deviational tendency of all average edge lines was in a clockwise direction equalling 6 20 mm In terms of the average intestinal length dissected (9 2 inches) the deviation of an average edge line was 0 24 mm Such an amount would be the equivalent of one full turn in 115 feet of large intestine

2 Hog Man Both mammals have taeniae with an intervening longitudinal layer so thin as to defeat attempts at removal by stripping The taenia themselves pursue a straight course in relation to the mesentery In the hog the large intestine is wholly free portions of a taenia were stripped off as a ribbon as long as six feet but these strips showed no noticeable deviation in any of the five colons examined Similar dissections of two human colons also failed to show any evidence of spiralling within the taeniae

RESULTS ON THE CIRCULAR COAT

A Method

The best method of preparation and a reasonably satisfactory one was to mount a 12 inch segment of the intestine on a test tube of appropriate diameter Beginning at the antimesenteric border, the serosa and longitudinal muscle coat were slit through and then removed by blunt dissection As the mesentery was approached vessels and nerves were divided small openings in the circular coat remained as markers of the mesenteric border

A second method of preparation that used by Carey (21) consisted of inverting the segment of intestine over a test tube and then removing the mucosal and submucosal linings This was satisfactory if done carefully but the muscular tube so prepared was quite flimsy and the circular fibers on stripping tended to adhere to the longitudinal coat

Dissections began at one side or the other of the mesenteric border where the muscular layer was thinnest by picking up and freeing a small band of circular fibers A straight pull then caused the bundle to follow a complete course around the intestinal wall It could be seen with the naked eye whether the strip returned directly to its starting position or whether it spiralled in one direction or the other In no trial did the strip make more than one turn Measurements were not done but a recording was made of the location of each strip and whether its course was strictly circular a clockwise spiral or a counterclockwise spiral When the intestine was inverted corrections had to be made in the records because the direction of spiralling as then observed is the reverse of that of the uninverted intestine when viewed externally Incidentally there was no mention by Carey (21) that this correction was made in his report of consistent counter clockwise spirality

B Small intestine

1 Dog This coat is a thick firm and compact layer It is considerably thicker than the longitudinal layer and separates easily both from that layer and from the submucosa Four well developed intestines were selected for study and segments at all levels were tested With the segment in its normal uninverted relation on the supporting test tube 659 bands of the circular coat were stripped off the jejuno ileum Also a total of 142 trials were made on the duodenum As a further check 105 strippings were made from the jejunum ileum after it had been inverted The results of all of these strippings are recorded in table 3

The relatively small number of bands from the jejunum ileum that showed a spiralling tendency were not consistent as to direction although the clockwise tendency prevailed One animal used in the duodenal trials showed such a large number of clockwise spirals at the duodeno jejunal junction that its frequency of occurrence rose to 35% It was this figure that raised the percentage for the group

TABLE 3

Records of stripping the circular muscle in the small intestine of four dogs

Portion of small intestine	Total trials	Undeviating ring	Clockwise deviation	Counter clockwise deviation
		%	%	%
Duodenum (outside dissection)	142	77 5	16.9	5 6
Jejunum ileum (outside dissection)	659	93 5	4 8	1 7
Jejunum ileum (inside dissection)	105	88 5	6 7	4 8
Jejunum ileum (weighted totals)	764	92.8	5 0	2 2

to probably an atypically high level This tendency was not present in the other two specimens recorded nor was it observed in two additional specimens not included in the table

2 *Cat* The circular muscle layer of the small intestine is 1 mm in thickness and of a rubbery consistency It was impossible to strip off complete circular bands Even when a strip began as large groups of fibers it would dwindle away to nothing before the circuit was completed Hence no satisfactory results could be obtained

3 *Hog* The circular muscle layer of the small intestine visible as bundles through the outer layers is thin and composed of small bundles of fibers The tensile strength of these bundles is slight so that it was extremely difficult to free them from the submucosa or longitudinal muscle Apparently adhesion to surrounding tissue was greater than cohesion of the bundles themselves Yet since this relatively unfavorable animal was the sole one used by Carey (21) a series of tests was conducted

Only those regions of the intestine that are empty and collapsed are suitable for experiment Three such segments from the upper middle and lower levels were used in both the normal and inverted positions A total of 47 trials proved satisfactory for recording and in none of these was any tendency toward spiralling noticed

4 *Man* The circular muscle of the small intestine resembled that of the hog While this layer appeared to be composed of heavier bundles than in the hog in attempted dissections these would break when an anastomosis with another bundle was reached Because of this no bundle formed a complete ring and it was impossible to obtain data with respect to the presence or absence of spiralling other than that related to anastomoses

C *Large intestine*

1 *Dog* The circular muscle was studied in five animals In 159 tests by stripping 149 (93 7%) complete simple rings were obtained Of the remainder one spiralled clockwise (0 6%) and nine counterclockwise (5 7%)

2 *Hog Man* In both the circular muscle coat would not come off in satisfactory strips The taeniae and connective tissue associated with them presented impassable barriers as if the circular muscle made an insertion at that point Hence no data on fiber direction could be obtained

RESULTS ON THE SUBMUCOSA

A *Method*

This tubular stratum was freed from the muscularis by blunt dissection and from the mucosa by autolysis aided by blunt scraping These treatments produced a whitish glistening translucent tube A region of the submucosal tube was prepared for testing by immersing it in hot water and filling it with melted paraffin As the water cooled and the paraffin solidified the floating submucosal tube retained its natural coils and relations On removal from the water the submucosal tissue dried and adhered to its paraffin core

In order to discover the architectural plan of the submucosa a small local portion of this parchment like membrane was freed from the paraffin filler along three sides Grasping this tab of submucosa with fine tissue forceps stripping was then continued by progressive pulling in the direction of the intact membrane In relation to the first starting point other strips were pulled away in other radial directions The direction of traction was made to correspond to whatever course the strip began to take as it came separate so that the pulling force was always directed in the initial line of separation In this way no strip was made to deviate unnaturally by pulling at an angle to its easiest course

B *Experiments*

1 *Dog* This animal is important since it was used by Mall (1896) in his basic study A submucosal tube measuring 14 feet in length was removed by dissection intact from the entire intestine It was cut into five segments of different lengths and these were filled with a paraffin core as already described

After a series of preliminary tests 100 trials at representative levels of the intestine constituted a final series In all but four attempts the strips tore easiest when the pulling force was directed at an angle of approximately 45° to the long axis of the intestine These strips came off with equal ease and regularity when torn off the submucosal tube so as to make either a clockwise or a counterclockwise spiral They had even sharply defined borders and sometimes maintained their spiral course for one or more turns Frequently however when encountering the region corresponding to the line of mesenterial attachment a strip would abandon its spiral trend and follow along this border rather than crossing it

C 2 *Man* From the small intestine of a 25 year old individual three three foot segments of submucosa were filled with paraffin as before When strips were peeled off the results were identical with those obtained on the dog The strips tore free along spiralling lines in either direction at angles of about 45° to the long axis The results both from the dog and man imply that the fiber arrangement in the submucosa of both the small and large intestine is one of double intersecting spirals

3 *Other tests* Further tests were made with segments of the submucosa that had been drawn over test tubes and allowed to dry and adhere to them Thirty two segments from the dog and 20 segments from man were subjected to trials in which the submucosa had dried in lax taut and twisted positions All of the results of strippings argued for a double spiral as Mall (1896) described and against two spirals coursing in the same direction as Carey (21) contended

From one of the human segments a strip of submucosa was obtained that showed remarkably well the double intersecting structure of this layer The naked eye could see the latticework whose components intersected in a slanting manner with respect to the circular circumference and the longitudinal axis of the intestine This specimen was made into a permanent museum preparation

LITERATURE CITED

Alvarez Morujo A 1949 Anatomia de la con traccion intestinal Medicina 25 402–417

Boott P 1733 De intestinis tennibus 27 pp Lugd Bat G Wishoff

Brandt W 1923 Makroskopische Preparate von der Musculatur des menschlichen Dunn darms Verhand Anat Gesell 32 261–263

Braus H 1924 Anatomie des Menschen 2 277 Springer Berlin

Carey E J 1921 Studies on the structure and function of the small intestine Anat Rec 21 189–215

Clason E 1872 Upsala Lak Forh 7 182

Cole W 1676 A discourse concerning the spiral instead of the supposed annular structure of the fibers of the intestines etc Phil Trans Royal Soc London *11* 603–609

Franklin K J and G P Maker Loughnam 1938 The circular musculature of the small intestine J Physiol *94* 426–429

Goerttler K 1932 Der konstructive Bau der menschlichen Darmwand Morph Jahrb *69* 329–3"9

Lewis F T 1922 The spiral trend of intestinal muscle fibers Science *55* 704–706

Mall F 1896 A study of intestinal contraction Johns Hopkins Hosp Rep *1* 37–75

Reid P E A C Ivy and J P Quigley 1934 Spiral propulsion of a bolus in the intestine Am J Physiol *109* 483–487

An Electron Microscopic Visualization of Transport Across Rat Visceral Yolk Sac [1]

ROGER O LAMBSON [2]

Department of Anatomy Tulane University School of Medicine New Orleans Louisiana

ABSTRACT In an attempt to elucidate some of the mechanisms utilized in the placental transfer of large molecules morphological changes in the visceral yolk sac have been studied in relation to the disposition of ferritin molecules at different stages of gestation

From the tenth through the eighteenth days of pregnancy ferritin molecules were readily absorbed by the visceral endodermal cells when this material was injected either into the maternal blood stream or directly into the uterine lumen These large molecules entered the endodermal cells through a progressively developed apical canalicular system and became localized within relatively large heterogenous vacuoles These vacuoles were seen to retain the ferritin for long periods except during the last few days of gestation At the end of pregnancy when normally antibodies are being transferred in the largest quantities to the fetus relatively smaller vesicles which contain ferritin appeared to have migrated away from the larger apical storage vacuoles and to have approached the endodermal basal plasma membrane Once the large protein molecules left these cells they appeared to pass either directly into vitelline capillaries or through mesothelial cells which line the exocoelom

Transport of large protein molecules through visceral endodermal cells involves an apical tubular system large storage vacuoles and smaller vesicles which appear to migrate basally near the end of pregnancy Regulation of this process appears not to depend on the failure or success of entry of such a substance into these cells but rather on its subsequent disposition once it is intracellular

Any consideration of placental function is complicated in those animals where more than one membrane is present which can serve for materno-embryonic exchange In eutherian mammals where a chorioallontoic placenta is the usual structure for this exchange the yolk sac membranes are variably developed (Amoroso 52 Hamilton Boyd and Mossman 62) However there is increasing evidence in the literature to suggest that in several species these yolk-sac membranes not only are involved but are of considerable importance in placental transport In the rat in addition to the usual chorio-allantoic placenta a complex inverted yolk sac placenta develops (Huber 15) and persists to term

The observations made by Goldman (09 12) Everett (33 35) Gillman Gilbert Gillman and Spence (48) and others that visceral endodermal cells of the yolk sac absorb certain vital dyes while the chorioallantoic placenta does not indicate a difference in the specificities of these membranes On the basis of results obtained by surgically manipulating the visceral yolk sac Noer and Mossman (47) suggested that this membrane acts in a complementary fashion to the chorioallantoic placenta An example of this complementary action comes from the histochemical studies of Wislocki Deane and Dempsey (46) Their results suggested that the visceral yolk sac serves as the route of iron transport while the chorioallantois appears to be specific for calcium transfer Nylander (53) demonstrated rather conclusively that iron is transported through the visceral yolk sac

[1] This work i p rt of a di sert ti n submitted to the Departm nt of Anatomy Tul n Uni ersity School of M dicine a requirement f r th Doct r of Ph l osophy degree Th author grat fully a knowl dges his in re pprecl ti n t Dr William P Jollie for hi p ti nt und t nding nd techni l demon tration through ut thi in stig tion nd fin lly for his crit i l s i t n e in the prep ration of the m nuscript Th i tigati n wa s pported by N I H Re r h g t GM 11484 nd in p rt by N I H T ining gr nt 5T1-GM 793

[2] Present ddre Dep rtment of An tomy Uni sity of Kentucky M dic l Cent Lexington Kentucky 40506

and described as well possible regulating mechanisms for this process

The placental transfer of maternal antibodies which in part are responsible for fetal and neonatal immunity demonstrates again the possible complementary nature of materno fetal exchange In the rat Brambell and Halliday (56) have demonstrated that the passage of specific antibodies which occurs during the last part of gestation takes place through the visceral yolk sac with its vitelline circulation and not through the chorioallantoic placenta Similarly Mayersbach (58) visually traced fluorescent labeled antibodies from maternal blood into the uterine lumen and across the yolk sac to the fetus during the last part of gestation

By explanting the visceral yolk sac to the chick chorioallantoic membrane Ferm and Beudoin (60) have shown that visceral yolk sac absorptive specificities are an inherent property of the endoderm and are not related to other embryonic membranes or particular maternal relationships Similarly Sorokin and Padykula (64) maintained visceral yolk sac in tissue culture Their observations led them to conclude that the yolk sac carries a timetable of differentiation that provides for metabolic accompaniment to the various morphological and functional events"

It thus appears that specificities among fetal membranes not only exist but, in addition seem to be intrinsically regulated

The prenatal passage of large antibody molecules (molecular weights 160 000–850 000) through the yolk sac has raised several important questions (Brambell 58) First how or by what mechanism do these large molecules move through this cellular structure? Second in what part of this barrier does selection between similar molecules occur? Third are these selective transport mechanisms limited solely to antibody movement late in gestation or might they have a wider application to include a variety of developmental transport problems and even to membrane transport in general?

Although diffusion solvent drag etc may be important in the movement of large molecules pinocytosis or phagocytosis seen both on the light and electron microscopic levels appears to be more directly involved in the transport of such materials Such morphological evidences for transport have been described in several tissues and cell types as follows lung (Karrer, '58 60), intestine (Clark 59 Palay and Karlan 59) endothelium (Palade 60) amebae, (Brandt and Pappas, 60) macrophages, (Essner, 60) kidney, (Farquhar and Palade 60 Miller 60 Trump, '61), liver and oocytes (Roth and Porter 62 64) thyroid (Wissig 63) and others Similarly in the first descriptions of placental ultrastructure (rat Wislocki and Dempsey 53 55 guinea pig Dempsey, 53) specializations of the plasma membrane particularly in the visceral yolk sac endodermal cells were noted

Because the visceral yolk sac with its structurally complex cells, has been shown to be involved in the transfer of large protein molecules in the present investigation yolk sac membranes were examined with the electron microscope at intervals from early in their development to term The normal ultrastructure of this membrane and its changes during gestation were examined and correlated with the route of entry intracellular localization and exit route of ferritin

MATERIALS AND METHODS

Sprague Dawley rats obtained from the Charles River Breeding Laboratory were used in this investigation As an aid in obtaining placentas of comparable gestational age timed pregnancies were obtained from animals fed and watered *ad libitum* and housed in an air conditioned light tight room where they received ten hours of darkness and 14 hours of artificial light Saline vaginal lavages were taken daily Mating was permitted during the night following proestrus and those females showing sperm were isolated and day one of pregnancy was indicated Parturition takes place on the twenty second day in females bred under these conditions

Control animals were anesthetized with an intraperitoneal injection of 5 mg/100 gm body weight sodium pentobarbital (nembutal–Abbott Laboratories) on days 10 12 14 16 18 20 and 21 of gestation

Experimental animals at similar gestational ages received horse spleen ferritin (Nutritional Biochemicals Corp) dialyzed against EDTA to remove traces of cadmium (Farquhar and Palade 61) Injections of 100 mg of this readily identifiable protein (Farrant 54 Muir 60) were made either intravenously or into the uterine lumen At suitable times after administering the protein (30 min –4 days) the animals were anesthetized and tissue specimens were removed for fixation embedding and observation

Because the entire ten-day conceptus required fixation a 3% glutaraldehyde solution in 0 1 M phosphate buffer (Sabatini Bensch and Barnett 63 Harkin 64) was used at 4 C for one hour fixation Following a 24 hour wash in 0 1 M phosphate buffer containing 2 5% glucose (Harkin 64) the tissues were post fixed in phosphate buffered 1% osmium tetroxide (Millonig 62) for two hours Visceral yolk sac membranes were dissected from embryos 12–21 days old and fixed either in the 3% glutaraldehyde as above or minced in a cold 1% osmium tetroxide solution made with Millonig's buffer diluted 1 1 with distilled water After 30 minutes fixation osmium fixed tissues were rinsed briefly in cold water and rapidly dehydrated in ethyl alcohol Small pieces were embedded in British Araldite (Richardson Jarett and Finke 60) Sections of 60–120 mμ thick were cut with glass knives on a Porter Blum ultramicrotome mounted on naked 200 × 200 or 100 × 400 mesh copper grids stained with lead hydroxide (Millonig 61) and viewed in a RCA EMU 3G electron microscope

OBSERVATIONS

I *Normal yolk sac*

The visceral wall of the yolk sac is composed of three concentric cellular layers (fig 2) which are separated by two fibrous sheets (fig 4) The first or outer most cellular layer is composed of visceral endoderm At first this simple epithelium lines the inner aspect of the yolk cavity (fig 1) However after rupture of the investing decidua capsularis and the parietal yolk sac at the outer aspect of the yolk cavity the epithelium becomes exposed to the uterine cavity (fig 1) The endodermal cells rest on a basement membrane (fig 5) which in turn rests upon a thin outer fibrous sheet (fig 4) Internal to this "visceral basement membrane" (Wislocki and Padykula 53) is found the second cellular layer Depending upon the stage of development and the area of the wall under consideration it consists of scattered mesenchymal or fibroblast like elements fetal capillaries or both (fig 2) Directly internal to these elements is the second fibrous sheet a thick "serosal basement membrane" (Wislocki and Padykula 53) This sheet separates the second cellular layer from flattened mesothelial cells which line the exocoelom The mesothelium constitutes the third cellular layer of the visceral yolk sac (figs 2 and 4)

At ten days of gestation numerous microvilli are seen to extend into the yolk cavity from the visceral endodermal cells (fig 2) The microvilli are long slender and at times branched

Between the bases of the microvilli the plasma membrane shows variably developed invaginations all of which are lined with a delicate brush like material 200–300 A deep Adjacent to such invaginations are similarly coated circular profiles (fig 2)

The next deeper layer of the cytoplasm contains scattered strands of rough surfaced endoplasmic reticulum large mitochondria numerous ribonucleoprotein granules and membrane bound globules which approximate 0 2–3 0 μ in diameter In many instances the endoplasmic reticulum bears an intimate spatial relationship to both mitochondria and the globules (fig 2)

The nuclei of the epithelial cells are basally located and are commonly pleomorphic Golgi elements either as small smooth vesicles or as parallel membranes occupy a paranuclear position primarily laterally or basally placed Typically between the nucleus and basal plasma membrane large lipid drops are found Occasionally small lipid droplets are found within the nuclear envelop as well

The intercellular spaces on the luminal side of the cells are invariably occluded by

a terminal bar or *zonula occludens* (Farquhar and Palade 63) The intercellular spaces in the apical two thirds of the cells at ten days show limited areas of dilation where the lateral cell margins are moderately convoluted The basal one third of these spaces on the other hand frequently are dilated and the cell margins are markedly folded The basal plasma membrane is quite irregular and a subepithelial basement membrane is indistinct at this time (fig 2)

Electron micrographs of visceral yolk sac 12 days old show many features similar to those seen at ten days The coated invaginations of the apical plasma membrane seem to have increased in depth and more circular profiles are seen than before Figure 3 shows the dense fibrous 200–300 Å deep material which lines these membrane invaginations

By 14 days some of the tall slender microvilli which were seen earlier have been replaced in certain areas either by highly branched thin villi or by villi which appear swollen in a pseudopod like arrangement The apical invaginations still retain their fuzzy coat but appear deeper curved and often branched (fig 6) In addition numerous Golgi vesicles often are seen in association with the lateral cell plasma membrane These vesicles contain a granular material which is optically similar to that in adjacent intercellular spaces (fig 7) The basal plasma membrane shows some evidence of micropinocytosis and a subepithelial basement membrane is well developed at this time (fig 5) In addition to the mesenchymal elements still found in the middle cellular layer of the yolk sac the fetal blood cells within vitelline capillaries have become rounded and have assumed an erythroblast like appearance (fig 5) Fibrous elements of the visceral and serosal basement membranes also appear about this time

The fine structure of the visceral yolk sac which is seen at 16 days of gestation differs little from that at 14 days However from the tenth day there has been a gradual loss of free ribonucleoprotein granules from the cytoplasm and the number of large lipid drops scattered throughout the endodermal cells appears greater From the sixteenth day on relatively more sections indicate that a direct structural relationship exists between the apical invaginations and the large globules (fig 8)

From the sixteenth to twenty first days these membranous infoldings develop further to form an extensive interconnected apical canalicular system (fig 9) Some of these canals connect directly to large vacuoles which may contain small lipid droplets myeloid figures and/or small vesicles of varying electron density Rough surfaced endoplasmic reticulum is well developed at this time it is either scattered in the cytoplasm or is found as spirals which are formed of several turns The visceral and serosal basement membranes are now quite thick (fig 4) and surround scattered mesodermal elements and vitelline blood vessels In addition to demonstrating a considerable amount of ergastoplasm numerous mitochondria and abundant Golgi material the mesothelial cells which line the exocoelom show evidence of micropinocytotic activity (fig 4)

Visceral yolk sac epithelium from animals on the day preceding parturition (fig 9) shows numerous microvilli and an extensive array of apical canaliculi Lateral and basal cell margins are highly tortuous The intercellular spaces especially near the base are filled with a granular material which was noted first at 14 days Golgi elements which contain a similar material are found in a supranuclear and lateral position The numerous small vesicles which earlier in gestation were limited to a narrow apical zone are now scattered throughout the cytoplasm (fig 9)

II Ferritin injected animals

Ferritin which was used in this study as a marked protein molecule was injected into rats at two-day intervals from day 10 to day 21 of pregnancy from 30 minutes to four days before autopsy In different experiments injection was made either into the maternal venous system or into the uterine lumen At all stages which have been investigated intravenously administered ferritin was readily found in the uterine lumen within a short time

Visceral yolk sac endodermal cells on days 10 through 18 contained ferritin after maternal administration The cytoplasm of 10-day visceral endodermal cells contained numerous ferritin filled vacuoles of varying size and density (fig 10) The heterogeneity noted at times within a single vacuole might be accounted for by a possible fusion between vesicles In addition to the ferritin laden vacuoles individual ferritin molecules were sometimes found scattered free in the cytoplasm The disposition of ferritin at 12 and 14 days was similar to that at ten days

As in the control animals on the sixteenth day sections from ferritin injected animals showed membrane invaginations which connected directly to apical vacuoles Figures 11 and 12 demonstrate several features of the transport process of ferritin into the endodermal cells Ferritin molecules were found within the delicate brush like material which lines the apical canalicular system (fig 11) Figure 12 demonstrates ferritin within these canals as well as within apical vacuoles Visceral yolk sac epithelium from animals 18 days pregnant which had been given ferritin either two hours or four days previously exhibited ferritin containing vacuoles in the apical cytoplasm At all stages through the eighteenth day except for a few scattered ferritin particles both in the cytoplasm and outside these cells the ferritin molecules were located within apical vacuoles

On the twentieth and twenty first days the disposition of ferritin was somewhat different On these two days for the first time 60 minutes after injection ferritin was found within the visceral and serosal basement membranes and within capillary endothelial cells as well as apically (figs 13 and 15) Small dense ferritin-containing vesicles could be seen at deeper levels within the endodermal cytoplasm (fig 13) and near the basal plasma membrane (fig 14) The epithelial basement membrane appeared not to act as a barrier to ferritin since no concentrations of this material were found between the basal plasma membrane and this structure In addition to the ferritin which was found within vacuoles inside capillary endothelial cells (fig 15) ferritin was also noted within small vacuoles of some of the mesothelial cells which line the exocoelom (fig 16)

DISCUSSION

The ultrastructure of visceral yolk sac epithelium which has been described sequentially from 10 to 21 days clearly indicates a series of morphological changes during this interval For the most part the present findings agree both with other descriptions of yolk sac ultrastructure (guinea pig Dempsey 53 rat Wislocki and Dempsey 55 Padykula and Wilson 60 Wislocki and Padykula 61 Sorokin and Padykula 64) and with histochemical analyses of this membrane (Wislocki and Padykula 53 Padykula 58a b Padykula and Richardson 63) However in the present study in which visceral yolk sac has been examined from early in development until the day preceding parturition several features of the visceral endodermal cells which previously have been either unemphasized or perhaps unnoticed have become evident

During gestation the apical canalicular system of visceral endodermal cells demonstrates a dramatic development from a number of simple membrane invaginations to a complex interconnected series of canaliculi which are directly continuous with large vacuoles Even at ten days when this apical system is composed of simple invaginations the plasma membrane at these invaginated sites is thickened by a fine filamentous material Later in gestation when these infoldings have increased in depth they still retain their extraneous coating Coatings similar to those which are described here have been found around membrane invaginations in a variety of different cell types (Roth and Porter 62 and 64 and others) and are believed to be involved in protein absorption Bennett (56) postulated that the polysaccharide coating which he found on membrane invaginations was responsible for the selectivity demonstrated by membranes In his proposal specific materials were selectively adsorbed by this extraneous material and were later carried into the cell through membrane flow and vesiculation In addition to selectivity Roth

and Porter (62 and 64) speculated that the small spines of this coating might be involved in the process of membrane in folding Although several investigators are studying these surface coatings with a variety of methods (Ito 65 Luft 64) their exact function remains speculative

Although rather extensive apical plasma membrane invaginations precede vacuole formation in yolk sac endodermal cells the overall structure is modified for bulk uptake as in pinocytosis or phagocytosis Similarly as in phagocytosis these mem brane specializations appear to be a likely mechanism for the transfer of large mole cules across membranes Schectman (56) pointed out however that where trans port across cells is concerned a distinc tion should be made between the simple uptake of a substance by pinocytosis and its transcellular movement In other words entrapment of materials within pinocytotic vacuoles in no way insures either confinement within the cell or pas sage across the cell unaltered Unlike Palade s (60) demonstration of bulk trans port directly across endothelial cells by pinocytosis many examples of pinocyto sis or phagocytosis in other cells involve a modification of the vesicles and their contents before anything is released from the cell Thus the formation of and ac tivities within cytoplasmic vesicles of pino cytotic origin may be an integral part of a transferring mechanism

For example Miller (60) and Miller and Palade (64) showed that hemoglobin was absorbed by the proximal convoluted tubules of the mouse kidney through in vaginations of the apical plasma mem brane However the hemoglobin was then transported to more deeply lying vacuoles where complex phospholipid membranes and ferritin particles were later formed Similarly Oliver MacDowell and Lee (54) in their study on the fate of ab sorbed protein in the kidney proximal tubules suggested that droplet formation is an accessory mechanism in the meta bolic process by which the renal cell dis poses of absorbed protein They also conclude that "The droplet is therefore not a cytological structure of fixed char acteristics but a locus of metabolic activity and varied structural aspect"

The discriminative selectivity and stor age of various vital dyes within large cytoplasmic vacuoles of visceral yolk sac cells which has been noted by several investigators (Wislocki 21 Ferm Free and Shires 59 Barber and Geer 64 and others) demonstrates the importance of these apical structures Both Ferm and Beudoin (60) and Sorokin and Padykula (64) showed that the yolk sac epithelium retained these capabilities whether it was tested while explanted to the chick chorio allantoic membrane, or to tissue culture

A new feature of the visceral endo dermal cells noted in this investigation is the fine granular material found inside Golgi vesicles and the intercellular spaces The presence of this material suggests to us that some material is either being transported through the epithelium by this route as was shown in the intestine by Weiss (55) and Palay and Karlan (59) or is manufactured in these cells and then elaborated intercellularly (Siekevitz and Palade 58 and 60 Peterson and Leblond 64) An abundance of ergastoplasm in these cells is also consistent with the dem onstration that yolk sac membranes are able to produce enzymes which can act on material outside of these cells in tissue culture (New and Stein 64) as well as to synthesize several compounds *in vitro* from labeled glucose (Popp 58) Another aspect of active enzyme production in the endodermal cells may be important in antibody and ferritin transfer

The absorption of ferritin and its vari ous dispositions within the endodermal cells of the visceral yolk sac at different periods of gestation not only raises several questions but demonstrates as well some of the functional aspects of structures which have been described

Although ferritin is a normal constit uent in regulating the amount of iron absorbed from the gut (Granick 46) and transferred across the rat yolk sac mem branes (Nylander 53 Wohler 55) fer ritin molecules were not found in the cytoplasm of visceral endodermal cells from uninjected controls However as has been described above exogenous fer ritin is capable of passing from the mater nal blood stream to the fetal blood intact as a macromolecule How this relates to

or affects normal iron transfer is unknown

The attachment of ferritin to the fuzzy coating of apical invaginations of visceral endodermal cells may be important in the uptake of large molecules Such has been suggested in the case of the ameba by Brandt and Pappas (60) and for yolk protein uptake in mosquito oocytes (Roth and Porter 64) On the other hand in our study ferritin molecules were found within apical invaginations which appeared to be unattached to the surface coating Since another unpublished experiment by the author showed that other unrelated compounds i e thorotrast and saccharated iron oxide can enter the apical vacuoles through the same canals specific attachment to the surface coating may not be necessary for the entrance of protein into these cells

Although direct connections between the apical canalicular system and large vacuoles have been noted there are indications particularly in the earlier stages which were investigated that fusion of vesicles occurs as well The heterogeneity of the ferritin within many vesicles as well as the disposition of some vesicle membranes suggests this A similar process of vesicle interaction has been noted in intestinal epithelium (Palay and Karlan 59) and in proximal convoluted kidney tubules (Straus 57 Miller 60 Trump 61 Maunsbach 63 and Miller and Palade 64)

It thus appears that yolk sac endodermal cells are capable of absorbing ferritin at all stages of gestation but show evidence of significant passage only late in gestation Some change must occur within these cells near the end of pregnancy therefore which allows in addition to an uptake of ferritin passage as well The relatively smaller 160 mμ more electron dense ferritin filled vesicles which appear to move through these cells late in development may be important in this process These small vesicles were sometimes found closely related to the large ferritin filled apical vacuoles particularly on their basal aspect The fine structure of these vesicles appears similar to the microvesicles described by Nachmias and Marshall (61) as being closely related to pinocytotic vesicles in amebae which had been exposed to ferritin On the other hand the microvesicles described by them did not at any time contain ferritin These investigators did suggest however that such microvesicles might be important for transfer either into or out of the larger pinocytotic vesicles In the case of ferritin transfer in visceral endodermal cells movement appears to be away from the larger vacuoles particularly by way of these microvesicles late in gestation

The selectivity of the yolk sac placenta for ferritin as well as its delayed transfer through this structure is in many respects consistent with the extensive work done in the laboratories of Brambell Brierley Halliday and Hemmings on the transfer of maternal antibodies to the fetus First of all the rather rapid transfer of ferritin from the maternal blood into the visceral endodermal cells throughout gestation is similar to findings of Brambell (58) He reported that while both homologous and heterologous proteins pass into and out of the uterine lumen with equal ease only a small amount of heterologous protein reaches the fetal circulation (Hemmings and Brambell 61) Brambell and Hemmings (54) explained that such a selectivity could be accounted for by a differential destruction within the uterine lumen by a differential destruction after reaching the fetus or by selection at the placental barrier

There is little evidence for proteolysis of antiserum within the uterine lumen before it reaches fetal endoderm (Brambell 58) Furthermore there appears to be no evidence for protein selection after reaching fetal blood (Brambell and Hemmings 54) Therefore selectivity within the placental barrier remains as a possible explanation for the limited population of proteins circulating within the neonatal bloodstream As Brambell (58) has suggested the apparently non selective uptake of homologous and heterologous protein from the uterus by the visceral yolk sac epithelium is consistent with the bulk uptake of droplets by pinocytosis On the other hand selective transfer might be explained by a specific immunological type of intracellular en

zyme substrate breakdown (Hemmings 56) Hemmings (56 and 58) demonstrated in fact that breakdown does occur within these cells When I[131] labeled rabbit and bovine serum globulins were introduced into the uterine lumens of pregnant rabbits both proteins were taken up by the fetal cells in equal amounts However only a small portion depending on the species of origin was passed into the fetal circulation that which was retained was broken down Thus while intact labeled antibodies were found in the fetal serum in addition free label was detected in the non protein fraction of the fetal serum The hydrolytic enzymes which have been detected both in tissue extracts of visceral yolk sac (Brambell 58) and in histochemical preparations of this tissue (Padykula 58a b) are perhaps involved in this process

The suggestion of Nachmias and Marshall (61) for the ameba that there must be therefore highly selective exchange mechanisms operating in both directions across the vesicle membrane or between the primary vesicle and the microvesicles coupled with Brambell s (58) hypothesis of an immunological type of enzyme substrate breakdown for specific molecular movement is consistent both with much of the literature relative to this problem and with the morphology seen in this investigation as well

After macromolecules pass through the visceral endodermal barrier two routes can be used to enter the fetus The presence of ferritin molecules in the visceral basement membrane as well as within vacuoles of vitelline endothelial cells suggests one direct pathway Another route is suggested by the presence of ferritin filled vesicles inside mesothelial cells lining the exocoelom This latter finding substantiates the findings of Brambell and Halliday (56) and Mayersbach (58) that some protein transport can take place through the exocoelomic cavity across the amnion and into the fetus through swallowed amniotic fluid which subsequently is absorbed by the gut endoderm

Our observations on normal ultrastructure of the yolk sac throughout gestation clearly demonstrates changes during this interval The present work with ferritin suggests in addition that such structural changes reflect a series of steps in the differentiation and function of this membrane These findings support the conclusions that in rats the yolk sac serves an important placental function in the transfer of specific materials The results also demonstrate the dynamic nature of this function and indicate some of the ultrastructural modifications which are associated with the transport process

LITERATURE CITED

Amoroso E C 1952 Placentation In Marshall s *Physiology of Reproduction* 3rd ed (A S Parkes ed) Longmans Green and Co New York 2 127–312

Barber A N and J C Geer 1964 Studies on the teratogenic properties of trypan blue and its components in mice J Embryol Exp Morph *12* 1–14

Bennett H S 1956 The concepts of membrane flow and membrane vesiculation as mechanisms for active transports and ion pumping J Biophys Biochem Cytol 2 (*Suppl*) 99–103

Brambell F W R 1958 The passive immunity of the young mammal Biol Rev *33* 488 531

Brambell F W R and R Halliday 1956 The route by which passive immunity is transmitted from mother to foetus in the rat Proc Roy Soc (Biol) *145* 170–178

Brambell F W R and W A Hemmings 1954 Active transport through embryonic membranes Sympos Soc Exp Biol *8* 476–489

Brandt P W and G D Pappas 1960 An electron microscopic study of pinocytosis in ameba I The surface attachment phase J Biophys Biochem Cytol *8* 675–688

Clark S L Jr 1959 The ingestion of proteins and colloidal materials by columnar absorptive cells of the small intestine in suckling rats and mice J Biophys Biochem Cytol 5 41 50

Dempsey E W 1953 Electron microscopy of the visceral yolk sac epithelium of the guinea pig Am J Anat *93* 331–363

Essner E 1960 An electron microscopic study of erythrophagocytosis J Biophys Biochem Cytol 7 329–335

Everett J W 1933 Structure and function of the yolk sac placenta in *Mus norvegicus albinus* Proc Soc Exp Biol Med *31* 77–79

——— 1935 Morphological and physiological studies of the placenta in the albino rat J Exp Zool *70* 243–277

Farquhar M G and G E Palade 1960 Segregation of ferritin in glomerular protein absorption droplets J Biophys Biochem Cytol 7 297–305

——— 1961 Glomerular permeability II Ferritin transfer across the glomerular capillary wall in nephrotic rats J Exp Med *114* 699–716

——— 1963 Junctional complexes in various epithelia J Cell Biol 17 375–412

Farrant J L 1954 An electron microscopic study of ferritin Biochem Biophys Acta 13 569–576

Ferm V H and A R Beudoin 1960 Absorptive phenomena in the explanted yolk sac placenta in the rat Anat Rec 137 89–92

Ferm V H H J Free and D L Shires 1959 Concentration of azoproteins in yolk sac placenta of the rat Proc Soc Exp Biol Med 100 456–459

Gillman J C Gilbert T Gillman and I Spence 1948 A preliminary report on hydrocephalus spina bifida and other congenital anomalies in the rat produced by trypan blue S Afr J Med Sci 13 47–90

Goldman E E 1909 Die aussere und innere Sekretion des gesunden und kranken Organismus im Lichte der vitalen Farbung Teil I Beitrage zur Klinischen Chirurgie 64 192–266

——— 1912 Die aussere und innere Sekretion des gesunden und kranken Organismus im Lichte der vitalen Farbung Teil II Beitrage zur Klinischen Chirurgie 78 1–109

Granick S 1946 Ferritin IX Increase of the protein apoferritin in the gastro-intestinal mucosa as a direct response to iron feeding The function of ferritin in the regulation of iron absorption J Biol Chem 164 737–746

Hamilton W J J D Boyd and H W Mossman 1962 Human Embryology The Williams and Wilkins Company Baltimore

Harkin J C 1964 A series of desmosomal attachments in the Schwann sheath of myelinated nerves Z Zellforsch 64 189–196

Hemmings W A 1956 Protein selection in the yolk sac splanchnopleur of the rabbit the distribution of isotope following injection of I labeled serum globulin into the uterine cavity Proc Roy Soc (Biol) 145 186–195

——— 1958 Protein selection in the yolk sac splanchnopleur of the rabbit the total uptake estimated as loss from the uterus Proc Roy Soc (Biol) 148 76–83

Hemmings W A and F W R Brambell 1961 Protein transfer across the fetal membranes Brit Med Bull 17 96–101

Huber G C 1915 The development of the albino rat *Mus Norvegicus Albinus* I From the pronuclear stage of mesoderm anlage end of the first to the end of the ninth day J Morph 26 247–358

Ito S 1965 Radioactive labeling of the surface coat on enteric microvilli (Abstract) Anat Rec 151 489

Karrer H E 1958 The ultrastructure of mouse lung the alveolar macrophage J Biophys Biochem Cytol 4 693–700

——— 1960 Electron microscopic study of the phagocytosis process in the lung J Biophys Biochem Cytol 7 357–366

Luft J H 1964 Electron microscopy of cell extraneous coats as revealed by ruthenium red staining (Abstract) J Cell Biol 23 54A

Maunsback A B 1963 Electron microscopic observations on ferritin absorption in microperfused renal proximal tubules J Cell Biol 19 48A–49A

Mayersbach H 1958 Zur Frage des Proteinuberganges von der Mutter zum Foeten I Befunde an Ratten am ende der Schwangerschaft Z Zellforsch 48 479–504

Miller F 1960 Hemoglobin absorption by the cells of the proximal convoluted tubule in mouse kidney J Biophys Biochem Cytol 8 689–718

Miller F and G Palade 1964 Lytic activities of renal protein absorption droplets An electron microscopical and cytochemical study J Cell Biol 23 519–553

Millonig G 1961 A modified procedure for lead staining of thin sections J Biophys Biochem Cytol 11 736–739

——— 1962 Further observations on a phosphate buffer for osmium solutions in fixation In 5th International Congress for Electron Microscopy (S S Breese Jr ed) Academic Press Inc New York 2 P-8

Muir A R 1960 The molecular structure of isolated and intracellular ferritin Quart J Exp Physiol 45 192–201

Nachmias V T and J M Marshall 1961 Protein uptake by pinocytosis in amoebae Studies on ferritin and methylated ferritin In Biological Structure and Function (T W Goodwin and O Linberg Ed) Academic Press Inc New York 2 604–619

New D A T and K F Stein 1964 Cultiva tion of post implantation mouse and rat embryos on plasma clots J Embryol Exp Morph 12 101–111

Noer H R and H W Mossman 1947 Surgical investigation of the function of the inverted yolk sac placenta in the rat Anat Rec 98 31–37

Nylander G 1953 On the placental transfer of iron An experimental study in the rat Acta Physiol Scand 29 Suppl 107 1–105

Oliver J M MacDowell and Y C Lee 1954 Cellular mechanisms of protein metabolism in the nephron I The structural aspects of proteinuria tubular absorption droplet formation and the disposal of proteins J Exp Med 99 589–604

Padykula H A 1958a Histochemistry of the rat s placenta In Environmental Influences on Prenatal Development (Beatrice Mintz Ed) University of Chicago Press Chicago pp 34–38

——— 1958b A histochemical and quantitative study of enzymes of the rat s placenta J Anat 92 118–129

Padykula H W and D Richardson 1963 A correlated histochemical and biochemical study of glycogen storage in the rat placenta Am J Anat 112 215–242

Padykula H A and T H Wilson 1960 Differentiation of absorptive capacity in the visceral yolk sac of the rat (Abstract) Anat Rec 136 254

Palade G E 1960 Transport of quanta across the endothelium of blood capillaries (Abstract) Anat Rec 136 254

Palay S L and L J Karlan 1959 An electron microscopic study of the intestinal villus II

The pathway of fat absorption J Biophys Biochem Cytol 5 373–384
Peterson M R, and C P Leblond 1964 Synthesis of complex carbohydrates in the Golgi zone as revealed by autoradiography (Abstract) Anat Rec *148* 322
Popp R A 1958 Comparative metabolism of blastocysts extraembryonic membranes and uterine endometrium of the mouse J Exp Zool *138* 1–23
Richardson K C L Jarett and E H Finke 1960 Embedding in epoxy resins for ultra thin sectioning in electron microscopy Stain Techn *35* 313–323
Roth T F and K R Porter 1962 Specialized sites on the cell surface for protein uptake In 5th International Congress for Electron Microscopy (S S Breese Jr ed) Academic Press Inc New York *2* LL-4
——— 1964 Yolk protein uptake in the oocyte of the mosquito *Aaedes Aegypti* L J Cell Biol *17* 96–101
Sabatini D D K Bensch and R J Barnett 1963 Cytochemistry and electron microscopy The preservation of cellular ultrastructure and enzyme activity by aldehyde fixation J Cell Biol *17* 19–58
Schectman A M 1956 Uptake and transfer of macromolecules by cells with special reference to growth and development Inter Rev Cytol 5 303–322
*Siekevitz P and G E Palade 1958 A cyto*chemical study on the pancreas of the guinea pig II Functional variations in the enzyme activity of microsomes J Biophys Biochem Cytol *4* 309–319
——— 1960 A cytochemical study on the pancreas of the guinea pig V *In vivo* incorporation of leucine 1 C^{14} into the chymotrypsinogen of various cell fractions J Biophys Biochem Cytol *7* 619–630
Sorokin S P and H A Padykula 1964 Differentiation of the rat s yolk sac in organ culture *Am J Anat 114* 457–479
Straus W 1957 Segregation of an intravenously injected protein by droplets of the cells of rat kidneys J Biophys Biochem Cytol 3 1037–1040
Trump B F 1961 An electron microscopic study of the uptake transport and storage of colloidal materials by the cells of the vertebrate nephron J Ultrastructure Res 5 291–310
Weiss J M 1955 The role of the Golgi complex in fat absorption as studied with the electron microscope with observations on the cytology of duodenal absorptive cells J Exp Med *102* 775–783
Wislocki G B 1921 III The behavior of the fetal membranes and placenta of the guinea pig toward trypan blue injected into the maternal bloodstream IV The behavior of the placenta and fetal membranes of the rabbit toward trypan blue injected into the maternal blood *stream Contributions* to Embryology (Carnegie Institution of Washington) Washington D C *13* 89–102
Wislocki G B and E W Dempsey 1953 Electron microscopy of the rat s placenta (Abstract) Anat Rec *117* 581
——— 1955 Electron microscopy of the placenta of the rat Anat Rec *123* 33–63
Wislocki G B and H A Padykula 1953 Reichert s membrane and the yolk sac of the rat investigated by histochemical means Am J Anat *92* 117–151
——— 1961 Histochemistry and electron microscopy of the placenta In Sex and Internal Secretions Third edition W C *Young* ed) The Williams and Wilkins Co Baltimore pp 883–957
Wislocki G B H W Deane and E W Dempsey 1946 The histochemistry of the rodents placenta Am J Anat *78* 281–347
Wissig S L 1963 The anatomy of secretion in the follicular cells of the thyroid gland II The effect of acute thyrotropic hormone stimulation on the secretory apparatus *J* Cell Biol *16* 93–119
Wohler V F 1955 Zur Physiologie und Path*ologie des Speichereisens* III Mitteilung Uber der intermediaren Eisenstoffwechsel der Plazenta Deutsch Med Wschr 80 30–32

The pathway of fat absorption J Biophys Biochem Cytol 5 373–384

Peterson M R and C P Leblond 1964 Synthesis of complex carbohydrates in the Golgi zone as revealed by autoradiography (Abstract) *Anat Rec 148* 322

Popp R A 1958 Comparative metabolism of blastocysts extraembryonic membranes and uterine endometrium of the mouse J Exp Zool *138* 1–23

Richardson K C L Jarett and E H Finke 1960 Embedding in epoxy resins for ultra thin sectioning in electron microscopy Stain Techn *35* 313–323

Roth T F and K R Porter 1962 *Specialized* sites on the cell surface for protein uptake In 5th International Congress for Electron Microscopy (S S Breese Jr ed) Academic Press Inc New York 2 LL-4

——— *1964 Yolk protein uptake in the oocyte* of the mosquito *Aaedes Aegypti* L J Cell Biol *17* 96–101

Sabatini D D K Bensch and R J Barnett 1963 Cytochemistry and electron microscopy The preservation of cellular ultrastructure and enzyme activity by aldehyde fixation J Cell Biol *17* 19–58

Schectman A M 1956 Uptake and transfer of macromolecules by cells with special reference to growth and development Inter Rev Cytol 5 303–322

Siekevitz P and G E Palade 1958 A cytochemical study on the pancreas of the guinea pig *II Functional variations in the enzyme* activity of microsomes J Biophys Biochem Cytol *4* 309–319

——— 1960 A cytochemical study on the pancreas of the guinea pig V *In vivo* incorporation *of leucine 1 C^{14} into the chymotrypsinogen* of various cell fractions J Biophys Biochem Cytol 7 619–630

Sorokin S P and H A Padykula 1964 Differentiation of the rat s yolk sac in organ culture Am *J Anat 114* 457–479

Straus W 1957 Segregation of an intravenously injected protein by droplets of the cells of rat kidneys J *Biophys* Biochem Cytol *3* 1037–1040

Trump B F 1961 An electron microscopic study of the uptake transport and storage of colloidal materials by the cells of the vertebrate *nephron J Ultrastructure Res 5* 291–310

Weiss J M 1955 The role of the Golgi complex in fat absorption as studied with the electron microscope with observations on the cytology of duodenal absorptive cells J Exp Med *102* 775–783

Wislocki G B 1921 III The behavior of the fetal membranes and placenta of the guinea pig toward trypan blue injected into the maternal bloodstream IV The behavior of the placenta and fetal membranes of the rabbit toward trypan blue injected into the maternal blood stream Contributions to Embryology (Carnegie Institution of Washington) Washington D C 13 89–102

Wislocki G B and E W Dempsey 1953 Electron microscopy of the rat s placenta (Abstract) Anat Rec *117* 581

——— 1955 Electron microscopy of the placenta of the rat Anat Rec *123* 33–63

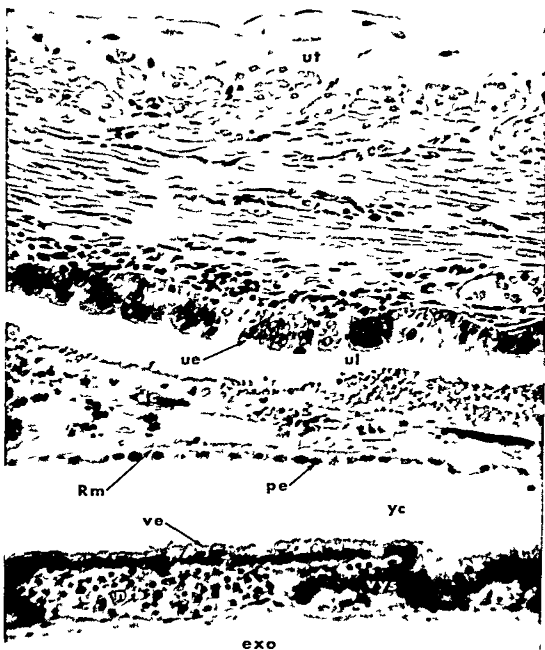
Wislocki, G B and H A Padykula 1953 Reichert s membrane and the yolk sac of the rat investigated by histochemical means Am J Anat *92* 117–151

——— 1961 Histochemistry and electron microscopy of the placenta In Sex and Internal Secretions Third edition W C Young ed) The Williams and Wilkins Co Baltimore pp 883–957

Wislocki G B H W Deane and E W Dempsey 1946 The histochemistry of the rodents placenta Am J Anat *78* 281–347

Wissig S L 1963 The anatomy of secretion in the follicular cells of the thyroid gland II The effect of acute thyrotropic hormone stimulation on the secretory apparatus J Cell Biol *16* 93–119

Wöhler V F 1955 Zur Physiologie und Pathologie des *Speichereisens III* Mitteilung Uber der intermediaren Eisenstoffwechsel der Plazenta Deutsch Med Wschr 80 30–32


ut
ue
ul
Rm
pe
yc
ve
vys
exo
1

Abbreviations

ac apical canaliculi
bm epithelial basement membrane
dc decidua capsularis
ER rough surfaced endoplasmic reticulum
exo exocoelom
G Golgi apparatus
is intercellular space
L lipid
M mitochondrion
mes mesothelial cell
mv microvilli
nfb nucleated fetal blood cell
pe parietal endodermal cell
Rm Reichert's membrane
sbm serosal basement membrane
tb terminal bar
ue uterine epithelium
ul uterine lumen
ut uterine wall
V vacuole
v microvesicle
vbm visceral basement membrane
vc vitelline capillary
ve visceral epithelium
vys visceral yolk sac
yc yolk cavity

PLATE 1

EXPLANATION OF FIGURE

1 A light micrograph of a section through the uterine wall and fetal membranes of the sixteenth day of gestation Nucleated fetal red blood cells can be identified within the visceral yolk sac membrane between the visceral endodermal cells and the mesothelial cells which face the exocoelom *The parietal yolk sac membrane composed of* parietal endoderm and Reichert's membrane covers one surface of the decidua capsularis while the opposite side faces uterine epithelium Fixed in formol sublimate dichromate stained with hematoxylin and eosin 435 ×

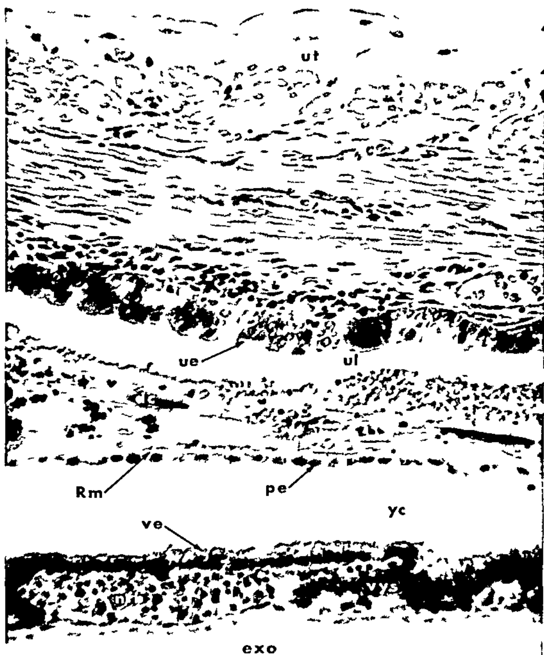

ut
ue
ul
Rm
pe
yc
ve
vys
exo
1

PLATE 2

EXPLANATION OF FIGURE

2 An electron micrograph of a section through the thickness of the visceral yolk sac membrane on the tenth day of gestation The ribo some rich cytoplasm contains rough surfaced endoplasmic reticulum and numerous vacuoles which are sometimes intimately apposed (arrows) Glutaraldehyde fixation 11 400 ×

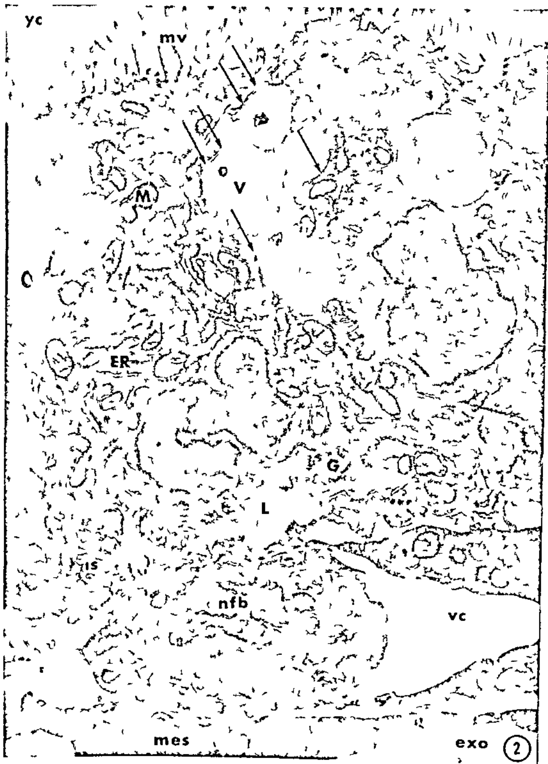

yc
mv
o
V
M
O
ER
G
L
is
nfb
vc
mes
exo
2

PLATE 2

EXPLANATION OF FIGURE

2 An electron micrograph of a section through the thickness of the visceral yolk sac membrane on the tenth day of gestation The ribo some rich cytoplasm contains rough surfaced endoplasmic reticulum and numerous vacuoles which are sometimes intimately apposed (arrows) Glutaraldehyde fixation 11 400 ×

ac
M
3

mes
vbm
sbm
G
exo
4

PLATE 3

EXPLANATION OF FIGURES

3 This electron micrograph shows at greater magnification details of the coated invaginations of the apical plasma membrane at 12 days Situated between the bases of the microvilli the invaginations demonstrate a dense fibrous material on their internal or luminal surface Osmium fixation 21 800 ×

4 By 20 days the visceral and serosal basement membranes are well developed and separate the visceral endodermal cells from the mesothelial cells which line the exocoelom Osmium fixation 6 700 ×


yc
ac
v
bm
vc
hfb
5

PLATE 4

EXPLANATION OF FIGURE

5 This section through the visceral yolk sac on the fourteenth day shows the columnar endodermal cells resting on a basement membrane which abuts on strands of collagen from the visceral basement membrane Nucleated fetal red blood cells can be seen within a vitelline capillary Osmium fixation 7 100 ×

6

GR
G
L
L
7

PLATE 5

EXPLANATION OF FIGURES

6 Some of the microvilli on these 14 day visceral endodermal cells have become fattened or branched and the apical canaliculi appear more extensive Osmium fixed 9 200 ×

7 In addition to the lipid droplets seen in the basal part of these 14 day endodermal cells a granular material is clearly visible both within Golgi vesicles and within intercellular spaces as indicated by the arrows Osmium fixed 11 800 ×

PLATE 6

EXPLANATION OF FIGURES

8 At 16 days direct connections can be seen between the apical canals and some of the vacuoles Osmium fixed 18 000 ×

9 On the twenty first day a complex interconnected system of apical canaliculi is evident Osmium fixed 10 700 ×

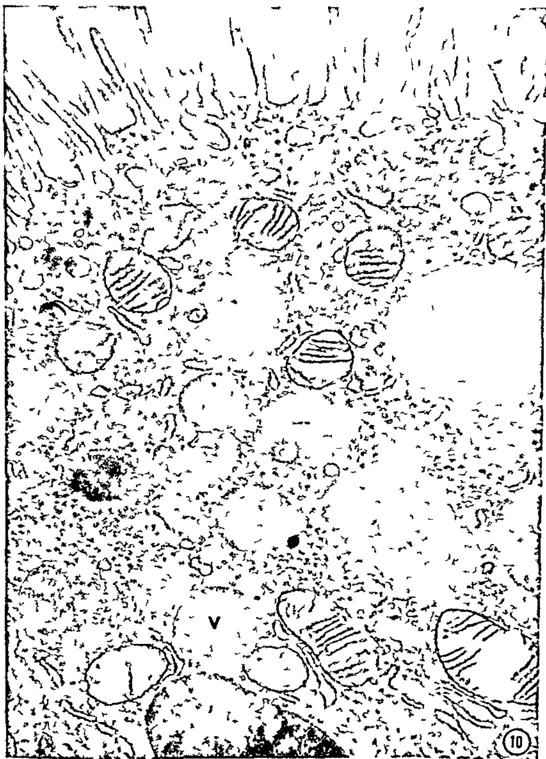

V
10

PLATE 7

EXPLANATION OF FIGURE

10 After maternal administration on the tenth day of gestation ferritin can be found within some of the short apical canaliculi as well as within cytoplasmic vacuoles Glutaraldehyde fixed 25 500 ×

PLATE 8

EXPLANATION OF FIGURES

11 Ferritin molecules (arrows) can be seen within the brush like material which lines the apical invaginations Twenty day Glutaraldehyde fixed 66 300 ×

12 Ferritin is again found associated with the fuzzy coating along the entire lengths of several apical canals in this section on the twenty first day Glutaraldehyde fixed 49 000 ×

PLATE 9

EXPLANATION OF FIGURES

13 On the twenty first day small electron dense microvesicles which contain ferritin are seen deep in the endodermal cytoplasm Ferritin is also scattered within the visceral basement membrane Glutaraldehyde fixed 23 000 ×

14 At higher magnification ferritin molecules are evident within the microvesicles adjacent to the basal plasma membrane of a visceral endodermal cell on the twentieth day Glutaraldehyde fixed 53 000 ×

vc

15

sbm

mes

exo

16

PLATE 10

EXPLANATION OF FIGURES

15 This portion of a vitelline capillary endothelial cell shows a ferritin filled vesicle in the cytoplasm adjacent to the fetal plasma Twenty day Glutaraldehyde fixed 77 600 ×

16 This electron micrograph demonstrates passage of ferritin through the serosal basement membrane and mesothelial cells into the exo coelom on the twentieth day of pregnancy Glutaraldehyde fixed 34 000 ×

vc

15

sbm

mes

exo

16

The Ultrastructure of the Gastric Mucosa in Normal and Hypophysectomized Rats [1,2]

RICHARD E CORPRON

Department of Anatomy The University of Michigan Medical School Ann Arbor Michigan

ABSTRACT The objectives of this study were to observe with the electron microscope (a) the epithelial cell types found in the neck and isthmus of the gastric fundic gland of the rat and (b) the effects of hypophysectomy on the gland The following cell types were distinguished in the neck of the fundic gland of the rat nondifferentiated cell immature surface cell mucous neck cell and neck parietal cell In the normal gland these cell types resembled each other in the possession of a ground cytoplasm and nucleoplasm of low density a poorly developed endoplasmic reticulum few mitochondria and numerous free ribosomes The most important structural difference between mucous neck and immature surface cells was the contrasting density of the secretory granules both cell types differed from the nondifferentiated cell primarily in the presence of their characteristic secretory granules The neck parietal cell appeared to be a developmental form between the immature surface cell and the mature parietal cell No changes were observed in these cells to result from hypophysectomy

Hypophysectomy caused marked involutional changes in the chief cell which involved mainly the organelles most directly concerned with protein synthesis i e the ergastoplasm and Golgi apparatus These effects were correlated with the loss of basophilia and secretory granules and with the reduction in cell size and capacity to secrete pepsinogen which were described previously In contrast the parietal cell which is concerned with electrolyte transport was affected much less

The extensive literature dealing with the ultrastructure of gastric epithelial cells has been summarized by Kurosumi (61) Helander (62) and Sedar (64) General agreement exists concerning most of the ultrastructural characteristics of the chief argyrophilic parietal and surface mucous cells However much conflict revolves around the fine structure and interrelations of the cell types found in the neck of the gland and deep portion of the pit

It is not agreed that a mucous neck cell can be differentiated with the electron microscope Lillibridge (64) working with man and Helander (62) with the mouse were unsuccessful in their attempts to do so Helander discounted the earlier identification and descriptions of mucous neck cells in the rat by Kurosumi et al (58) and Shibasaki (61) on the grounds of poor fixation The mucous neck cell as described by Sedar (64) in the dog bears only a superficial resemblance to that illustrated by Ito and Winchester (63) for the bat Only Shibasaki (61) has dealt with the possible existence of a nondifferentiated cell Furthermore only Lawn (60) has noted the striking structural differences between some parietal cells located in the neck as compared with those deeper in the gland The first objective of this investigation was to acquire information concerning the ultrastructure of the cell types found in the neck region of the fundic gland

A second objective was to observe the influence of hypophysectomy on the fine structure of chief and parietal cells As observed with the light microscope pituitary ablation in the rat caused a profound involution of chief cells accompanied by a decrease in cytoplasmic basophilia number of zymogenic granules and capacity to secrete pepsinogen (Baker and Abrams 54) These changes were evident within three days after the operation To a less significant degree parietal cells were somewhat smaller and contained fewer mitochondria (Baker and Abrams 54 Baker and Clark 61) The pH of the gastric juice was elevated and total acidity reduced (Crafts and Walker 47) It is im

S pported in p rt by rese rch gr nt from the USPHS (AM-00131 13) nd Th Upj hn Comp ny

From a thesi submitted in p rti l fulfillm nt of the requirement for th Docto of Philosophy d gree in An tomy Uni rsity of Mi hig n.

[3] Present ddre School of Denti try Uni rsity of Mi hig n Ann Arbor

portant to know how these modifications are reflected at the ultrastructural level

MATERIALS AND METHODS

Twelve young adult female white rats of the Sprague Dawley strain were used One member of each of the six pairs was hypophysectomized by the parapharyngeal approach and the other served as a control The control animal was pair fed against the hypophysectomized rat for 2–7 months following the operation The diet consisted of Purina Laboratory Chow Prior to termination of the experiment the rats were starved for 18 hours The mean initial and final body weights for the non hypophysectomized rats were 193 ± standard deviation 9 gm and 252 ± 6 gm respectively, and for the hypophysectomized rats 188 ± 17 gm and 176 ± 5 gm respectively Completeness of pituitary removal was verified by loss of body weight and by microscopic examination of the serially sectioned pituitary capsules

The stomach was removed while the rat was under sodium amytal anesthesia It was incised along the lesser curvature from the pyloroduodenal junction to the cardiac orifice and the luminal contents were washed out with 0 9% NaCl solution The stomach was pinned out flat on a cork block and the mucosal surface flooded with several drops of fixative Twelve to 16 pieces of mucosa measuring 1 mm^3 were taken from the greater curvature approximately half way between the horizontal ridge and the pyloric opening

Tissues from five pairs of rats were fixed for two hours at 4 C in 1% osmic acid buffered with Veronal acetate to pH 7 4 (Palade 52) Tissues from one pair of rats were fixed in Dalton s fluid (Dalton 55) at pH 7 2 for two hours at 4°C Subsequently the tissues were dehydrated in ethanol and propylene oxide prior to embedding in Epon 812 (50% mixture A 50% mixture B) according to Luft (61) Sections from 8 to 10 blocks per animal were cut on a Porter Blum microtome mounted on grids covered with carbon coated Formvar films They were stained with 2% uranyl acetate for 2 to 4 hours (Watson 58) The sections were photographed with an RCA EMU 3D electron microscope at an accelerating voltage of 50 kV with a 25 μ objective aperture Approximately 2 000 electron micrographs were taken at original magnifications of 1 400 to 42 000

OBSERVATIONS

Epithelial cells of normal rats

Nondifferentiated cell The nondifferentiated cell (fig 2) was columnar and often slightly wider at the base than at the apex The lateral plasmalemma was usually quite straight with only occasional interdigitations with contiguous cells Desmosomes were observed occasionally The basal plasmalemma was straight Stubby microvilli projected from the apical surface The nucleus was oval or of irregular shape and contained a nucleolus and nucleoplasm of low density

Other features were especially distinctive The cytoplasm was much less dense than that of neighboring parietal cells (fig 2) The endoplasmic reticulum was poorly developed its outer surface was sometimes smooth with ribosomes being attached in only restricted areas (fig 3) The cisternae contained a substance of moderate density Clusters of free ribosomes were distributed throughout the cytoplasm Components of the Golgi apparatus were distributed widely through the perinuclear cytoplasm being found lateral and even basal to the nucleus The Golgi apparatus consisted of indistinct flattened saccules small Golgi vesicles and occasional vacuoles Little dilation of the Golgi cisternae was observed Although the cell illustrated in figure 2 contained bodies which may have been secretory granules other nondifferentiated cells were observed which did not contain these questionable inclusions

Surface mucous cell The ultrastructure of the surface mucous cell in the rat has been described in detail by Kurosumi (61) My report is concerned only with observations which are new or different from those of Kurosumi and other workers The Golgi apparatus formed a high cap over the nucleus and extended laterally to occupy much of the supranuclear cytoplasm (fig 4) The peripheral portion of the Golgi apparatus was composed of stacks of 4 to 5 flattened saccules and a multitude of Golgi vesicles which accumu

lated chiefly at the ends of and inside the saccules Only the external cisternae showed slight dilation A unique feature of both Golgi saccules and vesicles was their high electron scattering capacity

Secretory granules were found usually within and superior to the Golgi apparatus In contrast to the observation of Kurosumi (61) the granules appearing within the Golgi apparatus were not of low density (fig 4) but usually showed greater electron scattering capacity than those in the apical cytoplasm Each secretory granule was enclosed at least partially by a membrane Thus the secretory granules which were associated closely with the Golgi apparatus may be the counterpart of the Golgi vacuoles containing material of low density which are found in many other types of cells Such vacuoles were never observed in the surface cell The dense secretory granules varied in size and the smaller ones approximated the size of the Golgi vesicles but there was no clear evidence that secretory granules arose by simple enlargement of Golgi vesicles The mucous granules appeared to stream out of the Golgi apparatus into the apical cytoplasm In contrast to Kurosumi (61) I saw no evidence of transformation of mitochondria to mucous granules

An apical cytoplasmic zone containing mucous granules was unique in several respects It was devoid of mitochondria and endoplasmic reticulum and its deeper portion contained only a few ribosomes This apical organelle free cytoplasm was separated from subjacent cytoplasm by abundant fibrils which seemed to form an irregular transverse band across the cell and to be continuous with those emanating from desmosomes

The endoplasmic reticulum was moderately well-developed and extended throughout the cytoplasm except for the apical zone For the most part it possessed attached ribosomes The cisternae were wide tortuous branched and contained material of moderate density Clusters of free ribosomes were found throughout the cytoplasm

In the neck region of the fundic gland an immature form of the surface mucous cell was readily identified by means of the mucous granules of high density which appeared in the apical region (fig 5) Except for this feature the immature surface cell resembled the nondifferentiated cell with respect to shape nuclear structure extent and form of the endoplasmic reticulum distribution and quantity of ribosomes number and structure of mitochondria and structure of the Golgi appartus

Mucous neck cell The mucous neck cell was distinguishable from other cell types by several distinctive structural characteristics as well as by the fact that it was located deeper in the gland than nondifferentiated and surface mucous cells Kurosumi et al (58) described the mucous neck cell of the rat in considerable detail However my observations differ in many respects

The mucous neck cell was high cuboidal (fig 6) except when compressed basally by the pressure exerted by adjacent parietal cells If filled with secretion the apical surface bulged slightly into the glandular lumen Only occasional short rounded microvilli were observed on the surface and if present were located near the lateral junction with adjacent cells The lateral plasmalemma was straight except for occasional interdigitations with contiguous cells Desmosomes occurred along the apical one third of the lateral plasmalemma inferior to the zonulae occludens and adherens The nucleus filled much of the basal portion of the cell and tended to be flattened against the base Its envelope was often deeply indented There was little cytoplasm lateral and basal to the nucleus

The round secretory granules differed distinctively from those of the surface cells and chief cells The density of individual granules as well as that of the total population in a cell was remarkably uniform The granules appeared finely granular in texture (fig 6) The overlying dust like particles described by Kurosumi et al (58) were not observed The secretory granules were far less dense than those of the surface cells Usually the secretory granules of chief cells were not well preserved If they were preserved their density was greater than that of the granules in mucous neck cells but less than that of the granules in surface cells A clearly defined enveloping

membrane was observed only around those granules in mucous neck cells which were *located* proximal to the Golgi apparatus (fig 7) The periphery of the apical granules was less clearly defined the granules often becoming confluent with one another Apically they appeared to be released from the cell by dissolution of the overlying plasmalemma Golgi vesicles were often in direct contact with the substance of the secretory granule (fig 7) The significance of this relationship with respect to formation of secretion could not be ascertained Contrary to Kurosumi et al (58), no foaminess at the periphery of the granules was observed this condition must have resulted from inadequate preservation as he suspected

The Golgi apparatus occupied the cytoplasm immediately superior to the nucleus and tended to spread across the cell (fig 7) It did not extend into the apical cytoplasm between the granules The Golgi apparatus consisted of stacks of flattened saccules the cisternae of the external saccules exhibiting considerable dilation Many dense vesicles were present at the ends of the saccules

The rough surfaced endoplasmic reticulum was poorly developed it and free ribosomes were distributed throughout the cell including the apical cytoplasm between secretory granules Thus the endoplasmic reticulum was not confined to the basal and peripheral cytoplasm as indicated by Kurosumi et al (58) The general appearance" of the ergastoplasm was equated by Kurosumi et al (58) to that of the chief cells In my material there was a vast difference in degree of development

A columnar cell believed to be an *immature mucous neck cell* was observed in the neck region of the fundic gland (fig 8) It resembled the nondifferentiated cell with respect to the ultrastructure of the nucleus mitochondria ground cytoplasm rough surfaced endoplasmic reticulum and in the number and distribution of free ribosomes Differentiation of the cell toward the mucous neck cell was indicated by the development of apical granules which on the basis of their density and structure resembled those of mature mucous neck cells

Neck parietal cell. Lawn (60) noted that neck parietal cells differ from those deeper in the gland (mature parietal cells) by having cytoplasm of less density, fewer cytoplasmic vacuoles collapsed and less extensive intracellular canaliculi more prominent rough surfaced endoplasmic reticulum and fewer and more scattered mitochondria My observations reveal that mature and neck parietal cells may occur side by side in the neck although the neck parietal cell is predominant Neck parietal cells were never found in the fundus of the gland

Most of the features cited by Lawn were confirmed The following additional observations were made The nucleus was spherical, basally located and contained a nucleolus and ribosomes in low concentration (fig 9) Rough surfaced endoplasmic reticulum was sparsely distributed (figs 5 and 9) being most common in the immediate perinuclear region Clusters of ribosomes were scattered throughout the cytoplasm being quite sparse in the apical portion Collapsed intracellular canaliculi extended as deeply as in the mature form of parietal cell (figs 5 and 9) often nearly approximating the basal side of the cell Microvilli were either long and of uniform density and width (fig 10) or bulbous and with a less dense interior (fig 5) Mitochondria varied in size the maximum being considerably greater than that of mitchondria in the mature cell They were pleomorphic and contained densely packed delicate cristae and a matrix of low density The peripherally located Golgi apparatus was made up of stacks of flattened saccules with little dilation of the cisternae no vacuoles and few vesicles (fig 10) Cytoplasmic vacuoles if present at all were restricted to the apical and pericanalicular region were usually collapsed and possessed a dense outer membrane Multivesicular bodies were present Granules having the density and size of the secretory granules in surface mucous cells were identified in the cytoplasm of some cells (figs 9 and 10)

The effects of hypophysectomy

No significant changes were observed after hypophysectomy in the mucous neck nondifferentiated surface and neck parie

tal cells However ultrastructural changes did occur in the chief and mature parietal cells Since the structure of each cell type varied somewhat in the control rats particularly in relation to its position in the gland it was necessary to study many cells in each case and to insure that the cells compared in control and hypophysectomized rats were located at approximately the same levels in the gland

Chief cell The following evaluations are based only on observation of chief cells located in the fundus of the gland this level being identified by the presence of argyrophilic cells and the dominance of chief over parietal cells After hypophysectomy chief cells were uniformly smaller (fig 12) than those of the controls (fig 11) and their form was altered While most cells in the controls were columnar and possessed a granule filled apical cytoplasm which bulged into the glandular lumen after pituitary ablation the cells were lower and usually had a flat apex

The technical methods employed did not preserve the large pepsinogen granules regularly The number of granules could be evaluated however by the vacuoles left following their dissolution In all six hypophysectomized rats the maximal number observed in any cell and the overall average number per cell were less than in the controls In one control rat numerous chief cells contained few granules Nevertheless those of the paired hypophysectomized rat were also poorly granulated Concurrently with fall in quantity of granules the volume of apical cytoplasm also became less

With depletion of the large secretory granules a zone of cytoplasm appeared beneath the apical plasmalemma (figs 14 and 15) from which these granules were absent Most superficially no organelles could be seen Small dense granules (fig 11) with smooth dense outer membranes and measuring 0 07–0 20 μ in diameter were present in the nonhypophysectomized rats In density the small granules resembled Golgi vesicles and granules of sizes transitional between the two were observed commonly After hypophysectomy they became relatively more prominent although probably not increased in absolute number (fig 15) Thus the small granules did not share in the regression which engulfed the large granules after hypophysectomy

As compared with nonhypophysectomized rats the average amount of ergastoplasm[4] was less in the chief cells of the hypophysectomized member of the five pairs in which this comparison could be made with certainty (figs 11 and 12) This involved in most cells a reduction in density of the ground cytoplasm usually in the number of ribosomes and often in the extent of the endoplasmic reticulum These changes were demonstrated after fixation in buffered osmic acid (figs 16 and 17) and Daltons fluid (figs 18 and 19) Polyribosomes (fig 13) occurred in both control and operated rats especially in the perinuclear area In 4 of 5 hypophysectomized rats they appeared to be increased in frequency but this observation could not be verified with certainty

The Golgi apparatus was affected severely by hypophysectomy The supranuclear position of the Golgi apparatus was maintained but its extent in the cell was reduced so that it became more compact (figs 20 and 21) Overall dilation of Golgi cisternae was usually reduced some large vacuoles were retained Golgi vesicles remained prominent and no alteration in their number or structure could be ascertained

Except for a possible increase in the irregularity of the nuclear envelope hypophysectomy caused no changes in the structure of the nucleus nucleolus or mitochondria (figs 16 and 17) Possible change in size of the nucleus was not accurately evaluated

Parietal cell In evaluating the parietal cell comparisons were made only between cells located in the body or fundus of the gastric gland in order to avoid the confusion which would be created by consideration of the neck parietal cell Cellular size was reduced For evaluation of canaliculi satisfactory micrographs were available from

---

"Erg stopl m" is used to encompa s endopl mic reticulum with it ci tern e th accomp nying att ch d and free ribosomes and intervening ground cytopl m. The term i pplied to those cytopla mic are s where the nd pla mic reticulum i quite con centr ted. Thi ultrastructure generally haracterizes b sophilic cyt pl m s seen with the light microscope Since "ergastopla m" wa applied originally to such re ten ion of its use to electron micrographs seem ppropri te

four nonhypophysectomized and from four hypophysectomized rats In all of the latter the maximal caliber of the intracellular canaliculi was reduced by hypophysectomy so that the lumen was often nearly occluded by the microvilli (figs 22 and 23) In contrast to the rather regular form and uniform caliber of intracellular microvilli in nonhypophysectomized rats the microvilli after hypophysectomy were greatly distorted No significant alteration was observed in number of cytoplasmic vacuoles mitochondria and microvilli nor in the ultrastructure of the nucleus Golgi apparatus or mitochondria

DISCUSSION

The normal gland

The observations presented show that the epithelial cells in the neck of the fundic gland may be differentiated into several closely related types on the basis of their ultrastructure

Nondifferentiated cell Most primitive cells when examined with the electron microscope have been distinguished by a paucity of endoplasmic reticulum few mitochondria and a ground cytoplasm and nucleoplasm of low density (Han 61) The nondifferentiated cell of the gastric gland possesses similar characteristics However it also contains numerous free ribosomes and a well developed Golgi apparatus

Mucous neck cell There can be little doubt that the mucous neck cell exists as a distinctive cell type in the rat and that its structural characteristics are as distinctive when viewed with the electron microscope as they are when observed with the light microscope With the exceptions and additions already cited the descriptions of Kurosumi et al (58) and Shibasaki (61) were supported by my observations The mucous neck cell of the rat resembles closely that of the bat as described by Ito and Winchester (63) In the rat the following minor differences are evident fewer apical microvilli, the limitation of secretory granules to the supranuclear cytoplasm and the absence of enveloping membranes around the apical secretory granules In both rat and bat secretory granules are of remarkable uniformity in density and are considerably less dense than those of the surface cells On the other hand in the mucous neck cell of the dog as illustrated by Sedar (64), the secretory granules are as dense as those in the surface cell

The failure of Helander (62) in the mouse and Lillibridge (64) in man to delimit a mucous neck cell is difficult to understand since in both species such distinctions can be made with the light microscope The mucous neck cells of the rat show some similarities to the mucoid cells as illustrated by Helander (62) for the mouse but can hardly be equated with them

The morphological involvement of the Golgi apparatus in the elaboration of secretion by the mucous neck cell was not clarified Fully formed secretory granules were present adjacent to the Golgi apparatus no Golgi vacuoles containing secretion of lower density, as is observed frequently in the pancreas were seen No transitional stages between the contents of Golgi cisternae and secretory granules nor between Golgi vesicles and granules were observed even though the vesicles were often in direct contact with the substance of the granule

Surface mucous cell The immature surface cell is almost identical in its ultrastructure to the nondifferentiated cell except for the presence of dense spherical mucous droplets in its apical cytoplasm Maturation of the immature surface cell as it moves into the wall of the gastric pit is accompanied by many changes (figs 4 and 5) Cytoplasm above the nucleus expands greatly and becomes delineated into a region proximal to the nucleus which contains organelles and into an apical organelle free zone which is utilized for storage of the secretory product These regions are separated by intracytoplasmic filaments During maturation of the cell endoplasmic reticulum undergoes considerable expansion and ribosomes increase in number The Golgi apparatus enlarges becomes more complex and assumes a supranuclear position, the electron scattering capacity of the flattened saccules and vesicles increases

The presence of mucous droplets in the cytoplasmic area surrounded by the Golgi

apparatus strongly suggests a direct involvement of this organelle in their formation Although others (Kurosumi et al 58 Ito and Winchester 63) have observed smaller granules of less density in the Golgi apparatus and interpreted them to represent stages in formation of secretion the precise manner in which the Golgi apparatus is involved in synthesis of secretion was not revealed in my preparations In view of the high electron scattering capacity of the granules it is particularly significant that the stacks of flattened saccules exhibit a similar property far in excess of that seen in the Golgi appartus of most other cells in the body Thus the synthesis of mucus in association with these membranes is suggested Indeed the addition of carbohydrate to protein in Golgi vacuoles of mucus secreting cells is indicated by the concentration of radioactivity therein following the administration of $S^{35}O_4$ (Lane et al 64) or of H^3 labeled glucose (Peterson Neutra 65)

Neck parietal cell Of the many workers who have examined the gastric mucosa with the electron microscope only Lawn ('60) appreciated the existence of two distinctive forms of parietal cells As suggested by Lawn the neck parietal cell is most likely an immature stage in formation of the parietal cell This conclusion may be supported by the low density of the ground cytoplasm and nucleoplasm the varied form size and densely packed delicate cristae of the mitochondria and the poorly developed endoplasmic reticulum The neck parietal cell occurs only in the superficial region of the gland the more typical mature form is located in the body and fundic region and frequently in the neck as well

The application of the electron microscope to experimental studies of the parietal cells in rats requires recognition of the existence of the neck parietal cell Valid comparisons between parietal cells in control and treated rats can be made only at comparable levels in the gland Although the occurrence of a neck parietal cell is yet to be demonstrated in other species its possible presence was not considered by Sedar and Friedman (61) in their experimental studies on the parietal cell of the dog nor by Ito (61) in his study of many species including the rat Ito concluded that the appearance of cytoplasmic vacuoles is a product of the action of technical factors on a tubular endoplasmic reticulum Two of the cells illustrated by Ito (61) (figs 1 and 6) on which he based his conclusions were located high in the mucosa because surface cells were shown adjacent to them Sedar (62) concurred with Ito s view with respect to the frog

Cell relationships There are numerous close ultrastructural similarities between the nondifferentiated immature surface immature mucous neck and neck parietal cells These include the low density of the ground cytoplasm and nucleoplasm poor development of the endoplasmic reticulum to which are attached only occasional ribosomes and the presence of numerous free ribosomes The only feature which differentiates the immature surface cell from the nondifferentiated cell is the presence of apical mucous granules Indeed clearly defined nondifferentiated cells lacking in these dense granules are uncommon The immature mucous neck cell is distinguished by the large size and moderate density of its secretory granules The neck parietal cell however possesses many distinctive characteristics

General agreement exists concerning the following aspects of the developmental interrelationships of cells in the gastric

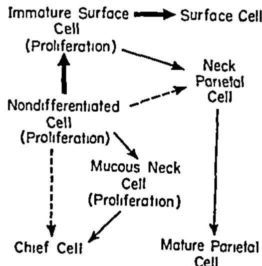


Figure 1

gland (1) Chief and parietal cells rarely divide by mitosis (2) Proliferation of cells occurrs in the neck of the gland and involves mucous neck and immature surface cells (Stevens and Leblond, 53, Leblond and Walker 56) (3) Immature surface cells undergo maturation and glide up onto the surface of the mucosa from whence they are sloughed into the lumen (Stevens and Leblond 53 Leblond and Walker 56 Messier, 60)

On the other points there is strong disagreement In dispute is the possibility that chief and parietal cells are replaced Messier (60) concluded from studies utilizing labeling with H^3 thymidine that chief and parietal cells are not formed by transformation of mucoid cells which divide in the neck Myhre (60) and Hunt and Hunt (62) came to the opposite conclusion and further showed that following stimulation of the mucosa the label which at first appears over mucous neck cells later is found deeper in the gland over chief and parietal cells indicating transformation of mucous neck cells to the other two types Townsend (61) demonstrated the apparent transformation of mucous neck cells to chief cells and of mucus containing cells to parietal cells by histochemical methods in both normal and regenerating gastric mucosa

With respect to the origin of the chief cell my observations are not helpful But the origin of the parietal cell from the immature surface cell is suggested by the presence of dense mucous granules in the neck parietal cell The occurrence of mucus in the apex of transforming parietal cells was described by Townsend (61) utilizing the light microscope he inferred that these apical portions are sloughed into the glandular lumen My observations further indicate that the neck parietal cell represents a stage in the development of the mature parietal cell from the immature surface cell Maturation of the parietal cell would then involve an increase in density of the cytoplasm reduction in average size of the mitochondria appearance of a canalicular lumen a reduction in caliber of the microvilli and appearance of cytoplasmic vacuoles or a tubular system The origin of the mucous neck cell from the nondifferentiated cell seems clear In no case was an interdevelopmental relationship between mucous neck cell and immature surface cell indicated by the presence within a single cell of the distinctive secretory granules characteristic of each cell type although transformation of surface cells to mucous neck cells has been described in a study utilizing the light microscope (Hunt 58) The probable cellular relationships are summarized in figure 1

The effects of hypophysectomy

Most experimental studies in which the electron microscope has been used have been characterized by a general lack of attention to the reproducibility of the observations being reported Without such information the reliability of the observations can hardly be ascertained In my study an attempt was made to alleviate this deficiency by the preservation of multiple blocks of tissue obtained from a carefully specified area of the mucosa by thorough examination of the ultrastructure of cells at various levels of the mucosa and by photographing a large number of cells in order to be certain that the differences described between control and hypophysectomized rats were regular in their appearance When a response was observed in only a portion of the hypophysectomized rats this information is given

Chief cell The ultrastructural changes observed after hypophysectomy in the chief cell confirm the observations of Baker and Abrams (54) with respect to reduction in size of the cell and depletion of zymogenic granules from the apical cytoplasm Since the secretory product pepsinogen is a protein and a host of biochemical (Hultin 64) and structural investigations (Siekevitz and Palade 59 Dalton 61 Caro 61 Caro and Palade 64) have demonstrated the involvement of ergastoplasm and Golgi apparatus in protein synthesis the changes induced in these cellular components by hypophysectomy are especially pertinent The marked loss of cytoplasmic basophilia which follows pituitary ablation (Baker and Abrams 54) indicates a reduction in the amount of ribonucleic acid (RNA) contained in the cell Since the RNA fraction which accounts for basophilia is unknown it is especially important that in my study a loss

of ribosomes was observed after hypophysectomy In addition the reduction in extent of the endoplasmic reticulum and in the density of the ground cytoplasm shows that the structures which appear to be involved in peptide synthesis (Caro and Palade 64 Hultin 64) undergo change upon withdrawal of pituitary hormones

The possible involvement of technical deficiencies in the induction of the ergastoplasmic changes observed after hypophysectomy merits consideration since somewhat similar characteristics in other cells are occasionally attributed to the influence of faulty fixation or embedding Hypophysectomy may have altered the tissue in such a way that cytoplasm could not be preserved in the usual manner The regularity in the appearance of the changes described in endoplasmic reticulum and in the ground cytoplasm of different cells of the hypophysectomized rats their rareness in the controls their demonstrableness with two different fixatives and adequate fixation of other adjacent cell types all indicate that hypophysectomy was either directly or indirectly responsible for the observations described Helander (64) reported alterations of the endoplasmic reticulum and ribosomes as well as the Golgi apparatus following refeeding of the starved mouse

Polyribosomes (Rich et al 63) were observed occasionally in the perinuclear area of control rats A chain was composed of as many at 16 ribosomes In more than half of the hypophysectomized rats polyribosomes appeared to be increased in number but the regularity of response could not be established Biochemical studies of polyribosomes (Rich et al 63) their depletion from fibroblasts in scorbutic guinea pigs and restoration following treatment with ascorbic acid (Ross and Benditt 64) lead one to associate the presence of polyribosomes with active protein synthesis Thus an increase in number of polyribosomes in chief cells at a time of depressed protein synthesis cannot be explained

In glandular cells a direct relationship between size of Golgi apparatus and secretory activity appears to exist (Kirkman and Severinghaus '38 Dalton 61) With the reduction in secretory activity which occurs in chief cells after hypophysectomy the Golgi apparatus becomes smaller and more compact However no alteration in number of saccules vesicles or vacuoles is evident although an overall reduction in dilation of the saccular cisternae appears to be present The apparent "budding off" of vesicles from the endoplasmic reticulum and their subsequent fusion with Golgi saccules as postulated by Zeigel and Dalton (62) and Essner and Novikoff (62) was rarely observed in the granulated chief cell of both nonhyophysectomized and hypophysectomized rats

In view of the evidence that chief cells may secrete intrinsic factor (Boass and Wilson 64) as well as pepsinogen the appearance within the cell of each secretion in a different morphological form must be considered It is possible that the dense granule represents a second secretion and its failure to regress following hypophysectomy suggests a different response to pituitary hormones Also because of its size and ultrastructural characteristics the small granule may be identical to the microbody of Rouiller and Bernhard (56) and the lysosome of de Duve (59)

Parietal cell The influence of hypophysectomy on the parietal cell as observed with the light microscope (Baker and Abrams 54) was far less pronounced than on the chief cell Similarly the production of hydrochloric acid (Crafts and Walker 47) was affected much less than the secretion of pepsinogen (Baker and Abrams 54) Pituitary ablation induced little change in the ultrastructure of the parietal cell this being limited to reduced canalicular caliber and distortion of microvilli Little is known of the role of cell structures in secretion of hydrochloric acid so meaningful interpretation is not possible

Modification of the canaliculi and associated microvilli have been observed under other experimental conditions Vial and Orrego (60) and Sedar and Friedman (61) noted that canaliculi and the surface area of their microvilli were increased in stomachs stimulated by several experimental means Following the claim of Ito (61) that patency of canaliculi cannot be correlated with the physiological state of

the animal because of the great normal variation Sedar (62) appears to have questioned his earlier results Although considerable variation in width of the canaliculi does exist, my observations indicate that one can detect differences in their average caliber following subjection of the rat to experimental procedures *providing* careful attention is given to the level of the cell in the gland and an adequate sampling is effected

ACKNOWLEDGMENT

I wish to thank Dr Burton L Baker for his guidance during this study

LITERATURE CITED

Baker B L and G D Abrams 1954 Effect of hypophysectomy on the cytology of the fundic glands of the stomach and on the secretion of pepsin Amer J Physiol, *177* 409–412
Baker B L and R H Clark 1961 Influence of hypophysectomy on oxidative enzymes and size of parietal cells in gastric mucosa Proc Soc Exp Biol Med *106* 65–67
Boass A and T H Wilson 1964 Cellular localization of gastric intrinsic factor in the rat Am J Physiol *206* 783–786
Caro L G 1961 Electron microscopic radio autography of thin sections The Golgi zone as a site of protein concentration in pancreatic acinar cells J Biophys Biochem Cytol *10* 37–46
Caro L G and G E Palade 1964 Protein synthesis storage and discharge in the pancreatic exocrine cell An autoradiographic study J Cell Biol *20* 473–495
Crafts R C and B S Walker 1947 The effects of hypophysectomy on gastric acidity of adult female rats Endocrinology *40* 395–402
Dalton A J 1955 A chrome-osmium fixative for electron microscopy Anat Rec *121* 281 Abstr
——— 1961 Golgi apparatus and secretion granules In The Cell J Brachet and A E Mirsky (ed) Academic Press New York vol II pp 603–619
de Duve C 1959 Lysosomes a new group of cytoplasmic particles In Subcellular Particles T Hayashi (ed) The Ronald Press Co New York pp 128–159
Essner E and A B Novikoff 1962 Cytological studies on two functional hepatomas Interrelations of endoplasmic reticulum Golgi apparatus and lysosomes J Cell Biol *15* 289–312
Han S S 1961 The ultrastructure of the mesenteric lymph node of the rat Am J Anat *109* 183–225
Helander H F 1962 Ultrastructure of fundus glands of the mouse gastric mucosa J Ultrastructure Res suppl 4 1–123
——— 1964 Ultrastructure of gastric fundus glands of refed mice J Ultrastructure Res *10* 160–175
Hultin T 1964 Ribosomal functions related to protein synthesis In International Review of Cytology G H Bourne and J F Danielli (ed) Academic Press New York and London vol 16 pp 1–36
Hunt T E 1958 Regeneration of the gastric mucosa in the rat Anat Rec *131* 193–212
Hunt T E and E A Hunt 1962 Radioautographic study of proliferation in the stomach of the rat using thymidine-H^3 and compound 48/80 Anat Rec *142* 505–517
Ito S 1961 The endoplasmic reticulum of gastric parietal cells J Biophys Biochem Cytol *11* 333–347
Ito S and R J Winchester 1963 The fine structure of the gastric mucosa in the bat J Cell Biol *16* 541–577
Kirkman H and A E Severinghaus 1938 A review of the Golgi apparatus Part III Anat Rec *71* 79–103
Kurosumi K 1961 Electron microscopic analysis of the secretion mechanism In International Review of Cytology G H Bourne and J F Danielli (ed) Academic Press New York vol 11 pp 1–124
Kurosumi K S Shibasaki G Uchida and Y Tanaka 1958 Electron microscope studies on the gastric mucosa of normal rats Arch Histol Jap *15* 587–624
Lane N L G Caro L R Otero-Vilardebó and G C Godman 1964 On the site of sulfation in colonic goblet cells J Cell Biol *21* 339–351
Lawn A M 1960 Observations on the fine structure of the gastric parietal cell of the rat J Biophys Biochem Cytol *7* 161–166
Leblond C P and B E Walker 1956 Renewal of cell populations Physiol Rev *36* 255–276
Lillibridge C B 1964 The fine structure of normal human gastric mucosa Gastroenterology *47* 269–290
Luft J H 1961 Improvements in epoxy resin embedding methods J Biophys Biochem Cytol *9* 409–414
Messier B 1960 Radioautographic evidence for the renewal of the mucous cells in the gastric mucousa of the rat Anat Rec *136* 242 Abstr
Myhre E 1960 Regeneration of the fundic mucosa in rats V An autoradiographic study on the effect of cortisone Arch Path *70* 476–485
Palade G E 1952 A study of fixation for electron microscopy J Exp Med *95* 285–298
Peterson Neutra M 1965 Synthesis of complex carbohydrates in Golgi saccules an electron microscope-radioautographic study Anat Rec *151* 399 Abstr
Rich A J R Warner and H M Goodman 1963 The structure and function of polyribosomes Cold Spring Harbor Symposia on Quantitative Biology *28* 269–285
Ross R and E P Benditt 1964 Wound healing and collagen formation IV Distortion of ribosomal patterns of fibroblasts in scurvy J Cell Biol *22* 365–390
Rouiller C and W Bernhard 1956 "Microbodies" and the problem of mitochondrial re

generation in liver cells J Biophys Biochem Cytol 2 (suppl) 355–360
Sedar A W 1962 Electron microscopy of the the oxyntic cell in the gastric glands of the bullfrog *Rana catesbiana* III Permanganate fixation of the endoplasmic reticulum J Cell Biol *14* 152–156
——— 1964 Stomach and intestinal mucosa In Electron Microscopic Anatomy S M Kurtz (ed) Academic Press New York pp 123–148
Sedar A W and M H F Friedman 1961 Correlation of the fine structure of the gastric parietal cell (dog) with functional activity of the stomach J Biophys Biochem Cytol *11* 349–363
Shibasaki S 1961 Experimental cytological and electron microscope studies on the rat gastric mucosa Arch Histol Jap *21* 251–288
Siekevitz P and G E Palade 1959 A cytochemical study on the pancreas of the guinea pig IV Chemical and metabolic investigation of the ribonucleoprotein particles J Biophys Biochem Cytol 5 1–10
Stevens C E and C P Leblond 1953 Renewal of the mucous cells in the gastric mucosa of the rat Anat Rec *115* 231–245
Townsend S F 1961 Regeneration of gastric mucosa in rats Am J Anat *190* 133–147
Vial J D and H Orreggo 1960 Electron microscope observations on the fine structure of parietal cells J Biophys Biochem Cytol 7 367–372
Watson M L 1958 Staining of tissue sections for electron microscopy with heavy metals J Biophys Biochem Cytol 4 475–478
Zeigel R F and A J Dalton 1962 Speculations based on the morphology of the Golgi systems in several types of protein-secreting cells J Cell Biol *15* 45–54

the animal because of the great normal variation Sedar ('62) appears to have questioned his earlier results Although considerable variation in width of the canaliculi does exist, my observations indicate that one can detect differences in their average caliber following subjection of the rat to experimental procedures providing careful attention is given to the level of the cell in the gland and an adequate sampling is effected

ACKNOWLEDGMENT

I wish to thank Dr Burton L Baker for his guidance during this study

LITERATURE CITED

Baker B L and G D Abrams 1954 Effect of hypophysectomy on the cytology of the fundic glands of the stomach and on the secretion of pepsin Amer J Physiol 177 409–412

Baker B L and R H Clark 1961 Influence of hypophysectomy on oxidative enzymes and size of parietal cells in gastric mucosa Proc Soc Exp Biol Med 106 65–67

Boass A and T H Wilson 1964 Cellular localization of gastric intrinsic factor in the rat Am J Physiol 206 783–786

Caro L G 1961 Electron microscopic radioautography of thin sections The Golgi zone as a site of protein concentration in pancreatic acinar cells J Biophys Biochem Cytol 10 37–46

Caro L G and G E Palade 1964 Protein synthesis storage and discharge in the pancreatic exocrine cell An autoradiographic study J Cell Biol 20 473–495

Crafts R C and B S Walker 1947 The effects of hypophysectomy on gastric acidity of adult female rats Endocrinology 40 395–402

Dalton A J 1955 A chrome-osmium fixative for electron microscopy Anat Rec 121 281 Abstr

——— 1961 Golgi apparatus and secretion granules In The Cell J Brachet and A E Mirsky (ed) Academic Press New York vol II pp 603–619

de Duve C 1959 Lysosomes a new group of cytoplasmic particles In Subcellular Particles T Hayashi (ed) The Ronald Press Co New York pp 128–159

Essner E and A B Novikoff 1962 Cytological studies on two functional hepatomas Interrelations of endoplasmic reticulum Golgi apparatus and lysosomes J Cell Biol 15 289–312

Han S S 1961 The ultrastructure of the mesenteric lymph node of the rat Am J Anat 109 183–225

Helander H F 1962 Ultrastructure of fundus glands of the mouse gastric mucosa J Ultrastructure Res suppl 4 1–123

——— 1964 Ultrastructure of gastric fundus glands of refed mice J Ultrastructure Res 10 160–175

Hultin T 1964 Ribosomal functions related to protein synthesis In International Review of Cytology G H Bourne and J F Danielli (ed) Academic Press New York and London vol 16 pp 1–36

Hunt T E 1958 Regeneration of the gastric mucosa in the rat Anat Rec 131 193–212

Hunt T E and E A Hunt 1962 Radioautographic study of proliferation in the stomach of the rat using thymidine H^3 and compound 48/80 Anat Rec 142 505–517

Ito S 1961 The endoplasmic reticulum of gastric parietal cells J Biophys Biochem Cytol 11 333–347

Ito S and R J Winchester 1963 The fine structure of the gastric mucosa in the bat J Cell Biol 16 541–577

Kirkman H and A E Severinghaus 1938 A review of the Golgi apparatus Part III Anat Rec, 71 79–103

Kurosumi K 1961 Electron microscopic analysis of the secretion mechanism In International Review of Cytology G H Bourne and J F Danielli (ed) Academic Press New York vol 11 pp 1–124

Kurosumi K S Shibasaki G Uchida and Y Tanaka 1958 Electron microscope studies on the gastric mucosa of normal rats Arch Histol Jap 15 587–624

Lane N L G Caro L R Otero-Vilardebó and G C Godman 1964 On the site of sulfation in colonic goblet cells J Cell Biol 21 339–351

Lawn A M 1960 Observations on the fine structure of the gastric parietal cell of the rat J Biophys Biochem Cytol 7 161–166

Leblond C P and B E Walker 1956 Renewal of cell populations Physiol Rev 36 255–276

Lillibridge C B 1964 The fine structure of normal human gastric mucosa Gastroenterology 47 269–290

Luft J H 1961 Improvements in epoxy resin embedding methods J Biophys Biochem Cytol 9 409–414

Messier B 1960 Radioautographic evidence for the renewal of the mucous cells in the gastric mucousa of the rat Anat Rec 136 242 Abstr

Myhre E 1960 Regeneration of the fundic mucosa in rats V An autoradiographic study on the effect of cortisone Arch Path, 70 476–485

Palade G E 1952 A study of fixation for electron microscopy J Exp Med 95 285–298

Peterson Neutra M 1965 Synthesis of complex carbohydrates in Golgi saccules an electron microscope-radioautographic study Anat Rec 151 399 Abstr

Rich A J R Warner and H M Goodman 1963 The structure and function of polyribosomes Cold Spring Harbor Symposia on Quantitative Biology 28 269–285

Ross R and E P Benditt 1964 Wound healing and collagen formation IV Distortion of ribosomal patterns of fibroblasts in scurvy J Cell Biol 22 365–390

Rouiller C and W Bernhard 1956 "Microbodies" and the problem of mitochondrial re

generation in liver cells J Biophys Biochem Cytol 2 (suppl) 355–360

Sedar A W 1962 Electron microscopy of the the oxyntic cell in the gastric glands of the bullfrog *Rana catesbuana* III Permanganate fixation of the endoplasmic reticulum J Cell Biol *14* 152–156

——— 1964 Stomach and intestinal mucosa In Electron Microscopic Anatomy S M Kurtz (ed) Academic Press New York pp 123–148

Sedar A W and M H F Friedman 1961 Correlation of the fine structure of the gastric parietal cell (dog) with functional activity of the stomach J Biophys Biochem Cytol *11* 349–363

Shibasaki S 1961 Experimental cytological and electron microscope studies on the rat gastric mucosa Arch Histol Jap *21* 251–288

Siekevitz P and G E Palade 1959 A cytochemical study on the pancreas of the guinea pig IV Chemical and metabolic investigation of the ribonucleoprotein particles J Biophys Biochem Cytol 5 1–10

Stevens C E and C P Leblond 1953 Renewal of the mucous cells in the gastric mucosa of the rat Anat Rec *115* 231–245

Townsend S F 1961 Regeneration of gastric mucosa in rats Am J Anat *190* 133–147

Vial J D and H Orreggo 1960 Electron microscope observations on the fine structure of parietal cells J Biophys Biochem Cytol 7 367–372

Watson M L 1958 Staining of tissue sections for electron microscopy with heavy metals J Biophys Biochem Cytol *4* 475–478

Zeigel R F and A J Dalton 1962 Speculations based on the morphology of the Golgi systems in several types of protein secreting cells J Cell Biol *15* 45–54

Abbreviations

A Axon
AC Argyrophilic cell
BI Basal infolding
BM Basement membrane
C Canaliculus
CAP Capillary
CC Chief cell
CE Centriole
CI Cisterna
D Desmosome
DC Dilated cisterna
E Endothelial cell
ER Endoplasmic reticulum
F Fibrils
G *Golgi apparatus*
GR Granule
GV Golgi vesicle
L Lumen
M Mitochondria
MNC Mucous neck cell
MV Microvillus
MVB Multivesicular body
N Nucleus
NC Neurilemmal sheath cell
NU Nucleolus
NPC Neck parietal cell
P Plasmalemma
PC Parietal cell
PV Pinocytotic vesicle
R Ribosome
RER Rough surfaced endoplasmic reticulum
SC Surface cell
SER, Smooth surfaced endoplasmic reticulum
SG Small granule
V Vacuole
ZO Zonula occludens

All tissues illustrated were preserved in Palade s osmic acid fixative unless stated to the contrary

PLATE 1

EXPLANATION OF FIGURES

2 Nondifferentiated cell The cell is columnar The nucleus (N) is large elongate basally located and contains a small nucleolus (NU) The endoplasmic reticulum (RER) is sparse and cisternae are of irregular shape There are many clusters of free ribosomes in the ground cytoplasm which is of low density The Golgi apparatus (G) is located lateral to the nucleus The apical plasmalemma (left) possesses short microvilli × 9 900

3 Nondifferentiated cell The lateral plasmalemma (P) is generally straight with few interdigitations with adjacent cells The thin amorphous basement membrane (BM) follows the basal contour of the cell The nucleus (N) is basal The endoplasmic reticulum (RER) is poorly developed and is found throughout the cell Portions of its external surface possess attached ribosomes elsewhere it is smooth A multitude of free ribosomes (R) are arranged in clusters The cisternae (CI) contain a material of low electron density The elongated or oval mitochondria (M) have transversely oriented cristae The Golgi apparatus (G) is extensive and consists of flattened saccules with little dilation small dense vesicles and a few larger vacuoles of irregular form × 17 800


M
N
MV
L
2
13

PLATE 2

EXPLANATION OF FIGURE

4 Surface mucous cell from the wall of a gastric pit The cell is high columnar the lumen (L) of the pit being at the upper end The oval nucleus (N) is basal and contains a nucleolus (NU) The lateral plasmalemma (P) is tortuous and interdigitated with adjacent cells Desmosomes (D) are occasionally present The apical plasmalemma is flat and generally lacking in microvilli The supranuclear Golgi apparatus (G) is large Its stacks of three or more flattened saccules are peripherally oriented with rare mild dilation of the external ones (DC) The flattened saccules show unusually intense electron density Many small vesicles are found internal to the saccules The rough surfaced endoplasmic reticulum (RER) is more extensively devel oped than in the nondifferentiated cell but is similar in having many areas with no attached ribosomes The irregularly shaped cisternae of the endoplasmic reticulum contain material of low electron density Free ribosomes are dispersed in the ground substance often being arranged in clusters Oval dense mucous granules (GR) occur within the Golgi apparatus and appear to move into the apical region where they become densely packed and more discoidal beneath the surface membrane The mitochondria are elongate pleomorphic and contain numerous wavy transversely oriented cristae and a few dense granules Cytoplasmic fibrils (F) abound in the apical cyto plasm × 15 000


GR
GR
GV
G
4

PLATE 3

EXPLANATION OF FIGURE

5 Immature surface cells and neck parietal cell At the left and right of the glandular lumen (L) are portions of three columnar immature surface cells (SC) The plasmalemmas (P) of contiguous surface cells are deeply interdigitated The nucleus (N) is of irregular shape and its nucleoplasm is of low density Rough surfaced endoplasmic reticulum (RER) is poorly developed There is a multitude of free ribosomes Mitochondria (M) are of irregular shape have cristae of variable form and density and are much smaller than the mitochondria of neighboring neck parietal cells (NPC) The apical cytoplasm contains mucous granules (GR) of high electron density The Golgi apparatus (G) is lateral to the nucleus

The neck parietal cell (NPC) is pyramidal and contains numerous pleomorphic mitochondria (M) with densely arranged cristae Microvilli (MV) both at the apex and within canaliculi (C) are densely packed and bulbous Cytoplasmic vacuoles are of irregular shape and distributed predominantly in the apex of the cell and in the vicinity of canaliculi The Golgi apparatus (G) is located laterally The plasmalemma (P) is somewhat folded laterally and basally $\times$ 9 900

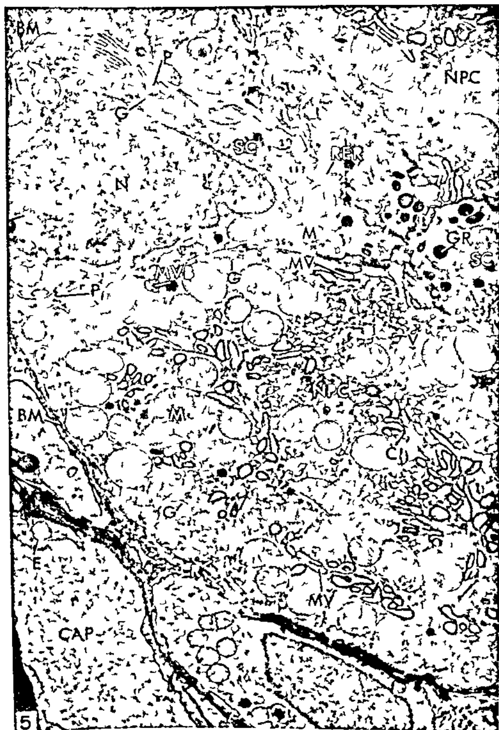

BM
P
G
NPC
SG
RER
N
M
GR
SC
MV
MVB
G
P
NPC
BM
M
CL
G
E
MV
CAP
5

PLATE 4

EXPLANATION OF FIGURES

6 Mucous neck cell The cell is low columnar and somewhat constricted basally The nucleus (N) is basal The lateral plasmalemma (P) is tortuous and interdigitates with adjacent cells Occasional desmosomes (D) are present The undulating apical plasmalemma is without microvilli except laterally near the junction with adjacent cells Basal cytoplasm is sparse and the rough surfaced endoplasmic reticulum (RER) is poorly developed Free ribosomes (R) are numerous The apical cytoplasm is filled with large round granules of mucoprotein of moderate electron density × 12 300

7 Mucous neck cell The supranuclear region reveals an extensive Golgi apparatus (G) composed of flattened saccules numerous dilated external saccules (DC) and dense vesicles (GV) The supranuclear region is packed with mucoprotein granules (GR) a limiting membrane (arrow) is sharply defined on the side of some granules near the Golgi apparatus Some Golgi vesicles (*) appear to be in direct contact with a secretory granule Ribosomes are attached to much but not all of the external surface of the endoplasmic reticulum Free ribosomes are frequent Mitochondria (M) are located laterally × 14 600

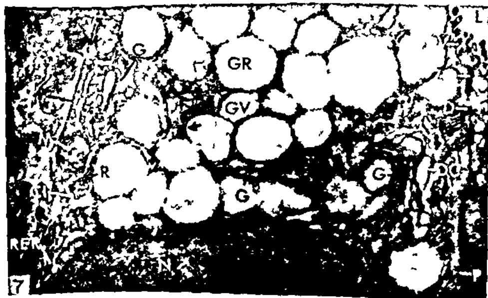

7
L
G
GR
GV
R
G
G
D
RER
N
P

PLATE 5

EXPLANATION OF FIGURE

8 Immature mucous neck cell This columnar cell is located in the neck region adjacent to neck parietal cells (NPC) The nucleus (N) is large oval basal and has a dense central nucleolus (NU) The lateral plasmalemma (P) is generally straight with only a few inter digitations with adjacent parietal cells A desmosome (D) appears apically The apical cytoplasm contains a few secretory granules (GR) of moderate density A centriole (CE) with attached cilium is located in the supranuclear area The rough surfaced endoplasmic reticulum (RER) is limited in extent and encompasses cisternae of irregular shape There are numerous free ribosomes The mito chondria (M) are oval and possess few cristae × 18 900


L
GR
N
IE
BM
8

PLATE 6

EXPLANATION OF FIGURES

9 Neck parietal cell The cell is pyramidal The nucleus (N) is basal and has a nucleoplasm of low density Cytoplasmic vacuoles are almost totally absent Intracellular canaliculi (C) extend deep into the cell and are occluded by long microvilli (MV) Mitochondria (M) are pleomorphic of variable size and contain many cristae Endoplasmic reticulum (RER) is exceedingly sparse Rosettes of ribosomes are randomly distributed throughout the cytoplasm Several dense mucous granules (GR) appear in the apical cytoplasm × 8 500

10 Neck parietal cell The tongue like apical cytoplasm projects into the glandular lumen (L) and contains densely packed vacuoles many of which seem to be collapsed An intracellular canaliculus (C) is partially occluded by long thick microvilli (MV) Several multi vesicular bodies (MVB) and mucous granules (GR) are present × 14 600

The Golgi apparatus (insert) consists chiefly of a few small vesicles and flattened saccules with minimal dilation × 12 500

PLATE 7

EXPLANATION OF FIGURE

11 Chief cell nonhypophysectomized rat The cell contains numerous zymogenic granules (GR) of varied size shape and density Occasional small dense granules (SG) which resemble similar bodies located in the neighborhood of the Golgi apparatus occur in the apical cytoplasm The Golgi apparatus (G) is supranuclear and widespread It consists primarily of flattened saccules whose cisternae show varying degrees of dilation (DC) Small Golgi vesicles (GV) are numerous Several short blunt microvilli (MV) project from the apical plasmalemma The oval nucleus (N) is surrounded by an extensive ergastoplasm consisting of well organized rough surfaced endoplasmic reticulum (RER) cisternae of fairly uniform caliber many free ribosomes and rather dense intervening ground cytoplasm × 15 000


MV
L
CC
G
IV
PC
GV
DC
N
MN
RT
11

PLATE 7

EXPLANATION OF FIGURE

11 Chief cell nonhypophysectomized rat The cell contains numerous zymogenic granules (CR) of varied size shape and density Occasional small dense granules (SG) which resemble similar bodies located in the neighborhood of the Golgi apparatus occur in the apical cytoplasm The Golgi apparatus (G) is supranuclear and widespread It consists primarily of flattened saccules whose cisternae show varying degrees of dilation (DC) Small Golgi vesicles (GV) are numerous Several short blunt microvilli (MV) project from the apical plasmalemma The oval nucleus (N) is surrounded by an extensive ergastoplasm consisting of well organized rough surfaced endoplasmic reticulum (RER) cisternae of fairly uniform caliber many free ribosomes and rather dense intervening ground cytoplasm × 15 000


SG
L
GR
N
M
BM
RER
12


M
13

PLATE 8

EXPLANATION OF FIGURES

12 Chief cell 74 days after hypophysectomy The cell is small with a flat apical surface and few microvilli Ergastoplasm is reduced in amount the rough surfaced endoplasmic reticulum (RER) being sparse and of irregular contour free ribosomes are depleted and the ground cytoplasm appears hydropic The Golgi apparatus (G) is compact Zymogenic granules (GR) are scarce and difficult to identify Several small granules (SG) are observed just beneath the apical plasmalemma × 15 000

13 Perinuclear area of a chief cell 74 days after hypophysectomy Numerous polyribosomes (arrows) are demonstrated A few cisternae of the rough surfaced endoplasmic reticulum (RER) are observed at the periphery of the micrograph × 28 600

MV
L
SG
RER
G
GV
GR
14

L
MV
G
G
RER
GR
GV
G
15

PLATE 9

EXPLANATION OF FIGURES

14 Apical region of a chief cell from a nonhypophysectomized rat Several round or oval zymogenic granules (GR) have accumulated in the apical region causing the surface to bulge into the glandular lumen (L) One granule approximates the apical plasmalemma The Golgi apparatus (G) is well developed and broadly expanded Several small dense granules (SG) extensive rough surfaced endoplasmic reticulum (RER) and many free ribosomes are present also × 26 000

15 Apical region of a chief cell 74 days after hypophysectomy Zymogenic granules (GR) are sparse and do not appear in the most superficial zone of cytoplasm Small granules (SG) are numerous and appear in intermediate sizes down to that of the Golgi vesicle (GV) A narrow zone free of organelles lies just beneath the apical plasmalemma Rough surfaced endoplasmic reticulum (RER) is poorly organized and the ground cytoplasm is of low density Several apical microvilli project into the lumen (L) × 26 000


R
R
M
Cl
16
RER
C
M
17

PLATE 10

EXPLANATION OF FIGURES

16 Basal portion of a chief cell from a nonhypophysectomized rat The ergastoplasm is well organized Free and attached ribosomes are numerous Cisternae (CI) contain electron dense material Ground cytoplasm between cisternae is fairly dense × 41 800

A mitochondrion (insert) of the chief cell illustrating its typical shape and position near the plasmalemma Several transversely oriented cristae span the entire width of the mitochondrion which exhibits a dense granular matrix with several intramitochondrial granules × 41 800

17 Basal region of a chief cell 58 days after hypophysectomy This micrograph illustrates in mild form the changes which followed hypophysectomy There may be some reduction in concentration of ribosomes but most striking is the reduced density of the ground cytoplasm which appears hydropic × 41 600

A mitochondrion (insert) from a hypophysectomized rat has trans versely oriented cristae a dense granular matrix and intramitochondrial granules × 41 800

G
GR
ER
M
18

GC
RER
M
19

PLATE 11

EXPLANATION OF FIGURES

18 Basal area of a chief cell from a nonhypophysectomized rat Dalton s fixative The ergastoplasm with its rough surfaced endoplasmic reticulum (RER) dense intervening ground cytoplasm free and attached ribosomes is compactly arranged × 21 600

19 Basal area of a chief cell 74 days after hypophysectomy Dalton s fixative Compared with figure 18 the amount of ergastoplasm is reduced the rough surfaced endoplasmic reticulum (RER) is less extensive ribosomes are fewer and ground cytoplasm is less dense Observe the excellent fixation of the parietal cell (PC) on the right × 21 600

L
GR
SG
GV
DC
GR
20



PLATE 12

EXPLANATION OF FIGURES

20 Golgi apparatus of a chief cell from a nonhypophysectomized rat The peripheral limits of the Golgi apparatus (G) are indicated by arrows It is spread extensively through the supranuclear region of the cell The Golgi apparatus consists of flattened saccules with considerably dilated cisternae small dense Golgi vesicles (GV) and some vacuoles (V) Large secretory granules (GR) are dispersed through the Golgi region A gradation in size and density can be observed between the small Golgi vesicle (GV) and the small granule (SG) The Golgi apparatus encompasses cytoplasm containing rough surfaced endoplasmic reticulum and free ribosomes × 15 400

21 Golgi apparatus in two chief cells 120 days after hypophysectomy The Golgi apparatus is outlined by arrows As compared with figure 20 the size of the Golgi apparatus is reduced and its cisternae (CI) are less dilated The large vacuoles may be secretory granules in an early stage of formation Golgi vesicles are numerous and compactly arranged × 15 400

PLATE 13

EXPLANATION OF FIGURES

22 Basal region of two parietal cells nonhypophysectomized rat The cells rest against the basement membrane (BM) Numerous basal infoldings (BI) are evident Canaliculi (C) are wide Microvilli (MV) are long and of uniform caliber Cytoplasmic vacuoles (V) border the canaliculi Mitochondria (M) contain many transversely oriented cristae and a dense matrix × 41 600

23 Basal region of a parietal cell 196 days after hypophysectomy The maximal width of canaliculi (C) is less than in figure 22 Microvilli (MV) are distorted and of irregular caliber and shape Cytoplasmic vacuoles (V) mitochondria and ribosomes appear unchanged × 41 600

Richard E. C rpr n

D
B
V
C
C
M
C
BM
R
MV
22

C
MV
V
M
23

[1] # Bone Formation and Resorption around Developing Teeth Transplanted into the Femur

RICHARD L HOFFMAN
Department of Histology College of Dentistry University of Illinois at the Medical Center Chicago Illinois

ABSTRACT Seven of 24 newborn hamsters developing maxillary molars which were transplanted to the femur for 28 days showed growth and development of crowns and roots Enamel dentin pulp cementum periodontal ligament and alveolar bone proper developed in their normal locations just as they had done previously in molars transplanted into subcutaneous connective tissues Several relationships were observed between alveolar bone proper developed in the foreign body environment and under the inductive influence of the tooth root and femoral bone Femoral bone was con tinuous with alvolar bone and supported the tooth socket In some areas near trans planted molar roots femoral bone was built out to join and support alveolar bone In other areas femoral bone was resorbed by the development of a molar root or the molar root was diverted from its normal direction of development Despite the effort to orient transplanted molars for eruption the orientation was altered and no evidence for tooth eruption was observed

Transplantation of newborn hamster (*Cricetus auratus*) developing maxillary molars into the subcutaneous connective tissues of hosts has demonstrated that sur viving transplants not only complete for mation of appropriate crowns and roots but also possess the ability to induce the de velopment of their own periodontal liga ment and shell of alveolar bone proper around their roots (Hoffman 60) Since these supporting tissues were not trans planted cells responsible for their produc tion were presumed to have been contrib uted by host subcutaneous tissues

The present investigation reports the transplantation of developing maxillary molars into prepared sites in non oral bone Each tooth germ was removed from its normal environment and transferred to the femur to determine whether the tooth could produce its own periodontal ligament and alveolar bone in a foreign bony en vironment to determine how alveolar bone proper which is under the formative in fluence of the developing tooth root might relate to bone of the femur diaphysis and to determine whether transplanted molars might erupt from the femur shaft as they normally do from the jaw

METHODS AND MATERIALS

Twenty four maxillary first molars were transpl nted from newborn hamsters into prepared crypts in the medial aspect of the right femoral diaphysis of 30-day-old ham ster hosts These molars had developed to the shell stage (Schour 63) ameloblasts and odontoblasts were differentiated over growth centers at the tips of the cusps and dentin formation had begun in these cen ters Root formation had not begun it commences at five days after birth In newborn hamsters the dental sac is a scantily cellular and primitive connective tissue with a few collagenous fibers ar ranged circularly around the enamel organ and the dental papilla

Removal of this enamel organ and dental papilla from the bony crypt is done under a dissecting microscope The oral mucosa covering the tooth germ is incised and spread With an iridectomy knife the enamel organ and dental papilla are lifted from the sac and transplanted into holes prepared in the medial side of the femoral diaphysis These holes are made in the host femur with a dental burr and engine after shaving and incision of the skin and blunt dissection of overlying musculature Hemorrhage invariably occurred when the bony shaft was penetrated Clot formation was rapid but the clot was partially re moved to accomodate the transplant which was oriented so that it might erupt from

[1] This investigation was supported by PHS grant DE 01971-02

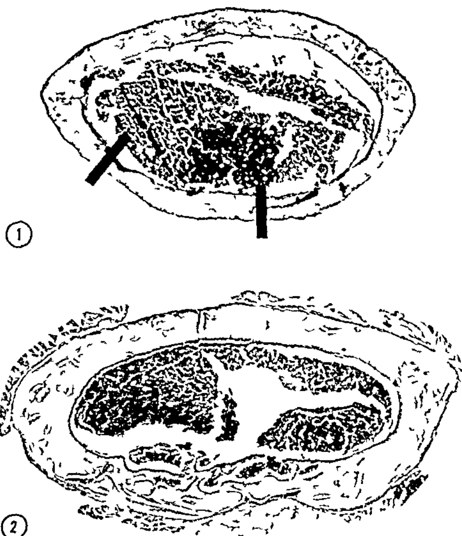


Fig 1 Cross section of a 30 day-old hamster control femur diaphysis with the transplantation site indicated by markers × 31

Fig 2 Cross section of a 58-day-old hamster control femur which was operated but received no transplant × 31

Abbreviations

AB alveolar bone proper	MR molar root
B bone	O odontoblasts
C cementum	OD osteodentin
CF collagen fibers	P pulp
D dentin	PD predentin
ES enamel space	PDL periodontal ligament
FB femoral bone	

the femur bone Muscles were repositioned and the skin sutured

The right femur carried the transplanted molar the left femur served as the experimental control Some left femurs were unoperated to provide examples of the normal femur while others were subjected to the preparation of a hole to receive a transplant although no tooth was transplanted

After four weeks host animals were sacrificed Right and left femurs were dissected free of musculature fixed in 10%

formalin decalcified in ethylenediamine tetraacetic acid embedded in paraffin cross sectioned at 10 μ and stained with hematoxylin and eosin Photographic re constructions of each specimen were made to assist in evaluating the growth and de velopment of transplants Surviving and developing transplanted molars and their surrounding tissues were compared to molars not surviving to operated femur controls receiving no transplant and to unoperated femur controls

OBSERVATIONS

Control femurs Figure 1 is representa tive of six unoperated femur diaphyses ex amined The femur shaft is egg shaped in cross section and measures about 3 mm in length and 1 5 mm in width The sharper bony crest to the left is anterior and the lower side is medial The medial side of the femur was seen to be narrower in width with a range of 160 to 230 μ and made up usually of denser bone The lateral side of the femur has internal and external circumferential lamellae and a somewhat more loosely arranged central bone Its thickness is about 260 μ the measured ranges were 200 to 300 μ The femur bone is covered externally by peri osteum and internally by endosteum and the central cavity contains myeloid tissue

Five femurs were operated but did not receive transplants Figure 2 shows that trabeculated bone of the endosteal or in ternal callus remains in about one fifth of the femur medullary cavity at the operated site after 28 days Bone remodeling was continuing neither the external nor the internal circumferential lamella were re-established after 28 days Marrow was found in the trabecular spaces in contrast to connective tissues found in trabecular spaces around all surviving transplants Two of the sham operated femurs showed a small hole remaining in the femur dia physis at the site of the operation Away from the operated site the femur diaphysis was somewhat thicker than unoperated control femurs The apposition line is vis ible on the figure where new bone was added to the external surface of the femur

Recovered transplants showing growth and development Seven out of 24 or 29% of transplanted molars demonstrated growth and development in the host femur Figures 3 4 and 5 show sections of three of these molars figures 3 and 4 are frontal sections of the molars and figure 5 is a sagittal section through the lingual cusps and one root Formative cells for enamel dentin and pulp survived transplantation In some crown areas however ameloblasts failed to survive and lay down enamel Odontoblasts laid down appropriate quan tities of dentin in both the crowns and roots of transplants despite the appearance of some irregularly wide predentin along the pulpal surfaces of the root dentin and osteodentin formation in crown cusps (fig 5) Irregularly wide predentin and osteo-dentin reflect disturbances in normal den tinogenesis Areas of resorption were seen in cusp dentin not covered by enamel Fol lowing transplantation the pulp tissue was revascularized and many areas of normal odontoblasts could be seen at the pulp dentin border of developed transplanted molars (fig 3)

In addition to the dental tissues of the tooth proper the supporting dental tissues periodontal ligament and alveolar bone proper were formed around the roots of all developed transplanted molars Figures 3 4 and 5 show typical periodontal ligament and alveolar bone formed in their normal relationship to the roots of the tooth Fig ures 6 and 7 illustrate the characteristic orientation of collagen fibers in the perio-dontal ligament between the alveolar bone proper and the tooth

The growth and development of the tooth the periodontal ligament and the alveolar bone were seen to affect several kinds of relationships with bone of the femoral diaphysis Figure 8 demonstrates a thinning of diaphyseal bone where a root developed resorbed an area of femur bone This root apex was not in the operated site it had femoral bone of normal width on each side of it as well as a periodontal ligament around it Figure 9 shows dia physis bone which was built out in the area of a tooth root This increased width in the femur shaft was found only in rela tion to the tooth root In all of the photo-graphs of transplants direct continuity be tween alveolar bone proper and femur bone can be seen Figures 10 11 12 and 13 further illustrate the supporting relation

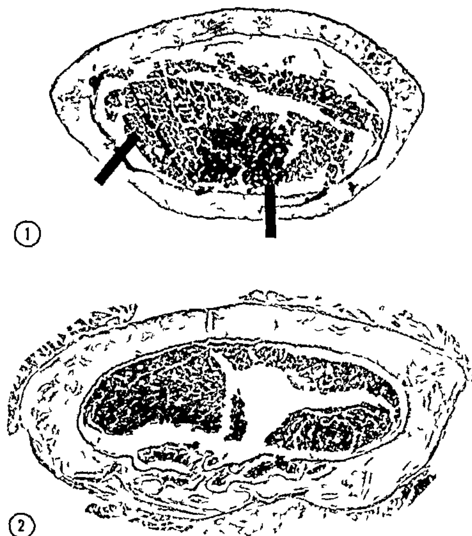


Fig 1 Cross section of a 30 day-old hamster control femur diaphysis with the transplantation site indicated by markers × 31

Fig 2 Cross section of a 58-day-old hamster control femur which was operated but received no transplant × 31

Abbreviations

AB alveolar bone proper	MR molar root
B bone	O odontoblasts
C cementum	OD osteodentin
CF collagen fibers	P pulp
D dentin	PD predentin
ES enamel space	PDL periodontal ligament
FB femoral bone	

the femur bone Muscles were repositioned and the skin sutured

The right femur carried the transplanted molar the left femur served as the experimental control Some left femurs were unoperated to provide examples of the normal femur while others were subjected to the preparation of a hole to receive a transplant although no tooth was transplanted

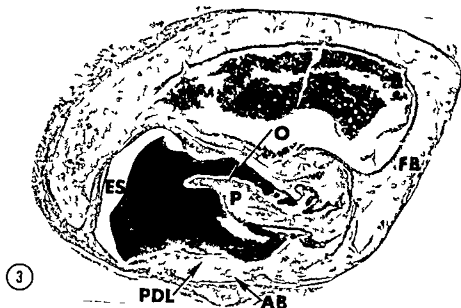
After four weeks host animals were sacrificed Right and left femurs were dissected free of musculature fixed in 10%

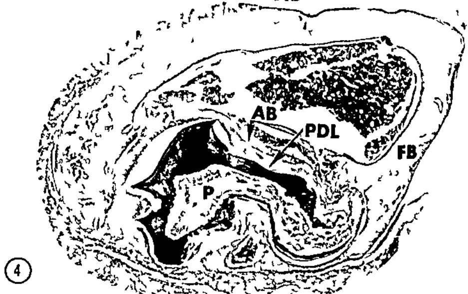


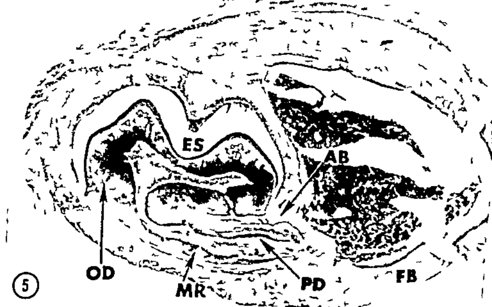
Figs 6 and 7 Histological details of periodontal tissues developed around the roots of molars transplanted into the femur × 85 and × 462

ship of diaphysis bone to the alveolar bone proper Trabeculae are seen to connect diaphysis and the alveolar socket of the root of the tooth

The presence of femoral bone in the area of the growth and development of the transplanted molar is seen to affect the morphology of developing roots Figure 5 shows a molar root which has been diverted almost 90 from its normal developmental direction apparently due to its contact with femur bone Similarly figures 3 and







Figs 3 4 and 5 Transplanted molars after 28 days of growth and development in the femur × 31



Figure 10



Figure 11

Fig 10 11 12 and 13 Sequential sections of a transplanted molar root its periodontal ligam nt alveolar bone proper and the upporting trabecular femoral bone × 85

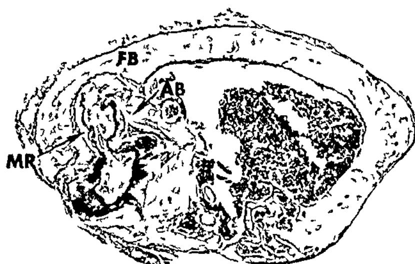


Fig 8 Cross section of the femur with transplanted molar showing resorption of femoral bone in the area of the developed root × 31

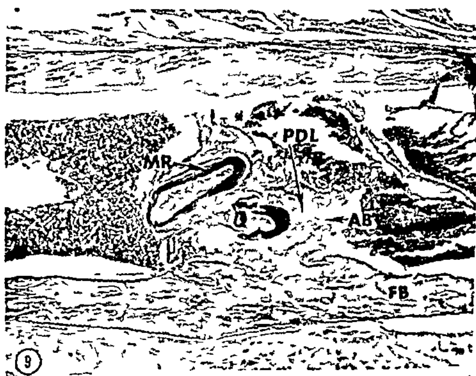


Fig 9 Longitudinal section of the femur showing transplanted molar roots developed periodontal tissues and their relationship to femoral bone × 31

in resorption bays in dentin of the enamelless cusp tip in the same area There was no evidence that transplanted molars had erupted

Recovered transplants not showing root development Eight or 33% of the transplanted molars showed limited growth or no growth after being transplanted In some no pulp tissue survived no additional dentin was laid down and no roots were formed In two cases pulp survived in one cusp where odontoblasts laid down limited additional dentin In other cusps where pulp tissue was seen to be more fibrous than normal or had been replaced by a more fibrous connective tissue bone formed in pulpal areas and approached the internal dentinal surface of dentin at about the normal periodontal width (fig 14) Bone approaches the external surface of dentin at a slightly greater distance

Figure 15 shows a developmentally arrested transplant in which a limited amount of crown dentin was added following transplantation but no roots were formed Connective tissue resembling primitive dental sac is seen interposed between the enamel space and osteodentin and the bone of the femur diaphysis

DISCUSSION

New bone formation within the femur medullary cavity and near the transplanted molars could be attributed to two separate and distinct influences or processes There was new bone formation related to the reconstitution or regeneration of the diaphysis bone removed in producing the bony crypt for the transplanted molars In this experimental site some of the new bone formed was a part of the wound healing or regeneration in a skeletal area The other new bone formation was the formation of alveolar bone proper related to the developing roots of the tooth and presumably occurred under the inductive influence of the transplanted tooth Because teeth do not ordinarily develop in the femur alveolar bone formed around the roots could be considered ectopic In the development of the jaw however one might consider that both formations of the jaw itself and of the alveolar bone proper were normal for the area but that they developed under separate influences

Regeneration in skeletal bone Regeneration of the diaphysis bone in prepared transplant crypts required healing and regeneration of the bone removed Wound

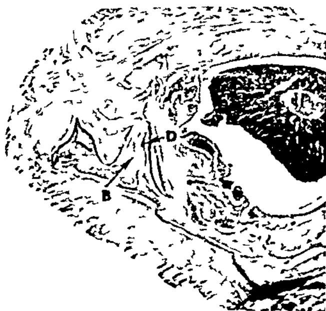


Fig 14 Cross section of the femur with a transplant which failed to develop but containing bone in the remaining coronal pulp tissue × 31

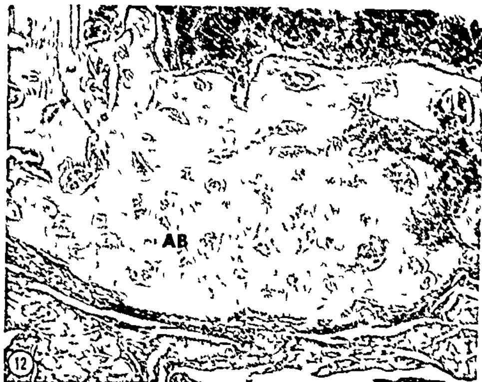


Figure 12



Figure 13

4 show some irregularities in root direction which seem to begin where the developing root contacted femur bone

In spite of the effort to orient transplanted molars so that they might erupt through the hole in the femur the orientations were either imperfect or altered following transplantation Osteoclasts were observed in resorption bays in bone opposite cusp tips but they were also observed

in resorption bays in dentin of the enamel less cusp tip in the same area There was no evidence that transplanted molars had erupted

Recovered transplants not showing root development Eight or 33% of the transplanted molars showed limited growth or no growth after being transplanted In some no pulp tissue survived no additional dentin was laid down and no roots were formed In two cases pulp survived in one cusp where odontoblasts laid down limited additional dentin In other cusps where pulp tissue was seen to be more fibrous than normal or had been replaced by a more fibrous connective tissue bone formed in pulpal areas and approached the internal dentinal surface of dentin at about the normal periodontal width (fig 14) Bone approaches the external surface of dentin at a slightly greater distance

Figure 15 shows a developmentally arrested transplant in which a limited amount of crown dentin was added following transplantation but no roots were formed Connective tissue resembling primitive dental sac is seen interposed between the enamel space and osteodentin and the bone of the femur diaphysis

DISCUSSION

New bone formation within the femur medullary cavity and near the transplanted molars could be attributed to two separate and distinct influences or processes There was new bone formation related to the reconstitution or regeneration of the diaphysis bone removed in producing the bony crypt for the transplanted molars In this experimental site some of the new bone formed was a part of the wound healing or regeneration in a skeletal area The other new bone formation was the formation of alveolar bone proper related to the developing roots of the tooth and presumably occurred under the inductive influence of the transplanted tooth Because teeth do not ordinarily develop in the femur alveolar bone formed around the roots could be considered ectopic In the development of the jaw however one might consider that both formations of the jaw itself and of the alveolar bone proper were normal for the area but that they developed under separate influences

Regeneration in skeletal bone Regeneration of the diaphysis bone in prepared transplant crypts required healing and regeneration of the bone removed Wound

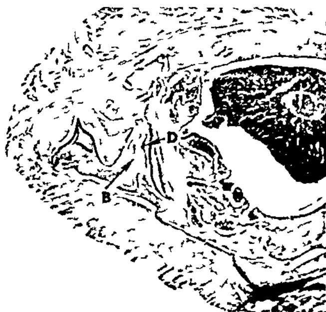


Fig 14 Cross section of the femur with a transplant which failed to develop but containing bone in the remaining coronal pulp tissue 31



Fig 15 Arrested development of a transplanted molar crown embedded in the femur × 85

healing in bone fractures has been well described (Urist and Johnson 43 Weinmann and Sicher 55 Boyd 61) It occurred by the formation of new bone After the clotting of the blood in the wound debrisment of the wound by phagocytes and invasion of the clot by capillaries fibroblasts produced collagen fibers converting the granulation tissue into fibrous or soft callus In a long bone such as the femur the soft callus extended beyond the wound site both external and internal to the shaft bone The callus cuff width was considerably greater than that of the shaft alone Osteoblast migrating from the inner layers of periosteum or endosteum laid down bony trabeculae within the soft callus Before calcification these trabeculae were osteoid in character and constituted the primary bony callus after calcification the secondary bony callus was formed Transformation of the cancellous bone and restitution of the lamellar character of the diaphysis bone involve remodeling of bone

Differences have been pointed out between the healing of fractures and the healing of experimentally produced bone wounds Bast Sullivan and Geist (25) sawed 10–20 mm longitudinal cuts in rabbit tibias and found the external or periosteal callus larger than the internal or endosteal callus Ely (27) Bourne (11) and Melcher and Irving (62) found more extensive endosteal callus formation with circumscribed defects produced by drilling into the medullary cavity of a long bone These authors stressed the importance of the endosteal callus as it established itself and then grew well into the defect before the external callus and the periosteum bridged the defect Periosteal callus was resorbed first some trabeculae of the endosteal callus remained in the medullary cavity adjacent to the operative site More than a year passed before inner circumferential lamellae were laid down in the remodeling of the diaphysis shaft according to these investigators

Using the figures and descriptions presented by these authors as a standard the operated control femurs in this experiment progressed in their healing in 28 days as far as the resorption of periosteal callus and the persistence of some endosteal callus near the defect site (fig 2) It seemed reasonable to assume that the wound healing in the femur had followed the general course of bone fracture wound

healing with the modifications for circumscribed experimentally produced bony defects This suggested that the molar transplantation environment had undergone a tissue transition from hemorrhage clot to granulation tissue to fibrous connective tissue to cancellous bone with medullary spaces during the growth and development of the transplanted tooth A tooth developing normally in the jaw undergoes environmental tissue change from mesenchyme to young fibrous connective tissue to cancellous bone

Bone formation related to tooth development Alveolar bone proper can be distinguished from femoral bone both developmentally and histologically Experimental transplantation of developing molars into subcutaneous connective tissues has shown that the shell of bone immediately adjacent to the root of the tooth the tooth socket is part of the developmental dental organ (Hoffman 60) With no host bone present in the area of transplantation each developed transplant formed this shell of bone with embedded fibers of the periodontal ligament The author assumed that the growth and development of the periodontal ligament and alveolar bone proper were induced from the host connective tissues Since these tooth supporting tissues were not transplanted they are believed to develop under the influence of the developing root of the tooth All tooth transplants which completed their development in the femur also showed the typical shell of alveolar bone proper adjacent to the roots and embedding the fibers of the periodontal ligament

Identification of alveolar bone proper can also be accomplished by its location adjacent to the roots of the tooth and histologically by its typical cribriform arrangement and content of bundle bone By definition the alveolar bone proper is the socket bone adjacent to the roots of the tooth Its typical cribriform arrangement can be seen in figure 12 It is denser bone than the supporting trabecular femoral bone in figure 13 or the trabecular endosteal callus seen in figure 2 Further alveolar bone proper is distinguished from the trabecular femoral bone by the presence of connective tissue fibers and cells of the periodontal ligament in its perforations figure 12 The intertrabecular tissue in the supporting femoral bone is hemopoetic figure 13

The term bundle bone is widely used among oral histologists particularly those having studied with Sicher Schour or Orban or having used either Orban s Oral Histology and Embryology or Schour s Oral Histology and Embryology as texts Ham and Leeson (61) recognized the locations of tendon insertions and periodontal ligament fiber insertion into bone as being a special situation While they refer to the collagen fibers embedded in the surface of bone as Sharpey s fibers they do not call the bony tissue which embeds them bundle bone According to Sicher (62) the term bundle bone was chosen because the principal fiber bundles of the periodontal ligament continue into the bone as Sharpey s fibers Bundle bone has very few fibrils in the intercellular substance these are arranged at right angles to Sharpey s fibers The predominance of a highly calcified cementing substance in bundle bone gives the tooth socket greater radiopacity than surrounding bone Depending upon the tooth s past and present functional requirements the socket bony composition may vary from being made up entirely of bundle bone to having areas of bundle bone on its inner surface which are backed by lamellated bone Figure 7 shows several areas with collagen fibers of the periodontal ligament entering the bone between osteoblasts The typical orientation of the periodontal ligament fibers between cementum and alveolar bone proper requires the embedding of the fibers in each tissue

Bone induction in general and its relationship to transplanted teeth have been discussed elsewhere (Hoffman 60) It can be added however that an area of bone wound healing in which the basic processes of proliferation growth and differentiation processes shared by both normal ontogenic development and regeneration are believed to be reactivated (Weiss 39) might be expected to be an excellent field and tissue for the developing root to stimulate Weinmann and Sicher (55) claim however that the young connective tissues which react to bone inducing stimuli in heteroplastic bone formation are not to be considered the same as embryonic mesen

chyme The connective tissue loses some of its potency or developmental possibilities as it matures In regeneration cells either dedifferentiate to a more primitive and pleuropotent type or reserve cells retaining embryonic pleuropotency differentiate and form the new tissues (Barth 55) These cells differentiate into osteoblasts and form bone

Relationships between bone of the callus and diaphysis and the alveolar proper Transplant root growth produced alterations in the femur diaphysis Roots have resorbed part of the femur shaft to accommodate the growth of their apices Additional bone was laid down on the endosteal surface of the shaft and bone which borders the roots and their periodontal ligament and is also continuous with bone of the femur diaphysis Both resorption of the femur and increases above its normal thickness appear directly related to the roots of the transplanted teeth Moreover figures 10 11 12 and 13 demonstrate the relationship of femur bone in the support of the bone and the tooth socket Since transplantations into subcutaneous connective tissues or muscle have not shown trabeculated supporting bone around the tooth bony socket only alveolar bone proper and interradicular bone the assumption that the trabecular bone supporting the tooth socket is a contribution of the femur bony callus seems reasonable Similarly one might expect the alveolar bone proper to be the contribution of the developing tooth root while the supporting bone is supplied by the adjacent jaw growth and development This would suggest that the developmental union of tooth to jaw was at the junction of the alveolar bone proper and supporting trabecular bone and not at the junction of the periodontal ligament and the cementum

ACKNOWLEDGMENTS

The author is indebted to Mrs Geno veva Bielskus for technical assistance and to Mr William Winn for photographs

LITERATURE CITED

Barth L G 1955 Regeneration — invertebrates In Analysis of Development Ed by B H Willier P Weiss and V Hamburger W B Saunders Co Philadelphia

Bast T H W E Sullivan and F D Geist 19?5 The repair of bone Anat Rec 31 255–280

Bourne G H 1944 The relative importance of periosteum and endosteum in bone healing and the relationship of Vit C to their activities Proc Roy Soc Med 37 275–279

Boyd W 1961 A Textbook of Pathology Lea and Febiger Philadelphia

Ely L W 1927 The internal callus An experimental study Arch of Surg 15 936–94?

Ham A W and T S Leeson 1961 Histology L B Lippincott Co Philadelphia

Hoffman R L 1960 *Formation* of periodontal tissues around subcutaneously transplanted hamster molars *J Dent Res 39* 781–798

Melcher A H and J T Irving 1962 The healing mechanism in artificially created circumscribed *defects in the femora of* albino rats J Bone and Joint Surg *44B* 928–936

Schour I 1963 Oral Histology and Embryology Lea and Febiger Philadelphia

Sicher H 1962 Orban s Oral Histology and Embryology C V *Mosby Co St Louis*

Urist M R and R W Johnson 1943 *Calcification* and ossification IV Healing of fractures in man under clinical conditions J Bone and Joint Surg 25 375–426

Weinmann J P and H Sicher 1955 *Bone and* Bones The C V Mosby Co St Louis

Weiss P 1939 Principles of Development Henry Holt and Co New York

Some Structural and Developmental Characteristics of Cetacean (Odontocete) Radii A Study of Adaptive Osteogenesis [1]

WILLIAM J L FELTS AND FRANCIS A SPURRELL [2]
University of Minnesota Minneapolis Minnesota

ABSTRACT Odontocete radii are short flattened longer than the humeri and lacking in open medullary cavities Their cross section is essentially a semi stream lined wedge End-on articulation at the elbow is a synchondrosis In the streamlined amuscular antebrachium the radius sustains loadings predominantly in the medial lateral transverse plane as flipper movements (at the shoulder) counter body inertia and water resistance in controlling body attitude

This study treats secondary marine adaptation as reflected in radial development growth and mechanical organization Early osteogenesis is similar to that we reported for cetacean humeri and parallels conditions in the manatee Later differential growth is analyzed *in extenso* Geometry of growth is visualized radiographically in the relationship of endochondral to periosteal bone in the absence of medullary cavitation Furthermore the neonatal outline is distinguishable within the porous structure of (only) beluga radii so that pre and postnatal phases may be differentiated Radiographs and models demonstrate that as elongation occurs circumferential increments to growth cartilages are eccentric i e minimal anteriorly moderate medially and laterally and maximal posteriorly By this method the centers of epiphyseal cartilage plates migrate posteriad with time Periosteal depositions follow the same pattern and are deepest posteriorly Eccentric growth of the ulna is in the opposite sense Additionally proximal growth cartilages of radii tilt posteriad as the bone elongates Some alterations in growth occur at birth and later Eccentric growth is an adaptation by which anterior and posterior margins respectively of radius and ulna move apart as the bones elongate and by which functional cross-sections are maintained in ante brachial bones singly and as a pair

Bone is concentrated on medial and lateral sides of the radius This feature and porosity of the central region varies with species Radii like humeri thus mimic an engineered box beam and trabecular orientation resembles trajectorial distribution in a loaded beam

Radii have higher absolute densities than do humeri although both bones have the same range of mineralization as typical mammalian bones The beluga radius is half again as dense as that of the pilot whale and thus is intermediate in density between those of most odontocetes and that of the hypothyroid pachyostotic manatee The possible evolution of odontocete bones from a more dense dense form as well as the phylogenetic implications of density changes are discussed It is suggested that some of the characteristics of growth and structure including an apparent periodicity in structural density may be related to temperature and vascular supply in the high area low volume flipper in colder waters

> There is a certain large class of morphological problems bound up with the general question of form and its determination as a result of growth The phenomena are those where *adaptation* in the strictest sense is obviously present in the clearly demonstrable form of mechanical fitness for the exercise of some particular function or action which has become inseparable from the life and well being of the organism — (D A W Thompson 42)

This paper reports on some specific and unusual features of structure and development in the radii of two small cetaceans the beluga (*Delphinapterus leucas*) the small white whale of Arctic and Sub-Arctic waters (Vladykov 44) and the pilot whale (*Globicephala melaena*) the blackfish or pothead of the North Atlantic (Sergeant 62) The limb skeletons of the cetaceans like those of many other extant and extinct marine mammals reptiles and birds (Howell 30 Meister 62) are foreshortened in their proximal segments have radical modifications of joints and the

[1] S pported by Nation l Science Fou d tion grant G-13348

[2] Dep rtme t of An tomy School of Medi ine Mi ne pol C mpu
Dep rtm nt of Veterin ry S rgery and Radiology Coll g of Veterin ry Medicine St Paul C mpu

chyme The connective tissue loses some of its potency or developmental possibilities as it matures In regeneration cells either dedifferentiate to a more primitive and pleuropotent type or reserve cells retaining embryonic pleuropotency differentiate and form the new tissues (Barth 55) These cells differentiate into osteoblasts and form bone

Relationships between bone of the callus and diaphysis and the alveolar proper Transplant root growth produced alterations in the femur diaphysis Roots have resorbed part of the femur shaft to accommodate the growth of their apices Additional bone was laid down on the endosteal surface of the shaft and bone which borders the roots and their periodontal ligament and is also continuous with bone of the femur diaphysis Both resorption of the femur and increases above its normal thickness appear directly related to the roots of the transplanted teeth Moreover figures 10 11 12 and 13 demonstrate the relationship of femur bone in the support of the bone and the tooth socket Since transplantations into subcutaneous connective tissues or muscle have not shown trabeculated supporting bone around the tooth bony socket only alveolar bone proper and interradicular bone the assumption that the trabecular bone supporting the tooth socket is a contribution of the femur bony callus seems reasonable Similarly one might expect the alveolar bone proper to be the contribution of the developing tooth root while the supporting bone is supplied by the adjacent jaw growth and development This would suggest that the developmental union of tooth to jaw was at the junction of the alveolar bone proper and supporting trabecular bone and not at the junction of the periodontal ligament and the cementum

ACKNOWLEDGMENTS

The author is indebted to Mrs Genoveva Bielskus for technical assistance and to Mr William Winn for photographs

LITERATURE CITED

Barth L G 1955 Regeneration — invertebrates In Analysis of Development Ed by B H Willier P Weiss and V Hamburger W B Saunders Co Philadelphia

Bast T H W E Sullivan and F D Geist 1925 The repair of bone Anat Rec 31 255-280

Bourne G H 1944 The relative importance of periosteum and endosteum in bone healing and the relationship of Vit C to their activities Proc Roy Soc Med 37 275-279

Boyd W 1961 A Textbook of Pathology Lea and Febiger Philadelphia

Ely L W 1927 The internal callus An experimental study Arch of Surg 15 936-91?

Ham A W and T S Leeson 1961 Histology L B Lippincott Co Philadelphia

Hoffman R L 1960 Formation of periodontal tissues around subcutaneously transplanted hamster molars J Dent Res 39 781-798

Melcher A H and J T Irving 19?2 The healing mechanism in artificially created circumscribed defects in the femora of albino rats J Bone and Joint Surg 44B 928-936

Schour I 1963 Oral Histology and Embryology Lea and Febiger Philadelphia

Sicher H 1962 Orban s Oral Histology and Embryology C V Mosby Co St Louis

Urist M R and R W Johnson 1943 Calcification and ossification IV Healing of fractures in man under clinical conditions J Bone and Joint Surg 25 375-426

Weinmann J P and H Sicher 1955 Bone and Bones The C V Mosby Co St Louis

Weiss P 1939 Principles of Development Henry Holt and Co New York

Some Structural and Developmental Characteristics of Cetacean (Odontocete) Radii A Study of Adaptive Osteogenesis [1]

WILLIAM J L FELTS AND FRANCIS A SPURRELL [3]
University of Minnesota Minneapolis Minnesota

ABSTRACT Odontocete radii are short flattened longer than the humeri and lacking in open medullary cavities Their cross section is essentially a semi stream lined wedge End-on articulation at the elbow is a synchondrosis In the streamlined amuscular antebrachium the radius sustains loadings predominantly in the medial lateral transverse plane as flipper movements (at the shoulder) counter body inertia and water resistance in controlling body attitude

This study treats secondary marine adaptation as reflected in radial development growth and mechanical organization Early osteogenesis is similar to that we reported for cetacean humeri and parallels conditions in the manatee Later differential growth is analyzed *in extenso* Geometry of growth is visualized radiographically in the relationship of endochondral to periosteal bone in the absence of medullary cavitation Furthermore the neonatal outline is distinguishable within the porous structure of (only) beluga radii so that pre and postnatal phases may be differentiated Radiographs and models demonstrate that as elongation occurs circumferential increments to growth cartilages are eccentric i e minimal anteriorly moderate medially and laterally and maximal posteriorly By this method the centers of epiphyseal cartilage plates migrate posteriad with time Periosteal depositions follow the same pattern and are deepest posteriorly Eccentric growth of the ulna is in the opposite sense Additionally proximal growth cartilages of radii tilt posteriad as the bone elongates Some alterations in growth occur at birth and later Eccentric growth is an adaptation by which anterior and posterior margins respectively of radius and ulna move apart as the bones elongate and by which functional cross-sections are maintained in ante brachial bones singly and as a pair

Bone is concentrated on medial and lateral sides of the radius This feature and porosity of the central region varies with species Radii like humeri thus mimic an engineered box beam and trabecular orientation resembles trajectorial distribution in a loaded beam

Radii have higher absolute densities than do humeri although both bones have the same range of mineralization as typical mammalian bones The beluga radius is half again as dense as that of the pilot whale and thus is intermediate in density between those of most odontocetes and that of the hypothyroid pachyostotic manatee The possible evolution of odontocete bones from a more dense dense form as well as the phylogenetic implications of density changes are discussed It is suggested that some of the characteristics of growth and structure including an apparent periodicity in structural density may be related to temperature and vascular supply in the high area low volume flipper in colder waters

> There is a certain large cla s of mor phological problems bound up with the general question of form and its de termination as a result of growth The phenomena are those where *adaptation* in the strictest sense is obvi ously present in the clearly demonstra ble form of mechanical fitne s for the exercise of some particular function or action which has become inseparable from the life and well being of the or ganism — (D A W *Thompson* 42)

This paper reports on some specific and unusual features of structure and development in the radii of two small cetaceans the beluga (*Delphinapterus leucas*) the small white whale of Arctic and Sub-Arctic waters (Vladykov 44) and the pilot whale (*Globicephala melaena*) the blackfish or pothead of the North Atlantic (Sergeant 62) The limb skeletons of the cetaceans like those of many other extant and ex tinct marine mammals reptiles and birds (Howell 30 Meister 62) are foreshort ened in their proximal segments have radical modifications of joints and the

[1] Supported by National Science Foundation grant G 13348

[2] Department of Anatomy School of Medicine Minneapolis Campus
[3] Department of Veterinary Surgery and Radiology College of Veterinary Medicine St Paul Campus

individual bones are lacking in medullary cavities In an investigation of cetacean osteogenesis bone structure and bone density (Felts 65 Felts and Spurrell 65) our interest has been in the manner and extent to which growth and development and the mechanical arrangement of bone tissue have been adapted to the conditions of the modified limb in the marine environment In the course of our study it was found that embryonic development postnatal growth and internal and external architecture of the small odontocete radius combine in such a striking illustration of adaptation that a separate report was warranted

The pectoral limb or flipper of the whales represents a very advanced adaptation of a primitive mammalian extremity to the marine environment (Howell 30 Slijper 62 Felts 65) This evolutionary process has encompassed function overall configuration musculature and tissue composition and bones and joints The flipper does not bear weight in the terrestrial sense rather this streamlined hydroplane is subjected to loads (predominantly perpendicular to the broad medial and lateral surfaces) imposed by body inertia and water resistance as it is employed in control of direction of movement and of body attitude Unlike the pectoral limbs of seals and sea lions cetacean flippers are only of incidental use in locomotion that function is carried out by the horizontally disposed tail flukes while the flattened caudal region acts as the prime rudder The flippers can be compared in external form and in function with the control surfaces of the contemporary submarine

Internal anatomy of the flipper is an interesting mixture of retention suppression and modification of the usual hard and soft tissue elements of the mammalian limb The shoulder complex is the only musculature retained in the limbs of all cetacean species and it is the only one in the flippers of the beluga and pilot whales The enarthroidal shoulder articulation is the only deliberately and freely movable joint in the limb The elbow at which the flat broad radius and ulna articulate end on with the humerus is a synchondrosis strongly reinforced by thick ligaments The wrist the carpals and the metacarpals beyond are related through nearly flat joint surfaces movements of which also are limited by ligaments most likely derived from tendons of the suppressed flexor and extensor muscles A very dense matted connective tissue surrounds the bones and ligaments in the amuscular portion of the limb and fills in the interdigital spaces and completes the streamlined form Over most of the limb the subcutaneous tissues are thin and firmly bind the subcutaneous layer to the deeper more dense connective tissues At the root of the flipper this layer becomes continuous with the thick blubber of the body

The skeleton contains the usual mammalian bones but with drastic modifications of proportions and articulations (fig 1) In addition the five digits in odontocetes (four in some mysticete or toothless species) possess more than the typical complement of phalanges (hyperphalangism Howell 30) The number of phalanges from thumb to fifth digit is 3 8 7 5 4 in the beluga and 4 15 10 3 and 2 in the pilot whale The manus together with the carpus comprises the larger portion of the free extremity The relatively short flat radius and ulna articulating edge to edge (through two facets) with each other and end on with the humerus lie in the basal portion of the free extremity while the line of the elbow joint is approximately at the body contour The humerus (Felts and Spurrell 65) also a short robust bone and relatively shorter than the radius and ulna is buried within the body in the shoulder musculature Major limb bones of cetaceans therefore are far more modified from the terrestrial antecedent than are the same bones in the amphibious seals and sea lions (Howell 30) and even the marine adapted manatee (Fawcett 42)

This summary of the anatomical and functional characteristics of the flipper should serve to define the conditions under which the radius exists and grows A discussion of the way in which the structure and development of the radius fit into the overall adaptation of the flipper will be found in the final section of this paper The scant literature dealing with the cetacean radius will be introduced and discussed where pertinent

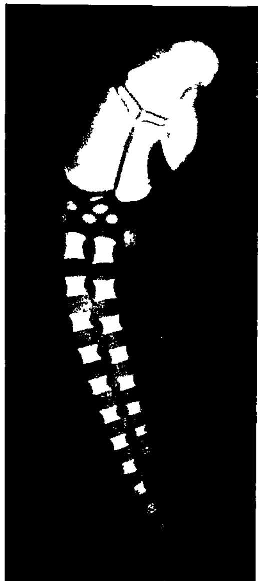


Fig 1 Rad ograph (do al or lateral view) of left flippe of yearling pilot whale Specimen was divested of marginal ti ue ithout d turbing bony or cartilagenou elements Contour of body diagonal acros elbo v is indicated by cuff of skin and blubber Distal econdary center of radius seen as two thin placode Other more distal centers are 4 carpals 5 metacarpals and (first to fifth digit) 2 11 8 2 and 0 phalanges Compare with description of appearance and fusion of primary and s condary centers on p 112 Exposure at 200 M S and 120 KV 1 3 natural size

MATERIALS AND METHODS

Most of the radii and fetal material used in this study were collected during field trips to small shore whaling operations in Canada At Churchill Manitoba on Hudson s Bay beluga are harpooned from powered canoes in the estuary of the Churchill River This form of hunting selects only the profitable larger animals which are processed in the adjacent plant for oil and as food for the fur industry In Trinity Bay Newfoundland entire pilot whale herds (numbering often in the hundreds of animals) are driven by catcher vessels into small bays and coves where they are slaughtered almost indiscriminately by teams of villagers in small boats The animals are processed at these villages and the blubber and meat are trucked to a central plant The conditions and aims of these whaling methods influence the availability of embryonic fetal and postnatal developmental series quite as much as the breeding periods of the animals themselves

Beluga material available for this study consisted of 12 embryos and fetuses (over half of these donated by Dr David E Sergeant Fisheries Research Board of Canada Montreal) irregularly distributed over the period of development of primary centers in humerus radius and ulna three circumnatal pectoral limbs and the flippers of 43 animals that were estimated to be between six months and more than four years of age The collection was limited in many respects but adequate for this report (as will be seen ossification progresses so slowly that no truly critical stage was missing) The pilot whale collection was more complete 28 fetuses (8 from D E Sergeant) and 8 flippers of late fetuses covering skeletal development from the pre-osseous stage to term and virtually a complete postnatal skeletal series

Information on early stages of ossification was obtained primarily from the pilot whale Comparison with available beluga material indicated no important species differences except in the timing of events Small specimens were fixed in the field in 10% neutral formalin In the laboratory flippers of one side were removed by transection of the shoulder capsule and then

were carefully divested of skin and placed in 5% KOH for clearing Addition of Alizarin Red S facilitated visualization of calcified cartilage and bone after these whole mounts had been run through glycerin series and stored in 100% glycerin These preparations then were compared with sections of the opposite flipper cut at 10–25 μ and stained with hemotoxylin and eosin

Flippers of older specimens were fixed by immersion in 10% neutral formalin or by perfusion or multiple hypodermic injections Often none of these alternatives was completely successful All late fetal neonatal and advanced postnatal flippers were radiographed to record limb anatomy and the state of the secondary centers Such radiographs generally were of less than satisfactory quality for detailed skeletal analysis due to fluid content of the tissues and secondary radiation by the fatty tissue component

Late fetal neonatal and older radii were dissected from the flippers mascerated in a temperature controlled hot water bath (96 C) cleaned and dried in an 80 oven Humeri (Felts and Spurrell 65) and ulnae were processed at the same time

Radiographs used in this presentation were made with a diagnostic Westinghouse 125 KVP 200 Ma machine utilizing a Machlett Super Dynamax rotating tungsten anode tube with a 1 mm focal spot Specimen tube distance was 250 cm The film used was Eastman Industrial Type M in no screen holders and with an aluminum foil filter between subject and cassette The KV and MaS values for illustrated sections are given (together with section thickness where appropriate) in the figure legends

For gross radiographs sections were cut on a Do All bandsaw with the specimens mounted on wooden blocks with Plastic Wood to insure proper orientation Before radiography the sawed sections were washed and cleaned further in an ultrasonic bath then were dried under weights to prevent warping In figures 7 and 8 section thickness was 5 mm in figure 9 3 mm

Microradiographs were made after band sawed sections had been reduced further in thickness on a Buehler metallurgical grinding wheel As grinding progressed test microradiographs were made to determine whether maximum optimum thickness was being approached In this way a compromise was made between retention of total section integrity and the attainment of the best possible resolution of microstructure In figure 13 the whole section microradiograph is of a 0 75 mm section while the enlarged microradiographs of regions of such a section were made from one ground to just over 100 μ

Microradiographic exposures were made on Eastman High Resolution plates with a locally produced apparatus employing a Machlett Type A 2 chromium target thin window x ray tube The tube was energized just above the voltage at which the copper absorber produced K characteristic radiation and the beam was filtered with a vanadium filter Sections were placed directly on the film and no vacuum was used in the column between x ray tube and plate Target film distance was 25 cm The relatively thick whole section radiograph in figure 13 serves to illustrate the orientation of the companion views and was made with an exposure of 480 minutes The remaining microradiographs in that figure are photographic enlargements of the thinner whole section exposed for 300 minutes

OBSERVATIONS AND DISCUSSION

Observations to be presented here concern the external anatomy of radii of adult beluga and pilot whales microscopic and macroscopic aspects of early development and radiographic anatomy of intact bones and of longitudinal and transverse sections This is accompanied by an analysis of differential growth in the odontocete radius (carried out with the aid of a series of models representing endochondral and periosteal bone relationships during growth) and by an examination of structural orientation and density

External anatomy of beluga and pilot whale radii

As befits its limited functional range and its position within the amuscular portion of the streamlined flipper (fig 1) the adult odontocete radius has a relatively uncomplicated form (figs 2 and 3) Certain of the gross features of mature beluga and pilot whale radii are described here to

establish essential morphology as an aid to understanding development and growth and to facilitate the interpretation of sections and radiographs Although each species has its characteristic proportions and slight differences in shape the radii of other small odontocetes e g the narwhal (*Monodon monoceros*) bottlenose dolphin (*Tursiops truncatus*) and common dolphin (*Delphinus delphis*) generally fall within the following description

The radius has broad medial and lateral surfaces a narrow posterior surface a thin anterior margin and proximal and distal surfaces largely occupied by articular facets (Due to the mean angular position of the flipper the lateral surface actually is dorsolateral in orientation) In the anterior posterior plane the radius is broadest just proximal to the distal surface and is narrowest across the proximal end (fig 2) In both pilot whale and beluga radii and especially in adult specimens from the beluga the distal portions of the anterior and posterior margins tend to be expanded or flared out from the rather straight proximal contour In the medial lateral plane the greatest thickness is at the margin of the proximal surface (fig 3) from there thickness decreases abruptly to the medial and lateral surfaces and then increases toward the distal end of the bone In typical cross section (figs 3 and 9) the radius approximates a semi streamlined wedge From thin anterior margin to flat posterior surface the pilot whale has essentially the same convexity across the medial and lateral surfaces The beluga radius however is flat to slightly concave on the lateral side and curved like that of the pilot whale on the medial side of the cross section The anterior margin (leading edge) of the radius comes to a thinner nearly sharp edge in the pilot whale radius the edge of the beluga radius is more rounded In the medial lateral plane the posterior surfaces of both beluga and pilot whale radii are flat to slightly concave (figs 3 and 8) (The ulna is flat on its anterior surface and rounded on the posterior To gether radius and ulna form an incompletely streamlined core for the streamlined antebrachium the trailing edge of which is completed by skin subcutaneous blubber and dense matted fibrous connective tissue)

The proximal and distal surfaces of beluga and pilot whale radii are quite similar (fig 2) In the anterior posterior plane the profile of the proximal surface slopes posterodistally more so in the pilot whale than in the beluga The anterior posterior profile of the distal surface consists of two segments meeting at a low angle This angle is approximately the same in the radii of both species but in the pilot whale the entire surface is inclined posteriorly this feature is reflected in the caudad deflection of the wrist in the pilot whale In superior view (fig 3) the proximal (radiohumeral) articular facet is alike in the two species It is half an oval slightly convex anteriorly and strongly convex posteriorly In neither form does the facet cover the entire proximal surface of the bone but in each it is continuous onto the posterior surface as the hemicircular superior radioulnar facet In end-on view the inferior surface and its articular facets are co-extensive In the beluga both facets are flat to slightly concave in the medial lateral plane In the pilot whale the anterior facet is slightly concave and the posterior facet strongly so In each the inferior radioulnar facet is hardly distinguishable at the edge of the posterior articular facet

Despite the appearance of a large nutrient vascular channel in lateral radiographs of the radius (fig 6) no corresponding aperture is found on the narrow posterior surface of the adult bone Over the medial and lateral surfaces there are a large number of small openings (fig 2) Those in the distal region of these surfaces are directed inward and proximad at a low angle to the surface In the proximal region of the medial and lateral surfaces the channels are inclined distad at a higher angle Near the posterior margins of these surfaces and on the posterior surface itself the vessel channels are directed anteriorly It will be seen later that the orientation of these channels as they enter the surface correlates with the differential growth of the radius as a whole On proximal and distal surfaces (fig 3) the vascular apertures are numerous throughout development with maturity these decrease in number and size

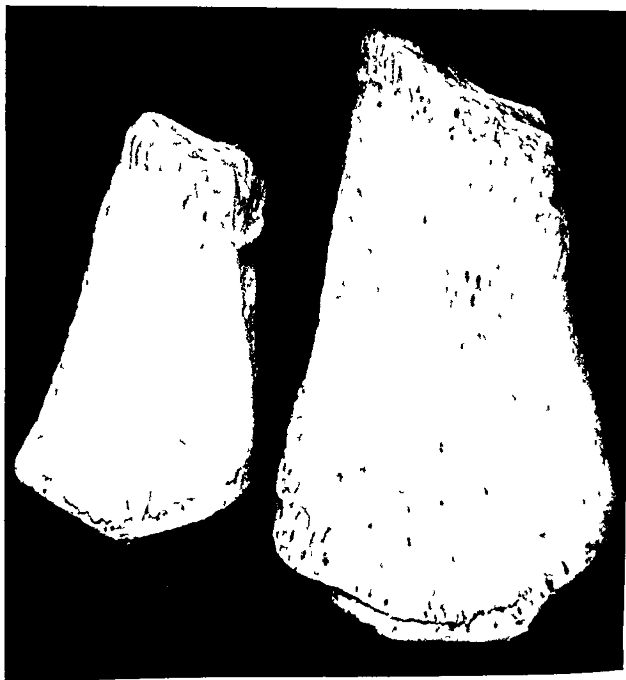


Fig 2 Radii of young adult beluga (left) and pilot whale in lateral view Anterior margins to left inferior margin down Proximal secondary centers fused in both bones distal center completely fused in beluga bone but fused only in posterior region in pilot whale specimen Described on p 107 × 4/5 natural size

Early development of the radius

The essential features of early development are shown in an anterior posterior longitudinal section of the antebrachium of the fetal pilot whale in figure 4 There are several striking departures from the histogenesis of cartilage and bone as observed in more typical mammals (e g the humerus of man Streeter 49) There are no significant differences in the early development of the radius and the humerus of the pilot whale (Felts and Spurrell 65) and a strong parallel to these bones can be found in the limb skeleton of the fetal manatee (Fawcett 12)

Streeter (49) has described the gradient of chondrocyte maturation in the pre osse

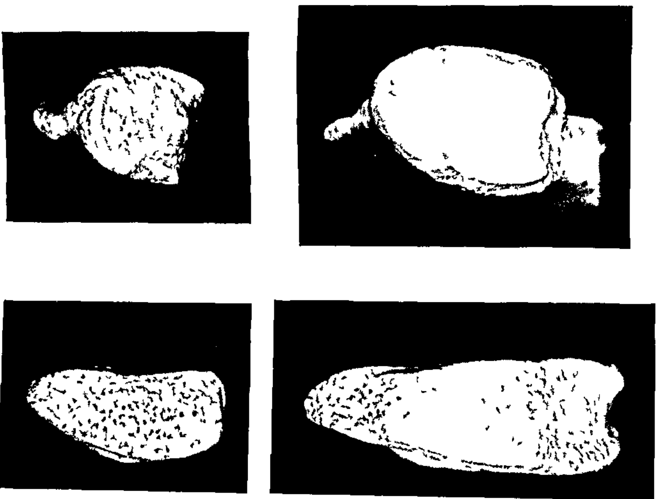


Fig 3 Superior (upper row) and inferior views of beluga (left) and pilot whale radii Lateral surfaces are down in superior views and up in inferior views Anterior margins to left Described on p 107 × 4/5 natural size

ous cartilage model and in the proximal and distal cartilage masses of the ossifying humerus of man His designation of zones may be paraphrased in simpler form for contrast with conditions in the cetacean In the humerus at the time of formation of the perichondral osseous sheath the epiphyses and adjacent portions of the metaphyses consist of small rounded cells in an ample matrix In the metaphyseal diaphyseal region cells are flattened in the transverse plane due to polarized mitosis and to pressure Extending from these cells onward to the middle of the diaphysis is a series of progressively more hypertrophic and vacuolated cells terminating in the central diaphyseal mass of degenerate cells Prior to ossification the sparse matrix of the degenerate region becomes calcified The perichondral osseous sheath is deposited superficial to the calcified cartilage and overlaps a small portion of the hypertrophic cell region With the advent of endochondral ossification the accumulated degenerate cells and thin matrix septa are removed and thereafter only a few degenerate cells are found at the end of the chondrocyte gradient The gradient soon is characterized by more distinctly arranged longitudinal cell rows having isogenous nests in the zone of flattened cells (Lacroix 51) and separated from adjacent rows by a substantial wall of intercellular matrix (Ham 32)

Our rather small series of embryonic and fetal radii of both species reveals clearly enough that the cetacean does not have all the zones of cellular maturation found in the humerus of man The entire central region of the flattened cartilage model (fig 5) consists of degenerate and hypertrophic cells Beyond this mass there is a deep zone of irregular isogenous nests interspersed here and there by rather large islands of matrix Without an intervening region of flattened cells this zone fades off into the small rounded cells in the enlarged ends of the model This pattern is retained through fetal (fig 4) and postnatal development rather than becoming more organized and linear With the onset of endochondral ossification and the erosion of the accumulated degenerate cells many large and small irregular islands of acellular calcified cartilage remain and are covered with a shell of bone In addition the absense of even the most simple form of linear arrangement of cartilage cells against the ossification front results in the isolation of a large number of bone encased cartilage remnants of varying size lying between irregular and generally meandering invasions of primitive vascular connective tissue Nearly all this primary spongiosa eventually is resorbed and replaced in the process of internal reorganization and no open medullary cavity forms in the radius In time as we will describe and discuss in a later section this mode of endochondral ossification gives rise to flattened proximal and distal cones of relatively very porous bone while marrow of a light fibrous and vascular type lacking in hematopoietic elements is restricted to the intra osseous channels Throughout this paper this mass of bone will be referred to as *endochondral bone* and that which covers it as *periosteal bone* These convenient terms acknowledging the mode of origin do not of course denote a difference in the bone substance *per se* nor do they imply an indefinite retention of bone laid down in the fetus

In cleared whole mounts the first evidence of periosteal ossification is an array of flattened trabeculae on the posterior margin of the calcified central region of the cartilage model (fig 5) (The calcified masses of cartilage are revealed so intensely in alizarin stained limb preparations and exist for so long a period before either perichondral or endochondral ossification that only histological sections of the opposite limb can demonstrate that they are not deep centers of ossification) Perichondral ossification progresses anteriad until a complete sheath of coarse trabeculae has formed increasing in length concurrently with elongation of the model and of the calcified region In typical mammalian limb bones (Streeter 49) cessation of growth in the degenerate central diaphysis and continuing growth in the younger cartilage proximal and distal to it results in a mid diaphyseal constriction that remains until periosteal ossification has produced a more robust shaft In the cartilage of cetacean radii and humeri as well this constriction is very pronounced but it is filled in rapidly by a deep deposit



Fig 4 Low power (× 8) of anterior posterior longitudinal section through radius and ulna of 165 mm (snout tail notch) fetal pilot whale Note union at elbow and proximal radio-ulnar articulations lack of regular cell rows in cartilage deep irregular ossification front large irregular endochondral spicules in light fibrous marrow deep periosteal deposit Anterior margin to left See p 110

of trabeculae that in section (fig 4) is easily distinguishable from the endochondral spicules central to it

The fetal radius has the same general form as the adult bone an incomplete oval in cross section and in the anterior posterior plane ossification however dimensions of the two ends are more alike than in the adult radius When first formed the proximal and distal endochondral cones (fig 5) are more alike than in the postnatal radius (fig 6) and periosteal bone is nearly as deep on the anterior as on the posterior side In the stage represented by the last drawing in figure 5 however there are initial indications of the growth pattern that will dominate the history of the radius i e a longer distal than proximal endochondral cone as measured from the conjunction of the cones a posterior in

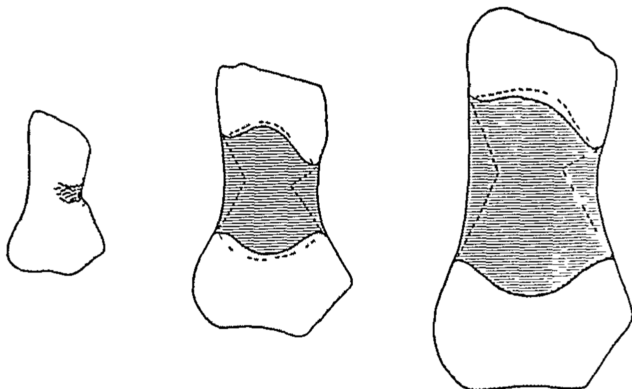


Fig 5 Schematic representation of progress of ossification in fetal pilot whale radii as seen in cleared specimens under transmitted light *Left* Stage immediately preceeding endochondral ossification Transverse dashed lines (here and in other two views) delimit zone of cellular hypertrophy Thick lines represent incipient periosteal ossification *Middle* Same state as in photomicrograph in figure 4 Horizontally lined region represents periosteal bone Dashed lines within that region show division between periosteal and endochondral bone *Right* Radius of a 200 mm fetus Same coding as in middle view Discussion on p 110 × 4 natural size

clination of the proximal chondro osseous junction and higher angles of endochondral to periosteal bone (and thus deeper periosteal bone) on the posterior side of the radius It will be noted that the angles of the sides of the endochondral cones actually are higher in the fetal specimens in figure 5 than in the postnatal radii in figures 6, 7 and 8 This feature is an indication of the early dominance of transverse growth over longitudinal growth in cartilage As will be seen in the radiographic anatomy of postnatal bones the ratio of transverse to longitudinal growth soon is reduced slightly but remains high throughout development The structure of the early fetal stages is in a manner of speaking lost in the relatively coarse texture of bone at the intersection of the endochondral and periosteal moieties of the older radius

The maturation of radial ossification centers is part of a total pattern that with some exceptions strongly parallels that found in the typical mammalian limb skeleton (Patten 53) Precise dating is impossible in the absence of requisite age/size/ossification data on the small odontocetes The primary center of the humerus apparently is the first to appear as part of a general proximal distal gradient extending out through the long series of phalanges The time differential between this center and the radial and ulnar primary centers however is very slight All three are present far back in the fetal period and there is a long time lag between these three and their secondary centers The sequence of *appearance* of secondary centers is proximal humeral distal humeral proximal radial and ulnar (nearly coincidental with the distal humeral) and after a long period the distal radial and ulnar The position of the distal radial and ulnar centers at the end of this sequence is a departure from the typical mammalian pattern i e they might be expected to appear before the elbow centers

The sequence of *fusion* of secondary to primary centers is distal humeral proximal radial and ulnar (the humeral only slightly earlier than the latter two) proximal humeral and distal radial and ulnar Thus the cetacean elbow centers are the first to fuse as in mammals in general The time lag between fusion of the proximal humeral center and those at the distal end of the radius and ulna however is a very considerable one in the odontocetes while it is very short in man The proximal humeral center fuses at about one year in the pilot whale and beluga and the distal radial center usually is incompletely fused even in old animals Tardiness of appearance of the distal centers does not mean that the distal antebrachial growth cartilages do not contribute the most to longitudinal growth of the radius and ulna lateness of their fusion early fusion at the elbow and the internal geometry of the radius establish that they do so

Radiographic anatomy

External configuration and internal structure of postnatal radii are such as to require a multiple radiographic approach Intact bones are shown in lateral views in figure 6 In figures 7 and 8 pilot whale and beluga radii respectively are represented by longitudinal sections cut in anterior posterior and medial lateral planes together with interpretative line drawings In figure 9 radiographs of selected transverse sections of both radii are displayed Contact microradiographs of transverse sections are shown in figure 13

Lateral radiographs of intact bones (fig 6) demonstrate absence of an open medullary cavity lack of a true compacta and retention of the fetal disposition of bone of endochondral and periosteal origins Intact adult pilot whale radii are very poor radiographic subjects only by comparison with section radiographs (fig 7) can the presence of a thin rather uniform cortical layer be verified There is extremely low contrast in radio-opacity between the geometrically delimited regions of the spongy interior Beluga radii with a similar geometric format have a higher overall radio-opacity and greater regional contrasts in radio-opacity (figs 6 and 8) In young and mature radii of both species a strong comparison can be made with the distribution of bone in fetal radii (figs 4 and 5) Flattened proximal and distal endochondral cones of differing lengths and sides have their bases on the epiphyseal plates (or lines of epiphyseal fusion) and are continuous at their apices The only visible space other than the intertrabecular labyrinth is a large vascular channel intersecting the apices of the endochondral cones In lateral views periosteal bone is most obvious posterior to the endochondral cones The masking effect of the medial and lateral sides of the radius and the radiographic artifacts introduced by its cross sectional shape limit visualization of many other details of internal structure and density

Anterior posterior and medial lateral longitudinal sections (figs 7 and 8) reveal more details of structural density of the distribution of endochondral and periosteal bone and of the anatomical evidence of differential growth than do lateral radiographs of intact bones The less complicated *pilot whale* sections will be examined first the complexities of equivalent sections of beluga radii are best approached from such a background In anterior posterior longitudinal sections (fig 7A) the the edochondral cones of the intact bone (fig 6) appear as proximal and distal triangles the bases of which are coextensive with the respective epiphyseal lines The sinuous proximal epiphyseal line is inclined posteriorly the distal epiphyseal line is symmetrically curved and nearly is bisected by the long axis of the radius The apical conjunction of the triangles is located approximately 32% of section width posterior to its anterior margin and about 31% of the distance along a line from the proximal to the distal epiphyseal line This conjunction is intersected by the large transverse vascular channel Extending from this eccentric fixed point to the distal epiphyseal line (fig 7C X to Dp to Dp′) the posterior side of the long distal endochondral triange has an angle of 40 to the long axis of the radius for approximately 84% of its length (to Dp) To an extent varying with individual specimens this line is curved posteriad in the remainder of its length (to Dp) The ante

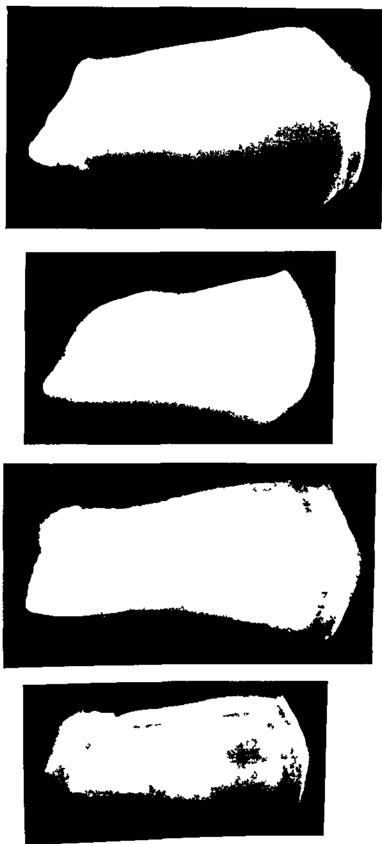


Fig 6 Lateral radiographs of yearling and adult beluga (two at left) and pilot whale radii Anterior margins to left Size relationship of beluga bones is natural one relative sizes of pilot whale bones somewhat distorted by reproducing both fetal and both adult bones at same heights The small incomplete distal secondary centers are omitted In young pilot whale specimen proximal center was lost in preparation Compare internal structure with figures 7 and 8 Exposures at 500 and 700 MaS (for pilot whale and beluga respectively) and 120 KV

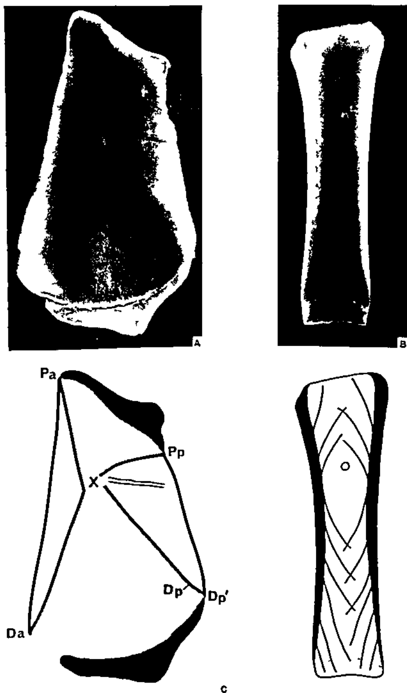


Fig 7 Rad ogr phs and interpretative line drawings of 5 mm thick anterior posterior (at left) and m dial lateral longitudinal sections of radu of the adult pilot whale Both from same animal M 1 section intersects a p plane through apex of periosteal bone triangle posterior to point X Angular relationships of endochondral and periosteal bone shown at lower left and de cribed on p 113 Abbreviations explained in text Line drawing at lower right represents mechanical organization in m 1 plane and is described and discussed on p 127 Expo ure at 350 MaS and 120 KV 2/5 natural size

rior side of the same triangle (X to Da) is essentially straight with an angle of approximately 20° for most of its length, in some specimens one can barely visualize a slight anteriad curve near its end The shorter proximal endochondral cone is curved on its posterior margin (X to Pp), and straight along its anterior side (X to Pa) with an angle of about 10° Asymmetrical triangles of periosteal bone complete the outline of the section the posterior triangle being deep and the anterior shallow Low contrast in radiographic and structural density between endochondral and periosteal components in pilot whale sections makes total visual separation difficult in many specimens The same will be found true for the anterior periosteal triangle in the beluga radius

Lateral radiographs (fig 6) and anterior posterior longitudinal sections (fig 7A) of young adult and adult *pilot whale* radii display a relatively low radio opacity within as well as a low contrast between endochondral and periosteal components Medial lateral longitudinal sections (fig 7B) and transverse sections (fig 9) however show that the medial and lateral sides of the radius consist of more dense bone These relatively thin layers of lower porosity act as a uniform screen in lateral radiographs and of course are absent in the anterior posterior longitudinal sections It cannot readily be determined in adult radii how much of the finely trabeculated bone deep to these surfaces is also of periosteal origin but in the very young pilot whale the distinction between components is as clear as in equivalent sections from the beluga Furthermore the periosteal triangles in radii from newborn and immature pilot whales are noticeably more radio opaque than in older specimens (figs 1 and 6)

Internal anatomy of *beluga* radii differs from that of pilot whale radii primarily in the degree and distribution of bone density In anterior posterior longitudinal section (fig 8A) the distal endochondral triangle again is the longer and larger and the orientation of epiphyseal lines is essentially the same as in pilot whale radii The apical conjunction of the triangles is located further anterior (24% of section width in from the anterior margin) but approximately the same distance from the proximal epiphyseal line (33%) as in the pilot whale Greater radiographic contrast between periosteal and endochondral bone permits better resolution of the junction between them except for the anterior periosteal triangle Only in radii of advanced age in which the entire bone becomes more radio opaque, does this resolution fade With the more anterior position of the fixed point far less periosteal bone is on the anterior side of the section and relatively more on the posterior side than in the pilot whale radius

In both lateral radiographs (fig 6) and those of anterior posterior longitudinal sections (figs 8A and 8C) the *beluga* radius presents a secondary pattern of contrasts in structural and radiographic density that is absent in the pilot whale radius Central in this is the outline of the neonatal radius a fact confirmed by comparison with the profile of the actual bone at birth (i e the primary center only at that stage) The anterior margin of this outline is located very close to that of the intact bone its proximal end is closer to the proximal epiphyseal line than its distal end is to the distal epiphyseal line Within its confines regions of periosteal and endochondral origin are quite homogeneous The posterior periosteal triangle is sharply distinguished from the endochondral regions although its radiodensity is not quite as great as that of periosteal bone of postnatal origin Beyond the neonatal outline, both components especially the periosteal display periodic or alternating zones of higher and lower density (The neonatal outline is identifiable in early postnatal pilot whale radii thereafter the outline fades into the texture of the rest of the radius see fig 6)

The retained neonatal outline and the alternations in density provide further information on the relationship between endochondral and periosteal bone Actually radiographs of young adult and older radii yield the same visual effect as the superimposition of tracings from several younger bones of increasing order of age and size In such radiographs (figs 8A and 8C) a line from X to *Dp* at the posterodistal corner of the neonatal outline is essentially straight (at approximately

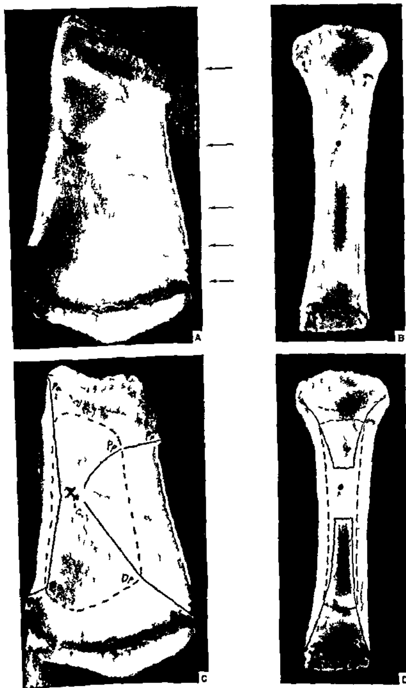


Fig 8 Radiographs and interpretative line drawings of 5 mm thick anterior posterior (at left) and medial lateral longitudinal sections of radii of adult beluga Both from same animal M l se t on intersects a p plane through apex of periosteal triangle posterior to point X Relat n h ps of periosteal and endochondral bone as delimited at lower left and right are desc b d and discussed on p 116 Abbreviations explained in text Exposure at 500 MaS and 90 KV × 3/5 natural size (Arrows indicate levels of transverse sections shown in figur 9

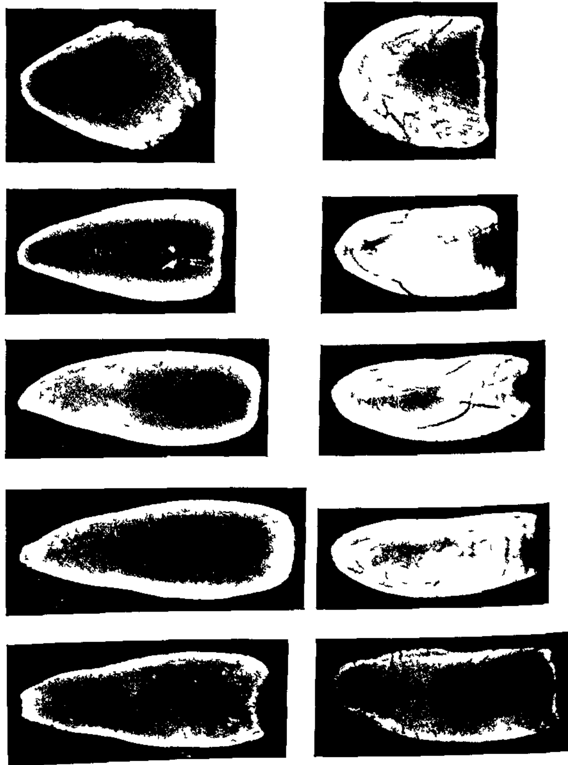


Fig 9 Radiographs of 3 mm transverse sections of beluga (right) and pilot whale radii From proximal at top to distal at bottom levels are or are equivalent to those indicated by arrows in figure 8A Anterior margin left and lateral surface up Exposure at 250 and 350 MaS (for pilot whale and beluga respectively) and 120 KV

29 to the radial axis) A line from Dp to Dp outside the neonatal outline and ending at the posterodistal corner of the primary center is straight or nearly so but has a higher angle (about 51) than the line from X to Dp At the opposite end of the section a line from X to Pp at the posteroproximal corner of the neonatal outline is a consistent curve flattening out near its termination Outs de the neonatal outline the line from Pp to Pp is essentially straight and nearly horizontal In most radiographs the line from X to Pa to Pa is straight The line from X to Da is most difficult to visualize although it usually is straight however the very short line from Da to Da outside the neonatal outline is most sharply deflected having an angle of 40 to 60 over a large series of radiographs

Radiographs of medial lateral longitudinal sections (fig 8) reveal that as in the pilot whale the medial and lateral surfaces of the *beluga* radius consist of less porous bone (having higher regional radio-opacity) than does most of the central region In the beluga however these slabs of near compacta are relatively and absolutely thicker and are of approximately the same radiodensity as the parts of the posterior periosteal triangle (fig 8A) laid down after birth All gross and microscopic evidence indicates that the medial and lateral dense masses (as delimited in fig 8D) are periosteal bone and that the less dense bone central to them is of endochondral origin

In transverse sections of the *beluga* radius (figs 9 and 13) the neonatal outline and the geometry of periosteal and endochondral bone are most evident The neonatal radius is distinguished by a very porous endochondral component and by the larger pores along the line of junction of its periosteal component with the postnatal bone immediately adjacent to it (fig 13) In the most proximal and distal levels of the adult radius beyond the neonatal mass endochondral bone of relatively fine uniform texture occupies virtually the entire section and the more dense periosteal bone is restric d to a mere surface layer (fig 9) At l els progressively closer to the fixed poin (X) periosteal bone of pre and postnat rigin comprises relatively more of the tion and endochondral bone (of prenatal origin) is limited to small areas of anterocentral position Periosteal bone in the adult radius thus is thinnest around the anterior margin progressively thicker posteriad along medial and lateral sides and is thickest on the posterior side of all but the most proximal and distal levels The extreme condition of course exists in midlength of the primary center

In gross radiographs of *beluga* transverse sections periosteal bone appears to be stratified due to alternations in pore size rather than in mineralization (figs 9 and 13) The innermost line of larger pores lies immediately external to the neonatal radius (figs 8A 8B 9 13A and 13F) The remaining irregular lines of larger and smaller pores can be traced entirely around some sections lying closer together where the periosteal bone layer is thin and further apart where it is thick The greatest regional porosity is posterior on all sections (fig 13E) These lines of pores correspond to the vertical striations in longitudinal sections (compare with figs 8A and 8B) The concentration of large pores (fig 13A) or longitudinal channels (depending on the section viewed) partially accounts for the low regional radio-opacity and poor resolution of the anterior periosteal bone in figures 7 and 8A Beyond the ends of the neonatal radius there are several transverse zones of more open structure (lower regional radio-opacity) in the endochondral bone roughly corresponding to the larger pores or longitudinal channels in the periosteal bone (figs 8A 8B 13A 13E and 13F)

In the course of this investigation radii of some other odontocete species were examined by lateral radiographs The radius of the narwhal (the other specifically Arctic odontocete) is a very close parallel of the beluga radius in density and internal geometry while radii of the common and bottlenose dolphins have essentially the same internal characteristics as that of the pilot whale

Differential growth

Information presented thus far has established several important ontogenetic and structural distinctions between odontocete radii and those of terrestrial mammals Growth of the odontocete radius is

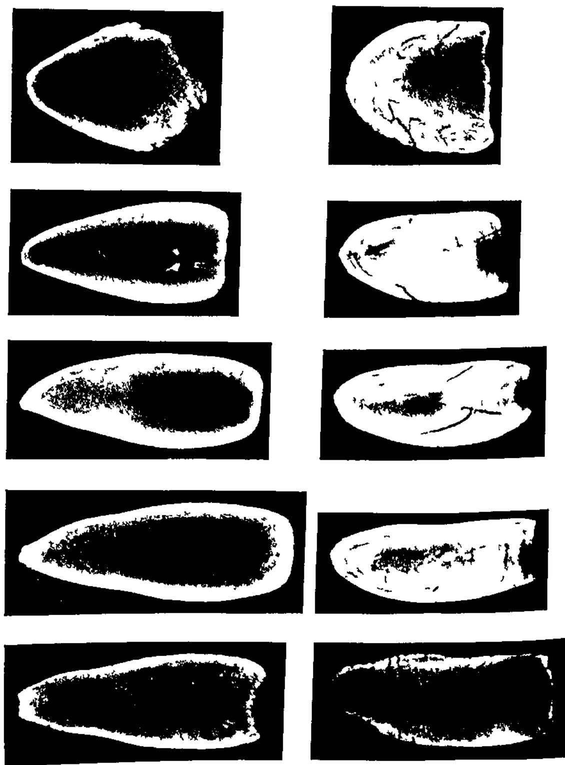


Fig 9 Radiographs of 3 mm transverse sections of beluga (right) and pilot whale radii From proximal at top to distal at bottom levels are or are equivalent to those indicated by arrows in figure 8A Anterior margin left and lateral surface up Exposure at 250 and 350 MaS (for pilot whale and beluga respectively) and 120 KV

Fig 10 Models depicting differential growth in idealized cylindrical limb bones in which endochondral bone produced in wake of epiphyseal growth cartilages is not resorbed See p 120 for description

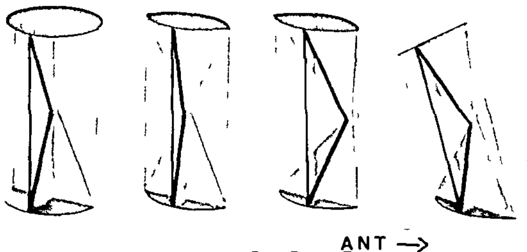


Fig 11 Models depicting differential growth in idealized limb bones having elliptical cross-section in which endochondral bone is not resorbed See p 120 for description

not accompanied by the creation and enlargement of a marrow cavity (figs 4, 5 6 and 9) Thus indications of the chronicle of depositions and of spatial relationships of periosteal and endochondral bone are retained in the substance of mature radii (figs 7 and 8) In typical mammalian long bones contrariwise the process of cavitation involves removal of endochondral spicules formed in the wake of migrating (separating) epiphyseal cartilage plates as well as the resorption of the inner surface of the periosteal bone of the shaft (Enlow 62) In the cetacean radius the lack of cavitation allows the outlines of neonatal and immature radii to be oriented knowledgably within the contour of adult radii and against the retained geometry of periosteal and endochondral bone depositions (figs 7 and 8) In the typical mammalian situation conversely the appropriate relationships between over all length diaphysial length and diameter and size and shape of the metaphysis and epiphysis are maintained by constant remodelling (Felts 54 Enlow 62) Consequently the position of the younger bone eventually is pre-empted by the medullary cavity of the older bone and above the microscopic level only the most immediate history of periosteal and endochondral bone is evident

A concept of the significance of temporal and spatial relationships of endochondral and periosteal bone in the growing cetacean radius (as revealed by figs 4 through 9) can be developed from the sequence of models in figures 10 11 and 12 The construction of these simple models presupposes the absence of internal cavitation and the lack of external remodelling and for simplicity it ignores the formation of secondary centers Figure 10 introduces the model sequence and develops the concept of endochondral periosteal bone relationships as a function of ratios of transverse to longitudinal growth in epiphyseal cartilage plates in the presupposed circumstances Figure 11 depicts individual growth processes that will be shown to operate in cetacean radii Figure 12 illustrates how these processes are implicated specifically in radial growth Endochondral bone is represented by proximal (upper) and distal (lower) intersecting triangles marking perpendicular central planes along the length of endochondral cones Discs or ellipsoids (depending on the model) indicate the final position of epiphyseal cartilage plates former areas and dimensions of which would be those of transverse sections anywhere along the endochondral cones Epiphyseal cartilage growth plates increase in diameter by the proliferation and differentiation of additional cells on their peripheries and contribute to longitudinal growth of the bone by proliferation of cells in their reserve zones as rapidly as on the opposite face of the plate degenerate terminal cells are removed and bone is deposited on matrix remnants Apical conjunction of the cones represents the starting point for growth and development i e the center of initial endochondral ossification deep to the perichondral osseous sheath in the embryonic cartilage model (present examples the center of the erosion cavity in fig 4 and X in figs 7 and 8) Longitudinal wires indicate the surface of the periosteal bone deposited about the endochondral cones It is presumed in these models that periosteal bone extends in depth from the wires to the wooden triangles representing the endochondral cones

The *first three models* in figure 10 depict the result of identical transverse (appositional) growth rates and differing rates of longitudinal (interstitial) growth in the epiphyseal cartilage plates over equal periods of time Final ratios of breadth to length are 1 6 1 4 and 1 2 respectively Angles of the sides of endochondral cones vary with ratios of fixed transverse to differing longitudinal growth rates in the epiphyseal cartilage plates Indeed they constitute regression lines of differential growth Periosteal bone depositions unresorbed from the interior and unremodelled from the exterior form cylinders of differing proportions with symmetrical lumina occupied by endochondral bone The relative amounts of periosteal and endochondral bone in any cross section depend on the level of the section but the depth of periosteal bone is uniform on all sides of a given section

The *fourth and fifth models* in figure 10 illustrate variations on the second 1 4 model in the series In the previous models

The *fourth model* in figure 11 depicts another process by which posterior movement of the centers of epiphyseal cartilage plates and of endochondral cones may occur during elongation of a bone In this case the lines of migration or separation of the epiphyseal plates from the embryonic starting point are not aligned with the longitudinal axis of the bone but are inclined or canted posteriorly The individual endochondral cones are symmetrical but the anterior sides of the two cones as in the previous model are nearly in a straight line while the posterior sides are almost perpendicular to each other (The model could be viewed with the wires vertical showing both ends canted or with the one epiphyseal plate horizontal and the wires tilted as in the figure) Periosteal bone therefore is deeper on the posterior than on the anterior side and it is of intermediate depth on medial and lateral sides Except for the canted ends which might be obscured or compensated for by the shape of the missing secondary centers this model has the same external form as the previous one

Differential growth in odontocete radii can be analyzed with reference to the several models just discussed General proportions of beluga and pilot whale radii fit well within those of the short broad types in figure 10 (third model) and figure 11 (all models) In lateral view the flattened endochondral cones (other features of their geometry ignored for the moment) are wide at their bases relative to their lengths (compare with figs 6 7 and 8) while those of the more slender models might be associated with the general proportions of more typical mammal bones Differences in proximal and distal proportions and internal geometry suggest partial comparison with the fourth and fifth models in figure 10 and of course comparison with the canted and eccentric models in figure 11 is immediate However simple direct comparisons between the entire cetacean radius and any one model *in toto* are misleading and inadequate This is true because of three facts (1) growth at the proximal end of the radius is neither as rapid nor of as long duration as at the distal end (2) there are differences in morphology between embryonic and adult radii neither of which are as simple in form as the models and (3) each model depicts but one or two processes while growth of the radius involves a number of interrelated processes

In the previous models growth was depicted as being of equal duration at the two ends with geometry dependent only on the ratios of transverse to longitudinal growth rates during fixed periods of time In the radius however the distal endochondral cone continues to lengthen and become wider at its base after the proximal line is closed Further the rate of longitudinal growth is higher in the distal epiphyseal plate than in the proximal plate This is documented in the beluga radius (figs 6 and 8) where the quite sharp neonatal outline permits comparison of proximad and distad growth away from a known point during a finite interval The position of the fixed point in pilot whale radii also demonstrates unequal growth even though the lack of a neonatal outline rules out temporal comparison Measurements from the fixed point (pp 113 and 116) show that the distal epiphyseal plate is responsible for approximately 69% of radial (i e primary center) length in the pilot whale and 67% in the beluga In this respect growth of the odontocete radius is comparable to that of the typical mammalian radii (Lacroix 51)

A difference in overall configuration between embryonic and adult radii of both pilot whale and beluga indicates a differential growth process involving (1) the rate and extent of elongation at the two ends of the bone and (2) the mechanisms of transverse growth depicted in the last three models in figure 11 and combined in a model of a composite odontocete radius in figure 12 In the early stages of ossification the pilot radius has proximal and distal ends that are far more alike than in the adult (figs 4 and 5 and p 111) Cross-sectional shape is an ellipse or oval with only a narrow flat area along the posterior margin The high ratio of transverse to longitudinal growth in the cartilages is such that the characteristic form of the endochondral cones is established almost at once (figs 4 and 5) From this morphologic beginning the distal portion of the radius grows in a manner suggested by the *third model* in figure 11 and it does so

it was assumed that the proximal and distal epiphyseal cartilage plates had the same rate of transverse growth and that with different rates in each example the matched plates migrated away from the embryonic center at equal velocities The fourth model depicts the result of a higher rate of longitudinal growth in one epiphyseal plate than in the other with a common transverse growth rate Compared with the second model the longitudinal growth rate in the proximal disc is lower (absolutely and relative to transverse growth) than in the distal The sum of the proximal and distal components in this instance equals the balanced growth represented by the second model Angles of the sides of the two endochondral cones vary with the ratios of transverse to longitudinal growth Externally the bones represented by the *second* and *fourth models* have identical shapes due to common epiphyseal diameters and to deposition of periosteal bone but the center of the second is filled with matched endochondral cones while that of the fourth is occupied by cones of dissimilar lengths and therefore, dissimilar angles of sides

The *fifth model* in figure 10 portrays the results of equal longitudinal growth but unequal transverse growth at the two ends of the bone The longitudinal growth rate is the same as in the second model and equal to the sum of the proximal and distal components in the fourth model The rate of transverse growth in the distal epiphyseal cartilage plate is the same as that at either end of previous models but across the proximal plate the rate is far lower Consequently the angles of proximal and distal cones differ although their lengths are the same Concurrent deposition of periosteal bone in the space around the lengthening unmatched endochondral cones completes the external form of a truncated cone Although this model assumes a difference in rates of transverse growth at the two ends of the bone the same proportions and form would result were the embryonic cartilage model of asymmetrical form (e g tapered like the definitive bone) and the inherent growth rates across the two plates identical

Transverse growth (i e addition of new cells on the periphery) thus far has been presumed to be uniform about the circumference of the epiphyseal cartilage plates In figure 11 this still is true of the *first model* The *second model* however illustrates the consequence of either a higher transverse growth rate in one axis of the plate (the anterior posterior) than in the other or uniform growth of the plate beginning with an embryonic model of ellipsoidal cross section In the first case the endochondral cones would become progressively ellipsoidal along their lengths In the second case (as in the model) the endochondral cones would have an ellipsoidal cross section at any level In either alternative the surrounding periosteal deposition produces a configuration having the same length and the same anterior posterior diameter as the first model but with a lesser medial lateral diameter At any level more periosteal bone would be found in the anterior posterior plane than in the medial lateral plane about the flattened cones

The *third model* in figure 11 depicts an alternative mechanism in maintaining an oval or ellipsoidal cross section during growth The previous model suggested symmetrical growth with uniform *concentric* increments about elliptical epiphyseal plates The third model demonstrates *eccentric* transverse growth a low rate of appositional growth on the anterior margin of the epiphyseal plates a progressive increase in rate along the medial and lateral margins and a high rate on the posterior margin eccentrically increase plate area In this circumstance the centers of the epiphyseal plates and the intersections of the major planes through the endochondral cones would migrate posteriorly as the bone elongates Periosteal bone deposition about this configuration results in an external form identical to that in the last model In cross sections however more periosteal bone would be found posterior to the asymmetric endochondral cones than on their medial and lateral sides and by far the least periosteal bone would be found on the anterior margin of the section Eccentric transverse growth and its consequences could occur of course in a structure having a circular or any other form of cross section

of growth in the proximal end of the radius eccentric growth of the cartilage plate probably is concurrent with canting Between birth and the time of epiphyseal closure however eccentric growth dominates During that interval the proximal cone in the beluga radius increases only about a seventh in length but approximately a third in the anterior posterior diameter of its base (fig 8)

In the medial lateral longitudinal plane of the beluga radius (figs 8B and D) the sides of the proximal endochondral cone appear curvilinear and are so depicted on (the lateral side of) the composite model in figure 12 On the basis of sections from younger radii rather than the mature bone in figure 8 the side of the distal endochondral cone in figure 12 is shown as straight in the equivalent of the prenatal period and slightly curved laterad in the postnatal period Thus the geometry of growth corresponds in anterior posterior and medial lateral planes

As represented by the third and fourth models in figure 11 and by the composite model in figure 12 the shallowest periosteal bone is on the anterior side of the radius and the deepest on the posterior side with an anterior posterior gradient of depth along the medial and lateral sides of the endochondral cones (figs 6 7 8 and 9) This distribution reflects a gradient in periosteal activity around the sides of the radius correlated with the eccentric growth and canting that progressively move the centers of the plates posteriad This differential in periosteal activity exists from a very early stage of development (i e beginning with the stages shown in figs 4 and 5) Throughout most of development bone of periosteal origin has a distribution approximating that seen in cross sections of adult radii (fig 9) through a differential process related directly to the dominantly posteriad movement of the epiphyseal plates

The disposition of small vascular channels entering the radius (i e proximad on distal surfaces and anteriad on posterior surfaces — see p 107) correlates with the pattern of differential growth This disposition corroborates Lacroix s (51) suggestion that the inclination of the channels for nutrient vessels is due to greater traction on the periosteum toward the more rapidly growing side or end of a bone

Rationale for the singular manner of growth of the radius is found in its position within the flipper Specifically the relationship of the radius to the ulna the humerus and to the cross sectional form of the antebrachium must be considered Early development is essentially identical in the radius and ulna i e each has the same retention of endochondral bone and distribution of periosteal bone (fig 4) As befits its more slender form the angles of the endochondral cones are lower in the ulna In later development (fig 1) there is more periosteal bone on the anterior than on the posterior side of the ulna Its internal geometry therefore is fundamentally a mirror image of that in the radius as a resultant of anteriad rather than posteriad eccentric growth Thus the antebrachial bones matched in longitudinal growth between elbow and wrist grow transversely in such a manner that their opposite margins progressively separate while their adjacent margins maintain an essentially constant relative position In short *posteriad* eccentric growth within the radius results in an *anteriad* shift of the center of the bone while the posterior margin remains nearly static In the ulna the reverse is true

A second phenomenon augments eccentric transverse growth of individual bones in anterior posterior widening of the antebrachium While growth of the radius and ulna away from the elbow is overwhelmingly distad there are anteriad and posteriad components respectively in their elongation Some growth in the proximal epiphyses (i e in the cartilage surrounding the secondary centers) must be perpendicular to the bifaceted distal surface of the humerus (fig 1) The more significant anteriad and posteriad components however are a function of longitudinal growth of the canted proximal epiphyseal cartilage plates of the radius and ulna The angle of these plates relative to the longitudinal axes of the radius ulna humerus and the antebrachium proper is in each case substantially greater than the angles of the elbow articulation (especially in the pilot whale) (figs 1 6 7 and 8) Thus the combination of eccentric growth and

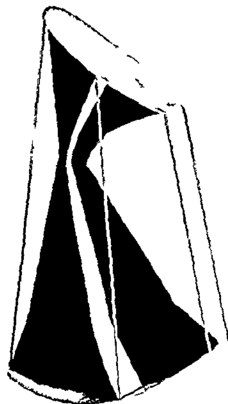


Fig 12 Model depicting relationship of internal geometry of an odontocete radius to patterns of differential growth suggested by figures 10 and 11 See p 120 for description

more rapidly and for a longer period of time than the proximal end The almost symmetrically curved distal epiphyseal plate remains essentially perpendicular to the long axis of the radius (figs 7 8 and 12) The posterior side of the distal endochondral cone acquires a higher angle to that axis than does the anterior side This is a clear example of eccentric growth of the epiphyseal cartilage as represented by the third model whereby differential increments on the margins result in a posterior shift of the disc s center as the endochondral cone elonagtes Posteriad eccentric growth (at both proximal and distal ends) is greater in the beluga than in the pilot whale radius as can be seen in a comparison of the positions of the fixed points and the sides of the endochondral cones in figure 7 and 8 Outside the neo*natal outline* in the beluga radius there is *indication* of an event not depicted in any of the theoretical models both the posterior and anterior sides of the distal cones are deflected to higher angles after birth than they held before birth (figs 6 7 and 12) The deflection of the *posterior* side indicates an absolute or relative increase (or both) in the rate of eccentric transverse growth in the postnatal beluga In the absence of experimental data (e g tracer or marker pin studies) it cannot be established which alternative is operative The corresponding deflection is not as clearly defined in pilot whale radii although it is evident in most specimens (figs 6 and 7) the angulation is not sharp nor is it related to birth Postnatal deflection of the *anterior* side of the distal cone in the beluga radius is not due to the same phenomenon as that of the posterior side At or about term (see p 116) the anterior end of the distal epiphyseal plate begins to take on a greater curvature than the rest of the plate and as development progresses a short segment comes to lie at about 45° to the radial axis Thus while the plate as a whole grows eccentrically with a posteriad shift of its center the small anterior segment is directed in nearly the opposite direction Elongation of this deviating anterior segment accompanied by periosteal depositions produces the anteriad flaring of the end of the mature radius This feature is only slightly manifested in the pilot whale radius

The proximal epiphyseal plates of beluga and pilot whale radii and the axes of their proximal endochondral cones are canted in the posterior direction This inclination is more pronounced in the pilot whale and in that species at least it begins early in fetal life (fig 5) The growth pattern of this end of the bone therefore generally resembles the geometry of the *fourth model* in figure 11 However growth at the proximal end of the radius cannot be explained by this one mechanism alone In both beluga and pilot whale radii the curvature of the posterior side of the proximal endochondral cone (figs 7 8 and 12) indicates a continuous rather than an abrupt alteration in the ratio of transverse to longitudinal growth rates Outside the neonatal outline of the beluga radius the posterior line becomes nearly horizontal (as does the equivalent portion of the line in the pilot whale radius) During the entire period

tribution is strongly mimetic of a box beam a configuration appropriate for sustaining greater (alternating) tensile and compressive forces in the medial lateral than in the anterior posterior plane Rather than constituting a low density filler between medial and lateral high-density masses trabeculae are so orientated as to complement the density distribution trabecular lines arising from the medial and lateral dense masses spread out and cross each other in a fashion comparable to the trajectories that might be drawn in a loaded beam (Murray 36 Evans 57) The humerus of the beluga whale differs from the others primarily in its middle region which is relatively more slender and more uniformly thick walled its overall trabecular orientation however is like that in the finback and pilot whale humeri

The radius of the adult pilot whale has a density distribution and trabecular orientation strongly comparable to that in the humerus The greatest concentration of bone (figs 7B and 9) is on the medial and lateral sides and in the absence of a high contrast between periosteal and endochondral bone there is an obvious entoectad gradient of increasing density in most transverse sections Actually the small density difference between periosteal and endochondral bone is reflected by slightly more dense posterocentral than anterocentral regions in such sections Thickness of the medial and lateral concentrations diminishes proximad and distad from a maximum at the level of the embryonic center point X Within individual transverse sections the posterior margin is without a superficial concentration of bone and where medial and lateral sides converge at the thin anterior margin the density concentration is diminished Despite asymmetry of cross section density distribution within the radius is a reasonable parallel of the box beam configuration in the humerus with bone concentrated toward the sides that carry alternately the greater tensile and compressive forces

Trabecular orientation within the pilot whale radius is visible in the medial lateral longitudinal section in figure 7B and in the accompanying line drawing (fig 7D) the main features of this orientation are suggested Lines of trabeculae extended from the medial and lateral concentrations across the central region intersecting those from the opposite side or doing so after passing at slight angles into the plane of adjacent sections Trabeculae in the mid length of the radius sweep centrad at lower angle and near the ends of the bone some terminate in the fine structure deep to the articular surface This organization clearly is advantageous in mechanically relating the articular surfaces to the medial and lateral concentrations of bone as well as relating the medial and lateral surfaces to each other in a system that undergoes loadings comparable to those on a main spar of an aircraft wing In its position in the limb as well as its more simple over all configuration the radius is perhaps even a better example for this analogy than is the cetacean humerus

To our knowledge the only previous illustrations of the mechanical organization in the odontocete radius are those by Roux (1893) His line drawing delineating the dense medial and lateral walls and the orientation of trabeculae in a medial lateral longitudinal section of the dolphin (*Delphinus delphis*?) radius was modified by Benninghoff (25) The latter investigator added his "split line" analysis of the "compacta The Benninghoff modification and Roux s additional line drawing of a transverse section of the radius were combined in a single figure in Murray's (36) classic discussion of the mechanical structure of bones These illustrations warrant discussion in terms of our findings

Roux s visualization of trabecular orientation in the medial lateral plane of the radius is for all practical purposes the same as ours His illustration is a complete schematic parallel of figure 7D Roux apparently was aware that dense bone is restricted to the medial and lateral sides although he did not show or describe the arrangement of bone in the anterior posterior longitudinal plane In his drawings (see Murray 36) especially that of the transverse section some liberties seem to have been taken In his longitudinal section the surface concentrations are too thick and of course give the same impression of solidarity as our figure 7D In transverse sections the dense medial and lateral masses again drawn in excessive

canting in the proximal end of the elongating radius not only contributes to transverse growth of the primary center but also drives it slightly anteriad as the proximal secondary center and the contiguous distal end of the humerus increase in size This phenomenon is not of long duration due to early closure of the epiphyses at the elbow, nor is the rate a high one due to the slower growth rate in the proximal compared with the distal end of the radius While the process operates however some of the increment on the posterior side of the radius must simply compensate for anteriad shift of the whole bone

The mode of transverse growth of the radius definitely is relatable to the cross sectional form of the flipper In an earlier report (Felts and Spurrell 65) it was shown that the cross sectional shape of the cetacean humerus (surrounded by muscles and lying entirely within the body contour and very basal region of the flipper) is broadly oval in the distal region oval to roughly triangular in the middle region and is expanded proximally into a massive head and tubercle As the humerus develops and is to a degree refined in shape by interaction with muscles its internal geometry remains basically symmetrical and approximates that depicted by the first and second models in figure 11 The radius contariwise develops in an amuscular environment and from the time of chondrogenesis its cross sectional shape conforms to that of the streamlined flipper In comprising the semistreamlined core of the antebrachium the radius and ulna are overlaid only thinly by soft tissues The eccentric growth of both radius and ulna is an ideal mechanism by which proportions of anterior posterior to medial lateral dimensions can be maintained inside a streamlined flipper that functions definitively from birth By simple experimentation with pencil and paper it can be shown that a series of uniform increments about the cross section will alter the ratio of minor to major axes In the odontocete radius and companion ulna by contrast non uniform increments in a gradient about the periphery of cartilage and bone result in maintenance of essential proportions as the bones and the limb grow and function

In the absence of data on absolute rates of transverse and longitudinal growth in prenatal and postnatal radii little may be said concerning the obvious increase in the rate of anterior posterior growth in the distal end of the maturing radius It should be noted that the greater change in the ratio of transverse to longitudinal growth occurs in the relatively narrower radius of the beluga Although we lack adequate information on the dimensions of the carpus and manus in older specimens from both species the slow maturation in and distal to the ends of the antebrachial bones suggests that widening of their ends may be part of a regional increase in breadth occurring as antebrachial elongation nears culmination The apparent co incidence of an increase in the rate of anterior posterior transverse growth with birth in the beluga will be discussed in the final section of this paper

Stuctural orientation and density

There certainly is nothing in lateral radiographs of the radius nor in radiographs of anterior posterior longitudinal sections (figs 6 7 and 8), resembling the classic illustrations of mechanical organization in limb bones (Wolff 1892 Murray 36 Evans 57) Indeed the asymmetrical disposition of more and less dense periosteal and endochondral bone in this plane could be considered *a priori* a mechanical disadvantage It should be remembered however that this is not the plane in which the radius sustains maximum loading As suggested in the Introduction the streamlined form of the flipper and the manner in which it is rotated in the waterstream result in the transmission of far greater tensile and compressive forces to one and the other broad medial and lateral surfaces of the antebrachial bones than to their anterior and posterior margins

In humeri of the finback whale (*Balaenoptera physalus*) and the pilot whale (Felts and Spurrell 65) the greatest concentration of bone is on the medial and lateral sides Bone immediately deep to these concentrations and filling in the anterior and posterior margins is approximately half as dense In the central region the density is only a quarter of that on the medial and lateral sides This density dis

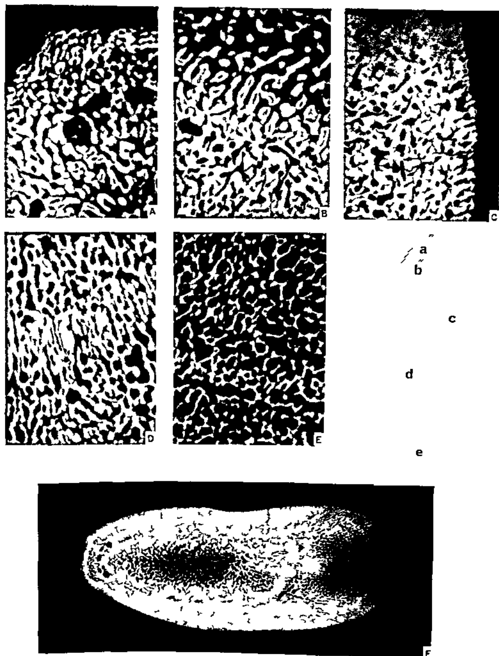


FIG 13 Contact microradiographs of a midlength transverse section of radius of late juvenile beluga Schematic at right shows position of all enlargements (× 7) in A through E and is relat ble to low power (× 1¾) whole section radiograph at bottom See p 106 for technique and p 130 for description and discussion

thickness are connected posteriorly by perpendicular lines while a circular pattern of lines in the center of the section is carried forward to the anterior margin as an intersecting pattern of lines The posterior perpendicular lines might be taken as a graphic representation of the moderately dense bone to which we have ascribed a periosteal origin However, the lines Roux drew in the central (endochondral) region and then carried into the anterior (periosteal) region apparently are intended to show a trabecular pattern that in reality does not exist Transverse sections of such dolphin radii we have examined differ in no significant manner from those of pilot whale sections (fig 9)

It is not clear whether Benninghoff based his trajectorial drawing on his knowledge of split lines in typical limb bones or if he actually decalcified and tested a section identical to that pictured by Roux In any case his lines through the medial and lateral concentrations of bone are continuous into Roux s trabecular lines The result is a classic biological analogy to the engineered beam under transverse loading one in which the dense bone is assumed to represent massed parallel trajectorial lines In reality our equivalent section of the pilot whale radius (fig 7B) has such a density characteristic that the lines drawn by Benninghoff could almost all be traced from proximal to distal trabecular arches without recourse to split line analysis Whether or not this is taken as anatomical evidence of trajectorial continuity in compacta and spongiosa depends upon whether one considers the radius to have a sparse or diffuse compacta or simply a medial and lateral concentration of spongiosa

It will be noted that the internal anatomy of beluga radii has been of prime importance in analysis of differential growth while that of pilot whale radii has contributed the most to visualization of mechanical organization This disparity is based of course on species differences in the amount of bone within the radius We have seen that overall radiodensity as well as the contrast in radiodensity between periosteal bone and endochondral bone never are as strong in the pilot whale as in the beluga Additionally internal geometry and the faint neonatal outline fade early in the pilot whale s postnatal life doubtlessly as a consequence of the differential process of resorption and deposition that produces the mechanically significant arrangement of dense and more porous bone in the adult In the beluga however the contrast between the two osseous components persists and the neonatal outline can be traced in the adult bone Internal reorganization is slow and incomplete (discussion below, and fig 13) Although there are medial and lateral concentrations of bone these are thick not sharply delimited and of about the same regional density as the posterior mass of periosteal origin Further there is no discrete trabecular pattern visible in the radius of the beluga (compare figs 7B and 8B) In view of the virtually identical general form and function of the radius in the two species it only can be concluded that the quantity of bone in that of the beluga (whatever the rationale) either obscures or obviates such a fine mechanical organization as is found in the less dense radius of the pilot whale

It can be demonstrated that the difference in radiodensity in the two odontocete radii is overwhelmingly a function of structural density (i e , the amount of bone per se encountered by the x ray beam) rather than of mineral density (i e the amount of mineral per unit bone encountered by the x ray beam) The ratios of post to pre ashing weights are 0 682 for the beluga and 0 673 for the pilot whale These means for ten entire radii of each species represent broadly overlapping ranges entirely within that for mineral proportion in human limb bones (Trotter and Peterson 62) and in the humerus of the finback whale (0 64 to 0 68 Felts and Spurrell 65) The absolute densities (weight/volume of intact clean dry bones without consideration of internal space) however are more striking Pilot whale radii (10 adult bones) have a mean A D of 0 75 gm/cm³ (range 0 72 to 0 79) The mean A D for the same number of beluga radii is 1 18 gm/cm³ (range 1 12 to 1 23) with the highest value in the oldest specimen The radius of the pilot whale thus is in the same range of absolute density as the more dense of human limb bones (Trotter et al

clearly visible in thin section radiographs (fig 13F) especially the large anterior most ones that obscure the anterior margin of the neonatal radius in lateral views (fig 8A)

A striking feature of contact microradiographs of the beluga radius is the microregional density pattern within the confines of the prenatal radius In bone of both periosteal and endochondral origin (figs 13A B and D) within the neonatal outline the centers of trabeculae are more radiolucent than are corresponding portions of postnatal ones however the superficial portions of trabeculae are more radiodense than any postnatal bone (It must be remembered that slightly more than the posterior one third as well as the periphery of the neonatal outline within the young adult section in figure 13F is of periosteal origin) This unexplained feature is an additional identification for the neonatal radius previously delimited on the basis of shape size and internal geometry These microregional differences in mineral content do not have an effect on radiodensity of intact bones for they appear to average out so that there is no appreciable difference in ash weight of small excised samples of prenatal and postnatal bone in the adult radius

The prime remaining question in this study is the rationale for lack of an open medullary cavity and for the relatively high but differing absolute densities in the two odontocete radii Certainly these characteristics cannot be explained *prima facie* as adaptations to local functional requirements within the evolving flipper as can external shape differential growth and the modification of joints Indeed contrasts in the densities of otherwise quite similar beluga and pilot whale bones suggests that density may be a relatively independent feature Moreover evidence exists that density may be one of the requirements for secondary marine adaptation of the mammalian body as a whole Zangerl (35) has suggested that increased density (or pachyostosis) was a means of compensating for lung volume and overall buoyancy in the early stages of the return to marine life Early (Cretaceous) marine reptiles had extremely dense limb bones but later fossil examples from the same lines possessed a less dense even spongy bone structure In such a phylogenetic cycle the only obvious requirement would be for modulation of the process of resorption as proposed by Gebhardt (01) for the manatee The present manatee it should be noted is somewhat less pachyostotic than its ancestor from the Eocene (Fawcett 42) In applying this line of reasoning to the cetacean humerus it has been postulated (Felts and Spurrell 65) that the protocetacean acquired heavy bone structure prior to modification of joints and adaptation of bone configuration a situation existing in the extant manatee and penguin (absolute density of 0 98 gm/cm^3 Meister 62) With subsequent changes in body organization tissue composition and anatomy of the flipper the less dense humerus evolved (and with a "new" mechanical organization befitting limb function) Our present information on radii indicates that odontocetes still like the classic pachyostotic forms (Zangerl 35 and personal communication) have higher absolute densities in the distal than in the proximal elements of the limb skeleton In the pilot whale the distinction between humeral and radial density is small in the beluga the difference is great and the radius is fully in the range of what has come to be regarded as pachyostosis Actually absolute density of the beluga radius is almost exactly intermediate between those of the pilot whale and manatee bones This suggests the possibility that the beluga has lagged behind other cetaceans in the trend away from an early condition of high density It might also be conjectured that the beluga a rather obese animal even for a cetacean has a greater need for dense bones Finally it is possible that other factors related neither to buoyancy nor to biomechanics may be important in the phylogeny and ontogeny of whale limb bones

Alternative theories in explanation of pachyostosis have implicated anoxia and the state and function of the thyroid Although these concern the manatee in particular a broader application to the evolution and to the present condition in other secondary marine forms has been implied Nopsca ('23) postulated that anoxia incurred in adjustment to marine existence

60) and is approximately 1 12 times as dense as its own humerus (0 67 gm/cm³ Felts and Spurrell 65) The beluga radius however is more dense than any normal limb bone in man and is about 1 74 times as dense as its own humerus (0 69 gm/cm³), and it is 1 57 times as dense as the radius of the pilot whale

The high absolute density of the beluga radius brings to focus a point we have alluded to only in passing i e the comparability of several developmental and structural characteristics in odontocete limb bones and those of the manatee (*Trichechus latirosteresis*) Externally the major limb bones of the wholly aquatic manatee are of a far more typical mammalian form than those of cetaceans and the shoulder elbow (humeroulnar) and wrist articulations are freely movable The radius and ulna are fused at the margin of the elbow joint and their distal articulation is partly a synchondrosis partly a synostosis Fawcett s (42) study of osteogenesis in the manatee revealed these features we now see are shared with odontocetes non linear arrangement of chondrocytes irregular endochondral ossification failure of development of an open medullary cavity and persistence of numerous endochondral spicules Consequently one can trace the development of proximal and distal endochondral cones within a thick trabeculated mass of periosteal bone In terms of our models depicting differential growth Fawcett s illustrations show the manatee humerus (like that of cetaceans) to have a concentric mode of transverse growth with the proximal the longer endochondral cone The radius appears to grow concentrically as well but ulnar growth is slightly eccentric laterad away from the radius As in the odontocete antebrachium the longer endochondral cones are distal in both radius and ulna of the manatee Meister (62) has described essentially the same fetal development for penguin bones without illustrating postnatal geometry

Although Fawcett s sections show that the endochondral and periosteal moieties can be distinguished microscopically even in adult manatee bones the continuing deposition of bone in the absence of substantial resorption and reorganization produces a limb bone that is exceedingly dense (pachyostotic) Indeed one can see almost nothing of internal structure in radiographs of intact adult bones Even radiographs of longitudinal sections (Bechtol 64) reveal an overall density that largely obscures internal geometry and is far in excess of that in equivalent sections from beluga radii The absolute density of a conjoint radius and ulna in our possession is 1 63 gm/cm³ or 1 38 times that for the beluga radius

Some histological features of the retained internal geometry and the high structural density of beluga radii are shown by contact microradiographs in figure 13 It is apparent in paraffin sections from the fetus (fig 4) and in ground sections of older beluga and pilot whale radii that periosteal osteogenesis produces a heavy spongiosa rather than a series of lamellae In limb bones of the manatee (Fawcett 42) and of two odontocetes the subsequent deposition of bone within the primary vascular spaces gives rise to a protohaversian structure (term of Enlow and Brown 56) In the manatee this process is carried to an extreme and together with meager resorption and secondary haversianation leads to the extremely dense bone structure of the adult animal In the pilot whale there is a substantial amount of resorption and new bone formation in the less dense central region while protohaversian and secondary haversian bone comprises a high proportion of the medial and lateral concentrations

Microscopic structure of the beluga radius is in many ways intermediate between that found in the manatee and the pilot whale The medial and lateral concentrations (fig 13F and C) are largely protohaversian and tend to become more densely structured with full maturity In the anterior region (fig 13A) the coarse primary spongiosa is retained while the posterior region consists of a more open or delicate spongiosa The more recent portions of the posterior periosteal bone (fig 13E) demonstrate that the gross striations seen in radiographs of thicker sections and of whole bones are due to lines of large pores rather than to periodic differences in mineralization Similarly the larger vascular channels lying immediately superficial to the neonatal outline are

mean and extremes of environmental tem perature or the occurrence of a change in transverse versus longitudinal growth at or just after term when the young beluga has entered the cold water or whether or not the alternating porosity of postnatal bone may reflect seasonal or subseasonal vascular responses to the environmental temperature

ACKNOWLEDGMENTS

The authors are indebted to many per sons and groups who were of assistance during collection and analysis of anatom ical material and in the preparation of this paper Dr David E Sergeant Fisher ies Research Board of Canada Arctic Unit Montreal was of great assistance through out the field operations and was the donor of valuable anatomical material before our collection was made Field work by one of us (W F) was facilitated at Churchill Manitoba by the Canadian Department of National Defence (Defence Research Northern Laboratory) and the Adanac Fish and Whale Co Ltd and their personnel At Dildo Trinity Bay Newfoundland work would not have been possible without the many courtesies extended by the Arctic Fisheries Products Ltd and Fur Farmers Feed Co-op management and personnel and by the fisherman of Dildo New Harbor and Bellvue and the crew of the catcher *Arctic Venture* Radiographs were pre pared with the assistance of Mr Bradford Yoho and photographs were by Messrs O V Heath and Leroy Christenson

LITERATURE CITED

Bechtol C 1964 Personal Communications with the loan of radiographs of sections of manatee radius and ulna from C Bechtol M D Department of Orthopedic Surgery Uni versity of California Los Angles

Benninghoff A 1925 Spaltlinien am Knochen eine Methods zur Ermittlung der Architektur platter Knochen Anat Anz 60 189–206

Enlow D H 1962 A study of the post natal growth and remodeling of bone Am J Anat *110* 79–102

Enlow D H and S O Brown 1956 A com parative histological study of fossil and recent bone tissues Texas J Sci *8* 405–443

Evans F G 1957 Stress and Strain in Bones Their Relation to Fracture and O teogenesis Charles C Thomas Springfield Ill

Fawcett D W 1942 The amedullary bones of the Florida manatee Am J Anat *71* 271–309

Felts W J L 1954 The prenatal development of the human femur Am J Anat *94* 1–44

——— 1965 Some structural and functional characteristics of flippers and flukes in ceta ceans In Whales Porpoises and Dolphins K S Norris ed University of California Press Los Angeles

Felts W J L and F A Spurrell 1965 Struc tural orientation and density in cetacean hu meri Am J Anat *116* 171–203

Gebhardt W 1901 Uber funktionell wichtige Anordnungsweisen der groberen und feiner Bauelemente des Wirbelthiereknochens Arch f Entw Mech *11* 383–498

Ham A W 1932 Cartilage and bone In Cowdry s Special Cytology (second edition) Hoeber New York

Howell A B 1930 Aquatic Mammals Their Adaptations to Life in the Water Charles C Thomas Springfield Ill

Lacroix P 1951 The Organization of Bones (translated by S Gilder) Blakiston Co Phila delphia

Meister W 1962 Histological structure of the long bones of penguins Anat Rec *143* 377–388

Murray P D F 1936 Bones A Study of the Development and Structure of the Vertebrate Skelton Cambridge University Press

Nopsca F 1923 Vorlaufige Notiz uber Pachyo stose und Osteosclerose einiger mariner Wirbel tiere Anat Anz *56* 353–359

Patten B M 1953 Human Embryology (sec ond edition) Blakiston Co Philadelphia

Roux W 1893 Das Estez der Transformation der Knochen Berliner Klin Wochenschr 30 509–511

Scholander P F and W E Schevill 1955 Counter-current vascular heat exchange in the fins of whales J Applied Physiol *8* 279–282

Sergeant D E 1962 The biology of the pilot or pothead whale (*Globicephala melaena*) (Traill) in Newfoundland waters Bull Fish Res Board Canada no 132

Sickenberg O 1931 Morphologie und Stam mesgeschichte der Sirenen Palaeobiologica *4* 405–444

Slijper E J 1962 Whales (translated by A J Pomerans) Basic Books Inc New York

Streeter G L 1949 Developmental horizons in human embryos (fourth issue) A review of the histogenesis of cartilage and bone Contr Embryol Carnegie Inst 33 149–168

Thompson D A W 1942 On Growth and Form (second edition) Cambridge University Press Cambridge

Trotter M and R R Peterson 1962 The rela tionship of ash weight and organic weight of human skeletons J Bone and Joint Surg 44 A 669–681

might have been reflected in pachyostosis through a sequence of medullary hyperplasia then aplasia and finally osseous replacement Nopsca suggested as well that the manatee might by hypothyroid due to the high iodine content of its marine vegetable diet Sickenberg (31) also believed that anoxia was a primary factor in pachyostosis but that the effect was upon the thyroid gland directly and that the structure of the skeleton evidenced hypothyroidism Fawcett (42) discounted the direct action of anoxia by pointing out the dissimilarity of bone histology in the manatee and in osteosclerotic humans who had undergone medullary aplasia He concluded however that the retardation of osteogenesis and the lack of remodelling together with the diet low physiological rates and the actual histology of the thyroid all implicated hypothyroidism as the prime causative factor in pachyostosis He showed that far more than a superficial comparison can be drawn between manatee bones and those of experimental animals in which the thyroid has been suppressed or removed

Certainly it is difficult to visualize increased density as a direct response to an overall body requirement for lower buoyancy However advantageous it might be in secondary marine adaptation there is enough direct and indirect evidence to postulate that pachyostosis in the manatee is at least partially an effect of anoxia or hypothyroidism or both In extant cetaceans however neither anoxia nor hypothyrodism is a likely factor for these animals are more evolved structurally and are very active carnivores with a high metabolic rate (discussed by Slijper 62) It cannot be discounted that either anoxia or hypothyroidism or both were important factors in early cetacean evolution just as the limb skeletons of protocetaceans may generally have resembled that of present day Sirenians The species differences in density of the radius and in the ratio of radial to humeral density may be taken to represent physiological as well as structural evolution away from the pachyostotic condition The strong similarity between early fetal osteogenesis in the odontocetes and the manatee may represent an advantageous recapitulation of phylogeny or the lack of a selective value in evolution or a transient anoxia or hypothyroidism during intrauterine life This problem certainly requires further study

On the basis of evidence presented in this paper, the possibility of another environmental influence on radial growth and development can be advanced To our knowledge attention has never been drawn to the possible effects of water temperature and flipper thermodynamics on osteogenesis and bone structure The flipper (like the dorsal fin and the tail flukes) is of high area and low volume and has a complex counter current vascular system (Scholander and Schevill 55 Felts 65) The flippers are therefore very effective variable heat sinks that are of importance in ridding the body of heat in periods of high activity (or in warm water) and in conserving body heat during times of low activity (or in cold water) The range of temperature encountered by cetaceans may be considered slight compared with the extremes to which terrestrial forms are exposed Slijper (62) states that the difference in mean temperature between tropical and polar seas is about 45°F However one of the odontocetes used in this study the pilot whale is from the open Atlantic while the other the beluga is from the circumpolar region where it lives in open water adjacent to the ice pack in winter and in shallow coastal waters and river estuaries in the summer The growing limb skeleton is encased in an essentially amuscular limb of high area and low volume that projects into a highly conductive liquid medium that may in the case of the beluga range in temperature from perhaps 60°F to below freezing Vascular supply to the limb varies with the level of body heat production and water temperature At this time there is no significant body of data on bodily activity flipper temperature and blood flow and the relationship of these to bone growth is unknown No study has been made of the bone structure of belugas reared or maintained in water of constant temperature or in water temperatures of controlled range and periodicity Until these experimental data are available one can only speculate as to the relationship of species differences in bone growth and reorganization to the

A Time Sequence Study of Fat Absorption in the Rat Jejunum

RALPH A JERSILD JR
Department of Anatomy Indiana University Medical Center Indianapolis Indiana

ABSTRACT Fat absorption and transport in rat intestinal epithelial cells were followed by electron microscopy and radioautography Physiological fatty-chyme prepared from fat fed donor rats was injected into ligated segments of the upper jejunum of fasting recipient animals Samples of tissue were removed in a time sequence from 1 to 30 minutes Oleic acid H^3 was added to the chyme for light and electron microscopic radioautography The results indicate that fat is absorbed and transported through the epithelium very rapidly Within 1 minute fat droplets can be seen in the endoplasmic reticulum and the Golgi apparatus Fat is shown to be absorbed during not prior to experimentation by the radioautographic identification of labeling in the vicinity of fat droplets throughout the cell Evidence of accumulation of fat within the Golgi apparatus appears between 1 and 2 minutes Such accumulation may be indicative of a rate limiting step in absorption It is suggested that phenomena occurring within the Golgi apparatus are in part responsible for the appearance of cellular saturation with fat which is evident in 8 to 10 minutes The sequential pattern can be followed in cells along the entire length of the villus

The pathway of fat absorption in the intestinal epithelium was described in a high resolution study by Palay and Karlin (59) Following this work formation and transport of lipid droplets across the epithelium have been examined and found similar in a number of mammalian species (Ladman et al 63 — human Strauss 63 — hamster Palay and Revel 64 — rat) Experiments have also been performed to understand better the functional concepts of fat absorption and transport within the intact cell (Millington et al 62 Rostgaard and Barrnett 64 Strauss 64a 64b Sabesin and Isselbacher 65)

Dietary lipids are presumed to be absorbed chiefly in the form of monoglycerides and fatty acids (see Wilson 62 Mattson and Volpenhein 64) These are then resynthesized to triglycerides within the epithelium by way of enzymatically controlled steps which have been shown to be primarily associated with the microsome fraction from the intestinal mucosa (Senior and Isselbacher 60 61 62) These authors (61 62) have shown that monoglycerides are rapidly converted to di and triglycerides (40% to 50% in 5 min) when incubated in a complete medium containing palmityl CoA and the microsome fraction Personal observations have also suggested that the transport of lipids through the epithelial cells is quite rapid

The present study was undertaken to examine the absorptive process in a time sequence in order to gain some insight into the rate of transport of fat across the epithelium and to observe morphological changes in the absorptive process with increasing length of exposure to lumenal fats In experiments involving oral or gastric administration of fats it is not possible to ascertain when the resultant fatty chyme reaches a given section of intestine or how long the cells are exposed to the lumenal contents To determine the length of time the fat is actually available for absorption in a specific area of the intestinal lumen the fat source was injection directly into a ligated segment of intestine In order to present the fat in a physiological form and circumvent possible complications with artificial preparations fatty chyme derived from donor animals was used in modification of the procedure described by Adamstone and Taylor (59)

MATERIALS AND METHODS

Wistar strain white rats (100 to 350 gm) were used throughout All animals were fasted about 24 hours with ample

Trotter M G E Broman and R R Peterson 1960 Densities of bones of White and Negro skeletons J Bone and Joint Surg, *42 A* 50–58

Vladykov V D 1944 Etudes sur les mammiferes aquatique III Chasse biologie et valeur economique du Marsouin Blanc ou Beluga (*Delphinapterus leucas*) du fleuve et du golfe Saint Laurent Department of Fisheries Province of Quebec Quebec Canada

Wolff J 1892 Das Gesetz det Transformation der Knochen Berlin

Zangerl R 1935 IX *Pachypleurosaurus edwardsi* Cornalia sp Ostelogie Variationsbreite — Biologie In B Peyer Dis Triasfauna der Tessiner Kalkalpen Abh Schweiz Pal Ges *56* 1–80

apical region of the cell or in abundance throughout the entire supranuclear cytoplasm (fig 5) The profiles of the Golgi apparatus correspondingly appear as clusters of flattened cisternae and small vesicles or with enlarged vacuolar dilations of the cisternae which contain slight or moderate accumulations of small fat droplets (figs 6 7) The cells along the remainder of the villus usually contain a few scattered droplets of fat

Examination of the fasting control specimens shows the absorptive cells to be void of any visible fat accumulations in most instances However some of the samples examined contain fat droplets with a distribution similar to that observed after brief exposure to chyme Thus the latter presumably could represent either the early stages of fat absorption or the presence of fat prior to the injection of chyme Radioautographic experiments using oleic acid H^3 were therefore employed to confirm the rapid absorption and transport of fat

Light microscopic radioautographs of specimens removed after a 1 minute exposure to labeled chyme do indicate that considerable label has already entered the cells along the upper half of the villus Grains are fairly evenly distributed over the supranuclear cytoplasm being concentrated mainly in the area extending from beneath the striated border to the nucleus Grains are also present lateral to and below the nuclei but generally in fewer numbers (fig 1) A light but definite labeling is also present in the cells at the proximal end of most villi Labeling in the core of the villus is very light and evenly distributed among the cellular elements and remains this way until much later (approximately 10 min) when clusters of fat droplets appear within the interstitial connective tissue and the lacteals Electron microscopic radioautography shows most of the grains to be located over areas of the endoplasmic reticulum and the Golgi apparatus containing small droplets of fat (figs 6 8) Very few grains appear over other cell structures including the microvilli and terminal web Few grains are found below the nuclei however their location suggests that the labeling seen by light microscopy is mainly over small scattered intracellular fat droplets No chylomicrons or radioactivity appear in the occasional lacteals observed

2 to 5 Minutes After 2 minutes exposure to chyme the absorptive process has progressed considerably The cells on the villous tips now contain numerous fat droplets predominately 60 to 130 mμ in diameter within the channels of the endoplasmic reticulum (fig 9) Enlarged vacuolar dilations of the Golgi cisternae contain larger accumulations of fat (figs 10 12) These droplets of fat display little or no coalescence during this time period and are in the same size range as those enclosed by profiles of endoplasmic reticulum

The amount of fat absorbed by the cells progressively decreases toward the base of the villus (figs 8 12) A few small droplets are evident in cells near the base in some of the villi These are located mainly in the extreme apical region or throughout the entire supranuclear cytoplasm similar to those seen at the villous tips in 1 minute preparations The Golgi apparatus however rarely contains accumulations of fat

In radioautographic experiments the distribution of grains seen during this time period is similar to but of greater density than the 1 minute samples Although labeling below the epithelial cell nuclei is considerably less than that above a distinct decrease in grain concentration is evident at the basal surface of these cells (fig 2) The grain density over the lamina propria remains very low Moderate to heavy labeling in the proximal cells of the villi was frequently observed (fig 4)

Small clusters of fat droplets are often observed in the lateral intercellular spaces during the shorter absorption intervals primarily below the level of the Golgi zone However similar clusters are also readily seen in specimens from fasting animals It is not until 5 minutes that intercellular clusters near the villous tips become appreciably larger and more numerous Following the injection of labeled chyme radioautographic grains are readily visible over such clusters at 5 minutes

water supply prior to experimentation All procedures were carried out under nembutal anesthesia (3 mg/100 gm body weight) Fatty chyme was usually collected from the donor animals by inserting a cannula into the lower duodenum or upper jejunum Safflower oil (or linoleic acid for four recipients) was then given by gastric intubation The resulting chyme rich in small clear globules of fat was collected in ice packed tubes in small amounts and immediately frozen until used

Segments of the upper jejunum of 15 recipients were ligated to form short sacs 1 to 3 cm in length One to two isolated segments were used per animal with at least 3 cm separating the segments when two were used Care was taken to prevent ligation of the blood vessels or lymphatics serving the isolated segments Approximately 0 1 cm^3 of the fatty chyme warmed to room temperature was then injected into the segments without over distention of the wall the abdominal wound closed and absorption allowed to proceed for varying lengths of time Tissue samples were removed at varying intervals either by tying off small blebs of the intestinal wall and removing with a sharp scissors or by clamping off the entire segments with hemostats and cutting free The pieces of tissue were immediately placed in fixative and cut into small pieces for electron microscopy Samples from the intestine were removed after the injection of chyme at the following time intervals 1 through 5 8 10 12 20 and 30 minutes Portions of intestine adjacent to the ligated areas served as fasting controls

The tissue was fixed for 4 hours in 1% phosphate buffered osmium tetroxide pH 7 1 to 7 2 (Millonig 61) dehydrated through ascending grades of ethanol and embedded in epon (Luft, 61) The intestinal villi were sectioned longitudinally and lead stained by Karnovsky's (61) or Reynolds (63) modifications

Radioautographic experiments

The absorption of fat after very short absorption periods (1 to 2 min) required additional support (see Observations) The actual absorption and transport of fat after short periods were tested by using tritium labeled fat in conjunction with radioautography The experimental procedures were as described above Before the injection 250 to 500 μc of oleic acid 9 10 H^3 (specific activity 730 mc/mM) were mixed with the chyme Tissue samples were embedded in methacrylate or epon The radioautographic procedures were essentially as described by Caro and van Tubergen (62) Ilford K 5 emulsion was applied to 0 5 μ methacrylate sections for light microscopy and L-4 as a monolayer over thin sections for electron microscopy Emulsions were applied to sections from the fasting control segments to check for non specific labeling of the tissue The thin sections were initially examined with or without lead staining Staining with the subsequent removal of gelatin facilitated the identification of the smallest fat droplets and therefore was routinely employed for observations and illustrations

OBSERVATIONS

In any given specimen variations in the absorptive process within the intestinal epithelium are evident Differences in the abundance and distribution of absorbed fat can be observed among neighboring villi and quite frequently from one side of a single villus to the other In addition a progressive decrease in absorption in the cells toward the base of the villus as described by Weiner ('28) is often apparent (Ladman et al 63) The villi from each time interval were therefore examined along the entire length The typical pattern of absorption from each of these intervals is presented Similarities were observed among different time intervals which are grouped accordingly into three periods 1 minute 2 to 5 minutes and 8 to 30 minutes

1 Minute Absorptive cells observed following a 1 minute exposure to chyme appear either without visible evidence of absorption or more frequently, with a variable number of small fat droplets about 40 to 70 mμ in diameter These droplets are characteristically within the channels of the endoplasmic reticulum At the tip of the villus their distribution may be predominately within the smooth elements of the reticulum in the extreme

apical region of the cell or in abundance throughout the entire supranuclear cytoplasm (fig 5) The profiles of the Golgi apparatus correspondingly appear as clusters of flattened cisternae and small vesicles or with enlarged vacuolar dilations of the cisternae which contain slight or moderate accumulations of small fat droplets (figs 6 7) The cells along the remainder of the villus usually contain a few scattered droplets of fat

Examination of the fasting control specimens shows the absorptive cells to be void of any visible fat accumulations in most instances However some of the samples examined contain fat droplets with a distribution similar to that observed after brief exposure to chyme Thus the latter presumably could represent either the early stages of fat absorption or the presence of fat prior to the injection of chyme Radioautographic experiments using oleic acid H^3 were therefore employed to confirm the rapid absorption and transport of fat

Light microscopic radioautographs of specimens removed after a 1 minute exposure to labeled chyme do indicate that considerable label has already entered the cells along the upper half of the villus Grains are fairly evenly distributed over the supranuclear cytoplasm being concentrated mainly in the area extending from beneath the striated border to the nucleus Grains are also present lateral to and below the nuclei but generally in fewer numbers (fig 1) A light but definite labeling is also present in the cells at the proximal end of most villi Labeling in the core of the villus is very light and evenly distributed among the cellular elements and remains this way until much later (approximately 10 min) when clusters of fat droplets appear within the interstitial connective tissue and the lacteals Electron microscopic radioautography shows most of the grains to be located over areas of the endoplasmic reticulum and the Golgi apparatus containing small droplets of fat (figs 6 8) Very few grains appear over other cell structures including the microvilli and terminal web Few grains are found below the nuclei however their location suggests that the labeling seen by light microscopy is mainly over small scattered intracellular fat droplets No chylomicrons or radioactivity appear in the occasional lacteals observed

2 to 5 Minutes After 2 minutes exposure to chyme the absorptive process has progressed considerably The cells on the villous tips now contain numerous fat droplets predominately 60 to 130 mμ in diameter within the channels of the endoplasmic reticulum (fig 9) Enlarged vacuolar dilations of the Golgi cisternae contain larger accumulations of fat (figs 10 12) These droplets of fat display little or no coalescence during this time period and are in the same size range as those enclosed by profiles of endoplasmic reticulum

The amount of fat absorbed by the cells progressively decreases toward the base of the villus (figs 8 12) A few small droplets are evident in cells near the base in some of the villi These are located mainly in the extreme apical region or throughout the entire supranuclear cytoplasm similar to those seen at the villous tips in 1 minute preparations The Golgi apparatus however rarely contains accumulations of fat

In radioautographic experiments the distribution of grains seen during this time period is similar to but of greater density than the 1 minute samples Although labeling below the epithelial cell nuclei is considerably less than that above a distinct decrease in grain concentration is evident at the basal surface of these cells (fig 2) The grain density over the lamina propria remains very low Moderate to heavy labeling in the proximal cells of the villi was frequently observed (fig 4)

Small clusters of fat droplets are often observed in the lateral intercellular spaces during the shorter absorption intervals primarily below the level of the Golgi zone However similar clusters are also readily seen in specimens from fasting animals It is not until 5 minutes that intercellular clusters near the villous tips become appreciably larger and more numerous Following the injection of labeled chyme radioautographic grains are readily visible over such clusters at 5 minutes

but are only occasionally encountered at 2 minutes

8 to 30 Minutes In the cells along the upper three fourths of the villus, the size of the fat droplets within the channels of the endoplasmic reticulum gradually become larger ranging predominately from 120 to 200 mμ by 10 minutes (fig 13) and 200 to 300 mμ by 20 minutes (fig 15) The number of villi showing similar absorptive activity in the more proximal cells (fig 14) increases substantially by 20 minutes In addition to the membrane enclosed droplets much larger masses of fat up to 1 μ in diameter appear in the cytoplasmic matrix after 8 minutes exposure to chyme (fig 11) These become progressively more numerous up to the 30 minute interval

The Golgi cisternae becomes extremely dilated by 10 minutes enclosing numerous tightly packed droplets of fat (fig 14) Together they appear as a distinctive band in the immediate supranuclear cytoplasm In many of the Golgi vacuoles the droplets show a tendency to coalesce which becomes most pronounced by 20 minutes (figs 16 17) The fat droplets in the lateral intercellular spaces become much more abundant (figs 16 18) and large clusters can be observed at and below the level of the Golgi apparatus along the entire extent of the villus These droplets range from 40 to 140 mμ in diameter They are approximately the same size as the droplets within the endoplasmic reticulum and Golgi apparatus of cells from the 1 to 5 minute time intervals (figs 5–10, 12) During longer time intervals occasional Golgi vacuoles usually closer to the nucleus contain droplets about equal in size to those within the intercellular spaces (figs 16 17) In addition the droplets enclosed within smooth surfaced vesicular profiles present in the Golgi zone (figs 16 17) and those within the channels of the endoplasmic reticulum toward the base of the cells (fig 18) are in this smaller size range

In radioautographic preparations from this time period heavy labeling in the Golgi zone is evident along the distal one half to two-thirds of the villus (fig 3) There is still a distinct decrease in grain concentration at the basal surface of the epithelial cells By electron microscopy clusters of fat droplets found in the connective tissue spaces and the lacteals are frequently observed to be labeled

DISCUSSION

Injection of fatty chyme into the intestinal lumen has made it possible to observe the pattern of absorption in the epithelial cells in a sequence of exact time intervals The interpretation of a proper sequence of events is possible when fat is administered by feeding or gastric intubation (Palay and Karlin 59 Palay and Revel 64) however the length of time required to bring about these changes is difficult to obtain by these methods The earliest evidence for absorption by the limits of light microscopy following fat feeding is at 10 minutes (Verzar and McDougall 36) When unmodified corn oil is injected into the intestine fat droplets are observed after 15 minutes (Laschi and Gasbarrini 63)

It is evident under the experimental conditions in the present study that fat absorption and transport through the epithelial cells is extremely rapid Correlation of standard electron microscopic with radioautographic preparations indicates that within 1 minute after exposure to chyme a substantial amount of fat is absorbed In addition the fat droplets found within the endoplasmic reticulum may reach the nuclear, and to some extent the infranuclear level of the cell

In the fasting state droplets may be seen in the epithelial cells and in the intercellular spaces This fat may be derived from lipids released during the digestion of epithelial cells sloughed into the lumen or from lipids secreted into the lumen (Bernhard et al 56 Johnston 59) The use of radioautography however readily demonstrates that fat is absorbed during the 1 minute interval Electron microscopic radioautography shows that the newly absorbed labeled fat is located in the same regions of the cytoplasm as the enclosed droplets of fat

After 2 minutes the absorptive process is well established with an array of medium size droplets present throughout the cell The earliest definite indication of the discharge of fat in this study is at

5 minutes when the number of intercellular droplets increases and becomes clearly labeled

The rapid transport of fat through the cell suggests a rapid synthesis of triglycerides from absorbed lipid moieties This is in accord with the rate of synthesis utilizing isolated microsomal systems as described by Senior and Isselbacher (61 62) It further suggests that the system of enzymes involved is highly organized for controlling the sequential reactions in triglyceride synthesis A specific association with the membranes of the endoplasmic reticulum would permit such control (McLaren and Babcock 59) Whether the triglycerides are totally synthesized before or following droplet formation is a question still open for speculation (Ashworth et al 60 Ashworth and Johnston 63 Palay and Revel 64)

It would seem that the smallest fat droplets present in the initial phases of the absorptive process are transported with little impedence through the cell However the rate at which fat is absorbed by the cells appears to be more rapid than the ability to discharge it (Morehouse et al 56) Shepherd and Simmonds (59) suggest the discharge occurs at a limited rate These conditions may lead to the appearance of saturation of the cells with fat as observed in the 8–30 minute time period The increase in fat content begins very soon after the onset of absorption The accumulation of fat droplets within the Golgi apparatus early in the absorptive process (within 1 to 2 min) is the first evidence of a site where transport might be retarded The extent to which the Golgi apparatus contributes to processes related to fat absorption is still unresolved however its involvement in fat metabolism has been suggested (Cramer and Ludford 25 Emmel 45 Dalton 61) Indications that the fat droplets can be discharged into the lateral intercellular spaces from this organelle have been discussed by Lacy and Taylor (62) It is apparent that this organelle has a considerable capacity for retaining fat through a distention of the cisternal elements This becomes more pronounced with longer exposure to chyme The coalescence of droplets observed when the accumulation is excessive appears to be a typical phenomenon (Ladman et al 63 Palay and Revel 64) During the early stages of absorption the Golgi-contained droplets are about the same size as the small droplets within the endoplasmic reticulum and intercellular spaces Later as the droplets within the endoplasmic reticulum become larger there is a tendency to coalesce Golgi vacuoles also contain either the larger (apical sized) or smaller (intercellular sized) droplets during these longer time intervals It is possible to infer from this a sequential pattern of events in which droplets enter the Golgi cisternae from the endoplasmic reticulum and are transformed into smaller size droplets These smaller droplets may then be transferred either directly to the lateral cell surface or to channels of the endoplasmic reticulum more proximally located in the cell The transfer of droplets to and from the Golgi apparatus may be mediated through smooth-surfaced vesicles such as are seen in the Golgi area These vesicles appear to be similar to the transitional elements described in various cell types by Zeigel and Dalton (62) and Essner and Novikoff (62)

The total chemical composition of the droplets as they leave the cells has not been established (Wilson 62) The potential ability of the mucosal cells presumably the epithelial cells to synthesize chylomicrons from absorbed lipids has been reported with evidence that this may be one of the rate limiting steps in fat transport (Isselbacher 65) Droplets in the apical endoplasmic reticulum like chylomicrons are apparently stabilized by the presence of protein (Sabesin and Isselbacher 65) Although these droplets maintain their individuality an increase in their size does occur with longer absorption time It may be that an alteration in stabilizing forces leading to a change in droplet size during longer time intervals is essential following triglyceride synthesis and prior to the discharge of the droplets from the cell (i e chylomicron formation) Such an alteration could permit the droplets to coalesce as observed in the Golgi vacuoles The possibility of

other modifications in the fat molecules during this time cannot be excluded

Light microscopic radioautographs from the present study show a marked reduction in grain concentration at the base of the cells A similar reduction has been shown to occur during the absorption of labeled sugars and amino acids which suggests the possibility of an exit barrier to these molecules (Kinter, 61) Fat does not accumulate in large quantities in the para and infranuclear cytoplasm which would suggest a retardation to its transport from the cell surface The fat droplets may be quickly transported from this area into the connective tissue and dissipated

The evidence presented here therefore suggests that the events occurring in the Golgi apparatus take place at a rate slower than the absorption of fat at the lumenal surface A decrease in rate of transport through the endoplasmic reticulum could follow leading to an increase in the size of the droplets in the apical cytoplasm Ultimately large masses of fat may coalesce in the matrix of the cell as though representing an overflow from the endoplasmic reticulum as suggested by Palay and Revel (64)

The observations in this study indicate that a complete sequence in the pattern of absorption and transport can occur along the entire length of the villus The delay in absorption toward the proximal end of the villus may be due to the fact that the cells at the villous tip are more readily in contact with the lumenal contents (Verzar and McDougall, 36)

ACKNOWLEDGMENTS

This investigation was supported in part by a USPHS GRS grant FR 05371 04 and a National Science Foundation grant GB 1841

The author wishes to acknowledge the skillful technical assistance of Mrs Joan Simpson and Mrs Doris DeBruler

LITERATURE CITED

Adamstone F B and A B Taylor 1959 Golgi response in intestinal epithelial cells of rats to chyme received from fat fed donors J Morph 105 389–400

Ashworth C T and J M Johnston 1963 The intestinal absorption of fatty acid A biochemical and electron microscopic study J Lipid Res 4 454–460

Ashworth C T V A Stembridge and E Sanders 1960 Lipid absorption transport and hepatic assimilation studied with electron microscopy Am J Physiol 198 1326–1329

Bernhard K E Seelig and H Wagner 1956 Die Sezernierung von Körperfett in das Darmlumen Hoppe Seyler s Zeitschr Physiol Chem 304 138–147

Caro L G and R P van Tubergen 1962 High resolution autoradiography I Methods J Cell Biol 15 173–188

Cramer W and R J Ludford 1925 On cellular changes in intestinal fat absorption. J Physiol 60 342–346

Dalton A J 1961 Golgi apparatus and secretion granules In The Cell J Brachet and A E Mirsky eds Academic Press New York 2 603–619

Emmel V M 1945 Alkaline phosphatase in the Golgi zone of absorbing cells of the small intestine Anat Rec 91 39–47

Essner E and A B Novikoff 1962 Cytological studies on two functional hepatomas Interrelations of endoplasmic reticulum Golgi apparatus and lysosomes J Cell Biol 15 289–312

Isselbacher K J 1965 Metabolism and transport of lipid by intestinal mucosa Fed Proc 24 16–22

Johnston J M 1959 The absorption of fatty acids by the isolated intestine J Biol Chem 234 1065–1067

Karnovsky M J 1961 Simple methods for staining with lead at high pH in electron microscopy J Biophys Biochem Cytol 11 729–732

Kinter W 1961 Autoradiographic study of intestinal transport In Proceedings of the 12th Annual Conference on the Nephrotic Syndrome J Metcoff ed National Kidney Disease Foundation pp 59–68

Lacy D and A B Taylor 1962 Fat absorption by epithelial cells of the small intestine of the rat Am J Anat 110 155–186

Ladman A J H A Padykula and E W Strauss 1963 A morphological study of fat transport in the normal human jejunum Am J Anat 112 389–419

Laschi R and G Gasbarrini 1963 Contributo allo studio dell assorbimento intestinale mediante la microscopia elettronica Lo Sperimentale 113 239–250

Luft J H 1961 Improvements in epoxy resin embedding methods J Biophys Biochem Cytol 9 409–414

Mattson F H and R A Volpenhein 1964 The digestion and absorption of triglycerides J Biol Chem 239 2772–2777

McLaren A D and K L Babcock 1959 Some characteristics of enzyme reaction surfaces In Subcellular Particles T Hayashi ed Ronald Press New York pp 23–35

Millington P F O C Forbes J B Finean and A C Frazer 1962 Studies of the effects of aminopterin on the small intestine of rats

II Fat absorption defects following a single intramuscular injection Exp Cell Res 28 179–191

Millonig G 1961 The advantages of a phosphate buffer for OsO_4 solutions in fixation J Applied Phys 32 1637

Morehouse M G W P Skipski R L Searcy and L Spolter 1956 Absorption and distribution in the rat of lipids utilizing labeled glycerides and components In Biochemical Problems of Lipids G Popjak and E LeBreton eds Interscience New York pp 341–346

Palay S L and L J Karlin 1959 An electron microscopic study of the intestinal villus II The pathway of fat absorption J Biophys Biochem Cytol 5 373–384

Palay S L and J P Revel 1964 The morphology of fat absorption In Proc of an Internat'l Symp on Lipid Transport, H C Meng ed Charles C Thomas Springfield pp 33–43

Reynolds E S 1963 The use of lead citrate at high pH as an electron-opaque stain in electron microscopy J Cell Biol *17* 208 212

Rostgaard J and R. J Barrnett 1964 Absorption of lipid as micelles by microvilli of rat small intestine J Cell Biol 23 79A (abstract)

Sabesin S M and K J Isselbacher 1965 Protein synthesis inhibition mechanism for the production of impaired fat absorption Science *147* 1149–1151

Senior J R and K J Isselbacher 1960 Activation of long-chain fatty acids by rat-gut mucosa Biochim Biophys Acta *44* 399-400

——— 1961 Formation of higher glycerides from monopalmitin and palmityl-CoA by microsomes of rat intestinal mucosa Biochem Biophys Res Comm 6 274–278

——— 1962 Direct esterification of monoglycerides with palmityl coenzyme A by intestinal epithelial subcellular fractions J Biol Chem 237 1454–1459

Shepherd P and W J Simmonds 1959 Some conditions affecting the maintainance of a steady lymphatic absorption of fat Austral J Exp Biol 37 1–9

Strauss E W 1963 The absorption of fat by intestine of golden hamster *in vitro* J Cell *Biol 17 597–607*

——— 1964a Absorption of fat from solutions of mixed bile salt micelles by hamster intestine *in vitro* J Cell Biol 23 90A (abstract)

——— 1964b Fat absorption from oil in water emulsions by sacs of everted intestine from golden hamster *in vitro* J Cell Biol 23 124A (*abstract*)

Verzár F and E J McDougall 1936 Absorption from the Intestine Longmans Green London.

Wilson T H 1962 Intestinal Absorption Saunders Philadelphia

Weiner P 1928 Über Fettablagerung und Fettresorption im Darm Zeitsch mikr anat Forsch 13 197–268

Zeigel R F and A J Dalton 1962 Speculations based on the morphology of the Golgi systems in several types of protein-secreting cells J Cell Biol. *15* 45–54

PLATE 1

EXPLANATION OF FIGURES

1 Radioautograph of the upper one third of a villus after a one minute exposure to oleic acid H^3 chyme Grains are evenly distributed over the supranuclear cytoplasm of the epithelial absorptive cells Some grains are also present below the nuclei At the tip of the villus *grains are quite abundant in this location (arrow placed at the base* of the cells) The nuclei (n) and goblet cell (g) are relatively free of labeling Twenty-one day exposure Phase contrast × 600

2 Radioautograph of the side of a villus after two minutes exposure to labeled chyme Labeling is most intense in the supranuclear cytoplasm of the epithelial cells Less labeling is present below the nuclei The nuclei (n) appear to be unlabeled A distinct decrease in grain concentration is evident at the base of the epithelium (arrows) Less absorptive activity at the proximal end of this villus is indicated by the smaller number of grains present Ten day exposure Phase contrast × 600

3 Radioautograph of the upper one half of a villus after 20 minutes exposure to labeled chyme The greatest concentration of grains lies over the Golgi zone (arrow) of the epithelial cells The remaining grains are distributed as in figure 2 Few grains are present over the lamina propria Seven day exposure Phase contrast × 800

4 Radioautograph of the villus-crypt junction after two minutes exposure to labeled chyme Considerable labeling in the proximal villous absorptive cells is evident The junction is indicated by the arrow Fourteen day exposure Phase contrast × 800


1


2


3


4

PLATE 1

EXPLANATION OF FIGURES

1 Radioautograph of the upper one third of a villus after a one minute exposure to oleic acid H^3 chyme Grains are evenly distributed over the supranuclear cytoplasm of the epithelial absorptive cells Some grains are also present below the nuclei At the tip of the villus grains are quite abundant in this location (arrow placed at the base of the cells) The nuclei (n) and goblet cell (g) are relatively free of labeling Twenty-one day exposure Phase contrast × 600

2 Radioautograph of the side of a villus after two minutes exposure to labeled chyme Labeling is most intense in the supranuclear cytoplasm of the epithelial cells Less labeling is present below the nuclei The nuclei (n) appear to be unlabeled A distinct decrease in grain concentration is evident at the base of the epithelium (arrows) Less absorptive activity at the proximal end of this villus is indicated by the smaller number of grains present Ten day exposure Phase contrast × 600

3 Radioautograph of the upper one half of a villus after 20 minutes exposure to labeled chyme The greatest concentration of grains lies over the Golgi zone (arrow) of the epithelial cells The remaining grains are distributed as in figure 2 Few grains are present over the lamina propria Seven day exposure Phase contrast × 800

4 Radioautograph of the villus-crypt junction after two minutes exposure to labeled chyme Considerable labeling in the proximal villous absorptive cells is evident The junction is indicated by the arrow Fourteen day exposure Phase contrast × 800


5

PLATE 2

EXPLANATION OF FIGURE

5 Electron micrograph of the apical cytoplasm of an absorptive cell from near the tip of a villus Exposure to chyme was less than one minute Very small dense droplets of fat are present in the lumen of vesicular and elongate profiles of the endoplasmic reticulum throughout the cell × 19 000



PLATE 3

EXPLANATION OF FIGURE

6 Electron microscopic radioautograph of the apical cytoplasm of an absorptive cell at the tip of a villus The size and distribution of the fat droplets is similar to those in figure 5 A few small fat droplets are within slight vacuolar dilations of the Golgi apparatus (arrows) All grains are associated with areas of endoplasmic reticulum Most of these grains lie very close to or over droplets of fat × 22 000


6

PLATE 4

EXPLANATION OF FIGURES

7 Supranuclear cytoplasm of an absorptive cell after a one minute exposure to chyme Smooth membrane profiles belonging primarily to the Golgi *apparatus occupy much of the area to the* right of the nucleus (N) Accumulations of small fat droplets within vacuolar dilations are evident Vesicular profiles parallel to the Golgi cisternae (arrows) suggest that fat droplets might be separated from the main components of this organelle by pinching off of small fat containing vesicles Other vesicles in the field may represent simi lar products of this process or possibly portions of smooth endo plasmic reticulum × 25 000

8 Electron microscopic radioautograph Cross section near the apex of the nucleus of an absorptive cell from the middle side of a villus Two minutes exposure to labeled chyme The Golgi apparatus forms a crescent peripheral to the nucleus A few small droplets of fat are present in the endoplasmic reticulum (arrows) Golgi vacuoles (V) and intercellular space (IF) Note that the grains lie very close to some of the droplets × 22 000

7

8

I LATL 5

EXPLANATION OF FIGURES

9 Apical cytoplasm of an absorptive cell from near the tip of a villus after two minutes exposure to chyme Clearly defined droplets of fat are in abundance within the channels of the endoplasmic reticulum × 27 000

10 A portion of the Golgi apparatus from a cell near the tip of a villus exposed to chyme for two minutes The vacuoles are filled with numerous small droplets of fat Anastomosing tubular profiles project toward the lateral cell surface (PM) with indications of vesicle formation at the arrow × 33 000

11 A portion of the apical cytoplasm of a cell at the tip of a villus exposed to chyme for eight minutes The large masses of fat which form in the cell matrix is illustrated Although the edges of these dense masses are darkened there is no indication that they are enclosed by membranes Numerous smaller fat droplets prevail in the lumen of the endoplasmic reticulum × 35 000


10



PLATE 6

EXPLANATION OF FIGURE

12 Apical cytoplasm of an absorptive cell from the middle side of a villus after two minutes exposure to chyme The absorptive activity appears somewhat less than at the tip of the villus Small droplets of fat are present within the endoplasmic reticulum and are more numerous in the extreme apical cytoplasm The Golgi apparatus (G) is in separate clusters of smooth membrane components A considerable amount of fat has accumulated within this organelle producing vacuolar distentions of varying size ×16 000


G
G
G
12

PLATE 7

EXPLANATION OF FIGURE

13 Apical cytoplasm of a cell from near the tip of a villus exposed to chyme for 12 minutes The cell presents an appearance of being nearly saturated with droplets of fat The dilations of the endoplasmic reticulum surrounding the droplets are more enlarged owing to the increased size of the droplets and most of the profiles take on the appearance of individual vesicles Occasionally continuity of the lumen between the vesicular and flattened components of the reticulum are observed (arrows) × 22 000



PLATE 8

EXPLANATION OF FIGURE

14 Apical cytoplasm of two absorptive cells from near the base of a villus exposed to chyme for 12 minutes Numerous enlarged fat droplets are present within the lumen of the endoplasmic reticulum The fat content in the Golgi apparatus has increased substantially and the organelle is distended to form a band at the apex of the nucleus × 10 000


14

PLATE 9

EXPLANATION OF FIGURES

15 Apical cytoplasm of an absorptive cell at the tip of a villus exposed to chyme for 20 minutes The droplets enclosed within the endoplasmic reticulum are large and occupy much of the cytoplasm × 24 000

16 Supranuclear cytoplasm of a cell at the proximal end of a villus exposed to chyme for 20 minutes A thick band of fat filled Golgi vacuoles occupies much of the area above the nucleus (N) The vacuoles observed here can be roughly divided into three groups (1) those more apically located which contain large fat droplets equal in size to droplets in the apical endoplasmic reticulum at this time interval (2) vacuoles in which droplets have coalesced into larger aggregates and (3) vacuoles in which the droplet size resembles the smaller droplets present in the lateral intercellular spaces (IF) Smaller droplets can also be seen in smooth surfaced vesicular profiles (v) × 17 000

PLATE 9

EXPLANATION OF FIGURES

15 Apical cytoplasm of an absorptive cell at the tip of a villus exposed to chyme for 20 minutes The droplets enclosed within the endo plasmic reticulum are large and occupy much of the cytoplasm × 24 000

16 Supranuclear cytoplasm of a cell at the proximal end of a villus exposed to chyme for 20 minutes A thick band of fat filled Golgi vacuoles occupies much of the area above the nucleus (N) The vacuoles observed here can be roughly divided into three groups (1) those more apically located which contain large fat droplets equal in size to droplets in the apical endoplasmic reticulum at this time interval (2) vacuoles in which droplets have coalesced into larger aggregates and (3) vacuoles in which the droplet size resembles the smaller droplets present in the lateral intercellular spaces (IF) Smaller droplets can also be seen in smooth surfaced vesicular profiles (v) × 17 000

PLATE 10

EXPLANATION OF FIGURES

17 Conditions are the same as for figure 16 The three groups of Golgi vacuoles described in figure 16 are distinguishable here In places (arrows) portions of the endoplasmic reticulum closely approach the Golgi apparatus both on the distal and proximal aspects This juxtaposition may facilitate a transfer of fat droplets to and from the Golgi apparatus Note that the membranes of the endoplasmic reticulum lying closest to the Golgi vacuoles lack RNA granules × 23 000

18 Infranuclear cytoplasm of a cell near the proximal end of a villus exposed to chyme for 20 minutes The base of the cell is to the left Droplets of fat are present in the endoplasmic reticulum but in much smaller numbers than in the apical cytoplasm at this time interval The infranuclear droplets are about the same size as those in the intercellular spaces (IF) At the arrow the endoplasmic reticulum appears to fan out against the plasma membrane This suggests an imminent discharge of the enclosed fat droplets into the intercellular space × 21 000

Vestibular Projections to the Nuclei of the Extraocular Muscles [1]

DEGENERATION RESULTING FROM DISCRETE PARTIAL LESIONS OF THE VESTIBULAR NUCLEI IN THE MONKEY

ROBERT E McMASTERS [2] ARTHUR H WEISS [3]
AND MALCOLM B CARPENTER
Department of Anatomy College of Physicians and Surgeons Columbia University New York

ABSTRACT In 35 monkeys attempts were made to produce localized unilateral lesions in individual vestibular nuclei in order to study vestibular projections to nuclei of the extraocular muscles Portions of the medial superior and inferior vestibular nuclei were destroyed selectively lesions in Deiters nucleus involved small portions of either the superior or inferior vestibular nuclei Fiber degeneration was studied by the Nauta-Gygax technic

Exclusively ascending fibers from the superior vestibular nucleus project to ipsilateral extraocular nuclei Ascending fibers from the inferior vestibular arise only from rostral portions of the nucleus are not numerous and pass to all extraocular nuclei The medial vest bular nucleus projects ascending fibers via the MLF bilaterally asymmetrically and differentially to all extraocular nuclei Prominent projections pass to (a) the contralateral trochlear nucleus and (b) the contralateral intermediate cell column and the ipsilateral ventral nucleus of the oculomotor complex Ascending fibers from Deiters nucleus arising only from ventral portions of the nucleus project primarily to (a) the contralateral abducens and trochlear nuclei and (b) specific asymmetrical portions of the oculomotor complex

Ascending vestibular fibers f om the medial and lateral vestibular nuclei appear capable of mediating all patterned eye movements resulting from stimulation of ampullary nerves from individual semicircular canals Vestibular projections to nuclei of the extraocular muscles are most abundant to those nuclei innervating muscles whose primary functions concern horizontal and rotatory eye movements

The labyrinths the vestibular nuclei and secondary vestibular pathways projecting to the nuclei of the extraocular muscles appear to play a major role in the control of conjugate eye movements Anatomical evidence that the vestibular nuclei are concerned with conjugate eye movements appears to have a secure foundation since secondary vestibular fibers ascending in the medial longitudinal fasciculus project to all the nuclei of the extraocular muscles (Szentágothai 43 Brodal and Pompeiano 57 Carpenter 60 Carpenter and McMasters 63) Physiological studies (Szentagothai 52 Fluur 59 Cohen Suzuki and Bender 64) provide clear evidence of a precise functional correlation between particular semicircular canals and eye movements in specific directions The investigations of Szentágothai (50) leave little doubt that functionally the most important impulses mediating ocular movements in response to stimulation of the semicircular canals ascend in the medial longitudinal fasciculus (hereafter abbreviated MLF) These results suggest that impulses from individual semicircular canals must ultimately be transmitted differentially to all the nuclei of the extraocular muscles including specific subdivisions of the oculomotor nuclear complex Szentagothai s (43) studies of the distribution of degenerated fibers in the nuclei of the extraocular muscles following extensive unilateral lesions of the vestibular nuclei suggest a pattern of termination correlated with the representation of indi

[1] Thi I ti ti n w support d by a grant (NB-01538-06) from th In t tut of N urol gi l Dise ses nd Bl ndn of th N tion l In tit t of H lth Beth d 14 M ryl nd

[2] Postdoct l t in e in n o nat my suppo ted by g nt 2B 5242(C2) from th In t tut of N urol gi l Dise ses nd Blindnes

[3] Speci l f llow in neuro n t my supported by gr nt 7F11 NB-1225-01A1 from th In t tute of N urol gi l Dise se nd Blindn s

with respect to the median sulcus of the fourth ventricle and electrodes entered the brain stem at a small angle from the ventricular surface After electrode placement stimulating square wave currents of low voltage were used in attempts to identify the location of the electrode tip At what appeared to be optimal locations lesions were produced by a direct current of 2 or 3 ma at 400 volts applied for intervals of 10 or 15 seconds (timed electrically) After the lesions were produced the dura was carefully closed with 6–0 silk muscle layers were sutured and the skin closed with Michel clips

Following surgery physiological observations and neurological examinations were recorded at frequent intervals Photographs and cinematographic records were made of animals with noteworthy physiological disturbances In some animals attempts were made to stimulate the labyrinths calorically with ice water Animals were permitted to survive postoperatively for variable periods of time ranging from 12 to 34 days

At the conclusion of the observation period animals were anesthetized and perfused via the left ventricle of the heart with 500 ml of normal isotonic saline followed by 500 ml of 10% neutral formalin After adequate fixation the brains were sectioned in blocks perpendicular to the axis of the brain stem The brains and selected segments of the spinal cord of animals with appropriate lesions were cut serially at 20 μ on the freezing microtome all sections were preserved in multiunit plastic containers Multiple sections through the region of the lesion were stained with cresyl violet or by the Weil technic to facilitate determination of the location disposition and extent of the lesions Representative sections from all levels of the brain stem and various spinal segments were stained according to the Laidlaw modification of the Nauta and Gygax (54) technic

The nomenclature for the subdivisions of the oculomotor complex used in this study was that of Warwick (53) The representation of the extraocular muscles in the oculomotor complex is shown in figure 1 The cell column (white) medial to the dorsal nucleus and the intermediate cell column was not named by Warwick for convenience of description this nucleus which innervates the superior rectus muscle has been referred to as the medial nucleus (Carpenter and Strominger 64)

OBSERVATIONS

Lesions in the medial vestibular nucleus

In three monkeys discrete stereotaxic lesions were produced in the right medial vestibular nucleus The lesion in rhesus C 668 began in the rostral third of the medulla and terminated rostrally near the level of the abducens nucleus Although some fibers of the right facial nerve were destroyed by the lesion no part of the sixth nucleus was involved Throughout its extent the lesion was confined to the central part of the right medial vestibular nucleus without encroaching upon other vestibular nuclei or the reticular formation In rhesus C 672 two small lesions consisting actually of enlarged electrode tracks were limited to the right medial vestibular nucleus The ventral most lesion destroying a small part of the nucleus cuneatus and nucleus prepositus caudally was situated dorsal to the ventral border of the medial vestibular nucleus Both lesions terminated at levels caudal to the abducens nucleus

The lesion in rhesus C 710 began caudally in the dorsolateral part of the medial vestibular nucleus at the level of the dorsal acoustic tubercle As the lesion extended rostrally it destroyed the lateral part of the medial vestibular nucleus as well as a few fibers of the dorsal acoustic stria and the juxtarestiform body The lesion terminated at the level of the abducens nucleus without encroaching upon any part of the lateral or superior vestibular nuclei the abducens nucleus or the facial nerve A tiny dorsomedial part of the inferior vestibular nucleus was injured but there was no damage to the nucleus prepositus

In only one of these three animals were retrograde cell changes seen in adjacent vestibular nuclei In rhesus C 668 two unequivocally chromatolytic large cells were seen in the lateral vestibular nucleus Cells of the inferior vestibular nucleus appeared normal in all of these animals

vidual extraocular muscles in these nuclei The above concepts appear well supported even though the exact regions of termination of primary afferent fibers from the various parts of the receptor organ within the vestibular nuclei are not known (Lorente de No 26 31 33)

While it is recognized widely that conjugate eye movements can be induced by stimulation of areas of the frontal and occipital cortex (see reviews by Crosby and Henderson 48 and Crosby 53) it has not been possible to define fully the anatomical pathways involved in the transmission of these impulses (Brodal Pompeiano and Walberg 62) No direct fibers to the vestibular nuclei appear to originate from the cerebral cortex corpus striatum superior colliculus nucleus of the posterior commissure nucleus of Darkschewitsch or the periaqueductal gray (Szentágothai 43, Pompeiano and Walberg 57) The only known descending pathway to the vestibular nuclei consists of fibers originating from the interstitial nucleus of Cajal coursing in the MLF and terminating in the medial vestibular nucleus (Pompeiano and Walberg 57) Although corticofugal projections to the interstitial nucleus of Cajal have been reported in Marchi stained material (Mettler 35a 35b 35–36 Crosby and Henderson 48) and in Gross Bielschowsky preparations (Szentagothai 43) Pompeiano and Walberg (57) were unable to find any evidence of terminal degeneration in this nucleus after extensive cortical lesions Nevertheless it has been shown that stimulation of this nucleus in animals gives rise to vertical and rotatory eye movements (Szentagothai 43 Hyde and Toczek 62)

It is also known that electrical stimulation of middle regions of the cerebellar vermis (Hoshino 21 Mussen 27 Hare Magoun and Ranson 37 Dow and Moruzzi 58) produced ipsilateral conjugate horizontal eye movements Similar ipsilateral conjugate horizontal deviation of the eyes has been reported with stimulation of the interior of the cerebellum in cats and monkeys (Magoun Hare and Ranson 35 Hare Magoun and Ranson 37) It has been suggested (Dow and Moruzzi 58) that lobules VI and VII of the cerebellum might be particularly concerned with the coordination of ocular movements brought about by visual and auditory stimuli Even though these physiological data are clear and particular parts of the cerebellum have a massive projection to the vestibular nuclei (Thomas Kaufman Sprague and Chambers 56 Carpenter, 59 Walberg and Jansen 61 Walberg Pompeiano Brodal and Jansen 62) correlation of these physiological and anatomical findings is extremely difficult One further finding of note is the observation (Carpenter and Strominger 64) that some efferent fibers from the dentate nucleus project to specific parts of the oculomotor complex

Previous studies (Carpenter and McMasters 63 Carpenter and Strominger 65) have shown that discrete lesions of the MLF in the monkey result in retrograde cell changes in localized portions of the vestibular nuclear complex and preterminal fiber degeneration distributed differentially within the oculomotor nucleus These findings suggested that the individual vestibular nuclei may have a differential projection to the nuclei of the extraocular muscles including the subdivisions of the oculomotor nuclear complex The object of the current study was to determine the secondary vestibular projections from the individual vestibular nuclei to the nuclei of the extraocular muscles

MATERIAL AND METHODS

Thirty five rhesus monkeys were used in this study Attempts were made to produce discrete stereotaxic lesions in the individual vestibular nuclei on the right side Lesions worthy of analysis were produced in 20 animals Coordinate systems used were determined from dissections of formalin fixed heads with brains *in situ* (Carpenter and Whittier 52) Surgery was performed aseptically under Nembutal anesthesia and operative procedures were similar to those previously described (Carpenter McMasters and Hanna 63 Carpenter and McMasters 63) Briefly these consisted of a suboccipital craniotomy incision of the dura and introduction of electrodes according to prior calculations Lateral measurements were made

with respect to the median sulcus of the fourth ventricle and electrodes entered the brain stem at a small angle from the ventricular surface After electrode placement stimulating square wave currents of low voltage were used in attempts to identify the location of the electrode tip At what appeared to be optimal locations lesions were produced by a direct current of 2 or 3 ma at 400 volts applied for intervals of 10 or 15 seconds (timed electrically) After the lesions were produced the dura was carefully closed with 6–0 silk muscle layers were sutured and the skin closed with Michel clips

Following surgery physiological observations and neurological examinations were recorded at frequent intervals Photographs and cinematographic records were made of animals with noteworthy physiological disturbances In some animals attempts were made to stimulate the labyrinths calorically with ice water Animals were permitted to survive postoperatively for variable periods of time ranging from 12 to 34 days

At the conclusion of the observation period animals were anesthetized and perfused via the left ventricle of the heart with 500 ml of normal isotonic saline followed by 500 ml of 10% neutral formalin After adequate fixation the brains were sectioned in blocks perpendicular to the axis of the brain stem The brains and selected segments of the spinal cord of animals with appropriate lesions were cut serially at 20 μ on the freezing microtome all sections were preserved in multi unit plastic containers Multiple sections through the region of the lesion were stained with cresyl violet or by the Weil technic to facilitate determination of the location disposition and extent of the lesions Representative sections from all levels of the brain stem and various spinal segments were stained according to the Laidlaw modification of the Nauta and Gygax (54) technic

The nomenclature for the subdivisions of the oculomotor complex used in this study was that of Warwick (53) The representation of the extraocular muscles in the oculomotor complex is shown in figure 1 The cell column (white) medial to the dorsal nucleus and the intermediate cell column was not named by Warwick for convenience of description this nucleus which innervates the superior rectus muscle has been referred to as the medial nucleus (Carpenter and Strominger 64)

OBSERVATIONS

Lesions in the medial vestibular nucleus

In three monkeys discrete stereotaxic lesions were produced in the right medial vestibular nucleus The lesion in rhesus C 668 began in the rostral third of the medulla and terminated rostrally near the level of the abducens nucleus Although some fibers of the right facial nerve were destroyed by the lesion no part of the sixth nucleus was involved Throughout its extent the lesion was confined to the central part of the right medial vestibular nucleus without encroaching upon other vestibular nuclei or the reticular formation In rhesus C 672 two small lesions consisting actually of enlarged electrode tracks were limited to the right medial vestibular nucleus The ventral most lesion destroying a small part of the nucleus cuneatus and nucleus prepositus caudally was situated dorsal to the ventral border of the medial vestibular nucleus Both lesions terminated at levels caudal to the abducens nucleus

The lesion in rhesus C 710 began caudally in the dorsolateral part of the medial vestibular nucleus at the level of the dorsal acoustic tubercle As the lesion extended rostrally it destroyed the lateral part of the medial vestibular nucleus as well as a few fibers of the dorsal acoustic stria and the juxtarestiform body The lesion terminated at the level of the abducens nucleus without encroaching upon any part of the lateral or superior vestibular nuclei the abducens nucleus or the facial nerve A tiny dorsomedial part of the inferior vestibular nucleus was injured but there was no damage to the nucleus prepositus

In only one of these three animals were retrograde cell changes seen in adjacent vestibular nuclei In rhesus C-668 two unequivocally chromatolytic large cells were seen in the lateral vestibular nucleus Cells of the inferior vestibular nucleus appeared normal in all of these animals

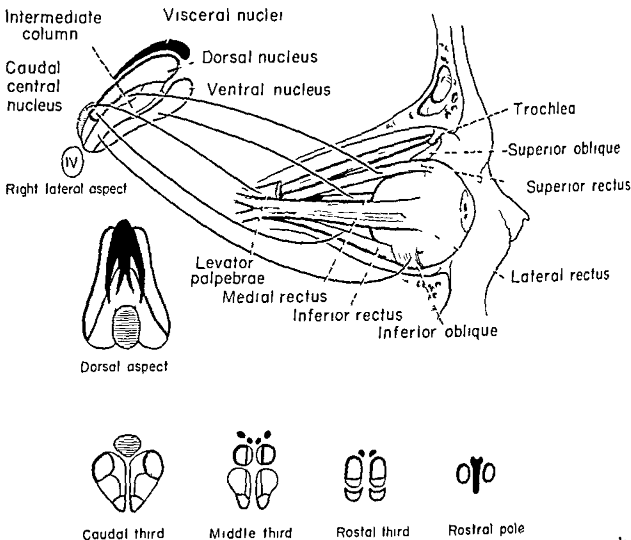


Fig 1 Schematic representation of the localization of the extraocular muscles within the oculomotor nuclear complex based upon studies in the rhesus monkey (Warwick 53) Cell columns composing the nucleus are shown in lateral and dorsal views and in transverse sections through various levels The visceral motor nuclei are shown in black The ventral nucleus (blue) innervates the medial rectus muscle The dorsal nucleus (red) innervates the inferior rectus muscle The intermediate cell column (yellow) innervates the inferior oblique muscle The cell column (white) medial to the dorsal nucleus and the intermediate cell column referred to as the medial nucleus innervates the superior rectus muscle The caudal central nucleus (lined) supplies fibers to the levator palpebrae superioris Fibers innervating the medial rectus inferior rectus and inferior oblique muscles are uncrossed fibers to the superior rectus muscle are crossed while those to the levator palpebrae muscle are both crossed and uncrossed The drawing in the upper right shows the positions of all the extraocular muscles in relation to the globe and bony orbit This figure from Truex and Carpenter (64) is reproduced with the permission of The Williams and Wilkins Company Baltimore Maryland

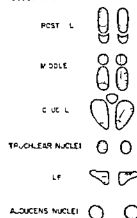
Preterminal degeneration Fiber degeneration resulting from the described lesions was remarkably similar and can be presented conveniently in a single composite description

At the level of the lesion abundant preterminal degeneration issuing from the ventral border of the medial vestibular nucleus coursed medially and somewhat rostrally Some of these fibers appeared to arborize about reticular neurons lateral to the medial longitudinal fasciculus while others passed between the fascicles of the MLF crossed the median raphe and were distributed to dorsomedial parts of the contralateral reticular formation and to the opposite vestibular nuclei Profuse degeneration was present in all parts of the right medial vestibular nucleus while on the left side degeneration in this

nucleus was found only in rostral parts In the lateral vestibular nuclei moderate degeneration was seen bilaterally with the greatest amount on the right side Degenerated fibers within Deiters nucleus distributed mainly to medial and ventral regions did not appear to arborize about large neurons Relatively modest preterminal degeneration was present bilaterally in the superior vestibular nucleus some of the degenerated fibers in this nucleus appeared to project to the cerebellum via the juxtarestiform body A considerable number of degenerated fibers was present bilaterally in all parts of the inferior vestibular nucleus particularly on the right side

The principal ascending fiber projections from the medial vestibular nucleus were to the nuclei of the extraocular muscles via the MLF Moderate preterminal degeneration from the medial vestibular nucleus passed bilaterally and asymmetrically to the abducens nuclei Preterminal degeneration in the left abducens nucleus was greatest in medial regions while on the right degeneration tended to be located in lateral parts of the nucleus Slightly more degeneration in the right abducens nucleus may have been due to the fact that degenerated fibers from the lesion partially traversed the nucleus *en route* to the MLF and nucleus of the opposite side No root fibers of the abducens nerve were degenerated Degenerated fibers from the medial vestibular nucleus entered the MLF in the region of the abducens nucleus and areas immediately rostral and caudal to it The greatest number of these fibers crossed the median raphe caudal to the rostral pole of the abducens nucleus entered the opposite MLF and were localized in the most ventromedial part of the bundle A smaller number of degenerated fibers entering the ipsilateral MLF tended to occupy more dorsal and lateral positions within the bundle Degenerated fibers in the ipsilateral MLF occasionally were seen in the lateral wing like process Preterminal degeneration in the trochlear nucleus contralateral to the lesion was profuse and evenly distributed throughout the nucleus Ipsilateral degeneration in the trochlear nucleus was sparse

In the oculomotor nuclear complex degeneration was bilateral and in general more profuse on the left side in caudal parts of the nucleus (fig 2) Progressively less fiber degeneration was seen in sections through the rostral parts of the nucleus Fiber degeneration within the oculomotor nucleus was distributed differentially In the caudal third of the left nuclear complex moderately heavy degeneration was present in the intermediate cell column and in the ventral nucleus On the right side caudally degeneration was localized to the dorsal nucleus and a tiny part of the ventral nucleus Through the middle third of the oculomotor complex most of the degeneration on the left side was in the dorsal nucleus and in the dorsal part of the intermediate cell column while on the right side degeneration was abundant in the ventral nucleus Through rostral portions of the oculo-



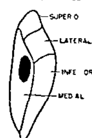


Fig 2 Schematic diagram of the distribution of secondary vestibular fibers passing to the nuclei of the extraocular muscles from a lesion in the medial vestibular nucleus In this and succeeding text figures the visceral nuclei and the rostral pole of the oculomotor complex have been omitted The vestibular nuclei are represented as seen in horizontal sections of the brain stem The area of the lesion is shown in black.

few if any ascending fibers in the MLF and (2) no fibers that descend in the MLF

In one other animal (C 732) a lesion destroyed the ventrolateral part of the superior vestibular nucleus and the dorsal part of the lateral vestibular nucleus No fibers of the brachium conjunctivum were interrupted by this lesion Ascending de generation confined to the lateral process of the ipsilateral MLF was distributed to the ipsilateral trochlear nucleus and the lateral somatic cell column of the oculo motor complex Although the amount of ascending degeneration in this case was not as great as in others of this group the distribution of degenerated fibers in the oculomotor nucleus was similar to that described above Degeneration in the ipsilateral oculomotor nucleus was vir tually limited to the dorsal nucleus in the rostral two thirds of the complex No preterminal degeneration was seen in the left half of the oculomotor nucleus De scending degeneration was present only in the ipsilateral vestibulospinal tract

Lesions in the inferior vestibular nucleus

In three animals small lesions were produced in parts of the right inferior vestibular nucleus without destroying por tions of other vestibular nuclei Rostral portions of this nucleus were destroyed selectively in two animals (C 741 and C 750) while a large part of the nucleus was destroyed caudally in a third animal (C 831)

The lesion in rhesus C 750 began in the middle third of the inferior vestibular nucleus and extended nearly to its rostral pole without involving any part of Deiters nucleus Throughout its extent the lesion was located in dorsal parts of the nucleus and did not infringe upon adjacent struc tures In rhesus C 741 the lesion destroyed the most lateral region of the rostral part of the inferior vestibular nucleus includ ing that part of this nucleus situated ven tral to the lateral vestibular nucleus Other structures concomitantly involved by this lesion included (1) small portions of the inferior cerebellar peduncle (2) small dorsal parts of the spinal trigeminal tract (3) some vestibular root fibers and (4) ventral portions of the superior sensory nucleus of the trigeminal nerve

The caudally situated lesion in rhesus C 831 began in the lateral part of the nucleus cuneatus and continued rostrally to destroy at least the caudal half of the inferior vestibular nucleus Neither the rostral part of this nucleus nor any part of the other vestibular nuclei was destroyed by the lesion Non vestibular structures damaged by this lesion included (1) a small dorsal part of the spinal trigeminal nucleus (2) root fibers of the glosso-pharyngeal nerve and (3) lateral portions of the tractus solitarius

Preterminal degeneration Although these lesions destroyed only portions of the inferior vestibular nucleus profuse preterminal degeneration was distributed to all parts of this nucleus and to ventro-lateral parts of the medial vestibular nu cleus In rhesus C 741 considerable pre terminal degeneration also was present in parts of the lateral and superior vestibular nuclei degeneration in these locations ap peared to be due to interruption of vesti bular root fibers Relatively sparse degen eration in these vestibular nuclei was seen in the other two animals of this group In all animals a large number of vestibular arcuate fibers coursed ventro-medially through the reticular formation crossed the median raphe and swept dorso-laterally into the opposite inferior vesti bular nucleus These fibers entered the ventral border of the nucleus by traversing parts of the spinal trigeminal nucleus Within the contralateral inferior vestibular nucleus preterminal degeneration usually was most profuse in rostral regions and tended to be greater in more medial areas A modest number of degenerated fibers also was seen in ventral portions of the left lateral vestibular nucleus Degenera tion in other contralateral vestibular nu clei was sparse

Ascending degeneration resulting from these lesions of the inferior vestibular nu cleus resulted only from lesions in the rostral part of the nucleus and was small compared with that seen in association with lesions in other parts of the vestibular complex Degeneration resulting from rostrally located lesions in rhesus C 741 and C 750 was remarkably similar Rela

tively sparse degeneration seen in the abducens nuclei tended to be greatest in rostral parts Rostral to the abducens nuclei a small amount of degeneration was seen in the right MLF These few fibers were located dorsally in the central part of the bundle Although degenerated fibers could not be detected in the left MLF in these transverse sections preterminal degeneration was seen clearly in the left trochlear nucleus No degenerated fibers from the right MLF could be followed into the right trochlear nucleus

Preterminal degeneration entering the oculomotor nuclear complex was bilateral sparse and asymmetrical Most of the degenerated fibers were seen on the right side in rostral portions of the ventral nucleus (fig 4) A very small number of fibers was seen in the right dorsal nucleus caudally The only degeneration seen in the lateral somatic cell columns on the left side was scattered in the caudal third of the intermediate cell column

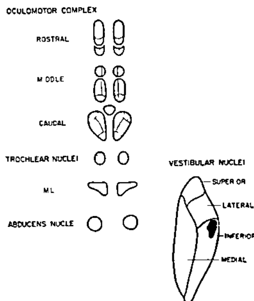


Fig 4 Schematic diagram of the distribution of secondary vestibular fibers passing to the nuclei of the extraocular muscles from a lesion in the rostral part of the inferior vestibular nucleus Ascending fibers from this vestibular nucleus appear relatively sparse compared with those from other vestibular nuclei and no ascending fibers originated from the caudal half of the inferior vestibular nucleus The lesion is shown in black

this degeneration was sparse No degeneration was seen in the interstitial nucleus of Cajal the nucleus of Darkschewitsch or in the nucleus of the posterior commissure on either side

Descending degeneration in rhesus C 741 and C 750 was confined to the dorsal part of the right MLF caudal to the lesion Although the amount of degeneration was small it could be followed for a short distance in the medulla No descending degeneration in the MLF was seen lateral to the corticospinal decussation or in the sulcomarginal area of the spinal cord No fibers of the vestibulospinal tract were degenerated in either of these animals

The lesion destroying caudal portions of the inferior vestibular nucleus (C-831) produced no ascending or descending degeneration in the MLF on either side No preterminal degeneration was found in any of the nuclei of the extraocular muscles Moderate ascending degeneration in the contralateral medial lemniscus appeared to be due to concomitant injury to the nucleus cuneatus the spinal trigeminal nucleus and the nucleus solitarius No degeneration was seen in multiple sections of the spinal cord

Lesions involving the lateral and inferior vestibular nuclei

In six monkeys well localized lesions on the right side destroyed portions of the lateral and inferior vestibular nuclei without injuring any part of the medial or superior vestibular nuclei Electrodes used to produce these lesions entered the dorsal surface of the lower brain stem slightly caudal to the dorsal acoustic tubercle traversed the oral part of the inferior vestibular nucleus in an oblique manner and entered the central or ventral parts of the lateral vestibular nucleus Although the lesions in these animals were not identical they were strikingly similar Destruction within the inferior vestibular nucleus in all instances was confined to the rostral third of the nucleus and included the oral pole of the nucleus ventral to the caudal part of Deiters nucleus Destruction within the rostral part of the inferior vestibular nucleus was least in rhesus C-727 and C-736 The lesions in the lateral vestibular nuclei destroyed ventral parts

of the nucleus caudally and virtually the entire nucleus in more rostral areas Small groups of large cells were preserved in the dorsocaudal part of the lateral vestibular nucleus in all animals While the lesions did not terminate precisely at the rostral border of the lateral vestibular nucleus, they did not extend into the superior vestibular nucleus because of the ventral inclination of the electrode Vestibular root fibers appeared to be completely interrupted by the lesions in all except one animal In rhesus C 755 the more dorsally located root fibers which in large part pass to the superior vestibular nucleus and the cerebellum, were spared Adjacent structures concomitantly involved by the electrode track included (1) a modest number of primary and secondary auditory fibers near the dorsal cochlear nucleus and (2) a minute dorsal part of the inferior cerebellar peduncle (rhesus C 755) Rostrally the lesions extended ventral to the vestibular nuclear complex and involved variable numbers of facial nerve root fibers and secondary trigeminal fibers arising from the dorsal part of the superior sensory nucleus of the trigeminal nerve (i e the dorsal trigeminal tract)

Preterminal degeneration Fiber degeneration resulting from these lesions involving parts of the lateral and inferior vestibular nuclei was remarkably similar and can be presented in a single composite description

Profuse preterminal degeneration was present in all parts of the ipsilateral lateral vestibular nucleus not destroyed by the lesion and in the lateral two thirds of the adjacent medial vestibular nucleus A considerable number of degenerated fibers could be followed dorsally into the cerebellum via the juxtarestiform body A moderate number of degenerated fibers coursed ventromedially into the dorsal part of the reticular formation where some fibers arborized extensively about large neurons At levels through the abducens nucleus bundles of degenerated fibers coursed medially ventral to this nucleus some of these fibers entered the ipsilateral abducens nucleus while a larger number crossed the median raphe to enter the contralateral nucleus Fiber degeneration within the contralateral abducens nucleus was quantitatively much greater particularly in rostral parts of the nucleus (fig 5)

The principal ascending secondary vestibular fibers entered the medial longitudinal fasciculi in the vicinity of the abducens nuclei In sections through the abducens nuclei fiber degeneration within the MLF was bilateral with the greatest number of degenerated fibers in the left fasciculus On the left side these fibers were located in the ventromedial part of the bundle, while degenerated fibers on the right side seemed somewhat scattered at this level Rostral to the abducens nuclei the preponderance of ascending degeneration in the left *MLF* was more evident Fiber degeneration in the left MLF was largely localized in a ventromedial zone while that in the right MLF was located more dorsally and somewhat removed from the medial border of the bundle Although the configuration of

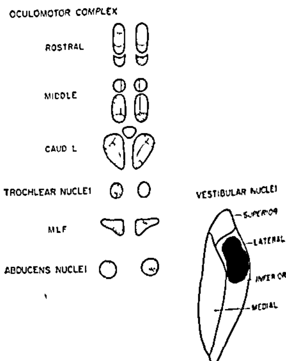


Fig 5 Schematic diagram of the distribution of secondary vestibular fibers passing to the nuclei of the extraocular muscles from a lesion involving the lateral vestibular nucleus and the rostral pole of the inferior vestibular nucleus This is the only lesion of the vestibular nuclei that produced degeneration passing to the medial nucleus Ascending fibers from the lateral vestibular nucleus arise only from ventral portions of the nucleus The lesion is shown in black

the MLF changes in the upper pons and isthmus region ascending degenerated fibers in these fasciculi retained their same relative positions at all levels No degenerated ascending fibers of the MLF were observed to cross the median raphe in the upper pons or isthmus region

Sections through the trochlear nuclei revealed relatively profuse preterminal degeneration confined to the left side in five of the six animals in this group Degenerated fibers entered the ventral surface of the left trochlear nucleus and were distributed to all parts Relatively few of these fibers arborized extensively about individual cells No degenerated fibers were seen in the right trochlear nucleus In one animal (C-736) no preterminal degeneration was seen in the trochlear nucleus on either side

Preterminal degeneration passed bilaterally into the oculomotor nuclear complex and was distributed differentially in the lateral somatic cell columns (fig 5) The most abundant degeneration seen on the left side was distributed selectively to the intermediate cell column and the medial nucleus Degeneration in these cell columns was present in the caudal two-thirds of the complex with the most profuse degeneration caudally Sparse degeneration in the rostral third of the complex on the left was confined to the ventral part of the dorsal nucleus Less profuse preterminal degeneration in the right somatic cell columns was discretely localized to (1) the ventral nucleus throughout its caudorostral extent and (2) the caudal third of the dorsal nucleus Other somatic cell columns were free of degeneration No degenerated fibers ascending in the MLF were observed to enter the caudal central nucleus or the midline visceral nuclei Preterminal degeneration passing into the interstitial nucleus of Cajal was seen only on the left side in three animals (C-727 C-734 and C 748) and was predominantly on the left side in two other animals (C-742 and C 755) Although degeneration entering the left interstitial nucleus was relatively profuse many of these fibers did not arborize about the soma of these cells in the manner frequently seen in association with lesions of the MLF (Carpenter and McMasters 63) In one animal (C 736) no unequivocal preterminal degeneration was seen in the interstitial nucleus of Cajal on either side

Other ascending degeneration observed in the brain stem appeared to be the result of concomitant injury to adjacent non vestibular structures In three animals (C 742 C-748 and C-755) a modest number of secondary auditory fibers was degenerated in the contralateral lateral lemniscus as a consequence of injury to the dorsal cochlear nucleus These fibers could be followed into the nucleus of the lateral lemniscus and the ventral part of the inferior colliculus A small number of these fibers bypassing the inferior colliculus projected to the magnocellular part of the medial geniculate body Injury to the dorsal part of the superior sensory nucleus of the trigeminal nerve and the area medial to it was associated with ascending degeneration in the dorsal trigeminal tract (Carpenter 57) The uncrossed fibers in this tract could be followed into the medial part of the arcuate nucleus of the thalamus

Caudal to the principal part of the lesion degenerated vestibular arcuate fibers originated from the rostral part of the inferior vestibular nucleus in three animals (C-742 C 748 and C-755) These fibers coursed through the reticular formation in small bundles and crossed the median raphe the greatest number of fibers was present at more rostral levels Contralaterally most of these fibers entered the inferior vestibular nucleus though some appeared to enter caudal and ventral portions of the lateral vestibular nucleus The overall appearance and distribution of these arcuate fibers was similar to that seen in animals with lesions limited to the rostral part of the inferior vestibular nucleus

Descending degeneration resulting from these lesions of the lateral and inferior vestibular nuclei was similar Caudal to the abducens nuclei moderate degeneration was present in the ventromedial part of the left MLF A smaller number of degenerated fibers occupied a dorsolateral location in the right MLF At more caudal levels in the medulla the relative amounts of descending degeneration in the MLF on

each side seemed to change though the locations of these degenerated fibers remained constant At levels through mid portions of the hypoglossal nuclei a greater number of degenerated fibers was found in the right MLF, the number of degenerated fibers in the left MLF diminished gradually so that at the level of the corticospinal decussation no degenerated fibers could be detected on that side A modest amount of descending degeneration persisted in the dorsal part of the right MLF lateral to the pyramidal decussation These fibers entered the sulcomarginal area of the spinal cord and descended as far as midcervical spinal levels (C 734 C 742 C 748 and C 755) The number of descending degenerated fibers in this location was modest

Relatively profuse degeneration was seen ipsilaterally in medial portions of the medullary reticular formation lateral to the MLF Occasional degenerated fibers arborized about reticular neurons in this region A considerable part of the degeneration in this location probably represented fastigioreticular fibers concomitantly interrupted by the lesions in the vestibular nuclei

Degeneration in the ipsilateral vestibulospinal tract could be followed throughout the medulla, but was identified most readily at caudal levels where fibers formed a discrete bundle in the retro olivary region These fibers entered the ventral part of the lateral funiculus of the spinal cord Although no systematic study of the vestibulospinal tract in the spinal cord was made in these animals degenerated fibers in this tract could be clearly identified in different animals in all spinal segments studied including those of the sacral spinal cord Preterminal degeneration in the spinal gray in all cases was relatively more abundant in cervical and lumbar segments than in thoracic segments Degeneration confined to the right side was distributed mainly to the region corresponding to lamina VIII of Rexed (52) Relatively few of these fibers arborized about large motor neurons Virtually no degeneration was found in lamina IX of Rexed

Physiological observations

Although the major purpose of this study was to determine the secondary vestibular projections to the nuclei of the extraocular muscles certain noteworthy physiological observations were made during the postoperative period

Animals with lesions involving portions of the superior vestibular nucleus tended to develop head tilting towards the opposite shoulder Lesions in other vestibular nuclei usually were associated with tilting of the head towards the side of the lesion The degree and persistence of this postural abnormality was greatest in those animals with lesions which destroyed portions of the inferior and lateral (ventral part) vestibular nuclei Destruction of portions of the medial vestibular nucleus resulted in only mild transient ipsilateral head tilt

Nystagmus seen postoperatively in ten animals with verified unilateral lesions in the vestibular nuclei was transient relatively mild and disappeared two to three days following surgery All of the animals (three) with lesions of the inferior vestibular nucleus exhibited nystagmus In two of these animals the nystagmus was predominantly rotatory in a clockwise direction in the third animal (C 831) positional nystagmus mainly vertical could be demonstrated by holding the animal in a supine position Clockwise rotary nystagmus was seen in two of the three animals with lesions in the medial vestibular nucleus Only one of the eight animals with lesions involving the superior vestibular nucleus had detectable nystagmus Nystagmus associated with lesions of the lateral and inferior vestibular nuclei usually was compound involving rotatory and horizontal components

Most of the animals exhibited a mild but definite gaze preference to the side opposite the lesion in the immediate postoperative period This gaze preference was not a forced deviation of the eyes to the opposite side as seen with lesions in the abducens nucleus (Carpenter McMasters and Hanna 63) and could not be correlated with destruction of any particular vestibular nucleus In only one animal (C 727) was a dissociation of eye movements seen This animal appeared to have a paresis of left ocular adduction

on attempted lateral gaze to the right side No nystagmus of any kind was seen The significance of this observation is questionable since other animals with almost identical lesions did not show this dissociation of eye movements

DISCUSSION

While physiological studies (Szentagothai 52 Fluur 59 Cohen Suzuki and Bender 64) provide a clear correlation between particular semicircular canals and eye movements in specific directions anatomical data regarding the pathways by which these impulses are conducted differentially to individual extraocular nuclei and their subdivisions are incomplete Studies of Walberg Bowsher and Brodal (58) provide detailed information concerning the differential distribution of primary vestibular fibers within the vestibular nuclear complex but the precise regions of the vestibular nuclei which receive primary vestibular fibers from particular parts of the receptor organ are not known Golgi studies by Lorente de No (33) indicate that fibers from the maculae and cristae of the semicircular ducts have in part a different central representation though no clearly selective distribution of afferents from the various receptor portions of the labyrinth to the subdivisions of the vestibular nuclear complex has been established Electro physiological evidence (Eckel 54) suggests that fibers from the crista of the horizontal duct probably are distributed to parts of the lateral and medial vestibular nuclei

Szentágothai (43 52) attempted to correlate the patterns of conjugate eye movements obtained by stimulaing individual semicircular canals with anatomical data derived from extensive unilateral lesions of the vestibular nuclei Degeneration resulting from these lesions passed via the MLF chiefly to the contralateral abducens and trochlear nuclei and bilaterally and asymmetrically to subdivisions of the oculomotor nuclear complex Although the somatotopic localization of cell groups within the oculomotor complex used in his study was less precise than that later determined by Warwick (53) degeneration was reported to pass to (1) ipsilateral middle portions of the complex considered to innervate the medial rectus muscle (2) contralateral caudal parts of the complex innervating the superior rectus muscle and (3) contralateral rostral parts of the complex innervating the inferior rectus and inferior oblique muscles Root fibers from all of these cell groups were regarded as uncrossed except for those passing to the superior rectus muscle These observations were considered to provide an anatomical explanation compatible with the reported physiological results Thus stimulation of one semicircular canal would provoke simultaneous contractions in a single pair of extraocular muscles as follows (1) *horizontal canal* ipsilateral medial rectus and contralateral lateral rectus (2) *anterior canal* ipsilateral superior rectus and contralateral inferior oblique and (3) *posterior canal* ipsilateral superior oblique and contralateral inferior rectus Subsequent anatomical studies (Szentagothai 64) disclosed that fiber projections arising from the rostral part of the medial vestibular nucleus and the superior vestibular nucleus were chiefly responsible for the pattern of differential degeneration in the nuclei of the extraocular muscles described above Ascending fibers from other parts of the vestibular nuclear complex were considered to be related to the functional effects of the utricular macula upon extraocular muscles

The physiological studies of Fluur (59) were similar to those of Szentágothai (52) with respect to the horizontal canal but electromyographic data demonstrated activation of the appropriate medial and lateral rectus muscles and reciprocal inhibition in the antagonistic muscles Conjugate upward eye movements elicited by stimulating the nerve from the anterior canal produced electromyographic activation bilaterally in the superior rectus and inferior oblique muscles and bilateral reciprocal inhibition in the inferior rectus and superior oblique muscles Conjugate downward movement of the eyes elicited by stimulating the nerve from the posterior canal was shown to activate bilaterally the inferior rectus and superior oblique muscles and reciprocally inhibit bilaterally the superior rectus and inferior oblique muscles

The physiological results of Cohen Suzuki and Bender (64) differed from those of Fluur in that these authors found upward and downward eye movements resulting from stimulation of single anterior or posterior ampullary nerves were dissociated rather than conjugate These experimental results indicated that the extraocular muscle activity evoked by electrical stimulation of ampullary nerves in the alert cat is highly organized and exceedingly complex Ocular movements produced in unanesthetized cats by stimulation of ampullary nerves was accomplished by a pattern of contractions and relaxations involving all extraocular muscles No eye movement was produced by contraction of a single extraocular muscle Stimulation of a single ampullary nerve produced much stronger activation of one extraocular muscle on each side and weaker activation of two other extraocular muscles on each side According to these authors each of the six extraocular muscles attached to each eye receives primary excitatory synaptic activation from one of the six semicircular canals and synergistic excitatory activation from two other canals Three of the six semicircular canals in addition, are said to exert inhibitory influences on each of the extraocular muscles These experiments demonstrating the potent control which the semicircular canals indirectly exert upon extraocular muscles indicate that primary and synergistic excitatory and inhibitory influences from the semicircular canals must be summated in a precise fashion to produce eye movements in particular directions

Anatomical evidence (Brodal and Pompeiano 57) based upon retrograde cell changes indicates that ascending vestibular projections contained largely in the MLF originate from all vestibular nuclei and are diffusely organized The majority of ascending fibers in the MLF are assumed to be ascending branches of dichotomizing axons, but some fibers undoubtedly are axons of cells with only ascending processes These authors suggest that ascending fibers to the oculomotor and trochlear nuclei are derived with some preponderance from the medial and superior vestibular nuclei, relatively more ascending fibers considered to bypass the oculomotor nucleus were thought to arise from the lateral and inferior vestibular nuclei

Most authors (Muskens 14 Leidler 16 Gray 26 Rasmussen 32 Buchanan '37 Gerebtzoff 41) agree that fibers from the superior vestibular nucleus only ascend in the MLF and are exclusively uncrossed Ascending fibers from the medial vestibular nucleus have been described as crossed (Muskens 14 Gray 26 P van Gehuchten 28, Rasmussen 32) though other authors (Satoh 29 Buchanan 37 Ferraro Pacella and Barrera 40 van Beusekom 55) report both crossed and uncrossed ascending fibers Findings with respect to ascending fibers from the lateral vestibular nucleus also vary but most investigators (Russell 1897 Probst 00, Fraser 01 Leidler 16 Sachs and Alvis 21 Kaida 29 Satoh 29 Buchanan 37 Gerebtzoff '40) regard these fibers as both crossed and uncrossed While oral portions of the inferior vestibular nucleus may give rise to a few fibers which ascend in the MLF such fibers do not appear numerous (Carpenter 60)

Even though these studies provide important information concerning the origins and courses of ascending secondary vestibular fibers details concerning their terminations and differential distribution within the extraocular nuclei are incomplete

The current study of secondary vestibular projections to the nuclei of the extraocular muscles is based upon preterminal degeneration resulting from localized lesions in subdivisions of the vestibular nuclear complex Because of the spatial disposition of these nuclei it was not possible to produce lesions confined strictly to each anatomical subdivision of this complex However it was possible to produce localized lesions in the inferior medial and superior vestibular nuclei which did not involve other subdivisions of this complex While it is possible that lesions in the medial vestibular nucleus may concomitantly interrupt some secondary vestibular fibers from the lateral and inferior vestibular nuclei as suggested by Szentágothai (64) it was our impression that most of these fibers coursed ventral to the medial vestibular nucleus or through ventral portions of it (Ferraro Pacella and Barrera 40) rather than through central regions of the nucleus Other data obtained in this study

support this view In two animals (C-667 and C-728) attempts to produce lesions in the medial vestibular nucleus destroyed localized areas immediately ventral to the nucleus These lesions interrupted large numbers of efferent fibers from both the medial and lateral vestibular nuclei as evidenced by (1) marked retrograde cell changes in these nuclei (2) profuse degeneration in the vestibulospinal tract and descending MLF and (3) degeneration passing to all of the nuclei of the extraocular muscles distributed in a pattern characteristic of efferent fibers from both the medial and lateral vestibular nuclei The amount of degeneration seen in the nuclei of the extraocular muscles greatly exceeded that found following lesions confined to either the medial or lateral vestibular nuclei

Lesions of the lateral vestibular nucleus always involved portions of either the inferior or superior vestibular nuclei In most cases it was possible to distinguish ascending secondary vestibular fibers arising from the superior vestibular nucleus from those originating in Deiters nucleus We were unable to make any similar distinction between ascending fibers arising from Deiters nucleus and rostral parts of the inferior vestibular nucleus Although the patterns of preterminal degeneration in the nuclei of the extraocular muscles following lesions of the inferior medial and lateral vestibular nuclei show basic similarities certain qualitative and quantitative differences are apparent

Although variable amounts of degeneration commonly were seen in the ipsilateral medullary reticular formation in association with these lesions of the vestibular nuclei a considerable part of this degeneration appeared to be due to concomitant interruption of efferent cerebellar fibers that traverse the vestibular nuclei In contrast sections of the brain stem above the level of the abducens nuclei revealed either no degeneration or very sparse degeneration in the reticular formation No secondary vestibular fibers ascending in the brain stem reticular formation could be traced into the trochlear or oculomotor nuclei on either side These findings suggest that ascending vestibular impulses transmitted via the reticular formation to nuclei of the extraocular muscles must involve multisynaptic pathways

Secondary vestibular fibers projecting to the nuclei of the extraocular muscles ascend exclusively in the MLF Fibers from the superior vestibular nucleus enter the lateral process of the MLF rostral to the facial genu are all uncrossed and are distributed differentially to ipsilateral nuclei of the extraocular muscles Ascending fibers from the inferior medial and lateral vestibular nuclei are crossed and uncrossed and enter the MLF in the immediate vicinity of the abducens nuclei Fibers crossing to the opposite MLF all appear to decussate near the abducens nuclei Ascending fibers from the inferior vestibular nucleus appear to arise mainly from the rostral third of this nucleus and are less numerous than those from other vestibular nuclei Fibers from the inferior medial and lateral vestibular nuclei project bilaterally assymmetrically and differentially upon the abducens nuclei and subdivisions of the oculomotor nuclei Certain anatomical subdivisions of the oculomotor nuclear complex appear to receive overlapping projections from these three vestibular nuclei Fibers projecting to the oculomotor complex are confined to the lateral somatic cell columns

Preterminal degeneration resulting from small lesions in the medial vestibular nucleus is distributed bilaterally and asymmetrically to all the nuclei of the extraocular muscles Degeneration in the abducens nuclei is confined virtually to the half of the nucleus ipsilateral to the lesion (fig 2) The greatest number of ascending fibers are in the ventromedial part of the contralateral MLF Degeneration within the trochlear nuclei is overwhelmingly greatest contralaterally In the oculomotor nuclear complex ipsilateral degeneration is present in the ventral nucleus at all levels with the greatest concentration in the rostral two-thirds of the nucleus degeneration in the dorsal nucleus is present caudally while scattered degeneration is present in the intermediate nucleus further rostrally Contralaterally degeneration is present mainly in portions of the intermediate cell column and dorsal nucleus at different levels

The pattern of projection of secondary vestibular fibers from the medial vestibular nucleus suggests that impulses from this nucleus could influence the activity of both abducens nuclei (asymmetrically) and the contralateral trochlear nucleus (ipsilateral superior oblique muscle) Impulses conveyed by these fibers to the oculomotor complex would seem capable of influencing the activity of (1) the ipsilateral medial rectus muscle (also the inferior oblique and inferior rectus to a lesser degree) and (2) the contralateral inferior oblique muscle (and to a lesser extent the inferior and medial rectus muscles)

Lesions of the superior vestibular nucleus concomitantly destroyed portions of the brachium conjunctivum in seven animals As a consequence of these lesions degenerated fibers from the superior vestibular nucleus entered the ipsilateral MLF rostral to the genu of the facial nerve No ascending degeneration was seen in the contralateral MLF Degenerated fibers located in the most ventral part of the brachium conjunctivum decussated and passed to the contralateral red nucleus and thalamus After crossing to the opposite side a small number of cerebellar efferent fibers passed dorsally medial to the red nucleus and entered mainly the middle third of the oculomotor complex The largest number of these cerebello oculomotor fibers passed into the area of the medial nucleus a cell group innervating the superior rectus muscle on the opposite side In animals with lesions involving only the brachium conjunctivum and the superior vestibular nucleus these degenerated cerebellar efferent fibers constituted the only degeneration seen on the left side in the oculomotor complex Crossed cerebello-oculomotor fibers have been commented upon by several authors (Klimoff 1896 Wallenberg 05 A van Gehuchten 05 Allen 24 Clark 36 Gerebtzoff 41) and are considered in detail in a recent paper (Carpenter and Strominger 64)

Szentagothai (64) has produced lesions in the superior vestibular nucleus which like ours have involved portions of the brachium conjunctivum His illustrations demonstrate the degeneration in the contralateral somatic cell columns of the oculomotor nucleus as described above but he considered the crossed degeneration to arise from the superior vestibular nucleus This interpretation does not seem to be supported by other anatomical evidence because (1) lesions destroying the superior vestibular nucleus and the dorsal part of Deiters nucleus (C 732) produce ascending degeneration only in the ipsilateral MLF and (2) lesions of the dentate nucleus produce degeneration that can be followed into the contralateral oculomotor nucleus (Carpenter and Strominger 64)

Exclusively ascending fibers from the superior vestibular nucleus pass only to ipsilateral nuclei of the extraocular muscles (fig 3) The secondary vestibular projection to the abducens nucleus is sparse but that to the trochlear nucleus is profuse In the oculomotor nuclear complex fibers from this nucleus are distributed exclusively to subdivisions which innervate the inferior rectus and the inferior oblique muscles These observations suggest that ascending fibers from the superior vestibular nucleus may provide controlling influences for muscles involved primarily in vertical or rotatory eye movements Consideration of these anatomical findings in conjunction with recent physiological data (Cohen Suzuki and Bender 64) suggests that some of the secondary vestibular fibers arising from the superior vestibular nucleus may be concerned with inhibitory activities The latter authors noted that no excitatory influences from any of the semicircular canals were observed in the ipsilateral inferior oblique or the contralateral superior oblique muscles The superior vestibular nucleus is the only vestibular nucleus which gives rise to secondary fibers distributed in this manner On the basis of these data secondary vestibular fibers passing from the superior vestibular nucleus to the rostral part of the dorsal nucleus may be concerned with synergistic activation of the ipsilateral inferior rectus muscle a response reported to occur following selective stimulation of the ampullary nerve from the posterior canal Judging from our findings the projection to the dorsal nucleus (inferior rectus) is quantitatively greater than that to the intermediate cell column (inferior oblique)

The only lesions of the inferior vestibular nucleus which appear to give rise to

ascending degeneration in the MLF are those involving the rostral third of this nucleus (fig 4) The number of ascending fibers from this nucleus is small and may only indicate that lesions were not optimally located Studies of retrograde cell changes in the vestibular nuclei following discrete lesions in the MLF near the abducens nuclei (Carpenter and Mc Masters 63 Carpenter and Strominger 65) indicate that chromatolytic cells in the inferior vestibular nucleus are most numerous in ventromedial regions Fibers passing to the abducens nuclei are more modest in amount and more symmetrical in distribution than those seen following lesions in either the medial or lateral vestibular nuclei Rostral to the abducens nuclei most of the degenerated fibers are in the ipsilateral MLF The small number of fibers in the left MLF project to the trochlear nucleus and the caudal portions of the intermediate cell column No degeneration was found in the ipsilateral trochlear nucleus Within the oculomotor nucleus ipsilateral degeneration was moderate in the rostral parts of the ventral nucleus and sparse in the dorsal nucleus caudally Ipsilateral degeneration in the oculomotor nuclear complex was qualitatively similar to that associated with lesions of the lateral vestibular nucleus

Evidence from this study indicates that ascending secondary vestibular fibers arising from the dorsal part of the lateral vestibular nucleus are either very sparse or completely lacking Lesions destroying the superior vestibular nucleus and the dorsal part of the lateral vestibular nucleus produced ascending degeneration only in the ipsilateral MLF distributed in a pattern identical with that found following lesions involving only the superior vestibular nucleus Since the dorsal part of Deiters nucleus receives relatively few primary vestibular fibers (Brodal Pompeiano and Walberg 62) it has been referred to as the "non vestibular part of Deiters nucleus Afferent fibers to this part of Deiters nucleus are derived from anterior portions of the cerebellar vermis (lobules IV and V) (Walberg and Jansen 61) and from rostral parts of the ipsilateral fastigial nucleus (Walberg Pompeiano Brodal and Jansen 62) Even so it is possible that some units in the so-called "non vestibular" part of Deiters nucleus may respond to labyrinthine stimulation via feed back systems from the cerebellum

The bulk of the ascending secondary vestibular fibers from the lateral vestibular nucleus arise from ventral portions of the nucleus that receive primary vestibular fibers Although most of our lesions of the lateral vestibular nucleus concomitantly involved the rostral pole of the inferior vestibular nucleus the pattern and amount of degeneration suggest that a far greater number of ascending fibers arise from the lateral vestibular nucleus On the basis of our data the greatest difference between ascending fibers from the lateral and inferior vestibular nuclei is the extensive contralateral projection arising from the lateral vestibular nucleus Fibers entering the contralateral abducens nucleus are much more numerous than in the ipsilateral nucleus (fig 5) The contralateral trochlear nucleus receives a large number of secondary vestibular fibers from the lateral vestibular nucleus none appear to enter the ipsilateral trochlear nucleus The distribution of secondary vestibular fibers in the oculomotor nuclear complex is asymmetrical differential and remarkably similar to that associated with lesions in the medial vestibular nucleus (cf figs 2 and 5) Notable differences include the lack of a projection from the lateral vestibular nucleus to the ipsilateral intermediate cell column and a relatively modest contralateral projection to the medial nucleus (superior rectus)

These observations indicate that secondary vestibular fibers passing to the nuclei of the extraocular muscles from the superior vestibular nucleus are different from those of all other vestibular nuclei These fibers differ in that they (1) are entirely uncrossed and (2) project only sparsely to nuclei of the extraocular muscles receiving fibers from other vestibular nuclei Regions of these nuclei where fibers from the superior vestibular nucleus minimally overlap ipsilateral projections from the medial or lateral vestibular nuclei include (1) the oral pole of the abducens nucleus (2) the trochlear nucleus which receives a sparse projection only from the medial vestibular nucleus and (3) the caudal part

The pattern of projection of secondary vestibular fibers from the medial vestibular nucleus suggests that impulses from this nucleus could influence the activity of both abducens nuclei (asymmetrically) and the contralateral trochlear nucleus (ipsilateral superior oblique muscle) Impulses conveyed by these fibers to the oculomotor complex would seem capable of influencing the activity of (1) the ipsilateral medial rectus muscle (also the inferior oblique and inferior rectus to a lesser degree) and (2) the contralateral inferior oblique muscle (and to a lesser extent the inferior and medial rectus muscles)

Lesions of the superior vestibular nucleus concomitantly destroyed portions of the brachium conjunctivum in seven animals As a consequence of these lesions degenerated fibers from the superior vestibular nucleus entered the ipsilateral MLF rostral to the genu of the facial nerve No ascending degeneration was seen in the contralateral MLF Degenerated fibers located in the most ventral part of the brachium conjunctivum decussated and passed to the contralateral red nucleus and thalamus After crossing to the opposite side, a small number of cerebellar efferent fibers passed dorsally medial to the red nucleus and entered mainly the middle third of the oculomotor complex The largest number of these cerebello oculomotor fibers passed into the area of the medial nucleus a cell group innervating the superior rectus muscle on the opposite side In animals with lesions involving only the brachium conjunctivum and the superior vestibular nucleus these degenerated cerebellar efferent fibers constituted the only degeneration seen on the left side in the oculomotor complex Crossed cerebello oculomotor fibers have been commented upon by several authors (Klimoff 1896 Wallenberg 05 A van Gehuchten 05 Allen 24 Clark '36 Gerebtzoff 41) and are considered in detail in a recent paper (Carpenter and Strominger 64)

Szentagothai (64) has produced lesions in the superior vestibular nucleus which like ours have involved portions of the brachium conjunctivum His illustrations demonstrate the degeneration in the contralateral somatic cell columns of the oculomotor nucleus as described above but he considered the crossed degeneration to arise from the superior vestibular nucleus This interpretation does not seem to be supported by other anatomical evidence because (1) lesions destroying the superior vestibular nucleus and the dorsal part of Deiters nucleus (C 732) produce ascending degeneration only in the ipsilateral MLF and (2) lesions of the dentate nucleus produce degeneration that can be followed into the contralateral oculomotor nucleus (Carpenter and Strominger 64)

Exclusively ascending fibers from the superior vestibular nucleus pass only to ipsilateral nuclei of the extraocular muscles (fig 3) The secondary vestibular projection to the abducens nucleus is sparse but that to the trochlear nucleus is profuse In the oculomotor nuclear complex fibers from this nucleus are distributed exclusively to subdivisions which innervate the inferior rectus and the inferior oblique muscles These observations suggest that ascending fibers from the superior vestibular nucleus may provide controlling influences for muscles involved primarily in vertical or rotatory eye movements Consideration of these anatomical findings in conjunction with recent physiological data (Cohen Suzuki and Bender 64) suggests that some of the secondary vestibular fibers arising from the superior vestibular nucleus may be concerned with inhibitory activities The latter authors noted that no excitatory influences from any of the semicircular canals were observed in the ipsilateral inferior oblique or the contralateral superior oblique muscles The superior vestibular nucleus is the only vestibular nucleus which gives rise to secondary fibers distributed in this manner On the basis of these data secondary vestibular fibers passing from the superior vestibular nucleus to the rostral part of the dorsal nucleus may be concerned with synergistic activation of the ipsilateral inferior rectus muscle a response reported to occur following selective stimulation of the ampullary nerve from the posterior canal Judging from our findings the projection to the dorsal nucleus (inferior rectus) is quantitatively greater than that to the intermediate cell column (inferior oblique)

The only lesions of the inferior vestibular nucleus which appear to give rise to

Also important is the apparent total absence of secondary vestibular fibers passing to the caudal central nucleus of the oculomotor complex a nucleus reported to give rise to crossed and uncrossed fibers innervating the levator palpebrae muscle (Warwick 53)

While it is possible that secondary vestibular fibers to the caudal central nucleus and the ipsilateral medial nucleus might arise from portions of vestibular nuclei not destroyed by the lesions in this study there is some evidence that afferents to one of these nuclei arise from non vestibular sources A considerable number of crossed cerebello-oculomotor fibers are projected to the medial nucleus following lesions of the dentate nucleus and brachium conjunctivum (Carpenter and Strominger 64) Although the origins of fibers passing to the caudal central nucleus are not known lesions of the MLF provoke modest degeneration in it (Carpenter and McMasters 63 Carpenter and Strominger 65) indicating that some fibers to the nucleus ascend from more caudal regions of the brain stem

Evidence presented here appears to confirm data indicating that the vestibular nuclei and their ascending secondary projections play a more important role in conjugate horizontal eye movements than in eye movements in other planes This thesis is supported by the fact that lesions of the MLF in the monkey (Bender and Weinstein 44 50 Shanzer Wagman and Bender 59 Carpenter and McMasters 63 Bender and Shanzer 64 Carpenter and Strominger 65) produce dissociated eye movements only in a horizontal plane Other physiological observations (Spiegel and Teschler 29 Spiegel 33) indicating that bilateral destruction of the vestibular nuclei abolishes conjugate horizontal eye movements in response to stimulation of frontal and occipital cortex likewise support this view

The vestibular nuclei and their projections to the nuclei of the extraocular muscles also appear to play a role in rotatory eye movements though this may not be a unique function Stimulation of certain non vestibular structures in the brain stem give rise to rotatory eye movements Szentágothai (43) found that stimulation of the interstitial nucleus of Cajal produced both vertical and rotatory eye movements Recently Hyde and Toczek (62) have confirmed this finding with respect to rotatory eye movements they further indicate that rotatory eye movements can be obtained by stimulating the pretectal area and the zona incerta It is possible that some of these responses actually may be mediated by descending fibers from the interstitial nucleus of Cajal that project to the medial vestibular nucleus (Pompeiano and Walberg 57)

The paucity of persistent physiological disturbances following discrete lesions of the particular vestibular nuclei is of special interest Abnormal posturing of the head appears to be the most enduring disturbance Considering the relatively profuse projection of secondary vestibular fibers upon the nuclei of the extraocular muscles and the demonstrated physiological importance of these fibers it is surprising that disturbances of coordinated eye movements are so mild and transient

SUMMARY AND CONCLUSIONS

In a series of 35 rhesus monkeys attempts were made to produce discrete localized lesions unilaterally in individual vestibular nuclei in order to study the secondary vestibular projections to the nuclei of the extraocular muscles Lesions worthy of detailed anatomical study were produced in 20 monkeys These lesions destroyed portions of the medial superior and inferior vestibular nuclei without concomitantly involving other vestibular nuclei Lesions primarily localized in the lateral vestibular nucleus invariably destroyed small portions of either the superior or inferior vestibular nuclei Fiber degeneration resulting from these lesions was studied in multiple representative sections from all levels of the brain stem stained by the Nauta-Gygax technic

The following conclusions were drawn from this study

1 Efferent fibers from the superior vestibular nucleus ascend exclusively enter the lateral process of the MLF rostral to the abducens nucleus and project only to the ipsilateral nuclei of the extraocular muscles

of the dorsal nucleus of the oculomotor complex

The physiological observations of Cohen, Suzuki and Bender ('64) viewed with respect to the current findings, suggest that secondary fibers from the superior vestibular nucleus to the ipsilateral trochlear nucleus (contralateral superior oblique) and the ipsilateral intermediate cell column (ipsilateral inferior oblique) probably are concerned with inhibitory activities

Ascending secondary vestibular fibers from the lateral and medial vestibular nuclei project asymmetrically and differentially to the nuclei of the extraocular muscles in a pattern demonstrating considerable overlap While it is possible that this similar projection pattern for the medial vestibular nucleus may in part be due to concomitant interruption of efferent fibers from the lateral vestibular nucleus our findings indicate that most of these fibers pass along the ventral border of the medial vestibular nucleus an area not infringed upon by lesions in the medial vestibular nucleus

Ascending secondary vestibular fibers arising from the medial and lateral vestibular nuclei appear capable of mediating all of the patterned eye movements in different planes obtained by stimulating individual semicircular canals (Szentagothai 52) or the ampullary nerves from the semicircular canals (Cohen Suzuki and Bender 64) In order not to overinterpret these data, only extraocular muscles whose contractions are regarded as primary will be considered Since stimulation of the ampullary nerve from one horizontal canal produces conjugate movement of the eyes to the opposite side secondary vestibular fibers conveying excitatory impulses must reach the contralateral abducens nucleus and the ipsilateral ventral nucleus of the oculomotor complex The only secondary vestibular fibers distributed in this manner arise from the medial and lateral vestibular nuclei This suggests that secondary vestibular fibers to the ipsilateral abducens nucleus may be concerned with reciprocal inhibitory activities

Since stimulation of the ampullary nerve from the right posterior canal produces primary contractions in the right superior oblique and the left inferior rectus muscles excitatory impulses must reach the contralateral trochlear nucleus and dorsal nucleus of the oculomotor complex Only secondary vestibular fibers arising from the medial and lateral vestibular nuclei are distributed to these nuclei contralaterally

Since stimulation of the ampullary nerve from the right anterior canal produces primary contractions in the right superior rectus and the left inferior oblique muscles it must be assumed that excitatory impulses reach the medial nucleus and the intermediate cell column on the left side Fibers from the medial nucleus innervate the contralateral superior rectus muscle while fibers from the intermediate cell column innervate the ipsilateral inferior oblique muscle (see fig 1) Secondary vestibular fibers that could mediate responses in these particular extraocular muscles appear to originate only from the medial and lateral vestibular nuclei While ascending secondary vestibular fibers to the contralateral intermediate cell column arise from both the medial and lateral vestibular nuclei only fibers from the lateral vestibular nuclei project to the contralateral medial nucleus

It seems likely that ascending secondary vestibular fibers arising from the rostral portions of the inferior vestibular nucleus also may mediate some of the primary responses discussed above but due to the relative paucity of demonstrated fibers from this source in this study additional data will be necessary before definite conclusions can be drawn

Review of the findings presented indicates that secondary vestibular fibers from the medial and lateral vestibular nuclei to the nuclei of the extraocular muscles and their subdivisions are (1) most abundant to those nuclei innervating muscles whose primary functions concern horizontal and rotatory movements of the eyes (2) moderate to nuclei innervating muscles whose primary function is concerned with downward eye movements and (3) relatively modest to nuclei innervating muscles concerned primarily with upward eye movements Particularly notable is the relatively small projection of vestibular fibers to the medial nucleus a cell group innervating the superior rectus muscle

Bender M B and S Shanzer 1964 Oculomotor pathways defined by electric stimulation and lesions in the brainstem of the monkey In Symposium The Oculomotor System Ed M B Bender Hoeber New York Chap 4 pp 81–140

Bender M B and E A Weinstein 1944 Effects of stimulation and lesion of the median longitudinal fasciculus in the monkey Arch Neur Psychiat 52 106–113

——— 1950 The syndrome of the median longitudinal fasciculus Res Publ Assoc nerv ment Dis 28 414–420

Beusekom G T van 1955 Fibre analysis of the anterior and lateral funiculi of the cord in the cat Thesis Eduard Ijdo N V Leiden 143 pp

Brodal A and O Pompeiano 1957 The origin of ascending fibers of the medial longitudinal fasciculus from the vestibular nuclei. An experimental study in the cat Acta Morph Neerl Scand *1* 306–328

Brodal A O Pompeiano and F Walberg 1962 The Vestibular Nuclei and Their Connections Anatomy and Functional Correlations Charles C Thomas Springfield Ill 193 pp

Buchanan A R 1937 The course of the secondary vestibular fibers in the cat J Comp Neur 67 183–204

Carpenter M B 1957 The dorsal trigeminal tract in the rhesus monkey J Anat London *91* 82–90

——— 1959 Lesions of the fastigial nuclei in the rhesus monkey Am J Anat *104* 1–34

——— 1960 Fiber projections from the descending and lateral vestibular nuclei in the cat Am J Anat *107* 1–22

Carpenter M B and R E McMasters 1963 Disturbances of conjugate horizontal eye movements in the monkey II Physiological effects and anatomical degeneration resulting from lesions of the medial longitudinal fasciculus Arch Neur 8 347–368

Carpenter M B R E McMasters and G R Hanna 1963 Disturbances of conjugate horizontal eye movements in the monkey I Physiological effects and anatomical degeneration resulting from lesions of the abducens nucleus and nerve Arch Neur *8* 231–247

Carpenter M B and N L Strominger 1964 Cerebello-oculomotor fibers in the rhesus monkey J Comp Neur *123* 211–230

——— 1965 The medial longitudinal fasciculus and disturbances of conjugate horizontal eye movements in the monkey J Comp Neur 125 41–66

Carpenter M B and J R Whittier 1952 Study of methods for producing experimental lesions of the central nervous system with special reference to stereotaxic techniques J Comp Neur *97* 73–132.

Clark W E L 1936 The termination of ascending tracts in the thalamus of the macaque monkey J Anat *71* 7–40

Cohen B J Suzuki and M B Bender 1964 Eye movements from semicircular canal stimulation in the cat Ann Oto Rhinol and Laryngol 73 153–169

Crosby E C 1953 Relations of brain centers to normal and abnormal eye movements in the horizontal plane J Comp Neur *99* 437–480

Crosby E C and J W Henderson 1948 The mammalian midbrain and isthmus regions Part II Fiber connections of the superior colliculus B Pathways concerned with automatic eye movements J Comp Neur *88* 53–91

Dow R W and G Moruzzi 1958 The Physiology and Pathology of the Cerebellum Univ Minn Press Minneapolis Chap 3 p 143 Chap 4 p 245

Eckel W 1954 Elektrophysiologische und histologiche Untersuchungen im Vestibulariskern gebiet bei Drehreizen Arch f Ohr Nas u Kehlkopfhlk *164* 487–513

Ferraro A B L Pacella and S E Barrera 1940 Effects of lesions of the medial vestibular nucleus An anatomical and physiological study in *Macacus rhesus* monkeys J Comp Neur 73 7–36

Fluur E 1959 Influences of semicircular ducts on extraocular muscles Acta Oto-Laryng Suppl *149* 1–46

Fraser E H 1901 An experimental research into the relations of the posterior longitudinal bundle and Deiters nucleus J Physiol London 27 372–397

Gehuchten A van 1905 Les pédoncules cerebelleux supérieurs Névraxe 7 29–86

Gehuchten P van 1928 Les voies nervuses du nystagmus Rev Neur 2 849–869

Gerebtzoff M A 1940 Recherches sur la projection corticale du labyrinthe II Étude anatomo-experimentale de la voie vestibulo-cerebrale J Belge Neur Psychiat 40 417–432

——— 1941 Les bases anatomiques de la physiologie due cervelet. La Cellule 49 71–166

Gray L P 1926 Some experimental evidence on the connections of the vestibular mechanism in the cat. J Comp Neur 41 319–346

Hare W K H W Magoun and S W Ranson 1937 Localization within the cerebellum of reactions to faradic cerebellar stimulation J Comp Neur 67 145–182

Hoshino T 1921 Beiträge zur Funktion des Kleinhirnwurmes beim Kaninchen Acta Oto-Laryng Suppl 2 1–72

Hyde J E and S Toczek 1962 Functional relation of interstitial nucleus to rotatory movements evoked from zona incerta stimulation J Neurophysiol 25 455–465

Kaida Y 1929 Uber den zentralen Verlauf des N vestibularis und der Fasern aus dem Deitersschen Kerne Fukuoka Ikwadaigaku Zasshi 22 3–4

Klimoff J 1896 Concerning the connection of the cerebellum with the nucleus of the oculomotor nerve (In Russian) Vrach St. Petersburgh 17 1013–1014

——— 1899 Über die Leitungsbahnen des Kleinhirns Arch f Anat u Entwicklungsgesch Anat Abt Leipzig 11–27

Leidler R 1916 Experimentelle Untersuchungen über das Endigungsgebiet des Nervus ves-

2 The major projections of the superior vestibular nucleus are to (a) the trochlear nucleus, and (b) the dorsal nucleus of the oculomotor complex smaller numbers of fibers pass to the abducens nucleus and the intermediate cell column of the oculomotor complex

3 Ascending secondary vestibular fibers from the inferior vestibular nucleus appear less numerous than those from other vestibular nuclei arise mainly from the rostral third of the nucleus and pass (a) bilaterally to the abducens and oculomotor nuclei and (b) to the contralateral trochlear nucleus Within the oculomotor complex fibers project to (a) the ipsilateral ventral and dorsal nuclei and (b) the contralateral intermediate cell column

4 Caudal portions of the inferior vestibular nucleus do not appear to project ascending or descending fibers in the MLF although numerous vestibular arcuate fibers from this part of the nucleus pass to the contralateral inferior vestibular nucleus

5 Ascending secondary vestibular fibers from the medial vestibular nucleus project via the MLF bilaterally asymmetrically and differentially to all of the nuclei of the extraocular muscles Particularly prominent among these projections are fibers to (a) the contralateral trochlear nucleus (b) the contralateral intermediate cell column of the oculomotor complex and (c) the ipsilateral ventral nucleus of the oculomotor complex, other fibers from this nucleus pass bilaterally to asymmetrical portions of the dorsal nucleus and intermediate cell column of the oculomotor complex and a few pass to the ipsilateral trochlear nucleus

6 Ascending vestibular projections from the lateral vestibular nucleus arise only from ventral portions of the nucleus

7 Ascending secondary vestibular fibers from the lateral vestibular nucleus project primarily to (a) the contralateral abducens and trochlear nuclei and (b) asymmetrically to specific portions of the oculomotor complex bilaterally The projection within the oculomotor complex is to (a) the ipsilateral ventral and dorsal nuclei and (b) the contralateral intermediate cell column and the medial and dorsal nuclei

8 Ascending fibers from the medial lateral and superior vestibular nuclei project to the interstitial nucleus of Cajal fibers from the medial and lateral vestibular nuclei are predominantly crossed while those from the superior vestibular nucleus are uncrossed

9 No ascending secondary vestibular fibers from any of the vestibular nuclei appear to project to the caudal central nucleus the visceral nuclei or the ipsilateral medial nucleus of the oculomotor complex

10 Secondary vestibular fibers descending in the MLF appear to arise mainly from the medial vestibular nucleus are present bilaterally in the MLF at medullary levels but appear to project only ipsilaterally to cervical spinal segments

11 Localized unilateral lesions of individual vestibular nuclei in the monkey produce transient nystagmus and sometimes a mild gaze preference abnormal posturing of the head associated with some lesions is more enduring

12 Ascending secondary vestibular fibers arising from the medial and lateral vestibular nuclei appear capable of mediating all the patterned eye movements in different planes obtained by stimulating the ampullary nerves from the individual semicircular canals

13 Vestibular fibers from the medial and lateral vestibular nuclei projecting to the nuclei of the extraocular muscles and their subdivisions are (a) most abundant to those nuclei innervating muscles whose primary functions concern horizontal and rotatory movements of the eyes (b) moderate to nuclei innervating muscles whose primary function is concerned with downward eye movements and (c) relatively modest to nuclei innervating muscles concerned primarily with upward eye movements

It is hypothesized that the vestibular nuclei and their projections to nuclei of the extraocular muscles may play a relatively more important role in horizontal and rotatory eye movements than in eye movements in vertical planes

LITERATURE CITED

Allen F W 1924 Distribution of the fibers originating from the different basal cerebellar nuclei J Comp Neur 36 399–439

Bender M B and S Shanzer 1964 Oculomotor pathways defined by electric stimulation and lesions in the brainstem of the monkey In Symposium The Oculomotor System Ed M B Bender Hoeber New York Chap 4 pp 81–140

Bender M B and E A Weinstein 1944 Effects of stimulation and lesion of the median longitudinal fasciculus in the monkey Arch Neur Psychiat 52 106–113

——— 1950 The syndrome of the median longitudinal fasciculus Res Publ Assoc nerv ment Dis 28 414–420

Beusekom G T van 1955 Fibre analysis of the anterior and lateral funiculi of the cord in the cat Thesis Eduard Ijdo N V Leiden 143 pp

Brodal A and O Pompeiano 1957 The origin of ascending fibers of the medial longitudinal fasciculus from the vestibular nuclei An experimental study in the cat Acta Morph Neerl Scand *1* 306–328

Brodal A O Pompeiano and F Walberg 1962 The Vestibular Nuclei and Their Connections Anatomy and Functional Correlations Charles C Thomas Springfield Ill 193 pp

Buchanan A R 1937 The course of the secondary vestibular fibers in the cat J Comp Neur 67 183–204

Carpenter M B 1957 The dorsal trigeminal tract in the rhesus monkey J Anat London *91* 82–90

——— 1959 Lesions of the fastigial nuclei in the rhesus monkey Am J Anat *104* 1–34

——— 1960 Fiber projections from the descending and lateral vestibular nuclei in the cat Am J Anat *107* 1–22

Carpenter M B and R E McMasters 1963 Disturbances of conjugate horizontal eye movements in the monkey II Physiological effects and anatomical degeneration resulting from lesions of the medial longitudinal fasciculus Arch Neur *8* 347–368

Carpenter M B R E McMasters and G R Hanna 1963 Disturbances of conjugate horizontal eye movements in the monkey I Physiological effects and anatomical degeneration resulting from lesions of the abducens nucleus and nerve Arch Neur *8* 231–247

Carpenter M B and N L Strominger 1964 Cerebello-oculomotor fibers in the rhesus monkey J Comp Neur 123 211–230

——— 1965 The medial longitudinal fasciculus and disturbances of conjugate horizontal eye movements in the monkey J Comp Neur 125 41–66

Carpenter M B and J R Whittier 1952 Study of methods for producing experimental lesions of the central nervous system with special reference to stereotaxic techniques J Comp Neur 97 73–132

Clark W E L 1936 The termination of ascending tracts in the thalamus of the macaque monkey J Anat 71 7–40

Cohen B J Suzuki and M B Bender 1964 Eye movements from semicircular canal stimulation in the cat Ann Oto Rhinol and Laryngol "3 153–169

Crosby E C 1953 Relations of brain centers to normal and abnormal eye movements in the horizontal plane J Comp Neur *99* 437–480

Crosby E C and J W Henderson 1948 The mammalian midbrain and isthmus regions Part II Fiber connections of the superior colliculus B Pathways concerned with automatic eye movements J Comp Neur *88* 53–91

Dow R W and G Moruzzi 1958 The Physiology and Pathology of the Cerebellum Univ Minn Press Minneapolis Chap 3 p 143 Chap 4 p 245

Eckel W 1954 Elektrophysiologische und histologiche Untersuchungen im Vestibulariskern gebiet bei Drehreizen Arch f Ohr Nas u Kehlkopfhlk *164* 487–513

Ferraro A B L Pacella and S E Barrera 1940 Effects of lesions of the medial vestibular nucleus An anatomical and physiological study in *Macacus rhesus* monkeys J Comp Neur 73 7–36

Fluur E 1959 Influences of semicircular ducts on extraocular muscles Acta Oto-Laryng Suppl *149* 1–46

Fraser E H 1901 An experimental research into the relations of the posterior longitudinal bundle and Deiters nucleus J Physiol London 27 372–397

Gehuchten A van 1905 Les pedoncules cérébelleux supérieurs Névraxe 7 29–86

Gehuchten P van 1928 Les voies nervuses du nystagmus Rev Neur 2 849–869

Gerebtzoff M A 1940 Recherches sur la projection corticale du labyrinthe II Étude anatomo-experimentale de la voie vestibulo-cérébrale J Belge Neur Psychiat 40 417–432

——— 1941 Les bases anatomiques de la physiologie due cervelet La Cellule *49* 71–166

Gray L P 1926 Some experimental evidence on the connections of the vestibular mechanism in the cat J Comp Neur *41* 319–346

Hare W K H W Magoun and S W Ranson 1937 Localization within the cerebellum of reactions to faradic cerebellar stimulation J Comp Neur 67 145–182

Hoshino T 1921 Beitrage zur Funktion des Kleinhirnwurmes beim Kaninchen Acta Oto-Laryng Suppl 2 1–72

Hyde J E and S Toczek 1962 Functional relation of interstitial nucleus to rotatory movements evoked from zona incerta stimulation J Neurophysiol 25 455–465

Kaida Y 1929 Über den zentralen Verlauf des N vestibularis und der Fasern aus dem Deitersschen Kerne Fukuoka Ikwadaigaku Zasshi 22 3–4

Klimoff J 1896 Concerning the connection of the cerebellum with the nucleus of the oculomotor nerve (In Russian) Vrach St Petersburgh *17* 1013–1014

——— 1899 Über die Leitungsbahnen des Kleinhirns Arch f Anat u Entwicklungsgesch Anat Abt Leipzig 11–27

Leidler R 1916 Experimentelle Untersuchungen über das Endigungsgebiet des Nervus ves-

tibularis 2 Mitteilung Arb a d Neur Inst Wien Univ 21 151–212
Lorente de Nó R 1926 Études sue l anatomie et la physiologie du labyrinthe de l oreille et du VIII nerf Deuxième partie Quelques données au sujet de l anatomie des organes sensoriels du labyrinthe Trav Lab Rech Biol Univ Madrid, 24 53–153
——— 1931 Ausgewahlte Kapitel aus der vergleichenden Physiologie des Labyrinthes Die Augenmuskelreflexe beim Kaninchen und ihre Grundlagen Ergebn Physiol 32 73–242
——— 1933 Anatomy of the eighth nerve The central projection of the nerve endings of the internal ear Laryngoscope 43 1–38
Magoun H W W K Hare and S W Ranson 1935 Electrical stimulation of the interior of the cerebellum in the monkey Am J Physiol 112 329–339
Mettler F A 1935a Corticifugal fiber connections of the cortex of Macaca mulatta The frontal region J Comp Neur 61 509–542
——— 1935b Corticifugal fiber connections of the cortex of Macaca mulatta The parietal region J Comp Neur 62 263–291
——— 1935–36 Corticifugal fiber connections of the cortex of Macaca mulatta The temporal region J Comp Neur 63 25–47
Muskens L J J 1914 An anatomico physiological study of the posterior longitudinal bundle in its relation to forced movements Brain 36 352–426
Mussen A T 1927 Experimental investigations on the cerebellum Brain 50 313–349
Nauta W J H, and P A Gygax 1954 Silver impregnation of degenerated axons in the central nervous system A modified technique Stain Tech 29 91–93
Pompeiano O and F Walberg 1957 Descending connections to the vestibular nuclei An experimental study in the cat J Comp Neur 108 465–503
Probst M 1900 Experimentelle Untersuchungen über die Schleifenendigung die Haubenbahnen das dorsale Langsbundel und die hintere Commissur Arch f Psychiat u Nervenkr 33 1–57
Rasmussen A T 1932 Secondary vestibular tracts in the cat J Comp Neur 54 143–159
Rexed B 1952 The cytoarchitectonic organization of the spinal cord in the cat J Comp Neur 96 415–495
Russell J S R 1897 The origin and destination of certain afferent and efferent tracts in the medulla oblongata Brain 20 409–440
Sachs E and B Y Alvis 1921 Anatomic and physiologic studies of the eighth nerve Arch Neur Psychiat 6 119–145
Satoh, K 1929 Experimentelle Untersuchungen uber die Beziehungen zwischen dem Vestibularis Deiters und dem Kerngebiete des dorsalen Langsbundels nach Edinger Folia Anat Japon 7 45–91
Shanzer S, I H Wagman and M B Bender 1959 Further observations on the median longitudinal fasciculus Trans Am Neur Assoc 84 14–17
Spiegel E A 1933 Role of vestibular nuclei in cortical innervation of the eye muscles Arch Neur Psychiat 29 1084–1097
Spiegel E A and L Teschler 1929 Experimentalstudien am Nervensystem XII Mitteilung Über die Beziehung der Blickbahn zu den Vestibulariskernen Arch ges Physiol 222 359–370
Szentágothai J 1943 Die zentrale Innervation der Augenbewegungen Arch f Psychiat u Nervenkr 116 721–760
——— 1950 The elementary vestibulo-ocular reflex arc J Neurophysiol 13 395–407
——— 1952 Die Rolle der einzelnen Labyrinthrezeptoren bei der Orientation von Augen und Kopf im Raume Adademiai Kiado Budapest, 129 pp
——— 1964 Pathways and synaptic articulation patterns connecting vestibular receptors and oculomotor nuclei In Symposium The Oculomotor System Ed M B Bender Hoeber New York Chap 8 pp 205–222
Thomas D M, R P Kaufman J M Sprague and W W Chambers 1956 Experimental studies of the vermal cerebellar projections in the brain stem of cat (fastigio bulbar tract) J Anat London 90 371–385
Truex R C and M B Carpenter 1964 Strong and Elwyn s Human Neuroanatomy 5th Ed Williams and Wilkins Co Baltimore Chap 17 pp 345–348
Walberg F D Bowsher and A Brodal 1958 The termination of primary vestibular fibers in the vestibular nuclei of the cat An experimental study with silver methods J Comp Neur 110 391–419
Walberg, F and J Jansen 1961 Cerebellar corticovestibular fibers in the cat Exp Neur 3 32–52
Walberg F O Pompeiano A Brodal and J Jansen 1962 The fastigiovestibular projection in the cat An experimental study with silver impregnation methods J Comp Neur 118 49–76
Wallenberg A 1905 Sekundäre Bahnen aus dem frontalen sensibeln Trigeminuskerne des Kaninchens Anat Anz 26 145–155
Warwick R 1953 Representation of the extra ocular muscles in the oculo-motor nuclei of the monkey J Comp Neur 98 449–504

PLATE 1

EXPLANATION OF FIGURES

6 Rhesus C 668 Photomicrograph of lesion confined to the medial ves tibular nucleus Nissl × 10

7 Rhesus C-669 Photomicrograph of ascending degeneration in the left medial longitudinal fasciculus Degenerated fibers are localized in ventromedial portions of the bundle Nauta Gygax × 80

8 Rhesus C 668 Photomicrograph of preterminal degeneration in the medial part of the left abducens nucleus Nauta-Gygax × 200

9 Rhesus C 668 Photomicrograph of degeneration in the left trochlear nucleus Nauta Gygax × 75

10 Rhesus C-668 Photomicrograph showing the distribution of preter minal degeneration in the caudal third of the oculomotor nuclear complex Degeneration on the left is present in the ventral nucleus and in the intermediate cell column on the right degeneration is localized in the dorsal nucleus Nauta Gygax × 30

11 Rhesus C-668 Photomicrograph of preterminal degeneration in the right ventral nucleus of the middle third of the oculomotor complex Almost no degeneration is seen in this nucleus on the left side Nauta Gygax × 80

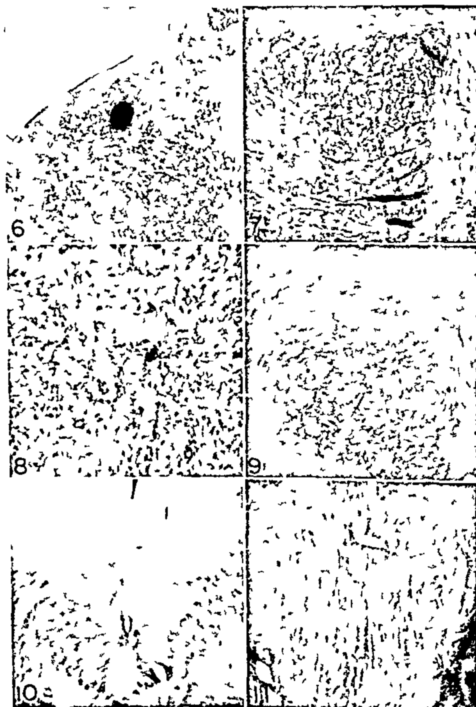

6
7
8
9
10

PLATE 2

EXPLANATION OF FIGURES

12 Rhesus C 675 Photomicrograph of a lesion in the superior vestibular nucleus Nissl × 10

13 Rhesus C 733 Photomicrograph of a lesion in the superior vestibular nucleus that concomitantly destroyed some fibers in the ventral part of the superior cerebellar peduncle and some cells in the dorsal part of the lateral vestibular nucleus Ascending degeneration confined to the ipsilateral MLF was identical in rhesus C 675 and C 733 Nissl × 8

14 Rhesus C 733 Photomicrograph of ascending degeneration localized in the lateral process of the ipsilateral medial longitudinal fasciculus Nauta Gygax × 80

15 Rhesus C 733 Photomicrograph of abundant preterminal degeneration in the right trochlear nucleus No degeneration was seen in the opposite trochlear nucleus Nauta Gygax × 85

16 Rhesus C 733 Photomicrograph of degeneration in the dorsolateral part of the medial longitudinal fasciculus passing selectively to the dorsal nucleus of the oculomotor complex Nauta Gygax × 70

17 Rhesus C 733 Higher magnification of degeneration in the ipsilateral dorsal nucleus of the oculomotor complex Nauta Gygax × 200


12
13
14
15
16
17

PLATE 2

EXPLANATION OF FIGURES

12 Rhesus C 675 Photomicrograph of a lesion in the superior vestibular nucleus Nissl × 10

13 Rhesus C 733 Photomicrograph of a lesion in the superior vestibular nucleus that concomitantly destroyed some fibers in the ventral part of the superior cerebellar peduncle and some cells in the dorsal part of the lateral vestibular nucleus Ascending degeneration confined to the ipsilateral MLF was identical in rhesus C 675 and C 733 Nissl × 8

14 Rhesus C 733 Photomicrograph of ascending degeneration localized in the lateral process of the ipsilateral medial longitudinal fasciculus Nauta Gygax × 80

15 Rhesus C 733 Photomicrograph of abundant preterminal degeneration in the right trochlear nucleus No degeneration was seen in the opposite trochlear nucleus Nauta Gygax × 85

16 Rhesus C 733 Photomicrograph of degeneration in the dorsolateral part of the medial longitudinal fasciculus passing selectively to the dorsal nucleus of the oculomotor complex Nauta Gygax × 70

17 Rhesus C 733 Higher magnification of degeneration in the ipsilateral dorsal nucleus of the oculomotor complex Nauta Gygax × 200

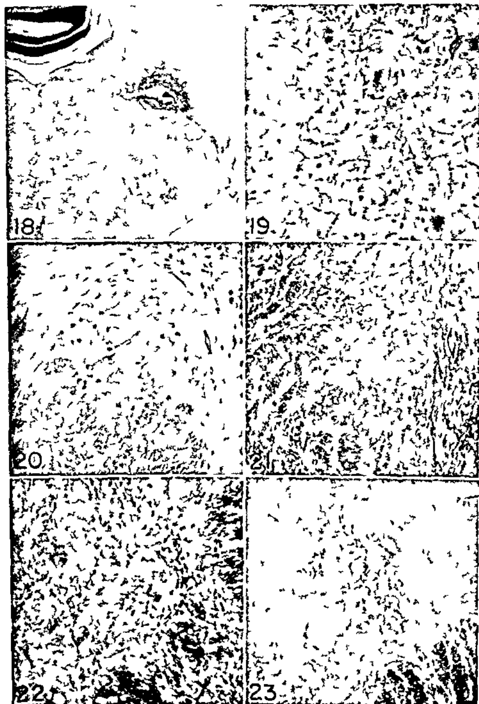

18
19
20
21
22
23

PLATE 3

EXPLANATION OF FIGURES

18 Rhesus C 734 Photomicrograph of lesion in the lateral vestibular nucleus at the level of the vestibular nerve root Nissl × 8

19 Rhesus C 734 Photomicrograph of profuse degeneration in the left abducens nucleus Nauta Gygax × 200

20 Rhesus C 734 Photomicrograph of degeneration in the left trochlear nucleus No degeneration was present in the right trochlear nucleus Nauta Gygax × 80

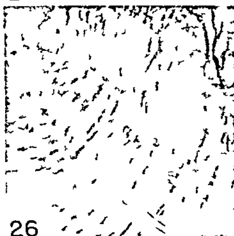
21 Rhesus C 734 Photomicrograph of preterminal degeneration in the intermediate cell column and medial nucleus of the left half of the oculomotor complex Only the lateral vestibular nucleus was found to project fibers to the medial nucleus Note the virtual absence of degeneration in the ventral nucleus Nauta Gygax × 75

22 Rhesus C 734 Photomicrograph of preterminal degeneration in the middle third of the ventral nucleus of the oculomotor complex on the right side Nauta Gygax × 150

23 Rhesus C 734 Photomicrograph of selectively distributed fibers in the dorsal nucleus of the oculomotor complex on the right side Nauta Gygax × 100


24


25


26


27


28


29

PLATE 4

EXPLANATION OF FIGURES

24 Rhesus C 831 Photomicrograph of lesion in the caudal half of the right inferior vestibular nucleus Nissl × 5

25 Rhesus C 741 Photomicrograph of lesion in the oral pole of the inferior vestibular nucleus which spared the lateral vestibular nucleus Nissl × 8

26 Rhesus C 831 Photomicrograph of vestibular arcuate fibers passing from the inferior vestibular nucleus through the reticular formation to the opposite side of the brain stem Nauta-Gygax × 30

27 Rhesus C 831 Photomicrograph of preterminal degeneration in the left inferior vestibular nucleus A considerable part of the vestibular arcuate fibers were distributed to this nucleus Nauta Gygax × 175

28–29 Rhesus C 741 Photomicrographs of relatively modest degeneration from the inferior vestibular nucleus projecting selectively to the ipsilateral ventral nucleus of the oculomotor complex Nauta Gygax × 75 × 190

Reproduction in the Ferret (*Mustela furo*)

I UTERINE HISTOLOGY AND HISTOCHEMISTRY DURING PREGNANCY AND PSEUDOPREGNANCY

G DALE BUCHANAN
Department of Anatomy University of Tennessee Medical Units Memphis Tennessee

ABSTRACT Similar histological and histochemical changes occur in the uteri of pregnant and pseudopregnant ferrets The pre implantation period is characterized by general growth of the tissue and moderate secretory activity At the time of implan tation the luminal epithelium undergoes hypertrophy and hyperplasia and shows much secretory activity This area of altered activity sweeps progressively toward the gland fundi and the epithelium behind it becomes greatly enlarged and forms sym plasmic masses Symplasma formation occurs in all regions of the uterus in con trast to other carnivores where it occurs only next to trophoblast and in response to uterine trauma

The principal uterine secretions are mucoproteins and glycoproteins There is some evidence that pseudopregnant uteri but not pregnant uteri secrete acid muco-polysaccharides Glycogen is present in moderate amounts at estrus declines during the pre implantation period and is absent during gestation A light to moderate dif fuse sudanophilia is seen during pregnancy and pseudopregnancy becoming more pronounced toward the end of the gestation period Occasional cholesterol crystals are seen in macrophages in the stroma of pregnant but not pseudopregnant uteri Macrophages containing hemosiderin were seen in all uteri examined being most abundant in estrous and early pre implantation uteri Uterine mast cells were abun dant at estrus declined during the pre implantation period and decreased markedly at the time of implantation The results are compared with data from other carnivore species

Several features make the ferret well suited for studies in reproductive phys iology There is a well defined breeding season and estrus is easily determined by the degree of vulval enlargement Since the animals are induced ovulators the various events of pregnancy can be timed rather accurately Pregnancy lasts 40–42 days and consists of a relatively long pre implantation period of 10–12 days and an active gestation period of 30 days A period of pseudopregnancy which is ex actly the same length as pregnancy follows sterile mating The influence of the amount of daylight on the reproductive cycle has been much exploited in prior studies of the relationship of environment to neural control of reproduction The basic features of the ferret reproductive cycle were first described by F H A Marshall (04) Although a more detailed description of the cycle and the histolog ical changes of the reproductive tract dur ing estrus pseudopregnancy and preg nancy was published by Hammond and Marshall (30) very little information is available concerning the histochemistry of the ferret uterus Hamilton and Gould (40) reported relatively small amounts of glycogen in the uterus of estrous ferrets and recently Nicol and Vernon Roberts (63) have described the distribution of lipoid and glycogen in ferret uteri during the follicular phase of the estrous cycle and during pseudopregnancy

In this study the reproductive tracts of pregnant and pseudopregnant ferrets have been examined by several histological and histochemical methods in order to provide a base of reference by which to gauge the effects of experimental modification of the reproductive cycle

MATERIALS AND METHODS

Estrous female ferrets were mated to either fertile or vasectomized males the day of mating being designated as day zero At various times post coitum (p c) hemihysterectomy was performed thus

much crowding and many areas are pseudostratified (fig 3) By the time of nidation essentially all the luminal epithelium is pseudostratified Mitoses are frequently seen in the luminal epithelium of estrous animals but are rare in pre implantation uteri

The endometrial glands undergo concomitant changes during the same period They are compact straight except for a slight basal twist and relatively short during the anestrum As estrus is attained the glands elongate and encroach upon the cores of the endometrial folds The uterine glands dilate especially the basal portion (fig 2) All fundi dilate detectably but some (usually about 15–20 in a single cross section) dilate considerably The gland cells of anestrous animals are low columnar with oval basal nuclei and somewhat scanty cytoplasm In estrous animals they are columnar being somewhat taller in the neck region than in the fundi A few mitotic figures are seen in the glands of estrous animals mostly in the basal portions Following mating there is a continued general growth of the glands and considerable coiling of the portion within the area spongiosa (fig 3) The cells of the neck region continue to be columnar with basal nuclei which are more often round than oval A large number of mitotic figures is seen in the neck region of the glands during the early pre implantation period but only a few are seen just prior to implantation At the same time the cells of the gland fundi are becoming tall columnar especially in the more dilated ones (This is the reverse of the case in estrus where neck cells were taller) The nuclei of the fundic cells become predominantly round rather than oval except in the more dilated fundi where they are elongate and the cells are obviously more crowded During the latter portion of the pre implantation period nuclei of fundic cells are often sub-central Mitotic figures are numerous in the fundic portion of the glands during the first half of the pre implantation period but not so numerous as in the neck portion

The changes seen in the endometrial stroma are passive and are caused by the growth of the glands rather than any real change in the stromal elements During anestrus the stroma is homogeneous throughout the endometrium except next to the myometrium where it appears somewhat less dense and less cellular As the glands begin to enlarge the stromal elements between them are compressed and consequently appear more dense At the same time the cores of the folds are being encroached upon by the developing gland bases of the area spongiosa As the fundi dilate the stroma of the cores is compressed into laminae which carry in them the blood vessels supplying the endometrium The stroma of the area compacta is relatively less changed due to the lesser degree of enlargement of the gland necks and the fact that the necks diverge from their almost parallel alignment to approach the luminal surface perpendicularly Thus there are relatively wide interglandular spaces in the upper area compacta Immediately subjacent to the luminal epithelium there is some increase in density of the connective tissue elements and in estrous and mated animals they form a cushion of fairly compact connective tissue Endometrial blood vessels from estrus onward are prominent but extravasation of blood has not been seen

The myometrium is similar in estrous animals and unimplanted pregnant animals contributing about 35% of the total diameter of the uterine horn The area vasculosa while prominent shows no distinctive changes

Following implantation the endometrium changes greatly in appearance A wave of epithelial hypertrophy and hyperplasia sweeps progressively from the uterine lumen toward the bases of the glands Behind this wave of hypertrophy the epithelial cells become extraordinarily enlarged (nuclei 90–100 μ in diameter may be seen) and the most superficial (luminal) cells lose their integrity and form masses of protoplasm containing whole or fragmented nuclei This degenerate tissue is termed a symplasma after Bonnet s suggestion since although technically a syncytium it is not an active tissue (Amoroso 52) The term also helps to distinguish it from the syncytial trophoblast next to which it lies in the placenta No special term seems to have been employed for the remarkably hypertrophied epithe

each animal furnished two items of data in the results reported below

The surgical procedure and tissue handling routine was standardized to insure uniform treatment of all material Animals were anesthetized with Nembutal The uterine horn was removed quickly placed upon a piece of bibulous paper and photographed with a camera mounted on the operating table Horns from pregnant non implanted animals were flushed with normal saline and the flushings saved for subsequent examination for conceptuses Each horn was rapidly divided into segments which were placed in a variety of fixatives (*vide infra*) For later enzyme study one segment was frozen in isopentane which was chilled in a dry ice alcohol bath Corresponding segments were always placed in the same fixative and in the same time sequence (e g the proximal most segment was always fixed in calcium formol and was fixed second) Uteri from pseudopregnant and implanted animals were handled in the same fashion except that they were not flushed with saline Tissue from implanted horns was taken from the interembryonic regions to exclude placental tissue and facilitate comparisons with non pregnant pseudopregnant and non implanted pregnant horns

For routine histology sections of Zenker s fixed material were stained in hematoxylin ponceau fuchsin light green and in hematoxylin eosin Serra s fixed material was used in a general histochemical survey Several serial sets of ten slides were made each slide containing 4–5 sections cut at 5 µ or 7 µ in thickness Adjacent slides were subjected to different staining procedures in order to allow comparison of contiguous sections by different methods Sections were stained by the Feulgen technique for DNA (Pearse 60 p 822) with eosin methylene blue at pH 4 5 for cytoplasmic basophilia (Burgos and Wislocki 56) by the PAS method for polysaccharides (Gurr 58 p 79) and with 0 10% toluidine blue for metachromasia (Pearse 60 p 834) Hemosiderin was determined by Perl s method for ferric iron (Pearse 60 p 931) Material fixed in cold Rossman s fluid was stained with PAS with and without prior diastase extraction for polysaccharides and glycogen Frozen sections of material fixed in 10% calcium formol were stained with Sudan Black in propylene glycol for lipids (Pearse 60 p 855) and subjected to the Schultz Smith test for cholesterol and its esters (Gurr 58 p 134) Phospholipids were determined by Sudan Black staining of paraffin embedded sections fixed in weak Bouin s solution

RESULTS

Histology of the uterus during the reproductive cycle

The ferret uterus is bicornuate The horns unite distally to form a common corpus uteri The endometrium is seen to be thrown into four (rarely 5 or 6) large longitudinal folds At the bottom of the troughs between the folds there may be smaller folds which vary in size and extent The endometrial glands lie with their axes essentially parallel to the apices of the large folds and consist of a straight neck region and a coiled basal portion In the non pregnant state the glands are short so that each endometrial fold has a non glandular core consisting of stromal elements only There is also a narrow area of gland free endometrial stroma immediately subjacent to the inner myometrium Accordingly for descriptive purposes the endometrium can be divided into four regions an area compacta occupied by the necks of the glands an area spongiosa occupied by the basal portion of the glands a non glandular core of the folds and a sub-myometrial area (fig 1)

The myometrium consists of a circular inner layer of smooth muscle and a longitudinal outer layer of smooth muscle Between the two layers is a well defined area vasculosa from which blood vessels pierce the inner myometrial layer to enter the cores of the endometrial folds

The changes occurring in the endometrial epithelium during the reproductive cycle are quite remarkable and are the same in pregnant and pseudopregnant uteri The luminal epithelium which is cuboidal during anestrus becomes tall columnar at estrus with elongate basally situated nuclei In the troughs there are occasional areas of pseudostratification (fig 2) After mating growth continues and at 4 days *p c* the luminal epithelium shows

was present in the lumen The gland neck cells showed even less PAS+ material in the brush border but in a few cells strongly PAS+ granules were seen in the apical cytoplasm Fundic cells had relatively more PAS+ material The fundic lumina had usually a moderate amount of strongly PAS+ granules and flakes Most cells had a moderate sprinkling of granules in the apical cytoplasm the brush border stained distinctly and some material was adherent to the apical surface of the cells The basement membrane of both luminal epithelium and glands was distinct and smooth The stroma was mildly PAS+

At estrus the brush border of the luminal epithelial cells was strongly PAS+ over the entire surface Only an occasional bit of PAS+ material was seen in the uterine lumen (fig 7) The neck region of the glands had moderate to small amounts of strongly PAS+ material in the lumina The brush borders of the gland neck cells stained distinctly but not so strongly as the luminal epithelium A few PAS+ granules were seen in the apical cytoplasm of an occasional cell Gland fundi had moderate amounts of strongly PAS+ material in the lumina in the form of flakes and large granules A loose granular fringe of PAS+ material was adherent to the apical end of the cells and apically and centrally disposed PAS+ cytoplasmic granules were numerous The more dilated glands contained relatively more PAS+ material The basement membrane was distinct and fairly smooth The stroma was mildly PAS+

The uterine luminal epithelium on day 4 *p c* was similar to that seen at estrus Luminal contents could not be assessed as the uterine horns had been flushed for conceptuses Gland neck lumina contained moderate amounts of strongly PAS+ flakes the brush border stained prominently and strongly PAS+ granules were adherent to the apical surface Although scarce PAS+ cytoplasmic granules were seen apically in some cells Gland fundi had essentially no PAS+ material in the lumina but a very heavy layer of strongly PAS+ material was adherent to the apical ends of the cells The brush border was strongly PAS+ and numerous PAS+ cytoplasmic granules were present in the apical cytoplasm and to a lesser extent in the central cytoplasm The basement membrane of the luminal epithelium was distinct but undulating while that of the glands was fairly smooth

In uteri removed on days 6 through 10 *p c* increasing amounts of strongly PAS+ material were seen in the gland lumina and by day 10 *p c* most neck lumina had moderately heavy concentrations of flaky material or solid plugs of PAS+ material and gland fundic lumina were nearly filled with granules and flakes (fig 8) Appreciable quantities of strongly PAS+ material remained in the uterine lumen on days 9 and 10 *p c* in spite of flushing for blastocysts The cells of all regions nonetheless showed relatively less PAS+ staining The brush border of the luminal epithelial cells and gland neck cells was strongly PAS+ but thin and no cytoplasmic granules were found Fundic cells showed moderate to strongly PAS+ brush borders with some PAS+ material adherent to the apical ends of the cells The more dilated glands showed relatively more staining in the brush border and relatively more adherent material A few apical cytoplasmic granules were seen in the fundic cells the number of granules per cell and the number of cells with granules being larger in the more dilated glands The apical cytoplasm of about one half of the fundic cells was moderately PAS+ in uterine tissue removed on day 10 p c The basement membrane was no different than in the earlier stages The stroma was mildly PAS+

In uterine tissue removed on day 11 *p c* the gland lumina were similarly filled with strongly PAS+ plugs or flakes Much strongly PAS+ material remained in the uterine lumen also Brush borders of both luminal cells and gland cells continued to stain strongly and the cytoplasm of both neck and fundic cells was moderately PAS+ Cytoplasmic granules were not seen except in occasional fundic gland cells

Tissue from the earliest post implantation stage (day 12 *p c*) was similar to the previous stage except that the luminal epithelium had a very thick fringe of strongly PAS+ material adherent to the

lium from which the symplasma is derived Since symplasma formation is continuous and there is no clear demarkation between the greatly enlarged cells and the symplasma it is suggested that the area of greatly enlarged cells be called the pre symplasma

Already by day 12 *p c* the luminal epithelium shows moderate hypertrophy (fig 4) Cell nuclei are detectably larger and the cytoplasm appears more dense and stains more intensely than the cells of the glands Mitoses are numerous in both the luminal epithelium and the gland necks

The gland neck cells in the area compacta are hypertrophied on day 15 *p c* and are indistinguishable from the luminal epithelium As the hypertrophy develops the cells become columnar rather than pseudostratified and the nuclei are central or subcentral in position Mitoses are very numerous in the hypertrophied area but scarce in the gland fundi At this time the cross sections of the longitudinal folds are beginning to assume a characteristic frond shape with the much compressed connective tissue core of the fold forming the stem of the frond and the adjacent walls of the gland necks with an extremely thin lamina of connective tissue between forming as it were the pinnae

The wave of hypertrophy has extended into the glandular tissue of the area spongiosa by day 20 *p c* (fig 5) The luminal epithelium by this time is a pre symplasma with very large cells of irregular shape and symplasmic masses are sloughing off into the lumen Mitoses are not seen in the pre symplasmic epithelium It appears that the more luminal portion of the glands in the area spongiosa hypertrophy and become indistinguishable from the portions in the compacta At any rate the spongiosa is reduced in extent and contains gland fundi which are of two types One shows extreme dilation and exhibits an epithelium similar to that of the neck region These greatly dilated glands are relatively few in number (4 to 6 in a cross section) and may in fact be invaginations of the luminal epithelium The greatly dilated glands are usually found in the base of one of the longitudinal folds The other gland fundi are moderately dilated and as the cells hypertrophy, they become cuboidal with centrally placed nuclei A large amount of mucoid secretion is present in the glands as well as the central lumen at this time

The endometrium at day 25 *p c* presents a further elaboration of the picture just described The symplasma which is sloughing off has pyknotic nuclei and occasional masses of nuclear material are seen without any surrounding cytoplasm The moderately dilated fundi are found in the sub myometrial portion of the endometrium and in the central core of the longitudinal folds Their cells are large and cuboidal or low cuboidal with central nuclei Mitoses are no longer seen in the endometrium Large amounts of mucoid secretion are found in the gland lumina and central lumen

Beyond day 25 *p c* no essential changes are noted The whole uterus of course enlarges grossly There is a more intense formation of symplasmic masses in the later stages and large spicules and globules of nuclear material are seen in the lumen Almost all of the moderately dilated fundi have a low cuboidal epithelium (fig 6)

Save for compression due to enlargement of the epithelial elements no changes occur in the endometrial stroma during the post implantation period The capillaries in the cores of the folds show some endothelial hypertrophy but this is moderate compared to that seen in placental tissue The myometrium becomes relatively thinner after implantation coming to represent only 15–20% of the diameter of the uterus The area vasculosa of the myometrium becomes enlarged as gestation progresses

Between days 35 and 40 *p c* the endometrium breaks down and by day 45 *p c* again resembles the anestrous state

Carbohydrates

Diastase resistant PAS+ material was examined in both Rossman s fixed and Serra s fixed material

The brush border of the luminal epithelium in anestrous animals exhibited a thin and discontinuous PAS+ reaction A very small amount of PAS+ material

Cytoplasmic basophilia

At anestrus estrus and during the pre implantation period the epithelial elements of the endometrium exhibited a moderate cytoplasmic basophilia which could be abolished by prior extraction with ribonuclease The basophilia in the gland cells was slightly less strong than that in the luminal epithelial cells and in the fundic cells the apical cytoplasm commonly stained more than the basal cytoplasm (fig 15)

At implantation the cells of the luminal epithelium and the upper portion of the gland necks showed a moderately strong cytoplasmic basophilia However the cells of the deeper portions of the glands showed no change in staining intensity Throughout gestation the hypertrophied epithelium and the pre symplasma developed from it exhibited strong basophilia Those gland fundi which became greatly dilated likewise developed a strong basophilia but the non-dilated and most of the moderately dilated fundi had a light or moderate basophilia (fig 16) Tissue from pseudopregnant animals showed changes which corresponded to similar stages from pregnant animals

Throughout all stages the luminal epithelium showed an apical cap of intensely basophilic material not removed by ribonuclease This apical cap corresponded to the diastase resistant PAS+ apical cap A similar apical cap of strong basophilic material was seen in the gland necks of implanted animals and in corresponding pseudopregnant animals However gland neck cells from pre implantation stages as well as estrous uteri showed little or no basophilia in the apical cap Fundic cells had either thin basophilic caps or none There appeared to be no pattern to the presence or absence of basophilic apical caps in the fundi

Neither the uterine lumen nor the gland lumina contained any noteworthy amount of basophilic material during anestrus and estrus Material remaining in the uterine lumen after flushing during the pre implantation period showed a weak to mild basophilia and occasionally small aggregates of acidophilic material were noted The material in the lumina of the gland necks was faintly basophilic during the early pre implantation period but became decidedly acidophilic as the time of implantation approached Fundic lumina exhibited little or no staining reaction

At the earliest post implantation stages strongly basophilic ribonuclease resistant material was present in the uterine lumen corresponding to the PAS+ material described above The gland neck lumina were filled with strongly acidophilic material and the gland fundi appeared empty The contents of the uterine lumen continued to exhibit strong basophilia through day 25 *p c* after which mixtures of moderately basophilic material and non stainable material was seen Toward the end of gestation masses of acidophilic necrotic cell debris were also seen The contents of the neck lumina which were acidophilic at early implantation became progressively more basophilic and at the end of gestation were strongly basophilic Most of the material in the moderately dilated gland fundi gave either a neutral reaction at pH 4 5 or a very slight basophilia Material from pseudopregnant animals was no different than material from pregnant animals

Metachromasia

At anestrus the uterus exhibited a faint metachromasia in both luminal epithelial cells and gland cells The stroma was faintly metachromatic The amount of metachromatic material increased at estrus and the luminal epithelium showed a mild metachromasia which was slightly more marked at the apical end of the cells The gland cells likewise showed a mild degree of metachromasia

During the early pre implantation period the gland cells showed only a faint metachromasia which was more apparent in the larger gland bases than elsewhere The luminal cells were somewhat variable but in general appeared to stain a bit less intensely than at estrus Just before implantation the metachromasia of the luminal cells increased becoming moderate to strong at implantation The apical ends of the cells stained more intensely than the cytoplasm in general A parallel but lesser increase in the amount of metachromatic staining was seen in the glands The stroma continued to be faintly meta

cell apices and the fundic lumina were mostly empty The basement membrane was somewhat less distinct than previously

On day 15 *p c* at which time the luminal epithelium and the gland necks had undergone hypertrophy, there was a thick refractile rim of very strongly PAS+ material adherent to the apical end of the cells (fig 9) Most luminal cells contained fair numbers of apical granules a lesser number of central granules and a fine sprinkling of basal granules The neck cells although histologically similar had little material adherent to the strongly PAS+ brush borders and only a modest scattering of apical granules In a small number of gland neck cells vacuoles of strongly PAS+ material were noted usually in a basal or central position (fig 9) The greatly dilated gland fundi resembled the luminal epithelium The cells of the moderately dilated and undilated fundi had a thin brush border and a weakly PAS+ cytoplasm The uterine and glandular lumina contained large amounts of strongly PAS+ material in the form of large flakes or solid plugs

Tissue removed at later periods of gestation was generally similar The presymplasmic epithelium showed increasing numbers of strongly PAS+ vacuoles and the cytoplasm was moderately to strongly PAS+ (fig 10) Few cytoplasmic granules were noted although the cytoplasm often had a grainy appearance The uterine and glandular lumina continued to have relatively large amounts of PAS+ material The basement membrane remained distinct but became smooth rather than undulating

Glycogen

At estrus the ferret uterus contained moderate amounts of glycogen (diastase extractable PAS+ material) in the luminal epithelium and cells of the gland necks (fig 11) However no glycogen was detectable in the cells of the gland fundi Most glycogen granules in the luminal epithelium were seen as basally situated aggregates or as columns" of granules which often gave the appearance of being between cells Occasionally glycogen granules were found in the apical cytoplasm and rarely in the central cytoplasm of the cells Cells of the gland necks had somewhat more glycogen than the luminal cells but the pattern of distribution was similar In addition to granules the cytoplasm of the cells in both regions gave a diffuse PAS+ reaction which was almost completely abolished by diastase extraction

The amount and distribution of glycogen in uterine tissue removed on day 4 *p c* was essentially the same as at estrus However the glycogen content of tissue removed on days 6 through 11 was highly variable The luminal epithelium had an abundance of glycogen granules on days 6 and 10 *p c* (fig 12) but at other times only traces of glycogen were seen Gland neck cells contained moderate to abundant numbers of glycogen granules on days 8 and 10 *p c* (fig 12) but only occasional granules were seen at other times Glycogen was found in the gland fundic cells on day 6 *p c* and thereafter until implantation The amount of glycogen in the fundic cells was correlated roughly with the degree of dilation of the fundi those showing little or no dilation being practically devoid of glycogen (fig 13) As in other parts of the endometrium glycogen was seen as aggregates of basally situated granules columns of granules occasional granules in the apical cytoplasm and a diffuse distribution in the cytoplasm In addition glycogen granules were seen in moderate numbers in the gland lumina in one or two specimens The number of dilated gland fundi increased during the pre implantation period and consequently the amount of glycogen in the fundic region (area spongiosa) increased However the degree of deposition in individual cells showed no detectable increase

Uterine tissue removed on day 12 *p c* (the earliest implantation stage) contained a small amount of glycogen as widely scattered basal granules in the cytoplasm of the luminal epithelium and neck cells (fig 14) Occasional fundic cells contained apically situated glycogen granules and a few granules were seen in the lumen of the gland fundi Uterine tissue removed from day 15 *p c* onward did not contain detectable amounts of glycogen

At estrus the number of cells contain ing Schultz positive granules in an entire cross section averaged one in the sub-myo metrial stroma and two in the core of the folds Sections from early pre implanta tion uteri averaged 7 to 8 positive cells in the sub myometrial region and one in the cores Late pre implantation stages had 3 to 5 positive cells per section in the sub-myometrial area and 3 to 4 cells per section in the cores Early post implanta tion material was virtually devoid of Schultz positive material Sections of tis sue removed on day 15 *p c* contained an average of one positive cell in the sub myometrial area and two in the core Uterine tissue removed on day 18 *p c* had an average of 11 positive cells per section in the sub-myometrial area and seven per section in the cores Tissue examined from later stages of gestation was essen tially negative

Pseudopregnant uteri were Schultz neg ative except for one case Sections from material removed on day 6 *p c* contained one or two macrophages with positive granules in about one half of the sections examined

Mast cells

The relative number and distribution of mast cells was recorded in a few of the toluidine blue stained sections Distribu tion was noted with respect to quadrants of the section (i e mesometrial antimeso-metrial or lateral) as well as tissue layer (i e endometrial stroma inner myome trium or outer myometrium)

The largest number of mast cells was observed in sections from estrous uteri Approximately 40 mast cells were seen per section in the endometrial stroma be ing found mostly in the connective tissue cores of the folds and in the sub myome trial region The outer myometrium con tained roughly twice as many mast cells per section (94/section) located primarily in or near the area vasculosa and the serosa Only an occasional mast cell was found in the inner myometrial layer The mast cells in the endometrial stroma showed no distributional pattern by quad rant however in the outer myometrium the largest number of cells were found in the mesometrial quadrant and the least in the antimesometrial Variation between sections was large enough however to suggest that the differences were not sig nificant

During the pre implantation period the number of mast cells in the stroma de creased to about one half the estrous fig ure The number in the myometrium while fluctuating averaged about the same as during estrus There was a defi nite tendency for mast cells to be concen trated in the mesometrial and antimeso metrial quadrants but there was no apparent difference in concentration be tween them

At implantation and afterward the total number of mast cells showed a marked decrease Fewer than ten cells on the average were found in the endometrial stroma and the myometrium with one or two exceptions contained 20–30 mast cells per section During gestation there ap peared to be a tendency for mast cells to be concentrated in the lateral quadrants although the pattern was not clear cut Mast cells in pseudopregnant animals cor responded in numbers and pattern to equivalent pregnant material

Ferric iron

The endometrial stroma of all tissue examined contained appreciable numbers of macrophages laden with pigment which appeared yellow or brownish regardless of the staining procedure employed Similar yellow brownish granules were seen in the cytoplasm of fundic gland cells of some animals during active gestation Applica tion of Perl s technique produced the clas sic Prussian blue color demonstrating ferric iron in the macrophages but in no case was iron found in the gland cells

Macrophages containing ferric iron were abundant in the endometrial stroma at estrus except in the area compacta where only a few were found (fig 19) A few iron containing macrophages were found in the myometrium being slightly more frequent in the area vasculosa

Following mating there was a definite decrease in the number of iron containing macrophages however a moderate num ber were always seen in the stroma next to the myometrium A lesser number was found in the connective tissue cores and

chromatic throughout this period Uteri from pseudopregnant animals during the same period exhibited somewhat less metachromasia but showed a qualitatively similar increase in staining toward the time of implantation

The degree of metachromatic staining seen in pregnant uteri removed from days 15 *p c* to 35 *p c* was variable ranging from mild to moderately strong No pattern was discerned except that the amount of metachromasia was less intense than at implantation The gland cells in any section showed less metachromasia than did the luminal epithelium The greatly dilated glands which contained pre symplasma cells stained like the luminal epithelium Occasionally a small amount of strongly metachromatic material was seen in the uterine lumen or gland lumina The pseudopregnant uteri removed after day 15 *p c* showed moderate metachromasia especially in the apical cytoplasm Fairly large amounts of moderately strong metachromatic material were seen in both glandular and uterine lumina

A possible clue to the variable staining seen in the post implantation uteri was provided by some uterine tissue in which some fetal trophoblast was present In this tissue the metachromasia was strong in the glandular epithelium just under the trophoblast but was progressively lighter as the distance from the fetal tissue increased

Lipids

The epithelial portions of the calcium formol fixed endometria from pregnant animals exhibited a diffuse sudanophilia ranging from moderate to very slight However except in one case lipid droplets were not seen Anestrous and estrous uteri showed a very slight sudanophilia in both luminal and gland cells A moderate sudanophilia was seen in the luminal epithelium on day 4 *p c* Although there was some variation in individual animals later stages showed progressively less sudanophilia the staining being almost negligible in tissue removed shortly after implantation (day 15 *p c*) Somewhat more staining was seen in later post implantation material as the pre symplasma developed The cells which were at the tips of the pre symplasmic fronds contained detectably more sudanophilic material than the other pre symplasmic cells (fig 17) The cells of the gland fundi were in general more sudanophilic than the luminal cells although the difference was not great

The only variations from the pattern of diffuse sudanophilia noted were seen in some uteri prior to implantation About one third of the non dilated glands in a uterine horn removed on day 4 *p c* contained numerous intracellular droplets which stained intensely (fig 18) The luminal epithelial cells in tissue removed on day 6 *p c* and the gland cells of tissue removed on day 9 *p c* had basal deposits of material which stained fairly heavily in Sudan Black Under low power examination these deposits had a fuzzy tufted appearance but under oil immersion some granularity was evident in the center of the stained area The appearance suggests that streaming of the sudanophilic material occurred during tissue preparation Both the luminal epithelial cells and the gland cells of tissue removed on day 11 *p c* had numerous basal tufts of sudanophilic material

Not all of the pseudopregnant material was suitably fixed for lipid staining but all stages examined corresponded to the equivalent pregnant material

The pattern of sudanophilia seen in tissue fixed in weak Bouin s fluid for the preservation of phospholipids was similar to that seen in calcium formol fixed material except that the basal tufts and granules mentioned above were not seen

Cholesterol and/or its esters

No Schultz positive material was found in the epithelial components of the uterine endometrium However Schultz positive granules were found within macrophages in the stroma of most pregnant animals Practically all of the cells containing Schultz positive material were located in the sub myometrial stroma or the cores of the endometrial folds Quite rarely isolated cells with Schultz positive granules were seen in the area spongiosa or compacta and occasionally such cells were seen in the area vasculosa or in the myometrium close to the area vasculosa

occurs on day 13 or 14 p c Amoroso 52) changes corresponding to the wave of hypertrophy in the ferret are seen Formation of pre symplasma and symplasma has not been described in the pseudopregnant cat and is said to occur in pregnant cats only at the implantation sites (Wislocki and Dempsey 46) Courrier and Gros (32) point out that they did not find "syncytiums épitheliaux" in the sterile horn of a unilaterally pregnant cat Mulligan (42) described post coital changes in the canine uterus which paralleled those in the cat The period of metestrum which is actually spontaneous pseudopregnancy is characterized by moderate hypertrophy and heightened secretion by the epithelial elements but neither pre symplasma nor symplasma formation occur A C Enders (57) observed greatly enlarged cells and symplasmic masses in a deciduoma produced by scratching the endometrium of a pseudopregnant mink and suggested that the production of the symplasma was a response to non specific trauma The spontaneous appearance of the pre symplasma and the production of symplasmic masses in both non placental regions of pregnant uteri and in pseudopregnant uteri represents a marked difference between the reproductive cycle of the ferret and the other carnivores which have been studied Whether this reflects a different hormonal balance in the ferret or a difference in intrauterine physiology is at present not clear It does suggest that the pseudopregnant ferret uterus may provide a better model of the maternal placenta" than other species for a variety of studies

The production of large amounts of histopoietic material is a notable characteristic of the endometrium of carnivores and other forms which have an endothe liochorial placenta (Amoroso 52) This material together with the symplasma comprises the histotrophe which is presumably an important source of nutrition for the embryo Previous histochemical studies of the endometrium of other carnivores have paid particular attention to glycogen and lipids and have shown that both are conspicuous features of the tissue In view of the strong histological similarity of the ferret uterus to other carnivore uteri it is somewhat surprising that neither glycogen nor lipid appear to play any considerable role in the uterine physiology of ferrets

The major secretory product of both luminal epithelium and the uterine glands is apparently glycoprotein and/or mucoprotein since it consists of diastase resistant PAS+ material which is non metachromatic and usually basophilic The present data do not permit a more precise identification but it is apparent that the exact composition of the secretory material varies in different portions of the endometrium and at different stages The material in the central lumen was always basophilic at pH 4 5 whereas the material in the gland neck lumina was acidophilic during the last half of the pre implantation period and the first week of active gestation Differences in the staining reaction of the fundic secretions were also seen during the latter part of gestation Most of this material appeared a neutral gray in the EMB stain although it was strongly PAS+

The only suggestion that acid mucopolysaccharides might form a part of the endometrial secretions in pregnant animals was the occurrence of occasional patches of strongly metachromatic material in the lumina of some uteri The consistent occurrence of moderately strong metachromasia in the contents of both central and glandular lumina of pseudopregnant uteri during the active gestation phase is most interesting as it represents one of the few differences noted between pregnant and pseudopregnant animals

Very little information is available concerning the histochemical nature of the uterine secretions in other carnivores A C Enders (61) found plugs of PAS+ diastase resistant material in the gland neck lumina and variable amounts of similar material in gland fundi of mink uteri during delayed implantation The picture resembles that seen in ferret uteri during the last half of the pre implantation period except that the ferret has a thicker apical cap of PAS+ material adherent to the luminal epithelium Erichsen (53) reported that the cells of the uterine glands and crypts of pro-estrous and estrous canine uteri were crowded with diastase resistant PAS+ granules in the

area spongiosa but only occasionally were any seen in the area compacta (fig 20) A few macrophages were located along the blood vessels in the area vasculosa Only rarely were they seen in the muscle layers and then in company with blood vessels

Essentially the same pattern was seen after the time of implantation that is moderate numbers of iron containing macrophages in the sub myometrial stroma and somewhat lesser numbers in the cores of the folds and the area spongiosa There was the impression that the number of macrophages increased in late pregnancy but this change was not significant The number of iron containing macrophages in the area vasculosa of the myometrium definitely increased in late pregnancy and there was a scattering in the muscle layer again usually next to the blood vessels

DISCUSSION

The general histological appearance of the ferret uterus resembles closely that of other carnivores for which adequate descriptions are available (mink Hansson 47 R K Enders 52 cat Dawson and Kosters 44 dog Mulligan 42) Mink and ferret uteri are virtually identical in appearance The cat differs chiefly in lacking the prominent connective tissue core in the longitudinal folds of endometrium, with the result that the glands have more of a simple radial orientation to the uterine lumen than do the glands of the ferret The canine uterus differs from the ferret in having a stromal layer interposed between the basal or crypt portion of the glands and the area spongiosa

The present study correlates well with prior descriptions of ferret uterine histology (Marshall 04 Hammond and Marshall 30 Hamilton and Gould 40) except on two points Marshall (04) described hemorrhage and extravasation of blood into the stroma during estrus such as occurs in the dog Such extravasation was not seen in the present study although blood vessels were more apparent during estrus and early pregnancy than previously Hammond and Marshall (30) described the anestrous uterus as having a large lumen and lacking the characteristic longitudinal endometrial folds Such an appearance was not seen in the present study and has only been noted in some experimental animals shortly after the end of pseudopregnancy

Before proceeding with the discussion of results it seems appropriate to reemphasize that the tissue from implanted animals was taken from the interembryonic areas of the uterus and it cannot be assumed that the morphological and physiological changes seen in this tissue are comparable to changes that occur in the placental areas

The changes seen in the ferret uterus during pregnancy and pseudopregnancy may conveniently be described as occurring in two phases However it must be recognized that the changes seen actually form a continuum of events all of which are evoked by the coital stimulus The first phase covers the entire 11 or 12 day pre implantation period This phase is characterized by general growth of the epithelial components especially the glands which dilate slightly become considerably elongated with basal coiling and exhibit considerable mitotic activity While secretory products of both glands and luminal epithelium show a steady increase during this phase the cytoplasmic basophilia does not suggest a highly accelerated secretory rate The second phase covers the period of active gestation and begins with the appearance in the luminal epithelium of frank hypertrophy and great mitotic activity As this hypertrophic zone sweeps toward the gland fundi the pre symplasma and symplasma appear behind it The intense cytoplasmic basophilia of both the hypertrophied zone and the pre symplasma indicates a high secretory rate and copious secretions are evident

Essentially the same sequence of uterine change and development occurs in other carnivores although there are several noteworthy differences regarding the stage of the cycle at which they occur and the conditions which elicit some of them Dawson and Kosters (44) describe two pre implantation phases in the cat uterus The first of these lasts one week and corresponds to the entire pre implantation phase in the ferret During the second week post coitum in the cat (implantation

coupled with Fitch s observations that glycogen is absent from the portion of the canine uterine gland which is secreting similar material is interesting and deserves further investigation

The distribution of uterine lipids seen in the present study differs in several respects from the work of Nicol and Vernon Roberts (63) who studied anestrous estrous and peudopregnant ferrets They found no lipid material prior to the twenty first day after mating when a small number of droplets appeared in the luminal epithelium Thereafter increasing amounts of lipid were found becoming heavy on the thirty fifth day and reaching a maximum on the forty seventh day The findings of diffuse sudanophilia in the present investigation in stages reported negative by Nicol and Vernon Roberts may be due to the use of calcium formol fixation and propylene glycol as a staining vehicle since both are stated to enhance lipid retention and staining (Pearse 160 p 308) The increase in lipid material in the most luminal portion of the pre symplasma which Nicol and Vernon Roberts reported from day 20 *p c* onward was seen in the present study also However they found droplets of lipid rather than a diffuse staining reaction It should be noted that the material in the present study does not extend beyond day 35 *p c* and it is possible that lipid droplets would have been seen in more advanced material

The occurrence and distribution of uterine lipids in other species of carnivores presents a diverse and confusing picture due in part to lack of data Erichsen (53) was unable to demonstrate lipid in the endometria of dogs during pro-estrus estrus or progressive metestrus Lipids were present in the epithelium during regressive metestrus suggesting fatty degeneration On the other hand Wislocki and Dempsey (46) examined the endometrium from the inter placental region of a dog uterus during mid pregnancy and found lipids in the cytoplasm of both luminal and glandular epithelium especially the former which was packed with droplets In the cat lipid is not present in the endometrium at estrus but appears in the luminal epithelium and gland neck cells around the middle of the pre implantation period (Dawson and Kosters 44) The only relevant data from other mustelids is that of A C Enders (61) who found only occasional lipid droplets in the intermediate gland segments during delayed implantation Although the limitations of the data make comparison difficult it is apparent that lipid metabolism in the ferret uterus is unlike either the dog or cat Certainly lipids do not play an important role in the uterine physiology of the ferret and their increase toward the latter part of pregnancy or pseudopregnancy is suggestive of cellular degeneration rather than any active process

Shelesnyak s suggestion that there is a relationship between histamine release uterine mast cell depletion and nidation in the rat (60) has focused attention on changes in uterine mast cells during the reproductive cycle The data concerning mast cell distribution in the ferret while not adequate for quantitative analysis do show qualitative changes which are similar to that seen in other species The observation that the myometrium contains more mast cells than the endometrium is consonant with results obtained in guinea pigs (Iverson 62) hamsters (Harvey 64) and in other rodents but differs from the cow in which stromal mast cells are more numerous than myometrial mast cells (Likar and Likar 64) The high mast cell count at estrus and the decline during the beginning of the luteal phase resembles the changes seen in the hamster (Harvey 64) The noticeable decrease at the time of implantation while less dramatic is similar to that which occures in the rat (Shelesnyak 60) The changes in uterine mast cells in the ferret seem to be related to the reproductive cycle and could be used as evidence for histamine release at nidation However in view of the fact that decidualization in the ferret involves the epithelium rather than the stroma it seems more likely that they reflect changes in the hormonal balance

Data from the material stained for ferric iron demonstrate that in the ferret as in other carnivores (Amoroso 52) iron is not concentrated or secreted by the uterine epithelium The pigment present in the stromal macrophages was undoubtedly hemosiderin since it possessed a character

supranuclear cytoplasm which is consistent with the findings in the ferret On the contrary Fitch (63) found PAS+ material in the neck cells but none in the deeper parts of the gland Both authors found plugs of PAS+ diastase resistant material in the gland lumina during metestrus It is of interest that Fitch found the luminal plugs in the upper portion of the gland only, not in the deeper coiled portions where glycogen was abundant The coating of diastase resistant PAS+ material seen to be adherent to the apical end of both luminal and glandular epithelia in the present study varied in appearance and amount When thin as in estrus and early post coital stages, it was granular but became thicker and homogeneous in later stages Fuxe and Nilsson (63) have observed a similar gluey secretion on the apical surface of the luminal epithelia in mice The amount of material varies during the estrous cycle being greatest in estrus but is apparently always homogeneous and never granular These authors correlate the thickness of the apical coat with estrogen levels but the present data from the ferret indicate that the apical cap reflects only the secretory activity of the cell regardless of the agents producing the activity

Glycogen, which plays a prominent role in the uterine physiology of most mammals is strikingly deficient in the ferret uterus Hamilton and Gould (40) found very little glycogen in anestrous ferret uteri and increasing but highly variable amounts in proestrous and estrous animals especially just prior to ovulation Similar results were recorded by Nicol and Vernon Roberts (63) who further reported that glycogen decreased in pseudopregnant ferrets disappearing altogether after day 10 *p c* The present study reveals a similar pattern in uteri of pregnant as well as pseudopregnant ferrets Both previous studies recorded the highest concentration of glycogen in the gland necks which was true in the present study However Nicol and Vernon Roberts found no glycogen in the luminal epithelium and Hamilton and Gould found relatively little The present study shows substantial amounts (relatively speaking) in the luminal epithelium

The glycogen pattern in ferret uteri is much different from that seen in other carnivores Glycogen in the canine uterus has been studied recently by Fitch (63) Proestrous uteri showed no glycogen in the luminal epithelium moderate amounts throughout the glands and in the stroma and an abundance in the myometrium In estrus glycogen increased in gland fundi but decreased elsewhere During early metestrus (pseudopregnancy) heavy deposits were present in the deep glands but absent from the necks which Fitch notes were the segments of the glands containing heavy deposits of diastase resistant PAS+ material In the cat Dawson and Kosters (44) have shown that glycogen is not present in the uterus until shortly after mating first appearing as supranuclear droplets in the gland cells Subsequently basal deposits are seen becoming so large as to displace the nuclei apically The luminal epithelium although lagging behind the glands undergoes a similar cycle During the second half of the pre implantation period glycogen is depleted being virtually absent by the time of implantation but reappearing in the non placental portions of the endometrium during gestation

Only fragmentary information is available concerning glycogen in uteri of other mustelids A C Enders (57) found highly variable deposits of glycogen in the luminal epithelium and glands of mink during delayed implantation Hansson (47) stated that glycogen was absent from mink uteri until the beginning of nidation However he appears to have been judging glycogen by nuclear displacement rather than histochemical identification

Interest in uterine glycogen has been largely due to its possible role in nourishing the embryo Certainly such a role is not indicated in the ferret although it might be of some value in nourishing the free blastocyst The disappearance of glycogen during the pre implantation period is consistent with the idea that progesterone decreases glycogen production or hastens its utilization The fact that glycogen disappears from the ferret uterus at the time the glands begin to secrete large amounts of diastase resistant PAS+ material

coupled with Fitch s observations that gly cogen is absent from the portion of the canine uterine gland which is secreting similar material is interesting and deserves further investigation

The distribution of uterine lipids seen in the present study differs in several re spects from the work of Nicol and Vernon Roberts (63) who studied anestrous estrous and peudopregnant ferrets They found no lipid material prior to the twenty first day after mating when a small num ber of droplets appeared in the luminal epi thelium Thereafter increasing amounts of lipid were found becoming heavy on the thirty fifth day and reaching a maximum on the forty seventh day The findings of diffuse sudanophilia in the present inves tigation in stages reported negative by Nicol and Vernon Roberts may be due to the use of calcium formol fixation and pro-pylene glycol as a staining vehicle since both are stated to enhance lipid retention and staining (Pearse 160 p 308) The increase in lipid material in the most lu minal portion of the pre symplasma which Nicol and Vernon Roberts reported from day 20 *p c* onward was seen in the present study also However they found droplets of lipid rather than a diffuse staining re action It should be noted that the mate rial in the present study does not extend beyond day 35 *p c* and it is possible that lipid droplets would have been seen in more advanced material

The occurrence and distribution of uter ine lipids in other species of carnivores presents a diverse and confusing picture due in part to lack of data Erichsen (53) was unable to demonstrate lipid in the endometria of dogs during pro-estrus estrus or progressive metestrus Lipids were present in the epithelium during re gressive metestrus suggesting fatty degen eration On the other hand Wislocki and Dempsey (46) examined the endometrium from the inter placental region of a dog uterus during mid pregnancy and found lipids in the cytoplasm of both luminal and glandular epithelium especially the former which was packed with droplets In the cat lipid is not present in the endometrium at estrus but appears in the luminal epi thelium and gland neck cells around the middle of the pre implantation period (Dawson and Kosters 44) The only relevant data from other mustelids is that of A C Enders (61) who found only oc casional lipid droplets in the intermediate gland segments during delayed implanta tion Although the limitations of the data make comparison difficult it is apparent that lipid metabolism in the ferret uterus is unlike either the dog or cat Certainly lipids do not play an important role in the uter ine physiology of the ferret and their in crease toward the latter part of pregnancy or pseudopregnancy is suggestive of cellu lar degeneration rather than any active process

Shelesnyak s suggestion that there is a relationship between histamine release uterine mast cell depletion and nidation in the rat (60) has focused attention on changes in uterine mast cells during the reproductive cycle The data concerning mast cell distribution in the ferret while not adequate for quantitative analysis do show qualitative changes which are simi lar to that seen in other species The obser vation that the myometrium contains more mast cells than the endometrium is conso-nant with results obtained in guinea pigs (Iverson 62) hamsters (Harvey 64) and in other rodents but differs from the cow in which stromal mast cells are more numer ous than myometrial mast cells (Likar and Likar 64) The high mast cell count at estrus and the decline during the beginning of the luteal phase resembles the changes seen in the hamster (Harvey 64) The noticeable decrease at the time of implan tation while less dramatic is similar to that which occures in the rat (Shelesnyak 60) The changes in uterine mast cells in the ferret seem to be related to the repro-ductive cycle and could be used as evi dence for histamine release at nidation However in view of the fact that decidual ization in the ferret involves the epithelium rather than the stroma it seems more likely that they reflect changes in the hor monal balance

Data from the material stained for ferric iron demonstrate that in the ferret as in other carnivores (Amoroso 52) iron is not concentrated or secreted by the uter ine epithelium The pigment present in the stromal macrophages was undoubtedly hemosiderin since it possessed a character

supranuclear cytoplasm which is consistent with the findings in the ferret On the contrary Fitch (63) found PAS+ material in the neck cells but none in the deeper parts of the gland Both authors found plugs of PAS+ diastase resistant material in the gland lumina during metestrus It is of interest that Fitch found the luminal plugs in the upper portion of the gland only not in the deeper coiled portions where glycogen was abundant The coating of diastase resistant PAS+ material seen to be adherent to the apical end of both luminal and glandular epithelia in the present study varied in appearance and amount When thin as in estrus and early post coital stages it was granular but became thicker and homogeneous in later stages Fuxe and Nilsson (63) have observed a similar gluey secretion on the apical surface of the luminal epithelia in mice The amount of material varies during the estrous cycle being greatest in estrus but is apparently always homogeneous and never granular These authors correlate the thickness of the apical coat with estrogen levels but the present data from the ferret indicate that the apical cap reflects only the secretory activity of the cell regardless of the agents producing the activity

Glycogen which plays a prominent role in the uterine physiology of most mammals is strikingly deficient in the ferret uterus Hamilton and Gould (40) found very little glycogen in anestrous ferret uteri and increasing but highly variable amounts in proestrous and estrous animals especially just prior to ovulation Similar results were recorded by Nicol and Vernon Roberts (63) who further reported that glycogen decreased in pseudopregnant ferrets disappearing altogether after day 10 *p c* The present study reveals a similar pattern in uteri of pregnant as well as pseudopregnant ferrets Both previous studies recorded the highest concentration of glycogen in the gland necks which was true in the present study However Nicol and Vernon Roberts found no glycogen in the luminal epithelium and Hamilton and Gould found relatively little *The present study shows substantial amounts (relatively speaking) in the luminal epithelium*

The glycogen pattern in ferret uteri is much different from that seen in other carnivores Glycogen in the canine uterus has been studied recently by Fitch (63) Proestrous uteri showed no glycogen in the luminal epithelium moderate amounts throughout the glands and in the stroma and an abundance in the myometrium In estrus glycogen increased in gland fundi but decreased elsewhere During early metestrus (pseudopregnancy) heavy deposits were present in the deep glands but absent from the necks which Fitch notes were the segments of the glands containing heavy deposits of diastase resistant PAS+ material In the cat Dawson and Kosters (44) have shown that glycogen is not present in the uterus until shortly after mating first appearing as supranuclear droplets in the gland cells Subsequently basal deposits are seen becoming so large as to displace the nuclei apically The luminal epithelium although lagging behind the glands undergoes a similar cycle During the second half of the pre implantation period glycogen is depleted being virtually absent by the time of implantation but reappearing in the non placental portions of the endometrium during gestation

Only fragmentary information is available concerning glycogen in uteri of other mustelids A C Enders (57) found highly variable deposits of glycogen in the luminal epithelium and glands of mink during delayed implantation Hansson (47) stated that glycogen was absent from mink uteri until the beginning of nidation However he appears to have been judging glycogen by nuclear displacement rather than histochemical identification

Interest in uterine glycogen has been largely due to its possible role in nourishing the embryo Certainly such a role is not indicated in the ferret although it might be of some value in nourishing the free blastocyst The disappearance of glycogen during the pre implantation period is consistent with the idea that progesterone decreases glycogen production or hastens its utilization The fact that glycogen disappears from the ferret uterus at the time the glands begin to secrete large amounts of diastase resistant PAS+ material

PLATES

istic yellow brown color in routine stains and gave a positive Perl s reaction Mulligan (42) found iron containing macrophages in the endometrium of all dogs which he studied except immature animals Fitch on the other hand, found only one such case in a series of 35 dogs (63) Mulligan found the highest number of iron containing macrophages in pro estrus and post partum uteri a pattern which bears a striking resemblance to the pattern seen in the ferret Since the presence of hemosiderin in macrophages presumably represents phagocytosis of erythrocytes an increased number of such cells toward the end of pregnancy would be expected as endometrium is breaking down The abundance of hemosiderin laden macrophages at *pro-estrus in the* dog coincides with the extravasation of blood which occurs at the beginning of the heat period A similar extravasation of blood was not seen in the ferret and it is suggested that the abundance of hemosiderin containing cells at this time is a reflection of a prior pregnancy

ACKNOWLEDGMENTS

The author would like to express his appreciation to Lynn B Goldner and Maxi Archibald for their invaluable technical assistance in this work especially in the preparation of tissues This investigation was supported by Public Health Service grant HD 00504 from the National Institute of Child Health and Human Development

LITERATURE CITED

Amoroso E C 1952 Placentation in Marshall s Physiology of Reproduction vol 2 Ed by A S Parkes Longmans Green and Co New York Chapter 15

Burgos M H and G B Wislocki 1956 The cyclic changes in the guinea pig's uterus cervix vagina and sexual skin investigated by histological and histochemichal means Endocrinology 59 93–118

Courrier R and G Gros 1932 Contribution a l étude du cycle génital chez la Chatte C R Soc Biol *110* 51–53

Dawson A B and B A Kosters 1944 Preimplantation changes in the uterine mucosa of the cat Am J Anat *75* 1–37

Enders A C 1957 Histological observations on *the chorio*-allantoic placenta of the mink Anat Rec *127* 231–246

——— 1961 Comparative studies on the endometrium of delayed implantation Anat Rec *139* 483–497

Enders R K 1952 Reproduction in the mink (*Mustela vison*) Proc Am Phil Soc *96* 691 755

Erichsen S 1953 Histochemical changes in the endometrium of the dog during the oestrous cycle Acta Path et Microbiol Scand 33 263–267

Fitch K L. 1963 A study of uterine glycogen during the estrous cycle of the dog J Morph *113* 331–344

Fuxe K and O Nilsson 1963 The mouse uterine surface epithelium during the estrous cycle Anat Rec *145* 541–548

Gurr E 1958 Methods of Analytical Histology and Histo-chemistry Leonard Hill (Books) Ltd London

Hamilton W J and H J Gould 1940 The normal oestrus cycle of the ferret The correlation of the vaginal smear and the histology of the genital tract with notes on the distribution of glycogen the incidence of growth and the reaction to intravitam staining by trypan blue Trans Roy Soc Edinb *60* 87–105

Hammond J and F H A Marshall 1930 Oestrus and pseudo-pregnancy in the ferret Proc Roy Soc B *105* 607–629

Hansson A 1947 The physiology of reproduction in the mink (*Mustela vison* Schreb) with special reference to delayed *implantation* Acta Zool 28 1–136

Harvey E B 1964 Mast cell distribution in the uterus of cycling and pregnant hamsters Anat Rec *148* 507–516

Iversen O H 1962 The influence of es[illegible] genic and androgenic hormones on mast cells and connective tissue in uterus of guinea pig Acta Path et Microbiol Scand *56* 215–[illegible]

Likar I N and I J Likar 1964 Acid mucopolysaccharides and mast cells in the bovine uterus at different stages of the sexual cycle Acta Endocrinol *46* 493–506

Marshall F H A 1904 The oestrous cycle in the common ferret Quart J Micr Sci *48* 323–345

Mulligan R M 1942 Histological studies on the canine female genital tract J Morph [illegible] 431–448

Nicol T and B Vernon Roberts 1963 The distribution of lipoid and glycogen in the uterine horns of the ferret during the oestrous cycle J Obstet and Gynec Brit Commonwealth 70 851–858

Pearse A G E 1960 Histochemistry Theoretical and Applied 2nd ed Little Brown and Company Boston

Shelesnyak M C 1960 Nidation of the fertilized ovum Endeavour *19* 81–86

Wislocki G B and E W Dempsey 1946 Histochemical reactions in the placenta of the cat Am J Anat *78* 1–45


G
4
2
3
6

PLATE 1

EXPLANATION OF FIGURES

1 Cross section of non pregnant uterus Note area compacta (C) containing gland necks area spongiosa (S) containing gland bases gland free core of fold (X) and sub myometrial zone (Z) of the endometrial stroma Area vasculosa (AV) separates inner circular muscularis and outer longitudinal muscularis Hematoxylin ponceau fuchsin light green × 40

2 Estrous endometrium Luminal cells are tall columnar with elongate nuclei Epithelium is pseudostratified in trough upper right Glands are slightly dilated Feulgen × 127

3 Pre implantation endometrium Luminal epithelium is becoming crowded and pseudostratified Glands show considerable growth and basal coiling Fundic cells are tall columnar and many fundi are dilated Feulgen × 127

4 Endometrium at early implantation Luminal epithelium is undergoing hypertrophy and hyperplasia Mitoses (arrows) are common in luminal and gland neck epithelia Feulgen × 127

5 Endometrium at mid pregnancy Luminal epithelium and gland necks are pre symplasmic Wave of hypertrophy is entering area spongiosa Gland fundi are enlarged and mucus filled Fundic epithelium is becoming cuboidal *lower right* Feulgen × 127

6 Endometrium during late pregnancy (day 30 *p c*) Luminal epithelium and gland necks show pre symplasma Symplasmic masses are present at luminal surface Gland fundi have cuboidal or low cuboidal epithelia Feulgen × 127


7
11
8
12
13
10
14

PLATE 2

EXPLANATION OF FIGURES

Figs 7 8 9 10 Distribution of diastase resistant PAS+ material during pregnancy Rossman s fixation PAS after diastase extraction × 187

7 Estrus Brush border of luminal epithelium is strongly PAS+ Gland cells have apical granules and a small amount of PAS+ material is present in the gland lumina

8 Late pre implantation Some PAS+ material is adherent to the brush border Gland lumina contain much PAS+ material

9 Early gestation Brush border is very strongly PAS+ Much positive material is present in the lumen and adherent to the luminal surface There are several vacuoles of PAS+ material in the pre symplasma (arrows) Cytoplasm of cells is slightly PAS+

10 Mid pregnancy Cytoplasm of cells is more strongly PAS+ than in early gestation Pre symplasma cells are much larger Copious secretory material in the lumen Vacuoles are numerous (arrows)

Figs 11 12 13 14 Distribution of glycogen during pregnancy Rossman s fixation PAS × 187

11 Estrus A few basal granules of glycogen are seen in luminal epithelium Fairly large amounts are present in neck cells Granules are often crowded to periphery of cells by nuclei and appear to be in columns at edge of cell Compare with figure 7 which is the adjacent section

12 Late pre implantation Large granules of glycogen are present in both basal and apical cytoplasm of luminal cells Granules are mostly basal in neck cells Cytoplasm shows moderate diffuse PAS+ reaction before diastase extraction Compare with figure 8 which is the adjacent section

13 Late pre implantation Gland fundic cells show some basal granules Fine granules of glycogen are also present apically

14 Early implantation A few basal granules of glycogen are still present in luminal and neck cells (arrows)

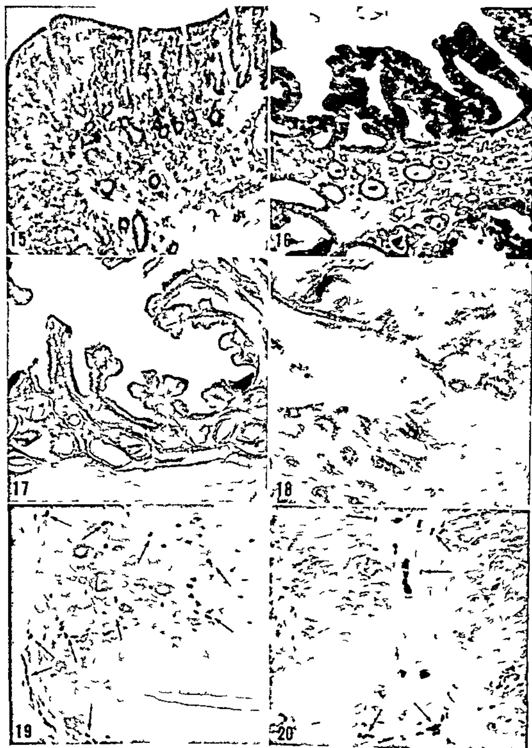

15
16
17
18
19
20

PLATE 3

EXPLANATION OF FIGURES

15–16 Cytoplasmic basophila Before implantation there is a moderate basophilia in luminal epithelium and gland fundi Neck cells show slightly less basophilia (fig 15) During gestation the pre symplasma shows a strong basophilia (fig 16) The relatively un modified glands show a moderate basophilia Eosin methylene blue at pH 4 5 × 105

17 Sudanophilia during mid gestation The apical cytoplasm of pre symplasma cells shows a moderate sudanophilia Calcium formol fixation Sudan Black B × 94

18 Sudanophilic droplets in gland neck cells of uterus removed on day four *p c* The cytoplasm shows a moderate sudanophilia Calcium formol fixation Sudan Black B × 94

19 Hemosiderin containing macrophages at estrus Macrophages (arrows) are very numerous in the area spongiosa and cores of the folds Fair numbers are also seen in the sub-myometrial stroma Perl s reaction × 72

20 Hemosiderin containing macrophages after implantation Modest numbers of macrophages (arrows) are present in the cores of the folds and in the sub myometrial stroma Perl s reaction × 72

Studies on the Nerve Endings in the Visceral Pleura[1]

FRANK I DWINNELL JR.
Department of Anatomy University of California School of Medicine San Francisco California

ABSTRACT The visceral pleura of 12 dogs eight lambs nine monkeys and four rabbits was studied by methylene blue immersion Nerve terminations were found in the pleura of all specimens The following types of nerve endings and patterns of innervation were observed (1) Free fiber endings arose from small myelinated fibers and terminated in the caudo-ventral lips of the lobes The parent fibers of these and all other endings arose in the lamb rabbit and dog from nerve bundles radiating from the hilus onto the inter lobar and diaphragmatic pleural surfaces In the monkey parent fibers arose from a complex hilar plexus of nerve bundles before spreading out within the pleural surfaces (2) Complex unencapsulated endings were seen in all specimens distributed evenly over the inter lobar and diaphragmatic pleural surfaces These arose from myelinated fibers which terminated in two or more complex endings In the monkey parent fibers may form an anastomotic network before terminating (3) In the dog an end net formation was found which appears to be a type of complex unencapsulated ending This "end net" is formed by the anastomosis of the terminal branches of several small myelinated fibers

Although nerve endings have been found in almost all tissues very few workers have reported them in the visceral pleura The first observation of nerve endings in the visceral pleura was reported by Larsell (22) in rabbits McLaughlin (33) then described pleural nerve endings in the cat Larsell (35) in the human infant Mizukoshi (53) in the human embryo Numata (56) in the bat and Honjin (56) in the mouse During the present decade Fukase (60) has studied the Formosan Macaque Honma (60) the Hedgehog and Saito (61) the Guinea pig and Flying squirrel

Although the description of nerve terminations and their distribution in the visceral pleura by these authors is excellent only Larsell (35) confined himself to the study of the visceral pleura Further most of the reports were based on observations using silver impregnation methods while Larsell's use of methylene blue had the advantage of demonstrating both the finer terminations as well as the full extent of nerve endings Finally only authors reporting in the latter half of this century have presented photographs while most others have illustrated their observations with drawings

The present study is an attempt to describe the distribution and types of nerve endings seen in the visceral pleura of the lamb rabbit monkey and dog and to present good photographs

MATERIALS AND METHODS

The visceral pleura of eight lambs four rabbits nine monkeys and 12 dogs was studied by methylene blue immersion In all cases only tissue from freshly sacrificed animals was used Whole lungs were cut into individual lobes and immersed in 0 01% methylene blue in normal saline for 30 minutes according to the method of Meyling (53) Tissues were fixed in cold 8 0% ammonium molybdate for 24 hours followed by thorough washing in distilled water

Pieces of lamb pleura were stripped from the lobes and dehydrated in alcohol The dog monkey and rabbit pleura could not be peeled from the lung Therefore pieces approximately 4 mm thick were cut from the surface of the lobes and dehydrated in alcohol

Sections were cleared in xylene and prepared for study in benzyl benzoate according to the method of Miller et al (58) Tissues prepared in this manner permit one to focus through the entire thickness of the section Therefore the distribution and course of the nerve endings and their par

[1] Th in estigati n was upport d by I SPHS grants 1 SO 1 FR 5355-04-5 and 5 T 5 GM 43-04

faces At this point single myelinated parent fibers extend to the edges of the lobes where they terminate in branched or unbranched free fiber endings

Other myelinated fibers after breaking away from the parent bundle terminate in complex unencapsulated endings There are two types of these endings The first of these a compact type of ending is seen to terminate shortly after anastomosis of the parent fibers (fig 4) It is formed from fine branches of one or more parent fibers which interdigitate prior to a very abrupt termination Greater detail of this type of ending is presented in figure 7 The second type (figs 9 10 and 13) is more coarse in construction and there is no anastomosis of parent fibers prior to termination This ending resembles more those seen in the lamb and rabbit An ending intermediate between these two types is seen in figure 12 This ending is formed from a single parent fiber and there is no anastomosis with other fibers prior to termination The structure is quite fine but not compact All these complex unencapsulated endings are found together in the same area of visceral pleura

Dog visceral pleura

In the dog the course of the fiber bundles away from the hilus is the same as that in the lamb and rabbit Free fiber and arborized endings similar to those of the lamb and rabbit are seen in the same distribution However in the dog a different type of complex unencapsulated ending is found This is the "end net formation shown in figure 8 This termination is formed from fine myelinated fibers which anastomose to cover a wide area of pleura approximately 0 1 mm There are no free fiber or arborized endings associated with this termination

DISCUSSION

The pleural nerve endings described in this paper may be classified according to the scheme presented by Miller and Kasahara (64) In all four animals (lamb rabbit monkey and dog) free fiber and complex unencapsulated endings were observed in the visceral pleura between the lobes and on the diaphragmatic surfaces The terminations are similar to those described in the visceral pleura of other animals the same types of ending have been reported by Larsell (35) and Numata (56) in such widely divergent animals as the human and the bat

The physiological evidence presented by Larsell and Coffey (28) leaves little doubt that the complex unencapsulated endings in the visceral pleura are "stretch" receptors They are therefore morphologically and functionally homologous with similar endings found elsewhere in the mammalian body such as in tendons (Ralston et al 60) blood vessels (Polley 55) and the heart (Miller and Kasahara 64) However without resort to dorsal and ventral root sections as well as vagotomies the nature of the central pathways of these endings cannot be ascertained

The true nature and function of the "end net" formation has not yet been determined It has not been described before in the visceral pleura of any animal but has been described in the heart (Holmes 57 Miller and Kasahara 64) Likewise in view of the evidence presented by Capps (11) the function of the free fiber endings with respect to the mediation of pain must remain in doubt

While numerous drawings of visceral pleural nerve endings have been published very few good photographs have been presented Since further study will involve description of the results of nerve section and since interpretation plays such an important role in any study of this type it is essential that photographic evidence be presented for comparison in any descriptive account

ACKNOWLEDGMENT

The author wishes to express thanks to Dr M R Miller and Miss M Kasahara for their advice encouragement and material support during work on this project

LITERATURE CITED

Capps J A 1911 An experimental study of the pain sense in the pleural membranes Archives of Internal Medicine 8 717–733

Fukase K 1960 On nerve supply especially sensory nerve supply of the lung in Formosan Macaque Archivum Histologicum Japonicum 19 75–93

ent fibers may be studied in relation to the visceral pleural surface

OBSERVATIONS

Before describing the types of nerve endings found in the visceral pleura it is necessary to describe briefly the general classes of nerve terminations found in other tissues In general according to the work of Miller and Kasahara (64), there are three types of nerve terminations which have been arbitrarily divided into 1 Free fiber endings which are little branched or unbranched terminations of small myelinated or unmyelinated fibers 2 Complex unencapsulated endings resulting from repeated branching of terminal fibers and which are distinctly discrete but unencapsulated structures (e g, Ruffini Ruffini like or Golgi type endings) 3 Encapsulated endings characteristically discrete and surrounded by a capsule of modified Schwann cells or connective tissue elements (e g Meissner s corpuscles Krause end bulbs Golgi Manzzoni ends or the various sized Vater Pacinian corpuscles) Although free fiber endings are often seen, the dominant type of nerve termination in the visceral pleura is the complex unencapsulated ending

In general distribution of parent fiber bundles is similar in all animals studied although there are some variations which will be discussed under specific headings Nerve fibers and terminations are observed consistently in certain regions of the visceral pleura and are never seen in others Nerves enter the pleura at the hilus fan out from this point and pass onto the pleura between the lobes and onto the diaphragmatic surface of the lower lobes Nerve fibers and endings are not seen on the costal surface of the visceral pleura Fibers do not enter the pleura by way of inter lobular connective tissue septa or with nervi vasorum Nerve bundles or parent fibers never terminate in more than one type of ending although there may be several endings of the same type formed from one fiber bundle

Lamb visceral pleura

Nerve bundles in the hilar region contain an average of 20 fibers each From the hilus fibers pass through the medial pleural surface into the interlobar and diaphragmatic surfaces where they separate into smaller parent bundles containing about five fibers each Parent fibers then break away to terminate in nerve endings which are distributed evenly over the pleural surface

Free fiber endings are observed in the pleura of the caudo ventral lips as single or branched terminations of myelinated parent fibers These fibers may extend a great distance from the parent bundle traveling over one half the width of the pleural surface before terminating

The majority of complex unencapsulated endings are formed by diffuse arborization of the parent fiber (fig 1) These endings are found in the pleura between the lobes and on the diaphragmatic surface of the lower lobes Detail and the relationship of this branching to the parent fiber may be seen more clearly in figure 11 Single fiber bundles give off parent fibers which terminate in several endings in an area approximately 5 mm² (fig 5) Another but less extensive example of this type of termination is presented in figure 3

A different type of complex unencapsulated ending (fig 2) is also found in the visceral pleura of the lamb These endings are less common They are formed by the fine branching of a single parent fiber and appear spherical in form

Rabbit visceral pleura

The course and distribution of fiber bundles and nerve endings is the same in the rabbit as in the lamb An arborized complex unencapsulated ending (fig 6) similar to that in the lamb is also seen In addition there are also free fiber endings present in the caudo ventral lips of the lobes In the rabbit spherical complex unencapsulated endings (fig 2) are not observed

Monkey visceral pleura

In the monkey the distribution of fiber bundles differs in that from the hilus fibers from one bundle will cross over to travel with those of another bundle This forms a complex network in the pleura of the medial lung surface From this medial pleura fiber bundles course toward the inter lobar and diaphragmatic pleural sur


1
2
3
4

Holmes R L 1957 Structures in the atrial endocardium of the dog which stain with methylene blue and the effects of unilateral vagotomy J Anat *91* 259–266

Honjin R 1956 On the nerve supply of the lung of the mouse with special reference to the peripheral vegetative nervous system J Comp Neur *105* 587–625

Honma H 1960 Histological study on the innervation especially sensory innervation of the lung in Hedgehog Archivum Histologicum Japonicum *19* 617–637

Larsell O 1922 The ganglia plexuses and nerve terminations of the mammalian lung and pleura pulmonalis J Comp Neur *35* 97–132

——— 1935 Nerve endings in the human pleura pulmonalis J Comp Neur *61* 407–411

Larsell O and J R Coffey 1928 The effect on respiration of stimulating the nerve terminations in the visceral pleura Anat Rec *38* 20

McLaughlin A I G 1933 Nerves and nerve endings in the visceral pleura of the cat J Physiol *80* 101–104

Meyling H A 1953 Structure and significa[nce] of the peripheral extension of the autonom[ic] nervous system J Comp Neur *99* 495–5[..]

Miller M R and M Kasahara 1964 Studies on nerve endings in the heart Am J Anat 11[.] 217–234

Miller M R H J Ralston III and M Kasahar[a] 1958 The pattern of cutaneous innervation [of] the human hand Am J Anat 10[.] 183 1[..]

Mizukoshi T 1953 Histological studies on [the in]nervation of lung of human embryo Tohok[u] Journal of Experimental Medicine 58 223 23[.]

Numata T 1956 Histology and innervation [of] lung in bat Archivum Histogicum Japoni[cum] 9 491–506

Polley E H 1955 The innervation of bl[ood] vessels in striated muscle and skin J Com[p] Neur *103* 253–267

Ralston *H J III M R Miller and* M Kasaha[ra] 1960 Nerve endings in human fasciae t[en]dons ligaments, periosteum and joint synov[ial] membrane Anat Rec *136* 137–148

Saito R 1961 Fine structure and innervat[ion] especially *sensory* innervation of the lungs [of] Guinea pig and Flying squirrel Archivum Hi[s]tologicum Japonicum *21* 299–322

PLATE 1

EXPLANATION OF FIGURES

The nerve endings demonstrated in all figures were stained by methylene blue immersion

The straight black line at the bottom of each photograph represents 100 μ of distance

In the explanation of figures C U E *is the abbreviation for complex* unencapsulated ending

1 Lamb Left lower lobe diaphragmatic surface A diffuse arborized type of C U E Endings similar to this are often seen in ventricular epicardium fasciae and periosteum

2 Lamb Right upper lobe inferior surface near hilus A C U E which takes a spherical form This type of ending is seen only rarely in the lamb and not at all in rabbit monkey or dog

3 Lamb Right middle lobe inferior surface A C U E similar to that shown in figure 1

4 Monkey Right lower lobe superior surface A compact type of C U E Three fiber bundles give off parent fibers to this area The parent fibers of the four endings shown appear to anastomose prior to termination


1
2
3
4

PLATE 2

EXPLANATION OF FIGURES

5 Lamb Right middle lobe, inferior surface A field of several diffuse arborized complex unencapsulated endings It will be seen that only one type of ending is formed from these parent fibers

6 Rabbit Left lower lobe diaphragmatic surface A diffuse arborized type of C U E This ending is similar to those seen in the lamb

7 Monkey Right upper lobe inferior surface A compact type of C U E

8 Dog Right cardiac lobe inferior surface A sensory end net formation which appears to be formed from the anastomosis of several small myelinated fibers This type of ending is seen only in the dog

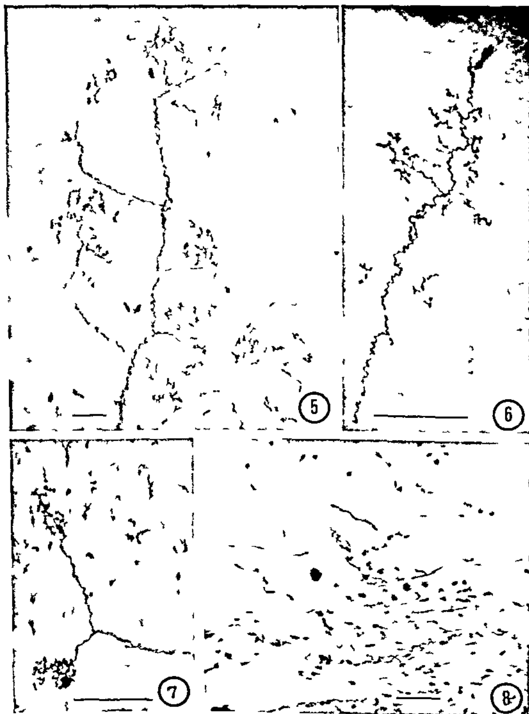

5
6
7
8

PLATE 2

EXPLANATION OF FIGURES

5 Lamb Right middle lobe inferior surface A field of several diffuse arborized complex unencapsulated endings It will be seen that only one type of ending is formed from these parent fibers

6 Rabbit Left lower lobe diaphragmatic surface A diffuse arborized type of C U E This ending is similar to those seen in the lamb

7 Monkey Right upper lobe inferior surface A compact type of C U E

8 Dog Right cardiac lobe inferior surface A sensory "end net" formation which appears to be formed from the anastomosis of several small myelinated fibers This type of ending is seen only in the dog

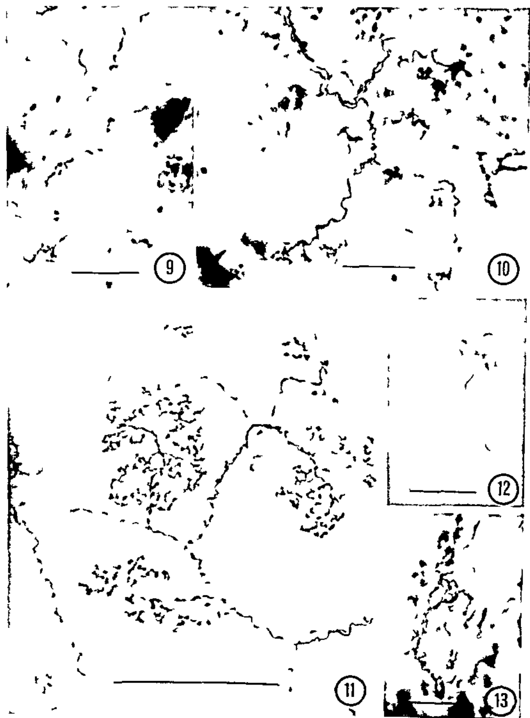

9
10
11
12
13

PLATE 3

EXPLANATION OF FIGURES

9 Monkey Right upper lobe inferior surface A coarse type of C U E There is no anastomosis of the parent fibers which give rise to this type of ending

10 Monkey Right upper lobe inferior surface A coarse type of C U E

11 Lamb Left lower lobe superior surface A diffuse arborized type of C U E

12 Monkey Right middle lobe superior surface A diffuse type of C U E similar to those seen in lamb and rabbit

13 Monkey Right middle lobe superior surface A coarse type of C U E

Morphologic Distinctions Between Oligodendrocytes and Microglia Cells in the Rabbit Cerebral Cortex

JAN CAMMERMEYER

Laboratory of Neuropathology National Institute of Neurological Diseases and Blindness Bethesda Maryland[1]

ABSTRACT In the rabbit cerebral cortex preserved by perfusion and stained by the silver carbonate method of Del Rio-Hortega modified by Naoumenko and Feigin for paraffin sections the oligodendrocytes are situated next to blood vessels or are placed at a short distance from the blood vessels which they contact with a thickening

The microglia cells are usually situated in juxtaposition to neurons and are rarely found along blood vessels They give off long tortuous thick processes with delicate secondary branches which contact numerous neighboring neurons and terminate either at short distances from branches of adjacent microglia cells or next to vascular walls Although there are regional variations in the appearance and number of microglia cells their processes are so profuse that they seem to supply all neurons these processes cover a small portion of the neuronal surface

In the cerebral cortex of the rabbit the oligodendrocytes because of their rare occurrence would seem to have a more restricted function while the microglia cells because of their profuse distribution seem to have a more universal function than is usually attributed to them

Although in light microscopic studies there is general agreement about the distribution of oligodendrocytes and the behavior of microglia cells (Del Rio-Hortega 19 32 and others) some recent observations would indicate that current concepts about the ubiquitous presence of oligodendrocytes and the mobility of microglia cells may not be correct (Cammermeyer 60b c d 65a b) In electron micrographs the oligodendrocytes are frequently referred to while the microglia cells even in regions with a rich supply are only rarely recognized (Herndon 64) or are not demonstrable (Westrum and Blackstad 62 Blackstad 63 Walberg 63)

A renewed investigation of oligodendrocytes and microglia cells in silver carbonate stained sections was initiated for the purpose of exploring (1) the characteristics of the two cell types (2) their relationship to blood vessels and neurons (3) the extent of cell processes and (4) the degree of approximation of processes from neighboring microglia cells The cerebral cortex of the rabbit was selected because in this animal fixation by perfusion can be performed rapidly and because in its cerebral cortex the cells are spaced far apart and the nuclei of various cell types are distinctive all prerequisites for accurate identification

MATERIAL AND METHOD

Male rabbits of known age were narcotized by an intravenous injection of sodium pentobarbital mixed with heparin Immediately thereafter the chest was opened a silk ligature placed in the transverse pericardial sinus a hemostat attached on the tip of the right ventricle and the right auricle cut The chest was filled with the same solution as that to be used in the first perfusate for flushing the blood vessels With the heart held under the fluid surface with the hemostat the left ventricle was incised and then a glass cannula attached to the perfusion system and filled with a composite saline solution was introduced into the ascending aorta through the incision and tied with the ligature Sucking of air into the arterial system was avoided by keeping the ventricular incision submerged this modification in the procedure used since the autumn of 1962 has proved to be essential for successful and uniform fixation by perfusion First the blood vessels were flushed with an amount corresponding to 15 or 20% of body weight of a composite saline solution (Elliott s "B" Irrigating Solution Baxter Laboratories Inc Morton

[1] N tion l Institut of He lth U S Public Health Servic Departm nt of H lth Edu tion nd Welf re B th d M ryl nd 20014

brane of the vascular wall (figs 1 18) If the oligodendrocyte and the blood vessel are superimposed then the close relation ship between the two is evidenced by the very slight change in focal plane necessary to bring each of them into sharp focus and to depict them at their greatest diameters (approximately 3 units on the microscrew of the Zeiss Ultraphot separates the two levels of figs 2 and 3 and of figs 4 and 5) The other type of oligodendrocyte is situ ated at a short distance from the vascular wall (fig 7)

The oligodendrocytes are distributed singly (figs 1 2 7 18 x in figs 25–27) or in small groups of 2 to 3 cells (fig 4 z in fig 25) but not in the large clusters seen in the rabbit facial nucleus (Cammer meyer 63b)

In a close up view of the oligodendro cytes their perikarya vary slightly from round to pear shape and the eccentric nuclei are usually round and are smaller than those of astrocytes (figs 1 2 4 7 8 o in fig 18) The cytoplasm is not uni formly black as the figures may indicate but consists of a silver impregnated net work enclosing minute vacuoles this lends a sieve like appearance to the perikaryon (fig 1 top cell of two in the center of fig 4) Along the periphery the vacuoles may become larger (between arrows c in fig 8) In the PASH stained sections the nuclei as characteristic for this species (compare Cammermeyer 63a) are noted for the diffuse distribution of small chro- matin granules and for a distinct larger chromatin mass connected by poorly stained lines The larger mass which covers the nucleolus is usually situated near the inner aspect of the nuclear mem branes in the central part of the peri karyon

A few extremely delicate processes ex tend from the perikaryon in various direc tions From a single oligodendrocyte situ ated next to a blood vessel (x and v in fig 3) one process after circumventing the blood vessel encroaches upon a juxta vascular neuron (upper arrow and n in fig 2) and another process converges with a dendron further away (lower arrow near d in fig 2) This can also be seen when two oligodendrocytes abut each other next to a blood vessel (figs 4 5) From oligo- dendrocytes situated near blood vessels (fig 7) numerous barely recognizable short processes radiate from the perikarya to the vascular walls (top cell in fig 7) One of the processes can be more intensely stained (bottom cell in fig 7) and may terminate in a bell shaped thickening close to the vascular wall (t in fig 8) In this instance the terminal structure encloses a vacuole with an oval minute granule

Under certain circumstances a classifi cation of cell type may be difficult or am biguous One of the inserts is of a cell which meets with most of the criteria here indicated for the juxtavascular oligoden drocytes (fig 6) however the ovoid shape of the nucleus and the relatively thick undulating process along the vascular wall are more characteristic of the microglia cell

Microglia cells

In sections prepared by a modified silver carbonate method numerous juxtaneu ronal microglia cells are stained through out the cerebral cortex

A close up view of the cells situated next to or over the periphery of neuronal peri karya (n in figs 9 10 13 15) reveals an ovoid or rarely a rounded nucleus with coarse chromatin granules

The perikarya are quite irregular in shape but are usually elongated with one two or more processes taking off from each pole of the cytoplasm (figs 9 10 13 15 16 18) These processes divide at varying distances into a few large branches which give off many smaller branches The angle of arborization varies and may reach 90 In order to demonstrate the processes in their entire length it is neces sary because of their extremely irregular and tortuous course to take photomicro- graphs at several different levels from 4 to 6 photomicrographic pictures may be represented in one composite figure

The silver impregnated cytoplasm is pervaded by myriads of minute vacuoles giving the cell a sieve like appearance as

[2] Th oligodendrocyt s in m thyl green pyronin t ined secti n di pl y a faintly pink c lored rim of cytopl m with se eral intensely pink t ined gr n ul which a b ly re gnizabl with immersion il Th perik rya are sm ll than in the sil er impregn ted ecti ns. In th methyl green pyronin t in d secti n th a trocyte e hib t mod t con tent f pink st in d parti l s and the microglia c ll practi lly non

Grove, Ill), thereupon the same amount or up to 50% of body weight of Bouin s picric acid solution Conn and Darrow s ammonium bromide solution or 6 25% glutaraldehyde solution was introduced The free flow of the perfusates was controlled by means of a glass tubing introduced through a rubber stopper into the fluid of each perfusion bottle the lower end of this tubing was maintained at a level 105 cm above the heart The duration of flow depended on the amounts used The time which elapsed from the moment of injection of the barbiturate to the moment of beginning perfusion of the fixative varied from 4 to 8 minutes

The animal was left untouched on the table for varying lengths of time up to six hours when the skull was opened and the brain extracted Pieces from various regions were placed in 95% alcohol which was renewed after 24 hours and on the third and fourth days they were transferred to 100% alcohol After being left in xylene over night they were embedded in paraffin in a vacuum oven

Microscopic sections of 10 μ were deparaffinized and stained according to a modified Del Rio Hortega silver carbonate method for selective impregnation of oligodendrocytes and microglia cells (Naoumenko and Feigin 63) Some of these sections were mounted without any supplementary staining while others immediately after being processed were subjected to periodic acid Schiff treatment alone (abbreviated PAS) or followed by a brief staining with Harris hematoxylin (abbreviated PASH) just enough to give a distinct color to nuclear chromatin

MICROSCOPIC EXAMINATION

Qualities of the microscopic sections

Sections from the Bouin fixed material displayed uniform staining regardless of whether the autopsy was performed shortly after the perfusion or after a prolonged delay In the ammonium bromide fixed material the results were equally good however since capillaries were often contracted and nuclei pyknotic in the white matter and since scattered neurons were hyperchromatic in the gray matter, this material was of limited usefulness The glutaraldehyde fixed material was discarded because the cells were not impregnated

The silver carbonate procedure was not sufficiently standardized to give consistent results thereby precluding reconstruction of cells in companion sections In some sections the astrocytes and the vascular walls would be impregnated as well as the oligodendrocytes and the microglia cells and in others the microglia cells were stained selectively or only faintly Optimal results with concomitant staining of the oligodendrocytes and the microglia cells were obtained when the sections were left for four hours in 5% sodium carbonate solution and when the silver nitrate solution was very faintly turbid

In the most successfully stained sections which were selected for this study the following observations were made All silver impregnated structures were sharply outlined against an unstained background delicate cellular processes could be followed to their terminal endings and the relationship between fibers could be determined with immersion oil objective for either transmitted light or phase contrast The vascular walls which were not impregnated by silver acquired an intense pink color after PAS treatment of the sections If thereafter the sections were stained with hematoxylin then the nuclear chromatin and membranes could be identified This triple staining procedure had the added advantage that the contours of neurons were recognizable Along the cut surface of the sections the upper aspect of the largest cortical neurons displayed a silver impregnated network a so-called outer Golgi net Since this network does not appear over other neurons below the surface of the microscopic section it is regarded as a non specific artifactual staining of polysaccharides

Oligodendrocytes

The cerebral cortex contains a very few scattered oligodendrocytes which in silver carbonate stained sections stand out by their dark color rounded shape and small size

According to their distribution two types of cells can be recognized One type abuts the PAS stained red basement mem

ner after circumventing a number of neu rons The processes from one cell reach out to form incomplete connections with those from cells all around

On many occasions a minute PAS stained red granule is enclosed in the meshwork formed by the perikaryon where it covers a nerve cell (large granule at the tip of long horizontal arrow in fig 13)

Nowhere did the cell body or processes show spine or thorn like minute expan sions perpendicular to the surface How ever many of the thinnest branches can be cut off near the point where they attach to the surface of a perikaryon (twig emerg ing from the left side of the thickening t in fig 10) thereby simulating spines

Although its typical position is juxta neuronal the microglia cell may on rare occasions be situated near a blood vessel or even along the vascular wall (fig 11) The antler like processes penetrating the tissue in various directions reach numerous neurons As elsewhere delicate terminal branches seem to coalesce and form a network (x in fig 11)

Along the surface of vascular walls i e on the outside of the basement membrane a cell referred to as a histiocyte (Cammer meyer 65a b) sometimes displays a nar row rim of an unimpregnated cytoplasm with no processes

Cytoarchitectural characteristics

The oligodendrocytes characterized by perikarya of uniform shape and by their position next to or near blood vessels are in the rabbit sparse in the fourth through the sixth cortical layers (x next to blood vessels indicated by arrows in fig 25) apparently absent in the second and third cortical layers (fig 24) and absent from and situated outside both the pyramidal cell layer of the Ammon s horn (x in fig 26) and the granular layer of the fascia dentata (x in fig 27)

The microglia cells usually located next to neurons are of varying shape with long processes reaching vascular walls they occur in large numbers throughout gray matter (m in figs 24–27) They line up along the granular layer bordering the hilus of the fascia dentata with a larger process penetrating the granular layer and several small ones entering the hilus scattered cells along the side bordering the molecular layer send processes in different directions Fragments of processes some short and some long are recognizable throughout gray matter giving the im pression that all neurons are connected with microglia cells (black dots and lines in figs 4 7 24 25)

The general principles of arrangement noted in the cerebral cortex are applicable to other parts of the central nervous sys tem The number of oligodendrocytes is high in the thalamus and white matter The microglia cells are plentiful in the cerebellar molecular layer less numerous in the cerebellar granular layer and mod erately frequent in the white matter In the white matter the long processes of the microglia cells as they wind along and across the myelinated fibers may display a remarkable tortuosity an undulating course or a corkscrew like shape Under neath the ependyma the microglia cells are flattened and have bulbous thicken ings not encountered in those of the cere bral cortex (Cammermeyer 65c) Along the free surface of the thalamus a super ficial layer of flattened microglia cells is demonstrable

DISCUSSION

This discussion restricted to the condi tions in the cerebral cortex is concerned with the cytologic and histologic peculiari ties of the oligodendrocytes and the micro-glia cells as seen in perfused fixed mate rial in comparison with other descriptions based on the study of immersed fixed ma terial A review of methods material and nomenclature used by various investiga tors may be helpful in clarifying contro versial concepts about the occurrence of the two cell types but any opinion about their functional role must be expressed with reservation

Cytologic characteristics

The silver impregnated oligodendrocytes have rounded perikarya with eccentric nu clei one type is distinguished by few long processes and another type by many short processes some of which may show a vari cose termination near the vascular wall (compare Pruijs '27 fig 67 in Del Río-Hortega '28) The finely vacuolated cyto-

noticeable where the cytoplasm covers the surface of a neuronal perikaryon (fig 9, lower cell in fig 13 and neuron n, in fig 14) or crosses a dendron (d in fig 9) Immediately after leaving the microglia cell body the processes may pass over the surface of the neuronal perikaryon (n in figs 9 10) follow along its periphery (fig 9), bend around the base of dendrons (d in fig 9), and after having traversed the intervening tissue affix themselves to other neuronal perikarya, astrocytes or vascular walls (figs 9, 10) The length of contact with a neuron, as demonstrable with the highest power of the light microscope varies greatly Silver impregnated fragments which are vacuolated and irregular in shape characteristic of microglia cell processes are discerned around most neurons (fragment m, in fig 4 passes over neuron n in fig 5 perineuronal fragment arrows in fig 7)

From its perineuronal position, a microglia cell gives off processes which after contacting numerous neurons may pass one blood vessel and contact others over a wide area The processes in their course may reach the vascular wall (x in fig 12 detail of fig 13 in a different focal plane) leave it and return to it (lower cell in fig 13), cross the wall (short arrow in fig 10), or terminate with a vacuolated silver impregnated thickening on the outside of the PAS stained red basement membrane (t in figs 10 13) When a process passes across the vascular wall its diameter is small and its appearance rather compact (small arrow in fig 10) However the process may be broad and vacuolated if it is attached to the neuronal perikaryon where it lies over a blood vessel (angled long arrows in fig 13) As depicted in such an instance the contours of the neuron are barely visible (short arrows in fig 13) but by a slight change of the focal plane the entire neuron becomes visible (n in fig 14) while the microglia cell is reduced to a mere shadow (x in fig 14) Another fact is brought out by this set of figures namely that the perikaryon and large processes of a microglia cell when seen in a flat view form a narrow band indicating that they cover only a small part of the neuronal surface If a larger portion or the entire surface were covered then the shape of the stained portion of the microglia cell body, contained between the surfaces of the microscopic section, would be more or less round and follow the outline of the neuron

In many instances a process car end abruptly with a small end foot on the surface of the polygonal clear perikaryon of a protoplasmic astrocyte (a in fig 10)

During these studies, particular attention was paid to possible connections between oligodendrocytes and microglia cells Microglia cell processes were seen to cross over or pass near oligodendrocytes but never to fuse with their processes A juxtaneuronal microglia cell (m in fig 18) is seen to send a delicate process to the nearest blood vessel (ascending branch x in fig 18) and a thicker process toward another blood vessel to which it is attached by a delicate terminal branch (arrow in fig 17) just beside a juxtavascular oligodendrocyte (o in figs 17 18) The continuation of this process can be followed at a different microscopic level as indicated by the connected arrows in the two latter figures

Where several microglia cells occur in the same microscopic field the highly twisted secondary or thin tertiary processes are seen to terminate opposite each other and so close that they seem to blend at one (f in fig 15) or several places (f in fig 16) After scrutiny with phase contrast optics of sections stained by the silver carbonate method alone whereby the microglia cell processes can be followed into their finest ramifications no instance of fusion was detected in the cerebral cortex or elsewhere Two apparently crossing processes (fig 19) are in fact in different microscopic planes when viewed with immersion oil (fig 20) Even if the two tips are seen in the same microscopic plane they will be separated by a few microns (fig 21) the top tip ends in a minute thickening indicated by an arrow However the presence between the two tips of a tiny fiber so delicate that it can barely be recognized with the resolution of the light microscope (planapochromat fig 21 phase contrast fig 22) and of minute granules (fig 23) may be an indication of some transfer of material The processes approach each other in a rather devious man

mann 57 Fernandez Moran 57 Scholz 57 Schlote 59 De Robertis Gerschenfeld and Wald 60 De Robertis and Gerschenfeld 61 Mugnaini and Walberg 64 Kruger 65 and others) but in this position it can be seen to be either adjacent to a vascular wall or separated from the neuron by a capillary (compare Cammermeyer 58 59 60b)

The microglia cells are distributed evenly and abundantly throughout the cerebral cortex of the rabbit as they are in man (Del Rio-Hortega 19 20 21b Schlote 59) where however they have been said to be less constant (Bauer 53) All regions are richly supplied with microglia cells — some as e g the cerebellar molecular layer (Schroeder, 29) and the inferior olivary nuclei (Dewulf 37) have more than others as e g the hippocampus (Dewulf 37) Since a microglia cell in juxtaposition to one neuron tends to project its processes onto neighboring neurons the length of the processes will depend on the distance between the neurons The greater separation between cortical neurons which occurs with increasing phylogenetic development (Haug 53 58 Tower 54) may explain a concomitant increase in length of the microglia cells (Glees 55) The profuse development of processes seems to enable them to supply all neurons and many astrocytes and to contact at widely separated points most blood vessels (compare Del Rio-Hortega 19 20 21b Metz and Spatz 24 Rand and Courville 32 Tronconi 35) Such a behavior is reminiscent of that exhibited by microglia cells in tissue cultures where they can attach themselves also to heterogeneous cell elements (Costero 30) Although the perikarya of microglia cells may be appended to the vascular wall the most common position is next to neurons clasping their cell bodies (compare Del Rio-Hortega 20 Ramón y Cajal 20 25 26 Penfield 24b '28 Metz and Spatz 24 Roussy Lhermitte and Oberling 30 Wells and Carmichael 30 Luse 56 Sulzmann 61) This feature is also depicted in older publications using different terminology (satellitic neuroglial cells or "elementos en bastoncito" in Achucarro 10 Achucarro and Gayarre 14 "astrocitos" in Ramón y Cajal 13) and in recent publications where the microglia cell is visualized because of its content of thymidine H³ (Adrian and Walker 62 Altman 62a b) or incorporation of fluorescein labeled protein (Klatzo and Miquel 60 Klatzo Miquel and Otenasek 62 Rubinstein Klatzo and Miquel 62) Approximately 10% of the cells in the vicinity of neurons are said to be microglia cells (Brownson 56) In electron micrographs microglia cells have been demonstrated in material fixed either by immersion (Farquhar and Hartmann 57 Hartmann 58 De Robertis and Gerschenfeld 61 Blinzinger and Hager 62 64 and others) or by perfusion (Herndon 64) and have been detected near a neuronal perikaryon (Wykoff and Young 56) and in apposition to an axon at the node of Ranvier (Sulzmann 64) however according to several other studies they are rather scarce (cerebellar cortex in Herndon 64) are encountered very rarely (Mugnaini and Walberg 64) or are not detectable (inferior olivary nuclei in Walberg 63 64) and they are sometimes not referred to (hippocampus in Westrum and Blackstad 62 Blackstad 63)

Source of controversy

There may be several reasons for the discrepancies in interpretation of the cytologic and histologic characteristics of oligodendrocytes and microglia cells whereby the two cell types have been confused

(1) *Inadequate procedure of preservation* As a consequence of injury incurred during removal of unfixed tissues the size and stainability of scattered perikarya and nuclei are altered In such material different cell types are less readily distinguishable (Cammermeyer 60a) and small neurons may even be mistaken for microglia cells (unfixed tissue subjected to histochemical test fig 7 in Brownson Suter and Diller 63) The dark cell *identified in* electron micrographs as a microglia cell is now associated with a neuron damaged during handling of the unfixed tissue (Gray 61 64 Blinzinger and Hager 62 Mugnaini 65 Kruger 65) If the cells are isolated by grinding the tissue the alteration of nuclei is severe enough to preclude classification (Nurnberger 58) In teased preparations as used for cyto-

plasm is dense near the nucleus unlike the cytoplasm in materials fixed by immersion where it is transformed to a clear zone (Cone 28, Belezky 31) The perikarya appear larger when silver impregnated than when stained by various aniline dyes After use of methyl green pyronin, their cytoplasm stands out by its pink hue and by its content of minute pink stained granules which are more numerous than in any of the other non neuronal elements These granules as indicated by their staining properties are composed of ribonucleic acids

The microglia cells have variform perikarya with irregular often elongated nuclei and tortuous long processes terminating in delicate branches or in a small bulbous swelling near blood vessels (compare Ramón y Cajal 26) Situated next to neurons they can be stellate in shape as in the neopallium elongated as in the pyramidal cell layer of the Ammon s horn or bulb like as along the granular layer of the fascia dentata (compare Achucarro 11, Achucarro and Gayarre 14) This variability is not an indication of different types (Costero, 30 Glees 55) but is an expression of their adaptability and the plasticity of their cytoplasm The cytoplasm is finely vacuolated (compare fig 14 in Achucarro and Gayarre 14 Del Rio Hortega 20 32 Ramón y Cajal 26 Cone '28) as in cells in tissue cultures (Costero 30) The origin of these vacuoles is demonstrated within damaged tissue when after injection of fluorescein labeled proteins this substance is incorporated as granular particles in the cytoplasm of microglia cells (Klatzo and Miquel 60 Klatzo Miquel Tobias and Haymaker 61 Klatzo Miquel Haymaker Tobias and Wolfe 62 Klatzo Miquel and Otenasek 62 Rubinstein Klatzo and Miquel 62) However in the intact tissue the cytoplasm contains either very sparse amounts of RNA stained particles or none and only a few small PAS stained inclusions (Cammermeyer 65b) suggesting that in these cells most of the vacuolar appearance may be due to uptake of solutes In the present material as in tissue cultures (Costero 30) the processes are free of the spines usually regarded as an important differential diagnostic feature (Del Rio-Hortega '20 '21b 28, 30 Penfield 24b '28 Metz '26 Ramón y Cajal, 26 Pruijs 27, Cone '28 Klatzo 52), accordingly their formation in other materials is associated with fragmentation of the delicate terminal branches during preparation of frozen sections Although the processes from neighboring cells seem to interdigitate (Ramón y Cajal 26 Rodriguez-Somoza 26) the tips of the finest branches are usually opposite each other (see the figures in Del Rio-Hortega 20 21b 32 Marshall 53 Field 57 and others) and are of.e so close that a fusion which may occur temporarily during cytogenesis (Del Rio-Hortega 30 32) and in tissue culture (Costero 30) is simulated (fig C i Achucarro 10 fig 8 in Achucarro 11 figs 12 14 in Achucarro and Gayarre 14 Scholz 22 figs 107 165 in Spielmeyer 22 Pruijs 27, fig 11 in Tronconi 3 figs 4B 16C in Finley and Brenner 41 fig 11a in Ferraro and Roizin 43 fig 5 in Ferraro and Roizin 46) Scrutiny of th terminal branches discloses that there is separation (compare Ramón y Cajal '2 Glees 55) and that each cell is in fact a isolated element (Metz and Spatz '24 D Rio-Hortega 28 30 32 Tronconi 3 Marshall 53) Although an anatomic co nection is dismissed a transfer of son material from one cell to another may ta place as suggested by the alignment granular particles between the termin branches

Histologic characteristics

The oligodendrocytes are poorly rep sented in the rabbit cerebral cortex (Ca mermeyer 60d) In the neopallium which the small variant with short pr esses is said to prevail (Penfield 24b 32 they tend to accumulate in the deep cor cal layers as in man (Schroeder 3 Schlote 59) They are distributed n to or at a short distance from blood v sels (see figures in Del Rio Hortega 21 28 30 Tronconi 35 Kulenkampff a Krbek 59 Sulzmann 61) The oli dendrocyte is repeatedly described as satellitic cell next to a neuron (Penfie 24b 28 32 Pruijs 27 Tronconi 3 Kryspin Exner 43 Bauer 53 Scharc berg 53 Luse 56 Farquhar and Ha

drocyte A figure in which elongated cells — again typical microglia cells — were designated "cellules emigrantes" (Auchu carro 15) is reprinted with reference to these cells as migratory polar spongioblasts" (Jones 32)

The use of collective terms instead of specific terms may also be misleading Astrocytes oligodendrocytes and microglia cells are grouped together as "neuroglia" in some publications (Glees 55) and as glia" in others in which the term neuro glia" is applied to astrocytes and oligoden drocytes only (Rubinstein Klatzo and Miquel 62) The oligodendrocytes and microglia cells are lumped together as Mesoglia" (Belezky 31 32a b) or "Mikro glia (Belezky 31 32a b Bauer 53) while microglia cells have been referred to as Histiocyten (Belezky 31 32a b) The term "macroglia " which in older liter ature refers to astrocytes only is applied to astrocytes and oligodendrocytes as a class as opposed to "microglia" (Glees 55 Schultz 64)

Functional role

Until a unanimous opinion is reached about the appearance and distribution of oligodendrocytes and microglia cells it would seem almost futile to speculate about a functional interaction between these two cell types astrocytes neurons and blood vessels

For the oligodendrocytes several different functions have been proposed namely that they act as (1) an intermediary in neuronal metabolism (Del Rio-Hortega 28 Hyden 60) (2) a cell forming the myelin sheath (Penfield 24b Del Rio-Hortega 28 Bunge Bunge and Pappas 62 Peters 62) (3) a drainage cell (Belezky 31 Bauer 53 Luse 62) (4) a massaging or stirring device for various tissue elements (Lumsden and Pomerat 51 Pomerat 52 55 58 59) or an energizer to neurons (Lumsden 62) or (5) an element for control of intrinsic blood flow (Cammermeyer 60b c d Sulzmann 61) It is intriguing that when the oligodendrocyte is situated in the angle between a neuron and a contacting blood vessel there is a tendency of the nucleus to be near the neuron and of the toplasm to expand toward the blood vessel this is indicative of a functional polarity the significance of which is not clear

A tendency of the oligodendrocytes to be more numerous in the deep cortical layers and to occur in columns may indi cate that the distribution of these cells is influenced by the cortical myeloarchitec ture favoring the original suggestion that the oligodendrocytes are concerned with myelin formation (Penfield 24b Del Rio-Hortega 28) Continuity of the myelin sheath with the cytoplasm of oligodendrocytes even when separated by some distance has been demonstrated in electron micrographs during maturation of white matter in the spinal cord (Bunge Bunge and Pappas 62) and in the optic nerve (Peters 62) In pathologic material the results have been equivocal Severe changes of oligodendrocytes associated with demyelination either alone (D Agostino Kernohan and Pease 63) or in com bination with necrosis of both gray and white matter have been described (Åstrom Mancall and Richardson 58) On the other hand after exposure of the brain to ultrasound oligodendrocytes were found to be unaltered in the zone of demyelina tion (Zeman 58) In laminar cortical lesions caused by alpha particle irradia tion the remyelination of fibers discerni ble within the "Bragg peak zone" was not attributed to an action of oligodendrocytes because of their paucity (Estable Puig de Estable Tobias and Haymaker 64) These observations may lend support to the view that the oligodendrocytes may serve differ ent functions in gray and white matter (Lumsden 62)

If the oligodendrocytes in the intact brain are capable of a pulsatile activity similar to that exhibited in tissue cultures (Lumsden and Pomerat 51 and others) then because of their proximity to a blood vessel with only a sheet of astrocytic cytoplasm interposed (Mugnaini and Walberg 64) these cells during a phase of "dia stole " will be in a position to compress the blood vessel The firm attachment between membranes of neighboring oligodendrocytes as seen in electron micrographs (Peters 62 Mugnaini and Walberg 64) ensures that the relative position of these cells in groups of two or three or more

chemical studies (Hyden, 60), the diag nostic difficulties are compounded because the cell during separation changes shape and loses relationship to environment

(2) *Inappropriate sampling of material* The distinction between the nuclei of oligo dendrocytes astrocytes and microglia cells depends both on the animal species se lected (identification is almost impossible in the guinea pig rather difficult in the rat and quite easy in the chinchilla and other mammals Cammermeyer 63a difficult in the rat Duncan 65), and on the regions studied (it is more difficult in white matter than in gray matter, Jones 32 Cammer meyer, 63a) However even with selec tion of a region which is optimal for sepa ration of the three cell types not all of those seen in a given field may be classi fied (Palay '58 De Robertis and Gerschen feld 61, Duncan 65) this may be due to the angle in which they present themselves to the viewer or because of the manner in which they were divided by the microtome Thus a visual impression of transition be tween cell types has on occasion led to the postulation that transformation of one cell type to another takes place throughout life as e g between oligodendrocytes and either microglia cells (Pruijs 27 Belezky 32b) or astrocytes (Rydberg 32 Far quhar and Hartmann 57 Hartmann 62 Sulzmann, 62) or between astrocytes and microglia cells(Farquhar and Hartmann 57)

(3) *Non specificity of the staining tech nique* Because most of the silver tech niques used for staining of the non neu ronal elements are not sufficiently selec tive oligodendrocytes and microglia cells are usually stained simultaneously (Del Rio Hortega 20–32 Metz and Spatz 24, Metz 26, Pruijs 27 King 37 Bauer 53 Clemente and Holst 54 Polak 56 Field 57 Estable Puig de Estable Tobias and Haymaker 64) resulting in a confusion of the two cell types Indeed there are many publications in which a cell labeled oligodendrocyte should because of the ap pearance of its processes be referred to as a microglia cell (fig 15 in Del Rio Hortega 21a cells around lower neuron in fig 5 in Penfield '24b reprinted in fig 10a in Glees 55 figs 2 3 and 28 in Tronconi 35 fig 35 in Bauer 53 fig 2 in Field '57 fig 10 in Kulenkampff and Krbek and others) or vice versa (figs 5a, b Niessing 52) Processes from the two types may blend into a common (fig 36 in Bauer, 53) An staining of microglia cells may lead to conclusion that they are not of the normal central nervous (Bauer '53) or that they are (Naoumenko and Feigin 63)

In sections prepared by the methy green pyronin or the gallocyanin-chrom alum method the perikarya of oligoder drocytes are stained more intensely t those of microglia cells indicative of ferences in their content of RNA, this dif ference is not apparent along their proc esses which seem to be free of partic matter After treatment with silver bonate the cytoplasm and processes both cell types react so much alike as suggest close similarities in their biochem ical composition and molecular tion As a consequence the two cell may not be readily distinguishable in very thin sections when only a small part of either cytoplasm or process is represented A procedure of tagging one of the cells (compare Vogel and Kemper, 62) or of reconstructing a field in companion sec tions may be required in order to define the submicroscopic characteristics of both the oligodendrocyte and the microglia cell in electron micrographs

(4) *Inconsistency of terminology* Use of different terminology may make it diffi cult to interpret older studies Under the general heading of neuroglial satellite cells, metal impregnated cells — typical micro glia cells — situated along each side of a pyramidal cell were labeled lateral astro cytes and one at the base was labeled a 'fusiform astrocyte (fig 10 in Ramón y Cajal 13) The same figure was reprinted as an example of the manner in which these cells can exert their massaging ac tion on the neuron they were said to be either glial cells implicating oligodendro cytes by inference (Pomerat 52 58) or oligodendroglial satellites (fig 11 in Pomerat 59) Under the base of the neu ron in question another cell with a typical halo originally captioned a corpusculo satélite adendrítico" (fig 10 in Ramón y Cajal 13) is without doubt an oligoden

Brownson R H 1956 Perineuronal satellite cells in the motor cortex of aging brains J Neuropath Exp Neur 15 190–195

Brownson R H D B Suter and D A Diller 1963 Acute brain damage induced by low dosage x irradiation Neurology 13 181–191

Bunge M B R P Bunge and G D Pappas 1962 Electron microscopic demonstration of connections between glia and myelin sheaths in the developing mammalian central nervous system J Cell Biol 12 448–453

Cammermeyer J 1958 Discussion In Biology of Neuroglia W F Windle ed Charles C Thomas Springfield Illinois pp 47 287

——— 1959 Discussion In The Process of Aging in the Nervous System J E Birren H A Imus and W F Windle eds Charles C Thomas Springfield Illinois p 90

——— 1960a Differences in shape and size of neuroglial nuclei in the spinal cord due to individual regional and technical variations Acta Anat (Basel) 40 149–177

——— 1960b Is the perivascular oligodendrocyte another element controlling the blood supply to neurons? Angiology 11 508–517

——— 1960c Reappraisal of the perivascular distribution of oligodendrocytes Am J Anat 106 197–231

——— 1960d The distribution of oligodendrocytes in cerebral gray and white matter of several mammals Am J Anat 107 107–127

——— 1963a Similarities between oligodendrocyte and cerebellar granule cell nuclei in Mammalia and Aves Am J Anat 112 111–139

——— 1963b Differential response of two neuron types to facial nerve transection in young and old rabbits J Neuropath Exp Neur 22 594–616

——— 1965a Juxtavascular karyokinesis and microglia cell proliferation during retrograde reaction in the mouse facial nucleus Ergebn Anat Entwicklungsgesch 38 1–22

——— 1965b Histiocytes juxtavascular mitotic cells and microglia cells during retrograde changes in the facial nucleus of rabbits of varying age Ergebn Anat Entwicklungsgesch 38 195–229

——— 1965c The hypependymal microglia cell Z Anat Entwicklungsgesch 124 543–561

Clemente C D and E A Holst 1954 Pathological changes in neurons neuroglia and blood brain barrier induced by x irradiation of heads of monkeys Arch Neur Psychiat 71 66–79

Cone W 1928 Acute pathologic changes in neuroglia and in microglia Arch Neur Psychiat 20 34–68

Costero I 1930 Estudio del comportamiento de la microglia cultivada in vitro" Mem Real Soc Espan Hist Nat 14 (2) 123–182

D Agostino A N G L Pease and J W Kernohan 1963 Cerebral demyelination associated with polycythemia vera J Neuropath Exp Neur 22 138–147

Del Rio-Hortega P 1919 El tercer elemento" de los centros nerviosos Bol Soc Espan Biol 8 68–82 91–103 108–120 154–166

——— 1920 La microglia y su transformación en células en bastoncito y cuerpos granuloadiposos Trab Lab Invest Biol Univ Madrid 18 37–82 and Arch Neurobiol. 1 171–208

——— 1921a Estudios sobre la neuroglia La glia de escasas radiociones Arch Neurobiol 2 16–43

——— 1921b Histogenesis y evolucion normal éxodo y distribución regional de la microglia Arch Neurobiol 2 212–255

——— 1928 Tercera aportacion al conocimiento morfológico e interpretacion functional de la oligodendroglia Mem Real Soc Espan Hist Nat 14 (1) 5–122

——— 1930 Concepts histogénique morphologique et physio-pathologique de la microglie Rev Neur (Paris) 37 (1) 956–986

——— 1932 Microglia In Cytology and Cellular Pathology of the Nervous System W Penfield ed P B Hoeber New York N Y

De Robertis E and H M Gerschenfeld 1961 Submicroscopic morphology and function of glial cells Int Rev Neurobiol 3 1–65

De Robertis E H M Gerschenfeld and F Wald 1960 Ultrastructure and function of glial cells In Structure and Function of the Cerebral Cortex Proc 2nd Int Meeting Neurobiol Amsterdam 1959 D B Tower and J P Schadé ed Elsevier Publishing Company Amsterdam London New York Princeton pp 69–78

Dewulf A 1937 La microglie normal chez le singe (Macacus rhesus) J Belge Neur Psychiat 37 341–365

Duncan D 1965 Light and electron microscopic study of neuroglia in the normal spinal cord of the rat Anat Rec 151 345

Estable-Puig J F R F De Estable C Tobias and W Haymaker 1964 Degeneration and regeneration of myelinated fibers in the cerebral and cerebellar cortex following damage from ionizing particle radiation Acta Neuropath 4 175–190

Farquhar M G and J F Hartmann 1957 Neuroglial structure and relationships as revealed by electron microscopy J Neuropath Exp Neur 16 18–39

Fernandez Morán H 1957 Electron microscopy of nervous tissue In Metabolism of the Nervous System D Richter ed Pergamon Press Inc New York London Paris Los Angeles

Ferraro A and L Roizin 1943 Histopathology of the central nervous tissue in experimental vitamin K deficiency (vitamin K deficiency hemorrhagic diathesis) J Neuropath Exp Neur 2 392–410

——— 1946 Hemorrhagic diathesis experimentally induced by deficiency in vitamin K Am J Path 22 1109–1179

Field E J 1957 Histogenesis of compound granular corpuscles in the mouse brain after trauma and a note on the influence of cortisone J Neuropath Exp Neur 16 48–56

Finley K H and C Brenner 1941 Histologic evidence of damage to the brain in monkeys treated with metrazol and insulin Arch Neur Psychiat 45 403–438

Glees P 1955 Neuroglia morphology and function Charles C Thomas Springfield Illinois

is maintained during pulsation Moreover because of the attachment between many oligodendrocytes clustered next to a blood vessel the pressure resulting from the sum activity of all the cells in various phases of pulsation will be exerted on the vascular wall

The microglia cell, originally considered to be capable of removing waste products was supposed to free the tissue of products of degeneration by a complex process involving metamorphosis mitotic multiplication and migration of the cell and incorporation of these products by the cytoplasm in a similar manner as peripheral macrophages (Del Rio Hortega 19 20 30 32 Penfield 24a b 28) Since the cells leave no telltale traces of a migration such an ability was conjectured from two main observations (1) the presence of the numerous delicate terminal branches mimicking a cell performing ameboid movements and (2) the apparent position of microglia cells at different distances from the blood vessel and the neuron suggesting a displacement (reviewed in Cammermeyer 60b) In order to penetrate the tissue the cells would have either to insinuate themselves with considerable force between fixed cells (Lumsden 62) to loosen the adhesion between cell membranes (Herndon 64) or to follow preformed pathways of communicating intercellular spaces (Sulzmann 62) In a study on the spatial relationship of histiocytes juxtavascular mitotic cells and microglia cells (Cammermeyer 65a b) the conclusion was reached that microglia cells attain their position next to both neurons and blood vessels during cytogenesis and not by migration In this position they may serve as a bridge between neuron and blood vessel for transportation and storage of substances necessary for neuronal metabolism There was no histologic evidence to indicate that microglia cells could enter into mitotic division an increase in their number was related to karyokinesis of histiocytes

ACKNOWLEDGMENTS

The author is indebted for the histologic preparation to Miss I Mercado and for assistance in writing of the manuscript to Mrs J Phelps (both of this laboratory) and for photographic assistance to Mr E Moodhe (Laboratory of Neuroanatomical Sciences)

LITERATURE CITED

Achucarro N 1910 Algunos datos relativos la naturaleza de las células en bastoncito de corteza cerebral humana obtenidos con el método de Cajal Trab Lab Invest Biol Univ Madrid 8 169–196

——— 1911 Neuroglia y elementos intersticiales patológicos del cerebro impregnados los métodos de reducción de la plata ó por modificaciones Trab Lab Invest Biol Univ Madrid 9 161–179

——— 1915 De l'évolution de la névroglie spécialement de ses relations avec l'appareil vasculaire Trab Lab Invest Biol Univ Madrid 13 169–212

Achucarro N and M Gayarre 1914 La corteza cerebral en la demencia paralitica con el nuevo método del oro y sublimado de Cajal Trab Lab Invest Biol Univ Madrid 1? 1-38

Adrian E K Jr and B E Walker 1962 Incorporation of thymidine-H³ by cells in normal and injured mouse spinal cord J Neuropath Exp Neur 21 597–609

Altman J 1962a Are new neurons formed in the brains of adult mammals? Science 135 1127–1128

———1962b Autoradiographic study of degenerative and regenerative proliferation of neuroglia cells with tritiated thymidine Exp Neur 5 302–318

Astrom K E E L Mancall and E P Richardson Jr 1958 Progressive multifocal leukoencephalopathy a hitherto unrecognized complication of chronic lymphatic leukemia and Hodgkin s disease Brain 81 93–111

Bauer K F 1953 Organisation des Nervengewebes und Neurencytiumtheorie Urban & Schwarzenberg Munchen Berlin

Belezky W K 1931 Die Pyridinsodamethode zur Imprägnation der Mesoglia (Hortegazellen Oligodendroglia Drenagezellen) und Reticuloendothelzellen (fur Gelatin und Celloidinschnitte) Virchow s Arch Path Anat 282 214–224

——— 1932a Über die Histogenese der Mesoglia Virchow s Arch Path Anat 284 295–311

——— 1932b Über die Rolle der Mesoglia bei akuten nichteitrigen Infektionen des Zentralnervensystems Virchow s Arch Path Anat 285 494–505

Blackstad T W 1963 Ultrastructural studies on the hippocampal region Progr Brain Res 3 122–148

Blinzinger K and H Hager 1962 Elektronenmikroskopische Untersuchungen über die Feinstruktur ruhender und progressiver Mikroglia zellen im Saugetiergehirn Beitr Path Anat 127 173–192

——— 1964 Elektronenmikroskopische Untersuchungen zur Feinstruktur ruhender und progressiver Mikrogliazellen im ZNS des Goldhamsters Progr Brain Res 6 99–112

Brownson R H 1956 Perineuronal satellite cells in the motor cortex of aging brains J Neuropath Exp Neur *15* 190–195
Brownson R H D B Suter and D A Diller 1963 Acute brain damage induced by low dosage x irradiation Neurology *13* 181–191
Bunge M B R P Bunge and G D Pappas 1962 Electron microscopic demonstration of connections between glia and myelin sheaths in the developing mammalian central nervous system J Cell Biol *12* 448–453
Cammermeyer J 1958 Discussion In Biology of Neuroglia W F Windle ed Charles C Thomas Springfield Illinois pp 47 287
——— 1959 Discussion In The Process of Aging in the Nervous System J E Birren H A Imus and W F Windle eds Charles C Thomas Springfield Illinois p 90
——— 1960a Differences in shape and size of neuroglial nuclei in the spinal cord due to individual regional and technical variations Acta Anat (Basel) *40* 149–177
——— 1960b Is the perivascular oligodendrocyte another element controlling the blood supply to neurons? Angiology *11* 508–517
——— 1960c Reappraisal of the perivascular distribution of oligodendrocytes Am J Anat *106* 197–231
——— 1960d The distribution of oligodendrocytes in cerebral gray and white matter of several mammals Am J Anat *107* 107–127
——— 1963a Similarities between oligodendrocyte and cerebellar granule cell nuclei in Mammalia and Aves Am J Anat *112* 111–139
——— 1963b Differential response of two neuron types to facial nerve transection in young and old rabbits J Neuropath Exp Neur *22* 594–616
——— 1965a Juxtavascular karyokinesis and microglia cell proliferation during retrograde reaction in the mouse facial nucleus Ergebn Anat Entwicklungsgesch 38 1–22
——— 1965b Histiocytes juxtavascular mitotic cells and microglia cells during retrograde changes in the facial nucleus of rabbits of varying age Ergebn Anat Entwicklungsgesch 38 195–229
——— 1965c The hypependymal microglia cell Z Anat Entwicklungsgesch *124* 543–561
Clemente C D and E A Holst 1954 Pathological changes in neurons neuroglia and blood brain barrier induced by x irradiation of heads of monkeys Arch Neur Psychiat *71* 66–79
Cone W 1928 Acute pathologic changes in neuroglia and in microglia Arch Neur Psychiat 20 34–68
Costero I 1930 Estudio del comportamiento de la microglia cultivada in vitro" Mem Real Soc Espan Hist Nat *14* (2) 123–182
D Agostino A N G L Pease and J W Kernohan 1963 Cerebral demyelination associated with polycythemia vera J Neuropath Exp Neur 22 138–147
Del Rio-Hortega P 1919 El tercer elemento de los centros nerviosos Bol Soc Espan Biol 8 68–82 91–103 108–120 154–166
——— 1920 La microglia y su transformación en células en bastoncito y cuperpos granulo-adiposos Trab Lab Invest Biol Univ Madrid *18* 37–82 and Arch Neurobiol *1* 171–208
——— 1921a Estudios sobre la neuroglia La glia de escasas radiociones Arch Neurobiol 2 16–43
——— 1921b Histogénesis y evolución normal éxodo y distribución regional de la microglia Arch Neurobiol 2 212–255
——— 1928 *Tercera aportación al conocimiento* morfológico e interpretación functional de la oligodendroglia Mem Real Soc Espan Hist Nat *14* (1) 5–122
——— 1930 Concepts histogénique morphologique et physio-pathologique de la microglie Rev Neur (Paris) 37 (1) 956–986
——— 1932 Microglia In Cytology and Cellular Pathology of the Nervous System W Penfield ed P B Hoeber New York N Y
De Robertis E and H M Gerschenfeld 1961 Submicroscopic morphology and function of glial cells Int Rev Neurobiol *3* 1–65
De Robertis E H M Gerschenfeld and F Wald 1960 Ultrastructure and function of glial cells In Structure and Function of the Cerebral Cortex Proc 2nd Int Meeting Neurobiol Amsterdam 1959 D B Tower and J P Schadé ed Elsevier Publishing Company Amsterdam London New York Princeton pp 69–78
Dewulf A 1937 La microglie normal chez le singe (Macacus rhesus) J Belge Neur Psychiat 37 341–365
Duncan D 1965 Light and electron microscopic study of neuroglia in the normal spinal cord of the rat Anat Rec *151* 345
Estable Puig J F R F De Estable C Tobias and W Haymaker 1964 Degeneration and regeneration of myelinated fibers in the cerebral and cerebellar cortex following damage from ionizing particle radiation Acta Neuropath *4* 175–190
Farquhar M G and J F Hartmann 1957 Neuroglial structure and relationships as revealed by electron microscopy J Neuropath Exp Neur *16* 18–39
Fernandez Morán H 1957 Electron microscopy of nervous tissue In Metabolism of the Nervous System D Richter ed Pergamon Press Inc New York London Paris Los Angeles
Ferraro A and L Roizin 1943 Histopathology of the central nervous tissue in experimental vitamin K deficiency (vitamin K deficiency hemorrhagic diathesis) J Neuropath Exp Neur 2 392–410
——— 1946 Hemorrhagic diathesis experimentally induced by deficiency in vitamin K Am J Path 22 1109–1179
Field E J 1957 Histogenesis of compound granular corpuscles in the mouse brain after trauma and a note on the influence of cortisone J Neuropath Exp Neur *16* 48–56
Finley K H and C Brenner 1941 Histologic evidence of damage to the brain in monkeys treated with metrazol and insulin Arch Neur Psychiat *45* 403–438
Glees P 1955 Neuroglia morphology and function Charles C Thomas Springfield Illinois

Gray E G 1961 The granule cells mossy synapses and Purkinje spine synapses of the cerebellum light and electron microscope observations J Anat 95 345–356

——— 1964 Tissue of the central nervous system In Electron Microscopic Anatomy S M Kurtz *ed Academic Press New York and* London pp 369–370

Hartmann J F 1958 Two views concerning criteria for identification of neuroglia cell types by electron microscopy Part A In Biology of Neuroglia W F Windle ed Charles C Thomas Springfield Illinois pp 51–56

——— 1962 *Identification of neuroglia in elec*tron micrographs of normal nerve tissue In IV Internationaler Kongress fur Neuropathologie Proceedings H Jacob ed Georg Thieme Stuttgart Vol II pp 32–35

Haug H 1953 Der Grauzellkoeffizient des Stirnhirnes der Mammalia in einer phylogenetischen Betrachtung Acta Anat *19* 60–100 153–190 239–270

——— 1958 Über die Beziehungen des Hirngewichtes zum Grauzellkoeffizienten der Schrinde bei den Primaten und einigen primitiven Saugern J Hirnforsch *4* 189–204

Herndon R M 1964 The fine structure of the rat cerebellum II The stellate neurons granule cells and glia J Cell Biol 23 277–293

Hydén H 1960 A functional relationship between oligodendroglia and the nerve cell Acta Morph Neerl Scand *3* 170–178

Jones O W 1932 Cytogenesis of oligodendroglia and astrocytes Arch Neur Psychiat 28 *1030–1045*

King L S 1937 Method for rapid impregnation of microglia and oligodendroglia in material fixed in formaldehyde Arch Neur Psychiat 38 362–364

Klatzo I 1952 A study of glia by the Golgi method Lab Invest *1* 345–350

Klatzo I and J Miquel 1960 Observations on pinocytosis in nervous tissue J Neuropath Exp Neur *19* 475–487

Klatzo I J Miquel and R Otenasek 1962 The application of fluorescein labeled serum proteins (FLSP) to the study of vascular permeability in the brain Acta Neuropath 2 144–*160*

Klatzo I J Miquel C Tobias and W Haymaker 1961 Effects of alpha particle radiation on the rat brain (including vascular permeability and glycogen studies) J Neuropath Exp Neur *20* 459–483

Klatzo I J Miquel W Haymaker C Tobias and L S Wolfe 1962 Observations on appearance of histochemically-demonstrable glycogen in the rat brain as effect of alpha particle irradiation In Effects of Ionizing Radiation on the Nervous System International Atomic Energy Agency Vienna

Kruger L 1965 The spectrum of oligodendrocytes in normal rat cerebrum Anat Rec *151* 375

Kryspin Exner W 1943 Beitrage zur Morphologie der Glia im Nissl Bilde Z Anat Entwicklungsgesch *112* 389–416

Kulenkampff H and F Krbek 1959 Morphologische Untersuchungen an Glia und Ependym des Mauseruckenmarkes Z Anat Entwicklungsgesch *121* 165–178

Lumsden C E 1962 New horizons in the physiology of the glia In Livre Jubilaire du Dr L van Bogaert Acta Medica Belgica, Bruxelles

Lumsden C E and C M Pomerat *1951 Nor*mal oligodendrocytes in tissue culture A preliminary report on the pulsatile glial cells in tissue cultures from the corpus callosum of the normal adult rat brain Exp Cell Res 2 103 114

Luse S A 1956 Electron microscopic observations of the central nervous system *J Biophys* Biochem Cytol 2 531–542

——— 1962 Transport of water and metabolites in the central nervous system as studied by electron microscopy A M A Arch Neur 7 245

Marshall A H E 1953 The reticular tissue and the reticulo-endothelial system " *J Path* Bact 65 29–48

Metz A 1926 Die drei Gliazellarten und der Eisenstoffwechsel Z Ges Neur Psychiat *100* 428–449

Metz A and H Spatz 1924 Die Hortegaschen Zellen (=das sogenannte dritte Element) und uber ihre funktionelle Bedeutung *Z Ges* Neur Psychiat *89* 138–170

Mugnaini E 1965 Dark cells in electron micrographs from the C N S of vertebrates J Ultrastruct Res *12* 235–236

Mugnaini E and F Walberg 1964 Ultrastructure of neuroglia Ergebn Anat Entwicklungsgesch *37 194–236*

Naoumenko J and I Feigin 1963 A modification for paraffin sections of silver carbonate impregnation for microglia Acta Neuropath 2 402–406

Niessing K 1952 Zellformen und Zellreaktionen der Mikroglia des Mausegehirns Gegenbaurs *Morph Jahrb 92 102–122*

Nurnberger J I 1958 Direct enumeration of cells of the brain In Biology of Neuroglia W F Windle ed Charles C Thomas Springfield Illinois pp 193–202

Palay S L 1958 An electron microscopical study of neuroglia In Biology of Neuroglia W F Windle ed Charles C Thomas Springfield Illinois pp 24–38

Penfield W G 1924a Microglie et son rapport avec la dégéneration névrogliale dans un gliome Trab Lab Invest Biol Univ Madrid 22 277–293

——— 1924b Oligodendroglia and its relation to classical neuroglia Brain *47* 430–452

——— 1928 Neuroglia and microglia *The* interstitial tissue of the central nervous system In Special Cytology E V Cowdry ed P B Hoeber New York N Y pp 1031–1068

——— 1932 Neuroglia normal and pathological In Cytology and Cellular Pathology of the Nervous System W Penfield ed P B Hoeber *New York N Y pp 421–479*

Peters A 1962 Plasma membrane contacts in the central nervous system J Anat *96* 237–248

Polak M 1956 Sobre una variante a la técnica de Rio Hortega para la impregnación de células

reticuloendotheliales normales y patológicas micro y oligodendroglia "barrera epitelial argentofila" (Polak) elementos neurogliocos blastomatosos etc Arch Histol Norm Pat 6 220–222
Pomerat C M 1952 Dynamic neurogliology Texas Rep Biol Med *10* 885–913
——— 1955 Dynamic neuropathology J Neuropath Exp Neur *14* 28–38
——— 1958 Functional concepts based on tissue culture studies of neuroglia cells In Biology of Neuroglia W F Windle ed Charles C Thomas Springfield Illinois
——— 1959 Dynamic activities of cellular elements of the nervous system Alfred Korzybski Mem Symposium 11 April 1959 New York Gen Semantics Bull nos 24–25 (Printed 1960)
Pruijs W M 1927 Über Mikroglia ihre Herkunft Funktion und ihr Verhältnis zu anderen Gliaelementen Z Ges Neur Psychiat *108* 298–331
Ramon y Cajal S 1913 Contribución al conocimiento de la neuroglia del cerebro humano Trab Lab Invest Biol Univ Madrid *11* 254–315
——— 1920 Algunas consideraciones sobre la mesoglia de Roberston y Rio-Hortega Trab Lab Invest Biol Univ Madrid *18* 109–127
——— 1925 Contribution à la connaissance de la névroglie cérébrale et cérébelleuse dans la paralysie generale progressive Trab Lab Invest Biol Univ Madrid *23* 157–216
——— 1926 Beitrag zur Kenntnis der Neuroglia des Gross und Kleinhirns bei der progressiven Paralyze mit einigen technischen Bemerkungen zur Silberimpragnation des pathologischen Nervengewebes Z Ges Neur Psychiat *100* 738–793
Rand C W and C B Courville 1932 Histologic changes in the brain in cases of fatal injury to the head Arch Neur Psychiat 27 605–644
Rodriguez Somoza R 1926 La macroglie et la mi roglie dans un cas de paralysie générale Trab Lab Invest Biol Univ Madrid *24* 289–317
Roussy G J Lhermitte and C Oberling 1930 La névroglie et ses réactions pathologiques Rev Neur (Paris) *37* (1) 878–955
Rubinstein L J I Klatzo and J Miquel 1962 Histochemical observations on oxidative enzyme activity of glial cells in a local b ain injury J Neuropath Exp Neur *21* 116–136
Rydberg E 1932 Cerebral injury in new born children consequent on birth trauma with an inquiry into the normal and pathological anatomy of the neuroglia Acta Path Microbiol Scand *10* (Suppl) 1–247
Scharenberg K 1953 Degeneration regeneration and readjustment in the human brain J Neuropath Exp Neur *12* 90–92
Schlote W 1959 Zur Gliaarchitektonik der menschlichen Grosshirnrinde im Nissl Bild Arch Psychiat Nervenkr *199* 573–595
Scholz W 1922 Über herdformige protoplasmatische Gliawucherungen von syncytialen Charackter Z. Ges Neur Psychiat *79* 114–179
——— 1957 Erkrankungen des zentralen Nervensystems In Nervensystem W Scholz ed Handbuch der speziellen pathologischen Anatomie und Histologie O Lubarsch F Henke und R Rossle eds Springer Verlag Berlin Gottingen Heidelberg Band 13 1 Teil Band teil A S 1–265
Schroeder A H 1929 Die Gliaarchitektonik des menschlichen Kleinhirns J Psychol Neur *38* 234–257
——— 1935 Gliaarchitektonik des Zentralner vensystem In Anatomie W Spielmeyer ed Handbuch der Neurologie O Bumke und O Foerster eds Julius Springer Berlin Band 1 S 791–810
Schultz R L 1964 Macroglial identification in electron micrographs J Comp Neur *122* 281–295
Spielmeyer W 1922 Histopathologie des Nervensystems Julius Springer Berlin
Sulzmann R 1961 Zur Frage der interfibraren bzw interfascicularen Bildung von myelinoider Substanz unter besonderer Berucksichtigung des Verhaltens der Makro- und Mikroglia Deutsch Z Nervenheilk *183* 28–47
——— 1962 Die mikroskopiche Morphologie der zentralen markhaltigen Nervenfaser Wis Z Friedrich Schiller Univ Jena *11* 197–245
——— 1964 Erstmaliger elektronenoptischer Nachweis von Austauschvorgangen zwischen Mikroglia und markhaltiger Nervenfaser im Meerschweinchenruckenmark Naturwissenschaften *51* 16–17
Tower D B 1954 Structural and functional organization of mammalian cerebral cortex the correlation of neuron density with brain size J Comp Neur *101* 19–51
Tronconi V 1935 Studio sulla nevroglia umana Riv Pat Nerv Ment *45* 223–396
Vogel F S and L Kemper 1962 Modification of Hortega s silver impregnation methods to assist in the identification of neuroglia with electron microscopy In IV Internationaler Kongress fur Neuropathologie Proceedings H Jacob ed Georg Thieme Stuttgart Vol II pp 66–71
Walberg F 1963 An electron microscopic study of the inferior olive of the cat J Comp Neur *120* 1–17
——— 1964 Further electron microscopical investigations of the inferior olive of the cat Progr Brain Res *6* 59–75
Wells A Q and E A Carmichael 1930 Microglia an experimental study by means of tissue culture and vital staining Brain *53* 1–10
Westrum L E and T W Blackstad 1962 An electron microscopic study of the stratum radiatum of the rat hippocampus (regio superior CA 1) with particular emphasis on synaptology J Comp Neur *119* 281–309
Wyckoff R. W G and J Z. Young 1956 The motorneuron surface Proc Roy Soc Series B *144* 440–450
Zeman W 1958 Discussion J Neuropath Exp Neur *17* 535

Gray E G 1961 The granule cells mossy synapses and Purkinje spine synapses of the cerebellum light and electron microscope observations J Anat 95 345–356
——— 1964 Tissue of the central nervous system In Electron Microscopic Anatomy S M Kurtz ed Academic Press New York and London pp 369–370
Hartmann J F 1958 Two views concerning criteria for identification of neuroglia cell types by electron microscopy Part A In Biology of Neuroglia W F Windle ed Charles C Thomas Springfield Illinois pp 51–56
——— 1962 Identification of neuroglia in electron micrographs of normal nerve tissue In IV Internationaler Kongress fur Neuropathologie Proceedings H Jacob ed Georg Thieme Stuttgart Vol II pp 32–35
Haug H 1953 Der Grauzellkoeffizient des Stirnhirnes der Mammalia in einer phylogenetischen Betrachtung Acta Anat 19 60–100 153–190 239–270
——— 1958 Über die Beziehungen des Hirngewichtes zum Grauzellkoeffizienten der Sehrinde bei den Primaten und einigen primitiven Saugern J Hirnforsch 4 189–204
Herndon R M 1964 The fine structure of the rat cerebellum II The stellate neurons granule cells and glia J Cell Biol 23 277–293
Hyden H 1960 A functional relationship between oligodendroglia and the nerve cell Acta Morph Neerl Scand 3 170–178
Jones O W 1932 Cytogenesis of oligodendroglia and astrocytes Arch Neur Psychiat 28 1030–1045
King L S 1937 Method for rapid impregnation of microglia and oligodendroglia in material fixed in formaldehyde Arch Neur Psychiat 38 362–364
Klatzo I 1952 A study of glia by the Golgi method Lab Invest 1 345–350
Klatzo I and J Miquel 1960 Observations on pinocytosis in nervous tissue J Neuropath Exp Neur 19 475–487
Klatzo I J Miquel and R Otenasek 1962 The application of fluorescein labeled serum proteins (FLSP) to the study of vascular permeability in the brain Acta Neuropath 2 144–160
Klatzo I J Miquel C Tobias and W Haymaker 1961 Effects of alpha particle radiation on the rat brain (including vascular permeability and glycogen studies) J Neuropath Exp Neur 20 459–483
Klatzo I J Miquel W Haymaker C Tobias and L S Wolfe 1962 Observations on appearance of histochemically-demonstrable glycogen in the rat brain as effect of alpha particle irradiation In Effects of Ionizing Radiation on the Nervous System International Atomic Energy Agency Vienna
Kruger L 1965 The spectrum of oligodendrocytes in normal rat cerebrum Anat Rec 151 375
Kryspin Exner W 1943 Beitrage zur Morphologie der Glia im Nissl Bilde Z Anat Entwick lungsgesch 112 389–416
Kulenkampff H and F Kirbek 1959 Morphologische Untersuchungen an Glia und Ependym des Mauseruckenmarkes Z Anat Entwicklungsgesch 121 165–178
Lumsden C E 1962 New horizons in the physiology of the glia In Livre Jubilaire du Dr L van Bogaert Acta Medica Belgica Bruxelles
Lumsden C E and C M Pomerat 1951 Normal oligodendrocytes in tissue culture A preliminary report on the pulsatile glial cells in tissue cultures from the corpus callosum of the normal adult rat brain Exp Cell Res 2 103–114
Luse S A 1956 Electron microscopic observations of the central nervous system J Biophys Biochem Cytol 2 531–542
——— 1962 Transport of water and metabolites in the central nervous system as studied by electron microscopy A M A Arch Neur 7 245
Marshall A H E 1953 The reticular tissue and the reticulo endothelial system J Path Bact 65 29–48
Metz A 1926 Die drei Gliazellarten und der Eisenstoffwechsel Z Ges Neur Psychiat 100 428–449
Metz A and H Spatz 1924 Die Hortegaschen Zellen (=das sogenannte dritte Element) und uber ihre funktionelle Bedeutung Z Ges Neur Psychiat 89 138–170
Mugnaini E 1965 Dark cells in electron micrographs from the C N S of vertebrates J Ultrastruct Res 12 235–236
Mugnaini E and F Walberg 1964 Ultrastructure of neuroglia Ergebn Anat Entwick lungsgesch 37 194–236
Naoumenko J and I Feigin 1963 A modification for paraffin sections of silver carbonate impregnation for microglia Acta Neuropath 2 402–406
Niessing K 1952 Zellformen und Zellreaktionen der Mikroglia des Mausegehirns Gegenbaurs Morph Jahrb 92 102–122
Nurnberger J I 1958 Direct enumeration of cells of the brain In Biology of Neuroglia W F Windle ed Charles C Thomas Springfield Illinois pp 193–202
Palay S L 1958 An electron microscopical study of neuroglia In Biology of Neuroglia W F Windle ed Charles C Thomas Springfield Illinois pp 24–38
Penfield W G 1924a Microglie et son rapport avec la dégéneration névroglialc dans un gliome Trab Lab Invest Biol Univ Madrid 22 277–293
——— 1924b Oligodendroglia and its relation to classical neuroglia Brain 47 430–452
——— 1928 Neuroglia and microglia The interstitial tissue of the central nervous system In Special Cytology E V Cowdry ed P B Hoeber New York N Y pp 1031–1068
——— 1932 Neuroglia normal and pathological In Cytology and Cellular Pathology of the Nervous System W Penfield ed P B Hoeber New York N Y pp 421–479
Peters A 1962 Plasma membrane contacts in the central nervous system J Anat 96 237–248
Polak M 1956 Sobre una variante a la técnica de Rio Hortega para la impregnación de células


n
v
c
m
v
n
v
n
v
x
x
d
2
3
4
5
n
6
v
v
n
n
a
c
7
8
v

PLATES

Material used for photomicrography

With the few exceptions indicated all figures are from a five month old rabbit (Ra1 103162C) Figures 19 and 20 are from a four month old rabbit (RA1 021065C) Both of these animals were perfused with Bouin s solution they were autopsied after a delay of six and five hours respectively Figures 21–23 are from a three month old rabbit (RA? 062664C) perfused with Conn and Darrow s solution and autopsied one hour later Figures 15–18 and 21–23 are from sections stained by the silver carbonate method alone and the other figures are from a section stained by a combined method of silver carbonate and PASH

Planapochromat immersion oil objective was used for all photomicrographs taken at a magnification of × 1 500 or more except as indicated Dry plan objectives were used for photomicrographs at lesser magnifications

PLATE 1

EXPLANATION OF FIGURES

1 Juxtavascular oligodendrocyte × 1 500

2 Perineuronal oligodendrocyte × 1 500

3 Blood vessel next to shadow of oligodendrocyte (x) seen at a different microscopic level in figure 2 × 1 500

4 Twin oligodendrocytes × 1 500

5 Blood vessel over shadow of oligodendrocytes (x) seen at a different microscopic level in figure 4 × 1 500

6 Juxtavascular cell of questionable type oligodendrocyte or microglia cell × 1 500

7 Oligodendrocytes at short distances from blood vessels (v) × 1 500

8 Oligodendrocyte at a short distance from blood vessel (v) with a thickened ending near vascular wall (t) × 2 450


n
v
c
m
v
n
n
v
v
x
v
x
d
2
3
4
5
n
6
v
v
n
c
n
a
c
t
v
7
8

PLATE 2

EXPLANATION OF FIGURES

9 Juxtaneuronal microglia cell with processes encircling perikaryon of neuron (n) crossing dendrons (d d) and reaching a blood vessel (v) × 1 500

10 Juxtaneuronal microglia cell with processes reaching several other neurons an astrocyte (a) and a blood vessel (v) and terminating with a swelling near the vascular wall (t) or crossing the blood vessel (short arrow) × 1 500

11 Juxtavascular microglia cell × 1 500

12 Process of microglia cell represented at bottom of figure 13 reaching vascular wall × 1 500

13 Top juxtaneuronal microglia cell (n) with a terminal swelling (t) on adjacent blood vessel (v) Lower microglia cell with one process winding along a blood vessel to a terminal ending (t) and a broader process crossing a blood vessel (arrows in angle) Contours of adjacent neuron represented in figure 14 indicated by short arrows × 1 500

14 Neuron (n) next to shadow of a microglia cell (x) seen at a different microscopic level in figure 13 × 1 500

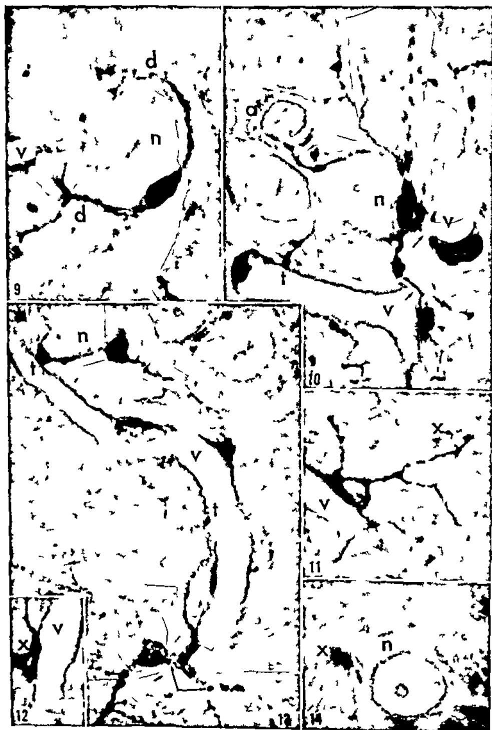

d
n
v
d
9
a
n
v
t
v
10
n
t
v
t
x
v
11
x
v
12
13
x
n
14

PLATE 3

EXPLANATION OF FIGURES

15 Apparent fusion (f) between single processes from neighboring microglia cells (x y) Phase contrast × 1 500

16 Apparent fusion (f f ?) between several processes from neighboring microglia cells (x y) Phase contrast × 1 500

17 Delicate terminal branch of a microglia cell process (arrow) passing near a juxtavascular oligodendrocyte (o) before reaching a blood vessel (v) Phase contrast × 1 500

18 Microglia cell (m) sending processes to blood vessels (v) bypassing an oligodendrocyte (o) as indicated in figure 17 Phase contrast × 1 500

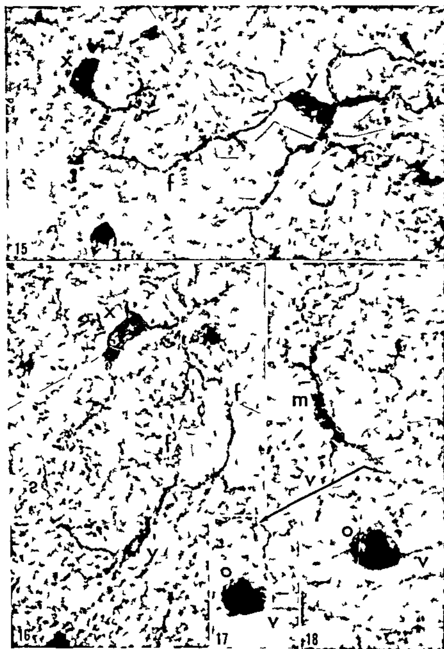

x
y
f
15
x
f
f
m
v
o
o
v
v
16
17
18

PLATE 3

EXPLANATION OF FIGURES

15 Apparent fusion (f) between single processes from neighboring microglia cells (x y) Phase contrast × 1 500

16 Apparent fusion (f f ?) between several processes from neighboring microglia cells (x y) Phase contrast × 1 500

17 Delicate terminal branch of a microglia cell process (arrow) passing near a juxtavascular oligodendrocyte (o) before reaching a blood vessel (v) Phase contrast × 1 500

18 Microglia cell (m) sending processes to blood vessels (v) bypassing an oligodendrocyte (o) as indicated in figure 17 Phase contrast × 1 500

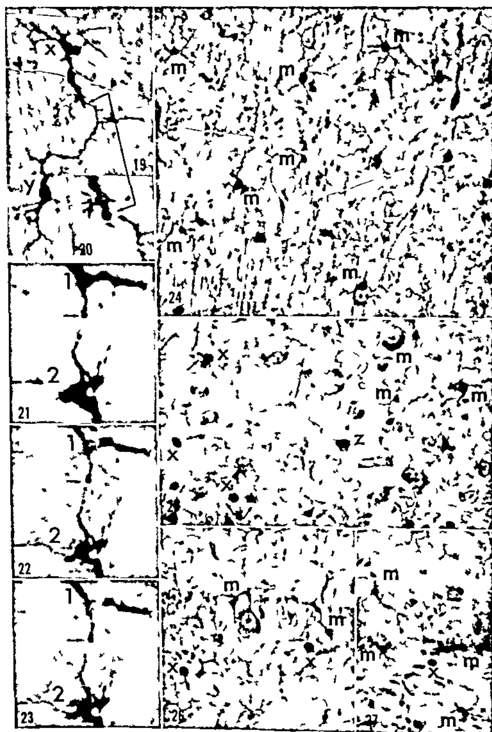

x
y
19
20
m
m
m
m
m
m
m
24
1
2
21
1
2
22
1
2
23
x
m
m
m
z
x
x
m
m
x
x
m
m
m
x
m

PLATE 4

EXPLANATION OF FIGURES

19 Apparent fusion (arrow) between single processes of two microglia cells (x y) × 600

20 Insert showing crossing of the two processes at different levels at the point indicated by arrow × 1 500

21 Separation between terminal branches from two different microglia cells (1 2) at the same microscopic level × 2 500

22 Same as in figure 21 Phase contrast immersion oil × 2 500

23 Same as in figure 22 with a slight change of microscopic level Phase contrast immersion oil × 2 500

24 Microglia cells (m) in cerebral cortex × 320

25 Microglia cells (m) with single oligodendrocytes (x) next to blood vessels (arrow) and a cluster of three oligodendrocytes (z) in the cerebral cortex × 320

26 Microglia cells (m) in pyramidal cell layer of Ammon s horn Oligo dendrocytes (x) one next to blood vessel (arrow) along the border of the pyramidal cell layer Lower clear zone is the stratum oriens and top clear zone is the stratum radiatum × 320

27 Microglia cells (m) lined up along the granular layer of the fascia dentata bordering the *hilus (lower clear zone) in which scattered* microglia cells (m) and oligodendrocytes (x) occur More prominent microglia cells (m) along the other side send processes into the molecular layer (top clear zone) × 320

Changes in Endometrial Vascularity during Implantation and Pregnancy in the Rabbit [1]

E S E HAFEZ AND Y TSUTSUMI [2]
Department of Animal Sciences Washington State University Pullman Washington

ABSTRACT Sixty five pregnant rabbits were autopsied at different stages of pregnancy 2 to 28 days *post coitum* (*p c*) The vascularity of the endometrium and placenta was studied using intervascular injections of neoprene latex cast by clearing injected specimens and by the study of frozen and paraffin embedded sections At 6 days *p c* the implantation sites were identified the endometrium at the interconceptus was similar to that during pseudopregnancy The subepithelial capillary plexus increased in thickness reaching a maximum at 6–11 days *p c* Marked endometrial branching occurred 10 days *p c* After 15 days *p c* the endometrium formed a thin irregular layer Most of the endometrial epithelial cells showed cytoplasmic projections at 6 days *p c* and were transformed into syncytial epithelial cells 8 days *p c* At 24–28 days *p c* the conceptus and interconceptus areas were unidentifiable

The size of the obplacental folds diminished at 6 days *p c* and the placental folds increased in size after 7 days *p c* At 9 days *p c* blastocyst attachment was observed histologically The surface capillaries were dilated and changed into surface sinuses Networks of blood pathways were established the pathways connected with large veins in the core of the fold The veins extended to the hemorrhage areas representing the origin of fetal placenta The fetal vessels were recognizable near the base of the fetal placenta at 11 days *p c* The maternal circulation in the fetal placenta started before the fetal vessels reached the fetal placenta At 10 days *p c* the perivascular sheath of the maternal vessels in the placental folds developed markedly as to replace most of the connective tissue With advancing pregnancy the number of vessels within the maternal placenta decreased and some vessels increased in size At 13 days *p c* the zone of separation was formed At 15 days *p c* the lobes were formed in the fetal placenta all placental elements were established anatomically Subsequent stages were characterized by developmental changes in the fetal placenta and degenerative changes in the maternal placenta

The histological physiological and biochemical interactions between the embryo and the endometrium have been extensively studied (Boyd and Hamilton 58 Amoroso 58 Lutwak Mann et al 60 Noyes and Dickmann 60 Dickmann and Noyes 60 Hafez 62 63a b 64 Boving 63) At the time of implantation there is a transition from the histotrophic type of embryonic nutrition to the hemotrophic nutrition The blood circulation of the endometrium plays an important role in embryonic survival and fetal development (Reynolds 37 49 Hafez 64b) Prior to implantation there is a rich blood supply underneath the endometrial surface (Bascich and Wyburn 40 Phelps 46) In the rabbit the trophoblast penetrates the uterine epithelium to connect with the subepithelial vasculature (Boving 54 59 62) During pregnancy there are rhythmic changes in the vascularity of the endometrium of intact uteri (Markee 31 32) and of transplanted endometrium (Markee and Andersen 34 Markee and French 34 Krichesky 43)

The blood volume in the uterus also undergoes marked changes during pregnancy In the estrous rabbit the uterine blood is less than 2 ml by 5–6 days post *coitum* (*p c*) the blood volume is some 10 ml The blood volume reaches a maximum of 30 ml at 28–29 days *p c* (Barcroft and Rothschild 32) The rate of increase in blood volume coincides with the increase in the vascular bed and the

---

[1] This inv t g tion w s upport d in p rt by USPHS re e h grant HD 00585-03 from the N ti nal Institut of Child H lth nd Human De lopment. Sci ntific P per no 2672 Wash ngton Agri ultur l Experim ntal Stati ns Pullman Proj ct 1698

[2] Lalor F undati n Po t Doct l F ll w Present ddre Dep rtm nt of Animal Scienc F ulty of Agri ulture Hokkaido Uni ersity S pporo J pan

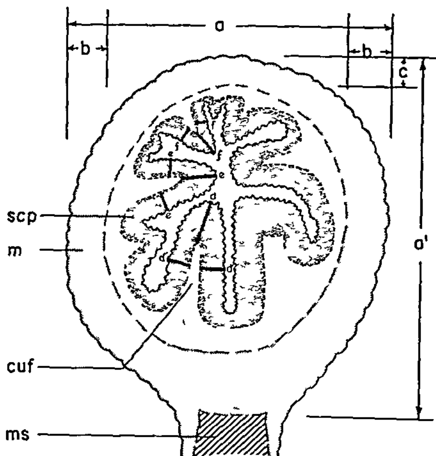


Fig 1 Technique used to measure the vascular supply in a cross section of the rabbit uterus

Abbreviations (a a) diameter of uterus (b c) thickness of myometrium thickness of subepithelial capillary plexus in the placental (d d) periplacental (e e) and obplacental (f,f') folds *cuf* core of uterine fold *m* myometrium *ms* mesometrium *scp* subepithelial capillary plexus

parent cross section of the conceptus (fig 3)

RESULTS

The circular arteries in the uterine muscular layer gave off arterioles that pass radially through the endometrium to the uterine lumen These arterioles broke up into capillaries which ran among the uterine glands and formed the subepithelial capillary plexus This plexus was connected with venules which passed through the endometrium to the myometrium and connected with the circular veins which ran in the myometrium in parallel with the arteries These venules formed an endometrial vascular plexus at the base of the endometrium

Changes in vascularity of endometrium and placenta

2–4 days p c There was no marked change in the endometrium At 4 days *p c* marked branching of the folds of mucosa occurred The uterine glands elongated and increased in number these changes were marked in the placental folds The capillaries in the subepithelial

growth of fetal tissue A critical change in the rate of blood flow through the rabbit uterus takes place after the twenty second day of pregnancy Between 22 and 24 days of pregnancy the blood flowing through the maternal vessels of the uterus diminishes thus this stage is critical for fetal survival (Reynolds, 37) In polytocous species the blood supply to each implantation site is related to the number of the implantations When the number of implantations is increased by superovulation or embryo transfer the placental development is restricted leading to a high post implantation mortality (Parkes, 42, Adams '60 Hafez, 64)

Histological characteristics of implantation and placentation in the rabbit have been reported (Mossman 26 Allen 49 Amoroso 58 Harvey 59 Larsen 61 62 63) Amoroso (58) classified the fully developed placenta of the rabbit as hemoendothelial but Larsen (62) using electron microscopy classified the placenta as hemochorial Other classical investigations were reported on the gross structure of the pregnant uterus (Reynolds 49) and the vascular pattern of the placental uterine mucosa (Krichesky 43 Parry 50 Ando and Yamashita 52) Quantitative aspects of the mitoses in the myometrium (Crandall 38) and histological analysis of uterine growth (Krichesky 42) during pregnancy were also reported However little is known about the vascular system of the endometrium during pregnancy

The present investigation is carried out to study the cyclical changes in the fine architecture of the endometrial vasculature throughout pregnancy in the rabbit with particular reference to the process of implantation

MATERIALS AND METHODS

Sixty five nulliparous and multiparous New Zealand white rabbits weighing 7 to 11 pounds were bred twice to fertile bucks and the uteri removed at 2 4 6 7 8 9 10 11 13 15 18 20 24 and 28 days *post coitum (p c)* Blood vessels of the uteri were studied using intervascular injections of neoprene latex, by clearing injected specimens and by the study of frozen and paraffin embedded sections

(1) *Neoprene latex cast* Water dispersible colors (DuPont) were added to neoprene latex 601A (from Cementex) which was diluted three times The middle uterine arteries and veins were cannulated using a dull needle and the colored latex injected using Mayer s injectors of different sizes To prevent leakage of the latex solution, the ovarian arterial and venous vessels and the vagina were ligated The injected uteri were placed for several days in concentrated HCl for maceration or were preserved in 10% formalin solution These specimens were examined under water, macroscopically and microscopically

(2) *Cleared sections* Segments of the uteri which were previously injected with latex (as described under 1) were preserved in 10% formalin solution washed in running water for 2 hours frozen by freezing microtome and sliced at 50 μ or more in thickness or cut in sections as thin as possible with a razor blade The sections were directly mounted in polyvinyl pyrrolidine solution without dehydration

(3) *Frozen sections* The segments of the uteri were fixed for 2 days in a mixed solution of formalin sodium chloride and potassium ferricyanide washed with water for 2 hours, frozen on the freezing microtome cut into sections with freezing microtome or a razor blade stained with benzidine treated with alcohol cleared in methyl benzoate and mounted in Permount (*cf* Slonimski and Cunge 48)

(4) *Histological sections* Segments of the uteri were preserved in 10% neutral formalin solution and were used for the histological observations They were stained with hematoxylin-eosin

All these specimens were observed macroscopically and microscopically The following measurements were taken from the transparent sections using a micrometric eyepiece (× 37 5) diameter of uterus thickness of myometrium and thickness of subepithelial capillary plexus at the placental periplacental and obplacental folds (fig 1) The thickness of the subepithelial plexus did not include the uterine epithelium The dimensions of the fetal placenta were also measured in the trans

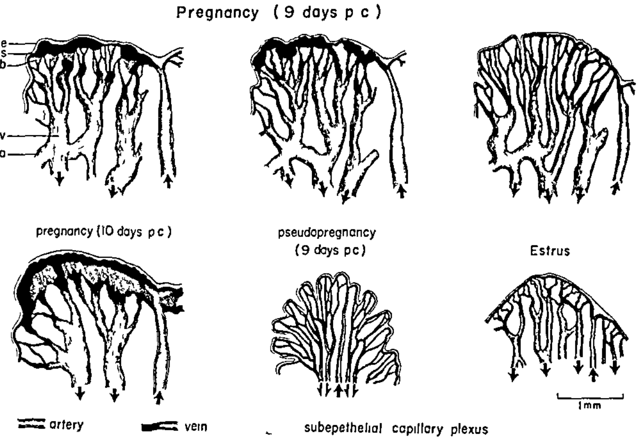


Fig 2 Diagrammatic illustration of the major vascular changes at the upper portion of the placental folds At the time of implantation the blood vessels in the core were dilated and the subepithelial capillary plexus was thicker The surface blood vessels increased in size and formed blood sinuses In the hemorrhage area the blood pathways were evident At 10 days p c the hemorrhage area expanded to form a thin layer of fetal placenta and the subepithelial capillary plexus was lost During pseudopregnancy there was more branching of the fold than during estrus *Abbreviations* *a* arcuate vein *b* blood pathway *e* epithelium of placental fold *s* blood sinus *v* large veins

capillary plexus were slightly elongated The vessels in the cores of the folds increased in diameter and the endometrial vascular plexus at the base of the endometrium was well developed, especially at the placental folds

6–8 days p c At 6 days *p c* areas of the conceptus and interconceptus within the uterus could be identified The capillaries in the subepithelial capillary plexus increased in thickness and length The free surface of the epithelium was irregular as a result of the cytoplasmic projections of the cells At 7 days *p c* the glandular lumina expanded slightly and the epithelium was transformed into syncytium in some parts of the interconceptus most parts of the glandular epithelium did not change in appearance At 8 days *p c* the epithelium of the interconceptus increased in thickness and most parts of the epithelium changed into syncytium except for the glands situated near the myometrium Sloughing off of many syncytial masses occurred into the uterine lumen (plates 1 and 2)

In some conceptuses the obplacental fold was completely lost and the endometrial glandular layer seemed to connect directly with the muscular layer The thickness of the subepithelial capillary plexus decreased although the branching of the folds was marked The capillaries of the plexus became slightly tortuous The arteries in the placental folds seemed to be more developed than before At 7 and 8 days *p c* the endometrial and muscular layer of the obplacental uterine wall became very thin Many shallow depressions were recognizable on the endometrial surface, which seemed to interlock the fetal and maternal tissues The subepithelial capillary plexus became thin and the capillary network was running along these shallow depressions

The periplacental folds diminished in size and the placental folds became larger and the cores of the folds increased in size (plates 2 and 3) The capillaries in the placental folds were longer than at 6 days p c On the surface of the placental folds deep grooves were formed by the branching of the folds

At 6 days *p c* the histological characteristics of the epithelial cells were similar in the conceptal and interconceptal areas At 7 days *p c* the transformation to the syncytium in the epithelium was more advanced in the conceptal area than in the interconceptal area At 8 days p c many vacuoles appeared in the epithelium of the periplacental and placental folds The vessels in the cores of these folds had marked perivascular sheaths although the capillaries of the subepithelial capillary plexus had no such sheath The decidual cells appeared in the interglandular area of the placental folds

9–10 days p c In the interconceptal area the branching of the folds reached a maximum The cores of the folds became narrow and the capillaries were stretched Most of the epithelium was transformed into syncytium except the basal portions of the glands situated near the muscular layer Sloughing off of the syncytial masses from the epithelium occurred and the thickness of the epithelium was decreased In some animals at 10 days p c the uterine lumen was dilated and the folds were decreased in size The folds showed a marked decrease in the cores

At the conceptus at 9 days p c the obplacental wall was very thin and the endometrium was similar to that at 8 days *p c* The periplacental folds became smaller At 10 days p c the periplacental folds disappeared completely or developed to knobs The vascular structure of the knobs was similar to that of the placental fold The placental folds developed in size and their surface was covered with fetal tissues Specialized areas of implantation were clearly recognizable on the surface of each placental fold In these areas the grooves formed by the branching of the fold were filled with fetal tissues and clearly identified from the surrounding tissues The implantation area was swollen and crescent shaped (called "dark horse shoe shaped area by Duval 1889) The vessels of the core were dilated markedly and formed large arcuate veins underneath the subepithelial capillary plexus In some animals small hemorrhagic areas were formed at the surface

ered gradually at the base of the fetal placenta and connected with the large venous vessels of the maternal placenta (plate 5)

In the placenta of 15 days *p c* the vascular structure was the same as above The convex projections of the fetal placenta increased in diameter and the fetal placenta was constructed of numerous lobes The large vessels on the fetal placenta were well developed These vessels gave off very short branches and tufts of capillaries in each lobe independently (plates 6 7)

Histologically the trophoblastic columns which accompanied allantoic mesenchyme were more developed at 11 days *p c* than before and the fetal vessels appeared near the base of the fetal placenta In the fetal placenta many mitoses were observed In the maternal placenta the number of small vessels decreased due to the marked development of the perivascular sheaths of the large vessels At 13 days *p c* a zone of separation was formed at the base of the maternal placenta the intermediary region became thin The trophoblastic tubules were branched and became more tortuous than before The general structure of the placenta seemed accomplished by 15 days *p c*

16–18 days p c In the interconceptal site the shape of the cross section of endometrium was variable because the uterine lumina showed different degrees of dilation In general the endometrium was thin and was covered with syncytial epithelium

The epithelium was constructed with syncytial and single columnar cells The sloughing off of the cells from the epithelium was marked The lobes of the fetal placenta were clearly formed and the zone separation was well developed (plate 7) At 18 days *p c* the surface vessels of the fetal placenta were running along the shallow grooves formed within the lobes The capillaries running in parallel through each lobe connected into venous branches then connected with the large venous vessels of the maternal placenta under the middle portion of fetal placenta In the maternal placenta the vessels were dilated especially under the fetal placenta Fewer vessels were seen In the zone of separation a few small vessels were distributed In the periplacental knobs the vessels were reduced in number and few dilated vessels were observed

20–28 days p c In the interconceptus of 20 days *p c* the uterine lumina were markedly dilated and no folds were seen (plate 8) The endometrium was covered with syncytium At 24–28 days *p c* the conceptal and interconceptal areas could be identified in the uterine wall of the peri and obplacental folds Areas of simple columnar epithelial cells appeared in the endometrium The giant cells were still evident

In the conceptus at 20 days *p c* the obplacental uterine wall was very thin Sloughing off of simple columnar epithelial cells occurred The capillary plexus showed polygonal meshlike network The lobes of the fetal placenta were crowded and well developed The intermediary region was divided into many islands

In the upper portion of the maternal placenta very large blood sinuses were formed at 24 days *p c* Some of the other vessels in the maternal placenta were clearly occluded The placenta at 28 days *p c* remained unchanged

The vascular changes in the endometrium and placenta during pregnancy are summarized in tables 1 2 and 3 The morphological changes in the folds of uterine mucosa and the placenta are shown throughout pregnancy (figs 3 4) The attachment between the maternal and fetal placentas (fig 5) is limited to the inner side and top area of the placental fold The fetal placenta was the newly formed tissue in the interglandular area and the maternal placenta was transformed mainly from the placental fold

Measurements of vascular structures in uterus and fetal placenta

The vascular structures in the uterus were measured throughout early pregnancy in transparent cross sections During later stages of pregnancy 13–28 days *p c* measurements were not taken because of the wide variability in the dilation of uterine lumina The subepithelial capillary plexus showed marked increase in

of each placental fold The capillaries along the surface of the folds and surrounding the crescent area were connected with the dilated and congested vessels on the surface of the crescent (plates 3 and 4) The large venous plexus in the cores were extended to reach under the dilated surface vessels In advanced stages small hemorrhages occurred from the dilated vessels in the area of the subepithelial capillary plexus in the crescents In the hemorrhagic areas very complicated net works of small pathways of blood were formed (fig 2)

Histologically the glandular lumina of the upper portion of the placental fold were filled with swollen glandular syncytium and the crescent area was covered with a layer of the trophoblast The dilated vessels at the crescent were recognized as the surface sinuses of the blood vessels In some parts of these blood sinuses the endothelium was broken up this led to hemorrhages in the intergland ular area The myometrium in the mesometrial side was reduced markedly in thickness and the endometrial vascular plexus became indistinct at 9–10 days *p c*

At 10 days *p c* the large vessels in the core of the placental fold were well developed and the area of the plexus of large vessels was extended The dilated vessels reached the subepithelial capillary plexus beyond the arcuate veins situated at the base of the plexus The capillaries changed into large vessels sparsely distributed near the surface of the placental fold The area of hemorrhage extended to cover the placental fold On the surface of the fetal placenta large vessels originated from the capillaries were running along the surface The large veins of the placental fold were connected with the base of the fetal placenta Among these two kinds of vessels there was a layer of blood pathways which formed a network After 9 days *p c* the placental fold could be considered as the maternal placenta

Histologically the perivascular sheaths of the vessels in the maternal placenta increased very extensively as they replaced the connective tissue The vascular sheaths were developed in the intergland ular area The large vessels increased in size and this vascular area of the maternal placenta had been referred to by Amoro (58) as the region of the 'uterine sinu A zone of the large decidual cells appear between the fetal and maternal placer (intermediary region) The large maten blood sinuses reached the base of t fetal placenta running through this int mediary region (fig 2) The fetal vess at 10 days *p c* reached the fetal place and the fetal capillaries were ming with the maternal capillaries on the s face of the fetal placenta (plates 4 5)

The surface sinuses were well develo at 9 days *p c* Newly formed trophobla tubules were connected with the surf of the sinuses The maternal blood fl the sinuses was flowing to the large nuses in the intermediary region thro the trophoblastic tubules The histolog changes in the periplacental knobs v similar to that in the placenta At obplacental area the endometrium for minute folds The arrangement of epithelial cells was very irregular giant cells appeared in some areas of endometrium

11–15 days p c The characteristic the folds in the interconceptal area a days *p c* were similar to those at 1 15 days The endometrium was m covered with syncytial epithelium w was sloughing off in masses In s animals large uterine lumina appe At 15 days *p c* the uterine lumina filled with mucus and debris

In the conceptal site at 11 days the obplacental uterine wall increase thickness The capillary plexus was i ularly arranged and the capillaries sho a network of polygonal meshes with low depressions at the surface The per cental fold was lost in some concepti whereas in others the folds developed knobs The endometrium was mostly ered with syncytium These feature the ob and periplacental folds were same at 13 and 15 days *p c* At 11 *p c* the maternal placenta was well veloped although the vascular pattern reduced markedly The large vessels w covered the fetal placenta branched formed a network numerous tortuous illaries were given off into the fetal maternal placenta The capillaries g

ered gradually at the base of the fetal placenta and connected with the large venous vessels of the maternal placenta (plate 5)

In the placenta of 15 days p c the vascular structure was the same as above The convex projections of the fetal placenta increased in diameter and the fetal placenta was constructed of numerous lobes The large vessels on the fetal placenta were well developed These vessels gave off very short branches and tufts of capillaries in each lobe independently (plates 6 7)

Histologically the trophoblastic columns which accompanied allantoic mesenchyme were more developed at 11 days p c than before and the fetal vessels appeared near the base of the fetal placenta In the fetal placenta many mitoses were observed In the maternal placenta the number of small vessels decreased due to the marked development of the perivascular sheaths of the large vessels At 13 days p c a zone of separation was formed at the base of the maternal placenta the intermediary region became thin The trophoblastic tubules were branched and became more tortuous than before The general structure of the placenta seemed accomplished by 15 days p c

16–18 days p c In the interconceptal site the shape of the cross section of endometrium was variable because the uterine lumina showed different degrees of dilation In general the endometrium was thin and was covered with syncytial epithelium

The epithelium was constructed with syncytial and single columnar cells The sloughing off of the cells from the epithelium was marked The lobes of the fetal placenta were clearly formed and the zone separation was well developed (plate 7) At 18 days p c the surface vessels of the fetal placenta were running along the shallow grooves formed within the lobes The capillaries running in parallel through each lobe connected into venous branches then connected with the large venous vessels of the maternal placenta under the middle portion of fetal placenta In the maternal placenta the vessels were dilated especially under the fetal placenta Fewer vessels were seen In the zone of separation a few small vessels were distributed In the periplacental knobs the vessels were reduced in number and few dilated vessels were observed

20–28 days p c In the interconceptus of 20 days p c the uterine lumina were markedly dilated and no folds were seen (plate 8) The endometrium was covered with syncytium At 24–28 days p c the conceptal and interconceptal areas could be identified in the uterine wall of the peri and obplacental folds Areas of simple columnar epithelial cells appeared in the endometrium The giant cells were still evident

In the conceptus at 20 days p c the obplacental uterine wall was very thin Sloughing off of simple columnar epithelial cells occurred The capillary plexus showed polygonal meshlike network The lobes of the fetal placenta were crowded and well developed The intermediary region was divided into many islands

In the upper portion of the maternal placenta very large blood sinuses were formed at 24 days p c Some of the other vessels in the maternal placenta were clearly occluded The placenta at 28 days p c remained unchanged

The vascular changes in the endometrium and placenta during pregnancy are summarized in tables 1 2 and 3 The morphological changes in the folds of uterine mucosa and the placenta are shown throughout pregnancy (figs 3 4) The attachment between the maternal and fetal placentas (fig 5) is limited to the inner side and top area of the placental fold The fetal placenta was the newly formed tissue in the interglandular area and the maternal placenta was transformed mainly from the placental fold

Measurements of vascular structures in uterus and fetal placenta

The vascular structures in the uterus were measured throughout early pregnancy in transparent cross sections During later stages of pregnancy 13–28 days p c measurements were not taken because of the wide variability in the dilation of uterine lumina The subepithelial capillary plexus showed marked increase in

TABLE 1
Changes of the endometrial vascularity in the interconceptal area during pregnancy

Days post coitum	Endometrial folds	Proliferation index[1]	Endometrium
2	No marked change	1	Many mitoses in Ep
4	Marked branching number of uterine glands increased	3	Few mitoses in Ep SECP increased in thickness
6	Marked branching conceptus and interconceptus sites are identified	4	Cytoplasmic projections of epithelial cells SECP increased in thickness
7	Delicately branched very narrow cores	4	Some parts of Ep transformed into syncytium glandular lumina slightly expanded
8	Delicately branched very narrow cores	4	Most parts of Ep transformed into syncytium many syncytial masses sloughing off from Ep
9	More marked branching	4	Capillaries in SECP stretched in length and became slender arteries well developed Ep decreased in thickness
10	In some areas uterus had large lumen folds decreased in size branching of endometrium still marked		Layer of SECP is thick
11 13	In some areas uterus had large lumen folds decreased in size branching of endometrium still marked		Well branched folds covered with syncytium
15	Lumen expanded and filled with mucus and degenerated matter		Endometrium formed thin irregular layer SECP directly connected with endometrial vascular plexus
16	Endometrium very variable in shape		Endometrium formed thin irregular layer SECP directly connected with endometrial vascular plexus
18	Endometrial swelling in some animals		Endometrium formed thin irregular layer SECP directly connected with endometrial vascular plexus
20	No large folds		Endometrium formed thin irregular layer SECP directly connected with endometrial vascular plexus
24–28	Interconceptus not identified from conceptus area		Thin endometrium in Ep areas of syncytial cells and simple columnar cells

[1] Values based on method of McPhail (34)
Abbreviations Ep Epithelium SECP Subepithelial capillary plexus

thickness especially in the placental folds In the interconceptus the ratio of the thickness of capillary plexus to the uterine diameter reached a maximum of 6 days p c and was maintained until mid pregnancy At 6 days p c the thickness of this capillary plexus in the conceptus decreased This coincided with the rapid expansion of the blastocyst However at 7 and 8 days p c this thickness increased markedly

The length and depth of the fetal placenta were measured in transparent cross section at the center of the conceptuses (table 4) The maximum growth rate of the fetal placenta occurred between 10 to 13 days *p c*

DISCUSSION

The vasculature of the uterus is of special physiological significance in relation to the cyclical changes taking place during the estrous cycle pseudopregnancy and pregnancy (Stafford 30 Markee 31 Barcroft and Rothschild 32 Barcroft et al 33 Markee and French 34 Reynolds

D y pc	Conc ptu	Obpl nt l t ine w ll	Pe pl ent l f ld	Pl cent l f ld	
				F t l pl ent	M t rn l placenta
6	Ep similar to intercon ceptus SECP thinner than in interconceptus	Endometrial folds diminished in size by presence of blastocyst especially in ob-periplacental folds obplacental fold completely lost endometrial vascular plexus well developed especially under placental folds			
7	Transformation into syn cytium in Ep more ad vanced than intercon ceptus	Thin wall endometrium showed minute branching	Well branched	Cores of folds more developed capillaries in SECP slightly tortuous vessels in the core dilated and tortuous	
8	Many shallow depressions recognizable on endome trial surface SECP formed network	Vacuolation in Ep peri vascular sheath	Cores of folds more extended vessels well developed vacuolation in Ep perivascular sheath decidual cells in interglandular area		
9	Thickness of myometrium reduced endometrial vas cular plexus degenerated	Shallow holes increase in diameter	Smaller	Fetal and maternal tissues attached glandular lumina of upper portion of folds filled with swollen glandular syncytium folds covered with a layer of trophoblast subepithelial capillaries at attachment site in some animals small hemmorhages occurred at crescent area on surface of folds; at hemmorhage area inter or intra cellular blood pathways formed many mitoses occurred in various cell types	
10	Fetal vessels reached crescent areas on surface of placental folds fetal maternal placentae clearly identified	Well stretched giant cells appeared	Some folds developed to knobs vascular structure same as in placental fold glandular syncytium filled glandular lumina peri vascular sheath	Fetal vessels reached cres cent of fold fetal vessels mingled with maternal vessels at surface area of crescent trophoblastic tu bules appeared	Perivascular sheath so in creased as to nearly re place connective tissue dilation of vessels into SECP size of vessels in creased zone of large decidual cells between fetal and maternal pla centa (intermediary re gion)
11	Fetal vessels reached crescent areas on surface of placental folds fetal maternal placentae clearly identified	Well stretched giant cells appeared	Some folds developed to knobs vascular structure same as in placental fold glandular syncytium filled glandular lumina peri vascular sheath	Trophoblastic columns which accompanied al lantoic mesenchyme were more developed fetal ves sels near base of pla centa many mitoses fe tal placenta covered with dilated large maternal vessels which showed branching and gave off capillaries into fetal pla centa tortuous capillaries ran toward maternal pla centa through tropho-blastic tubules	Small vessels became few in number by develop ment of perivascular sheaths

previatio s: Fp Epith lium SECP Subepithelial capillary plexus

TABLE 3

Changes in endometrial and placental vascularity at the conceptal site during late pregnancy

Conceptus	Obplacental uterine wall	Periplacental fold	Placental fold: Fetal placenta	Placental fold: Maternal placenta
Fetal vessels reached crescent areas on surface of placental folds fetal maternal placentae identified	Well stretched giant cells	Some folds developed to knobs vascular structure same as in placental fold glandular syncytium filled glandular lumina peri vascular sheaths	Trophoblastic tubules branched and more tortuous trophoblastic columns became thin	Large vessels sparsely distributed zone of separation appeared intermediary region became thin
Placentae accomplished in general structure	Sloughing off of syncytial mass of Ep single columnar Ep predominated	Some folds developed to knobs vascular structure same as in placental fold glandular syncytium filled glandular lumina peri vascular sheaths	Convex surfaces of lobes clearly formed trophoblastic tubules became more definite vessels tubules increased in number length and complexity	*Zone of separation* clearly formed with few distributions of vessels
Placentae accomplished in general structure	Ep formed with syncytial and single columnar cells giant cells well developed	Ep almost degenerated	Convex surfaces of lobes clearly formed trophoblastic tubules became more definite vessels tubules increased in number length and complexity	Zone of separation clearly formed with few distributions of vessels
Placentae accomplished in general structure	Marked sloughing off of syncytial masses from Ep	Vessels reduced in number	Lobes grew in size	Vessels dilated distribution of vessels became more sparse zone of separation extended laterally to obmesometrial limits of periplacenta
Placentae accomplished in general structure	Stretched and thin smooth endometrial surface most parts of endometrium covered with simple columnar or cubic cells giant cells still evident	Knobs decreased in size	Lobes well developed and crowded tissues between fetal and maternal blood streams very thin	Intermediary zone irregularly divided by forming many islands
No identification between conceptus and interconceptus site of uterine wall	Thin endometrium syncytial cells and simple columnar cells mixed in Ep giant cells evident	Knobs decreased in size	Lobes well developed and crowded tissues between fetal and maternal blood streams very thin	At upper port on of maternal placenta very large sinuses some ves els clearly occluded

tion Ep Epithelium SECP Subepith ll l c pillary plex

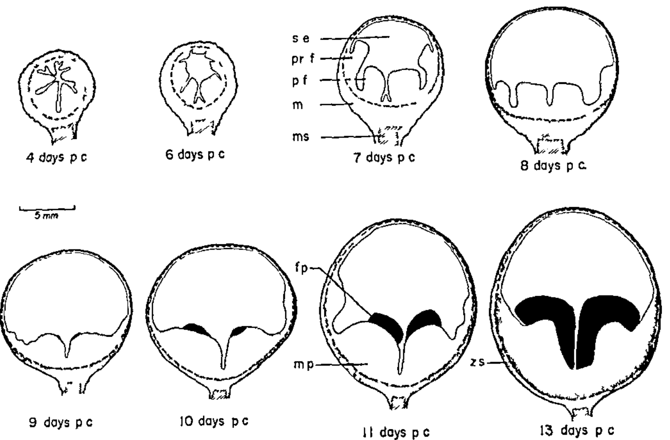


Fig 3 Diagrammatic illustration of the changes in the *endometrium* and fetal placenta at the conceptal site during early pregnancy *in the rabbit* The obplacental folds diminished at 6 days *p c* whereas the placental folds developed in size at 7–8 days *p c* At 9 days *p c* implantation occurred and the origin of fetal *placenta was evident* At 11 days *p c* the fetal placenta is situated on the top of *the placental folds* whereas at 13 days *p c* the fetal placenta was extended downward An irregular zone of separation between the placentome and the uterus occurred at 13 days *p c*

Abbreviations *f p* fetal placenta *m* musculature *m p* maternal placenta *m s* mesometrium *p f* placental fold *pr f* preplacental fold *s e* site of embryo *z s* zone of *separation*

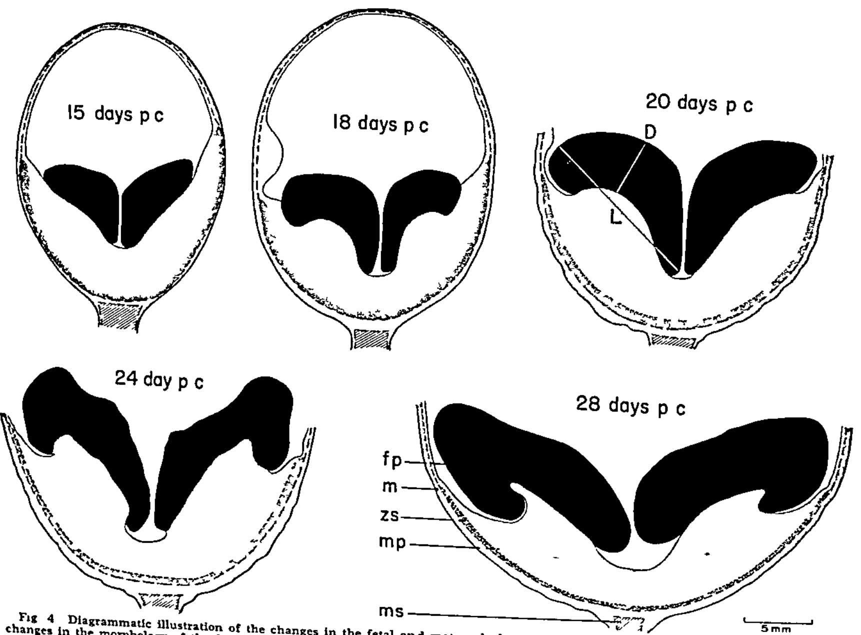


Fig 4 Diagrammatic illustration of the changes in the fetal and maternal placenta during late pregnancy in the rabbit Note the changes in the morphology of the fetal and maternal placenta the fetal placenta was superficial throughout pregnancy and became flattened at 28 days p c After 20 days p c the zone of separation was thin

Abbreviations L and D show the technique used to measu e the length and depth of fetal placenta; *f p* fetal placenta; *m* musculature *m p* mate nal placenta; *m* mesomet ium z zone of sepa a ion

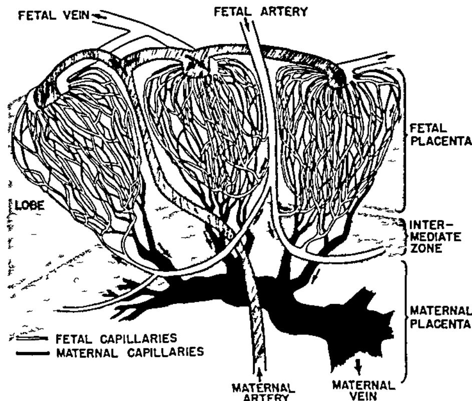


Fig 5 Diagrammatic illustration showing vascular distribution of the allantochorionic placenta in the rabbit The branches of uterine arteries penetrate into the maternal placenta and extend to the surface of the fetal placenta and are distributed thereon giving off a tuft of capillaries The capillaries form a network by anastomosis and the fetal capillaries mingle with the maternal ones The branches of the umbilical artery give off arterial branches into the intermediate zone and connect with fetal capillary network in each lobe The fetal capillaries unite at the upper portion of lobe and connect with the umbilical vein

TABLE 4

Measurements of fetal placenta in transparent cross sections of uteri in pregnant rabbits (all measurements are in microns)

D y p c	(L) Length of plac nt	Rat f growth of length of pl centa	(D) ι Depth f pl centa	Rat of growth of d pth of pla enta
		%		ơ
9	1896	—	777	—
10	5113	269	1528	197
11	6441	126	2545	167
13	9155	142	3773	148
15	11768	129	3711	98
16	11632	99	4138	112
18	14248	122	4140	100
20	17353	122	4957	120
24	15206	88	4870	98
28	19939	131	6041	124

For me surem nt of L nd D see figure 3

M urem nt in rea of extrav ti n of th impl ntati n site of the placental f ld.

Rate of growth of pl nt equ ls incre se in length or depth of pl centa a a percentag to th t on the previ us d y

'37 Gillman 41 Krichesky 43, Parry 50) Moreover the classification of mammalian placenta is usually based on its vascular structure (Mossman, 26 Ando and Yamashita 52 Amoroso 58, Larsen 61 62 Tsutsumi 62 Haynes, 63)

In the present study the changes in the endometrial vascularity of the placental folds have been examined more closely especially at the time of implantation of the blastocyst In the maternal circulation at 10 days p c the newly formed tubes which connect with the surface blood sinuses open into spaces between the multinucleate cells Mossman (26) reported that the extravasation can be observed in the interglandular veins In the present studies, small hemorrhages are found at the crescent area on the placental fold in some animals at 9 days p c In these hemorrhage areas the blood pathways form a network of minute meshes The blood in the surface sinuses which are connected with maternal arterial vessels seems to flow to the dilated maternal vessels in the placental core through these blood pathways The hemorrhage areas are extended and the fetal vessels appear on the surface of the crescent 10 days p c The implantation site in the rabbit has been examined by electron microscopy (Larsen 61) The vacuoles formed in the syncytial trophoblast merge into lacunae which become filled with maternal blood when the trophoblast invades the maternal vessels 10 days p c This time coincides with the appearance of the blood pathways described in the present studies

The blood pathways develop into capillaries in the fetal placenta at later stages of pregnancy The time of implantation varies in different conceptuses within the uterine horn The characteristic structures which normally appear at 9 days p c are not recognizable in some conceptuses This variability may be related to the size of blastocyst and may be correlated with subsequent embryonic survival At 10 days p c the homorrhage areas are recognized in all conceptuses

The branches of uterine arteries penetrate into the maternal placenta from the mesometrial side of the uterine wall they become large vessels and extend to the surface of the fetal placenta These branches, which resemble the venous vessels because of their thin wall give off a tuft of capillaries radially in each lobe (fig 3) The capillaries are dilated and connect to the surface blood sinuses of the crescent area at the time of implantation In the rabbit implantation occurs superficially and the fetal placenta is the newly developed tissue on the surface of the placental fold It is confirmed that the large vessels which cover the fetal placenta are derived from the maternal capillaries running along the surface of the placental fold

The yolk sac attachment on the obplacenta occurs at 7 days p c (Sansom 27 Parry 50 Boving 63) It was suggested that the greater vascular development of this region is associated with implantation (Bascish and Wyburn 40 Phelps 46 Amoroso 58) However Parry (50) could not confirm this phenomenon He reported that when the fusion areas are first formed they have a very poor vascular supply The present studies also show that the vascularity of the obplacental endometrium becomes poor because of the rapid expansion of the conceptus and stretching of the uterine wall

The identification of the conceptus and interconceptus sites is possible at 6 days p c In the interconceptal site the changes in the vascularity during early pregnancy seem to be similar to that during pseudopregnancy At 6 days p c the thickness of the subepithelial capillary plexus is increased and the capillaries of the plexus are well stretched Histologically the endometrial epithelium in pseudopregnant rabbits shows cytoplasmic projections in most cells at 6 days p c (Tsutsumi and Hafez 66) Similar histological characteristics are recognized in the interconceptal site at 6 to 8 days of gestation The endometrium is restored to the normal estrous state some 20 days p c in pseudopregnant rabbits whereas in the interconceptal area the syncytial epithelium is maintained until the time of delivery Deanesly and Parkes (31) described the changes taking place in the sterile horn during 16 to 28 days p c of pregnancy The endometrial characteristics in the interconceptal area seem to be different to that in the sterile horn The uterine lumen in

the interconceptus is expanded in some animals at 10 days p c and the endometrial folds become very irregular in shape In the present study no difference is recognizable between the conceptal and interconceptal area at 24 to 28 days p c The changes taking place in the shape of conceptus have been described by Reynolds (46)

The maternal placenta of the rabbit is actively growing up to the sixteenth day of pregnancy (Hammond 37) There is an interaction among the placenta ovary and hypophysis during pregnancy Progesterone levels in the ovarian vein blood throughout pregnancy increases gradually reaching a maximum by midpregnancy the levels decreasing gradually thereafter (Mikhail et al 61) As shown by histochemical evidence glycogen appears in the maternal placenta of the rabbit at about the eighth day of pregnancy and increases in amount until a maximum is reached at the 12–16 day (Chipman 03) It would appear that the rabbit placenta is well established anatomically and physiologically by the sixteenth day of pregnancy

Further studies are needed to evaluate the physiological significance of endometrial vascularity in relation to postimplantation morality and the rate of fetal development

LITERATURE CITED

Adams C E 1960 Studies on prenatal mortality in the rabbit *Oryctolagus cuniculus* the amount and distribution of the loss before and after implantation J Endocrin 19 325–344
Amoroso E C 1958 Placentation In Marshall s Physiology of Reproduction A S Parkes ed Longmans London vol 2 ch 15
Allen P 1949 Cited by Brambell and Hemmings J Physiol 108 177–184
Ando Y and R Yamashita 1952 The distribution of the minute blood vessels of the pregnant rabbit s uterus Hiroshima Igaku 5 41–44
Bascich P and G M Wyburn 1940 Cited from H J Parry Trans Roy Soc Edinb 60 79
Barcroft J and P Rothschild 1932 The volume of blood in the uterus during pregnancy J Physiol 76 447–459
Barcroft J W Herker and S Hill 1933 The rate of blood flow and gaseous metabolism of the uterus during pregnancy J Physiol 77 194–206
Boyd J D and W J Hamilton 1958 Cleavage early development and implantation of the egg In Marshall s Physiology of Reproduction A S Parkes ed Longmans London vol 2 chapter 14
Boving B G 1954 Blastocyst uterine relationships Cold Spring Harbor Symp Quant Biol 19 9–28
——— 1959 Implantation Ann N Y Acad Sci 75 700–725
——— 1962 Anatomical analysis of rabbit trophoblast invasion Contribution to Embryology 37 33–55
——— 1963 Implantation mechanisms In Conference on Physiological Mechanisms Concerned with Conception Pergamon Press chapter 7 pp 321–396
Chipman W 1903 Observations on the placenta of the rabbit with special reference to the presence of glycogen fat and iron Lab Reports of Royal College of Physicians Edinburgh 8 227–485
Crandall W 1938 A quantitative study of the influence of the ovarian hormones on hyperplasia by mitosis in the rabbit uterus in early pregnancy Anat Rec 72 195–210
Deanesly R. and A S Parkes 1931 The functions of the corpus luteum V Changes in the sterile horn during pregnancy and their relation to changes in the corpus luteum Proc Roy Soc B 109 196–212
Dickmann Z and R W Noyes 1960 The fate of ova transferred into the uterus of the rat J Reprod Fertil 1 197–212
Duval M 1889 Le placenta des rongens le placenta du lapin Cited by Larsen 61 J Anat Paris 25 399–573
Gillman J 1941 Profound vascular changes induced in the uterus of the castrated rabbit by combinations of estradiol benzoate and progesterone Endocrinology 29 336–342
Hafez E S E 1962 Effect of progestational stage of the endometrium on implantation fetal survival and fetal size in the rabbit *Oryctolagus cuniculus* J Exp Zool 151 217–226
——— 1963a Physiological mechanisms of implantation Cornell Veterinarian 53 348–368
——— 1963b Physio-genetic interaction between mammalian blastocyst and endometrium J Exp Zool 154 163–168
——— 1964 Effects of over-crowding in utero on implantation and fetal development in the rabbit J Exp Zool 156 269–287
Hammond J 1937 Pregnancy and nutrition of the embryo in the rabbit. Cited by Huggett and Hammond 58 In Marshall s Physiology of Reproduction chapter 16
Harvey E B 1959 Placentation in Ochotonidae Amer J Anat 104 61–85
Haynes D M 1963 Experimental abruptio placentae in the rabbit Amer J Obst and Gynec 85 626–645
Krichesky B 1942 A histologic analysis of uterine growth during pregnancy in the rabbit. Anat Rec 82 551–564

——— 1943 Vascular changes in the rabbit uterus and in intraocular endometrial transplants during pregnancy Anat Rec 87 221–234

Larsen J F 1961 Electron microscopy of the implantation site in the rabbit Amer J Anat 109 319–334

——— 1962 Electron microscopy of the chorioallantoic placenta of the rabbit I The placental labyrinth and the multinucleated giant cells of the intermediate zone J Ultrastructure Res 7 535–549

——— 1963 Electron microscopy of the chorioallantoic placenta of the rabbit II The decidua and the maternal vessels J Ultrastructure Res 8 327–338

Lutwak Mann C J C Boursnell and J P Bennett 1960 Blastocyst uterine relationships Uptake of radioactive ions by the early rabbit embryo and its environment J Reprod Fertil 1 169–185 no 2

Markee J E 1931 Modification of the vascular rhythm in the rabbit uterus by follicular hormone Anat Rec 48 (Supplement) 28 (abstr)

——— 1932 Rhythmic vascular uterine changes Amer J Physiol 100 32–39

Markee J E and E Andersen 1934 The growth of intraocular endometrial transplants in pregnant rabbits Anat Rec 58 (Supplement) 78 (abstr)

Markee J E and H M French 1934 The vascular changes in intraocular endometrial and myometrial transplants in pregnant rabbit Anat Rec 58 (Supplement) 78–79 (abstr)

Mikhail G M W Noall and W M Allen 1961 Progesterone levels in the rabbit ovarian vein blood throughout pregnancy Endocrinology 69 504–509

Mossman H W 1926 The rabbit placenta and the problem of placental transmission Amer J Anat 37 433–497

Noyes R W and Z Dickmann 1960 Relationship of ovular age to endometrial development J Reprod Fertil 1 186–196

Parkes A S 1942 Induction of superovulation and superfecundity in rabbit J Endocrin 3 268–279

Parry H J 1950 The vascular structure of the extra placental uterine mucosa of the rabbit J Endocrin 7 86–99

Phelps D 1946 Endometrial vascular reactions and the mechanism of nidation Amer J Ana 79 167–197

Reynolds S R M 1937 Haemodynamic factors in the uterus during the latter part of gestation Nature (Lond) 140 546

——— 1946 The relation of hydrostatic conditions in the uterus to the size and shape of the conceptus during pregnancy a conceptus of uterine accommodation Anat Rec 95 283–296

——— 1949 Adaptation of maternal uterine blood vessels and uterine accommodation of the products of conception Contrib to Embryol 33 1–19

Sansom G S 1927 The giant cells in the placenta of the rabbit Proc Roy Soc Lond B 101 354–368

Slonimski P and A Cunge 1949 In Mikroskopische Technik B Romeis ed Verlag Leibzig p 470

Stafford E S 1930 The origin of the blood of the placental sign Anat Rec 47 43–57

Tsutsumi Y 1962 The vascular pattern of the placenta in farm animals (horse pig cow sheep and rabbit) J Faculty of Agriculture Hokkaido Univ 52 372–482

Tsutsumi Y and E S E Hafez 1966 Endometrial vascularity during pseudopregnancy in the rabbit J Morphol 118 43–56

PLATE 1

EXPLANATION OF FIGURES

Vascular supply of the endometrium in pregnant rabbits

6 Surface lining of endometrium at 6 days *p c* showing the site of im plantation (arrow) The uterine wall was cut to expose the lumen note the flat folds surrounding the embryo (latex injected specimen × 3 6)

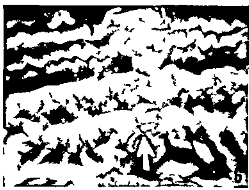
7 Same as above Note the obplacental folds and the implantation site (arrow) (latex injected specimen × 3 6)

8 Cross section of the conceptus at 6 days *p c* The size of the folds was diminished especially the obplacental folds (transparent sec tion × 9)

9 Vascularity at the interconceptal site 6 days *p c* Note marked branching of folds (transparent section × 9)

10 *Longitudinal section of uterus showing the conceptal and* intercon ceptal sites at 6 days *p c* (histological section × 9)

11 The conceptal site at 7 days *p c* Note the marked development of the placental folds and the winding grooves (latex injected specimen × 3 6)


6




8


9


10


11

PLATE 1

EXPLANATION OF FIGURES

Vascular supply of the endometrium in pregnant rabbits

6 Surface lining of endometrium at 6 days *p c* showing the site of im plantation (arrow) The uterine wall was cut to expose the lumen note the flat folds surrounding the embryo (latex injected specimen × 3 6)

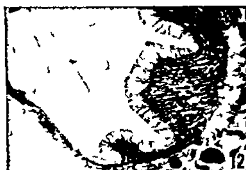
7 Same as above Note the obplacental folds and the implantation site (arrow) (latex injected specimen × 3 6)

8 Cross section of the conceptus at 6 days *p c* The size of the folds was diminished especially the obplacental folds (transparent sec tion × 9)

9 Vascularity at the interconceptal site 6 days *p c* Note marked branching of folds (transparent section × 9)

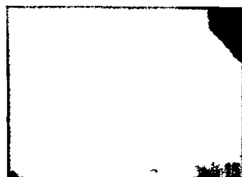
10 Longitudinal section of uterus showing the conceptal and intercon ceptal sites at 6 days *p c* (histological section × 9)

11 The conceptal site at 7 days *p c* Note the marked development of the placental folds and the winding grooves (latex injected specimen × 3 6)


12


13


14




16

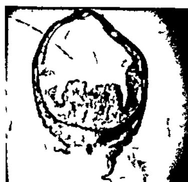


PLATE 2

EXPLANATION OF FIGURES

Vascular supply of the endometrium in pregnant rabbits

12 A cross section of the conceptus at 7 days *p c* Note the branching and the vascularity of the fold (transparent section × 9)

13 Vasculature of the uterine mucosa in the interconceptus site at 7 days *p c* Note the marked branching of the folds and the well developed vasculature (transparent section × 9)

14 The placental folds at the conceptal site 8 days *p c* after removing the obplacental uterine wall Note the distribution of the capillaries on the surface of the placental folds (latex injected specimen × 3 6)

15 Surface capillaries of the placental fold at 8 days *p c* (latex injected specimen × 17 6)

16 Cross section of the placental fold in the conceptal site at 8 days *p c* Large arteries reached the surface of the placental folds and dispersed into capillaries (transparent section × 9)

17 General structure of the conceptus 8 days *p c* (frozen section × 3 6)


12


13


14




16



PLATE 3

EXPLANATION OF FIGURES

Vascular supply of the endometrium in pregnant rabbits during implantation

18 Cross section of the placental folds at the conceptus 8 days p c Note the vacuoles in the branches of the folds (histological section × 17 6)

19 *Cross section of the interconceptus 8 days p c Note the syncytial* masses of epithelium (histological section × 17 6)

20 Embryo situated on the placental folds at 9 days p c The membrane lined the inner surface of the conceptus (latex injected specimen × 3 6)

21 Surface of the placental folds at 9 days p c On the surface of the placental fold attachment occurred and the crescent was slightly apparent (latex injected specimen × 3 6)

22 Well developed crescents on the placental folds at 9 days p c Compare with previous figure of the same stage In the crescent the vessels were dilated (latex injected specimen × 3 6)

23 Blood vessels of the crescent connected (arrow) with the surface capillaries on one placental fold 9 days p c (latex injected specimen × 17 6)


18


19


20


21


22


23

PLATE 4

EXPLANATION OF FIGURES

Vascular supply of the endometrium in pregnant rabbits

24 Small hemorrhage areas in the crescent 9 days p c (frozen section × 17 6)

25 The surface capillaries of the placental folds were dilated at 9 days p c (transparent section × 9)

26 Dilated vessels and small hemorrhage areas in the crescent area on top of the placental fold 9 days p c Note the complicated and irregular network of blood pathways in the hemorrhage area (transparent section × 3 6)

27 Embryo *in situ* 10 days p c Note the development of the vascular splanchnopleur (latex injected specimen × 3 6)

28 Same specimen 10 days p c embryo and embryonic membranes removed Note the development and swelling of the crescent on the placental folds this is the origin of the fetal placenta (latex injected specimen × 3 6)

29 Cross section of conceptus 10 days p c The fetal placentae were clearly formed covering the top and inner surface of the folds Maternal vessels were markedly dilated in the maternal placenta (frozen section × 3 6)













PLATE 5

EXPLANATION OF FIGURES

Vascular supply of the endometrium in pregnant rabbits

30 Vasculature of the fetal and maternal placentae 10 days *p c* The vessels in the maternal placenta were markedly dilated (transparent section × 9)

31 Fetal and maternal vessels on the surface of the fetal placenta 11 days *p c* The umbilical cord is represented by a white central spot (latex injected specimen × 3 6)

32 A cross section showing the vascularity of the fetal and maternal placenta 11 days *p c* Note the swollen and the dilated vessels in the maternal placenta (transparent section × 9)

33 The vascularity in the fetal placenta 11 days *p c* Note the capillaries forming network (transparent section × 36)

34 Cross section of the interconceptus 11 days *p c* The uterine lumen was expanded and the folds became small and irregular in shape (transparent section × 9)

35 Surface vascularity of the fetal placenta 13 days *p c* (latex injected specimen × 3 6)


30


31






34



PLATE 5

EXPLANATION OF FIGURES

Vascular supply of the endometrium in pregnant rabbits

30 Vasculature of the fetal and maternal placentae 10 days *p c* The vessels in the maternal placenta were markedly dilated (transparent section × 9)

31 Fetal and maternal vessels on the surface of the fetal placenta 11 days *p c* The umbilical cord is represented by a white central spot (latex injected specimen × 3 6)

32 A cross section showing the vascularity of the fetal and maternal placenta 11 days *p c* Note the swollen and the dilated vessels in the maternal placenta (transparent section × 9)

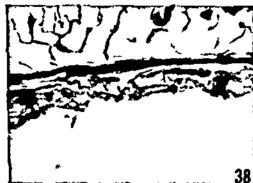
33 The vascularity in the fetal placenta 11 days *p c* Note the capillaries forming network (transparent section × 36)

34 Cross section of the interconceptus 11 days *p c* The uterine lumen was expanded and the folds became small and irregular in shape (transparent section × 9)

35 Surface vascularity of the fetal placenta 13 days *p c* (latex injected specimen × 3 6)


36




38


39

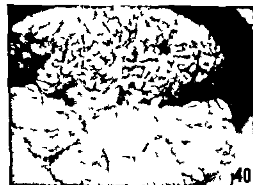

40



PLATE 6

EXPLANATION OF FIGURES

Vascular supply of the endometrium in pregnant rabbits

36 Same specimen 13 days *p c* The surface of the fetal placenta was formed by many small convex surfaces (latex injected specimen × 9)

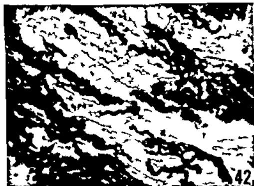
37 Surface of the periplacental knob and obplacental endometrium 13 days *p c* The shallow depressions increased in diameter (latex injected specimen × 9)

38 Cross section of the obplacental uterine wall 13 days *p c* The thin layer of the subepithelial capillary plexus appear below the myometrium (transparent section × 36)

39 Endometrial capillaries formed a network with shallow holes (the intact obplacental uterine wall was mounted in polyvinyl pyrrolidone solution transparent specimen × 36)

40 Fetal and maternal vasculature on the surface of the fetal placenta *15 days p c Note the formation of lobes (latex injected specimen* × 3 6)

41 Maternal vasculature in the fetal placenta 15 days *p c* Large dilated arteries reached the surface of the fetal placenta from the maternal placenta (arrow) (transparent section × 9)


42


43




45



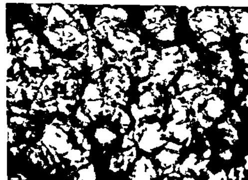


PLATE 7

EXPLANATION OF FIGURES

Vascular supply of the endometrium in pregnant rabbits

42 Maternal capillaries in the fetal placenta 15 days *p c* Note the complicated network (transparent section × 36)

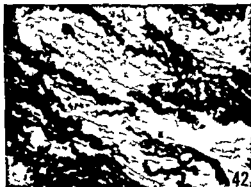
43 Cross section of the interconceptal site 15 days *p c* Note the small folds irregularly arranged and the uterine lumen filled with degenerated matter (histological section × 9)

44 Maternal vasculature on the surface of the fetal placenta 15 days *p c* *Note the formation of the lobes (latex injected specimen* × 3 6)

45 Maternal vasculature on the surface of the fetal placenta 16 days p c Note the tufts of capillaries from the large maternal vessels (latex cast specimen × 17 6)

46 *Periplacental knob and obplacental endometrial surface 16 days p c* The capillaries formed a network with shallow holes (latex injected specimen × 3 6)

47 Endometrial capillary network of the obplacental wall 16 days *p c* (the intact uterine wall was mounted in polyvinyl pyrrolidone solution transparent specimen × 36)


42


43


44


45



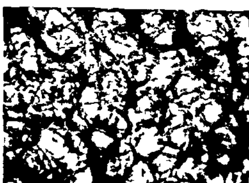

47

PLATE 7

EXPLANATION OF FIGURES

Vascular supply of the endometrium in pregnant rabbits

42 Maternal capillaries in the fetal placenta 15 days *p c* Note the complicated network (transparent section × 36)

43 Cross section of the interconceptal site 15 days *p c* Note the small folds irregularly arranged and the uterine lumen filled with degenerated matter (*histological section* × 9)

44 Maternal vasculature on the surface of the fetal placenta 15 days *p c* Note the formation of the lobes (latex injected specimen × 3 6)

45 Maternal vasculature on the surface of the fetal placenta 16 days *p c* Note the tufts of capillaries from the large maternal vessels (latex cast specimen × 17 6)

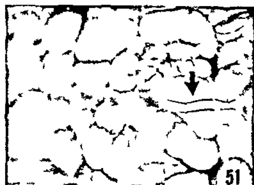
46 Periplacental knob and obplacental endometrial surface 16 days *p c* The capillaries formed a network with shallow holes (latex injected specimen × 3 6)

47 Endometrial capillary network of the obplacental wall 16 days *p c* (the intact uterine wall was mounted in polyvinyl pyrrolidone solution transparent specimen × 36)


48


49


50


51

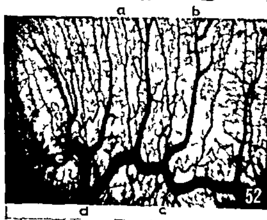

a
b
52
d
c

PLATE 8

EXPLANATION OF FIGURES

Vascular supply of the endometrium in pregnant rabbits

48 Maternal vasculature in the fetal and maternal placenta 18 days *p c* In the maternal placenta the vessels formed large sinuses (transparent section × 9)

49 *Maternal vessels on the surface of the fetal placenta 20 days p c* Maternal vessels gave off tufts of capillaries for each lobe (latex cast specimen × 17 6)

50 Maternal vasculature in the fetal placenta 20 days *p c* The maternal capillaries were arranged longitudinally more or less in parallel *within each lobe They were connected with the blood sinus in the* maternal placenta gradually joining with each other (transparent section × 17 6)

51 Maternal vasculature on the surface of the fetal placenta 21 days *p c* Note the fetal vessel running along the surface (arrow) (latex injected specimen × 9)

52 Maternal vasculature of the obplacental uterine wall 24 days *p c* (specimen was mounted in polyvinyl pyrrolidone solution transparent specimen × 3 6)

Abbreviations *a* ventral uterine artery *b* ventral collecting vein *c* circumferential uterine artery *d* circumferential collecting vein *e* lateral arcuate vein

Histogenesis of Choroid Plexus in Man [1]

SAMRUAY SHUANGSHOTI AND MARTIN G NETSKY
Department of Pathology University of Virginia School of Medicine Charlottesville Virginia

ABSTRACT Four stages of development can be recognized in the histogenesis of the human telencephalic choroid plexus Division into stages is based on alterations of outline of the plexus characteristic appearance and biochemical content of the epithelial cells and the components of the stroma The stages are less distinctive in the myelencephalic and diencephalic plexus where differentiation is accomplished sooner than in the telencephalic plexus Neuroepithelial lined tubules are common in the choroid plexus and are formed by folding of choroidal epithelium into the stroma Some tubules are large enough to be designated as incipient neuroepithelial (colloid) cysts Cysts having only connective tissue walls are also present The choroidal epithelial cells proliferate focally stratify and desquamate into intervillous clefts or flow into the stroma by disruption of the epithelial basement membrane or tubular wall These findings are confirmed by use of serial sections The size of the developing telencephalic plexus relative to the ventricular system is small at first then large occupying almost the entire telencephalon but gradually decreases during development Glycogen is prominent in developing choroidal epithelial cells but disappears in the mature plexus Both epithelial and mesenchymal mucin and mucopolysaccharides are identified in the plexus The paraphysis is re-emphasized as an extraventricular choroid plexus on the basis of a common neuroepithelial origin It is rudimentary and inconstant in man

We have reviewed in another publication the developmental and comparative anatomy of choroid plexus ependyma and other derivatives of the primitive neuroepithelium in relation to the development of neuroepithelial (colloid) cysts (Shuangshoti Roberts and Netsky 65) It was emphasized in that paper that the paraphysis is an extra ventricular choroid plexus Because our data indicated a close relationship between the neuroepithelial cyst and the choroid plexus we decided to study the histogenesis of the choroid plexus in detail We described in the same paper the finding of mucin and PAS reactive materials in neuroepithelial cysts and in fragments of choroid plexus attached to the cysts Histochemical tests for these substances were therefore conducted on developing choroid plexus to clarify these observations

A few investigators have described the times of appearance of the primordia of telencephalic and myelencephalic plexuses in some mammals as in pig (Weed 17) guinea pig rabbit and rat (Cohen and Davies 38 Strong 56) but the full histogenesis has not been presented Kiszely (51) and Kappers (58) studied human embryos incompletely and more recently Tennyson and Pappas (64) investigated the problem ultrastructurally in material from rabbits An extensive morphologic study of human material is still lacking

MATERIALS AND METHODS

Eighteen brains obtained from embryos and fetuses ranging from 13 to 100 mm crown rump (C-R) length (about 4 to 14½ weeks of gestation) were examined The material was obtained from abortions but none of the specimens were grossly abnormal microscopic observation failed to disclose malformations or other evidence of disease The tissues were fixed immediately after they were obtained and all observations reported were consistent with in groups of comparable ages Ten brains were sectioned sagittally and six coronally In two cases only the choroid plexuses of lateral third and fourth ventricles were examined but the entire brain was sectioned in the remaining 16 Additional

[1] This investigation was supported in part by grant NB-5383 from the National Institute of Neurological Diseases and Blindness Public Health Service

Histogenesis of Choroid Plexus in Man [1]

SAMRUAY SHUANGSHOTI AND MARTIN G NETSKY
Department of Pathology University of Virginia School of Medicine Charlottesville Virginia

ABSTRACT Four stages of development can be recognized in the histogenesis of the human telencephalic choroid plexus Division into stages is based on alterations of outline of the plexus characteristic appearance and biochemical content of the epithelial cells and the components of the stroma The stages are less distinctive in the myelencephalic and diencephalic plexus where differentiation is accomplished sooner than in the telencephalic plexus Neuroepithelial lined tubules are common in the choroid plexus and are formed by folding of choroidal epithelium into the stroma Some tubules are large enough to be designated as incipient neuroepithelial (colloid) cysts Cysts having only connective tissue walls are also present The choroidal epithelial cells proliferate focally stratify and desquamate into intervillous clefts or flow into the stroma by disruption of the epithelial basement membrane or tubular wall These findings are confirmed by use of serial sections The size of the developing telencephalic plexus relative to the ventricular system is small at first then large occupying almost the entire telencephalon but gradually decreases during development Glycogen is prominent in developing choroidal epithelial cells but disappears in the mature plexus Both epithelial and mesenchymal mucin and mucopolysaccharides are identified in the plexus The paraphysis is re-emphasized as an extraventricular choroid plexus on the basis of a common neuroepithelial origin It is rudimentary and inconstant in man

We have reviewed in another publication the developmental and comparative anatomy of choroid plexus ependyma and other derivatives of the primitive neuroepithelium in relation to the development of neuroepithelial (colloid) cysts (Shuangshoti Roberts and Netsky 65) It was emphasized in that paper that the paraphysis is an extra ventricular choroid plexus Because our data indicated a close relationship between the neuroepithelial cyst and the choroid plexus we decided to study the histogenesis of the choroid plexus in detail We described in the same paper the finding of mucin and PAS reactive materials in neuroepithelial cysts and in fragments of choroid plexus attached to the cysts Histochemical tests for these substances were therefore conducted on developing choroid plexus to clarify these observations

A few investigators have described the times of appearance of the primordia of telencephalic and myelencephalic plexuses in some mammals as in pig (Weed 17) guinea pig rabbit and rat (Cohen and Davies 38 Strong 56) but the full histogenesis has not been presented Kiszely (51) and Kappers (58) studied human embryos incompletely and more recently Tennyson and Pappas (64) investigated the problem ultrastructurally in material from rabbits An extensive morphologic study of human material is still lacking

MATERIALS AND METHODS

Eighteen brains obtained from embryos and fetuses ranging from 13 to 100 mm crown rump (C R) length (about 4 to 14½ weeks of gestation) were examined The material was obtained from abortions but none of the specimens were grossly abnormal microscopic observation failed to disclose malformations or other evidence of disease The tissues were fixed immediately after they were obtained and all observations reported were consistent within groups of comparable ages Ten brains were sectioned sagittally and six coronally In two cases only the choroid plexuses of lateral third and fourth ventricles were examined but the entire brain was sectioned in the remaining 16 Additional

[1] Thi in estig tion w support d in p rt by grant NB-5383 from the N tional Institute f Neurologi l Diseases and Blindness Publi He lth Servi

TABLE 1

Stages of differentiation of human telencephalic plexus

	Stag I	Stage II	St ge III	*Stage IV*
Time of dev lopment	7th week	9th week	17th week	29th w ek
D rati n f d v l pment	2 w eks	8 weeks	12 weeks	11 we ks
Epithelium	Pseudostratified tall *predominantly central* nuclei	Low columnar apical nuclei	*Cuboidal apical* and central nuclei	Cuboidal or squamous cen tral and basal nuclei
Glycogen	Absent?	Abundant	Moderate	*Minimal and finally absent*
Villi	Absent lobules present	Sparse primary villi	Mostly primary villi	*Villi with multiple fronds*
Tubules	May be present	Several	Numerous	*Numerous*
Stroma	Loose mesenchyme	Extremely loose mesen *chyme* small amount of connective tissue fibers	Loose mesenchyme moderate amount of connective tissue fibers	Scant *mesenchyme* large amount of connective tis sue fibers and meningo cytes
Stromal blood vessels	Islets of nucleated blood cells surrounded by ill defined vascular walls blood islets located subepithelially	Definite vascular *walls* capillaries located sub epithelially large blood vessels in central inter stitium	Well *formed* vascular walls capillaries in *villous core large* blood vessels in central stroma	Same
Size of plexus in relation to ventricle	Minute	Extremely large	Moderately large	*Small*

materials were studied from human fetuses or premature full term or new born infants The choroid plexuses from lateral, third and fourth ventricles were examined in these cases, but the entire brains were not sectioned The ages ranged from four months of intra uterine life to one post natal month Most specimens were fixed in 10% formaldehyde Some fresh material was preserved in nine parts of absolute alcohol plus one part of 40% formaldehyde to study glycogen content of cells The staining methods employed were hematoxylin and eosin (H & E) Mayer s mucicarmine periodic acid Schiff (PAS) with and without diastase Mallory s phosphotungstic acid hematoxylin (PTAH) Wilder s reticulum Verhoeff s elastic and Sudan IV All fetuses and much of the remainder of the material were serially sectioned The gestational age of the embryo fetus or premature infant was calculated from the chart of the National Pituitary Agency if C R length or body weight were known This chart was modified from data of Streeter (20)

OBSERVATIONS

The first indication of the myelencephalic plexus consisting of an invagination of mesenchyme into the thin roof area was found in a six week embryo (16 mm C R length) In the telencephalic area the first invagination became visible in a seven week embryo (19 mm C R length) and in the diencephalic area of the eighth week (23 mm C R length) The invaginations are covered by pseudostratified columnar neuroepithelium Histogenesis of the telencephalic plexus will be described in detail the other plexuses less extensively

Based on the shape of the plexus characteristic features of the epithelial cells and their biochemical and stromal components four stages of histogenesis are recognized in the telencephalic plexus A comparison of various features of these stages is shown in the table

Stage I (figs 1 2 3) The primordium of the telencephalic plexus is club shaped has a short stalk and is covered by pseudo stratified tall neuroepithelium ranging from 50 to 60 μ in thickness (figs 1 2) The epithelial cells have indistinct borders the size of individual cells therefore is difficult to determine The nuclei are large elongated or ovoid hyperchromatic and predominantly centrally located They contain one or more small nucleoli and are surrounded by fine granular eosinophilic cytoplasm Nuclei in mitosis are rarely seen and if present are located toward the apices of the epithelial cells (fig 2 at arrow) A brush border is seen at the luminal side of the epithelium Cilia are not observed and the basement membrane is indistinct The neuroepithelium in the region distal to the stalk (fig 1 at upper arrow) is 70 μ thick and many mitotic nuclei are present at the luminal side of the epithelium

The stroma is loose mesenchyme interspersed with numerous islets of nucleated blood cells within ill-defined vascular walls Many islets are closely applied to the base of the epithelium (fig 2) more closely than to the neuroepithelium of the neural tube Vascularization is greater in the plexus than in the primitive leptomeninges

Toward the end of Stage I the club-shaped invagination is slightly lobulated (fig 3) The epithelium is reduced to 20 to 30 μ in thickness A few primitive endothelial cells appear around the islets of immature blood corpuscles to form the vascular walls

Glycogen seems to be absent in this stage but lacking fresh specimens we were not able to test for its presence Vacuoles are not seen in the cytoplasm of the epithelial cells

Stage II (figs 4 5 6A 7) This stage begins during the ninth week and lasts until about the sixteenth week of gestation A moderate increase in the size of the primordium (fig 4) occurs in the 30 mm embryo (about 9 weeks of gestation) The stromal mesenchyme becomes extremely loose accumulating a large amount of mucin as revealed by Mayer s mucicarmine reaction The choroid plexus becomes more lobulated and occupies about one third of the lateral ventricle (fig 4) and reaches its maximal size (fig 5A) filling about three fourths of the lateral ventricle at 50 mm C R length (about 11 weeks of gestation) The pseudostratified tall columnar epithelium is spread and

is scant or absent (fig 6D) being gradually replaced by mucin and granular acidophilic PAS reactive but diastase resistant material (fig 10 inset at upper arrow) Throughout this stage of development areas of simple pseudostratified and stratified epithelium can be identified but simple cuboidal epithelium predominates The villi become more delicate branching frequently into multiple fronds with cores of scant connective tissue (fig 10) In some specimens however the epithelium throughout the process of differentiation may show features characteristic of Stage III

Mesenchymal elements are gradually replaced by large amounts of connective tissue fibers mainly collagenous and reticular Stellate mesenchymal cells are rarely seen Delicate fibers develop primarily around the stromal blood vessels and subsequently become coarse and wavy spreading throughout the interstitium The vascular walls thicken intimal medial and adventitial layers are clearly recognized including well-defined elastic lamellae Meningocytic cells appear many arranged in whorls around blood vessels (fig 10 at lower arrow) Tubules (fig 12) and incipient neuroepithelial cysts (fig 11) are always present In addition cysts having connective tissue fibrous walls rather than an epithelial lining are occasionally seen in the stroma (fig 11 inset) Macrophages and foamy cells are widely scattered (fig 12) The formation of tubules by folding of epithelium is clearly shown in figure 12C

Neo-natal period (up to one month after birth) The epithelium (fig 13) consists chiefly of small cuboidal or squamous cells with predominantly central and basal nuclei The individual cell is about 10 × 10 μ Cytoplasmic glycogen is replaced by PAS reactive diastase resistant acidophilic granules and mucin (fig 13 inset at lower arrow) Stratified proliferative epithelium is present in some places The stroma is more compact and is made denser by infiltration with newly formed connective tissue fibers and meningocytes The latter cells occur only in the central interstitium and are not seen in the stroma of villous fronds The epithelium and stromal blood vessels especially capillaries are separated by thin layers of connective tissue In many areas especially in the villous cores only a thin membrane of connective tissue is seen between the stromal blood vessels and the choroidal epithelium of the surface Psammoma bodies are not seen in any specimen examined

Differences among plexuses Histologic differentiation of the myelencephalic and diencephalic plexuses is different from that of the telencephalic plexus The former arise from a remarkably thinned-out pseudostratified neuroepithelium of the myelencephalic and diencephalic roofs by invaginated mesenchymal *tela choroidea* (figs 14 15) The thickness of epithelium in both roofs ranges from 20 to 25 μ Stage I of differentiation is therefore extremely short or absent The fully grown plexus consists mainly of simple cuboidal epithelium but areas of stratification and proliferative epithelium are also present such as occur in the telencephalic plexus Pseudostratified columnar epithelium is present throughout the stalk of each plexus Tubules and incipient neuroepithelial cysts are also noted

Completed differentiation of the myelencephalic and diencephalic plexuses occurs sooner than in the telencephalon Three fetuses in which all plexuses were examined histologically and histochemically have remarkable differences among the plexuses In one fetus of 7 5 cm C-R length (about 13 weeks of gestation) the telencephalic plexus has features characteristic of Stage II but the diencephalic and myelencephalic plexuses are in Stage III of differentiation

Another fetus of 17 0 cm C R length (about 21 weeks of gestation) also shows noteworthy differences (fig 16) The telencephalic plexus is in Stage III (fig 16A) The diencephalic (fig 16B) and myelencephalic (fig 16C) plexuses are in Stage IV Similar findings are also encountered in the third fetus weighing 1 500 gm (about 31 weeks of gestation) Some features of Stage III still can be seen in the telencephalic plexus but the diencephalic and myelencephalic plexuses have features characteristic of the adult plexus

A significant difference is noted in amount of glycogen in epithelial cells of

becomes mostly simple low columnar (fig 5B 5C at arrow) to cover a wider area In some places, as in the stalk (fig 5 C) or the tips of interlobular clefts pseudo stratified epitheluim persists Abundant glycogen appears in the cytoplasm of the epithelial cells especially in the basal portion (fig 6A) as revealed by the PAS reaction in the fresh specimen preserved in alcohol formaldehyde solution the reactive material disappears after digestion with diastase In the usual formaldehyde fixed specimen the basal parts of the cells are clear because of dissolution of glycogen in the fixative (fig 5B 5C at arrow fig 7) The epithelial cells in the stalk of the plexus contain little glycogen and this substance is absent from the ependymal lining of the ventricle

During this stage the cellular membrane is well delineated (fig 5B) The individual epithelial cell measures 25 μ in height and 20 μ in width The nuclei are located apically and are surrounded by a thin rim of fine granular eosinophilic cytoplasm which is PAS reactive but diastase fast and positive for mucin Nucleoli are rarely seen Tips of the interlobular clefts are occasionally pinched off entrapping multiple neuroepithelial lined tubules in the interstitium (fig 5A at two upper arrows) The epithelia both at the surface and in tubules proliferate manifested by stratification of a few cells thickness in some places pyknosis of nuclei shadowy outlines of cells and finally desquamation and replacement of effete cells by those adjacent These findings are confirmed by serial sectioning A few fibroblasts and connective tissue fibers appear in the stromal mesenchyme particularly around the vascular walls The fibers are delicate and chiefly reticular Occasionally collagenous fibers are present in the vascular walls but elastic fibers are lacking Many macrophages and cells with foamy cytoplasm are scattered throughout the stroma Islets of immature blood corpuscles gradually decrease in number and size and the primitive endothelial cells subsequently form the vascular walls (fig 5B) The smaller blood vessels tend to be located subepithelially the larger ones are scattered in the deeper part of the stroma They are engorged with predominantly non nucleated erythrocytes

Toward the end of the second stage (100 mm C R length or 15 weeks of gestation), the plexus continues to be lobulated and some primary villi develop (fig 7) The stroma contains a few mesenchymal cells with large numbers of fibroblasts fibers of connective tissue and mucin

Stage III (figs 6B 8 9) This stage begins to appear in an embryo of about 120 mm C R length (seventeenth week of gestation) and lasts until about the twenty eighth week (1 000 gm body weight) Relative to the ventricle the plexus gradually decreases in size and primary villi develop further (figs 8 9) The epithelium changes from low columnar to cuboidal The individual epithelial cell is approximately 15 × 15 μ Some apical nuclei shift toward central parts of the epithelial cells Cytoplasmic glycogen is moderate in amount (fig 6B) More PAS reactive diastase fast material and mucin are present in the cytoplasm of the epithelial cells Many tubules (fig 9 at lower arrow) appear in the interstitium of the plexus some large enough to be designated as incipient neuroepithelial cysts using the criterion that a cyst is more than five times the diameter of most tubules Desquamated epithelial cells are scattered in the stroma of the plexus (fig 9 at upper arrow) and in the intervillous clefts (fig 8) Frequently these desquamated cells become round and foamy resembling lipid laden macrophages and contain free fat demonstrated by Sudan stains The loose mesenchyme decreases in amount while connective tissue fibers increase moderately (fig 9) These fibers react like collagen in PTAH stains Small numbers of reticular and elastic fibers are also present as indicated by their reactions in Wilder s and Verhoeff s preparations Elastic fibers are mainly in vascular walls

Stage IV (figs 6C 10 11 12) From about the twenty ninth week of gestation until term the large cuboidal epithelial cells are replaced by smaller ones Each cell is now approximately 10 × 10 μ The nuclei are situated more basally their characteristic position in adult epithelium Glycogen in the cytoplasm decreases in amount (fig 6C) until after birth when it

toses should be seen in the basal or central zones as well as the luminal side

Most authors state that the choroidal epithelium after Stage I of development is simple cuboidal In every specimen examined by us some areas of simple stratified and pseudostratified epithelium could always be identified and the finding confirmed by serial sections The epithelium is always pseudostratified at the stalk of the plexus even in post natal life These findings indicate that choroidal epithelium is of multiple types although largely simple cuboidal

Steiner and Shanklin (64) reported pathologic changes in telencephalic plexuses from newborn infants who died with hyaline membrane disease of the lungs within 12 hours after birth The alterations were less severe after 24 hours of age The changes in choroid plexus were characterized by stromal edema and swollen choroidal epithelial cells with clear cytoplasm The authors did not mention the fixatives used for preservation of the specimens We are not certain that the swelling of the choroidal epithelial cells with clear cytoplasm is related to the hyaline membrane disease of the lung During the first few days of post natal life the telencephalic plexus may retain some immature features of Stage IV or even Stage III of histologic differentiation The large cuboidal epithelial cells with cytoplasmic glycogen can usually be detected for a few days after birth The clear cytoplasm described by these authors may merely represent sites of glycogen not retained by the technics used for study

Blood and blood vessels The presence of large numbers of immature blood cells and primitive endothelial cells in the stroma of the plexus in Stage I led Kappers (58) to postulate that the embryonic choroid plexus was a blood forming organ but this observation was denied by Tennyson and Pappas (64) who argued that immature blood cells are always present in vascular lumens hence are merely the usual circulation of the choroid plexus The latter seems the more likely explanation

Tubules and cysts Ciaccio and Scaglione (13) described a case of hyperplasia of follicles" of the telencephalic plexus associated with status thymo-lymphaticus in a child Cameron (53) described "vesicles" in the plexus of rat rabbit and chick in tissue culture and believed that these "vesicles are formed by outgrowth of the epithelium Klosovskii (63) found "follicles" embedded in the stroma of the telencephalic plexus and suggested a possible endocrine function or activity related to growth of brain in post natal life In addition this author believed that these "follicles" may atrophy and be transformed into amyloid bodies in the aged He denied the existence of "follicles in diencephalic and myelencephalic plexuses

We believe that the "vesicles" and "follicles" described by these authors are structures analogous to the tubules we find are formed by folding of the surface epithelium into the stroma during differentiation of the plexus (figs 5A at upper arrows 9 at lower arrow 12 13 at left arrow) Thirty three of 40 specimens of choroid plexus from various ventricles of the brain contain these structures and only seven specimens in the early stages of development do not The number of tubules increase at the same rate as the number of lobules or villi of the plexus indicating that formation is closely related to interlobular or intervillous clefts The tubules are formed when the tips of these clefts are pinched off We find these tubules in all three major plexuses Tubules in seven specimens are large enough to be designated as incipient neuroepithelial cysts (fig 11) The presence of neuroepithelial cysts even in fetal life suggest that the cysts found in adult man are congenitally formed

The epithelium in the tubules undergoes similar histologic differentiation as on the surface These tubules show frequent divisions as revealed by serial sections and therefore are not follicles or vesicles In addition to neuroepithelial cysts we also find cysts consisting of a space in the connective tissue without epithelial lining (fig 11 inset) These cysts have been regarded as evidence of retrogression (Wolf Cowen and Graham 50 Dunn and Kernohan 55 Ham 57 and Millen and Woolam 62) but their presence even in fetal life is evidence against such a mechanism Morphologically these cysts in

the various plexuses in the same embryo or fetus The glycogen content of cells of the myelencephalic plexus is greater than in the diencephalic plexus but it is much less than in the telencephalic

Primordium of paraphysis With regard to the paraphysis, the extraventricular choroid plexus of the third ventricle (Studnicka 00 McMurrich 15 Brachet 21 Kingsley 26 Zimmerman and German 33 Shuangshoti Roberts and Netsky 65) only 4 of 16 fetuses at 19 23 30 and 41 mm C R length (about 7 8 9 and 10 weeks gestation) have the primordium of this structure Pseudostratified neuroepithelium of the diencephalic roof folds into the mesenchyme at the rostral end of the roof (figs 4 15 17 18) The microscopic structure of the first indication of the paraphysis is similar to the primordium of the diencephalic plexus (fig 15)

DISCUSSION

Time of development of choroidal primordia Much variation is noted in journals and standard textbooks of embryology regarding the embryonic age in which the primordium of the choroid plexus first appears It varied from 4 to 5 weeks for the myelencephalic (Streeter 12 Jordan and Kindred 48 Klosovskii 63) and five to six and one half weeks (Minot 1892 Heisler 07 Kappers 58) or during the second month (Klosovskii 63) for the telencephalic plexus Frazer (32) stated the primordium of the diencephalic plexus appears early in the third month but Klosovskii (63) said it is seen in the first month

We found primordia of the myelencephalic telencephalic and diencephalic plexuses in embryos of 16 19 and 23 mm C R length respectively (about 6 7 and 8 weeks of intrauterine life) We may state generally that all primordia of the choroid plexuses develop during the second month of gestation Studies of pig and rabbit are consistent in showing that the primordium of the myelencephalic plexus appears first followed by the telencephalic (Weed 17 Cohen and Davies 38 Tennyson and Pappas 64) This sequence also occurs in man as found by Kappers (58) and by ourselves Our findings also agree with Kappers (58) who stated that the diencephalic primordium developed last

Morphology of choroidal epithelium During intra uterine life the telencephalic plexus undergoes the most complex changes Our observation of four stages of differentiation is slightly different than those described in another study of human embryo (Kappers 58) and in the rabbit (Tennyson and Pappas 64) Klosovskii (63) characterized the developing choroidal epithelial cell as vesicular because of the huge mass of cytoplasm in comparison to the nucleus This cell may be the same as the epithelial cells in our Stages II and III (figs 5B 7, 8 9 16A) Although cilia have been described by some authors using animals and human material (Davis and Cushing 25 Freeman 33 Zimmerman and German 33 Chu 42 Kappers 49 Greep 54 Millen and Woollam 60 Bloom and Fawcett 62 Tennyson and Pappas 64) and in plexuses in tissue culture (Cameron 53 Lumsden 58) we do not find these structures in any specimen examined Brush borders however are present (fig 2) Only the ependyma bears cilia Better preservation of the material and special staining methods might have revealed them in the plexus

Sauer (35) found that the nucleus of the primitive neuroepithelial cells in the neural tube always migrated toward the luminal side of the epithelium before undergoing mitosis Our observation of mitotic nuclei at the luminal end of the choroidal epithelium in Stage I (fig 2 at arrow) and in the epithelial lining of the neural tube confirms this finding as do both the colchicine technic (Woodard and Estes 44 Watterson Veneziano and Bartha 56) and radioautographic studies (Sidman Miale and Feder 59 Fujita 60 63)

The nature of the epithelium during Stage I of histogenesis has been controversial It has been described as pseudostratified (Kappers 58) pseudostratified or stratified (Tennyson and Pappas 64) and stratified (Klosovskii 63) neuroepithelium The presence of nuclei in mitosis only in the luminal zone of the epithelium strongly suggests that the epithelium in Stage I is composed of a single layer of cells If the epithelium is stratified mi

Components of choroidal stroma The components of the choroidal interstitium have been much debated In spite of the accepted origin from mesenchyme the argument still remains as to whether the matrix is composed of only pia mater or arachnoid or both Histologically the arachnoid contains meningocytes (arachnoidal cells) but the pia mater does not We found meningocytes only in the central portion of the stroma of the developing choroid plexus (figs 10 at lower arrow 13 at arrow at right) There are no meningocytes in the interstitium of the choroidal villi Such findings are also commented on by Dunn and Kernohan (55) in studying the mature choroid plexus in man In this respect the central stroma of the choroid plexus is composed of arachnoid and those in the villi are pial in origin

Role of ante natal choroidal glycogen

The presence of glycogen in fetal choroidal epithelium and its complete disappearance in post natal life (fig 6) raises the question of the role of this substance in the nervous system In Stage II large amounts of glycogen are present in the epithelium of the telencephalic plexus but only moderate amounts in the myelencephalic plexus and glycogen is minimal in the diencephalic plexus Klosovskii (63) made similar observations in the plexus of the cat The glycogen laden epithelium secretes large amounts of protein into the cerebrospinal fluid (Weed 17) The cerebrospinal fluid in the fetal pig has a higher protein content than in the adult and the concentrations of other ions is similar to that in the plasma up to the fortieth day of intrauterine life (Flexner 38) Otila (48) found greater concentrations of glucose and protein in the cerebrospinal fluid of premature infants than in older children or adults Although most investigators agree that fetal choroidal glycogen serves as a carbohydrate depot for the tissue of the developing brain we suggest also that it may account for some biochemical differences between fetal and adult cerebrospinal fluid

Morphologic and biochemical differences between developing and mature choroid plexuses may indicate other functional differences Disappearance of glycogen from choroidal epithelium after birth or at the beginning of aerobic oxidation suggests that the developing nervous tissue uses energy by anaerobic metabolism of glycogen Meek (07) observed a difference in nuclear position and height of choroidal epithelial cells during fetal and post natal life This phenomenon may be directly related to the glycogen content of the cell Accumulation of glycogen in the basal part of the cell pushes the nucleus apically and the cell becomes columnar Decrease of glycogen in the late fetal period and its complete disappearance from cells in newborn and adult man is followed by movement of the nucleus centrally or basally and the cell becomes cuboidal or flat

This physiologic change may be compared with those occurring in endometrium during the menstrual cycle under the influence of sex hormones The endometrium proliferates being stimulated by estrogen The glandular epithelial cells become columnar and the nuclei basal characteristics of the proliferative phase Under the influence of progesterone secretory products (glycogen mucin and fat) appear in the basal part of the glandular epithelial cells and the nuclei are pushed apically features of secretory endometrium Toward the end of the menstrual cycle the secretory products decrease in amount until undetectable during menstruation The glandular epithelial cells become cuboidal and the nuclei are central or basal The similar physiologic changes of the choroid plexus therefore suggest the influence of hormones from placenta or other sources upon its development

Mucin PAS reactive materials in the cytoplasm of the choroidal epithelial cells (fig 10 in inset at arrow) not specific for glycogen and thought to be a mucopolysaccharide have been described by many workers We are unable however to find references concerning production of mucin (a glycoprotein) in normal choroid plexus Voetmann (49) and Mosberg and Blackwood (54) stated that it is *not* a property of the choroidal epithelium to secrete mucin In our study both epithelial and mesenchymal mucins are identified (figs 12A 13 in inset at lower arrow 16B) This confirms previous observations (Shuangshoti Roberts and Netsky 65)

connective tissue *resemble lymphatic* vessels but the absence of an endothelial lining makes this possibility unlikley As far as we are aware, only Findlay (1898 1899) mentioned lymphatics of the choroid plexus but his statement has not been confirmed It is generally believed that lymphatics do not exist in the central nervous system including the choroid plexus (Wolf Cowen and Graham 50, Ayres and Haymaker, 60)

Proliferation of choroidal epithelium In spite of absence of mitoses except in Stage I we suggest that slow proliferation of choroidal epithelium occurs and is characterized by stratification and desquamation of superficial epithelial cells followed by replacement *from adjacent underlying* cells (figs 8 9 12A and B 13 in inset at *upper arrow*) Such proliferation can be *seen* either in epithelium at the surface or *in tubules (fig* 12B) Miale and Sidman (61) *found* labeling by tritiated thymidine in the choroidal epithelial cells of embryos *of* mice A similar observation was also made in the epithelial cells of the plexuses in adult mouse rat (Messier and Leblond 60) and man (Johnson et al 60) We *found labeling by tritiated* thymidine in ependyma and choroidal epithelial cells in adult mouse (unpublished) These finding indicate proliferative capabilities of the epithelium of the choroid plexus and ependyma Desquamated cells if derived from surface epithelium may float freely in the intervillous space (fig 8) or flow into the stroma if they arise from tips of intervillous clefts (figs 9 at middle arrow 12A at upper arrow) or tubular epithelium (fig 12B) In the latter case the tubules may be filled with these cells Subsequent breaking of the tubular wall releases individual cells into the surrounding interstitium (fig 12B) This interpretation is made with the aid of deep multiple sectioning to rule out artefact due to the plane of the cut These cells become round then degenerate and accumulate fatty material in the cytoplasm Their foamy appearance makes them hardly distinguishable from lipid laden macrophages It is likely that the hyperplastic follicles described by Ciaccio and Scaglione (13) represent the usual proliferative phenomena of the tubular epithelium without relationship to status thymo-lymphaticus

In young dogs removal of both the telencephalic and myelencephalic plexuses or of telencephalic plexus only is followed by hypertrophy and hyperplasia of the diencephalic plexus In addition regeneration occurs if the stump of the removed plexus remains This phenomenon is accomplished by mitosis of the choroidal epithelial cells (Volzhina 57, 58) Knudsen (64) used Colcimid (R) to demonstrate mitoses in choroidal epithelial cells in embryos of *mice* These experiments clearly demonstrate proliferative capabilities of the developing and even mature epithelium

Size of developing choroid plexus The telencephalic plexus is extremely large in relation to the lateral ventricle in Stages II (figs 4 5A) and III This observation has been made by previous investigators (Bailey 16a Boyd 20 Kiszely 51 Kappers 58 Klosovskii 63) but Voetmann (49) *suggested that the* enlargement may represent hydropic degeneration of the plexus similar to the appearance of placental villi in hydatidiform mole The telencephalic plexuses in Stages II and III are of tremendous size occupying almost the entire lateral ventricle but the elements comprising the plexus are intact Although the stroma is extremely loose we see no similarity to the pathologic features observed in the placental villi of hydatidiform mole We therefore regard this appearance as a physiologic enlargement of the plexus

The loose and bulky stroma is related to formation of large amounts of mesenchymal mucin Such physiologic enlargement spreads the thick pseudostratified surface epithelium to become the simple cuboidal type The stroma in the stalk is scant hence this epithelium remains pseudostratified throughout the course of development and even in post natal life In addition the surface epithelium folds easily into such loose stroma to form the lobules and villi resulting in tremendous increase in surface area of the plexus During Stage IV a gradual absolute decrease in size occurs as a result of replacement of mesenchyme by connective tissue fibers meningocytes and blood vessels

der Beitr Path Anat Ztschr Allg Path 55 131
Cohen H and S Davies 1938 The morphology and permeability of the roof of the fourth ventricle in some mammalian embryos J Anat 72 430
Davis L E and H Cushing 1925 Papillomas of the choroid plexus Arch Neurol Psychiat 13 681
Dunn J and J W Kernohan 1955 Histologic changes within the choroid plexus of the lateral ventricle Their relation to age Proc Staff Meeting Mayo Clinic 30 607
Findlay W 1898 Observations on the normal and pathological histology of the choroid plexuses of the lateral ventricles of the brain J Ment Sci (Lond) 44 744
——— 1899 The choroid plexus of the lateral ventricle of the brain their histology normal and pathological Brain 22 161
Flexner L B 1938 Change in the chemistry and nature of the cerebrospinal fluid during fetal life in the pig Am J Physiol *124* 131
Francotte P 1894 Note sur l oeil pariétal l epiphyse la paraphyse et les plexus choroides du troisieme ventricule Bull de l Acad royale des Sci d Belg 3 Serie 27 84
Frazer J E 1932 A manual of embryology William Wood New York p 170
Freeman W 1933 Neuropathology the anatomical foundation of nervous system Saunders Philadelphia p 53
Fujita S 1960 Mitotic pattern and histogenesis of the central nervous system Nature *185* 702
——— 1963 The matrix cell and cytogenesis in developing central nervous system J Comp Neur *120* 37
Gladstone R J and C P G Wakeley 1940 The pineal organ Baillière Tindall & Cox London p 184
Greep R O 1954 Histology Blakiston New York pp 256–257
Ham A W 1957 Histology 3rd ed Lippincott Philadelphia pp 453–455
Heisler J C 1907 A textbook of embryology for students of medicine Saunders Philadelphia pp 306–308
Johnson H A W E Haymaker J R Rubin T M Fliedner V P Bond E P Cronkite and W E Hughes 1960 A radioautographic study of a human brain and glioblastoma multiforme after *in vivo* uptake of tritiated thymidine Cancer *13* 636
Jordan H E and J E Kindred 1948 Textbook of embryology 5th ed Appleton-Century New York p 340
Kappers J A 1949 Preliminary data on the function of the paraphysis cerebri in Urodeles Experientia 5 162
——— 1950 The development and structure of the paraphysis cerebri in Urodeles with experiments on its function in Amblystoma mexicanum J Comp Neur 39 93
——— 1955 The development of the paraphysis cerebri in man with comments on its relationship to the intercolumnar tubercle and its significance for the origin of cystic tumors in the third ventricle J Comp Neur *102* 425
——— 1958 Structural and functional changes in the telencephalic choroid plexus during human ontogenesis In The Ciba Foundation Symposium on the Cerebrospinal Fluid eds G E W Wolstenholme and C M O Connor Little Brown Boston pp 3–31
Kingsley J S 1926 Outlines of comparative anatomy of vertebrates 3rd ed Blakiston Philadelphia p 161
Kiszely G 1951 Contribution to the morphology and functioning of the choroid plexus Acta Morph Acad Sci Hung 1 263
Klosovskii B N 1963 The development of the brain and its disturbance by harmful factors Ed B Haigh Macmillan New York, pp 3–43 and 83–105
Knudsen P A 1964 Mode of growth of the choroid plexus in mouse embryos Acta Anat 57 172
Krabbe K H 1936 Studies on the existence of a paraphysis in mammalian embryos Brain 59 483
Lumsden C E 1958 Observation on the choroid plexus maintained as an organ in tissue culture In The Ciba Foundation Symposium on the Cerebrospinal Fluid eds G E W Wolstenholme and C M O Connor Little Brown Boston pp 97–123
McMurrich J P 1915 Development of the human body 5th ed Blakiston Philadelphia pp 393–394
Meek W J 1907 A study of the choroid plexus J Comp Neur *17* 286
Messier B and C P Leblond 1960 Cell proliferation and migration as revealed by radioautography after injection of thymidine H in male rats and mice Am J Anat *106* 247
Miale I L and P L Sidman 1961 An autoradiographic analysis of histogenesis in the mouse cerebellum Exp Neurol *4* 277
Millen J W and D H M Woollam 1962 The anatomy of the cerebrospinal fluid Oxford London pp 60–90
Minot C S 1892 Human embryology William Wood New York p 681
Mosberg W H and W Blackwood 1954 Mucus secreting cells in colloid cysts of the third ventricle J Neuropath Exp Neurol 13 417
Otila E 1948 Studies on the cerebrospinal fluid in premature infants Acta Paediat (Uppsala) *35* 1 (Suppl 8)
Sauer F C 1935 Mitosis in the neural tube J Comp Neur *62* 377
Shuangshoti S M P Roberts and M G Netsky 1965 Neuroepithelial (colloid) cysts Pathogenesis and relation to choroid plexus and ependyma Arch Path 80 214–224
Sidman R L I L Miale and N Fedar 1959 Cell proliferation and migration in the primitive ependymal zone An autoradiographic study of histogenesis in the nervous system Exp Neurol *1* 322
Steiner M L and D R Shanklin 1964 The choroid plexus in hyaline membrane disease Am J Path *44* 452 (abstr)
Streeter G L 1912 The development of the nervous system In Handbook of Human Em

Paraphysis in man The presence of a paraphysis seems to be variable Francotte (1894) found this structure in a human embryo of 12 weeks According to Bailey (16a, b), the paraphysis never appears in mammalia except as an arch of the telencephalic roof rostral to the *velum transversum* in early stages of development and Bailey called it the paraphyseal arch He could not identify this arch in human embryos of more than 32 mm C R length Warren (17) found the paraphysis in only 8 of 30 human embryos ranging from 15 to 44 3 mm C R length Krabbe (36) in human embryos of 21 22 5 25 5 mm C R length According to Kappers (55) this structure is present in embryos of 17 to 100 mm C R length Only 4 to 16 human embryos examined serially by us are found to bear the paraphyseal primordium (figs 4 15 17 18) In all four this primordium arises from the rostal end of the diencephalic roof intermingled with the primordium of diencephalic choroid plexus (fig 15) The paraphyseal primordium does not contain glandular or tubular formations only a single fold is seen The paraphysis probably has glandular or tubular formations only in lower vertebrates such as *Urodeles* We believe however that the mode of formation of tubules in the paraphysis is similar to their formation in the choroid plexus as demonstrated in figure 12C The paraphysis in man is inconstant variable and rudimentary

The location of the paraphysis has been controversial It was regarded by some workers as arising from the most rostral part of the diencephalic roof and by others from the most caudal part of the telencephalic roof The latter view was held by Bailey (16a b) and Kappers (55) They rejected the paraphysis described by Francotte (1894) because of its diencephalic location Bailey also cast out the description of Streeter (12) of the human paraphysis for the same reason According to Kappers (50 55) evaginations from the rostral part of the diencephalic roof are not paraphyseal but diencephalic tubules diverticula or recesses He further distinguished the epithelial lining of the paraphysis from that of the diencephalic roof by stating that the epithelial cells of the latter derive from less differentiated ependyma and bear cilia Our view is that *velum transversum* is a purely descriptive boundary of the primary and secondary fore brain and is not easily located in embryos of higher vertebrates especially man The epithelia of the telencephalic and diencephalic roofs and *velum transversum*, moreover are neighboring derivatives of the same primitive neuroepithelium Cilia and location of the epithelium are not a fundamental distinction The neuroepithelial out pouchings developing in this immediate region either rostrad or caudad to the *velum transversum* are all extraventricular choroid plexus of the third ventricle (fig 15) In addition the *velum transversum* is itself choroid plexus Bailey (16b) called it velar plexus In some tailed amphibia the *velum* serves as an unpaired choroid plexus (Gladstone and Wakeley 40)

ACKNOWLEDGMENTS

We are indebted to Dr James E Kindred for six embryos and five fetuses and to Dr Leo Erbele for ten embryos Mrs Margaret Tennant and Mrs Evans Townsend did the histologic sections and Miss Anne Russell the photomicrographs

LITERATURE CITED

Ayers W W and W Haymaker 1960 Xanthoma and cholesterol granuloma of the choroid plexus J Neuropath Exp Neurol 19 280

Bailey P 1916a Morphology of the roof plate of the forebrain and the lateral choroid plexuses in the human embryo J Comp Neur 26 79

——— 1916b The morphology and morphogenesis of the choroid plexuses with special reference to the development of the lateral telencephalic plexus in *Chrysemys marginata* J Comp Neur 26 507

Bloom W and D W Fawcett 1962 A textbook of histology 8th ed Saunders Philadelphia p 257

Boyd W 1920 Physiology and pathology of cerebrospinal fluid Macmillian New York p 44

Brachet A 1921 Traité D Embryologie des vertébrés Masson Paris p 344

Cameron G 1953 Secretory activity of the choroid plexus in tissue culture Anat Rec 117 115

Chu H Y 1912 Ciliary movement and circulation of cerebrospinal fluid within brain ventricles in larval and adult Anurans Am J Physiol 136 223

Ciaccio C and S Scaglione 1913 Beitrag zur cellularen physiopathologie der plexus chorol

der Beitr Path Anat Ztschr Allg Path 55 131

Cohen H and S Davies 1938 The morphology and permeability of the roof of the fourth ventricle in some mammalian embryos J Anat 72 430

Davis L E and H Cushing 1925 Papillomas of the choroid plexus Arch Neurol Psychiat 13 681

Dunn J and J W Kernohan 1955 Histologic changes within the choroid plexus of the lateral ventricle Their relation to age Proc Staff Meeting Mayo Clinic 30 607

Findlay W 1898 Observations on the normal and pathological histology of the choroid plexuses of the lateral ventricles of the brain J Ment Sci (Lond) 44 744

——— 1899 The choroid plexus of the lateral ventricle of the brain their histology normal and pathological Brain 22 161

Flexner L B 1938 Change in the chemistry and nature of the cerebrospinal fluid during fetal life in the pig Am J Physiol 124 131

Francotte P 1894 Note sur l oeil pariétal l épiphyse la paraphyse et les plexus choroides du troisieme ventricule Bull de l Acad royale des Sci d Belg 3 Serie 27 84

Frazer J E 1932 A manual of embryology William Wood New York p 170

Freeman W 1933 Neuropathology the anatomical foundation of nervous system Saunders Philadelphia p 53

Fujita S 1960 Mitotic pattern and histogenesis of the central nervous system Nature 185 702

——— 1963 The matrix cell and cytogenesis in developing central nervous system J Comp Neur 120 37

Gladstone R J and C P G Wakeley 1940 The pineal organ Balillière Tindall & Cox London p 184

Creep R O 1954 Histology Blakiston New York pp 256–257

Ham A W 1957 Histology 3rd ed Lippincott Philadelphia pp 453–455

Heisler J C 1907 A textbook of embryology for students of medicine Saunders Philadelphia pp 306–308

Johnson H A W E Haymaker J R Rubin T M Fliedner V P Bond E P Cronkite and W E Hughes 1960 A radioautographic study of a human brain and glioblastoma multiforme after in vivo uptake of tritiated thymidine Cancer 13 636

Jordan H E and J E Kindred 1948 Textbook of embryology 5th ed Appleton-Century New York p 340

Kappers J A 1949 Preliminary data on the function of the paraphysis cerebri in Urodeles Experientia 5 162

——— 1950 The development and structure of the paraphysis cerebri in Urodeles with experiments on its function in Amblystoma mexicanum J Comp Neur 39 93

——— 1955 The development of the paraphysis cerebri in man with comments on its relationship to the intercolumnar tubercle and its significance for the origin of cystic tumors in the third ventricle J Comp Neur 102 425

——— 1958 Structural and functional changes in the telencephalic choroid plexus during human ontogenesis In The Ciba Foundation Symposium on the Cerebrospinal Fluid eds G E W Wolstenholme and C M O Connor Little Brown Boston pp 3–31

Kingsley J S 1926 Outlines of comparative anatomy of vertebrates 3rd ed Blakiston Philadelphia p 161

Kiszely G 1951 Contribution to the morphology and functioning of the choroid plexus Acta Morph Acad Sci Hung 1 263

Klosovskii B N 1963 The development of the brain and its disturbance by harmful factors Ed B Haigh Macmillan New York pp 3–43 and 83–105

Knudsen P A 1964 Mode of growth of the choroid plexus in mouse embryos Acta Anat 57 172

Krabbe K H 1936 Studies on the existence of a paraphysis in mammalian embryos Brain 59 483

Lumsden C E 1958 Observation on the choroid plexus maintained as an organ in tissue culture In The Ciba Foundation Symposium on the Cerebrospinal Fluid eds G E W Wolstenholme and C M O Connor Little Brown Boston pp 97–123

McMurrich J P 1915 Development of the human body 5th ed Blakiston Philadelphia pp 393–394

Meek W J 1907 A study of the choroid plexus J Comp Neur 17 286

Messier B and C P Leblond 1960 Cell proliferation and migration as revealed by radioautography after injection of thymidine H^3 in male rats and mice Am J Anat 106 247

Miale I L and R L Sidman 1961 An autoradiographic analysis of histogenesis in the mouse cerebellum Exp Neurol 4 277

Millen J W and D H M Woollam 1962 The anatomy of the cerebrospinal fluid Oxford London pp 60–90

Minot C S 1892 Human embryology William Wood New York p 681

Mosberg W H and W Blackwood 1954 Mucus secreting cells in colloid cysts of the third ventricle J Neuropath Exp Neurol 13 417

Otila E 1948 Studies on the cerebrospinal fluid in premature infants Acta Paediat (Uppsala) 35 1 (Suppl 8)

Sauer F C 1935 Mitosis in the neural tube J Comp Neur 62 377

Shuangshoti S M P Roberts and M G Netsky 1965 Neuroepithelial (colloid) cysts Pathogenesis and relation to choroid plexus and ependyma Arch Path 80 214–224

Sidman R L I L Miale and N Fedar 1959 Cell proliferation and migration in the primitive ependymal zone An autoradiographic study of histogenesis in the nervous system Exp Neurol 1 322

Steiner M L and D R Shanklin 1964 The choroid plexus in hyaline membrane disease Am J Path 44 452 (abstr)

Streeter G L 1912 The development of the nervous system In Handbook of Human Em

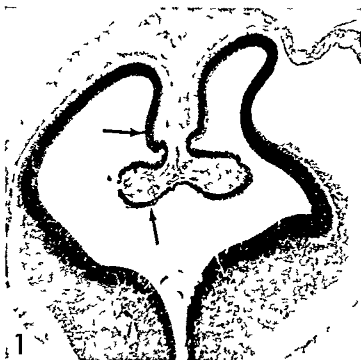
bryology Vol II eds F Keibel and P F Mall Lippincott Philadelphia pp 59-61 and 80
——— 1920 Weight sitting height head size *foot length and menstrual age of the human* embryo Contr Embryol Carneg Inst no 55 *11* pp 143-170
Strong L H 1956 Early development of the ependyma and vascular pattern of the fourth *ventricular choroid plexus in the rabbit* Am J Anat 99 249
Studnicka F K 1900 Zur Kenntnis der Parietalorgane und der sog Paraphyse der Niederen Wirbeltiere Verh Anat Ges Verslg *Pavia 14 101*
Tennyson V M and G D Pappas 1964 Fine structure of the developing telencephalic and myelencephalic choroid plexus in the rabbit J Comp Neur *123* 379
Volzhina N S 1957 *Compensatory* hypertrophy of the vascular network of the brain in experiment Arkhiv Pathologii (Moscow) 7 52
——— 1958 On regeneration of the brain vascular plexus Arkhiv Anatomii Gistologii i Embryiologii (Moscow) 35 68
Voetmann E 1949 On the structure and surface area of the human choroid plexus A quantitative anatomical study Acta Anat, *8 (suppl 10)* 1
Watterson R L P Veneziano and A Bartha 1956 Absence of a true germinal zone in neural tube of young chick embryos as demonstrated by colchicine technique Anat Rec *124* 379
Warren J 1917 The development of the paraphysis and pineal region in mammalia J Comp Neur 27 75
Weed L H 1917 The development of the cerebrospinal spaces in pig and man Contr Embryol Carneg Inst 14 5 91
Wolf A D Cowen and S Graham 1950 Xanthomas of the choroid plexus in man J Neuropath Exp Neurol 9 286
Woodard T M Jr and S B Estes 1944 Effect of colchicine on mitoses in the neural tube of the 48 hour chick embryo Anat Rec *90* 51
Zimmerman H M and W J German 1933 Colloid tumors of the third ventricle Arch Neurol Psychiat 30 309

PLATE 1

EXPLANATION OF FIGURES

1 Photomacrograph of coronally sectioned human brain from embryo of 19 mm C R length Note the club shaped telencephalic choroid plexus covered by pseudostratified tall neuroepithelium The neuro epithelium of the telencephalon (upper arrow) is thicker than the choroidal epithelium (lower arrow) The choroidal primordium is more vascular than the developing leptomeninx Hematoxylin and eosin stain × 32

2 Photomicrograph of the same brain as in figure 1 to show microscopic details of the choroidal epithelium in Stage I *Note pseudostratified* tall epithelial cells with mainly central nuclei The epithelial basement membrane is indistinct Nuclei in mitosis are present toward the luminal ends of the epithelial cells (arrow) Note brush border Many islets of immature blood cells are surrounded by ill defined vascular walls in this early stage of development Hematoxylin and eosin stain × 710



2

PLATE 2

EXPLANATION OF FIGURES

3 Photomicrograph of telencephalic choroid plexus toward the end of Stage I (23 mm C R length) to show slight lobulation of the plexus Many mitoses are present Islets of immature blood cells are surrounded by primitive endothelial cells Hematoxylin and eosin stain × 225

4 Photomacrograph of brain of fetus of 30 mm C R length to show lobulation of the telencephalic choroid plexus at beginning of Stage II Note extremely loose mesenchymal stroma and thin stalk Arrow indicates folding of the paraphysis from the rostral end of diencephalic roof into the mesenchyme Hematoxylin and eosin stain × 22

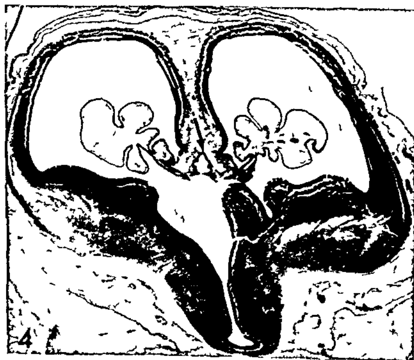

4

PLATE 3

EXPLANATION OF FIGURE

5 A Photomacrograph of coronally sectioned brain from embryo of *50 mm C R* length to show extreme enlargement and lobulation of the telencephalic plexus filling about three fourths of the lateral ventricle A few faintly outlined tubules are scattered in the stroma (two upper arrows) The stalk is slender (right lower arrow) Hematoxylin and eosin stain × 32

B Photomicrograph of the surface epithelium at the area corresponding to the left lower arrow Note low columnar epithelial cells with apical nuclei vacuolated cytoplasm and extremely loose stroma Mesenchymal cells and blood vessels with definite wall are present Hematoxylin and eosin stain × 710

C Photomicrograph of the stalk indicated by the right arrow in figure 5A to show pseudostratified neuroepithelium Note change of the pseudostratified tall neuroepithelium to simple low columnar type with the cells having apical nuclei at the site distal to the stalk (arrow) Hematoxylin and eosin stain × 220

5A

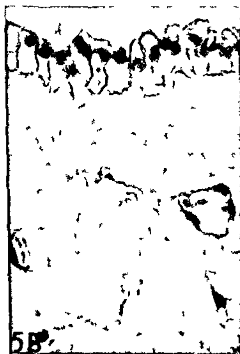




PLATE 4

EXPLANATION OF FIGURE

6 Photomicrographs of telencephalic choroid plexuses showing glycogen during various stages of development

A Embryo of 8 0 mm C R length (Stage II) × 120

B Embryo of 17 0 cm C R length (Stage III) × 116

C Embryo of 28 0 cm C R length (Stage IV) × 125

D Full term newborn weighing 4 200 gm × 138

All photomicrographs are of PAS stains and are taken from areas of greatest concentration of glycogen Note gradual decrease in amount


6A


6B


6C


6D

PLATE 4

EXPLANATION OF FIGURE

6 Photomicrographs of telencephalic choroid plexuses showing glycogen during various stages of development

A *Embryo of 8 0 mm C R length (Stage II)* × 120

B Embryo of 17 0 cm C R length (Stage III) × 116

C Embryo of 28 0 cm C R length (Stage IV) × 125

D Full term newborn weighing 4 200 gm × 138

All photomicrographs are of PAS stains and are taken from areas of greatest concentration of glycogen Note gradual decrease in amount


7

PLATE 5

EXPLANATION OF FIGURES

7 Photomicrograph of the telencephalic plexus in embryo of 100 mm C R length showing extreme lobulation of the plexus Note epithelial cells with apical nuclei and vacuolated cytoplasm The mesenchymal ground substance is infiltrated with a small amount of connective tissue fibers Note aggregation of fibers around blood vessels Hematoxylin and eosin stain × 200

8 Photomicrograph of telencephalic choroid plexus during Stage III in specimen obtained from fetus of 17 cm C R length The cuboidal epithelium contains some epithelial cells having central nuclei Stratification proliferation and desquamation of epithelial cells are shown Note the deep folding of epithelium into the stroma to form primary villi Desquamated cells are scattered in the intervillous clefts Mayer s mucicarmine stain × 230



PLATE 6

EXPLANATION OF FIGURE

9 Photomicrograph of telencephalic choroid plexus (Stage III) from a fetus weighing 840 gm (26 weeks) Note primary villi moderate amount of connective tissue stroma and formed blood vessels Many clusters of foamy cells probably desquamated choroidal epithelial cells are scattered in the interstitium (upper arrow) Groups of proliferative epithelial cells protrude from the tip of intervillous cleft into the stroma (middle arrow) One tubule is present at the lower arrow and nearby proliferative tubular epithelial cells protrude into the surrounding ground substance Mayer's mucicarmine stain × 120



11

PLATE 7

EXPLANATION OF FIGURES

10 Photomicrograph of telencephalic choroid plexus of a premature in fant weighing 2 270 gm showing characteristics of the plexus toward the end of Stage IV Note numerous villi with multiple fronds dense connective tissue stroma and well formed blood vessels A perivascular meningocytic whorl is present (lower arrow) Hematoxylin and eosin stain × 105 Inset shows epithelial cells with intracytoplasmic PAS reactive diastase resistant material (upper arrow) Note many cen tral nuclei PAS stain × 700

11 Same case as in figure 10 An incipient neuroepithelial cyst is shown Note cuboidal epithelium with cells having central or basal nuclei Mayer s mucicarmine stain × 225 Inset shows a cyst rimmed by a few fibroblasts in the connective tissue stroma PAS stain × 225



11

PLATE 8

EXPLANATION OF FIGURE

12 A Photomicrograph of telencephalic choroid plexus during Stage IV of differentiation (body weight 2 100 gm) Note numerous tubules in the stroma One tubule (lower arrow) contains mucin The upper arrow indicates a cluster of proliferative cells arising from the tip of an intervillous cleft Note centrally located nuclei of many epithelial cells Mayer s mucicarmine stain × 120

B Detail of one deep tubule filled with proliferative cells Note rupture of tubular wall with release of foamy cells into surrounding stroma × 700

C Photomicrograph showing the method of formation of tubules Arrow indicates folding of the surface epithelium from the ventricle into the stroma to create a tubule Mayer s mucicarmine stain × 690

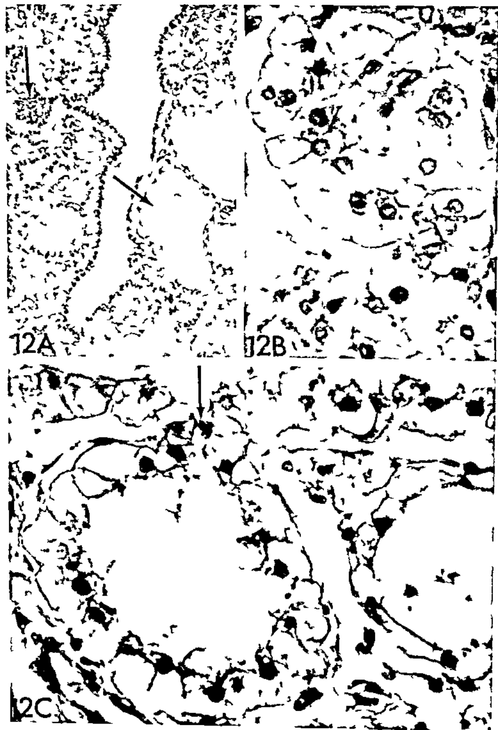

12A
12B
12C

PLATE 9

EXPLANATION OF FIGURES

13 Photomicrograph of telencephalic choroid plexus of one month old infant to show villi with multiple fronds covered by cuboidal or squamous epithelial cells having central or basal nuclei Note thin layers of connective tissue separating the surface epithelium and vascular walls in villous fronds Several tubules are scattered in the stroma one indicated by arrow at left Note cluster of meningocytes shown by arrow at right Mayer's mucicarmine stain × 113 Inset shows details of one villous frond Note flattened surface epithelium intracellular mucin (lower arrow) and desquamating cell in shadowy outline (upper arrow) Mayer's mucicarmine stain × 700

14 Photomicrograph of primordium of the myelencephalic plexus in embryo of 16 mm C.R. length Note pseudostratified low neuroepithelium covering the primordium and loose mesenchymal stroma Hematoxylin and eosin stain × 225

13

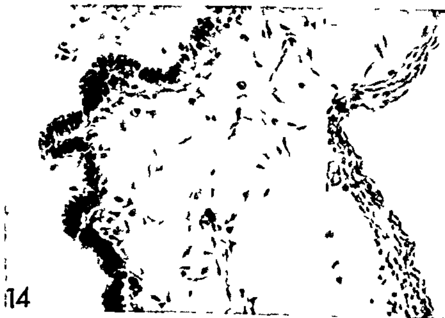


PLATE 9

EXPLANATION OF FIGURES

13 Photomicrograph of telencephalic choroid plexus of one month-old infant to show villi wih multiple fronds covered by cuboidal or squamous epithelial cells having central or basal nuclei Note thin layers of connective tissue separating the surface epithelium and vascular walls in villous fronds Several tubules are scattered in the stroma one indicated by arrow at left Note cluster of meningocytes shown by arrow at right Mayer s mucicarmine stain × 113 Inset shows details of one villous frond Note flattened surface epithelium intracellular mucin (lower arrow) and desquamating cell in shadowy outline (upper arrow) Mayer s mucicarmine stain × 700

14 Photomicrograph of primordium of the myelencephalic plexus in embryo of 16 mm C R length Note pseudostratified low neuroepithelium covering the primordium and loose mesenchymal stroma Hematoxylin and eosin stain × 225

13

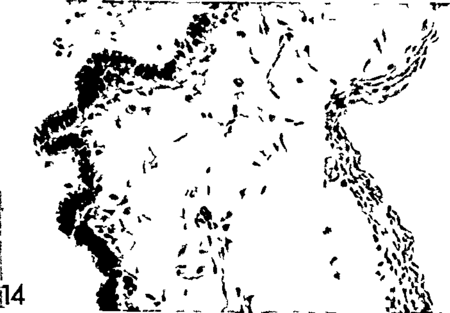


PLATE 10

EXPLANATION OF FIGURES

15 Photomicrograph of primordium of the diencephalic plexus and paraphysis (extraventricular choroid plexus) in embryo of 23 mm C R length The brain is sectioned sagittally The velum transversum (arrow) is at the anterior end All epithelial out pouchings (P) are paraphyseal primordia The epithelial infoldings (D) are primordia of diencephalic plexus Note pseudostratified low epithelium covering the primordia Large venous sinuses are embedded in the mesenchymal stroma Hematoxylin and eosin stain × 235

16 Photomicrographs of the three major choroid plexuses at the same magnification (× 116) from a fetus of 17 cm C R length to show the differences of development All are stained with Mayer s mucicarmine technic

A Telencephalic plexus in Stage III Note cuboidal epithelial cells with many apical and some central nuclei a primary villus and moderate amount of connective tissue Many desquamated cells are present in the stroma (arrow)

B Diencephalic plexus in Stage IV characterized by villi with multiple fronds replacement of mesenchymal stroma with dense connective tissue fibers and cuboidal epithelial cells with mostly central or basal nuclei Note intracellular mucin (dark in photomicrograph) of the epithelial cells

C Myelencephalic plexus in Stage IV Note similar features as described in B

15

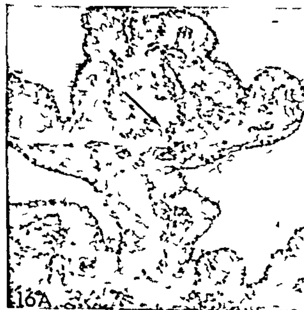




PLATE 11

EXPLANATION OF FIGURES

17 Photomicrograph of the brain of embryo in figures 1 and 2 (19 mm C R length) showing the primordium of the paraphysis formed by folding of the neuroepithelium into the mesenchyme at the rostral end of the diencephalic roof Hematoxylin and eosin stain × 800 The photomicrograph is taken from the area indicated by the arrow in the inset

18 Same case as in figure 4 to show microscopic details of the para physeal primordium (upper arrow) Stalk of the telencephalic plexus is indicated by the lower arrow Note similarity to the paraphyseal and choroidal epithelia Hematoxylin and eosin stain × 110


18

Development of the Flank Organ (Scent Gland) of the Syrian Hamster

II POSTNATAL DEVELOPMENT [1]

F THOMAS ALGARD [2] ALICE H DODGE [3] AND HADLEY KIRKMAN [3]
Department of Biological Sciences University of Victoria Victoria British Columbia Canada and Department of Anatomy Stanford University School of Medicine Stanford California

ABSTRACT In the first paper of this series the prenatal development of the flank organ (scent gland) of the Syrian hamster was described The present paper is concerned with the postnatal development of this organ The embryology of the organ actually continues into postnatal life until during the fifth day the organ attains the degree of development characteristic of general body skin at birth Subsequently an accelerated growth rate results in a conspicuous and characteristic hypertrophy of the gland relative to surrounding integument During the acquisition of this hypertrophy two opposite developmental gradients are involved i e a series of consecutive centripetal waves of hair cycling and a centrifugal gradient of sebaceous gland development Maturation of the gland including changes in its pigmentation and the onset of sexual dimorphism is discussed in relation to pertinent literature

The costovertebral scent gland (flank organ) of the hamster has been an object of attention from furriers (Hanicke 02 Petzsch 36) natural historians (Vrtiš 30 31 Lipkow 54 Lochbrunner 56) reproductive physiologists (Schaffer 40 Parkes and Bruce 61) endocrinologists (Kupperman 44 44a 46 Ortiz 47) embryologists (Shrader 49 LaVelle 51) ethologists (Dieterlen 59) and histochemists (Hamilton and Montagna 50) Flank organs have also been employed in studies of dimethylbenzanthrene induced melanotic tumors (Ghadially and Barker 60 Horning 58) The significance of these structures as favorable sites for the study of sex hormone tumorigenesis *in vivo* has been stressed by Kirkman (57 66) Kirkman and Algard (64 65) and Algard (60 61 63 65) have used tumorous flank organs as a model system for studying hormone dependency in cell and organotypic culture In conjunction with this study a base line of normal prenatal development has been drawn (Algard Dodge and Kirkman 64) Although the earlier literature took no cognizance of prenatal development several accounts describing certain aspects of postnatal development do exist (Kupperman 44 44a 46 Shrader 49 LaVelle 51 Markel 52 Lipkow 54 and Lochbrunner 56) These accounts are to some extent incomplete and in conflict

The scent glands are generally recognized as small slightly elevated organs consisting of epidermis hypertrophied skin adnexa and associated dermal connective tissue In colored hamsters these organs have traditionally been described as pigmented spots Although this description is adequate for sexually mature males it does not take into account the presence of a relatively unpigmented peripheral zone characteristic of immature or gonadectomized animals of both sexes mature females senile males and experimental animals treated with estrogen Undoubtedly the well known androgen induced expansion of the gland represents a maximal development of the total organ i e central active and peripheral quiescent zones rather than enlargement at the expense of surrounding integument

The purpose of this paper is to extend the base line of normal development

---

[1] Thi tudy w s supported by grant C2791-C8 nd C9 and CA 04516-07 from the N tion l C n r I ti tut N t on l In titut of H lth Public He lth Service nd Canad n N ti n l Rese rch Cou c l gr t A2351

[2] Departm nt of Bl logic l Sci nces Uni ersity of Vict ri Vi t ria British Col mbi Canad

[3] Dep rtment of An tomy St nf d University School of Medicine St nford California

against which organotypic cultures may be assessed and to extend and clarify previous observations on the gland (Algard Dodge and Kirkman, '64)

MATERIALS AND METHODS

Materials and techniques were similar to those already described (Algard, Dodge and Kirkman '64)

OBSERVATIONS

The observations described below will be confined almost entirely to development of the central (active) region of the flank organ

Days one through ten

At birth flank organs are still essentially embryonic structures in spite of the fact that differentiation of the basic components of adjacent skin are already well established (fig 1) e g in the latter coat hairs associated with heavily pigmented bulbs and small but well defined sebaceous glands are erupting (Algard Dodge and Kirkman 64) It is not until the fifth day that the degree of adnexal development in the flank organ approximates that observed in general body skin of the newborn animal although unlike the latter there is still no indication of the separation of subepidermal mesenchyme into the dermal and hypodermal layers already very evident in the adjacent skin Subsequently growth and differentiation of these structures accelerates to such an extent that by the tenth postnatal day all constitutents of the gland have surpassed their counterparts in adjacent skin and an easily discernible distinction between dermis and hypodermis is present

Day one

On day one flank organs appear as glabrous nonpigmented approximately oval areas of about 0 7 mm² each Histologically they are demarcated from adjacent skin by possession of relatively thickened epidermis compacted subepidermal connective tissue and scanty hair follicles none of which are beyond Stohr stage 5 (Pinkus 58) (fig 2) Epidermal and connective tissue components of the flank organ measure about 170 μ in thickness as compared with about 72 μ for surrounding skin

Day two

During the second day (fig 3) the periphery of the developing gland becomes faintly pubescent Emerging hairs are colorless and considerably finer than those already established in the adjacent coat In section these very fine hairs derive from elongating faintly pigmented anagen follicles In spite of the apparent centripetal gradient of hair emergence sebaceous glands develop at a more or less uniform rate throughout the organ

Day three

During the third day (fig 4) hair follicles in this centripetally progressing wave continue to elongate and to show an increased compliment of melanin although development still lags markedly behind that observed in skin elsewhere

Days four and five

During the fourth (fig 5) and fi[fth] (fig 6) days the sebaceous glands exhi[bit] a centrifugal gradient the central m[ost] glands beginning to exceed in size th[ose] in the periphery During this time inter[...] the separation of the subepidermal co[n]nective tissue into dermis and hypoderm[is] evident in adjacent skin during the f[...] day begins

Day six

Until the sixth day the growth and [dif]ferentiation of the flank organ has be[en] retarded relative to the general inte[gu]ment the average area approximating o[...] 1 mm² On the sixth day however [...] acceleration in growth significantly [in]creases surface area and results in a[...] to 10% increase in glandular thickn[ess] Subsequently the growth rate slows [...] remains relatively uniform until the ad[ult] condition is reached By the sixth day [...] centripetal wave of hair emergence reac[hes] the center of the gland and some of [...] peripheral follicles are producing so[me]what coarser pigmented hair initiatin[g] second centripetal wave

Day seven

During this time the second wave [of] hair differentiation reaches the central [re]gion of the gland resulting in a mixture [of] fine colorless hairs from the first wave [...]

slightly pigmented coarser hairs from the second wave

Day eight

On this day still coarser more heavily pigmented hairs begin to emerge in the peripheral region of the organ initiating a third wave of hair emergence No other significant events occur except for moderate increases in size of sebaceous glands

Day nine

At this time the flank organ is characterized by sufficient elongation of many of the centrally situated hairs to form a recognizable tuft It is during this day that dermal melanoblasts in close proximity to flank organ hairs have synthesized appreciable quantities of melanin

Day ten

This day is significant since in the majority of litters it is during this time that sexual dimorphism may first be recognized in the developing flank organ i e all components are quantitatively greater in the male

Days 11 through 19

During this nine day period sexual dimorphism gradually progresses due primarily to the more rapid rate of differentiation of flank organ components in the male than in the female The rate of growth and differentiation is somewhat decreased over that occurring during the first ten-day period By the end of the sixteenth day there is no longer any apparent difference in thickness of epidermis between flank organ and general body skin

Although the total amount of pigment increases from the tenth day onward (fig 7) the organ itself especially when viewed from the dermal surface may appear relatively depigmented starting at from 14 to 16 days and extending through the twenty fourth day due to the movement of pigment from bulbs into forming hairs This leads to the development of an adult hair which when examined microscopically consists of three segments a proximal solid black portion a middle portion consisting of alternating pigmented and relatively non pigmented segments and a finely tapering relatively short unpigmented distal portion Such hairs *en mass* present the golden brown hue characteristic of the golden hamster By the twenty-eighth day pigmentation of the next crop of growing hair bulbs has grossly repigmented the organ

The hairs comprising the tuft described for day nine are now being replaced by shorter coarser hairs from the next piliary cycle Whether or not comparable tufts are observed during the subsequent life history of the animals depends on whether or not the animals are examined sometime between the termination of one growth cycle and the beginning of another (telogen) (cf fig 4 in Kirkman and Algard 64)

At the termination of this period the successive waves of piliary development lead to the establishment of the typical adult pattern with the largest most heavily pigmented hairs emerging from the hypertrophied pilosebaceous complexes characteristic of the central region of the flank organ From this day on the chief developmental change is one of straight forward growth and differentiation although there will occur during the next 15 days some fluctuation in the disposition of melanin

Days 20 through 35 with notes on older animals

During this 15-day period the flank organs become nearly definitive in size and sexual dimorphism becomes fully developed Although individual variations in the surface areas of the organs may be noted there is in general about a twofold increase in area of the organ and a corresponding increase in sebaceous gland volume After the thirty fifth day there is a gradual increase in the size of the active portion culminating at 100 days in a volume of approximately 23 mm for the male and 8 mm for the female The first fat droplets are observable in centrally situated sebaceous glands between the thirtieth and thirty second days

From 20 to 27 days both male and female organs when shaved are flesh colored actually lighter than the shaved adjacent areas By the twenty-eighth day the surface of the male flank organ has a grayish cast correlated with the reappear

against which organotypic cultures may be assessed and to extend and clarify previous observations on the gland (Algard, Dodge and Kirkman, 64)

MATERIALS AND METHODS

Materials and techniques were similar to those already described (Algard Dodge and Kirkman 64)

OBSERVATIONS

The observations described below will be confined almost entirely to development of the central (active) region of the flank organ

Days one through ten

At birth flank organs are still essentially embryonic structures in spite of the fact that differentiation of the basic components of adjacent skin are already well established (fig 1) e g in the latter coat hairs associated with heavily pigmented bulbs and small but well defined sebaceous glands are erupting (Algard Dodge and Kirkman 64) It is not until the fifth day that the degree of adnexal development in the flank organ approximates that observed in general body skin of the newborn animal although unlike the latter there is still no indication of the separation of subepidermal mesenchyme into the dermal and hypodermal layers already very evident in the adjacent skin Subsequently growth and differentiation of these structures accelerates to such an extent that by the tenth postnatal day all constitutents of the gland have surpassed their counterparts in adjacent skin and an easily discernible distinction between dermis and hypodermis is present

Day one

On day one flank organs appear as glabrous nonpigmented approximately oval areas of about 0 7 mm² each Histologically they are demarcated from adjacent skin by possession of relatively thickened epidermis compacted subepidermal connective tissue and scanty hair follicles none of which are beyond Stohr stage 5 (Pinkus 58) (fig 2) Epidermal and connective tissue components of the flank organ measure about 170 μ in thickness as compared with about 72 μ for surrounding skin

Day two

During the second day (fig 3) th periphery of the developing gland becom faintly pubescent Emerging hairs ar colorless and considerably finer than th already established in the adjacent coa In section these very fine hairs derive fro elongating faintly pigmented anagen fo licles In spite of the apparent centripet gradient of hair emergence sebacec glands develop at a more or less unifor rate throughout the organ

Day three

During the third day (fig 4) hair licles in this centripetally progressing w continue to elongate and to show an creased compliment of melanin althou development still lags markedly beh that observed in skin elsewhere

Days four and five

During the fourth (fig 5) and (fig 6) days the sebaceous glands ex a centrifugal gradient the central glands beginning to exceed in size t in the periphery During this time int the separation of the subepidermal nective tissue into dermis and hypode evident in adjacent skin during the day begins

Day six

Until the sixth day the growth and ferentiation of the flank organ has retarded relative to the general in ment the average area approximating 1 mm² On the sixth day however acceleration in growth significantly creases surface area and results in to 10% increase in glandular thick Subsequently the growth rate slows remains relatively uniform until the condition is reached By the sixth da centripetal wave of hair emergence re the center of the gland and some o peripheral follicles are producing what coarser pigmented hair initiati second centripetal wave

Day seven

During this time the second wav hair differentiation reaches the centr gion of the gland resulting in a mixtu fine colorless hairs from the first wave

LaVelle (51) this early pigmentation is at first chiefly in the hair roots moving into hair shafts during the twenty first to twenty ninth day and dense aggregates of "melanophores" do not congregate in the flank organ until puberty i e between the twenty ninth and thirty first days the age range when Kupperman first observed the organ

ACKNOWLEDGMENT

The authors wish to express appreciation to Miss Sumiko Sakaguchi for technical help and to Mr Max Millsap for the photomicrography

LITERATURE CITED

Algard F Thomas 1960 Hormone induced tumors I Hamster flank organ and kidney tumors *in vitro* J Nat Cancer Inst 25 557–571

——— 1961 Hormone induced tumors II Flank-organ epithelioma of the Syrian hamster *in vitro* J Nat Cancer Inst 27 1493–1502

——— 1963 Action of sex hormones on dependent tumors in cell and organ-culture systems Nat Cancer Inst Monog 11 215–226

——— 1965 Characteristics of an androgen/estrogen induced dependent leiomyosarcoma of the ductus deferens of the Syrian hamster II In vitro Cancer Res 25 147–151

Algard F Thomas Alice H Dodge and H Kirkman 1964 Development of the flank organ (scent gland) of the Syrian hamster I Embryology Am J Anat 114 435–455

Dieterlen F 1959 Das Verhalten des syrischen Goldhamsters (*Mesocricetus auratus* Waterhouse) Untersuchungen zur Frage seiner Entwicklung und seiner angeborenen Anteile durch geruchsisolierte Aufzuchten Ztschr Tierpsychol 16 47–103

Ghadially F N and J F Barker 1960 The histogenesis of experimentally induced melanotic tumours in the Syrian hamster (*C icetus auratus*) J Path and Bact 79 263–271

Hamilton J B and W Montagna 1950 The sebaceous glands of the ham ter I Morphological effects of androgens on integumentary structures Am J Anat 86 191–234

Hanicke Heinrich 1902 Handbuch fur Kürschner Anleitung zum rationellen Betrieb der Kur chnerei Leipzig A Duncker

Horning E S 1958 Induction of pituitary tumours and melanomas in the golden hamster Ciba Found Colloq on Endoc 12 22–29

Kirkman H 1957 Steroid tumorigenesis Cancer 10 57–64

——— 1966 Androgen/estrogen hair follicle tumorigenesis (chaetepithelioma formation) in the scent gland of the Syrian hamster In Advances in Biology of Skin vol 5 W Montagna (editor) Carcinogenesis (In press)

Kirkman Hadley and F Thomas Algard 1964 Androgen-estrogen induced tumors I The flank organ (scent gland) chaetepithelioma of the Syrian hamster Cancer Res 24 1569–1593

Kirkman H and F T Algard 1965 Characteristics of an androgen/estrogen induced dependent leiomyosarcoma of the ductus deferens of the Syrian hamster I *In vivo* Cancer Res 25 141–145

Kupperman H S 1944 Hormone control of a dimorphic pigmentation area in the golden hamster (*Cricetus auratus*) Anat Rec 88 26 (abstr)

——— 1944a Sexual cycle and dimorphic pigmentation in the golden hamster (*Cricetus auratus* Waterhouse) Endoc 35 225–226 (abstr)

——— 1946 Dimorphic pigmentation in the golden hamster and its control by the sex steroids Anat Rec 96 530 (abstr)

LaVelle F W 1951 A study of hormonal factors in the early sex development of the golden hamster Carnegie contributions to embryology *no 223 vol 34 (222–230) publ 572* Washington D C 19–53

Lipkow J 1954 Über das Seitenorgan des Goldhamsters (*Mesocricetus auratus auratus* Waterh) Zietschr Morph u Ökol Tiere 42 333–372

Lochbrunner A 1956 Beitrage zur Biologie des Syrischen Goldhamsters *Mesocricetus auratus* (Nehring) Zool Jahrb abt allg Zool u Physiol der Tiere 66 389–428

Markel K 1952 Zur Kenntnis der Seitendrusen des Goldhamsters Zool Anz 149 216–225

Ortiz E 1947 The postnatal development of the reproductive system of the golden hamster (*Cricetus auratus*) and its reactivity to hormones Physiol Zool 20 45–67

Parkes A S and H M Bruce 1961 Olfactory stimuli in mammalian reproduction Science 134 1049–1054

Petzsch H 1936 Beitrage zur Biologie insbesondere Fortpflanzungsbiologie des Hamsters (*Cricetus cricetus* L) Kleintier und Pelztier 12 11–83

Pinkus H 1958 Embryology of hair In The Biology of Hair Growth W Montagna and R A Ellis (editors) pp 1–32 Acad Press New York

Schaffer J 1940 Die Hautdrusenorgane der Saugetiere Urban und Schwarzenberg/Berlin und Wien pp 1–464

Shrader R E 1949 Development of the dimorphic pigment spot of the Syrian hamster Anat Rec 105 561 (abstr)

Vrtiš V 1930 Glandular organ on the flancs of the hamster *Cricetus cricetus* (L) Biologické Spisy Acad Veter 9 1–31 (Article 13–4) (English summary)

——— 1931 Ueber die sogenannten Seitendrusen der Was erratte (*Arvicola*) und des Hamsters (*Cricetus*) Arch Zool ital 16 790–796

ance of heavy pigmentation in the dermis Gradually from approximately day 28 pigmentation in the male becomes more pronounced until finally by the thirty fifth day the flank organs may properly be said to be pigmented when viewed *in situ* The female flank organ however remains flesh colored except for clumps of dermal pigment associated with hair follicles

Histologically despite the lack of pigment visible when the organ is viewed *in situ* around 20 days (fig 8) there is a well established complement of black melanin granules in dermal melanocytes particularly around the larger sebaceous glands and pilosebaceous canals in the compact layer of the dermis There is a notable decrease in this pigmentation around the twenty fifth day by 30 days it has increased sharply to an even higher concentration than when first observed until by the thirty fifth day the male gland (fig 10) is definitely pigmented Subsequently despite variations the male gland slowly accumulates even more pigment In the mature female organ (fig 9) pigmentation is mainly restricted to clumps of large anagen hairs however even in the female at 100 days there is sufficient general pigmentation to impart a distinct darkness to the glandular area

DISCUSSION

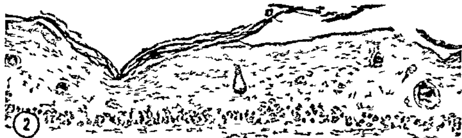
Although there is a slow progressive sexual dichotomy throughout much of the early postnatal developmental history of the hamster flank organ it is not well defined until the onset of puberty between the twenty sixth and twenty ninth days of life (Ortiz 47 LaVelle 51) Since the adult organ is such an obvious androgen target (Kupperman 44 46 Hamilton and Montagna 50) the possibilities of sex hormone influence during development should be examined

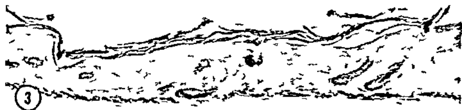
Because the gland develops equally in the two sexes prenatally and during the first ten postnatal days it seems reasonable to assume that this early growth and differentiation is essentially independent of sex hormones (LaVelle 51) Although the earliest indications of dimorphism suggest the possibility of some androgen activity in the ten day male other estimates of the time of onset of androgen activity place it at 25 to 26 days (Ortiz 4 LaVelle 51) There is good agreement be tween the observation that dimorphism o the flank organs is conspicuous by day 9 and those observations reported for th development and onset of function of ac cessory sex organs (LaVelle 51) Un doubtedly some androgen is present we before these key events take place on o about the twenty sixth day and it is possi ble that the very first influx of androge accounts for the inconspicuous dimorph ism we observe during the tenth da Since this early dimorphism remains qui inconspicuous until sexual maturity it i probable that the amounts of androge present in young animals of either se must be essentially equal In view o information available concerning the pos sible andromimetic action of the juxta medullary zone of the adrenal cortex in th female hamster and in view of the proba bility that even the adult adrenal gland se cretes some androgenic material it would again seem reasonable to attribute th similarity in flank organ development i both sexes from day 10 to 26 to the pres ence of essentially similar quantities o androgen in both sexes

In addition to the overall developmenta pattern of these glands in terms of andro gen reactivity we have been interested i the observation that the developing pilary component of these organs exhibits from the very beginning (day 2) a centripeta gradient of initial hair emergence and sub sequent successive centripetal waves of hair growth and pigmentation and in the observation that sebaceous gland develop ment starting uniformly throughout the organ on day two progresses thereafter in a centrifugal direction The exhibition of opposite gradients of development by two histogenetically related processes within a single organ requires two relatively inde pendent developmental mechanisms This constitutes an unusual phenomenon worthy of further investigation

The apparent contradiction between Kupperman s observation that the flank organ is absent prior to 30 to 35 days (44 44a 46) and Shrader s observation that pigment is first seen grossly in the organ at from 10 to 12 days (49) results from the fact that as fully recognized by


1


2


3


4



PLATE 1

EXPLANATION OF FIGURES

1 Section through term skin adjacent to flank organ (16 days) The basic components of the skin are well established 85 ×

2 Section through one day old flank organ in which none of the scanty hair follicles are beyond Stohr stage 5 95 ×

3 Section through two-day old flank organ in which sebaceous glands now appear 90 ×

4 Section through three day old flank organ An emerging hair is noted 90 ×

5 Section through four day-old flank organ The central most sebaceous glands are beginning to exceed in size those in the periphery 90 ×

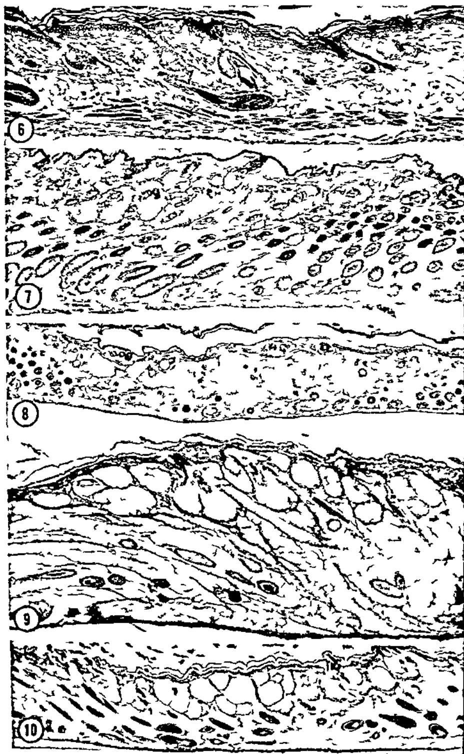

6
7
8
9
10

PLATE 2

EXPLANATION OF FIGURES

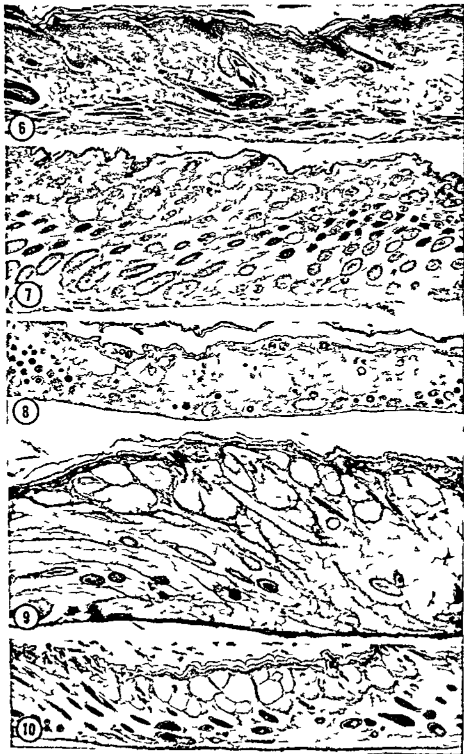
6 Section through five day old flank organ The degree of adnexal development approximates term condition of adjacent skin 55 ×

7 Section of 11 day-old male flank organ illustrating the large pigmented bulbs responsible for pigmented dermal disc 65 ×

8 Section of 20 day old male flank organ illustrating the young adult flank organ 65 ×

9 Section of 33 day old female flank organ 55 ×

10 Section of 35 day-old male flank organ 32 ×


6
7
8
9
10

On Anatomy of Nerves by Galen of Pergamon

CHARLES MAYO GOSS
George Washington University School of Medicine Washington D C

ABSTRACT In this treatise Galen gives a synopsis of the description of the nerves contained in his long anatomical work On Anatomical Procedures" He omits the olfactory nerves from the cranial group considering them a pa t of the brain Out of loyalty to his teacher Marinos he numbers seven cranial nerves but actually identifies ten misconstruing the fourth omitting the sixth and describing all the others The sympathetic is linked with the trigeminal but most parts of it are described The spinal nerves and their plexuses are b iefly but quite accurately described He leaves no doubt that he identified these nerves anatomically and understood much of their function

The publication of the present transla tion was undertaken as a tribute to Robert Montraville Green late Professor of Anat omy at Harvard Medical School He trans lated a number of Galen s works as a commission for Doctor Sidney Licht of New Haven who deposited the original manu script of these translations in the Yale Historical Library Doctor Licht gave me copies of most of them however and it is a pleasure to express my gratitude for his generosity

It soon became obvious from a transla tion which I had made at an earlier date that simple editing of Green s manuscript would not be possible Although it is well written and quite readable it is a free translation and contains a great many in accuracies and misinterpretations of Gal en s descriptions The present version therefore is a completely new translation from the Greek text in the Kuhn edition but with due acknowledgment of the bene fit derived from reference to Green s work

Typical of the reiteration by historians that Galen was unable to distinguish nerves from other structures is the following com ment by Charles Singer in the Introduction to his translation of Galen s surviving Greek text of On Anatomical Procedures" (56) Even greater difficulty arises from his theory of the nature of nerves Galen saw that a nerve NEURON passes into each muscle and that it then divides Knowing that many muscles end in a whitish tendon he thought that the branches of the nerves had reunited within the muscle to form this tendon which he naturally also called NEURON "

This is strangely at variance with Galen s own remarks in the following quotation from Duckworth s Galen on Anatomical Procedures the Later Books" (62) So now you must retain the significance of these names quite distinctly in your mem ory and remind yourself constantly that when we say nerve we only mean that which springs from the brain or the spinal marrow and when we say ligament we mean by it only that which grows out from the bones And when we say tendon then we only mean what takes origin and issue from a muscle "

The present translation of On Anatomy of Nerves" is a synopsis of the descriptions of nerves in Galen s long treatise "On Anatomical Procedures covered by the two translations just mentioned Only the first nine books have come down to us in a Greek text and although nerves are men tioned in passing the bulk of the nervous system is contained in Book Nine which ends abruptly after a few pages The rest of Book Nine and the other six books however are contained in an Arabic ver sion originally published by Simon (06) with a German translation The Arabic portion is available fortunately in an Eng lish translation of the German by Duck worth published after a comparison with the Arabic by Doctor C M Lyons Fellow of Pembroke College and University Lec turer in Arabic It is interesting that

On Anatomy of Nerves by Galen of Pergamon

CHARLES MAYO GOSS
George Washington University School of Medicine Washington D C

ABSTRACT In this treatise Galen gives a synopsis of the description of the nerves contained in his long anatomical work On Anatomical Procedures" He omits the olfactory nerves from the cranial group considering them a part of the brain Out of loyalty to his teacher Marinos he numbers seven cranial nerves but actually identifies ten misconstruing the fourth omitting the sixth and describing all the others The sympathetic is linked with the trigeminal but most parts of it are described The spinal nerves and their plexuses are briefly but quite accurately described He leaves no doubt that he identified these nerves anatomically and understood much of their function

The publication of the present translation was undertaken as a tribute to Robert Montraville Green late Professor of Anatomy at Harvard Medical School He translated a number of Galens works as a commission for Doctor Sidney Licht of New Haven who deposited the original manuscript of these translations in the Yale Historical Library Doctor Licht gave me copies of most of them however and it is a pleasure to express my gratitude for his generosity

It soon became obvious from a translation which I had made at an earlier date that simple editing of Greens manuscript would not be possible Although it is well written and quite readable it is a free translation and contains a great many inaccuracies and misinterpretations of Galens descriptions The present version therefore is a completely new translation from the Greek text in the Kuhn edition but with due acknowledgment of the benefit derived from reference to Greens work

Typical of the reiteration by historians that Galen was unable to distinguish nerves from other structures is the following comment by Charles Singer in the Introduction to his translation of Galens surviving Greek text of "On Anatomical Procedures (56) Even *greater difficulty arises from* his theory of the nature of nerves Galen saw that a nerve NEURON passes into each muscle and that it then divides Knowing that many muscles end in a whitish tendon he thought that the branches of the nerves had reunited within the muscle to form this tendon which he naturally also called NEURON

This is strangely at variance with Galens own remarks in the following quotation from Duckworths Galen on Anatomical Procedures the Later Books" (62) So now you must retain the significance of these names quite distinctly in your memory and remind yourself constantly that when we say nerve we only mean that which springs from the brain or the spinal marrow and when we say ligament we mean by it only that which grows out from the bones And when we say tendon then we only mean what takes origin and issue from a muscle"

The present translation of On Anatomy of Nerves is a synopsis of the descriptions of nerves in Galens long treatise On Anatomical Procedures" covered by the two translations just mentioned Only the first nine books have come down to us in a Greek text and although nerves are mentioned in passing the bulk of the nervous system is contained in Book Nine which ends abruptly after a few pages The rest of Book Nine and the other six books however are contained in an Arabic version originally published by Simon (06) *with a German translation* The Arabic portion is available fortunately in an English translation of the German by Duckworth published after a comparison with the Arabic by Doctor C M Lyons Fellow of Pembroke College and University Lecturer in Arabic It is interesting that

Chapter IV [834]

Lying next to this at its passage from the cranium but not at its first origin is a third pair of nerves (*n trigeminus*) Although they call it soft it is seen to be multiple at its very first root as a rule if you apply your attention to it closely but if you look more carelessly all will seem single to you Actually these nerves are softer than those in the previously mentioned second pair and those in the fourth and other succeeding pairs but they appear still more so because the rootlets are more numerous are slender as hair and lie beside one another without being made into felt and interwoven

Chapter V

Being a little harder than the latter the fourth pair[4] of nerves from the brain immediately after its origin mingles with the third pair It first penetrates the thick meninx and after this forthwith the bone of the cranium then in turn it separates toward the palate of the mouth

Now the third pair just as [835] it appears composed of many primary roots so also it breaks up in many ways For it makes no difference whether we say that the above mentioned aggregation of the nerves is loosed from each other or that the entirety if split up is of the separated parts Thus if anyone says that they are separate from one another or that each of the parts is produced from the whole aggregate it does not matter First then each part separates off one of them (*plexus caroticus sympathici*) running below the skull unknown to the anatomists goes downward through a foramen in the cranium in common with the continuing portion of the carotid artery which runs upward toward the brain one on each side Also even if it should not be stated sometimes it must always be understood after you have heard it this once that neither from the brain nor from the spinal cord do they exist unpaired but the one on the right and the one on the left are always exactly equal to each other in size [836] How these nerves course through the neck and the thorax[1] into the regions below the diaphragm and something of their distribution will be related as the discussion proceeds but now let us come to the remaining parts of the third pair

For leaving the cranium it touches the second but does not mingle with it as some of the others do and divides variously as I said To begin with at any rate a certain part of it (*n auriculotemporalis*) emerges beside the diarthrosis of the jaw at the front of the ears but how it happens to communicate with the fifth pair you will hear a little later This is indeed a small part of it But the trunk with all the parts growing out from it in a word like branches and twigs first splits into two and each of these in turn into many parts one being distributed to the temporal muscles the so-called masseters and the other muscles which take origin from the upper jaw and there are branches (*nn alveolares superiores*) from these nerves to the so-called gums and the teeth and [837] skin of the face Another branch (*n alveolaris inferior*) splits off to the roots of the teeth in the lower jaw in the same proportion as it divided into the upper and similarly it sends distributions to the gums and the lower lips as to the upper But the largest part of it (*n lingualis*) is distributed to the tunic of the tongue Some call this pair of nerves the gustatory [GEUSTIKOS] since through them the sensation of taste arises Some such then is the dissection of the third pair Also we have spoken about the fourth pair which Marinos correctly found separated from the third and going to the palate which I state in the book "On Anatomical Procedures"

This nerve is an enigma. It cannot be the motor root of the trigeminal as Duckworth (62) page 191 suggests because the latter does not go to the palate Galen is trying to maintain his loyalty to Marinos in sorting out the nerves related to the cavernous sinus as the next paragraph shows The best interpretation of this fourth nerve appears to be the trochlear abducens and cavernous sympathetic fusing with the ophthalmic division of the trigeminal and continued as the pterygopalatine nerve

This refers to the incorporation of the sympathetic into the third-fourth nerve complex.

Galen's long anatomical treatise "On Anatomical Procedures" has not survived in a complete Greek edition The first eight books and the first five chapters only are included in the Kühn edition of Greek text in volume 2 pages 215–731

The last part of the treatise has come down to us in an Arabic version first made available in a German translation by Simon in 1906 but now translated into English by W L H Duckworth.

The third and fourth pairs of nerves are described in Duckworth pages 189–195

Duckworth s translation through three languages Greek into Arabic, Arabic into German, and German into English is more accurate and carries the imprint of Galen s personality as revealed by the present translation much better than the some times inaccurate and quite disparaging rendition published by Singer (56)

It must be remembered that Galen is describing the anatomy of a monkey al though he does not mention this at the beginning as he does in some other trea tises During the course of the description however the monkey is specifically men tioned ten times

The following typographical conventions will be used

The numbers in square brackets refer to the pages in volume 2 of the Kuhn edition (1821–33)

Greek words taken directly into English are transliterated into Roman Capitals

Greek words are given their Greek endings

Titles of Galen s own works appear in quotes

Modern Anatomical terms where appro priate are taken from the 1965 Nomina Anatomica italicized and placed in peren theses

ON ANATOMY OF NERVES

Chapter I [831]

All the physicians agree that none of the parts of the living being [ZOON] has either sensation or motion which we call purposeful without a nerve [NEURON] and that if the nerve be cut the part immedi ately becomes motionless and insensitive It is not known to all however that the source of the nerves is the brain and the spinal marrow[1] and that some of them originate from the brain [ENKEPHALON] it self and others from the spinal cord al though this is the manner in which they are seen in the dissections [ANATOMAI]

Chapter II [832]

The most anterior cavities in the brain as they extend forward narrow gradually in a manner similar to a cone until they reach the beginning of the nose lying side by side and touching throughout so that there is nothing[2] between them but the thin meninx

At each side of these one on the right and one on the left a nerve (*nervus op ticus*) worthy of mention in thickness and almost the softest of all those growing out from the brain itself proceeds outside the [KRANION] to the eye through a foramen having exactly the same diameter as the thickness of the nerve This foramen is located where first the space for the eyes (*orbita*) begins to appear and as you look at these nerves they will seem to be like roots of the eyes They do not break up into many fibers however as all the othe nerves do when they are distributed to the receiving organs but terminate in a re markably different way which is not eas to explain and which perhaps you will no believe when you hear it unless [833] yo see it yourself For each of them passin inside the eye immediately adjacent broad ens out like a sphere (*retina*) encirclin the so called glass like [HYELOEIDES] liqui (*humor vitreus*) but even there not bein altered at all from the nature of brai substance In these nerves alone befor they enter the eye there is within a clearl perceptible pore[3] whence some of the ana omists [ANATOMIKOI] have called the canals not nerves Others term them opti [OPTIKA] nerves taking the name fro the function and they number this pa first of the nerves from the brain of a the others being softest

Chapter III

The pair next in order is distributed t the muscles moving the eyes (*n ocul motorius*) It is much harder and small than the above mentioned and it escape from the cranium near them being sep rated by the thinnest bone

---

[1] The Greek expression here is NOTIAION MYELO or spinal marrow Throughout the rest of the treati NOTIAION alone is used but it is an adjective for and therefore must refer to the spinal cord rath than the spine as translated by Green

[2] A simian characteri tic

[3] This apparently refers to the arteria central retinae

foramen which is at the end of the lamb doid suture Although almost everyone thinks they are a single nerve if we take up in a noose the one running along with the arteries (*n vagus*) the animal im mediately becomes speechless Indeed the muscles of the larynx also receive offshoots from it But of the other two one reaches each of the muscles of the pharynx and the root of the tongue (*n glossopharyngeus*) [842] but the other goes to the muscle of the scapula the flat and some others of those in that region (*n accessorius*) But it has escaped notice that those not small nerves running along the arteries course through the neck and thorax before enter ing the body of the stomach to which the principal part of these nerves is attached and distributed But it is remarkable that they say that some parts of them are dis tributed to the diaphragm although actu ally the diaphragm does not receive the least supply from this pair and again they do not even mention that some parts of these nerves return from the midst of the thorax to certain muscles of the larynx (*n recurrens*) nor say what function they have And yet these cause aphonia in ani mals if injured as well as the great pair of nerves with the arteries because these same are parts of the cause of the loss of voice if they are injured

Intricate also is the [843] plexus of dis tribution of these nerves beyond the dia phragm for it also receives some parts from the spinal cord in this region and is distributed to the viscera of this area and is mixed with the previously mentioned branches from the third pair said to de scend through the neck and the thorax (*n sympathicus*) And yet on the contrary *all* those descending along the roots of the ribs seem to be the same as offshoots from the sixth pair Intricate also is their mix ture with the nerves of the intercostal spaces and almost all of the small ones of the loins and the remainder going to the outlet of the hollow intestines (*colon*) Varied also is the distribution to the region outside the peritoneum with which we are not concerned to explain in exact de tail But it is fitting not to be ignorant that of the nerves from the brain the third pair on the one hand as was said and from the sixth pair on the other hand seem to reach the liver the spleen the kidneys and be fore these the whole stomach and all the viscera [844] Indeed all have recognized that the lungs and the heart receive some part of their nerves in the neck from the sixth pair

At all events this is sufficient for begin ners concerning the nerves from the brain We must speak next concerning the nerves coming from the spinal cord in which all the anatomists were in error But now is not the time to pursue the causes of their errors since I have already explained them in the book "On Anatomical Procedures "[1] But nevertheless I feel obliged to recall the ancients to mind for the reason that it may seem uncertain to those familiar with their books although not to those viewing the phenomena with me through dissection whether they are all in error or I alone

Chapter XI

Now the first pair of nerves f om the spinal cord originates from the first ver tebra penetrated by foramina present in common running through the first six ver tebrae for these are in the transverse processes and do not touch the marrow But [845] there are two others which do touch it through which the first pair of nerves escapes having a single root at the spine but immediately bifurcating one part extends to the posterior regions and the other lateralward Now this pair of nerves is small in those animals in which the first vertebrae are small as in mon keys but large in those in which the ver tebrae are large as in sharp toothed and in horned animals In these therefore on account of their size the nerve branches reaching to the side are distributed to most muscles those mentioned in "On Anatomi cal Procedures "[1] But in monkeys those animals resembling man in most other re gions but especially in the neck *the first* pair is distributed only to the muscles around the diarthrosis of the head which were not accurately known by the anato- mists

See Duckworth (62) Book 14 p g 203–217
See Duckw rth (62) Book 14 p ge 217 222
See Du kworth (62) Book 15 p ges 228 nd 231
See Duckworth (62) Book 15 p ge 229

Chapter VI

There is also another pair of nerves which which Marinos called fifth Although strictly not splitting off from one root the two nerves being close to each other each originates from the other In the more anterior [838] parts the one which they call AKOUSTIKON (*n vestibulo cochlearis*) penetrates the foramen (*meatus*) of the hearing organ [AKOE] at the same time as the outpouching of the thick meninx which widening out spreads into the passage But from the posterior parts (i e the depth of the meatus) the other nerve (*n facialis*) penetrates a particular orifice (*canalis facialis*) in the stone like bone the one called blind for thus the ancient anatomists named it not being able to bore out the winding course [HELIX] through which the nerve penetrates to the exterior behind the external ear (*foramen stylomastoideus*) And immediately this nerve joins with the fibers of the third pair mentioned above (*n auriculotemporalis*) said to escape outward near the diarthrosis of the jaw the latter not traveling toward the former but awaiting the former s approach to it But from both of them mingled it is better to say the greatest part is distributed to the flat muscle[7] the one underlying the skin moving the jowl without the chin which I discovered and which is from both sides For it is necessary to remember that we hear each paired even if it should be omitted [839] in the discourse Such then is the distribution of the fifth pair Let it therefore remain one for the sake of Marinos even though it is obviously double

Chapter VII

The sixth pair of nerves from the brain uses a foramen at the lower end of the lambdoid suture (*foramen jugulare*) At the primary origin from the brain it has three nerves (*nn glossopharyngeus vagus et accessorius*) but having emerged from the cranium these mingle with one another and with adjacent nerves in many ways which I shall state a little later

Chapter VIII

There is remaining the seventh pair of nerves from the brain distributing their proper branches for the most part to the muscles of the tongue For a small portion of them always reaches the common muscles of the thyroid cartilage of the larynx (*mm suprahyoidei*) and of the lower border of the lambdoid (hyoid) bone (*mm infrahyoidei*) but not always also to certain others

Chapter IX

The nerves descending below the head as I said combine with each other both those from the third pair [840] and also from the two pairs now mentioned last Moreover the first and the second pair of nerves from the spinal cord also make many communications with these nerves Oftentimes it will seem to you that the slip from one to another is like some single bond common to both and sometimes one of the nerves enlarges as if something had been added to it and the other diminishes as if something had been taken away from it Wherefore all the anatomists are confused in their knowledge of these nerves generally disagreeing with one another and for the most part being individually ignorant For they have confidently written some things as never occurring otherwise which not only are not always seen in all animals but not even in monkeys alone Similarly it was unknown to them that some things always occur not only in monkeys but also in other animals of which there are six existing kinds as I point out in the book On Anatomical Procedures[8] Take for example how the nerves from the sixth pair are distributed to the intrinsic muscles of the larynx by three branches from each side so that altogether they are six But some of them knew only two and some not even these

Chapter X

Now the muscles common to other parts of the larynx do not always receive nerves from the sixth pair just as neither do those muscles joining the bone called lambdoid or hyoid to the sternum about which it is accurately stated in the book On Anatomical Procedures and in which there is also a statement concerning the distribution of the three nerves said to emerge from the

[7] The platysma myoides which is much more extensive in monkeys than in man

[8] See Duckworth (62) Book 14 chapter 5 pages 197-203

foramen which is at the end of the lambdoid suture Although almost everyone thinks they are a single nerve if we take up in a noose the one running along with the arteries (*n vagus*) the animal immediately becomes speechless Indeed the muscles of the larynx also receive offshoots from it But of the other two one reaches each of the muscles of the pharynx and the root of the tongue (*n glossopharyngeus*) [842] but the other goes to the muscle of the scapula the flat and some others of those in that region (*n accessorius*) But it has escaped notice that those not small nerves running along the arteries course through the neck and thorax before entering the body of the stomach to which the principal part of these nerves is attached and distributed But it is remarkable that they say that some parts of them are distributed to the diaphragm although actually the diaphragm does not receive the least supply from this pair and again they do not even mention that some parts of these nerves return from the midst of the thorax to certain muscles of the larynx (*n recurrens*) nor say what function they have And yet these cause aphonia in animals if injured as well as the great pair of nerves with the arteries because these same are parts of the cause of the loss of voice if they are injured

Intricate also is the [843] plexus of distribution of these nerves beyond the diaphragm for it also receives some parts from the spinal cord in this region and is distributed to the viscera of this area and is mixed with the previously mentioned branches from the third pair said to descend through the neck and the thorax (*n sympathicus*) And yet on the contrary all those descending along the roots of the ribs seem to be the same as offshoots from the sixth pair Intricate also is their mixture with the nerves of the intercostal spaces and almost all of the small ones of the loins and the remainder going to the outlet of the hollow intestines (*colon*) Varied also is the distribution to the region outside the peritoneum with which we are not concerned to explain in exact detail But it is fitting not to be ignorant that of the nerves from the brain the third pair on the one hand as was said and from the sixth pair on the other hand seem to reach the liver the spleen the kidneys and before these the whole stomach and all the viscera [844] Indeed all have recognized that the lungs and the heart receive some part of their nerves in the neck from the sixth pair

At all events this is sufficient for beginners concerning the nerves from the brain We must speak next concerning the nerves coming from the spinal cord in which all the anatomists were in error But now is not the time to pursue the causes of their errors since I have already explained them in the book On Anatomical Procedures " But nevertheless I feel obliged to recall the ancients to mind for the reason that it may seem uncertain to those familiar with their books although not to those viewing the phenomena with me through dissection whether they are all in error or I alone

Chapter XI

Now the first pair of nerves from the spinal cord originates from the first vertebra penetrated by foramina present in common running through the first six vertebrae for these are in the transverse processes and do not touch the marrow But [845] there are two others which do touch it through which the first pair of nerves escapes having a single root at the spine but immediately bifurcating one part extends to the posterior regions and the other lateralward Now this pair of nerves is small in those animals in which the first vertebrae are small as in monkeys but large in those in which the vertebrae are large as in sharp-toothed and in horned animals In these therefore on account of their size the nerve branches reaching to the side are distributed to most muscles those mentioned in "On Anatomical Procedures " But in monkeys those animals resembling man in most other regions but especially in the neck the first pair is distributed only to the muscles around the diarthrosis of the head which were not accurately known by the anatomists

---

See Duckworth (62) Book 14 pages 203-217
See Duckworth (62) Book 14 pages 217 222.
See Duckworth (62) Book 15 pages 228 and 231
See Duckworth (62) Book 15 page 229

Chapter VI

There is also another pair of nerves which which Marinos called fifth. Although strictly not splitting off from one root the two nerves being close to each other each originates from the other. In the more anterior [838] parts the one which they call AKOUSTIKON *(n. vestibulo cochlearis)*, penetrates the foramen (*meatus*) of the hearing organ [AKOE] at the same time as the outpouching of the thick meninx which widening out spreads into the passage. But from the posterior parts (i e the depth of the meatus) the other nerve (*n facialis*) penetrates a particular orifice (*canalis facialis*) in the stone like bone the one called blind for thus the ancient anatomists named it not being able to bore out the winding course [HELIX] through which the nerve penetrates to the exterior behind the external ear (*foramen stylomastoideus*). And immediately this nerve joins with the fibers of the third pair mentioned above (*n auriculotemporalis*) said to escape outward near the diarthrosis of the jaw the latter not traveling toward the former but awaiting the former's approach to it. But from both of them mingled it is better to say the greatest part is distributed to the flat muscle[7] the one underlying the skin moving the jowl without the chin which I discovered and which is from both sides. For it is necessary to remember that we hear each paired even if it should be omitted [839] in the discourse. Such then is the distribution of the fifth pair. Let it therefore remain one for the sake of Marinos even though it is obviously double.

Chapter VII

The sixth pair of nerves from the brain uses a foramen at the lower end of the lambdoid suture (*foramen jugulare*). At the primary origin from the brain it has three nerves (*nn glossopharyngeus vagus et accessorius*) but having emerged from the cranium these mingle with one another and with adjacent nerves in many ways which *I shall state a little later*

Chapter VIII

There is remaining the seventh pair of nerves from the brain distributing their proper branches for the most part to the muscles of the tongue. For a small por[tion] of them always reaches the common mus[cles] of the thyroid cartilage of the lar[ynx] (*mm suprahyoidei*) and of the lower bor[der] of the lambdoid (hyoid) bone (*m[m] infrahyoidei*) but not always also to cer[tain] others

Chapter IX

The nerves descending below the hea[d] as I said combine with each other bot[h] those from the third pair [840] and al[so] from the two pairs now mentioned la[st]. Moreover, the first and the second pai[r of] nerves from the spinal cord also mak[e] many communications with these nerves. Oftentimes it will seem to you that the s[...] from one to another is like some sing[le] bond common to both and sometime[s] one of the nerves enlarges as if some[thing] had been added to it and the othe[r] diminishes as if something had bee[n] taken away from it. Wherefore all th[e] anatomists are confused in their knowl[edge] of these nerves generally disagreein[g] with one another and for the most par[t] being individually ignorant. For they have confidently written some things as never occurring otherwise which not only are no[t] always seen in all animals but not even in monkeys alone. Similarly it was unknown to them that some things always occur not only in monkeys but also in other animals of which there are six existing kinds as I point out in the book On Anatomical Procedures.[8] Take for example how the nerves from the sixth pair are distributed to the intrinsic muscles of the larynx by three branches from each side so that al[to]gether they are six. But some of them knew only two and some not even these.

Chapter X

Now the muscles common to other parts of the larynx do not always receive nerves from the sixth pair just as neither do those muscles joining the bone called lambdoid or hyoid to the sternum about which it is accurately stated in the book "On Anatomical Procedures" and in which there is also a statement concerning the distribution of the three nerves said to emerge from the

[7] The platysma myoides which is much more extensive in monkeys than in man.

[8] See Duckworth (62) Book 14 chapter 5 pages 197–203.

unique to each of the subsequent pairs From the fourth nerve which arises be tween the third and fourth vertebrae an altogether short nerve in monkeys goes to the next pair combining with it where it first emerges but in other animals we do not often see this combination occur ring Next to this the fifth pair arises after the fourth vertebra A certain small part of its extends downward destined if it receives some small parts from the next nerve to become the nerve of the dia phragm (*n phrenicus*) For from the fourth nerve Nature sends to the dia phragm a spiderweb like process and from the fifth [851] a considerable one and then from the sixth another smaller than this but larger than the first Another branch larger than the latter ascends to the top of the scapula (*n suprascapularis*) but all the rest was mentioned in the de scription of the common distribution And of the next pairs the sixth emerges after the fifth and the seventh after the sixth and eighth after the seventh vertebra from the common foramina as has been said and combining with one another (*plexus brachialis*) they extend to the hollow of the scapula and arm through the axilla

Chapter XVI

Another pair next to this springing from between the first and second thoracic ver tebrae combines for the most part with the above mentioned pairs Indeed a cer tain small part of it splits off into the first intercostal space and reaches to the posterior vertebral muscles but all the rest ascending above the first rib com bines with the nerve after the seventh vertebra Thus then both these and the others above course through the axilla [852] to the hollow of the scapula and the arm in a certain way combining and en twining with each other (*plexus brachi alis*) Much of them is distributed to the muscles of the arm and forearm what re mains is distributed to the tip of the hand The rule especially is for the last of the origins mentioned to send nerves to the hand but those to the forearm are from the one above this and those to the arm and those to parts still higher to reach the scapula from the highest pairs as a rule What course they take through the upper limb and how they are distributed to each of the muscles has already been stated in the book On Anatomical Procedures "[1] And in the same way nerves arise from all the vertebrae of the thorax (*nn inter costales*) all having a similar distribution except the one in the second intercostal space For from there clearly a nerve proceeds to the skin of the arm (*n inter costobrachialis*) But all the other pairs at their [853] origin immediately give some part to the spinal muscles and to the others in the broad of the back as well as to those moving the scapulae and to those extend ing up to the diarthrosis at the shoulder In short the remaining and largest part of them runs forward through the intercostal spaces as far as the bone at the sternum supplying the muscles in the intercostal spaces and those lying outside the thorax concerning the distributing of each individ ual part which was stated in the book On Anatomical Procedures " Now of the pairs of nerves from the spinal cord at the false ribs since false ribs do not reach the sterum each runs through its own space a short distance but all the rest escapes to the HYPOCHONDRION and is distributed to the first oblique muscles descending from the thorax above and to the vertical fleshy muscles

Chapter XVII [854]

After these the origins of the nerves at the lumbar region are not from a common foramen like those in the neck for here the overlying vertebra alone being perfo rated affords a suitable passage for the nerve Although a common foramen is formed from both vertebrae in the neck farther caudalward *the foramen is dis* placed gradually into the overlying verte bra so that first it is hollowed out consider ably then altogether then it extends up from the inferior surface of the vertebra *and the origin itself* becomes above the inferior surface It is usual also for all these nerves to go to the spinal and epi gastric muscles and to the PSOAS Also from the first vertebrae below the dia phragm a small nerve (*ramus communi*

Th w d CHEIR in G eek m n both h nd nd uppe limb, AKRA CHEIR th t p of th limb is th h nd HOLES CHEIR i th whol limb

See Du kw rth (62) Book 15 p g 239-256

See Duckw rth (62) Book 15 p ges 256-260

Chapter XII

The second pair of nerves from the spinal cord arises from the posterior aspect not [846] indeed through a foramen similar to the first *For at each side of the* spine of the vertebrae there is a place devoid of bone the interval through which the nerves arise They extend forward between the first and second *transverse processes* combining with the nerves of the first and third pairs as the third with those *springing from the brain The major part* of them is distributed to the muscles on the back of the neck by which the movements of the first vertebrae toward each other and the head arise after giving some supply also to the flat muscles moving the jowls But whatever is left of them ascends *to the head investing all its posterior aspect (n occipitalis major)* and the parts around the ears even as far as the crown and the top of the bregma Thus also the part extending anteriorly is distributed to almost all the anterior part of the head

Chapter XIII

Now the third pair of nerves from the spinal cord arises from the lateral parts [847] where the second and third vertebrae *touching each other form* a common rounded foramen equal in width to the thickness of the nerve Immediately splitting one of the two branches runs to the posterior parts of the deep muscles there giving them some branches of distribution and then ascending along the spinous *processes of the vertebrae From there this* nerve extends obliquely forward *(n auricularis magnus)* distributing to the muscles behind the ear one on each side for always I wish this understood by you even if I do not say so With the other of its branches extending forward the third pair about which we are speaking combines with adjacent branches and has some distribution both to the other bodies which are there to the flat muscles to those in front of the ear and *to those moving the jaws It is* also distributed to those nodding the whole neck backward with the entire head The part extending forward combines with two [848] pairs both the second one previously described and after this with the fourth about to be described The accurate distri*bution which* their combination involves in the anterior parts of the neck will be stated in another discourse But for the present it is necessary to know this much that the third and fourth pairs supply *nerves to the muscles common to the neck* and head and to those moving the jaws as also to all those parts behind the ears

Chapter XIV

The subsequent pairs of nerves all have a common foramen through which the nerves escape but they are also alike in bifurcating immediately at their origin with their smaller part running forward and with their larger branch running deep *at first toward the spine and then again* to the front of the flat muscle the one moving the jowl to the side with the lips without *moving the bone of the lower jaw* which the anatomists have not recognized although [849] it most clearly has this function And again also it is common to *all the subsequent pairs that immediately after the first origin* some small distribution of them spreads to the spinal muscles And yet even in extending back to the spine it is usual for all these nerves to give some branches to the muscles common to the neck and head For all the muscles in *the anterior parts of the neck and* in the lateral parts receive nerves from these pairs apart from those which I said before receive some distribution and supply from the pairs from *the brain (n accessorius)* On the whole then these things are indeed common to all of those in the entire neck *the neck being of seven vertebrae* in all those animals not being at all different in nature from man

Chapter XV

What is unique to the individual nerves has been accurately stated before in the book On Anatomical Procedures [11] but now it is necessary for me to speak *in summary* and comprehensively about their function in the briefest discourse [850] All the muscles in the anterior and lateral parts of the neck receive their nerves from these pairs except those muscles to which we have said before that there is distribu*tion from the brain And these being* known beforehand it is amply clear to anyone who applies his mind what is

[11] See Duckworth (62) Book 15 pages 227 239

In his description of the vagus nerve he passes over his experiments on the recur rent laryngeal branch with rather un wonted reticence These very remarkable experiments are given in the Duckworth translation and are rewarding to read Nor does he mention his still more remarkable experiments on the spinal cord Although he was well aware of the motor and sen sory function of various nerves he could only guess at the method of their segrega tion and was unable therefore to interpret correctly the communications of the nerves at the cavernous sinus or the base of the skull This also explains his tendency to describe cutaneous nerves as going to the underlying muscles

LITERATURE CITED

Duckworth W L H translator Lyons M C and B Towers editors 1962 Galen on Ana tomical Procedures the Later Books (From Simon s German and Arabic) xix + 279 pages Cambridge The University Press

Kuhn C G 1821–33 Galen Opera omnia Greek and Latin text 20 volumes in 22 Cnobloch Lipsiae 2 831–855

Simon M 1906 Sieben Bucher Anatomie des Galen 2 volumes J C Hinrichs Buchhand lung Leipzig

Singer C 1956 Galen on Anatomical Procedures Translation of the Surviving Books Oxford Uni versity Press London and New York xxvi + 289 pages

cans) from each combines with those descending from the brain above Below the last two lumbar vertebrae two very large roots of nerves emerge running to the legs Also other small ones unite with them (*plexus sacralis*) one lying above and one other [855] lower arising from the first foramen in the so called flat bone (*os sacrum*) These immediately diverging supply the first muscles moving the diarthrosis at the hip but all the rest descends into the legs (*n ischiadicus*) branching into each muscle as far as their extremities corresponding to those in the hands as has already been stated in the book On Anatomical Procedures [17] So also what nerves emerge through the remaining foramina of the sacrum and are distributed to the muscles existing there we have discussed carefully in each detail Now this alone is fitting to say that nerves from the spinal cord arising from the internal and external foramina in the sacred bone [18] are distributed to the muscles of the seat perineum and bladder to the genitalia themselves and to the muscles arising from the sacrum and from the inner surface of the pubic bone and to all structures lying outside the so called flat or sacred bone terminating in the so called coccyx bone So now we have made an outline and synopsis of those things accurately written in the book On Anatomical Procedures to be useful for beginners [19]

DISCUSSION

This treatise should dispel from everyone s mind all doubt concerning Galen s ability to identify nerves with commendable precision in his dissections

If Galen had not been deliberately honoring his teacher Marinos by following his numbering of the cranial nerves he would have identified and numbered ten rather than the seven with which he is accredited He missed the multiple small olfactory nerves but correctly identified the olfactory bulb and tract as parts of the brain He did not distinguish the sixth as motor to an ocular muscle He was indeed confused by the several nerves associated with the cavernous sinus and their fusion with various parts of the trigeminal His treatment of Marinos fourth nerve suggests that he was rather dissatisfied with it because he gave no details A nerve going to the palate could not have been a mistaken identification of the motor root It could have included the trochlear and in one place in Book 14 Chapter 3 (page 192 Duckworth 62) it also includes the sympathetic as follows (in cleaning the dura away from around the hypophysis' But if you make no mistake there in th application of the knife you will sometimes see in that position a nerve whicl the anatomists have neglected It is on which passes out from the skull throug an orifice beneath the auditory meatus i which the carotid artery mounts upwards

Now take care of this nerve and pr serve it uninjured from all damage If yo do that with it you will learn that it come from the fourth pair He identified an distinguished quite satisfactorily the f cial acoustic (vestibulocochlear) gloss pharyngeal vagus accessory and hyp glossal nerves

Except for including it as part of th trigeminal Galen gives a surprisingly cor plete description of the morphological fe tures of the sympathetic The cervic ganglia bewildered him because he cou not separate the nerve trunk from th swelling He identified the rami commun cantes the splanchnic nerves and th mingling with the vagus to form the celi plexus

It is unsatisfactory to dismiss the a ducens nerve as simply overlooked Galer skill in dissecting and accuracy of obser tion makes this unlikely It is probab that he saw it along with the trochlea sympathetic and trigeminal ophthalmi but had no other guidance to follow fro Marinos than to lump them together in th third fourth complex It is characterist of Galen that he described accurately if h has worked out an explanation which sa isfies him but slides over parts in whic he has not found a satisfactory answe The latter is his treatment of Marino fourth nerve

[17] *See Singer (56) Book 3 chapters 10 and 11 pages 83-87*

[18] The flat bone" and the sacred bone are both used for the sacrum The ilium is "the flat bone of the loins

[19] This sentence was moved from the beginning to the end of the paragraph

Histochemical and Electron Microscopic Observations on the Salt Secreting Lacrymal Glands of Marine Turtles

JOHN H ABEL JR AND RICHARD A ELLIS
Department of Biology Brown University Providence Rhode Island and Mt Desert Island Biological Laboratory Salisbury Cove Maine

ABSTRACT The lobular compound branched tubular salt-secreting lacrymal glands of two marine turtles *Chelonia mydas* and *Ca etta caretta* are similar in structure and in histochemical reactivity Blood from the centrolobular arteries flows through a rich capillary bed counter to the flow of tubule secretion The capillary endothelium is reactive for ad nosine triphosphatase (ATPase) Nerves containing cholinesterase pervade the connective tissue At the blind ends of the secretory tubules small basophilic peripheral cells contain an abundance of glycogen monoamine oxidase (MAO) and phosphorylase but little succinic dehydrogenase (SDH) or cytochrome oxidase (CTO) Non mitochondrial ATPase is concentrated at the luminal interface of these cells The larger principal cells lining the major portion of the secretory tubules are rich in SDH and CTO but contain relatively little glycogen MAO or phosphorylase Broad intercellular channels reactive for mucopolysaccharide are formed by intermeshing pleomorphic microvilli that fringe the extensive lateral surfaces of the principal cells The cytoplasm of these cells contains profiles of smooth surfaced endoplasmic reticulum (SSER) abundant mitochondria and prominent Golgi membranes Profiles of SSER and small membrane bound vesicles fill the apical cytoplasm but mitochondria are lacking The luminal secretory border of the cell is extremely limited in area

Two types of epithelial cells l ne the duct system basal cells that react strongly for non specific esterase and MAO and goblet cells containing mucopolysaccharide acid phosphatase cholinesterase and ATPase

The principal cells clo e to the arterial blood supply contain the highest con centrations of oxidative enzymes and have special modifications of the cell surface consistent with their role in salt concentration and secretion

Osmoregulation in marine reptiles is aided by head glands that have an extra renal function in the elimination of salt (Schmidt Nielsen and Fange 58) In the loggerhead turtle (*Caretta caretta*) and the Atlantic green turtle (*Chelonia mydas*) a salt solution hypertonic to blood is se creted by modified lacrymal glands that lie against the posterior wall of the orbit (Peters 1892 Schmidt Nielsen and Fange 58) Each gland consists of approximately 100 lobules that are filled with myriad closely packed secretory tubules

Histologically the salt glands of the sea turtles resemble in their organization other glands that are modified for osmoregula tion in different marine vertebrates The nasal glands of marine birds (Marples 32 Fange et al 58a) and the rectal glands of marine elasmobranchs (Fange and Fugelli 63 Bulger 63) are both compound branched tubular structures Many of the morphological similarities among these salt secreting glands are lost however when they are examined at the cellular level For example the principal secretory cells in the salt glands of marine turtles (Ellis and Abel 64) have speciali zations of the cell surface that are entirely different in form from the secretory cells in the nasal glands of marine birds (Doyle 60 Komnick 63c) or in the rectal glands of elasmobranchs (Bulger 63 Doyle 62a b) These are however merely vari ations in form since in each instance the same effect is achieved that is the area of the absorptive surfaces of the cell is greatly expanded

In this study the unusual features of the turtle salt gland as well as the char acteristics that it shares with the salt se creting glands of other marine vertebrates are explored by histochemical and elec tron microscopic techniques The sites of

nective tissue encloses each tubule Two types of nerve fibers course through the connective tissue of the glands one gives a strong positive reaction for cholinesterase the other is reactive for monoamine oxidase The large fibers that react for cholinesterase in the inter and intralobular connective tissue send branches that form a rich plexus around each tubule (fig 2) Nerves reactive for monoamine oxidase form a diffuse perilobular network

Many large arteries revealed by staining and by vascular perfusions lie embedded in the interlobular connective tissue Smaller arteries branch from the larger ones penetrate the lobules through broad sheaths of intralobular connective tissue and send 8–16 small arterioles along the central canals Radiating from these arterioles towards the periphery of the lobule are numerous extensions that branch and rebranch to form a rich capillary bed paralleling the branched secretory tubules (fig 1) Many circumtubular and intertubular connectives further augment this system so that at any one point each tubule is associated with 4–6 capillaries At the periphery of the lobules the capillaries enter venous sinuses that fuse together and drain into larger interlobular veins Some venous elements are present within the intralobular connective tissue and appear to drain the vessels supplying the central canal

The secretory tubules

The blind terminal segments of secretory tubules lie just beneath the interlobular connective tissue and run centripetally towards the center of each lobule In the loggerhead turtle the tubules average 1 mm in length and generally bifurcate two or three times within this distance Near the blind end of each tubule the central lumen is extremely small centripetally it increases slightly in size and reaches its largest diameter when the tubule joins with the central canal The fine bore of the lumen indicates that the single layer of truncated epithelial cells have a very limited secretory surface

Three distinct cell types may be identified among the cells lining the tubules At the blind ends of the tubule are small terminal cells with scant cytoplasm and a high affinity for basic dyes These comprise approximately a tenth of the cells lining the secretory tubules in the immature green turtles Most of the remainder of each tubule is paved with principal secretory cells These are small near the periphery of the lobule but they gradually increase in size as they approach the central canals Broad intercellular channels are apparent along the lateral surfaces of adjacent secretory cells except at their apex where they are joined by junctional complexes (fig 15) Cross sections of the secretory cells reveal large folds projecting from the main cell body that interlock with similar processes of adjacent cells The cell boundaries thus formed are extremely irregular and fit together like the pieces of a jigsaw puzzle (fig 4) The broad bases of the secretory cells rest upon a well-developed basement membrane that separates them from the adjacent peritubular connective tissue No myoepithelial elements have been detected with either the light or electron microscope

The principal and peripheral cells contain a large central nucleus with a single nucleolus bits of heterochromatin and a homogeneous karyoplasm There are no obvious differences in nuclear structures between the principal and peripheral cells

The third cell type of the tubules is morphologically unrelated to the secretory cells This small oval cell lies against the basement membrane of the tubule its apical surface never extends more than one quarter the distance to the lumen (fig 17) and the bases of adjoining secretory cells surround it on all sides The highest concentration of these cells is found in portions of tubules nearest the central canal while none occurs at the blind ends

Tubule cytochemistry

There are striking cytochemical differences between the peripheral cells and the principal secretory cells The peripheral cells are sudanophobic they have few mitochondria and little succinic dehydrogenase and cytochrome oxidase activity (figs 5 6) The centripetal principal cells however are sudanophilic (fig 7) have large numbers of mitochondria and exhibit a large amount of oxidative enzyme activity (figs 5 6) Conversely the pe

specific enzymatic activity are identified within the tissues of the gland and the fine structure of the principal secretory cells is delineated This data is correlated wherever possible with biochemical and cytological observations on other salt glands and with the general problem of salt secretion

MATERIALS AND METHODS

Ten vigorous young Atlantic green turtles (*Chelonia mydas*)[1] raised in aquaria at the marine laboratory of Duke University and two loggerhead turtles (*Caretta caretta*) captured fresh locally were used for these studies After the animals were drugged with chloral hydrate or with nembutal the salt glands were removed intact from the posterior wall of the orbit and weighed Single lobules were dissected from the salt gland and rapidly frozen in dry ice sectioned at 7–60 μ in an International cryostat and used to demonstrate monoamine oxidase (Glenner et al 57) phosphorylase (Takeuchi and Kuriaki 55 Ellis and Montagna 58) cytochrome oxidase (Burstone 59) and succinic dehydrogenase (Nachlas et al 57) activity Other segments of the glands were appropriately fixed in 10% neutral formalin formal calcium or chloral formalin sectioned on the cryostat and tested for alkaline phosphatase (Gomori 52 Pearse 61) acid phosphatase (Gomori 50 Burstone 58) a naphthyl esterase (Nachlas and Seligman 49) non mitochondrial ATPase (Wachstein and Meisel 57) and cholinesterase (Koelle and Friedenwald 49) Sudan black B staining was used to demonstrate lipids and phospholipids (Gomori 52) alcian blue was used to demonstrate acid mucopolysaccharides (Pearse 61)

Still other portions of the glands were fixed in Zenkers Bouins or Hellys fluids for histological study The following techniques were applied to 2–6 μ paraffin sections toluidine blue at pH 2 5 3 8 4 5 5 5 and 7 (Montagna et al 51) toluidine blue for permanent metachromasia (Hess and Hollander 47) toluidine blue following sulfation (Mowry 58) toluidine blue following hyaluronidase digestion (Gersh and Catchpole 48) PAS (McManus 48) with saliva diastase and or hyaluronidase digestions as controls hematoxylin and eosin and Mallorys triple connective tissue stain (Holde and Isler 58 Baker 58) Mitochondria were demonstrated by the Altman technique following fixation in Regauds fluid The glands of two turtles were perfused by the method of Williams (48) to demonstrate blood vessels

Tissue for electron microscopy was fixed in phosphate buffered 2% osmium tetroxide (Millonig 61) and dehydrated with acetone the fixed tissue was embedded in Epon (Luft 61) sectioned and stained either with lead hydroxide (Karnovsky 61) or lead citrate (Reynolds 63) The sections were examined in an RCA EMU 3F electron microscope equipped with a double condenser and a 40 μ platinum objective aperture Electron micrographs were taken at initial magnifications 4 100 to 12 000 and enlarged photographically as desired One micron thick sections of epon embedded tissues were mounted on glass slides and stained with toluidine blue

RESULTS AND OBSERVATIONS

Gross morphology

The two species of marine turtles that were examined have salt glands which are essentially similar in all histological details These paired lacrymal glands located within the orbits posterior and dorsal to the eye constitute between 0 05 to 0 1% of the total body weight In lateral view they are roughly pyrimidal in form with the bulges of individual secretory lobules clearly visible at the surface Dense sheaths of interlobular connective tissue separate the lobules Internally each of the 100 or more secretory lobules consists of myriad tightly packed branched tubules that radiate from a central excretory canal (fig 1) The central canals coalesce into one large tortuously infolded duct which opens externally to the posterior canthus of the eye Histologically therefore the modified lacrymal glands of marine turtles may be classified as compound branched tubular glands

Broad sheaths of intralobular connective tissue surround the central canals while only a thin sleeve of peritubular con

[1] Green turtles were secured through the courtesy of Dr Klaus Fisher Duke University

in the apical cytoplasm bordering the tubular lumen The mitochondria take a variety of forms but most are seen as long or short rodlets Numerous tightly packed cristae are oriented more or less parallel to the short axis of the mitochondria and a variable number of large dense granules are suspended within the matrix The intramitochondrial granules are nearly spherical in outline and although some are larger they average 200–300 A in diameter

Glycogen granules are very abundant within the basal cytoplasm of the tubule cells Clumps of glycogen are frequently sequestered within alternated looped mitochondria

The small basal cells that lie flat against the basement membrane of the tubule are covered by the microvilli of overlying secretory cells Unlike the secretory cells the basal cells have a nearly smooth plasma membrane There are only a few mitochondria but numerous smooth surfaced vesicles and some glycogen granules are present in the cytoplasm The nucleus is prominent comprising nearly one half of the cell volume Small filaments tentatively identified as tonofilaments may be clumped in twisted masses or scattered diffusely through the cytoplasm they are a distinguishing characteristic of the basal cells (fig 16)

The central canals

Two distinct cell types form the stratified mucous epithelium that lines the central canals Immediately subjacent to the surrounding capsule of intralobular connective tissue are several layers of small cells with scant cytoplasm and large nuclei Along the epithelial surface lining the lumen of the canal itself is a single row of large closely packed goblet cells with basal nuclei (figs 7 8) The goblet cells appear to be in various stages of mucus synthesis and release since there are many transitional intermediate sized ones lining the canal Those that have discharged their contents into the lumen show only a vacuolated membrane bound sac projecting outward into the lumen

Central canal cytochemistry

Central canal cells may be distinguished readily from the tubule cells since their cytoplasm contains extremely high concentrations of a naphthyl esterase (fig 12) and a few mitochondria (figs 5–7) The large mucus cells differ from the small underlying epithelial cells in giving intense reactions for cholinesterase (fig 2) acid phosphatase (fig 8) and ATPase in their apical caps The mucous secretion of the goblet cells is highly PAS positive and stains metachromatically with toluidine blue above pH 3 These staining reactions are unaffected by previous digestion of the tissue section with saliva diastase or hyaluronidase

DISCUSSION

The salt secreting lacrymal glands of marine turtles are comprised of a heterogeneous population of cells Along the length of the branched secretory tubules from the center to the periphery of each lobule the cells vary progressively in size shape and chemical reactivity At the blind ends of the secretory tubules the terminal cells are small in size they contain glycogen monoamine oxidase and phosphorylase in high concentration but only low levels of succinic dehydrogenase and cytochrome oxidase The apical surfaces of these cells are reactive for adenosine triphosphatase Centripetally there is a gradual transition between the terminal cells and the principal secretory cells and the principal secretory cells themselves also change progressively in size and increase in histochemical reactivity toward the center of the lobule The principal cells contain lipids succinic dehydrogenase and cytochrome oxidase in high concentration but little glycogen monoamine oxidase or phosphorylase The intercellular channels between the principal cells become progressively more conspicuous toward the center of the lobule and the mitochondria within the cells become more numerous Small basal cells that are found among the principal secretory cells in the turtle salt gland have not been reported in the salt glands of birds (Komnick 63a b c) and seem to be unique in the turtle Where the secretory tubules join the central canal the strikingly different cells of the central canal are admixed with the principal cells The central canal cells contain high concentrations of non specific esterase and

ripheral cells contain more glycogen and react more intensely for phosphorylase and monoamine oxidase than do the principal cells Occasionally small basophilic clumps are evident in the peripheral cells

Different phosphatases are extremely abundant within these glands but are separately and discretely localized to specific areas Acid phosphatase activity is strongest nearest the central canal and appears as a sharply localized band near the cell membrane at the basal surface of the principal secretory cells (fig 8) Alkaline phosphatase is restricted to the connective tissue (fig 9) and blood vessel endothelium Non mitochondrial ATPase is sharply localized as a dense line on or near the plasma membrane at the apical cell surfaces of the peripheral cells (fig 10) ATPase activity is also evident within the connective tissue the endothelial cells lining the vascular system and as a thin perinuclear ring in each of the tubule cells

The broad intercegllular channels between adjacent tubule cells contain abundant mucopolysaccharides They stain a bright blue green with alcian blue and an intense pink after the PAS reaction even when the sections are treated with diastase saliva or hyaluronidase (fig 11) A red γ metachromasia is evident following sulfation with toluidine blue at pH 5 or after the technique of Hess and Hollander (fig 4) The lateral borders of the peripheral cells are not as strongly metachromatic as the borders of the principal cells The basement membrane is PAS positive but does not stain metachromatically (fig 11) Using these same techniques it is also possible to make distinctions between the ground substance of the connective tissue and the intercellular mucopolysaccharides since the sugary constituents associated with the connective tissue at best exhibit only a purple (β) metachromasia and are faintly PAS positive A negative image of the intercellular channels is apparent when the tissues are stained with acid dyes The intercellular channels are not readily demonstrated by hematoxylin and eosin staining

The small "basal" cells are differentiated cytochemically from the remainder of their tubule cells by the positive reaction of their cytoplasm for α naphthyl esterase (fig 3) The secretory cells have no esterase activity In addition the basal cells contain few mitochondria are low in oxidative enzymes and have an acidophilic cytoplasm

Cytology of principal secretory cells

Electron micrographs show that the channels between opposed secretory cells are packed with long pleomorphic microvilli that extend from and fringe the cell margins (fig 13) In some regions the microvilli are truly digitiform while in other areas they appear as flat folds The microvilli of adjacent secretory cells intermesh loosely with one another and are linked by occasional desmosomes Irregularly arranged clear spaces appear between them forming tortuous intercellular channels that average 1 5 μ in width (fig 14) At the base of each cell the microvilli are sparse and may be flattened against the basement membrane (fig 16) No fibrous elements or other cytoplasmic organelles extend outward into the microvilli

Scant irregular short microvilli extend outward from the apical cell surface into the lumen of the tubule (fig 15) No open or direct connection was observed between the intercellular channels and the lumen of the secretory tubules Without exception the lateral and luminal surfaces of the cell are separated by a continuous system of prominent terminal bars and intermittent desmosomes that resemble the junctional complexes found in other epithelia (fig 15)

A large number of small irregularly shaped profiles of endoplasmic reticulum predominantly of the smooth surface form are distributed evenly throughout the central and basal cytoplasm (fig 13) Smooth surfaced vesicles are sometimes evident near the lateral margins of the cells immediately subjacent to the microvillous borders (fig 14) and they are always present in large numbers in the cell apex (fig 15) In addition vesicles are often associated with the stacked cisternae of the Golgi apparatus that usually assume a supranuclear position

Abundant mitochondria are distributed evenly throughout the basal cytoplasm None of these organelles are located in the villous processes fringing the cells o

surfaces of salt secreting cells in the lacrymal gland of turtles in the nasal glands of birds and in the rectal glands of elasmobranchs supports the hypothesis that the glycocalyx is linked with electrolyte transport

Mitochondria are packed within the cytoplasm of the secretory cells in the turtle salt glands Abundant mitochondria are also conspicuous within the secretory cells of the avian salt gland (Doyle 60 Fawcett 62 Komnick 63c) and elasmobranch s rectal gland (Bulger 63) They are concentrated at the absorptive surfaces of these cells Strong reactions for both cytochrome oxidase and succinic dehydrogenase occur in the principal cells suggesting a high level of oxidative phosphorylation The large numbers of mitochondria their production of high energy compounds and their close association with the plasma membranes of the absorptive surfaces suggest a primary role in salt secretion

The peculiar vascular architecture of the salt gland of the turtle probably contributes to its capacity to concentrate and secrete electrolytes Arteries in the central lobular connective tissue ramify into a capillary plexus paralleling the secretory tubules and the capillaries eventually empty into venous sinuses at the periphery of each lobule In the salt glands of marine birds (Fange et al 58) the blood flow is counter to the pathway of salt secretion and the arterial blood circulates first through the mid portion of each lobule Schmidt Nielsen (61) has shown that such a countercurrent flow cannot function in ion concentration like the countercurrent multiplier system found in the mammalian kidney The circulatory pattern in the turtle salt gland however does expose the most metabolically active secretory cells (i e those near the center of the lobule) to fresh arterial blood A similar pattern is repeated in the non homologous salt secreting nasal glands of marine birds This system may be adaptive for optimal salt secretion

From the histochemical evidence presented the lacrymal salt secreting glands of marine turtles appear to have a double innervation The nerves positive for cholinesterase are probably cholinergic fibers of the parasympathetic nervous system and the nerves reactive for monoamine oxidase are probably adrenergic fibers of the sympathetic nervous system The cholinergic fibers ramify through the peritubular connective tissue but the adrenergic fibers seem to be restricted primarily to the perilobular connective tissue This suggests that the cholinergic secretory fibers may affect the interlobular arteries Metacholine evokes secretion in the turtle salt gland (Schmidt Nielsen and Fange 58) and in the avian salt gland epinephrine blocks secretion (Fange et al 58b) Indications of the effect of acetylcholine on the secretory cells may also be drawn from the literature Borut and Schmidt Nielsen (63) showed that metacholine causes an increase in the rate of respiration in avian salt gland tissue slices but NaCl in increased concentration inhibits respiration Salt secretion then is mediated at least partially by the nervous system and is not a direct effect of an osmotic load on the secretory epithelium

LITERATURE CITED

Baker J R 1958 Principles of Biological Technique Methuen and Co Ltd London

Bennett H S 1963 Morphological aspects of extracellular polysaccharides J Histochem Cytochem *11* 14–23

Borut A and K Schmidt Nielsen 1963 Respiration of avian salt-secreting gland in tissue slice experiments Am J Physiol 204 573–581

Bulger R E 1963 Fine structure of the rectal (salt-secreting) gland of spiny dogfish *Squalus acanthias* Anat Rec *147* 95–127

Burstone M S 1958 Histochemical comparison of naphthol AS phosphates for the demonstration of phosphatases J Natl Cancer Inst *20* 601–616

——— 1959 New histochemical techniques for the demonstration of tissue oxidase (cytochrome oxidase) J Histochem Cytochem 7 112–122

Doyle W L 1960 The principal cells of the salt-gland of marine birds Exptl. Cell Res *21* 386–393

——— 1962a Secretory cells of the rectal salt gland of an elasmobranch *Urolophus* Anat Rec 142 228 (abstr)

——— 1962b Tubule cells of the rectal salt gland of *Urolophus* Am J Anat. 111 223–238

Ellis R A and J H Abel 1964 Intercellular channels in the salt secreting glands of marine turtles Science *144* 1340–1342

Ellis R A C C Goertemiller Jr R A DeLellis and Y H Kablotsky 1963 The effect of a salt water regimen on the development of the

monoamine oxidase but they have low levels of succinic dehydrogenase and cytochrome oxidase Small peripheral and large principal secretory cells have also been reported in the salt gland of the duck (Scothorne 58 59 Ellis et al 63) in the herring gull (Fange et al 58) and in the rectal gland of the dogfish (Bulger 63) There is therefore overwhelming evidence that the epithelium of the salt secreting glands in birds reptiles and fishes cannot be considered as a homogeneous cell population

The salt secreting nasal glands of marine birds the rectal glands of elasmobranchs and the lacrymal glands of marine turtles have many common cytochemical and cytological features All are lobulated branched tubular glands In all these species the secretory segments of the glands are composed of two different cell types small terminal cells that probably have a generative function (Ellis et al 63) and larger principal cells that are active in salt secretion (Doyle 60 Komnick 63c) The principal cells have abundant mitochondria high levels of succinic dehydrogenase and cytochrome oxidase they stain deeply for phospholipid and have a surface coat of mucopolysaccharide Acid phosphatase is usually present at the base of the principal cells Both the basal and lateral absorptive surfaces of the principal cells are extensively folded to increase their surface area while the apical secretory surface of the principal cells is very small The principal cells usually contain little glycogen phosphorylase or monoamine oxidase All of these factors are probably relevant to the salt secreting function of the glands but three seem particularly significant (1) the absorptive surface of the principal cells is vast relative to the restricted secretory surface (2) a mucopolysaccharide is associated with the absorptive surfaces of the principal cells and (3) the principal cells are packed with mitochondria rich in the oxidative enzymes that aid in the synthesis of ATP

The surface area of the principal cells that is exposed to the extracellular fluid is extensive in constrast the cell surface that borders the lumen is extremely narrow (fig 16) By a conservative approximation the area of the absorptive surface of these cells exceeds the area of the s tory surface by a factor greater 1000 1 The intercellular channels run from the perimeter of the tubu the junctional complexes borderin lumen allow extracellular fluid to both the lateral and basal surfaces T surfaces are expanded by the irre outlines of the principal cells and b fringe of microvilli that border the i cellular channels The pleomorphis the microvilli suggests that this surfa the cell is active in pinocytosis and is evidence of pinocytotic vesicles i adjacent cytoplasm In the rectal gla elasmobranchs the salt secreting cell have highly folded basal surfaces different modification of the cell su the principal cells in the salt glan marine birds achieve the same goal Fawcett (62) cites this cell type a ultimate example of a cell with an e sive basal absorptive surface The si cance of these observations in salt s tion is not entirely clear but possibilities present themselves (1 expanded surface area provides for exchange of metabolites permitting cells to sustain high levels of activity the expanded surface area may permi more efficient trapping of ions

Cytochemical techniques reveal tha broad intercellular channels betwee lateral margins of the principal cel the turtle salt gland are intensely positive and exhibit a variable degre metachromasia indicating that a n tively charged carbohydrate probab mucopolysaccharide or glycoprotein sides between the secretory cells M polysaccharides have been reported tween the secretory cells in the rectal g of the dogfish (Bulger 63) and w the principal cells of the nasal gland ducks (Ellis et al 63) Many cells a surface coat of mucopolysaccharide "glycocalyx and Bennett (63) has posed that the anionic charge of the cocalyx could produce an effective m of attracting trapping and concentra cations In fact some mucopolysacchar do have the capacity for binding cat and can function as ion exchange re (Farber 60) The abundant mucop saccharides associated with the absorp

salt glands of domestic ducklings Dev Biol 8 286
Ellis R A and W Montagna 1958 Histology and cytochemistry of human skin XV Sites of phosphorylase and amylo 1 6 glucosidase activity J Histochem Cytochem 6 201–207
Fange R and K Fugelli 1963 The rectal salt gland of elasmobranchs and osmoregulation in Chimaeroid Fishes Sarcia 10 27–34
Fange R K Schmidt Nielsen and H Osaki 1958a The salt gland of the herring gull Biol Bull 115 161–171
Fange R K Schmidt Nielsen and M Robinson 1958b The control of secretion from the avian salt gland Am J Physiol 195 321–326
Farber S J 1950 Mucopolysaccharides and sodium metabolism Circulation 21 941–953
Fawcett D W 1962 Physiologically significant specializations of the cell surface Circulation 26 1105–1126
Gersh I and H R Catchpole 1948 The organization of ground substance and basement membrane and its significance in tissue injury disease and growth Am J Anat 85 457–523
Glenner G G H G Burtner and G W Brown Jr 1957 The histochemical demonstration of monoamine oxidase activity by tetrazolium salts J Histochem Cytochem 5 591–600
Gomori G 1950 An improved histochemical technique for acid phosphatase Stain Tech 25 81–86
——— 1952 Microscopic Histochemistry Principles and Practice Univ of Chicago Press Chicago Ill
Hess M and F Hollander 1947 Permanent metachromatic staining of mucus in tissue sections and smears J Lab Clin Med 32 905
Holde P and H Isler 1958 The effect of phosphomolybdic acid on the stainability of connective tissue by various dyes J Histochem and Cytochem 6 265–270
Karnovsky M J 1961 Simple methods for staining with lead at high pH in electron microscopy J B B C 11 729
Koelle G B and J S Friedenwald 1949 A histochemical method for localizing cholinesterase activity Proc Soc Exp Biol Med 70 617–622
Komnick H 1963a Elecktronenmickroskopische Untersuchungen zur funktionellen Morphologie des Ionentransportes in der Salzdruse von Larus argentatus (I Bau und Feinstruktur der Salzdruse) Protoplasma 56 274–314
——— 1963b Elecktronenmickroskopische Untersuchungen zur funktionellen Morphologie des Ionentransportes in der Salzdruse von Larus argentatus (II Funktionelle Morphologie Blutgefasse) Protoplasma 56 385–419
——— 1963c Electronenmickroskopische Untersuchungen zur funktionellen Morphologie des Ionentransportes in der Salzdruse von Larus argentatus (III Funktionelle Morpholog[...] Tubulusepithelzellen) Protoplasma 56 636
Luft J H 1961 Improvements in epoxy embedding methods J B B C 9 409–[...]
Marples B J 1932 The structure and de[...]ment of the nasal glands of birds Proc Soc (London) 4 820–844
McManus J F A 1948 The periodic [...] routine applied to the kidney Am J Pa[...] 24 643–653
Millonig G 1961 A modified procedure [...] lead staining of thin sections J C B [...] 736–740
Montagna W H B Chase and H P Melar[...] 1951 Histology and cytochemistry of hu[...] skin I Metachromasia in the mons p[...] J Natl Cancer Inst 12 591–597
Mowry R 1958 Observations on the us[...] sulfuric acid in ether J Histochem Cytoch[...] 6 82
Nachlas M M and S M Seligman 1949 [...] histochemical demonstration of esterase [...] Natl Cancer Inst 9 415–425
Nachlas M M K C Tsou E DeSouza [...] Cheng and S M Seligman 1957 Cytoc[...]ical demonstration of succinic dehydroge[...] by the use of a new p nitrophenyl substit[...] ditetrazole J Histochem Cytochem 5 [...] 436
Pearse A G F 1961 Histochemistry T[...]retical and Applied Little Brown and [...] Boston
Peters A 1892 Beitrog zur kenntniss [...] harder schen druse Arch Mikr Anat [...] 192
Reynolds E S 1963 The use of lead cit[...] at high pH as an electron opaque stain in [...]tron microscopy J C B 17 208–212
Schmidt Nielsen K 1961 Concentrating m[...]anism of the kidney from a comparative [...] point Amer Heart J 62 579–586
Schmidt Nielsen K and R Fange 1958 [...] glands in marine reptiles Nature 182 784
Scothorne R J 1958 A histochemical st[...] of the nasal (supraorbital) gland of the d[...] Nature 181 732
——— 1959 The nasal glands of birds A [...]tological and histochemical study of the [...] active gland in the domestic duck J An[...] 93 246–256
Takeuchi T and H Kuriaki 1955 Hi[...]chemical method for glucosan phosphoryl[...] and transglycolase J Histochem Cytoche[...] 3 153–160
Wachstein M and E Meisel 1957 Histoche[...]istry of hepatic phosphatases at a physiologi[...] pH Am J Clin Pathol 27 13
Williams T W 1948 The visualization [...] vertebrate capillary beds by intravascular p[...]cipitation of lead chromate Anat Rec 1[...] 115–126

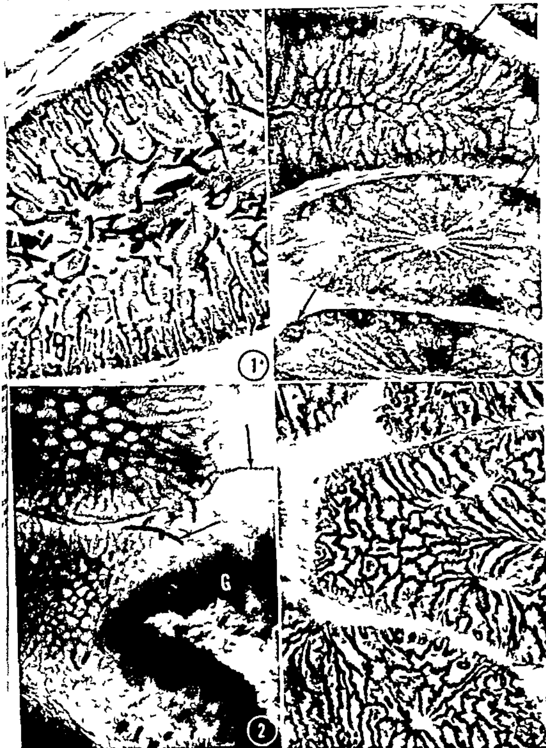

1
G
2

PLATE 1

EXPLANATION OF FIGURES

1 This photomicrograph illustrates the basic histological organization and the vascular system of a lobule in the lacrymal gland of the green turtle The branching secretory tubules are small at the periphery of the lobule and increase steadily in size centripetally where they join the central canal (arrows) At the left a large artery (*A*) penetrates the lobule and branches to form arterioles that extend along the central canal From the arterioles capillaries radiate between the secretory tubules to the periphery of the lobule where they empty into venous sinusoids Lead chromate perfusion counterstained with hematoxylin and eosin (× 70)

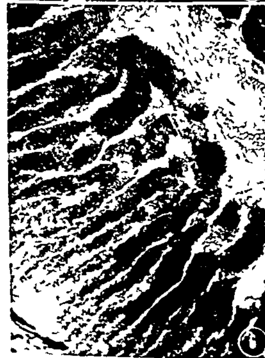
2 Cholinesterase activity is restricted to large interlobular nerve fibers (arrows) smaller intralobular fibers that form a peritubular net work and the goblet cells (G) lining the central canals Acetylthiocholine iodide substrate 60 μ formalin fixed cryostat section incubation one hour (× 60)

3 Strong alpha naphthol esterase activity may be demonstrated in the small basal cells near the perimeter of each tubule (arrows) In this preparation the channels between the principal cells were also reactive for this enzyme but this was not a consistent finding Ten microns cryostat section α naphthol acetate substrate 5 minutes incubation at room temperature (× 450)

4 The broad intercellular channels between the secretory cells stain metachromatically with toluidine blue The irregular surfaces of the cells intermesh with one another to form a jigsaw puzzle pattern Hess and Hollander technique for permanent metachromasia (× 430)


5




6


G
B
8

PLATE 2

EXPLANATION OF FIGURES

5 The principal secretory cells have cytochrome oxidase within cytoplasmic granules the intercellular channels and the nuclei are unstained The peripheral cells and the cells lining the central canal react weakly Paraphenylene Diamine base Incubation 15 minutes (× 100)

6 The pattern of succinic dehydrogenase activity in the gland parallels that of cytochrome oxidase the reaction is weak in the cells at the periphery of the lobule intense in the principal secretory cells and weak in the cells lining the central canals Tetranitro blue tetrazolium incubated 15 minutes (× 110)

7 This micrograph shows only a small portion of a lobule in the area of its central canal The cytoplasm of the principal secretory cells is intensely sudanophilic while the nuclei and intercellular channels are unstained The cells lining the central canal as well as the surrounding connective tissue contain little stainable lipid A large artery (arrow) bisects the field Ten microns cryostat section Sudan black B (× 190)

8 Acid phosphatase activity is restricted to a narrow band along the base of the principal secretory cells (*B arrows*) and to the goblets of the mucous cells lining the central canal (*G arrows*) Twelve microns cryostat section Naphthol AS B1 tion Sudan black B (× 190)

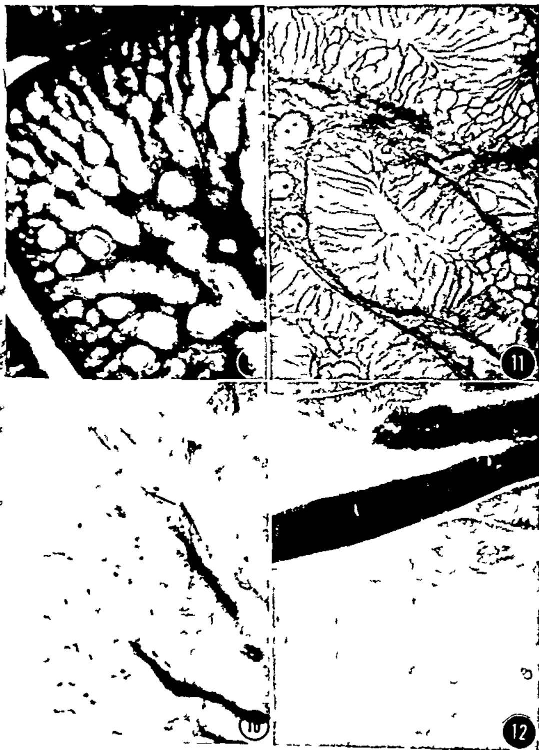

11
10
12

PLATE 3

EXPLANATION OF FIGURES

9 Alkaline phosphatase activity is restricted to the blood vessels and connective tissue in the turtle salt gland Twenty microns cryosat section sodium a naphthyl phosphate substrate 20 minute incubation (× 100)

10 Non mitochondrial ATPase activity is demonstrated within the blood vessels and the connective tissue A thin dense line of ATPase is also present along the lumen at the periphery of each tubule (arrows) None of the enzyme is detect able along the borders or within the principal secretory cells Twelve microns cryostat section Wachstein and Meisel method substrate disodium salt ATP 30 minutes incubation (× 200)

11 Intense PAS positive diastase resistant material is found within the well devel oped basement membrane surrounding each tubule within the broad intercellular channels at the lateral surfaces of the secretory cells and around each of the blood vessels The ground substance of the connective tissue and cytoplasm of the secretory cells is also moderately reactive Five microns paraffin section 30 minutes digestion with diastase at 37 C PAS stain (× 400)

12 Alpha napthylesterase activity is restricted primarily to the cytoplasm of cells lining the central canal The tubule cells do not give any more reaction than in the control sections incubated without substrate Twelve micron cryostat sec tion a naphthyl acetate substrate 5 minutes incubation at room temperature (× 300)

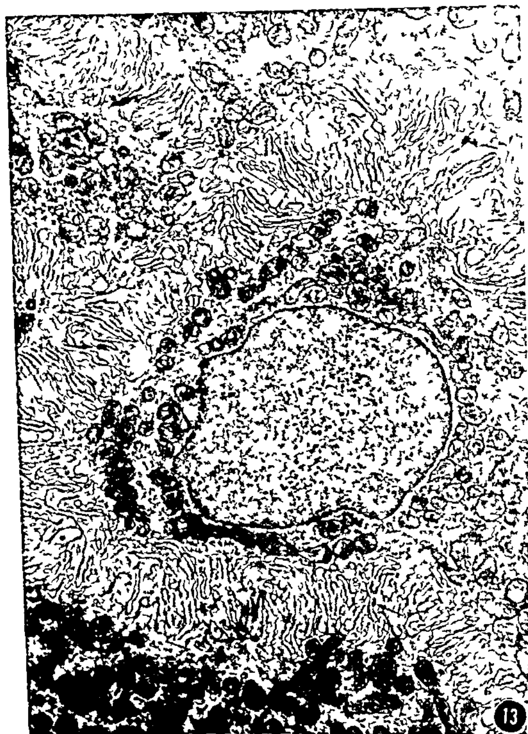

13

PLATE 4

EXPLANATION OF FIGURE

13 A secretory cell sectioned at the level of the nucleus and the cyto plasm of the several adjacent cells are shown in this electron micro graph Mitochondria glycogen and small smooth surfaced vesicles of endoplasmic reticulum fill the cytoplasm around the nucleus Tall pleomorphic microvilli pack the intercellular spaces forming broad tortuous intercellular channels The microvilli of adjacent cells in terdigitate and are connected by occasional desmosomes (arrows) (× 10 800)

14

15

PLATE 5

EXPLANATION OF FIGURES

14 Portions of the intercellular channels surrounding three cells are shown in this electron micrograph the intercellular spaces lying between the projecting microvilli of adjacent cells are irregular and variable in width Cytoplasmic organelles are excluded from the microvilli but mitochondria and small smooth surfaced vesicles (arrows) are evident near their bases (× 24 120)

15 In this electron micrograph seven cells are sectioned at their apices Junctional complexes separate the lateral and luminal surfaces of the cells and the interdigitating microvilli on the adjoining lateral surfaces end abruptly at these points The apical cytoplasm is packed with numerous vesicles of nearly uniform size but there are no mitochondria and little glycogen in this zone The small tubular lumen contains a few villous projections from the apical surface (× 26 300)

PLATE 6

EXPLANATION OF FIGURES

16 In this electron micrograph the basal portions of several salt secreting cells are extended along their apposed basement membranes The long villous processes on the sides of the principal cells intermesh laterally and they are flattened against the basement membrane A small basal cell (arrows) wedged among the principal cells contains few mitochondria and little glycogen but numerous profiles of SSER and some filamentous cytoplasmic elements The surface of the basal cell is nearly smooth and bears no villous process (× 14 700)

17 Portions of three secretory tubules with adjoining connective tissue and capillaries are included in this photomicrograph The large principal cells outlined by the negative images of broad intercellular channels extend from the small central lumen to the basement membrane Small basal cells are interposed between bases of the secretory cells (arrows) One micron section stained with toluidine blue epon embedded (× 640)

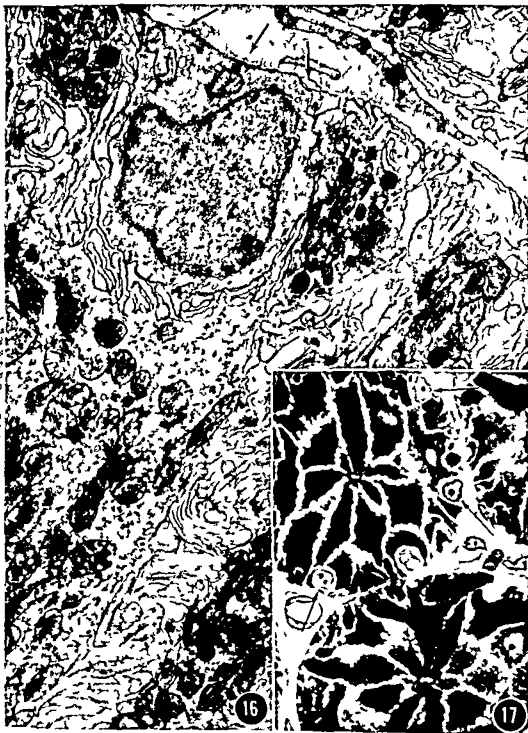

16
17

PLATE 6

EXPLANATION OF FIGURES

16 In this electron micrograph the basal portions of several salt secreting cells are extended along their apposed basement membranes The long villous processes on the sides of the principal cells intermesh laterally and they are flattened against the basement membrane A small basal cell (arrows) wedged among the principal cells contains few mito chondria and little glycogen but numerous profiles of SSER and some filamentous cytoplasmic elements The surface of the basal cell is nearly smooth and bears no villous process (× 14 700)

17 Portions of three secretory tubules with adjoining connective tissue and capillaries are included in this photomicrograph The large principal cells outlined by the negative images of broad intercellular channels extend from the small central lumen to the basement mem brane Small basal cells are interposed between bases of the secretory cells (arrows) One micron section stained with toluidine blue epon embedded (× 640)

ıne Structure of the Photoreceptor Cells of the ɹround Squırrel (*Cıtellus trıdecemlıneatus* ıdecemlıneatus)[1]

MARTIN J HOLLENBERG[2] AND MAURICE H BERNSTEIN
Department of Anatomy Wayne State Unıversıty School of Medıcıne
Detroıt Mıchıgan

ABSTRACT The structure of the photoreceptor cells of the ground squırrel retına has been studıed by lıght and electron mıcroscopy The ground squirrel photoreceptor cells are of partıcular morphologic interest because this mammal is believed to possess a pure cone retına Light mıcrographs show that the ground squırrel retına possesses an unusually narrow outer nuclear layer a characterıstıc feature of pure cone or predominantly cone retınae By light mıcroscopy all the photoreceptor outer segments appear unıform in size shape and posıtıon and resemble cones more closely than rods Electron mıcrographs of ground squırrel photoreceptor cells also reveal a uniform struc ture typical of cones of other vertebrates Each of the photoreceptor outer segments is formed by flattened saccules lying one on top of the other and many of the saccules as is characterıstıc of cones are continuous with the overlying plasma membrane The basal processes of the photoreceptor cells also are cone lıke in nature sınce each contains several synaptic lamellae and makes contact with a large number of dendrıtıc processes arising from cells ın the inner nuclear layer It is concluded that the ground squirrel retina from a purely morphologıc standpoınt is exclusıvely or almost exclu sively pure cone in type

The fine structure of mammalian photo- ceptor cells has previously been studıed ı both mıxed rod and cone retinae of ıurnal mammals such as monkey (Cohen 1a b) and man (Mıssotten 60) and ın reponderantly rod retınae of prımarıly octurnal animals such as the albıno rat Ladman 58) and guinea pıg (Sȷostrand 8 61) The present report deals with ıe photoreceptor cells of the ground squir l (*Cıtellus trıdecemlıneatus trıdecem neatus*) an animal of predominantly dı rnal habits believed to possess a pure one type of retına (Walls 42 Karli 51 ılter 54 Arden and Tansley 55 Cresci llı 61 Tansley 61 Vaıdya 64)

The ground squırrel is a member of the ımily Sciurıdae which also includes the yıng squirrels and the gray squırrels The yıng squirrels are nocturnal animals ʼhose retinae are thought to be predomi antly rod in type (Walls 42) whereas he gray squırrels generally diurnal ani nals have recently been shown to possess mixed rod and cone retina (Cohen 64) The histologic structure of the retina of the lıurnal ground squirrel has recently been tudied by Vaıdya (64) The results of his light microscopic investigation indi cate that the retına of the ground squırrel (*Cıtellus trıdecemlıneatus trıdecemlınea tus*) contaıns only one varıety of photo- receptor which conforms in morphology to the cone type of vısual cell

The results of the present lıght and elec tron mıcroscopıc study also ındıcate that at least from a purely morphologıc stand point the ground squırrel retına ıs exclu sıvely or almost exclusıvely pure cone in type Only one variety of receptor has been found in the anımals studıed and this cell has the ultrastructural characterıstıcs which have come to be assocıated with the cone receptor

MATERIALS AND METHODS

Electron mıcroscopy

The retinae of 20 adult ground squirrels were used for this study The animals were placed under pentobarbıtal anesthesia the eyes removed and dıvided at the ora ser

[1] Supported in part by g nts from th Nation l In titut of Neurologic l Dise se and Blindnes (NB-02010-06) U S Publi H lth Service Th Lif In u nce Medi l Rese rch Fund (G-64-62) and a postdoct l fellow hip from The American H rt A soci tion (M J H.)

[2] Present ddres Dep rtment of An tomy Medical Sci n s B ilding Uni e ity of Western Ont rio London Ont rio Can d

ıne Structure of the Photoreceptor Cells of the ɹround Squirrel (*Citellus tridecemlineatus* ıdecemlineatus) [1]

MARTIN J HOLLENBERG [2] AND MAURICE H BERNSTEIN

Department of Anatomy Wayne State University School of Medicine Detroit Michigan

ABSTRACT The structure of the photoreceptor cells of the ground squirrel retina has been studied by light and electron microscopy The ground squirrel photoreceptor cells are of particular morphologic interest because this mammal is believed to possess a pure cone retina Light micrographs show that the ground squirrel retina possesses an unusually narrow outer nuclear layer a characteristic feature of pure cone or predominantly cone retinae By light microscopy all the photoreceptor outer segments appear uniform in size shape and position and resemble cones more closely than rods Electron micrographs of ground squirrel photoreceptor cells also reveal a uniform structure typical of cones of other vertebrates Each of the photoreceptor outer segments is formed by flattened saccules lying one on top of the other and many of the saccules as is characteristic of cones are continuous with the overlying plasma membrane The basal processes of the photoreceptor cells also are cone like in nature since each contains several synaptic lamellae and makes contact with a large number of dendritic processes arising from cells in the inner nuclear layer It is concluded that the ground squirrel retina from a purely morphologic standpoint is exclusively or almost exclusively pure cone in type

The fine structure of mammalian photoreceptor cells has previously been studied in both mixed rod and cone retinae of diurnal mammals such as monkey (Cohen 61a b) and man (Missotten 60) and in preponderantly rod retinae of primarily nocturnal animals such as the albino rat (Ladman 58) and guinea pig (Sjostrand 58 61) The present report deals with the photoreceptor cells of the ground squirrel (*Citellus tridecemlineatus tridecemlineatus*) an animal of predominantly diurnal habits believed to possess a pure cone type of retina (Walls 42 Karli 51 Vilter 54 Arden and Tansley 55 Crescitelli 61 Tansley 61 Vaidya 64)

The ground squirrel is a member of the family Sciuridae which also includes the flying squirrels and the gray squirrels The flying squirrels are nocturnal animals whose retinae are thought to be predominantly rod in type (Walls 42) whereas the gray squirrels generally diurnal animals have recently been shown to possess a mixed rod and cone retina (Cohen 64) The histologic structure of the retina of the diurnal ground squirrel has recently been studied by Vaidya (64) The results of this light microscopic investigation indicate that the retina of the ground squirrel (*Citellus tridecemlineatus tridecemlineatus*) contains only one variety of photoreceptor which conforms in morphology to the cone type of visual cell

The results of the present light and electron microscopic study also indicate that at least from a purely morphologic standpoint the ground squirrel retina is exclusively or almost exclusively pure cone in type Only one variety of receptor has been found in the animals studied and this cell has the ultrastructural characteristics which have come to be associated with the cone receptor

MATERIALS AND METHODS

Electron microscopy

The retinae of 20 adult ground squirrels were used for this study The animals were placed under pentobarbital anesthesia the eyes removed and divided at the ora ser

[1] Supported in part by grants from the National Institute of Neurological Diseases and Blindness (NB-02010-06) U S Public Health Service The Life Insurance Medical Research Fund (C-64-62) and postdoctoral fellowship from The American Heart Association (M.J H)

[2] Present address Department of Anatomy Medical Science Building University of Western Ontario London Ontario Canada.

rata The posterior halves were placed in cold 2% osmium tetroxide buffered with veronal to pH 7 4 and containing 4 5% sucrose The tissues were fixed for one hour in the cold and then for one hour at room temperature Following fixation the retinae were cut into small pieces rapidly dehydrated in alcohol transferred to ace tone and embedded in Vestopal W Thin sections were cut on a L K B or Porter Blum microtome and then placed on Form var or carbon coated grids The sections were stained with uranium or lead salts or both and examined in a RCA EMU 3E or Hitachi Model HS 6 electron microscope operated at 50 K V The photographic plates were developed in Dektol (Kodak) at 28°C

Light microscopy

Retinal specimens obtained as above were fixed in 10% formalin for three or four days Following dehydration the speci mens were embedded in paraffin sectioned serially in various planes at thicknesses ranging from 3 to 5 μ and stained with hematoxylin and eosin Sections were ex amined in a Leitz Ortholux photomicro scope and photographed in black and white using 35 mm Panatomic X (Kodak) film

OBSERVATIONS

Light microscopy (figs 1 and 2)

Histologic sections of the ground squir rel retina (figs 1 and 2) show two out standing features First the outer nuclear layer is unusually narrow a structural peculiarity usually associated with the pre dominantly cone or pure cone type of ret ina (Walls 42) In the example shown from the upper half of the retina (fig 1) only a single layer layer of nuclei is pres ent Vaidya (64) has noted however that in the thicker lower half of the retina there are 2 to 3 strata of photoreceptor nuclei The uniformity of size shape and position of the photoreceptor outer segments is the second striking feature The outer seg ments are all relatively short and thick tapering to a small degree at their outer extremities In addition they maintain a constant relationship both to each other and to the line formed by the external limiting membrane (figs 1 and 2)

Electron microscopy
Pigment epithelium — photoreceptor junction (figs 3 and 4)

The pigment epithelium of the ground squirrel retina is formed by a single layer of rectangular cells containing spherical nuclei large granules of varying density scattered mitochondria and an almost agranular endoplasmic reticulum (fig 3) The cells are connected at the apices of their lateral borders by a prominent sys tem of terminal bars (fig 3)

In its apical zone the pigment epithe lium is broken up into numerous cyto plasmic prolongations varying in thickness from 0 1 to 2 0 μ (fig 3) between which are placed the outer segments of the photo receptor cells (fig 4) The thicker apical processes contain large dense granules similar to those present within the main body of the epithelial cell (fig 4) The apical processes are generally found in close proximity to the plasma membrane of the photoreceptor outer segments (fig 4)

Outer segments of the photoreceptor cells (figs 4 and 5)

All the outer segments of the ground squirrel retina studied have a similar ap pearance They are cylindrical averaging 7 μ in length and 1 to 2 μ in diameter Each is composed of a series of flattened sac cules averaging 150 A in width lying one on top of the other (figs 4 and 5) In the basal third of the outer segments adja cent to the ellipsoid many of the saccules are continuous with infoldings of the plasma membrane (fig 5) At the lateral borders the membranes forming a saccule diverge in opposite directions turn back on themselves and unite with adjoining membranes to form new units Commonly the turning membranes contain within their borders the terminations of 1 to 4 sac cules which in the plane of section have not reached the periphery of the outer seg ment As they loop back the membranes which fuse with their neighbors form the continuous outer boundary of the basal portion of the outer segment (fig 5) Towards their apices in contrast the outer segments are formed by a series of discrete discs lying one on top of the other en closed by a continuous but apparently separate plasma membrane (figs 4 and 5)

In addition to their complex inner struc ure the outer segments also possess an itricate array of external supports At ieir outer ends they are enveloped by the igment rich apical prolongations of the pithelial cells (figs 3 and 4) The inner ortions of the outer segments are more losely supported by thin cytoplasmic ex ensions called calycal processes by Cohen 63) arising from the periphery of the oncentration of mitochondria forming the llipsoid (fig 5) Similar cytoplasmic for nations have been recently described by Brown (63) in the retina of the mud puppy *Necturus* and have been known to exist in the vertebrate retina since the early descriptions by Schultze (1873)

Inner segments of the photoreceptor cells (figs 6 and 7)

The inner segments of the ground squir rel photoreceptor cells (fig 6) are cylin drical structures measuring from 14 to 18 μ in length and 1 to 3 μ in diameter Their internal structure is similar in most respects to that reported in this region of other mammalian retinae (Sjostrand 53 Cohen 60 61)

The mitochondria of the ellipsoid (fig 6) vary considerably in size and shape but most are orientated with their longest di ameter parallel to the long axis of the inner segment The cristae of the mito chondria appear to run in all directions without specific orientation Deeper in the inner segment the mitochondria are grad ually replaced by a zone of ergastoplasm (fig 6) marked by the presence of long narrow canaliculi and prominent Golgi complexes

External limiting membrane (fig 7)

The external limiting membrane in the ground squirrel retina is formed by a prom inent terminal bar system encircling the photoreceptor cells at the inner segment nuclear junction The terminal bars ap pear as local thickenings of the plasma membranes joining the photoreceptor cells to outer prolongations of the Muller or supporting cells (fig 7) The Muller cell processes broaden as they approach the terminal bar system occupy most of the space between the outer ends of the photo receptor nuclei and then divide above the external limiting membrane into a number of microvillous processes forming a pali sade around the inner segments of the photoreceptor cells (fig 7) The cytoplasm of the Muller cells is much less dense than that of the adjacent photoreceptor cells (fig 7)

The outer nuclear layer (figs 7 and 8)

The photoreceptor nuclei are oval in shape and lie with their long axis per pendicular to the retinal surface (fig 8) They average 5 μ in length 2 μ in width are separated by intervals ranging from 0 5 μ to 3 μ and commonly contain a prom inent nucleolus surrounded by clumped coarsely granular chromatin Each nu cleus is surrounded by a narrow zone of dense granular cytoplasm lying adjacent to relatively clear Muller cell prolongations (fig 8) Filamentous components are a prominent feature of the cytoplasm of both Muller and photoreceptor cells (fig 8)

Receptor synapses (figs 9 and 10)

The basal processes of the photoreceptor cells are dense club shaped structures usu ally separated by relatively lightly stained Muller cell extensions (fig 10) Occasion ally however the photoreceptor bases lie directly in contact with each other (fig 9) affording an anatomical basis for synaptic transmission of an inhibitory or excitatory nature between photoreceptor cells Lat eral receptor connections of this nature have also been described in other mam malian retinae including that of the gray squirrel (Sjostrand 58 Cohen 64) Each of the photoreceptor basal processes is in vaded by a large number of dendritic proc esses arising in the inner nuclear layer (figs 9 and 10) and the junctional sites are marked by a thickening of adjacent plasma membranes (figs 9 and 10) In ternally each basal process contains sev eral synaptic lamellae or ribbons (Smith and Sjostrand 61 Fine 62) and large numbers of synaptic vesicles grouped around the lamellae and dispersed through out the cell cytoplasm

The basal processes of the photoreceptor cells are separated from the nuclei of the inner nuclear layer by a complex zone

composed of numerous cytoplasmic processes arising in the inner nuclear zone and running outwards towards the photoreceptor bases (figs 9 and 10)

DISCUSSION

The structural organization of the ground squirrel retina as revealed by the foregoing data is virtually unique amongst vertebrates and points to the presence of a pure cone or nearly pure cone retina Several outstanding morphologic features lead to this conclusion

First the narrow outer nuclear layer present in the ground squirrel retina (fig 1) is a structural peculiarity which has come to be associated with cone rich retinae of predominantly diurnal animals (Walls 42) The presence of a narrow outer nuclear layer reflects a relatively small degree of convergence of nerve impulses traveling inwards to the ganglion cell layer and emphasizes the relative importance of individual photoreceptor impulses in this retinal type

Secondly the light micrographs of the ground squirrel retina (figs 1 and 2) reveal a remarkable consistency in the size shape and position of the photoreceptor outer segments The single morphologic variety of outer segment present is short and slightly tapered in appearance It more closely resembles the cone type of receptor than the long slender appearance of the typical rod

Finally many features which are characteristic of the cone type of receptor can be distinguished in electron micrographs of ground squirrel photoreceptor cells The basal third of the ground squirrel outer segment is formed by flattened saccules many of which are continuous with the plasma membrane of this portion of the cell (fig 5) Only towards their apices are the ground squirrel outer segments formed by discrete saccules lying within but separate from the overlying plasma membrane (fig 4) This structural arrangement has come to be recognized as characteristic of extra foveal vertebrate cones (Cohen 63 Dartnall and Tansley 63) Vertebrate rods in contrast are formed almost entirely by discs lying within but apparently separate from the overlying plasma membrane Only occasionally and only in a small region of the rod outer segment has it been possible to see direct communications between saccules and the surrounding plasma membrane (Cohen 63)

The basal processes of the ground squirrel photoreceptor cells also have a structural organization more typical of the cone type of receptor Each of the club shaped ground squirrel basal processes is invaded by many dendrites from the inner nuclear layer and each contains several synaptic lamellae or ribbons (figs 9 and 10) To date basal processes of this nature have been found in vertebrate cones only (Dartnall and Tansley 63) Basal processes of vertebrate rods are less complex They are spherical in shape and usually are penetrated by the dendrites of a single cell only (Dartnall and Tansley 63) Also they generally contain only a single synaptic ribbon although several may be present within rod spherules in the human retina (Missotten 60)

Taken together all of the above findings support the view that the ground squirrel retina is exclusively or almost exclusively pure cone in type It must be emphasized however that although some confirmation has already been obtained from electroretinographic studies (Bornschein 54 Arden and Tansley 55 Tansley 57 61 Crescitelli 61 Tansley Copenhaver and Gunkel 61) this conclusion is primarily based on consideration of morphologic evidence alone It is evident that final determination of the exact nature of the ground squirrel retina must await the results of further study in other fields

ACKNOWLEDGMENT

We wish to acknowledge the invaluable technical assistance of Wesley A Heiple

LITERATURE CITED

Arden G B and K Tansley 1955 The spectral sensitivity of the pure-cone retina of the souslik (*Citellus citellus*) J Physiol *130* 225-232

Bornschein H 1954 Elektrophysiologischen Nachweis einer I Retina bei einem Säuger (*Citellus citellus*) Naturwiss *41* 435

Brown P K I R Gibbons and G Wald 1963 The visual cells and visual pigment of the mudpuppy necturus J Cell Biology *19* 79-106

Cohen A I 1960 The ultrastructure of the rods of the mouse retina. Am J Anat *107* 23–48

——— 1961a Some preliminary electron microscopic observations of the outer receptor segments of the *Macaca rhesus* In The Structure of the Eye Edited by G K. Smelser Academic Press New York.

——— 1961b The fine structure of the extrafoveal receptors of the Rhesus monkey Exp Eye Res *1* 128–136

——— 1963 Vertebrate retinal cells and their organization Biol Rev *38* 427–459

——— 1964 Some observations on the fine structure of the retinal receptors of the American gray squirrel Invest Ophthal *3* 198–216

Crescitelli F 1961 The electroretinogram of the antelope ground squirrel Vision Res *1* 139–153

Dartnall H J A and K Tansley 1963 Physiology of vision Retinal structure and visual pigments Ann Rev Physiol 25 433–458

Fine B S 1962 Synaptic lamellae in the human retina an electron microscopic study J Neuropathology and Exp Neurology 22 255–262

Karli P 1951 Sur la structure de la retine du spermophile (*Citellus citellus* L) C R Soc Biol *145* 1376–1378

Ladman A J 1958 The fine structure of the rod bipolar cell synapse in the retina of the albino rat J Biophys and Biochem Cytol 4 459–466

Missotten L 1960 Étude des bâtonnets de la rétine humaine au microscope electronique Ophthalmologica *140* 200–214

Schultze M 1873 Manual of Human and Comparative Histology The New Sydenham Society London

Sjostrand F S 1953 The ultrastructure of the inner segments of the retinal rods of the guinea pig eye as revealed by electron microscopy J Cell and Comp Physiol 42 45–70

——— 1958 Ultrastructure of retinal rod synapses of the guinea pig eye as revealed by three dimensional reconstructions from serial sections J Ultrastructure Res 2 122–170

——— 1961 Electron microscopy of the retina In The Structure of the Eye Edited by G K Smelser Academic Press New York.

Smith C A and F S Sjostrand 1961 A synaptic structure in the hair cells of the guinea pig cochlea J Ultrastructure Research 5 184 192

Tansley K 1957 Some observations on mammalian cone electroretinograms Ophthalmology *133* Suppl *48* 7–14

——— 1961 Comparative anatomy of the mammalian retina with respect to the electroretinographic response to light In The Structure of the Eye Edited by G K Smelser Academic Press New York

Tansley K R M Copenhaver and R D Gunkel 1961 Spectral sensitivity curves of diurnal squirrels Vision Res *1* 154–165

Vaidya P G 1964 The retina and optic nerve of the ground squirrel *Citellus tridecemlineatus tridecemlineatus* J Comp Neurology *122* 347–353

Vilter V 1954 Histologie et activite electrique de la retine d un mammifere strictement diurne le spermophile (*Citellus citellus*) C R Soc Biol *148* 1768–1771

Walls G 1942 The vertebrate eye Bloomfield Hills Michigan Cranb ook

composed of numerous cytoplasmic processes arising in the inner nuclear zone and running outwards towards the photoreceptor bases (figs 9 and 10)

DISCUSSION

The structural organization of the ground squirrel retina as revealed by the foregoing data is virtually unique amongst vertebrates and points to the presence of a pure cone or nearly pure cone retina Several outstanding morphologic features lead to this conclusion

First the narrow outer nuclear layer present in the ground squirrel retina (fig 1) is a structural peculiarity which has come to be associated with cone rich retinae of predominantly diurnal animals (Walls 42) The presence of a narrow outer nuclear layer reflects a relatively small degree of convergence of nerve impulses traveling inwards to the ganglion cell layer and emphasizes the relative importance of individual photoreceptor impulses in this retinal type

Secondly the light micrographs of the ground squirrel retina (figs 1 and 2) reveal a remarkable consistency in the size shape and position of the photoreceptor outer segments The single morphologic variety of outer segment present is short and slightly tapered in appearance It more closely resembles the cone type of receptor than the long slender appearance of the typical rod

Finally many features which are characteristic of the cone type of receptor can be distinguished in electron micrographs of ground squirrel photoreceptor cells The basal third of the ground squirrel outer segment is formed by flattened saccules many of which are continuous with the plasma membrane of this portion of the cell (fig 5) Only towards their apices are the ground squirrel outer segments formed by discrete saccules lying within but separate from the overlying plasma membrane (fig 4) This structural arrangement has come to be recognized as characteristic of extra foveal vertebrate cones (Cohen 63 Dartnall and Tansley 63) Vertebrate rods in contrast are formed almost entirely by discs lying within but apparently separate from the overlying plasma membrane Only occasionally and only in a small region of the rod outer segment has it been possible to se direct communications between saccules and the surrounding plasma membrane (Cohen 63)

The basal processes of the ground squirrel photoreceptor cells also have a structural organization more typical of the cone type of receptor Each of the club shaped ground squirrel basal processes is invaded by many dendrites from the inner nuclear layer and each contains several synaptic lamellae or ribbons (figs 9 and 10) To date basal processes of this nature have been found in vertebrate cones only (Dartnall and Tansley 63) Basal processes of vertebrate rods are less complex They are spherical in shape and usually are penetrated by the dendrites of a single cel only (Dartnall and Tansley 63) Also they generally contain only a single synaptic ribbon although several may be present within rod spherules in the human retin (Missotten 60)

Taken together all of the above findin support the view that the ground squirr retina is exclusively or almost exclusivel pure cone in type It must be emphasize however that although some confirmatio has already been obtained from electr retinographic studies (Bornschein 54 Arden and Tansley 55 Tansley 57 61 Crescitelli 61 Tansley Copenhaver an Gunkel 61) this conclusion is primaril based on consideration of morphologic ev dence alone It is evident that final dete mination of the exact nature of the grour squirrel retina must await the results of further study in other fields

ACKNOWLEDGMENT

We wish to acknowledge the invaluab technical assistance of Wesley A Heipl

LITERATURE CITED

Arden G B and K Tansley 1955 The spectr sensitivity of the pure-cone retina of the so slik (*Citellus citellus*) J Physiol 130 2? 232

Bornschein H 1954 Elektrophysiologische *Nachweis einer I Retina bei einem Säuger (Ci tellus citellus)* Naturwiss 41 435

Brown P K I R Gibbons and C Wald 196 *The visual cells and visual pigment of th* mudpuppy necturus J Cell Biology 19 7? 106

S C 1 2 3 4 5 6 7 8

1

ELM

PRN

2

Note In the following micrographs the direction of the choroid is indicated by the encircled arrow

PLATE 1

EXPLANATION OF FIGURES

Paraffin section from the upper half of the ground squirrel retina

1 The outer nuclear layer *(4)* is unusually narrow comprising in this example only a single layer of photoreceptor nuclei A narrow outer nuclear layer is a characteristic feature of predominantly cone retinae of diurnal mammals (Walls 42) The photoreceptor outer segments *(2)* which have pulled away from the pigment epithelium *(1)* during preparation of the specimen are clearly visible and demonstrate a uniformity of size shape and position *(S)* sclera *(C)* choroid *(1)* pigment epithelium *(2)* outer segments *(3)* external limiting membrane *(4)* outer nuclear layer *(5)* outer plexiform layer *(6)* inner nuclear layer *(7)* inner plexiform layer *(8)* layer of ganglion cell nuclei Hematoxylin and Eosin × 730

Paraffin section showing outer segments of the photoreceptor cells

2 At higher magnification the uniformity in size and shape of the outer segments *(OS)* is readily apparent The outer segments are short and taper slightly at their outer extremities All the outer segments are approximately the same distance from the external limiting membrane *(ELM)* and the layer of photoreceptor nuclei *(PRN)* Hematoxylin and Eosin × 1 950

PLATE 2

EXPLANATION OF FIGURES

Inner pigment epithelium

3 The inner portions of two pigment epithelial cells are shown in this micrograph The epithelial cells contain spherical nuclei *(N)* with clumped marginated chromatin a largely agranular endoplasmic reticulum and large dense granules *(DG)* both within the main body of the cell and the apical processes Prominent terminal bars *(TB)* can be seen affixing the epithelial cells at their apices The inner border of the pigment epithelium is broken up into numerous processes of varying thicknesses × 9 900

Pigment epithelium — photoreceptor junction

4 At the pigment epithelium — photoreceptor junction the distal portion of an outer segment *(OS)* is visible lying between inner prolongations of the pigment epithelium *(PE)* This region of the outer segment is formed by discrete flattened saccules enclosed by but not continuous with the overlying plasma membrane × 27 000

PLATE 3

EXPLANATION OF FIGURES

Photoreceptor outer segment

5 This figure shows the outer segment as it appears adjacent to the ellipsoid In this region the saccules forming the outer segment are continuous with the plasma membrane of the receptor cell Towards the pigment epithelium (to the left of the arrow) however the sac cules are separate from the overlying plasma membrane Cytoplasmic prolongations *(CP)* arising in the ellipsoid the calycal processes lie adjacent to the outer segment × 33 700

Photoreceptor inner segments

6 The inner segments of the receptor cells are composed of two distinct zones The ellipsoids (to the left) contain numerous mitochondria oriented so that their long axis is parallel to the plasma membrane of this portion of the receptor cell Further inwards the mitochon drial region is gradually replaced by a zone of granular endoplasmic reticulum marked by the presence of long narrow canaliculi and Golgi complexes × 14 700

CP

CP

5

6

PLATE 3

EXPLANATION OF FIGURES

Photoreceptor outer segment

5 This figure shows the outer segment as it appears adjacent to the ellipsoid In this region the saccules forming the outer segment are continuous with the plasma membrane of the receptor cell Towards the pigment epithelium (to the left of the arrow) however the sac cules are separate from the overlying plasma membrane Cytoplasmic prolongations (*CP*) arising in the ellipsoid the calycal processes lie adjacent to the outer segment × 33 700

Photoreceptor inner segments

6 The inner segments of the receptor cells are composed of two distinct zones The ellipsoids (to the left) contain numerous mitochondria oriented so that their long axis is parallel to the plasma membrane of this portion of the receptor cell Further inwards the mitochon drial region is gradually replaced by a zone of granular endoplasmic reticulum marked by the presence of long narrow canaliculi and Golgi complexes × 14 700

IS IS IS IS
P P
TB
M N M N
7



PLATE 4

EXPLANATION OF FIGURES

Cross section through the external limiting membrane

7 The external limiting membrane is revealed as a prominent system of terminal bars (*TB*) joining the dense granular inner segments (*IS*) of the photoreceptor cells to relatively clear outer Muller cell (*M*) prolongations Beyond the external limiting membrane the Muller cells divide into a number of microvillous processes (*P*) lying immediately adjacent to the inner segments Portions of two photoreceptor nuclei (*N*) are visible at the bottom of the figure immediately beneath the external limiting membrane × 15,300

Outer nuclear layer

8 The photoreceptor nuclei (*N*) are oval in shape and contain a dense uneven chromatin They are surrounded by a narrow zone of granular cytoplasm containing fine filaments (*F*) The sub terminal expansions of the Muller cells can be seen forming relatively clear areas between photoreceptor cells Fine filaments (*FM*) are also present within the cytoplasm of the Muller cells × 15 700

IS IS IS IS
P P
TB
M N M N
7



PLATE 5

EXPLANATION OF FIGURES

Photoreceptor basal processes

9 The basal processes (*BP*) of the photoreceptor cells are relatively dense club shaped expansions filled with small synaptic vesicles In this figure several of the basal processes are directly in contact with each other affording a structural basis for interreceptor synaptic transmission Others are separated by lighter Muller cell prolongations (*M*) Each of the basal processes also contains several synaptic lamellae (*SL*) and is invaded in a complex manner by numerous dendritic processes arising in the inner nuclear layer × 12 300

Outer plexiform layer

10 The entire thickness of the outer plexiform layer is shown in this micrograph A portion of a photoreceptor nucleus (*PN*) is present in the upper right and a portion of a nucleus from the inner nuclear layer (*IN*) is present in the lower left The basal processes (*BP*) of the receptor cells in this case are each separated by Muller cell prolongations (*M*) so that no interreceptor contacts are visible Each of the basal processes however receives a large number of dendritic processes from the inner nuclear layer and junctional sites are *marked by a thickening of contiguous plasma membranes* Several synaptic lamellae (*SL*) are present within each of the photoreceptor basal processes × 12 300

The Fine Structure of Nerve Endings in the Nucleus of the Trapezoid Body and the Ventral Cochlear Nucleus

NICHOLAS J LENN AND T S REESE[1]

Laboratory of Neuroanatomical Sciences National Institute of Neurological Diseases and Blindness National Institutes of Health Bethesda Maryland

ABSTRACT Large calyciform axonal endings as well as typical terminal boutons have been previously described in the ventral cochlear nucleus and the nucleus of the trapezoid body by light microscopists In the present study these endings were examined with the electron microscope in chinchillas rats and a cat after perfusion fixation with osmium tetroxide The calyces were found to consist of elongated processes arising from myelinated axons and making multiple synaptic contacts with perikarya and dendrites This finding suggests that an important property of calyces is the large amount of synaptic activity that they can bring to bear on a single post synaptic structure Adjacent to the calyciform endings were variable numbers of boutons that made synaptic contacts with the same perikarya and dendrites The majority of boutons contained smaller synaptic vesicles than those present in the calyces implying both anatomical and functional differences between these two types of ending It is suggested that many of these boutons in the ventral cochlear nucleus are endings of centrifugal inhibitory fibers described by previous workers

Held (1893) and others (e g Ramon y Cajal 34 Harrison and Irving 65) have described calyciform terminations of axons in mammalian auditory nuclei When impregnated with the Golgi method these calyces of Held appear at the terminations of axons as expansions of variable size from which arise processes of variable shape These elongated processes provide for large areas of apposition between a single axonal ending and a perikaryon or dendrite It has been shown that similar calyciform axonal endings in chick ciliary ganglia are electrically coupled with ganglion cells (Martin and Pilar 63a b 64) and thorough cytological studies of these calyces are available (e g Takahashi and Hama 65) It therefore seemed of interest to examine the auditory calyces with the electron microscope and to compare their structure to that of the chick ciliary ganglion calyces

Among the calyciform endings in mammalian auditory nuclei are other axonal endings which appear as typical terminal boutons in Golgi preparations (Ramón y Cajal 09) They are distinguished from calyces by their smaller size and simple shape In the cochlear nucleus many of these appear to be endings of axons from higher auditory centers (Rasmussen 60) which are probably inhibitory (Pfalz 62) A second objective of this study was to identify these endings and to determine their synaptic relationships with the calyces and adjacent neurons

MATERIALS AND METHODS

The material for the present report consisted of four adult rats three adult chinchillas and one adult cat The regions studied most intensively were the nucleus of the trapezoid body in rat and the ventral cochlear nucleus in chinchilla

Animals were first anesthetized with chloral hydrate and the body temperature lowered to 26 C (Wolfe 65) The brains were fixed by perfusion through the aorta with balanced salt solution (McEwen 55) followed by 1 or 2% osmium tetroxide in phosphate buffer (Millonig 62 without glucose pH 7 0) Brain stem slices were dehydrated in methanol and embedded in Maraglas (Spurlock et al 63) or Araldite The anterior ventral cochlear nucleus and

[1] P rt f this work w s done in the Dep rtment of An tomy H rv rd Medi l School Boston 15 M husetts. Thi i Dr Reese prese t ddre s. The work done t the H rv rd Medical School w sup ported in p rt b gr nt GM 11182 10 from the N tion l In titutes f H lth U ited States Public H lth Servic

the nucleus of the trapezoid body were identified with the light microscope in transverse sections of brain stem slices after staining with toluidine blue (Richardson et al 60) From the ventral cochlear nucleus a region analogous to the area III of Harrison and Irving (65) was selected for electron microscopy Ultrathin sections were stained with lead citrate (Reynolds 63) or uranyl acetate (Watson 58) and lead citrate Three ribbons of 25–35 serial sections from the nucleus of the trapezoid body of a rat were also examined using an RCA EMU 3D electron microscope

The diameters of synaptic vesicles were measured on electron micrographs at a magnification of 100 000 with a Zeiss TGZ3 particle size analyzer

RESULTS

By means of light microscopic techniques which can show a complete synaptic ending in one section calyces or bulbs of Held in the ventral cochlear nucleus have been distinguished from calyces of Held in the nucleus of the trapezoid body (Ramon y Cajal 34) Each calyx in the nucleus of the trapezoid body has several irregularly shaped processes which arise from an axon to encircle a considerable portion of a single perikaryon The pattern of the processes from calyces in the ventral cochlear nucleus is less symmetrical and the processes are generally smaller In the ventral cochlear nucleus more than one perikaryon may be contacted by a calyx and more than one calyx may contact a perikaryon However in electron micrographs only portions of one or two branches of a single calyx of Held could be seen and these were remarkably similar in both nuclear regions in the three species of mammal examined The description below therefore applies equally to the endings in both regions of all three species Because the branches of the calyces of Held in both locations wrapped around the cells with which they synapsed it was convenient to call them all calyceal processes By using this one term the similarity between individual branches of calyces of Held in the two nuclear regions as seen with the electron microscope is emphasized Differences in the arrangement of these branches could not be found electron microscopically without extensive serial reconstruction Therefore the present study adds nothing on this point to the previous light microscopic descriptions Figure 1 is intended to supplement the following description by summarizing pictorially the principal findings

The characteristic form of the calyceal processes was seen in favorable planes of section where individual processes up to 20 μ in length encircled part of a perikaryon and made up to 14 synaptic contacts with it It was common to find calyceal processes originating from myelinated axons 1–5 μ in total diameter to which they were usually connected by short preterminal segments (fig 5) A preterminal segment might join either the center or end of a calyceal process or it might first bifurcate In one instance the preterminal segment apparently arose from a myelinated axon at the site of a node in the myelin sheath (fig 7) (cf Bodian and Taylor 63) Calyceal processes were often found making synaptic contacts with both a perikaryon and one of its dendrites (fig 4) Planes of section containing dendrites alone often showed calyceal processes contacting them but it was not clear whether these processes also contacted perikarya lying outside the plane of section It was common in the anterior ventral cochlear nucleus for the same portion of calyceal processes to make synaptic contact both with a perikaryon and other processes of unknown origins which were presumably dendrites (fig 2) Similar contacts occurred less commonly in the nucleus of the trapezoid body The degree of heterogeneity of these dendrites with respect to such factors as location of cell of origin was not determined

The synaptic contacts which the calyceal processes made with dendrites and perikarya (fig 2 inset) were similar to those found in other regions of the mammalian nervous system (Palay 58) The calyceal processes were always presynaptic Each synaptic contact consisted of a presynaptic accumulation of small vesicles of uniform size near a short segment of cell membrane which at the magnifications used in this study appeared thickened The extracellular space in this region was widened and contained a dense material



Fig 1 Di gram summarizing synaptic relationships in anterior ventral cochlear nucleus and n leus of the trape oid body Curved arrows indicate direction of synaptic activity as determined fr m morphological polarities of synaptic contacts *Abbreviat ons* *B* bouton C calyceal process *D* dendrite *P* perikaryon.

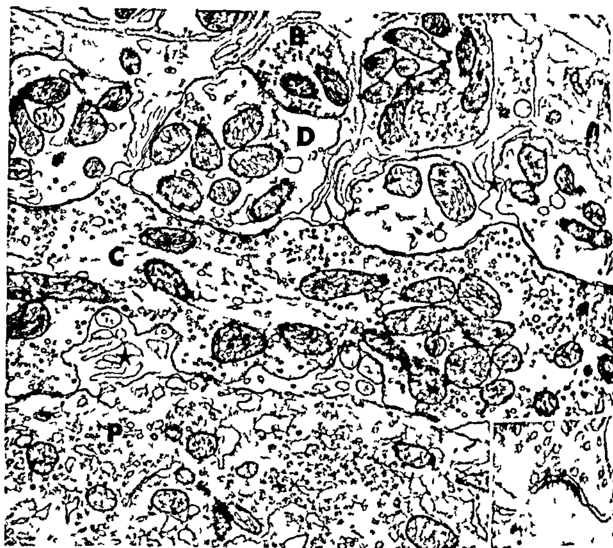


Fig 2 Calyceal process (C) with synaptic contacts on a perikaryon (P) and a small dendrite (D). The dendrite is also post synaptic to a bouton (B) which is distinguished from the calyceal process by the simple shape of its profile and smaller synaptic vesicles Processes of astrocytes in places attenuated to thin sheets are loosely packed into the spaces between neural processes Stars mark regions of the extracellular space which are unusually large Anterior ventral cochlear nucleus chinchilla × 20 000

Inset Higher magnification of a synaptic contact between a calyceal process and a perikaryon. Nucleus of the trapezoid body rat × 47 000

in which an even denser discontinuous zone often could be distinguished lying both parallel to and closer to the post synapatic cell membrane A segment of the post synaptic cell membrane coextensive with the thickened presynaptic cell membrane also appeared thickened and had a variable amount of dense material on its cytoplasmic surface That these synaptic contacts were of uniform size in all planes of section implied that they were roughly circular

Large numbers of synaptic vesicles not associated with synaptic contacts tended to be concentrated in the periphery of the calyceal processes while numerous mitochondria and neurofilaments as well as a few neurotubules were dispersed in the central regions (figs 4 5) The frequent occurrence of profiles of smooth surfaced endoplasmic reticulum was reflected in the long upper tail of the frequency distribution curve of synaptic vesicle size in the calyces (fig 3) Small numbers of multivesiculate bodies granular vesicles and coated vesicles some of the last continuous with the plasma membrane were also present in the calyceal processes

Many endings which appeared to be simple boutons were present in both nuclei in all three species although the frequency of their occurrence was variable (fig 6) These boutons characteristically made one synaptic contact with either a dendrite or a perikaryon In a few instances such contacts were found on a perikaryon being situated in the space between two calyceal synaptic contacts The bouton synaptic contacts were similar to those formed by calyceal processes but the boutons lacked neurofilaments neurotubules and abundant endoplasmic reticulum Also differing from the calyceal processes was the tendency of the boutons to occur side by side with their membranes closely apposed (fig 6) However the interpretation that boutons were indeed distinct from calyceal processes was complicated by the finding that some boutons were connected to calyceal processes by narrow stalks (fig 8) This continuity was seen in many single sections and in one series of sequential sections from the nucleus of the trapezoid body where several boutons were traced to a calyceal process Boutons arising from calyces are also commonly seen in Golgi preparations (Ramón y Cajal 09) Further the possiblity could not be eliminated that some of the profiles which appeared to be boutons in single sections were actually skewed sections of regions of calyceal processes that did not contain neurofilaments or endoplasmic reticulum

Calyceal processes and a few boutons appeared visually to differ from the majority of the boutons in having uniformly larger synaptic vesicles (fig 6) To test this hypothesis the diameters of 1 200 synaptic vesicles from eight endings of both types from the anterior ventral cochlear nucleus of a chinchilla were measured The median vesicle size for each ending was thus obtained and the mean value for the three obvious calyceal processes compared with the mean value for the five boutons The difference between the means was significant ($p < 0.01$) The frequency distribution curves for the two populations are presented in figure 3 Measurements of synaptic vesicle diameters from the rat material showed that a similar difference in vesicle size existed between obvious calyceal processes and other endings Furthermore it was found that visual estimations of the relative vesicle size in these endings which had been made before the measurements agreed with the measurements in every instance Having thus confirmed objectively our ability to determine vesicle size visually all available micrographs were surveyed and in both nuclei of all animals studied the calyceal processes were found to consistently contain the larger type of synaptic vesicles (see fig 6) Micrographs of the cochlear nucleus of a rat where the primary fixation was with glutaraldehyde (available from another study Lenn 65) also showed obviously larger synaptic vesicles in calyceal processes While the sizes of synaptic vesicles can undoubtedly be changed during preparation the constant association of larger vesicles with calyceal processes after preservation with either OsO or glutaraldehyde suggested that the difference in vesicle size might be of fundamental importance The presence of unswollen endoplasmic reticulum in the calyceal processes also favored the interpretation that the larger vesicles in these processes were not the result of artifactual swelling

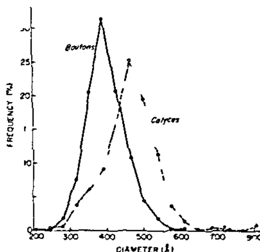


Fig 3 Frequency distribution curves of synaptic vesicle diameters for three typical calyceal processes and five boutons from the anterior ventral cochlear nucleus of a chinchilla The means are significantly different ($p < 0.01$) The long upper tail on the calyceal curve reflects the presence of vesicular endoplasmic reticulum



Fig 2 Calyceal process (*C*) with synaptic contacts on a perikaryon (*P*) and a small dendrite (*D*). The dendrite is also post synaptic to a bouton (*B*) which is distinguished from the calyceal process by the simple shape of its profile and smaller synaptic vesicles Processes of astrocytes in places attenuated to thin sheets are loosely packed into the spaces between neural processes Stars mark regions of the extracellular space which are unusually large Anterior ventral cochlear nucleus chinchilla × 20 000

Inset Higher magnification of a synaptic contact between a calyceal process and a perikaryon. Nucleus of the trapezoid body rat × 47 000

in which an even denser discontinuous zone often could be distinguished lying both parallel to and closer to the post synapatic cell membrane A segment of the post synaptic cell membrane coextensive with the thickened presynaptic cell membrane also appeared thickened and had a variable amount of dense material on its cytoplasmic surface That these synaptic contacts were of uniform size in all planes of section implied that they were roughly circular

Large numbers of synaptic vesicles not associated with synaptic contacts tended to be concentrated in the periphery of the calyceal processes while numerous mitochondria and neurofilaments as well as a few neurotubules were dispersed in the central regions (figs 4 5) The frequent occurrence of profiles of smooth surfaced endoplasmic reticulum was reflected in the long upper tail of the frequency distribution curve of synaptic vesicle size in the calyces (fig 3) Small numbers of multivesiculate bodies granular vesicles and coated vesicles some of the last continuous with the plasma membrane were also present in the calyceal processes

Many endings which appeared to be simple boutons were present in both nuclei in all three species although the frequency of their occurrence was variable (fig 6) These boutons characteristically made one synaptic contact with either a dendrite or a perikaryon In a few instances such contacts were found on a perikaryon being situated in the space between two calyceal synaptic contacts The bouton synaptic contacts were similar to those formed by calyceal processes but the boutons lacked neurofilaments neurotubules and abundant endoplasmic reticulum Also differing from the calyceal processes was the tendency of the boutons to occur side by side with their membranes closely apposed (fig 6) However the interpretation that boutons were indeed distinct from calyceal processes was complicated by the finding that some boutons were connected to calyceal processes by narrow stalks (fig 8) This continuity was seen in many single sections and in one series of sequential sections from the nucleus of the trapezoid body where several boutons were traced to a calyceal process Boutons arising from calyces are also commonly seen in Golgi preparations (Ramón y Cajal 09) Further the possiblity could not be eliminated that some of the profiles which appeared to be boutons in single sections were actually skewed sections of regions of calyceal processes that did not contain neurofilaments or endoplasmic reticulum

Calyceal processes and a few boutons appeared visually to differ from the majority of the boutons in having uniformly larger synaptic vesicles (fig 6) To test this hypothesis the diameters of 1 200 synaptic vesicles from eight endings of both types from the anterior ventral cochlear nucleus of a chinchilla were measured The median vesicle size for each ending was thus obtained and the mean value for the three obvious calyceal processes compared with the mean value for the five boutons The difference between the means was significant ($p < 0.01$) The frequency distribution curves for the two populations are presented in figure 3 Measurements of synaptic vesicle diameters from the rat material showed that a similar difference in vesicle size existed between obvious calyceal processes and other endings Furthermore it was found that visual estimations of the relative vesicle size in these endings which had been made before the measurements agreed with the measurements in every instance Having thus confirmed objectively our ability to determine vesicle size visually all available micrographs were surveyed and in both nuclei of all animals studied the calyceal processes were found to consistently contain the larger type of synaptic vesicles (see fig 6) Micrographs of the cochlear nucleus of a rat where the primary fixation was with glutaraldehyde (available from another study Lenn 65) also showed obviously larger synaptic vesicles in calyceal processes While the sizes of synaptic vesicles can undoubtedly be changed during preparation the constant association of larger vesicles with calyceal processes after preservation with either OsO or glutaraldehyde suggested that the difference in vesicle size might be of fundamental importance The presence of unswollen endoplasmic reticulum in the calyceal processes also favored the interpretation that the larger vesicles in these processes were not the result of artifactual swelling

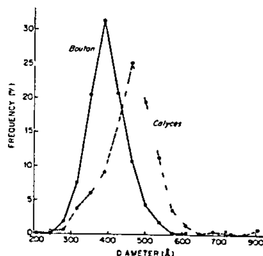


Fig 3 Frequency distribution curves of synaptic vesicle diameters for three typical calyceal processes and five boutons from the anterior ventral cochlear nucleus of a chinchilla The means are significantly different ($p < 0.01$) The long upper tail on the calyceal curve reflects the presence of vesicular endoplasmic reticulum

The neuronal perikarya on which the calyceal processes ended (figs 2 4–6) were typical of those elsewhere in the brain stem prepared by similar techniques (see Lenn 65, for references) The contour of the cell membrane was typically smooth but in places small projections of cyto plasm extended a short distance to receive a synaptic contact from a calyceal process (fig 5) In many sections a typical den drite containing most of the components of the perikaryal cytoplasm was found emerging from a perikaryon but no axons were recognized arising from perikarya

In the regions around the perikarya and calyceal processes were dendrites mye linated axons and processes of astrocytes containing glycogen granules and fine fila ments (figs 2 4–8) The astrocytic proc esses were most prevalent in the regions immediately surrounding the perikarya where they often formed stacks of thin sheets which lay on the outer surfaces of calyceal processes and boutons (fig 5) However this glial investment was not present at all points and the calyceal proc esses and their subjacent cells were not invested with loose myelin as are the calyces in the chick ciliary ganglion (Hess 65)

Between the calyceal processes and the subjacent perikarya in regions free of synaptic contacts there were extracellular spaces of variable size often containing small glial processes (fig 2) From single sections and a series of sequential sections it was apparent that these spaces were con tinuous with the extracellular space sur rounding the calyces (fig 6) When the origin of the glial processes could be as certained as was often possible they were seen to arise from astrocytes identified by their content of glycogen and filaments Spaces between some of the glial processes surrounding the calyceal processes were also much larger than the 150–200 A spaces which are so commonly found in osmium fixed brain tissue including other regions of the brains used in the present study While it is likely that these enlarged extracellular spaces are an artifact of fixa tion (e g Torack et al 65) it remains to be explained why certain regions of the brain and not others should consistently react in this manner The techniques used here do not help resolve this question However it should be stressed that in the present ma terial the perfusion was complete through out the primarily cellular areas of the brains as judged by the blackening and hardening of the brain In the electron micrographs the crispness of detail the lack of broken membranes the absence of cytoplasmic and nucleoplasmic displace ments and the unswollen appearance of the endoplasmic reticulum were all indica tions of good structural preservation

DISCUSSION

That the processes of calyces of Held as seen with the light microscope are indeed identical with the structures which we have identified as calyceal processes in electron micrographs is evident for severa reasons In the electron micrographs ca lyceal processes were elongated structure arising from myelinated axons an appea ance that correlates well with their appea ance with the light microscope The processes had large areas of close associa tion with perikarya or dendrites which le the light microscopists to conclude th they made synaptic contact In the ele tron micrographs these areas of clo association were typified by multiple in dividual synaptic contacts That the stru ture of these synaptic contacts was foun to be like that of most other synaptic co tacts in the nervous system suggested th here too the transmission of impulses d pends on the release of a chemical tran mitter The main difference provided b the multiple synaptic contacts is the lar amount of synaptic activity that a sing ending can bring to bear on a single po synaptic structure

Calyciform axonal endings are al found on chick ciliary ganglion cells wi which they make multiple synaptic co tacts similar to those in mammalian au tory calyces (de Lorenzo 60 Hámori a Dyachkova 64) The recent studies Martin and Pilar (63a b) indicate th the avian calyces depolarize contacted ga glion cells by direct electrical couplin and in addition failing this by the app ent release of a depolarizing transmit substance It has been proposed (Hess 65) that investment of the calyx and gan glion cell by loose myelin is a major fac

tor in promoting electrical coupling How ever according to *Martin and Pilar* (64) the synaptic membranes must be of low resistance and capacitance which implies that the presence of myelin alone is not *sufficient* to explain the presence of electrical coupling The close membrane appositions demonstrated by Takahashi and Hama (65) are similar to the quintuple layered junctions found in other sites of electrical transmission and therefore might represent the essential anatomical feature making electrical coupling possible in the chick ciliary ganglion In any case if *either myelin or quintuple* layered junctions are the morphological features responsible for electrical coupling in avian calyces then such coupling should not be expected in the mammalian auditory system where the calyces although grossly similar lack both of these features

Ramón y Cajal (09) described nerve endings in the nucleus of the trapezoid body and ventral cochlear nucleus which appeared to be typical terminal boutons In the present study two types of bouton were found on cells and dendrites that received *calyces Both were differentiated* from the calyceal processes by their smaller size and simple shape The less frequent type contained the larger synaptic vesicles which have proven to be characteristic of the calyceal processes It is likely that these profiles represented skewed sections of calyceal processes or boutons arising from these processes The majority of the boutons *contained smaller synaptic* vesicles We might tentatively assume that all the endings of a single axon contain the same size of synaptic vesicles although this is obviously a basic problem of considerable interest This assumption would lead us to doubt in the case of the ventral cochlear nucleus the importance of two possible sources of the boutons with small vesicles *namely additional* endings of primary afferent fibers and recurrent collaterals of the fibers going to the nucleus of the trapezoid body (Ramón y Cajal 09) both of which end as calyces containing large vesicles Other possible sources of boutons including the endings of intranuclear connections and recurrents of other axons leaving the nucleus cannot be excluded *Previous studies* of the ventral cochlear nucleus have however shown *that many of the boutons there are end*ings of axons from higher auditory centers (Rasmussen 60) A reasonable hypothesis therefore is that an important source *of the boutons with smaller vesicles* found in the ventral cochlear nucleus is axons originating in higher auditory centers These axons and their terminations have been characterized in the cat by their positive reaction with the thiocholine method for cholinesterase (Rasmussen 64) Also higher auditory centers appear to exert an inhibitory influence on the cells in the cochlear nucleus in the cat and guinea pig (Pfalz 62) Both a positive cholinesterase reaction and an inhibitory function might then be correlated with the smaller synap*tic vesicles A similar argument can be* made in the case of the nucleus of the trapezoid body although comparable evidence is lacking That the smaller vesicles in the boutons contain a different neurotransmitter than the larger vesicles found in calyceal processes is at once the most obvious and most attractive hypothesis for the significance of their smaller size

ACKNOWLEDGMENT

The authors wish to express their appreciation to Mr K C Richardson for provid*ing two of the rat brains studied and for* his guidance and encouragement throughout We are also indebted to Dr G L Rasmussen for advice and encouragement Figure 1 was drawn by Mrs G Turner

LITERATURE CITED

Bodian D and N Taylor 1963 Synapse arising at central node of Ranvier and note on fixation of the central nervous system Science 139 330–332

De Lorenzo A J 1960 The fine structure of synapses in the ciliary ganglion of the chick J Biophys Biochem Cytol 7 31–36

Hámori J and L N Dyachkova 1964 Electron microscope studies on developmental differentiation of ciliary ganglion synap es in the chick Acta Biol Hung 15 213–230

Harrison J M and R Irving 1965 The anterior ventral cochlear nucleus J Comp Neurol 124 15–42

Held H 1893 Die centrale Gehorleitung Arch Anat u Physiol 201–248

Hess A 1965 Developmental changes in the structure of the synapse on the myelinated cell bodies of the chicken ciliary ganglion J Cell Biol 25 1–19

The neuronal perikarya on which the calyceal processes ended (figs 2 4–6) were typical of those elsewhere in the brain stem prepared by similar techniques (see Lenn 65 for references) The contour of the cell membrane was typically smooth but in places small projections of cytoplasm extended a short distance to receive a synaptic contact from a calyceal process (fig 5) In many sections a typical dendrite containing most of the components of the perikaryal cytoplasm was found emerging from a perikaryon but no axons were recognized arising from perikarya

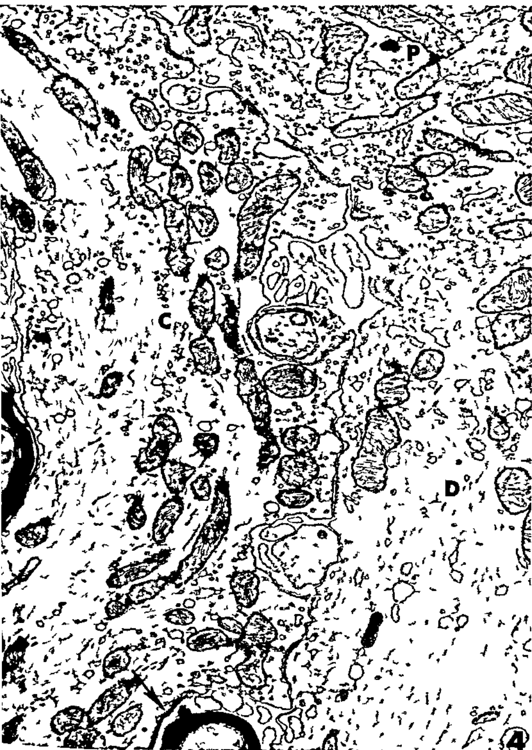
In the regions around the perikarya and calyceal processes were dendrites myelinated axons and processes of astrocytes containing glycogen granules and fine filaments (figs 2 4–8) The astrocytic processes were most prevalent in the regions immediately surrounding the perikarya where they often formed stacks of thin sheets which lay on the outer surfaces of calyceal processes and boutons (fig 5) However this glial investment was not present at all points and the calyceal processes and their subjacent cells were not invested with loose myelin as are the calyces in the chick ciliary ganglion (Hess 65)

Between the calyceal processes and the subjacent perikarya in regions free of synaptic contacts there were extracellular spaces of variable size often containing small glial processes (fig 2) From single sections and a series of sequential sections it was apparent that these spaces were continuous with the extracellular space surrounding the calyces (fig 6) When the origin of the glial processes could be ascertained as was often possible they were seen to arise from astrocytes identified by their content of glycogen and filaments Spaces between some of the glial processes surrounding the calyceal processes were also much larger than the 150–200 Å spaces which are so commonly found in osmium fixed brain tissue including other regions of the brains used in the present study While it is likely that these enlarged extracellular spaces are an artifact of fixation (e g Torack et al 65) it remains to be explained why certain regions of the brain and not others should consistently react in not help resolve this question However it should be stressed that in the present material the perfusion was complete throughout the primarily cellular areas of the brains as judged by the blackening and hardening of the brain In the electron micrographs the crispness of detail the lack of broken membranes the absence of cytoplasmic and nucleoplasmic displacements and the unswollen appearance of the endoplasmic reticulum were all indications of good structural preservation

DISCUSSION

That the processes of calyces of Held as seen with the light microscope are indeed identical with the structures which we have identified as calyceal processes in electron micrographs is evident for several reasons In the electron micrographs calyceal processes were elongated structures arising from myelinated axons an appearance that correlates well with their appearance with the light microscope These processes had large areas of close association with perikarya or dendrites which led the light microscopists to conclude that they made synaptic contact In the electron micrographs these areas of close association were typified by multiple individual synaptic contacts That the structure of these synaptic contacts was found to be like that of most other synaptic contacts in the nervous system suggested that here too the transmission of impulses depends on the release of a chemical transmitter The main difference provided by the multiple synaptic contacts is the large amount of synaptic activity that a single ending can bring to bear on a single postsynaptic structure

Calyciform axonal endings are also found on chick ciliary ganglion cells with which they make multiple synaptic contacts similar to those in mammalian auditory calyces (de Lorenzo 60 Hámori and Dyachkova 64) The recent studies of Martin and Pilar (63a b) indicate that the avian calyces depolarize contacted ganglion cells by direct electrical coupling and in addition failing this by the apparent release of a depolarizing transmitter substance It has been proposed (Hess 65) that investment of the calyx and gan


P
C
D
4

Lenn N J 1965 Electron microscopic observations on monoamine-containing brain stem neurons in normal and drug treated rats Anat Rec *153* 399–406

Martin A R and G Pilar 1963a Dual mode of synaptic transmission in the avian ciliary ganglion J Physiol *168* 443–463

——— 1963b Transmission through the ciliary ganglion of the chick J Physiol *168* 464–475

——— 1964 An analysis of electrical coupling at synapses in the avian ciliary ganglion J Physiol *171* 454–475

McEwen L M 1956 The effect on the isolated rabbit heart of vagal stimulation and its modification by cocaine hexamethonium and ouabain J Physiol *131* 678–689

Millonig G 1962 Further observation on a phosphate buffer for osmium solutions in fixation Vth Int Cong for Electron Microscopy S S Breese Jr ed Academic Press, New York Vol 2 p P8

Palay S L 1958 The morphology of synapses in the central nervous system Exptl Cell Res suppl *5* 275–293

Pfalz R K J 1962 Centrifugal inhibition of afferent secondary neurons in the cochlear nucleus by sound J Acoust Soc Am *34* 1472–1477

Ramón y Cajal S 1909–11 Histologie du Système Nerveux de l Homme et des Vertébrés Trans by L Azoulay Maloine Paris Vol 1 774–812

——— 1934 Les preuves objectives de l unité anatomique des cellules nerveuses Trav du Lab de Rech Biol *29* 1–137 Trans by M Ubeda Purkiss and C A Fox 1954 Instituto Ramón y Cajal Madrid Chap 4 27–39

Rasmussen G L 1960 Efferent fibers of the cochlear nerve and cochlear nucleus. In Neural Mechanisms of the Auditory and Vestibular Systems G L Rasmussen and W W[illegible] eds Charles C Thomas Springfield Ill Chap 8 105–115

——— 1964 Anatomic relationships of the ascending and descending auditory systems In Neurological Aspects of Auditory and Vestibular Disorders W S Fields and B R Alford eds Charles C Thomas Springfield Ill pp 1–19

Reynolds E S 1963 The use of lead citrate [illegible] high pH as an electron-opaque stain in electron microscopy J Cell Biol *17* 208–212.

Richardson K C L Jarrett and E Finke 19[illegible] Embedding in epoxy resins for ultrathin sectioning in electron microscopy Stain Technol *35* 313–323

Spurlock B O V C Kattine and J A Freem[illegible] 1963 Technical modifications in Mara[illegible] embedding J Cell Biol *17* 203–207

Takahashi K and K Hama 1965 Some o[illegible] servations on the fine structure of the synap[illegible] area in the ciliary ganglion of the chick [illegible] Zellforsch *67* 174–184

Torack R M M L Dufty and J M Hay[illegible] 1965 The effect of anisotonic media up[illegible] cellular ultrastructure in fresh and fixed [illegible] brain Z Zellforsch *66* 690–700

Watson M L 1958 Staining of tissue sectio[illegible] for electron microscopy with heavy metals. [illegible] Biophys Biochem Cytol *4* 475–478

Wolfe D E 1965 The epiphyseal cell an ele[illegible] tron microscopic study of its intercellular [illegible] lationships and intracellular morphology in t[illegible] pineal body of the albino rat Prog in Bra[illegible] Res *10* 332–386

PLATE 1

EXPLANATION OF FIGURE

4 Calyceal process (*C*) with synaptic contacts on a perikaryon (*P*) and its dendrite (*D*) The extreme end of the myelin sheath that covered the preterminal axon of the calyceal process is indicated by an arrow at the bottom Cut off at the top of plate is the continuation of the calyceal process over the surface of the perikaryon where it formed several additional synaptic contacts Filaments in the calyceal process contrast with tubules in the dendrite Anterior ventral cochlear nucleus chinchilla × 26 000


P
C
5

PLATE 2

EXPLANATION OF FIGURE

5 Calyceal process (*C*) with multiple synaptic contacts on a perikaryon (*P*) Myelin sheath of preterminal fiber ends at origin of the process Microtubules are exceptionally abundant At top (arrow) a cytoplasmic projection of the perikaryon juts out to contact the calyceal process At bottom (arrow) is a stack of glial sheets Anterior ventral cochlear nucleus cat × 18 000


B
P
C
6

PLATE 3

EXPLANATION OF FIGURE

6 Boutons (*B*) and a calyceal process (*C*) with synaptic contacts on a perikaryon (*P*) Boutons are distinguished by their smaller size simple shape and their tendency to lie side by side with their cell membranes closely apposed Their cytoplasm contrasts with that in calyces in lacking filaments or vesicular endoplasmic reticulum and their synaptic vesicles are distinctly smaller It is from thin astrocytic processes (arrow) that the small processes under the calyceal processes originate Anterior ventral cochlear nucleus chinchilla × 27 000


C
P
7

PLATE 4

EXPLANATION OF FIGURES

7 Calyceal process arising from a node in a myelinated axon *Abbreviations* C calyceal process P perikaryon Anterior ventral cochlear nucleus chinchilla × 24 000

8 A short neck (arrow) connecting a bouton to a calyceal process (C) The synaptic vesicles in both the bouton and the calyceal process were larger than those found in other boutons in this nucleus *Abbreviations* C calyceal process P perikaryon Nucleus of the trapezoid body rat × 26 000



C
P
8

pontaneous and Diet induced Hepatic Fibrosis n Mice of the C Strain [1]

BEN R CLOWER [2] AND W LANE WILLIAMS
Department of Anatomy University of Mississippi School of Medicine Jackson Mississippi

ABSTRACT Mice of the highly inbred C strain were used Of these 146 were fed a completely adequate diet These were 10–66 weeks old when killed Beginning at 3–4 months of age 45 mice were fed a diet high in fat (40% lard) low in protein (8% casein) and deficient in lipotropic substances for 4–66 weeks

Livers were not fatty in mice fed the adequate diet Hepatic fibrosis developing within 24 weeks of age and increasing with age was observed in more than 60% of these control mice Fibrosis was usually subcapsular but in some instances was perivenous or intralobular Reticular fibers were the chief component

In those fed the atypical diet the livers were fatty in all mice killed during the 4–66 weeks of the study At approximately 20 weeks liposis declined from the large amounts present earlier (4–18 weeks) Until 52 weeks most of the lipid was located in fatty cysts Subsequently the livers became excessively fatty Parenchymal necrosis was limited to three mice Parenchymal hyperplasia was lacking

In the dietary group of mice there were three patterns of hepatic fibrosis Subcapsular fibrosis developed within a month and was the most common type Another type consisted of fibrous septa extending chiefly from central veins Linkage of septa produced pseudolobulation or pseudoencapsulation of areas of parenchyma The least common type was an intralobular fibrosis which was unrelated to the capsule or to veins All three types consisted initially of reticular fibers Collagen was present in subcapsular and perivenous fibrosis within 16 weeks and in the intralobular type by 52 weeks

The feeding of a diet high in fat low in rotein and deficient in lipotropic sub tances *produces rapid cytoplasmic liposis* of the hepatic parenchyma in several spe ies including rats and mice (Gyorgy and Goldblatt 39 Hartroft 50 Buckley and Hartroft 55 Meader and Williams 57) The results of numerous studies are contradictory in demonstrating whether or not extensive fibrosis occurs in these fatty livers Data obtained (Ball 64) by feeding high fat low protein hypolipotropic diets to mice do not confirm that the course of events is the production of a chronologically progressive hepatic liposis which is followed by nodular parenchymal hyperplasia and then by fibrosis or severe stromal distortion and compression (Hoffbauer 57) The lack of definitive information concerning the amount of fibrosis has been due in part to the short term survival of animals fed these atypical diets In the present study extensive longevity (as long as 66 weeks on the diet) was attained

This study also demonstrated that a diet which produced fatty livers also enhanced and *accelerated a spontaneous* hepatic fibrosis which was associated with aging in C mice fed a completely adequate *diet*

MATERIALS AND METHODS

Control mice The highly inbred C strain also known as BALB/C was originated in 1913 by Bagg (Snell et al 60 Staff of R B Jackson Memorial Lab 62) Mice of the C strain have been used extensively for nutritional studies because they have no significant incidence of spontaneous lesions (Williams 60 Williams and Oliver 61) A total of 146 female mice of the C strain were used as controls After weaning they were fed an adequate commercial diet Age ranged from 10–66 weeks when killed All mice seemed in excellent health at the time they were killed

Mice in dietary group Forty five female mice of the C strain 3 to 4 months

[1] S ppo ted by g nt HE-07318 from th Nat onal In titut s of He lth U S P H S

[2] N I H U S P H S Predocto l T ainee in th Ana t m 1 5 1 n s (2T1 GM 287 A5) Th e d ta were in luded n a the i bmitt d t th G d at F culty f the Uni rs ty of M s ipp in cand da y f th deg of Ma t f Sci nce

TABLE 1

Hepatic liposis in C mice fed a high fat (40%) low protein hypolipotropic diet

Weeks on diet	No of mice	Chiefly central and midzonal liposis	Liposis of all zones	Fatty cysts	Generalized liposis without lobular patterns	Minimal liposis with no lobular patterns and with fat pre dominantly in cysts	Ceroid pigment
4	10	0	+(10)	0	0	0	0
6 10	6	+(5)	+(1)	+(6)	0	0	0
14 16 18	9	0	+(9)	+(9)	0	0	+(4)
20 26 28 32 38 52	6	0	0	+(6)	0	+(6)	+(6)
54 60 62 66	14	0	0	+(14)	+(14)	0	+(14)

\+ Present as indicated by column heading 0 Absent
Numbers in parentheses no of mice

TABLE 2

Hepatic fibrosis in C mice

Weeks fed 40% fat low protein hypolipotropic diet	No of mice	Location of fibrosis		
		Subcapsular	Extensions (septa) from central veins	Intralobular
4	10	0	0	0
6	2	+(R)	0	0
10	4	+(R)	+(R)	0
14	2	+(R C)	+(R)	0
16	4	+(R C)	+(R C)	+(R)
18	3	+(R C)	+(R C)	0
20 26	2	+(R C)	+(R C)	+(R)
28 32 38	3	+(R C)	+(R C)	0
52 64 60 63 66	15	+(R C)	+(R C)	+(R C)
Mice fed normal diet				
Age				
10–20 weeks	20	0	0	0
24 weeks	16	+ (R in 62%)	0	0
32–42 weeks	34	+ (R in 82% C&R in 6%)	+ (R in 12%)	0
52–66 weeks	76	+ (R in 76% C&R in 42%)	+ (R in 7%)	+ (R in 3

0 ab ent + present R reticular fibers C collagenous fibers

old and weighing 21 to 23 gm at the beginning of the study were fed the experimental diet (tables 1 and 2) During the experiment three mice were kept in each plastic cage Raised wire floors were used in the cages to prevent coprophagia Mice were weighed weekly up to four months and monthly thereafter (table 3) Ten mice were killed after receiving the d for four weeks 20 after 6–38 weeks a 15 after 52–66 weeks (see table 2) Mi were killed by compression of the cervic spinal cord The simple statistical analy of the data on body weights (table 3) w based on the methods presented by Croxt (59)

TABLE 3

Summary of weight changes in C mice fed a high fat (40%) low protein hypolipotropic diet

Weeks fed diet	Total no of mice	Mean weight change	Per cent of mice	
			Gained weight	Lost weight
		%		
4	45	+2 9 ±8 2	83 (5 6) ±6 2	17 (10 18) ±7 4
20	20	+6 9 ±11 2	75 (12.3) ±7 1	25 (9 1) ±9 4
36	16	+6 7 ±11 0	75 (11 9) ±6 5	19 (11 4)
52	15	+1 4 ±12 6	67 (9 1) ±4 3	27 (17 6)
60	12	+4 5 ±14 8	75 (11 9) ±3 6	17 (27 2)
66	9	+10 ±7 4	89 (11 8) ±4 5	11 (4 0) *

Numbers in parentheses are mean of weight change (%) in animals (% of total in group) listed directly above

Standard deviations of those of changes in body weight (i.e. the mean listed directly above) and were not determined for groups smaller than five mice

Experimental diet

Prior to this experiment all mice had been fed an adequate commercial diet The composition of the experimental diet was as follows

	gm/100 gm of diet
Sugar	45 5
Lard	40 0
Vitamin free casein	8 0
Salt mixture no 2 (U S P XIII)	4 0
L-cystine	0 5
Vitamin mixture	2 0

This diet was not supplemented with a lipotropic material Mice were given fresh diet twice a week unless needed sooner For feeding the food was kept in metal containers constructed with partitions and wire mesh covers to restrict contact with the diet to the mouth and snout The diet and fresh water were available at all times

Histological methods These have been described previously (Williams 60) and follow the technics as presented by Lillie (54) Organs were fixed in 10% aqueous formaldehyde (U S P) or in Lavdowsky s solution (formaldehyde water ethanol and acetic acid) Reticular fibers were demonstrated by a silver method (Gordon and Sweets 36) In addition the PAS (periodic acid Schiff s reagent) Mallory aniline blue and Van Gieson methods were used to show fibrosis and also the PAS (with and without diastase hydrolysis) to demonstrate glycogen and recent myocardial lesions (Kent and Diseker 55 Yokoyama Jennings Clabaugh and Wartmann 55 Ashburn Williams and Cobb 63) The Verhoeff method was used to show elastic fibers Frozen sections of formalin fixed livers were stained with oil red O and with sudan black to show lipid For routine survey of organs PAS (with hematoxylin) and H and E were used as stains

Vitamin content per kilogram of diet was
Vit A concentrate (containing 200 000 unit /gm)	0 10 gm
Vit D concentrate (containing 400 000 unit /gm)	0 005
Alpha tocopherol	0 11
Ascorbic acid	1 0
Inositol	0 11
Menadione	0 05
P aminobenzoic acid	0 11
Niacin	0 10
Riboflavin	0 02
Thiamin hydrochloride	0 02
Ca pantothenate	0 06
Folic acid	2 00 mg
Biotin	0 44 mg
Vit B	0 03 mg

TABLE 1

Hepatic liposis in C mice fed a high fat (40%) low protein hypolipotropic diet

Weeks on diet	No of mice	Chiefly central and midzonal liposis	Liposis of all zones	Fatty cysts	Generalized liposis without lobular patterns	Minimal liposis with no lobular patterns and with fat pre dominantly in cysts	Ceroid pigment
4	10	0	+(10)	0	0	0	0
6 10	6	+(5)	+(1)	+(6)	0	0	0
14 16 18	9	0	+(9)	+(9)	0	0	+(4)
20 26 28 32 38 52	6	0	0	+(6)	0	+(6)	+(6)
54 60 62 66	14	0	0	+(14)	+(14)	0	+(14)

\+ Present as indicated by column heading 0 Absent
Numbers in parentheses no of mice

TABLE 2

Hepatic fibrosis in C mice

Weeks fed 40% fat low protein hypolipotropic diet	No of mice	Location of fibrosis		
		Subcapsular	Extensions (septa) from central veins	Intralobula[r]
4	10	0	0	0
6	2	+(R)	0	0
10	4	+(R)	+(R)	0
14	2	+(R C)	+(R)	0
16	4	+(R C)	+(R C)	+(R)
18	3	+(R C)	+(R C)	0
20 26	2	+(R C)	+(R C)	+(R)
28 32 38	3	+(R C)	+(R C)	0
52 64 60 63 66	15	+(R C)	+(R C)	+(R C
Mice fed normal diet				
Age				
10–20 weeks	20	0	0	0
24 weeks	16	+(R in 62%)	0	0
32–42 weeks	34	+(R in 82% C&R in 6)	+(R in 12%)	0
52–66 weeks	76	+(R in 76% C&R in 42%)	+(R in 7%)	+(R i[n]

0 ab ent + present R reticular fibers C collagenous fibers

old and weighing 21 to 23 gm at the be ginning of the study were fed the experi mental diet (tables 1 and 2) During the experiment three mice were kept in each plastic cage Raised wire floors were used in the cages to prevent coprophagia Mice were weighed weekly up to four months and monthly thereafter (table 3) Ten mice were killed after receiving the di[et] for four weeks 20 after 6–38 weeks and 15 after 52–66 weeks (see table 2) Mice were killed by compression of the cervical spinal cord The simple statistical analysis of the data on body weights (table 3) was based on the methods presented by Croxton (59)

ntralobular increases in reticulum (figs 5 and 7) in a few of the older mice (table 2) The parenchyma adjacent to areas of fibrosis appeared normal The increases in subcapsular fibrosis were concurrent with aging in control mice The fibrosis was accentuated as to precocity and extent by feeding the experimental diet (table 2)

Other changes in control group

Thickening of glomerular basement membranes was common in the older mice A current study shows a 50% or greater incidence of this in old mice of several strains (Ball and Williams 65)

In the four groups of control mice (table 2) body weights had increased progressively with age When one year old the control mice weighed an average of 20% more than those receiving the experimental diet

Livers of dietary group
Parenchymal liposis

The results are presented in table 1 Early stages of this type of liposis have been described in such detail that these phases are considered briefly here Cytoplasmic liposis begins with 24 hours is first concentrated as droplets in centrolobular cells and all lobular zones are involved within 3–7 days (Buckley and Hartroft 55 Meader and Williams 57 Williams Cardle and Meader 59) Initially the intracytoplasmic fat consisted of numerous droplets Then the droplets fused to form a single large mass of sudanophilic material Progressive increase of cytoplasmic fat may produce rupture of such cells Fusion of these remnants forms fatty cysts (Hartroft 50) In the group killed after receiving the diet for four weeks the parenchymal cytoplasm of all lobular zones was filled with fat (fig 1)

In summary the pattern of parenchymal liposis in subsequent chronologic stages was as follows (see table 1)

6 and 10 weeks (6 mice) In peripheral zones of lobules the amount of fat was less than at 30 days With this exception liposis was extensive Numerous cells or remnants were sufficiently enlarged and aggregated to be designated as fatty cysts Liposis was more irregular as to intralobular (zonal) distribution than after feeding the diet for four weeks

14 16 and 18 weeks (9 mice) All zones contained fat some as fatty cysts Earliest appearance of ceroid pigment (Meader and Williams 57 Williams and Oliver 61) was in a mouse killed at 16 weeks Limited amounts of ceroid were characteristic of mice fed the diet for more than 16 weeks

20 26 28 32 38 and 52 weeks (6 mice) The amount of fat had decreased Distribution was irregular Lipid was predominantly in the form of fatty cysts (fig 2) that had no constant intralobular (zonal) location or distribution Numerous lobules were free of fat The decrease in fat observed during this period (20–52 weeks) agrees with the earlier observations of Ball (64) in mice fed a similar diet

54 60 62 and 66 weeks (14 mice) The amount of fat was much greater than in the 20–52 weeks group (fig 3) By 54 weeks all portions of lobules were abundantly fatty No specific zonal patterns of fat distribution were predominant within lobules Fatty cysts were numerous

Sites of hepatic fibrosis

Subcapsular fibrosis This was the most common type of fibrosis in the dietary group and in the controls (figs 8 9 15) It consisted of numerous reticular and a smaller number of collagenous fibers both distributed irregularly beneath the capsule The fibrosis seemed perivenous and perisinusoidal as to origin and location rather than to be extensions from the capsule The arrangement of the fibers resembled pseudotrabeculation from the capsule in a few instances (fig 8) The fibrosis often had distorted the sinusoidal pattern Numerous intraluminal erythrocytes indicated sinusoidal compression in some sites No parenchymal changes including the amount or pattern of liposis could be associated with sites of subcapsular fibrosis

Subcapsular fibrosis was much more extensive in the dietary group than in the controls The fibrosis consisted entirely of reticular fibers during the initial 6–10 weeks of feeding the diet By 14 weeks collagenesis had occurred within these

Sections were made through whole lobes of livers through entire lungs kidneys (with attached adrenals) and through the whole heart in a frontal plane The sections of heart also included thymus lymph nodes bronchi esophagus and great vessels The large sizes of the sections and the use of several staining methods provided sufficient material for an extensive survey of the organs

OBSERVATIONS

General aspects of hepatic fibrosis

The increments in fibrous connective tissue are described here as subcapsular (beneath the hepatic capsule figs 6 8 9 15) perivenous (chiefly related to central veins figs 5 7 11–13 16–19) and intralobular (figs 12 14) The major features of the fibrosis are summarized in table 2 Small argyrophilic fibers identical to those forming the normal intralobular stroma of the liver have been designated here as reticular fibers Such fibers were components of all three types of fibrosis There was no increase in elastic fibers

Collagenous fibers were observed in areas of subcapsular fibrosis in control mice fed a normal diet and in all three types of fibrosis in the experimental (dietary) group Such fibers were a more frequent and more extensive component of fibrosis in the dietary group than in the controls (table 2) Collagenous fibers were stained poorly (pink red) by the Van Gieson method and very clearly (blue) by the Mallory technic These collagenous fibers were also well demonstrated by the silver method for reticulum Then their large size and blue gray (or purple) color contrasted clearly with the black and thread like reticular fibers When such preparations were counterstained with eosin the collagenous fibers were red brown in color while the reticular fibers continued to be black In normal and fibrotic livers the reticular (i e argyrophilic) fibers were not stained by aniline blue or by the Van Gieson procedure Therefore the large fibers stained by these methods particularly those stained heavily by aniline blue are considered to be collagenous

Livers of mice fed normal diet

Parenchyma Staining with H and E and with the PAS method showed norma liver cells Cytoplasmic glycogen was abu dant Fat was limited to very small suda ophilic droplets within cytoplasm This usual in livers of normal mice (Willia 60 Ball 64)

Vessels Blood vessels including lobular sinusoids appeared normal exc in some areas of fibrosis In such the walls of central veins and the ret lum of (or adjacent to) sinusoids seen to be the sources of fibrosis Lymph in the portal areas appeared normal

Biliary system This system appe normal except in one mouse (12 mo of age) where there was an area contai small, epithelium lined tubular struct These resembled small bile ducts and so-called biliary hyperplasia that has associated with diet induced hepatic by (Buckley and Hartroft 55 Popper netto Schaffner and Perez 61)

Normal stroma In young adult (2½–6 months of age) collagenous were limited to the capsule and to restricted amounts in periductal and vascular (excluding sinusoids) sites amounts of collagen were adjacen portal veins and the large tributar the hepatic vein system Central were not surrounded by collagen F lar (argyrophilic) fibers were also lo in the extralobular sites described a Within lobules there was the usual porting pattern of reticulum which predominantly perisinusoidal Sub lar increases in reticular fibers we served in 62% of the control mice i six months age group (table 2)

Fibrosis Among those fed an ade diet 110 mice were 32–66 weeks c when killed In approximately 80 these mice reticular fibers had inc (figs 4–7 14 18 19 and table 2) most frequent site of such fibrosi within and between the lobules that located immediately subjacent to th patic capsule In some areas of inc reticulum a minimal collagenesis ha curred (table 2) Numerous fibro were present in a minority of these (figs 18–19) There were perivenou

intralobular increases in reticulum (figs 5 and 7) in a few of the older mice (table 2) The parenchyma adjacent to areas of fibrosis appeared normal The increases in subcapsular fibrosis were concurrent with aging in control mice The fibrosis was accentuated as to precocity and extent by feeding the experimental diet (table 2)

Other changes in control group

Thickening of glomerular basement membranes was common in the older mice A current study shows a 50% or greater incidence of this in old mice of several strains (Ball and Williams 65)

In the four groups of control mice (table 2) body weights had increased progressively with age When one year old the control mice weighed an average of 20% more than those receiving the experimental diet

Livers of dietary group
Parenchymal liposis

The results are presented in table 1 Early stages of this type of liposis have been described in such detail that these phases are considered briefly here Cytoplasmic liposis begins with 24 hours is first concentrated as droplets in centrolobular cells and all lobular zones are involved within 3–7 days (Buckley and Hartroft 55 Meader and Williams 57 Williams Cardle and Meader 59) Initially the intracytoplasmic fat consisted of numerous droplets Then the droplets fused to form a single large mass of sudanophilic material Progressive increase of cytoplasmic fat may produce rupture of such cells Fusion of these remnants forms fatty cysts (Hartroft 50) In the group killed after receiving the diet for four weeks the parenchymal cytoplasm of all lobular zones was filled with fat (fig 1)

In summary the pattern of parenchymal liposis in subsequent chronologic stages was as follows (see table 1)

6 and 10 weeks (6 mice) In peripheral zones of lobules the amount of fat was less than at 30 days With this exception liposis was extensive Numerous cells or remnants were sufficiently enlarged and aggregated to be designated as fatty cysts Liposis was more irregular as to intralobular (zonal) distribution than after feeding the diet for four weeks

14 16 and 18 weeks (9 mice) All zones contained fat some as fatty cysts Earliest appearance of ceroid pigment (Meader and Williams 57 Williams and Oliver 61) was in a mouse killed at 16 weeks Limited amounts of ceroid were characteristic of mice fed the diet for more than 16 weeks

20 26 28 32 38 and 52 weeks (6 mice) The amount of fat had decreased Distribution was irregular Lipid was predominantly in the form of fatty cysts (fig 2) that had no constant intralobular (zonal) location or distribution Numerous lobules were free of fat The decrease in fat observed during this period (20–52 weeks) agrees with the earlier observations of Ball (64) in mice fed a similar diet

54 60 62 and 66 weeks (14 mice) The amount of fat was much greater than in the 20–52 weeks group (fig 3) By 54 weeks all portions of lobules were abundantly fatty No specific zonal patterns of fat distribution were predominant within lobules Fatty cysts were numerous

Sites of hepatic fibrosis

Subcapsular fibrosis This was the most common type of fibrosis in the dietary group and in the controls (figs 8 9 15) It consisted of numerous reticular and a smaller number of collagenous fibers both distributed irregularly beneath the capsule The fibrosis seemed perivenous and perisinusoidal as to origin and location rather than to be extensions from the capsule The arrangement of the fibers resembled pseudotrabeculation from the capsule in a few instances (fig 8) The fibrosis often had distorted the sinusoidal pattern Numerous intraluminal erythrocytes indicated sinusoidal compression in some sites No parenchymal changes including the amount or pattern of liposis could be associated with sites of subcapsular fibrosis

Subcapsular fibrosis was much more extensive in the dietary group than in the controls The fibrosis consisted entirely of reticular fibers during the initial 6–10 weeks of feeding the diet By 14 weeks collagenesis had occurred within these

Sections were made through whole lobes of livers through entire lungs kidneys (*with attached adrenals*) and through the whole heart in a frontal plane The sec*tions of heart also* included thymus lymph nodes bronchi esophagus and great ves sels The large sizes of the sections and *the use of several* staining methods pro vided sufficient material for an extensive *survey of the* organs

OBSERVATIONS

General aspects of hepatic fibrosis

The increments in fibrous connective tissue are described here as subcapsular (beneath the hepatic capsule figs 6 8 9 15) perivenous (chiefly related to central veins figs 5 7 11–13 16–19) *and intra* lobular (figs 12 14) The major features of the fibrosis are summarized in table 2 Small argyrophilic fibers identical to those *forming the normal intralobular stroma of* the liver have been *designated here as* reticular fibers Such fibers were com*ponents of all three types of fibrosis* There was no increase in elastic fibers

Collagenous fibers were observed in areas of subcapsular fibrosis in control mice fed a normal diet and in all three types of fibrosis in the experimental (die tary) group Such fibers were a more fre quent and more extensive component of fibrosis in the dietary group than in the controls (table 2) Collagenous fibers were stained poorly (pink red) by the Van Gie son method and very clearly (blue) by the Mallory technic These collagenous fibers were also well demonstrated by the silver method for reticulum Then their large size and blue gray (or purple) color contrasted clearly with the black and thread like reticular fibers When such prep arations were counterstained with eosin the collagenous fibers were red brown in color while the reticular fibers continued to be black In normal and fibrotic livers the reticular (i e argyrophilic) fibers were not stained by aniline blue or by the Van Gieson procedure Therefore the large fi bers stained by these methods particularly those stained heavily by aniline blue are considered to be collagenous

Livers of mice fed normal diet

Parenchyma Staining with H and I and with the PAS method showed norm liver cells Cytoplasmic glycogen was abu dant Fat was limited to very small suda ophilic droplets within cytoplasm This usual in livers of normal mice (Williams 60 Ball 64)

Vessels Blood vessels including t lobular sinusoids appeared normal exce in some areas of fibrosis In such sit the walls of central veins and the retic lum of (or adjacent to) sinusoids seem to be the sources of fibrosis Lympha in the portal areas appeared normal

Biliary system This system appear normal except in one mouse (12 mont of age) where there was an area containi small epithelium lined tubular structur These resembled small bile ducts and t so called biliary hyperplasia that has be associated with diet induced hepatic lipo (Buckley and Hartroft 55 Popper Pa netto Schaffner and Perez 61)

Normal stroma In young adult m (2½–6 months of age) collagenous fib were limited to the capsule and to v restricted amounts in periductal and pe vascular (excluding sinusoids) sites Sm amounts of collagen were adjacent portal veins and the large tributaries the hepatic vein system Central ve were not surrounded by collagen Retic lar (argyrophilic) fibers were also local in the extralobular sites described abo Within lobules there was the usual su porting pattern of reticulum which w predominantly perisinusoidal Subcap lar increases in reticular fibers were served in 62% of the control mice in t six months age group (table 2)

Fibrosis Among those fed an adequ diet 110 mice were 32–66 weeks of a when killed In approximately 80% *these mice reticular fibers had increas (figs 4–7 14 18 19 and table 2)* T most frequent site of such fibrosis w within and between the lobules that we located immediately subjacent to the h patic capsule In some areas of increas reticulum a minimal collagenesis had c curred (table 2) Numerous fibroblas were present in a minority of these are (figs 18–19) There were perivenous ar

ıtralobular increases in reticulum (figs and 7) in a few of the older mice (table) The parenchyma adjacent to areas of brosis appeared normal The increases ı subcapsular fibrosis were concurrent ıth aging in control mice The fibrosis ıas accentuated as to precocity and ex nt by feeding the experimental diet table 2)

Other changes in control group

Thickening of glomerular basement nembranes was common in the older mice \ current study shows a 50% or greater ncidence of this in old mice of several trains (Ball and Williams 65)

In the four groups of control mice (table) body weights had increased progres ıvely with age When one year old the control mice weighed an average of 20% nore than those receiving the experimental liet

Livers of dietary group
Parenchymal liposis

The results are presented in table 1 Early stages of this type of liposis have been described in such detail that these phases are considered briefly here Cytoplasmic liposis begins with 24 hours is first con centrated as droplets in centrolobular cells and all lobular zones are involved within 3–7 days (Buckley and Hartroft 55 Meader and Williams 57 Williams Cardle and Meader 59) Initially the in tracytoplasmic fat consisted of numerous droplets Then the droplets fused to form a single large mass of sudanophilic mate rial Progressive increase of cytoplasmic fat may produce rupture of such cells Fusion of these remnants forms fatty cysts (Hartroft 50) In the group killed after receiving the diet for four weeks the parenchymal cytoplasm of all lobular zones was filled with fat (fig 1)

In summary the pattern of parenchy mal liposis in subsequent chronologic stages was as follows (see table 1)

6 and 10 weeks (6 mice) In peripheral zones of lobules the amount of fat was less than at 30 days With this exception liposis was extensive Numerous cells or remnants were sufficiently enlarged and aggregated to be designated as fatty cysts Liposis was more irregular as to intralobu lar (zonal) distribution than after feeding the diet for four weeks

14 16 and 18 weeks (9 mice) All zones contained fat some as fatty cysts Earliest appearance of ceroid pigment (Meader and Williams 57 Williams and Oliver 61) was in a mouse killed at 16 weeks Limited amounts of ceroid were character istic of mice fed the diet for more than 16 weeks

20 26 28 32 38 and 52 weeks (6 mice) The amount of fat had decreased Distribution was irregular Lipid was pre dominantly in the form of fatty cysts (fig 2) that had no constant intralobular (zonal) location or distribution Numer ous lobules were free of fat The decrease in fat observed during this period (20–52 weeks) agrees with the earlier observa tions of Ball (64) in mice fed a similar diet

54 60 62 and 66 weeks (14 mice) The amount of fat was much greater than in the 20–52 weeks group (fig 3) By 54 weeks all portions of lobules were abun dantly fatty No specific zonal patterns of fat distribution were predominant within lobules Fatty cysts were numerous

Sites of hepatic fibrosis

Subcapsular fibrosis This was the most common type of fibrosis in the dietary group and in the controls (figs 8 9 15) *It consisted of numerous reticular and a* smaller number of collagenous fibers both distributed irregularly beneath the capsule The fibrosis seemed perivenous and perisi nusoidal as to origin and location rather than to be extensions from the capsule The arrangement of the fibers resembled pseudotrabeculation from the capsule in a few instances (fig 8) The fibrosis often had distorted the sinusoidal pattern Numer ous intraluminal erythrocytes indicated sinusoidal compression in some sites No parenchymal changes including the amount or pattern of liposis could be as sociated with sites of subcapsular fibrosis

Subcapsular fibrosis was much more extensive in the dietary group than in the controls The fibrosis consisted entirely of reticular fibers during the initial 6–10 weeks of *feeding the diet* By 14 weeks collagenesis had occurred within these

subcapsular sites in the dietary group (table 2 fig 15) The areas of subcapsular fibrosis observed in the older control mice were also composed of reticular and collagenous fibers

Feeding of the experimental diet seemed to accelerate and increase a spontaneous subcapsular fibrosis that also occurred in older mice receiving a normal diet Subcapsular fibrosis was the initial and most extensive stromal change in the dietary group In control mice it was the only significant fibrosis (table 2)

Perivenous fibrosis Thin and irregular septa (Popper Szanto and Elias 55) extended from the adventitia or the perivascular tissue of veins chiefly the central veins of lobules The walls of these vessels were so thin that separation of mural layers from immediately adjacent fibrous elements was obscure These septa (or trabeculae) seemed to link one central vein to another (or to an intercalated vein) The result was an appearance of subdivision of lobules or encapsulation of masses of parenchyma (figs 11–13 16 17) The terms pseudoencapsulation and pseudolobulation seem appropriate to describe the relation of these septa to parenchyma Portal canals were in some instances the central structure of the encapsulated pseudolobules The fibrous septa were still thin (figs 11 12) in their most advanced state as observed after feeding the diet for 52–66 weeks Demonstration of the extent and arrangement of this fibrous tissue depended upon use of stains that showed reticular fibers and or collagen selectively The predominance of perivenous fibrosis in the centrolobular sites of initial and continuing liposis indicates a relationship of this stromal change to the pattern of fat deposition

The origin of septa from portal veins was restricted to a few examples in four mice fed the experimental diet for 38–66 weeks (fig 11) The limited incidence of origin of such septa from portal veins suggests that their real significance is their scarcity or absence

Except for an increase of reticular fibers in some of the older control mice (table 2) perivenous fibrosis was limited to those fed the experimental diet for at least 10 weeks In the dietary group collagen was a component of perivenous fibrosis during the 16–66 week period (table 2)

Intralobular fibrosis This fibrosis was not subcapsular or perivenous in location (fig 10) It consisted chiefly of an in crease in reticular fibers originating from the walls of sinusoids The distribution and extent were irregular Intralob[illegible] fibrosis was not extensions from central or portal veins or from the capsule [illegible] developed in areas of minimal and max[illegible] mal liposis Reticular fibers were the [illegible] component in mice fed the experimen[illegible] diet for as long as 38 weeks (table 2) small amount of collagen had develop[illegible] by 52 weeks

Relation of non parenchymal cells to fibrosis

Increases in fibroblasts or mesenc[illegible] mal cells were questionable in even most extensively fibrotic livers of the [illegible] tary group (Schaffner Barka and Pop[illegible] 63) Fibrosis accompanied by numer[illegible] fibroblasts was best demonstrated in [illegible] capsular areas of two old mice fed a [illegible] mal diet (figs 18 19)

In the older mice of the dietary [illegible] control groups there were focal area[illegible] perivascular cuffing by numerous lym[illegible] cytes and plasma cells and a few ma[illegible] phages and fibroblasts This perivasc[illegible] reaction seemed unrelated to fibrosis [illegible] was limited almost exclusively to p[illegible] areas which were rarely sites of fibro[illegible]

Other non stromal hepatic change[illegible]

Areas of parenchymal necrosis us[illegible] at the surface of lobes and comprisi[illegible] much as 20% of such lobes were se[illegible] three mice killed after receiving the [illegible] perimental diet for 10 18 and 62 w[illegible] The necrosis appeared recent and [illegible] represent a lesion that occurs in mic[illegible] diets inadequate in protein (Williams [illegible] Aronsohn 56) These areas of nec[illegible] were excluded from the appraisal of [illegible] enchymal and stromal changes No [illegible] enchymal hyperplasia was observed [illegible] few mitoses were seen in all livers of [illegible] trol and dietary mice

Changes in other organs

Kidneys In ten of the 45 mice fed the experimental diet glomerular basement membranes were thickened as observed previously in older mice receiving an adequate diet (Ball and Williams 65)

Hearts There was massive atrial (mural) thrombosis in 4 of 16 mice killed after receiving the experimental diet for 10–28 weeks and in one mouse at 54 weeks This relatively low incidence of atrial thrombosis is in striking contrast to one of 100% observed in some stocks of mice fed a diet similar to the one used here (Ball Williams and Collum 63 Ball 64 Ball Clower and Williams 65)

Changes in body weight

Body weights varied considerably within groups at comparable chronologic intervals Maintenance of body weight and a slight trend toward weight gain seemed significant (table 3) At specific intervals the livers of mice losing weight did not differ from those maintaining or gaining weight Weight loss initially was most severe in mice with atrial thrombosis During 20–52 weeks liver fat decreased This decrease in fat was not associated with gain or loss in body weight Later (52–66 weeks) the greatest weight loss was not associated with any type of lesion During this period weight maintenance (or gain) was excellent (table 3) and hepatic liposis and fibrosis were extensive (tables 1 and 2)

DISCUSSION

Fibrosis in control mice

In C mice fed a normal diet fibrosis seemed to be a spontaneous process associated with aging and unrelated to hepatic damage including liposis The livers of young adult mice showed the normal stromal pattern but as aging occurred there was an increase of fibrous tissue The most striking increase in fibrous tissue was beneath the capsule The origin of the fibrosis seemed to be perivenous and perisinusoidal Fibrous strands linking central vein to central vein were present but to a much lesser degree than in the dietary group In rare instances there were fibrous extensions from portal areas After receiving the diet for 6–10 weeks and thus attaining an age of 20–30 weeks members of the experimental (dietary) group showed stromal changes equivalent to those in livers of control mice 52–66 weeks of age Therefore older control mice fed a normal diet and much younger mice fed the experimental diet demonstrated fibrotic changes which were comparable

The subcapsular fibrosis seen here in old control mice and in the dietary group is similar to that described by MacDonald (62) MacDonald s study was limited to rats fed a high fat low protein choline deficient diet and did not include old rats receiving normal diet Spontaneous hepatic fibrosis associated with aging has received little if any attention in relation to experimental dietary cirrhosis

The number of strains of mice that develop spontaneous hepatic fibrosis when fed adequate diets is yet to be determined Little information is available concerning strain limited reactions of mice or of other species to the fibrogenic and cirrhogenic actions of diets that produce fatty livers Patek and de Fritsch (63) observed that 20%–30% of male Sprague Dawley rats were usually resistant to the "cirrhosis producing" actions of a low protein choline-deficient diet Inbreeding of the descendants of these rats increased this resistance for three generations Subsequently there was a loss of resistance and an increase in susceptibility to the production of cirrhosis

Hepatic fibrosis in the dietary group of mice

When compared with Ball s study (64) of mice receiving a hypolipotropic diet the present data indicate that the feeding of a diet containing a larger amount of fat (40% instead of 28%) and in some instances for a longer period of time produced more extensive and prolonged liposis and greater fibrosis The fibrosis observed here was less than described in earlier studies of younger mice fed a high fat choline-deficient diet that differed from the present one in protein composition and vitamin supplementation (Buckley and Hartroft 55 Meader and Williams 57) In choline-deficient young rats the amounts of hepatic liposis and fibrosis were pro-

portional to the level of dietary fat but not to that of protein (Zaki Bandt and Hoffbauer, 63)

MacDonald (62) described fibrosis as developing first around central veins later around portal areas and then along the lobular sinusoids in rats fed a high fat, low protein, choline deficient diet Lymphatics and blood vessels beneath the capsule were involved early and to a greater extent than those deeper within the liver substance Bands of fibrous tissue eventually connected nearly all central and portal veins When there was parenchymal regeneration in the fatty and cirrhotic liver it occurred diffusely throughout the organ and was not organized in a nodular pattern The present findings concur in general with those of MacDonald The amount of fibrosis was less but the pattern was similar to that observed by MacDonald Likewise there was extensive subcapsular fibrosis MacDonald did not describe subcapsular fibrosis in rats fed a normal diet Perivascular sources and patterns of dietary induced fibrosis have been described in detail by Popper (54) and Popper and Schaffner (57)

Some of the similarities between the present results and those of MacDonald (62) may have been due to his use of young adult rats in contrast to the much younger rats in Hoffbauers study (57) In the present study and in MacDonalds the animals were fed similar diets for more than a year In Hoffbauers younger rats the nodular regeneration and extensive fibrosis occurred within 4–6 months MacDonald and Mallory (59) emphasized active fibrogenesis in fatty cirrhosis while Hoffbauer (57) stressed the mechanical effects of fatty cysts and of expanding nodules of parenchyma (Baggenstoss 55)

Hoffbauer (57) concluded that fatty cirrhosis in young rats was the result of development and enlargement of regenerative nodules of hepatic parenchyma which were surrounded by fibrous tissue Earlier compression of stroma and perhaps a true fibrosis had resulted from pressure exerted by large fatty cysts and by rupture of the cysts Subsequently periportal parenchymal hyperplasia formed distinct nodules of new liver cells Regenerative nodules were not observed in the livers of the mice studied here or earlier (Ball 64)

The currently described perivenous fibrosis originated in centrolobular zones and consisted of increases in reticulum and a subsequent collagenesis in sites of initial and incremental parenchymal lipo[...]sis Subsequently there was great enlarge[...]ment and distortion of cells by their in[...]creasing content of fat and formation of fatty cysts Hartroft (50 54) has de[...]scribed in detail the sequence of events in rats that follows rupture of fatty cysts and results in condensation of their remnants into fibrous trabeculae (Hartroft and R[...]out 51) In pattern but not in amount the perivenous septa observed here were similar to those described by Hartroft [...] the present mice the amount of liposis [...] formation of fatty cysts, and the extent of fibrosis were less than in rats fed sim[...] diets (Hartroft '50 54 MacDonald [...]

The observations indicate that experi[...]mental diet may have produced fibrosis [...] accelerating and expanding a spontane[...] process which occurs with aging in C[...] fed a normal diet Also when fed a h[...] fat low protein hypolipotropic diet th[...] mice developed fattier livers and more [...]patic fibrosis but less cardiovascular [...] age than other strains of mice (Ball [...]liams and Collum 63 Ball 64 Clower and Williams 65)

LITERATURE CITED

Ashburn A D W L Williams and F R [...] 1963 Cardiovascular hepatic a d ren[...] sions in mice receiving cortisone estron[...] progesterone Yale J Biol and Med 35 [...] 340

Baggenstoss H A 1955 The significa[...] nodular regeneration in cirrhosis of the [...] Am J Clin Path 25 936–939

Ball C R 1964 Actions of betaine ca[...] and choline on the pattern of hepatic [...] in mice fed a high fat low protein diet [...] Rec 149 677–689

Ball C R Ben R Clower and W L Wi[...] 1965 Dietary induced atrial thrombos[...] mice Arch Path 80 391–396

Ball C R and W L Williams 1965 [...]taneous and dietary induced cardiovascu[...] sions in DBA mice Anat Rec 152 19[...]

Ball C R W L Williams and J M C[...] 1963 Cardiovascular lesions in Swiss [...] fed a high fat low protein diet with and [...]out betaine supplementation Anat Rec [...] 49–60

ckley G F and W S Hartroft 1955 Pathology of choline deficiency in the mouse Arch Path 59 185-197
oxton F E 1959 Elementary Statistics with Applications in Medicine and Biology Dover New York
rdon H and H H Sweets 1936 A simple method for silver impregnation of reticulum Am J Path 12 545-552
yorgy P and H Goldblatt 1939 Hepatic injury on a nutritional basis in rats J Exp Med 70 185-192
artroft W S 1950 Accumulation of fat in liver cells and in lipodiastemata preceding experimental dietary fatty cirrhosis Anat Rec 106 61-87
—— 1954 The sequence of pathologic events in the development of experimental fatty liver and cirrhosis Ann N Y Acad Scs 57 633-645
Hartroft W S and J H Ridout 1951 Pathogenesis of the cirrhosis produced by choline deficiency Escape of lipid from fatty hepatic cysts into the biliary and vascular system Am J Path 27 951-989
Hoffbauer F W 1957 Experimental fatty cirrhosis Minnesota Med 40 603-614
ent S P and M Diseker 1955 Early myocardial ischemia Lab Invest 4 398-405
illie R D 1954 Histologic Technic and Practical Histochemistry The Blakiston Co Inc New York
MacDonald R A 1962 Pathogenesis of nutritional cirrhosis Arch Int Med 110 424-434
MacDonald R A and K Mallory 1959 Fibrous tissue in nutritional cirrhosis Autoradiographic studies with use of tritiated thymidine Arch Path 67 119-127
Meader R D and W L Williams 1957 Choline deficiency in the mouse Am J Anat 100 167-204
Patek A J Jr and N M de Fritsch 1963 Evidence for genetic factors in the resistance of the rat to dietary cirrhosis Proc Soc Exp Biol and Med 113 820-824
Popper H 1954 Liver disease morphologic considerations Am J Med 16 98-117
Popper H F Paranetto F Schaffner and V Perez 1961 Studies on hepatic fibrosis Lab Invest 10 265-290
Popper H and F Schaffner 1957 Liver Structure and Function McGraw Hill New York
Popper H P B Szanto and H Elias 1955 Transition of fatty liver into cirrhosis Gastroenterology 28 183-192
Schaffner F T Barka and H Popper 1963 Hepatic mesenchymal cell reaction in liver disease Exp Molec Path 2 419-441
Snell G D J Staats M F Lyon L C Dunn H Gruneberg P Hertwig and W E Heston 1960 Standardized nomenclature for inbred strains of mice — Second Listing Cancer Research 20 145-169
Staff Roscoe B Jackson Memorial Laboratory 1962 Handbook on Genetically Standardized JAX Mice Roscoe B Jackson Memorial Laboratory Bar Harbor Times Publishing Co Bar Harbor Maine
Williams W L 1960 Hepatic liposis and myocardial damage in mice fed choline-deficient or choline supplemented diets Yale J Biol Med 33 1-14
Williams W L and R B Aronsohn 1956 Cardiac and hepatic lesions in mice fed yeast protein diets I Diets containing British bakers yeast Yale J Biol Med 28 515-524
Williams W L J B Cardle and R D Meader 1959 The nature of dietary fat and the pattern of hepatic liposis in choline-deficient mice Yale J Biol Med 31 263-270
Williams W L and R I Oliver 1961 The relation of types of dietary fat to hepatic liposis and myocardial damage in mice Anat Rec 141 97-108
Yokoyama H O R B Jennings G Clabaugh and W B Wartman 1955 Histochemical studies of early experimental myocardial infarction Periodic acid Schiff method Arch Path 59 347-354
Zaki F G C Brandt and F W Hoffbauer 1963 Fatty cirrhosis in the rat III Liver lipid and collagen content in various stages IV The influence of different levels of dietary fat Arch Path 75 648-660

portional to the level of dietary fat but not to that of protein (Zaki Bandt and Hoffbauer 63)

MacDonald (62) described fibrosis as developing first around central veins later around portal areas and then along the lobular sinusoids in rats fed a high fat low protein choline deficient diet Lymphatics and blood vessels beneath the capsule were involved early and to a greater extent than those deeper within the liver substance Bands of fibrous tissue eventually connected nearly all central and portal veins When there was parenchymal regeneration in the fatty and cirrhotic liver it occurred diffusely throughout the organ and was not organized in a nodular pattern The present findings concur in general with those of MacDonald The amount of fibrosis was less but the pattern was similar to that observed by MacDonald Likewise there was extensive subcapsular fibrosis MacDonald did not describe subcapsular fibrosis in rats fed a normal diet Perivascular sources and patterns of dietary induced fibrosis have been described in detail by Popper (54) and Popper and Schaffner (57)

Some of the similarities between the present results and those of MacDonald (62) may have been due to his use of young adult rats in contrast to the much younger rats in Hoffbauer s study (57) In the present study and in MacDonald s the animals were fed similar diets for more than a year In Hoffbauer s younger rats the nodular regeneration and extensive fibrosis occurred within 4–6 months MacDonald and Mallory (59) emphasized active fibrogenesis in fatty cirrhosis while Hoffbauer (57) stressed the mechanical effects of fatty cysts and of expanding nodules of parenchyma (Baggenstoss 55)

Hoffbauer (57) concluded that fatty cirrhosis" in young rats was the result of development and enlargement of regenerative nodules of hepatic parenchyma which were surrounded by fibrous tissue Earlier compression of stroma and perhaps a true fibrosis had resulted from pressure exerted by large fatty cysts and by rupture of the cysts Subsequently periportal parenchymal hyperplasia formed distinct nodules of new liver cells Regenerative nodules were not observed in the livers of the mice studied here or earlier (Ball '64

The currently described perivenous fibrosis originated in centrolobular zones and consisted of increases in reticulum and a subsequent collagenesis in sites of initial and incremental parenchymal lipos sis Subsequently there was great enlargement and distortion of cells by their increasing content of fat and formation of fatty cysts Hartroft (50 54) has described in detail the sequence of events in rats that follows rupture of fatty cysts and results in condensation of their remnants into fibrous trabeculae (Hartroft and R out 51) In pattern but not in amou the perivenous septa observed here w similar to those described by Hartroft the present mice the amount of liposis formation of fatty cysts and the exten fibrosis were less than in rats fed sim diets (Hartroft 50 54 MacDonald

The observations indicate that ex mental diet may have produced fibros accelerating and expanding a spontan process which occurs with aging in C fed a normal diet Also when fed a h fat low protein hypolipotropic diet t mice developed fattier livers and mor patic fibrosis but less cardiovascular age than other strains of mice (Ball llams and Collum 63 Ball 64 Clower and Williams 65)

LITERATURE CITED

Ashburn A D W L Williams and F R 1963 Cardiovascular hepatic and re sions in mice receiving cortisone estro progesterone Yale J Biol and Med 35 340

Baggenstoss H A 1955 The significa nodular regeneration in cirrhosis of the Am J Clin Path 25 936–939

Ball C R 1964 Actions of betaine ca and choline on the pattern of hepatic in mice fed a high fat low protein diet Rec 149 677–689

Ball C R Ben R Clower and W L W 1965 Dietary induced atrial thrombo mice Arch Path 80 391–396

Ball C R and W L Williams 1955 taneous and dietary induced cardiovasc sions in DBA mice Anat Rec 152 19

Ball C R W L Williams and J M 1963 Cardiovascular lesions in Swiss fed a high fat low protein diet with and out betaine supplementation Anat Rec 49–60

…tley G F and W S Hartroft 1955 Path…ogy of choline deficiency in the mouse Arch …ath 59 185–197

…tton F E 1959 Elementary Statistics with …pplications in Medicine and Biology Dover …lew York

…don H and H H Sweets 1936 A simple …nethod for silver impregnation of reticulum …m J Path 12 545–552

…orgy P and H Goldblatt 1939 Hepatic in…ury on a nutritional basis in rats J Exp …Med 70 185–192

…rtroft W S 1950 Accumulation of fat in …iver cells and in lipodiastemata preceding ex…perimental dietary fatty cirrhosis Anat Rec 106 61–87

—— 1954 The sequence of pathologic events in the development of experimental fatty liver and cirrho is Ann N Y Acad Scs 57 633–645

…artroft W S and J H Ridout 1951 Pathogenesis of the cirrhosis produced by choline deficiency Escape of lipid from fatty hepatic cysts into the biliary and vascular system Am J Path 27 951–989

…offbauer F W 1957 Experimental fatty cir…rhosis Minnesota Med 40 603–614

…ent S P and M Diseker 1955 Early myocardial ischemia Lab Invest 4 398–405

…llie R D 1954 Histologic Technic and Prac…tical Histochemistry The Blakiston Co Inc New York

…acDonald R A 1962 Pathogenesis of nutri…tional cirrhosis Arch Int Med 110 424–434

…acDonald R A and K Mallory 1959 Fibrous tissue in nutritional cirrhosis Autoradiographic studies with use of tritiated thymidine Arch Path 67 119–127

…eader R D and W L Williams 1957 Choline deficiency in the mouse Am J Anat 100 167–204

…itek A J Jr and N M de Fritsch 1963 Evidence for genetic factors in the resistance of the rat to dietary cirrhosis Proc Soc Exp Biol and Med 113 820–824

…opper H 1954 Liver disease morphologic con…siderations Am J Med 16 98–117

Popper H F Paranetto F Schaffner and V Perez 1961 Studies on hepatic fibrosis Lab Invest 10 265–290

Popper H and F Schaffner 1957 Liver Structure and Function McGraw Hill New York

Popper H P B Szanto and H Elias 1955 Transition of fatty liver into cirrhosis Gastroenterology 28 183–192

Schaffner F T Barka and H Popper 1963 Hepatic mesenchymal cell reaction in liver disease Exp Molec Path 2 419–441

Snell G D J Staats M F Lyon L C Dunn H Gruneberg P Herturg and W E Heston 1960 Standardized nomenclature for inbred strains of mice — Second Listing Cancer Research 20 145–169

Staff Roscoe B Jackson Memorial Laboratory 1962 Handbook on Genetically Standardized JAX Mice Roscoe B Jackson Memorial Laboratory Bar Harbor Times Publishing Co Bar Harbor Maine

Williams W L 1960 Hepatic liposis and myocardial damage in mice fed choline-deficient or choline-supplemented diets Yale J Biol Med 33 1–14

Williams W L and R B Aronsohn 1956 Cardiac and hepatic lesions in mice fed yeast protein diets I Diets containing British bakers yeast Yale J Biol Med 28 515–524

Williams W L J B Cardle and R D Meader 1959 The nature of dietary fat and the pattern of hepatic liposis in choline-deficient mice Yale J Biol Med 31 263–270

Williams W L and R I Oliver 1961 The relation of types of dietary fat to hepatic liposis and myocardial damage in mice Anat Rec 141 97–108

Yokoyama H O R B Jennings G Clabaugh and W B Wartman 1955 Histochemical studies of early experimental myocardial infarction Periodic acid Schiff method Arch Path 59 347–354

Zaki F G C Brandt and F W Hoffbauer 1963 Fatty cirrhosis in the rat III Liver lipid and collagen content in various stages IV The influence of different levels of dietary fat Arch Path 75 648–660

Abbreviations

(All figures show livers)

Aniline blue Mallory method for fibrous connective tissue
(*wks*) Weeks fed the high fat low protein choline deficient diet
C Central vein
Control mice Mice 12–16 months of age fed an adequate diet
E Eosin
H Hematoxylin
P Portal vein
PAS Periodic acid Schiff's reagent procedure
Ret Silver method for demonstrating reticular fibers

PLATE 1

EXPLANATION OF FIGURES

Frozen sections of livers of dietary mice stained with sudan black to show fat × *100*

1 Abundant liposis with concentration of fat in central and middle zones of lobules (*4 wks*)

2 Most of the fat is in large cysts (*20–52 wks*)

3 Extensive liposis without a predominant zonal pattern (*54–66 wks*)

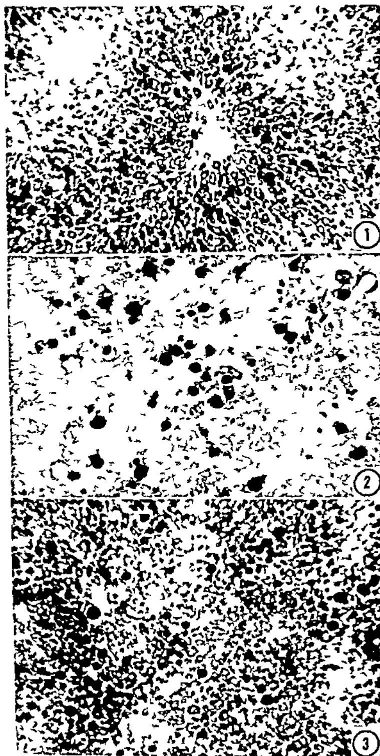

1
2
3

PLATE 2

EXPLANATION OF FIGURES

Reticulum stain livers of control mice

4–6 (× 100) and 7 (× 60) show range in quantity and distribution of reticulum in livers of mice fed an adequate diet In figure 4 the reticulum is heavily stained There is no focal or general increase but the amount is maximal within the normal range In figures 5 and 7 the increase in reticulum consists of perivenous extensions The increase in subcapsular in figure 6 Except for the increased reticulum (figs 5 6 7) the livers were normal The areas in figures 4 5 and 7 are deep within lobes

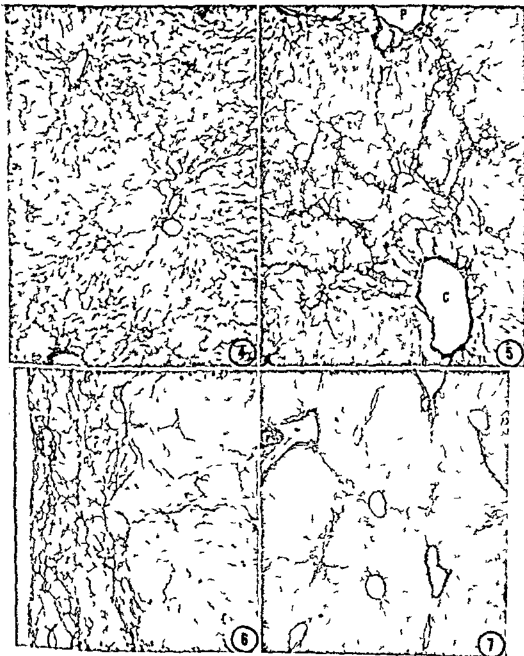

P
C
4
5
6
7

PLATE 2

EXPLANATION OF FIGURES

Reticulum stain livers of control mice

4–6 (× 100) and 7 (× 60) show range in quantity and distribution of reticulum in livers of mice fed an adequate diet In figure 4 the reticulum is heavily stained There is no focal or general increase but the amount is maximal within the normal range In figures 5 and 7 the increase in reticulum consists of perivenous extensions The increase in subcapsular in figure 6 Except for the increased reticulum (figs 5 6 7) the livers were normal The areas in figures 4 5 and 7 are deep within lobes

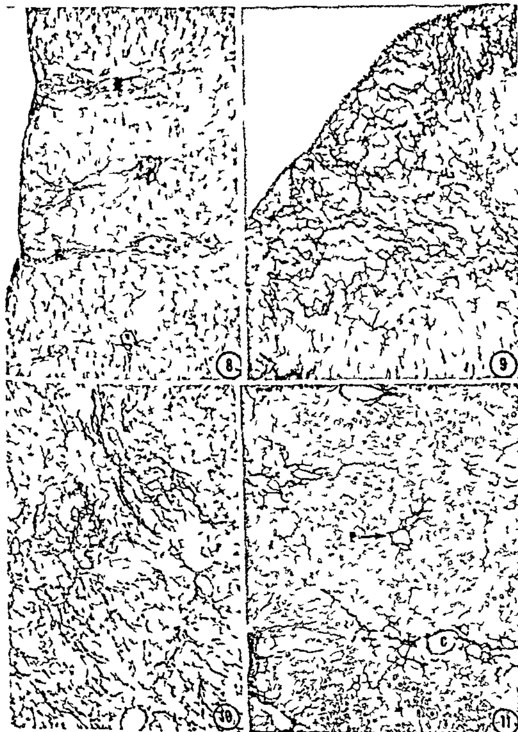

8
9
10
11
P
C

PLATE 3

EXPLANATION OF FIGURES

Livers of dietary mice Ret stain × 100

8–9 Figure 8 (*10 wks*) and 9 (*30 wks*) Sites of subcapsular fibrosis In figure 8 the perivenous fibers form a pattern of pseudotrabeculation extending internally from the subcapsular area The more common type of subcapsular fibrosis is shown in figure 9 There was no parenchymal necrosis in these sites and the increase in reticulum was not related to the amount of parenchymal liposis Liposis was greater in the liver shown in figure 8

10 (*66 wks*) Intralobular fibrosis in an area of extreme liposis Identical fibrosis occurred in less fatty areas

11 (*54 wks*) Typical pseudolobulation or pseudoencapsulation resulting from perivenous (chiefly central veins) extensions A portal canal (*P*) is in the center of the pseudolobule


12
13
14
15

PLATE 4

EXPLANATION OF FIGURES

12–13 Figure 12 (*66 wks*) and 13 (*52 wks*) Perivenous projections appear to surround or encapsulate areas of parenchyma The site in figure 12 is immediately beneath the hepatic capsule while that in figure 13 is deep in the lobe *Ret* × 100

14 Area of intralobular fibrosis in an old (*66 wks*) control mouse fed an adequate diet The parenchymal cells appear normal *Ret H and E* × 200

15 (*16 wks*) Collagenous fibers in a subcapsular area of extensive liposis *Aniline blue* × 200

16
17
C
18
P
19

PLATE 5

EXPLANATION OF FIGURES

All show collagenous fibers stained with aniline blue

16–17 Figure 16 (*66 wl s*) and 17 (*14 wl s*) The collagenesis is extensive Both areas are directly beneath the capsule In the upper left area of figure 17 there is obvious perivenous fibrosis Liposis is extensive but there is no parenchymal necrosis × 200

18–19 There are small amounts of collagen in livers of control mice 52 and 66 weeks of age Numerous fibroblasts are seen in figure 18 × 200


16


17


C
18


P
19

ectron Microscopy of Oligodendrocytes Normal Rat Cerebrum

LAWRENCE KRUGER AND DAVID S MAXWELL
Department of Anatomy School of Medicine and Brain Research Institute University of California Los Angeles California and Veterans Administration Hospital Long Beach California

ABSTRACT Electron microscopic examination of rat cerebral gray and white matter following formaldehyde or glutaraldehyde vascular perfusion reveals distinctive morphological features for identification of oligodendrocytes These elements are situated as satellites of neurons (perikarya dendrites and axons) and display a wide range of nuclear and cytoplasmic densities which tend to parallel each other Cytoplasmic density appears to be an uncertain criterion for neuroglial identification but oligodendrocytes are recognizable by the following distinctive features large quantities of free ribosomes or ribosomal rosettes numerous nuclear pores and light patches of otherwise dense chromatin adjacent to the pores extensive cytoplasmic microtubules absence of broad processes seen in other cerebral elements but presence of numerous fine processes which can occasionally be traced to form the outer mesaxon of *myelin sheaths* absence of glycogen and fine gliofibrils *uniquely present in astrocytes* and the usual presence of thin rims of perinuclear cytoplasm frequently associated with large dilatations of the nuclear cleft Arguments are adduced for rejecting the identification of "dark glial elements as microglia The relation of oligodendrocytes to myelin and the functional significance of the wide spectrum in cytoplasmic density are considered in relation to the synthetic demands of adjacent neurons

In the electron microscopic literature here appears to be a consensus regarding he characteristic features of oligodendro ytes (Farquhar and Hartmann 57 chultz et al 57 Hartmann 58 Palay 58 Schultz and Pease 59 Bunge et al 60 Peters 60 De Robertis and Gerschenfeld 61 Palay et al 62 Gray 64 Gregoire 63 Terry and Weiss 63 Coulter 64 Herndon 64 Maxwell and Kruger 64 Schultz 64 Bodian 64 Mugnaini and Walberg 64) In conventional microscopy nuclear size and density (Smart and Leblond 61) and configuration of processes (Penfield 32) have been suggested as the bases for subclassification of oligodendroglia However a similar recognition of morphological diversity and a clear specification of the range of oligodendrocyte morphology has not yet occurred in electron microscopy The difficulties posed by this diversity have been compounded by some authors (Luse 58 62 Vogel and Kemper 61) who have designated the more dense glial elements as astrocytes and the less dense as oligodendrocytes Oligodendrocytes in light and electron microscopy are easily found in white matter commonly in rows and are often arranged as neuronal satellites in gray matter Recent studies following aldehyde fixation have provided additional criteria for the electron microscopic identification of astrocytes on the basis of distinctive organelles (Maxwell and Kruger 65a) and therefore for distinguishing between them and non astrocytic glia

In light microscopy the nuclei of oligodendrocytes are difficult to distinguish from those of microglia which are said to be irregular or rod shaped and smaller than the round or oval nuclei of oligodendrocytes These two categories of cells comprise the third element of Cajal (11) which was subdivided by Rio-Hortega (32) on the basis of his silver carbonate method This method displays the cytoplasmic configuration of cells of the third element and by manipulation of such poorly understood factors as pH or the duration of fixation and staining or post mortem changes (Rio-Hortega et al 43) can be made to more or less preferentially impregnate oligodendrocytes or microgliacytes The cells which Rio Hortega classified as microglia he believed were derived from mesoderm and were to be distinguished from oligodendrocytes (of ectodermal origin) by their slen

der but elaborately branched processes The identification of a variety of glial cell in electron microscopy which might correspond with the microglial cell of silver carbonate impregnation has met with difficulty Numerous authors have designated cells displaying marked nuclear and cytoplasmic density as microglia (Schultz et al 57 De Robertis and Gerschenfeld 61 Palay et al 62 Terry and Weiss 63 Bodian 64 Mugnaini and Walberg 64 Yasuzumi et al 64) although there has usually been appropriate caution expressed regarding the tentative nature of such identification

The present study constitutes part of a continuing effort (Maxwell and Kruger 65b) to examine the electron microscopic basis for Rio Hortega s subdivision of Cajal s third element and an attempt to specify the normal range of fine structure of oligodendrocytes in the cortex and white matter of the cerebrum The reactive changes which occur in oligodendrocytes in response to focal injury are described in the accompanying publication (Maxwell and Kruger 66)

MATERIALS AND METHODS

The tissue on which this report is based was taken from normal adult rats All animals were sacrificed under pentobarbital anesthesia The chest was opened and the animal was rapidly perfused by means of a tube introduced into the ascending aorta via the left ventricle The perfusion fluid was either phosphate buffered 4% formaldehyde or phosphate or cocodylate buffered 6 25% glutaraldehyde at pH 7 2–7 4 Excised pieces of cerebrum were post fixed for one to two hours in 1% OsO_4 in the same buffer as the perfusion solution Rapid dehydration was followed by embedment in Araldite All of the illustrations in the present report are of thin sections stained with lead citrate and photographed with the aid of the RCA EMU 3E or the Hitachi HU 11A electron microscopes All technical procedures employed are described in detail by Pease (64)

In our experience aldehyde perfusion followed by OsO_4 post fixation has been characterized by consistently satisfactory preservation and remarkable uniformity the cerebral cortex for a large series normal and experimental animals T white matter of these animals has ev ited less uniform fixation and it is co mon to find patches of apparently enlar extracellular spaces and swollen astroc processes These signs of less satisfact preservation may be due in part to chanical distortions of the tissue du preparation or they may reflect a diffic in obtaining uniformly good fixation vascular perfusion in a region not n endowed with blood vessels

RESULTS

Electron microscopy of cerebral w matter The linearly arranged inte cicular glia of white matter provides most appropriate site to begin a stud electron microscopy (Rio Hortega 32 field 24 32) Astrocytes intermi with these cells can be identified with sonable certainty by the unique pres of glycogen granules and bundles o proximately 60 Å filaments (fig 3 Maxwell and Kruger 65a) The str absence of these two components in glial elements in formaldehyde or g aldehyde perfused material renders i sible to classify cells lacking these o elles as non astrocytic glia The wide r of nuclear and cytoplasmic matrix sities displayed by this class of cells i interfascicular glia suggests two diff cell types with a range of interme forms (figs 1–8) and which we shall to as oligodendrocytes for descriptive poses Those elements with lighter plasm and nucleus are present in l numbers than the dark variety but and dark varieties are abundantly rounded by axons and form a typical fascicular row of cells (figs 1 4 5 numerous instances the perinuclear plasm on at least one surface is narr to a thin rim as shown in figures Eccentric nuclear position renders th terion of scanty cytoplasm unsui for identification when plane of secti taken into account The irregular con of these elements the wide variety o clear shapes evident and eccentric pos of nucleus emphasize the difficult

interpreting profiles on the basis of nuclear/cytoplasmic ratio or form of nucleus

The absence of extensive *broad* processes which are displayed by other cerebral elements (e g the astrocyte in fig 3) is striking in the whole range of oligodendrocytes of varying nuclear and cytoplasmic density This feature could account for the paucity of processes seen in light microscopic examination of metallic impregnation material and also provides one satisfactory criterion for identification in electron microscopy However examination of the fine structure of oligodendrocytes reveals the presence of numerous *very fine* processes in intimate relation to surrounding axons (figs 7–9)

Oligodendrocytes studied in the cerebral white matter have many cytoplasmic features which emphasize their common nature in spite of the range of cytoplasmic matrix density which can be observed The granular endoplasmic reticulum is commonly dilated into cisterns (figs 1 3–5) Free ribosomes and occasional ribosomal rosettes are much more abundant than in astrocyte cytoplasm The Golgi membranes are conspicuous as are the profiles of smooth endoplasmic reticulum Glutaraldehyde perfusion preserves the microtubular component of the cytoplasm noted by Mugnaini and Walberg (64) in OsO immersed tissue and similar to the microtubular systems preserved with glutaraldehyde in some other tissues These tubules are approximately 200 Å in diameter and appear to have no consistent orientation *to each other* or to other organelles They are readily found in the perinuclear cytoplasm (figs 2–5 11 13) and in the entrapped oligodendrocyte cytoplasm of nodes of Ranvier (fig 9) They are usually less well preserved with formaldehyde fixation (figs 6–8) By contrast the microtubules of astrocyte cytoplasm are sparse (fig 3) In general the nuclei of oligodendrocytes contain more densely packed chromatin than astrocytes (fig 3) Large dilatations of the nuclear cleft (figs 1 5 7) are fairly frequent in oligodendrocytes and were recognized by Bodian (64) as a useful criterion for identification but this is not a striking feature in the denser elements (figs 1 3 8 13)

The highest density of inhomogeneously distributed chromatin material occurs at the nuclear membrane (figs 1 3–5 7 11 12) Irregular light patches interrupt the dense chromatin at the nuclear membrane and are usually identifiable as the sites of nuclear pores (fig 7) Nuclear pores may be observed in other cortical elements but their prominence and number in oligodendrocytes serves to provide another criterion for identification These pores may account for the parallel of nuclear and cytoplasmic density encountered in the wide spectrum of oligodendrocytes by providing an extensive channel system for interchange between nucleus and cytoplasm (Feldherr 65)

A crucial factor in designating the above described elements oligodendrocytes is their relation to the surrounding axons (figs 3–9) Excellent examples showing that the plasma membrane of similar cells forms the outer mesaxon continuous with the spiral lamellae of the myelin sheath have been published in studies of developing optic nerve (Peters 60 Maturana 60) A similar relationship has been found in cat spinal cord following recovery from experimental demyelination by Bunge Bunge and Pappas (62) (although these workers did not designate this cell as an oligodendrocyte) and in normal mouse spinal cord by Gregoire (63)

The difficulty in establishing that the axons surrounding a presumed oligodendrocyte are indeed myelinated by its processes is due to the rarity with which the outer loop or tongue of cytoplasm forming the outer mesaxon can be traced into continuity with the generally thin rim of perinuclear cytoplasm in adult material (fig 6) Evidently most of the processes are sufficiently fine and tortuous to obscure this continuity in a single thin section However even the occasional propitious example would seem to suggest that the small tongues forming the outer mesaxon of fibers surrounding the oligodendrocytes are probably derived from this cell The trapped cytoplasm which may display a wide range of matrix density also usually displays the same matrix density as the juxtaposed cell Despite wide variations in cytoplasmic matrix densities it is usually

simple to distinguish oligodendrocyte contacts from those of the prominent astrocyte processes (fig 3) It should also be emphasized that we have never seen more than a single inner and outer mesaxon in any of our material

Electron microscopy of gray matter In normal adult cerebral cortex the oligodendrocytes with denser matrix described above are less numerous and although they resemble their interfascicular counterpart only a few myelinated axons adhering to the surface are ever encountered in a single section Furthermore the complexity and compactness of the surrounding small processes renders it generally impossible to trace the continuity between the outer tongue and the parent cell body However there can be no doubt concerning the similarity of the cytoplasmic and nuclear features of these cells in white (figs 1–10) and gray (figs 11–13) matter and it is possible that the differences are related to the nature of the neuronal relationship Within the cortical gray the oligodendrocyte is often in contact with the neuron perikaryon (figs 12 13) It may be relevant that these satellite cells frequently display the lowest cytoplasmic and nuclear densities (fig 12) and that oligodendrocytes with dense matrix cytoplasm (figs 11 13) are less common in the cortex

The oligodendrocytes of high cytoplasmic and nuclear density of gray matter are generally agreed to constitute the most difficult problem in identification These elements are frequently darker than the common dense oligodendrocytes of white matter and appear to possess a very dense and almost homogeneous nucleus Because of unusually high matrix density only the ribosomes are prominent and even mitochondria are difficult to delimit The cytoplasmic microtubules (figs 11 13) Golgi membranes and granular endoplasmic reticulum with prominent dilatations suggest a similarity between the dense elements of both gray and white matter Some thin rims of cytoplasm and the consistent absence of broad processes provide additional support for regarding these somewhat different elements as oligodendrocytes It might also be noted that the dense oligodendrocytes of both gray (figs 11 13) and white (figs 1 3 4 6) matter display a less prominent nuclear cleft than their paler counterparts

Large osmiophilic cytoplasmic organelles in oligodendrocytes are occasionall[y] encountered in both gray and white mat[ter] but their nature and factors affectin[g] their incidence are poorly understoo[d] These are membrane bound granula[r] crystalline or amorphous bodies of hi[gh] electron density occasionally associat[ed] with vacuoles The number of these den[se] organelles appears to be higher in cortic[al] tissue from older animals and in tissue [in] which degenerative processes are evide[nt] (Maxwell and Kruger 66)

DISCUSSION

The diversity of oligodendrocyte m[or]phology implied by the above descripti[on] and illustrations raises some questions c[on]cerning alternative classifications and [the] possibility of transitional forms (Ram[ón-] Moliner 58) The oligodendrocytes [dis]playing low cytoplasmic matrix den[sity] superficially resemble astrocytes Howev[er] oligodendrocytes can be distinguished [by] the presence of thin cytoplasmic rims ([fre]quently associated with an expanded [nu]clear cleft) large quantities of free ri[bo]somes and ribosomal rosettes numer[ous] nuclear pores abundant cytoplasmic [mi]crotubules (Mugnaini and Walberg 6[4]) and the relation of their processes to [my]elin sheaths In contrast to astrocy[tes] they lack broad processes cytoplasmic [fi]brils and glycogen granules (Maxwell [and] Kruger 65a) Transitional types displ[ay]ing features of both astrocytes and oli[go]dendrocytes have not been observed in [our] material The oligodendrocytes of h[igh] matrix density have been recognized [by] numerous authors (Schultz Maynard a[nd] Pease 57 Farquhar and Hartmann [57] Palay et al 58 Schultz and Pease [59] Peters 60 Bunge Bunge and Pappas [6.] Gray 61 64 Gregoire 63 Bodian [6.] Herndon 64 Mugnaini and Walberg [6.] Schultz 64 Yasuzumi et al 64 Krug[er] 65 et al) but many of these same a[u]thors have tentatively identified profiles [of] the densest elements of this group as m[i]crogliacytes However it must be reco[g]

nized that cytoplasmic quantity or density provide uncertain criteria and the micro glia recently illustrated by several authors (Bodian 64 Herndon 64 Yasazumi et al 64) would appear essentially similar to the micrographs of oligodendrocytes shown by these same authors if the latter cells were sectioned perpendicular to the plane of the micrograph The poor visibil ity of the nuclear membrane in the densest glial elements (Mugnaini and Walberg 64 and figs 11 13) may be suggestive of varying preservation reduction of the nu clear cleft or tangential plane of section rather than a criterion for a distinct cell type It has been suggested that microglia possess smaller mitochondria than those in oligodendrocytes and that conspicuous spaces abut the plasma membrane of mi croglia (Herndon 64) thereby providing easier means of mobility in a tissue strik ingly sparse in channels as would appear appropriate for migrating elements How ever neither mitochondrial size nor extra cellular space constitute consistent fea tures for distinguishing the lightest and darkest oligodendrocytes of the present description and it remains doubtful that some of the densest elements could be identified as microglia on *morphological* grounds

It is perhaps possible that microglia have been difficult to identify in normal cerebral tissue because they represent a peculiar group of oligodendrocytes which display extensive processes in silver carbonate preparations Evidence has been adduced to show that vascular pericytes or circulat ing leukocytes are the only elements which undergo transformation into phagocytic cells (Maxwell and Kruger 65b Konigs mark and Sidman 63) and that the dark oligodendrocytes do not display the macrophage properties ascribed to mi croglia (Maxwell and Kruger 64 65c Vaughn 65) If the present interpretation should prove correct mesodermally de rived elements cannot be identified in brain neuropil and white matter because they are absent and the only glial cells present are the easily distinguished neuro glia — astrocytes and oligodendrocytes

The wide range in nuclear and cyto plasmic densities displayed by oligodendro cytes might conceivably be related to the extent of the plasma membrane and a correlation may exist between surface area and the density of both nucleus and cyto-plasm Thus the "darkest" oligodendro-cytes appear to be related to more numerous myelinated fiber contacts than intermediate or pale density varieties It appears reasonable to suggest that a larger surface area would require greater syn thetic activity of the cell and that this might be reflected in an increased nuclear and cytoplasmic basophilia The attractive feature of this hypothesis is that it would help explain how such apparently dissim ilar cells can belong to the same morpho-logical category However several incon sistencies are immediately apparent The oligodendrocyte with dense cytoplasmic matrix generally has been shown to be related to myelin in the interfascicular glia and the tongues of cytoplasm asso ciated with myelinated axons are often of high density However "dark" cells are also found in cerebral gray matter (albeit with less frequency) despite the relative paucity of large myelinated axons in rat cerebral cortex Furthermore cells in white matter with lighter cytoplasmic density are often found surrounded by a larger number of myelinated axons than cells of the same density in the cortex itself It is also clear that examination of a single section through a cell does not necessarily provide an adequate sample of its environ ment Thus a correlation of nuclear and cytoplasmic density with the extent of the surface membrane clearly cannot be di rectly established

The principal reasons for evading a sub-division of oligodendrocytes on the basis of cytoplasmic density aside from defer ence to an already existing terminology are as follows (1) The finely granular nuclear chromatin and ribosomal arrange ments show a greater similarity between the dark and light oligodendrocytes than to any other element (2) There are nu merous examples of intermediate forms in both nuclear and cytoplasmic densities rendering a clear division into two distinct types virtually impossible (3) Although the cytoplasm trapped in the myelin wrap-ping is usually of the dense variety cyto-

plasm of pale and intermediate density surrounding the inner mesaxon and in the outer tongue can be seen in all areas containing a large number of myelinated axons (4) The wide range of oligodendrocytes are clearly distinguished from astrocytes and neurons (although not with equal ease) on the basis of cytoplasmic features (5) We have seen a comparable range of cytoplasmic matrix densities in the analagous cells of peripheral nerve *Schwann cells using the same methods* of tissue preparation The use of cytoplasmic density as a criterion for subclassification of myelin forming cells would be difficult to defend for peripheral nerve and consequently is not easily justifiable for the central nervous system It would therefore seem reasonable to assign to the interfascicular glia displaying a wide range of densities the designation oligodendrocyte provided that astrocytes can be excluded on independent grounds The striking differences in the density of oligodendrocytes is offset by the common features and the transitional types frequently encountered The different proportions of pale and dark cells in gray and white matter are presumably related to some still unknown factor perhaps the metabolic demands of the adjacent neuronal tissue Unfortunately there is nothing known concerning the relationship of oligodendrocytes to the enormous number of unmyelinated axons found in cerebral tissue

The relation of oligodendrocytes to myelin formation is exceedingly difficult to demonstrate because the tongues of cytoplasm which constitute the outer loop are attached to long thin processes which render their attachment to the cell body difficult to trace in a single thin section When they can be traced the oligodendrocyte plasma membrane can be seen in continuity with the outer lamina of myelin (fig 6) Indeed it appears probable that a single oligodendrocyte can form a large number of myelin sheaths with no morphologically obvious contribution from other elements

Luse (56 62) has suggested that multiple glial processes are continuous with central myelin sheaths and that these processes flatten and fuse to form myelin A similar view has been offered to interpret myelination in tissue culture preparations of cerebellum (Ross et al 62) Luse (62) has also argued that the thickness of myelin is not uniform on all surfaces and that inner mesaxons are sometimes absent This can be ambiguous in the cerebral cortex but can easily be refuted in micrographs of cerebral white matter (figs 6-8) optic nerve (Peters 60 62) and spinal cord (Bunge Bunge and Pappas 62 Grégoire 63) where a spiral arrangement and single inner mesaxons have been demonstrated

De Robertis Gerschenfeld and Wald (58 61) have also reported single mesaxons in brain and spinal cord of immature cat and rat but considered this to be a rare finding They also deny a uniform spiral at all stages and have suggested that myelin is formed by the fusion of intracytoplasmic membranes which are deposited by oligodendrocytes onto or around the axon It is more difficult to visualize the manner in which these membranes could wrap around the axon as a membrane secretion or to reconcile the suggested intracytoplasmic formation of myelin (De Robertis and Gerschenfeld 61) with the numerous examples in which mesaxons have been demonstrated The failure to demonstrate the mesaxons for all sheaths is an insufficient argument against their existence when one considers such crucial factors as plane of section and the frequently encountered poor preservation of myelin lamellae The principal difference in myelination as performed by oligodendrocytes when compared with the better understood relations of Schwann cells is the apparent dependence of segments of several myelinated axons on a single cell and because they are distributed in all directions it is certain that the oligodendrocyte cell body is incapable of spiralling around each axon It may be worth noting that we have never seen astrocytes (Bunge Bunge and Ris 61 62) forming myelin in normal and recuperative lesion material (Maxwell and Kruger 65a) and would strongly support the notion that myelinogenesis is performed uniquely by oligodendrocytes

ACKNOWLEDGMENT

This work was supported by United States Public Health Service grants B 3604 and B 2684 and the Atomic Energy Commission grant AT(11 1) 34 Project no 68

We are indebted to Mrs Olga Fiorello Mrs Sharon Sampogna and Mrs Reid Severin for technical assistance to Mrs Diana Brinton for preparation of the manuscript and to Drs Daniel C Pease Anselmo Pineda and James E Vaughn for helpful discussions

LITERATURE CITED

Bodian D 1964 An electron microscopic study of the monkey spinal cord Bull Johns Hopk *Hosp 114 13–119*

Bunge M B R P Bunge and G D Pappas 1962 Electron microscopic demonstration of connections between glia and myelin sheaths in the developing mammalian central nervous system J *Cell Biol 12 448–453*

Bunge M B R P Bunge and H Ris 1961 Ultrastructural study of remyelination in an experimental lesion in adult spinal cord J Biophys Biochem *Cytol 10* 67

Bunge R P M B Bunge and H Ris 1960 Electron microscopic study of demyelination in an experimentally induced lesion in adult cat spinal cord J Biophys Biochem Cytol 7 685–696

Cajal S Ramon y 1911 Histologie du systèm de l'homme et des vertebres A Maloine Paris

Coulter H D 1964 Electron microscopic identification of glial cells in the central nervous system of adult mice and rats after perfusion fixation *Anat Rec 148* 273

De Robertis E and H M Gerschenfeld 1961 Submicroscopic morphology and function of glial cells Inter rev Neurobiol 3 1–65

De Robertis E H M Gerschenfeld and F Wald 1958 *Cellular* mechanism of myelination in the central nervous system J Biophys Biochem Cytol 4 651–658

Farquhar M B and J F Hartmann 1957 Neuroglial structure and relationships as revealed by electron microscopy J Neuropath Exp Neurol *16* 18–39

Feldherr C M 1965 The effect of the electron opaque pore material on exchang s through the nuclear annuli *J Cell Biol 2, 43–53*

Gray E G 1961 Ultrastructure of synapses of the cerebral cortex and of certain specializations *of the* neuroglial membranes In Electron Microscopy in Anatomy J D Boyd F R Johnson and J D Lever eds Edward Arnold London pp 54–73

——— 1964 Tissues of the central nervous system In *Electron Microscopy* in Anatomy S M Kurtz ed Academic Press New York pp 369–417

Grégoire A 1963 Utilisation de la double fixation gluta aldehyde — osmium pour l etude du système nerveux central au microscope electronique J *Microscopie 2 613–620*

Hartmann J F 1958 Two views concerning criteria for identification of neuroglia cell types in electron microscopy Part A In Biology of Neuroglia W F Windle ed Charles C Thomas Springfield Illinois pp 50–56

Herndon R M 1964 The fine structure of the rat cerebellum II The stellate neurons granule cells and glia J Cell Biol 23 277–293

Konigsmark B W and R L Sidman 1963 Origin of brain macrophages in the mouse J Neuropath Exp Neurol 22 643–676

Kruger L 1965 The spectrum of oligodendrocyte in normal rat cerebrum Anat Rec *151* 375

Luse S L 1958 The ultrastructure of normal and reactive astrocytes Lab Investig 7 401–417

——— 1962 Ultrastructure of the brain and its relation to transport of metabolites Res Publ Assn nerv ment Dis 40 1–24

Maturana H R 1960 The fine anatomy of the optic nerve of Anurans — an electron microscopic study J Biophys Biochem Cytol 7 107–120

Maxwell D S and L Kruger 1964 Electron microscopy of radiation induced laminar lesions in the cerebral cortex of the rat 2nd Int Sympos In The Response of the Nervous System to Ionizing Radiation T Haley ed Little Brown and Company pp 54–83

——— 1965a The fine structure of ast ocytes in the cerebral cortex and their response to focal injury produced by heavy ionizing particles J Cell Biol 25 141–157

——— 1965b Small blood vessels and the origin of phagocytes in the rat cerebral cortex following heavy particle irradiation Exptl Neurol *12* 33–54

——— 1965c Changes in oligodendrocyte organelles during neuronal degeneration VIII Int Anat Cong pp 76–77

——— 1966 The reactive oligodendrocyte An electron microscopic study of cerebral cortex following alpha particle irradiation Am J Anat *118* 437–460

Mugnaini E and F Walberg 1964 Ultrastructure of neuroglia Ergebn Anat EntwGesch *3" 194–236*

Palay S L 1958 An electron microscopical study of neuroglia In Biology of Neuroglia W F Windle ed Charles C Thomas Springfield Illinois pp 24–38

Palay S L S M McGee G Spencer Jr and M A Grillo 1962 Fixation of neural tissues for electron microscopy by perfusion with solutions of osmium tetroxide J Cell Biol 12 385–410

Pease D C 1964 Histological Techniques for Electron Microscopy Second Edition Academic Press New York

Penfield W 1924 Oligodendroglia and its relation to classical neuroglia Brain 47 430–452

——— 1932 Neuroglia normal and pathological In Cytology and Cellular Pathology of the Nervous System Vol II W Penfield ed P Hoeber New York pp 421–480

Peters A 1960 The formation and structure of myelin sheaths in the central nervous system J Biophys Biochem Cytol *8* 431–446

——— 1962 Plasma membrane contacts in the central nervous system J Anat (Lond) *96* 237–248

Ramón Moliner E 1958 A study on neuroglia The problem of transitional forms J Comp Neurol *110* 157–171

Rio Hortega P Del 1932 Microglia In Cytology and Cellular Pathology of the Nervous System W Penfield ed , Vol I pp 483–534

Rio Hortega P Del M Ojea and L Zimman 1943 Investigaciones respecto a los cambios post mortem de la microglia en el conejo sacrificado en estado normal Arch Histol (B Aires) 2 203–218

Ross L L M B Bornstein and G M Lehrer 1962 Electron microscopic observations of rat and mouse cerebellum in tissue culture J Cell Biol *14* 19–30

Schultz R L 1964 Macroglial identification in electron micrographs J Comp Neurol *122* 281–295

Schultz R L E A Maynard and D C Pease 1957 Electron microscopy of neurons and neuroglia of cerebral cortex and corpus callosum Am J Anat *100* 369–408

Schultz R L and D C Pease 1959 Cicatrix formation in rat cerebral cortex as revealed by electron microscopy Amer J Path 35 101 1042

Smart I and C P Leblond 1961 Evidence for division and transformation of neuroglia cells in the mouse brain as derived from radio autography after injection of thymidine H³ J Comp Neurol *116* 349–367

Terry R D and M Weiss 1963 Studies i Tay Sachs disease II Ultrastructure of th cerebrum J Neuropath Exp Neurol 2 18–55

Vaughn J E 1965 Electron microscopic stud of the vascular response to axonal degener tion in rat optic nerve Anat Rec 151 4

Vogel F A and L Kemper 1961 Modific tions of Hortega s silver impregnation metho to assist in the identification of neuroglia w electron microscopy IV Internat Cong Neu path Proc *2* 66–71

Yasuzumi G I Tsubo R Sugihara and Y Na 1964 Analysis of the development of Japan B encephalitis (JBE) virus I Electron mic scope studies of microglia infected with J virus J Ultrastruct Res *11* 213–229

PLATE 1

EXPLANATION OF FIGURES

1 Interfascicular glia in normal subcortical white matter Adjacent oligodendrocytes (*O*) display extremes of nuclear and cytoplasmic matrix densities The paler cells usually possess a prominent nuclear cleft and nuclear pores (arrow) The trapped cytoplasm associated with the inner mesaxon of myelinated axons on the right also differ in matrix density Formaldehyde perfusion Bar in this and all subsequent figures represents 1 μ unless otherwise indicated

2 Typical cytoplasm in an oligodendrocyte of intermediate density The cytoplasm trapped in the adjacent paranodal tongues (*T*) (lower left) is strikingly similar Free ribosomes (*r*) are irregularly scattered The variety of circular profiles includes smooth endoplasmic reticulum (*er*) alveolate vesicles (*av*) a multivesiculate body (*mv*) and a widespread microtubular (*mt*) array Glutaraldehyde perfusion



——— 1962 Plasma membrane contacts in the central nervous system J Anat (Lond) *96* 237–248

Ramón Moliner E 1958 A study on neuroglia The problem of transitional forms J Comp Neurol *110* 157–171

Rio Hortega P Del 1932 Microglia In Cytology and Cellular Pathology of the Nervous System *W Penfield ed Vol I pp 483–534*

Rio Hortega P Del M Ojea and L Zimman 1943 Investigaciones respecto a los combios post mortem de la microglia en el conejo sacrificado en estado normal Arch Histol (B Aires) 2 203–218

Ross L L M B Bornstein and G M Lehrer 1962 Electron microscopic observations of rat and mouse cerebellum in tissue culture J Cell Biol *14* 19–30

Schultz R L 1964 Macroglial identification in electron micrographs *J Comp Neurol 122* 281–295

Schultz R L E A Maynard and D C Pease *1957 Electron microscopy of neurons* and neuroglia of cerebral cortex and corpus callosum Am J Anat *100* 369–408

Schultz R L and D C Pease 1959 Cicatrix formation in rat cerebral cortex as revealed by electron microscopy Amer J Path 35 101–1042

Smart I and C P Leblond 1961 Evidence for division and transformation of neuroglia cells in the mouse brain as derived from radioautography after injection of thymidine H³ J Comp Neurol *116* 349–367

Terry R D and M Weiss 1963 Studies in Tay Sachs disease II Ultrastructure of the cerebrum J Neuropath Exp Neurol 22 18–55

Vaughn J E 1965 Electron microscopic study *of the vascular response to* axonal degeneration in rat optic nerve Anat Rec 151 4..

Vogel F A and L Kemper 1961 Modifica*tions of Hortega s silver impregnation* method to assist in the identification of neuroglia with electron microscopy IV Internat Cong Neuropath *Proc 2 66–71*

Yasuzumi G I Tsubo R Sugihara and Y Nak.. 1964 Analysis of the development of Japanese *B encephalitis (JBE) virus I Electron* microscope studies of microglia infected with Jo.. virus J Ultrastruct Res *11* 213–229

PLATE 1

EXPLANATION OF FIGURES

1 Interfascicular glia in normal subcortical white matter Adjacent oligodendrocytes (O) display extremes of nuclear and cytoplasmic matrix densities The paler cells usually possess a prominent nuclear cleft and nuclear pores (arrow) The trapped cytoplasm associated with the inner mesaxon of myelinated axons on the right also differ *in matrix density Formaldehyde perfusion* Bar in this and all subsequent figures represents 1 μ unless otherwise indicated

2 Typical cytoplasm in an oligodendrocyte of intermediate density The cytoplasm trapped in the adjacent paranodal tongues (*T*) (lower left) is strikingly similar Free ribosomes (*r*) are irregularly scattered The variety of circular profiles includes smooth endoplasmic reticulum (*er*), alveolate vesicles (*av*) a multivesiculate body (*mv*) and a widespread microtubular (*mt*) array Glutaraldehyde perfusion


mt
O
d
G
AP
er
O
mt
nf
3

PLATE 2

EXPLANATION OF FIGURE

3 Subcortical white matter interfascicular glia An astrocyte with a broad process (*AP*) contains numerous fibrillar (*f*) aggregates The cytoplasm of two adjacent oligodendrocytes (*O*) is readily distinguished by its numerous microtubules (*mt*) granular endoplasmic reticulum (*er*) with prominent dilatations and richer content of free ribosomes and dense matrix material Golgi zones (*G*) and mitochondria and dense bodies (*d*) appear similar in both glial types Glutaraldehyde perfusion



PLATE 3

EXPLANATION OF FIGURE

4 Linear array of three interfascicular oligodendrocytes in subcortical white matter Note the greater nuclear and cytoplasmic matrix density displayed by the upper two cells With this method of preservation occasional blistering of mitochondria is apparent Glutaraldehyde perfusion

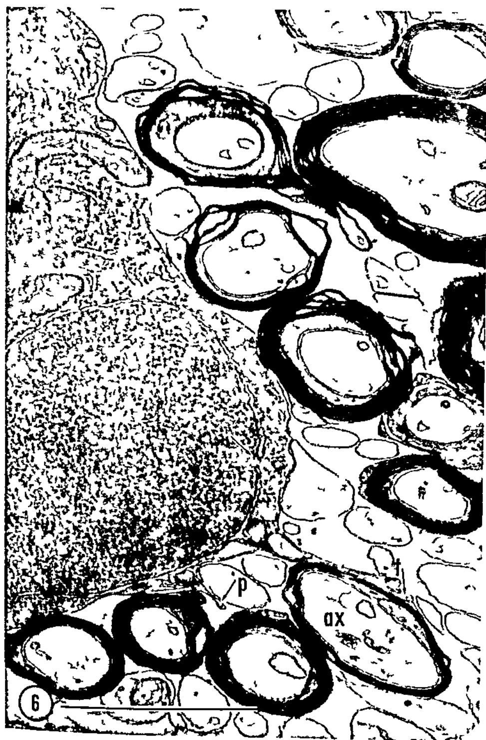

p
f
ax
6

PLATE 5

EXPLANATION OF FIGURE

6 Typical dark oligodendrocyte in subcortical white matter The thin cytoplasmic rim can occasionally be traced into a very fine process forming the outer tongue (*t*) of cytoplasm trapped within a myelinated axon (*ax*) Another fine process (*p*) and a nuclear pore (arrow) are also indicated Note that the nuclear cleft is not conspicuously dilated in the darker variety of oligodendrocyte Formaldehyde perfusion


C
7
5 μ
8
0 5

PLATE 6

EXPLANATION OF FIGURES

7 A pale oligodendrocyte in subcortical white matter (nucleoplasm to the left) displaying a narrow cytoplasmic rim surrounded by axons a prominent nuclear cleft (*c*) and nuclear pores (arrows) Formal dehyde perfusion

8 A dark oligodendrocyte (nucleoplasm to the right) in subcortical white matter The typically narrow nuclear cleft (*c*) of this variety is much less conspicuous than of the pale cell in figure 7 The outer mesaxons of several myelin sheaths are indicated by arrows Formal dehyde perfusion


e
c
n
mi
R


R


mi
11
ax

PLATE 7

EXPLANATION OF FIGURES

9 Oligodendrocyte in subcortical white matter adjacent to a node of Ranvier (*R*) The nucleus (*n*) nuclear cleft (*c*) dilated granular endoplasmic reticulum (*er*) and microtubules (*mt*) of the cell are indicated Note the similarity of cytoplasm trapped in tongues of the paranodal region (*t*) A periodic structure associated with the zones of trapped cytoplasm (arrows) is characteristic of the paranodal region of central nervous system axons with this method of preservation Glutaraldehyde perfusion

10 Node of Ranvier (*R*) in cerebral cortex with dense matrix oligodendrocyte cytoplasm trapped in the paranodal tongues (*t*) The periodic paranodal structures are less conspicuous than in figure 9 but clearly present (arrows) Glutaraldehyde perfusion

11 Dark oligodendrocyte in cerebral cortex Note the similar matrix density of the cytoplasm (*t*) trapped inside of the myelin sheath of an axon (*ax*) Matrix density free ribsomes thin cytoplasmic rim (lower margin of the cell) and extensive microtubules (*mt*) are characteristic Glutaraldehyde perfusion


B
D
O
D
D
b
d
Ax
N
12

PLATE 8

EXPLANATION OF FIGURE

12 Oligodendrocyte (*O*) in cerebral cortex displaying a thin pale cytoplasmic rim in contact with a large neuron perikaryon (*N*) several dendrites (*D*) myelinated axon (*ax*) and synaptic bouton sac (*B*) Dense bodies (*d*) containing granular lamellar fat and vacuolar zones are occasionally present Fine processes presumably of astro cytes separate the plasma membrane from the basal lamina (*b*) at arrow Formaldehyde perfusion


N
13

PLATE 9

EXPLANATION OF FIGURE

13 Dark perineuronal satellite oligodendrocyte in cerebral cortex with a typically narrow cytoplasmic rim is adjacent to a large neuron (*N*) Characteristic narrow nuclear cleft microtubules and free ribosomes are evident Formaldehyde perfusion

The Reactive Oligodendrocyte

AN ELECTRON MICROSCOPIC STUDY OF CEREBRAL CORTEX FOLLOWING ALPHA PARTICLE IRRADIATION

DAVID S MAXWELL AND LAWRENCE KRUGER

Department of Anatomy School of Medicine and Brain Research Institute University of California Los Angeles California and Veterans Administration Hospital Long Beach California

ABSTRACT The ultrastructural features of oligodendrocytes have been studied in a zone of cerebral cortex in which all neurons are destroyed and numerous processes damaged by heavy ionizing particles This type of lesion fails to reveal signs of vascular inflammation and classical "gitter cells" in light microscopy or any signs of debris fragments in electron microscopy Oligodendrocyte satellites of neurons or their processes display an acute swelling associated with signs of neuronal damage This is followed by a marked increase in a morphologically rich variety of dense osmiophilic organelles of granular lamellar crystalline or amorphous sub-structure Acid phosphatase activity has been demonstrated in some of these organelles thus implying a participation in "lysosomal" intracellular breakdown Invasion by microgliacytes and phagocytosis was not observed Present evidence supports the efficacy of intracellular mechanisms in the breakdown of degenerating material and suggests a re-evaluation of the evidence for identification of microglia on the basis of granular inclusions

Focal degeneration in the cerebral cortex is accompanied by distinctive changes in both of the clearly-defined neuroglial cell varieties (Maxwell and Kruger 64) The study of the morphological response of neuroglia to cortical injury may provide some clues to the functional role of these cells and some further criteria for identification of glial cell types In a study of the response of astrocytes to heavy particle irradiation it was possible to distinguish these cells from other glia by the presence of cytoplasmic components which increase markedly following tissue damage (Maxwell and Kruger 65a)

In a previous publication (Maxwell and Kruger 65b) we have presented evidence for the participation of non glial cells in the phagocytosis of debris following extensive injury and necrosis of cortical tissue produced with high-dose irradiation The classification of a group of glial cells as microglia was called into question and alternative sources for gitter cells (compound granular corpuscles) was considered A sequence of events compatible with the classic concepts of gitter cell formation was not observed electron microscopically following injury insufficiently severe to cause extensive necrosis and accumulation of extracellular debris The present report deals with morphological changes occurring in a distinctive group of neuroglia under such circumstances and the relation of these changes to destruction of adjacent neurons and their processes This group of cells possesses cytoplasmic features which we believe are characteristic of oligodendrocytes (Kruger and Maxwell 66) It is proposed that the oligodendrocyte participates in the disposal of degeneration products and that cytoplasmic alterations can be related to this process A preliminary report of these findings has been presented (Maxwell and Kruger 65c)

MATERIALS AND METHODS

The present report constitutes a portion of a more extensive study of morphological aspects of focal lesions in the cerebral cortex produced with heavy ionizing particles All animals in this study were female rats 28–30 days of age at the time of irradiation

Experimental lesions were produced with a monoenergetic beam of 41 6 MeV alpha particles (10 4 MeV per nucleon) at the Heavy Ion Linear Accelerator of the Law

ound to change in appearance and these altered cells will be considered reactive oligodendrocytes The identification of these cells as oligodendrocytes is supported by the following (1) they appear to retain many similarities to normal oligodendrocytes (see Kruger and Maxwell 66) and a spectrum of changes is demonstrable which serves to relate them to their normal counterparts (2) the frequency with which the reactive oligodendrocytes are found in satellite position to neurons (see figs 1–3) suggests they originated as satellite oligodendrocytes and (3) the distinctive features of reactive astrocytes in the lesion zone (Maxwell and Kruger 65a and see fig 4) prevents confusion of these two glial cell types

There are several features of reactive oligodendrocytes which are indicative of a pathological process The most prominent of these include (1) nuclear changes (2) some infolding of the plasma membrane (3) occasional appearance of cell processes which are more robust than those of normal oligodendrocytes and an expanded cytoplasmic volume (4) cytoplasmic swelling and (5) extensive accumulation of pleomorphic and generally electron-dense cytoplasmic inclusions Neuronal chromatolysis and myelin and axon degeneration can frequently be identified in association with the earlier phases of these reactive changes

The nuclei of reactive oligodendrocytes often display a clumping of the chromatin into large masses usually at the periphery of the nucleus and in several central patches (figs 1 2 4 6 7 9) Nuclear profiles are frequently elongated (figs 1 4) and usually are irregular in outline (figs 1 4 6 7) Such nuclear changes may be observed throughout the post irradiation period studied Some of the oligodendrocytes particularly during the first days following irradiation display a few infoldings of the plasma membrane (fig 1) These appear analagous to a short mesaxon except that the deepest part of the fold does not contain an axon or evidence of any axonal remnant Conceivably this transient occurrence reflects some sort of activity of the plasma membrane There is apparently an increase in the total cytoplasmic volume of the acutely reactive cells The perinuclear cytoplasm seems more prominent and stout processes of oligodendrocytes may be observed (figs 2 4 6) Such large processes and the generally increased bulk of cytoplasm displayed by reactive cells appear only transiently and after a few months the oligodendrocytes in the laminar lesion appear to approach normal volume and nuclear/cytoplasmic ratio and large processes are less frequently encountered

During the first two weeks following irradiation oligodendrocytes in the developing laminar lesion which display other indications of response to tissue injury are found to be acutely swollen" The present observations seem to support the general view (Penfield and Cone 26 Ferraro 28) that oligodendrocytes can swell to some extent in response to local tissue injury "Swollen" oligodendrocytes in the present study are characterized at first by the occurrence of clear patches of cytoplasm (figs 1 2) and then by the clustering of cytoplasmic organelles around the nucleus leaving a relatively clear rim between the organelles and the plasma membrane (figs 3 4 6 9) This distribution of organelles and electron lucent areas of cytoplasm is also observed in the roots of the larger processes (fig 4) but apparently not at any great distance from the cell body

It is impossible to draw firm conclusions regarding water distribution in the brain following our preparative procedures The fact that "swelling" is restricted to limited areas of the cytoplasm of this variety of cell in the developing laminar lesion for a short period following irradiation and not in other cells or other parts of the same brain suggests that the swollen appearance is not entirely artifactitious

Numerous dense organelles can be seen in the cytoplasm of reactive oligodendrocytes in the lesion zone shortly after irradiation (figs 11–14) Most of the organelles in the first three weeks of neuronal degeneration exhibit some internal structure either granular (figs 3–9 11–14) or lamellar (figs 8 9 11) Other organelles display irregular internal form (fig 6) These organelles may exceed a micron in one or more dimensions and may occasionally exhibit complex external configurations as well as internal structure (fig

rence Radiation Laboratory University of California Berkeley Details of the method have been described in some detail else where (Malis et al 60 Brustad et al 60 Maxwell and Kruger 65a) The essential feature of the lesion produced can best be described as a laminar destruction of neu ron perikarya and their processes within a narrow band of the neuronal layers of the cortex This is accomplished by employing the unique feature of maximal energy re lease occurring near the end of the range (the Bragg effect) The sharp spatial de cay (approximately 10 μ) renders it pos sible to study unirradiated tissue 10–20 μ below the band in which all neurons are destroyed Intact neuronal layers that have received a lower dose of irradiation can be studied above the laminar lesion Dosages presented in this paper represent measured surface dose — details for making calcu lations of energy distribution within cortex and for measurement are presented else where (Malis et al 60 Brustad et al 60)

Five dose ranges were studied 5 9 12 20 and 30 thousand rads (1 rad = 100 erg gm or 6 25 × 10' MeV gm) The high doses produced extensive vascular inflam mation or destruction the results of which will not be presented here (see Maxwell and Kruger 65b) Animals were sacri ficed by vascular perfusion following bar biturate anesthesia at intervals of 1 2 3 5 10 11 22 35 49 and 84 days and 5 6 8 9 10 12 and 22 months following irra diation In most cases tissue of satisfac tory quality for electron microscopy was obtained for each dose and time A portion of each lesion was taken for light micros copy embedded in paraffin sectioned at 10 μ and studied with a Nissl stain All of the animals were perfused with phosphate buffered 4% formaldehyde according to the method of Pease (64) except for the animals studied for acid phosphatase local ization which were perfused with either phosphate or cacodylate buffered 6 25% glutaraldehyde All tissue was post fixed in 1% OsO_4 in the same buffer as the alde hyde The electron microscopic methods were the same as in the preceding paper (Kruger and Maxwell 66) Acid phospha tase localization was studied by methods similar to those described by Sabatini et al (61) Free hand sections of cortex were incubated in the Gomori acid phosphata medium with appropriate controls th post fixed in OsO_4 and embedded for th sectioning

RESULTS

Irradiation within the dose range e ployed in the present study (6 000 to 12 0 rad alpha particles) will result in the p duction of a laminar lesion with minir destruction of neurons in the overly layers Light microscopic examination the laminar lesion zone after a dose-dep dent interval reveals the degeneration disappearance of all neuron perikarya distinctive features of the laminar les relevant to the present study are (1) number of glial nuclei does not decre and with progressively higher doses a tinct increase in glial nuclei appears wi the laminar lesion (2) extra cellular d which might constitute a substrate phagocytosis is consistently absent studied electron microscopically (3) macrophages found in necrotic areas lowing 20 000 to 30 000 rad alpha pa irradiation are absent (Maxwell and Kr 65b) (4) there is evidence of severe ronal damage for short periods after diation followed by the appearance aneuronal band of cortex (5) there is age to many neuron processes in th veloping laminar lesion (Kruger and mente 64 Kruger and Malis 64) (6) glycogen granules accumulate in cytes presumably initially as a dire sponse to irradiation then later as sponse to local tissue damage (Ma and Kruger 65a)

The response of oligodendrocytes t production of laminar lesions can b lated to the rate of development o lesion In contrast to the astrocyte oligodendrocyte probably undergoes phological changes only in respon damage to neurons or their processes the initiation of the oligodendrocyt sponse is closely correlated with the ea indications of neuronal damage W 48 hours following irradiation neuror hibiting chromatolytic changes ma found in the developing laminar lesion some myelinated fibers appear disti abnormal From this time forward dendrocytes in the laminar lesion zon

ind to change in appearance and these ered cells will be considered reactive godendrocytes The identification of se cells as oligodendrocytes is supported the following (1) they appear to re in many similarities to normal oligoden rocytes (see Kruger and Maxwell 66) nd a spectrum of changes is demonstrable which serves to relate them to their normal counterparts (2) the frequency with which the reactive oligodendrocytes are found in satellite position to neurons (see figs 1–3) suggests they originated as satellite oligodendrocytes and (3) the distinctive features of reactive astrocytes in the lesion zone (Maxwell and Kruger 65a and see 4) prevents confusion of these two glial cell types

There are several features of reactive oligodendrocytes which are indicative of a pathological process The most prominent of these include (1) nuclear changes (2) some infolding of the plasma membrane (3) occasional appearance of cell processes which are more robust than those of normal oligodendrocytes and an expanded cytoplasmic volume (4) cytoplasmic "swelling" and (5) extensive accumulation of pleomorphic and generally electron-dense cytoplasmic inclusions Neuronal chromatolysis and myelin and axon degeneration can frequently be identified in association with the earlier phases of these reactive changes

The nuclei of reactive oligodendrocytes often display a clumping of the chromatin into large masses usually at the periphery of the nucleus and in several central patches (figs 1 2 4 6 7 9) Nuclear profiles are frequently elongated (figs 1 4) and usually are irregular in outline (figs 1 4 6 7) Such nuclear changes may be observed throughout the post irradiation period studied Some of the oligodendrocytes particularly during the first days following irradiation display a few infoldings of the plasma membrane (fig 1) These appear analagous to a short mesaxon except that the deepest part of the fold does not contain an axon or evidence of any axonal remnant Conceivably this transient occurrence reflects some sort of activity of the plasma membrane There is apparently an increase in the total cytoplasmic volume of the acutely reactive cells The perinuclear cytoplasm seems more prominent and stout processes of oligodendrocytes may be observed (figs 2 4 6) Such large processes and the generally increased bulk of cytoplasm displayed by reactive cells appear only transiently and after a few months the oligodendrocytes in the laminar lesion appear to approach normal volume and nuclear/cytoplasmic ratio and large processes are less frequently encountered

During the first two weeks following irradiation oligodendrocytes in the developing laminar lesion which display other indications of response to tissue injury are found to be acutely swollen" The present observations seem to support the general view (Penfield and Cone 26 Ferraro 28) that oligodendrocytes can swell to some extent in response to local tissue injury Swollen" oligodendrocytes in the present study are characterized at first by the occurrence of clear patches of cytoplasm (figs 1 2) and then by the clustering of cytoplasmic organelles around the nucleus leaving a relatively clear rim between the organelles and the plasma membrane (figs 3 4 6 9) This distribution of organelles and electron lucent areas of cytoplasm is also observed in the roots of the larger processes (fig 4) but apparently not at any great distance from the cell body

It is impossible to draw firm conclusions regarding water distribution in the brain following our preparative procedures The fact that "swelling" is restricted to limited areas of the cytoplasm of this variety of cell in the developing laminar lesion for a short period following irradiation and not in other cells or other parts of the same brain suggests that the swollen appearance is not entirely artifactitious

Numerous dense organelles can be seen in the cytoplasm of reactive oligodendrocytes in the lesion zone shortly after irradiation (figs 11–14) Most of the organelles in the first three weeks of neuronal degeneration exhibit some internal structure either granular (figs 3–9 11–14) or lamellar (figs 8 9 11) Other organelles display irregular internal form (fig 6) These organelles may exceed a micron in one or more dimensions and may occasionally exhibit complex external configurations as well as internal structure (fig

8) They commonly do not have a uniform internal structure but display homogeneous zones of electron opacity and clear vacuolar zones as well as granular or lamellar regions This pattern of mixed high and low electron opacity persists in the apparently coalesced aggregates of granules characteristic of the longer survival periods long after the dense bodies have lost most of the other internal structure characteristic of earlier forms (fig 10)

Accompanying the accumulation of organelles is an apparent proliferation of Golgi membranes and several Golgi zones may be apparent in a single cell profile (figs 5 9) Surrounding these zones a tubular or vesicular component of the cytoplasm is usually prominent and this component frequently exhibits electron dense material within its membrane bound borders (figs 5 9) This material resembles that found in the dense regions of the organelles and may represent stages in the formation of the larger organelles This likelihood is supported by recent views on the origin and life history of the members of the lysosome family of cell inclusions which the dense organelles of this study resemble (see Gordon Miller and Bensch 65)

Acid phosphatase activity as revealed by the Gomori method adapted for electron microscopy (Sabatini Bensch and Barrnett 63) can be demonstrated in the dense organelles in the first weeks following irradiation (figs 11–14) The reaction product is most readily deposited in those parts of the organelle which display some internal structure (figs 11–14) We have been less successful in demonstrating acid phosphatase activity in the more homogeneous regions of the organelles or in organelles of the predominantly homogeneous electron dense variety These latter enzymatically inactive dense bodies of long post irradiation survival times are quite similar to lipofuscin inclusions seen in neurons (Duncan Nall and Morales 60 Palay and Palade 55 Samorajski Ordy and Keefe 65) The latter authors have emphasized the probable relation of lipofuscin to lysosomes These pigment bodies do not differ except in quantity from the dense organelles found in some oligodendrocytes of normal cortex (Kruger and Maxwell 66)

DISCUSSION

The most striking feature of low and moderate dose laminar lesions is that particle irradiation has resulted in marke[d] neuronal damage in the absence of marke[d] gliosis gitter cells or phagocytes in ligh[t] microscopic examination and the absenc[e] of identifiable neuronal fragments as eith[er] extra or intra cellular debris in the ele[c]tron microscope The oligodendrocytes [i]n these lesions exhibit a series of compl[ex] cytoplasmic alterations, which seem clea[rly] related to neuronal injury These cytopl[as]mic changes may be representative of t[he] response of oligodendrocytes to the pr[od]ucts of normal degenerative process[es] such as those related to aging If the pr[es]ence of dense bodies in lesser numbers [in] normal material (Kruger and Maxwell [66]) can be assigned a similar functional [sig]nificance

Acute swelling of oligodendrocytes [w]as emphasized in light microscopy as an e[arly] pathological change (Penfield and Co[ne] 26 Cone 28 Ferraro 28 Penfield 3[2]) Such changes are difficult to assess in e[lec]tron microscopy because of technical c[on]siderations and because there is diffic[ulty] in recognizing such slight and transient [de]partures from the broad range of nor[mal] oligodendrocyte morphology The only [sub]stantial criterion of oligodendrocyte sw[ell]ing in the present study is the occurre[nce] of an electron lucent rim of cytoplasm [ad]jacent to the plasma membrane and a c[lus]tering of the cytoplasmic organelles aro[und] the nucleus The resulting pale" oligo[den]drocyte can readily be distinguished f[rom] either normal or reactive astrocytes or[an] organelle basis however (Maxwell [and] Kruger 65a) The pattern of swellin[g in] the present study is also quite diffe[rent] from that occurring in oligodendroc[ytes] during other types of pathological proce[sses] (Hirano Zimmerman and Levine [65] O Leary et al 65) It is not possibl[e to] determine which or if all of these patt[erns] of swelling correspond to the acu[tely] swollen oligodendrocytes of the earlier l[ight] microscopic literature The significanc[e of] oligodendrocyte swelling in the pres[ent] study remains obscure but its transi[ent] nature suggests it is not the crucial m[or]phological change in the elucidation of

role of the oligodendrocyte during neuronal degeneration

The striking absence of debris fragments in the present study and in some disease states (Terry and Weiss 63) may be explained by a capacity of nervous tissue to reduce degenerating material to molecular dimensions more amenable to transport than large cell fragments It would be difficult to interpret the dense organelles of the reactive oligodendrocytes as ingested particulate debris in spite of the frequent incidence of a lamellar structure reminiscent of myelin sheath fragments Such an interpretation would fail to explain the absence of extra-cytoplasmic debris The likelihood that cell fragmentation is accompanied by phagocytosis so rapid that no debris is ever seen seems remote at best The efficacy of "lysosomal digestion compared to phagocytosis by a wandering cell is apparent when one considers the sparse extracellular space available for a wandering macrophage and the complex guiding forces that would therefore be required for such a cell to identify and reach the one element among many which is degenerating at a given time In degenerating peripheral nervous tissue where connective tissue spaces contain numerous macrophages phagocytosis by mobile macrophages is more easily imagined But even in this circumstance most of the phagocytosis described (Nathaniel and Pease 64) can be appropriately interpreted as auto-digestion since the myelin ingested by Schwann cells was originally the plasma membrane of that cell The semantic distinction is important because the phagocytosis of destroyed cells by another element has not yet been clearly demonstrated in non inflammatory lesions of the central nervous system Furthermore ingested debris would not *a priori* be rich in acid phosphatase In any case the myelin like inclusions could not be entirely accounted for by the ingestion of myelin fragments since the supragranular cortex of the rat contains too few myelinated fibers for so many laminated inclusions

A phagocytic mechanism in disposing of debris associated with inflammatory processes and tissue disruption has been observed (Blinzinger and Hager 64 Gonatas Levine and Shoulson 64 Maxwell and Kruger 65b) Vaughn (65) has implicated astrocytes in phagocytosis of myelin in degenerating optic nerve However it is difficult to identify "ingested material in many other circumstances of experimental degeneration It has been suggested that axon terminals undergoing degeneration can be removed by dendrites (Walberg 63) and glial processes surrounding degenerating axo-dendritic contacts have been interpreted as a stage in the phagocytosis of degenerating boutons together with the portion of the apposed dendrite (Colonnier and Guillery 64 Colonnier 64) The presence of degenerated axonal material in direct contact with the cytoplasm of another cell (rather than merely being surrounded by its plasma membrane) would seem an important requirement for recognizing phagocytosis which has not yet been fulfilled It would also seem desirable at our present state of knowledge to adhere to the caution expressed by Webster (64) in interpreting myelin like lamellar inclusions many are evidently not derived from axonal ingestion and can be related to mitochondria (Sjostrand Cedergen and Karlsson 64) or lysosome and lipofuscin configurations (Samorajski Ordy and Keefe 65)

The accumulation of dense organelles following irradiation endow the oligodendrocytes with the appearance of fat granule laden cells in light microscopy Numerous osmiophilic rosettes can be seen in laminar lesions and surrounding neurons where the Marchi method presumably displays secondary axon terminal degeneration (Kruger and Malis 64) The distribution of Marchi positive material may be better correlated with the presence of dense bodies in satellite cells rather than myelin degeneration especially in regions sparsely populated with myelinated axons Presumably the dense homogeneous bodies characteristic of the *late* stages of the laminar lesion correspond to the residual lipofuscin usually associated with chronic pathological alterations A relationship between lipofuscin granules and lysosomes has recently been suggested (Gordon Miller and Bensch 65 Samorajski Ordy and Keefe 65) although there is no direct morphological evidence that the dense lipid organelles associated with vacuoles represent a

8) They commonly do not have a uniform internal structure but display homogeneous zones of electron opacity and clear vacuolar zones as well as granular or lamellar regions This pattern of mixed high and low electron-opacity persists in the apparently coalesced aggregates of granules characteristic of the longer survival periods long after the dense bodies have lost most of the other internal structure characteristic of earlier forms (fig 10)

Accompanying the accumulation of organelles is an apparent proliferation of Golgi membranes and several Golgi zones may be apparent in a single cell profile (figs 5 9) Surrounding these zones, a tubular or vesicular component of the cytoplasm is usually prominent and this component frequently exhibits electron dense material within its membrane bound borders (figs 5 9) This material resembles that found in the dense regions of the organelles and may represent stages in the formation of the larger organelles This likelihood is supported by recent views on the origin and life history of the members of the lysosome family of cell inclusions which the dense organelles of this study resemble (see Gordon Miller and Bensch, 65)

Acid phosphatase activity as revealed by the Gomori method adapted for electron microscopy (Sabatini Bensch and Barrnett 63) can be demonstrated in the dense organelles in the first weeks following irradiation (figs 11–14) The reaction product is most readily deposited in those parts of the organelle which display some internal structure (figs 11–14) We have been less successful in demonstrating acid phosphatase activity in the more homogeneous regions of the organelles or in organelles of the predominantly homogeneous electron dense variety These latter enzymatically inactive dense bodies of long post irradiation survival times are quite similar to lipofuscin inclusions seen in neurons (Duncan Nall and Morales 60 Palay and Palade 55 Samorajski Ordy and Keefe 65) The latter authors have emphasized the probable relation of lipofuscin to lysosomes These pigment bodies do not differ except in quantity from the dense organelles found in some oligodendrocytes of normal cortex (Kruger and Maxwell 66)

DISCUSSION

The most striking feature of low and moderate dose laminar lesions is that pa ticle irradiation has resulted in marked neuronal damage in the absence of marked gliosis gitter cells or phagocytes in ligh microscopic examination and the absenc of identifiable neuronal fragments as eithe extra or intra-cellular debris in the elec tron microscope The oligodendrocytes i these lesions exhibit a series of comple cytoplasmic alterations which seem clear related to neuronal injury These cytopla mic changes may be representative of th response of oligodendrocytes to the pro ucts of normal degenerative process such as those related to aging if the pre ence of dense bodies in lesser numbers normal material (Kruger and Maxwell 6 can be assigned a similar functional s nificance

Acute swelling of oligodendrocytes w emphasized in light microscopy as an ea pathological change (Penfield and Co 26 Cone 28 Ferraro 28 Penfield 3 Such changes are difficult to assess in el tron microscopy because of technical c siderations and because there is difficu in recognizing such slight and transient partures from the broad range of norm oligodendrocyte morphology The only s stantial criterion of oligodendrocyte sw ing in the present study is the occurre of an electron lucent rim of cytoplasm jacent to the plasma membrane and a cl tering of the cytoplasmic organelles arou the nucleus The resulting pale oligod drocyte can readily be distinguished fr either normal or reactive astrocytes on organelle basis however (Maxwell a Kruger 65a) The pattern of swelling the present study is also quite differ from that occurring in oligodendrocy during other types of pathological proces (Hirano Zimmerman and Levine, O Leary et al 65) It is not possible determine which or if all of these patte of swelling correspond to the acut swollen oligodendrocytes of the earlier li microscopic literature The significance oligodendrocyte swelling in the prese study remains obscure but its transie nature suggests it is not the crucial mo phological change in the elucidation of th

role of the oligodendrocyte during neuronal degeneration

The striking absence of debris fragments in the present study and in some disease states (Terry and Weiss 63) may be explained by a capacity of nervous tissue to reduce degenerating material to molecular dimensions more amenable to transport than large cell fragments It would be difficult to interpret the dense organelles of the reactive oligodendrocytes as ingested particulate debris in spite of the frequent incidence of a lamellar structure reminiscent of myelin sheath fragments Such an interpretation would fail to explain the absence of extra-cytoplasmic debris The likelihood that cell fragmentation is accompanied by phagocytosis so rapid that no debris is ever seen seems remote at best The efficacy of lysosomal" digestion compared to phagocytosis by a wandering cell is apparent when one considers the sparse extracellular space available for a wandering macrophage and the complex guiding forces that would therefore be required for such a cell to identify and reach the one element among many which is degenerating at a given time In degenerating peripheral nervous tissue where connective tissue spaces contain numerous macrophages phagocytosis by mobile macrophages is more easily imagined But even in this circumstance most of the phagocytosis described (Nathaniel and Pease 64) can be appropriately interpreted as auto-digestion since the myelin ingested by Schwann cells was originally the plasma membrane of that cell The semantic distinction is important because the phagocytosis of destroyed cells by another element has not yet been clearly demonstrated in non inflammatory lesions of the central nervous system Furthermore ingested debris would not *a priori* be rich in acid phosphatase In any case the myelin like inclusions could not be entirely accounted for by the ingestion of myelin fragments since the supragranular cortex of the rat contains too few myelinated fibers for so many laminated inclusions

A phagocytic mechanism in disposing of debris associated with inflammatory processes and tissue disruption has been observed (Blinzinger and Hager 64 Gonatas Levine and Shoulson 64 Maxwell and Kruger 65b) Vaughn (65) has implicated astrocytes in phagocytosis of myelin in degenerating optic nerve However it is difficult to identify "ingested material" in many other circumstances of experimental degeneration It has been suggested that axon terminals undergoing degeneration can be removed by dendrites (Walberg 63) and glial processes surrounding degenerating axo-dendritic contacts have been interpreted as a stage in the phagocytosis of degenerating boutons together with the portion of the apposed dendrite (Colonnier and Guillery 64 Colonnier 64) The presence of degenerated axonal material in direct contact with the cytoplasm of another cell (rather than merely being surrounded by its plasma membrane) would seem an important requirement for recognizing phagocytosis which has not yet been fulfilled It would also seem desirable at our present state of knowledge to adhere to the caution expressed by Webster (64) in interpreting myelin like lamellar inclusions many are evidently not derived from axonal ingestion and can be related to mitochondria (Sjostrand Cedergen and Karlsson 64) or lysosome and lipofuscin configurations (Samorajski Ordy and Keefe 65)

The accumulation of dense organelles following irradiation endow the oligodendrocytes with the appearance of fat granule laden cells in light microscopy Numerous osmiophilic rosettes can be seen in laminar lesions and surrounding neurons where the Marchi method presumably displays secondary axon terminal degeneration (Kruger and Malis 64) The distribution of Marchi positive material may be better correlated with the presence of dense bodies in satellite cells rather than myelin degeneration especially in regions sparsely populated with myelinated axons Presumably the dense homogeneous bodies characteristic of the *late* stages of the laminar lesion correspond to the residual lipofuscin usually associated with chronic pathological alterations A relationship between lipofuscin granules and lysosomes has recently been suggested (Gordon Miller and Bensch 65 Samorajski Ordy and Keefe 65) although there is no direct morphological evidence that the dense lipid organelles associated with vacuoles represent a

late enzymatically inactive stage in the transformation of the structured organelles seen in the acute stage of reactivity It is of interest in this connection to note that it is our distinct impression that more dense homogeneous granules of the lipo fuscin type are found in oligodendrocytes of older animals though by no means in as large numbers as we find in the long survival laminar lesions

The lysosome concept of de Duve sug gests that membrane bound packets of acid hydrolases constitute the digestive system of individual cells and morphological and biochemical evidence in support of this concept has been obtained in studies of several tissues (see Reuck and Cameron 63 Novikoff 61) The occurrence of large numbers of electron dense organelles some of which are acid phosphatase posi tive may serve to relate the absence of debris in the present studies to the lyso some concept

Caution might be exerted in the use of several recent terms such as lysosome phagosome siderosome or cytoly some to designate the dense organelles in reactive oligodendrocytes because of the wide morphological variety in this organ elle population and the cytochemical im plications of such terms Furthermore a single generic term cannot be applied to all of the dense bodies until some property common to all of them can be demon strated or a sequence of developmental stages from one variety to another firmly established (Gordon Miller and Bensch 65)

The lysosome is presently a biochemical concept rather than a morphological entity and on chemical grounds could include such diverse structures as the bodies dis playing granular crystalline or lamellar sub structure as well as the dense homo geneous lipofuscin bodies characteristic of later stages of the reactive oligodendrocyte The application of this concept to the pres ent study need not be limited by the mor phological diversity exhibited by the organ elle population It seems likely that some of the pleomorphic inclusions are the result of ingestion of molecular products of neu ronal dissolution These products may be further degraded in the sites of lytic en zyme activity The arrest of such degrada tion by fixation and the resulting dense body morphology would be dependent upon its chemical composition and stage of activity at the time of fixation No doubt other members of the dense body popula tion in reactive oligodendrocytes reflects the degradation of myelin by the parent cell since the breakdown of myelin may reasonably be regarded as auto digestion in central and peripheral nerves (Nathan iel and Pease 64)

In the classical literature it is generally accepted that a distinct class of cells known as microglia can be recognized as phago cytes in central nervous system pathology At the electron microscopic level these ele ments have been difficult to identify and the published illustrations to date are vir tually impossible to distinguish from cer tain profiles of oligodendrocytes (Bodian 64 Kruger and Maxwell 66) The form of microglia in metallic impregnation is remarkably similar to vascular pericytes and evidence has been adduced showing that the phagocytes of radiation disrupted lesions can be derived from vessel walls and do not originate from the brain paren chyma (Maxwell and Kruger 65b) The identity of cells containing cytoplasmic granules which can be counterstained with fat stains and which have been demon strated with the Rio Hortega silver carbo nate method in pathological material is subject to reinterpretation It is clear that the method impregnates oligodendroglia as well as microglia (distinguished on the basis of their processes) and that the variety of cell preferentially revealed is determined by such tenuous factors as pH and the duration of fixation and staining It should be emphasized that fat stained or phagocytosed material (Ferraro and Davidoff 26 Cramer and Alpers 32) was identified in reactive oligodendrocytes and that such inclusions might easily corre spond to the dense organelles described in the present report It should also be noted that compound granular corpuscles or gitter cells which are presumed to repre sent the more advanced stages of reactive microgliacytes are apparently absent in non inflammatory lesions (e g low dose particle irradiation lesions or retrograde thalamic atrophy) The role of microglia" in pathology indeed their actual existence

remains open to question (Adams 58 Maxwell and Kruger 65b Kruger and Maxwell 66)

The association of myelin manufacture to the dense varieties and dense bodies (or lysosomes in the generic sense) with pale oligodendrocytes might be a relevant clue to the wide spectrum of cytoplasmic density seen even in normal tissue (Kruger and Maxwell 66) It is of interest that the reactive oligodendrocytes do not display the wide range of cytoplasmic matrix densities observed in their normal counterparts Most of the dense organelles (of oligodendrocytes) were found within pale cytoplasm although this was not uniformly the case The palest cells appear to contain the largest array of structures related to degenerative and presumably lytic activity whereas the darkest variety displays little evidence of such processes but instead may possess properties related to membrane (myelin) synthesis In at least a qualitative sense there is a suggestive correlation of cytoplasmic matrix density ribosomes and nuclear density with the synthetic activity of oligodendrocytes A similar hypothesis has been offered to explain the larger proportion of dark" oligodendrocytes in white matter than in the cerebral cortex where the quantity of myelin (and consequently plasma membrane) requiring synthetic activity is considerably less (Kruger and Maxwell 66)

ACKNOWLEDGMENT

This work was supported by United States Public Health Service grants B 3604 and B 2684 and the Atomic Energy Commission grant AT(11 1) 34 Project no 68

We are indebted to Mrs Olga Fiorello Mrs Sharon Sampogna and Mrs Reid Severin for technical assistance to Mrs Diana Brinton for preparation of the manuscript and to Drs Daniel C Pease Anselmo Pineda and James E Vaughn for helpful discussions

LITERATURE CITED

Adams R D 1958 Implications of the biology of the neuroglia and microglia cells for clinical neuropathology In Biology of Neuroglia W F Windle ed Charles C Thomas Springfield Illinois pp 245–263

Blinzinger K H and H Hager 1964 Elektronmikroskopische Untersuchungen zur Feinstruktur ruhender und progessiver Mikrogliazellen in ZNS des Goldhamsters Prog Brain Res 6 99–112

Bodian D 1964 An electron microscopic study of the monkey spinal cord Bull Johns Hopkins Hosp 114 13–119

Brustad T P Ariotti and J Lyman 1960 Experimental setup and dosimetry for investigating biological effects of densely ionizing radiations Univ of Cal Rad Lab Report 9454 30 pp

Colonnier M 1964 Experimental degeneration in the cerebral cortex J Anat (Lond) 98 47–54

Colonnier M and R W Guillery 1964 Synaptic organization in the lateral geniculate nucleus of the monkey Zeitschr f Zellforschung 62 333–355

Cone W 1928 Acute pathologic changes in neuroglia and in microglia Arch Neurol Psychiat 20 34–68

Cramer F and B J Alpers 1932 Functions of glia in secondary degeneration of spinal cord Oligodendroglia as phagocytes Arch Path 13 23–55

Duncan D D Nall and R Morales 1960 Observations on the fine structure of old age pigment J Gerontol 15 366–372

Ferraro A 1928 Acute swelling of oligodendroglia and grapelike areas of disintegration Arch Neurol Psychiat 20 1065–1079

Ferraro A and L M Davidoff 1928 Reaction of oligodendroglia to injury of brain Arch Path 6 1030–1053

Gonatas N K S Levine and R Shoulson 1964 Phagocytosis and regeneration of myelin in an experimental leukoencephalopathy Am J Path 44 565–583

Gordon G B L R Miller and K G Bensch 1965 Studies on the intracellular digestive process in mammalian tissue culture cells J Cell Biol 25 41–55

Hirano A H M Zimmerman and S Levine 1965 Fine structure of cerebral fluid accumulation VI Intracellular accumulation of fluid and cryptococcal polysaccharide in oligodendroglia Arch Neurol 12 189–196

Kruger L and C D Clemente 1964 Anatomical and functional studies of the cerebral cortex by means of laminar destruction with ionizing radiation In Response of the Nervous System to Ionizing Radiation T J Haley and R S Snider eds Little Brown and Co Boston pp 84–104

Kruger L and L I Malis 1964 Distribution of afferent and efferent fibers in the cerebral cortex of the rabbit revealed by laminar lesions produced by heavy ionizing particles Exper Neurol 10 509–524

Kruger L and D S Maxwell 1966 Electron microscopy of oligodendrocytes in normal rat cerebrum Am J Anat 118 411–436

Malis L I C P Baker L Kruger and J E Rose 1960 Effects of heavy ionizing monoenergetic particles on the cerebral cortex I Production of laminar lesions and dosimetric considerations J Comp Neur 115 219–242

late enzymatically inactive stage in the transformation of the structured organelles seen in the acute stage of reactivity It is of interest in this connection to note that it is our distinct impression that more dense homogeneous granules of the lipofuscin type are found in oligodendrocytes of older animals though by no means in as large numbers as we find in the long survival laminar lesions

The lysosome concept of de Duve suggests that membrane bound packets of acid hydrolases constitute the digestive system of individual cells and morphological and biochemical evidence in support of this concept has been obtained in studies of several tissues (see Reuck and Cameron 63 Novikoff 61) The occurrence of large numbers of electron dense organelles some of which are acid phosphatase positive may serve to relate the absence of debris in the present studies to the lysosome concept

Caution might be exerted in the use of several recent terms such as lysosome phagosome siderosome or cytolysome to designate the dense organelles in reactive oligodendrocytes because of the wide morphological variety in this organelle population and the cytochemical implications of such terms Furthermore a single generic term cannot be applied to all of the dense bodies until some property common to all of them can be demonstrated or a sequence of developmental stages from one variety to another firmly established (Gordon Miller and Bensch 65)

The lysosome is presently a biochemical concept rather than a morphological entity and on chemical grounds could include such diverse structures as the bodies displaying granular crystalline or lamellar sub structure as well as the dense homogeneous lipofuscin bodies characteristic of later stages of the reactive oligodendrocyte The application of this concept to the present study need not be limited by the morphological diversity exhibited by the organelle population It seems likely that some of the pleomorphic inclusions are the result of ingestion of molecular products of neuronal dissolution These products may be further degraded in the sites of lytic enzyme activity The arrest of such degradation by fixation and the resulting dense body" morphology would be dependent upon its chemical composition and sta[illegible] of activity at the time of fixation No doubt other members of the dense body population in reactive oligodendrocytes reflect the degradation of myelin by the paren[illegible] cell since the breakdown of myelin ma[illegible] reasonably be regarded as auto digestion in central and peripheral nerves (Nathaniel and Pease 64)

In the classical literature it is genera[illegible] accepted that a distinct class of cells know[illegible] as microglia can be recognized as pha[illegible]cytes in central nervous system patholog[illegible] At the electron microscopic level these el[illegible]ments have been difficult to identify a[illegible] the published illustrations to date are vi[illegible]tually impossible to distinguish from ce[illegible]tain profiles of oligodendrocytes (Bodia[illegible] 64, Kruger and Maxwell 66) The for[illegible] of microglia in metallic impregnation [illegible] remarkably similar to vascular pericyte[illegible] and evidence has been adduced showin[illegible] that the phagocytes of radiation disrupt[illegible] lesions can be derived from vessel wal[illegible] and do not originate from the brain pare[illegible]chyma (Maxwell and Kruger 65b) T[illegible] identity of cells containing cytoplasm[illegible] granules which can be counterstained wi[illegible] fat stains and which have been demo[illegible]strated with the Rio Hortega silver ca[illegible]nate method in pathological material [illegible] subject to reinterpretation It is clear th[illegible] the method impregnates oligodendroglia [illegible] well as "microglia (distinguished on t[illegible] basis of their processes) and that t[illegible] variety of cell preferentially revealed [illegible] determined by such tenuous factors as p[illegible] and the duration of fixation and stainin[illegible] It should be emphasized that fat stained phagocytosed material (Ferraro a[illegible] Davidoff 26 Cramer and Alpers 32) w[illegible] identified in reactive oligodendrocytes a[illegible] that such inclusions might easily cor[illegible]spond to the dense organelles described [illegible] the present report It should also be not[illegible] that compound granular corpuscles gitter cells which are presumed to repr[illegible]sent the more advanced stages of reacti[illegible] microgliacytes are apparently absent [illegible] non inflammatory lesions (e g low do[illegible] particle irradiation lesions or retrograd[illegible] thalamic atrophy) The role of microgli[illegible] in pathology indeed their actual existence


g
N

Maxwell D S and L Kruger 1964 Electron microscopy of radiation induced laminar lesions in the cerebral cortex of the rat In 2nd Int Symp on The Response of the Nervous System to Ionizing Radiation T Haley Ed Little Brown and Co Boston pp 54–83

——— 1965a The fine structure of astrocytes in the cerebral cortex and their response to focal injury produced by heavy ionizing particles *J Cell Biol* 25 141–157

——— 1965b Small blood vessels and the origin of phagocytes in the rat cerebral cortex following heavy particle irradiation Exper Neurol *12* 33–54

——— 1965c Changes in oligodendrocyte organelles during neuronal degeneration VIII Int Anat Cong pp 76–77

Nathaniel E J and D C Pease 1963 Regenerative changes in rat dorsal root following Wallerian degeneration J Ultrastr Res 9 533–549

Novikoff A B 1961 Lysosomes and related particles In The Cell Vol II J Brachet and A E Mirsky eds Academic Press New York pp 423–488

O Leary J L A B Harris R R Fox J H Smith and M Tidwell 1965 Ultrastructural lesions in rabbit hereditary ataxia Arch Neurol *13* 238–262

Palay S L and G E Palade 1955 The fine structure of neurons J Biophys Biochem Cytol *1* 69–88

Pease D C 1964 Histological Techniques for Electron Microscopy Second Edition Academic Press New York

Penfield W 1932 Neuroglia Normal and pathological In Cytology and Cellular Pathology of the Nervous System Paul B Hoeber New York pp 423–479

Penfield W and W Cone 1926 Acute swelling of oligodendroglia Arch Neurol and Psychiat (Chicago) *16* 131–153

Reuck A V S and M P Cameron (editors) 1963 Lysosomes — Ciba Foundation Symposium Little Brown and Co Boston 4?8 pp

Sabatini D D K G Bensch and R J Barrnett 1963 Cytochemistry and electron microscopy The preservation of cellular ultrastructure and enzymatic activity by aldehyde fixation J Cell Biol *17* 19–58

Samorajski T J M Ordy and J R Keefe 1965 The fine structure of lipofuscin age pigment in the nervous system of aged mice J Cell Biol 26 779–795

Sjostrand F S E A Cedergren and U Karlsson 1964 Myelin like figures formed from mitochondrial material Nature *202* 1075–1078

Terry R D and M Weiss 1963 Studies in Tay Sachs disease II Ultrastructure of the cerebrum J Neuropath Exp Neurol 22 18–55

Vaughn J E 1965 Electron microscopic study of the vascular response to axonal degeneration in rat optic nerve Anat Rec *151* 4?8

Walberg F 1963 Role of normal dendrites in removal of degenerating terminal boutons Exp Neurol *8* 112–124

Webster H de F 1964 Some ultrastructural features of segmental demyelination and myelin regeneration in peripheral nerve Prog Brain Res *13* 151–172

PLATE 1

EXPLANATION OF FIGURE

1 *Early stage of oligodendrocyte reactivity Clear spaces in the perinuclear cytoplasm suggest acute swelling At several points apparent invaginations of plasma membrane are indicated by arrows The contacts of this cell include neuron cytoplasm (N) and processes of reactive astrocytes indicated by dense black glycogen granules (g) Five days following irradiation with 9 000 rads Bar in this and all subsequent figures represents one micron*


N
O

PLATE 2

EXPLANATION OF FIGURE

2 Reactive satellite oligodendrocyte (*O*) displaying moderate swelling near the edge of the laminar lesion The adjacent neuron (*N*) shows little indication of pathological change Eleven days following irradiation with 6 000 rads


13

PLATE 3

EXPLANATION OF FIGURE

3 Chromatolytic neuron (*N*) with a reactive satellite oligodendrocyte (O) containing granular and homogeneous dense organelles The nucleus (*n*) has been sectioned tangentially The neuron displays peripherally clustered Nissl bodies (granular endoplasmic reticulum *er*) Eleven days following irradiation with 9 000 rads


3

PLATE 4

EXPLANATION OF FIGURE

4 Swollen reactive oligodendrocyte (*O*) containing a range of pathological dense organelles juxtaposed to a reactive astrocyte (*A*) The latter cell in contrast to the oligodendrocyte contains prominent cytoplasmic fibrils (*f*) and glycogen granules In this example the cytoplasmic matrix density of the astrocyte is higher than that of the oligodendrocyte A moderately chromatolytic neuron (*N*) can be seen near the lower right edge Eleven days following irradiation with 9 000 rads


O
A
N
4

PLATE 5

EXPLANATION OF FIGURES

5 Cytoplasm of a reactive oligodendrocyte displaying two prominent Golgi zones (*G*) associated with profiles of vesicles or tubules which may be part of the smooth endoplasmic reticulum A spectrum of dense bodies can be found ranging from these small profiles to large granular and lamellar organelles Twenty two days following irradiation with 9 000 rads

6 Reactive swollen oligodendrocyte containing a range of sizes of dense bodies and displaying a diversity of internal structure The large denser varieties exhibit the more common granular and crystalline contents and the dense body at the extreme left contains an electron opaque plate A bulge (arrow) suggests extrusion or coalescence Eleven days following irradiation with 9 000 rads

5

6

PLATE 5

EXPLANATION OF FIGURES

5 Cytoplasm of a reactive oligodendrocyte displaying two prominent Golgi zones (*G*) associated with profiles of vesicles or tubules which may be part of the smooth endoplasmic reticulum A spectrum of dense bodies can be found ranging from these small profiles to large granular and lamellar organelles Twenty two days following irradiation with 9 000 rads

6 Reactive swollen oligodendrocyte containing a range of sizes of dense bodies and displaying a diversity of internal structure The large, denser varieties exhibit the more common granular and crystalline contents and the dense body at the extreme left contains an electron opaque plate A bulge (arrow) suggests extrusion or coalescence Eleven days following irradiation with 9 000 rads


7
8

PLATE 6

EXPLANATION OF FIGURES

7 Reactive oligodendrocyte containing granular dense bodies some of these (arrows) are bounded by a double membrane and one (*double arrow*) is bounded by a complex structure containing a dense line *Eleven days following irradiation with 9 000 rads*

8 A highly structured dense body of a reactive oligodendrocyte The lamellar and granular portions are in continuity The elongate tails often display a dense central core similar to that of small dense *bodies seen in figures 5 7 and 9 Eleven days following irradiation* with 9 000 rads

9

10

PLATE 7

EXPLANATION OF FIGURES

9 Reactive oligodendrocyte The highly developed Golgi membranes (*G*) may be related to the cluster of small dense bodies (arrows to the left of the nucleus) whose form suggests development within a tubular system This section of cytoplasm reveals two larger organelles with granular and lamellar internal structure (*l*) Twenty two days fol lowing irradiation with 9 000 rads

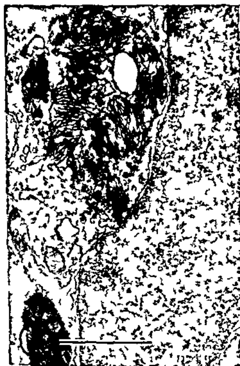
10 Oligodendrocyte cytoplasm commonly encountered in long standing lesions The organelles are typically highly vacuolated irregular homogeneous masses of electron dense material and probably corre spond to lipofuscin bodies Twenty two months following irradiation with 9 000 rads


10

PLATE 8

EXPLANATION OF FIGURES

11–14 Four figures illustrating lysosomes in reactive oligodendrocyte cytoplasm after incubation in Gomori substrate Electron opaque reaction product of the Gomori acid phosphatase procedure is deposited in the site of acid phosphatase activity The lysosomes contain granular and lamellar internal structure Seven days following irradiation with 9 000 rads




12




14

Histochemical Studies on the Pacinian Corpuscle

T R. SHANTHAVEERAPPA AND G H BOURNE
Yerkes Regional Primate Research Center and Laboratory for Ophthalmic Research Emory University Atlanta Georgia

ABSTRACT Detailed studies on the localization of various oxidative and hydrolytic enzymes were made of the Pacinian corpuscle nerve fiber inner core and lamellae The nerve fiber of the corpuscle was found to be rich in specific and nonspecific cholinesterases simple esterase lactic dehydrogenase succinic dehydrogenase cytochrome oxidase alkaline phosphatase adenosine triphosphatase thiamine pyrophosphatase and 5-nucleotidase enzymes It showed moderately positive activity for acid phosphatase and negligible activity for monoamine oxidase The lamellar cells and the inner core cells showed mild to moderate positive activity for all these enzymes excepting monoamine oxidase specific and nonspecific cholinesterases for which they were negative The relationship between these cells and the perineural epithelium of peripheral nerves and the pia arachnoid mater of the central nervous system was discussed

The cholinesterase activity of the Pacinian corpuscle has been studied in detail by Hebb and Hill (55) Beckett et al (56) and cauna (61) and the physiological properties by Hubbard (56 58) and Danysz and Malofiejew (63) Histological detail of the corpuscle as seen under the light microscope has been described by Cauna and Mannan (58) Quilliam and Sato (55) and Shanthaveerappa and Bourne (63a b) Electron microscope studies have been made by Pease and Quilliam (57) There are few studies on the localization of various oxidative and dephosphorylating enzymes attempted in the Pacinian corpuscle Such studies of the corpuscle would be of interest because of the complexity of its organization and might help to shed some light on the transducer mechanisms operating in the functioning of this tactile corpuscle

MATERIAL AND METHODS

Young adult male and female cats were used in this study The animals were anesthetized by proper doses of nembutal (Abbott) The adominal cavity was opened by using scalpel and dissecting scissors The small intestines were drawn out on a clean towel and then the mesentery was exposed Areas of mesentery containing large numbers of Pacinian corpuscles were selected and cut and folded into small blocks These were put on aluminum foil and frozen in isopentane to dry ice temperature (78 C) These peritoneal blocks containing the Pacinian corpuscles were removed from the isopentane mounted on a cryostat chuck and 10 μ thick sections were cut at 20 C These sections were gradually brought to the room temperature by being placed in a refrigerator for some time Then they were dried under a fan for 2 to 3 minutes and various histochemical tests were applied on the sections

Various enzymes were demonstrated by the following methods
Alkaline phosphatase (Gomori 39)
Acid phosphatase (Barka and Anderson 62)
Adenosine triphosphatase (Wachstein and Meisel 57a)
Thiamine pyrophosphatase (Novikoff and Goldfischer 61)
5-Nucleotidase (Wachstein and Meisel 57b)
Succinic dehydrogenase (Nachlas et al 57)
Cytochrome oxidase (Burstone 60)
Monoamine oxidase (Glenner et al 57)
Lactic dehydrogenase (Hess et al 58)
Specific and nonspecific cholinesterases (Coupland and Holmes 57 and Gerebtzoff 59)

Thiamine pyrophosphatase (TPPase) method was applied on 10% neutral calcium formalin post fixed sections Controls were carried out by leaving out the appropriate substrate Diisopropyl fluorophosphate inhibition tests were carried out for nonspecific cholinesterase

RESULTS

Three distinct areas can be recognized in the Pacinian corpuscle with both the light and the electron microscope (1)

Histochemical Studies on the Pacinian Corpuscle

T R SHANTHAVEERAPPA AND G H BOURNE
Yerkes Regional Primate Research Center and Laboratory for Ophthalmic Research Emory University Atlanta Georgia

ABSTRACT Detailed studies on the localization of various oxidative and hydrolytic enzymes were made of the Pacinian corpuscle nerve fiber inner core and lamellae The nerve fiber of the corpuscle was found to be rich in specific and nonspecific cholinesterases simple esterase lactic dehydrogenase succinic dehydrogenase cytochrome oxidase alkaline phosphatase adenosine triphosphatase thiamine pyrophosphatase and 5-nucleotidase enzymes It showed moderately positive activity for acid phosphatase and negligible activity for monoamine oxidase The lamellar cells and the inner core cells showed mild to moderate positive activity for all these enzymes excepting monoamine oxidase specific and nonspecific cholinesterases for which they were negative The relationship between these cells and the perineural epithelium of peripheral nerves and the pia arachnoid mater of the central nervous system was discussed

The cholinesterase activity of the Pacinian corpuscle has been studied in detail by Hebb and Hill (55) Beckett et al (56) and cauna (61) and the physiological properties by Hubbard (56 58) and Danysz and Malofiejew (63) Histological detail of the corpuscle as seen under the light microscope has been described by Cauna and Mannan (58) Quilliam and Sato (55) and Shanthaveerappa and Bourne (63a b) Electron microscope studies have been made by Pease and Quilliam (57) There are few studies on the localization of various oxidative and dephosphorylating enzymes attempted in the Pacinian corpuscle Such studies of the corpuscle would be of interest because of the complexity of its organization and might help to shed some light on the transducer mechanisms operating in the functioning of this tactile corpuscle

MATERIAL AND METHODS

Young adult male and female cats were used in this study The animals were anesthetized by proper doses of nembutal (Abbott) The adominal cavity was opened by using scalpel and dissecting scissors The small intestines were drawn out on a clean towel and then the mesentery was exposed Areas of mesentery containing large numbers of Pacinian corpuscles were selected and cut and folded into small blocks These were put on aluminum foil and frozen in isopentane to dry ice temperature (78 C) These peritoneal blocks containing the Pacinian corpuscles were removed from the isopentane mounted on a cryostat chuck and 10 µ thick sections were cut at 20 C These sections were gradually brought to the room temperature by being placed in a refrigerator for some time Then they were dried under a fan for 2 to 3 minutes and various histochemical tests were applied on the sections

Various enzymes were demonstrated by the following methods

Alkaline phosphatase (Gomori 39)
Acid phosphatase (Barka and Anderson 62)
Adenosine triphosphatase (Wachstein and Meisel 57a)
Thiamine pyrophosphatase (Novikoff and Goldfischer 61)
5-Nucleotidase (Wachstein and Meisel 57b)
Succinic dehydrogenase (Nachlas et al 57)
Cytochrome oxidase (Burstone 60)
Monoamine oxidase (Glenner et al 57)
Lactic dehydrogenase (Hess et al 58)
Specific and nonspecific cholinesterases (Coupland and Holmes 57 and Gerebtzoff 59)

Thiamine pyrophosphatase (TPPase) method was applied on 10% neutral calcium formalin post fixed sections Controls were carried out by leaving out the appropriate substrate Diisopropyl fluorophosphate inhibition tests were carried out for nonspecific cholinesterase

RESULTS

Three distinct areas can be recognized in the Pacinian corpuscle with both the light and the electron microscope (1)

the nerve fiber zone found in the center (II) the inner core area lying next to and completely surrounding the nerve fiber and (III) the external lamellar sheath surrounding the inner core area consisting of several layers of flat squamous cells Histochemical descriptions were made on these three zones

(1) *Dephosphorylating enzymes* The nerve fiber of the corpuscle was strongly positive for alkaline phosphatase (fig 1) adenosine triphosphatase (figs 2 3) 5 nucleotidase (fig 6) moderately positive for thiamine pyrophosphatase and mildly positive for acid phosphatase (fig 5) The lamellar sheath was moderately positive for all these enzymes In adenosine triphosphatase thiamine pyrophosphatase and acid phosphatase preparations we observed some lamellar cells showing much stronger positive reactions than others (figs 2 4 5) The blood vessels found inside the corpuscles were strongly positive for adenosinetriphosphatase (fig 3) One of the corpuscles contained about 10 to 12 blood vessels which were all positive for adenosine triphosphatase (fig 3) The inner core showed the same type of enzyme activity as the lamellar sheath and the positive activity was much stronger as compared to the lamellar sheath

(2) *Esterases* The nerve fiber in the center of the corpuscle was strongly positive for specific cholinesterase (fig 8) nonspecific cholinesterase (figs 9 11) and for simple esterase (fig 7) Simple esterase activity was found to be granular as well as diffuse in character The specific and nonspecific cholinesterase activity was diffuse The inner core and lamellar sheath were negative for specific and non specific cholinesterases but showed a very mild type of simple esterase activity Sections pretreated with diisopropyl fluoro phosphate at 10^{-6} concentration showed negative activity for nonspecific (fig 10) and moderate positive activity for specific cholinesterase in the nerve fiber

(3) *Oxidative enzymes* The nerve fiber in the center of the corpuscle was strongly positive for succinic dehydrogenase (figs 12 13) and lactic dehydrogenase (fig 14) moderately positive for cytochrome oxidase (fig 15) and showed mild activity for monoamine oxidase (fig 16) The positive activity was both granular and diffuse in type The inner core showed moderately strong positive activity for succinic and lactic dehydrogenases (figs 12 14) and was mildly positive for cytochrome oxidase The monoamine oxidase test showed negative activity in the inner core as well as in the lamellar sheath Some of the lamellae showed moderately strong positive activity for lactic and succinic dehydrogenases as compared to other lamellar cells

No positive activity was observed in the connective tissue component of the corpuscle that is found in between the lamellae and was indistinct in most of our preparations The perineural epithelium found on the nerve fiber fasciculi in the mesentery showed the same type of enzyme distribution as observed in the inner core and lamellar sheath of the corpuscle

Staining with silver nitrate and cresyl violet showed that the lamellae of the Pacinian corpuscle are made up of flat squamous cells laid one on top of the other (fig 17) and are the continuation of the perineural epithelium as observed in our previous studies (Shanthaveerappa and Bourne 63a b)

DISCUSSION

Cauna (61) and Beckett et al (56) found the inner core of the corpuscle showing both specific and nonspecific cholinesterase activity whereas Hebb and Hill (55) think that the inner core contains nonspecific but no specific cholinesterase Loewenstein and Hollins (58) in their biochemical analysis of the cat Pacinian corpuscle found the concentration of cholinesterase around the non myelinated endings negligible amounts of it in the capsular zone Our studies show that the positive activity is exclusively found in the nerve fiber of the corpuscle However we also observed that when the sections were treated with diisopropyl fluorophosphate and incubated for specific cholinesterase localization they showed the reduction in degree of specific cholinesterase positive activity Diisopropyl fluorophosphate completely inhibits the nonspecific cholinesterase This tends to indicate that nonspecific cholinesterase is present in the nerve fiber as well as in the

innermost aspect of the inner core adja ent to the nerve terminal Further it in dicated that the heavy CuSO deposits ob served in specific cholinesterase activity are not only due to specific cholinesterase activity but are also due to nonspecific cholinesterase activity

Pease and Quillium (57) have shown under the electron microscope that the nerve fiber in the Pacinian corpuscle con tains abundant mitochondria as well as a few synaptic vesicles The presence of synaptic vesicles and high cholinesterase activity and the presence of mild mono-amine oxidase activity indicate that the Pacinian corpuscles are more cholinergic than adrenergic in nature In view of the presence of large numbers of mitochon dria high oxidative enzyme activity in the nerve fiber is not surprising Small round granules of positive areas were observed in succinic dehydrogenase (fig 13) lactic dehydrogenase and cytochrome oxidase (fig 15) preparations in the nerve ter minal These probably represent the posi tive activity (oxidative enzymes) in the mitochondria

It is now well recognized that the thi amin pyrophosphatase technique acts as a marker of Golgi apparatus (Novikoff and Goldfischer 61 Goldfischer 64 Novi koff and Essner 62 Baker 63 and Shan thaveerappa and Bourne 65a f g,h,i) But still we could not find a distinctly stained Golgi apparatus in the terminal nerve fiber of the corpuscle The terminal nerve fiber was diffusely stained and the lamellae also showed a diffuse type of activity which was of a mild type Some darkly stained specks were seen here and there indicat ing the Golgi complex in the lamellar cells Though the nerve fiber terminal does not have any thiamine pyrophosphatase posi tive Golgi complex it has the enzyme thiamine pyrophosphatase The blood ves sels the mesothelial lining of peritoneum the pia arachnoid mater choroid of the eye and the perineural epithelium of peripheral nerves all give a diffuse reac tion with this technique (Shanthaveerappa and Bourne 62a b 63c 64b c 65c g) So in these structures thiamine pyrophos phatase is probably not restricted to the Golgi complex but is distributed diffusely as it is seen in the nerve terminal of the corpuscle

The lamellae of the Pacinian corpuscle represent the extension of the perineural epithelium cells from the nerve which supplies it (Shanthaveerappa and Bourne 63a 65b) We have shown that these cells are not fibroblasts but are flat squa mous epithelial cells forming continuous lamellae laid one on top of the other In this study also the above observations were confirmed

Our electronmicrographs of the peri neural epithelium (Shanthaveerappa et al 63) resemble those of the lamellar cells of the Pacinian corpuscle (Pease and Quil liam 57) and the inner and outer cap-sular sheaths of the muscle spindle (Rob-ertson 60) Electron microscopic studies of the perineural epithelium have shown conclusively that these cells are not fibro blasts because they have a basement membrane on both upper and lower sur faces It is important to point out here that if these lamellar cells were fibroblasts the corpuscle would contain much fibrous tissue On the contrary little collagen is found between lamellar cells

In this study we noted that the lamellae of the Pacinian corpuscle showed the same type of enzyme distribution as the perineural epithelium the pia arachnoid mater choroid of the eye and the capsule of the muscle spindle thus helping to confirm the idea that all these structures are identical and represent the continua tion of the pia arachnoid mater from the central nervous system (Shanthaveerappa and Bourne 62a b 63a b c d 64a b c 65b c) The lamellar cells undergo divi sion (Pease and Quilliam 57) It is pos sible that high enzyme activity seen in some of the cells of the lamellae may be related to the age or state of division of the lamellar cells

The adenosine triphosphatase alkaline phosphatase acid phosphatase found in the nerve fiber may be in some way con cerned with membrane permeability and ion exchange at the nerve terminal as sociated with the initiation of the nerve impulse of this end-organ The areas of exclusive synapses like glomeruli in the olfactory bulb and the cerebellum in the squirrel monkey also show high activity

for these enzymes (Shanthaveerappa and Bourne 65d e f g) Thus both nerve end organs and the synaptic areas are rich in these enzymes The glomeruli also showed high activity for oxidative enzymes and simple esterase The Pacinian corpuscle nerve terminal has specific and nonspecific cholinesterases and thiamine pyrophosphatase but negligible monoamine oxidase whereas the glomeruli has moderate specific cholinesterase and high monoamine oxidase enzyme activity, and does not show any thiamine pyrophosphatase or nonspecific cholinesterase activity

ACKNOWLEDGMENTS

This work was supported by grant NB 01914 from the National Institute of Neurological Diseases and Blindness grants FR 00165 and FR 05235 from the Division of Research facilities and Resources National Institutes of Health and grant HE 05691 of the National Heart Institute

LITERATURE CITED

Baker J R 1963 New developments in the Golgi controversy J Roy Micr Soc 82 145-147

Barka T and P J Anderson 1962 Histochemical method for acid phosphatase using hexazonium pararosanilin as coupling J *Histochem Cytochem 10* 741-753

Beckett E B G H Bourne and W Montagna 1956 *Histology and cytochemistry of human skin The distribution of cholinesterases in the finger of the embryo and the adult* J Physiol 134 202-206

Burstone M S 1962 Enzyme Histochemistry and its Application in the Study of Neoplasms Academic Press Inc New York and London

Danysz A and M Malofiejew 1963 The reaction of vater Pacini corpuscles to chemical and physical factors acting on the small intestine mucosa Arch int Pharmacodyn *143* 34-41

Cauna N 1961 Cholinesterase activity in cutaneous receptors of man and of some quadrupeds *Bibl anat* 2 128-138

Cauna N and G Mannan 1958 The structure of the human digital Pacinian corpuscles (corpuscula lamellosa) and its functional significance *J Anat Lond 92* 1-20

Coupland R E and R L Holmes 1957 The use of cholinesterase techniques for the demonstration of peripheral nervous structures Quart J micr Sci 98 327-330

Gerebtzoff M A 1959 Cholinesterases Pergamon Press New York

Glenner G G H J Burtner and G W Brown Jr 1957 The histochemical demonstration of monoamine oxidase activity by tetrazolium salts J Histochem Cytochem 5 591-600

Goldfischer D 1964 The Golgi apparatus and the endoplasmic reticulum in neurons of the rabbit J Neuropath exp Neur 23 36-4[illegible]

Gomori G 1939 Microtechnical demonstration of phosphatases in tissue sections Proc Soc Exp Biol N Y 42 23-26

Hebb C O and K J Hill 1955 Pseudocholinesterase in Pacinian corpuscles Nature *175* 597

Hess R D G Scarpelli and A G E Pearse 1958 Cytochemical localization of oxidative enzymes II Pyridine nucleotidase linked dehydrogenases J Biophys Biochem Cytol 4 753-760

Hubbard S J 1956 The mechanical properties of Pacinian corpuscles J Physiol 13[illegible] 23

——— 1958 A study of rapid mechanical events in a mechanoreceptor J Physiol 14[illegible] 198-218

Loewenstein W R and D Molins 1958 Cholinesterase in a receptor Science 128 1[illegible]

Nachlas M M L C Tsou E D Souza C Cheng and A M Seligman 1957 Cytochemical demonstration of succinic dehydrogenase by the use of a new p nitrophenyl substituted ditetrazole J Histochem Cytochem 5 4[illegible] 436

Novikoff A B and E Essner 1962 Pa[illegible] logical changes in cytoplasmic organelles [illegible] Proc 21 1130-1142

Novikoff A B and S Goldfischer 1961 [illegible] leosidediphosphatase activity in the Golgi apparatus and its usefulness for cytolo[illegible] studies Proc N A S 47 802-810

Pease D C and T A Quilliam 1957 [illegible] tron microscopy of the Pacinian corpuscle Biophys Biochem Cytol 3 331-342

Quilliam T A and M Sato 1955 The d[illegible] bution of myelin on nerve fibers from Pac[illegible] corpuscles J Physiol 129 167-176

Robertson J D 1960 Electron microsco[illegible] the motor end plate and the neuromus[illegible] spindle Amer J Phys Med 39 1-42

Shanthaveerappa T R and G H Bourne [illegible] A perineural epithelium J Cell Biol 14 346

——— 1962b The perineural epitheliu[illegible] metabolically active continuous protopl[illegible] cell barrier surrounding peripheral fasciculi J Anat Lond 96 527-537

——— 1963a New observations on the [illegible] ture of the Pacinian corpuscle and its re[illegible] to the perineural epithelium of peri[illegible] nerves Am J Anat 112 97-109

——— 1963b Demonstration of perineur[illegible] thelium in whale and shark peripheral n[illegible] Nature 197 577-579

——— 1963c The perineural epithelium [illegible] ture and significance Nature 199 577[illegible]

——— 1963d Demonstration of perineur[illegible] thelium in vagus nerves Acta anat 5[illegible] 100

——— 1964a The perineural epitheliu[illegible] sympathetic nerves and ganglia and its [illegible] tion to the pia arachnoid of the central n[illegible] system and perineural epithelium of th[illegible] ripheral nervous system Z Zellforsch 742-753

——— 1964b The effects of transection of the nerve trunk on the perineural epithelium with special reference to its role in nerve degeneration and regeneration Anat Rec 150 35–50
——— 1964c Histochemical studies on the distribution of oxidative and dephosphorylating enzymes of the rabbit eye Acta anat 57 192–219
——— 1965a Histochemical demonstration of thiamine pyrophosphatase and acid phosphatase in the Golgi region of the cells of the eye J Anat Lond 99 103–117
——— 1965b A simple method for preparation and staining of the whole Pacinian corpuscle Acta anat 60 199–206
——— 1965c Histological and histochemical studies of the choroid of the eye and its relation to the pia arachnoid mater of the central nervous system and the perineural epithelium of the peripheral nervous system Acta anat 379–398
——— 1965d Histochemical studies on the distribution of dephosphorylating and oxidative enzymes and esterases in the olfactory bulb of the squirrel monkey J Nat Cancer Inst. 35 153–165
——— 1965e Histochemical studies on the olfactory glomeruli of the squirrel monkey Histochemie 5 125–129
——— 1965f The thiamine pyrophosphatase technique as an indicator of the morphology of the Golgi apparatus in the neurons II Studies on the cerebral cortex La Cellulle 65 201–209
——— 1965g The thiamine pyrophosphatase technique as an indicator of the morphology of the Golgi apparatus in the neurons III Studies on the olfactory bulb Exp Cell Res 292–300
——— 1965h The thiamine pyrophosphatase technique as an indicator of the morphology of the Golgi apparatus in the neurons I Studies on ganglion cells Acta histochem 22 155–178
——— 1965i The thiamine pyrophosphatase technique as an indicator of the morphology of the Golgi apparatus in the neurons IV Studies on the cerebellum of rat and squirrel monkey Z Zellforsch 68 699–710
——— 1965j Histochemical studies on the localization of oxidative and dephosphorylating enzymes and esterases in the peritoneal mesothelial cells Histochemie 5 331–338
Shanthaveerappa T R James Hope and G H Bourne 1963 Electron microscopic demonstration of the perineural epithelium in rat peripheral nerve Acta anat 52 193–201
Wachstein M and E Meisel 1957a Histochemistry of hepatic phosphatases at a physiological pH with special reference to the demonstration of bile canaliculi Amer J Clin Path 27 13–23
——— 1957b A comparative study of enzymatic staining reactions in the rat kidney with necrobiosis induced by ischemia and nephrotoxic agents (mercuhydrin and dl-serine) J Histochem Cytochem 5 204–220

for these enzymes (Shanthaveerappa and Bourne 65d e f g) Thus both nerve end organs and the synaptic areas are rich in these enzymes The glomeruli also showed high activity for oxidative enzymes and simple esterase The Pacinian cor puscle nerve terminal has specific and nonspecific cholinesterases and thiamine pyrophosphatase but negligible mono amine oxidase whereas the glomeruli has moderate specific cholinesterase and high monoamine oxidase enzyme activity and does not show any thiamine pyrophos phatase or nonspecific cholinesterase ac tivity

ACKNOWLEDGMENTS

This work was supported by grant NB 01911 from the National Institute of Neu rological Diseases and Blindness grants FR 00165 and FR 05235 from the Division of Research facilities and Resources Na tional Institutes of Health and grant HE 05691 of the National Heart Institute

LITERATURE CITED

Baker J R 1963 New developments in the Golgi controversy J Roy Micr Soc 82 145–147

Barka T and P J Anderson 1962 Histo chemical method for acid phosphatase using hexazonium pararosanilin as coupling J Histochem Cytochem 10 741–753

Beckett E B G H Bourne and W Montagna 1956 Histology and cytochemistry of human skin The distribution of cholinesterases in the finger of the embryo and the adult J Physiol 134 202–206

Burstone M S 1962 Enzyme Histochemistry and Its Application in the Study of Neoplasms Academic Press Inc New York and London

Danysz A and M Malofiejew 1963 The reac tion of vater Pacini corpuscles to chemical and physical factors acting on the small intestine mucosa Arch int Pharmacodyn 143 34–41

Cauna N 1961 Cholinesterase activity in cu taneous receptors of man and of some quad rupeds Bibl anat 2 128–138

Cauna N and G Mannan 1958 The struc ture of the human digital Pacinian corpuscles (corpuscula lamellosa) and its functional sig nificance J Anat Lond 92 1–20

Coupland R E and R L Holmes 1957 The use of cholinesterase techniques for the demon stration of peripheral nervous structures Quart J micr Sci 98 327–330

Gerebtzoff M A 1959 Cholinesterases Per gamon Press New York

Glenner G G H J Burtner and G W Brown Jr 1957 The histochemical demonstration of monoamine oxidase activity by tetrazolium salts J Histochem Cytochem 5 591–600

Goldfischer D 1964 The Golgi appa atus ar the endoplasmic reticulum in neurons of th rabbit J Neuropath exp Neur 23 36–45

Gomori G 1939 Microtechnical demonstra c of phosphatases in tissue sections Proc So Exp Biol N Y 42 23–26

Hebb C O and K J Hill 1955 Pseudoch linesterase in Pacinian corpuscles Natu 175 597

Hess R D G Scarpelli and A G E Pear 1958 Cytochemical localization of oxidat enzymes II Pyridine nucleotidase linked d hydrogenases J Biophys Biochem Cytol 753–760

Hubbard S J 1956 The mechanical prop ties of Pacinian corpusel s J Physiol 13 23

——— 1958 A study of rapid mechanic events in a mechanoreceptor J Physiol 14 198–218

Loewenstein W R and D Molins 19 8 Ch linesterase in a receptor Science 128 1284

Nachlas M M L C Tsou E D Souza C Cheng and A M Seligman 1957 Cytoche cal demonstration of succinic dehydrogena by the use of a new p nitrophenyl substitut ditetrazole J Histochem Cytochem 5 42 436

Novikoff A B and E Essner 1962 Pat logical changes in cytoplasmic organelles Fe Proc 21 1130–1142

Novikoff A B and S Goldfischer 1961 Nu leosidediphosphatase activity in the Golgi a paratus and its usefulness for cytologi studies Proc N A S 47 802–810

Pease D C and T A Quillium 1957 El tron microscopy of the Pacinian corpuscle Biophys Biochem Cytol 3 331–342

Quillium T A and M Sato 1955 The dist bution of myelin on nerve fibers from Pacini corpuscles J Physiol 129 167–176

Robertson J D 1960 Electron microscopy the motor end plate and the neuromuscul spindle Amer J Phys Med 39 1–42

Shanthaveerappa T R and G H Bourne 196 A perineural epithelium J Cell Biol 14 34 346

——— 1962b The perineural epithelium metabolically active continuous protoplasm cell barrier surrounding peripheral ner fasciculi J Anat Lond 96 527–537

——— 1963a New observations on the stru ture of the Pacinian corpuscle and its relatio to the perineural epithelium of peripher nerves Am J Anat 112 97–109

——— 1963b Demonstration of perineural ep thelium in whale and shark peripheral nerve Nature 197 577–579

——— 1963c The perineural epithelium na ture and significance Nature 199 577 579

——— 1963d Demonstration of perineural ep thelium in vagus nerves Acta anat 52 95 100

——— 1964a The perineural epithelium o sympathetic nerves and ganglia and its rela tion to the pia arachnoid of the central nervou system and perineural epithelium of the pe ripheral nervous system Z Zellforsch 61 742–753

—— 1964b The effects of transection of the nerve trunk on the perineural epithelium with special reference to its role in nerve degeneration and regeneration Anat Rec 150 35–50
—— 1964c Histochemical studies on the distribution of oxidative and dephosphorylating enzymes of the rabbit eye Acta anat 57 192–219
—— 1965a Histochemical demonstration of thiamine pyrophosphatase and acid phosphatase in the Golgi region of the cells of the eye J Anat Lond 99 103–117
—— 1965b A simple method for preparation and staining of the whole Pacinian corpuscle Acta anat 60 199–206
—— 1965c Histological and histochemical studies of the choroid of the eye and its relation to the pia arachnoid mater of the central nervous system and the perineural epithelium of the peripheral nervous system Acta anat. 379–398
—— 1965d *Histochemical studies on the* distribution of dephosphorylating and oxidative enzymes and esterases in the olfactory bulb of the squirrel monkey J Nat Cancer Inst 35 153–165
—— 1965e Histochemical studies on the olfactory glomeruli of the squirrel monkey Histochemie 5 125–129
—— 1965f The thiamine pyrophosphatase technique as an indicator of the morphology of the Golgi apparatus in the neurons II Studies on the cerebral cortex La Cellulle 65 201–209
——— 1965g The thiamine pyrophosphatase technique as an indicator of the morphology of the Golgi apparatus in the neurons III Studies on the olfactory bulb Exp Cell Res 292–300
——— 1965h The thiamine pyrophosphatase technique as an indicator of the morphology of the Golgi apparatus in the neurons I Studies on ganglion cells Acta histochem 22 155–178
——— 1965i The thiamine pyrophosphatase technique as an indicator of the morphology of the Golgi apparatus in the neurons IV Studies on the cerebellum of rat and squirrel monkey Z Zellforsch 68 699–710
——— 1965j Histochemical studies on the localization of oxidative and dephosphorylating enzymes and esterases in the peritoneal mesothelial cells Histochemie 5 331–338
Shanthaveerappa T R James Hope and G H Bourne 1963 Electron microscopic demonstration of the perineural epithelium in rat peripheral nerve Acta anat 52 193–201
Wachstein M and E Meisel 1957a Histochemistry of hepatic phosphatases at a physiological pH with special reference to the demonstration of bile canaliculi Amer J Clin Path 27 13–23
——— 1957b A comparative study of enzymatic staining reactions in the rat kidney with necrobiosis induced by ischemia and nephrotoxic agents (mercuhydrin and dl-serine) J Histochem Cytochem 5 204–220

PLATE 1

EXPLANATION OF FIGURES

Figures 1 through 16 are all sections of the Pacinian corpuscle of the cat mesentery

1 Alkaline phosphatase test The nerve terminal in the Pacinian corpuscle is very strongly positive for the test Note the positive activity in the lamellar cells also × 370

2 Adenosine triphosphatase test The nerve terminal in the corpuscle is very strongly positive (arrow = *n*) The inner core (arrow = *c*) next to the nerve terminal and some of the lamellar cells also show moderately strong positive activity (arrow = *p*) × 370

3 Adenosine triphosphatase test There are two corpuscles in the micrograph One corpuscle has two nerve terminals showing strong positive activity (arrow = *n*) It also contains about 10 to 12 blood vessels found all over the corpuscle which also give strong adenosine triphosphatase positive activity × 370

4 Thiamine pyrophosphatase test The nerve terminal in the corpuscle gives moderate positive activity of a diffuse type (arrow = *n*) The lamellar cells also give positive activity (plain arrows) × 370

5 Acid phosphatase reaction The nerve terminal in the corpuscle gives mild positive activity (arrow = *n*) wheras the inner core and lamellar cells showed much milder positive activity × 370

6 5 Nucleotidase reaction showing the strongly positive activity in the nerve terminal of the corpuscle × 370

7 Simple esterase reaction showing the strongly positive activity in the nerve terminal of the corpuscle × 370

8 Specific cholinesterase reaction The nerve terminal of the corpuscle is strongly positive for the test Note the negative activity in the inner core and lamellar cells × 370

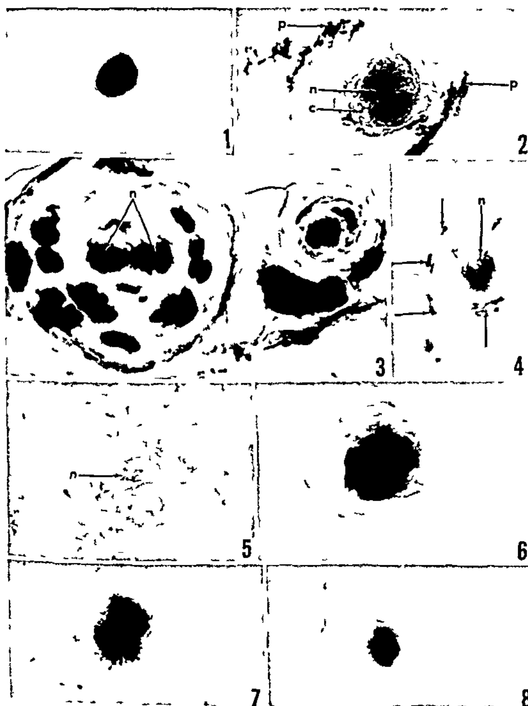

p
n
c
p
1
2
n
3
n
4
n
5
6
7
8

PLATE 2

EXPLANATION OF FIGURES

9 Nonspecific cholinesterase test Note the strongly positive activity in the nerve terminal (arrows) Lamellar cells are completely negative × 148

10 Section of the Pacinian corpuscle pretreated with diisopropyl fluorophosphate (10^{-6}) and then tested for nonspecific cholinesterase activity Note the complete inhibition of nonspecific cholinesterase activity in the nerve terminal (arrow = *n*) of the corpuscle × 370

11 Nonspecific cholinesterase reaction Note the strongly positive activity at the nerve terminal of the corpuscle The inner core is negative × 1 400

12 Succinic dehydrogenase test The nerve terminal is strongly positive (arrow = *n*) The inner core shows moderately strong positive activity (arrows = c) The lamellar cells show moderate positive activity × 370

13 High power photomicrograph of the inner core of the corpuscle showing large granular type of succinic dehydrogenase positive activity probably located in the mitochondria (arrows) × 1 480

14 Lactic dehydrogenase test The nerve terminal gives very strong positive activity (arrow = *n*) The inner core is strongly positive (arrow = *c*) The lamellar cells show moderately strong positive activity × 592

15 Cytochrome oxidase test Note the positive activity is granular in character and is found located at the peripheral part of the nerve terminal of the corpuscle (arrows) × 1 370

16 Monoamine oxidase test Note the mild positive activity in the nerve terminal The inner core and lamellar cells are negative × 1 370

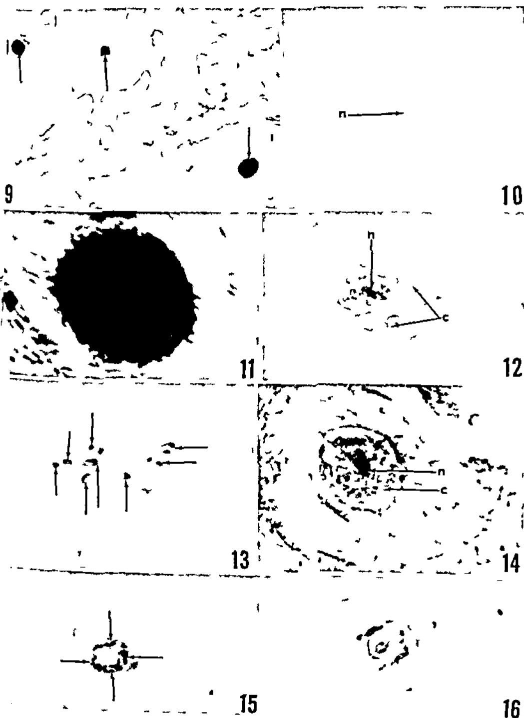

9
10
n
11
12
n
c
13
14
n
c
15
16

PLATE 2

EXPLANATION OF FIGURES

9 Nonspecific cholinesterase test Note the strongly positive activity in the nerve terminal (arrows) Lamellar cells are completely negative × 148

10 Section of the Pacinian corpuscle pretreated with diisopropyl fluorophosphate (10^{-6}) and then tested for nonspecific cholinesterase activity Note the complete inhibition of nonspecific cholinesterase activity in the nerve terminal (arrow = *n*) of the corpuscle × 370

11 Nonspecific cholinesterase reaction Note the strongly positive activity at the nerve terminal of the corpuscle The inner core is negative × 1 400

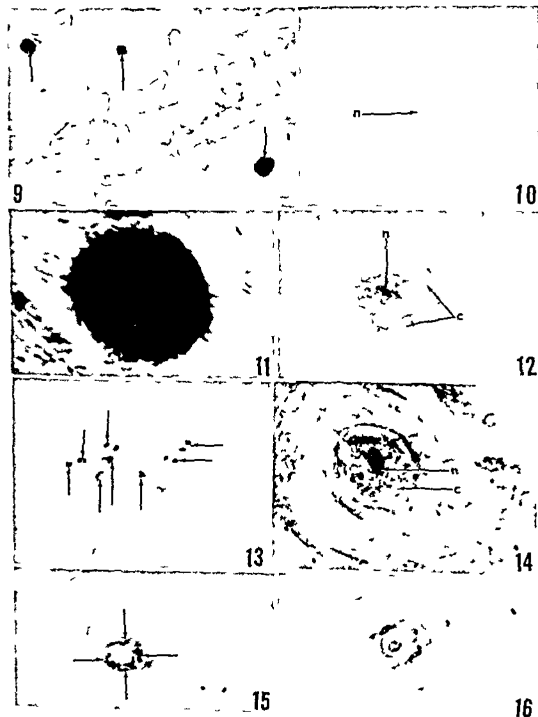
12 Succinic dehydrogenase test The nerve terminal is strongly positive (arrow = *n*) The inner core shows moderately strong positive activity (arrows = *c*) The lamellar cells show moderate positive activity × 370

13 High power photomicrograph of the inner core of the corpuscle showing large granular type of succinic dehydrogenase positive activity probably located in the mitochondria (arrows) × 1 480

14 Lactic dehydrogenase test The nerve terminal gives very strong positive activity (arrow = *n*) The inner core is strongly positive (arrow = *c*) The lamellar cells show moderately strong positive activity × 592

15 Cytochrome oxidase test Note the positive activity is granular in character and is found located at the peripheral part of the nerve terminal of the corpuscle (arrows) × 1 370

16 Monoamine oxidase test Note the mild positive activity in the nerve terminal The inner core and lamellar cells are negative × 1 370


9
10
n
11
12
n
c
13
14
n
c
15
16



17

EXPLANATION OF FIGURE

17 Whole mount of the Pacinian corpuscle stained with silver nitrate and counterstained *with cresyl violet* Note the whole corpuscle is made up of continuous sheets of flat squamous cells laid one on top of the other some of which are continuous with the perineural epithelium covering the nerve which supplies the corpuscle × 110

Electron Microscope and Ultracentrifugation Studies on the Rat Reticulocyte [1]

H W BEAMS AND R G KESSEL
Department of Zoology University of Iowa Iowa City Iowa

ABSTRACT Reticulocytosis was induced in rats by the daily injections of phenyl hydrazine The reticulocytes were studied by supravital staining ultracentrifugation and phase-contrast and electron microscopy Electron micrographs of sectioned retic ulocytes reveal the presence of hemoglobin polyribosomes mitochondria micropino-cytosis vesicles tubules of varying size and in some cases Heinz body material When subjected to ultracentrifugation these materials are readily stratified in the order of their relative densities from the centrifugal to the centripetal end as follows hemo-globin mitochondria ribonucleoprotein material (ribosomes) and Heinz body material The centrifuged reticulocytes may be stretched two or three times their normal diam eter and even pulled into two parts without hemolysis Of interest is the observation that in ultracentrifuged reticulocytes the ribosomes are not displaced from the region of the cortex a condition which is interpreted as strong evidence that this region is of a greater consistency (viscosity) than the remainder of the cell Evidence was observed to show that as maturation of the reticulocyte occurs the cell gradually decreases in size and increases in density concomitantly with these changes is a progressive degra dation of the mitochondria and ribonucleoprotein material so that by the time the erythrocyte stage is reached these materials seem to have completely disappeared

The reticulocyte is an enucleated red blood cell characterized by the presence of a basophilic staining reticulum These cells originate in the bone marrow where they eventually enter the circulation at a rela tively constant rate In normal human blood 0 05 to 2% of the red corpuscles are reticulocytes (Bessis 56 Jones 61) Here they complete their maturation and differ entiate into erythrocytes

Much discussion has centered around the question of the structure of the reticulo-cyte particularly as it concerns the reticu lum and the ribonucleoprotein component The reticulum is not observed in the living cell unless it has been injured or stained with supravital dyes such as brilliant cresyl blue new methylene blue Azure II neutral red etc For this reason it is considered an artifact produced in some manner by the action of the supravital dyes upon a diffuse basophilic staining substance which has been identified as ribonucleoprotein (Dustin 51 Ponder 55 Bessis 56 Chal fin 56 Lowenstein 59 Jones 61 Win trobe 61 and others)

Several electron microscope studies on the fine structure of the reticulocytes and erythrocytes have been made The early studies were mainly whole mounts of ghosts and the results of these have been extensively reviewed by Ponder (55) and Bessis (56) Studies of sectioned reticulo-cytes have revealed the presence of mitochondria polyribosomes vacuoles ferritin granules and endoplasmic reticu lum (Grasso Swift and Ackerman 62 Hallinan Eden and North 62 Rifkind Danon and Marks 64 Bessis and Breton Gorius 64 Jensen Moreno and Bessis 65) Electron dense globules said to be Heinz bodies have also been described (Rifkind Danon and Marks 64 Rifkind and Danon 65)

The ribonucleoprotein is revealed in the form of ribosomes and polyribosomes and these have been the subject of intense bio-chemical studies because they are easily isolated appear in groups of different size and seem to be directly related to the syn thesis of hemoglobin (Marks Burka and Schlessinger 62 Warner Rich and Hall 62 Gierer 63 Rich 63 Warner Knopf and Rich 63 Burka and Marks 64 Mathias Williamson Huxley and Page 64)

[1] Thi tudy was upported by rese rch grants GM 3479 4706 9*29 HD-00699 from the N tion l In tit tes f H alth Public H alth S rvice and gr nt G-9879 from the Nati n l Scien Foundation Dr K sel i th recipient of C re r Development Aw rd 1 K3-GM 11,524 from the Nat nal In titute f Gene l Med cal Scien e

The present study offers additional in formation concerning the fine structure and physical nature of the reticulocyte It describes the stratification upon ultracen trifugation of the different materials in the order of their relative specific gravities Evidence has been revealed for the pres ence of a cortex composed of a much higher viscosity than the remainder of the cell

MATERIAL AND METHODS

Young adult white rats weighing 250 to 300 gm were injected daily over a period of seven days with 2 cm³ of a 1% solution of phenylhydrazine Blood drawn from the tail or heart 6 to 7 days after the first injec tion usually showed 80 to 90% of the red cells to be reticulocytes The blood was prepared for study by several methods To demonstrate the reticulum for light micro scope study it was stained in new meth ylene blue (Brecher, 49) and in 1% bril liant cresyl blue followed by Wright s stain Some cells were smeared fixed and stained for the demonstration of RNA by the method of Korson (51) Wet smears were also fixed in Bouin s solution and stained in Heidenhain s hematoxylin or they were fixed in Carnoy s solution followed by treat ment with the Feulgen method Samples of all cells whether centrifuged or uncen trifuged were studied by aid of the phase contrast microscope

Blood cells from animals injected 5 to 7 days with phenylhydrazine were washed in 0 9% sodium chlorde and placed in small plastic tubes (about 1 cm³ capacity) which had been partly filled with a 20 to 30% solution of gum acacia The tubes were spun in an air turbine ultracentrifuge (Beams Weed and Pickels 33) at speeds generating forces varying from 100 000 to 400 000 times gravity for periods varying from 5 to 30 minutes After ultracentrifu gation the cells were immediately exam ined with the phase contrast microscope and stained with brilliant cresyl blue fol lowed by Wright s stain or fixed in cold 1% solution of osmium tetroxide buffered with acetate veronal (Palade 52) to a pH of 7 2 to 7 6 Other samples of the blood were fixed in 3 to 6% phosphate buffered glutaraldehyde (Sabatini Bensch and Barr nett 63) followed by treatment with 1% phosphate buffered osmium tetroxide a 7 4 (Millonig 62) The cells were d drated rapidly in a series of cold etha treated with propylene oxide and embe in Epon 812 (Luft 61) Thin sect were cut on a Porter Blum ultramicrot stained with uranyl acetate (Watson and studied by aid of an RCA EMU or 3G electron microscope Uncentrifu reticulocytes were prepared in a sim way for electron microscope study

RESULTS

I Uncentrifuged reticulocytes

A Light microscope observations

Reticulocytes are a stage in the mat tion of red blood cells between the nor blast and erythrocyte When stained certain supravital dyes such as brill cresyl blue or new methylene blue striking basophilic reticulum is reve (figs 1 and 4) It may vary from a c pact densely stained reticulum (fig 1 a more loosely arranged network (fig The quantity complexity and density the reticulum may vary somewhat depe ing upon the age of the reticulocyte the methods used to demonstrate it reticulum decreases concomitantly with maturation and diminution in size of cell until the erythrocyte stage is reach whereupon it completely disappears (4 E)

We have not observed the reticulum unstained and uncentrifuged reticulocyt however some cells may show under phase contrast microscope isolated gr ules and vacuoles The reticulum as be seen in the electron micrographs to f low is an artifact rather than a preform morphological structure How this artif is formed is obscure but it seems to characteristic of reticulocytes and does r readily occur in other types of cells e leucocytes or ascites tumor cells wh stained in a similar way

A few reticulocytes and erythrocytes d play a basophilic and Feulgen positi granule the Howell Jolly body which considered a nuclear remnant (fig 4 HJ This body probably signifies a your erythrocyte and it soon disappears eith through extrusion or more likely throug dissolution

B *Electron microscope observations*

Essentially what follows is a fine structural analysis of cells taken from the same experimental animals and except for the method of preparation treated in a similar way to those photographed and described above

1 *Polyribosomes* The fine structure of a relatively young reticulocyte is illustrated in figures 15 to 17 Distributed throughout the cytoplasm are groups of granules termed polyribosomes (Warner Rich and Hall 62) These are said to be characteristic of young reticulocytes and to play an important role in the synthesis of hemoglobin (e g Rifkind Danon and Marks 64) The polyribosmoes are usually composed of 2 to 6 ribosomes each and constitute the ribonucleoprotein component of the cell (figs 15 16 and 17) No special arrangement of the ribosomes within the aggregate is evident some appear rather tightly bunched while others are more loosely organized No clear evidence was observed for the presence of a strand (messenger RNA) which has been described in homogenates of reticulocytes as connecting the ribosomes within an aggregate However if the strand is not present the nature of the forces involved in holding the ribosomes together within a polyribosome is unexplained

This study supports the view that as the reticulocytes mature the number of ribonucleoprotein particles within an aggregate becomes less until a stage is reached where they exist only as single or double ribosome (figs 21 23 and 25) and as the maturation of the reticulocyte is completed all ribosomes disappear probably through dissolution within the cytoplasm

As mentioned above when the reticulocytes are stained with brilliant cresyl blue or new methylene blue the ribosomes aggregate to form a large body of anastomosing strands the so-called reticulum (figs 19 and 20) An apparent stage in the formation of the reticulum is seen in figure 18 This cell was briefly stained with new methylene blue and subsequently fixed in glutaraldehyde The polyribosomes appear in the process of flocculating and aggregating into a loose network or reticulum and the cytoplasm between the forming strands is relatively free of polyribosomes The reticulum appears composed in addition to the ribosomes of a continuous and homogeneous substance (fig 19) As the reticulum forms it undergoes a marked contraction and condensation giving rise to a body typifying the reticulocyte (fig 20) Both the Golgi complex and endoplasmic reticulum are greatly reduced or absent in the reticulocytes herein studied They seem to be the first organelles affected by the changes in morphology associated with the maturation of these cells

2 *Mitochondria* Mitochondria especially of young reticulocytes are filamentous and display well-defined membranes and cristae (figs 15 16 and 18) However they are comparatively few and as the reticulocytes undergo differentiation the number becomes less probably through dissolution until the erythrocyte stage is reached whereupon they disappear completely Concomitant with the progressive differentiation of the reticulocyte is a gradual degradation in the structure of the mitochondria such as the loss of cristae and the appearance of poorly defined or ruptured membranes (figs 19 to 23) Sometimes the mitochondria are seen to collect around vesicles such as that seen in figure 25 the significance of this is not clear Within many of the mitochondria especially those in advanced stages of atrophy are dense granules often massed together (figs 21 to 23 M F) These have been identified by Bessis (61 63) as ferritin

3 *Cytoplasmic tubules and vesicles* Many of the younger reticulocytes show groups of tubular structures (figs 17 and 21) which vary considerably in diameter the larger ones measure 600 Å and the smaller ones about 200 Å in width (fig 17 T and M T respectively) The size and structure of the latter is reminiscent of the cytoplasmic microtubules commonly observed in many different types of cells (Ledbetter and Porter 63 Slautterback 63) Micropinocytosis vesicles are frequently observed at the surface of the cell where the membrane is invaginated in a cup-like shape (figs 15 16 and insert M V) Eventually the forming vesicles are separated from the surface membrane and migrate into the deeper regions of the cytoplasm (fig 15 S V) These vesicles

y carry with them extracellular the identity of which has not mined Some of the vesicles re dense lining which may be : to the inner dense filamentous ved by Roth and Porter (62) ıted by them to be involved in ake Much larger vesicles which ntly formed by the fusion of ıes (fig 15 arrow) possess l more dense vesicles or tubules n Other large vesicles contain arranged membranes may also l (fig 25) Whether or not the esent intravesicular bodies or e membranes pulled away from of the vesicles is not clear In hey are probably by products of 'e changes occurring in the ma and they do not seem to repre ınt structures of the reticulo ıes composed of concentrically ense structures are sometimes ig 24) These are reminiscent ıgement of the mitochondria in nebenkern (Beams Tahmisian Roth 54) However since no evident within them a positive on of this body cannot be made seem to be a consistent struc probably the result of organelle r degradation within the matur

ll Jolly body It has long been t a certain percentage of eryth ow bodies which are Feulgen d which are thought to repre ants of the discarded nucleus 'hese bodies are relatively com emic blood but probably are not ıal occurrence The body in s found in a preparation which tained briefly in new methylene subsequently fixed in buffered troxide The significance of its medulla and cortex) is unknown its staining reaction the outer ıld appear to be composed of However not enough electron ıs of these bodies were observed ıe whether or not the fine struc n figure 2 is a typical one Sur he Howell Jolly body are a series ; these are probably artifacts caused by the staining in new methylene blue before fixation in osmium tetroxide

5 *Heinz bodies* Large refractile bodies are observed in erythrocytes under certain clinical conditions they can be produced *in vitro* and *in vivo* by many toxic sub stances including phenylhydrazine (Bren ner and Allison 53) Among the compo nents of the Heinz body are thought to be denatured hemoglobin and lipid this mate rial typically collects near the surface of the erythrocyte causing a bulging of its plasma membrane (fig 3) As evident here the Heinz body is so electron dense that no detailed structure can be observed within it

It is generally stated that Heinz bodies are found only in erythrocytes (Cruz 41 Lowenstein 59) however Rifkind Danon and Marks (64) and Rifkind and Danon (65) have described numerous dense finely granular bodies in reticulocytes which they have interpreted as Heinz body ma terial We have confirmed this observation and as in the mature erythrocytes the bodies are dense but much smaller and more loosely arranged (figs 22 and 23 H B) Apparently as maturation progresses the smaller bodies fuse giving rise to the typical Heinz bodies of the erythrocyte (fig 3)

II *Ultracentrifuged reticulocytes*

A *Light microscope observations*

When reticulocytes are ultracentrifuged they may become stretched to three or four times their normal diameter assume dumbbell shapes and in extreme cases fragment into two usually unequal parts (figs 5 to 14) The materials layer out in the order of their relative specific gravities with the hemoglobin at the centrifugal end the mitochondria above the hemoglobin and the basophilic or ribosomal material at the centripetal end (figs 6 to 14) The centripetal layer is compact and in addi tion to the basophilic staining substance (polyribosomes) it contains larger bodies which have been interpreted as Heinz bodies (figs 8 10 and 14) It should be emphasized that considerable variation in the effects of ultracentrifugation occurs depending upon the quantity of the differ ent materials present the intensity of the

centrifugal force position of the cell within the centrifuge and the time the centrifuge is allowed to operate If only slightly stretched the cells usually regain their shape however if stretched more than two cell diameters they rarely completely recover and the sharply stratified layers do not redistribute

B *Electron microscope observations*

The stratified layers observed in the reticulocyte under the light microscope described above display more detail when viewed with the electron microscope The fine structure of the displaced materials namely mitochondria ribonucleoprotein particles vacuoles Heinz bodies and hemoglobin are readily observed they appear from the centrifugal to the centripetal end as follows hemoglobin mitochondria ribosomes and Heinz bodies (figs 26 to 33)

1 *Ribonucleoprotein particles* Because of their relatively low density the ribosomes are displaced centripetally causing the cell to elongate in the axis of the centrifugal field The series of electron micrographs to follow display different degrees of elongation and stratification of the reticulocytes Early effects of the centrifugal force are seen in figures 26 and 27 where the separation of the components has occurred and the cells are somewhat elongate Of interest is the high percentage of ribosomes which seem to have formed a loose reticulum at the centripetal end simulating the structure sometimes seen in the nucleoloneme of the nucleolus (figs 26 27 and 33) However not all of the displaced ribosomes appear to form a reticulum some although packed at the centrifugal end still appear discrete (figs 29 and 32) Before ultracentrifugation the ribosomes were distributed in the cells like those seen in figures 15 and 16 and when displaced through the cytoplasm they were probably forced in contact with each other a condition favorable for the formation of a reticulum The reticulum seems to be composed in addition to the ribosomes of a more dense component of the cytoplasm (figs 26 27 and 33) Upon ultracentrifugation the polyribosome arrangement is lost and the ribosomes become evenly distributed in the strands of the reticulum

Not all the ribosomes appear to be displaced at the same rate (figs 26 to 28) Probably regions of different density exist in the reticulocytes causing the ribosomes to fall in jerks as has been described for the crystals in amoeba when observed in the centrifuge microscope (Harvey and Marsland 32) Of interest is the fact that the ribosomes are not displaced from the cortex by ultracentrifugation a condition which demonstrates that it possesses a much higher viscosity than the remainder of the cell (figs 26 to 29 and 32) For example the region between the arrows in figure 27 measures about 100 mμ in thickness however its thickness may vary from 50 to 150 mμ This peripheral cortical layer or ectoplasm is bounded externally by a 75 Å thick plasma membrane (fig 27 single arrow) and it is composed of two layers the outer one is 200 to 300 Å thick relatively dense and granule free the inner one contains a layer of undisplaced ribosomes and is of variable thickness

Even the most affected cells that is those most extensively stretched show the ribosomes undisplaced in the cortical region The presence of a cortex has been postulated for the red cell and it has been thought to serve as a possible mechanism for maintaining its biconcave shape (Ponder 55) The cytoplasm in the centripetal end of the cell where the ribosomes are concentrated has probably been squeezed out and displaced from between the packed hemoglobin molecules

2 *Heinz bodies* Like the ribosomes Heinz bodies of the reticulocytes collect at the centripetal ends of the ultracentrifuged cells (figs 30 and 31 H B) Here they still maintain the same form as in the uncentrifuged cells (figs 22 and 23 H B) When displaced centripetally they may show a close association with the ribosomes In fact the ribosomes in some instances appear stuck to the surface of the globules of Heinz body material (figs 30 and 31) Possibly this condition arises as both the ribosomes and Heinz body material are forced in contact as they are displaced through the cell

3 *Mitochondria* Mitochondria commonly collect in a rather compact layer between the ribosomes and hemoglobin (figs 26 to 28 and 32 and 33) More

specifically they are usually located at the *centripetal end of the hemoglobin layer* As the cells are stretched and pulled into a light and heavy fragment the mitochondria generally remain associated with the heavy or hemoglobin portion Most of the mitochondria show evidence of degeneration they are swollen and the cristae on the whole are ill defined because of their apparent atrophy which accompanies the maturation of the cell Bodies are sometimes seen among the ribosomes which appear larger than mitochondria but this may be due to degenerative changes within the mitochondria affecting both their structure and density (fig 33 arrow)

4 *Hemoglobin* It is evident in all of the ultracentrifuged cells examined that the hemoglobin is the most dense component of the reticulocyte It is always found at the centrifugal end and occupies more *than half the volume of the cell (figs 26* to 28) Reticulocytes nearing the end of maturation and differentiation would appear to possess a greater amount of hemoglobin but this is deceiving since most of the hemoglobin is said to be formed by the time the reticulocyte stage is reached (Lowenstein 59) *and the difference in* relative size of the centrifugal and centripetal ends of the cells is due mainly to the variation in amount of other cellular materials present

Except for the cortex little characteristic structure is revealed in the hemoglobin end of the cell It is composed of fine granules (hemoglobin?) closely packed (figs 27 and 28) The cortex of this region and other regions of the cell displays clearly the granules (ribosomes) as unaffected by the ultracentrifugation a fact which demonstrates a difference in density between the cortex and the remainder of the cell Except for the cortex most but not all of the ribosomes are displaced from the hemoglobin end Possibly this is due to local regions of high viscosity such as occur in amoeba (Harvey and Marsland 32)

A few vesicles sometimes containing granules are observed in the centrifugal *end of the cell* In all cases they are located in the cortical region and are probably recently formed micropinocytosis vesi*cles* Their position in the gelled cortex presumably accounts for the fact that t| *are not displaced by the ultracentrifuge*

5 *Fragmentation of cells* Reticulocy are readily fragmented into a light heavy component by the action of h centrifugal forces An elongate cell cau in a stage of apparent fragmentation seen in figure 32 Cells distorted to t degree will not recover their shape or re tribute their stratified materials yet th seldom undergo hemolysis As mentior above the mitochondria usually rem with the hemoglobin layers when the ce are separated into two parts

DISCUSSION

The results herein reported for the fi structure of the reticulocyte are for t most part consistent with those found certain other investigators (Bessis a Breton Gorius 64 Rifkind Danon a Marks 64 Jensen Moreno and Bess *65 and Rifkind and Danon 65) Ho*ever additional information has been vealed concerning the nature of the ret ulocyte such as its fine structure relati density of its various cytoplasmic ma rials property of its plasma membrane stretch demonstration of a differential viscosity between the cortex and the r mainder of the cytoplasm and the proper of the cell to separate into two parts wit out becoming hemolyzed

Because of the small size and relative high viscosity of the reticulocyte a cor paratively high centrifugal force is nece sary to effect a displacement and stratific tion of its contents By the time th reticulocyte stage is reached in the erythr cyte series most of the hemoglobin h *been synthesized (Thorell 47)* howeve some of the machinery for protein synthe sis still remains (ribosomes mitochondri and vacuoles) How these structures ar eventually disposed of by the reticulocyt is debatable Chalfin (56) suggests tha they may be degraded enzymatically to product which diffuses through the plasm membrane or that they may be expelle through the plasma membrane in a man ner similar to that which happens to th *nucleus of the normoblast* Bertles an Beck (62) have studied the biochemica aspects of rabbit reticulocyte maturation *in vitro* and have suggested that a conver

sion of the cellular ribonucleic acid into low molecular weight extracellular products occurs Our results show that as maturation progresses the reticulum mitochondria and large vacuoles gradually diminish until the erythrocyte stage is reached whereupon they are completely lost to view The first organelles to be affected by the morphological changes accompanying maturation of the reticulocyte seem to be the centrioles Golgi apparatus and endoplasmic reticulum for in our studies these organelles were not observed save possibly for small bits of rough surfaced endoplasmic reticulum

After reviewing the literature on the structure of the red cell especially the mammalian erythrocyte Bessis (61) states that two hypotheses have been formulated that the structure is a sac containing hemoglobin or that it is a spongework in which the hemoglobin is contained Certainly the reticulocyte is something more than a sac containing hemoglobin as is evidenced by its cytoplasmic organelles Unpublished results indicate that this is also true for erythrocytes but to a much lesser degree Hematologists usually refer to the colorless framework" of the red cells as stroma and it is composed of protein lipid and a little carbohydrate (Crosby 57) It is known that both the reticulocytes and erythrocytes are to a limited extent metabolically active some of the energy is required for active transport the remainder is probably used for maintaining their shape and cytoplasmic motion (Prankerd 61) The stroma of the living reticulocyte probably includes a large part of the cytoplasmic matrix and in ultracentrifuged cells the matrix like the cytoplasm in centrifuged *Arbacia* eggs (Harvey 36) may be only stretched and not completely displaced in which case each stratified layer would contain a portion of the matrix Stratified and slightly elongate reticulocytes may in time assume their original shape but remixing of the stratified layers does not readily occur this is probably due in part to the high density of the packed hemoglobin layer at the centrifugal end of the cell Mature red cells are composed of 33% hemoglobin and the hemoglobin molecules which are free to rotate are said to be spaced about 8 to 10 Å apart within the matrix In centrifuged cells the molecules are probably more densely packed Improved methods of tissue preparation for electron microscopy have failed to reveal in red cells the dense fibrous stroma reported by early electron microscopists (Grasso Swift and Ackerman 62 Bessis and Breton Corius 64 Rifkind Danon and Marks 64)

One of the major problems of red cell cytology is an explanation of the mechanism involved in producing and maintaining their biconcave shape and in spite of the fact that this problem was first raised nearly 200 years ago " the shape of the red cell still presents an unsolved problem" (Lehmann and Huntsman 61) It is generally agreed that the red cell shape is consistent with increased efficiency of function Theories concerning the shape of the red cells must be compatible with their ability to change shape as occurs in the case of the target cell and spherocyte or more dramatically in the case of the "disc sphere transformation" (Ponder 55) Some investigators maintain that the shape of the mammalian red cell is due to a supporting stroma extending in part or throughout the cell and adhering to the plasma membrane others hold the forces involved are localized at or near the surface of the cell (cf Ponder 55 Beiss 56 61 Lehmann and Huntsman 61 and Prankerd 61 for literature) Prankerd (61) suggests that since the changes in shape of the red cell are reversible this would imply the absence of structure traversing the interior of the cell He thinks therefore that some special arrangement of the protein fibers at the surface is responsible for maintaining the shape (see also Rand and Burton 64)

We have not observed a formed fibrillar network within the red cells nor a marginal band of microtubules which occur in certain nucleated erythrocytes and which are postulated to play an important role in maintaining their shape (cf Fawcett and Witebsky 64 for literature) However the demonstration that the reticulocyte possesses a cortex of a much greater density than the remainder of the cell may be important in the formulation of theories concerning the shape of red cells that is the cortex and plasma membrane may pos-

mainly due to the presence of degenerating cytoplasmic materials These being much lighter than the hemoglobin they are displaced and moved in a centripetal direction causing the cell to elongate and the membrane to stretch Mature erythrocytes may be stretched by this treatment but much less so than the reticulocytes (unpublished observations) However ultracentrifuged erythrocytes do show some stratification and the layers thus formed may be differentially stained (Beams and Hines 44 unpublished observations)

It should be emphasized that the reticulocytes studied here like those of most other similar investigations have been produced by experimental means and therefore it cannot be assumed that they are identical in structure with those in "normal blood However it has been shown by Hallinan and Eden (62) that they possess the same amount of phospholipid and ATP as reticulocytes from normal animals and in discussing this matter they state that "definite experimental evidence that they are abnormal is lacking

LITERATURE CITED

Beams H W and E B Hines 1944 Stratification of the rat erythrocyte by ultracentrifuging Anat Rec 90 155–159

Beams H W T N Tahmisian R Devine and E Roth 1954 Phase-contrast and electron microscope studies on the nebenkern a mitochondrial body in the spermatids of the grasshopper Biol Bull 107 47–56

Beams J W A J Weed and E G Pickels 1933 The ultracentrifuge Science 77 338–340

Bertles J F and W S Beck 1962 Biochemical aspects of reticulocyte maturation J Biol Chem 237 3770–3777

Bessis M 1956 Cytology of the Blood and Blood forming Organs Translated by E Ponder Grune and Stratton New York

——— 1961 The blood cells and their formation In The Cell (J Brachet and A E Mirsky eds) Academic Press Inc New York vol 5 pp 163–217

——— 1963 Cytological aspects of hemoglobin production In The Harvey Lectures Academic Press Inc New York series 58 pp 125–156

Bessis M and J Breton-Gorius 1964 Le réticulocyte Colorations vitales et microscopie électronique Nouv Rev Fr D Hémat 4 77–94

Brecher G 1949 New Methylene blue as a reticulocyte stain Am J Clin Path 19 895–896

Brenner S and A C Allison 1953 Catalase inhibition a possible mechanism for the production of Heinz bodies in erythrocytes Experientia 9 381–383

Burka E R and P A Marks 1964 Protein synthesis in erythroid cells II Polyribosome function in intact reticulocytes J Mol Biol 9 439–451

Chalfin E 1956 Differences between young and mature rabbit erythrocytes J Cell and Comp Physiol 47 215–244

Crosby W 1957 Diseases of the reticulo-endothelial system and hematology The red cell and some of its problems Ann Rev Med 8 151–176

Cruz W O 1941 Acetyphenylhydrazine anemia I The mechanism of erythrocyte destruction and regeneration Am J Med Sci 202 781–789

Dustin P 1951 Ribonucleic acid and the vital staining of cytoplasmic vacuoles in animal cells In Symposia of the Society for Experimental Biology Cambridge University Press England no 1 pp 114–126

Fawcett D W and F Witebsky 1964 Observations on the ultrastructure of nucleated erythrocytes and thrombocytes with particular reference to the structural basis of their discoidal shape Zeit Zellforsch 62 785–806

Gierer A 1963 Function of agg egated reticulocyte ribosomes in p otein synthesis J Mol Biol 6 148–157

Grasso J A H Swift and G A Ackerman 1962 Observations on the development of erythrocytes in mammalian fetal liver J Cell Biol 14 235–254

Hallinan T and E Eden 1962 The structure and composition of rat reticulocytes II Phospholipid and total cholesterol in reticulocytes Blood 20 557–565

Hallinan T E Eden and R North 1962 The structure and composition of rat reticulocytes I The ultrastructure of reticulocytes Blood 20 547–556

Harvey E B 1936 Parthenogenetic merogony or cleavage without nu lei in *Arbacia punctulata* Biol Bull 71 101–121

Harvey E N and D A Marsland 1932 Tension at the surface of *Amoeba dubia* with direct observations on the movement of cytoplasmic particles at high centrifugal speeds J Cell and Comp Physiol 2 75–98

Hawes J B 1909 A study of reticulated red blood corpuscles by means of vital staining Its relation to polychromatophilia and stippling Boston Med and Surg J 161 493–499

Jensen W N G D Moreno and M C Bessis 1965 An elect on microscope description of basophilic stippling in red cells Blood 25 933–943

Jones O P 1961 The influence of disturbed metabolism on the morphology of blood cells In Functions of the Blood (R G MacFarland and A H T Robb Smith eds) Academic Press Inc New York pp 171–270

Key J A 1921 Studies on erythrocytes with special refe ence to reticulum polychromatophilia and mitochondria Arch Int Med 28 511–549

Korson R 1951 A differential stain for nucleic acids Stain Tech 26 265–270

Ledbetter M C and K R Porter 1963 A "microtubule" in plant cell fine structure J Cell Biol 19 239–250

Lehmann H and R H Huntsman 1961 Why are red cells the shape they are? The evolution

sess a molecular arrangement capable of exerting the necessary forces for maintain ing the shape of these cells However, by measuring the pressure required to suck a red cell into a pipette Rand and Burton (64) were unable to detect a difference in stiffness between the rim and bicon cavity of the cell They also observed that the membrane can withstand large bend ing strains but limited tangential or stretching strains These observations on the erythrocyte would seem to be in conflict with the results herein reported for the reticulocyte namely, that a difference in physical nature exists between the cortex and the interior of the cell and also that the plasma membrane is capable of exten sive stretching (Seifriz 27) In this con nection it is important to emphasize that a substantial difference in physical consist ency may exist between the reticulocyte and the erythrocyte and that a close com parison of the physical nature of the two cells is not at this time wholly justified

Early studies by a variety of methods show a wide variation in thickness (50 to 5 000 A) of the surface membrane of hem olyzed cells (Ponder 55 Prankerd 61) In these studies it is not always clear what was being measured In some instances it may have been the plasma membrane only in others it may have been the membrane plus the cortical layer herein described Probably the most reliable measurements of the red cell membrane are those of Robertson (64) who found it to be com posed of two 20 A thick membranes sepa rated by an intermembrane space of 35 A Robertson has found this basic triple lay ered structure in all plasma membranes examined and has referred to it as a unit membrane structure We have observed the plasma membrane to measure approxi mately 75 A in thickness (fig 27 arrow) No plaques or coarse fibers as reported by early electron microscopists were ob served within it (cf Ponder 55 Bessis 56) these are probably artifacts

Of special interest is the nature and dis tribution of the ribonucleoprotein in retic ulocytes It has been proposed that the polyribosomes are composed of a number of 78 S ribosomes attached to a strand of messenger RNA along which they move as the peptide chain grows (Marks Burka Rifkind and Danon 63) Much of the evi dence for this view is based upon biochem ical studies and electron micrographs of polyribosomes in the lysate of reticulocytes (Warner, Rich and Hall 62 Warner Knopf and Rich 63 Gierer 63) Our studies have not revealed the messenger RNA filament between the ribosomes which is so clearly observed in the lysate of reticulocytes Rifkind Danon and Marks (64) saw short filaments between the ribo somes in sectioned cells but they state these may or may not represent artifacts Perhaps some condition associated with their extracellular environment permits the polyribosomes to straighten out and thus render the messenger RNA filament more conspicuous It is somewhat surprising that the messenger RNA filament is able to withstand the rigors of cell lysis and ultra centrifugation in a sucrose density gradient (Warner Rich and Hall 62, Rich Warner and Goodman 63)

Histochemical methods together with studies with the electron microscope have confirmed the view that the classical retic ulum of the reticulocyte is an artifact How ever it should be emphasized that the artifact is a consistent one under certain uniform procedures of staining a fact which has allowed the counting of them to serve as an important diagnostic precedure for certain hemolytic diseases Insofar as we know the behavior of the ribosomes in forming a reticulum when exposed to supravital staining is unique and from the work of Hawes (09) Key (21) and Jen sen Moreno and Bessis (65) it seems prob able that most of the basophilic staining material (reticulum basophilic stippling polychromasia) is derived wholly or in part from ribonucleoprotein That is vari ation in supravital staining which we have also observed may cause different degrees of precipitation of the ribonucleoprotein materials

Bessis (61 63) has studied the incor poration of iron containing substance (fer ritin) into the erythroblast It takes place by a process termed rhopheocytosis and involves the taking in of bits of ferritin bearing reticuloendothelia cytoplasm Fer ritin is still found in the reticulocyte stage especially within the mitochondria and how it enters the mitochondria is an in triguing but unanswered question

The stratification and elongation of the reticulocytes by ultracentrifugation is

mainly due to the presence of degenerating cytoplasmic materials These being much lighter than the hemoglobin they are displaced and moved in a centripetal direction causing the cell to elongate and the membrane to stretch Mature erythrocytes may be stretched by this treatment but much less so than the reticulocytes (unpublished observations) However ultracentrifuged erythrocytes do show some stratification and the layers thus formed may be differentially stained (Beams and Hines 44 unpublished observations)

It should be emphasized that the reticulocytes studied here like those of most other similar investigations have been produced by experimental means and therefore it cannot be assumed that they are identical in structure with those in "normal blood However it has been shown by Hallinan and Eden (62) that they possess the same amount of phospholipid and ATP as reticulocytes from normal animals and in discussing this matter they state that "definite experimental evidence that they are abnormal is lacking

LITERATURE CITED

Beams H W and E B Hines 1944 Stratification of the rat erythrocyte by ultracentrifuging Anat Rec *90* 155–159

Beams H W T N Tahmisian R Devine and E Roth 1954 Phase-contrast and electron microscope studies on the nebenkern a mitochondrial body in the spermatids of the grass hopper Biol Bull *107* 47–56

Beams J W A J Weed and E G Pickels 1933 The ultracentrifuge Science 77 338–340

Bertles J F and W S Beck 1962 Biochemical aspects of reticulocyte maturation J Biol Chem 237 3770–3777

Bessis M 1956 Cytology of the Blood and Blood forming Organs Translated by E Ponder Grune and Stratton New York

——— 1961 The blood cells and their formation In The Cell (J Brachet and A E Mirsky eds) Academic Press Inc New York vol 5 pp 163–217

——— 1963 Cytological aspects of hemoglobin production In The Harvey Lectures Academic Press Inc New York series 58 pp 125–156

Bessis M and J Breton-Gorius 1964 Le reticulocyte Colorations vitales et microscopie electronique Nouv Rev Fr D Hémat 4 77–94

Brecher G 1949 New Methylene blue as a reticulocyte stain Am J Cl n Path *19* 895–896

Brenner S and A C Allison 1953 Catalase inhibition a possible mechanism for the production of Heinz bodies in erythrocytes Experientia 9 381–383

Burka E R and P A Marks 1964 Protein synth sis in erythroid cells II Polyribosome function in intact reticulocytes J Mol Biol *9* 439–451

Chalfin E 1956 Differences between young and mature rabbit erythrocytes J Cell and Comp Physiol 47 215–244

Crosby W 1957 Diseases of the reticulo-endothelial system and hematology The red cell and some of its problems Ann Rev Med *8* 151–176

Cruz W O 1941 Acetyphenylhydrazine anemia I The mechanism of erythrocyte destruction and regeneration Am J Med Sci *202* 781–789

Dustin P 1951 Ribonucleic acid and the vital staining of cytoplasmic vacuoles in animal cells In Symposia of the Society for Experimental Biology Cambridge University Press England no 1 pp 114–126

Fawcett D W and F Witebsky 1964 Observations on the ultrastructure of nucleated erythrocytes and thrombocytes with particular reference to the structural basis of their discoidal shape Zeit Zellforsch 62 785–806

Gierer A 1963 Function of aggregated reticulocyte ribosomes in protein synthesis J Mol Biol 6 148–157

Grasso J A H Swift and G A Ackerman 1962 Observations on the development of erythrocytes in mammalian fetal liver J Cell Biol *14* 23‿–254

Hallinan T and E Eden 1962 The structure and composition of rat reticulocytes II Phospholipid and total cholesterol in reticulocytes Blood *20* 557–565

Hallinan T E Eden and R No th 1962 The structure and composition of rat reticulocytes I The ultrastructur of reticulocytes Blood *20* 547–556

Harvey E B 1936 Parthenogenetic merogony or cleavage without nuclei in *Arbacia punctulata* Biol Bull *71* 101–121

Harvey E N and D A Marsland 1932 Tension at the surface of *Amoeba dubia* with direct observations on the movement of cytoplasmic particles at high centrifugal speeds J Cell and Comp Physiol 2 75–98

Hawes J B 1909 A study of reticulated red blood corpuscles by means of vital staining Its relation to polych omatophilia and stippling Boston Med and Surg J *161* 493–499

Jensen W N G D Moreno and M C Bessis 1965 An electron microscope description of basophilic stippling in red cells Blood *25* 933–943

Jones O P 1961 The influence of disturbed metabolism on the morphology of blood cells In Functions of the Blood (R G MacFarland and A H T Robb Smith eds) Academic Press Inc New York pp 171–270

Key J A 1921 Studies on erythrocytes with special reference to reticulum polychromatophilia and mitochondria Arch Int Med 28 511–549

Korson R 1951 A differential stain for nucleic acids Stain Tech 26 265–270

Ledbetter M C and K R Porter 1963 A "microtubule" in plant cell fine structure J Cell Biol *19* 239–250

Lehmann H and R H Huntsman 1961 Why are red cells the shape they are? The evolution

sess a molecular arrangement capable of exerting the necessary forces for maintaining the shape of these cells However by measuring the pressure required to suck a red cell into a pipette Rand and Burton (64) were unable to detect a difference in stiffness between the rim and biconcavity of the cell They also observed that the membrane can withstand large bending strains but limited tangential or stretching strains These observations on the erythrocyte would seem to be in conflict with the results herein reported for the reticulocyte namely that a difference in physical nature exists between the cortex and the interior of the cell and also that the plasma membrane is capable of extensive stretching (Seifriz 27) In this connection it is important to emphasize that a substantial difference in physical consistency may exist between the reticulocyte and the erythrocyte and that a close comparison of the physical nature of the two cells is not at this time wholly justified

Early studies by a variety of methods show a wide variation in thickness (50 to 5 000 A) of the surface membrane of hemolyzed cells (Ponder 55 Prankerd 61) In these studies it is not always clear what was being measured In some instances it may have been the plasma membrane only in others it may have been the membrane plus the cortical layer herein described Probably the most reliable measurements of the red cell membrane are those of Robertson (64) who found it to be composed of two 20 A thick membranes separated by an intermembrane space of 35 A Robertson has found this basic triple layered structure in all plasma membranes examined and has referred to it as a unit membrane structure We have observed the plasma membrane to measure approximately 75 A in thickness (fig 27 arrow) No plaques or coarse fibers as reported by early electron microscopists were observed within it (cf Ponder 55 Bessis 56) these are probably artifacts

Of special interest is the nature and distribution of the ribonucleoprotein in reticulocytes It has been proposed that the polyribosomes are composed of a number of 78 S ribosomes attached to a strand of messenger RNA along which they move as the peptide chain grows (Marks Burka Rifkind and Danon 63) Much of the evidence for this view is based upon biochemical studies and electron micrographs of polyribosomes in the lysate of reticulocytes (Warner Rich and Hall 62 Warner Knopf and Rich, 63 Gierer 63) Our studies have not revealed the messenger RNA filament between the ribosomes which is so clearly observed in the lysate of reticulocytes Rifkind Danon and Marks (64) saw short filaments between the ribosomes in sectioned cells but they state these may or may not represent artifacts Perhaps some condition associated with their extracellular environment permits the polyribosomes to straighten out and thus render the messenger RNA filament more conspicuous It is somewhat surprising that the messenger RNA filament is able to withstand the rigors of cell lysis and ultracentrifugation in a sucrose density gradient (Warner Rich and Hall, 62 Rich Warner and Goodman 63)

Histochemical methods together with studies with the electron microscope have confirmed the view that the classical reticulum of the reticulocyte is an artifact However it should be emphasized that the artifact is a consistent one under certain uniform procedures of staining a fact which has allowed the counting of them to serve as an important diagnostic precedure for certain hemolytic diseases Insofar as we know the behavior of the ribosomes in forming a reticulum when exposed to supravital staining is unique and from the work of Hawes (09) Key (21) and Jensen Moreno and Bessis (65) it seems probable that most of the basophilic staining material (reticulum basophilic stippling polychromasia) is derived wholly or in part from ribonucleoprotein That is variation in supravital staining which we have also observed may cause different degrees of precipitation of the ribonucleoprotein materials

Bessis (61 63) has studied the incorporation of iron containing substance (ferritin) into the erythroblast It takes place by a process termed rhopheocytosis and involves the taking in of bits of ferritin bearing reticuloendothelia cytoplasm Ferritin is still found in the reticulocyte stage especially within the mitochondria and how it enters the mitochondria is an intriguing but unanswered question

The stratification and elongation of the reticulocytes by ultracentrifugation is


1
2
3

of the human red cell In Functions of the Blood (R G MacFarland and A H T Robb Smith eds) Academic Press Inc New York pp 71–148
Lowenstein L M 1959 The mammalian retic ulocyte *Int Rev Cytol* *8* 135–174
Luft J H 1961 Improvements in epoxy resin embedding methods J Biophysic and Bio chem Cytol *9* 409–414
Marks P A E R Burka R A Rifkind and D Danon 1963 Polyribosomes active in retic ulocyte protein synthesis Cold Spring Harbor Symp Quant Biol 28 223–226
Marks P A E R Burka and D Schlessinger 1962 Protein synthesis in erythroid cells I Reticulocyte ribosomes active in simulating amino acid incorporation Proc Nat Acad Sci 48 2163–2171
Mathias A P R Williamson H E Huxley and S Page 1964 Occurrence and function of polysomes in rabbit reticulocytes J Mol Biol 9 154–167
Millonig G 1962 Further observations on a phosphate buffer for osmium solutions in fixa tion In Proceedings of the 5th International Congress for Electron Microscopy (S S Breese Jr ed) Academic Press Inc New York vol 2 p 8
Palade G E 1952 A study of fixation for elec tron microscopy J Exp Med *95* 285–297
Ponder E 1955 Red cell structure and its breakdown Protoplasmatologia *10* 1–123
——— 1961 The cell membrane and its prop erties In The Cell (J Brachet and A E Mirsky eds) Academic Press Inc New York vol 2 pp 1–84
Prankerd T A J 1961 The Red Cell An Account of its Chemical Physiology and Path ology *Blackwell Scientific Publications* Oxford
Rand R P and A C Burton 1964 Mechani cal properties of the red cell membrane I Membrane stiffness and intracellular pressure Biophysic J 4 115–135
Rich A 1963 Polyribosomes Sci Amer *209* 44–53
Rich A *J R Warner and M Goodman 1963* The structure and function of polyribosomes Cold Spring Harbor Symp Quant Biol *28* 269–285
Rifkind R A and D Danon 1965 Heinz body anemia — an ultrastructural study I Heinz body formation Blood *25* 885–896
Rifkind R A D Danon and P A Marks 1964 Alterations in polyribosomes during erythroid cell maturation With an appendix by William Perl J Cell Biol 22 599–611
Robertson J D 1964 Unit membranes a re view with recent new studies of experimental alterations and a new subunit structure in synaptic membranes In Cellular Membranes in Development (M Locke ed) Academic *Press Inc New York*
Roth T F and K R Porter 1962 Specialized sites on the cell surface for protein uptake In Proceedings of the 5th International Con gress for Electron Microscopy (S S Breese Jr ed) Academic Press Inc New York vol 2 p 114
Sabatini D D K Bensch and R J Barrnett 1963 Cytochemistry and electron microscopy The preservation of cellular ultrastructure and *enzymatic activity by aldehyde fixation J Cell* Biol *17* 19–58
Seifriz W 1927 The physical properties of erythrocytes Protoplasma *1* 345–365
Slautterback D B 1963 Cytoplasmic micro tubules II Hydra J Cell Biol *18* 367–388
Thorell B 1947 The relation of nucleic acids to the formation and differentiation of cellular proteins Cold Spring Harbor Symp Quant Biol 12 247–255
Warner J R P M Knopf and A Rich 1963 A multiple ribosomal structure in protein syn thesis Proc Nat Acad Sci *49* 122–129
Warner J R A Rich and C E Hall 1962 Electron microscope studies of ribosomal clus ters synthesizing hemoglobin Science *138* 1399–1403
Watson M L 1958 Staining of tissue sections for electron microscopy with heavy metals J Biophysic and Biochem Cytol *4* 475–485
Wintrobe M 1961 Clinical Hematology Lea and Febiger Philadelphia

PLATE 1

EXPLANATION OF FIGURES

All cells are from blood of phenylhydrazine injected rats The centri petal end of the cells is directed toward the top of the plates

1 Reticulocytes in different stages of maturation as evidenced by the amount and complexity of the reticulum present New methylene blue staining × 4 914

2 Electron micrograph of reticulocyte showing Howell Jolly body Two regions of different density are present cortex and medulla Vacuoles surrounding body are probably artifacts caused by the supravital staining in new methylene blue *Glutaraldehyde osmium tetroxide* × 48 230

3 Electron micrograph of erythrocyte containing Heinz body Osmium tetroxide × 18 200

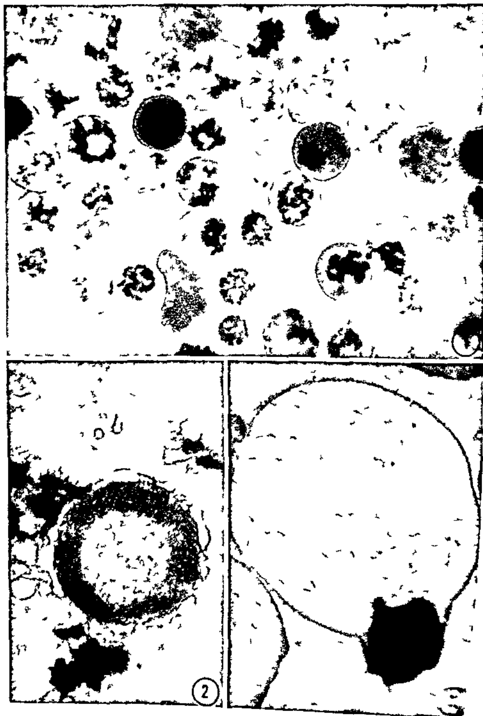

2

PLATE 2

EXPLANATION OF FIGURES

4 Blood from animal injected over a three day period with phenyl hydrazine About 25% of the cells show different degrees of reticulation Howell Jolly bodies appear at *HJ* Brilliant cresyl blue and Wright s staining × 4 914

5 Low power view of ultracentrifuged reticulocytes Phase-contrast photomicrograph × 455


HJ
E
4
5

PLATE 2

EXPLANATION OF FIGURES

4 Blood from animal injected over a three day period with phenyl hydrazine About 25% of the cells show different degrees of reticulation Howell Jolly bodies appear at *HJ* Brilliant cresyl blue and Wright s staining × 4 914

5 Low power view of ultracentrifuged reticulocytes Phase contrast photomicrograph × 455

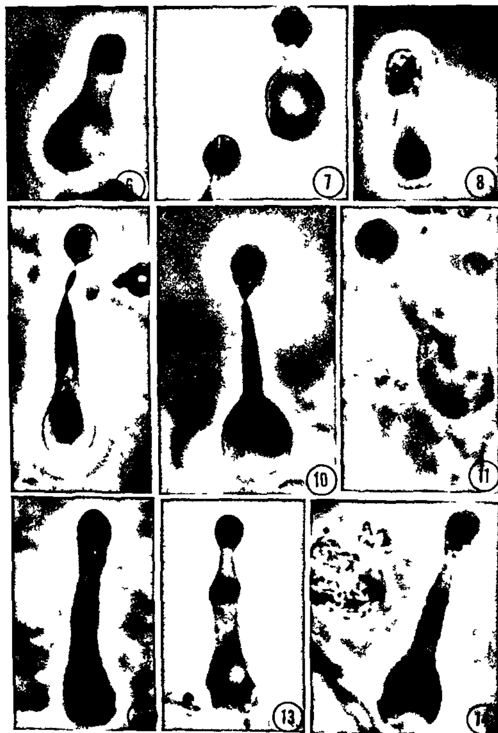

7
8
10
11
13

PLATE 3

EXPLANATION OF FIGURES

6–14 Stages showing stratification and elongation of reticulocytes Treated as in figure 5 Three layers are revealed in most figures a granular basophilic staining layer at the centripetal ends a layer of mitochondria near the middle and a dense hemoglobin layer at the centrifugal ends Phase contrast photomicrographs × 6 000

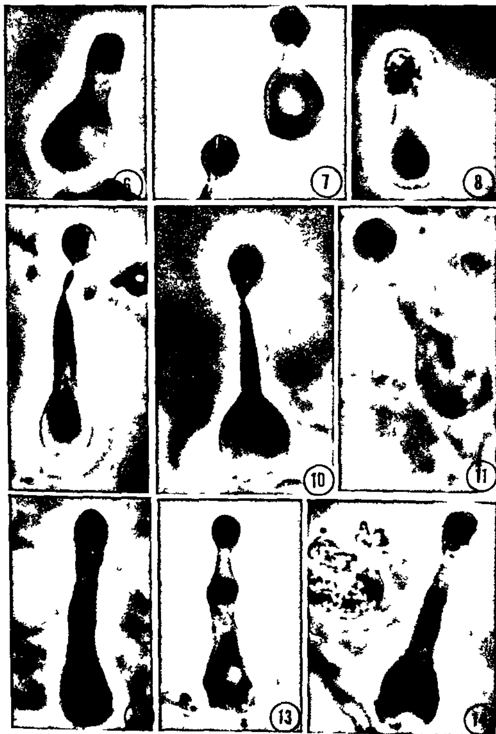

6
7
8
10
11
13
14

PLATE 4

EXPLANATION OF FIGURES

15–16 Relatively young reticulocytes with groups of ribosomes (poly ribosomes) distributed throughout the cytoplasm Note mitochon dria small vesicles (*SV*) micropinocytosis vesicles (*MV*) and larger vesicles The larger vesicle (fig 15) contains dense bodies and it is apparently formed by fusion of smaller ones (vesicles) (fig 15 arrow) Glutaraldehyde osmium tetroxide Figure 15 × 50 000 figure 16 × 30 940 insert × 29 120


SV
SV
15

PLATE 4

EXPLANATION OF FIGURES

15–16 *Relatively young reticulocytes with groups of ribosomes* (poly ribosomes) distributed throughout the cytoplasm Note mitochon dria small vesicles (*SV*) micropinocytosis vesicles (*MV*) and larger vesicles The larger vesicle (fig 15) contains dense bodies and it is apparently formed by fusion of smaller ones (vesicles) (fig 15 arrow) Glutaraldehyde osmium tetroxide Figure 15 × 50 000 figure 16 × 30 940 insert × 29 120


MV
MV
16
M
17

PLATE 5

EXPLANATION OF FIGURES

15–16 Relatively young reticulocytes with groups of ribosomes (poly ribosomes) distributed throughout the cytpoplasm Note mitochon dria small vesicles (*SV*) micropinocytosis vesicles (*MV*) and larger vesicles The larger vesicle (fig 15) contains dense bodies and it is apparently formed by fusion of smaller ones (vesicles) (fig 15 arrow) Glutaraldehyde osmium tetroxide Figure 15 × 50 000 figure 16 × 30 940 insert × 29 120

17 Groups of various size tubules Some appear like elongate vesicles (*T*) others may be similar to the microtubules of other types of cells (*MT*) Glutaraldehyde osmium tetroxide ×45 500



PLATE 6

EXPLANATION OF FIGURES

18 Early stages in the formation of the reticulum Stained briefly in new methylene blue and subsequently fixed in osmium tetroxide × 48 230

19 Stained to show reticulum by new methylene blue Cell was subsequently fixed in osmium tetroxide Note ribosomes within the reticulum Mitochondria show poorly preserved cristae × 48 230

18

19

PLATE 7

EXPLANATION OF FIGURE

20 Similar to figure 19 but lower magnification × 32 00


20

PLATE 8

EXPLANATION OF FIGURES

21 Mitochondria (*MF*) show dense staining granules (ferritin) Groups of tubules (*MT*) are similar to those in figure 17 Glutaraldehyde osmium tetroxide × 29 120

22 Here both reticulum (*RT*) and Heinz body material (*HB*) are revealed Mitochondria show dense ferritin bodies and evidence of degeneration Osmium tetroxide × 29 120

MF
MT
21

RT
HB
MF
22

PLATE 8

EXPLANATION OF FIGURES

21 Mitochondria (*MF*) show dense staining granules (ferritin) Groups of tubules (*MT*) are similar to those in figure 17 Glutaraldehyde osmium tetroxide × 29 120

22 Here both reticulum (*RT*) and Heinz body material (*HB*) are revealed Mitochondria show dense ferritin bodies and evidence of degeneration Osmium tetroxide × 29 120

HB
MF
23

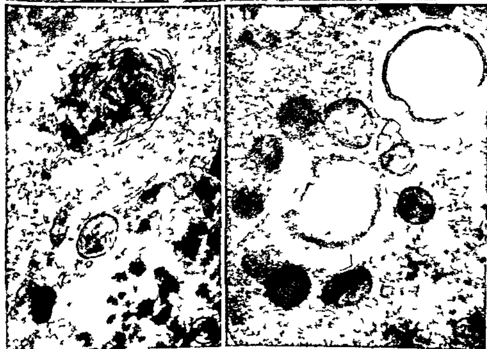


PLATE 9

EXPLANATION OF FIGURE

23 Forming Heinz body material (*HB*) The dense bodies will fuse *by the time the erythrocyte stage is reached (fig 2) The mito* chondria contain ferritin (*MF*) Osmium tetroxide × 30 940

24–25 Unidentified bodies that sometimes occur in reticulocytes They probably result from degradation of organelles which accompany *the maturation of the cell Osmium tetroxide Figure* 24 × 29 120 figure 25 ×30 940

PLATE 10

EXPLANATION OF FIGURE

26 Slightly elongate ultracentrifuged reticulocytes Stratified from the centripetal to the centrifugal ends are the ribosomes mitochondria and hemoglobin Note especially the undisplaced ribosomes in the *cortex adjacent the plasma membrane In figure 27 the plasma mem* brane is indicated by the single arrow the cortex by the region be tween the arrows Glutaraldehyde osmium tetroxide × 32 000

PLATE 10

EXPLANATION OF FIGURE

26 Slightly elongate ultracentrifuged reticulocytes Stratified from the centripetal to the centrifugal ends are the ribosomes mitochondria and hemoglobin Note especially the undisplaced ribosomes in the cortex adjacent the plasma membrane In figure 27 the plasma mem brane is indicated by the single arrow the cortex by the region be tween the arrows Glutaraldehyde osmium tetroxide × 32 000


27

PLATE 11

EXPLANATION OF FIGURE

27 Slightly elongate ultracentrifuged reticulocytes Stratified from the centripetal to the centrifugal ends are the ribosomes mitochondria and hemoglobin Note especially the undisplaced ribosomes in the cortex adjacent the plasma membrane In figure 27 the plasma membrane is indicated by the single arrow the cortex by the region between the arrows Glutaraldehyde osmium tetroxide × 32 000


27

PLATE 12

EXPLANATION OF FIGURE

28 Centrifugal end of reticulocyte showing finely granular material (hemoglobin?) (see also fig 27) Evident are a few patches of ribo *somes a well defined cortical region composed in part of undisplaced* ribosomes and a few vesicles (arrow) Mitochondria are compactly layered at the centripetal end of the hemoglobin layer Glutaralde hyde osmium tetroxide $\times$ 32 000


28

PLATE 12

EXPLANATION OF FIGURE

28 *Centrifugal end of reticulocyte showing finely granular material* (hemoglobin?) (see also fig 27) Evident are a few patches of ribosomes a well defined cortical region composed in part of undisplaced ribosomes and a few vesicles (arrow) Mitochondria are compactly layered at the centripetal end of the hemoglobin layer Glutaraldehyde osmium tetroxide × 32 000

29

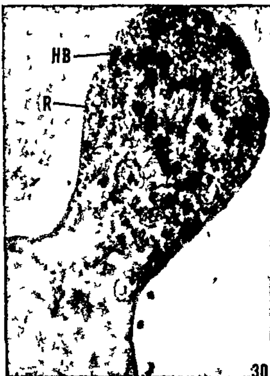




PLATE 13

EXPLANATION OF FIGURES

29 Extensively stretched reticulocyte displaying intact plasma membrane *discrete ribosomes at centripetal end and cortex of undisplaced* ribosomes Glutaraldehyde osmium tetroxide × 22 000

30 Centripetal end of relatively mature reticulocyte showing displaced ribosomes (*R*) and Heinz body material (*HB*) Only a relatively few ribosomes are present in this cell Osmium tetroxide × 32 000

31 Similar to figure 30 except a close association of Heinz body material (*HB*) and ribosomes is evident Osmium tetroxide × 32 000

29

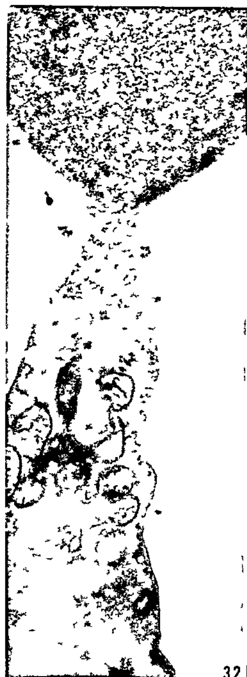




PLATE 14

EXPLANATION OF FIGURES

32–33 Stretched reticulocytes showing variation in shape as they become elongate to the point of separation into two parts The materials are layered in their usual order from the centripetal to the centrifugal ends as follows ribosomes mitochondria and hemoglobin Glutaraldehyde osmium tetroxide Figure 32 × 32 000 figure 33 × 53 000


32
3

Renewal of Spermatogonia in Man

YVES CLERMONT
Department of Anatomy McGill University Montreal Canada

ABSTRACT The spermatogonia of normal adult human testis were investigated in view of clarifying their mode of proliferation and renewal Three main types of sper matogonia were identified the dark type A spermatogonia (*Ad*) tentatively considered as the stem cells the pale type A spermatogonia (*Ap*) and the type B spermatogonia (B) these being the more and more differentiated elements giving rise to preleptotene spermatocytes The dark and pale type A spermatogonia were present in all stages of the cycle of the seminiferous epithelium the type B spermatogonia were found in stages VI I and II of the cycle and the preleptotene spermatocytes in stages III and IV of the cycle The type A spermatogonia divided preferentially in stage V of the cycle and the type B spermatogonia in stage II of the cycle

Quantitative data on spermatogonia and preleptotene spermatocytes revealed that the cell ratio Ad Ap B Pl was equal to 1 1 2 4 This indicated that the spermatogonial stem cells divided to produce equal numbers of new stem cells (*Ad*) and of the more differentiated pale type A spermatogonia (*Ap*) Each one of the latter gave rise to two type B spermatogonia which in turn produced four spermatocytes

The arrangement in pairs of the dark and pale type A spermatogonia throughout the duration of the cycle indicated that the mitoses of spermatogonial stem cells are "equivalent" in nature therefore the possibility of having "differential mitoses to explain the renewal of spermatogonial stem cells should be abandoned Lastly the frequent arrangement of the two classes of type A spermatogonia in homogeneous clusters indicated that the impetus which facilitates the differentiation of stem cells into the more differentiated elements (*Ap*) may affect homogeneous and compact groups of stem cells

The kinetics of the spermatogonial population has been subjected to detailed investigations in some mammals (see reviews by Roosen Runge 62 Leblond et al 63) In man however with the exception of the study by Roosen Runge and Barlow (53) no systematic attempt has been made to clarify the mode of spermatogonial proliferation differentiation and renewal Branca (24) in his classical study of the human testis lucidly formulated the following questions pertinent to the behavior of spermatogonia "Through how many mitoses does a spermatogonium pass before its transformation into a spermatocyte? Is this number of mitoses fixed? Is it variable? Are the two daughter cells of a given mitosis always two spermatogonia or two spermatocytes? Or does one of the two daughter cells become a spermatogonium and the other a spermatocyte?"

Branca himself failed to answer these questions because as he wrote of individual variations of the process of spermatogenesis" — variations not only from testis to testis but from one seminiferous tubule to the next The more recent attempts of Roosen Runge and Barlow (53) to resolve these same problems were impaired by two major difficulties Firstly these authors were unable to distinguish the more primitive from the more differentiated spermatogonia or indeed from the newly formed spermatocytes Secondly they lacked specific landmarks which would enable them to time the successive steps in the life history of the spermatogonium The nature of this second difficulty may be appreciated if one recalls that an analysis of spermatogonial development is dependent largely upon the characterization of cell groupings formed by the spermatogonia spermatocytes and spermatids which make up the seminiferous epithelium Because each step of spermatogenesis is precisely timed spermatids at a given step of spermiogenesis are always associated with spermatocytes and spermatogonia at given steps in their respective development This results in a series of distinct cellular associations of constant composition which have been designated as stages of a cycle of a the seminiferous epithelium The cycle in turn has been defined as a complete series

of cell associations appearing successively in any given area of the seminiferous epithelium (Leblond and Clermont 52) and is therefore a precise phenomenon which unfolds over a set period of time[1] In the case of the rat and other mammalian species the stages of the cycle were the key to a study of the kinetics of the spermatogonial population allowing the steps in the development of spermatogonia to be analyzed in a time sequence

In man this tool for the analysis of the spermatogonia was apparently lacking Branca (24) emphasized the absence of any regular arrangement of germ cells in the seminiferous epithelium Roosen Runge and Barlow (53) pointed out that in man in contrast to most other mammals there is little if any correlation between the developmental stages of spermatogonia spermatocytes and spermatozoa in any restricted area of the seminiferous tubules More recently however Clermont (63) demonstrated that in the human testis a cycle of the seminiferous epithelium exists and may be divided into six characteristic stages (fig 1) These stages have been used in the present article to investigate the kinetics of the spermatogonial population and from this data to propose a model for the development and renewal of spermatogonia in man

MATERIAL AND METHODS

Testicular biopsies from healthy prisoners obtained for us through the kindness of Dr Carl G Heller Seattle Washington provided material for the present study The biopsies were collected in such a manner as to avoid damage to the seminiferous epithelium (see details in Clermont 63) and fixed in Zenker formol This fixative was found to be the best suited for a cytological study of the spermatogonia In fact while Zenker formol preserves the chromatin in a spread condition (see description below) most other fixatives such as formol Bouin Cleland Carnoy Flemming Steive s solution precipitate the chromatin into clumps of various sizes The latter fixatives therefore tend to make the nuclei of the various classes of spermatogonia and of the newly formed spermatocytes look more or less alike

Following fixation in Zenker formol (16–24 *hours*) the specimens were washed in water and when necessary stored in 70% alcohol After dehydration with dioxane they were impregnated with paraffin Five micron sections were stained with Harris hematoxylin and eosin A few sections from each biopsy were stained with the periodic acid Schiff technique but these were not used in the quantitative analysis

Ten biopsies were quantitatively analyzed eight of these were serially sectioned and used in the reconstruction of spermatogonial maps Such maps were constructed as follows seminiferous tubules which happened to be cut parallel to the basement membrane were utilized Then using a camera lucida the nuclei of spermatogonia were drawn onto sheets of transparent tracing paper This procedure was repeated in 4 to 8 consecutive sections of the same tubule These drawings subsequently were superimposed over one another on an illuminated x ray viewing screen and a single aggregate map representing all the spermatogia was prepared Care was taken not to draw the same nucleus twice on this map

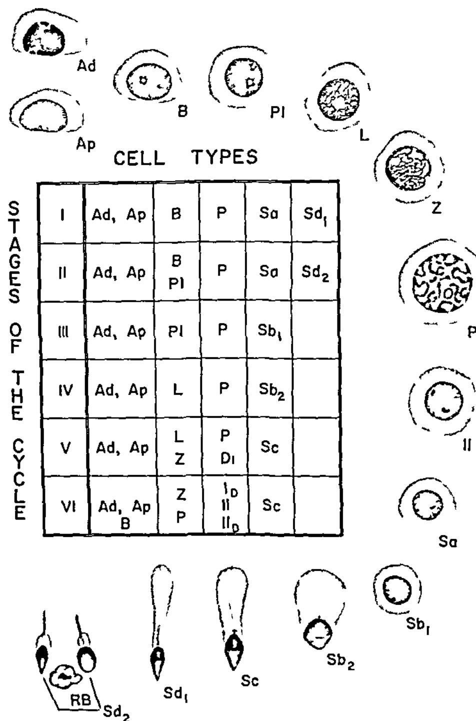
Serial sections were also used to study groups of dividing spermatogonia along the basement membrane of tubules in this

[1] In this respect the cycle of the seminiferous epithelium is fundamentally different from the wave of the seminiferous epithelium described in the rat and some other mammalian species The wave concerns the distribution of the cellular associations along the seminiferous tubules and has no dynamic connotations (Percy Clermont and Leblond 61)

Fig 1 Starting from the upper left hand corner of the figure and encircling the table drawings illustrate the steps of spermatogenesis in *man*

Lettering *Ad* dark type A spermatogonium *Ap* pale type A spermatogonium *B* type B spermatogonium *Pl* resting or preleptotene primary spermatocyte *L* leptotene spermatocyte *Z* zygotene spermatocyte *P* pachytene spermatocyte *II* secondary spermatocyte *Sa Sb* Sb_2 *Sc* Sd_1 Sd_2 correspond to steps of spermiogenesis *Rb* residual body

The table in the center of the figure gives the cellular composition of the six stages of the cycle of the seminiferous epithelium (Roman numerals *I VI*) Lettering same as above in addition *Di* diakinesis *ID* and *IID* first and second maturation divisions of spermatocytes (modified from Clermont 63)



I	Ad, Ap	B	P	Sa	Sd$_1$
II	Ad, Ap	B Pl	P	Sa	Sd$_2$
III	Ad, Ap	Pl	P	Sb$_1$	
IV	Ad, Ap	L	P	Sb$_2$	
V	Ad, Ap	L Z	P Di	Sc	
VI	Ad, Ap B	Z P	I$_D$ II II$_D$	Sc	

Figure 1

cell associations appearing successively any given area of the seminiferous epi elium (Leblond and Clermont 52) and therefore a precise phenomenon which ifolds over a set period of time [1] In the se of the rat and other mammalian spe :s the stages of the cycle were the key a study of the kinetics of the spermato nial population allowing the steps in the velopment of spermatogonia to be ana :ed in a time sequence

In man this tool for the analysis of the ermatogonia was apparently lacking anca (24) emphasized the absence of y regular arrangement of germ cells the seminiferous epithelium Roosen nge and Barlow (53) pointed out that man *in contrast to most other mam* ils there is little if any correlation be een the developmental stages of sperma gonia spermatocytes and spermatozoa in y restricted area of the seminiferous bules More recently however Cler *mt (63) demonstrated that in the* man testis a cycle of the seminiferous thelium exists and may be divided into characteristic stages (fig 1) These ges have been used in the present article investigate the kinetics of the spermato *nial population and from this data to* pose a model for the development and newal of spermatogonia in man

MATERIAL AND METHODS

Testicular biopsies from healthy pris ers obtained for us through the kindness Dr Carl G Heller Seattle Washington vided material for the present study biopsies were collected in such a man as to avoid damage to the seminiferous thelium (see details in Clermont 63) *fixed in Zenker formol This fixative* found to be the best suited for a cyto cal study of the spermatogonia In fact ile Zenker formol preserves the chroma in a spread condition (see description ow) most other fixatives such as for *Bouin* Cleland Carnoy Flemming ves solution precipitate the chroma into clumps of various sizes The latter tives therefore tend to make the nu of the various classes of spermatogonia of the newly formed spermatocytes *more* or less alike

Following fixation in Zenker formol (16–24 hours) the specimens were washed in water and when necessary stored in 70% alcohol After dehydration with di oxane they were impregnated with paraf fin Five micron sections were stained with Harris hematoxylin and eosin A few sec tions from each biopsy were stained with the periodic acid Schiff technique but these were not used in the quantitative analysis

Ten biopsies were quantitatively ana lyzed eight of these were serially sectioned and used in the reconstruction of sperma togonial maps Such maps were con structed as follows seminiferous tubules which happened to be cut parallel to the basement membrane were utilized Then using a camera lucida the nuclei of sper matogonia were drawn onto sheets of transparent tracing paper This procedure was repeated in 4 to 8 consecutive sections of the same tubule These drawings sub sequently were superimposed over one an other on an illuminated x ray viewing screen and a single aggregate map repre senting all the spermatogia was prepared Care was taken not to draw the same nucleus twice on this map

Serial sections were also used to study groups of dividing spermatogonia along the basement membrane of tubules In this

[1] In this respect the cycle of the seminiferous epithelium is fundamentally different from the wave of the seminiferous epithelium described in the rat and some other mammalian species The wave con cerns the distribution of the cellular associations along the seminiferous tubules and has no dynamic connotations (Percy Clermont and Leblond 61)

Fig 1 Starting from the upper left hand cor ner of the figure and encircling the table draw ings illustrate the steps of spermatogenesis in man

Lettering *Ad* dark type A spermatogonium *Ap* pale type A spermatogonium *B* type B sper matogonium *Pl* resting or preleptotene primary spermatocyte *L* leptotene spermatocyte *Z* zygo tene spermatocyte *P* pachytene spermatocyte *II* secondary spermatocyte *Sa* Sb_1 *Sb* *Sc* Sd_1 Sd_2 correspond to steps of spermiogenesis *Rb* resi dual body

The table in the center of the figure gives the cellular composition of the six stages of the cycle of the seminiferous epithelium (Roman numerals *I VI*) Lettering same as above in addition *Di* diakinesis *ID* and *IID* first and second ma turation divisions of spermatocytes (modified from Clermont 63)

matin adhered to the nuclear membrane which then appeared more clearly de lineated some also adhered to the nucleo lus which was now detached from the nuclear membrane As this cell approached prophase more chromophilic chromatin accumulated in the nucleoplasm The cytoplasm of these spermatogonia like that of the pale type A spermatogonia lacked any appreciable amount of gly cogen

The spherical nuclei of the *resting or preleptotene spermatocytes* (fig 1) bore great resemblance to those of the type B spermatogonia and except for their slightly smaller size (6 0 µ) could be easily mis taken for them The nucleus contained both pale and deep staining chromatin although the latter was relatively more abundant than in the nuclei of type B sper matogonia More numerous chromophilic chromatin flakes had become adherent to the nuclear membrane and to the centrally located nucleolus The pale staining chro matin was clearly more granulated and as the cell approached the leptotene step of meiotic prophase it acquired a progres sively filamentous texture The cytoplasm of these cells contained no glycogen The cells themselves were displaced away from the tubular wall toward the lumen

The dark and the pale type A spermato gonia were found at all six stages of the cycle the type B spermatogonia were pres ent predominantly in stages VI I and II and the preleptotene spermatocytes in stages III and IV of the cycle (fig 1)

Counts of spermatogonia and resting (preleptotene) spermatocytes at various stages of the cycle of the seminiferous epithelium

Because in man typical cell associations occupied relatively small areas of semi niferous epithelium a single tubular sec tion often contained several of them side by side Furthermore due to the mixing of cells the demarcation between adjacent cell associations was often imprecise and difficult to define Taking these histologi cal characteristics into consideration the cell counts were done as follows in cross oblique or longitudinal sections of tubules only the portions of the tubular wall cut perpendicularly to the basement mem brane were considered The spermato gonia and spermatocytes were scored along the basement membrane and the cell asso ciation to which they belonged was identi fied Counts were made so as to avoid Abercrombie s correction for differences of nuclear diameters i e only the nuclei with geometrical centers within the section were enumerated In the tabulation of data counts obtained for stages I and II of the cycle were pooled This was similarly done with the counts obtained for stages III or IV and for stages V and VI of the cycle, respectively

In a first series of counts the numbers of dark and pale type A spermatogonia were pooled and the ratios of these to the numbers of type B spermatogonia or of pre leptotene spermatocytes were estimated The results (table 1) revealed that in stages I–II of the cycle the proportion of type A to type B spermatogonia was very close to 1 1 with little variation from one biopsy to another In stages III IV of the cycle the proportion of type A spermatogonia to the number of preleptotene or early lepto tene spermatocytes was close to 1 2 with again relatively little variation from one biopsy to another

In a second series of counts the dark and pale type A spermatogonia were enum erated separately at the three main phases of the cycle (I–II III–IV V–VI) The pro portion of the dark to the pale type A spermatogonia for each one of these three phases approximated a 1 1 ratio (table 2)

Counts of spermatogonial mitoses at the various stages of the cycle

Mitoses were counted at the various stages of the cycle the absolute numbers obtained were recorded in a histogram (fig 4) This histogram indicated that spermatogonia divided preferentially at stages II and V of the cycle although mitoses were found at other stages

Distribution of dark and pale type A spermatogonia along the basement membrane of the seminiferous tubules

For reasons that will be made clear in the discussion the topographical distribu tion of type A spermatogonia along the

case transversely cut tubules were utilized and a large number of consecutive sections of the same tubule were examined

RESULTS

Description of spermatogonia and of resting (preleptotene) spermatocytes

On the basis of the morphological configuration of chromatin and nucleoli spermatogonia were classified (Clermont 63) as dark type A (*Ad*) pale type A (*Ap*) and type B (*B*) (figs 1 2 and 3) In the following description some additional cytological features of these cells will be given

The *dark type A spermatogonium* (fig 2 *Ad*) was characterized by a spherical or slightly ovoid nucleus which contained a very finely granulated chromatin The chromatin was uniformly and intensely stained by hematoxylin except for a single large and unstained space near the center of the nucleus Despite the vacuole like appearance of this unstained area close examination revealed the presence of some pale eosinophilic material in it One or two other hemispherical spaces seen on the inner surface of the nuclear membrane contained deeply eosinophilic nucleoli of various sizes (fig 1 *Ad*) The cytoplasm of these cells was usually vacuolated and pale stained In PA Schiff stained sections however the cytoplasm was filled with positive granulations which after amylase treatment were identified as glycogen

The *pale type A spermatogonium* (figs 2 3 *Ap*) had an ovoid nucleus containing a granular chromatin with little affinity for hematoxylin These chromatin particles were somewhat coarser than those of the dark type A nuclei and gave a ground glass texture to the nucleus Several globular chromatin masses more deeply stained with hematoxylin were also visible One to three eosinophilic nucleoli were attached to the nuclear membrane They were free of deeply stained or chromophilic chromatin granules The PA Schiff technique revealed little or no glycogen in the cytoplasm of these cells

Both the dark and the pale type A spermatogonia varied somewhat in size the majority of them having an average nuclear diameter of 6 0 μ and 6 8 μ respectively

The *type B spermatogonia* (fig 3 *B*) displayed a spherical nucleus (average diameter 7 0 μ) which contained a finely granulated and pale stained chromatin as well as several flakes and granules of chromophilic chromatin Some of this chro-



matin adhered to the nuclear membrane which then appeared more clearly de lineated some also adhered to the nucleo lus which was now detached from the nuclear membrane As this cell approached prophase more chromophilic chromatin accumulated in the nucleoplasm The cytoplasm of these spermatogonia like that of the pale type A spermatogonia lacked any appreciable amount of gly cogen

The spherical nuclei of the *resting or preleptotene spermatocytes* (fig 1) bore great resemblance to those of the type B spermatogonia and except for their slightly smaller size (6 0 μ) could be easily mis taken for them The nucleus contained both pale and deep staining chromatin although the latter was relatively more abundant than in the nuclei of type B sper matogonia More numerous chromophilic chromatin flakes had become adherent to the nuclear membrane and to the centrally located nucleolus The pale staining chro matin was clearly more granulated and as the cell approached the leptotene step of meiotic prophase it acquired a progres sively filamentous texture The cytoplasm of these cells contained no glycogen The cells themselves were displaced away from the tubular wall toward the lumen

The dark and the pale type A spermato gonia were found at all six stages of the cycle the type B spermatogonia were pres ent predominantly in stages VI I and II and the preleptotene spermatocytes in stages III and IV of the cycle (fig 1)

Counts of spermatogonia and resting (preleptotene) spermatocytes at various stages of the cycle of the seminiferous epithelium

Because in man typical cell associations occupied relatively small areas of semi niferous epithelium a single tubular sec tion often contained several of them side by side Furthermore due to the mixing of cells the demarcation between adjacent cell associations was often imprecise and difficult to define Taking these histologi cal characteristics into consideration the cell counts were done as follows in cross oblique or longitudinal sections of tubules only the portions of the tubular wall cut perpendicularly to the basement mem brane were considered The spermato gonia and spermatocytes were scored along the basement membrane and the cell asso ciation to which they belonged was identi fied Counts were made so as to avoid Abercrombie s correction for differences of nuclear diameters i e only the nuclei with geometrical centers within the section were enumerated In the tabulation of data counts obtained for stages I and II of the cycle were pooled This was similarly done with the counts obtained for stages III or IV and for stages V and VI of the cycle respectively

In a first series of counts the numbers of dark and pale type A spermatogonia were pooled and the ratios of these to the numbers of type B spermatogonia or of pre leptotene spermatocytes were estimated The results (table 1) revealed that in stages I–II of the cycle the proportion of type A to type B spermatogonia was very close to 1 1 with little variation from one biopsy to another In stages III–IV of the cycle the proportion of type A spermatogonia to the number of preleptotene or early lepto tene spermatocytes was close to 1 2 with again relatively little variation from one biopsy to another

In a second series of counts the dark and pale type A spermatogonia were enum erated separately at the three main phases of the cycle (I–II III–IV V–VI) The pro portion of the dark to the pale type A spermatogonia for each one of these three phases approximated a 1 1 ratio (table 2)

Counts of spermatogonial mitoses at the various stages of the cycle

Mitoses were counted at the various stages of the cycle the absolute numbers obtained were recorded in a histogram (fig 4) This histogram indicated that spermatogonia divided preferentially at stages II and V of the cycle although mitoses were found at other stages

Distribution of dark and pale type A spermatogonia along the basement membrane of the seminiferous tubules

For reasons that will be made clear in the discussion the topographical distribu tion of type A spermatogonia along the

TABLE 1

Counts of type A, type B spermatogonia and spermatocytes at various stages of the cycle

Stages I–II of the cycle

Biopsy no.	Type A spermatogonia	Type B spermatogonia	Ratio A:B	Number of tubular sections examined
1	141	136	1:0.96	36
2	527	535	1:1.01	82
3	279	259	1:0.92	35
4	63	68	1:1.07	24
Total	1010	991	1:0.98	177

Stages III–IV of the cycle

Biopsy no.	Type A spermatogonia	Preleptotene or Leptotene spermatocytes	Ratio A:Pl	Number of tubular sections examined
5	904	1896	1:2.09	134
6	621	1319	1:2.12	101
7	159	316	1:2.02	36
8	393	700	1:1.78	50
9	282	550	1:1.94	34
Total	2359	4781	1:2.02	358

TABLE 2

Counts of "dark" and "pale" type A spermatogonia at various stages of the cycle

Stages of the cycle	Biopsy no.	Type Ad spermatogonia	Type Ap spermatogonia	Ratio Ad:Ap	Number of tubular sections examined
I–II	9	222	201	1:0.90	39
	10	147	132	1:0.89	53
III–IV	7	71	88	1:1.23	36
	9	46	52	1:1.13	16
	10	84	62	1:0.73	14
V–VI	9	70	66	1:0.85	20
	10	27	33	1:1.22	10
Total		667	634	1:0.95	188

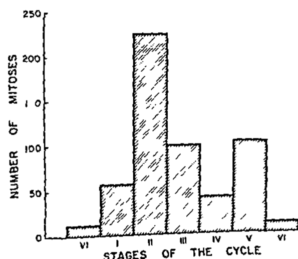


Figure 4

Fig. 4. Diagram showing the location of mitotic figures within the cycle of the seminiferous epithelium. The total number of mitotic figures found in each stage of the cycle is indicated on the ordinate.

Since the relative frequency with which the stages appear in seminiferous tubules is variable, the heights of the columns have no real significance. This data indicated that mitoses were found preferentially in stages *II* and V of the cycle.

Fig. 5a, b. Map showing the distribution of dark and pale type A spermatogonia along the limiting membrane of the seminiferous tubule in stage V of the cycle.

In (b) the spermatogonia *were tentatively* arranged in pairs, the members of the pairs being identical Ad or Ap cells. Formation of pairs of different cells was comparatively more difficult if not impossible.

a

b

Figure 5

TABLE 1

Counts of type A type B spermatogonia and spermatocytes at various stages of the cycle

Stages I–II of the cycle

Biopsy no	Type A spermatogonia	Type B spermatogonia	Ratio A B	Number of tubular sections examined
1	141	136	1 0 96	36
2	527	535	1 1 01	82
3	279	259	1 0 92	35
4	63	68	1 1 07	24
Total	1010	991	1 0 98	177

Stages III–IV of the cycle

Biopsy no	Type A spermatogonia	Preleptotene or Leptotene spermatocytes	Ratio A II	Number of tubular sections examined
5	904	1896	1 2 09	131
6	621	1319	1 2 12	104
7	159	316	1 2 02	36
8	393	700	1 1 78	50
9	282	550	1 1 94	34
Total	2359	4781	1 2 02	358

TABLE 2

Counts of dark and pale type A spermatogonia at various stages of the cycle

Stages of the cycle	Biopsy no	Type Ad spermatogonia	Type Ap spermatogonia	Ratio Ad Ap	Number of tubular sections examined
I–II	9	222	201	1 0 90	39
	10	147	132	1 0 89	53
III–IV	7	71	88	1 1 23	36
	9	46	52	1 1 13	16
	10	84	62	1 0 73	14
V–VI	9	70	66	1 0 85	20
	10	27	33	1 1 22	10
Total		667	634	1 0 95	188

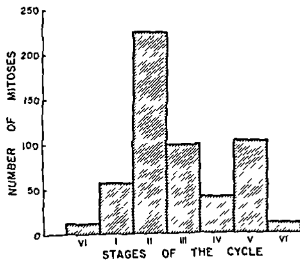


Figure 4

Fig 4 Diagram showing the location of mitotic figures within the cycle of the seminiferous epithelium The total number of mitotic figures found in each stage of the cycle is indicated on the ordinate

Since the relative frequency with which the stages appear in seminiferous tubules is variable the heights of the columns have no real significance This data indicated that mitoses were found preferentially in stages *II* and *V* of the cycle

Fig 5a b Map showing the distribution of dark and pale type A spermatogonia along the limiting membrane of the seminiferous tubule in stage V of the cycle

In (b) the spermatogonia were tentatively arranged in pairs the members of the pairs being identical Ad or Ap cells Formation of pairs of different cells was comparatively more difficult if not impossible

a

b

Figure 6a and 6b

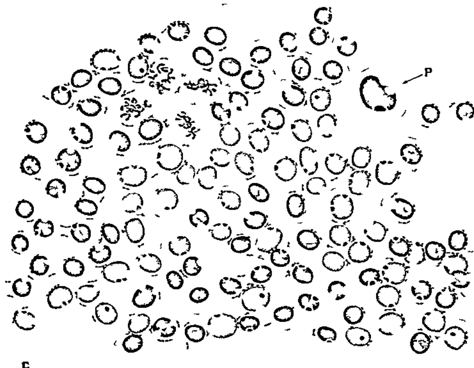


Figure 6c

Figs 6a b c Map showing the distribution of dark and pale type A spermatogonia along the tubular basement membrane in stage V of the cycle

A cluster of four mitotic figures is visible in the upper left quadrant of the field

In (*b*) contour lines indicate the tendency of the cells to form clusters composed of identical cells areas I (*I*) point to clusters of dark type A spermatogonia area II (*II*) indicates a cluster of pale type A spermatogonia area III (*III*) shows a territory in which the two classes of type A spermatogonia are mixed

In (*c*) the spermatogonia were tentatively arranged in pa rs the members of the pairs being cytologically identical The large isolated dark type A spermatogonium in the upper right corner of the map was conside ed as a polyploid cell (*P*)

basement membrane of the seminiferous tubule was examined Fifteen maps showing resting and dividing cells were reconstructed ten of these showed dark and pale type A spermatogonia at stage V of the cycle (figs 5 6 7) while the remaining five maps showed in addition to type A cells some type B spermatogonia associated with stages I and II

Spermatogonia were found to be remarkably abundant and constituted an almost continuous layer of cells along the basement membrane The nuclei of Sertoli cells were usually on the luminal side of the spermatogonial layer their cytoplasm reached the basement membrane through delicate interstices seen between spermatogonia From these maps the following main facts emerged While over some areas the dark and pale type A spermatogonia were mixed (fig 6b area III) in many other places the dark and pale type A spermatogonia were segregated into homogeneous groups (fig 6b areas I and II) Furthermore it was soon discovered that within both the mixed and homogeneous regions all spermatogonia could be arranged into pairs of identical cells (figs 5b 6c) The pairing of the spermatogonia was done by using two criteria close apposition and similarity in the nuclear morphology such as texture of chromatin and

a

I

II

III

b

Figure 6a and 6b

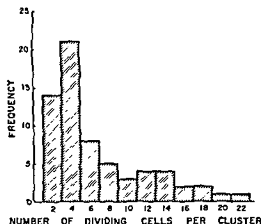


Fig 8 Diagram giving on the abscissa the siz of clusters of mitotic figures found along th tubular wall (the size r ferring to the number of dividing cells per cluster) and on the ordinate their frequency

In this series a total of 65 clusters of dividing cells were mapped and scored in stage V of the cycle Although clusters of four mitotic figures predominated this wa not found to be signifi cant (the distribution observed being compatible with a random distribution curve)

main parts the first will deal with the existence of three classes of spermatogonia and their filiation the second one will attempt to build a model for the development and renewal of spermatogonia and the third one will present some considerations on the impetus involved in the initiation of spermatogenesis

Classes of spermatogonia and their filiation

On the basis of their nuclear morphology in Zenker formol fixed biopsies three types of spermatogonia were described in the seminiferous epithelium of man Despite some variability in chromatin configuration and in nuclear size most spermatogonial nuclei were readily classified as one of these three types There remained however some dark staining nuclei that were difficult to identify since these often occurred in proximity to clusters of dividing cells they were tentatively regarded as nuclei in late telophase in which the nuclear chromatin had not yet assumed its definitive spread configuration Roosen Runge and Barlow (53) in their quantitative analysis of human spermatogonia concluded to the existence of seven classes of spermatogonia on the basis of sixty four mitotic figures seen in the largest clusters of dividing spermatogonia found along the tubular wall they regarded the apparent existence of seven class sizes in the metaphase plates of dividing spermatogonia as confirmation of this conclusion In this approach the largest metaphase plates would belong to the most immature or stem spermatogonia and the smallest ones to most evolved spermatogonia The view that the largest (excluding polyploid) nuclei pertained exclusively to stem cells is difficult to support in man Roosen Runge and Barlow (53) themselves observed a marked variation of volume in intermitotic spermatogonial nuclei and in the present work it was found that the average nuclear diameter of type B spermatogonia was larger than that of pale type A spermatogonia which in turn was larger than that of dark type A spermatogonia Furthermore the conclusion that there were seven classes or types of spermatogonia was seemingly based on the assumption that the stem cells when they entered spermatogenesis did so singly The present study on the other hand demonstrated that stem cells divided in pairs

The present classification of human spermatogonia could not be correlated in any way with the description of spermatogonia presented by Mancini and his colleagues (60) who investigated prepuberal testes fixed in Bouin s fluid

It was of interest to compare the spermatogonia in man with those described in the Rhesus monkey (Clermont and Leblond 59) The dark type A spermatogonia in man bore strong resemblance to the type A cells of the monkey Although the pale vesicle seen in the center of the nucleus of the human dark type A spermatogonium was missing from its counterpart in the monkey glycogen was present in the cytoplasm of these cells in both species

The pale type A spermatogonia in man were identical to the type A cells described in the monkey The type B spermatogonia in man were clearly the morphological equivalent of the type B cells in monkey but while there seemed to be only one generation of type B cells in man there were three generations of type B cells in the monkey (Clermont and Leblond 59)

number and appearance of nucleoli (fig 5) Occasionally a large nucleus of the dark or the pale class had no partner (fig 6c *P*) Such a nucleus was considered atypical and probably polyploid

The arrangement of spermatogonia into pairs was confirmed in maps showing only dividing type A spermatogonia (fig 7) Some 70 islands or clusters of dividing type A cells were thus analyzed without attempting to identify the type of spermatogonia in mitosis (*Ad* or *Ap*) This indicated that in 65 out of 70 areas all spermatogonia divided in groups of two or multiples of two (fig 8) Furthermore when the phase (prophase metaphase etc) of mitosis was considered it was obvious that two cells at the same step of division were very close to each other so as to constitute the two members of a pair (fig 7) In five instances a dividing cell had no partner but in two of these cases the isolated mitotic figures were tripolar Therefore to summarize the observations made from maps the dark and pale type A spermatogonia were generally arranged in pairs which in turn had a definite tendency to form larger groups of identical cells

DISCUSSION

The purpose of the present discussion will be to determine the mode of proliferation differentiation and renewal of spermatogonia This discussion will have three

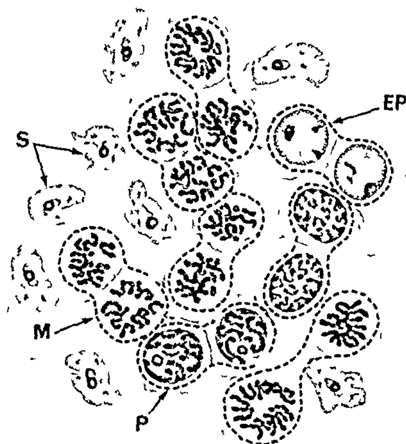


Fig 7 Map showing a cluster of dividing pale type A spermatogonia in stage V of the cycle Sertoli nuclei are also indicated (*S*)

The dividing cells were clearly arranged in pairs *the two members of a pair being at the same phase of mitosis*

Lettering *EP* early prophase *P* prophase *M* metaphase

spermatogonial population they were not considered to be numerically capable of distorting the cell ratios

On the basis of these assumptions the quantitative data were interpreted as follows The cell ratios indicated that for each dark type A spermatogonium there was one pale type A cell at all times in the cycle of the seminiferous epithelium ($Ad\ Ap = 1\ 1$) The ratio of $Ad + Ap$ to type B cells at stages I–II of the cycle was also equal to 1 1 meaning that the proportion of either of these two classes of type A spermatogonia to type B cells was equal to 1 2 Since the pale type A spermatogonia were regarded as the immediate precusors of type B cells then each type *Ap* cell should produce two type B spermatogonia Finally the ratio of $Ad + Ap$ spermatogonia to preleptotene spermatocytes found at stages III–IV of the cycle was equal to 1 2 (table 1) Again the ratio of any one of the two classes of type A cells to preleptotene spermatocytes must be equal to 1 4 Since the ratio of *Ap* to B was equal to 1 2 and that of *Ap* to *Pl* was equal to 1 4 then the ratio of B to *Pl* should equal 1 2 and each type B cell produced should give rise to two primary spermatocytes In summary therefore the proportion of the various cells counted was as follows

Ad Ap B *Pl* was equal to 1 1 2 4

The simplest model that could be built from these cell ratios to illustrate the behavior of spermatogonia is presented in figure 9 Thus a dark type A cell would divide at stage V of the cycle to yield one dark plus one pale type A spermatogonia The pale type A cell (*Ap*) in stage V of the next cycle would divide to produce two type B spermatogonia which in stage II of the following cycle would give rise to four preleptotene spermatocytes According to this model the dark type A spermatogonia would in stage V of each cycle undergo a "differential mitosis" i e a division giving rise to two morphologically distinct spermatogonia a dark type A considered as a new stem cell and a pale type A spermatogonium considered as a differentiated cell Were such a differential mitosis to occur then following the divisions of type *Ad* cells in stage V of the cycle pairs of mophologically different cells i e one

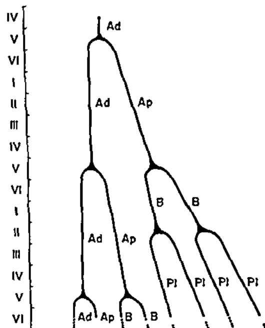


Fig 9 Diagram showing the simplest possible model illustrating the development of spermatogonia It is built on the cell ratio *Ad Ap B Pl* being equal to 1 1 2 4 and on a number of assumptions (see text)

On the left the stages of the cycle are indicated (Roman numerals) The divisions of cells are indicated by the junction of three lines and are located in stages *V* and *II* of the cycle According to this model the mitoses of dark type A spermatogonia (*Ad*) are differential" i e giving rise to two morphologically distinct cells The divisions of pale type A (*Ap*) and type B (B) spermatogonia are "equivalent" i e producing two morphologically similar cells This model would explain the continuous renewal of stem cells (*Ad*) and the production of preleptotene primary spermatocytes (*Pl*) (For a discussion of this model see text)

dark plus one pale spermatogonium should be found along the tubular limiting membrane However spermatogonial maps disclosed clusters of identical cells within which spermatogonia formed identical pairs Furthermore it became apparent that these pairs of identical cells persisted throughout the cycle and after a 16-day interval (i e the duration of one cycle in man Heller and Clermont 64) divided in pairs the two cells in every pair being at the same phase (prophase metaphase etc) of mitosis This last observation was not in accord with the data of Roosen Runge and Barlow (53) who reported that

The next question to arise concerned ; filiation of the three types of spermato nia in man which of these cells was ; most primitive element or stem cell ; intermediate and the most differenti ed ones? To answer this question it was ınd convenient to begin with the most ferentiated elements and proceed back rd The cells arising from spermato nia are the spermatocytes These cells their preleptotene phase are usually n in stages III and IV of the cycle i e er the peak of division observed in ge II Of the three types of spermato nia the type B should be selected as ; immediate precursor of spermatocytes the following reasons Firstly except a small difference in nuclear volume ; two cell types were morphologically nilar Both had spherical nuclei with mps of chromophilic chromatin along ; nuclear membrane and on the centrally ated nucleolus Secondly the type B ermatogonia were found in stages VI I I II of the cycle i e before the peak of ision noted in stage II Lastly as it will demonstrated later the number of sper tocytes was twice that of the type B ls

Between the dark and the pale type A rmatogonia the latter was tentatively ected as the immediate precursor of the e B spermatogonia for the following son In the early prophasic nucleus of pale type A spermatogonium some omophilic clumps of chromatin ap ared in proximity to the nuclear mem ne and nucleolus These nuclei there ; acquired a great similarity to those of e B spermatogonia The position of the in nucleolus remained however a dis ctive cytological feature between the classes of cells Similar criteria were d in the investigation of spermatogen ; in the monkey where it was con ded that the type A₁ cells were the nediate precursor of type B₁ spermato nia (a similar approach is taken to study differentiation in hemopoietic sys ns) However more direct proofs are ecessary to affirm this conclusion and it mains possible that the dark instead of e pale type A spermatogonia give rise to pe B spermatogonia

Since the pale type A spermatogonia were considered to be the immediate pre cursors of type B cells the remaining dark type A spermatogonia were obviously re garded as stem cells and as the progenitors of new stem cells and of the pale type A spermatogonia

Model of spermatogonial development

From the data collected an attempt was made to build a model illustrating the pro liferation and renewal of spermatogonia To do so several assumptions were made The first assumption was that once sper matogonia embarked on their course of differentiation into spermatocytes their evolution was unidirectional and irreversi ble In other words the pale type A sper matogonia more differentiated than the stem cells necessarily gave rise to type B cells which in turn inevitably produced spermatocytes None of these elements would revert to the stem cell condition or even stopped progress along the path of differentiation Such an assumption found strong support from studies on species in which the evolution of spermatogonia could be followed after tagging a radio active tracer element onto the nucleus (Clermont Leblond and Messier 59 Monesi 62) Indications that a similar condition prevailed in man was noted in ³H thymidine injected testicles by Heller and Clermont (64)

A second assumption was that the sper matogonia of each type divided only once during the cycle This assumption sug gested by the yield of spermatocytes from a spermatogonial stem cell (4 1) was in fact difficult to ascertain in man Again this assumption found support from data collected in rodents in which counting and tracing of labeled cells during a cycle of the seminiferous epithelium could be done more easily and systematically than in man (Clermont Leblond and Messier 59 Monesi 62)

Lastly interpretation of data and con struction of a model was dependent on the assumption that there was no degeneration of spermatogonia In fact degenerating spermatogonia as well as some polyploid nuclei were observed in the human semi niferous tubules but because these repre sented only a very small proportion of the

spermatogonial population they were not considered to be numerically capable of distorting the cell ratios

On the basis of these assumptions the quantitative data were interpreted as follows The cell ratios indicated that for each dark type A spermatogonium there was one pale type A cell at all times in the cycle of the seminiferous epithelium ($Ad\ Ap = 1\ 1$) The ratio of $Ad + Ap$ to type B cells at stages I–II of the cycle was also equal to 1 1 meaning that the proportion of either of these two classes of type A spermatogonia to type B cells was equal to 1 2 Since the pale type A spermatogonia were regarded as the immediate precusors of type B cells then each type *Ap* cell should produce two type B spermatogonia Finally the ratio of $Ad + Ap$ spermatogonia to preleptotene spermatocytes found at stages III–IV of the cycle was equal to 1 2 (table 1) Again the ratio of any one of the two classes of type A cells to preleptotene spermatocytes must be equal to 1 4 Since the ratio of Ap to B was equal to 1 2 and that of *Ap* to *Pl* was equal to 1 4 then the ratio of B to *Pl* should equal 1 2 and each type B cell produced should give rise to two primary spermatocytes In summary therefore the proportion of the various cells counted was as follows

Ad Ap B *Pl* was equal to 1 1 2 4

The simplest model that could be built from these cell ratios to illustrate the behavior of spermatogonia is presented in figure 9 Thus a dark type A cell would divide at stage V of the cycle to yield one dark plus one pale type A spermatogonia The pale type A cell (*Ap*) in stage V of the next cycle would divide to produce two type B spermatogonia which in stage II of the following cycle would give rise to four preleptotene spermatocytes According to this model the dark type A spermatogonia would in stage V of each cycle undergo a "differential mitosis" i e a division giving rise to two morphologically distinct spermatogonia a dark type A considered as a new stem cell and a pale type A spermatogonium considered as a differentiated cell Were such a differential mitosis to occur then following the divisions of type *Ad* cells in stage V of the cycle pairs of mophologically different cells i e one

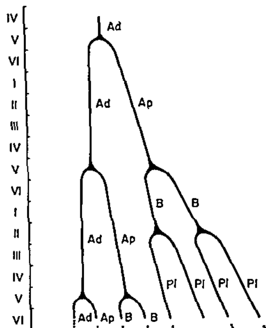


Fig 9 Diagram showing the simplest possible model illustrating the development of spermatogonia It is built on the cell ratio *Ad Ap B Pl* being equal to 1 1 2 4 and on a number of assumptions (see text)

On the left the stages of the cycle are indicated (Roman numerals) The divisions of cells are indicated by the junction of three lines and are located in stages *V* and *II* of the cycle According to this model the mitoses of dark type A spermatogonia (*Ad*) are differential i e giving rise to two morphologically distinct cells The divisions of pale type A (*Ap*) and type B (*B*) spermatogonia are "equivalent" i e producing two morphologically similar cells This model would explain the continuous renewal of stem cells (*Ad*) and the production of preleptotene primary spermatocytes (*Pl*) (For a discussion of this model see text)

dark plus one pale spermatogonium should be found along the tubular limiting membrane However spermatogonial maps disclosed clusters of identical cells within which spermatogonia formed identical pairs Furthermore it became apparent that these pairs of identical cells persisted throughout the cycle and after a 16-day interval (i e the duration of one cycle in man Heller and Clermont 64) divided in pairs the two cells in every pair being at the same phase (prophase metaphase etc) of mitosis This last observation was not in accord with the data of Roosen Runge and Barlow (53) who reported that

clusters of mitotic cells were composed of either odd or even numbers of dividing spermatogonia

Thus the differential mitosis postulated in the first model (fig 9) had to be replaced by an equivalent mitosis i e a mitosis giving rise to two morphologically identical cells This was done in figure 10 which presents a model of cell renewal in which the spermatogonia were arranged in pairs According to this scheme therefore one member of a pair of stem cells (*Ad*) would give rise to a pair of new stem cells while the other member would produce a pair of the more differentiated spermatogonia (*Ap*) These in turn would produce type B spermatogonia which would give rise to spermatocytes The existence of equivalent mitoses instead of differential mitoses during the proliferative cycle of spermatogonia was also reported in the seminiferous epithelium of the monkey (Clermont and Leblond 59) and of the rat (Clermont 62) Equivalent mitoses were also observed in the actively renewing esophageal epithelium of the rat by Pereira and Leblond (65) indicating that the phenomenon was not exclusive to the seminiferous epithelium

Consideration of the initial impetus for the differentiation of spermatogonia into spermatocytes

One portion of the present model however had to be examined more closely (heavy line of fig 10) The division of a stem cell which maintained the stock of

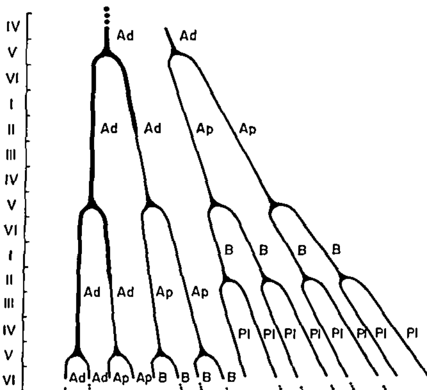


Fig 10 A more elaborate diagram to illustrate the mode of development and renewal of spermatogonia in man The Roman numerals on the left of the diagram indicate the stages of the cycle

Lettering *Ad* dark type A spermatogonia *Ap* pale type A spermatogonia *B* type B spermatogonia *Pl* preleptotene primary spermatocytes

This model takes into account the arrangement in pairs of the dark and pale type A spermatogonia Thus a pair of dark type A spermatogonia starts proliferating in stage V of the cycle and gives rise by equivalent mitoses to pairs of dark and pale type A spermatogonia While the pair of dark type A spermatogonia repeats the sequence in stage V of the next cycle the pale type A *spermatogonia yield type B spermatogonia which in stage II of* the following cycle produce preleptotene spermatocytes This model gives a statistical representation of the behavior of the spermatogonial population as a whole (see text)

stem cells gave rise to two potentially different type *Ad* cells (one *Ad* precursor of new *Ad*s and one *Ad* precursor of *Ap*s) Since there was no morphological expression of these potentialities it was not possible to verify by cytological means the existence of pairs of such differently fated cells But there was one fact which seemed to indicate that the heavy line part of the model did not necessarily represent the exact behavior of every stem cell this was the fact that spermatogonia of both types (*Ad* and *Ap*) had a clearcut tendency to form clusters of identical cells This would suggest that during the mitosis of type A spermatogonia groups of dark type A cells would give rise exclusively to clusters of new dark type A stem cells while other groups of dark type A spermatogonia under the influence of some unidentified impetus would yield clusters of the more differentiated pale type A spermatogonia Since the dark and the pale type A spermatogonia were produced in such a way as to maintain an exact 1 1 proportion to one another it may be further speculated that the spermatogonia themselves exerted an autoregulatory control and the impetus (stimulatory or inhibitory) mentioned previously would have its origin in the spermatogonial population itself Autoregulatory mechanisms of this nature have already been proposed for other systems (Stich 58 Weiss 53)

At any rate the model proposed (fig 10) may still be taken as a correct statistical representation of the behavior of the spermatogonial population as a whole and may be used to answer Branca's (24) questions To his first question "Through how many mitoses does a spermatogonium pass before its transformation into a spermatocyte? the answer would be that a spermatogonial stem cell (*Ad*) passed through three successive mitoses before giving rise to a generation of spermatocytes (fig 10 progeny of *Ad* on the right) To the second query Is this number of mitoses fixed? Is it variable? it appeared judging from the constancy of cell ratios from one biopsy to another that this number of mitoses was fixed Lastly to the questions Are the two daughter cells of a given mitosis always two spermatogonia or two spermatocytes? Or does one of the two daughter cells become a spermatogonium and the other a spermatocyte?" one is led to answer in view of the fact that the spermatogonia of various types are generally arranged in pairs that in the series of spermatogonial divisions the first two give rise to pairs of identical spermatogonia (*Ap* or *B*) and the third spermatogonial divisions yield pairs of preleptotene spermatocytes The existence of differential mitoses implied in the second part of Branca's question to explain the continuous renewal of the spermatogonial population does not appear to take place The new stem cells (*Ad*) and the more differentiated spermatogonia (*Ap*) are both formed by ordinary "equivalent divisions

ACKNOWLEDGMENTS

This work was supported by a grant from the Population Council Inc The assistance of Drs Claire Huckins and C P Leblond in the preparation of the manuscript is gratefully acknowledged Dr Carl G Heller Pacific Northwest Research Foundation Seattle Washington is given thanks for providing the biopsies The illustrations were prepared by Mrs Margot Oeltzschner

LITERATURE CITED

Branca A 1924 Les canalicules testiculaires et la spermatogenese de l homme (Etude cytologique) Arch Zool exp 62 53-252

Clermont Y 1962 Quantitative analysis of spermatogenesis of the rat A revised model for the r newal of spermatogonia Am J Anat *111* 111-130

——— 1963 The cycle of the seminiferous epithelium in man Am J Anat 112 35-52

Clermont Y and C P Leblond 1959 Differentiation and renewal of spermatogonia in the monkey *Ma acus hesus* Am J Anat *104* 237-274

Cle mont Y C P Leblond and B Messier 1959 Duree du cycle d l epithelium seminal du rat Arch Anat micr morph exp *48bis* 37-56

Heller C G and Y Clermont 1964 Kinetics of the germinal epithelium in man Rec Progr Horm Res 20 545-575

Leblond C P and Y Clermont 1952 Definition of the stages of the cycle of the seminiferous epithelium in the rat Ann N Y Acad Sci 55 548-573

Leblond C P E Steinberg r and E C Roosen Runge 1963 Conference on Physiological Mechani ms Concerned with Conception Perg m n Press N Y 1-72

Mancini R E R Narbaitz and J C Lavieri 1960 Origin and d elopment of the germina

clusters of mitotic cells were composed of either odd or even numbers of dividing spermatogonia

Thus the differential mitosis postulated in the first model (fig 9) had to be replaced by an equivalent mitosis i e a mitosis giving rise to two morphologically identical cells This was done in figure 10 which presents a model of cell renewal in which the spermatogonia were arranged in pairs According to this scheme therefore one member of a pair of stem cells (*Ad*) would give rise to a pair of new stem cells while the other member would produce a pair of the more differentiated spermatogonia (*Ap*) These in turn would produce type B spermatogonia which would give rise to spermatocytes The existence of equivalent mitoses instead of differential mitoses during the proliferative cycle of spermatogonia was also reported in the seminiferous epithelium of the monkey (Clermont and Leblond 59) and of the rat (Clermont 62) Equivalent mitoses were also observed in the actively renewing esophageal epithelium of the rat by Pereira and Leblond (65) indicating that the phenomenon was not exclusive to the seminiferous epithelium

Consideration of the initial impetus for the differentiation of spermatogonia into spermatocytes

One portion of the present model however had to be examined more closely (heavy line of fig 10) The division of a stem cell which maintained the stock of

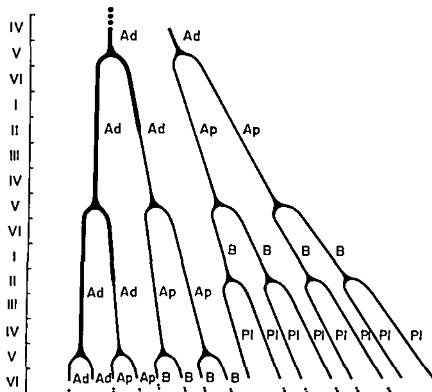


Fig 10 A more elaborate diagram to illustrate the mode of development and renewal of spermatogonia in man The Roman numerals on the left of the diagram indicate the stages of the cycle

Lettering *Ad* dark type A spermatogonia *Ap* pale type A spermatogonia *B* type B spermatogonia *Pl* preleptotene primary spermatocytes

This model takes into account the arrangement in pairs of the dark and pale type A spermatogonia Thus a pair of dark type A spermatogonia starts proliferating in stage V of the cycle and gives rise by equivalent mitoses to pairs of dark and pale type A spermatogonia While the pair of dark type A spermatogonia repeats the sequence in stage V of the next cycle the pale type A spermatogonia yield type B spermatogonia which in stage II of the following cycle produce preleptotene spermatocytes This model gives a statistical representation of the behavior of the spermatogonial population as a whole (see text)

stem cells gave rise to two potentially different type *Ad* cells (one *Ad* precursor of new *Ad*'s and one *Ad* precursor of *Ap*'s) Since there was no morphological expression of these potentialities it was not possible to verify by cytological means the existence of pairs of such differently fated cells But there was one fact which seemed to indicate that the heavy line part of the model did not necessarily represent the exact behavior of every stem cell this was the fact that spermatogonia of both types (*Ad* and *Ap*) had a clearcut tendency to form clusters of identical cells This would suggest that during the mitosis of type A spermatogonia groups of dark type A cells would give rise exclusively to clusters of new dark type A stem cells while other groups of dark type A spermatogonia under the influence of some unidentified impetus would yield clusters of the more differentiated pale type A spermatogonia Since the dark and the pale type A spermatogonia were produced in such a way as to maintain an exact 1 1 proportion to one another it may be further speculated that the spermatogonia themselves exerted an autoregulatory control and the impetus (stimulatory or inhibitory) mentioned previously would have its origin in the spermatogonial population itself Autoregulatory mechanisms of this nature have already been proposed for other systems (Stich 58 Weiss 53)

At any rate the model proposed (fig 10) may still be taken as a correct statistical representation of the behavior of the spermatogonial population as a whole and may be used to answer Branca's (24) questions To his first question "Through how many mitoses does a spermatogonium pass before its transformation into a spermatocyte?" the answer would be that a spermatogonial stem cell (*Ad*) passed through three successive mitoses before giving rise to a generation of spermatocytes (fig 10 progeny of *Ad* on the right) To the second query Is this number of mitoses fixed? Is it variable? it appeared judging from the constancy of cell ratios from one biopsy to another that this number of mitoses was fixed Lastly to the questions Are the two daughter cells of a given mitosis always two spermatogonia or two spermatocytes? Or does one of the two daughter cells become a spermatogonium and the other a spermatocyte? one is led to answer in view of the fact that the spermatogonia of various types are generally arranged in pairs that in the series of spermatogonial divisions the first two give rise to pairs of identical spermatogonia (*Ap* or *B*) and the third spermatogonial divisions yield pairs of preleptotene spermatocytes The existence of differential mitoses implied in the second part of Branca's question to explain the continuous renewal of the spermatogonial population does not appear to take place The new stem cells (*Ad*) and the more differentiated spermatogonia (*Ap*) are both formed by ordinary "equivalent" divisions

ACKNOWLEDGMENTS

This work was supported by a grant from the Population Council Inc The assistance of Drs Claire Huckins and C P Leblond in the preparation of the manuscript is gratefully acknowledged Dr Carl G Heller Pacific Northwest Research Foundation Seattle Washington is given thanks for providing the biopsies The illustrations were prepared by Mrs Margot Oeltzschner

LITERATURE CITED

Branca A 1924 Les canalicules testiculaires et la spermatogenese de l homme (Etude cytologique) Arch Zool exp 62 53–252

Clermont Y 1962 Quantitative analysis of spermatogenesis of the rat A revised model for the renewal of spermatogonia Am J Anat 111 111–130

——— 1963 The cycle of the seminiferous epithelium in man Am J Anat 112 35–52

Clermont Y and C P Leblond 1959 Differentiation and renewal of spermatogonia in the monkey *Macacus rhesus* Am J Anat 104 237–274

Clermont Y C P Leblond and B Messier 1959 Durée du cycle de l epithelium seminal du rat Arch Anat micr morph exp 48b s 37–56

Heller C G and Y Clermont 1964 Kinetics of the germinal epithelium in man Rec Progr Horm Res 20 545–575

Leblond C P and Y Clermont 1952 Definition of the stages of the cycle of the seminiferous epithelium in the rat Ann N Y Acad Sci 55 548–573

Leblond C P E Steinberge and E C Roosen Runge 1963 Conference on Physiological Mechanisms Concerned with Conception Pergamon Press N Y 1–72

Mancini R E R Narbaitz and J C Lavieri 1960 Origin and development of the germina

clusters of mitotic cells were composed of either odd or even numbers of dividing spermatogonia

Thus the differential mitosis postulated in the first model (fig 9) had to be replaced by an equivalent mitosis i e a mitosis giving rise to two morphologically identical cells This was done in figure 10 which presents a model of cell renewal in which the spermatogonia were arranged in pairs According to this scheme therefore one member of a pair of stem cells (*Ad*) would give rise to a pair of new stem cells while the other member would produce a pair of the more differentiated spermatogonia (*Ap*) These in turn would produce type B spermatogonia which would give rise to spermatocytes The existence of equivalent mitoses instead of differential mitoses during the proliferative cycle of spermatogonia was also reported in the seminiferous epithelium of the monkey (Clermont and Leblond 59) and of the rat (Clermont 62) Equivalent mitoses were also observed in the actively renewing esophageal epithelium of the rat by Pereira and Leblond (65) indicating that the phenomenon was not exclusive to the seminiferous epithelium

Consideration of the initial impetus for the differentiation of spermatogonia into spermatocytes

One portion of the present model however had to be examined more closely (heavy line of fig 10) The division of a stem cell which maintained the stock of

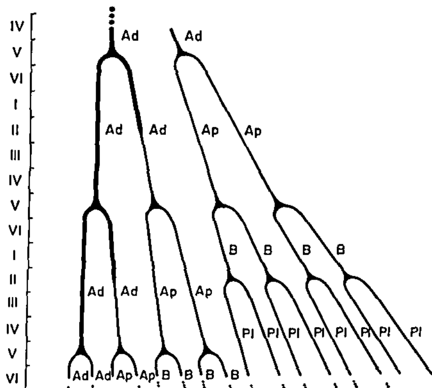


Fig 10 A more elaborate diagram to illustrate the mode of development and renewal of spermatogonia in man The Roman numerals on the left of the diagram indicate the stages of the cycle

Lettering *Ad* dark type A spermatogonia *Ap* pale type A spermatogonia *B* type B spermatogonia *Pl* preleptotene primary spermatocytes

This model takes into account the arrangement in pairs of the dark and pale type A spermatogonia Thus a pair of dark type A spermatogonia starts proliferating in stage V of the cycle and gives rise by equivalent mitoses to pairs of dark and pale type A spermatogonia While the pair of dark type A spermatogonia repeats the sequence in stage V of the next cycle the pale type A spermatogonia yield type B spermatogonia which in stage II of the following cycle produce preleptotene spermatocytes This model gives a statistical representation of the behavior of the spermatogonial population as a whole (see text)

stem cells gave rise to two potentially different type *Ad* cells (one *Ad* precursor of new *Ad*s and one *Ad* precursor of *Ap*s) Since there was no morphological expression of these potentialities it was not possible to verify by cytological means the existence of pairs of such differently fated cells But there was one fact which seemed to indicate that the heavy line part of the model did not necessarily represent the exact behavior of every stem cell this was the fact that spermatogonia of both types (*Ad* and *Ap*) had a clearcut tendency to form clusters of identical cells This would suggest that during the mitosis of type A spermatogonia groups of dark type A cells would give rise exclusively to clusters of new dark type A stem cells while other groups of dark type A spermatogonia under the influence of some unidentified impetus would yield clusters of the more differentiated pale type A spermatogonia Since the dark and the pale type A spermatogonia were produced in such a way as to maintain an exact 1 1 proportion to one another it may be further speculated that the spermatogonia themselves exerted an autoregulatory control and the impetus (stimulatory or inhibitory) mentioned previously would have its origin in the spermatogonial population itself Autoregulatory mechanisms of this nature have already been proposed for other systems (Stich 58 Weiss 53)

At any rate the model proposed (fig 10) may still be taken as a correct statistical representation of the behavior of the spermatogonial population as a whole and may be used to answer Branca s (24) questions To his first question "Through how many mitoses does a spermatogonium pass before its transformation into a spermatocyte? the answer would be that a spermatogonial stem cell (*Ad*) passed through three successive mitoses before giving rise to a generation of spermatocytes (fig 10 progeny of *Ad* on the right) To the second query Is this number of mitoses fixed? Is it variable? it appeared judging from the constancy of cell ratios from one biopsy to another that this number of mitoses was fixed Lastly to the questions Are the two daughter cells of a given mitosis always two spermatogonia or two spermatocytes? Or does one of the two daughter cells become a spermatogonium and the other a spermatocyte?" one is led to answer in view of the fact that the spermatogonia of various types are generally arranged in pairs that in the series of spermatogonial divisions the first two give rise to pairs of identical spermatogonia (*Ap* or *B*) and the third spermatogonial divisions yield pairs of preleptotene spermatocytes The existence of differential mitoses implied in the second part of Branca s question to explain the continuous renewal of the spermatogonial population does not appear to take place The new stem cells (*Ad*) and the more differentiated spermatogonia (*Ap*) are both formed by ordinary "equivalent" divisions

ACKNOWLEDGMENTS

This work was supported by a grant from the Population Council Inc The assistance of Drs Claire Huckins and C P Leblond in the preparation of the manuscript is gratefully acknowledged Dr Carl G Heller Pacific Northwest Research Foundation Seattle Washington is given thanks for providing the biopsies The illustrations were prepared by Mrs Margot Oeltzschner

LITERATURE CITED

Branca A 1924 Les canalicules testiculaires et la spermatogenese de l'homme (Etude cytologique) Arch Zool exp 62 53–252

Clermont Y 1962 Quantitative analysis of spermatogenesis of the rat A revised model for the renewal of spermatogonia Am J Anat 111 111–130

——— 1963 The cycle of the seminiferous epithelium in man Am J Anat 112 35–52

Clermont Y and C P Leblond 1959 Differentiation and renewal of permatogonia in the monkey *Macacus rhesus* Am J Anat 104 237–274

Clermont Y C P Leblond and B Messier 1959 Duree du cycle de l ep th lium sem nal du rat Arch Anat micr morph exp 48bis 37–56

Heller C G and Y Clermont 1964 Kinet cs of the germinal epithel um in man Rec Progr Horm Res 20 545–575

Lebl nd C P and Y Clermont 1952 Definition of the stages of the cycle of the seminiferous epithel um in the at Ann N Y Acad Sci 55 548–573

Leblond C P E Steinbe ge and E C Roosen Runge 1963 Conference on Physiological Mech nism Concerned with Conception Pergamon Press N Y 1–72

M ncini R E R Na baitz and J C Lavieri 1960 Origin and development of the germina

tive epithelium and Sertoli cells in the human testis cytological cytochemical and quantitative study Anat Rec *136* 477–490

Marques Pereira J P and C P Leblond 1965 Mitosis and differentiation in the stratified squamous epithelium of the rat esophagus Am J Anat *117* 73–90

Monesi V 1962 Autoradiographic study of DNA synthesis and the cell cycle in spermatogonia and spermatocytes of mouse testis using tritiated thymidine J Cell Biol *14* 1–18

Perey B Y Clermont and C P Leblond 1961 The wave of the seminiferous epithelium in the rat Am J Anat *108* 47–77

Roosen Runge E C 1962 The process of spermatogenesis in mammals Biol Rev 37 343–377

Roosen Runge E C and F D Barlow 1953 Quantitative studies on human spermatogenesis I Spermatogonia Am J Anat *92* 143–170

Stich H F and M L Florian 1958 The presence of a mitosis inhibitor in the serum and liver of adult rats Canad J Biochem Physiol *36* 855–859

Weiss P 1953 Some introductory remarks on the cellular basis of differentiation J Embryol Exp Morphol *1* 181–211

Cell Dynamics in the Intestine of the Mouse from Late Fetal Life to Maturity [1]

THOMAS M O CONNOR [2]
Department of Zoology Washington University St Louis Missouri

ABSTRACT A normal developmental pattern of the mitotic index growth of villi and crypts rate of cell extrusion and number of villi per duodenal cross section is presented for mice ranging in age from the seventeenth day of gestation through 48 days after birth These patterns are correlated with the normal increases in both length and weight of the intestine as a whole during this period Two periods were observed during which there is a 25% reduction in the mitotic index There is essentially no change in the mitotic index after the twenty first postnatal day Approximately 43% of the 48-day villus-crypt height is reached by birth and approximately 83% of the 48-day level is reached by the twenty first day No extrusion zones were observed in mice before birth and a threefold increase in the rate of extrusion was observed between the fifteenth and twenty first postnatal day Growth of the villus crypt epithelial cell population appears to be a result of a rate of cell extrusion which is much lower in the young than in the adult animal

The histology of the small intestine of mammals is well known (Bloom and Fawcett 62) Functionally its most important part is the intestinal epithelium which consists of a single layer of columnar cells This epithelium invests the crypts of Lieberkuhn and the slender folds and fingerlike projections of the small intestinal mucosa known as the villi Histologists have been aware for many years that the crypt epithelium is the locus of very intensive mitotic activity More recently it has been established that the new cells continuously being formed in the crypts glide up the sides of the villi to their tips where they are extruded into the intestinal lumen at the so-called "extrusion zones (Hooper 56 Leblond and Messier 58 Leblond Stevens and Bogoroch 48 Messier and Leblond 60 Quastler and Sherman 59)

All of the studies which have been reported in the literature concerning cell proliferation and migration in the intestinal epithelium have dealt with the adult animal after growth has ceased This obviously neglects a very important period in the life of this cell population — the period from fetal life to maturity During this period the intestine is growing Much of this growth is due to an increase in the number and the size of the villi During this period the cell loss at the extrusion zones cannot balance the cell production in the crypts as it apparently does after the attainment of adult size

The following study was undertaken in an attempt to determine the growing pattern of the villus-crypt epithelial cell population in relation to the growth of the intestine as a whole A normal developmental pattern of the mitotic index growth of villi and crypts rate of cell extrusion and number of villi per duodenal cross section will be presented for mice ranging in age from the seventeenth day of gestation through 48 days after birth An attempt will be made to correlate these patterns with the normal increases in both length and weight of the intestine as a whole during this period

MATERIALS AND METHODS

The animals used in this study were from a colony of White Swiss mice maintained in this laboratory They were fed Purina Lab Chow and had free access to water The 318 mice used ranged in age from the seventeenth day of gestation until 48 days after birth Seventeen-day fetal mice were chosen as a starting point because true villi are clearly present in the duodenum at this time Fetal ages were determined by noting the time of copulation allowing approximately six hours for

[1] Aid d by U S P bl H lth S rv c gr nts 2T1 HD-12 nd GM 03937

[2] P nt dd s Departm nt f B logy W h bu n U v ty of T pek T p k K n s

fertilization and counting the days from this point For all of the postnatal stages only litters consisting of nine mice were used The young remained with the mother for about 25 days All mice were sacrificed between 2 and 4 P M

Each animal used was weighed and then sacrificed by decapitation Of the nine mice of a litter two were used as sources of tissue for histological study the remaining seven were used for determining the weight and length of the intestine In all cases the sex of the animal was recorded When tissue was prepared the abdomen was opened immediately after decapitation and a piece of duodenum approximately one half to three fourth centimeter long was removed about 5 mm posterior to the pylorus and fixed in cold Zenker s fluid overnight Cross sections of the duodenum were cut at 4 μ and stained with hematoxylin and eosin

The number of interphase and mitotic epithelial cells in histological sections was determined by counting their nuclei The nuclei of chief and goblet cells were included in the counts but not those of migrating lymphocytes and Paneth cells Nuclear fragments that were too small to be identified with certainty were not included in the counts All counts were made with oil immersion (970 ×)

All stages of mitosis of the epithelial cells lining the crypts were counted Only crypts which were sectioned throughout their entire length were chosen Mitosis normally occurs only in the cells lining the crypts and in the present study no mitotic figures were ever found on the villi The identification of metaphase anaphase and telophase stages of the mitotic cycle was comparatively easy but the decision as to when a given nucleus had entered prophase was often more difficult A nucleus was judged to be in prophase when the chromatin was collected into clumps and accumulated along the nuclear membrane

The number of mitotic figures per 1 000 crypt cells was recorded An average of 6 000 cells was counted per animal The results are expressed as the percentage of crypt cells undergoing mitosis at the moment of fixation

To determine the changes in the height of the crypt and villus cell population during the above stated time period the number of nuclei were counted Only areas which showed a continuous epithelial layer from the tip of the villus to the base of the crypt were selected to insure that the full length of both structures was seen The number of nuclei lining one side of such a villus and crypt was then recorded Paneth cells were included in this count It was difficult to find many such perfect sections The number of cells in approximately six crypts and villi were counted per animal There was very little variation in the height of the villi and crypts within a given animal

In determining the percentage of villi with extrusion zones only those villi were examined in which the section passed through the tip as shown by the presence of a continuous single layer of nuclei in the epithelium Forty to eighty villus tips were examined per animal and classified as to whether they did or did not have extrusion zones The results are expressed as the per cent of villi having extrusion zones

Any change in the number of villi per cross section of the mouse duodenum was determined by counting the bases of the villi in six cross sections per animal The individual sections used were approximately 40 μ apart The number of villi per cross section did not vary by more than two in any given mouse

For the remaining seven mice of the litter the abdomen was opened and the intestine cut at the pylorus and at the most caudal part of the large intestine at the anus The coils were teased apart and freed from adjacent fat connective tissue and mesenteries Care was taken to avoid stretching the tube The entire tube was laid on a glass plate and straightened as much as possible without stretching and the total length and the length of its various parts were measured The intestine as a whole as well as the large intestine and the cecum were then weighed quickly on a torsion balance In most cases the intestinal contents were not removed In those in which the contents were removed the intestine was slit lengthwise and the material contained was very gently brushed out

RESULTS

1 Mitotic index

The mitotic indices of the crypt cell population of the developing mouse duodenum are presented in figure 1 Throughout this study the term "birth or "newborn" (NB) refers to mice sacrificed within 4 to 6 hours after birth Since crypts were not well developed from the seventeenth day of gestation through birth mitotic counts at these ages were made on nuclei which are found between the bases of the villi No mitotic figures were ever observed to be located anywhere but in spaces at the base of the villi

On the nineteenth day of gestation a significant drop in the mitotic index was observed and at birth the mitotic index was 25% lower than observed on the seventeenth and eighteenth days of gestation The mitotic activity increased after the second day of postnatal life and by the fifth day it reached a level approximating the earlier high value From the fifth through the twelfth day the mitotic index remained more or less constant Between the twelfth and thirteenth day there was again a significant drop in the mitotic index to a level of mitotic activity that lasted for six days with the lowest per cent of dividing nuclei being observed on the

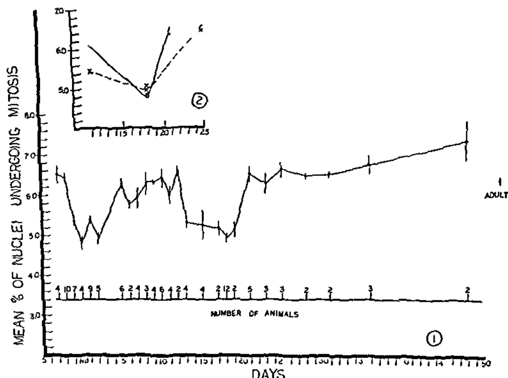


Fig 1 Mean per cent of crypt nuclei undergoing mitosis at any one time (mitotic index) Each dot indicates the mean of the mitotic indices of a group of mice at a particular age The vertical lines on either side of the dots indicate s the standard errors of the means With the exception of the seventeenth eighteenth nineteenth days of gestation newborn and the first postnatal day only two mice were used from a litter Mice on the seventeenth day of gestation are from one litter as are the newborn mice and the mice on the first postnatal day Mice on the eighteenth day of gestation are from three litters and mice on the nineteenth day of gestation are *from two litters*

Fig 2 Per cent of crypt nuclei undergoing mitosis at any one time in mice of the same litter at various days This graph shows the mitotic indices of two litters Each mark (or X) indicates the mitotic index of one mouse based on the number of mitotic figures per 6 000 crypt cells

eighteenth day The mitotic activity from the thirteenth to the nineteenth day after birth is 25% lower than the period from the fifth to the twelfth day

Twenty one day old mice showed a cryptal mitotic activity which had again returned to the previously attained high level From the twenty first to the thirty first day there was no change in the mitotic index and from the thirty first to the forty eighth day a slight increase was observed

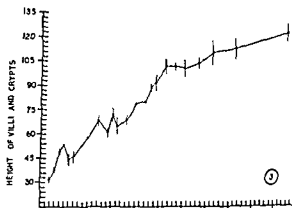
Since the mitotic activity appeared to be increasing somewhat at 48 days it was of interest to determine the mitotic index of the adult Three adult mice (wt 25 gm) were used and the results are shown in figure 1 The mitotic index of 6 33% does not differ significantly from the values obtained during the periods of high mitotic activity already reported To further establish the 25% reduction in mitotic activity observed on the eighteenth postnatal day (fig 1) mitotic counts of littermates were made on the eleventh eighteenth and twenty first or twenty fifth days after birth Figure 2 shows that 18 day old mice had mitotic indices 25% lower than those of 11 and 21 or 25 day old littermates

2 *Growth of villi and crypts*

The height of the villi and crypts which was determined by counting the number of epithelial nuclei from the tip of the villus to the base of the crypt increases rapidly from the seventeenth day of gestation up to birth (fig 3) This rapid increase is interrupted on the first day after birth by a slight reduction in the mean height of the villi and crypts By the second day after birth the height of the villi and crypts has increased somewhat and from this day until the seventh day the mean height increases rapidly From the seventh day to the thirteenth day no noticeable height increase occurs but from the thirteenth to the twenty first day the mean height of the villi and crypts is again increasing rapidly After the twenty first day the growth of the villi and crypts levels off Approximately 13% of the 48 day villus crypt height has been reached by birth and approximately 83% of the 48 day level has been reached by the twenty first day Most of this height increase is due to an increase in the height of the villus The crypts remain shallow during the first two postnatal weeks and only deepen markedly late in the third week

3 *Occurrence of extrusion zones*

On the seventeenth eighteenth and nineteenth day of gestation no extrusion zones were observed in any of the 21 mice examined (fig 4) Of the villi of the four newborn mice examined however 14% were observed to have extrusion zones The number of villi having extrusion zones



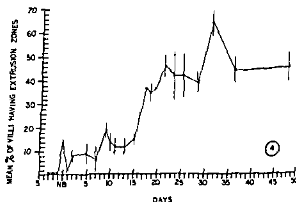


Fig 3 Height of villi and crypts based on the number of cells (nuclei) from the villus tip to the base of the crypt Each dot indicates the mean villus crypt height of a group of mice at a particular age The vertical lines = standard errors of the means

Fig 4 Mean per cent of villi having extrusion zones Each dot indicates the mean per cent of the villi showing extrusion zones for a group of mice at a particular age The vertical lines standard errors of the means Dots on the seventeenth eighteenth and nineteenth days of gestation indicate that no extrusion zones were observed Dots on the seventeenth and nineteenth postnatal days indicate only one mouse used

remains less than 10% from the first until the ninth day after birth when a value of 19% is reached From the ninth through the fifteenth day there is no increase in the per cent of villi with extrusion zones but between the fifteenth day and the twenty first day the per cent with extrusion zones increases threefold At 21 days 46% of the villi have extrusion zones and this level is maintained up through the forty eighth day with the exception of two 31 day-old mice Therefore as figure 4 shows the increases in the per cent of villi having extrusion zones occur in a step like manner

4 *Number of villi per duodenal cross section*

Figure 5 shows that the number of villa per duodenal cross section increases rapidly from the seventeenth through the nineteenth day of gestation This rapid increase does not continue over the next few days however At birth the newborn mouse exhibits essentially the same number of villi per cross section (26 ± 2 30) as was observed on the previous day (27 ± 1 07) and mice of 1 and 2 days of age are seen to have fewer villi per cross section (24 ± 1 53 and 23 ± 0 85 respectively) than mice on the day before birth The number of villi per cross section increases after the second postnatal day and levels off at a high value of 37 by the ninth day From the fifteenth to the eighteenth day a reduction in villi number is noticed This reduced level is significantly ($P < 0\,001$) lower than the level found on the ninth through eleventh days

5 *Weight and length changes*

The absolute and relative weight of the intestine and its component parts are shown in figures 6 and 7 The intestine is

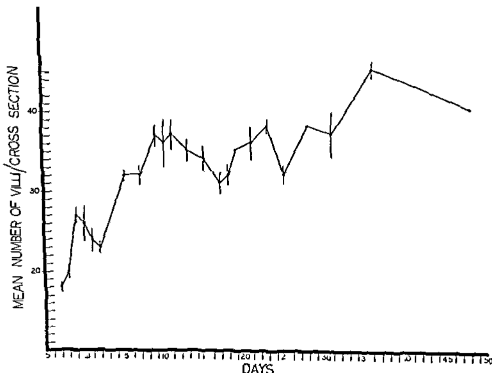


Fig 5 Mean number of villi per duodenal cross section Each dot indicates the mean number of villi per cross-section of a group of mice at a particular age Only one mouse was used on the nineteenth and twenty eighth postnatal days The mean at 48 days represents two mice who showed exactly the same number of villi

increasing in both absolute and relative weight from the seventeenth day of gestation through birth After birth a reduction in weight is observed during the first day From the second day through the fifteenth day the absolute weight of the intestine increases slowly but no increase is observed in relative weight After the fifteenth day after birth both the absolute and relative weight increase significantly however whereas the relative weight begins leveling off at 23 days the absolute weight does not This indicates that from the twenty third to the forty eighth day the intestine and the body weight are increasing at approximately the same rate

Only a small percentage of the rapid increase in both absolute and relative weight of the intestine during the period from 15 days to 21 days is due to the increase weight and or retention of the solid food in the intestinal lumen after weaning This was indicated by testing 13 day and 23 day old mice Using six litters it was found that the relative weight of the intestine with its contents increased 148% from the thirteenth to the twenty third day without the intestinal contents a 109% increase was recorded Although the difference in the intestinal contents does account for some of the increase observed during this period by far the greatest increase is due to actual increase in the substance of the intestine itself

The absolute length of the intestine increases continually from the seventeenth day of gestation to 48 days after birth (fig 8) The relative length of the intestine (length of intestine gram body weight) shows a different pattern (fig 9) Early

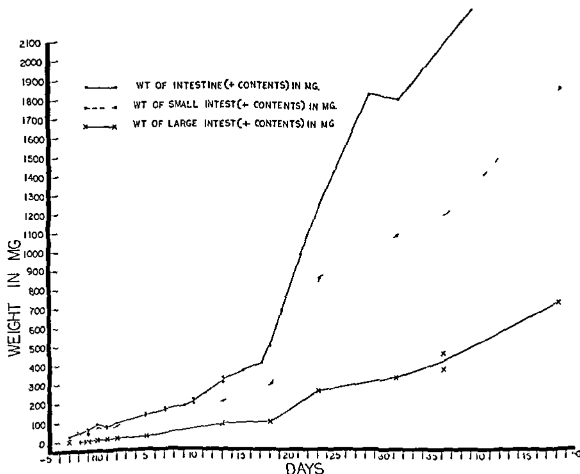


Fig 6 Weight of the ... e small intestine and large intestine in milligram The weight of the large in... eight minu the weight of the cecum The weight of the cecum if plotted woul... actly the ame values as are shown for the large intestine Each mark indicates ... ained from approximately six littermate mice

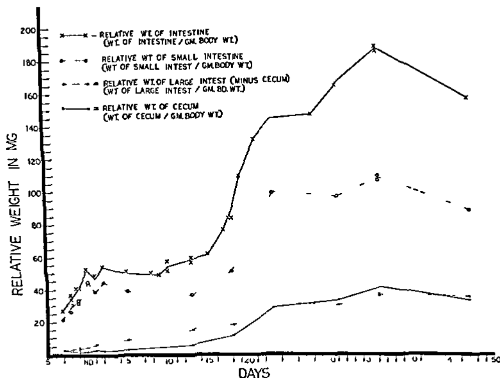


Fig 7 Relati e weights of the whole intestine small int stine large intestine and cecum in milli grams Ea h m rk indicates a mean value obtained from approximately six littermate mice

in the development of the mouse the in testine is very long compared to the weight of the body From the seventeenth day of gestation to 48 days after birth however the body of the animal increases in weight faster than the intestine increases in length so that the relative length decreases steadily The slight increase in the rela tive length of the intestine on the day after birth is to be expected since there is a loss of body weight on that day with no cor responding decrease in the absolute length of the intestine

6 *Sex differences*

From the seventeenth day of gestation through 18 days after birth there were no significant differences in body weights be tween the two sexes At 19 days male mice weighed approximately one half gram more than did their female littermates and from this day on the male mice al ways weighed more on an average than did the female mice At 48 days the differ ence in weight between the two sexes was approximately 2 gm The intestines of male mice 19 days or older weighed slightly more and were somewhat longer than those of female mice at the same age However there was no difference in the relative weight and relative length of the intestine between the two sexes The weight of the cecum the weight of the large intestine and the length of the large intestine did not reflect the body weight increase observed in the males when com pared to females therefore the relative weight of the cecum and large intestine and the relative length of the large intestine were slightly higher in the female mice than in the male mice during this period It can be concluded then that between 19 to 48 days of age both the weight and the length of the intestine of the male mouse are somewhat greater than in the female mouse and that most if not all of this difference is due to the greater size of the small intestine in males

increasing in both absolute and relative weight from the seventeenth day of gestation through birth. After birth a reduction in weight is observed during the first day. From the second day through the fifteenth day the absolute weight of the intestine increases slowly but no increase is observed in relative weight. After the fifteenth day after birth both the absolute and relative weight increase significantly; however, whereas the relative weight begins leveling off at 23 days, the absolute weight does not. This indicates that from the twenty third to the forty eighth day the intestine and the body weight are increasing at approximately the same rate.

Only a small percentage of the rapid increase in both absolute and relative weight of the intestine during the period from 15 days to 21 days is due to the increase weight and or retention of the solid food in the intestinal lumen after weaning. This was indicated by testing 13 day and 23 day old mice. Using six litters it was found that the relative weight of the intestine with its contents increased 148% from the thirteenth to the twenty third day; without the intestinal contents a 109% increase was recorded. Although the difference in the intestinal contents does account for some of the increase observed during this period, by far the greatest increase is due to actual increase in the substance of the intestine itself.

The absolute length of the intestine increases continually from the seventeenth day of gestation to 48 days after birth (fig. 8). The relative length of the intestine (length of intestine gram body weight) shows a different pattern (fig. 9). Early

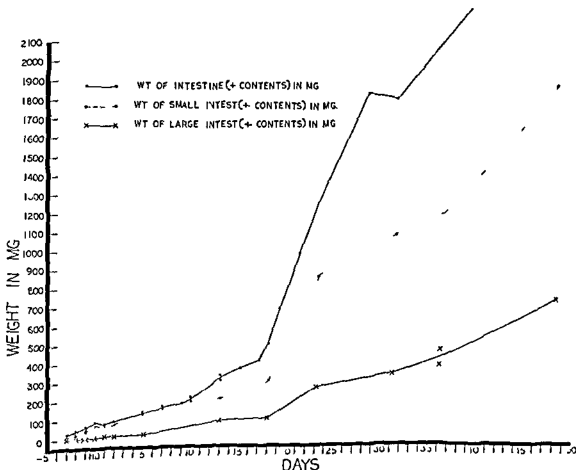


Fig 6 Weight of the whole intestine, small intestine and large intestine in milligram. The weight of the large intestine is the weight minus the weight of the cecum. The weight of the cecum if plotted would show almost exactly the same value as are shown for the large intestine. Each mark indicates a mean value obtained from approximately six littermate mice.

mental period On this same day 14% of the villi were observed to have extrusion zones The result of this decreased cell production and increased cell loss presumably leads to the reduction in the villi crypt height observed on the following day

From the thirteenth to the nineteenth day the per cent of villi showing extrusion zones increases threefold It is during this period that a 25% reduction in mitotic activity occurs Under these circumstances one would expect either a decrease in villus-crypt height or at least a reduction in the rapidity with which the height of the villus and crypts is increasing in comparison with the rate observed on the preceding days However figure 3 shows that there is no such effect on the mean height increase from the thirteenth through nineteenth day The period just preceding this also presents a puzzling situation which is unexplainable with the data at hand From the ninth through the twelfth day the mitotic index is high and the rate of cell extrusion is at a low level Yet during this time the villus-crypt height does not increase

Currently there are two main theories as to the causes of cell loss The first holds that loss of cells from the villus tip is to some extent a consequence of the pressure exerted by the cells crowded up from the regions of cell formation Recently Grad and Stevens (50) Hughes et al (58) and Sherman and Quastler (60) have shown that pressure from mitotic activity is not the only cause of cell extrusion The second theory has to do with muscular contraction Villus motility is affected by contractions of strands of smooth muscle which arise from the muscularis mucosae and insert into connective tissue underlying the villus tips (Hooper 56) It is conceivable that such muscle contractions could flex the epithelial basement membrane and thus help to dislodge the cells at the tip

This study tends to support the idea that pressure from mitotic activity is not the only cause of cell extrusion By comparing figures 1 and 4 it can be seen that during the period from the thirteenth to the nineteenth postnatal day the mitotic index is at a low level However an increase in the per cent of extrusion zones is observed during this period Although the "pressure" or "push" from the region of cell proliferation is reduced extrusion increases

The role of muscular contraction of the villi in the extrusion mechanism may be strengthened by the work presented here On the seventeenth eighteenth and nineteenth days of gestation no extrusion zones were observed as indicated by figure 4 During this period the intestinal lumen is essentially empty Histological examination of these intestines showed none of the villi in a contracted condition Villi in a contracted state were observed however in many of the older mice Therefore it is assumed that there is probably little or no contraction of the villi during this period thus resulting in no cell extrusion and in rapid villi growth The newborn mouse however shows 14% of the villi having extrusion zones This increase may be the result of muscular contractions of the villi in response to their new environment — milk and its attendant enzymes After the fifteenth day there is a rapid increase in the per cent of villi with extrusion zones On about the seventeenth day the young mouse begins sampling solid food Since most of the increase in extrusion rate is observed before the switch to solid food it cannot be said that the threefold increase in extrusion activity is a result of a change in diet The increased extrusion rate appears to be a response to the general physiological changes occurring at this time

Sherman and Quastler (60) and Messier and Leblond (60) suggest that crypt cells are made to leave the crypt by the continuous loss of cells from the tip of the villus Presumably the cell loss from the surface induces nearby cells to wander in to cover the gap and the neighboring cells to follow suit so that eventually the whole epithelium glides towards the surface This may be true of the adult intestine but such a mechanism does not seem entirely adequate to explain migration in the developing intestine If the loss of one cell was replaced by only one cell which was induced to migrate by the loss of the former growth would not occur During the growing period "migration must exceed extrusion If migration was solely dependent upon the "inducing action of extrusion

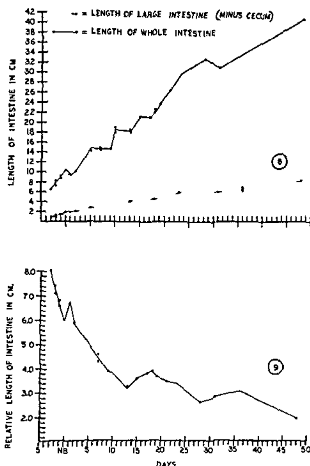


Fig 8 Changes in the length of the whole intestine and the large intestine during the course of this study Each dot indicates a mean value obtained from approximately six mice taken from the same litter

Fig 9 Changes in the relative length of the intestine (length of intestine in cm/gm body weight) during the course of this study Each dot indicates a mean value obtained from approximately six littermate mice

The mitotic index showed no sex difference during the period from the seventeenth day of gestation through 48 days after birth Similarly there were no sex differences observed for the height of the villi and crypts number of extrusion zones or number of villi per duodenal cross section during this time period

DISCUSSION

It has been shown above (figs 3 and 5) that much of the growth of the small intestine of the mouse involves an increase in both the number and in particular the size of the villi Growth or increase in cell number of the villus crypt cell population could occur in a number of ways Growth might result from a very high mitotic index This mitotic index would of necessity have to be much higher than the adult level since the mitotic activity in the adult intestinal epithelium results in essentially no growth It has been shown in this work however that villus growth is not the result of mitotic activity greater than that found in the adult A mitotic index of 6 33% was found in the crypt cell population of the adult mice of this colony *At no period during the growth of the villi* is a significantly higher mitotic index observed (fig 1)

Villus growth appears to be the result of a cell extrusion rate which is below that of the adult level (fig 4) From the twenty first through the forty eighth day 35 to 50% of the villi possess extrusion zones with no significant increase or decrease during this period In the adult rat 33% of the villi of the duodenum show extrusion zones (Leblond and Stevens 48) Earlier than the twenty first day however extrusion zones becomes increasingly scarce It has been shown that 43% of the 48 day villus crypt height has been reached by birth During this period no extrusion zones were observed Presumably then all mitoses found in the epithelial cell population during this period add to the population size Another 40% of the 48 day villus crypt height is achieved between the first and twenty first day During the greater part of this period only 8 to 15% of the villi have extrusion zones (fig 4) This is well below the post 21 day or adult level From these observations it is concluded that growth of the villus cell population is not a result of a mitotic activity which is greater in the young than in the adult but to a rate of cell extrusion which is much lower during the period of greatest villus growth

By comparing figures 1 3 and 4 other features of villus crypt growth can be illuminated First the leveling off of the height of the villus crypt population after 21 days is explained by the threefold increase in cell extrusion observed at this time Second as mentioned earlier there is a reduction in the mean height of the villi and crypts on the first day after birth On the day of birth the mitotic index was observed at its lowest level of the develop

day and therefore the above explanation may fit the decrease in villi number per cross section observed at this time

The observed increase in intestinal mass might result from (1) increase in the number of cells (2) enlargement of the cells and (3) increase of intercellular material An increase in weight per nucleus with age would provide an index of weight gain which is not due to an increase in the number of cells Enesco and Leblond (62) have found that the intestine of rats shows no significant change in the weight per nucleus between 7 and 95 days of age but the number of nuclei (cells) increases continually If the same is true for the mouse the rapid increase in absolute and relative weight observed from the fifteenth through the twenty third postnatal day would appear to be the result of cellular increase There is however no corresponding rapid increase in intestinal length during this period (fig 8) nor is there a disproportionate growth in villi crypt height (fig 3) although both show a steady increase at this time Apparently much of the weight increase of the intestine during this period must be due to the multiplication of non-crypt cells This view is supported by the fact that the thickness of the mucosal wall (i e the radial distance from the villi bases to the adventitia) doubles between the nineteenth and twenty second postnatal days in the mouse duodenum (Moog 51) This doubling plus the normal increases in the epithelial cell population of the villus could explain the observed weight gain

ACKNOWLEDGMENT

I am greatly indebted to Dr Florence Moog for her suggestions and helpful comments throughout the course of this work

LITERATURE CITED

Bloom W and D W Fawcett 1962 A Text book of Histology W B Saunders Company Philadelphia

Chaud y A P F Halbe g and J J Bittner 1956 Reduction of mitotic activity in pinna epidermis of mice given cortisol or 9 fluorocortisol Proc Soc Exp Biol Med *91* 602–604

Enesco M and C P Leblond 1962 Increase in cell number as a factor in the growth of the organs and tissues of the young male rat J Embryol Exp Morph *10* 530–56.

Grad B and C E Stevens 1950 Histological changes produced by a single large injection of radioactive phosphorus (P^{32}) into albino rats and C_3H mice Cancer Res *10* 289–296

Hooper C E 1956 Cell turnover in epithelial populations J Histochem and Cytochem 4 531–540

Hughes W L V P Bond G Brecher E P Cronkite R B Painter R Quastler and F G Sherman 1958 Cellular proliferation in the mouse as revealed by autoradiography with tritiated thymidine Proc Natl Acad Sci *44* 476–483

Josimovich J B A J Ladman and H W Deane 1954 A histophysiological study of the developing adrenal cortex of the rat during fetal and early postnatal stages Endocrinology *54* 627–639

Leblond C P and R Carriere 1955 The effect of growth hormone and thyroxine on the mitotic rate of the intestinal mucosa of the rat Endocrinology *56* 261–266

Leblond C P and B Messier 1958 Renewal of chief cells and goblet cells in the small intestine as shown by radioautography after injection of thymidine H into mice Anat Rec *132* 247–259

Leblond C P and C E Stevens 1948 The constant renewal of the intestinal epithelium in the albino rat Anat Rec *100* 357–378

Leblond C P C E Stevens and R Bogoroch 1948 Histological localization of newly formed desoxyribonucleic acid Science *108* 531–533

Leblond C P and B E Walker 1956 Renewal of cell populations Physiol Rev *36* 255–276

MacDowell E C W Gates and C MacDowell 1930 The influence of the quantity of nutrition upon the growth of the suckling mouse J Gen Physiol *13* 529–545

Messier B and C P Leblond 1960 Cell proliferation and migration as revealed by radioautography after injection of thymidine H into male rats and mice Am J Anat *106* 247–285

Moog F 1951 The functional differentiation of the small intestine II The differentiation of alkaline phosphomonoesterase in the duodenum of the mouse J Exp Zool *118* 187–208

——— 1953 The functional differentiation of the small intestine III The influence of the pituitary adrenal system on the differentiation of phosphatase in the duodenum of the suckling mouse J Exp Zool *124* 329–346

——— 1961 Regional differences in the alkaline phosphatases of the small intestine of the mouse from birth to one year Devel Biol 3 153–174

——— 1965 Acceleration of the normal and corticoid induced increas of alkaline phosphatase in the duodenum of the nursling mouse by actinomycin D puromycin colchicine and ethionine Advances in Enzyme Regulation 3 221–236

zones migration should be absent during the late periods of gestation when no extrusion zones were observed Yet this is the most active period of villus crypt height increase Migration must be taking place from the site of cell proliferation The inducing action of extrusion zones cannot account for all the migration observed during the period of growth

The fluctuations in the mitotic index of the developing duodenal crypt population (fig 1) raise the question of a controlling mechanism It may be significant that the *mitotic index is* reduced at two periods (the first begins before and continues through birth the second begins before *and continues through weaning) when far* reaching physiological changes are taking place within the mouse Both these periods precede and coincide with times when the mouse is experiencing either the availability of food (milk) for the first time or experiencing a change in diet One might expect that during these transition periods there may be a slight reduction in the amount of nutrients in the blood stream An involuntary reduction in food consumption has been reported in the mouse preceding and during weaning by MacDowell *et al* (30) *From the work of Hughes* et al (58) Leblond and Messier (58) Leblond and Stevens (48) and Leblond and Walker (56) it would appear to be extremely unlikely that a moderate reduction in food consumption would have any effect on the mitotic index of the intestine

During the period under consideration the epithelial cells of the duodenum show changes in their biochemistry Moog (51) *has shown that during this time there are* two periods of rapid increase in alkaline phosphatase activity — one just before birth and the second just before weaning The highest levels of phosphatase activity are reached in the duodenum by a 15 fold upsurge beginning at the end of the second week of postnatal life and *continuing into* the middle of the third week The upsurge in activity is accompanied by a pronounced shift in *the rapidity* with which the enzyme hydrolyzes phenylphosphate relative to B glycerophosphate (Moog 61) Figure 1 shows that it is precisely during this period that a 25% reduction in *mitotic* activity is observed This finding is consistent *with the idea expressed* by Moog (65) that mitotic retardation might possibly contribute to the conversion of duodenal phosphatase from a less active B glycerophosphate preferring to a more active phenylphosphate preferring type

Both periods showing a low mitotic index (fig 1) coincide with times of cortical stimulation (Josimovich et al 54 Moog 53) Recently it has been shown that various cortical hormones have the effect of reducing mitotic activity (Chaudry et al 56 Rasanen 62 Rasanen 63) Of the various tissues studied *the intestine* appears to be the least affected by the cortical substances This is in agreement with *Moog (65) who observed no* significant effect on the mitotic index of the duodenum six hours after hydrocortisone injection It is not possible therefore at this time to relate the observed reductions in the mitotic index to adrenal activity however the possibility of cortical influence does exist

Leblond and Carriere (55) and Leblond and Walker (56) have shown that growth hormone from the hypophysis is needed for the maintenance of the normal high level of mitotic activity in the intestine *The low mitotic index observed from* the thirteenth to the nineteenth postnatal day may then be part of a general growth decrease observed during this period (MacDowell et al 30)

During the period of intestinal growth the number of villi per duodenal *cross section* increases By the ninth postnatal day the adult level has about been reached (fig 5) Two observed decreases are be*lieved to be significant The first occurs* during the first few days after birth and the second occurs from the eleventh through the seventeenth postnatal day It is very doubtful that these observed decreases are due to an actual disappearance of villi already formed It might be as*sumed that these decreases* are due *to* lengthening of the intestine with the consequent increase in the spacing between villi Such an explanation however clearly fails to fit the decrease at birth for the intestine does not increase in length at that time (fig 8) The intestine is *rapidly increasing in length* from the eleventh through the seventeenth postnatal

dav and therefore the above explanation may fit the decrease in villi number per cross section observed at this time

The observed increase in intestinal mass might result from (1) increase in the number of cells (2) enlargement of the cells and (3) increase of intercellular material An increase in weight per nucleus with age would provide an index of weight gain which is not due to an increase in the number of cells Enesco and Leblond (62) have found that the intestine of rats shows no significant change in the weight per nucleus between 7 and 95 days of age but the number of nuclei (cells) increases continually If the same is true for the mouse the rapid increase in absolute and relative weight observed from the fifteenth through the twenty third *postnatal day would appear to be the result* of cellular increase There is however no corresponding rapid increase in intestinal length during this period (fig 8) nor is there a disproportionate growth in villi crypt height (fig 3) although both show a steady increase at this time Apparently much of the weight increase of the intestine during this period must be due to the multiplication of non crypt cells This view is supported by the fact that the thickness of the mucosal wall (i e the radial distance from the villi bases to the adventitia) doubles between the nineteenth and twenty second postnatal days in the mouse duodenum (Moog 51) This doubling plus the normal increases in the epithelial cell population of the villus could explain the observed weight gain

ACKNOWLEDGMENT

I am greatly indebted to Dr Florence Moog for her suggestions and helpful comments throughout the course of this work

LITERATURE CITED

Bloom W and D W Fawcett 1962 A Text book of Histology W B Saunde s Comp ny Philadelph a

Chaud y A P F Halberg and J J Bitt ier 1956 Reduction of mitoti a tivity in pinna epi de mis of mice g ven corti ol or 9 fluorocort sol P o Soc Exp Biol Med 91 602–604

Enes o M and C P Leblond 1962 I crea e in cell number a a factor in the growth of the organs and tissues of the young male rat J Embryol Exp Morph 10 530–562

Grad B and C E Stevens 1950 Histological changes produced by a single large injection of radioactive phosphorus (P ²) into albino rats and C H mice Cancer Res 10 289–296

Hooper C E 1956 Cell turnover in epithelial populations J Histochem and Cytochem 4 531–540

Hughes W L V P Bond G Brecher E P Cronkite R B Painter R Quastler and F G Sherman 1958 Cellular proliferation in the mouse as revealed by autoradiography with *tritiated thymidine Proc Natl Acad Sci 44* 476–483

Josimovich J B A J Ladman and H W Deane 1954 A histophysiological study of the developing adrenal cortex of the rat during fetal and early postnatal stages Endocrinology *54* 627–639

Leblond C P and R Carriere 1955 The effect of growth hormone and thyroxine on the mitotic rate of the intestinal mucosa of the rat Endocrinology 56 261–266

Leblond C P and B Messier 1958 Renewal *of chief cells and goblet cells in the small* intestine as shown by radioautography after injection of thymidine H into mice Anat Rec *132* 247–259

Leblond C P and C E Stevens 1948 The constant renewal of the intestinal epithelium in the albino rat Anat Rec *100* 357–378

Leblond C P C E Stevens and R Bogoroch 1948 Histological localization of newly formed desoxyribonucleic acid Science *108* 531–533

Leblond C P and B E Walker 1956 Renewal of cell populations Physiol Rev *36* 255–276

MacDowell E C W Gates and C MacDowell 1930 The influence of the quantity of nutrition upon the growth of the suckling mouse J Gen Physiol *13* 529–545

Messier B and C P Leblond 1960 Cell proliferation and migration as revealed by radioautography after injection of thymidine H into male rats and mice Am J Anat *106* 247–285

Moog F 1951 The functional differentiatio i of the small intestine II The differentiation of alkal ne phosphomonoesterase in the duodenum of the mouse J Exp Zool *118* 187–208

——— 1953 The functional diffe entiat on of the small intestine III The influence of the pituitary adrenal system on the differentiation of ph sphatase in the duodenum of the suckling mouse J Exp Zool *124* 329–346

——— 1961 Regional diffe ences in the alkaline phosphatases of the small intestine of the mouse from bi th to one yea Devel Biol 3 153–174

——— 1965 Acceleration of the normal and *o ticoid nduced increase of alkaline* phosphatase in the duode um of the nursling mouse by act nomycin D pu omycin colchicine and eth onine Advances in Enzyme Regulation *3* 221–236

Quastler H and F G Sherman 1959 Cell *population kinetics in the intestinal epithelium* of the mouse Exp Cell Res *17* 420–438

Rasanen T 1962 Mitotic activity in rat epi dermis and gastric mucosa after gluco and mineralocorticoid administration Growth *26* 1–14

——— 1963 Fluctuations in the mitotic fre *quency of the glandular stomach and intestine* of rat under the influence of ACTH gluco corticoids stress and heparin Acta Physiol Scand 58 201–210

Sherman F G and H Quastler 1960 DNA synthesis in irradiated intestinal epithelium Exp Cell Res *19* 343–360

Cytological Changes in Hepatic and Reticuloendothelial Cells in Rabbit Liver Following Gonadectomy [1]

DORIS R NATHANIEL AND EDWARD J H NATHANIEL

Division of Laboratories Cedars of Lebanon Hospital Los Angeles California and Department of Pathology and Anatomy Medical College of Georgia and Eugene Talmage Memorial Hospital Augusta Georgia

ABSTRACT Male rabbits of the New Zealand strain were castrated and sacrificed after two four and six weeks The animals were maintained on normal diet *ad libitum* Alterations in hepatic and reticuloendothelial cells were studied with the electron microscope The response of the hepatic cell was as follows The most significant change during the second week was a considerable increase in agranular reticulum which was concentrated along the cell borders as well as within the cells It was associated with glycogen particles Accumulation of glycogen was progressive from the second week onward There was a decrease in the smooth surfaced reticulum as the glycogen content increased It is suggested that the agranular reticulum is related to glycogen metabolism An increase in lipids was also present It is observed that gonadectomy has induced an increase in glycogen and lipid content of the cell In addition the nucleus showed a moderate condensation of chromatin along the inner margin There was a slight increase in the rough surfaced endoplasmic reticulum Castration also produced changes in the Kupffer cell This was characterized by the shortening of the cell processes resulting in reduction in cell size There were fewer inclusions within the cell

There is evidence in the literature that estrogenic hormones have a profound effect on the phagocytic property of the reticuloendothelial cells of the liver (Biozzi et al 57 Heller et al 57) Nicol and Bilbey (60) in their study of the effects of various steroids on the phagocytic activity of the reticuloendothelial system found that estradial benzoate was a powerful stimulant On the other hand testosterone and progestrone had little or no effect while cortisone had a strong depressant property Light microscope studies (Nathaniel 61a b) showed that castration of male rabibts depressed the phagocytic function of the Kupffer cells as revealed by the sparse and diffuse pick up of the carbon administered intravenously

There are relatively few studies on the morphological responses of the hepatic cell to steroids Recently MacCullum et al (65) reported that castrated and intact rats when treated with testosterone and estrogen showed a decrease in glycogen and increase in lipids acid phosphatase and non specific esterases in the hepatic cell However no ultrastructural features have been reported

In this paper the ultrastructural changes in the hepatic and reticuloendothelial cells of the rabbit were studied following castration

MATERIALS AND METHODS

Adult male rabbits of the New Zealand strain weighing about 2–3 kg were used They were castrated under pentobarbital anesthesia The animals were maintained on normal diet *ad libitum* and sacrificed at the end of two four and six weeks following gonadectomy Normal male rabbits of the same strain and weight were used as controls At the time of sacrifice the animals were perfused with buffered formaldehyde (Pease 62) In order to sample several areas of the liver small pieces of the tissue were taken from various sites of both the lobes These pieces were fixed for a further period of 20 minutes in buffered formaldehyde and post

[1] Support d by U S Publ c H lth Service gr nts NB-05850 and HE-09126

Quastler H and F G Sherman 1959 Cell population kinetics in the intestinal epithelium of the mouse Exp Cell Res *17* 420–438

Rasanen T 1962 Mitotic activity in rat epidermis and gastric mucosa after gluco and mineralocorticoid administration Growth 26 1–14

——— 1963 Fluctuations in the mitotic frequency of the glandular stomach and intestine of rat under the influence of ACTH glucocorticoids stress and heparin Acta Physiol Scand 58 201–210

Sherman F G and H Quastler 1960 DNA synthesis in irradiated intestinal epithelium Exp Cell *Res 19* 343–360

Cytological Changes in Hepatic and Reticuloendothelial Cells in Rabbit Liver Following Gonadectomy [1]

DORIS R NATHANIEL AND EDWARD J H NATHANIEL

Division of Laboratories Cedars of Lebanon Hospital Los Angeles California and Department of Pathology and Anatomy Medical College of Georgia and Eugene Talmage Memorial Hospital Augusta Georgia

ABSTRACT Male rabbits of the New Zealand strain were castrated and sacrificed after two four and six weeks The animals were maintained on normal diet *ad libitum* Alterations in hepatic and reticuloendothelial cells were studied with the electron microscope The response of the hepatic cell was as follows The most significant change during the second week was a considerable increase in agranular reticulum which was concentrated along the cell borders as well as within the cells It was associated with glycogen particles Accumulation of glycogen was progressive from the second week onward There was a decrease in the smooth surfaced reticulum as the glycogen content increased It is suggested that the agranular reticulum is related to glycogen metabolism An increase in lipids was also present It is observed that gonadectomy has induced an increase in glycogen and lipid content of the cell In addition the nucleus showed a moderate condensation of chromatin along the inner margin There was a slight increase in the rough surfaced endoplasmic reticulum Castration also produced changes in the Kupffer cell This was characterized by the shortening of the cell processes resulting in reduction in cell size There were fewer inclusions within the cell

There is evidence in the literature that estrogenic hormones have a profound effect on the phagocytic property of the reticuloendothelial cells of the liver (Biozzi et al 57 Heller et al 57) Nicol and Bilbey (60) in their study of the effects of various steroids on the phagocytic activity of the reticuloendothelial system found that estradial benzoate was a powerful stimulant On the other hand testosterone and progestrone had little or no effect while cortisone had a strong depressant property Light microscope studies (Nathaniel 61a b) showed that castration of male rabibts depressed the phagocytic function of the Kupffer cells as revealed by the sparse and diffuse pick up of the carbon administered intravenously

There are relatively few studies on the morphological responses of the hepatic cell to steroids Recently MacCullum et al (65) reported that castrated and intact rats when treated with testosterone and estrogen showed a decrease in glycogen and increase in lipids acid phosphatase and non specific esterases in the hepatic cell However no ultrastructural features have been reported

In this paper the ultrastructural changes in the hepatic and reticuloendothelial cells of the rabbit were studied following castration

MATERIALS AND METHODS

Adult male rabbits of the New Zealand strain weighing about 2–3 kg were used They were castrated under pentobarbital anesthesia The animals were maintained on normal diet *ad libitum* and sacrificed at the end of two four and six weeks following gonadectomy Normal male rabbits of the same strain and weight were used as controls At the time of sacrifice the animals were perfused with buffered formaldehyde (Pease 62) In order to sample several areas of the liver small pieces of the tissue were taken from various sites of both the lobes These pieces were fixed for a further period of 20 minutes in buffered formaldehyde and post

[1] S pp rt d by U S Publ H alth Servi gr nt NB 05850 nd HE-09126

fixed in Millonig s buffered osmium tetroxide for two hours (Millonig 61) Tissues were processed in the usual manner and embedded in araldite Thin sections were stained with uranyl acetate and lead citrate (Reynolds 63) and visualized with the R C A EMU 3F and Phillips E M 200 electron microscopes

OBSERVATIONS

Normal hepatic cells of the control animals presented the usual features (fig 1) The nucleus of each hepatic cell was round or oval in shape with very little chromatin along its inner nuclear membrane The rough surfaced endoplasmic reticulum which was moderate in amount was usually found close to the nucleus The glycogen was evenly distributed without being confined to any particular area of the cell The mitochondria were oval or spherical with abundant matrix Vesicles of smooth surfaced reticulum were not prominent and were generally located throughout the cell

The reticuloendothelial cells of the controls also presented the usual characteristics The shape of the nucleus was variable The cytoplasm was watery and the cell membrane was thrown into folds and processes which were long and attenuated These processes extended considerable distance in the sinusoid (fig 2) often overlapping other cells and their processes (fig 3) The cytoplasm contained many inclusions (figs 2 3) some of which resembled lysosomes The rough surfaced endoplasmic reticulum was small in amount A well defined Golgi complex (fig 2) was often found at one pole of the cell

Significant morphological changes were observed in the hepatic and reticuloendothelial cells following castration of male rabbits The changes in the hepatic cells will be described first

Changes in the hepatic cells A significant morphological change at the end of two weeks following castration was an increase in the agranular reticulum Large numbers of vesicular profiles were found in the cytoplasm (figs 4 5 6 7) They were most numerous along the sinusoidal border (fig 5) and extended throughout the cytoplasm in streaks as seen in figure 7 reaching the vicinity of the nucleus (fig 4) Ribonucleoprotein particles mitochondria and glycogen were located in between the channels of agranular reticulum The glycogen content of the cells did not appear to have been significantly altered at this period At the end of four weeks the agranular reticulum had diminished though it was still present to a certain degree along the borders of the cells The glycogen content was increased and formed aggregated masses occupying large areas of the cytoplasm This accumulation of glycogen persisted in a similar manner at the end of six weeks (fig 8) These glycogen masses were stained heavily by lead citrate In sections stained with uranyl acetate alone the glycogen particles could not be seen and glycogen holes (Steiner and Baglio 63) occurred in the same locations where they were observed in lead stained sections (fig 9)

In addition to the increase in smooth surfaced reticulum vacuoles of varying sizes were seen in hepatic cells They were associated with glycogen (fig 6) The vacuoles became larger by the end of four and six weeks following gonadectomy and were distributed throughout the cytoplasm (figs 8 9) The vacuoles present in the glycogen areas in figure 9 contain electron dense material which probably could be lipid in nature Such vacuoles with similar contents may be visualized in figures 6 and 8 It is thus seen that orchidectomy produced an increase in the glycogen and probably the lipid content of the cell

A less prominent change in hepatic cells following castration was a condensation of chromatin along the inner nuclear margin The rough surfaced reticulum was slightly increased and became more conspicuous than the normal It often ended in dilatations at their lateral ends (fig 4) There was a slight increase in the number of mitochondria Some of them lying in close apposition to the granular reticulum were markedly elongated aligning themselves parallel to the axis of the reticulum (fig 4)

Changes in the reticuloendothelial cells The reticuloendothelial cells responded to castration so that changes were obvious at the end of two weeks Figure 10 represents a reticuloendothelial cell manifesting the characteristic alterations The nucleus

became condensed and regular in shape The whole cell appeared more rounded and smaller This effect was brought about by the withdrawal of the cell processes so typical of a Kupffer cell Those processes that were present were short unlike the long thin arms found normally The inclusions were relatively few and the cytoplasm less watery The increase in cytoplasmic protein may be only apparent because it may have been concentrated in a cell much reduced in size The changes mentioned persisted at the end of four and six weeks The regular nucleus the retracted cell processes decreased inclusions and the reduction in cell size indicate that castration affected the activity of the cell

DISCUSSION

These observations mentioned above provide evidence that the hepatic cell of the rabbit undergoes morphological changes when the animal is deprived of the male sex hormone from the testes

A most striking cytoplasmic change in hepatic cells of the castrate was seen in smooth surface reticulum It was evident two weeks after castration and consisted of elaboration of numerous vesicles which were found in considerable numbers along the edge as well as within the hepatic cell It is said that in animals fed *ad libitum* the amount of smooth surface reticulum in liver is insignificant (Porter and Bruni 59) Fawcett (55) reported the appearance of great amounts of smooth surfaced membranes after fasting and refeeding and related it to regeneration of the rough form of E R In addition Porter and Bruni (59) Millonig and Porter (60) and Porter (61a b) have shown that there is an accumulation of smooth surfaced membranes near glycogen deposits In animals fed with the dye dimethylaminobenzene (3 Me DAB) the loss of glycogen was associated with increase in smooth vesicles (Porter and Bruni 59) Yamada (60) reported the association of agranular reticulum in relation to glycogen rich paraboloid of the retina of the turtle The glycogen storage in relation to the complex agranular patterns have been referred to as finger print of glycogen bodies by Steiner et al (64) It is becoming more apparent that the endoplasmic reticulum is enzymatically active Ernster et al (62) in their study of enzyme structure relationships in endoplasmic reticulum of rat liver found that R N P particles were practically devoid of enzyme activity and were also poor in phospholipids On the other hand the membrane subfraction from liver microsomes was rich in enzymes such as NADH-cytochrome c reductase glucose six phosphotase ATPase and others More recently fractionation studies by Dallner Orrenius and Bergstrand (63) showed that glucose six phosphotase was almost exclusively confined to rough surfaced reticulum In the light of the above findings it is suggested that endoplasmic reticulum may be related to enzymes responsible for glycogen metabolism It may be well to emphasize that in the present study the increase in smooth reticulum was not associated with the loss of glycogen but rather with its formation It is to be noted that the rabbits in the present study were fed *ad libitum* on a normal diet and showed increase in weight at time of sacrifice It is only possible to say that agranular reticulum is in some manner involved in glycogenesis as well as glycogenolysis (Rouiller and Jezequel 63)

At the end of four and six weeks the hepatic cell continued to show increase in glycogen content However there was a diminution in the smooth surface reticulum It was still seen located along the sinusoidal border Gonadectomy or depletion of male hormone has enhanced the capacity of the liver to form and store glycogen The observations of MacCallum et al (65) that administration of testosterone and estrogen to castrate male rats resulted in marked diminution of glycogen are in keeping with the present findings

Besides the increase in glycogen vacuoles were also observed in the liver of castrated rabbits These vacuoles contained material which resembled lipid Such lipid vacuoles usually were surrounded by glycogen and vesicles of smooth surface membranes Normally the utilization and deposition of lipids occur at a rate sufficient to prevent accumulation of lipids Phospholipids are essential for the utilization of hepatic lipids Amick and Stenger (64) observed close relationship between lipid bodies and smooth surfaced

fixed in Millonig s buffered osmium tetroxide for two hours (Millonig 61) Tissues were processed in the usual manner and embedded in araldite Thin sections were stained with uranyl acetate and lead citrate (Reynolds 63) and visualized with the R C A EMU 3F and Phillips E M 200 electron microscopes

OBSERVATIONS

Normal hepatic cells of the control animals presented the usual features (fig 1) The nucleus of each hepatic cell was round or oval in shape with very little chromatin along its inner nuclear membrane The rough surfaced endoplasmic reticulum which was moderate in amount was usually found close to the nucleus The glycogen was evenly distributed without being confined to any particular area of the cell The mitochondria were oval or spherical with abundant matrix Vesicles of smooth surfaced reticulum were not prominent and were generally located throughout the cell

The reticuloendothelial cells of the controls also presented the usual characteristics The shape of the nucleus was variable The cytoplasm was watery and the cell membrane was thrown into folds and processes which were long and attenuated These processes extended considerable distance in the sinusoid (fig 2) often overlapping other cells and their processes (fig 3) The cytoplasm contained many inclusions (figs 2 3) some of which resembled lysosomes The rough surfaced endoplasmic reticulum was small in amount A well defined Golgi complex (fig 2) was often found at one pole of the cell

Significant morphological changes were observed in the hepatic and reticuloendothelial cells following castration of male rabbits The changes in the hepatic cells will be described first

Changes in the hepatic cells A significant morphological change at the end of two weeks following castration was an increase in the agranular reticulum Large numbers of vesicular profiles were found in the cytoplasm (figs 4 5 6 7) They were most numerous along the sinusoidal border (fig 5) and extended throughout the cytoplasm in streaks as seen in figure 7 reaching the vicinity of the nucleus (fig 4) Ribonucleoprotein particles mitochondria and glycogen were located in between the channels of agranular reticulum The glycogen content of the cells did not appear to have been significantly altered at this period At the end of four weeks the agranular reticulum had diminished though it was still present to a certain degree along the borders of the cells The glycogen content was increased and formed aggregated masses occupying large areas of the cytoplasm This accumulation of glycogen persisted in a similar manner at the end of six weeks (fig 8) These glycogen masses were stained heavily by lead citrate In sections stained with uranyl acetate alone the glycogen particles could not be seen and glycogen holes (Steiner and Baglio 63) occurred in the same locations where they were observed in lead stained sections (fig 9)

In addition to the increase in smooth surfaced reticulum vacuoles of varying sizes were seen in hepatic cells They were associated with glycogen (fig 6) The vacuoles became larger by the end of four and six weeks following gonadectomy and were distributed throughout the cytoplasm (figs 8 9) The vacuoles present in the glycogen areas in figure 9 contain electron dense material which probably could be lipid in nature Such vacuoles with similar contents may be visualized in figures 6 and 8 It is thus seen that orchidectomy produced an increase in the glycogen and probably the lipid content of the cell

A less prominent change in hepatic cells following castration was a condensation of chromatin along the inner nuclear margin The rough surfaced reticulum was slightly increased and became more conspicuous than the normal It often ended in dilatations at their lateral ends (fig 4) There was a slight increase in the number of mitochondria Some of them lying in close apposition to the granular reticulum were markedly elongated aligning themselves parallel to the axis of the reticulum (fig 4)

Changes in the reticuloendothelial cells The reticuloendothelial cells responded to castration so that changes were obvious at the end of two weeks Figure 10 represents a reticuloendothelial cell manifesting the characteristic alterations The nucleus

became condensed and regular in shape The whole cell appeared more rounded and smaller This effect was brought about by the withdrawal of the cell processes so typical of a Kupffer cell Those processes that were present were short unlike the long thin arms found normally The inclusions were relatively few and the cytoplasm less watery The increase in cytoplasmic protein may be only apparent because it may have been concentrated in a cell much reduced in size The changes mentioned persisted at the end of four and six weeks The regular nucleus the retracted cell processes decreased inclusions and the reduction in cell size indicate that castration affected the activity of the cell

DISCUSSION

These observations mentioned above provide evidence that the hepatic cell of the rabbit undergoes morphological changes when the animal is deprived of the male sex hormone from the testes

A most striking cytoplasmic change in hepatic cells of the castrate was seen in smooth surface reticulum It was evident two weeks after castration and consisted of elaboration of numerous vesicles which were found in considerable numbers along the edge as well as within the hepatic cell It is said that in animals fed *ad libitum* the amount of smooth surface reticulum in liver is *insignificant (Porter and Bruni* 59) Fawcett (55) reported the appearance of great amounts of smooth surfaced membranes after fasting and refeeding and related it to regeneration of the rough form of E R In addition Porter and Bruni (59) Millonig and Porter (60) and Porter (61a b) have shown that there is an accumulation of smooth surfaced membranes near glycogen deposits In animals fed with the dye dimethyiaminobenzene (3 Me DAB) the loss of glycogen was associated with increase in smooth vesicles (Porter and Bruni 59) Yamada (60) reported the association of agranular reticulum in relation to glycogen rich paraboloid of the retina of the turtle The glycogen storage in relation to the complex agranular patterns have been referred to as finger print of *glycogen bodies* by Steiner et al (64) It is becoming more apparent that the endoplasmic reticulum is enzymatically active Ernster et al (62) in their study of enzyme structure relationships in endoplasmic reticulum of rat liver found that R N P particles were practically devoid of enzyme activity and were also poor in phospholipids On the other hand the membrane subfraction from liver microsomes was rich in enzymes such as NADH-cytochrome c reductase glucose six phosphotase ATPase and others More recently fractionation studies by Dallner Orrenius and Bergstrand (63) showed that glucose six phosphotase was almost exclusively confined to rough surfaced reticulum In the light of the above findings it is suggested that endoplasmic reticulum may be related to enzymes responsible for glycogen metabolism It may be well to emphasize that in the present study the increase in smooth reticulum was not associated with the loss of glycogen but rather with its formation It is to be noted that the rabbits in the present study were fed *ad libitum* on a normal diet and showed increase in weight at time of sacrifice It is only possible to say that agranular reticulum is in some manner involved in glycogenesis as well as glycogenolysis (Rouiller and Jezequel 63)

At the end of four and six weeks the hepatic cell continued to show increase in glycogen content However there was a diminution in the smooth surface reticulum *It was still seen located along the* sinusoidal border Gonadectomy or depletion of male hormone has enhanced the capacity of the liver to form and store glycogen The observations of MacCallum et al (65) that administration of testosterone and estrogen to castrate male rats resulted in marked diminution of glycogen are in keeping with the present findings

Besides the increase in glycogen vacuoles were also observed in the liver of castrated rabbits These vacuoles contained material which resembled lipid Such lipid vacuoles usually were surrounded by glycogen and vesicles of smooth surface membranes Normally the utilization and deposition of lipids occur at a rate sufficient to prevent accumulation of lipids Phospholipids are essential for *the utilization of hepatic lipids* Amick and Stenger (64) observed close relationship between lipid bodies and smooth surfaced

reticulum and glycogen in fatty metamorphosis induced in rats by choline deficient diet

The nucleus of the hepatic cell exhibited a moderate condensation of chromatin along the nuclear margin There was also an increase in the granular endoplasmic reticulum of the cell These findings coupled together suggest a probable increase in the production of ribonucleic acid Mitochondria in the liver of the castrate were slightly increased in number and were located in close association with the endoplasmic reticulum In a study of hepatic regeneration Bernard and Rouiller ('56) observed a considerable increase in ergastoplasm associated with mitochondria They have been said to multiply by division (Fawcett '55) from microbodies (Rouiller and Bernard '56) and by budding (Bearcroft '62a b)

The primary effect of castration on the reticuloendothelial cell was the retraction of the cell process resulting in reduced surface area The nucleus was more compact and the cell as a whole appeared quiescent Previous light microscope studies (Nathaniel '61a b) revealed that the phagocytic property of the Kupffer cell in gonadectomized rabbits was reduced considerably However the administration of estrogen to these rabbits caused stimulation of phagocytosis This was shown by the qualitative increase in the carbon laden R E cells in the liver It is conceivable from the observations of the present ultrastructural studies that the reduced phagocytic property of the reticuloendothelial cell observed in the earlier light microscope studies mentioned above may be related to decreased surface area or altered property of the cell membrane

ACKNOWLEDGMENTS

We gratefully appreciate the advice and help rendered by Dr D C Pease in the early phase of the project The co-operation of Dr Nathan B Friedman Division of Laboratories Cedars of Lebanon Hospital is appreciated The authors wish to thank Dr L D Stoddard for the interest shown in this work and for reviewing the manuscript We are also indebted to Terry Sheehan Helene Merren and Jane Smith for the valuable technical assistance

LITERATURE CITED

Amick C J and R J Stenger 1964 Ultrastructural alterations in experimental acute hepatic fatty metamorphosis Lab Invest, 13 128–136

Bearcroft W G C 1962a Electron microscope studies on the livers of yellow fever infected African monkeys J Path Bact 83 59–64

——— 1962b Electron microscopic studies on the liver in infective hepatitis J Path Bact 83 383–388

Bernard W and Ch Rouiller 1956 Close topographical relationship between mitochondria and ergastoplasm of liver cells in a definite phase of cellular activity J Biophys Biochem Cytol 2 Suppl 73–76

Biozzi G B N Halpern D Bilbey C Stiffel B Benacerraf and D Mouton 1957 Oestrogènes et fonction phagocytaire du système réticuloendothélial (S R E) Compt Rend Soc Biol 151 1326–1331

Dallner G S Orrenius and A Bergstrand 1963 Isolation and properties of rough and smooth vesicles from rat liver J Cell Biol 16 426–430

Ernster L P Siekevitz and G E Palade 1962 Enzyme structure relationships in the endoplasmic reticulum of rat liver A morphological and biochemical study J Cell Biol 15 541–562

Fawcett D W 1955 Observations on the cytology and electron microscopy of hepatic cells J Nat Cancer Inst 15 Suppl 1475–1503

Heller J H R M Meir R A Zucker and G W Mast 1957 The effect of natural and synthetic estrogens on reticuloendothelial system function Endocrinol 61 235–241

MacCullum D P R Patek and V A de Mignard 1965 Long term study of the effect of sex steroids on the liver of carbon injected intact and castrated rats Anat Rec 151 380

Millonig G 1961 Advantages of a phosphate buffer for OsO_4 solutions in fixation J Appl Phys 32 1637

Millonig G and K R Porter 1960 Structural elements of rat liver cells involved in glycogen metabolism Proc European Regional Conf on Electron Microscopy Delft 2 655–659

Nathaniel D R 1961a The effects of sex hormones upon the reticuloendothelial cell responses to foreign particles and related arterial disease Thesis for Masters Degree University of Southern California Los Angeles

——— 1961b The effects of sex hormones upon the reticuloendothelial cell responses to foreign particles and related arterial disease Anat Rec 139 259

Nicol T and D L Bilbey 1960 The effect of various steroids on the phagocytic activity of the reticuloendothelial system In Reticuloendothelial Structure and Function Ed J H Heller Ronald Press Company New York p 301–320

Pease D C 1962 Buffered formaldehyde as a killing agent and primary fixative for electron microscopy Anat Rec 142 342

Porter K. R. 1961a The ground substance Observations from electron microscopy In The Cell Ed J Brachet and A E Mirsky New York Acad Press Vol 2 621–675

——— 1961b The endoplasmic reticulum Some current interpretations of its forms and functions In Biological Structure and Function Ed T W Goodwin and O Lindberg New York Acad Press Vol 1 127–155

Porter K. R and C Bruni 1959 An electron microscope study of the early effects of 3 Me DAB on rat liver cells Cancer Res 19 997–1009

Reynolds E S 1963 The use of lead citrate at high pH as an electron opaque stain in electron microscopy J Cell Biol 17 208–212

Rouiller Ch and W Bernard 1956 Microbodies and the problem of mitochondrial regeneration J Biophys Biochem Cytol 2 Suppl 355–360

Rouiller Ch and A M Jezequel 1963 Electron microscopy of the liver In The Liver Ed Ch Rouiller Acad Press New York and London Vol 1 195–264

Steiner J W and C M Baglio 1963 Electron microscopy of the cytoplasm of the parenchymal liver cells in a naphthyl isothiocynate induced cirrhosis Lab Invest 12 765–790

Steiner J W K Miyai and M J Phillips 1964 Electron microscopy of membrane particle arrays in liver cells of ethionine intoxicated rats Am J Path 44 169–213

Yamada E 1960 The fine structure of the paraboloid in the turtle retina as revealed by electron microscopy Anat Rec 136 352

reticulum and glycogen in fatty metamorphosis induced in rats by choline deficient diet

The nucleus of the hepatic cell exhibited a moderate condensation of chromatin along the nuclear margin There was also an increase in the granular endoplasmic reticulum of the cell These findings coupled together suggest a probable increase in the production of ribonucleic acid Mitochondria in the liver of the castrate were slightly increased in number and were located in close association with the endoplasmic reticulum In a study of hepatic regeneration Bernard and Rouiller (56) observed a considerable increase in ergastoplasm associated with mitochondria They have been said to multiply by division (Fawcett 55) from microbodies (Rouiller and Bernard 56) and by budding (Bearcroft 62a b)

The primary effect of castration on the reticuloendothelial cell was the retraction of the cell process resulting in reduced surface area The nucleus was more compact and the cell as a whole appeared quiescent Previous light microscope studies (Nathaniel 61a b) revealed that the phagocytic property of the Kupffer cell in gonadectomized rabbits was reduced considerably However the administration of estrogen to these rabbits caused stimulation of phagocytosis This was shown by the qualitative increase in the carbon laden R E cells in the liver It is conceivable from the observations of the present ultrastructural studies that the reduced phagocytic property of the reticuloendothelial cell observed in the earlier light microscope studies mentioned above may be related to decreased surface area or altered property of the cell membrane

ACKNOWLEDGMENTS

We gratefully appreciate the advice and help rendered by Dr D C Pease in the early phase of the project The co-operation of Dr Nathan B Friedman Division of Laboratories Cedars of Lebanon Hospital is appreciated The authors wish to thank Dr L D Stoddard for the interest shown in this work and for reviewing the manuscript We are also indebted to Terry Sheehan Helene Merren and Jane Smith for the valuable technical assistance

LITERATURE CITED

Amick C J and R J Stenger 1964 Ultrastructural alterations in experimental acute hepatic fatty metamorphosis Lab Invest 13 128–136

Bearcroft W G C 1962a Electron microscope studies on the livers of yellow fever infected African monkeys J Path Bact 83 59–64

——— 1962b Electron microscopic studies on the liver in infective hepatitis J Path Bact 83 383–388

Bernard W and Ch Rouiller 1956 Close topographical relationship between mitochondria and ergastoplasm of liver cells in a definite phase of cellular activity J Biophys Biochem Cytol 2 Suppl 73–76

Biozzi G B N Halpern D Bilbey C Stiffel B Benacerraf and D Mouton 1957 Oestrogènes et fonction phagocytaire du système réticuloendothélial (S R E) Compt Rend Soc Biol *151* 1326–1331

Dallner G S Orrenius and A Bergstrand 1963 Isolation and properties of rough and smooth vesicles from rat liver J Cell Biol *16* 426–430

Ernster L P Siekevitz and G E Palade 1962 Enzyme structure relationships in the endoplasmic reticulum of rat liver A morphological and biochemical study J Cell Biol *15* 541–562

Fawcett D W 1955 Observations on the cytology and electron microscopy of hepatic cells J Nat Cancer Inst *15* Suppl 1475–1503

Heller J H R M Meir R A Zucker and G W Mast 1957 The effect of natural and synthetic estrogens on reticuloendothelial system function Endocrinol *61* 235–241

MacCullum D P R Patek and V A de Mignard 1965 Long term study of the effect of sex steroids on the liver of carbon injected intact and castrated rats Anat Rec *151* 380

Millonig G 1961 Advantages of a phosphate buffer for OsO_4 solutions in fixation J Appl Phys 32 1637

Millonig G and K R Porter 1960 Structural elements of rat liver cells involved in glycogen metabolism Proc European Regional Conf on Electron Microscopy Delft 2 655–659

Nathaniel D R 1961a The effects of sex hormones upon the reticuloendothelial cell responses to foreign particles and related arterial disease Thesis for Masters Degree University of Southern California Los Angeles

——— 1961b The effects of sex hormones upon the reticuloendothelial cell responses to foreign particles and related arterial disease Anat Rec *139* 259

Nicol T and D L Bilbey 1960 The effect of various steroids on the phagocytic activity of the reticuloendothelial system In Reticuloendothelial Structure and Function Ed J H Heller Ronald Press Company New York p 301–320

Pease D C 1962 Buffered formaldehyde as a killing agent and primary fixative for electron microscopy Anat Rec *142* 342

Porter K R 1961a The ground substance Observations from electron microscopy In The Cell Ed J Brachet and A E Mirsky New York Acad Press Vol 2 621–675

——— 1961b The endoplasmic reticulum Some current interpretations of its forms and functions In Biological Structure and Function Ed T W Goodwin and O Lindberg New York Acad Press Vol 1 127–155

Porter K R and C Bruni 1959 An electron microscope study of the early effects of 3 Me DAB on rat liver cells Cancer Res 19 997–1009

Reynolds E S 1963 The use of lead citrate at high pH as an electron opaque stain in electron microscopy J Cell Biol 17 208–212

Rouiller Ch and W Bernard 1956 Microbodies and the problem of mitochondrial regeneration J Biophys Biochem Cytol 2 Suppl 355–360

Rouiller Ch and A M Jezequel 1963 Electron microscopy of the liver In The Liver Ed Ch Rouiller Acad Press New York and London Vol 1 195–264

Steiner J W and C M Baglio 1963 Electron microscopy of the cytoplasm of the parenchymal liver cells in a naphthyl isothiocynate induced cirrhosis Lab Invest 12 765–790

Steiner J W K Miyai and M J Phillips 1964 Electron microscopy of membrane particle arrays in liver cells of ethionine intoxicated rats Am J Path 44 169–213

Yamada E 1960 The fine structure of the paraboloid in the turtle retina as revealed by electron microscopy Anat Rec 136 352

PLATE 1

EXPLANATION OF FIGURES

1 *Electron micrograph of a normal male rabbit hepatic cell* The cell shows a binucleate condition Note mitochondria (*m*) endoplasmic reticulum (*er*) The glycogen (*gly*) is diffusely distributed through out the cell × 14 250

2 Portion of a normal rabbit reticuloendothelial cell (*Re*) within the sinusoid (*s*) of the liver A well developed Golgi (*g*) is located at one end of the cell Observe the attenuated cytoplasmic processes of the cell (arrows) The sinusoidal border of the hepatic cell characterized by *microvilli is closely related to the processes of the* Kupffer cell × 9 000

3 *Note overlapping of the processes of the reticuloendothelial cells* in a normal rabbit liver (arrows) × 12 500

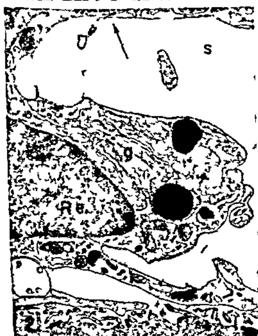

s
g
Re



PLATE 2

EXPLANATION OF FIGURES

4 Liver cell from male rabbit two weeks following castration Condensation of chromatin along the nuclear margin moderate development of rough surfaced endoplasmic reticulum with lateral dilatations (arrows) and streaks of *smooth surfaced reticulum (ser) are evident* × 30 750

5 Sinusoidal border of two hepatic cells in male rabbit two weeks after gonadectomy Observe numerous vesicles (ser) at the edge of the cell and areas of glycogen × 23 000

6 Demonstrates vesicles and vacuoles of various sizes in hepatic cells of male rabbit two weeks following castration Note the tendency for glycogen particles to be associated with vacuoles (arrows) Electron dense body presumably lysosome may be seen × 26 600


ser
ser
5


6

PLATE 3

EXPLANATION OF FIGURES

7 Micrograph to demonstrate the streaks of small vesicles of agranular reticulum (*ser*) traversing the cytoplasm of the hepatic cell Glycogen particles are present around the vacuoles Tissue from male rabbit two weeks after gonadectomy × 23 750

8 Electron micrograph of hepatic cell of male rabbit six weeks after castration Large masses of glycogen were present at this stage Vacuoles (*V*) probably containing lipids are located within the areas of glycogen × 14 200

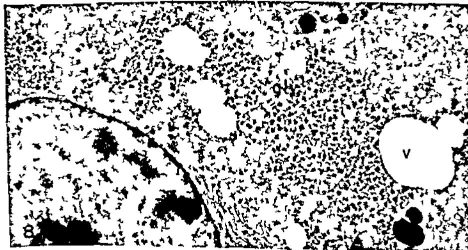

v
8

PLATE 4

EXPLANATION OF FIGURES

9 Section stained with uranyl acetate alone Unstained areas represent glycogen masses (*gly*) Vacuoles filled with lipid (*L*) are present in the areas of glycogen Section from liver of male rabbit six weeks after castration × 2 730

10 Reticuloendothelial cell of male rabbit liver six weeks after castration The nucleus shows increased chromatin and is more regular The cytoplasm is condensed the processes retracted and short There is also a decrease in the inclusions normally present × 16 600

The Fine Structure of Testicular Interstitial Cells in Mice [1]

A KENT CHRISTENSEN AND DON W FAWCETT

Departments of Anatomy Stanford School of Medicine Stanford California and Harvard Medical School Boston Massachusetts

ABSTRACT The testicular interstitial cells of mice contain an abundant agranular endoplasmic reticulum occurring as a network of interconnected tubules Unusual features of the reticulum are occasional extensive whorls of concentric membranes and the occurrence of bundles of parallel double walled tubules The mitochondria have tubular cristae and are occasionally very large

In contrast to the interstitial cells of other species that have been described the mouse interstitial cells show a segregation of the cytoplasm into areas of dense agranular reticulum and other areas where the agranular reticulum is relatively sparse The latter areas contain scattered cisternae of granular reticulum many free ribosomes in clusters mitochondria lipid droplets and small granules The mitochondria and lipid droplets are often encircled by cisternae of the reticulum

Biochemical evidence from other laboratories taken with the present results indicates that the membranes of the endoplasmic reticulum in mouse interstitial cells are the site of the enzymes that mediate the synthesis of testosterone from progester one There is also an indication that cholesterol biosynthesis is associated with the agranular reticulum The membranes of the agranular reticulum may also serve as a reservoir for the storage of cholesterol

The main source of androgens in the testes of laboratory mammals is the in terstitial or Leydig cell (Wattenberg 58 Levy et al 59 Christensen and Mason 65) These cells have been studied with the electron microscope in several species including opossums (Christensen and Faw cett 61 Fawcett 65) guinea pigs (Christ ensen 65) humans (Fawcett and Burgos 60 Gordon Miller and Bensch 64) rats (Leeson 63 Schwarz and Merker 65) and rabbits (Crabo 63) The most com mon characteristic of this cell type is the presence of a well developed agranular endoplasmic reticulum and there is good biochemical evidence in some species that this agranular reticulum is the site of many enzymes involved in androgen bio- synthesis (see review in Christensen 65)

Mouse interstitial cells have been stud ied in considerable detail with the light microscope (Sluiter 45) and have been shown to be the main source of testicular androgens in mice (Wattenberg 58 Hitz man 62 Baillie and Griffiths 64 Maier 65) but as yet there has been no com prehensive description of the fine structure of interstitial cells in this species Carr and Carr (62) described the membrane whorls that occur in these cells Porter and Bonneville (64) included an electron micrograph of a mouse interstitial cell in their atlas of cell fine structure Baillie (64) has dealt with several aspects of the fine structure in a paper on the histochem istry of mouse interstitial cells An illus trated abstract on interstitial cells in this species has appeared (Yasutake 62)

The present study describes the nor mal fine structure of testicular interstitial cells in mice after prefixation in glutaral dehyde (Sabatini et al 63) a method which seems to preserve the agranular endoplasmic reticulum particularly well The description is rendered more pertinent by the recent biochemical paper of Murota Shikita and Tamaoki (65) reporting that in mice as in some other species the conversion of progesterone to testosterone takes place in the microsome fraction of testis homogenates and therefore prob- ably in the endoplasmic reticulum of the intact interstitial cells

[1] Thi In e tig t on w s upported in part by Pub- lic H lth Rese rch G nt HD 01512 from the Na ti nal In titut of Child H lth and Human Dev lop- m nt and by RG 6729 from th Di ision of Gen ral Med l Sci nce Nati n l In titute f He lth Un t d St tes Publi Health Service

gesting that they actually are flattened cisternae If so these cisternae resemble somewhat those seen in guinea pig inter stitial cells (Christensen 65) although in guinea pigs the cisternae are usually fenestrated and are much more abundant filling large regions of the peripheral cyto-pla m of the interstitial cells

In mouse interstitial cells there is a cer tain degree of spatial segregation of the agranular endoplasmic reticulum from the much less abundant granular reticulum In certain areas of the cytoplasm the agranular reticulum is sparse and in its place are found scattered cisternae of granular reticulum bearing attached ribo-somes in irregular patches and between the cisternae are numerous clusters of free ribosomes or polyribosomes (see lower half of fig 2 upper half of fig 3 right half of fig 6 and also figs 7 10 and 11) The mitochondria and lipid droplets are more numerous in these areas than in regions of the cytoplasm where the agranular reti culum is abundant The membranous whorls tend to occur in these areas (figs 2 and 7)

The mitochondria vary considerably in size as indicated by the great disparity in their cross sectional area (figs 2 3 10 and 11) The diameter is commonly about 0 5 μ but occasionally much larger mito chondria are seen (figs 2 and 10) which may have a diameter of 2 μ or more The internal structure of the mitochondria con sists of numerous tubular cristae that are similar in size and appearance to the tub ules of the surrounding agranular reticu lum except that the tubules within the mitochondria show less tendency to branch The mitochondria are much more numerous in the areas where the agranular reticulum is sparse and in these areas they are often loosely enfolded by a cis terna of the endoplasmic reticulum which is commonly of the agranular type but often bears a few ribosomes (see figs 2 3 5 10 and 11) Mitochondrial granules are seen occasionally in the smaller mito-chondria (fig 3) but are more numerous in the large mitochondria (figs 2 and 10) The granules are small often resem bling small myelin figures (lower left in fig 3 and fig 10) No large mitochondrial granules were seen like those found in the mitochondria of opossum interstitial cells (Christensen and Fawcett 61)

Lipid droplets (figs 3 7–9) vary in size from about 0 5 to 2 μ in diameter They usually occur in the areas containing granular reticulum and like the mitochon dria in these areas the lipid droplets are often wrapped in a cisterna of either gran ular or agranular reticulum (figs 3 7 and 9)

Small granules about 0 2 μ in diameter occur in the areas of granular reticulum (figs 2 3 6 10 and 11) They are bounded by a single membrane and their content generally appears granular al though close examination often reveals in distinct profiles of lamellae or tubules Simi lar small granules have been described in opossum interstitial cells (Christensen and Fawcett 61) These small granules are not the same as the large granules de scribed by Porter and Bonneville (64) in mouse interstitial cells the large "gran ules" of these authors probably correspond to what in the present study are considered to be lipid droplets (see discussion)

DISCUSSION

Mouse interstitial cells resemble those of other species that have been described in having a well developed agranular endo-plasmic reticulum The reticulum is in the usual form of a network of intercon necting tubules and is approximately com parable in abundance to that described in opossum interstitial cells (Christensen and Fawcett 61 Fawcett 65) and generally more abundant than in the interstitial cells of rats (Leeson 61 Schwarz and Merker 65) rabbits (Crabo 63) or humans (Fawcett and Burgos 60 Gordon Miller and Bensch 64) The agranular reticulum is somewhat less well developed in mouse interstitial cells than in those of guinea pigs (Christensen 65)

The interstitial cells are the main source of androgens in the mouse testis (Watten berg 58 Hitzman 62 Baillie and Grif fiths 64 Maeir 65) In biochemical stud ies mouse testicular tissue is capable of synthesizing testosterone from progester one *in vitro* (Dominguez et al 50 Huseby et al 61) and more recently it has been shown in mice that androgen biosynthesis from pregnenolone passes both through

MATERIALS AND METHODS

The observations reported here are based upon the examination of the testes of approximately six adult male mice and two juvenile BALB/c mice The tissue was fixed by immersion in collidine buffered 6 5% glutaraldehyde (Sabatini Bensch and Barrnett 63 Bennett and Luft, 59) followed by a period of further fixation and staining in 1% osmium tetroxide After embedding in Epon (Luft 61) sections exhibiting silver to gold interference colors were cut with glass or diamond knives and stained with lead citrate (Reynolds 63) The sections were examined with RCA EMU 3F or 3G electron microscopes and electron micrographs taken at original magnifications of 4,000 to 10 000 times

OBSERVATIONS

A low power electron micrograph of mouse testis is presented in figure 1 showing a typical interstitial cell lying between two seminiferous tubules The cytoplasm contains scattered mitochondria between which are masses of agranular endoplasmic reticulum which is somewhat difficult to make out at this magnification In one area of the cytoplasm just below the nucleus the agranular reticulum is much less well developed and instead there are scattered cisternae of the granular endoplasmic reticulum In this area the mitochondria are more numerous and there are also two dense lipid droplets

At higher magnification the most striking feature of the cytoplasm is the agranular endoplasmic reticulum (figs 2 and 3) comprising an abundant network of interconnecting tubules about 400 A in diameter that extends throughout much of the cytoplasm The tubules are more or less uniform in diameter and do not tend to have vesicular dilatations in this glutaraldehyde fixed material

Two unusual modifications of the agranular reticulum occur in mouse interstitial cells — double walled tubules and systems of concentric membranes or whorls The double walled tubules occur in bundles containing from a few to 100 or more running parallel to one another In cross section (figs 4 and 5) they are arranged in a loose hexagonal array and each double walled tubule appears as two concentric tubules one inside the other The outer tubule has about the same diameter and appearance as nearby tubules of the agranular reticulum The inner tubules are of smaller diameter about 250 A and have thicker denser walls In longitudinal section (fig 6) it is clear that both the outer and inner tubules are continuous at their ends with the membranes of the agranular reticulum (asterisks) The double walled tubules are thus considered to be a modification of the agranular reticulum although their functional significance is unknown In figure 6 the lumen of the inner tubule seems continuous with the general cytoplasm while the space between the inner and outer tubules appears to be continuous with the cavity of the agranular endoplasmic reticulum The bundles of double walled tubules are somewhat reminiscent of the bundles of microtubules found in opossum interstitial cells (Christensen and Fawcett 61) although in opossums the tubules were not double walled were of smaller diameter (about 180 A) and the microtubules were interconnected by bridges

The concentric membrane systems or whorls (figs 2 and 7–9) have already been described in mouse interstitial cells by Carr and Carr (62) and consist of numerous concentric membranes arranged around a common center often a lipid droplet or other inclusion The whorl in figure 7 contains about 60 layers In favorable sections it can be seen that the membranes of the whorl are continuous with membranes of the surrounding endoplasmic reticulum a fact already noted by Carr and Carr (62) Figure 8 is an enlargement of the area enclosed in the rectangle at right in figure 7 and shows the continuity (asterisks) between the membranes of the whorl and those of the agranular endoplasmic reticulum Figure 9 shows more detail of the area indicated in the other rectangle in figure 7 and here the membranes are clearly continuous with the granular endoplasmic reticulum These continuities indicate that the whorls are regional modifications of the endoplasmic reticulum When viewed at high magnification (fig 9) the membranes within the concentric systems seem to be organized in pairs sug

interstitial cells (Toren et al 64) If the localization of this step is valid and is similar in the mouse testis it means that any cholesterol synthesized and stored in the membranes of the endoplasmic reticulum must migrate to the mitochondria to be transformed into pregnenolone which would then return to the reticulum for further metabolism to testosterone Since in mouse interstitial cells the mitochondria are more numerous in the regions where the agranular reticulum is sparse the problem of the translocation of cholesterol from agranular reticulum to mitochondria is more complex than in other species where most of the mitochondria are surrounded by agranular reticulum It is conceivable that the strands of endoplasmic reticulum often surrounding the mitochondria in the present study might in the living cell be part of a dynamic process of membrane circulation bringing cholesterol stored in the membranes to the mitochondria Biochemical studies are needed to establish whether the cholesterol side chain cleavage system is indeed in the mitochondria in mouse interstitial cells

In the interstitial cells of other species that have been described the agranular endoplasmic reticulum fills most of the cytoplasm not occupied by other organelles or inclusions However an interesting feature of mouse interstitial cells is the separation of the cytoplasm into areas rich in agranular reticulum and other areas that contain little agranular reticulum but instead show scattered cisternae of granular reticulum abundant free ribosomes mitochondria and some lipid droplets It is difficult to assign functional significance to this segregation of cytoplasmic components Granular reticulum and free ribosomes are now generally considered to be sites of protein synthesis and it is probable that the regions of the cytoplasm where these organelles are better developed are where the enzymes and structural proteins needed by the cell are synthesized Proteins may also be needed for protein binding of steroids if this device is used in mouse interstitial cells to make steroids more soluble for intracellular transport Protein for this purpose might be produced in the granular reticulum and transported to the regions of agranular reticulum within the lumen of the reticulum

The mitochondria of mouse interstitial cells contain the tubular cristae that are typical of mitochondria in many steroid secreting cells (Belt and Pease 56) These tubular cristae are common in mitochondria of adrenocortical cells although their occurrence varies in different species and in different layers of the adrenal cortex (for example see Sheridan and Belt 64) In addition to mouse interstitial cells tubular cristae are well developed in the interstitial cell mitochondria of rabbits (Crabo 63) and humans (Gordon et al 64) but are not particularly conspicuous in those of guinea pigs (Christensen 65) or opossums (Christensen and Fawcett 61) The significance of these tubular cristae is unknown but their similarity in size and appearance to the tubules of the agranular endoplasmic reticulum in the present study suggests that the two structures may share some common feature of chemical organization It was suggested above that the membranes of the agranular reticulum might contain unusual amounts of cholesterol and it is conceivable that the cristae of mitochondria might also sequester steroids if the mitochondria are involved in any stage of androgen biosynthesis The significance of the occasional very large mitochondria in mouse interstitial cells is unknown An unusual degree of variation in size of mitochondria is also found in other steroid producing organs (Belt and Pease 56)

It is necessary to distinguish between the small granules described here and other granules that have been reported in mouse interstitial cells by Sluiter (45) and by Porter and Bonneville (64) The granules seen in the present study are membrane bounded are about 0 2 μ in diameter and have a granular matrix Similar small granules are common in opossum interstitial cells (Christensen and Fawcett 61) The granules are clearly distinct from lipid droplets and their small size makes it improbable that they correspond to anything seen with the light microscope since they are at the lower limit of resolution of this instrument

progesterone and through an alternative pathway involving dehydroepiandrosterone (Ellis and Berliner, '65). The enzymes for the progesterone pathway are found mainly in the microsome fraction of mouse testis homogenates (Murota, Shikita and Tamaoki, '65). It is now generally agreed that the microsome fraction derives predominantly from the endoplasmic reticulum of intact cells, and thus the enzymes necessary to transform progesterone to 17-hydroxyprogesterone, androstenedione and finally testosterone are presumably associated with the abundant agranular endoplasmic reticulum of mouse interstitial cells reported in the present study. The same conclusion can be reached for guinea pig and rat interstitial cells (see Christensen, '65) and for human and rabbit interstitial cells (compare Murota, Shikita and Tamaoki, '65 with Fawcett and Burgos, '60 and Crabo, '63). Thus in a variety of species, including mice, the agranular endoplasmic reticulum of testicular interstitial cells is the main site of enzymes mediating the synthesis of testosterone from progesterone.

Christensen ('65) has reviewed the evidence that cholesterol, one of the main substrates of androgen biosynthesis, is synthesized from acetate in the endoplasmic reticulum and surrounding cytoplasmic matrix of rat and guinea pig interstitial cells. In addition to biochemical evidence, it was pointed out that the amount of agranular reticulum seems to correlate well with the extent of cholesterol synthesis (basing the correlation upon the biochemical data of Werbin and Chaikoff, '61) in the testes and adrenals of rats and guinea pigs. It is not known to what extent the mouse testis produces its own cholesterol rather than absorbing it from the plasma, but if cholesterol production and the abundance of agranular reticulum are indeed correlated, then one would expect considerable cholesterol production in mouse interstitial cells. Recent biochemical evidence in mouse testes indicates a high activity of the lanosterol demethylating system, one of the microsomal enzyme systems involved in cholesterol biosynthesis (Ying et al., '65). It is interesting to note that the activity of the lanosterol demethylating system is much higher in the testes of mice and guinea pigs, in which the interstitial cells have a richly developed agranular reticulum, than in the testes of rats and rabbits, where the agranular reticulum is less well developed.

In summary, then, the membranes of the agranular endoplasmic reticulum seem to play a broad role as sites for enzymes of androgen biosynthesis in interstitial cells of mice and other species. In addition to acting as a site for synthetic enzymes, the membranes of the agranular reticulum may also possibly serve to some extent as a reservoir for the storage of cholesterol, as has been suggested by Fawcett ('65). Cell membranes contain a considerable amount of cholesterol — approximately two out of every five lipid molecules in the plasma membranes that make up myelin sheath are cholesterol (see Finean, '62). Experiments *in vitro* have shown that phospholipid micelles can take up to 25% of their weight of cholesterol or other steroids, and by this means it is possible to attain a 10 or 20% solution of cholesterol in water (see comment by D. E. Green in Fawcett, '65, p. 38). It is therefore conceivable that the profusion of agranular membranes in the cytoplasm of interstitial cells might harbor an appreciable quantity of cholesterol for eventual use as a substrate for androgen biosynthesis. Some support for this notion may come from the finding of Baillie ('64) that the whole cytoplasm of interstitial cells in the adult mice is rich in cholesterol. If the agranular reticulum in interstitial cells contains unusual amounts of cholesterol, this might explain the instability which has made it difficult in the past to fix this reticulum adequately with many of the older techniques of specimen preparation that were very successful in fixing the granular reticulum. In mouse interstitial cells the membrane whorls may also constitute a depot for the storage of cholesterol.

If cholesterol is stored in the membranes, it would be satisfying to find that the enzymes initiating the conversion of cholesterol to androgen also occur there. However, the available evidence indicates, at least in rats, that the first step of cholesterol conversion, the cleavage of its side chain, occurs in the mitochondria of the

interstitial cells (Toren et al 64) If the localization of this step is valid and is similar in the mouse testis it means that any cholesterol synthesized and stored in the membranes of the endoplasmic reticulum must migrate to the mitochondria to be transformed into pregnenolone which would then return to the reticulum for further metabolism to testosterone Since in mouse interstitial cells the mitochondria are more numerous in the regions where the agranular reticulum is sparse the problem of the translocation of cholesterol from agranular reticulum to mitochondria is more complex than in other species where most of the mitochondria are surrounded by agranular reticulum It is conceivable that the strands of endoplasmic reticulum often surrounding the mitochondria in the present study might in the living cell be part of a dynamic process of membrane circulation bringing cholesterol stored in the membranes to the mitochondria Biochemical studies are needed to establish whether the cholesterol side chain cleavage system is indeed in the mitochondria in mouse interstitial cells

In the interstitial cells of other species that have been described the agranular endoplasmic reticulum fills most of the cytoplasm not occupied by other organelles or inclusions However an interesting feature of mouse interstitial cells is the separation of the cytoplasm into areas rich in agranular reticulum and other areas that contain little agranular reticulum but instead show scattered cisternae of granular reticulum abundant free ribosomes mitochondria and some lipid droplets It is difficult to assign functional significance to this segregation of cytoplasmic components Granular reticulum and free ribosomes are now generally considered to be sites of protein synthesis and it is probable that the regions of the cytoplasm where these organelles are better developed are where the enzymes and structural proteins needed by the cell are synthesized Proteins may also be needed for protein binding of steroids if this device is used in mouse interstitial cells to make steroids more soluble for intracellular transport Protein for this purpose might be produced in the granular reticulum and transported to the regions of agranular reticulum within the lumen of the reticulum

The mitochondria of mouse interstitial cells contain the tubular cristae that are typical of mitochondria in many steroid secreting cells (Belt and Pease 56) These tubular cristae are common in mitochondria of adrenocortical cells although their occurrence varies in different species and in different layers of the adrenal cortex (for example see Sheridan and Belt 64) In addition to mouse interstitial cells tubular cristae are well developed in the interstitial cell mitochondria of rabbits (Crabo 63) and humans (Gordon et al 64) but are not particularly conspicuous in those of guinea pigs (Christensen 65) or opossums (Christensen and Fawcett 61) The significance of these tubular cristae is unknown but their similarity in size and appearance to the tubules of the agranular endoplasmic reticulum in the present study suggests that the two structures may share some common feature of chemical organization It was suggested above that the membranes of the agranular reticulum might contain unusual amounts of cholesterol and it is conceivable that the cristae of mitochondria might also sequester steroids if the mitochondria are involved in any stage of androgen biosynthesis The significance of the occasional very large mitochondria in mouse interstitial cells is unknown An unusual degree of variation in size of mitochondria is also found in other steroid producing organs (Belt and Pease 56)

It is necessary to distinguish between the small granules described here and other granules that have been reported in mouse interstitial cells by Sluiter (45) and by Porter and Bonneville (64) The granules seen in the present study are membrane bounded are about 0 2 μ in diameter and have a granular matrix Similar small granules are common in opossum interstitial cells (Christensen and Fawcett 61) The granules are clearly distinct from lipid droplets and their small size makes it improbable that they correspond to anything seen with the light microscope since they are at the lower limit of resolution of this instrument

progesterone and through an alternative pathway involving dehydroepiandrosterone (Ellis and Berliner, '65). The enzymes for the progesterone pathway are found mainly in the microsome fraction of mouse testis homogenates (Murota, Shikita and Tamaoki, '65). It is now generally agreed that the microsome fraction derives predominantly from the endoplasmic reticulum of intact cells, and thus the enzymes necessary to transform progesterone to 17-hydroxyprogesterone, androstenedione and finally testosterone are presumably associated with the abundant agranular endoplasmic reticulum of mouse interstitial cells reported in the present study. The same conclusion can be reached for guinea pig and rat interstitial cells (see Christensen, '65) and for human and rabbit interstitial cells (compare Murota, Shikita and Tamaoki, '65 with Fawcett and Burgos, '60 and Crabo, '63). Thus in a variety of species, including mice, the agranular endoplasmic reticulum of testicular interstitial cells is the main site of enzymes mediating the synthesis of testosterone from progesterone.

Christensen ('65) has reviewed the evidence that cholesterol, one of the main substrates of androgen biosynthesis, is synthesized from acetate in the endoplasmic reticulum and surrounding cytoplasmic matrix of rat and guinea pig interstitial cells. In addition to biochemical evidence, it was pointed out that the amount of agranular reticulum seems to correlate well with the extent of cholesterol synthesis (basing the correlation upon the biochemical data of Werbin and Chaikoff, '61) in the testes and adrenals of rats and guinea pigs. It is not known to what extent the mouse testis produces its own cholesterol rather than absorbing it from the plasma, but if cholesterol production and the abundance of agranular reticulum are indeed correlated, then one would expect considerable cholesterol production in mouse interstitial cells. Recent biochemical evidence in mouse testes indicates a high activity of the lanosterol demethylating system, one of the microsomal enzyme systems involved in cholesterol biosynthesis (Ying et al., '65). It is interesting to note that the activity of the lanosterol demethylating system is much higher in the testes of mice and guinea pigs, in which the interstitial cells have a richly developed agranular reticulum, than in the testes of rats and rabbits, where the agranular reticulum is less well developed.

In summary, then, the membranes of the agranular endoplasmic reticulum seem to play a broad role as sites for enzymes of androgen biosynthesis in interstitial cells of mice and other species. In addition to acting as a site for synthetic enzymes, the membranes of the agranular reticulum may also possibly serve to some extent as a reservoir for the storage of cholesterol, as has been suggested by Fawcett ('65). Cell membranes contain a considerable amount of cholesterol — approximately two out of every five lipid molecules in the plasma membranes that make up myelin sheath are cholesterol (see Finean, '62). Experiments *in vitro* have shown that phospholipid micelles can take up to 25% of their weight of cholesterol or other steroids, and by this means it is possible to attain a 10 or 20% solution of cholesterol in water (see comment by D. E. Green in Fawcett, '65, p. 38). It is therefore conceivable that the profusion of agranular membranes in the cytoplasm of interstitial cells might harbor an appreciable quantity of cholesterol for eventual use as a substrate for androgen biosynthesis. Some support for this notion may come from the finding of Baillie ('64) that the whole cytoplasm of interstitial cells in adult mice is rich in cholesterol. If the agranular reticulum in interstitial cells contains unusual amounts of cholesterol, this might explain the instability which has made it difficult in the past to fix this reticulum adequately with many of the older techniques of specimen preparation that were very successful in fixing the granular reticulum. In mouse interstitial cells the membrane whorls may also constitute a depot for the storage of cholesterol.

If cholesterol is stored in the membranes, it would be satisfying to find that the enzymes initiating the conversion of cholesterol to androgen also occur there. However, the available evidence indicates, at least in rats, that the first step of cholesterol conversion, the cleavage of its side chain, occurs in the mitochondria of the

stitial cell tumors J Biol Chem 235 2608–2612
Ellis L C and D L Berliner 1965 Sequential biotransformation of 5-pregnenolone 7 H and progesterone-4 C into androgens by mouse testis Endocrinology 76 591–599
Fawcett D W 1965 Structural and functional variations in the membranes of the cytoplasm In Intracellular Membranous Structure Ed by S Seno and E V Cowdry Japan Society for Cell Biology Okayama Pp 15–40
Fawcett D W and M H Burgos 1960 Studies on the fine structure of the mammalian testis II The human interstitial tissue Am J Anat 107 245–269
Finean J B 1962 The nature and stability of the plasma membrane Circulation 26 1151–1162
Gordon G B L R Miller and K G Bensch 1964 Electron microscopic observations of the gonad in the testicular feminization syndrome Lab Invest 13 152–160
Hitzeman J W 1962 Development of enzyme activity in the Leydig cells of the mouse testis Anat Rec 143 351–361
Huseby R A O V Dominguez and L T Samuels 1961 Function of normal and abnormal testicular interstitial cells in the mouse Rec Prog in Hormone Res 17 1–51
Leeson C R 1963 Observations on the fine structure of rat interstitial tissue Acta Anat 52 34–48
Levy H H W Deane and B L Rubin 1959 Visualization of steroid-3β-ol-dehydrogenase activity in tissues of intact and hypophysectomized rats Endocrinology 65 932–943
Luft J H 1961 Improvements in epoxy resin embedding methods J Biophys and Biochem Cytol 9 409–414
Maeir D M 1965 Species variation in testicular Δ-3β hydroxysteroid dehydrogenase activity Absence of activity in primate Leydig cells Endocrinology 76 463–469
Murota S M Shikita and B Tamaoki 1965 Intracellular distribution of the enzymes related to androgen formation in mouse testes Steroids 5 409–413
Porter K R and M A Bonneville 1964 An Introduction to the Fine Structure of Cells and Tissues 2nd edition Lea and Febiger Philadelphia Plate 15
Reynolds E S 1963 The use of lead citrate at high pH as an electron-opaque stain in electron microscopy J Cell Biol 17 208–212
Sabatini D D K G Bensch and R J Barrnett 1963 Cytochemistry and electron microscopy The preservation of cellular ultrastructure and enzymatic activity by aldehyde fixation J Cell Biol 17 19–58
Schwarz W and H J Merker 1965 Die Hodenzwischenzellen der Ratte nach Hypophysektomie und nach Behandlung mit Choriongonadotropin und Amphenon B Z f Zellforsch 65 272–284
Sheridan M N and W D Belt 1964 Fine structure of the guinea pig adrenal cortex Anat Rec 149 73–97
Sluiter J W 1945 Experimentelle Untersuchungen uber die Funktion des Interstitiums der Gonade I Versuche an mannlichen und weiblichen juvenilen Mausen Z f Zellforsch 33 311–335
Toren D K M J Menon E Forchielli and R I Dorfman 1964 *In vitro* enzymatic cleavage of the cholesterol side chain in rat testis preparations Steroids 3 381–390
Wattenberg L W 1958 Microscopic histochemical demonstration of steroid-3β-ol dehydrogenase in tissue sections J Histochem and Cytochem 6 225–232
Werbin H and I L Chaikoff 1961 Utilization of adrenal gland cholesterol for synthesis of cortisol by the intact normal and ACTH treated guinea pig Arch Biochem and Biophys 93 476–482
Yasutake S 1962 Fine structure of the mouse testicular interstitial cell 5th Intern Congr Electron Microscopy Ed by S S Breeze Jr Academic Press Philadelphia TT 13
Ying B P Y J Chang and J L Gaylor 1965 Testicular sterols III Effect of gonadotrophins on the biosynthesis of testicular sterols Biochim et Biophys Acta 100 256–262

In contrast Sluiter (45) described fuchsinophilic granules that were usually somewhat larger than *mitochondria in the interstitial* cells of juvenile mice studied with the *light* microscope Sluiter s study is *one of the more* complete descriptions *of interstitial cells in* the light microscope literature However since it was done be fore the *advent* of electron microscopy in cytology *it was not possible* to see the endoplasmic reticulum *or to be certain* of the identification of cytoplasmic organel les In his preparations which were fixed with Champy s fluid and stained with acid fuchsin both the granules and the mito chondria were fuchsinophilic and there fore could only be distinguished from one another by their size and shape—the granules appeared round and generally larger than the rod shaped mitochondria In the present study no granules of the dimensions described by Sluiter were ob served with the electron microscope How ever the mitochondria were found to vary a great deal in size and shape and it *seems likely that* all the fuchsinophilic structures observed by Sluiter were ac tually mitochondria A comparison of his figures *with the present electron micro* graphs bears out this suggestion since his granules have the same size and pattern of distribution as the mitochondria in the electron micrographs There is one pos sible source of concern in this interpreta tion Sluiter studied juvenile mice and although his work suggests that the same granules would be present to some extent in adult animals it is conceivable that the granules might arise during puberty [2] and then become much less common in adults *To investigate this possibility with the elec* tron microscope we examined testis tissue from two juvenile BALB c mice weighing 10 8 and 14 6 gm which according to Sluiter should be optimal material for ob serving the large granules The fine struc ture of the interstitial cells in these two ani mals was basically similar to that described here for adult animals with polymorphic mitochondria and small 0 2 μ granules but no large granules It seems reasonable to conclude that Sluiter s granules were ac tually large mitochondria

Still another *type of* granule has been *described* in mouse interstitial cells by Porter and Bonneville (64) with the elec tron microscope These granules are up to 1μ in diameter are strongly osmiophilic and their matrix is relatively homogeneous without obvious granularity Although they appear to be membrane bounded closer scrutiny reveals that the membranes are actually cisternae of the endoplasmic reticulum wrapped around the structures as described here for lipid droplet and mitochondria—the granules themselves do *not appear to be bounded by a* distinc *membrane The granules of thes* au *thors thus closely resemble and may* wel be identical *to the* structures that ar interpreted as lipid droplets in the presen study

LITERATURE CITED

Baillie A H 1964 Further observations on th growth and histochemistry of the Leydig tissu in the postnatal prepubertal mouse testis Anat *98* 403–419

Baillie A H and K Griffiths 1961 3+H droxysteroid dehydrogenase activity in th mouse Leydig cell J Endocrinol *23* 9–17

Belt W D and D C Pease 1956 Mitocho drial structure in sites of steroid secretio J Biophys and Biochem Cytol 2 (suppl 369–374

Bennett H S and J H Luft 1959 s Collidi as a basis for buffering fixatives J Biophy and Biochem Cytol 6 113–114

Brokelmann J 1964 Über die Stütz und Zwi schenzellen des Froschhodens während de spermatogenetischen Zyklus Z f Zellforsch *64* 429–461

Carr I and J Carr 1962 Membranous whor in the testicular interstitial cell Anat Rec 144 143–147

Christensen A K 1965 The fine structure testicular interstitial cells in guinea pigs Cell Biol 26 911–935

Christensen A K and D W Fawcett 196 The normal fine structure of opossum testicul interstitial cells J Biophys and Biochen Cytol 9 653–670

Christensen A K and N R Mason 196 Comparative ability of seminiferous tubul and interstitial tissue of rat testes to synthe size androgens from progesterone-4 ¹⁴C *in vitro* *Endocrinology* *76* 646–656

Crabo B 1963 Fine structure of the inte stitial cells of the rabbit testes Z f Zel forsch 61 587–604

Dominguez O V H F Acevedo R A Huseb and L T Samuels 1960 Steroid 21 hydroxy lase in normal testes and malignant inter

[2] Large granules up to 0 7 μ in diameter do in fac occur in frog interstitial cells at certain times of the year (Brökelmann 64) Except for their larger size these granules resemble the 0 2 μ granule of the present study in being membrane bounded and con taining a granular matrix They are fuchsinophilic in light microscope preparations

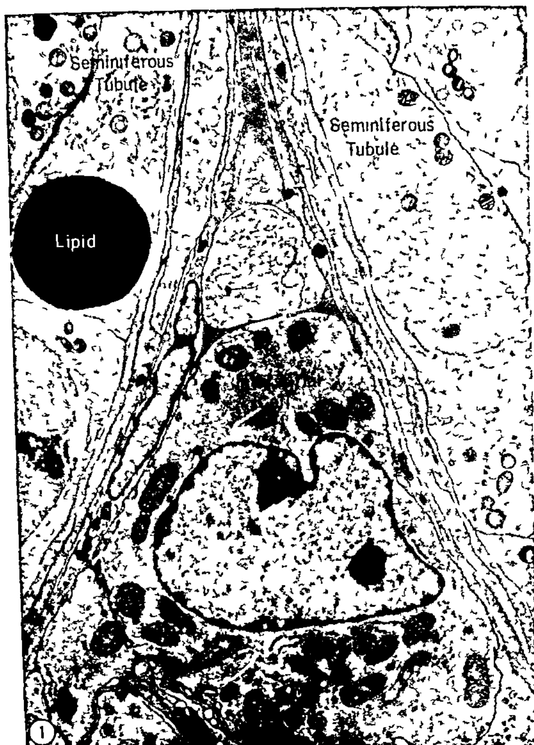

Seminiferous Tubule
Seminiferous Tubule
Lipid
1

PLATE 1

EXPLANATION OF FIGURE

1 Low power electron micrograph of a typical mouse interstitial cell lying between two seminiferous tubules The most abundant organelle in the interstitial cell cytoplasm is the agranular endoplasmic reticulum a network of small tubules filling the cytoplasm between the mitochondria In the area just below the nucleus the agranular reticulum is less well developed and in its place are scattered cisternae of the granular endoplasmic reticulum and numerous clusters of free ribosomes which are difficult to make out at this low magnification The mitochondria are more numerous in the area of granular reticulum and there are two dense lipid droplets The spatial segregation of the granular reticulum from the much more abundant agranular reticulum is a characteristic of mouse interstitial cells 10 000 ×

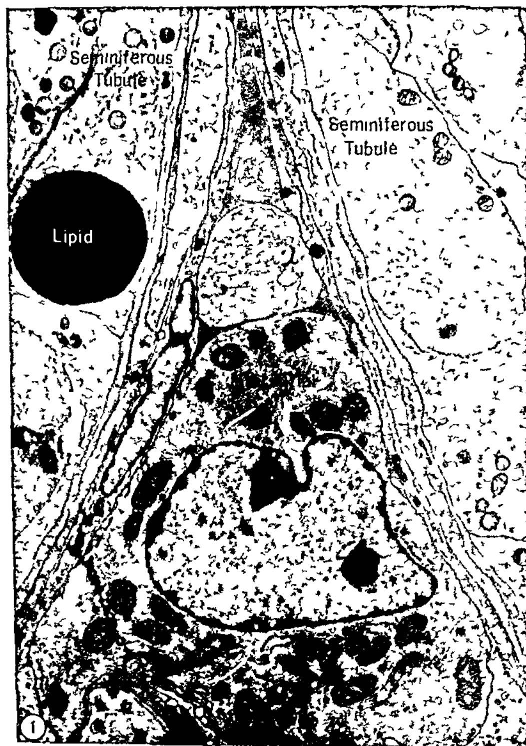

Seminiferous Tubule
Seminiferous Tubule
Lipid
1

PLATE 2

EXPLANATION OF FIGURE

2 Portions of the cytoplasm of two interstitial cells The abundant agranular endoplasmic reticulum is seen in the upper cell and at lower left The lower half of the micrograph illustrates an area of granular endoplasmic reticulum with occasional cisternae of granular reticulum and numerous free ribosomes The concentric membrane system or whorl is a regional modification of the endoplasmic reticulum and occurs frequently in these cells The mitochondria vary greatly in size (note the extremely large mitochondrion at lower right) and contain tubular cristae Small membrane bounded granules about 0 2 μ in diameter are also common 18 000 ×

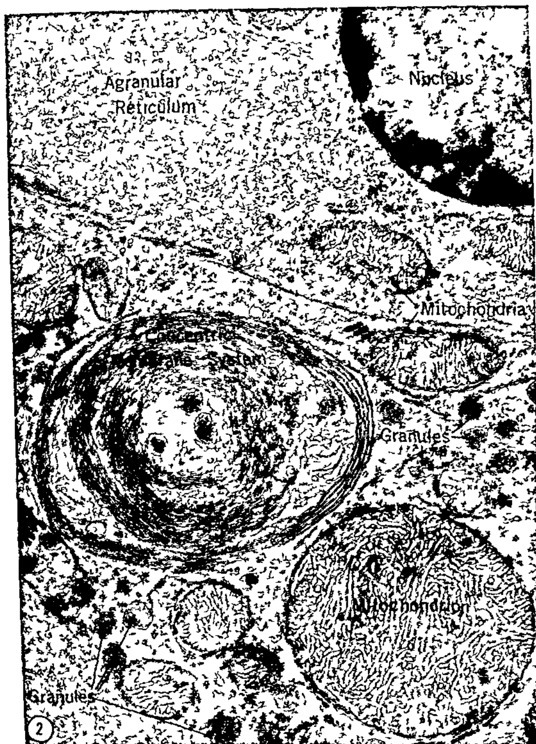

Agranular
Reticulum
Nucleus
Mitochondria
Granules
Mitochondrion
Granules
2

PLATE 3

EXPLANATION OF FIGURE

3 Cytoplasm of two interstitial cells The agranular endoplasmic reticulum is seen in the lower half of the figure and consists of a network of interconnected tubules about 400 A in diameter There is evidence from cell fractionation studies that this agranular reticulum is the principal site of the enzymes that transform progesterone to testosterone and also possibly of many of the enzymes involved in cholesterol biosynthesis Although the agranular reticulum extends nearly to the surface of the cell none of the tubules seem to connect with the plasma membrane In the upper half of the field is a region of granular reticulum showing a lipid droplet clusters of free ribosomes or polyribosomes and several small granules Many of the mitochondria in this figure and also the lipid droplet are enveloped by cisternae of the endoplasmic reticulum (*note especially the mitochondrion at lower left*) 30 000 ×


Lipid
Ribosomes
Granules
Agranular
Reticulum
3

PLATE 3

EXPLANATION OF FIGURE

3 Cytoplasm of two interstitial cells The agranular endoplasmic reticulum is seen in the lower half of the figure and consists of a network of interconnected tubules about 400 A in diameter There is evidence from cell fractionation studies that this agranular reticulum is the principal site of the enzymes that transform progesterone to testerone and also possibly of many of the enzymes involved in cholesterol biosynthesis Although the agranular reticulum extends nearly to the surface of the cell none of the tubules seem to connect with the plasma membrane In the upper half of the field is a region of granular reticulum showing a lipid droplet clusters of free ribosomes or polyribosomes and several small granules Many of the mitochondria in this figure and also the lipid droplet are enveloped by cisternae of the endoplasmic reticulum (note especially the mitochondrion at lower left) 30 000 ×


Lipid
Ribosomes
Granules
Agranular
Reticulum
3

PLATE 4

EXPLANATION OF FIGURES

4 Cross section through a bundle of double walled tubules These unusual structures are derived from the agranular reticulum The outer wall of the double walled tubules has about the same diameter and appearance as nearby tubules of the agranular reticulum The inner wall is more dense and has a diameter of about 250 A The significance of these structures is unknown 47 000 ×

5 Another cross section through a bundle of double walled tubules in which the tubules are more nearly perpendicular to the plane of section and are therefore seen more clearly 48 000 ×

PLATE 4

Double Walled
Tubules

Agranular
Reticulum

4

5

PLATE 5

EXPLANATION OF FIGURES

6 Longitudinal section of double walled tubules The walls of the tubules are continuous with the membranes of the agranular reticulum (asterisks) which suggests that the double walled tubules are a regional modification of the reticulum The central lumen of the double walled tubules seems to be in continuity with the general cytoplasm while the space between the inner and outer walls is continuous with the cavity of the agranular reticulum 52 000 ×

7 Concentric membrane system or whorl This whorl contains about 60 layers and is organized around two lipid droplets (one of them partially extracted) The areas within the rectangles at right and left in the figure are shown at higher magnification in figures 8 and 9 31 000 ×

PLATE 6

EXPLANATION OF FIGURES

8 Enlargement of the area within the rectangle at right in figure 7 showing connections (asterisks) between the membranes of a whorl and those of the agranular reticulum Such connections suggest that the whorls are derived from the endoplasmic reticulum Also shown in the figure are clusters of ribsomes (polyribosomes) and a lipid droplet 98 000 ×

9 Enlargement of the area within the rectangle at left in figure 7 showing a connection (asterisk) between the membranes of a whorl and those of the granular endoplasmic reticulum (note ribo somes attached to the membranes) The membranes of the whorl seem to occur in pairs which may indicate that the whorl is actually composed of flattened cisternae The lipid droplet at upper left is surrounded by a cisterna of the agranular reticulum 98 000 ×

Lipid

Ribosomes

8

Lipid

9

PLATE 6

EXPLANATION OF FIGURES

8 Enlargement of the area within the rectangle at right in figure 7, showing connections (asterisks) between the membranes of a whorl and those of the agranular reticulum Such connections suggest that the whorls are derived from the endoplasmic reticulum Also shown in the figure are clusters of ribsomes (polyribosomes) and a lipid droplet 98 000 ×

9 Enlargement of the area within the rectangle at left in figure 7 showing a connection (asterisk) between the membranes of a whorl and those of the granular endoplasmic reticulum (note ribosomes attached to the membranes) The membranes of the whorl seem to occur in pairs which may indicate that the whorl is actually composed of flattened cisternae The lipid droplet at upper left is surrounded by a cisterna of the agranular reticulum 98 000 ×

PLATE 6

EXPLANATION OF FIGURES

8 Enlargement of the area within the rectangle at right in figure 7 showing connections (asterisks) between the membranes of a whorl and those of the agranular reticulum Such connections suggest that the whorls are derived from the endoplasmic reticulum Also shown in the figure are clusters of ribsomes (polyribosomes) and a lipid droplet 98 000 ×

9 Enlargement of the area within the rectangle at left in figure 7 showing a connection (asterisk) between the membranes of a whorl and those of the granular endoplasmic reticulum (note ribo somes attached to the membranes) The membranes of the whorl seem to occur in pairs which may indicate that the whorl is actually composed of flattened cisternae The lipid droplet at upper left is surrounded by a cisterna of the agranular reticulum 98 000 ×

8

Lipid

Ribosomes

9

Lipid

PLATE 7

EXPLANATION OF FIGURES

10 Large mitochondria To the left and right of the nucleus at upper center are mitochondria of very large size up to 2μ in diameter—compare them with the three more typical mitochondria near the center of the figure The large mitochondria contain the usual tubular cristae and also dense inclusions which resemble small myelin figures The significance of this variation in mitochondrial size is unknown 25 000 ×

11 Mitochondria enveloped by cisternae of the endoplasmic reticulum The cisternae surrounding the mitochondria are agranular for the most part but there are occasional patches of attached ribsosomes 31 000 ×

10

11

Oocytogenesis in Rabbits

THE ROLE OF NEOGENESIS IN THE FORMATION OF THE DEFINITIVE OVA AND THE STABILITY OF OOCYTE DNA MEASURED WITH TRITIATED THYMIDINE

J J KENNELLY[1] AND R H FOOTE
Department of Animal Husbandry Cornell University Ithaca New York

ABSTRACT A series of six thymidine methyl H (thy H^3) injections one every 12 hours was administered to 35 Dutch belted female rabbits (does) commencing on the day of their birth Seventeen of the does were unilaterally ovariectomized as follows five does at 4 and 12 weeks of age five does at 4 and 20 weeks of age five does at 12 and 20 weeks of age and two does at 4 and 40 weeks of age Autoradiographs of ovarian tissue were prepared up to 600 oocytes per ovary were randomly chosen and the silver grains associated with the oocyte nuclei recorded The mean grain counts decreased significantly ($P < 0\,05$) from 4 to 12 weeks 13 5 vs 10 1 and from 4 to 20 weeks 14 7 vs 11 4 However the mean grain counts did not differ significantly ($P > 0\,1$) between 12 and 20 weeks of age 10 5 vs 9 6 Although the mean grain count decreased between 4 to 40 weeks of age 21 5 vs 14 6 the number of replications was too few to detect significant differences ($P > 0\,1$) At 40 weeks of age 91% of the oocytes were still labeled The reduction in grain counts from 4 to 12 weeks of age was attributed to the non random degeneration of the older more highly labeled oocytes located deep in the cortical zone The lack of significant differences between grain counts at 12 and 20 weeks of age suggests that (1) during this interval the desoxyribonucleic acid (DNA) is metabolically stable and (2) significant *de novo* oocyte formation did not occur Nine rabbits were superovulated at 20 weeks of age and of the 217 ova recovered 82 5% were radioactive This was similar to the 89 8% radioactive oocytes observed in the ovaries of the same animals

Artificial insemination of the remaining nine does at 35 and 60 weeks of age resulted in normal litters and superovulation and artificial insemination of this group at 52 weeks of age produced 73 8% radioactive ova

Five Dutch belted does injected at four weeks of age with thy H at the same rate and interval as the day-old rabbits showed a slight incorporation of the isotope into both oocyte nuclei and cytoplasm suggesting that most of the incorporation was not related to any synthesis of new chromosomal DNA A single thy H injection into three 20-week-old does did not result in appreciable uptake of the isotope by oocyte nuclei although many nuclei of parenchymal cells in the ovary were highly labeled

The results conclusively support the view that most if not all definitive ova are formed at birth and *de novo* oocytogenesis does not occur in the post-pubertal rabbit

The generally accepted view that in most mammals the definitive ova are formed in the natal or neonatal period and further that *de novo* oocyte formation through a cyclical proliferation of the germinal epithelium does not occur (Zuckerman 51 55) has been challenged from time to time Allen (23) reviewed arguments both for and against neoovogenesis and concluded from his own work in the mouse that several hundred oocytes were formed at each estrous cycle Swezy (29) and Evans and Swezy (31) reached the same general conclusions in the rat guinea pig dog cat monkey and man However in order to conclude this the authors had to assume that typical meiosis did not occur in the adult as the usual meiotic figures were not seen Meiotic figures in oocytes of some adult prosimians have been observed (Gerhard 32 Rao 27 Gerhard and Herlant 53) but the authors considered these to be exceptions rather than the rule Zuckerman (51 55) presented

[1] Present addres Denve Wildl f R search Center Bure u of Sport F sh rie nd Wildlife B ilding 45 Den Col ad

compelling arguments supporting the view point that new oocytes do not arise in the adult It has been difficult to obtain irrevocable evidence to support this view point

Recent students in mice (Rudkin and Griech 62) using tritiated thymidine as a cell marker have shown that oocytes formed in the natal period persist beyond puberty Vital staining techniques have been used to trace the origin of germ cells Latta and Pederson (44) concluded from studies with India ink that oocytes and follicle cells were derived from the ger minal epithelium However Jones (49) using the same technique found no evi dence to support Latta and Pederson (44) and concluded that technical artifacts led the authors to an erroneous interpreta tion Chiquoine (61) studied mouse ovaries vitally stained with colloidal gold and also found no evidence for the post natal formation of oocytes To be able to demonstrate unequivocally a link or lack of a link between the oocytes observed in meiosis during the late natal and neonatal period and the definitive ova would resolve this question and contribute much to our understanding of oogenesis

This investigation was undertaken in the rabbit to determine whether all the definitive ova of this species are formed at birth or whether significant numbers of oocytes develop in the post neonatal and post pubertal periods The rabbit was chosen because the majority of germ cells in the newborn females of this species enter Prophase I of meiosis during the first week of life (von Winiwarter 00 Teplitz and Ohno 63) and because a very suc cessful procedure for routinely superovulat ing rabbits and collecting ova had been developed (Kennelly and Foote 65) Consequently the oocytes may be labeled by injecting young females with tritiated thymidine and determining the radioac tivity of oocytes and ova as the animals age

METHODS

Animals and experimental design

The animals were divided into two major experimental groups based on their age at the start of the experiment In ex periment I 35 day old Dutch belted female rabbits were injected with thymidine methyl H^3 (thy H^3) [1] Each rabbit received six subcutaneous injections of thy H^3 in the mid dorsal region once every 12 hours at the rate of 0 5 microcuries per gram of body weight per injection Body weight was determined prior to the first third and fifth injections All young were returned to their dams between injections

Seventeen of the does hereafter referred to as group Ia were used to study whether significant changes occur in the mean grain counts or proportions of radioactive oocytes with respect to time Five does were unilaterally ovariectomized at 4 and 12 weeks of age (4–12 week group) five at 4 and 20 weeks of age (4–20 week group) two at 4 and 40 weeks of age (4 40 week group) and five at 12 and 20 weeks of age (12–20 week group) Left and right ovaries from these 17 does were removed alternately Nine does in experimental group Ib were superovulated at 20 weeks of age according to procedures reported previously (Kennelly and Foote 65) ex cepting the dose was 0 31 mg of FSH per injection instead of per day The animals were euthanized and ova from each doe flushed counted and fixed The ovaries were saved for histological study The remaining nine does in experimental group Ic were artificially inseminated and ovu lated with luteinizing hormone (Kennelly and Foote 65) at 35 52 and again at 60 weeks of age The does were permitted to kindle normally after the inseminations at 35 and 60 weeks of age At 52 weeks the does were superovulated and the ova were flushed from the live animal 26 to 30 hours after insemination All does in one age group were inseminated with semen from one male but different males were used from one age group to the next

In experiment II older females received thy H^3 Five 4 week-old Dutch belted fe males comprising group IIa were injected with thy H^3 at the same dose rate and interval described for the day old rabbits They were weaned at six weeks of age and thereafter were maintained in individual cages until the termination of the ex

[1] New England Nuclear Corp specific activity 6 7 curies per millimole prepared as 5 millicuries per 5 ml sterile aqueous solution per vial

periment Each of these five does were unilaterally ovariectomized 24 hours after the last thy H injection and the remaining ovary was removed at 12 weeks of age

Experimental group IIb contained three 20 week old virgin Dutch belted females Each of these does received a single sub cutaneous injection of thy H[3] in the mid dorsal region at the rate of 0 5 microcuries per gram of body weight These adult does were unilaterally ovariectomized 24 hours after the thy H injection and the remaining ovary was removed 96 hours after the thy H injection

Non injected animals were maintained to provide control ovarian tissue A sum mary of experiments I and II is as follows

I Does received thy H at birth

a Ovaries were removed at 4 and 12 4 and 20 4 and 40 and 12 and 20 weeks of age

b Does were superovulated and eu thanized at 20 weeks

c Does were superovulated at 52 weeks of age and were allowed to kindle at 35 and 60 weeks Ovaries were removed at 69–71 weeks of age

II Does received thy H when older

a Given thy H at four weeks ovaries removed at 4 and 12 weeks

b Given thy H at 20 weeks ovaries re moved at 20 weeks

Histological procedures

All ovaries were fixed in acetic acid absolute ethanol (1 3) for 5–7 hours dehydrated routinely and embedded in paraffin Transverse sections from several areas of each ovary were cut at 5 μ moun ted on acid-cleaned gelatin-coated slides and stained by a Feulgen fast green pro cedure In experiment II sections cut from ovaries of non treated rabbits at the cor responding ages were mounted on slides containing the radioactive tissue to serve as non radioactive standards

The ova from the unmated does in group Ib were flushed from the excised oviducts with oxalated blood plasma col lected in a watch glass and counted at 35 × Approximately 0 5 ml of Simplastin solution was added to the plasma contain ing the ova A clot formed within three minutes The clot was fixed in acetic acid absolute ethanol (1 3) for 30 minutes dehydrated routinely and embedded in paraffin Each clot was serially sectioned at 4 μ and stained by the Feulgen fast green procedure

The ova from the does artificially in seminated at 52 weeks of age were ob tained by in vivo flushing of the ova from the fimbriated end of the oviduct with oxalated blood plasma 26 to 30 hours after insemination During this time it was ex pected that fertilized ova would reach the 2-cell or 4-cell stage thus making possible a check of fertilization rates At the same time dilution of thy H which would ac company successive cell divisions was minimized The ova were examined and processed as described for the previous group excepting the sections were cut at 5 μ

Autoradiographic procedure

The stained slides were coated with Kodak NTB 3 liquid emulsion warmed to 40–45 C and applied with a stainless steel roller (Belanger 61) Slides containing standard non radioactive tissue (experi ment II) were coated so that the emulsion always covered the standard tissue first thereby eliminating the possibility of con tamination of the standard tissue by radio active particles The slides were placed in light tight plastic boxes containing about 15 gm of packaged Drierite (CaSO) and stored at 5 C for six weeks The slides were developed for ten minutes in Kodak D 19 developer rinsed in tap water fixed in Kodak acid fixer for ten minutes washed for 15 minutes in running tap water dehydrated routinely and mounted with Diaphane Development and dehy dration was done at 5 C up to the first absolute ethanol solution and at room tem perature thereafter The autoradiographs of the ova from group Ic underwent addi tional staining when it was discovered that the ova from experimental group Ib were difficult to locate due to loss of stain in the photographic development The addi tional staining consisted of a 1% eosin in 95% ethanol solution for two minutes prior to the first absolute ethanol step in the final dehydration

W rn r Ch lc tt Manuf t re

Autoradiographic evaluation

The procedures for counting grains in the autoradiographs (ARGs) are given in some detail because the interpretation of these results is crucial to the inferences regarding oocyte formation and DNA stability Grains were counted at a magnification of 970 ×

In group Ia grains over 600 oocyte nuclei selected at random (4 slides per ovary × 150 oocytes per slide) were counted in the 4–12 and 4–20 week groups In two animals with pronounced oocyte atresia less than 600 oocytes were found in the four slides In the 4–40 week group 100 oocytes per slide were examined making a total of 400 oocytes per ovary

The average background grain count was determined by counting the grains in a 5 062 μ^2 area of nuclear free tissue per slide The mean background count was 0 47 grains per 100 μ^2 Only nuclei with two or more grains over them were classified as labeled Mean grain counts unless otherwise noted are based on the population of labeled oocytes and not on the total population sampled To equalize the number of labeled cells in the different groups for the statistical analysis of the labeled oocyte population the first 125 labeled oocytes encountered were used for the 4–12 and 4–20 week group Later all labeled nuclei were included in the analysis

The oocyte nuclei change size with time Changes in nuclear size may influence the proportion of total nuclear tritium disintegrations which are recorded on film over a cross section partly as a result of coincidence The possible effects of compactness of the DNA on coincident grains was explored by making grain counts over a total of 2 400 oocyte nuclei from 4 week old and from 12 week old does after exposure of the ARGs for two and six weeks

ARGs of the ova in group Ib were scanned at 35 × to locate the ova and grains were counted over the chromosomes at 970 × Ova with three or more grains associated with the chromosomes were classified as labeled This presumably gave a conservative estimate of labeled ova because background counts averaged 0 50 grains per 100 μ^2 Care was taken to insure that labeled chromosomes and labeled polar bodies of the same ovum were not both counted The percentage of labeled oocytes in the ovaries from the animals producing these ova was estimated Grains over 300 randomly selected oocytes per ovary were recorded and nuclei with two or more grains were considered to be labeled

The ARGs in group Ic were examined in the same manner as that described for group Ib excepting that the polar bodies were used to determine whether or not an ovum was labeled it was difficult to determine whether the nuclei of cleaved ova were labeled or not Serial sections of each ovum were examined to be sure that where polar bodies were present in more than one section each ovum was counted only once

In experiment II it was particularly important to establish accurate background grain counts over nuclei and cytoplasm in order to determine whether or not thy H^3 injected into older animals was significantly incorporated into oocytes Low levels of isotope in the cells could result from incorporation into non chromosomal DNA or incorporation into other products of cell metabolism after thy H^3 had been degraded In group IIa (5 does) three slides per ovary per doe were prepared from the ovaries removed one day after thy H^3 injection in week four and a similar series was prepared for the remaining ovaries removed eight weeks later The same slides contained representative sections of ovaries removed from non injected does of the same age Background over 5 062 μ^2 of nuclear free tissue (primarily the cytoplasm of parenchymal and stromal cells) from injected as well as control animals was counted on each of 15 slides at each age This was compared with grain counts over 1 500 oocyte nuclei (300 nuclei per doe × 5 does) from injected animals vs controls at each age To make the comparisons between cytoplasm and nuclei more meaningful nuclear areas were calculated and all counts converted to grains per 1 000 μ^2 Nuclear areas were calculated from two diameter measurements made at right angles to each other on each of five oocytes in all ovaries stu

died The nuclei were found to be round and the area was calculated on this basis

Similar procedures were followed for group IIb injected with thy H³ at 20 weeks of age Grain counts over 1 200 oocyte nuclei in tissue removed 24 hours after thy H injection gave the same result as for 1 200 oocyte nuclei in tissue removed 96 hours post injection Therefore an additional set of slides was prepared from the tissue removed 96 hours post injection for comparison with tissue from non radioactive does Grain counts over cytoplasm and nuclei again were converted to grains per 1 000 μ

All data were statistically analyzed according to procedures described by Henderson (59) and Steel and Torrie (60)

RESULTS

Labeled oocytes were observed in all ovaries of the 17 does in group Ia (plate 1) The mean nuclear grain counts for all oocytes and for labeled oocytes of the 4–12 4–20 4–40 and 12–20-week groups are presented in table 1 In each treatment group the oocyte mean nuclear grain counts were greater in the ovaries removed at the younger age The proportion of cells labeled decreased with increasing age

The analysis of variance of the mean nuclear grain counts of the labeled oocytes is presented in table 2 for the 4–12 and 4–20 week treatment groups and in table 3 for the 4–40 and 12–20 week treatment groups Most of the variation was due to differences in grain counts among oocytes in the same ovary However with the exception of the 4–40 week treatment group composed of only two does does within each treatment group differed significantly ($P < 0\ 005$) This doe variation in oocyte labeling is believed to represent in part differences in doe development at the time they are born The decrease in mean grain counts between 4 and 12 weeks and 4 and 20 weeks was real ($P < 0\ 005$ and $P < 0\ 05$ respectively) but the decrease in grain counts between 12 and 20 weeks was not significant ($P > 0\ 1$) The decrease in mean grain count between 4 and 40 weeks was not statistically significant with only two animals but the results of the other treatment groups suggest that the difference probably was real At the same time it should be noted that 91% of the oocytes were still labeled at 40 weeks of age

The effect of coincident disintegrations on the oocyte mean grain counts of the tissue removed at 4 and 12 weeks is presented in table 4 The mean percentage of actual grains counted compared to the number of grains expected was 83 8 and 86 4% of the 4 and 12 week tissue respectively Student s t test indicated that coincident disintegrations affected the grain counts at 4 and

TABLE 1

Labeled oocyte nuclei in ovaries removed at 4 12 20 and 40 weeks of age from animals injected with thy H at birth

T tm nt group	N mber of doe pe tre tm nt	Age wh n y w s s mpl d	Number f oocyt observed	Grain count			Rad o- cti oocyte
				Me n of ll oocyt	L beled oocyt s		
					Me n	S E	
							%
4–12	5	4 weeks	600	12 2	13 5	9 43	90 3
		12 weeks	600	8 4	10 1	6 87	82 5
4–20	5	4 weeks	600	13 6	14 7	10 09	91 7
		20 weeks	600	10 1	11 4	7 87	86 5
4–40	2	4 weeks	400	21 0	21 5	14 44	96 6
		40 weeks	400	13 8	14 6	10 04	91 0
12–20	5	12 weeks	600	9.3	10 5	7 13	88.8
		20 weeks	600	8.3	9 6	6 29	86 0

Due to atre i th number of oocytes observ d fo one doe at 12 and 20 weeks w s 162 and 138 and f r a second doe 550 nd 440 re pecti ly The s m number f sl des prep red w s more th n d q te to count 600 oocy s in ll other bbits

TABLE 2

Analysis of variance of labeled oocytes in the 4–12 and 4–20 week groups

Source of variation[1]	d f	Expectation of mean square	4–12 week group				4–20-week group			
			Mean square	F ratio	Probability level	Total variance	Mean square	F ratio	Probability level	Total variance
D	4	$\sigma^2_w + \sigma^2_d + 150\sigma^2_d + 600\sigma^2_d + 1200\sigma^2_d$	2 904 9	7 1	$< 0\ 005$	3 2	8 661 0	32 1	$< 0\ 005$	8 6
A	1	$\sigma^2_w + \sigma^2_d + 150\sigma^2_d + 600\sigma^2_d + 3000\sigma^2$	14 526 6	39 1	$< 0\ 005$	7 1	12 884 1	11 6	$< 0\ 05$	4 8
DA	4	$\sigma^2_w + \sigma^2_d + 150\sigma^2_d + 600\sigma^2_d$	371 7	0 9	$> 0\ 10$	—	111 5	4 1	$< 0\ 01$	1 7
S DA	30	$\sigma^2_w + \sigma^2_d + 150\sigma^2_d$	407 5	6 0	$< 0\ 005$	3 4	270 0	3 3	$< 0\ 005$	1 5
O SDA	4960	$\sigma^2_w + \sigma^2_d$	68 0	—	—	86 2	81 8	—	—	83 4

[1] Does (D) slides (S) and observations (O) were all considered to be random variables whereas age (A) was considered to be fixed

12 weeks equally and so probably can be ignored here when comparing relative counts at the different ages However coincidence must be taken into account when absolute values are being estimated

The results of the superovulatory procedure and the proportion of recovered ova which were radioactive for group Ib does sacrificed at 20 weeks of age are p e sented in table 5 Although 360 ova were collected only 217 ova were located in the autoradiographs and identified Of the 217 ova 179 or 82 6% were classified as radioactive This is slightly less than the 89 8% of the ovarian oocytes classified as radioactive but the difference is all due to one animal doe 5

The kindling results and proportion of cleaved and labeled ova of the group Ic does which underwent superovulation and/or artificial insemination are presented in table 6 The mean litter sizes of 7 0 and 6 6 for the first and second gestations were normal Surgery at 52 weeks may have reduced the pregnancy rate at 60 weeks Gestation length averaged 31 days The sex ratio apparently was unaffected by the thy H^3 incorporated into the oocyte nuclei as 42 males and 39 females were born The mean percentage of radioactive ova was 73 8% and of radioactive ovarian oocytes was 77 6%

The mean oocyte grain counts 1 000 μ^2 in rabbits receiving thy H^3 at four weeks of age (group IIa) is contrasted with noninjected controls in table 7 and the analysis of variance is presented in table 8 The grain counts for ages injected vs control animals for nuclei versus cytoplasm differed ($P < 0\ 005$) Incorporation of the label occurred in both the nucleus and cytoplasm However by 12 weeks most of the label appeared to be gone from the nuclei and all from the cytoplasm indicating that the initial incorporation was in components that turned over rapidly In no case was thy H^3 incorporated extensively The grain counts per nucleus were only 6–18% of the counts calculated on the basis of 1 000 μ^2 because oocyte nuclei ranged from 57 to 179 μ^2 in area depending upon the animal and its age when the ovaries were removed Mean oocyte nuclear grain counts for radioactive and control tissue at four weeks were 1 8 and 0 74

TABLE 3

Analysis of variance of labeled oocytes in the 4–40 and 12–20 week groups

4–40-week group					12–20-week group				
Source of variation	d f	Mean square	F ratio	Probability level	Source of variation	d f	Mean square	F ratio	Probability level
D	1	848.5	3.02	> 0.10	D	4	493.2	10.40	< 0.005
A	1	16 690.7	5.05	> 0.10	A	1	580.7	1.63	> 0.10
DA	1	3 306.0	11.78	< 0.005	DA	4	355.78	7.50	< 0.005
S DA	12	280.6	1.79	< 0.05	O DA	4233	47.40		
O SDA	1548	156.6							

[1] See footnote to table 2

TABLE 4

Coincident effect on oocyte grain counts from ovaries removed at 4 and 12 weeks of age

Doe	Mean grain count 4 weeks			Mean grain counts 12 weeks		
	Expected	Actual	Actual as a % of expected	Expected	Actual	Actual as a % of expected
1	11.2	8.9	79.5	7.6	6.8	89.5
2	12.5	11.0	88.0	10.8	9.0	83.3
Mean	11.8	10.0	83.8	9.2	7.9	86.4

Expected value is the actual count after two weeks of exposure × 3
Actual count after six weeks of exposure

TABLE 5

Proportion of radioactive ova and ovarian oocytes at 20 weeks of age in does injected with thy-H at birth

Doe	Number of ova collected	Number of ova found in ARG	Number of radioactive ova	Radioactive cells	
				Ova	Ovarian oocytes
				%	%
1	66	21	19	90.5	89.6
2	39	34	30	88.2	93.3
3	33	26	17	65.4	95.7
4	16	10	9	90.0	84.3
5	42	28	5	17.8	90.0
6	51	36	30	83.3	87.3
7	16	11	10	90.9	88.3
8	41	24	24	100.0	94.0
9	56	37	35	94.6	86.0
Total	360	217	179	—	—
Mean	40.0	24.1	19.9	82.6	89.8

Weighted mean
[2] Three hundred oocytes from each randomly selected ovary per doe were examined

and at 12 weeks were 0.31 and 0.19 respectively

The frequency distribution of grain counts and the mean nuclear and cytoplasmic counts of ovaries removed from 20-week-old does (group IIb) 24 and 96 hours after injection with thy H are presented in table 9. Calculation of χ^2 for the grain count distribution resulted in a value of 5.08 ($P > 0.4$) which suggests that the two ovaries sampled at different intervals give the same results. Likewise the mean nuclear counts per 1 000 μ of 3.50 and 3.68 grains in the two series of ovaries were similar. Thereafter only the ovaries removed 96 hours after injection were compared with standard non-radioactive tissue to estimate the extent of thy H utilization by adult ovaries. Results are presented in table 10. Grain counts

TABLE 6

Radioactivity and fertility of ova binding rates and radioactivity of ovarian oocytes in adult rabbits injected with thy H³ at birth

Does	Gestation at 35 weeks		Superovulation at 52 weeks					Gestation at 60 weeks		Labeled ovarian oocytes at 70 weeks [2]
					Ova labeled [1]					
	Litter size	Died before weaning	Total ova collected	Ova cleaved	Un cleaved	Cleaved	Total	Litter size	Died before weaning	
				%	%	%	%			%
1	5	2	29	86	17	43	60	9	0	80
2	9	0	11	0	100	0	100	2	0	78
3	0	0	22	100	0	77	77	0	0	84
4	6	1	10	0	75	0	75	8	0	67
5	9	0	46	78	4	56	60	0	0	74
6	0	0	31	0	81	0	81	0	0	81
7	5	0	26	12	13	48	61	0	0	86
8	9	7	42	7	74	10	84	8	0	74
9	6	0	23	13	82	12	94	6	0	— [4]
Mean	7 0 [3]	1 4 [3]	26 7	32 9	42 1	31 7	73 8	6 6 [3]	0	77 6

[1] Based upon the ova observed following autoradiography
[2] Based on 100 oocytes per doe classifying oocytes with three or more grains over them as *labeled* th same as was used for ova The percentage of labeled oocytes was 84 5 when two or more grains was take as evidence for labeling
[3] Based on rabbits producing young only Litter size is similar to non radioactive animals in the col n surgically treated between first and second pregnancies
[4] Doe died and tissue was unsuitable for study

TABLE 7

Grain counts in ovaries removed at 4 and 12 weeks of age from does injected at 4 weeks versus non radioactive controls (5 does per group)

Age at removal of ovary	Thy H³ injected			Non injected controls		
	Grains per 1000 μ² [1]		Oocytes with one or more grains	Grains per 1000 μ²		Oocytes with one or more grains
	Nuclei	Cytoplasm		Nuclei	Cytoplasm	
			%			%
4 weeks	13 70 [2]	6 26	43	3 76	4 15	30
	13 94	7 44	48	3 76	3 16	26
	19 15	8 23	69	4 20	3 23	36
	16 94	14 16	73	3 65	3 89	31
	11 11	9 68	67	2 75	3 42	26
Mean	14 97	9 16	59 9	3 62	3 57	29 8
12 weeks	3 02	2 77	11	1 92	1 98	6
	4 75	2 57	18	4 06	1 78	10
	6 94	3 95	28	4 64	4 21	15
	4 26	1 98	15	2 73	2 57	9
	4 20	2 44	13	3 42	1 65	10
Mean	4 64	2 74	16 9	3 35	2 44	10 3

[1] Grain counts per 1000 μ² are equivalent to an area from 6 to 18 times the size of the oocyte nucleus depending upon animals and age group
[2] Three hundred nuclei counted per tabular mean value

over both nuclei and cytoplasm were higher in the radioactive does than in the controls ($P < 0\ 1$) a finding similar to that obtained with the group IIa does injected at four weeks of age However since the cytoplasmic counts differed a much as the counts over nuclei the smal uptake of tritium at 20 weeks does no appear to be associated with chromosoma DNA in the oocytes Nuclei of paren

chymal and stromal cells in the group receiving thy H^3 often were heavily labeled but oocytes with several grains were not found more frequently than in the con trols

TABLE 8

Analysis of variance of nuclear and cytoplasmic grain counts/1000 μ^3 of radioactive ovaries in does injected with thy H^3 at four weeks and in non radioactive ovaries

Source	d f	Me n squ re	F ti	P bability l v l
A	1	618 12	39 45	< 0 005
T	3	290 00	27 36	< 0 005
AT	3	167 52	10 69	< 0 005
D T	16	10 60	4 00	< 0 005
DA T	16	7 72	2 91	< 0 005
S DAT	80	2 65		

Ag (A) nd t e tment (T) were cons dered t be fix d b t does (D) and slides (S) we e cons de ed to be a dom ari ble

DISCUSSION

The significant changes in the grain counts of the oocyte population with in creasing age in experiment I (tables 1 2 3) have several possible explanations (1) changes in nuclear volume with age causing estimated grain counts to vary without necessarily any other change taking place in the oocyte population (2) new oocytes arising *de novo* or from con tinued oogonial divisions (3) non random degeneration of existing oocytes and (4) isotope decay along with possible breakage of the chemical bonds by radiation energy and replacement with non radioactive ma terial

The oocyte nuclei decreased in diameter about 16% from 4 to 20 weeks of age This decrease would be expected to result

TABLE 9

Grain counts over oocyte nuclei and over cytoplasm in does injected with thy-H at 20 weeks of age

H rs aft thy H I j ct on	Does	Frequency d tribut n of oocyte gr in unt 0	1	2	3	4	> 4	Oocyte with one or more grains	G ain pe 1000 µ Oocyte nuclei	Cyt pl m
								%		
24	1	180	12	4	3	–	1	10	3 03	3 56
24	2	179	12	5	2	1	1	10	3 00	2 96
24	3	169	19	5	5	2	–	16	4 48	4 74
Total		528	43	14	10	3	2	—	—	—
Mean		176 0	14 3	4 7	3 3	2 0	0 7	12 0	3 50	3 75
96	1	174	14	8	2	2	–	13	3 34	4 35
96	2	172	17	6	2	–	3	14	3 63	3 56
96	3	165	16	13	5	–	1	18	4 08	2 96
Total		511	47	27	9	2	4	—	—	—
Mean		170 3	15 7	9 0	3 0	0 7	1 3	15 0	3 68	3 62

F hund d oocyt x mined per o ry

TABLE 10

G ain counts ove oocyte nuclei and cytoplasm in does injected with thy H at 20 weeks of age versus non rad oactive controls

Doe	Thy H injected: G ins pe 1000 µ Oocyt nu l i	Cytopl m	Oocyt s with n o mo e g in	Doe	Non injected ontrol: G ins p 1000 µ Oocyte nucl i	Cyt pl sm	Oocyt s with on o more g ain
			%				%
1	5 53	4 94	18	4	5 80	3 36	18
2	5 62	3 16	18	5	3 05	1.28	11
3	7 00	6 62	24	6	5 71	3 46	20
Mean	6 05	4 91	20 0		4 85	2 70	16 3

Fou hu d d oocyte mined pe doe

in a concomitant increase in the concentration of desoxyribonucleic acid (DNA) per unit of area as well as volume and an increase in the number of grains per cross section This could affect the number of coincident grains A study of coincident effects in the 4–12 week group (table 5) indicated that coincidence was similar at both ages and can be excluded from consideration However the reduction in mean grain count during a time when the opposite results might have been expected from the estimation procedure alone implies that the true differences between ages probably were greater than observed

Formation of new oocytes from oogonia or other precursor cells could decrease the mean grain count of oocytes because of the dilution of the radioactive DNA which occurs with new DNA synthesis preceding divisions leading to oocytes The proportion of labeled oocytes could be altered depending upon the proportion of precursor cells with sufficient thy H^3 to produce oocytes with detectable isotope This second hypothesis of new formation of oocytes is not a likely explanation of the observed changes because (1) meiotic figures never were observed in the older ovaries and (2) the proportion of labeled oocytes decreased little after 12 weeks of age Some of the early changes may have been due to new formation of oocytes as the formation of oocytes from oogonia is not completely synchronized throughout the ovary However no cytological evidence of new oocyte formation was observed in animals 12 weeks old or older The grain count over nuclei of most cells other than oocytes was much reduced in older ovaries Thus if any of these cells could give rise to oocytes the resultant oocyte nuclei would appear to be non labeled or only slightly labeled No increase in this type of oocyte nuclei was found

Finally the injection of thy H into animals at 4 and 20 weeks of age resulted in only slight incorporation of the isotope into oocyte nuclei at four weeks and no specific incorporation in these nuclei at 20 weeks The mean oocyte grain counts of the group IIa does injected at four weeks of age never approached the values obtained for the groups given the isotope at birth Among the 1 500 individual oocyte grain counts made at 4 weeks on the group IIa does only three or 0 2% exceeded ten grains above background The average oocyte count at 4 and 12 weeks of age averaged 1 8 and 0 31 grains respectively whereas the mean counts of the group Ia does ranged from 8 4 to 21 0 grains (table 1) The complete lack of any labeled oocytes in the three does injected at 20 weeks of age (IIb) confirms the finding at four weeks that oocytogenesis ceases at an early age

The third and most likely explanation of grain count changes is that oocytes degenerate extensively in a non random manner especially early in life (Kingsbury 13 Mandl and Shelton 59 Jones and Krohn 61 Mauleon 61) Kingsbury (13) suggested that oocyte atresia in the cat followed a centrifugal course" It occurred first among the cells in the deepest portions of the cortex and proceded peripherally Also von Winiwarter (00) has shown that meiosis in the rabbit ovary begins in the deeper cortical layer and proceeds toward the periphery In the present study the more advanced oocytes synthesizing DNA at the time of the thy H^3 injections appeared in the more central areas and these oocytes were more highly labeled Oogonia labeled at this time soon produced oocytes in which the thy H^3 had been diluted

The distribution of grain counts (figs 1 and 2) and the reduction in the standard errors of the means (table 1) of the grain counts over oocyte nuclei in the older ovaries clearly supports the view that the highly labeled oocytes formed early degenerated more frequently than other oocytes Whether the concentration of thy H^3 was responsible for oocyte atresia per se was not established The 0 5 microcuries per gram of body weight dose of thy H used was below the level reported by Johnson and Cronkite (61) to be detrimental to male germ cells

The fact that the grain counts decreased significantly ($P < 0.05$) at the early ages (table 2) but not between 12 and 20 weeks ($P > 0.1$ table 3) is consistent with the findings in mouse and rat ovaries (Mandl and Shelton 59 Mauleon 61) that large numbers of oocytes degenerate early an

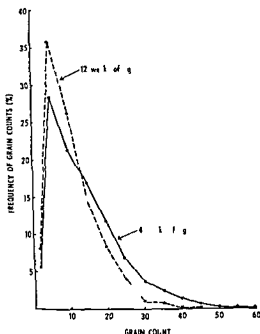


Fig 1 Distribution of grain counts over oocyte nuclei at 4 and 12 weeks of age in rabbits receiving thymidine H^3 at birth

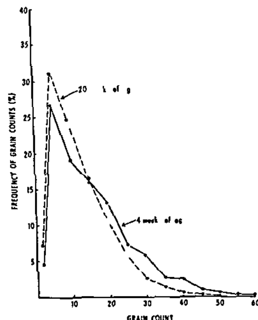


Fig 2 Distribution of grain counts over oocyte nuclei at 4 and 20 weeks of age in rabbits receiving thymidine-H^3 at birth

the rate of degeneration decreases with age

These findings also are consistent with the concept that the oocyte DNA is metabolically stable If large portions of chromosomal DNA had been replaced gradually by non radioactive DNA as the animal aged the grain count should have continued to decrease markedly Most of the decrease occurred between 4 and 12 weeks of age with little change thereafter Decay of the isotope would have little effect during this time The decline in grain counts occurred more rapidly in some does than in others as evidenced by the age × doe interactions ($P < 0\ 01$)

The recovery of radioactive ova from the does in groups Ib and Ic (figs 7 8 9 10) clearly indicates that at least the majority of the ovulated ova are formed during the neonatal period persist past puberty and are capable of fertilization The close agreement in group Ib (table 5) between the proportion of radioactive ovarian oocytes and the proportion of radioactive ova collected 89 8% vs 82 5% respectively further supports this view The difference between the two proportions appeared to be due entirely to one doe with only 17 8% labeled ova since the means of the other eight does are essentially equal It is not known why this animal ovulated so few radioactive ova as the ovaries appeared to be normal

The apparently normal litters which followed the insemination of the thy H^3 treated rabbits in group Ic (table 6) implies that the levels of isotope used did not adversely affect the development of young the sex ratio or the gestation length The cleavage rates are underestimates of true fertility since the time interval allowed between insemination and ova collection was sometimes insufficient to allow all fertilized eggs to cleave Unpublished studies in this laboratory have shown that on the average superovulated ova undergo the first cleavage division approximately three hours later than untreated does and undoubtedly many fertilized ova were collected prior to cleavage For example one doe with only three ova classified as definitely cleaved had an additional three labeled ova in the pronuclear stage Apparently sperm transport was a significant

in a concomitant increase in the concentration of desoxyribonucleic acid (DNA) per unit of area as well as volume and an increase in the number of grains per cross section This could affect the number of coincident grains A study of coincident effects in the 4–12 week group (table 5) indicated that coincidence was similar at both ages and can be excluded from consideration However the reduction in mean grain count during a time when the opposite results might have been expected from the estimation procedure alone implies that the true differences between ages probably were greater than observed

Formation of new oocytes from oogonia or other precursor cells could decrease the mean grain count of oocytes because of the dilution of the radioactive DNA which occurs with new DNA synthesis preceding divisions leading to oocytes The proportion of labeled oocytes could be altered depending upon the proportion of precursor cells with sufficient thy H^3 to produce oocytes with detectable isotope This second hypothesis of new formation of oocytes is not a likely explanation of the observed changes because (1) meiotic figures never were observed in the older ovaries and (2) the proportion of labeled oocytes decreased little after 12 weeks of age Some of the early changes may have been due to new formation of oocytes as the formation of oocytes from oogonia is not completely synchronized throughout the ovary However no cytological evidence of new oocyte formation was observed in animals 12 weeks old or older The grain count over nuclei of most cells other than oocytes was much reduced in older ovaries Thus if any of these cells could give rise to oocytes the resultant oocyte nuclei would appear to be non labeled or only slightly labeled No increase in this type of oocyte nuclei was found

Finally the injection of thy H^3 into animals at 4 and 20 weeks of age resulted in only slight incorporation of the isotope into oocyte nuclei at four weeks and no specific incorporation in these nuclei at 20 weeks The mean oocyte grain counts of the group IIa does injected at four weeks of age never approached the values obtained for the groups given the isotope at birth Among the 1 500 individual oocyte grain counts made at 4 weeks on the group IIa does only three or 0 2% exceeded ten grains above background The average oocyte count at 4 and 12 weeks of age averaged 1 8 and 0 31 grains respectively whereas the mean counts of the group Ia does ranged from 8 4 to 21 0 grains (table 1) The complete lack of any labeled oocytes in the three does injected at 20 weeks of age (IIb) confirms the finding at four weeks that oocytogenesis ceases at an early age

The third and most likely explanation of grain count changes is that oocytes degenerate extensively in a non random manner especially early in life (Kingsbury 13 Mandl and Shelton 59 Jones and Krohn 61 Mauleon 61) Kingsbury (13) suggested that oocyte atresia in the cat followed a centrifugal course It occurred first among the cells in the deepest portions of the cortex and proceeded peripherally Also von Winiwarter (00) has shown that meiosis in the rabbit ovary begins in the deeper cortical layer and proceeds toward the periphery In the present study the more advanced oocytes synthesizing DNA at the time of the thy H^3 injections appeared in the more central areas and these oocytes were more highly labeled Oogonia labeled at this time soon produced oocytes in which the thy H^3 had been diluted

The distribution of grain counts (figs 1 and 2) and the reduction in the standard errors of the means (table 1) of the grain counts over oocyte nuclei in the older ovaries clearly supports the view that the highly labeled oocytes formed early degenerated more frequently than other oocytes Whether the concentration of thy H^3 was responsible for oocyte atresia per se was not established The 0 5 microcuries per gram of body weight dose of thy H used was below the level reported by Johnson and Cronkite (61) to be detrimental to male germ cells

The fact that the grain counts decreased significantly ($P < 0\ 05$) at the early ages (table 2) but not between 12 and 20 weeks ($P > 0\ 1$ table 3) is consistent with the findings in mouse and rat ovaries (Mandl and Shelton 59 Mauléon 61) that large numbers of oocytes degenerate early and

Evans H and O Swezy 1931 Oogenesis and the normal follicular cycle in adult mammalia Mem Univ Calif *9* 119–224

Gerard P 1932 Etudes sur l ovogenese et l onto genese chez les lemuriens du genre *Galago* Arch Biol Paris *43* 93–151

Gerard P and M Herlant 1953 Sur la per sistence de phenomenes d oogenese chez les lemuriens adultes Arch Biol Paris *64* 97–111

Henderson C R 1959 Design and analysis of animal husbandry experiments In Techniques and Procedures in Animal Production Research The Ame ican Society of Animal P oduction 1–55

Jones R 1949 The use of vital staining in the study of the origin of germ cells in the female rat *Mus norwegicus* J Morph *84* 293–333

Jones E C and P L Krohn 1961 The rela tionships between age numbers of oocytes and fertility in virgin and multiparous mice J Endocrin *21* 469–495

Kennelly J J and R H Foote 1965 Ovarian response and supero ulation in pre and post pubertal rabbits treated with standard gona dotrophin prepa ations J Rep od Fert 9 177–188

Kingsbury B F 1913 The morphogenesis of the mammalian ovary *Felis domestica* Am J Anat *15* 345–387

Latta J S and E S Pederson 1944 The orig n of ova and follicle cells from the ger minal epithelium of the ovary of the albino rat as demonstrated by selecti e int avital staining with india ink Anat Rec *90* 23–25

Mandl A M and M Shelton 1959 A quan titative study of oocytes in young and old nul liparous laboratory rats J Endocrin *18* 444–450

Mauleon P 1961 Deroulement de l ovogenese compare chez differents mammiferes domesti ques IV Internat Cong Anim Reprod The Hague 348–354

Rao C R N 1927 On the structure of the ovary and the ovarian ovum of *Lo is lydek kerianus* Camb Quart J Micr Sci *71* 57–74

Rudkin G T and H A Griech 1962 On the persistence of oocyte nuclei from fetus to ma turity in the laboratory mouse J Cell Biol *12* 169–176

Steel R D G and J H Torrie 1960 Princi ples and Procedures of Statistics McGraw Hill Book Co Inc New York

Swezy O 1929 The ovarian chromosome cycle in a mixed rat strain J Morph *48* 445–473

Teplitz R and S Ohno 1963 Postnatal induc tion of ovogenesis in the rabbit (*Oryctolagus cuniculus*) Exp Cell Res *31* 183–189

von Winiwarter H 1900 Recherches sur l ovo genese et l organogenese de l ovaire des mam mife es (lapin et homme) Arch Biol *17* 33–199

Waldeyer W 1870 Eierstock und ei Engel mann Leipzig

Zuckerman S 1951 The number of oocytes in the mature ovary In Recent P ogress in Hor mone Research G Pincus ed *6* 63–109

——— 1955 The regenerative capacity of ovarian tissue In Ciba Foundation Colloquia on Aging *2* 31–58

contributing factor to the reduced cleavage rate since in at least one instance no sperm were found either in the ova or in the area in the clot surrounding the ova The percentage of labeled oocytes in the ovaries removed at 70 weeks of age was 84 5 when put on the same basis as the younger oocytes (classified as labeled with two or more grains) In addition the isotope should have decayed about 6% during 70 weeks Thus the proportion of labeled oocytes appears to have remained remarkably stable with increasing age

With respect to the group II animals which received thy H³ either at four weeks or 20 weeks of age it has already been noted that the isotope was only slightly incorporated into oocyte nuclei at the younger age (table 7) and at 20 weeks of age oocyte nuclei showed no more uptake than cytoplasm (table 10) These results clearly suggest that very little oocytogenesis persists until four weeks of age and none is occurring at 20 weeks of age The heavily labeled follicular and stromal cells shown in figure 11 demonstrate the availability of thy H³ for synthesis of DNA If any oocytes were undergoing any form of meiosis labeled oocytes should have been observed

The results shown in table 7 suggest that some thymidine incorporating material presumably DNA is present in the cytoplasm of the parenchymal and stromal cells at four weeks of age or that some tritium has become available from the degradation of thy H and has been reutilized Evidently the material is unstable or undergoes metabolic turnover since the cytoplasmic grain counts do not differ from background at 12 weeks of age Likewise most of the radioactivity of the oocyte nucleus has disappeared from these animals by 12 weeks suggesting that most of the material does not represent chromosomal DNA The small and equal increase in grain counts over both oocyte nuclei and cytoplasm in rabbits injected with thy H at 20 weeks of age (table 10) also suggests that the tritium is incoporated in substances other than chromosomal DNA The nature of the substances involved have not been characterized

From all the evidence obtained it is concluded that most if not all oocytes in the adult rabbit originate during the neonatal period and DNA is stored without appreciable turnover in the oocytes which survive the normal oocyte atresia characteristic of female mammals A summation of the results obtained supporting these conclusions is as follows (1) No cytological evidence was found of meiotic activity after the intense neonatal activity subsided (2) the concentration of radioactive DNA incorporated at birth remained relatively constant in older animals and no appreciable decrease in the percentage of labeled oocyte nuclei was observed (3) the changes noted in the population of oocytes were completely explainable by non random degeneration of oocytes at the earlier ages (4) the proportion of radioactive eggs obtained in the mature animal by superovulation was similar to the proportion of radioactive oocytes labeled neonatally and present in the ovaries of adults (5) the radioactive ova are capable of fertilization and give rise to normal litters (6) thy H³ incorporation into oocyte nuclei was very slight at four weeks of age and it was not incorporated into oocyte nuclei at 20 weeks of age Thus it is concluded that oocytogenesis ceases before reproductive life begins in rabbits and from this evidence and other published work it is inferred that this is characteristic for most mammals

ACKNOWLEDGMENTS

This investigation was supported in part by Public Health Research Service grant GM 10 263 and Fellowship GM 20 925 National Institute of General Medical Sciences Public Health Service The authors are grateful to F R Allaire and I D VanVleck for their aid with the statistical analysis and to Mrs W Piper and Mrs J Kimpland for technical assistance S Ohno kindly read the manuscript and offered helpful suggestions

LITERATURE CITED

Allen E 1923 Ovogenesis during sexual maturity Am J Anat 31 439–481
Belanger L F 1961 Staining processed radioautographs Stain Tech 36 313–317
Chiquoine A D 1961 An electron microscope study of vitally stained ovaries and ovaries from argyric mice Anat Rec 139 29–36

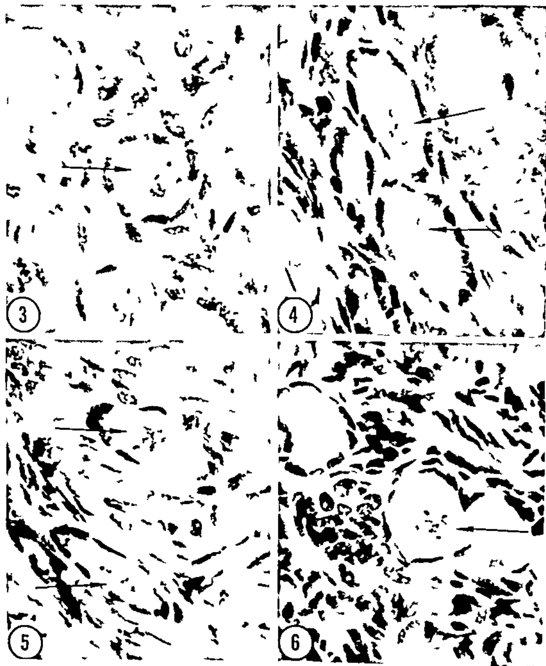

3
4
5
6

PLATE 1

EXPLANATION OF FIGURES

Photomicrographs of ovaries from rabbits injected with thymidine H^3 at birth Feulgen fast green stain magnification 870 ×

3 Ovary at four weeks of age showing a labeled primary oocyte (arrow) and some labeled stromal and follicular cell nuclei

4 Ovary at 12 weeks of age showing two labeled primary oocytes (arrows) Note that the follicular and stromal cell nuclei are less intensively labeled than those at four weeks of age

5 Ovary at 20 weeks of age showing two labeled primary oocytes (arrows)

6 Ovary at 40 weeks of age showing a labeled primary oocyte (arrow) Note the almost complete absence of grains over the follicular and stromal cell nuclei

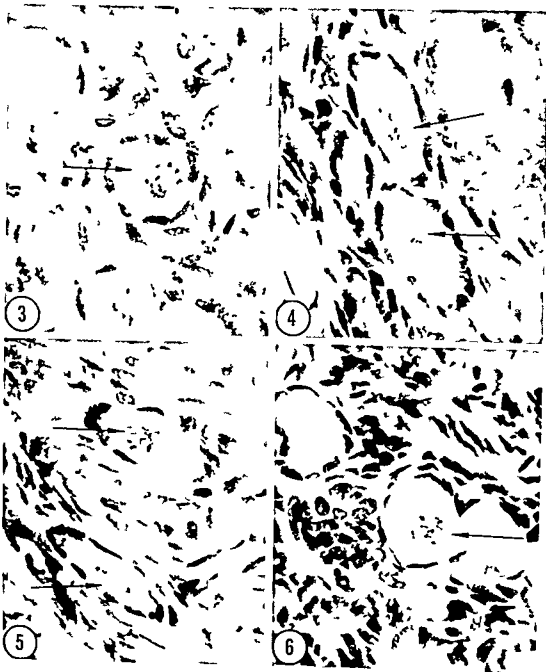

3
4
5
6

PLATE 2

EXPLANATION OF FIGURES

Autoradiographs of rabbit ova and an ovary stained with Feulgen fast green

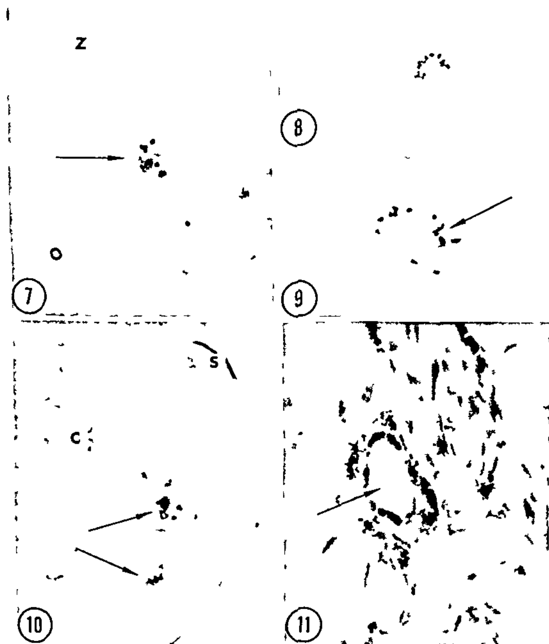
7 Photomicrograph of an unfertilized ovulated ovum collected from a 20 week-old rabbit injected with thymidine H^3 at birth Note the intensely labeled polar body (arrow) O ovum Z zona pellucida (2 000 ×)

8 A polar view of labeled metaphase chromosomes in an unfertilized ovulated ovum collected from a 20 week-old rabbit injected with thymidine H at birth (870 ×)

9 Same as figure 8 magnified 2 000 × Note the intense labeling of certain chromosomes (arrow)

10 Photomicrograph of a fertilized and cleaved ovum collected from a 20 week old rabbit injected with thymidine H^3 at birth Note the two labeled polar bodies (arrows) S sperm in zona pellucida C cleavage resulting in two blastomeres (870 ×)

11 Photomicrograph of an ovary from a rabbit injected with thymidine H^3 at 20 weeks of age Note the absence of grains from the area of the oocyte nucleus (arrow) but the intense labeling of the follicular cell nuclei Photograph was taken focusing on the grains of the emulsion (870 ×)


Z
O
7
8
9
S
C
10
11

An Electron Microscopic Investigation of Osteogenesis in the Embryonic Chick

JAY DONOVAN DECKER

Department of Biological Structure University of Washington Seattle Washington

ABSTRACT Cell matrix and bone matrix relationships have been studied by electron microscopy in the diaphysis of chick embryo tibio-tarsus Osteoblasts within the periosteum possess cytoplasmic machinery characteristic of cells involved in protein synthesis They contain abundant ergastoplasm and an extensive Golgi apparatus Small vesicles are associated with the juxtanuclear Golgi apparatus as well as with the extensive ergastoplasm This suggests that the mechanism of protein synthesis and its transfer to the external milieu may be similar to that of other protein secreting cells the fibroblast the odontoblast and the chondroblast

A rather wide variation in collagen fibril diameter is seen in those fibrils located between the osteoblasts and the initial ossification area The first nucleation of apatite crystals is seen as random aggregations distinct and separate from the collagen fibrils This appearance is independent of section orientation since there appeared to be no difference between sections oriented at right angles to or parallel with the diaphysis long axis

The observations of this study are consistent with proposed mechanisms for the nucleation phenomenon involving the ground substance and collagen fibrils In addition the observations suggest a concept of cellular control over the extracellular environment effecting the initial crystal nucleation The morphologic evidence indicates that the molecular arrangement of collagen as fibrils probably does not provide the mechanism for apatite crystal nucleation

The process by which apatite crystals are incorporated into the matrix of bone remains obscure despite the efforts of many investigators in a number of disciplines over the past few years

There is definite controversy concerning the relative roles that collagen the extracellular milieu and the osteoblast play in the initial deposition or nucleation of the apatite crystals

Recently Glimcher (59) has focused attention on the role collagen plays in the nucleation phenomenon *in vitro* and *in vivo* His electron micrographs present evidence that the apatite crystals reinforce the native collagen periodicity and align themselves preferentially along the longitudinal axis of the collagen His conclusion was that collagen acts as a "catalytic heterogeneity for the nucleation of apatite crystals"

Cameron (63) in a recent review article has rejected this hypothesis based on his observations in the rat of a "random distribution of the patches of calcification and the absence of nuclei at regular sites in relation to bands on the collagen fibrils"

In light of this diversity of opinion it seems reasonable to examine again the process of apatite crystal nucleation or deposition at the electron microscopic level of resolution in another tissue to shed light on this apparent disagreement

First of all it seemed apparent that if the process of crystal nucleation was the subject to be investigated then logically a system where this process was occurring with some degree of assurance should be chosen For this reason a long bone rudiment in the embryonic chick was examined at the time of initial bone formation in its diaphysis Maturational changes in the crystal latticework could then be minimized as a complicating factor in this system

The results presented in this report show that the initial nucleation of apatite crystals does not occur on within or even necessarily near collagen fibrils but rather independent and unoriented with respect to the collagen fibril or fibril banding

MATERIALS AND METHODS

The tibio-tarsus from 12 10-day chick embryos was isolated by microdissection and quickly placed in ice cold 2 67% OsO buffered with s-collidine (Bennett and Luft 59) The entire bone was fixed

one to one and one half hours dehydrated in ascending grades of ethyl alcohol and embedded in either Epon or Araldite epoxy resins (Luft 61) without decalcification

Sections were cut with glass knives on either the Porter Blum or Cambridge (Huxley) ultramicrotomes and were selected for observation at the electron microscope according to interference colors in the range of light gold to silver The sections were picked up on carbon filmed copper grids and stained for 2–5 hours in a 2–3% aqueous solution of uranyl acetate (Watson 58) Thick sections of each block were examined at the light microscope for orientation purposes prior to thin sectioning

Section examination was done at either an RCA EMU2A or 2C electron microscope fitted with 40 u objective apertures Canalco stigmators and specially stabilized power supplies Negatives were taken on Kodak Fine Grain Positive film (Wood and Howard 59)

OBSERVATIONS

The middle third of the cartilaginous rudiment of the chick tibio tarsus is surrounded by a narrow ring of bone by the tenth embryonic day In cross section through the diaphysis bone separates cartilage its cells and matrix from the surrounding periosteum which may itself be positionally divided into osteoblastic and fibroblastic layers (fig 1) The cells of the osteoblastic layer are arranged concentrically about the bone with their longitudinal axes aligned parallel to it and are closely packed with relatively little intercellular space Two or three cell thicknesses peripherally the cells of the fibroblastic layer are similarly arranged but with relatively more intercellular space (figs 1 2)

The osteoblast cell outline is irregular and an interdigitation of processes from adjacent cells is common (fig 3) No cell surface modifications for attachment or adhesion are seen Many cell processes which are relatively small in cross sectional diameter are seen in all areas (fig 4 6)

The nuclei of the osteoblasts are eccentrically placed round to oval in profile and often exhibit prominent nucleoli (figs 1 2) The nucleus is bounded by a double layered nuclear envelope which is provided with ribonucleoprotein particles on the cytoplasmic surface (fig 5)

Although the Golgi complex is typically juxtanuclear in location the electron microscope occasionally reveals vacuoles and membranous lamellae in the peripheral cytoplasm that are similar to those in the juxtanuclear region (figs 5 6) Regardless of location the Golgi complex is comprised of the usual smooth surfaced cisternae or lamellae stacked in close array and associated vacuoles and vesicles

The ergastoplasm is not polarized within the cell but is distributed throughout the cytoplasm It tends to be more abundant at the periphery of the cell more or less encircling the juxtanuclear Golgi apparatus The ergastoplasm consists of cisternae or flattened membranous sacs which are interconnected to form a reticulum similar to that found in fibroblasts odontoblasts and hepatic or pancreatic acinar cells (figs 2 3 5 6) The diameter of the ribonucleoprotein granules attached to the cisternae varies from *ca* 125–150 A Smooth surfaced vesicles are found between the rough surfaced cisternae and are often closely associated with them The vesicles are similar to those associated with the Golgi region (fig 6)

Mitochondria are numerous and are randomly scattered in the areas rich in ergastoplasm but are less abundant in the Golgi region The ground substance of the cytoplasm contains some free ribonucleoprotein particles (figs 4 6)

In cross sections of the growing diaphysis the extracellular space between cells of the osteoblastic layer is occupied by collagen fibrils which also appear predominately in cross section The diameter of these fibers (*ca* 400 A) is quite uniform (figs 2 4) In the same sections the cross sectioned collagen fibrils lying between the osteoblasts and bone range in diameter from 400 A to over 1 200 A (figs 4 4a) (Decker 62) The typical 640 A periodicity characteristic of collagen is apparent in those few fibers longitudinally sectioned (fig 4)

Among these collagen fibrils in the extracellular space between the osteoblasts and bone one finds the initial aggregations of apatite crystals The aggregations consist of a few or many randomly arranged and oriented crystals with little or no obvious relation to collagen fibrils (figs 5 7 8) Crystal deposition appears independent of collagen periodicity and the intraperiod banding This appearance is independent of tissue orientation differences between sections parallel with or at cross section to the long axis of the bone rudiment were not observed (figs 8 9)

Within the newly formed bone collagen fibrils exhibit typical periodicity and sub banding Apatite crystals surround such fibrils but the crystals neither reinforce the collagen periodicity nor are they aligned preferentially along the collagen axis (figs 9 10)

DISCUSSION

Ample evidence that the osteoblast is capable of and is responsible for the synthesis of tropocollagen has been accumulated by the use of radioactive tracers in combination with radioautography (Carneiro and Leblond 59 Young 62) Cells with comparable cytoplasmic machinery odontoblasts and fibroblasts have similarly been shown to utilize tritiated proline one of collagen s precursors in the production of collagen fibrils (Ross and Benditt 62 Leblond 63)

It has been proposed that the fibroblast is capable of exerting an influence over the polymerization of tropocollagen and in general over its own environment (Ross and Benditt 61) Grobstein (61) has suggested that embryonic inductive effects might be closely associated with protein rich materials secreted by the cells Earlier work *implied that there is no requirement* for direct contact between inductive interactants (Grobstein 59 Grobstein and Dalton 57) The concept of such inductive processes remains limited however to short range effects

The pattern of the uptake and utilization of tritiated proline by chondrocytes in regenerating limb buds of salamanders (Revel and Hay 63) as well as in normal and scorbutic wound healing fibroblasts (Ross and Benditt 61 62) suggests that collagen is in the form of a soluble protein when it leaves the cell for it readily diffuses through the matrix and is precipitated at some distance from the cell The manner in which cells might control the distant polymerization of the collagen fibrils is unknown but some authors (Revel and Hay 63) have postulated that the cells do this by regulation of the chemical environment of the extracellular matrix Therefore it seems plausible to suggest that in the area of bone formation like mechanisms mediated by the osteoblasts are in operation both to influence the polymerization of tropocollagen and as will be suggested to effect the nucleation of apatite crystals

The variation of collagen fibril diameter seen in the area between the osteoblast and initial bone formation may be due to random side to-side polymerization of the tropocollagen under the cells influence Ross and Benditt (61) suggested that constant remodeling of fibril size occurs during the course of fibrillogenesis This also would have an effect upon fibril diameter within any given region Sheldon and Robinson (61) also described fiber diameter variation for the bone matrix in rats with experimentally produced rickets but attributed it to this deficiency situation The former suggestions would seem more likely until better data and adequate control experiments are available to document the contention that the large and small collagen fibril diameters are the result of pathology

The presence of vesicles associated with the ergastoplasm in the peripheral cytoplasm and within the smallest cell processes indicates that the osteoblast possesses an appropriate system for the transport of substances synthesized within the ergastoplasm *Larger vacuoles in the Golgi zone* may then represent sites of accumulation of some of this newly synthesized protein material Such an intracellular pathway has been proposed for chondrocytes by Revel and Hay (63) and although there is no direct experimental evidence from the present study to confirm this pathway for osteoblasts the morphologic evidence is consistent with this interpretation

No evidence of intracytoplasmic apatite crystals has been seen in the present study

This conforms with the findings of Leblond et al. (50) who in a radioautographic study of the uptake and utilization of radioactive phosphorous demonstrated its presence throughout all areas of bone within the first hour after injection but never within the soft tissues. Cameron (61) also found no apatite crystals within any osteoblast in his electron microscopic study of metaphyseal osteogenesis in the young rat.

Ossification in the diaphysis commences at the junction of cartilage and periosteum with the initial aggregations of apatite crystals appearing independent of collagen fibrils. Neither a preferential orientation nor a specific alignment of the crystals with the collagen fibrils has been seen in the present work. The observation of individual crystals or groups of crystals within the ground substance distinct and separate from any collagen fibril confirms the findings of Ascenzi and Benedetti (59), Knese and Knoop (58) and Cameron (63). Such random aggregations, isolated from one another, could be explained by assuming that the crystals are within and over a cross-sectioned fibril, a possibility rejected by Cameron (63) on the basis that the extremely haphazard arrangement of crystals precludes this. In addition, if this hypothesis were true one would expect to see apatite crystals within longitudinally sectioned fibrils. Fibrils containing such crystals, however, were never seen in sections either at right angles to or parallel with the long axis of the chick tibio-tarsus. This is negative evidence but there is no reason to think that pre-existing crystals may be lost or dissolved selectively during tissue preparation; however, neither can this possibility be completely excluded.

In between the aggregations of apatite crystals in the ossifying area, no small single crystals at repeating sites along the fibrils are seen. This is in contradiction to the findings of Jackson (57).

Finding clearly delineated collagen fibrils within and surrounded by newly mineralized bone does not support the hypothesis that collagen acts alone as the nucleation site for apatite crystals. Bone crystals surrounding such fibrils are not oriented with their long axes parallel to the fibril, nor do they seem associated with either the major period or sub-bands of collagen. Bachra, Sobel and Stanford (59) demonstrated that a chondroitin sulfate-collagen complex will act *in vitro* as a nucleation site for apatite crystals. They did not imply, however, that such a system duplicates the *in vivo* system, and they therefore concluded that since collagen exists in many parts of the body where it does not calcify, additional factors are necessary.

The above findings and considerations detract from Glimcher's (59) hypothesis that mineralization is initiated solely by regular repetition of a steric configuration of side chains along the collagen fibrils. Rather, the isolated aggregations suggest that there are additional factors existing at nucleation sites which, in combination with the underlying collagen, may initiate the development of crystals.

Cell directed control of the extracellular environment, postulated above for effecting the polymerization of molecular collagen, need not be limited to this function and may play the single most important factor in apatite nucleation.

In examining the importance of the ground substance in calcification, it is interesting to note the findings of Urist, Schjeide and McLean (58). These workers reported the presence of a phosphoprotein and a lipoprotein in estrogenized roosters identical to two proteins normally present in yolk granules of chicken eggs. The data showed that these proteins have a large capacity for combination with calcium and demonstrated that the dissociation constant pK Ca Pro does not differ materially from that of other proteins, e.g., serum albumin, serum globulin and casein. There are simply more calcium binding groups per molecule or per unit weight of the phosphoproteins than there are in the usual serum proteins.

These proteins may represent physiologic ion exchange resins for calcium in the chick. It is tempting to suggest that such resins could act within the ground substance as a source of supply for calcium during ossification, the osteoblast making this calcium available for bone formation through control of its extracellular environment.

After studying the blood disappearance curves of bone seeking isotopes Neuman and Neuman (58) found that the curves consisted of a series of exponentials of which the third rate term described in part isotope pickup by bone Transcapillary exchange and extracellular mixing dominated the first and second rate terms In view of the relatively slow fluid exchange and the known ratio of high cell volume to fluid volume in bone it is reasonable to postulate that the extracellular environment in and around the area of bone formation may differ considerably from a simple ultrafiltrate of plasma It is seen then that cellular control of the extracellular environment is conceivable and its effects multiple

Since groups of crystals are more frequently encountered than individual crystals it follows that nucleation occurs randomly within circumscribed areas and is followed rapidly by crystal growth This is in agreement with the conclusion reached by Cameron (63)

Increase in diameter size for the diaphysis of any long bone is extended over a longer time scale both grossly and microscopically than metaphyseal growth in the same bone Leblond et al (50) have presented evidence showing that metaphyseal bone is renewed about three times during an 8-day period while in the diaphysis approximately one tenth of the cortical bone is renewed within this same 8 day period This difference in rate of growth may explain why separate initial aggregations are seen in the diaphysis i e nucleation is occurring at a rate compatible with gross increase in size

Dudley and Spiro (61) reported that they saw either unmineralized collagen fibers or massively mineralized fibers in bone They suggested on the basis of this finding that once nucleation has occurred the rate of crystal growth is rapid Although consistent with their findings this concept does not consider that though crystal growth may be rapid nucleation need not be

One other important time affected parameter is the stage development in which any particular bone exists It is clear that maturational changes in the crystal framework must be distinguished conceptually as well as structurally from the initial nucleation phenomenon before the nucleation process can be completely understood

Cellular control of the aggregation of collagen fibrils and the equilibrium of the ground substance provide examples of the type of mechanism proposed to control the nucleation of apatite crystals Modifying factors including the organism s rate of growth and inherent metabolism of calcium and phosphate may in addition affect the initial position and orientation of the inorganic salt

ACKNOWLEDGMENTS

The author wishes to express his gratitude to Drs John H Luft and Richard Wood of the Department of Biological Structure who with their advice and suggestions made this work possible The investigation was supported by a post doctoral fellowship DPD 11 517 from the U S Public Health Service and by USPHS grants nos H 2698 and GM 136

LITERATURE CITED

Ascenzi Antonio and Ennio L. Benedetti 1959 An electron microscopic study of the foetal membranous ossification Acta Anat 37 370–385

Bachra B N A E Sobel and J W Stanford 1959 Calcification XXIV Mineralization of collagen and other fibers Arch Biochem Biophys 84 79–95

Bennett H S and J H Luft 1959 s-Collidine as a basis for buffering fixatives J Biophys Biochem Cytol 6 113–114

Cameron D A 1961 The fine structure of osteoblasts in the metaphysis of the tibia of the young rat J Biophys Biochem Cytol 9 583–595

——— 1963 The fine structure of bone and calcified cartilage Clin Orthopaedics 26 199–228

Carneiro J and C P Leblond 1959 Role of osteoblasts and odontoblasts in secreting the collagen of bone and dentin as shown by radioautography in mice given tritium labeled glycine Exp Cell Res 18 291–300

Decker J D 1962 Electron microscopy of fibril morphology in developing bone Anat Rec 142 225

Dudley H Robert and D Spiro 1961 The fine structure of bone cells J Biophys Biochem. Cytol. 11 627–649

Glimcher M J 1959 Molecular biology of mineralized tissues with particular reference to bone Rev Mod Phys 31 359–393

Grobstein Clifford 1959 Autoradiography of the interzone between tissues in inductive interaction J Exp Zool 142 203–213

——— 1961 Cell contact in embryonic induction Exp Cell Res Suppl 8 234–245
Grobstein Clifford and A J Dalton 1957 Kidney tubule induction in mouse metanephrogenic mesenchyme without cytoplasmic contact J Exp Zool 135 57–66
Jackson Sylvia Fitton 1957 The fine structure of developing bone in the embryonic fowl Proc Roy Soc (London) Ser B 146 270–280
Knese Karl Heinrich and Anne Marie Knoop 1958 Elektronenoptische untersuchungen uber die periostale osteogenese Z Zellforsch 48 455–478
Leblond C P 1963 Elaboration of dentinal collagen in odontoblasts as shown by radioautography after injection of labeled glycine and proline Ann Histochim 8 43–50
Leblond C P C W Wilkinson L F Belanger and J Robichon 1950 Radioautographic visualization of bone formation in the rat Am J Anat 86 289–327
Luft J H 1961 Improvements in epoxy resin embedding methods J Biophys Biochem Cytol 9 409–414
Neuman W F and M W Neuman 1958 The Chemical Dynamics of Bone Mineral University of Chicago Press Chicago Chaps V VI
Revel Jean Paul and E D Hay 1963 An autoradiographic and electron microscopic study of collagen synthesis in differentiating cartilage Z Zellforsch 61 110–144
Ross R and E P Benditt 1961 Wound healing and collagen formation I J Biophys Biochem Cytol 11 677–700
——— 1962 Wound healing and collagen formation III J Biophys Biochem Cytol 15 99–108
Sheldon H and R A Robinson 1961 Studies on rickets I The fine structure of uncalcified bone matrix in experimental rickets Z Zellforsch 53 671–684
Urist M R Ole A Schjeide and F C McLean 1958 The partition and binding of calcium in the serum of the laying hen and of the estrogenized rooster Endocrinology 63 570–584
Watson M L 1958 Staining of tissue sections for electron microscopy with heavy metals J Biophys Biochem Cytol 4 475–478
Wood R L and C C Howard 1959 Use of fine grain positive film for electron microscopy J Biophys Biochem Cytol 5 181–182
Young R W 1962 Autoradiographic studies on bone and cartilage matrix formation in young rats injected with glycine H³ Anat Rec 142 335

All illustrations are electron micrographs of chick embryo tibio tarsus fixed in buffered osmium tetroxide and embedded in epoxy resins All sections are cross sections through the diaphysis unless otherwise noted The tissues have been stained with uranyl acetate

PLATE 1

EXPLANATION OF FIGURE

An electron micrograph showing bone (*B*) separating the cartilage matrix (*CM*) and its cells the chondrocytes from the periosteum on the right The nuclei (*N*) of cells in the osteoblastic (*OBL*) and fibroblastic (*FBL*) layers of the periosteum exhibit prominent nucleoli 3 750 ×

OSTEOGENESIS IN THE EMBRYONIC CHICK
J y Donovan Decke



PLATE 2

EXPLANATION OF FIGURE

2 An electron micrograph showing the osteoblastic layer *(OBL)* and bone *(B)* Cartilage matrix *(CM)* appears in the upper left Cell nuclei *(N)* in the osteoblastic layer are round to oval in outline Collagen fibrils *(CF)* are seen in cross section extracellularly between osteoblasts and between the cells and bone Abundant ergastoplasm *(E)* is seen in most cells 8 900 ×


CF
CM
CF
B
B
CF
N
OBL
N

PLATE 3

EXPLANATION OF FIGURE

3 An electron micrograph showing a portion of one osteoblast (*OB*) its *nucleus* (*N*) *and cell processes* (*CP*) *from others Within the cell cyto* plasm ergastoplasm (*E*) Golgi apparatus (*GA*) and mitochondria (*M*) are seen Bone (*B*) lies extracellularly 22 500 ×

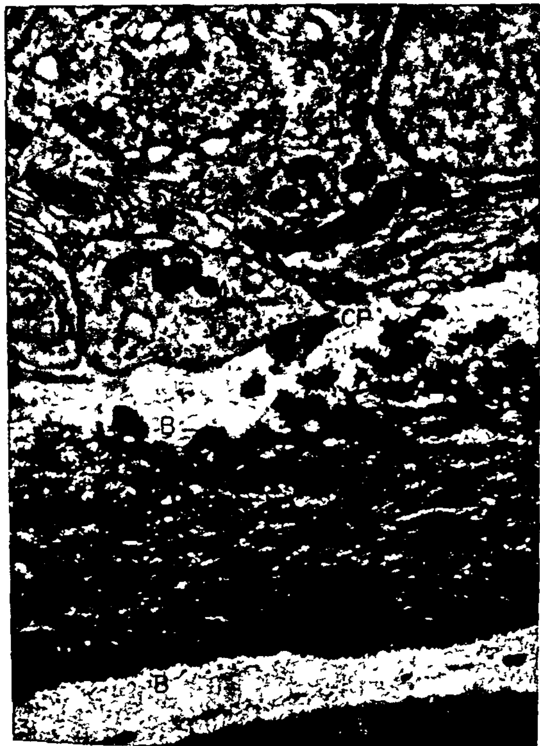

CP
B
B

PLATE 4

EXPLANATION OF FIGURES

4 *An electron micrograph showing collagen fibrils (CF) between an osteoblast and bone (B)* Near the cell surface the collagen fibril diameter is *ca* 400 A Away from the cell surface nearer the bone the diameters vary from *ca* 400 A to over 1 200 A Cartilage matrix *(CM)* is at the lower left Osteoblast cell processes *(CP)* are numerous Ribonucleoprotein particles *(RNP) ca* 125–150 A in diameter appear free within the cell cytoplasm 22 500 ×

4a Inset An electron micrograph showing the variation in diameter of the cross sectioned fibrils 32 000 ×

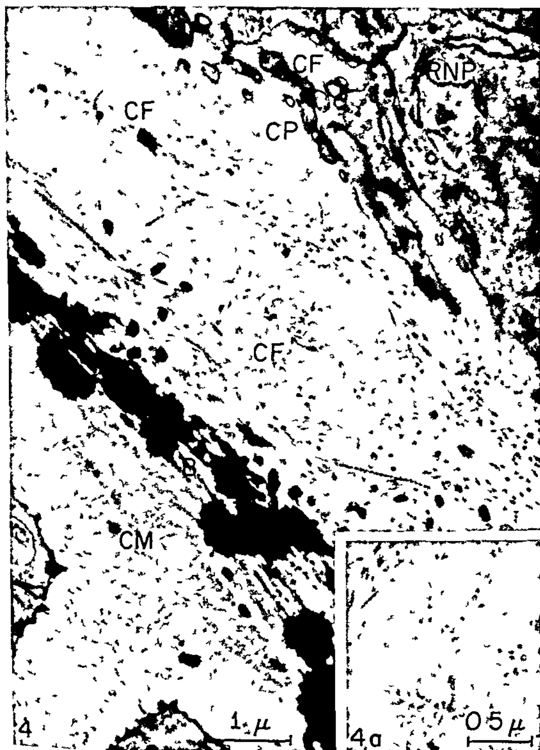

CF
RNP
CF
CP
CF
B
CM
4
1 μ
4a
0.5 μ

PLATE 5

EXPLANATION OF FIGURE

5 An electron micrograph showing portions of two osteoblasts their nuclei (*N*) exhibit a two layered nuclear membrane (*NM*) Vacuoles (*V*) and vesicles (*V*) are abundant in the area of the Golgi apparatus (*GA*) as well as in more peripheral regions Ribonucleoprotein parti cles (*RNP*) are abundant within the cytoplasm Mitochondria (*M*) surround the Golgi apparatus The initial deposits of bone crystals (*B*) appear extracellularly amongst the collagen fibrils (*CF*) 23 000 ×


B
CF
V
NM
N
M
B
V
CF
GA
V
NM
M
N
5

PLATE 6

EXPLANATION OF FIGURE

6 An electron micrograph showing a portion of one osteoblast and cell processes (*CP*) of others. The Golgi apparatus (*GA*) near the nucleus (*N*) consists of flattened lamellae and many vacuoles (*V*) and vesicles (*V*). Ribonucleoprotein particles (*RNP*) appear free within the cytoplasm and attached to the membranes of the ergastoplasm (*E*). 35 000 ×


N
E
CP
RNP
GP
V
GA
E
V
V
6

PLATE 6

EXPLANATION OF FIGURE

6 An electron micrograph showing a portion of one osteoblast and cell processes (*CP*) of others The Golgi apparatus (*GA*) near the nucleus (*N*) consists of flattened lamellae and many vacuoles (*V*) and vesicles (*V*) Ribonucleoprotein particles (*RNP*) appear free within the cytoplasm and attached to the membranes of the ergastoplasm (*E*) 35 000 ×

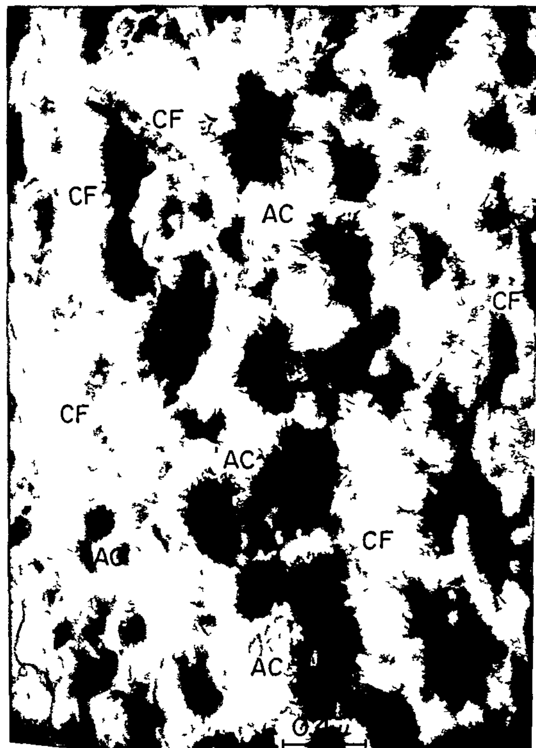

CF
CF
AC
CF
CF
AC
AC
CF
AC

PLATE 7

EXPLANATION OF FIGURE

7 An electron micrograph showing the initial groups of apatite crystals (*AC*) situated within the organic matrix among the collagen fibrils (*CF*) 55 300 ×

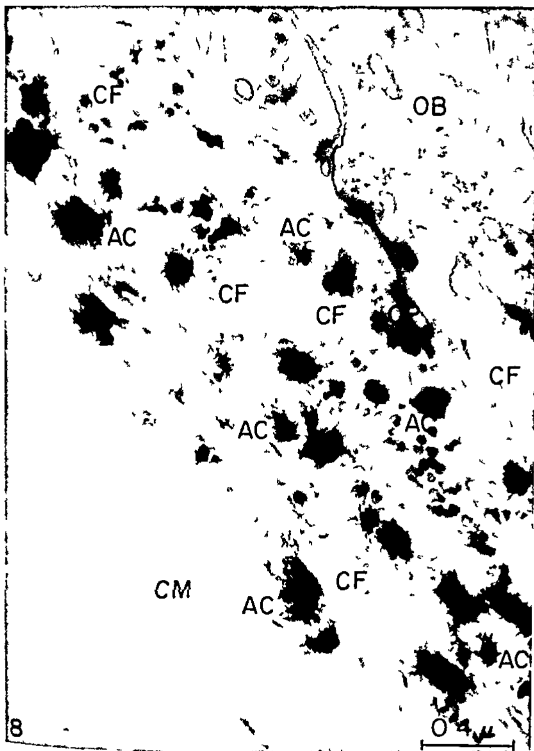

CF
OB
AC
AC
CF
CF
CF
AC
AC
CM
CF
AC
AC
O
8

PLATE 8

EXPLANATION OF FIGURE

8 An electron micrograph showing the initial deposits of apatite crystals *(AC)* separate and distinct from the collagen fibrils *(CF)* in the extra cellular matrix Cell processes *(CP)* from one or more osteoblasts *(OB)* are numerous Cartilage matrix *(CM)* appears at the lower left 58 000 ×

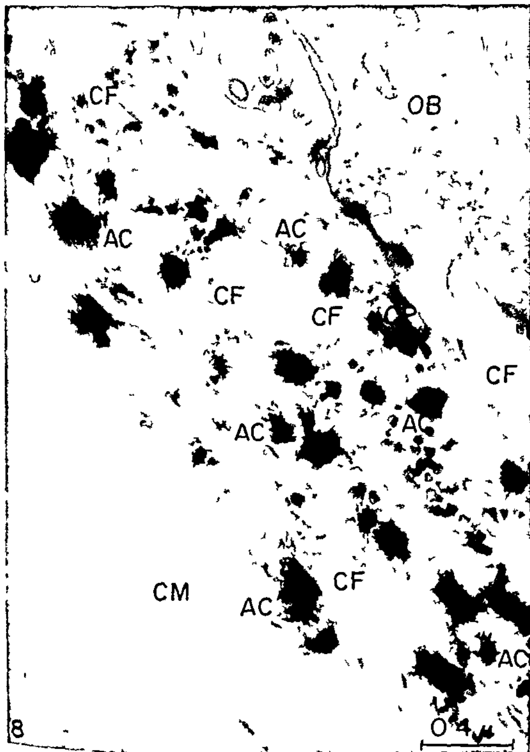

CF
OB
AC
AC
CF
CF
OP
CF
AC
AC
CF
CM
AC
AC
8
0·4 μ

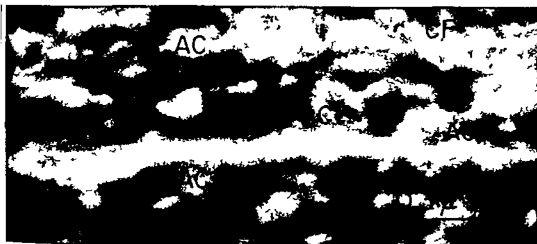
PLATE 9

EXPLANATION OF FIGURES

9 An electron micrograph showing apatite crystals (*AC*) surrounding a collagen fibril (*CF*) The crystals do not appear oriented to the fibrils 70 000 ×

10 An electron micrograph (longitudinal section of diaphysis) showing a number of collagen fibrils (*CF*) surrounded by apatite crystals (*AC*) No reinforcement of collagen periodicity or sub banding is apparent 82 000 ×

10a Inset An electron micrograph (longitudinal section) of an area directly adjacent to that pictured in figure 10 not undergoing ossification Collagen fibril (*CF*) periodicity and sub-banding is apparent 82 000 ×


AC
AC

CF
CF
AC
AC
AC
AC
AC
10
0 2 μ
10a
CF
0 2 μ

Differentiation of Adrenal Cortex like Tissue at the Hilum of the Gonads in Response to Adrenalectomy [1]

WILLIAM G SELIGER A JAMES BLAIR [2] AND H W MOSSMAN
Departments of Anatomy and Medicine University of Wisconsin Madison Wisconsin

ABSTRACT Following bilateral adrenalectomy the adrenal cortex like cells which appear in the ovaries of the 13 lined ground squirrel are in close relationship to the epithelial remnants of the rete ovarii and the medullary cords Identical cells form in the bilaterally adrenalectomized male around the efferent ductules of the testes

Histochemical tests on these periductular cells gave positive results with polarized light Sudan Black stain ultraviolet light and the Schultz test — all comparable to normal adrenal cortex cells

Electron microscopic studies of the periductular cells showed them to have ultra structural characteristics of a steroid secreting cell

Male and female animals adrenalectomized a year before and maintained on tap water died within four days when the gonads and adnexa were removed Male animals adrenalectomized a year before and maintained on tap water survived actively for two weeks when the testicles were removed provided that the efferent ductules and surrounding adrenal cortex like cells were left in place These animals died within four days after the adnexa were removed

The periductular cells were incubated with radioactively tagged progesterone which showed that these cells secrete corticosterone the normal primary corticosteroid of this animal and desoxycorticosterone which functions as a combination glucocorticoid and mineralocorticoid

The occurrence of adrenal cortex like cells at sites other than their usual location in the cortex of the suprarenal gland has been recorded many times These cells occur in the form of accessory adrenal glands adrenal cortical rests and adrenal cortical tumors Since the adrenal cortex forms from the nephrogenic ridge of the embryo in conjunction with the gonad and the duct system of the mesonephros it is not surprising that a great deal of the aberrant adrenal cortex tissue occurs in or near the gonad There are a number of animals in which these masses of adrenal cortex like tissue have been found routinely for example in the mesovarium of the armadillo (*Dasypus novemcinctus*) Enders (59) and in the pika (*Ochotona princeps*) Duke (52) They have also been observed in the head of the epididymis of the rabbit Lacassagne (35) and in the mediastinum of the testis of the red howler monkey (*Alouatta villosa*) in our laboratory

Growth of adrenal cortex like tissue has been stimulated by the administration of hormones Frantz et al (49) produced adrenal cortical adenomas in ovariectomized mice by injection of sex hormones This intimate relationship between the sex gland and the adrenal cortex is further illustrated by Groat s (43) work on the 13 lined ground squirrel Groat (44) subsequently reported the appearance of adrenal cortex like cells at the hilum of the ovary three days after bilateral adrenalectomy and in the medulla of the ovary at ten days The hilum cells were in close relationship to the epoophoron He believed that they were derived from mesenchymal like cells" associated with the epoophoron and from fibroblast like cells at the periphery of the primary mass of new adrenal cortex like cells Groat felt that in the medulla of the ovary these new cells were formed from fibroblast like cells of the stroma He reported that in bilaterally adrenalectomized females both ovaries presented a "similar picture" He did not find these cells in or near the ovaries of normal animals Adrenalectomized male animals survived under the same post

[1] Support d by N ti n l In t tut of H lth gr nt DPD-18 577 and Unit d St tes Publi He lth S rvice g nt AM-05068

[2] Present ddre Dep rtm nt f A tomy Col do St t Un er t Fort Collin Col do

[3] Present ddres H m nl bo t ri t K inn kl n ik n K rol n ka Sjukh set Stockholm Sweden

operative treatment given the female squirrels — i e maintenance on a 1% saline drinking solution for a minimum of three weeks He assumed that the male animals formed the new adrenal cortex like cells since like the females they would eventually survive without the saline drinking solution However he did not locate the cells in the male

Chester Jones (63) repeated Groat s work on the ground squirrel He records that in the absence of the adrenal glands the new tissue appears in the ovaries and more rarely at the hilum In normal female ground squirrels he found no adrenal rests either in or near the ovary or in the perirenal tissue Jones could not find stages of transformation between fibroblast like cells and the adrenal cortex like cells He states Both ovaries of an adrenalectomized animal showed about the same amount of development of the new cell type In general the longer the period after adrenalectomy the greater the development of new tissue though this relationship did not always hold

The present investigation was undertaken in the fall of 1962 (1) to investigate further the phenomenon described by Groat (2) to see if a similar differentiation occurred in the male and if so to establish the locus of the new cells (3) to identify the product or products of these cells

MATERIALS AND METHODS

The animal used in this investigation was the 13 lined ground squirrel (*Citellus tridecemlineatus* Mitchell) Prior to being used for an experiment the animals were kept in a pen as a colony They were maintained on tap water Purina rat pellets and tinned whale meat dog food

Adrenalectomized and mock operated animals were put in individual hanging cages They were all fed Purina rat pellets and had access to tap water and a 1% saline drinking solution was given by dropper bottles Over 400 animals both male and female were used in this study At least one mock operated or control animal was used for every six experimental animals for most phases of the work In special experiments such as inhibition experiments a one to one ratio was used

Surgical procedure All experimental animals both operated and mock operated were anesthetized with intraperitoneal injections of sodium pentobarbital (0 1 gr/100 gm body weight) This was supplemented with ether inhalation anesthesia when necessary to produce suitable relaxation for surgery Adrenalectomy was performed by means of a dorsal incision Mock adrenalectomy was performed by lifting and moving the perirenal fat containing the adrenal gland

Histological procedures For the fixation of all early tissues 10% neutral buffered formalin was used Later when more cytological detail was desired Helly s fixative was used Dehydration was carried out with a graduated series of ethyl alcohol solutions Clearing was accomplished with toluene Tissues were embedded in paraffin and sectioned on a rotary microtome Routine staining was done with Groat s (circa 40) tetrachrome stain [4]

Histochemical procedures Histochemical procedures were used on normal adrenal glands of the 13 lined ground squirrel the efferent ductules of normal and adrenalectomized males and the ovaries of normal and adrenalectomized females These tissues were fixed in 10% buffered formalin washed in tap water then mounted and sectioned on a cryostat microtome at a thickness of 16 μ and picked up on coverslips for processing After processing they were mounted in glycerol jelly These tissues were examined with Sudan Black stain polarized light the Schultz reaction (Lewis and Lobban 61) and with the fluorescence microscope

Electron microscope procedures An electron microscopic examination was made of the normal adrenal gland and of the adrenal cortex like cells around the efferent ductules of an adrenalectomized animal

The tissue was fixed in 6 25% glutaraldehyde postfixed in 1% osmium tetraoxide (both phosphate buffered at pH 7 5) embedded in Epon and sectioned The grids were examined on an R C A model E M U 3 electron microscope

[4] Groat s tetrachrome stain Harris hematoxylin Orange II Biebrich scarlet Fast green

Chromatographic procedures The methods for incubation with progesterone 4C[14] extracting separating with chromatography and counting are presented below in outline form

1 The tissue was removed weighed and placed in iced Ringer bicarbonate buffer

2 The tissue was minced pooled and incubated Two pools were made up of contralateral tissue from each donor One was ACTH treated and could be compared with non treated control pools of tissue from the identical donor

3 The tissue was incubated for a total of three and one half hours ACTH was added to the treated pools of tissue after a pre incubation period of one half hour to allow for equilibration The volume of incubated material was 5 ml

4 The tissue was homogenized and extracted with 50 ml of methylene chloride

5 The extract was dried by removing the methylene chloride under a stream of air at 50 C

6 Lipids were removed by passage through a 5 gm silica gel column The sample was applied in 10 ml of Skellysolve C and chloroform (1/1) and eluted with 25 ml of ethyl acetate and methyl alcohol (1 1)

7 The final eluate was taken to dryness under a stream of air at 50 C

8 Samples were run on thin layer silica gel plates in a system of chloroform and ethyl acetate (1/1)

The following R zones were eluted transferred to counting vials and evaporated

R	Steroid
0 9	Progesterone
0 7	Desoxycorticosterone
0 26	Corticosterone

9 Ten milliliters of phosphor solution were added to the vials and they were counted in a Packard Tri Carb Liquid Scintillator Spectrometer (The overall recovery of radioactive labeled progesterone standards for the extraction and chromatography averaged 41%)

OBSERVATIONS

Female In adrenalectomized female 13 lined ground squirrels adrenal cortex like cells appeared consistently in the mesovarium in close relationship to the epoophoron as described by Groat (fig 1) The cells were mature and active looking in three and one half to four days after adrenalectomy They also appeared later in the medulla of the ovary (fig 4) but because of the compactness of fibers and cells of the stroma it was impossible to establish the exact time of their appearance

Juvenile females were next adrenalectomized The adrenal cortex like cells appeared in 8 to 10 days in close and constant relationship with the medullary cords and the rete ovarii (fig 2) This observation was confirmed in the adult tissues by re-examining the slides of the mature adrenalectomized females The medullary cords and rete ovarii are compressed by the cells of the stroma of the adult ovary so that they are often very difficult to identify

Male Three and one half to four days after adrenalectomy adrenal cortex like cells appeared in clusters around the efferent ductules near the testes (fig 3) and in approximately equal amounts on the two sides of the same animal They were never seen to penetrate into the tunica albuginea testis or into the testis proper nor did they extend very far into the head of the epididymis In fact they were usually confined to the testicular three fifths of the efferent ductules

They appear in variable sized clusters which often surround an individual ductule (fig 9) There is usually a small amount of fibrous connective tissue between these adrenal cortex like cells and the bases of the epithelial cells of the efferent ductules and they are richly supplied with capillaries (figs 6 7)

Histology The efferent ductules are composed of simple columnar to pseudostratified ciliated columnar epithelium resting on a thin basement membrane At intervals there are clusters of the cells which differentiate into the adrenal cortex like cells (fig 5) These clusters are also covered with delicate fibrous connective tissue and usually appear to have an arteriole or two and a rich capillary supply The precursor cells are commonly ovoid with clear or very weakly stained cyto-

operative treatment given the female squirrels — i e maintenance on a 1% saline drinking solution for a minimum of three weeks He assumed that the male animals formed the new adrenal cortex like cells since like the females they would eventually survive without the saline drinking solution However he did not locate the cells in the male

Chester Jones (63) repeated Groat s work on the ground squirrel He records that in the absence of the adrenal glands the new tissue appears in the ovaries and more rarely at the hilum In normal female ground squirrels he found no adrenal rests either in or near the ovary or in the perirenal tissue Jones could not find stages of transformation between fibroblast like cells and the adrenal cortex like cells He states Both ovaries of an adrenalectomized animal showed about the same amount of development of the new cell type In general the longer the period after adrenalectomy the greater the development of new tissue though this relationship did not always hold

The present investigation was undertaken in the fall of 1962 (1) to investigate further the phenomenon described by Groat (2) to see if a similar differentiation occurred in the male and if so to establish the locus of the new cells (3) to identify the product or products of these cells

MATERIALS AND METHODS

The animal used in this investigation was the 13 lined ground squirrel (*Citellus tridecemlineatus* Mitchell) Prior to being used for an experiment the animals were kept in a pen as a colony They were maintained on tap water Purina rat pellets and tinned whale meat dog food

Adrenalectomized and mock operated animals were put in individual hanging cages They were all fed Purina rat pellets and had access to tap water and a 1% saline drinking solution was given by dropper bottles Over 400 animals both male and female were used in this study At least one mock operated or control animal was used for every six experimental animals for most phases of the work In special experiments such as inhibition experiments a one to one ratio was used

Surgical procedure All experimental animals both operated and mock operated were anesthetized with intraperitoneal injections of sodium pentobarbital (0 1 gr/100 gm body weight) This was supplemented with ether inhalation anesthesia when necessary to produce suitable relaxation for surgery Adrenalectomy was performed by means of a dorsal incision Mock adrenalectomy was performed by lifting and moving the perirenal fat containing the adrenal gland

Histological procedures For the fixation of all early tissues 10% neutral buffered formalin was used Later when more cytological detail was desired Helly s fixative was used Dehydration was carried out with a graduated series of ethyl alcohol solutions Clearing was accomplished with toluene Tissues were embedded in paraffin and sectioned on a rotary microtome Routine staining was done with Groat s (circa 40) tetrachrome stain [1]

Histochemical procedures Histochemical procedures were used on normal adrenal glands of the 13 lined ground squirrel the efferent ductules of normal and adrenalectomized males and the ovaries of normal and adrenalectomized females These tissues were fixed in 10% buffered formalin washed in tap water then mounted and sectioned on a cryostat microtome at a thickness of 16 μ and picked up on coverslips for processing After processing they were mounted in glycerol jelly These tissues were examined with Sudan Black stain polarized light the Schultz reaction (Lewis and Lobban 61) and with the fluorescence microscope

Electron microscope procedures An electron microscopic examination was made of the normal adrenal gland and of the adrenal cortex like cells around the efferent ductules of an adrenalectomized animal

The tissue was fixed in 6 25% glutaraldehyde postfixed in 1% osmium tetraoxide (both phosphate buffered at pH 7 5) embedded in Epon and sectioned The grids were examined on an R C A model E M U 3 electron microscope

---

[1] Groat s tetrachrome stain Harris hematoxylin Orange II Biebrich scarlet Fast green

Chromatographic procedures The meth ods for incubation with progesterone-4C[14] extracting separating with chromatogra phy and counting are presented below in outline form

1 The tissue was removed weighed and placed in iced Ringer bicarbonate buf fer

2 The tissue was minced pooled and incubated Two pools were made up of contralateral tissue from each donor One was ACTH treated and could be compared with non treated control pools of tissue from the identical donor

3 The tissue was incubated for a total of three and one half hours ACTH was added to the treated pools of tissue after a pre incubation period of one half hour to allow for equilibration The volume of in cubated material was 5 ml

4 The tissue was homogenized and ex tracted with 50 ml of methylene chloride

5 The extract was dried by removing the methylene chloride under a stream of air at 50 C

6 Lipids were removed by passage through a 5 gm silica gel column The sample was applied in 10 ml of Skellysolve C and chloroform (1/1) and eluted with 25 ml of ethyl acetate and methyl alcohol (1/1)

7 The final eluate was taken to dryness under a stream of air at 50 C

8 Samples were run on thin layer silica gel plates in a system of chloroform and ethyl acetate (1/1)

The following R zones were eluted transferred to counting vials and evapo rated

R	Steroid
0 9	Progesterone
0 7	Desoxycorticosterone
0 26	Corticosterone

9 Ten milliliters of phosphor solution were added to the vials and they were counted in a Packard Tri Carb Liquid Scintillator Spectrometer (The overall re covery of radioactive labeled progesterone standards for the extraction and chroma tography averaged 41%)

OBSERVATIONS

Female In adrenalectomized female 13 lined ground squirrels adrenal cortex like cells appeared consistently in the mesovarium in close relationship to the epoophoron as described by Groat (fig 1) The cells were mature and active looking in three and one half to four days after adrenalectomy They also appeared later in the medulla of the ovary (fig 4) but because of the compactness of fibers and cells of the stroma it was impossible to establish the exact time of their appear ance

Juvenile females were next adrenal ectomized The adrenal cortex like cells appeared in 8 to 10 days in close and con stant relationship with the medullary cords and the rete ovarii (fig 2) This observa tion was confirmed in the adult tissues by re-examining the slides of the mature adrenalectomized females The medullary cords and rete ovarii are compressed by the cells of the stroma of the adult ovary so that they are often very difficult to iden tify

Male Three and one half to four days after adrenalectomy adrenal cortex like cells appeared in clusters around the effer ent ductules near the testes (fig 3) and in approximately equal amounts on the two sides of the same animal They were never seen to penetrate into the tunica albuginea testis or into the testis proper nor did they extend very far into the head of the epididymis In fact they were usu ally confined to the testicular three fifths of the efferent ductules

They appear in variable sized clusters which often surround an individual duc tule (fig 9) There is usually a small amount of fibrous connective tissue be tween these adrenal cortex like cells and the bases of the epithelial cells of the efferent ductules and they are richly sup plied with capillaries (figs 6 7)

Histology The efferent ductules are composed of simple columnar to pseudo-stratified ciliated columnar epithelium resting on a thin basement membrane At intervals there are clusters of the cells which differentiate into the adrenal cortex like cells (fig 5) These clusters are also covered with delicate fibrous connective tissue and usually appear to have an arte riole or two and a rich capillary supply The precursor cells are commonly ovoid with clear or very weakly stained cyto-

plasm (figs 6 7) The cell outline is distinct and the nucleus is smoothly rounded and appears somewhat hyperchromatic because the nucleoplasm takes a heavy stain, the chromatin granules although distinct are closely packed When these cells become active they enlarge and tend to become polyhedral in shape The cytoplasm becomes distinctly acidophilic the nucleus enlarges and becomes clearer and vesicular in type Cytologically these new cells are like adrenal cortex cells (figs 8 9) They are large cells with cytoplasm which has a foamy or granular structure They have a large spheroidal semichromatic nucleus

Histochemistry Frozen sections of the efferent ductules of a six week postoperative animal and of a normal ground squirrel were examined with the histochemical tests mentioned in Materials and Methods Frozen sections of the adrenal glands of normal animals were also tested for comparison

The cytoplasm of the active periductular cells was birefringent with polarized light It stained positively with Sudan Black demonstrating the presence of lipoid substance The Schultz test also gave positive results This is strong evidence for the presence of steroid compounds The cytoplasm fluoresced when viewed with the fluorescence microscope The results of all of these tests were comparable to the results of the same tests performed on the normal adrenal cortex cells and strongly indicate that these cells are steroid secretors

Ultrastructure The efferent ductules were removed from a ground squirrel which had been adrenalectomized two weeks earlier The electron micrographs prepared from these tissues showed that the periductular cells possessed smooth endoplasmic reticulum a characteristic of steroid secreting cells (fig 11) Large mitochondria with tubular cristae and many glycogen granules were also observed in preparations of these cells These findings suggest that the new periductular cells could have a function similar to that of adrenal cortex cells They also show the presence of rough endoplasmic reticulum which indicates they possibly have an additional function

Abolition of adrenal cortex like tissues Five weeks after adrenalectomy 13 lined ground squirrels can be maintained on tap water Three to five months later they can withstand stress as well as normal animals can

Six male and six female animals were selected from a group which had been bilaterally adrenalectomized and maintained on tap water and rat pellets for one year They were all anesthetized with sodium pentobarbital and their gonads with adnexa were removed All were returned to their own cages The tap water and rat pellet diet was continued All 12 died within four days

Another group of eight one year post operative male animals was selected They were anesthetized and only the testis proper was removed bilaterally from each animal The head of the epididymis the efferent ductules and their surrounding adrenal cortex like cells were allowed to remain intact in each case All animals remained healthy and active for two weeks At that time the remaining duct systems and their surrounding cells were removed by another operation The tap water and rat pellets were continued Seven animals perished within four days The surviving ground squirrel was later sacrificed for examination and a small body was found at the hilum of the left kidney This body was identified histologically as an accessory adrenal gland

Inhibition and stimulation Initially it was believed that the cells which differentiated into the adrenal cortex like cells were spindle shaped or fibroblast like cells in the connective tissue surrounding the efferent ductules None of the normal efferent ductules which were examined earlier showed any periductular adrenal cortex like cells Groat (43) and Jones (63) noted that in the female these adrenal cortex like cells do not occur normally

The fact that the new cells develop bilaterally and the belief that they did not occur normally led to the use of one side of an animal as a control for the other

Animals were adrenalectomized and given cortisone acetate injections for five days while being maintained on 1% saline drinking solution The injection dosage varied from 0 25 mg to 1 mg per 100 gm

of body weight After five days one testicle was removed and fixed The animals were then maintained for five or six days on 1% saline solution to allow time for the uninhibited cells to differentiate The second testicle was then removed and fixed The inhibited and uninhibited periductular cells were compared histologically The object of this procedure was to see if cortisone acetate inhibited the cell differentiation of the first side and later whether the adrenalectomy had been complete and the cell did have the ability to differentiate when the inhibitory effect of the steroid had been removed

This experiment was repeated adding exogenous ACTH to the cortisone acetate inhibited animals At this time it was believed that the absence or presence of the adrenal cortex like cells was a very absolute thing The results of these experiments tended to substantiate the idea that ACTH stimulated the cell differentiation and that parenterally administered cortisone acetate inhibited it However they did not show as much contrast as had been anticipated

Corticosteroids are known to inhibit ACTH secretion by the pituitary (Sayers 62) but do not completely block its secretion So the fact that some partly differentiated cells and an occasional differentiated cell appeared on the inhibited side was not surprising

A more extensive examination was made of the efferent ductules of normal animals and a new observation was made In the late winter and early spring months it is common to see a few active looking adrenal cortex like cells around the efferent ductules of ground squirrels kept in captivity through the fall and winter

To gain better control of the inhibition experiments transplant operations were next used In the first transplant operations the ductules from three animals were placed in the rectus abdominis muscles of two adrenalectomized animals One was given cortisone acetate to inhibit formation of the new cells The other received ACTH gel to stimulate them into activity These animals were used during the late winter months so that some differentiated cells were probably normally present around the ductules In spite of this it was possible to separate the tissue of inhibited animals from that of stimulated animals Accurate identification was made in a blind study

The tissue from the ACTH stimulated ground squirrel showed numerous large cells which were typical of adrenal cortex cells With Groat s stain they had richly stained cytoplasm and vesicular nuclei

The inhibited cells were fewer and smaller and had almost colorless cytoplasm The nuclei appeared rather pycnotic The cells were irregular in shape

Colchicine studies Colchicine studies were done on adrenalectomized animals both male and female from the time of the operation until the end of the fourth day The dosage was regulated by trial and error to keep the animals alive for 24 hours after administration The dosage varied considerably from animal to animal probably due to the physiological state of the animal following surgery and the resultant corticosteroid insufficiency No mitotic figures were ever seen in the adrenal cortex like cells or their presumptive precursor cells

Incubation and chromatography studies In preparation for the chromatography experiments the adrenal glands were removed from two normal male ground squirrels chilled homogenized and extracted The lipid was removed with a silica gel column and the extract then run on thin layer chromatography plates with a system of chloroform and ethyl acetate 1/1 The primary corticosteroid of the normal ground squirrel adrenal gland was found to be corticosterone (compound B)

Tissue from 11 male animals which had been adrenalectomized various lengths of time was used for the incubation study Three of the animals had survived bilateral adrenalectomy for three months Four had survived for one month after adrenalectomy and the remaining four were two week postoperative animals Eleven recently caught spring males were used to furnish the normal efferent ductules

The following table shows the results of this study Included are the weights of the bilaterally separated tissues Half received ACTH and half did not The minced tissue was incubated with isotope tagged progesterone and the products were isolated with

plasm (figs 6 7) The cell outline is distinct and the nucleus is smoothly rounded and appears somewhat hyperchromatic because the nucleoplasm takes a heavy stain the chromatin granules although distinct are closely packed When these cells become active they enlarge and tend to become polyhedral in shape The cytoplasm becomes distinctly acidophilic the nucleus enlarges and becomes clearer and vesicular in type Cytologically these new cells are like adrenal cortex cells (figs 8 9) They are large cells with cytoplasm which has a foamy or granular structure They have a large spheroidal semichromatic nucleus

Histochemistry Frozen sections of the efferent ductules of a six week postoperative animal and of a normal ground squirrel were examined with the histochemical tests mentioned in Materials and Methods Frozen sections of the adrenal glands of normal animals were also tested for comparison

The cytoplasm of the active periductular cells was birefringent with polarized light It stained positively with Sudan Black demonstrating the presence of lipoid substance The Schultz test also gave positive results This is strong evidence for the presence of steroid compounds The cytoplasm fluoresced when viewed with the fluorescence microscope The results of all of these tests were comparable to the results of the same tests performed on the normal adrenal cortex cells and strongly indicate that these cells are steroid secretors

Ultrastructure The efferent ductules were removed from a ground squirrel which had been adrenalectomized two weeks earlier The electron micrographs prepared from these tissues showed that the periductular cells possessed smooth endoplasmic reticulum a characteristic of steroid secreting cells (fig 11) Large mitochondria with tubular cristae and many glycogen granules were also observed in preparations of these cells These findings suggest that the new periductular cells could have a function similar to that of adrenal cortex cells They also show the presence of rough endoplasmic reticulum which indicates they possibly have an additional function

Abolition of adrenal cortex like tissues Five weeks after adrenalectomy 13 lined ground squirrels can be maintained on tap water Three to five months later they can withstand stress as well as normal animals can

Six male and six female animals were selected from a group which had been bilaterally adrenalectomized and maintained on tap water and rat pellets for one year They were all anesthetized with sodium pentobarbital and their gonads with adnexa were removed All were returned to their own cages The tap water and rat pellet diet was continued All 12 died within four days

Another group of eight one year postoperative male animals was selected They were anesthetized and only the testis proper was removed bilaterally from each animal The head of the epididymis the efferent ductules and their surrounding adrenal cortex like cells were allowed to remain intact in each case All animals remained healthy and active for two weeks At that time the remaining duct systems and their surrounding cells were removed by another operation The tap water and rat pellets were continued Seven animals perished within four days The surviving ground squirrel was later sacrificed for examination and a small body was found at the hilum of the left kidney This body was identified histologically as an accessory adrenal gland

Inhibition and stimulation Initially it was believed that the cells which differentiated into the adrenal cortex like cells were spindle shaped or fibroblast like cells in the connective tissue surrounding the efferent ductules None of the normal efferent ductules which were examined earlier showed any periductular adrenal cortex like cells Groat (43) and Jones (63) noted that in the female these adrenal cortex like cells do not occur normally

The fact that the new cells develop bilaterally and the belief that they did not occur normally led to the use of one side of an animal as a control for the other

Animals were adrenalectomized and given cortisone acetate injections for five days while being maintained on 1% saline drinking solution The injection dosage varied from 0 25 mg to 4 mg per 100 gm

of body weight After five days one testicle was removed and fixed The animals were then maintained for five or six days on 1% saline solution to allow time for the uninhibited cells to differentiate The second testicle was then removed and fixed The inhibited and uninhibited periductular cells were compared histologically The object of this procedure was to see if cortisone acetate inhibited the cell differentiation of the first side and later whether the adrenalectomy had been complete and the cell did have the ability to differentiate when the inhibitory effect of the steroid had been removed

This experiment was repeated adding exogenous ACTH to the cortisone acetate inhibited animals At this time it was believed that the absence or presence of the adrenal cortex like cells was a very absolute thing The results of these experiments tended to substantiate the idea that ACTH stimulated the cell differentiation and that parenterally administered cortisone acetate inhibited it However they did not show as much contrast as had been anticipated

Corticosteroids are known to inhibit ACTH secretion by the pituitary (Sayers 62) but do not completely block its secretion So the fact that some partly differentiated cells and an occasional differentiated cell appeared on the inhibited side was not surprising

A more extensive examination was made of the efferent ductules of normal animals and a new observation was made In the late winter and early spring months it is common to see a few active looking adrenal cortex like cells around the efferent ductules of ground squirrels kept in captivity through the fall and winter

To gain better control of the inhibition experiments transplant operations were next used In the first transplant operations the ductules from three animals were placed in the rectus abdominis muscles of two adrenalectomized animals One was given cortisone acetate to inhibit formation of the new cells The other received ACTH gel to stimulate them into activity These animals were used during the late winter months so that some differentiated cells were probably normally present around the ductules In spite of this it was possible to separate the tissue of inhibited animals from that of stimulated animals Accurate identification was made in a blind study

The tissue from the ACTH stimulated ground squirrel showed numerous large cells which were typical of adrenal cortex cells With Groat s stain they had richly stained cytoplasm and vesicular nuclei

The inhibited cells were fewer and smaller and had almost colorless cytoplasm The nuclei appeared rather pycnotic The cells were irregular in shape

Colchicine studies Colchicine studies were done on adrenalectomized animals both male and female from the time of the operation until the end of the fourth day The dosage was regulated by trial and error to keep the animals alive for 24 hours after administration The dosage varied considerably from animal to animal probably due to the physiological state of the animal following surgery and the resultant corticosteroid insufficiency No mitotic figures were ever seen in the adrenal cortex like cells or their presumptive precursor cells

Incubation and chromatography studies In preparation for the chromatography experiments the adrenal glands were removed from two normal male ground squirrels chilled homogenized and extracted The lipid was removed with a silica gel column and the extract then run on thin layer chromatography plates with a system of chloroform and ethyl acetate 1/1 The primary corticosteroid of the normal ground squirrel adrenal gland was found to be corticosterone (compound B)

Tissue from 11 male animals which had been adrenalectomized various lengths of time was used for the incubation study Three of the animals had survived bilateral adrenalectomy for three months Four had survived for one month after adrenalectomy and the remaining four were two week postoperative animals Eleven recently caught spring males were used to furnish the normal efferent ductules

The following table shows the results of this study Included are the weights of the bilaterally separated tissues Half received ACTH and half did not The minced tissue was incubated with isotope tagged progesterone and the products were isolated with

plasm (figs 6 7) The cell outline is distinct and the nucleus is smoothly rounded and appears somewhat hyperchromatic because the nucleoplasm takes a heavy stain the chromatin granules although distinct are closely packed When these cells become active they enlarge and tend to become polyhedral in shape The cytoplasm becomes distinctly acidophilic the nucleus enlarges and becomes clearer and vesicular in type Cytologically these new cells are like adrenal cortex cells (figs 8 9) They are large cells with cytoplasm which has a foamy or granular structure They have a large spheroidal semichromatic nucleus

Histochemistry Frozen sections of the efferent ductules of a six week postoperative animal and of a normal ground squirrel were examined with the histochemical tests mentioned in Materials and Methods Frozen sections of the adrenal glands of normal animals were also tested for comparison

The cytoplasm of the active periductular cells was birefringent with polarized light It stained positively with Sudan Black demonstrating the presence of lipoid substance The Schultz test also gave positive results This is strong evidence for the presence of steroid compounds The cytoplasm fluoresced when viewed with the fluorescence microscope The results of all of these tests were comparable to the results of the same tests performed on the normal adrenal cortex cells and strongly indicate that these cells are steroid secretors

Ultrastructure The efferent ductules were removed from a ground squirrel which had been adrenalectomized two weeks earlier The electron micrographs prepared from these tissues showed that the periductular cells possessed smooth endoplasmic reticulum a characteristic of steroid secreting cells (fig 11) Large mitochondria with tubular cristae and many glycogen granules were also observed in preparations of these cells These findings suggest that the new periductular cells could have a function similar to that of adrenal cortex cells They also show the presence of rough endoplasmic reticulum which indicates they possibly have an additional function

Abolition of adrenal cortex like tissues Five weeks after adrenalectomy 13 lined ground squirrels can be maintained on tap water Three to five months later they can withstand stress as well as normal animals can

Six male and six female animals were selected from a group which had been bilaterally adrenalectomized and maintained on tap water and rat pellets for one year They were all anesthetized with sodium pentobarbital and their gonads with adnexa were removed All were returned to their own cages The tap water and rat pellet diet was continued All 12 died within four days

Another group of eight one year postoperative male animals was selected They were anesthetized and only the testis proper was removed bilaterally from each animal The head of the epididymis the efferent ductules and their surrounding adrenal cortex like cells were allowed to remain intact in each case All animals remained healthy and active for two weeks At that time the remaining duct systems and their surrounding cells were removed by another operation The tap water and rat pellets were continued Seven animals perished within four days The surviving ground squirrel was later sacrificed for examination and a small body was found at the hilum of the left kidney This body was identified histologically as an accessory adrenal gland

Inhibition and stimulation Initially it was believed that the cells which differentiated into the adrenal cortex like cells were spindle shaped or fibroblast like cells in the connective tissue surrounding the efferent ductules None of the normal efferent ductules which were examined earlier showed any periductular adrenal cortex like cells Groat (43) and Jones (63) noted that in the female these adrenal cortex like cells do not occur normally

The fact that the new cells develop bilaterally and the belief that they did not occur normally led to the use of one side of an animal as a control for the other

Animals were adrenalectomized and given cortisone acetate injections for five days while being maintained on 1% saline drinking solution The injection dosage varied from 0 25 mg to 4 mg per 100 gm

and are less constant They are in close and constant relationship to the rete ovarii and the medullary cords This is much more obvious in juvenile females where these epithelial structures are not obliterated or masked by other cells Figures 1 and 10 are inserted to show the location and character of these cells in normal female ground squirrels The ovary shown in figure 10 had a large active mass of adrenal cortex like tissue extending from the epoophoron region throughout the medulla This condition was not commonly seen in normal females in July but the illustration is included here to show the similarity between well-differentiated cells in the female and those of the male (figs 8 9) A careful year round study of the appearance of the adrenal cortex like cells in normal animals both young and adults of each sex would be worthwhile

Male Our work on the male ground squirrels has shown that adrenal cortex like cells similar to those of adrenalectomized females do differentiate in the same length of time in the male

Cytologically these cells appear like adrenal cortex cells The histochemical tests used were selected as the most reliable available to identify this type of cell The fact that these tests gave positive results does not prove that the cells are adrenal cortex cells but it supplies excellent evidence that the cells are steroid secretors The presence of smooth endoplasmic reticulum is also good evidence that they are steroid secreting cells In fact their ultra structure suggests that they could function like adrenal cortex cells

The gonadectomy experiments on male and female animals which had survived on tap water for one year following bilateral adrenalectomy showed that at least an essential amount of the corticosteroid secreting tissue was removed with the gonad All animals died within four days on tap water

To exclude the possibility that the steroids formed by the gonads were maintaining the male animals the efferent ductules and the surrounding cells were left intact in one group of animals while the testes proper were removed These animals survived two weeks on tap water Subsequent removal of the efferent ductules and surrounding cells caused all but one animal to die within four days The exception was found to have a small accessory adrenal gland which actually helped show that the second operation was not enough to over stress the animal and cause its death if it had even a small amount of active adrenal cortex tissue

The initial stimulation and inhibition experiments were performed using the periductular cells of one side as a control for the other The results were positive but the difference was not as striking as had been anticipated if total inhibition occurred This led to the observation that in the late winter and early spring months a few of these cells normally appear active

The later inhibition and stimulation experiments were done using transplanted efferent ductules They showed that ACTH did stimulate these cells to activity and that the presence of cortisone acetate inhibited the release of endogenous ACTH and kept the cells inactive This substantiates Groat s (44) observation that hypophysectomized adrenalectomized females did not differentiate these cells

The results of the chromatography and incubation work may be taken qualitatively not quantitatively The androgens and estrogens were separated from the corticosteroid fraction by the column chromatography The amount of radioactivity in the corticosteroid fractions cannot be used to calculate the actual amount of corticosteroid produced since the final specific activity of each fraction was not determined In addition to this the large losses involved (average 59% loss) limit the value of the results to qualitative interpretation However this experiment has shown that these periductular cells can produce corticosterone and desoxycorticosterone from a progesterone precursor

This experiment was conducted in the spring of the year when it is normal for a few periductular cells to be active This probably explains the positive reading on the control efferent ductules

The ACTH did not stimulate increased production in the incubated tisuses This was possibly because these animals were caught brought to the laboratory and anesthetized and as a result of this stress these cells were probably being stimulated

TABLE 1

Percentage of initial counts [1] recovered

Chromatographic zone	Efferent ductules of normal animals		Efferent ductules of adrenalectomized animals	
	Control	ACTH	Control	ACTH
Progesterone	33	16	14	16
Desoxycorticosterone	18	7	3	3
Corticosterone	3	4	10	10

The overall recovery of radioactively tagged progesterone standards for the extraction and chromatography averaged 41%

[1] 164 309 CPM as progesterone 4C[14]

thin layer chromatography The isolated and identified compounds were measured with a Packard Tri Carb Liquid Scintillator Spectrometer

The results of this incubation and chromatography study may be taken only qualitatively The reasons will be mentioned in the discussion The tissue weights are not of any true value in this type of study but are included for the record [3] The results do show that the adrenal cortex like cells associated with the efferent ductules do possess the ability to form corticosteroid compounds from a progesterone precursor

DISCUSSION

Embryology The gonad and the suprarenal cortex are two of the three organs known to develop cells which secrete steroid compounds They are derived directly from the nephrogenic ridge of the embryo The third organ is of course the placenta The actual differentiation of these cells has been described by a number of workers R E Mancini (63) P Gruenwald (44) R L Zwemer (38) D W Fawcett (60) A Schaberg (55) and R A Groat (44)

In the classical description of the suprarenal gland the fetal cortex is said to arise from the columnar mesothelial cells situated in the angle between the root of the mesentery and the developing gonad

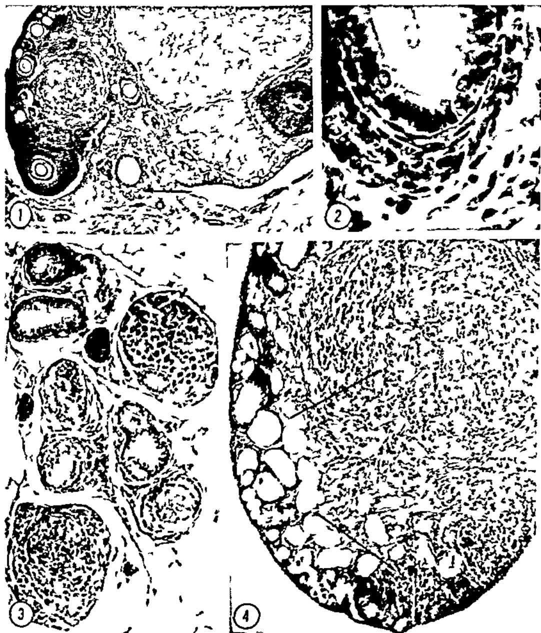
In 1885 Weldon stated that the adrenal blastema was derived from the Wolffian bodies According to him the cell mass proliferates from the walls of Bowman s capsule and separates into two masses One migrates dorsally and becomes the suprarenal body and the other passes caudally and enters the developing gonad to become the seminiferous tubules of the male Witschi (56) describes the adrenal cortex cells and parts of the gonad as being formed from cells derived from portions of the mesonephros in amphibians birds and man

In 1957, Crowder described three sources of cells which contribute to the fetal adrenal cortex of man He numbered them in the order of their addition to the adrenal blastema The first source he traces from the coelomic mesothelium and the second from the ventral surface of Bowman s capsules of the mesonephros The third like the first is from the coelomic mesothelium

These observations emphasize the intimate relationship between the blastema of the adrenal cortex and the gonad They also emphasize the intimate relationship between the mesonephros and the adrenal cortex cells Gillman (48) points out that the whole mesonephric unit contributes to the efferent ductules With these points in mind it becomes understandable that adrenal cortex like cells and cells which can differentiate into adrenal cortex like cells are found in such close and constant relationship with the derivatives of the mesonephrose the epoophoron and the efferent ductules and epididymis

Female Groat and Jones disagree on one point concerning the ovarian changes following bilateral adrenalectomy of the 13 lined ground squirrel Our observations to date substantiate Groat s work We found the constant locus of new cells in the mesovarium of the ovary in close relationship to the epoophoron Those cells which form in the medulla of the ovary appear later

[3] Total tissue weights
a Normal efferent ductules — untreated — 65 8 mg
b Normal efferent ductules — ACTH treated — 76 8 mg
c Efferent ductules of adrenalectomized animals — controls — 79 6 mg
d Efferent ductules of adrenalectomized animals — ACTH treated — 89 7 mg


1
2
3
4

to the maximum by endogenous ACTH The 13 lined ground squirrel normally forms corticosterone as its primary gluco corticoid the mineralocorticoid has not been ascertained These new adrenal cor tex like cells form a combination of cor ticosterone and desoxycorticosterone The latter steroid is a compound with a dual action, i e it acts both as a glucocorticoid and a mineralocorticoid This is probably the reason the adrenalectomized animals manage to survive on tap water in five weeks

Colchicine studies Colchicine studies show that the first adrenal cortex like cells appearing in the periductular region are produced from pre existing cells and not as a result of repeated divisions of a more primitive cell

LITERATURE CITED

Crowder R E 1957 The development of the adrenal gland in man Contrib Embryol Carnegie Institution of Washington D C 251 193

Duke K L 1952 Ovarian histology of *Ochotona princeps* the Rocky Mountain pika Anat Rec 112 737

Enders A C and G D Buchanan 1959 The reproductive tract of the female nine banded armadillo Tex Rep Biol and Med 17 323

Fawcett D W and M H Burgos 1960 Studies on the fine structure of the mammalian testis II The human interstitial tissue Am J Anat 170 245

Frantz M J and Arthur Kirschbaum 1949 Development of adrenal cortical adenomas in ovariectomized mice injected with physiologic doses of sex hormone Proc Soc Exp Biol Med 72 282

Gillman J 1948 The development of the gonads in man with a consideration of the role of fetal endocrines and the histogenesis of ovarian tumors Contrib Embryol Carnegie Institution of Washington D C 32 81

Groat R A Circa 1940 Unpublished data

——— 1943 The ovaries of the adrenalectomized ground squirrel Endocrinology 32 488

——— 1944 Formation and growth of adrenocortical like tissue in the ovaries of the ground squirrel Anat Rec 89 33

Gruenwald P and W M Konikov 1944 Cell replacement and its relation to the zona glomerulosa in the adrenal cortex of mammals Anat Rec 89 1

Jones I C 1963 Ovary of the thirteen lined ground squirrel after adrenalectomy Jour Endocrinol 26 265

Lacassagne A and W Nyka 1935 Constancy of phenomenon of appearance of aberrant portions of suprarenal cortex in region of head of epididymis in adult rabbit Compt rend Soc de Biol 118 1406

Lewis P R and M C Lobban 1961 The chemical specificity of the Schultz test for steroids Jour Histochem Cytochem 9 2

Mancini R E Oscar Vilar J C Lavieri J A Andrada and J Heinrich 1963 Development of Leydig cells in the normal human testis Am J Anat 112 203

Sayers G 1962 The Human Adrenal Cortex Currie Symington and Grant editors E & S Livingstone Ltd p 181

Schaberg A 1955 Regeneration of the adrenal cortex in vitro Anat Rec 122 205

Weldon W R F 1885 Suprarenal bodies of vertebrates Quart Jour Microsc Science XXV

Witschi E 1956 Development of Vertebrates pp 148 291 and 536 Saunders

Zwemer R L R M Wotton and M G Norkus 1938 A study of cortico adrenal cells Anat Rec 72 249

PLATE 1

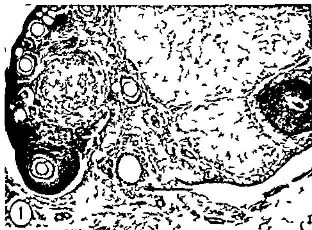
EXPLANATION OF FIGURES

1 Undifferentiated adrenal cortex like cells (arrow) surrounding epoophoron tubule of normal postpartum adult in June C 13 lined ♀ 85 × 70

2 Undifferentiated adrenal cortex like cells from epoophoron of 110 gm juvenile in August three days after adrenalectomy C 13 lined ♀ A15A × 620

3 Efferent ductules with associated adrenal cortex like tissue removed on May 8 1963 from an animal adrenalectomized October 4 1962 and given ACTH subcutaneously 24 hours and one hour before castration C 13 lined ♂ 75 × 120

4 Ovary removed October 5 from an animal adrenalectomized on August 18 Adrenal cortex like tissue (arrows) is differentiated in both the cortex and medulla C 13 lined ♀ A37A × 100


1


2


3

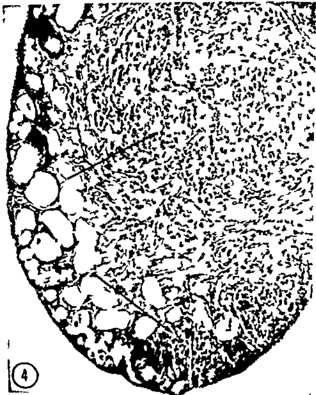

4

PLATE 2

EXPLANATION OF FIGURES

5 Adrenal cortex like tissue (arrows) associated with the testicular ends of the efferent ductules of a normal adult male C 13 lined ♂ 150 × 57

6 Partly differentiated adrenal cortex like cells (arrow) associated with an efferent ductule of a normal adult male C 13 lined ♂ 150 × 500

7 Partly differentiated adrenal cortex like cells (arrow) associated with an efferent ductule two and one half days after adrenalectomy C 13 lined ♂ 183D × 620



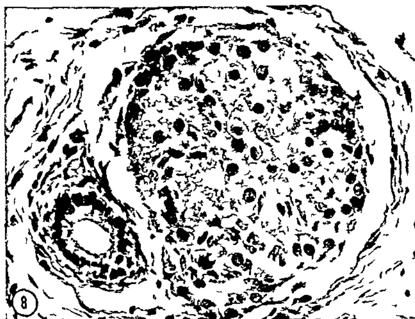
PLATE 3

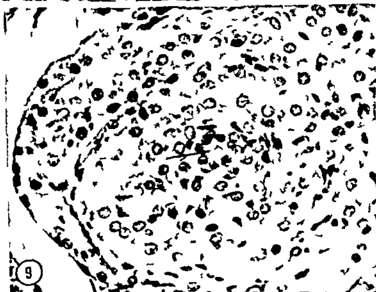
EXPLANATION OF FIGURES

8 Adrenal cortex like mass associated with efferent ductule of an animal adrenalectomized six days earlier C 13 lined ♂ 186A × 400

9 *Dense mass of adrenal cortex like tissue surrounding efferent ductule (arrow) removed on May 8 1963 from an animal adrenalectomized October 4 1962 and given ACTH subcutaneously 24 hours and one hour before castration C 13 lined ♂ 75 × 390*

10 Adrenal cortex like cells from tissue located in the medulla and hilar region of a normal parous non lactating adult on July 2 1962 Note the similarity to those of male animals shown in figures 3 and 9 C 13 lined ♀ 136 × circa 300


8


9

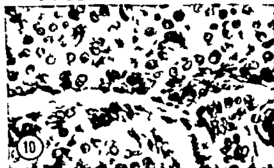

10

PLATE 3

EXPLANATION OF FIGURES

8 Adrenal cortex like mass associated with efferent ductule of an animal *adrenalectomized six days earlier C 13 lined ♂ 186A × 400*

9 *Dense* mass of adrenal cortex like tissue surrounding efferent *ductule* (arrow) removed on May 8 1963 from an animal adrenalectomized October 4 1962 and given ACTH subcutaneously 24 hours and one hour *before castration* C 13 lined ♂ 75 × 390

10 Adrenal cortex like *cells from* tissue *located in the medulla and hilar* region of a normal parous non lactating adult on July 2 1962 *Note* the similarity to those of male animals shown in figures 3 and 9 C 13 lined ♀ 136 × circa 300


11

PLATE 4

EXPLANATION OF FIGURE

11 Ultrastructure of part of a periductular adrenal cortex like cell from an adrenalectomized male ground squirrel Note the abundant smooth endoplasmic reticulum rough endoplasmic reticulum relatively large mitochondria containing tubular cristae most of which are in the formative stage (arrows) The cristae appear to bud from the inner unit membrane of the mitochondria and by dilation of the existing cristae of the precursor cells Lead acetate stain C 13 lined ♂ 2W × 55 000



The Fine Structure of the Stria Vascularis of the Cat Inner Ear [1]

R HINOJOSA [2] AND E L RODRIGUEZ-ECHANDIA [3]
Department of Anatomy Harvard Medical School Boston Massachusetts

ABSTRACT The fine structure of the cat stria vascularis was studied with the electron microscope It consists of three layers of epithelial cells in close association with intraepithelial capillaries The cells of the superficial row have a convex luminal surface bordering on the cochlear duct lumen The apical cytoplasm contains numerous coated vesicles and vesicular invaginations which are interpreted as a type of micropinocytosis Deep infoldings of the plasmalemma divide the lower two-thirds of these cells into thin compartments containing numerous mitochondria It is suggested that marginal cells are well adapted by their fine structure to participate in regulation of the ion composition of endolymph The cells of the intermediate and basal rows have pale cytoplasm and numerous processes Ascending processes of the basal cells form cup like structures which partially isolate each apical cell from the rest of the epithelium

The endothelium of the strial capillaries is not remarkable and no discontinuities of the endothelial lining were observed The endothelial basement lamina sends out numerous extensions into a system of interconnected extracellular passages that permeate the epithelium These are interpreted as pathways for the rapid diffusion of materials from the capillaries

The stria vascularis is a vascularized epithelium beneath the external wall of the cochlear duct (Pars acoustica of the inner ear) The literature of light microscopy is rich in excellent descriptions of the strial cells and the intraepithelial network of capillaries Corti (1851) was one of the first to identify the stria as an epithelial structure of the cochlear duct He also presented an excellent description of the strial vascularity A number of other light microscopic observations include those of Retzius (1882) Shambaugh (07) Held (26) Guild (27) v Fieandt and Saxen (36) Citron et al (56) and Chou (61) Electron microscopic observations on the stria vascularis of the guinea pig have been presented by Engstrom et al (55) Smith (57) and Rodriguez Echandia and Burgos (65)

Since the stria vascularis is presumed to be involved in the secretion of the endolymphatic fluid (Guild 27) the secretion of the endolymphatic oxygen (Misrahy 58 Vosteen 60) and the production and maintenance of the endocochlear D C potential (Davis et al 58) a detailed knowledge of the fine structure of this epithelium is necessary in order to understand its functional mechanism

The present paper is an electron microscopy analysis of the stria vascularis of the adult cat which offers new observations on the fine structure of the strial cells the strial capillaries and the basement lamina Special attention has been focused on the morphological features that may be of physiological significance

MATERIAL AND METHODS

Adult cats were anesthetized by intraperitoneal injection of pentobarbital sodium (Diabutal 60 mg/ml) in a dosage of 0 6 ml per kilo body weight The middle ear was exposed under a dissecting microscope and the cochlea was perfused with the fixative solution through the perilymphatic space (Hinojosa and Fernández technique)

The fixative used was 1% osmium tetroxide buffered with s-collidine (Bennett and Luft 59) at pH 7 4 In some instances calcium chloride in the amount of 0 78 gm 100 ml of fixative was added to achieve 307 milliosmols Osmolarity was measured in an Advanced Osmometer

---

[1] This study was supported by USPHS Research grant GM 10182 NB-682-11 and K3 NB 22 677-01

[2] Present address Department of Surgery (Otolaryngology) University of Chicago Chicago Ill 60637

[3] Fellow of the Rockefeller Foundation

The Fine Structure of the Stria Vascularis of the Cat Inner Ear [1]

R. HINOJOSA AND E. L. RODRIGUEZ ECHANDIA [2]
Department of Anatomy Harvard Medical School Boston Massachusetts

ABSTRACT The fine structure of the cat stria vascularis was studied with the electron microscope It consists of three layers of epithelial cells in close association with intraepithelial capillaries The cells of the superficial row have a convex luminal surface bordering on the cochlear duct lumen The apical cytoplasm contains numerous coated vesicles and vesicular invaginations which are interpreted as a type of micropinocytosis Deep infoldings of the plasmalemma divide the lower two-thirds of these cells into thin compartments containing numerous mitochondria It is suggested that marginal cells are well adapted by their fine structure to participate in regulation of the ion composition of endolymph The cells of the intermediate and basal rows have pale cytoplasm and numerous processes Ascending processes of the basal cells form cup-like structures which partially isolate each apical cell from the rest of the epithelium

The endothelium of the strial capillaries is not remarkable and no discontinuities of the endothelial lining were observed The endothelial basement lamina sends out numerous extensions into a system of interconnected extracellular passages that permeate the epithelium These are interpreted as pathways for the rapid diffusion of materials from the capillaries

The stria vascularis is a vascularized epithelium beneath the external wall of the cochlear duct (Pars acustica of the inner ear) The literature of light microscopy is rich in excellent descriptions of the strial cells and the intraepithelial network of capillaries Corti (1851) was one of the first to identify the stria as an epithelial structure of the cochlear duct He also presented an excellent description of the strial vascularity A number of other light microscopic observations include those of Retzius (1882) Shambaugh ('07) Held ('26) Guild ('27) v Fieandt and Saxen ('36) Citron et al ('56) and Chou ('61) Electron microscopic observations on the stria vascularis of the guinea pig have been presented by Engstrom et al ('55) Smith ('57) and Rodriguez Echandia and Burgos ('65)

Since the stria vascularis is presumed to be involved in the secretion of the endolymphatic fluid (Guild '27) the secretion of the endolymphatic oxygen (Misrahy '58 Vosteen '60) and the production and maintenance of the endocochlear D C potential (Davis et al '58) a detailed knowledge of the fine structure of this epithelium is necessary in order to understand its functional mechanism

The present paper is an electron microscopy analysis of the stria vascularis of the adult cat which offers new observations on the fine structure of the strial cells the strial capillaries and the basement lamina Special attention has been focused on the morphological features that may be of physiological significance

MATERIAL AND METHODS

Adult cats were anesthetized by intraperitoneal injection of pentobarbital sodium (Diabutal 60 mg ml) in a dosage of 0 6 ml per kilo body weight The middle ear was exposed under a dissecting microscope and the cochlea was perfused with the fixative solution through the perilymphatic space (Hinojosa and Fernandez technique)

The fixative used was 1% osmium tetroxide buffered with s-collidine (Bennett and Luft '59) at pH 7 4 In some instances calcium chloride in the amount of 0 78 gm/100 ml of fixative was added to achieve 307 milliosmols Osmolarity was measured in an Advanced Osmometer

[1] This study was supported by USPHS Research grants GM 10182 NB-68211 and K3 NB 22677-01

[2] Present address Department of Surgery (Otolaryngology) University of Chicago Chicago Ill. 60637
Fellow of the Rockefeller Foundation.

When perfusion was completed the living anesthetized animal was decapitated and the cochlea removed from the temporal bone under a dissecting microscope Part of the lateral bony capsule was rapidly removed with a fine chisel and the whole cochlea was immersed in the fixative for an additional period to a total of four hours

The material was then transferred to cold 70% ethanol and the cochlea was trimmed under a dissecting microscope into smaller pieces The specimens were dehydrated in ethanol and embedded in Epon 812 according to Luft (61) Sections were made with an LKB or a Porter Blum ultramicrotome and collected on Athene slit grids of Robertson s type covered with carbon film (Robertson 59) Sections were stained with a combination of saturated uranyl acetate (5 minutes at 60 C) followed by lead tartrate (Millonig 61) for 20 seconds The sections were examined in an RCA EMU 3F or in a Siemens Elmiskop Ib electron microscope Most of the micrographs obtained with the RCA electron microscope were made on a Dupont Ortho A lithographic sheet film with Cronar (polyester) base

Seriate sections 1 μ thick were stained with toluidine blue for study at the light microscope

OBSERVATIONS

Light microscopy

The stria vascularis can be described as made up of three ill defined layers of cells which can be distinguished by reason of differences in their location and cytoplasmic characteristics The apical layer borders on the lumen of the cochlear duct Its cells are large and chromatophilic with a smooth luminal border and a highly irregular basal surface sending processes downward among the cells of deeper layers of the epithelium (fig 1) The cytoplasm

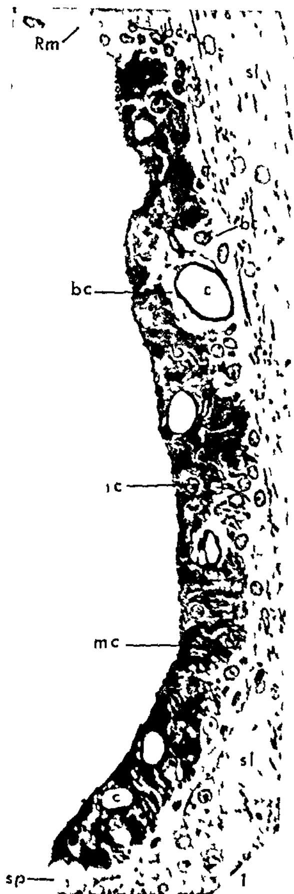


Fig 1 Photomicrograph of a section of the stria vascularis stained with toluidine blue showing the three layers of strial cells the marginal cells (*mc*) the intermediate cells (*ic*) and the basal cells (*bc*) Also the relationship of the strial epithelium to the spiral ligament (*sl*) the Reissner membrane (*Rm*) and the spiral prominence (*sp*) Six intraepithelial blood capillaries (*c*) have been comprised in the section × 460

contains numerous deeply stained spherical or elongated granules which are interpreted to be mitochondria The cells of the intermediate row are smaller than those of the superficial layer and have paler staining cytoplasm which may occasionally contain small deposits of brown pigment Intermediate cells are proportionate in number to the cells of the apical layer as revealed by the analysis of seriate 1 μ sections The cells of the basal layer that connect the stria vascularis to the adjacent spiral ligament are generally flattened but send long processes upward between the cells of the intermediate and superficial layers Their cytoplasmic characteristics are similar to those of the intermediate cells (fig 1) The shapes of the cells of all three layers are complex and are so elaborately interdigitated that it is impossible clearly to resolve their limits with the light microscope Special attention has been paid in this light microscopy analysis to the vascularity of the stria The intraepithelial capillaries lie parallel to one another in the direction of the cochlear turns and their relations with the strial cells may vary from one section to another

Observation of seriate sections revealed that capillaries which at one point in a given section are completely embedded among the cells of the basal layer come up progressively to the apical part of the epithelium and vice versa making smooth arcs or loops of approximately 80 μ in length Another interesting finding is the existence of smaller anastomotic branches which connect one capillary loop to another (fig 1) These run perpendicular to the loops and their number can be estimated to be one or two anastomoses in each 10 μ linear extent of the capillary loop

Electron microscopy

The marginal cells

In electron micrographs the large marginal cells comprising the superficial layer of the epithelium have a convex free surface exposed to the endolymph (fig 2) The surface is generally smooth contoured but may have occasional short microvilli Adjacent cells are attached near the lumen by typical junctional complexes each consisting of a zonula occludens zonula adherens and a small macula adherens or desmosome (figs 3 5) Farther down on the boundary the cell surfaces may have a meandering and interdigitated course

The nucleus is spherical or ellipsoidal with a homogeneous nucleoplasm and an eccentrically placed nucleolus (fig 2) The juxta nuclear Golgi complex consists of small parallel arrays of cisternae and clusters of associated small vesicles (fig 5) The granular endoplasmic reticulum is sparse and located mainly in the apical third of the cell The cisternae often appear somewhat distended and have a pale amorphous content Curving cisternal profiles are often wrapped around a mitochondria (fig 5) The mitochondria are few and tend to be clustered along the lateral aspects of the cell in its upper third but are more abundant and more uniformly distributed in the cytoplasm toward the basal part (fig 2) Judging from the frequency of elongate mitochondrial profiles the majority are presumed to be long rods They have numerous irregularly oriented cristae The cytoplasm at the apex of the cell contains a few large dense bodies of unknown nature (fig 5) occasional multivesicular bodies numerous small vesicles (figs 3 4) and many rosettes and beaded strands of ribosomes (figs 3 4 5) Filaments also occur in the cytoplasmic matrix either individually or associated in bundles that course parallel to the cell membrane and sometimes terminate in desmosomes or in the zonula adherens of the junctional complex (fig 5) These filaments are presumed to be cytoskeletal in their function

Of particular interest and possible functional significance is the apparent invagination of the free surface of the marginal cells to form numerous coated vesicles that accumulate in the apical cytoplasm Although the cell membrane is generally smooth it develops an external filamentous coating on highly localized areas of its surface (figs 3 4) At these sites of specialization of the luminal surface there is also a thin radially striated layer on the cytoplasmic surface of the membrane Various intermediate stages can be found

in the invagination of these plaques to form coated vesicles (fig 3) Thus the large numbers of such vesicles found in the apical cytoplasm evidently arise by invagination of the cell surface Deeper in the cell the coated vesicles become progressively smaller and their light center frequently disappears altogether leaving a moderately dense spherical granule with fuzzy ill defined outer limits (fig 4) These findings strongly suggest that the marginal cells are engaged in some kind of absorptive process

The basal portion of the marginal cells is characterized by an extraordinary degree of compartmentation Deep infoldings of the lateral and basal plasmalemma divide the lower two thirds of the cell into myriad thin foliate compartments (fig 6) Large numbers of mitochondria are lodged in lenticular expansions of the compartments which become so narrow between successive mitochondria that their limiting membranes are almost in contact (figs 2 6) Most other cell types with such elaborate compartmentation of the base rest directly upon a basal lamina (basement membrane)

The base of the marginal cells of the stria vascularis on the other hand reside in concavities of the upper surface of the basal cells (fig 2) The margins of the concavity are prolonged upward around the periphery of the marginal cell as the ascending processes of the basal cell The compartmented basal two-thirds of each marginal cell is thus more or less isolated from the rest of the epithelum by the cup shaped surrounding basal cell (fig 2) Smaller processes of the intermediate and basal cells penetrate the labyrinthine extracellular space in the base of the marginal cell demarcating groups of ten or more of its foliate compartments (figs 6 11)

Adjacent folia of the base of the marginal cells are for the most part separated from one another and from intermediate and basal cell processes by 150 to 200 Å intercellular cleft which often contain an amorphous substance of appreciable density (figs 6 7 8) However in addition to these narrow spaces there is a ramifying system of large extracellular passages (0 1 to 0 2 μ wide) which contain an interstitial material that in its fine structure and density is indistinguishable from that comprising the basement lamina of the intraepithelial capillaries (figs 7 8) The substance occupying the larger spaces among marginal cells processes thus appears to represent extensions of the capillary basement lamina into a branching system of extracellular passages permeating the epithelium Wherever processes of any of the three cell types in the epithelium are exposed to extracellular spaces containing this glycoprotein material they show a local specialization of their membrane and a condensation of the underlying cytoplasm (figs 7 8) These differentiations represent half desmosomes similar to those found along the basal plasmalemma of stratified squamous epithelial cells where they rest upon the basement lamina These canalicular extracellular spaces occupied by extensions of the basement lamina resemble a similar system of channels described by Coggeshall and Fawcett (64) in the ganglia of the avascular nervous system of the leech It seems likely that attachment of cell processes to the ramifying extensions of basement lamina may not only contribute to the structural stability of the epithelium but these channels may also constitute important pathways for the rapid exchange of materials between the capillaries and the surrounding epithelial cells

Intermediate cells

Of noticeably different appearance are the cells of the intermediate layer They are smaller elements of stellate form having a small cell body and long radiating cytoplasmic processes (figs 2 9 10) Some processes directed upward continue between the cells of the upper row approaching the luminal surface of the epithelium but never quite reaching it Other processes extending downward and lateralward are juxtaposed to the cells of the basal layer or make contact with the capillary wall as vascular feet (fig 2) These processes of the intermediate cells can usually be distinguished from adjacent processes of the marginal cells by reason of their differences in shape and in the density and texture of their cytoplasm Intermediate cells processes have a pale

cytoplasmic matrix possess typical profiles of endoplasmic reticulum and have few mitochondria The basal compartments of marginal cells are generally more slender They have a much denser cytoplasm and contain numerous mitochondria ribosomes microtubules and a variable number of vesicular structures (figs 6 7 8) The cell body of the intermediate cells contains the nucleus the Golgi complex the endoplasmic reticulum and a few rod shaped mitochondria (figs 9 10) The nucleus is spheroidal but may be irregular in outline It has a nucleolus which is centrally placed (fig 9)

Small parallel arrays of cisternae and vesicles of the Golgi complex are mainly located at the juxtanuclear cytoplasm while the granular and smooth endoplasmic reticulum are dispersed throughout the cell body and in the cytoplasmic processes (fig 10) An observation of some interest is the occurrence of large spheroidal bodies formed of closely spaced concentric cisternae of the smooth endoplasmic reticulum (figs 2 11) They are most often located in the cell processes and their outermost cisternae may be continuous with the granular endoplasmic reticulum In the interior of these bodies is a small core of cytoplasm usually containing one or two mitochondria and clusters of small dense granules (fig 11)

Other elements that have often been found in the cytoplasm of the intermediate cells are dense granular bodies of an extremely variable size (fig 10) Most of them are limited by a single membrane and contain a mixture of a fine granular material and a variable number of homogeneous dense droplets of larger size probably lipoidal in nature Similar dense bodies have been identified in other cells as lipofuscin pigment deposits or as lysosomes (Holt and Hicks 61) Another type of electron dense bodies having the characteristic fine structure of melanin was seldom found In addition the cytoplasm contains a few multivesicular bodies and there are small bundles of filaments which are similar to those described in the cytoplasm of the apical cells These are likewise interpreted to be cytoskeletal in their function

Basal cells

The cells of the basal layer are flattened elements with pale cytoplasm and long cytoplasmic processes (figs 2 11 12) They resemble the intermediate cells One of the most characteristic features of the basal cells is the presence of upward directed processes at the periphery of the cell which are insinuated between the apical cells and reach to the upper third of the epithelium (fig 2) These processes obviously make extensive contact not only with the two superincumbent rows of cells but also with the capillary wall The deep concavity between these ascending processes holds the elaborately compartmented basal part of each apical cell (figs 2 12) Extending laterally from the basal cells are a number of flattened processes that penetrate between the neighboring basal cells and the adjacent elements of the spiral ligament (figs 11 12) Owing to the absence of a distinct basement lamina separating these two different tissues this region at the base of the stria which is rich in flattened cytoplasmic processes has been interpreted in guinea pig and rat as a transitional zone between the stria and the spiral ligament (Rodriguez Echandia and Burgos 65 Iurato 62) These lateral processes of the basal cells can also be found connecting the stria and the adjacent epithelium of the spiral prominence and the epithelial cells of the Reissner membrane (figs 12 13)

Basal cells have relatively few organelles and inclusions Those present have characteristics similar to those described for the intermediate cells The form of cell to cell junction between basal cells and between basal and intermediate cells is a simple apposition with a 100 A gap between their membranes (fig 6) Small desmosomes were found infrequently along the junction of these cells It is interesting to note that the intercellular clefts between the cells of the intermediate and basal rows is significantly narrower than those separating adjacent compartments of the apical cells or those between the apical cells and the processes of the intermediate and basal cells

in the invagination of these plaques to form coated vesicles (fig 3) Thus the large numbers of such vesicles found in the apical cytoplasm evidently arise by invagination of the cell surface Deeper in the cell the coated vesicles become progressively smaller and their light center frequently disappears altogether leaving a moderately dense spherical granule with fuzzy ill defined outer limits (fig 4) These findings strongly suggest that the marginal cells are engaged in some kind of absorptive process

The basal portion of the marginal cells is characterized by an extraordinary degree of compartmentation Deep infoldings of the lateral and basal plasmalemma divide the lower two thirds of the cell into myriad thin foliate compartments (fig 6) Large numbers of mitochondria are lodged in lenticular expansions of the compartments which become so narrow between successive mitochondria that their limiting membranes are almost in contact (figs 2 6) Most other cell types with such elaborate compartmentation of the base rest directly upon a basal lamina (basement membrane)

The base of the marginal cells of the stria vascularis on the other hand reside in concavities of the upper surface of the basal cells (fig 2) The margins of the concavity are prolonged upward around the periphery of the marginal cell as the ascending processes of the basal cell The compartmented basal two-thirds of each marginal cell is thus more or less isolated from the rest of the epithelium by the cup shaped surrounding basal cell (fig 2) Smaller processes of the intermediate and basal cells penetrate the labyrinthine extracellular space in the base of the marginal cell demarcating groups of ten or more of its foliate compartments (figs 6 11)

Adjacent folia of the base of the marginal cells are for the most part separated from one another and from intermediate and basal cell processes by 150 to 200 A intercellular cleft which often contain an amorphous substance of appreciable density (figs 6 7 8) However in addition to these narrow spaces there is a ramifying system of large extracellular passages (0 1 to 0 2 μ wide) which contain an interstitial material that in its fine structure and density is indistinguishable from that comprising the basement lamina of the intraepithelial capillaries (figs 7 8) The substance occupying the larger spaces among marginal cells processes thus appears to represent extensions of the capillary basement lamina into a branching system of extracellular passages permeating the epithelium Wherever processes of any of the three cell types in the epithelium are exposed to extracellular spaces containing this glycoprotein material they show a local specialization of their membrane and a condensation of the underlying cytoplasm (figs 7 8) These differentiations represent half desmosomes similar to those found along the basal plasmalemma of stratified squamous epithelial cells where they rest upon the basement lamina These canalicular extracellular spaces occupied by extensions of the basement lamina resemble a similar system of channels described by Coggeshall and Fawcett (64) in the ganglia of the avascular nervous system of the leech It seems likely that attachment of cell processes to the ramifying extensions of basement lamina may not only contribute to the structural stability of the epithelium but these channels may also constitute important pathways for the rapid exchange of materials between the capillaries and the surrounding epithelial cells

Intermediate cells

Of noticeably different appearance are the cells of the intermediate layer They are smaller elements of stellate form having a small cell body and long radiating cytoplasmic processes (figs 2 9 10) Some processes directed upward continue between the cells of the upper row approaching the luminal surface of the epithelium but never quite reaching it Other processes extending downward and lateralward are juxtaposed to the cells of the basal layer or make contact with the capillary wall as vascular feet (fig 2) These processes of the intermediate cells can usually be distinguished from adjacent processes of the marginal cells by reason of their differences in shape and in the density and texture of their cytoplasm Intermediate cells processes have a pale

parotid gland the secretory duct of the submaxillary gland (Scott and Pease '59) the cells of the nasal salt gland of lizard (Philpott and Templeton 64) the renal tubule cells of a variety of animals (Pease 55 Rhodin 58 Christensen 63) are other examples of epithelia with a great amplification of their basal surface associated with numerous mitochondria To our knowledge the most extensive system of interdigitating processes or cytoplasmic compartments have been found in the principal cells of the salt gland of marine birds (Doyle 60) In these glands the entire epithelium is organized into an infinitely complex system of narrow compartments in which are numerous mitochondria The fine structure of these compartments closely resembles those we have observed here at the base of the apical cells of the stria vascularis of the cat

On the other hand the biochemical analysis of the endolymph of the cat (Citron et al 56) reveals that it contains an unusually high concentration of potassium (about 120 mEquiv l) and low concentration of sodium (about 60 m Equiv l) A more or less similar ion composition was previously found in the endolymph of guinea pig (Smith et al 54) Endolymph is therefore an extracellular fluid of unique ionic composition which can not be accounted for on the basis of simple diffusion due to concentration or voltage gradients According to Davis (57) it is more reasonable to assume that the concentration of cations of the endolymph is actively regulated by some one of the epithelial structures lining the cochlear duct lumen The present investigation suggests that it is the marginal cell of the stria vascularis that is best adapted by its location and fine structural differentiation to accomplish this function Further combined physiological and biochemical studies may resolve this problem

Another interesting aspect of the fine structure of the apical cells of the stria is the presence of many coated vesicles in the apical cytoplasm They are in close topographical relation to similar invaginations at the cells surface and resemble those found in the stria vascularis of guinea pig and also those described in many other cells as a type of pinocytosis vesicles (Roth and Porter 62 and 64)

Although experimental studies have never demonstrated incorporation by the stria vascularis of the various particulate markers presented to it by injection into the endolymph (Yamamoto et al 64) it is still probable that these coated vesicles may be involved in a kind of selective absorption

Intermediate and basal cells Much less elaboration of the surface was observed in the cells of the intermediate and basal layers An interesting new finding in the intermediate cells of the stria was the occurrence of concentric layers of cisternae of the smooth endoplasmic reticulum sometimes in communication with adjacent cisternae of the granular reticulum The significance of these structures is obscure at present

Of particular interest is the observation of slender processes which extend upward from the basal cells to form a cup-like structure surrounding the compartmented basal two-thirds of each marginal cell These have been recently described in guinea pig (Rodriguez Echandia and Burgos 65) and may be considered as columns or incomplete septa that support and partially isolate each marginal cell Since marginal cells are exposed to the most rapid changes in the pressure of endolymph this elaborate system of supporting cells may represent another example of adaptation tending to protect the essential marginal cells from damage

Strial capillaries Special attention has been paid to the distribution of the strial capillaries the fine structure of the endothelium and the basement lamina (basement membrane) One of the earliest investigations on the vascularity of the stria goes back to Corti (1851) who described the strial capillaries as tortuous blood vessels of variable diameter which are in turn resolved into a number of smaller anastomotic branches to form altogether an intraepithelial rete Our observations with the light microscope on seriate sections of the stria add little to these findings of Corti With the electron microscope we have observed that the endothelium is not remarkable As in other capillaries the endothelial cells appear to be closely

The strial capillaries

The capillaries of the stria vascularis have a continuous endothelial lining which varies in its thickness from 0 5 to 5 μ (fig 14) The endothelial cells possess a flattened nucleus sparse small mitochondria a few cisternae of the endoplasmic reticulum and a small Golgi complex which is located in the juxtanuclear zone At the peripheral part of contiguous endothelial cells one or both cells have a thin fold that generally lies flat against the capillary wall Scanty short microvillies can be also observed on the luminal surface of the endothelium (fig 14) Adjacent endothelial cells are closely attached by a typical attachment band and sometimes one or more small desmosomes

Along the luminal surface of the endothelium there are a few empty appearing vesicular invaginations of the plasma membrane which frequently communicate with the capillary lumen Vesicular invaginations of similar shape are also associated with the base of the endothelium adjacent to the perivascular basement lamina (figs 14 15 17) Such vesicles are very numerous in some micrographs and have a rather dense content resembling the substance of the subjacent basement lamina A few vesicular structures are situated deep in the cell These are frequently provided with minute radial spines on the cytoplasmic surface of the membrane (fig 14) The endothelial basement lamina is 0 3 to 0 6 μ in width At high magnification it appears to consist of a network of fine fibrillar elements (fig 14) Some of these fibrils show the characteristic striation of collagen (fig 16) As already noted above the basement lamina of the strial capillaries sends out a number of prolongations which extend into the interstice among the interdigitating processes of the strial cells (figs 14 15) As a result of this special distribution of channels occupied by extensions of the basement lamina the cellular elements of the three layers of the epithelium even those which are far away from the capillaries are in direct communication with the perivascular basement lamina It is interesting to note that vesicles and vesicular invaginations suggesting pinocytosis were infrequently observed in the cytoplasm of the cells that are adjacent to the basement lamina (figs 14 15) The capillary basement lamina splits to enclose prominent pericytes associated with the endothelium (fig 17)

The existence of pericapillary cells along the strial vessels was first reported by Smith (51) but it could not be determined with the light microscope whether they were smooth muscle cells or closely applied epithelial cells The existence of abundant pericytes in the stria vascularis of guinea pig has also been reported recently (Rodriguez Echandia and Burgos 65) The pericapillary cells of the stria vascularis of the cat resemble the endothelial cells in their fine structure but possess fewer micropinocytosis vesicles (fig 17)

DISCUSSION

Investigations with the light microscope have already drawn attention to the elaborate cytoarchitecture of the stria vascularis Electron microscopy studies (Engstrom et al 55 Smith 57 Rodriguez Echandia and Burgos 65) have confirmed these findings and have greatly extended the our knowledge of the finer details of the strial epithelium The results of the present investigation of the stria vascularis of the cat inner ear are in general agreement with these earlier studies all of which emphasize that the marginal cells are by far the most elaborately specialized elements of the stria

Marginal cells The extraordinary compartmentation of the lower two thirds of the apical cells into myriad thin foliate processes containing a large number of mitochondria is believed to have important physiological significance That this particular organization is essential to the function of the stria vascularis is suggested by the fact that an almost identical system of lateral and basal infoldings of the plasma membrane has also been found in apical cells of the stria vascularis of guinea pig (Rodriguez Echandia and Burgos 65) The resemblance of this compartmentation to that seen in various epithelia involved in an active transport of fluids and ions in very striking The epithelial cells of the striated duct of the

Shambaugh G E 1907 Über die Herkunft der in der tieferen Schicht der Stria vascularis sich findenden Zellen Z Ohrenheilk 53 301–314

Smith C A 1951 Capillary areas of the cochlea in the guinea pig Laryngoscope 61 1073–1095

—— 1957 Structure of the stria vascularis and the spiral prominence Ann Otol Rhin & Laryng 66 521–536

Smith C A O H Lowry and M L Wu 1954 The electrolytes of the labyrinthine fluids Laryngoscope 64 141–153

v Fieandt H and A Saxén 1936 Beitrage zur Histologie der Stria vascularis und der Prominentia spiralis bei Saugern (Hund und Mensch) Ztschr f Anat Entwickl -Gesch 106 424–446

Vosteen K H 1960 The histochemistry of the enzymes of oxygen metabolism in the inner ear Laryngoscope 70 351–362

Yamamoto K and Y Nakai 1964 Electron microscopic studies on the function of the stria vascularis and the spiral ligament in the inner ear Ann Otol Rhin & Laryng 73 332–347

attached by specific specializations of the cell surface (attachment bands and desmosomes) and no pores or discontinuities in the endothelial lining were observed Of special interest is the existence of extensions of the endothelial basement lamina into a branching system of extracellular passages permeating the epithelium A similar system of interstitial channels has been described recently in the ganglia of the avascular nervous system of the leech (Coggeshall and Fawcett 64) It has been suggested by these authors that they may well be of great importance to glial and ganglion cell function as channels for rapid diffusion deep into the ganglion It seems reasonable to speculate that the system of extracellular passages of the stria vascularis may also act as pathways for the rapid diffusion of materials from the strial capillaries

ACKNOWLEDGMENT

The authors wish to thank Dr Don W Fawcett for the advice and assistance in the critical reading of the manuscript

LITERATURE CITED

Bennet H S and J H Luft 1959 s Collidine as a basis for buffering fixatives J Biophys Biochem Cytol 6 113–114

Chou J T Y 1961 A cytological and histochemical study of the stria vascularis of the guinea pig s ear Quart J Micr Sci 102 75–82

Christensen A K 1963 Fine structure of an exceptional kidney in the salamander Batrachoseps J Cell Biol 19 13A (Abstract)

Citron L D Exley and C S Hallpike 1956 Formation circulation and chemical properties of the labyrinthine fluids Brit M Bull 12 101–104

Coggeshall R F and D W Fawcett 1964 The fine structure of the central nervous system of the leech Hirudo Medicinalis J Neurophysiol 27 229–289

Corti A 1851 Recherches su l organe de l ouie des mamifères Ztschr f wiss Zool 3 109–169

Davis H 1957 Biophysics and physiology of the inner ear Physiol Rev 37 1–49

Davis H B H Deatherage B Rosenblut C Fernandez R Kimura and C A Smith 1958 Modification of cochlear potentials produced by streptomycin poisoning and by extensive venous obstruction Laryngoscope 68 596–627

Doyle W L 1960 The principal cells of the salt gland of marine birds Exp Cell Res 21 386–393

Engstrom H F S Sjostrand and H Spoendlin 1955 Feinstruktur der Stria vascularis beim Meerschweinchen Pract oto rhino-laryng 17 69–79

Fawcett D W 1965 Surface specializations of absorbing cells J Histochem Cytochem 13 75–91

Guild S 1927 Circulation of the endolymph Am J Anat 39 57–81

Held H 1926 Handbuch der Normalen und Pathologischen Physiologie Vol I Julius Springer Berlin

Hinojosa R and C Fernandez To be published

Holt S J and M R Hicks 1961 The localization of acid phosphatase in rat liver cells as revealed by combined cytochemical staining and electron microscopy J Biophys Biochem Cytol 11 47–66

Iurato S 1962 Submicroscopic structure of the membranous labyrinth III The supporting structure of Corti s organ (basilar membrane limbus spiralis and spiral ligament) Z Zellforsch 56 40–96

Luft J H 1961 Improvements in epoxy resin embedding methods J Biophys Biochem Cytol 9 409–414

Millonig C 1961 A modified procedure for lead staining of thin sections J Biophys Biochem Cytol 11 736–739

Misrahy G A K M Hildreth E W Shinabarger L C Clark and E A Rice 1958 Endolymphatic oxygen tension in the cochlea of the guinea pig J Acoust Soc Am 30 247–250

Pease D C 1955 Electron microscopy of the tubular cells of the kidney cortex Anat Rec 121 723–744

Philpott C W and J R Templeton 1964 A comparative study of the histology and fine structure of the nasal salt secreting gland of lizard Dipsosaurus Anat Rec 148 394 (Abstract)

Retzius G 1882 Ueber ein Blutgefasse fu hrendes Epithelgewebe im membranosen Gehororgan Biol Untersuch 2 1–32

Rhodin J A G 1958 Anatomy of the kidney tubules Int Rev Cytol 7 485–534

Roberston J D 1959 The electron microscope In Tools of Biological Research H J B Atkins ed Blackwell Scient Pub Oxford pp 72–121

Rodriguez Echandia E L and M H Burgos 1965 The fine structure of the stria vascularis of the guinea pig inner ear Z Zellforsch 67 600–619

Roth T F and K R Porter 1962 Specialized sites on the cell surface for protein uptake 5th Internat Congr Electr Micr S S Breese Jr ed Academic Press New York Vol 2 LL-4

——— 1964 Yolk protein uptake in the oocyte of the mosquito Aedes aegypti L J Cell Biol 20 313–332

Scott B L and D C Pease 1959 Electron microscopy of the salivary and lacrimal glands of the rat Am J Anat 104 115–161

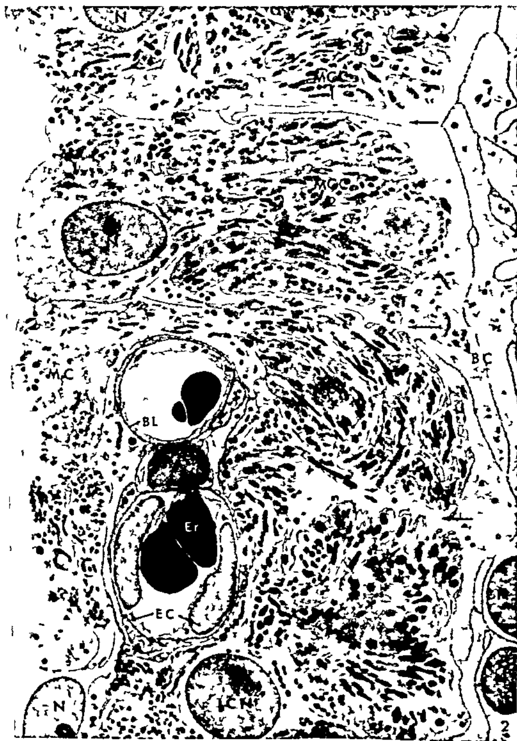

N
MCC
MCC
N
BC
MC
BL
Er
EC
N
ICN
2

PLATE 1

EXPLANATION OF FIGURE

2 Low power electron micrograph of the stria vascularis of the cat showing the arrangement of the strial cells and their relationship to the intraepithelial capillaries Marginal cells (*MC*) have a convex luminal surface and an apically placed nucleus (*N*) Deep infoldings of the lateral and basal plasmalemma divide the lower two thirds of these cells into myriad compartments in which are lodged numerous mitochondria (*MCC*) Intermediate cells (*ICN*) and basal cells (*BC*) have a pale cytoplasm and are irregular in outline Upward directed processes of the basal cells (arrows) are insinuated between the marginal cells (*MC*) and reach the upper third of the epithelium They partially isolate each marginal cell from the rest of the epithelium (*MCC 1 MCC 2 MCC 3 MCC 4*) The three types of cells of the stria are in close topographical relation with intraepithelial capillaries These show the endothelial cells (*EC*) the basement lamina (*BL*) and the pericapillary cells (*P*) Erythrocytes are visible inside capillaries (*Er*) × 3 038


CV
RI
GER

PLATE 2

EXPLANATION OF FIGURES

3 A portion of the apical cytoplasm of two adjacent marginal cells showing numerous coated vesicles and three different stages of vesicular invaginations of the free surface Vesicular invaginations (*1 2 3*) possess an external filamentous coating and a thin radially striated layer on the cytoplasmic surface of the membrane A one to four sequence in the formation of the coated vesicles is suggested Near the luminal surface there is a junctional complex attaching the lateral plasmalemmas of adjacent marginal cells *M* mitochondria × 36 135

4 A portion of the apical cytoplasm of a marginal cell showing vesicular invaginations of the free surface (arrows) and numerous coated vesicles Deep in the cell these vesicles apparently become progressively concentrated (CV) GER granular endoplasmic reticulum *Ri* ribosomes *M* mitochondria × 25 560


G
D
F
ger
R1
D
F
ger
R1
gera
HD
5

PLATE 3

EXPLANATION OF FIGURE

5 Peripheral cytoplasm of marginal cells (apical third) showing distended cisternae of the granular endoplasmic reticulum (*ger*) having an amorphous content of considerable density Some curving cisternal profiles are wrapped around mitochondria (*M*) Ribosomes are numerous throughout the cytoplasm (*Ri*) The cells are closely attached by small desmosomes (*D*) Bundles of filaments (*F*) are present in the cytoplasmic matrix most of them course parallel to the cell membrane *HD* half desmosome *GC* Golgi complex *DB* dense body × 63 000


G
D
F
ger
R1
D
F
ger
M
R1
ger
HD
5

PLATE 4

EXPLANATION OF FIGURE

6 An oblique section of a *marginal* cell (basal portion) Deep infoldings of the plasmalemma divide the cytoplasm of these cells into myriad thin foliate compartments (*MCC*) Large numbers of mitochondria are lodged in lenticular expansions of these compartments Intermediate cell processes (*ICP*) and basal cells processes (*BCP*) interdigitate with the marginal cell compartments (*MCC*) These processes have a pale cytoplasm possess profiles of the endoplasmic reticulum and have few mitochondria Adjacent compartments of marginal cells (*MCC*) are separated from one another and from intermediate (*ICP*) and basal cells processes (*BCP*) by a regular intercellular cleft (about 200 Å) The intercellular cleft between the cells of the intermediate and basal rows is narrower (arrow) Large irregular areas of extracellular spaces are frequent They contain interstitial material (*IM*) × 13 365


BCP
IM
ICP
MC
MC
ICP
IM
ICP
ICP
BCP
6

PLATE 5

EXPLANATION OF FIGURES

7–8 Two areas at the base of the marginal cells at high magnification showing the characteristics of the large extracellular passages They *contain an interstitial material with a line of condensation closely* applied to the outer surface of the cell processes This is interpreted as representing interstitial extensions of the endothelial basement lamina (*BL*) The 200 Å intercellular cleft between adjacent folia *of the cells also* contains an *interstitial material of similar density* (*IM*) Cytoplasmic processes that are exposed to the large extra cellular passages show a local specialization of the membrane and a condensation of the underlying cytoplasm (arrows) resembling half desmosomes Small desmosomes attaching adjacent cytoplasmic processes such as shown in the lower right corner of figure 8 (*D*) were occasionally observed *M* mitochondria *V* vesicles *ICP* intermediate cell processes *DB* dense body *T* microtubules Figure 7 × 40 500 Figure 8 × 79 114

PLATE 6

EXPLANATION OF FIGURE

9 A section of an intermediate cell at low magnification showing the nucleus (*Int CN*) the rod shaped mitochondria (*m*) the endoplasmic reticulum (*Er*) and numerous cytoplasmic processes which give these cells a stellate appearance (*ICP*) These processes (*ICP*) interdigitate with the cytoplasmic compartments of marginal cells (*MCC*) A labyrinthine system of large intercellular passages some of them very close to the nucleus of the intermediate cell (*Int CN*) contain an interstitial material of high density (*IM*) *Marg C* marginal cells *db* dense body × 12 690


db
m
Er
Er
m

PLATE 7

EXPLANATION OF FIGURE

10 Another section of an intermediate cell showing the nucleus (*Int CN*) the juxtanuclear Golgi complex (*Gc*) the endoplasmic reticulum (*Er*) and the presence of numerous dense bodies (*Db*) of variable size On the right side of the picture there is a long process of an intermediate cell having a few mitochondria (*m*) typical profiles of the endoplasmic reticulum (*Er*) and dense bodies resembling lysosomes (*Db*) The intermediate cell and its processes are embedded between compartments of the marginal cells (*MCC*) × 13 365

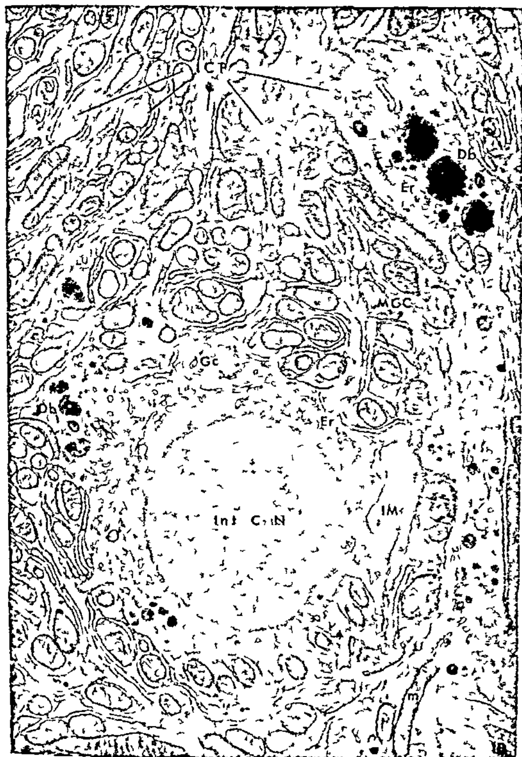

CP
Db
Er
MGC
Gc
Db
Er
Int Cy N
IMc
m
IB

PLATE 7

EXPLANATION OF FIGURE

10 Another section of an intermediate cell showing the nucleus (*Int CN*) the juxtanuclear Golgi complex (*Gc*) the endoplasmic reticulum (*Er*) and the presence of numerous dense bodies (*Db*) of variable size On the right side of the picture there is a long process of an intermediate cell having a few mitochondria (*m*) typical profiles of the endoplasmic reticulum (*Er*) and dense bodies resembling lysosomes (*Db*) The intermediate cell and its processes are embedded between compartments of the marginal cells (*MCC*) × 13 365


ICN
BCP
C
IM
MCC
PCP
BCP
MCC
BCP
G
N
DB
Basal
Cells
N
ER
St

PLATE 8

EXPLANATION OF FIGURE

11 Low power electron micrograph of the basal part of the stria showing in the upper right corner the cell body of an intermediate cell (*ICN*) Also numerous intermediate cell processes (*ICP*) which interdigitate with the marginal cell compartments (*MCC*) In one of these processes there is a system of concentric cisternae of the smooth endoplasmic reticulum (*er*) There are numerous intercellular passages which contain interstitial material (*IM*)

At the bottom two *Basal Cells* showing the nucleus (*N*) the endoplasmic reticulum (*ER*) the Golgi complex (*G*) and dense bodies which resemble melanin (*DB*) Upward directed processes of these cells (*BCP*) *are insinuated between marginal cell compartments* (*MCC*) Extending laterally from the cell body of the basal cells are flattened processes (arrows) that penetrate between the neighboring basal cells and the elements of the spiral ligament (*SL*) × 5 792


Sp Pr
Spiral Ligament
Basal C N
12

PLATE 9

EXPLANATION OF FIGURE

12 A section of the zone in which the stria vascularis (left) connects with the spiral prominence (*Sp Pr*) Basal cells connect the stria with the subjacent spiral ligament and the adjacent epithelium of the spiral prominence (*Sp Pr*) *Int CN* intermediate cell nucleus *N* nucleus *Marg C* marginal cell *Cytopl Comp* cytoplasmic compartments of marginal cells *Basal CN* Basal cell nucleus × 6 075


Sp Pr
Cytopl Comp
Cytopl Comp
N
Spiral Ligament
12

PLATE 10

EXPLANATION OF FIGURE

13 *A low power electron micrograph from the zone of connection of* the stria vascularis to the epithelial elements of the Reissner membrane (*Reissner M*) There is no transition between the large marginal cells of the stria and the small Reissner s cells Basal cells of the stria are insinuated between the marginal cells and the first *Reissner s cell (arrow) Basal cells are also insinuated below the* first elements of Reissner s membrane and separate them from the subjacent spiral ligament (*Spiral Lig*) Basal cells disappear at the point in which the basement lamina of Reissner s membrane is apparent (*Basem L*) The spiral ligament (*Spiral Lig*) shows a capillary (*Cap*) and large intercellular passages which contain interstitial material (*IM*) *N* Nucleus *Basal C* Basal cells × 4 631

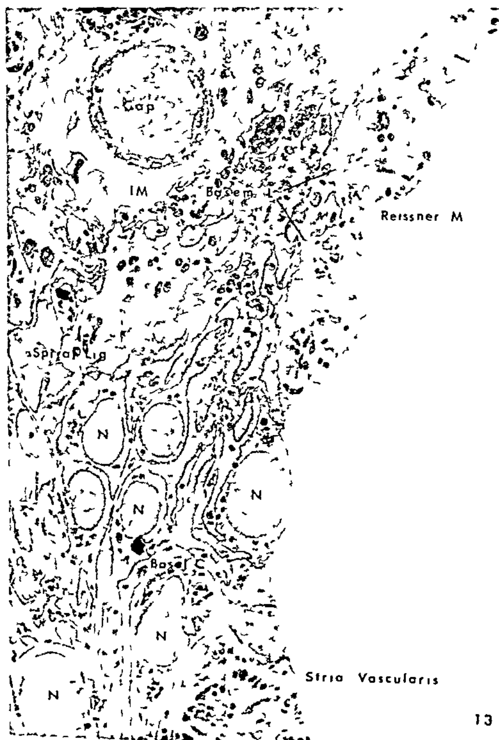

Cap
IM
Basem. L
Reissner M
Spiral Lig
N
N
N
N
N
Basal C
N
N
Stria Vascularis
13

PLATE 10

EXPLANATION OF FIGURE

13 A low power electron micrograph from the zone of connection of the stria vascularis to the epithelial elements of the Reissner membrane (*Reissner M*) There is no transition between the large marginal cells of the stria and the small Reissner s cells Basal cells of the stria are insinuated between the marginal cells and the first Reissner s cell (arrow) Basal cells are also insinuated below the first elements of Reissner s membrane and separate them from the subjacent spiral ligament (*Spiral Lig*) Basal cells disappear at the point in which the basement lamina of Reissner s membrane is apparent (*Basem L*) The spiral ligament (*Spiral Lig*) shows a capillary (*Cap*) and large intercellular passages which contain interstitial material (*IM*) *N* Nucleus *Basal C* Basal cells × 4 631

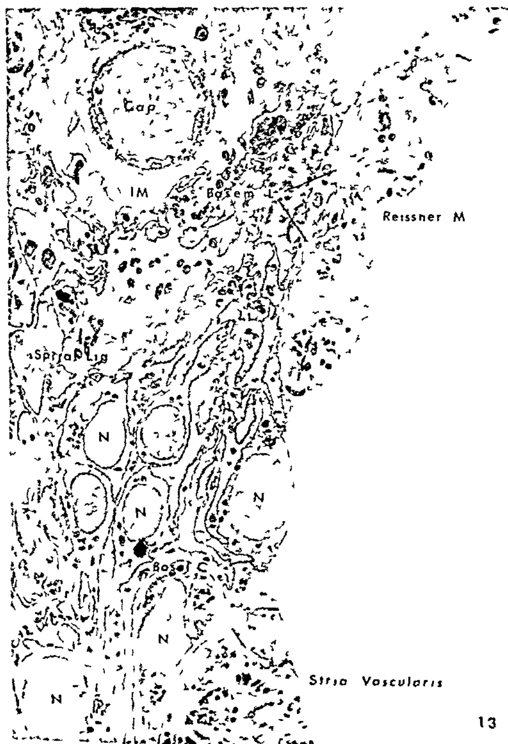

Cap
IM
Basem L
Reissner M
Spiral Lig
N
N
N
N
N
N
Basal C
Stria Vascularis
13

PLATE 10

EXPLANATION OF FIGURE

13 A low power electron micrograph from the zone of connection of the stria vascularis to the epithelial elements of the Reissner membrane (*Reissner M*) There is no transition between the large marginal cells of the stria and the small Reissner s cells *Basal cells* of the stria are insinuated between the marginal cells and the first Reissner s cell (arrow) Basal cells are also insinuated below the first elements of Reissner s membrane and separate them from the subjacent spiral ligament (*Spiral Lig*) Basal cells disappear at the point in which the basement lamina of Reissner s membrane is apparent (*Basem L*) The spiral ligament (*Spiral Lig*) shows a capillary (*Cap*) and large intercellular passages which contain interstitial material (*IM*) *N* Nucleus *Basal C* Basal cells × 4 631

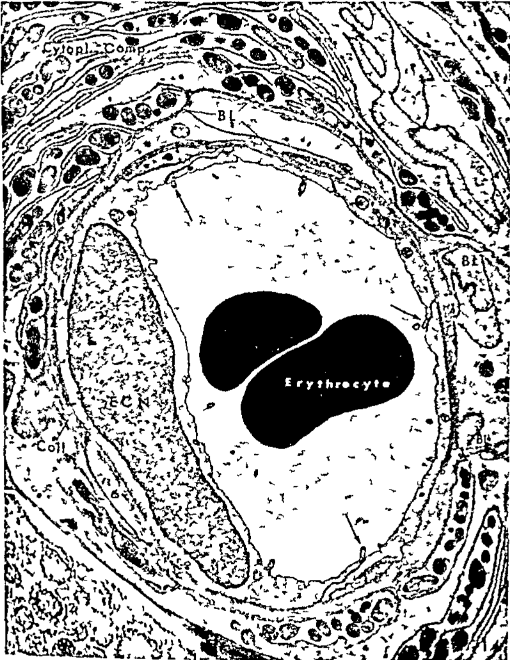

Cytopl. Comp.
BL
BL
Erythrocyte
ECN
Coll
BL

PLATE 11

EXPLANATION OF FIGURE

14 A section of a strial capillary which contains erythrocytes and possesses a continuous endothelial lining The endothelial cells have a flattened nucleus (*ECN*) a few mitochondria and scarce cisternae of the endoplasmic reticulum On the luminal surface marginal folds and microvilli are apparent (arrows) Numerous vesicular structures are present in the endothelial cytoplasm The endothelial basement lamina (*BL*) appears to consist of a network of fine fibrillar elements having the periodical striation of collagen (*Coll*) The basement lamina sends out numerous prolongations that extend into the interstices of the epithelium (*BL*) *Cytopl Comp* cytoplasmic compartments of marginal cells

A typical portion of the endothelium has been reproduced at higher magnification in the inset In this area an empty appearing vesicular structure lies next to the luminal border (*1*) Deep in the cell another vesicle shows minute radial spines on the cytoplasmic surface of the membrane (2) Next to the basement lamina there are two vesicles having a rather dense content (3) × 10 575 Inset × 99 000

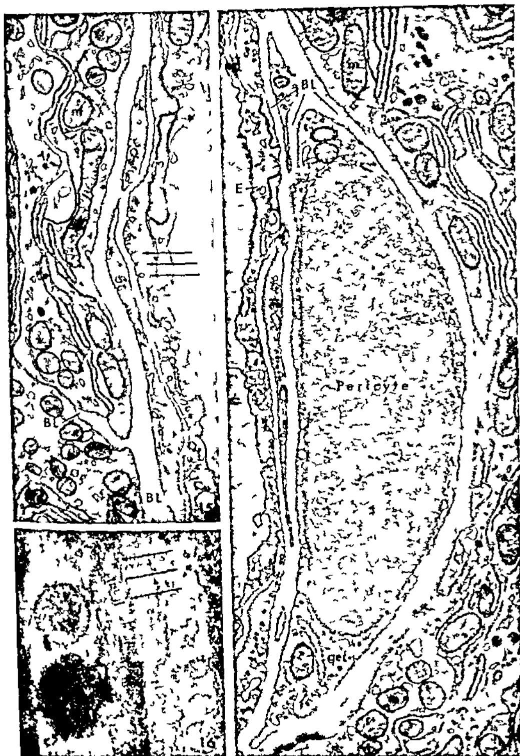

BL
BL
BL
E
Pericyte
gel

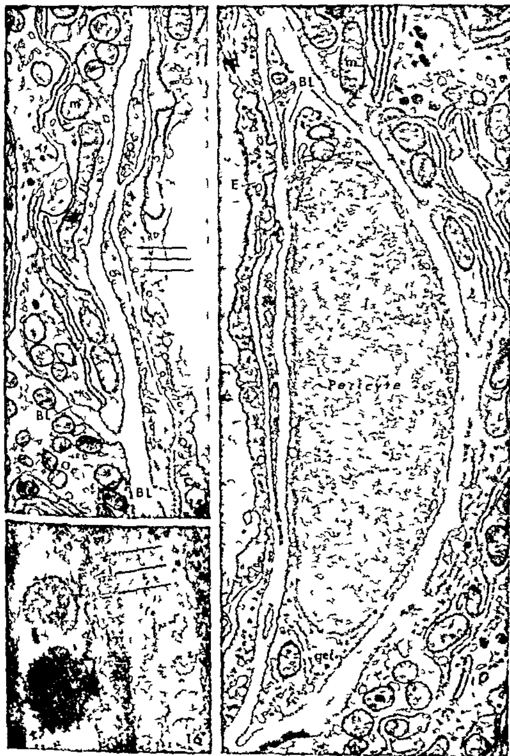
PLATE 12

EXPLANATION OF FIGURES

15 A portion of a strial capillary showing numerous vesicles and vesicular invaginations at the base of the endothelium (arrows) Splittings and interstitial prolongations of the basement lamina are apparent (BL) The strial cells are in direct contact with the endothelial basement lamina *m* mitochondria × 19 170

16 A portion of the endothelial basement lamina at high magnification showing the presence of fibrillar structures with the characteristic periodic striation of collagen (arrows) × 151 200

17 Another portion of a strial capillary showing the existence of pericapillary cells (*pericyte*) occupying lenticular clefts in the basement lamina (*BL*) The fine structure of these pericytes resembles the endothelial cell (*E*) *ger* granular endoplasmic reticulum *m* *mitochondria* × 14 850


m
BL
BL
BL
E
Pericyte
gel
1a

The Effects of High Fluoride Diets on Developing Enamel and Dentin in the Incisors of Rats [1]

JAMES A YAEGER
Department of Histology College of Dentistry University of Illinois Chicago Illinois

ABSTRACT Three groups of ten rats each were placed on diets containing 0 025 0 05 and 0 1% sodium fluoride and killed in pairs at intervals of 1 2 4 8 and 16 weeks Their maxillary incisors were embedded in methacrylate transverse and longitudinal sections were cut and microradiographs prepared A few teeth were demineralized embedded in paraffin and sectioned transversely These demineralized sections were stained with histochemical methods for polysaccharide protein complexes

In the dentin four abnormalities were commonly seen striations hypoplastic defects hypomineralized interglobular spaces and gross deformations of the external outline of the dentin The number and severity of these abnormalities increased with increasing fluoride levels in the diets and with increasing time on the diets Both hypo- and hypermineralized striations were seen in the microradiographs The previously hypomineralized layers and interglobular spaces stained weakly for polysaccharide protein complexes in the demineralized sections

In the enamel a hypermineralized surface layer covered a diffuse zone in which mineralization was inhibited Hypoplastic defects were also common

In the description of the effects of fluoride these abnormalities form part of a continuum of changes from the histologically distin t and well characterized responses to injected fluoride to the subtle changes seen in human chronic endemic dental fluorosis

The effects of diets containing high levels of fluoride on developing enamel and dentin in experimental animals have been described in a number of reports (Chaneles 30 Bethke Kick Hill and Chase 33 Schour and Smith 34 Hoffman Schuck and Furuta 42 Bélanger Lotz Visek and Comar 54 Belanger Visek Lotz and Comar 57 and 58) The related effects of single injections of fluoride have also been reported (Schour and Smith 34 Irving 43) Hematoxylin staining of demineralized materials has generally been accepted as an indication of the previous distribution of mineral More recently the responses in enamel and dentin produced by injected fluoride have been re-examined In both tissues microradiography disclosed a distribution of mineral which was not accurately reflected by the staining reactions of demineralized material (Osmanski and Yaeger 64 Weber and Yaeger 64) Combining microradiography with histochemical methods it was possible to demonstrate only a partial correlation between dentin matrix polysaccharide protein complexes and the distribution of mineral (Yaeger 63 Yaeger Hinrichsen and Cohen 64)

The relationships between those observations concerning the effects of injected fluoride and the previously published descriptions of the effects of dietary fluoride remain obscure Only two microradiographs have been published illustrating the effects of dietary fluoride which can be compared with the microradiographs from the injection experiments (Bélanger Lotz Visek and Comar 54 Belanger Visek Lotz and Comar 58) For that reason the present paper describes the results of a microradiographic and histochemical examination of the abnormal enamel and dentin resulting from diets containing high levels of fluoride The normal pattern of mineralization in the rat incisor and the changes induced by dietary fluoride are described In addition this study demon

[1] Thi in stigation was s pported by Public He lth Service rese rch g nt DE-01716 nd by research reer dev l pment w rd 5-K3-DE 7,272 from th N tional In t tute of Dent l R se rch I m ind bted t M Willi m Ay r nd Dr D l Eisenmann who prep red the micro diog phs during the tenure of mmer rese rch f llowships supported by Public H lth Servic gene l rese rch support gr nt IGS 10

strates a continuum in some respects from the dramatic changes seen after the injection of fluoride (acute fluorosis) through the somewhat less marked abnormalities in laboratory animals on diets containing fluoride to the histologically mild changes in human chronic endemic dental fluorosis (mottled enamel)

MATERIALS AND METHODS

Diets

Schour and Smith (34) have published the results of a thorough study of the effects of dietary fluoride on the incisors of rats Using demineralized material they described changes in the enamel and dentin in animals on diets containing 0 05% NaF but no changes at 0 025% NaF Therefore those fluoride levels were used as well as a third diet containing 0 1% NaF chosen to produce more severe changes Forty two male Sprague Dawley rats weighing about 200 gm each at the beginning of the experimental period were divided into four groups Three groups of ten animals each were placed on experimental diets containing 0 025% NaF (diet no 1) 0 05% NaF (diet no 2) or 0 1% NaF (diet no 3) respectively The dry sodium fluoride was mixed with ground Rockland pellets The fourth group (12 rats) was placed on a control diet of whole pellets without added fluoride All animals received tap water *ad libitum* Two animals from each of the groups on the experimental diets were killed after intervals of 1 2 4 8 and 16 weeks on the diets All animals in the control group were killed after four weeks

Microradiography

The maxillary incisors from all animals were removed with the sheath of alveolar bone and soft periodontal tissue which surrounds them and were fixed for several days in 10% formalin One incisor from each animal was embedded in methyl methacrylate after ethanol dehydration From each pair of incisors for each time period and diet one was sectioned longitudinally in a sagittal plane for the examination of enamel and the other was sectioned transversely for examination of the dentin The transverse sections were cut through the centers of the basal (posterior) middle and incisal (anterior) thirds of the teeth In the figures transverse sections of teeth from normal animals and from animals after one to eight weeks on the experimental diets are through the middle thirds while transverse sections from some animals after eight weeks and all animals after 16 weeks are through the incisal thirds These undemineralized sections were cut at a thickness of 80–100 μ on a sectioning machine equipped with a diamond disc and using water as a lubricant All of the incisors from the control group were sectioned longitudinally Transverse sections of normal animals from previous studies were also used as controls

Four microradiographs at different exposure times of each undemineralized section were prepared in a contact microradiographic apparatus An x ray tube with a copper target operated at 19 kilovolts and a nickel filter were used routinely The exposure factors were selected empirically to produce maximum contrast between areas with small differences in mineral content The microradiographs were prepared on Kodak Spectroscopic 649 0 plates and developed in Kodak X ray Developer

Histochemistry

Four of the undemineralized sections which had distinct dentin striations in microradiographs were immersed over night in acetone to remove the methacrylate demineralized in EDTA formalin and stained with hematoxylin Photomicrographs of the demineralized sections were enlarged to match photomicrographs of the same areas in the microradiographs These pairs of prints permitted direct comparisons between mineral distribution demonstrated in microradiographs and hematoxylin staining in demineralized sections and in turn with the histochemical methods used for other demineralized sections

Five teeth which had prominent dentin striations in the microradiographs (diet no 3 weeks 4 8 and 16 diet no 2 weeks 4 and 16) were selected for study with the histochemical methods The incisors contralateral to those used to prepare the transverse undemineralized sections were demineralized in EDTA formalin and embedded in paraffin Semi serial transverse

sections through their middle thirds were stained for polysaccharide protein complexes using the periodic acid Schiff procedure (Pearse 60) dialyzed iron ferrocyanide (Hale 46) and alcian blue (Mowry 56) Adjacent sections were stained with hematoxylin and eosin for comparison with the similarly stained sections which had been matched with microradiographs

Polarizing microscopy

To complete the comparisons with the previously described material from animals injected with fluoride some sections were examined in a polarizing microscope The demineralized sections used for histochemistry and the demineralized thick sections stained with hematoxylin were mounted in a synthetic resin (H S R) before examination

OBSERVATIONS

Table 1 summarizes the abnormalities of enamel and dentin found in microradiographs These abnormalities appeared earliest in animals on diet no 3 except for changes which occurred during the first week on all of the diets The severity of the abnormalities generally increased with longer times on the diets

The normal pattern of development of the rat incisor determines many of the differences and similarities between the abnormalities seen in enamel and those seen in dentin Since the rat incisor grows continuously dentin apposition at the internal surface of the dentin occurs at a nearly constant rate Therefore abnormalities appear in the dentin nearest the pulp (internal) in early weeks but not until after eight weeks has all of the dentin present in the tooth formed under the influence of the experimental diets (Schour and Massler 49) For that reason some of the figures include normal dentin formed before the animals were placed on the experimental diets as well as abnormal dentin formed while the animals were on the experimental diets Striations representing alternate layers of relatively normal and abnormal matrix were also common

Mineralization of enamel on the other hand does not occur in such a distinctly lamellar pattern The full thickness of enamel matrix is completed before the first formed matrix (nearest the dentinoenamel junction) is completely mineralized Abnormalities of enamel mineralization therefore may appear as relatively diffuse patches rather than as striations However the apposition of matrix (unlike its mineralization) occurs in much the same geometrical way in enamel and dentin and both odontoblast and ameloblast atrophy result in similar hypoplastic defects in the two tissues

Abnormalities in dentin

Striations Recognizable layers of normal and hypo- or hypermineralized dentin could be detected in all of the microradiographs of teeth from animals on the experimental diets (figs 1 and 6) Teeth from normal animals contained no or very

TABLE 1

Microradiographic abnormalities in the incisors of rats on high fluoride diets

			Diet		
			0 025% NaF	0 05% NaF	0 1% NaF
Abnormalities	Dentin	Striation	1	1	1
		Hypoplasia	4	2	1
		Interglobular spaces	16	8	4
		Gross deformation	none	8	4
	Enamel	Hypermineralized surface	1	1	1
		Hypoplasia	16	8	2

Weeks on diet (dry NaF mixed with ground pellets) at which abnormality was first detected

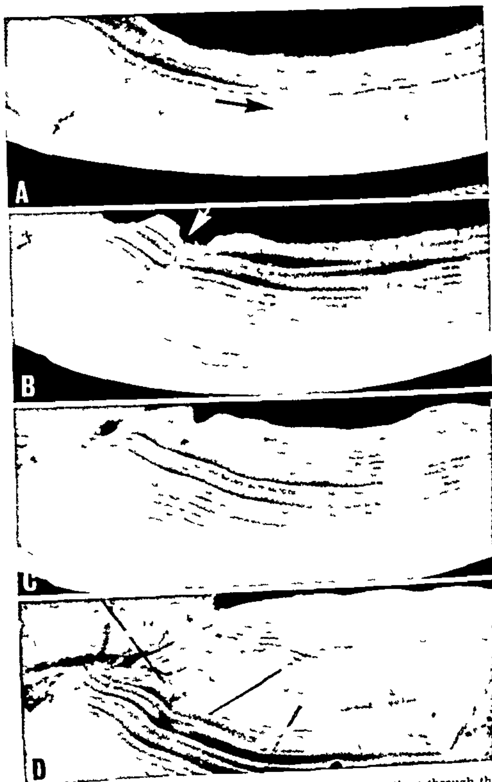


Fig 1 Microradiographs of the medial halves of transverse sections through the incisors of rats on a diet containing 0 05% NaF (diet no 2) The enamel of the labial (superior) surfaces are at the left the pulp chambers above *A* After one week on the experimental diet striations are evident only in the internal half of the dentin The arrow indicates the approximate line of junction between normal pre-experimental dentin (below) and abnormal dentin (above) *B* After four weeks the dentin striations are more obvious The arrow indicates a shallow hypoplastic defect on the internal surface of the medial labial corner of the dentin *C* After eight weeks and *D* 16 weeks on the experimental diet (× 80)

subtle striations of this kind (figs 7 and 10) Dentin formed in the pre experimental period (before the animals were placed on the high fluoride diets) was also normal in texture (fig 1*A*)

The severity of the alterations in mineralization increased from the first through the sixteenth week (fig 1) No particular pattern of distribution of hypo- or hypermineralized layers was obvious although hypermineralized layers were most frequent in animals on diet no 3 Such layers occurred at any level within the abnormal dentin at any time interval Hypo- and hypermineralized layers often but not always occurred in pairs The severity of this abnormality was greater at any time interval in animals on diet no 2 than in animals on diet no 1 In animals on diet no 3 some of the striations were obscured by the preponderance of interglobular dentin in weeks 8 and 16 (figs 5 and 6) In all microradiographs the dentinal tubules were seen to pass without interruption or deviation through the abnormally mineralized layers

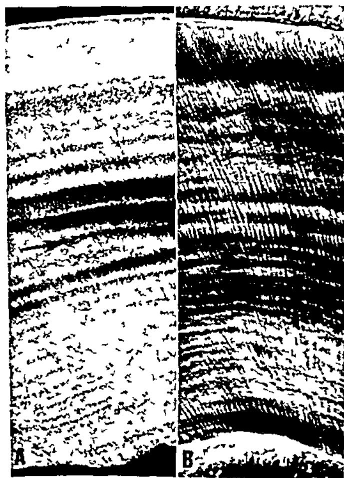


Fig 2 *A* Microradiograph of a portion of the medial wall in a transverse section through an incisor of a rat after four weeks on diet no 2 The pulp chamber is below *B* The same area after the section had been demineralized and stained with hematoxylin The print was enl rged to m tch the microradiograph Hypomineralized layers (arrow in *A*) correspond to l yers which are unstained by hematoxylin (arrow in *B*) Layers which stain intensely with h m toxylin are either normally mineralized or hypermineralized (Microradiograph 185 demineralized section × 260)

The thick sections which were demineralized and stained with hematoxylin shrank substantially so that it was necessary to enlarge the prints of the hematoxylin stained sections to match the prints of the microradiographs (fig 2) The presence of a number of rather closely spaced layers produced by high fluoride diets made matching the prints much more difficult than matching prints made from animals injected with fluoride since the injections produced only single pairs of abnormal layers (Yaeger 63 Yaeger Hinrichsen and Cohen 64) Nevertheless it could be demonstrated that most of the layers which were unstained by hematoxylin corresponded to hypomineralized layers in the microradiographs The layers staining more intensely with hematoxylin correspond to normally mineralized or hypermineralized layers in the microradiographs

With the relationships between hematoxylin staining and microradiographs established it was possible to compare the histochemical staining reactions with hematoxylin staining and indirectly with the microradiographs The variation in dimensional changes of sections during the various staining routines used was small so that the prints were relatively well matched (fig 3) All three of the methods used to demonstrate polysaccharide protein complexes yielded similar results with certain minor variations described previously (Yaeger Hinrichsen and Cohen 64) The layers which were unstained by hematoxylin (previously hypomineralized) were also unstained or weakly stained by the histochemical methods The layers which stained more intensely with hematoxylin (previously hypermineralized or normally mineralized) were also more intensely stained by the histochemical methods

Many of the demineralized sections were examined in the polarizing microscope The dentin formed while the animals were on the experimental diets contained a number of isotropic layers surrounded by nor



Fig 3 A portion of the medial wall in demineralized sections through an incisor of a rat after four weeks on diet no 2 The pulp is below An artifact separates the pulp from the predentin Sections stained with *A* Hematoxylin and eosin (the arrow indicates one of several layers which are only lightly stained with any of the routines used) *B* alcian blue *C* dialyzed *iron* ferrocyanide (the arrow indicates the presence of calcospherites in the relatively lightly stained layers) and *D* the periodic acid Schiff procedure Figure 2 demonstrates that the lightly stained layers were hypomineralized (× 260)

mally birefringent dentin (fig 4) These isotropic layers in demineralized sections were dark at all azimuths while the surrounding dentin passed through the usual light and dark phases as the stage was rotated (Schmidt and Keil 58) When the analyzer was removed the isotropic layers were seen to be unstained and therefore had been hypomineralized

Hypoplasia Table 1 indicates that hypoplastic defects appeared earlier with diets containing greater amounts of fluoride The first indications of the development of hypoplasia were relatively shallow depressions in the pulpal surfaces of the dentin (fig 1*B*) After longer experimental periods some hypoplastic defects extended through nearly the full thickness of the dentin (figs 5 and 6) In stained sections these depressions were found to be occupied by inclusions of pulp tissue surrounded by a layer of predentin or unmineralized dentin matrix Apparently small groups of odontoblasts diminished their rate of formation or ceased forming dentin matrix No evidence of dentin resorption was found The continued activity of the surrounding odontoblasts resulted in the formation of hypoplastic defects containing vascularized pulp tissue



Fig 4 An area in the medial wall of a demineralized thick transverse section through an incisor of a rat after four weeks on diet no 2 The pulp chamber is below The area was photographed through crossed pri ms in a polarizing microscope The arrows indicate two of several isotropic l yers With the analyzer removed these layer are seen to be unstained with hematoxylin and th refor they were hypomineralized (×60)

Hypoplasia was most marked in the medial and lateral labial (superior) corners of the teeth (fig 6) The odontoblasts most often and most severely affected were those whose processes reached the external surface of the dentin near the cementoenamel junction Hypoplastic defects occasionally occurred elsewhere in the dentin covered with cementum (medial lateral and lingual) but rarely in dentin covered with enamel (labial) The severity of the hypoplasia was proportional to the amount of fluoride in the diet and increased the length of the experimental period

Interglobular spaces Well after the appearance of striations and hypoplasia normally mineralized "calcospherites" (Schour 60) and hypomineralized angular patches of interglobular dentin between them were evident in the microradiographs (fig 5) In the demineralized sections stained with polysaccharide protein complexes the calcospherites within the hypomineralized layers stained more nearly as intensely as normal dentin matrix than did the surrounding nearly unstained interglobular matrix (fig 3) When the areas of calcospherites and interglobular dentin were sufficiently extensive they obscured the dentin striations (fig 5)

Gross deformation The most puzzling finding was the distortion of the dentinocemental junction outlining the periphery of the dentin This deformation was restricted to the teeth from animals on diets no 2 and no 3 Even after 16 weeks on diet no 1 the external outline of the dentin was normal With diet no 2 the deformation was first detectable at eight weeks and was somewhat more marked at 16 weeks With diet no 3 the deformation was present at four weeks and became progressively more severe at eight weeks (fig 6) and 16 weeks (fig 5)



Fig 5 Microradiograph of a transverse section through an incisor of a rat after 16 weeks on a diet containing 0 1% NaF (diet no 3) *A* The labial surface is above Many hypoplastic defects extend through the external half of the enamel Severe hypoplastic defects are present in the medial and lateral labial corners of the dentin (arrow at right) The arrow at the left indicates one of several areas in which hypomineralized interglobular dentin is particularly prominent The presence of interglobular dentin and calcospherites throughout the section obscures the dentin striations The gross deformation of the external dentin surface is more severe than at eight weeks (fig 6) (× 55) *B* Higher magnification of an area in the lateral wall in the same microradiograph Calcospherites and the hypomineralized interglobular dentin between them are visible (× 260)



Fig 6 Microrad ograph of a transverse section through the incisor of a rat after eight weeks on diet no 3 Hypoplastic defects are present in the medial and lateral labial corners of the dentin and hypomineral zed interglobular dentin obscures the striations in the labial dentin (above) Many shallow hypoplastic defects are present in the enamel The arrow indicates one of everal hypomineralized striations in the incompletely mineralized lateral enamel The external outline of the dentin is distinctly deformed (× 40)

The deformations had the same mor phology in all the teeth in which they occurred Three depressions were con stantly found on the lingual (inferior) halves of the teeth Two of the depressions were on the medial surface and one on the lateral surface Both surfaces were S shaped in outline The curves were approximately parallel and opposite each other resulting in an overall S" shape in which the curves diverged toward the la bial and joined lingually The alveolar bone was poorly adapted to these curvatures The widened space between tooth and bone was filled with apparently normal tissue of the periodontal ligament

Abnormalities in enamel

In the course of mineralization of enamel in the incisors of normal rats at least three phases or stages could be recognized histologically in microradiographs (figs 7 9A B) even though mineralization is probably a continuous process occurring at a nearly constant rate A short distance toward the incisal surface from the basal end the full thickness of enamel matrix was present In this phase the matrix was only lightly mineralized less so than the adjacent dentin which was almost fully mineralized shortly after it formed (fig 7A) Nearer the incisal end in about the middle of the basal third of the tooth the enamel matrix had accumulated mineral until its radiopacity was equal to that of the underlying dentin (fig 7B) At about the middle of the tooth the enamel was fully mineralized In this final phase the enamel was much more heavily mineralized than the dentin which had only a slightly greater mineral content than the dentin at the basal end (fig 7C)

Hypermineralized surface In the region of the tooth in which enamel and dentin were normally equally mineralized the teeth from animals on the experimental diets had a hypermineralized surface layer (figs 8 9C D E) This hypermineralized layer was demonstrable in the first week on all three diets (table 1) The term hypermineralized is used here in a comparative sense only This layer of enamel was about equal in mineral content to mature enamel (figs 9C D E) and was obvious only because the enamel beneath it was less mineralized than normal enamel in the same position The hypermineralized layer included approximately the outer third of the enamel (fig 8) It extended from the zone of lightly mineralized enamel through the zone in which enamel and dentin were equally mineralized and became obscured when the underlying enamel became as well mineralized as the surface layer

Frequently the incisal end of this hypermineralized layer was interrupted The area in which the hypermineralized layer

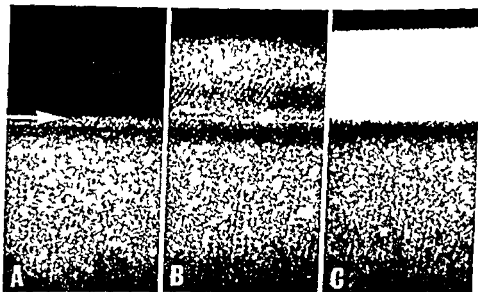


Fig 7 Microradiographs of portions of the labial wall in a longitudinal section through an incisor of a normal rat The dentin is below A Near the basal (posterior) end of the tooth the enamel matrix is less mineralized than the dentin The arrow indicates the position of the dentinoenamel junction The enamel is above the arrow the dentin below B Near the middle of the basal third of the tooth the enamel matrix and dentin are equally mineralized C Near the incisal (anterior) end of the basal third of the tooth the mature enamel is more heavily mineralized than the dentin The mineral content of the dentin is nearly equal in all of these regions and shows no or very faint striations in normal animals (× 260)

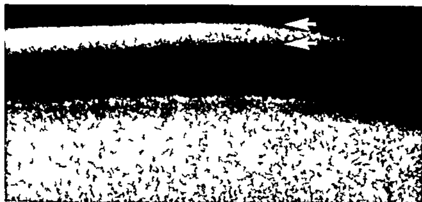


Fig 8 Microradiograph of a portion of the labial wall in a longitudinal section through the incisor of a rat after two weeks on diet no 2 The basal end of the tooth is toward the right the dentin below The outer third of the enamel matrix (indicated by the arrows) is hypermineralized (× 260)

was absent or thin occurred either within the zone in which enamel and dentin were equally mineralized or in the zone in which the underlying enamel matrix had accumulated a substantial fraction of its ultimate mineral content (fig 9C)

A generalized inhibition of enamel mineralization beneath the hypermineralized layer was demonstrated by measuring the lengths of the zones in which enamel and dentin were equally mineralized in microradiographs of longitudinal sections (fig 9) Since the lightly mineralized and fully mineralized enamel blended into the ends of this zone some uncertainty must be expected in these measurements In sections from 17 normal teeth the zones of equal mineralization had an average length of 0 9 mm and a range of 0 33–1 3 mm The mean length of this zone in three teeth from animals on the three experimental diets for eight weeks was 3 6 mm and the range was 1 4–5 1 mm It had therefore increased about four fold after eight weeks on the experimental diets After 16 weeks enamel hypoplasia was severe enough to render such measurements unreliable

The zone of lightly mineralized enamel matrix was limited to the basal third of normal teeth The microradiographs of teeth from animals on the experimental diets demonstrated that the same zone often extended well into the middle thirds of the teeth (figs 9C D E) Efforts to measure the extent of this manifestation of the inhibition of mineralization using cephalometric methods failed because the sections were not all cut in precisely equivalent planes Small variations in the plane of section caused substantial changes in relationships between the few landmarks present in these sections

Two thin layers of enamel could frequently be distinguished near the dentinoenamel junction in microradiographs of normal rat incisors (fig 10) The enamel immediately adjacent to the dentin was hypermineralized It was surrounded externally by a layer of hypomineralized enamel This pattern was absent from incisors of animals on the experimental diets Rarely hypo- or hypermineralized striations in enamel were visible in microradiographs of these teeth but these striations were not near the dentinoenamel junction (fig 6) None of the longitudinal sections showed such striations

Hypoplasia The depth and number of hypoplastic defects in enamel like those in dentin increased with the fluoride levels in the diet and with the length of the experimental period (table 1) Small surface depressions were common and defects reaching about half way through the enamel were even more frequent (figs 5 and 6) These defects did not reach the dentinoenamel junction Their depth and number were greatest at the medial and lateral sides of the enamel and least near

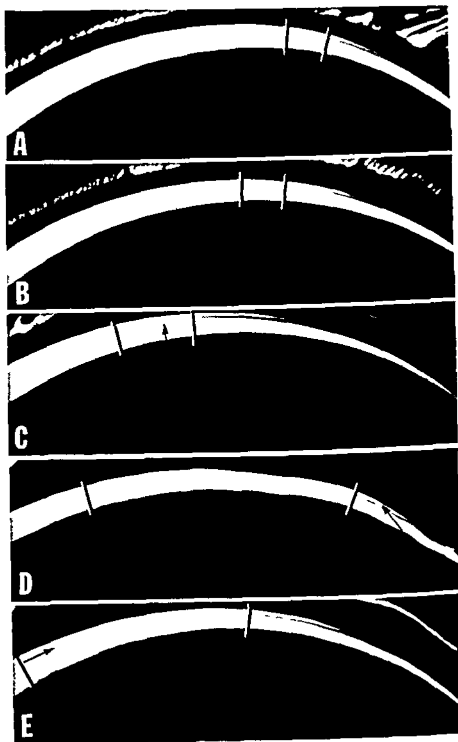


Fig 9 Microradiographs of the labial walls in longitudinal sections through the incisors of rats The pulp chambers are below The vertical bars enclose the zones in which enamel and dentin are equally mineralized The zones of lightly mineralized enamel matrix are toward the basal ends (right) and the zones of fully mineralized mature enamel are toward the incisal ends (left) *A* and *B* Normal rats The zones in which enamel and dentin are equally mineralized are shorter than in teeth from animals on the experimental diets C–E *C* After four weeks on a diet containing 0 025% NaF (diet no 1) The arrow indicates an interruption in the hypermineralized surface layer of enamel *D* After two weeks on diet no 2 The arrow indicates the hypermineralized surface layer of enamel which is also evident in C and E *E* After four weeks on diet no 2 The arrow indicates the position of the dentinoenamel junction Incompletely mineralized enamel is above the arrow dentin below (× 15) (The photomicrographs for this figure were prepared by Mr William Winn Biological Photographer)

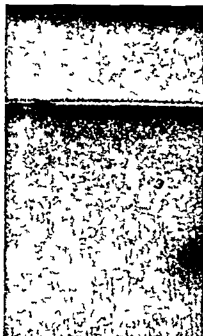


Fig 10 Microradiograph of a portion of the labial wall in a longitudinal section through the incisor of a normal rat The dentin is below The arrow indicates the hypermineralized layer of enamel at the dentinoenamel junction A hypomin ralized layer of enamel is immediately ex ternal to (above) the hypermineralized layer This normal dentin shows no striation (260)

the midline of the enamel Although the labial alveolar bone and labial alveolar periosteum were present in almost all of the sections used for microradiography no evidence was seen of displaced enamel fragments or mineralized masses in the space between enamel and alveolar bone as described by Hoffman Schuck and Furuta (42)

DISCUSSION

The principal matters of interest here are the effects of large doses of fluoride on the mechanism of mineralization and the pathogenesis of fluoride induced abnormal ities in the teeth of laboratory animals However it is also profitable to relate these experimental findings to the abnormalities seen in human fluorosed teeth (mottled enamel chronic endemic dental fluorosis)

The levels of fluoride used in the present experimental diets were chosen to cover the range of doses adequate to induce histological changes in developing enamel and dentin in rat incisors The previously published literature includes descriptions of teeth from men and laboratory animals receiving a wide range of fluoride doses from a fraction of a milligram of fluoride per kilogram per day to about 20 milligrams of fluoride per kilogram per day Not only do the doses vary but the experimental periods (from a few days to many years) and the route of administration (in drinking water in the diet by injection) vary from one investigation to another Efforts to reduce the doses reported to a common denominator have failed for a number of reasons In the present study for example the amount of fluoride in the diet influenced body weight On all three experimental diets the animals lost weight between weeks two and four but gained weight rapidly between weeks four and sixteen After 16 weeks the animals on diet no 3 weighed about 13% less than the animals on diet no 1 It is impossible therefore to attribute much significance to a calculation of fluoride intake based on an average body weight during the experimental period Furthermore food and water consumption may vary with variations in their fluoride contents (McClure 39) In any case the only really pertinent value is probably the level of fluoride in serum or extracellular fluid during the development of the abnormal tissues Such measurements have not been reported in studies which also describe the histological changes In spite of these limitations it is possible to describe a partial continuum of histological abnormalities resulting from various doses and routes of administration of fluoride The histologically discrete and relatively well-characterized effects of the injection of fluoride can be compared with the somewhat less distinct effects of high fluoride levels in the diet The latter abnormalities in turn can be profitably compared with the subtle alterations found in human fluorosed enamel resulting from a fluoride level of a few parts per million in community water supplies

Dentin striations

The layers of abnormally mineralized dentin illustrated here strongly resemble the similar abnormality resulting from the

injection of fluoride This comparison was first made by Schour and Smith (34) and the injection experiments were confirmed and extended by Irving (43) These investigators deduced the distribution of mineral from the pattern of staining with hematoxylin in demineralized sections Microradiographic studies of the response have in general confirmed the sequence of events in its development described by Irving (Osmanski and Yaeger 64 Yaeger Hinrichsen and Cohen 64) However the relationship between hypo and hypermineralized layers deduced from hematoxylin staining by Schour and Smith and by Irving is found to be reversed in microradiographs The hypermineralized layer is immediately external to the hypomineralized layer when mineral distribution is determined by microradiography (Osmanski and Yaeger 64) Although both hyper and hypomineralized layers are seen in teeth from animals on high fluoride diets they do not regularly occur in pairs Similar striations have been described by others in demineralized sections from animals on high fluoride diets (Chaneles 30 Hoffman Schuck and Furuta 42 Sutro 35) and they are also present in microradiographs of dentin from pigs on high fluoride diets (Belanger Lotz Visek and Comar 54 Bélanger Visek Lotz and Comar 58) but not in microradiographs of dentin in human fluorosed teeth which do show abnormalities in the enamel (Gustafson 61)

The significance of the decreased staining intensity for polysaccharide protein complexes in the hypomineralized layers of dentin is not yet clear A related but more generalized loss of metachromasia and periodic acid Schiff reactivity in dentin from pigs on high fluoride diets has been reported (Belanger Visek Lotz and Comar 58) An identical staining pattern exists in the hypomineralized components of the responses produced by injected fluoride (Yaeger 63 Yaeger Hinrichsen and Cohen 64) This was previously interpreted as indicating that less aggregated ground substances are lost from the hypomineralized layers during preparation of the demineralized sections (Yaeger Hinrichsen and Cohen 64) These observations do not clarify the role of ground substances in the mechanism of mineralization although they do add another item to the list of circumstantial associations of ground substance changes in areas of normal and abnormal mineralization These alterations in ground substances are also reflected in the pattern of staining with hematoxylin Specifically layers stained weakly with hematoxylin correspond to hypomineralized layers It is this pattern which has been described by others who have used demineralized material The interpretation that layers in demineralized sections staining intensely with hematoxylin were hypermineralized is not confirmed by microradiography Such layers are as often normally mineralized as they are hypermineralized

Polarizing microscopy demonstrates that the demineralized matrix of the hypomineralized layers is isotropic This is in contrast to teeth from animals injected with fluoride in which the matrix of the hypomineralized layer is birefringent (Grady and Yaeger 65) In the teeth from animals injected with fluoride the azimuth of extinction of the hypomineralized matrix is at about 45° to that of the surrounding normal dentin indicating a distortion in the normal pattern of orientation of matrix collagen fibrils The isotropy observed in the present material from animals on high fluoride diets suggests that collagen fibrils are absent or randomly arranged in the hypomineralized layers The difficulties associated with polarizing microscopy demand that these observations be confirmed and extended before interpretations are derived from them

Dentin hypoplasia

Irregularities in the outline of the internal edge of the predentin and variations in the thickness of the predentin occur frequently in teeth from animals on high fluoride diets (Chaneles 30 Sutro 35 Hoffman Schuck and Furuta 42) Inclusions of pulp tissue within hypoplastic defects in dentin are also common (Chaneles 30 Sutro 35 and Belanger Visek Lotz and Comar 58) With diet no 3 used in the present study the hypoplastic defects are more frequent and more severe than those previously illustrated These hypoplastic defects are suggestively similar to those occurring in vitamin A deficiency

calcium and phosphorus deficiency and after parathyroidectomy (Schour and Massler 49)

The f ct that hypoplastic defects may result from localized areas of odontoblast atrophy or death caused by fluoride is less surprising than the peculiar distribution of these defects Hypoplastic pits occur occasionally in all of the internal surfaces of the dentin although most rarely in the labial surface They are most frequent and deepest in the medial and lateral labial corners internal to the region of the cementoenamel junction The peculiar sensitivity of the odontoblasts in these positions cannot be explained by the present observations However this variation in odontoblast lability is reminiscent of similar differences in other abnormal situations For example in vitamin A deficiency in laboratory animals the rate of apposition of labial dentin increases while the rate of apposition of lingual dentin decreases In magnesium deficiency these changes in the rates of apposition are reversed and the lingual dentin develops marked striations while the labial dentin does not (Schour and Massler 49) Whatever the explanation of these variations in odontoblast reactivity they are not effects peculiar to the fluoride ion

Interglobular dentin

Calcospherites and the interglobular dentin surrounding them are only occasionally seen in untreated laboratory animals and have been attributed to an accentuation of a normal pattern due to a diet with only a marginal content of vitamin D (Schour and Massler 49) The enlargement and fusion of calcospherites is considered by some to be the normal mechanism of mineralization in human dentin (Schour 60) even though it is not regularly demonstrable in normal teeth from men or laboratory animals

The persistence or development of an obvious pattern of calcospherites and interglobular dentin is often detectable in stained sections through demineralized teeth from animals on high fluoride diets (Chaneles 30 Schour and Smith 34 Hoffman Schuck and Furuta 42 Rockert 63) A corresponding microradiographic image in which the calcospherites are more mineralized than the surrounding interglobular dentin has also been published (Belanger Lotz Visek and Comar 54) In two subsequent papers Belanger Visek Lotz and Comar (57 and 58) described the calcospherites ("globules" in their terminology) in considerable detail In demineralized sections calcospherites bind more Ca^{45} and $S^{35}O$ than does the surrounding matrix When demineralized sections are ashed the residue of the calcospherites is refractile in dark field illumination If the sections are treated with ammonium acetate before ashing a similar residue is not present These observations were interpreted as indicating that the calcospherites contain calcium fluoride (Belanger Visek Lotz and Comar 58)

In the microradiographs described here the calcospherites are about as well mineralized as normal dentin while the surrounding interglobular dentin is hypomineralized In the demineralized sections the calcospherites have the staining characteristics of normal dentin with hematoxylin dialyzed iron ferrocyanide and periodic acid Schiff while the surrounding interglobular dentin is lightly stained more nearly resembling predentin In the sections stained with alcian blue the calcospherites are difficult to distinguish Comparing microradiographs with stained sections reveals that most of the stains used reflect the pattern of hypomineralization as it appears in microradiographs This same relationship is also true for the dentin striations

Gross deformation of dentin

The distortion of the dentinocemental junction is proportional to both the amount of fluoride in the diet and the length of the experimental period Similar changes have been described by several authors but are rarely illustrated (Chaneles 30 Bethke Kick Hill and Chase 33 Hoffman Schuck and Furuta 42) The pattern of the deformation is the same in every case This strongly suggests a highly specific and localized effect of fluoride on the morphology of the teeth Once mineralized dentin is deposited the outline of the dentin is probably *too rigidly fixed* to allow such deformations to develop The fluoride therefore must act on the differentiating

injection of fluoride This comparison was first made by Schour and Smith (34) and the injection experiments were confirmed and extended by Irving (43) These investigators deduced the distribution of mineral from the pattern of staining with hematoxylin in demineralized sections Microradiographic studies of the response have in general confirmed the sequence of events in its development described by Irving (Osmanski and Yaeger 64 Yaeger Hinrichsen and Cohen 64) However the relationship between hypo and hypermineralized layers deduced from hematoxylin staining by Schour and Smith and by Irving is found to be reversed in microradiographs The hypermineralized layer is immediately external to the hypomineralized layer when mineral distribution is determined by microradiography (Osmanski and Yaeger 64) Although both hyper and hypomineralized layers are seen in teeth from animals on high fluoride diets they do not regularly occur in pairs Similar striations have been described by others in demineralized sections from animals on high fluoride diets (Chaneles 30 Hoffman Schuck and Furuta 42 Sutro 35) and they are also present in microradiographs of dentin from pigs on high fluoride diets (Belanger Lotz Visek and Comar 54 Belanger Visek Lotz and Comar 58) but not in microradiographs of dentin in human fluorosed teeth which do show abnormalities in the enamel (Gustafson 61)

The significance of the decreased staining intensity for polysaccharide protein complexes in the hypomineralized layers of dentin is not yet clear A related but more generalized loss of metachromasia and periodic acid Schiff reactivity in dentin from pigs on high fluoride diets has been reported (Belanger Visek Lotz and Comar 58) An identical staining pattern exists in the hypomineralized components of the responses produced by injected fluoride (Yaeger 63 Yaeger Hinrichsen and Cohen 64) This was previously interpreted as indicating that less-aggregated ground substances are lost from the hypomineralized layers during preparation of the demineralized sections (Yaeger Hinrichsen and Cohen 64) These observations do not clarify the role of ground substances in the mechanism of mineralization although they do add another item to the list of circumstantial associations of ground substance changes in areas of normal and abnormal mineralization These alterations in ground substances are also reflected in the pattern of staining with hematoxylin Specifically layers stained weakly with hematoxylin correspond to hypomineralized layers It is this pattern which has been described by others who have used demineralized material The interpretation that layers in demineralized sections staining intensely with hematoxylin were hypermineralized is not confirmed by microradiography Such layers are as often normally mineralized as they are hypermineralized

Polarizing microscopy demonstrates that the demineralized matrix of the hypomineralized layers is isotropic This is in contrast to teeth from animals injected with fluoride in which the matrix of the hypomineralized layer is birefringent (Grady and Yaeger 65) In the teeth from animals injected with fluoride the azimuth of extinction of the hypomineralized matrix is at about 45° to that of the surrounding normal dentin indicating a distortion in the normal pattern of orientation of matrix collagen fibrils The isotropy observed in the present material from animals on high fluoride diets suggests that collagen fibrils are absent or randomly arranged in the hypomineralized layers The difficulties associated with polarizing microscopy demand that these observations be confirmed and extended before interpretations are derived from them

Dentin hypoplasia

Irregularities in the outline of the internal edge of the predentin and variations in the thickness of the predentin occur frequently in teeth from animals on high fluoride diets (Chaneles 30 Sutro 35 Hoffman Schuck and Furuta 42) Inclusions of pulp tissue within hypoplastic defects in dentin are also common (Chaneles 30 Sutro 35 and Bélanger Visek Lotz and Comar 58) With diet no 3 used in the present study the hypoplastic defects are more frequent and more severe than those previously illustrated These hypoplastic defects are suggestively similar to those occurring in vitamin A deficiency

Thewlis 40) or perhaps because it is indistinct or absent in fully mineralized enamel This hypermineralized surface layer may be related to the high fluoride content of surface enamel (Brudevold 62) A diffuse hypomineralization of fluorosed human enamel similar to that seen in the present material has been illustrated and described in a number of reports (Applebaum 36 Gustafson 61 Gustafson and Gustafson 61 Newbrun and Brudevold 60) In demineralized material the amount of matrix which survives demineralizing solutions is greater in teeth from laboratory animals on high fluoride diets than it is in normal teeth (Bethke Kick Hill and Chase 33 Schour and Smith 34 Hoffman Schuck and Furuta 42) These authors interpreted this acid resistance of enamel matrix as indicating an inhibition of matrix maturation and mineralization

Enamel hypoplasia

Localized defects in the apposition of enamel matrix in laboratory animals on high fluoride diets are frequently described (Chaneles 30 Bethke Kick Hill and Chase 33 Schour and Smith 34 Sutro 35) Hypoplastic defects are also common in chronic fluorosis of human teeth (Dean 34 36)

The hypoplastic defects in enamel of laboratory animals are not as circumscribed as those seen in dentin In enamel the walls of the defects generally diverge toward the surface while the walls of the defects in dentin are more nearly parallel Using demineralized sections Schour and Smith (34) have described a gradient of ameloblast and matrix damage decreasing toward the periphery of the hypoplastic defects and a zone of acid resistant matrix with the staining characteristics of immature enamel matrix surrounding the defects The mode of development of hypoplastic defects is apparently similar in enamel and dentin Young ameloblasts in limited regions atrophy or die while the surrounding ameloblasts continue to form enamel matrix In this way areas of ameloblastic epithelium become surrounded by enamel matrix

Summary of the relationships between experimental dental fluorosis in laboratory animals and chronic endemic dental fluorosis in man

The continuum of changes from the animals injected with fluoride through animals on high fluoride diets and ending with the histologically mild effects of chronic endemic fluorosis is interrupted at several points The microradiographically and histochemically similar changes (striations) in the dentin of animals receiving fluoride either by injection or in their diets have not been described in human fluorosed teeth This may well prove to be the result of a process of recovery in dentin similar to the "healing" of the response to injected fluoride in enamel The partial recovery of dentin from the effects of injected fluoride can be demonstrated in rat incisors (Osmanski and Yaeger 64) In human teeth usually examined a number of years after their development has nearly ceased recovery from abnormal mineralization may be nearly complete

Hypoplastic defects in the dentin have been demonstrated only in laboratory animals on high fluoride diets Apparently the short period of action of fluoride in injection experiments does not cause odontoblast atrophy or death while the doses of fluoride which produce chronic fluorosis in human teeth are too small to damage odontoblasts Neither interglobular dentin nor gross deformations have been described in laboratory animals injected once with fluoride or in human fluorosed teeth

The hypermineralized surface diffuse subsurface hypomineralized zone and hypoplastic defects seen in the enamel of teeth from laboratory animals on high fluoride diets are closely related to similar changes demonstrated in human teeth and clarify the pathogenesis of such abnormalities The presence of hypoplastic defects in the enamel of human fluorosed teeth which contain apparently normal dentin indicates that ameloblasts are more susceptible to fluoride than are odontoblasts as suggested by Schour and Smith (34) Enamel hypoplastic defects are not present in the teeth from injected animals

odontogenic organ before dentin minerali zation begins

The presence and severity of these de formations was determined in the present study only by inspection of microradio graphs It is reasonable to expect more accurate measurements to disclose more subtle changes Kruger (62) has meas ured the influence of repeated injections of small doses of fluoride on the morphology of the mandibular first molars of young rats He found that the widths of the mesial fissures are increased while their depths are decreased the distal fissures show decreased depth and the mesial distal diameters of the crowns are de creased from normal values A similar reduction in crown diameter induced by dietary fluoride has also been reported by Paynter and Grainger (56) Since the morphology of teeth can be correlated with caries incidence (Grainger Paynter and Shaw 59) the mechanisms by which fluor ide can affect tooth morphology is of con siderable clinical interest The results de scribed here suggest that the influence of fluoride on the morphology of the incisors of rats is a promising experimental situa tion with which to pursue such studies

Hypermineralized surface enamel and enamel striations

In the present material the surface layer of enamel was hypermineralized only with respect to the relatively hypomineralized enamel beneath it For that reason it is necessary to discuss together hyper and hypomineralization of enamel

The subcutaneous injection of fluoride in rats produces in enamel a response con sisting of both hyper and hypomineralized components similar to the response pro duced in dentin (Weber and Yaeger 64) In demineralized material related stria tions have been described in enamel from animals on high fluoride diets (Chaneles 30 Schour and Smith 34 Sutro 35) In human fluorosed teeth hypomineralized layers of enamel parallel to the incremen tal lines can be demonstrated by micro radiography (Crabb and Darling 62 Gus tafson 61 Gustafson and Gustafson 61 Newbrun and Brudevold 60)

In spite of these descriptions of stria tions in enamel they are not seen in microradiographs of longitudinal sections through teeth from animals on the experi mental diets Rarely hypo or hypermin eralized layers of enamel are visible in microradiographs of transverse sections particularly in areas where the enamel is incompletely mineralized The relative in frequency of such striations in the radio graphs may be an artifact resulting from the technique used The sections were 80–100 μ thick and the exposure times used were compromises between shorter exposures most appropriate for dentin and longer exposures necessary for maximum contrast within fully mineralized enamel It is more likely however that variations in mineralization which may have been present in the youngest enamel in rat in cisors are obscured when the enamel be comes fully mineralized Such a healing process occurs in the response produced by injected fluoride (Weber and Yaeger 64) and in the present material the hyper mineralized surface enamel is obscured when the enamel beaneath it becomes fully mineralized This interpretation would ac count for the striations which have been described in the young enamel matrix which survives demineralization the pat terns seen in the present microradiographs where the enamel matrix is incompletely mineralized and would explain their ab sence from more fully mineralized enamel in laboratory animals It leaves unex plained however the persistence of ab normally mineralized layers in human fluorosed enamel This may be a deception based on the fact that the microradio- graphs chosen to illustrate previously pub- lished reports are only those showing nota ble changes

In human fluorosed teeth a distinctly hypermineralized surface layer of enamel similar to that illustrated here is some times visible in published microradiographs (Crabb and Darling 62 Gustafson 61 Gustafson and Gustafson 61) No one has commented on its presence perhaps because a hypermineralized surface is also sometimes seen in enamel considered to be normal (Gustafson and Gustafson 61

Thewlis 40) or perhaps because it is indistinct or absent in fully mineralized enamel This hypermineralized surface layer may be related to the high fluoride content of surface enamel (Brudevold 62) A diffuse hypomineralization of fluorosed human enamel similar to that seen in the present material has been illustrated and described in a number of reports (Applebaum 36 Gustafson 61 Gustafson and Gustafson 61 Newbrun and Brudevold 60) In demineralized material the amount of matrix which survives demineralizing solutions is greater in teeth from laboratory animals on high fluoride diets than it is in normal teeth (Bethke Kick Hill and Chase 33 Schour and Smith 34 Hoffman Schuck and Furuta 42) These authors interpreted this acid resistance of enamel matrix as indicating an inhibition of matrix maturation and mineralization

Enamel hypoplasia

Localized defects in the apposition of enamel matrix in laboratory animals on high fluoride diets are frequently described (Chaneles 30 Bethke Kick Hill and Chase 33 Schour and Smith 34 Sutro '35) Hypoplastic defects are also common in chronic fluorosis of human teeth (Dean 34 36)

The hypoplastic defects in enamel of laboratory animals are not as circumscribed as those seen in dentin In enamel the walls of the defects generally diverge toward the surface while the walls of the defects in dentin are more nearly parallel Using demineralized sections Schour and Smith (34) have described a gradient of ameloblast and matrix damage decreasing toward the periphery of the hypoplastic defects and a zone of acid resistant matrix with the staining characteristics of immature enamel matrix surrounding the defects The mode of development of hypoplastic defects is apparently similar in enamel and dentin Young ameloblasts in limited regions atrophy or die while the surrounding ameloblasts continue to form enamel matrix In this way areas of ameloblastic epithelium become surrounded by enamel matrix

Summary of the relationships between experimental dental fluorosis in laboratory animals and chronic endemic dental fluorosis in man

The continuum of changes from the animals injected with fluoride through animals on high fluoride diets and ending with the histologically mild effects of chronic endemic fluorosis is interrupted at several points *The microradiographically* and histochemically similar changes (striations) in the dentin of animals receiving fluoride either by injection or in their diets have not been described in human fluorosed teeth This may well prove to be the result of a process of recovery in dentin similar to the "healing" of the response to injected fluoride in enamel The partial recovery of dentin from the effects of injected fluoride can be demonstrated in rat incisors (Osmanski and Yaeger 64) In human teeth usually examined a number of years after their development has nearly ceased recovery from abnormal mineralization may be nearly complete

Hypoplastic defects in the dentin have been demonstrated only in laboratory animals on high fluoride diets Apparently the short period of action of fluoride in injection experiments does not cause odontoblast atrophy or death while the doses of *fluoride which produce chronic fluorosis in* human teeth are too small to damage odontoblasts Neither interglobular dentin nor gross deformations have been described in laboratory animals injected once with fluoride or in human fluorosed teeth

The hypermineralized surface diffuse subsurface hypomineralized zone and hypoplastic defects seen in the enamel of teeth from laboratory animals on high fluoride diets are closely related to similar changes demonstrated in human teeth and clarify the pathogenesis of such abnormalities The presence of hypoplastic defects in the enamel of human fluorosed teeth which contain apparently normal dentin indicates that ameloblasts are more susceptible to fluoride than are odontoblasts as suggested by Schour and Smith (34) Enamel hypoplastic defects are not present in the teeth from injected animals

odontogenic organ before dentin mineralization begins

The presence and severity of these deformations was determined in the present study only by inspection of microradiographs It is reasonable to expect more accurate measurements to disclose more subtle changes Kruger (62) has measured the influence of repeated injections of small doses of fluoride on the morphology of the mandibular first molars of young rats He found that the widths of the mesial fissures are increased while their depths are decreased the distal fissures show decreased depth and the mesial distal diameters of the crowns are decreased from normal values A similar reduction in crown diameter induced by dietary fluoride has also been reported by Paynter and Grainger (56) Since the morphology of teeth can be correlated with caries incidence (Grainger Paynter and Shaw 59) the mechanisms by which fluoride can affect tooth morphology is of considerable clinical interest The results described here suggest that the influence of fluoride on the morphology of the incisors of rats is a promising experimental situation with which to pursue such studies

Hypermineralized surface enamel and enamel striations

In the present material the surface layer of enamel was hypermineralized only with respect to the relatively hypomineralized enamel beneath it For that reason it is necessary to discuss together hyper and hypomineralization of enamel

The subcutaneous injection of fluoride in rats produces in enamel a response consisting of both hyper and hypomineralized components similar to the response produced in dentin (Weber and Yaeger 64) In demineralized material related striations have been described in enamel from animals on high fluoride diets (Chaneles 30 Schour and Smith 34 Sutro 35) In human fluorosed teeth hypomineralized layers of enamel parallel to the incremental lines can be demonstrated by microradiography (Crabb and Darling 62 Gustafson 61 Gustafson and Gustafson 61 Newbrun and Brudevold 60)

In spite of these descriptions of striations in enamel they are not seen in microradiographs of longitudinal sections through teeth from animals on the experimental diets Rarely hypo or hypermineralized layers of enamel are visible in microradiographs of transverse sections particularly in areas where the enamel is incompletely mineralized The relative infrequency of such striations in the radiographs may be an artifact resulting from the technique used The sections were 80–100 μ thick and the exposure times used were compromises between shorter exposures most appropriate for dentin and longer exposures necessary for maximum contrast within fully mineralized enamel It is more likely however that variations in mineralization which may have been present in the youngest enamel in rat incisors are obscured when the enamel becomes fully mineralized Such a healing process occurs in the response produced by injected fluoride (Weber and Yaeger 64) and in the present material the hypermineralized surface enamel is obscured when the enamel beaneath it becomes fully mineralized This interpretation would account for the striations which have been described in the young enamel matrix which survives demineralization the patterns seen in the present microradiographs where the enamel matrix is incompletely mineralized and would explain their absence from more fully mineralized enamel in laboratory animals It leaves unexplained however the persistence of abnormally mineralized layers in human fluorosed enamel This may be a deception based on the fact that the microradiographs chosen to illustrate previously published reports are only those showing notable changes

In human fluorosed teeth a distinctly hypermineralized surface layer of enamel similar to that illustrated here is sometimes visible in published microradiographs (Crabb and Darling 62 Gustafson 61 Gustafson and Gustafson 61) No one has commented on its presence perhaps because a hypermineralized surface is also sometimes seen in enamel considered to be normal (Gustafson and Gustafson 61

Thewlis 40) or perhaps because it is indistinct or absent in fully mineralized enamel This hypermineralized surface layer may be related to the high fluoride content of surface enamel (Brudevold 6?) A diffuse hypomineralization of fluorosed human enamel similar to that seen in the present material has been illustrated and described in a number of reports (Applebaum 36 Gustafson 61 Gustafson and Gustafson 61 Newbrun and Brudevold 60) In demineralized material the amount of matrix which survives demineralizing solutions is greater in teeth from laboratory animals on high fluoride diets than it is in normal teeth (Bethke Kick Hill and Chase 33 Schour and Smith 34 Hoffman Schuck and Furuta 42) These authors interpreted this acid resistance of enamel matrix as indicating an inhibition of matrix maturation and mineralization

Enamel hypoplasia

Localized defects in the apposition of enamel matrix in laboratory animals on high fluoride diets are frequently described (Chaneles 30 Bethke Kick Hill and Chase 33 Schour and Smith 34 Sutro '35) Hypoplastic defects are also common in chronic fluorosis of human teeth (Dean '34 36)

The hypoplastic defects in enamel of laboratory animals are not as circumscribed as those seen in dentin In enamel the walls of the defects generally diverge toward the surface while the walls of the defects in dentin are more nearly parallel Using demineralized sections Schour and Smith (34) have described a gradient of ameloblast and matrix damage decreasing toward the periphery of the hypoplastic defects and a zone of acid resistant matrix with the staining characteristics of immature enamel matrix surrounding the defects The mode of development of hypoplastic defects is apparently similar in enamel and dentin Young ameloblasts in limited regions atrophy or die while the surrounding ameloblasts continue to form enamel matrix In this way areas of ameloblastic epithelium become surrounded by enamel matrix

Summary of the relationships between experimental dental fluorosis in laboratory animals and chronic endemic dental fluorosis in man

The continuum of changes from the animals injected with fluoride through animals on high fluoride diets and ending with the histologically mild effects of chronic endemic fluorosis is interrupted at several points The microradiographically and histochemically similar changes (striations) in the dentin of animals receiving fluoride either by injection or in their diets have not been described in human fluorosed teeth This may well prove to be the result of a process of recovery in dentin similar to the "healing of the response to injected fluoride in enamel The partial recovery of dentin from the effects of injected fluoride can be demonstrated in rat incisors (Osmanski and Yaeger 64) In human teeth usually examined a number of years after their development has nearly ceased recovery from abnormal mineralization may be nearly complete

Hypoplastic defects in the dentin have been demonstrated only in laboratory animals on high fluoride diets Apparently the short period of action of fluoride in injection experiments does not cause odontoblast atrophy or death while the doses of fluoride which produce chronic fluorosis in human teeth are too small to damage odontoblasts Neither interglobular dentin nor gross deformations have been described in laboratory animals injected once with fluoride or in human fluorosed teeth

The hypermineralized surface diffuse subsurface hypomineralized zone and hypoplastic defects seen in the enamel of teeth from laboratory animals on high fluoride diets are closely related to similar changes demonstrated in human teeth and clarify the pathogenesis of such abnormalities The presence of hypoplastic defects in the enamel of human fluorosed teeth which contain apparently normal dentin indicates that ameloblasts are more susceptible to fluoride than are odontoblasts as suggested by Schour and Smith (34) Enamel hypoplastic defects are not present in the teeth from injected animals

odontogenic organ before dentin minerali zation begins

The presence and severity of these de formations was determined in the present study only by inspection of microradio graphs It is reasonable to expect more accurate measurements to disclose more subtle changes Kruger (62) has meas ured the influence of repeated injections of small doses of fluoride on the morphology of the mandibular first molars of young rats He found that the widths of the mesial fissures are increased while their depths are decreased the distal fissures show decreased depth and the mesial distal diameters of the crowns are de creased from normal values A similar reduction in crown diameter induced by dietary fluoride has also been reported by Paynter and Grainger (56) Since the morphology of teeth can be correlated with caries incidence (Grainger Paynter and Shaw 59) the mechanisms by which fluor ide can affect tooth morphology is of con siderable clinical interest The results de scribed here suggest that the influence of fluoride on the morphology of the incisors of rats is a promising experimental situa tion with which to pursue such studies

Hypermineralized surface enamel and enamel striations

In the present material the surface layer of enamel was hypermineralized only with respect to the relatively hypomineralized enamel beneath it For that reason it is necessary to discuss together hyper and hypomineralization of enamel

The subcutaneous injection of fluoride in rats produces in enamel a response con sisting of both hyper and hypomineralized components similar to the response pro duced in dentin (Weber and Yaeger 64) In demineralized material related stria tions have been described in enamel from animals on high fluoride diets (Chaneles 30 Schour and Smith 34 Sutro 35) In human fluorosed teeth hypomineralized layers of enamel parallel to the incremen tal lines can be demonstrated by micro radiography (Crabb and Darling 62 Gus tafson 61 Gustafson and Gustafson 61 Newbrun and Brudevold 60)

In spite of these descriptions of stria tions in enamel they are not seen in microradiographs of longitudinal sections through teeth from animals on the experi mental diets Rarely hypo or hypermin eralized layers of enamel are visible in microradiographs of transverse sections particularly in areas where the enamel is incompletely mineralized The relative in frequency of such striations in the radio graphs may be an artifact resulting from the technique used The sections were 80–100 μ thick and the exposure times used were compromises between shorter exposures most appropriate for dentin and longer exposures necessary for maximum contrast within fully mineralized enamel It is more likely however that variations in mineralization which may have been present in the youngest enamel in rat in cisors are obscured when the enamel be comes fully mineralized Such a healing process occurs in the response produced by injected fluoride (Weber and Yaeger 64) and in the present material the hyper mineralized surface enamel is obscured when the enamel beaneath it becomes fully mineralized This interpretation would ac count for the striations which have been described in the young enamel matrix which survives demineralization the pat terns seen in the present microradiographs where the enamel matrix is incompletely mineralized and would explain their ab sence from more fully mineralized enamel in laboratory animals It leaves unex plained however the persistence of ab normally mineralized layers in human fluorosed enamel This may be a deception based on the fact that the microradio graphs chosen to illustrate previously pub lished reports are only those showing nota ble changes

In human fluorosed teeth a distinctly hypermineralized surface layer of enamel similar to that illustrated here is some times visible in published microradiographs (Crabb and Darling 62 Gustafson 61 Gustafson and Gustafson 61) No one has commented on its presence perhaps because a hypermineralized surface is also sometimes seen in enamel considered to be normal (Gustafson and Gustafson 61,

size of rat molar teeth J Canad Dent Assoc 22 519-531

Pearse A G E 1960 Histochemistry Theoretical and Applied Second Edition Little Brown and Company Boston pp 239-248

Rockert H 1963 X ray absorption and X ray fluorescence microanalyses of mineralized tissue of rats which have ingested fluoridated water Acta Path Microbiol Scand 59 32-38

Schmidt W J and A Keil 1958 Die gesunden und die erkrankten Zahngewebe des Menschen und der Wirbeltiere im Polarisations mikroskop Hauser Munchen pp 45-50

Schour I 1960 Noyes Oral Histology and Embryology Eighth Edition Lea and Febiger Philadelphia p 122

Schour I and M Massler 1949 The teeth In The Rat in Laboratory Investigation Second Edition Ed by E J Farris and J Q Griffith Jr J B Lippincott Co Philadelphia pp 104-165

Schour I and M C Smith 1934 The histologic changes in the enamel and dentin of the rat incisor in acute and chronic experimental fluorosis University of Arizona College of Agriculture Agricultural Experimental Station Technical Bulletin No 52

Sutro C J 1935 Changes in the teeth and bone in chronic fluoride poisoning Arch Path 19 159-173

Thewlis J 1940 The structure of teeth as shown by X ray examination Medical Research Council (Great Britain) Special Report Series no 238 pp 52-58

Weber D and J A Yaeger 1964 A microradiographic interpretation of abnormal enamel formation induced by subcutaneous sodium fluoride J Dent Res 43 50-56

Yaeger J A 1963 Microscopy of the response of rodent dentin to injected fluoride Anat. Rec 145 139-147

Yaeger J A C F L Hinrichsen and M J Cohen 1964 Development of the response in rat incisor dentin to injected strontium and fluoride Am J Anat 114 255-272

The response produced in enamel by injected fluoride has its counterpart in the hypomineralized layers of enamel seen in human fluorosed teeth Striations of intermediate histological severity in the enamel of teeth from animals on high fluoride diets are present in demineralized material but are less frequent and less distinct in microradiographs The significance of this difference is not at all clear It may result from a recovery process in the laboratory animals or it may represent differences in the samples illustrated in published reports The microradiographs illustrated here include many which do not show striations in enamel and only a few that do show striations Of the human fluorosed teeth examined by microradiography probably only those showing some abnormality have been described in the literature Perhaps if equivalent samples of teeth from man and laboratory animals were prepared the incidence of enamel striations would be comparable

The undemineralized sections used here are much too thick to demonstrate individual enamel rods Images resembling individual rods are sometimes seen in microradiographs but they must result from the superimposition of several layers of rods and rod sheaths It was therefore impossible to confirm in rat incisors the observations that rod sheaths are less mineralized than normal in human fluorosed enamel (Newbrun and Brudevold 60 Crabb and Darling 62)

LITERATURE CITED

Applebaum E 1936 Mottled enamel Dent Cosmos *78* 969–980

Bélanger L F W E Lotz W J Visek and C L Comar 1954 Autoradiographic visualization with Ca^{45} of normal growth of the incisor of pigs and the effect of fluorine feeding Anat Rec *119* 53–69

Bélanger L F W J Visek W E Lotz and C L Comar 1957 The effects of fluoride feeding on the organic matrix of bones and teeth of pigs as observed by autoradiography after in vitro uptake of Ca^{45} and S^{35} J Biophysic Biochem Cytol 3 559–566

——— 1958 The effects of fluoride ingestion on the organic matrix of the teeth of growing pigs J Dent Res *37* 264–275

Bethke R M C H Kick T J Hill and S W Chase 1933 Effects of diets containing fluorine on jaws and teeth of swine and rats J Dent Res *13* 473–493

Brudevold F 1962 Chemical composition of the teeth in relation to caries In Chemistry and Prevention of Dental Caries Ed by R F Sognnaes Charles C Thomas Springfield pp 32–88

Chaneles J 1930 Estudios sobre el fluor y la fluorosis experimental Talleres Graficos Ferrari Hnos Buenos Aires pp 87–112

Crabb H S M and A I Darling 1962 The Pattern of Progressive Mineralisation in Human Dental Enamel International Series of Monographs on Oral Biology Volume 2 Pergamon Press New York

Dean H T 1934 Classification of mottled enamel diagnosis J Am Dent Assoc *21* 1421–1426

——— 1936 Chronic endemic dental fluorosis (mottled enamel) J Am Med Assoc *107* 1269–1272

Grady J E and J A Yaeger 1965 Polarizing microscopy of abnormal dentine produced by injections of strontium or fluoride Arch Oral Biol *10* 175–178

Grainger R M K J Paynter and J H Shaw 1959 Differences in the morphology and size of the teeth of a caries susceptible and a caries resistant strain of rats J Dent Res *38* 105–120

Gustafson A G 1961 The histology of fluorosed teeth Arch Oral Biol *4* 67–69

Gustafson G and A G Gustafson 1961 Human dental enamel in polarized light and contact micro radiography Acta Odont Scand *19* 259–287

Hale C W 1946 Histochemical demonstration of acid polysaccharides in animal tissues Nature *157* 802

Hoffman M M C Schuck and W J Furuta 1942 Histologic study on the effects of fluorine administered in dry and moist diets on teeth of young albino rats J Dent Res *21* 157–170

Irving J T 1943 The action of sodium fluoride on the dentin and predentin of the incisor teeth of rats consuming diets containing calcium and phosphorus in various ratios J Dent Res *22* 447–456

Kruger B J 1962 Trace elements in dental morphology University of Queensland Papers Department of Dentistry Vol I No 6 pp 101–125

McClure F J 1939 Fluorides in food and drinking water National Institutes of Health United States Public Health Service Bulletin no 172

Mowry W 1956 Alcian blue technics for the histochemical study of acidic carbohydrates J Histochem *4* 407

Newbrun E and F Brudevold 1960 Studies on the physical properties of fluorosed enamel — I Microradiographic studies Arch Oral Biol *2* 15–20

Osmanski C P and J A Yaeger 1964 Microradiography of rat incisor dentin during the development of the response to injected fluoride Anat Rec *148* 467–483

Paynter K J and R M Grainger 1956 The relation of nutrition to the morphology and

Fine Structure of the Rat Renal Papilla

RUTH ELLEN BULGER AND BENJAMIN F TRUMP
Department of Pathology University of Washington Medical School Seattle Washington

ABSTRACT The fine structure of the rat renal papilla was studied after fixation with various fixative solutions and by using three modes of fixative application immersion vascular perfusion and injection of fixative into the renal pelvis The morphology of the following was described thin limbs of Henle s loop collecting ducts capillaries interstitial cells and interstitium Several previously undescribed features were seen Two types of capillaries were identified on the basis of their fine structure Regions identified as limbs of Henle had at least two types of mural structure differing in degree of cellular interdigitation In addition numerous projections were seen extending from the basal cytoplasm of capillary endothelium and collecting duct epithelium through the basement membrane into the interstitium

It has long been assumed that the renal papilla is important in the production of concentrated urine (Marshall 34) Though the exact mechanisms involved are still the subject of considerable debate several groups of workers (Wirz and co-workers 51 Wirz 53 and others) hypothesized that the papilla was the site of a counter current multiplier a counter-current exchanger and an osmotic exchanger The loop of Henle is presumed to function as the counter current multiplier by creating an increasing gradient of solute concentration from the cortex to the papillary tip When the collecting duct (an osmotic exchanger) passes through the concentrated interstitium of this region water leaves the tubular lumen resulting in the production of hypertonic urine The capillaries form a counter-current exchange system allowing blood flow without abolition of the gradient Micropuncture studies by Gottschalk and Mylle (59) were consistent with this hypothesis The majority of other physiological experiments are also consonant with the counter-current hypothesis but some contradictory experiments have been reported (Hilger and co-workers 58 and Marsh and Solomon 65)

Although a few reports concerning selected aspects of papillary fine structure have been published (Rhodin 58a b 62 63 Sakaguchi and Suzuki 58 Novikoff 60 Thoenes 61 Lapp and Nolte 62 Robeson 63 Sabour and co-workers 64 Gloor and Neiditsch Halff 65 and Muehrcke and co-workers 65) a thorough study of all the structures in the papilla seems warranted as a basis for our morphological studies of this region in water diuresis and antidiuresis

MATERIALS AND METHODS

Sixteen Sprague Dawley and 14 Charles River male and female rats weighing 175–300 gm were used in this experiment The rats were allowed access to food and water at will until the time of sacrifice

The animals were anesthetized with pentobarbital and opened with a mid ventral incision Kidneys were fixed by three methods (1) The kidneys were removed and small (~ 1 mm) slices or pieces immersed in the fixative solutions for various time intervals (2) At the time of laparotomy with the blood supply still intact 5 ml of fixative solution were injected into the renal pelvis for a period of approximately five minutes with a needle and syringe The fixative could be seen to move down the ureter into the bladder if the needle was in the renal pelvis The kidney was then removed from the animal and pieces of papilla were post fixed by immersion for the remainder of the time interval utilized (3) Kidneys were also fixed by vascular perfusion To perfuse the kidney the major branches of the abdominal aorta with the exceptions of the renal arteries were ligated Loose sutures were placed around the aorta just medial to the left adrenal just rostral to its bifurcation and just caudal to the origin of the renal arteries A needle or a cannula was intro-

Fine Structure of the Rat Renal Papilla

RUTH ELLEN BULGER AND BENJAMIN F TRUMP
Department of Pathology University of Washington Medical School Seattle Washington

ABSTRACT The fine structure of the rat renal papilla was studied after fixation with various fixative solutions and by using three modes of fixative application immersion vascular perfusion and injection of fixative into the renal pelvis The morphology of the following was described thin limbs of Henle s loop collecting ducts capillaries interstitial cells and interstitium. Several previously undescribed features were seen Two types of capillaries were identified on the basis of their fine structure Regions identified as limbs of Henle had at least two types of mural structure differing in degree of cellular interdigitation In addition numerous projections were seen extending from the basal cytoplasm of capillary endothelium and collecting duct epithelium through the basement membrane into the interstitium

It has long been assumed that the renal papilla is important in the production of concentrated urine (Marshall 34) Though the exact mechanisms involved are still the subject of considerable debate several groups of workers (Wirz and co-workers 51 Wirz 53 and others) hypothesized that the papilla was the site of a counter current multiplier a counter-current exchanger and an osmotic exchanger The loop of Henle is presumed to function as the counter current multiplier by creating an increasing gradient of solute concentration from the cortex to the papillary tip When the collecting duct (an osmotic exchanger) passes through the concentrated interstitium of this region water leaves the tubular lumen resulting in the production of hypertonic urine The capillaries form a counter-current exchange system allowing blood flow without abolition of the gradient Micropuncture studies by Gottschalk and Mylle (59) were consistent with this hypothesis The majority of other physiological experiments are also consonant with the counter-current hypothesis but some contradictory experiments have been reported (Hilger and co-workers 58 and Marsh and Solomon 65)

Although a few reports concerning selected aspects of papillary fine structure have been published (Rhodin 58a b 62 63 Sakaguchi and Suzuki 58 Novikoff 60 Thoenes 61 Lapp and Nolte 62 Robeson 63 Sabour and co-workers 64 Gloor and Neiditsch Halff 65 and Muehrcke and co-workers 65) a thorough study of all the structures in the papilla seems warranted as a basis for our morphological studies of this region in water diuresis and antidiuresis

MATERIALS AND METHODS

Sixteen Sprague Dawley and 14 Charles River male and female rats weighing 175–300 gm were used in this experiment The rats were allowed access to food and water at will until the time of sacrifice

The animals were anesthetized with pentobarbital and opened with a mid ventral incision Kidneys were fixed by three methods (1) The kidneys were removed and small (~ 1 mm) slices or pieces immersed in the fixative solutions for various time intervals (2) At the time of laparotomy with the blood supply still intact 5 ml of fixative solution were injected into the renal pelvis for a period of approximately five minutes with a needle and syringe The fixative could be seen to move down the ureter into the bladder if the needle was in the renal pelvis The kidney was then removed from the animal and pieces of papilla were post fixed by immersion for the remainder of the time interval utilized (3) Kidneys were also fixed by vascular perfusion To perfuse the kidney the major branches of the abdominal aorta with the exceptions of the renal arteries were ligated Loose sutures were placed around the aorta just medial to the left adrenal just rostral to its bifurcation and just caudal to the origin of the renal arteries A needle or a cannula was intro-

generally ellipsoidal but frequently appeared indented A slight degree of clumping of the chromatin was seen in some of the nuclei While some tubules appeared similar to the thin limbs described here they lacked the abundant interdigitating processes All tubules were surrounded by a PAS positive basement membrane

Collecting ducts (figs 1–3 5)

The course of the collecting ducts was parallel to that of the two limbs of Henle s loop The cells that comprised the collect ing duct epithelium increased in height from low cuboidal to columnar as the duct approached the papillary tip Not all the cells at any given level appeared to be the same height Because the cell borders stained intensely it was evident that the cells were polyhedrons with an apex which bulged slightly into the lumen and had small microvilli projecting from it Short striations perpendicular to the basement membrane were seen in the basal cyto plasm In some collecting duct profiles vacuole like areas appeared along the lat eral borders and in the region of the basal striations A PAS positive basement mem brane surrounded the tubule Projections from the basal region of the collecting duct cells into the surrounding interstitium were frequently seen (figs 1 5) These were ex ceedingly frequent when the collecting duct was adjacent to a capillary and often seemed to run into similar projections from the capillary The cytoplasm of the col lecting duct cells was pale and contained small round or slightly elongate mitochon dria Some nonhomogeneous bodies larger than mitochondria with parts which stained intensely were seen adjacent to the nucleus Bodies with a similar size shape and distribution contained acid phos phatase activity and similar bodies were also seen to segregate trypan blue after in traperitoneal injection The nuclei con tained frequent nucleoli and were large and round with homogeneous chromatin Two types of cells were seen in the lu mens red blood cells and cells with clumped chromatin and few organelles

Blood vessels (figs 1–4 6)

Abundant capillaries were seen between the parenchymal tubules They were characterized by regions with extremely thin cytoplasmic layers although thicker regions of cytoplasm were seen near the nucleus or at other places along the circumference A few mitochondria were seen in the cytoplasm The nuclei contained nucleoli and were smaller than those of the tubules Their more irregular shape was accented by a slight peripheral clumping of the chromatin Erythrocytes and a material of moderate density were seen in some capil lary lumens The projections which ex tended from the capillaries into the inter stitium were particularly abundant when the capillary lay next to a collecting duct with its projections A material with the appearance of the basement membrane of ten bridged the gap between the projec tions of the capillary and the collecting duct (fig 5)

Interstitial cells (figs 1–6)

Lying in the interstitium between the parallel array of tubules and capillaries were the elongate interestitial cells which exhibited numerous processes In cross sections of the papilla however some of these cells were stellate The long axis of the cell lay perpendicular to that of the tubules and the cellular processes wrapped adjacent capillaries thin limbs of the loop of Henle and to a lesser extent the col lecting ducts The interstitial cells lay in rows between the parallel tubules In the densely staining cytoplasm the following structures were identified a variable num ber of lipid droplets (fig 6) round and ir regularly shaped vacuoles elongate mito chondria and some densely stained circu lar bodies Nuclei were smaller than those of the collecting duct and were irregular in shape with deep invaginations they often contained nucleoli Peripheral chromatin clumping was frequent (fig 6) and binucleate cells were seen A given cell often contacted more than one tubule in fact examples were seen where processes from one cell wrapped a thin limb a capil lary and a collecting duct Numerous small bodies demonstrated acid phospha tase activity Trypan blue administered in traperitoneally appeared in bodies of simi lar size and distribution When acid phosphatase activity was demonstrated on tissues containing trypan blue the bodies

duced into the aorta near its bifurcation (but caudal to the loose suture) and tied in place with the sutures which had been previously placed around the aorta below the level of the renal arteries An isotonic NaCl solution in the tubing that connected with the syringe containing fixative, was injected followed by the fixative After the injection had begun an assistant tied off the aorta (with the loose suture rostral to the renal artery) and quickly nicked the vena cava near the level of the kidneys Maunsbach (personal communication) stressed the importance of maintaining the blood pressure until the perfusion had begun and our experience supported this To determine what pressure should be applied to the syringe the kidney size was watched If any increase in volume was noted the pressure applied to the syringe was decreased It was easy to determine when adequate perfusion was obtained with osmium tetroxide (OsO_4) because the kidney turned entirely black with the exception of the papilla which turned a light brown After perfusion regions of the kidney were cut into approximately 1 mm pieces and fixed for the remainder of the time by immersion (Griffith and co workers)

The following fixative solutions and conditions were used (1) one hour at 0–4°C in 1 or 2% OsO_4 buffered with *s* collidine (pH 7 4) (*Bennett and Luft* 59) (2) three hours at 0–4 C in 6 25% glutaraldehyde buffered with 0 1 M sodium cacodylate (pH 7) followed by an overnight wash in 0 1 M cacodylate buffer (pH 7 4) containing 7 5% sucrose (Sabatini and co workers 63) (3) six hours at 0–4°C in 6 25% glutaraldehyde buffered with 0 1 M sodium cacodylate (pH 7 4) followed by an overnight wash in 0 1 M cacodylate buffer containing 7 5% sucrose and post osmicated for two hours at 0–4°C with 1 or 2% OsO_4 buffered with *s* collidine (Sabatini and co workers 63) (4) one hour at 0–4°C in a mixture containing 6 25% glutaraldehyde 1% OsO_4 and 0 067 M *s* collidine buffer (pH 7) (Trump and Bulger 65) or (5) 12 hours at room temperature in 4% phosphate buffered formaldehyde (Gridley 60)

All tissues were dehydrated in ethanol Those fixed with methods 1 3 and 4 were embedded in Epon epoxy resin (Luft 61) while those fixed with solutions 2 and 5 were embedded in paraffin or washed in gum acacia sucrose (Holt and co-workers 60) and then frozen and sectioned in a cryostat The cryostat sections were stained for neutral lipid with oil red O (Gridley, 60) or stained for acid phosphatase activity by the method of Gomori (Barka and Anderson 63) or using naphthol ASBI phosphate as a substrate and hexazonium pararosanilin as a coupler (Barka and Anderson '63) Two female rats were given intraperitoneal injections (1 ml/100 gm body weight) of 1% aqueous trypan blue (manufactured by National Aniline Division Allied Chemical Corporation) for seven days The kidneys from these animals were fixed in solutions 2 and 5 and embedded in paraffin or frozen and cut with a cryostat

Examples of tissues fixed in all the fixatives were studied with the light microscope after staining with Gomori trichrome (Gridley, 60) hematoxylin and eosin (H&E) (Gridley 60) periodic acid Schiff technique (PAS) (Gridley 60), or toluidine blue (Trump and co workers 61) Thin sections of material embedded in Epon epoxy resin were cut with glass or diamond knives on LKB and Porter Blum microtomes placed on grids supported with a thin carbon film double stained with uranyl acetate (Watson 58) and lead tartrate (Millonig 61) and examined using RCA EMU 3G electron microscopes

RESULTS

Light microscopy (figs 1–6)

Henle s loop (figs 1–4)

The thin limbs of Henle s loop coursed toward the tip of the renal papilla and then doubled back forming hairpin loops The thin limbs could best be distinguished from the other elements on the basis of their low epithelium which was frequently formed by interdigitation of small processes Sections tangential to the cell processes showed this to best advantage (fig 4) The cells were higher in the region of the nucleus The more abundant cytoplasm in this region contained only a few bodies which stained intensely with toluidine blue and were presumed to be mitochondria The nuclei which contained nucleoli were

Cytoplasmic ground substance In addition to the filaments running beneath the apical plasmalemma (figs 17 18) the cytoplasmic ground substance contained a few randomly disposed filaments (fig 10) A fine flocculent material filled the space between the structures described already After glutaraldehyde fixation with post-osmication or fixation in glutaraldehyde-osmium mixtures microtubules could be seen in the cytoplasm

Centrioles Centrioles were seen lying adjacent to the nucleus often in close association with the Golgi apparatus

Nucleus The nuclear profiles were generally round or ellipsoidal but small indentations were often seen There was a slight degree of chromatin clumping which was more marked after glutaraldehyde fixation Chromatin fibrils resembled those observed in other cells (Trump and co-workers 65b) Interchromatin granules were found The nuclear envelope with its pores was of usual structure Nucleoli had both filamentous and granular components

Basement membranes In some regions the basement membrane consisted of a single dense layer separated from the basal plasmalemma by a layer of intermediate density (figs 8 18) In most regions however the basement membrane was more complex consisting of two or more continuous layers with projections connecting them These projections extended into the interstitium or extended upwards between the interdigitating processes (figs 7–10 17)

Collecting ducts (figs 7 8 11 12–16)

The collecting ducts were composed of one cell type which increased in height as it approached the tip of the papilla

Cytoplasm Plasma membrane and associated structures The apical plasmalemma was thick The membrane formed a few short bulbous microvilli and had a thick coating of fuzz Extending down into the cytoplasm between the microvilli were alveolate vesicles lined with a fuzzy layer on either side of the cell membrane These were similar to the pits described by Roth and Porter (62 64) The lateral membranes were generally closely apposed with some small processes and lateral interdigitation but regions were found where large intercellular spaces separated the lateral plasmalemmas of adjacent cells (fig 3) In the basal region of the cell several specializations were seen the basal cell membrane invaginated the cell and returned along a parallel course forming true basal infoldings the basal cell membrane displayed regions of interdigitating processes generally from the same cell the basal plasma membrane seemed to infold slightly and the infoldings lay adjacent to a row of vesicles thought to result from fragmentation of parallel membranes and the basal plasma membrane formed what appeared to be intracellular canaliculi (fig 15) In some regions separations were seen between the specialized forms of the basal plasmalemma Some projections were seen extending from the basal region of the cell into the interstitium (fig 16) The processes had a filamentous matrix

The junctional complex consisted of a tight junction an intermediate junction and occasionally a desmosome Other desmosomes were seen along the lateral cell borders in a more basal region

Mitochondria Round or elongate mitochondrial profiles were small in size and number They contained few cristae or matrical granules and frequently appeared swollen with broken outer membranes In some mitochondria a crystalline intramatrical structure could be found (fig 14)

Endoplasmic reticulum and Golgi apparatus Small irregular vesicles and short cisternae were seen studded with RNP particles They contained a dense flocculent material especially prominent after glutaraldehyde fixation and post osmication (fig 11) Smooth surfaced elements consisted of a few irregular vesicles short cisternae and numerous round vesicles of varying size and matrix density Groups of RNP particles were found in the cytoplasm The Golgi apparatus was located above or lateral to the nucleus (fig 11) Multiple units consisted of a few short cisternae with frequent expanded areas In the vicinity of the Golgi membranes a cloud of vesicles with a moderately dense matrix was located

Cytosomes lipid droplets and multivesicular bodies Many small cytosomes

appeared to be purple *presumably* from the superposition of the trypan blue and the acid *phosphatase reactivity*

Interstitum (figs 1–6)

The interstitial space was abundant especially near the papillary tip Wisps of material which resembled the basement membranes were seen lying along regions of the interstitial cells and forming a net work throughout the interstitium This material was PAS positive

Electron microscopy

It was difficult to obtain what is con sidered satisfactory fixation of the renal papilla Pieces of tissue fixed by immer sion often showed several features that are regarded as inconsistent with well fixed normal cells broken cell membranes swollen mitochondria with broken mem branes swollen endoplasmic reticulum or swollen nuclear envelopes (fig 37) It was postulated that depriving the papilla of its blood supply caused cellular alterations re sulting in marked cellular swelling These alterations were minimized or eliminated by injecting the fixative into the renal pelvis or by vascular perfusion with the fixative

Thin limb of Henle s loop (figs 7–10 17 18 45)

Two types of tubular profiles were in terpreted as thin limbs of Henle s loop *They differed from each other only in* cell shape and height Numerous cross sec tions of interdigitating processes lined the tubular wall of type I (figs 7–10 17 18) The interdigitating processes consisted of large lateral extensions extending the full height of the cells and small extensions seen just in the basal region Type II (fig 10) lacked the complex interdigitating processes and showed long stretches of cytoplasm that were a little higher (al though still best considered as squamous) than that of type I It was not determined whether these two types of profiles repre sented ascending or descending thin limbs or just variations in cell shape in both limbs although it has been shown that the early part of the thin limb is of an elabo rate shape (Zimmermann 11 Rhodin 58a b, 62 63, and Osvaldo and Latta 65) *In longitudinal* sections of the papilla however each type of profile extended for a considerable distance Because the organ elles of the two types appeared identical they will be discussed together

Cytoplasm Plasma membrane and as sociated structures The apical plasmalem ma appeared to be much thicker than that of the rest of the cell (fig 17), a few small microvilli projected into the lumen The surface was coated with a thick layer of fuzz resembling the *antennulae microvil lares of gall bladder epithelium (Yamada* 56) The junctional complex (Farquhar and Palade 63) in this cell consisted of two parts tight and intermediate junc tions desmosomes were not found The tight junction was exceedingly short and the intermediate junction lying just basal to the tight junction was also fairly short A layer of fine filaments which coursed through the cytoplasm just beneath the apical plasmalemma lay in apposition to *the region of the intermediate junction*

Mitochondria Although the majority of the mitochondrial profiles appeared round, fortuitous sections showed that many were elongate The mitochondrial matrix contained *some dense flocculent* material and a few cristae matrical gran ules were rarely seen

Endoplasmic reticulum and Golgi ap paratus The endoplasmic reticulum was scanty and consisted of a few small irreg ular profiles and short cisternae studded with a few ribonucleoprotein (RNP) par *ticles (figs 8 9) After* glutaraldehyde fixation a dense flocculent material was seen in the cisternae *of the rough* sur faced endoplasmic reticulum Occasional smooth surfaced *vesicles with both* pale and dense matrix were seen Clusters of *free ribosomes were frequently identified* The Golgi apparatus found in a perinu clear position consisted of several *stacks* of cisternae and many vesicles of varying density Cisternal dilatations were fre quent (fig 10)

Cytosomes and multivesicular bodies A few small cytosomes containing filaments membranes and a dense component were seen The multivesicular bodies which were more frequently seen had a pale matrix and contained small vesicles

characterized by tight and intermediate junctions Although the basement membrane tended to be a single dense layer examples with multiple layers were seen (fig 18) Rare instances were found where basal processes of type I endothelial cells extended through the basement membrane into the surrounding interstitium (fig 25)

Type II (figs 7–9 16 19–24 26) In this type of capillary the cytoplasm of the endothelial cell had frequent pores which were spanned by a thin diaphragm A dense spot was often seen in the center of the diaphragm (fig 26) Areas lacking the pores were found and these often exhibited a curious configuration with processes of cytoplasm extending into the interstitium (figs 7 8 16 19–24) These processes which were either coated with a layer of basement membrane or sometimes extended through this extracellular coat came into apposition with similar processes from collecting ducts interstitial cells or processes from unidentifiable sources The cytoplasm contained elongate mitochondria with few cristae elements of the smooth and rough surfaced endoplasmic reticulum some free RNP particles a well developed Golgi apparatus and dense multivesicular bodies On both basal and apical surfaces indentations of the cell membrane were seen in which the membrane was coated with a fuzzy layer on its internal and external surfaces (fuzzy alveolate vesicles) The basement membrane generally was a single dense layer

The interstitial cell (figs 7–11 17–19 27–40)

Cytoplasm Plasma membrane and associated structures The interstitial cells had both large and small processes which came into close contact with the basement membranes of capillaries thin limbs and collecting ducts Wisps of material which were morphologically indistinguishable from basement membrane lay adjacent to the interstitial cells in many regions The entire cell however was not covered in this fashion Interstitial cells frequently were close to other interstitial cells In certain regions apposition of cell membranes resulted in the formation of structures that resembled tight junctions (figs 18 27 28) Similar areas of close apposition were seen between small processes some of which were thought to be interstitial cells or between two processes of the same interstitial cell

At various sites along the cell membrane invaginations occurred in which the cell membrane was coated on each surface by a fuzzy layer forming fuzzy alveolate vesicles (fig 17)

Mitochondria The mitochondria were in general elongate although circular and irregular profiles were seen The matrix material was of intermediate density and contained a moderate number of cristae Matrical granules were infrequent Large dense bodies similar to those seen in dying cells (Trump and co-workers 65a) were observed (fig 29)

Endoplasmic reticulum and Golgi apparatus The moderate amount of rough surfaced endoplasmic reticulum consisted mainly of long cisternae In some regions the lumens appeared dilated and contained a moderately dense flocculent material Stacks of these cisternae were frequently seen (fig 34) Smooth surfaced cisternae were also seen and in some areas formed several layers of whorls around areas of cytoplasm containing mitochondria and lipid droplets (fig 39) Vesicles were of frequent occurrence Membranes lacking granules were seen evaginating from rough surfaced membranes in the region of the Golgi apparatus forming the so-called transition elements The Golgi apparatus was complex and several units could be seen in a given cell profile Although some cisternae were short and others extremely long both showed areas of dilatation A cloud of vesicles was seen in the region of the Golgi apparatus Free RNP particles existed in clusters On rare occasions cylindrical bodies like those previously reported to occur in large numbers in interstitial cells of dehydrated rats (Bulger and co-workers 65) were seen (fig 33) The walls of these cylinders were continuous with the membranes of the endoplasmic reticulum

Cytosomes lipid droplets and multivesicular bodies A large number of cytosomes with varying internal morphology

(fig 11) were seen both lateral and apical to the nucleus They contained a variety of substances including a flocculent to dense matrix whorls of membranes, vacuoles of moderate density, vesicles and filaments Some appeared to contain lipofuscin pigment (fig 11) The external limiting membrane of the cytosomes showed interruptions which were thought to be artifacts of preparation These were more numerous in tissues fixed in OsO_4 buffered with s collidine Presumptive lipid droplets were located in the cytoplasm Frequently seen multivesicular bodies had a pale matrix and contained small vesicles

Cytoplasmic ground substance The cell sap frequently appeared to be exceedingly pale after OsO_4 fixation but was considerably denser after fixation with glutaraldehyde or glutaraldehyde OsO_4 mixtures These later two fixatives also preserved many microtubules in the cytoplasm Filaments observed throughout the ground substance were concentrated near the cell membranes A few membrane whorls were identified

Nucleus The nuclear profiles were generally circular with some indentations The chromatin often had a homogeneous distribution but slight clumping was observed in some cells The nucleoli had fibrillar and granular components A few ring shaped profiles consisting of a moderately dense filamentous network (figs 7 30) and interchromatin granules could be identified The nuclear envelope was of the usual structure with frequent nuclear pores In sections tangential to the nucleus, some component structures of the pore were easily seen The pore wall consisted of approximately 8–9 tubular units The pore also had a central dense spot Connections existed between the nuclear envelope and the endoplasmic reticulum

Basement membranes The basement membrane consisted of a single dense layer separated from the basal plasma lemma by a region of intermediate density The basement membrane frequently extended out to partially cover the projections of the collecting duct cells into the interstitium and therefore had a scalloped appearance In these regions the basement membrane was confluent with material of similar appearance that bridged across to the basement membrane of adjacent capillary projections The basement membrane seemed to be composed of a dense meshwork of filaments

Lumen In the lumens of some collecting ducts, cells could be seen which contained nuclei undergoing karyolysis and showing numerous bulbous processes of the plasmalemma (fig 12) Such cells are frequently found in control rats

Capillaries (figs 7–9, 16, 18–26)

Two distinct types of capillaries were identified in the renal papilla Because of their differing morphology, they will be discussed separately Also several distinctive features in the luminal contents were found The flocculent material in the capillary lumen varied greatly in density from animal to animal and from vessel to vessel After primary glutaraldehyde fixation the plasma always appeared dense Some erythrocytes were seen that lacked the usual homogeneous appearance (figs 19 20) In these cells the contents consisted of a varying number of multiple squarish areas separated by a continuous phase of flocculent material of lesser density The squarish areas were similar in density to the matrix of the normal erythrocytes In addition vessels from animals fixed by injection of fixative into the renal pelvis showed an increased number of platelets in their lumens (fig 20)

Type I (figs 18 and 25) The ultrastructure of this type of capillary was characterized by an unperforated squamous lining The cytoplasm contained a layer of little caves near the apical and basal cell membranes A few microvilli with thin fuzzy layers extended into the lumen The cytoplasm also contained a moderate number of elongate mitochondria with few cristae a network of fine filaments a well-developed Golgi apparatus some free RNP particles and some irregularly shaped vesicles and short cisternae of smooth and rough surfaced endoplasmic reticulum Dense material was sometimes seen in the lumen of the rough surfaced endoplasmic reticulum The ellipsoidal nuclei showed frequent indentations and peripheral chromatin clumping Nucleoli were seen Cell junctions were

laries two types of thin limb cells and the frequent basal projections of collecting ducts and capillaries

Because of the importance of the papilla to urine concentration recent studies have been focused on morphological differences seen in diuresis and antidiuresis These studies have reported varied and contradictory results on both the light and electron microscopic level (Ginetzinsky 58 Heller and Lojda 60 Breddy and co-workers 61 Stolarczyk and Manitius 62 Lapp and Nolte 62 Robeson 63 Sabour and co workers 64 Piel and co-workers 64 and Muehrcke and co workers 65) Studies in our laboratory (Griffith and co-workers) indicate that these inconsistent results may result in part from the following reasons First it appears that not enough is known about the normal variations in papillary structures seen in animals given food and water at will Secondly not enough is known about the alterations which take place during various fixing procedures The cells of the renal papilla are in a highly specialized environment and therefore may respond in a unique fashion to the interruption of their blood supply In our laboratory cells in the papilla fixed by immersion often showed broken cell membranes swollen mitochondria with broken membranes and swollen and dilated endoplasmic reticulum and nuclear envelopes This was particularly marked in the interstitial cells The membrane rupture and organelle swelling could have occurred subsequent to the interruption of the blood supply and before fixation or else this period of time could have altered the cells in such a way that they were more easily damaged by the preparatory procedures It is also difficult to assess how profoundly the various fixatives and procedures affected the volume relationships in the papilla It seems easy to imagine that variations in precedures could modify the size relationships and account for some of the inconsistencies reported Fixation by injection of fixative solutions into the renal pelvis or by vascular perfusion largely eliminated the swelling and membrane breakage often seen after immersion fixation and were judged by us to be more adequate techniques for fixation of the papilla Unless care is taken with the vascular perfusion however the intrarenal pressures may be altered leading to volume changes

Two types of capillaries were identified in the rat papilla The first type was lined by an unperforated squamous lining similar to that seen in the medulla of rabbit kidney (Sakaguchi and Suzuki 58) in the medulla of mouse kidney (Thoenes 61) and in the afferent vessels of the rat medullary rete mirabile (Longley and co-workers 60) and therefore most likely forms the proximal part of the papillary capillary bed The second type was lined by endothelial cells with frequent pores similar to the second type of capillary in the medulla of rabbit kidney (Sakaguchi and Suzuki 58) to that of the efferent vessels of the rat medullary rete mirabile (Longley and co-workers 60) and to the cortical peritubular capillaries (Rhodin 58a b 62 63) and probably forms the more distal capillary bed Longley and co-workers (60) postulated that the endothelium (particularly that of the arterial capillaries) may be able to modify its permeability because in his opinion the structural characteristics of the capillary walls go beyond what would be required for efficient passive exchange It therefore might exert some controlling influence on the medullary composition This possibility exists for the thick walled capillaries of the papilla as well

Two types of thin limbs were also seen those which demonstrated a moderate degree of interdigitation and those which had little interdigitation Since serial reconstructions were not attempted it is impossible to exclude the possibility that the two types of thin limbs cells existed at random in both ascending and descending limbs The careful studies of thin limbs from several species done by Zimmermann ('11) demonstrated however that the complex shape of the thin limb decreased along its course This study coupled with the fact that the first part of the medullary thin limb exhibits the most complex shape in electron micrographs (Rhodin 58a b 62 63 Osvaldo and Latta 65 and Trump and Bulger unpublished observations) make it seem likely that the papillary thin limb with the greater interdigitation was part of the descending limb The role pos

were seen These corresponded in size and location to the acid phosphatase and trypan blue positive droplets observed by light microscopy They contained a wide variety of materials of varying density and configuration including frequent my elin figures The cytoplasm also contained many lipid droplets but the size, shape and number varied with the animal (figs 7 19 32, 39) In some cells lipid drop lets almost completely filled areas of cyto plasm while few droplets were seen in others In some cells the lipid profiles appeared circular and in others they were irregular in shape The dense lipid drop lets appeared to be well preserved by the techniques used It was hard to deter mine if the dense lipid droplets were sur rounded by a membrane but in some cases they appeared to be The abundant multivesicular bodies contained a pale matrix and many vesicles

Cytoplasmic ground substance The cytoplasmic ground substance was filled with a flocculent material of moderate density Cytoplasmic filaments coursed through the cytoplasm and were especially concentrated just beneath the cell mem brane and in the processes In fact the small processes were filled with a dense array of filaments Following glutaralde hyde fixation, microtubules were easily found

Centrioles A pair of centrioles and associated satellite structures were often seen in the region of the Golgi apparatus Frequently one of the centrioles appeared to be involved with the organization of an aberrant cilium (figs 35 36)

Nucleus. The nuclei were often of irreg ular shape with frequent indentations The degree of chromatin clumping varied but clumping was often seen even after os mium collidine fixation (fig 7) Nucleoli and interchromatin granules were promi nent The nucleolonema was composed of peripheral granular and a more central fibrillar material The nuclear envelope showed frequent pores and communicated with the rough surfaced endoplasmic re ticulum Ring like profiles frequently seen were composed of a dense fibrillar outer ring with a lighter center similar to the interchromatin material (figs 7, 30)

The interstitium (figs 7–10, 41–45)

A *flocculent material* of low density filled the interstitial space and contained several other components The first con sisted of strands and patches of a material indistinguishable from basement mem brane and composed of a mat of extremely fine filaments (fig 43) The strands lay ad jacent to the interstitial cell and its proc esses and formed a network throughout the space connecting with the basement membranes of the tubules and capillaries

An array of fibrils of varying size was seen running throughout the interstitium A banded pattern could not be seen in the smallest fibrils but the larger ones had the banding pattern of collagen (figs 44 45) The interstitium also contained debris from degenerating cells, free lipid drop lets myelin figures, and some dense circu lar profiles (figs 41, 42)

DISCUSSION

Zimmermann (11) reviewed the early histologic descriptions of the thin limb cells and then clearly demonstrated the irregu lar interdigitating shape of these cells in several species He clearly showed that the cell shape became less elaborate over the length of the thin limb and was most sim ple just prior to the thick ascending limb of the loop of Henle Von Mollendorff (30) reviewed previous work and gave compre hensive descriptions of many of the papil lary elements including the presence and orientation of the lipid filled interstitial cells Histochemical and morphologic stud ies of the papilla with the light micro scope have been published (Vimtrup and Schmidt Nielsen 52 Sternberg and co-workers 56 Novikoff 60 Khalil and Tawfic 63 Young and Wissig 65 and others) Reports describing certain details of papillary structure as viewed with the electron microscope have also been pub lished (Rhodin 58a b 62 63 Sakaguchi and Suzuki 58 Novikoff 60 Oswaldo and Latta 65 and Gloor and Neiditsch Halff 65) None of these however has comprehensively reported the fine structure of all the elements in the renal papilla It is no surprise therefore, that several un described features have been identified during the course of this study including the identification of two types of capil

laries two types of thin limb cells and the frequent basal projections of collecting ducts and capillaries

Because of the importance of the papilla to urine concentration recent studies have been focused on morphological differences seen in diuresis and antidiuresis These studies have reported varied and contra dictory results on both the light and elec tron microscopic level (Ginetzinsky 58 Heller and Lojda 60 Breddy and co-workers 61 Stolarczyk and Manitius 62 Lapp and Nolte 62 Robeson 63 Sabour and co-workers 64 Piel and co-workers 64 and Muehrcke and co-workers 65) Studies in our laboratory (Griffith and co-workers) indicate that these inconsistent results may result in part from the follow ing reasons First it appears that not enough is known about the normal varia tions in papillary structures seen in ani mals given food and water at will Sec ondly not enough is known about the alterations which take place during various fixing procedures The cells of the renal papilla are in a highly specialized environ ment and therefore may respond in a unique fashion to the interruption of their blood supply In our laboratory cells in the papilla fixed by immersion often showed broken cell membranes swollen mitochondria with broken membranes and swollen and dilated endoplasmic reticulum and nuclear envelopes This was particu larly marked in the interstitial cells The membrane rupture and organelle swelling could have occurred subsequent to the in terruption of the blood supply and before fixation or else this period of time could have altered the cells in such a way that they were more easily damaged by the preparatory procedures It is also difficult to assess how profoundly the various fixa tives and procedures affected the volume relationships in the papilla It seems easy to imagine that variations in precedures could modify the size relationships and account for some of the inconsistencies re ported Fixation by injection of fixative solutions into the renal pelvis or by vascu lar perfusion largely eliminated the swell ing and membrane breakage often seen after immersion fixation and were judged by us to be more adequate techniques for fixation of the papilla Unless care is taken with the vascular perfusion however the intrarenal pressures may be altered leading to volume changes

Two types of capillaries were identified in the rat papilla The first type was lined by an unperforated squamous lining simi lar to that seen in the medulla of rabbit kidney (Sakaguchi and Suzuki 58) in the medulla of mouse kidney (Thoenes 61) and in the afferent vessels of the rat medul lary rete mirabile (Longley and co-workers 60) and therefore most likely forms the proximal part of the papillary capillary bed The second type was lined by endo thelial cells with frequent pores similar to the second type of capillary in the medulla of rabbit kidney (Sakaguchi and Suzuki 58) to that of the efferent vessels of the rat medullary rete mirabile (Longley and co-workers 60) and to the cortical peri tubular capillaries (Rhodin 58a b 62 63) and probably forms the more distal capil lary bed Longley and co-workers (60) postulated that the endothelium (particu larly that of the arterial capillaries) may be able to modify its permeability because in his opinion the structural characteris tics of the capillary walls go beyond what would be required for efficient passive ex change It therefore might exert some con trolling influence on the medullary compo sition This possibility exists for the thick walled capillaries of the papilla as well

Two types of thin limbs were also seen those which demonstrated a moderate de gree of interdigitation and those which had little interdigitation Since serial re constructions were not attempted it is im possible to exclude the possibility that the two types of thin limbs cells existed at random in both ascending and descending limbs The careful studies of thin limbs from several species done by Zimmermann (11) demonstrated however that the com plex shape of the thin limb decreased along its course This study coupled with the fact that the first part of the medullary thin limb exhibits the most complex shape in electron micrographs (Rhodin 58a b 62 63 Osvaldo and Latta 65 and Trump and Bulger unpublished observations) make it seem likely that the papillary thin limb with the greater interdigitation was part of the descending limb The role pos

were seen These corresponded in size and location to the acid phosphatase and trypan blue positive droplets observed by light microscopy They contained a wide variety of materials of varying density and configuration including frequent myelin figures The cytoplasm also contained many lipid droplets but the size, shape and number varied with the animal (figs 7 19 32 39) In some cells lipid droplets almost completely filled areas of cytoplasm while few droplets were seen in others In some cells the lipid profiles appeared circular and in others they were irregular in shape The dense lipid droplets appeared to be well preserved by the techniques used It was hard to determine if the dense lipid droplets were surrounded by a membrane but in some cases they appeared to be The abundant multivesicular bodies contained a pale matrix and many vesicles

Cytoplasmic ground substance The cytoplasmic ground substance was filled with a flocculent material of moderate density Cytoplasmic filaments coursed through the cytoplasm and were especially concentrated just beneath the cell membrane and in the processes In fact the small processes were filled with a dense array of filaments Following glutaraldehyde fixation microtubules were easily found

Centrioles A pair of centrioles and associated satellite structures were often seen in the region of the Golgi apparatus Frequently one of the centrioles appeared to be involved with the organization of an aberrant cilium (figs 35 36)

Nucleus The nuclei were often of irregular shape with frequent indentations The degree of chromatin clumping varied but clumping was often seen even after osmium collidine fixation (fig 7) Nucleoli and interchromatin granules were prominent The nucleolonema was composed of peripheral granular and a more central fibrillar material The nuclear envelope showed frequent pores and communicated with the rough surfaced endoplasmic reticulum Ring like profiles frequently seen were composed of a dense fibrillar outer ring with a lighter center similar to the interchromatin material (figs 7 30)

The interstitium (figs 7–10 41–45)

A flocculent material of low density filled the interstitial space and contained several other components The first consisted of strands and patches of a material indistinguishable from basement membrane and composed of a mat of extremely fine filaments (fig 43) The strands lay adjacent to the interstitial cell and its processes and formed a network throughout the space connecting with the basement membranes of the tubules and capillaries

An array of fibrils of varying size was seen running throughout the interstitium A banded pattern could not be seen in the smallest fibrils but the larger ones had the banding pattern of collagen (figs 44 45) The interstitium also contained debris from degenerating cells free lipid droplets myelin figures and some dense circular profiles (figs 41, 42)

DISCUSSION

Zimmermann (11) reviewed the early histologic descriptions of the thin limb cells and then clearly demonstrated the irregular interdigitating shape of these cells in several species He clearly showed that the cell shape became less elaborate over the length of the thin limb and was most simple just prior to the thick ascending limb of the loop of Henle Von Mollendorff (30) reviewed previous work and gave comprehensive descriptions of many of the papillary elements including the presence and orientation of the lipid filled interstitial cells Histochemical and morphologic studies of the papilla with the light microscope have been published (Vimtrup and Schmidt Nielsen 52 Sternberg and coworkers 56 Novikoff 60 Khalil and Tawfic 63 Young and Wissig 65 and others) Reports describing certain details of papillary structure as viewed with the electron microscope have also been published (Rhodin 58a b 62 63 Sakaguchi and Suzuki 58 Novikoff 60 Osvaldo and Latta 65 and Gloor and Neiditsch Halff 65) None of these however has comprehensively reported the fine structure of all the elements in the renal papilla It is no surprise therefore that several undescribed features have been identified during the course of this study including the identification of two types of capil

terstitial cells molecular rearrangement following water deprivation Submitted for publication
Farquhar M G and G E. Palade 1963 Junctional complexes in various epithelia J Cell Biol *17* 375–412
Friederici H H R 1965 Extrusion of basal endothelial projections through the capillary basement membrane Angiology *16* 163–169
Ginetzinsky A G 1958 Role of hyaluronidase in the re-absorption of water in renal tubules the mechanism of action of the antidiuretic hormone Nature *182* 1218–1219
Gloor F and L. A Neiditsch Halff 1965 Die Interstitiallen Zellen des Nierenmarker der Ratte Zeitschrift fur Zellforschung 66 488–495
Gottschalk C W and M Mylle 1959 Micropuncture study of the mammalian urinary concentrating mechanism evidence for the countercurrent hypothesis Am J Phqsiol *196* 927–936
Gridley M F 1960 Manual of Histologic and Special Staining Technics Second Edition The Blakiston Division McGraw Hill Book Company Inc New York
Griffith L. D B F Trump and R E Bulger Unpublished observations
Hilger H H J D Klumper and K. J Ullrich 1958 Wasserruckresorption und Ionentransport durch die Sammelrohrzellen der Saugetiermiere Arch Ger Physiol 267 218–237
Holt S J E E Hobbiger and G L. S Pawan 1960 Preservation of integrity of rat tissues for cytochemical staining purposes J Biophysic Biochem Cytol 7 383–386
Khalil F and J Tawfic 1963 Some observations on the kidney of the desert *J jaculus* and *G gerbillus* and their possible bearing on the water economy of these animals J Exp Zool *154* 259–271
Lapp H and A Nolte 1962 Vergleichende elektronenmikroskopische Untersuchungen am Mark der Rattenniere bei Harnkonzentrierung und Harnverdunnung Frankfurt z Path *71* 617–633
Longley J B W G Banfield and P C Brindley 1960 The structure of the rete mirabile in the kidney of the rat as seen with the electron microscope J Biophysic Biochem Cytol 7 103–106
Luft J H 1961 Improvements in epoxy resin embedding methods J Biophysi Biochem Cytol 9 409–414
Marsh D J and S Solomon 1965 Analysis of electrolyte movement in thin Henle s loops of hamster papilla Am J Physiol *208* 1119–1128
Marshall E K 1934 The comparative physiology of the kidney in relation to theories of enal secretion Physiol Rev *14* 133–159
Maunsbach A Personal communication
Millonig G 1961 A modified procedure for lead staining of thin sections J Biophysic Biochem Cytol *11* 736–739
Mollendorff W von 1930 Handbuch der Mikroskopischen Anatomie des Menschen Siebenter Band Harn und Geschlechtsapparat Julius Springer Berlin Vol 7
Muehrcke R C S Rosen and F I Volini 1965 The interstitial cells of the renal papilla Light and electronmicroscopic studies In Progress in Pyelonephritis Ed by E. H Kass F A Davis Philadelphia pp 422–433
Novikoff A B 1960 The rat kidney cytochemical and electron microscopic studies In Biology of Pyelonephritis Henry Ford Hospital International Symposium Ed by E. L. Quinn and E. Kass Little Brown and Company Boston pp 113–144
Osvaldo L. and H Latta 1965 Identification of ascending and descending thin limbs of the loop of Henle by electron microscopy Fed Proc *24* 618
Rhodin J A G 1958a Electron microscopy of the kidney Am J Med *24* 661–675
——— 1958b Anatomy of kidney tubules Intern Rev Cytol 7 485–534
——— 1962 Electron microscopy of the kidney In Renal Disease Ed by D A K. Black. Blackwell Scientific Publications F A Davis Company Philadelphia Pennsylvania.
——— 1963 Structure of the kidney In Diseases of the Kidney Ed by M B Strauss and L. G Welt Little Brown and Company Boston Massachusetts
Robson J S 1963 Factors affecting renal concentrating ability Electronmicroscopic study of the kidney during antidiuresis diuresis and potassium depletion In Memoirs of Soc for Endocrinol no 13 Hormones and the Kidney Ed by P C Williams Academic Press London
Roth T F and K R Porter 1962 Specialized sites on the cell surface for protein uptake *In* Fifth International Congress for Electron Microscopy Philadelphia Ed by S S Breese Jr Academic Press Inc New York 2 LL-4
——— 1964 Yolk protein uptake in the oocyte of the mosquito *Aedes aegypti L* J Cell Biol *20* 313–332
Sabatini P D K Bensch and R. S Barrnett 1963 Cytochemistry and electron microscopy The preservation of cellular ultrastructure and enzymatic activity by aldehyde fixation J Cell Biol 17 19–58
Sabour M S M K MacDonald A T Lambie and J S Robson 1964 The electron microscopic appearance of the kidney in hydrated and dehydrated rats Quarterly J Exp Physiol 49 162–170
Sakaguchi H and Y Suzuki 1958 Fine structure of renal tubule cells Keio J Med 7 17–26
Sternberg W H E. Farber and C E Dunlap 1956 Histochemical localization of specific oxidative enzymes II Localization of diphosphopyridine nucleotide and triphosphopyridine nucleotide and diaphorases and the succindehydrogenase system in the kidney J Histochem Cytochem 4 266–283
Stolarczyk J and A Manitius 1962 Morphology of the collecting tubules in diuretic and antidiuretic rats Proc Soc Exp Biol Med *110* 849–851
Thoenes W 1961 Die Mikromorphologie des Nephron in ihrer Beziehung zur Funktion Teil II Klinische Wochenschrift 39 827–839

tulated for the thin and thick ascending limb of the loop of Henle was to establish the counter current multiplier system (see review of Berliner) by active extrusion of sodium ions The structure of the thin limb poses a dilemma, therefore because the thin limb cells do not resemble many other cells believed to be specialized for ion transport This problem is only intensified if the thin ascending limbs are more simple in cell shape Either the relatively simple morphology of the cell still contains sufficient machinery to pump the required amount of sodium ion or the counter current hypothesis does not accurately describe the role of the thin limb cells and will have to be modified or replaced

Numerous projections were seen extending from the basal cytoplasm of capillaries and collecting ducts into the interstitium These projections often extended through the basement membrane and came into apposition with processes from other elements of the papilla Projections often occurred from collecting ducts and capillaries in adjoining regions forming a double scalloped pattern between the two structures The role, if any of these projections is unknown although certain functions might be considered Friederici (65) noted similar projections under conditions of increased permeability in peripheral capillaries and reviewed the literature finding several additional reports of endothelial processes He postulated that small vesicles formed from the projections and represented a mechanism of release of material In our studies vesicles did not seem to form from the processes From Friederici s literature review however it seems likely that small processes extending basally from the endothelium may be a more common feature than is presently realized A few endothelial processes were seen in rat kidney cortex (personal observation) Why the endothelial processes are closely related to processes of collecting ducts and interstitial cells is also unknown although some type of information might be transferred at these sites of contact The processes might also serve as some type of structural support for the elements of the papilla They were at least partially surrounded with basement membrane material which blends into similar material in the interstitium

The role of the abundant interstitial cells is also unknown, although as can be seen in this study and in the work of others (Vimtrup and Schmidt Nielsen '52 Sternberg and co workers, 56, and Novikoff 60) several possibilities exist The interstitial cell appeared to be able to phagocytize trypan blue given intraperitoneally It contains rough surfaced endoplasmic reticulum and a well developed Golgi apparatus and therefore could play a secretory role such as production and maintenance of the abundant interstitium Recent studies from our laboratory (Bulger and co-workers, 65) indicate that morphologic alterations can occur in interstitial cells during dehydration These involve the production of cylinders confluent with the endoplasmic reticulum The numerous filaments in the cytoplasm and cellular processes could be related to some contractile function

Two examples of cellular degeneration were observed in papillas from control animals These consisted of cellular debris in the interstitium and altered cells with karyolytic nuclei in collecting duct lumens In both cases the nature of the alterations seemed to preclude rapid production during or immediately preceding the fixation and embedding process and hence may represent some form of necrobiosis

ACKNOWLEDGMENTS

The authors wish to express their thanks to Liz Caldwell Ingrid Klock Rene Collman Franque Remington and Carla Reiter

LITERATURE CITED

Barka T and P J Anderson 1963 Histochemistry Theory Practice and Bibliography Hoeber Medical Division Harper and Row Publishers Inc New York

Bennett H S and J H Luft 1959 s Collidine as a basis for buffering fixatives J Biophysic Biochem Cytol 6 113–114

Berliner R W 1965 Some aspects of the function of the renal medulla In Progress in Pyelonephritis Ed by F H Kass F A Davis Philadelphia pp 417–421

Breddy P G F Cooper and J M N Boss 1961 Antidiuretic hormone and renal collecting tubules Nature 192 76

Bulger R E L D Griffith and B F Trump 1965 Endoplasmic reticulum in rat renal in


TL
CD
TL
C
C
CD
TL
C
TL
C

Trump B F and R E Bulger 1965 New ultrastructural characteristics of cells fixed in a glutaraldehyde-osmium tetroxide mixture Lab Invest in press

Trump B F P J Goldblatt and R E Stowell 1965a Studies on necrosis of mouse liver in vitro Ultrastructural alterations in the mitochondria of hepatic parenchymal cells Lab Invest 14 343–371

——— 1965b Studies of mouse liver necrosis in vitro Ultrastructural and cytochemical alterations in hepatic parenchymal cell nuclei Lab Invest in press

Trump B F E A Smuckler and E P Benditt 1961 A method for staining epoxy sections for light microscopy J Ultrastruc Res 5 343–348

Vimtrup B J and B Schmidt Nielsen 1952 The histology of the kidney of kangaroo rats Anat Rec 114 515–528

Watson M L 1958 Staining of tissue sections for electron microscopy with heavy metals J Biophysic Biochem Cytol 4 475–478

Wirz H 1953 Des osmotische Druck der Blutes in der Merenpapille Helv Physiol Pharmacol Acta 11 20–29

Wirz H B Hargitay and W Kuhn 1951 Lokalisation des Konzentrierungs prozesses in der Nier durch direkte Kryoskopie Helv Physiol Pharmacol Acta 9 196–207

Yamada E 1955 The fine structure of the gall bladder epithelium of the mouse J Biophysic Biochem Cytol 1 445–458

Young D and S L Wissig 1964 A histologic description of certain epithelial and vascular structures in the kidney of the normal rat Am J Anat 115 43–70

Zimmermann K W 1911 Zur Morphologie der Epithelzellen der Saugetierniere Arch Mikr Anat 78 199–231

Figures 1–8 represent photomicrographs of tissues fixed as indicated embedded in Epon epoxy resin sectioned at 0 5–1 μ and stained with toluidine blue

PLATE 1

EXPLANATION OF FIGURES

1 Light micrograph of a section from rat papilla showing the parallel array of thin limbs of Henle s loop (*TL*) collecting ducts (*CD*) capillaries (*C*) and rows of interstitial cells (*IC*) with their processes bridging between the parallel tubules Fixed by immersion with the osmium tetroxide glutaraldehyde mixture × 770

2 Light micrograph of a section from rat papilla showing thin limbs of Henle s loop (*TL*) a collecting duct (*CD*) and capillaries (*C*) The processes of the interstitial cells (*IC*) can be seen in close relation to the tubules and capillaries Fixed by immersion with the osmium tetroxide glutaraldehyde mixture × 1 600


CD
TL
C
IC
C
TL
3


TL


CD


LD

PLATE 2

EXPLANATION OF FIGURES

3 Light micrograph of a section from a rat papilla showing thin limbs (*TL*) a *collecting duct* (*CD*) *capillaries* (*C*) *and interstitial* cells (*IC*) with their cytoplasmic processes Strands of material can be seen in the interstitium Fixed by papillary injection of osmium tetroxide buffered with *s* collidine × 1 400

4 Light micrograph showing a thin limb of Henle s loop (*TL*) The terminal bar regions (arrows) indicate the irregular interdigitating processes of the thin limb cells Lipid droplets (*LD*) can be seen in the interstitial cell cytoplasm (*IC*) Fixed by papillary injection of osmium tetroxide buffered with *s* collidine × 2 900

5 Light micrograph showing a collecting duct (CD) Note the small extension from the basal region of these cells into the interstitium (arrow) Fixed by papillary injection of osmium tetroxide buffered with *s* collidine × 2 500

6 Light micrographs showing several interstitial cells (*IC*) Lipid drop lets (LD) are seen in the cytoplasm Fixed by papillary injection of osmium tetroxide buffered with *s*-collidine × 2 800


CD
C
IC
IC
TL

Figures 7–45 are electron micrographs of tissues fixed as indicated embedded in Epon epoxy resin and double stained with uranyl acetate and alkaline lead tartrate

PLATE 3

EXPLANATION OF FIGURE

7 Electron micrograph of a section from rat papilla showing portions of a collecting duct (*CD*) a type II capillary (*C*) two interstitial cells (*IC*) and a type I thin limb of Henle s loop (*TL*) Small endothelial processes (arrows) can be seen extending into the interstitium Note the lamellated structure of the basement membrane surrounding the thin limb Fixed by papillary injection of osmium tetroxide buffered with *s*-collidine × 8 800


CD
C
TL

PLATE 4

EXPLANATION OF FIGURE

8 Electron micrograph showing portions of a collecting duct (*CD*) type II capillary (*C*) and a type I thin limb Numerous profiles of small processes can be seen in the interstitial space (arrows) Fixed by papillary injection of osmium tetroxide buffered with s-collidine × 7 500


CD
C
TL
B

PLATE 4

EXPLANATION OF FIGURE

8 Electron micrograph showing portions of a collecting duct (*CD*) type II capillary (*C*) and a type I thin limb Numerous profiles of small processes can be seen in the interstitial space (arrows) Fixed by papillary injection of osmium tetroxide buffered with *s* collidine × 7 500


TL
IC
IC
C
C
TL I
TL II
30

PLATE 5

EXPLANATION OF FIGURES

9 Electron micrograph showing a type I thin limb (*TL*) two type II capillaries (*C*) and parts of several interstitial cells (*IC*) Fixed by perfusion with osmium tetroxide buffered with *s* collidine × 15 800

10 Electron micrograph showing both types of thin limbs Fixed by papillary injection of osmium tetroxide buffered with *s*-collidine × 13 200


TL
IC
IC
C
C
TL I
TL II

PLATE 6

EXPLANATION OF FIGURE

11 Electron micrograph showing a collecting duct cell The cytoplasm contains mitochondria (*M*) cytosomes (*C*) Golgi apparatus (*G*) free RNP particles lipofuscin (*L*) and rough surfaced endoplasmic reticulum (*ERG*) containing a flocculent material of moderate density Fixed by immersion in osmium tetroxide glutaraldehyde mixture × 15 100


ERG
C

PLATE 7

EXPLANATION OF FIGURES

12 Electron micrograph showing part of two collecting duct cells and a lumen containing a degenerating cell The chromatin in the nucleus (*N*) of the degenerating cell is clumped while the nucleus (*N*) of the collecting duct cell is more homogeneous Fixed by immersion in osmium tetroxide glutaraldehyde mixture × 8 900

13 Electron micrograph of the lateral cell borders of two collecting duct cells showing separations between the two plasma membranes Fixed by immersion in osmium tetroxide buffered with *s*-collidine × 15 300

14 Electron micrograph of mitochondria (*M*) from a collecting duct cell which contains bodies with a repeating substructure Cytosomes can also be seen Fixed by immersion in osmium tetroxide buffered with *s*-collidine × 17 900

15 Electron micrograph of the basal region of a collecting duct cell showing what appears to be a basal invagination similar to an intra cellular canaliculus Fixed by perfusion with osmium tetroxide buf fered with *s*-collidine × 16 900


12
N
M
15

PLATE 7

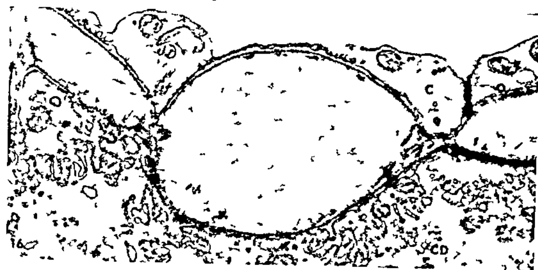
EXPLANATION OF FIGURES

12 Electron micrograph showing part of two collecting duct cells and a lumen containing a degenerating cell The chromatin in the nucleus (*N*) of the degenerating cell is clumped while the nucleus (*N*) of the collecting duct cell is more homogeneous Fixed by immersion in osmium tetroxide glutaraldehyde mixture × 8 900

13 Electron micrograph of the lateral cell borders of two collecting duct cells showing separations between the two plasma membranes Fixed by immersion in osmium tetroxide buffered with s collidine × 15 300

14 Electron micrograph of mitochondria (*M*) from a collecting duct cell which contains bodies with a repeating substructure Cytosomes can also be seen Fixed by immersion in osmium tetroxide buffered with *s*-collidine × 17 900

15 Electron micrograph of the basal region of a collecting duct cell showing what appears to be a basal invagination similar to an intra cellular canaliculus Fixed by perfusion with osmium tetroxide buf fered with *s*-collidine × 16 900



TL
AV
IC
17
C
IC
IC
18

PLATE 8

EXPLANATION OF FIGURES

16 Electron micrograph showing areas of close relationship between projections from the capillary endothelium (*C*) and the collecting ducts (*CD*) Fixed by immersion in osmium tetroxide buffered with s collidine × 18 000

17 Electron micrograph showing part of a type I thin limb of Henle's loop (*TL*) and an interstitial cell (*IC*) The interstitial cell cytoplasm contains a large Golgi apparatus An alveolate vesicle (*AV*) can be seen along the cell membrane Fixed by papillary injection of osmium tetroxide buffered with s collidine × 19 500

18 Electron micrograph of a type I capillary (*C*) and a type I thin limb (*TL*) The capillary has many little caves along its plasma membranes Processes from interstitial cells (*IC*) can be seen Areas of close contact (arrows) are present between adjacent profiles and between two processes of the same profile Fixed by papillary injection of osmium tetroxide buffered with s collidine × 17 100


19
20

PLATE 9

EXPLANATION OF FIGURES

19 Electron micrograph of a type II capillary showing two kinds of erythrocytes those of normal density and those with two phases Parts of two interstitial cells can also be seen Fixed by papillary injection of osmium tetroxide buffered with s collidine × 17 000

20 Electron micrograph of a type II capillary showing a two phase erythrocyte and a platelet An endothelial protrusion can also be seen (arrow) extending into the interstitium Fixed by papillary injection of osmium tetroxide buffered with s collidine × 24 000


19
20

PLATE 10

EXPLANATION OF FIGURES

21–24 Electron micrographs of parts of type II capillaries showing basal protrusions of cytoplasm into the interstitium Fixed with osmium tetroxide buffered with s-collidine × 21 900 × 36 000 × 30 000 × 30 100 × 37 500

25 Electron micrograph of a part of a type I capillary showing a basal protrusion of cytoplasm into the interstitium Fixed by perfusion of osmium tetroxide buffered with s-collidine × 36 200

26 Electron micrograph showing a tangential section of the pores of a type II capillary A central dense spot can be seen Fixed by perfusion of osmium tetroxide buffered with s collidine × 62 100

27–28 Electron micrographs showing areas of close apposition of plasma lemmas of processes in the interstitium Figure 27 fixed by immersion and figure 28 fixed by papillary injection in osmium tetroxide buffered with s collidine × 58 200 33 000


21
22
23
24
25
26
27
28

PLATE 10

EXPLANATION OF FIGURES

21–24 Electron micrographs of parts of type II capillaries showing basal protrusions of cytoplasm into the interstitium Fixed with osmium tetroxide buffered with *s*-collidine × 21 900 × 36 000 × 30 000 × 30 100 × 37 500

25 Electron micrograph of a part of a type I capillary showing a basal protrusion of cytoplasm into the interstitium Fixed by perfusion of osmium tetroxide buffered with *s*-collidine × 36 200

26 Electron micrograph showing a tangential section of the pores of a type II capillary A central dense spot can be seen Fixed by perfusion of osmium tetroxide buffered with *s*-collidine × 62 100

27–28 Electron micrographs showing areas of close apposition of plasma lemmas of processes in the interstitium Figure 27 fixed by immersion and figure 28 fixed by papillary injection in osmium tetroxide buffered with *s*-collidine × 58 200 33 000


ERG
29
30
31
32
33
34
36

PLATE 11

EXPLANATION OF FIGURES

29–36 Electron micrographs of areas of interstitial cells showing various features In figure 29 dense bodies (arrows) which are thought to be indicative of early cell degeneration are found in certain mitochondria In figure 30 three ringlet images can be seen in the nucleus (arrows) Expanded cisternae of the rough surfaced endoplasmic reticulum containing moderately dense flocculent material (*ERG*) can be seen in figures 30 and 31 In figure 32 six profiles of lipid droplets can be seen with a dense homogeneous matrix Figure 33 shows profiles of three cylindrical bodies (arrows) which are only rarely seen in control animals but frequently seen in dehydrated animals In figure 34 cisternae of rough surfaced endoplasmic reticulum are seen adjacent to an elongate mitochondrion Figures 35 and 36 show centrioles in the Golgi region In figure 36 an aberrant cilium is being formed Fixed with osmium tetroxide buffered with s-collidine × 22 300 × 25 500 × 12 400 × 33 000 × 55 000 × 32 900 × 37 500 × 19 800

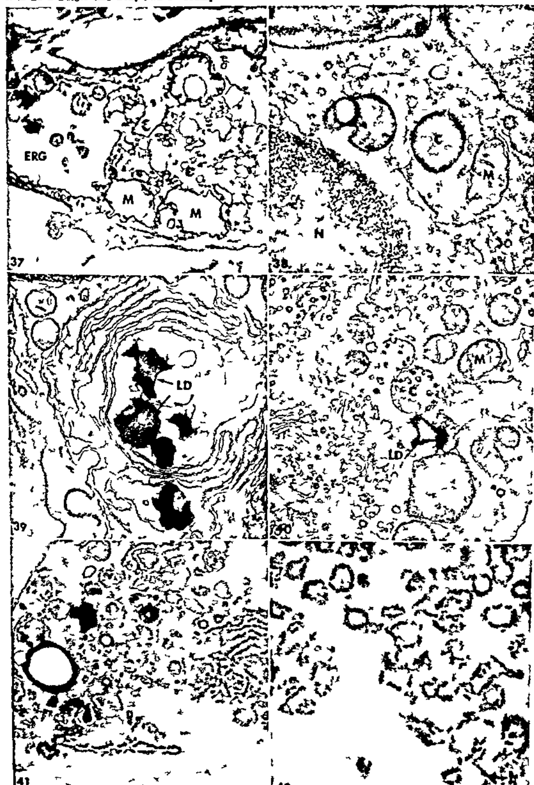

ERG
M
M
37
N
M
38
LD
39
M
C
LD
50
41

PLATE 12

EXPLANATION OF FIGURES

37 Electron micrograph of an interstitial cell fixed by immersion The cisternae of the endoplasmic reticulum (*FRG*) are expanded and the mitochondria (*M*) appear distorted and swollen and contain a pale matrix Fixed by immersion in osmium tetroxide buffered with s collidine × 12 000

38 Electron micrograph of an area of an interstitial cell showing part of a nucleus (*N*) cytosomes (*C*) mitochondria (*M*) rough surfaced endoplasmic reticulum and a cell membrane Fixed by papillary injection of osmium tetroxide buffered with s collidine × 20 400

39 Electron micrograph of an area of cytoplasm from an interstitial cell Several layers of smooth surfaced cisternae surround some lipid droplets (*LD*) Fixed by immersion in osmium tetroxide buffered with s collidine × 18 700

40 Electron micrograph of an area of interstitial cell cytoplasm showing a well developed Golgi apparatus mitochondria (*M*) cytosomes (*C*) and a lipid droplet (*LD*) Fixed by papillary injection of osmium tetroxide buffered with s collidine × 23 600

41–42 Electron micrographs showing debris in the interstitium which presumably marks the remains of degenerated interstitial cells Figure 41 fixed by perfusion and figure 42 fixed by immersion in osmium tetroxide buffered with s collidine × 20 700 × 23 600

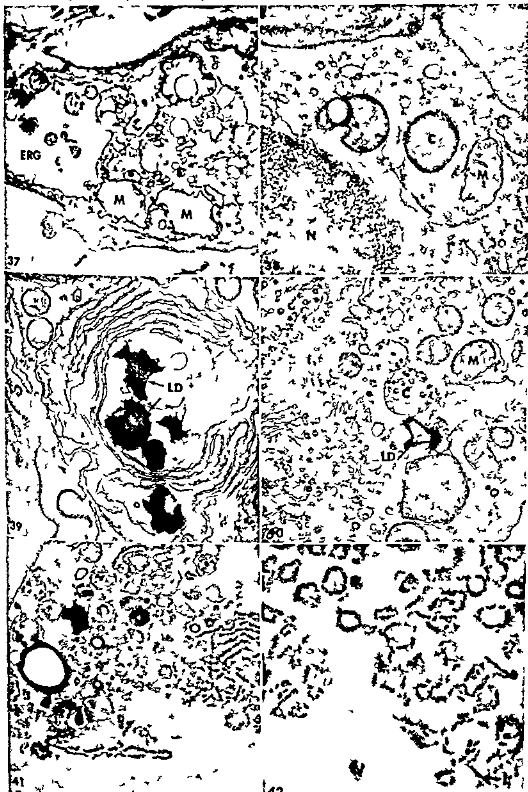

ERG
M
M
37
C
M
N
38
LD
39
M
C
LD
40
41
42

PLATE 13

EXPLANATION OF FIGURES

43 Electron micrograph of the interstitial space showing basement membrane (*BM*) material similar to basement membrane fibrils (*F*) and a flocculent material in the remaining space The material similar to basement membrane appears to consist of a mat of fine fibrils (arrows) Fixed by immersion in an osmium tetroxide glutaraldehyde mixture × 21 700

44–45 Electron micrographs showing the striated nature of some of the fibrils in the interstitium (arrows) Figure 44 is fixed by perfusion and figure 45 is fixed by papillary injection of osmium tetroxide buffered with *s*-collidine × 35 800 × 43 300


BM
45

PLATE 13

EXPLANATION OF FIGURES

43 Electron micrograph of the interstitial space showing basement membrane (*BM*) material similar to basement membrane fibrils (*F*) and a flocculent material in the remaining space The material similar to basement membrane appears to consist of a mat of fine fibrils (arrows) Fixed by immersion in an osmium tetroxide glutaraldehyde mixture × 21 700

44–45 Electron micrographs showing the striated nature of some of the fibrils in the interstitium (arrows) Figure 44 is fixed by perfusion and figure 45 is fixed by papillary injection of osmium tetroxide buffered with *s* collidine × 35 800 × 43 300


BM
43
44
45

The Visual Cells of the Chicken as Revealed by Phase Contrast Microscopy [1]

DAVID B. MEYER AND TERRANCE G. COOPER
Department of Anatomy, Wayne State University School of Medicine, Detroit, Michigan

ABSTRACT Phase microscopic investigations of Kolmer fixed, depigmented sections of the adult chicken retina have provided photomicrographic evidence of the existence of three different photoreceptors: single rods, single cones and double cones. The rod extends the entire thickness of the visual cell layer and is characterized by a uniformly thick outer segment and a hyperboloid-containing inner segment which is devoid of an oil droplet. The single cone is the shortest element; it contains a red oil droplet. The double cone consists of two unequal members, a tall, slender chief cone and a broad accessory cone. The chief component contains a large yellow oil droplet, whereas the accessory cone houses a small, oval, yellowish green droplet and a characteristically large, oval paraboloid. The rod hyperboloid and the accessory cone paraboloid contain glycogen. No colorless droplets have been observed. Owing to the close association between oil droplet color and cone type, three colored layers of oil droplets are formed within the thickness of the retina: a proximal row of red droplets (the short, single cones), an intermediate layer of yellowish green droplets (the accessory cones) and a distal row of yellow droplets (the tall chief cones).

Although the visual cells of the domestic chicken (*Gallus domesticus*) have been extensively examined since the pioneering researches of Max Schultze (1866, 1867, 1872), considerable controversy still exists regarding their morphological types and structural organizations. Chicken photoreceptors, like those of other animals, are extremely fragile cells which require rapid, delicate fixation and careful microtechnical manipulations, particularly with respect to the removal of the abundant pigment granules which surround and greatly interfere with their identification. In the present study, an excellent depigmentation method has been applied to fixed and unfixed sections of the chicken retina in order to obtain unobstructed visualizations of their various photoreceptors by phase contrast microscopy. Reliable cytological data as provided by this material are considered to be absolutely essential for a proper understanding and interpretation of the existing as well as future cytochemical and electron microscopic findings. Many such studies of the chicken retina have been published, but unfortunately the vast majority of these have not been correlated with an accurate knowledge of visual cell types or structure or have employed inconsistent descriptive terminologies. It is intended that the present investigation will help to eliminate this confusion with respect to the chicken retina, at least by providing photomicrographic evidence of the morphological appearance and cytological organization of the various types of visual elements residing in this species.

MATERIALS AND METHODS

The light adapted eyes of the domestic chicken (*Gallus domesticus*) were rapidly enucleated and sectioned with a razor through their equators. The resultant posterior halves with their intact retinas were then subjected to the following manipulations for subsequent phase and light microscopic examination. (1) Fresh, unfixed retinas were examined as *in toto* spread preparations after teasing in physiological saline (with or without trypsin) and as frozen sections (cryostat). (2) Chemically fixed (Kolmer's, Gendre's, Carnoy's, Zenker's, Bouin's, 10% formalin (neutral buffered), aqueous mercuric chloride, calcium acetate formalin, 4% buffered osmic acid) retinas were sectioned in the frozen state as well as after embedding in carbowax, gelatin, agar and paraffin (celloidin paraffin according to Peterfi's methyl ben

[1] This investigation was supported in part by research grant AM 06705 from the National Institutes of Health and in part by a Fight for Sight Grant-in-Aid of the National Council to Combat Blindness, Inc., New York, New York.

zoate method) (Carleton and Drury 58) All sections were cut at 6 μ (3) The freeze substitution method of Feder and Sidman (58) was also applied to retinas fixed in either 1% osmic acid in acetone or 1% picric acid in ethanol Most sections were subjected to the acidified permanganate depigmentation method as described by Chesterman and Leach (58), and were examined by bright field (after routine staining procedures e g hematoxylin and eosin iron hematoxylin PAS reaction) and phase contrast (unstained) microscopy (Zeiss Neofluar objectives)

Photomicrographs were taken with a Zeiss photomicroscope on Kodak plus X pan professional (figs 1 3–5) or high contrast copy (figs 2 6–7) film The latter film was overexposed and underdeveloped in Kodak D 76 developer in order to utilize in full the high resolution of this film and at the same time to retain the normal contrast

OBSERVATIONS

The combination of Kolmer fixation and acidified permanganate depigmentation resulted in the production of well preserved sections of chicken retina in which the visual elements were easily seen and appeared to have undergone minimal morphological or cytological changes None of the other fixatives produced equivalent results Freeze substitution procedures yielded poor cytological detail The use of fresh frozen cryostat sections for visualizing the different colored oil droplets *in situ* did not materialize because the cytology was not adequate for reliable identification of the various visual cell types in these preparations Likewise the droplets became easily displaced and did not appear to retain their normal localizations

The visual cell layer of the chicken is extraordinarily thick and comprises approximately one third of the thickness of the entire retina (fig 1) The photoreceptors are most easily recognized in the peripheral portions of the retina where they are broader (particularly the cones) and not as heavily concentrated as in the central areas For this reason the descriptions presented in this study have been obtained for the most part from the visual elements occupying the periphery of the retina

Three distinctly different visual cells are observed in the chicken retina single rods single cones and double cones The rods are the longest of the photoreceptors and extend the total distance of the visual cell layer (figs 2 3E) They are easily identified in the phase microscope because of their prominent uniformly thick outer segments the distal extremities of which appear to be embedded within the cytoplasm of the pigment epithelium Proximally, the rod outer segments join the equally thick ellipsoids which appear dark and granular owing to a dense accumulation of mitochondria The inner and outer segments of the rods are comparable in length their junction lies approximately in the middle of the visual cell layer Proximal to the ellipsoid the inner segment tapers gradually and becomes almost indistinguishable at its myoid region A striking and constant feature of the rod inner segment is the presence of an elongated conical shaped dark body just proximal to the ellipsoid (arrow fig 2) This structure which measures on the average about 1–2 μ in thickness and 7–10 μ in length represents the hyperboloid of Krause (1894) The slightly thicker distal or basal end of the hyperboloid lies close to the ellipsoid the proximal tapered apex terminates about half way between the ellipsoid and the external limiting membrane The hyperboloid often appears slightly curved as in figure 2 but this is undoubtedly due to slight distortions of the inner segments In contrast to the ellipsoid the hyperboloid appears smooth in texture it is everywhere surrounded by the clear cytoplasm of the inner segment In retinas fixed with picric acid-ethanol (freeze substitution) or Gendre s fluid and subjected to the periodic acid Schiff (PAS) reaction the hyperboloids become brilliant magenta in color The loss of this cytochemical reaction when similar retinal sections are treated with malt diastase prior to the PAS procedure identifies this material as glycogen



Fig 1 Phase contrast photomicrograph of entire thickness of peripheral portion of chicken retina fixed in Kolmer's fluid and depigmented (Chesterman and Leach 58) The retina is approximately 127 μ in thickness about one third of which comprises the visual cell layer The large photoreceptors with their conspicuous oil droplet vacuoles are easily recognized Unstained 6 μ section 800 ×

Fig 2 Phase contrast photomicrograph of a double cone and a single rod In the rod the thick outer segment adjoins the equally thick but darker ellipsoid A slightly curved hyperboloid (arrow) is evident below the latter Unstained 6 μ section Kolmer fixation and bleached 2000 ×

No oil droplet vacuoles are observed in the rods

The single cones (figs 3B F G 4) represent the shortest of the chicken photoreceptors their conical but relatively long outer segments comprise approximately one third of their total length Each inner segment is characterized by the presence of a single large circular oil droplet (approximately 4 μ in diameter) which occupies almost the entire thickness at its distal end A delicate rim of cytoplasm surrounds the oil droplet however so that the latter can also be conveniently described as occupying the distal extremity of the ellipsoid The single cone ellipsoid which like that in the rods also appears granular owing to the presence of abundant mitochondria occupies approximately the distal third of the inner segment The proximal portion of the ellipsoid ends rather abruptly only to appear to continue again as a thinner rectangular body likewise granular which fades out a considerable distance from the external limiting membrane The significance of this appearance is unknown However additional evidence that these are perhaps two independent structures is indicated by the rare presence (we have only observed three of them) of a peculiar

zonte method) (Carleton and Drury 58) All sections were cut at 6 μ (3) The freeze substitution method of Feder and Sidman (58) was also applied to retinas fixed in either 1% osmic acid in acetone or 1% picric acid in ethanol Most sections were subjected to the acidified permanganate de pigmentation method as described by Chesterman and Leach (58) and were examined by bright field (after routine staining procedures e g hematoxylin and eosin iron hematoxylin PAS reaction) and phase contrast (unstained) microscopy (Zeiss Neofluar objectives)

Photomicrographs were taken with a Zeiss photomicroscope on Kodak plus X pan professional (figs 1 3–5) or high contrast copy (figs 2 6–7) film The latter film was overexposed and underdeveloped in Kodak D 76 developer in order to utilize in full the high resolution of this film and at the same time to retain the normal contrast

OBSERVATIONS

The combination of Kolmer fixation and acidified permanganate depigmentation resulted in the production of well preserved sections of chicken retina in which the visual elements were easily seen and appeared to have undergone minimal morphological or cytological changes None of the other fixatives produced equivalent results Freeze substitution procedures yielded poor cytological detail The use of fresh frozen cryostat sections for visualizing the different colored oil droplets *in situ* did not materialize because the cytology was not adequate for reliable identification of the various visual cell types in these preparations Likewise the droplets became easily displaced and did not appear to retain their normal localizations

The visual cell layer of the chicken is extraordinarily thick and comprises approximately one third of the thickness of the entire retina (fig 1) The photoreceptors are most easily recognized in the peripheral portions of the retina where they are broader (particularly the cones) and not as heavily concentrated as in the central areas For this reason the descriptions presented in this study have been obtained for the most part from the visual elements occupying the periphery of the retina

Three distinctly different visual cells are observed in the chicken retina single rods single cones and double cones The rods are the longest of the photoreceptors and extend the total distance of the visual cell layer (figs 2 3E) They are easily identified in the phase microscope because of their prominent uniformly thick outer segments the distal extremities of which appear to be embedded within the cytoplasm of the pigment epithelium Proximally the rod outer segments join the equally thick ellipsoids which appear dark and granular owing to a dense accumulation of mitochondria The inner and outer segments of the rods are comparable in length their junction lies approximately in the middle of the visual cell layer Proximal to the ellipsoid the inner segment tapers gradually and becomes almost indistinguishable at its myoid region A striking and constant feature of the rod inner segment is the presence of an elongated conical shaped dark body just proximal to the ellipsoid (arrow fig 2) This structure which measures on the average about 1–2 μ in thickness and 7–10 μ in length represents the hyperboloid of Krause (1894) The slightly thicker distal or basal end of the hyperboloid lies close to the ellipsoid the proximal tapered apex terminates about half way between the ellipsoid and the external limiting membrane The hyperboloid often appears slightly curved as in figure 2 but this is undoubtedly due to slight distortions of the inner segments In contrast to the ellipsoid the hyperboloid appears smooth in texture it is everywhere surrounded by the clear cytoplasm of the inner segment In retinas fixed with picric acid ethanol (freeze substitution) or Gendre s fluid and subjected to the periodic acid Schiff (PAS) reaction the hyperboloids become brilliant magenta in color The loss of this cytochemical reaction when similar retinal sections are treated with malt diastase prior to the PAS procedure identifies this material as glycogen



Fig 4 Single cone Phase contrast Unstained Kolmer fixation bleached 2000 ×

Fig 5 Peculiar single cone The oil droplet has apparently been displaced and is located proximal to the ellipsoid Phase contrast Unstained Kolmer fixation bleached 2000 ×

The outer segment of the accessory cone is very slender (the thinnest of all outer segments) and is most difficult to detect It is thickest at its base and gradually tapers to a relatively fine point near the pigment epithelium it does not appear to reach the latter however The outer segment represents approximately one third the total length of the accessory cone

The inner segment of the accessory cone on the other hand is extremely broad (fig 3C) and consists of an ellipsoid paraboloid and myoid The ellipsoid is conical in shape and consists of dark staining granules the mitochondria Within its distal apex is a small oval oil droplet which measures about 4 μ in its greatest diameter and 2 μ in its shortest It lies in close association with the oil droplet of the chief cone and is best seen when both components of the double cone lie side by side in section (fig 3C) or when the accessory element is sectioned alone (fig 7) In other views of the double cone the oil droplet vacuole of the accessory element is superimposed upon that of the chief cone and therefore is not visible (figs 2 3A 6) Perhaps this may account for the failure of the majority of investigators to recognize the existence of this oil droplet

The paraboloid constitutes the bulk of the accessory cone inner segment It is a diagnostic feature of the latter and provides an excellent criterion for its identifi



Fig 6 Double cone sectioned through both components The upper half of the inner segment is dominated by the ellipsoid and oil droplet of the chief cone whereas the proximal half represents the paraboloid of the accessory element Phase contrast Unstained Kolmer fixation bleached 2400 ×

Fig 7 Same cell as shown in figure 6 at depth which reveals the accessory cone alone

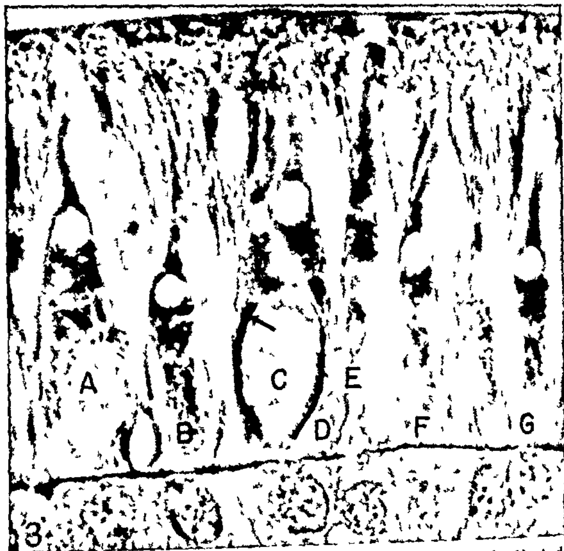


Fig 3 Phase contrast photomicrograph of chicken visual cells (enlargement of fig 1) A double cone B single cone C accessory and D chief components of double cone F rod F and G single cones In the accessory cone note the oval oil droplet and the dark body (arrow) between the ellipsoid and paraboloid The hyperboloid of the rod (F) is not in focus Unstained Kolmer fixation bleached 2000 ×

visual element (fig 5) which has all the charcteristics of a single cone except that the oil droplet is situated, not at the apex of the inner segment but at precisely the junction between the two previously described portions of the ellipsoid (compare figs 4 and 5) The ellipsoid of this cone consequently appears larger (it no longer relinquishes space for the oil droplet) Likewise, the rectangular body is separated from the ellipsoid as a distinct entity although a thin layer of cytoplasm appears to extend around the oil droplet Whether both of these structures are similar in ultrastructural organization requires additional electron microscopic studies

The double cones consist of two unequal but independent components a tall thin chief cone and a broad accessory cone which are in close proximity along most of the extent of their inner segments (fig 3C D) The fusion of these two elements has yet to be established in the chicken their individuality however is represented by separate nuclei The double cone represents one of the most obscure elements of the vertebrate retina (Walls 42) and this becomes readily apparent when one begins to identify their components microscopically Double cones are most easily distinguished when both components lie parallel to the plane of section (fig 3C D)



Fig 4 Single cone Phase contrast Unstained Kolmer fixation bleached 2000 ×

Fig 5 *Peculiar single cone* The oil droplet has apparently been displaced and is located proximal to the ellipsoid Phase contrast Unstained Kolmer fixation bleached 2000 ×

The outer segment of the accessory cone is very slender (the thinnest of all outer segments) and is most difficult to detect It is thickest at its base and gradually tapers to a relatively fine point near the pigment epithelium it does not appear to reach the latter however The outer segment represents approximately one third the total length of the accessory cone

The inner segment of the accessory cone on the other hand is extremely broad (fig 3C) and consists of an ellipsoid paraboloid and myoid The ellipsoid is conical in shape and consists of dark staining granules the mitochondria Within its distal apex is a small oval oil droplet which measures about 4 μ in its greatest diameter and 2 μ in its shortest It lies in close association with the oil droplet of the chief cone and is best seen when both components of the double cone lie side by side in section (fig 3C) or when the accessory element is sectioned alone (fig 7) In other views of the double cone the oil droplet vacuole of the accessory element is superimposed upon that of the chief cone and therefore is not visible (figs 2 3A 6) Perhaps this may account for the failure of the majority of investigators to recognize the existence of this oil droplet

The paraboloid constitutes the bulk of the accessory cone inner segment It is a diagnostic feature of the latter and provides an excellent criterion for its identifi



Fig 6 Double cone sectioned through both components The upper half of the inner segment is dominated by the ellipsoid and oil droplet of the chief cone whereas the proximal half represents the paraboloid of the accessory element Phase contrast Unstained Kolmer fixation bleached 2400 ×

Fig 7 Same cell as shown in figure 6 at depth which reveals the accessory cone alone

cation Like the rod hyperboloid it appears to be completely filled with glycogen (positive PAS reaction with diastase control) as also demonstrated by Rabinovitch et al (54) and O'Rahilly and Meyer (63) The paraboloid appears relatively clear and structureless in unstained phase contrast preparations (glycogen loss) except for a slightly darker crescent shaped marginal area in the distal half which appears to be continuous with a thinner dense area proximally (fig 3C) Within the cytoplasm surrounding the paraboloid is an extremely dark body which is thickest distally (arrow fig 3C) It does not appear to separate completely the ellipsoid from the paraboloid however except at the periphery This body appears to form a dense ring between the paraboloid and the ellipsoid which continues around the paraboloid toward the proximal portion of the inner segment At times it often appears to be continuous with the external limiting membrane and at other times to continue around the base of the paraboloid Further insight into this structure requires electron microscopic studies

Owing to the great development of the paraboloid the myoid comes to represent the scant portion of the inner segment situated lateral and proximal to the paraboloid Its true morphology is not evident in Kolmer fixed phase microscopic sections

The chief component of the double cone (fig 3D) is the tallest of the cones it extends almost the entire thickness of the visual cell layer

The outer segment of the chief cone closely resembles that of the single cone in height and thickness but accounts for only about one fourth of the total length of the cone

The inner segment possesses a very prominent circular oil droplet approximately 5 μ in diameter which like the others completely fills the distal extremity of the inner segment The ellipsoid of the chief cone lies in the contour of the ellipsoid of the accessory element and consequently lies at an angle with respect to the other visual cells It is thicker distally where it houses the oil droplet and tapers proximally (at the level of the distal end of the paraboloid) where it becomes condensed into a prominent conical shaped body which gradually fades out toward the myoid

The myoid is extremely difficult to identify It appears thinner distally where it lies adjacent to the greatest diameter of the paraboloid and thicker proximally where it seems to undercut the basal portion of the paraboloid

The spatial relationship of the chief and accessory cones is not constant so that in any one section of the retina the chief cone may be observed in front behind or on either side of the accessory element As mentioned previously a better understanding of the structure of these components is obtained when they are visualized side by side or sectioned separately (fig 3C D 7) Unfortunately however double cones are more often seen as large bizarre looking cells actually representing a composite of both components (figs 2 3A 6) This appearance is produced when the double cones are sectioned at right angles to the plane in which their two components lay side by side (as in fig 3C D) The large oil droplet vacuole is that of the chief cone whereas the broad basal portion of the inner segment corresponds to the paraboloid of the accessory cone The oil droplet and ellipsoid of the accessory cone are obscured by the corresponding parts of the chief cone the myoid of the latter is obscured by the paraboloid

The examination of fresh unfixed teased preparations of the chicken retina with the light microscope reveals the presence of three differently colored oil droplets red golden yellow and yellowish green Colorless droplets are not observed The red and golden yellow droplets are spherical and of approximately the same size whereas the yellowish green are smaller and oval shaped

When viewed with phase objectives the yellowish green droplets assume a definite green shade and are seen to occupy the accessory components of the double cone Many accessory and chief cones are readily discernible in teased preparations as independent elements The chief cones however are upright not arched as shown in Kolmer fixed preparations It is assumed therefore that double cones in the

chicken do not represent solidly fused ele ments but rather two independent com ponents which for some unknown reason are always found together *in situ* The chief cones are the tallest visual cells observed in teased preparations and they always possess the golden yellow oil droplet The red droplet on the other hand appears to be confined to the shorter single cones

Microscopic examination of flattened spread preparations of fresh chicken ret inas does not reveal any circumscribed colored fields (orange or yellow) as de scribed in the chicken (Waelchli 1883 Krause 1894) Instead the retina appears a uniform reddish yellow color

DISCUSSION

The phase contrast photomicrographs of Kolmer fixed chicken visual cells as demonstrated in the present study pre sent for the first time reliable evidence of the morphological appearance and structural arrangement of these once highly obscure elements More signifi cantly however an understanding of the anatomy of the various types of photoreceptors in the chicken retina will now permit a more accurate evaluation and interpretation of data (past and present) on the ultrastructure cytochemistry and physiology of these cells For example the rods of the striated mannikin (*Uroloncha striata* var *domestica* Flower) which have been observed in the electron microscope by Yasuzumi et al (58) to be three to four and one half times thicker than the cones undoubtedly due to the presence of a peculiar navicular profile are now seen to be in reality double cones the navicular profiles merely representing the inner segments of the chief cones (compare figs 1 and 6 (Yasuzumi et al 58) with fig 29 of Okuda et al 61) With respect to the chicken retina Meller (64) Meller and Breipohl (65) and Meller and Glees (65) have very re cently described ultrastructural altera tions occurring in the developing "receptor cells (6–21 days of incubation) but their failure to identify the specific types of visual elements in this species has greatly hindered interpretation of their data

Rods

The phase microscopic observations of the chicken rods have revealed in agree ment with the majority of investigators that these visual elements are character ized by long (approximately 35 µ) uni formly thick (approximately 3 5 µ) outer segments (Hoffmann 1877 Wolken 58) and the absence of oil droplets (fig 8a,f j,l) Oil droplets have been described in chicken rods (Uchiyama 30) but ade quate evidence has not been presented to account for this unique localization The hyperboloids are an additional constant feature of rod structure having been de scribed by many early microscopists (Schultze 1872 Hoffmann 1877 Ritter 1891 Krause 1894) (fig 8f j) In the corn-crake (*Crex pratensis*) and honker (*Charadrius pluvialis*) it measures 3 µ in length and 1 5 µ in width (Ritter 1891) It was originally believed to be a presist ent and resistant axis fiber (Schultze 1867) but subsequently considered as a refractive medium (Schultze 1872) Rabinovitch et al (54) believes the chicken hyperboloids correspond to the paraboloids of the rods of *Passer domesticus* as illustrated by Walls (42) (p fig 8n o) According to our findings how ever the chicken hyperboloid is located more distally close to the ellipsoid (fig 8s) and in contrast to Walls diagram does not assume the same morphological appearance as the paraboloid of the pe ripheral rod (fig 8n) or the same microscopic appearance as the chicken cone paraboloid The hyperboloid appears uni formly dark in phase contrast microscopy whereas the cone paraboloid is relatively clear Nevertheless both of them defi nitely contain histochemically demonstra ble glycogen (Rabinovitch et al 54 Yamada 62 O'Rahilly and Meyer 63) and this is apparently the only cytochemical clue to their functional significance

Cones

The cones of the chicken which com prise single and double types are char acterized by the presence of brightly col ored oil droplets Since their discovery

Uchiy ma (30) ecogn z d only on type of cone in the chi ken Rab n vitch et al (54) f lled to recogni e s mpl c ne

cation Like the rod hyperboloid it appears to be completely filled with glycogen (positive PAS reaction with diastase control) as also demonstrated by Rabinovitch et al (54) and O Rahilly and Meyer (63) The paraboloid appears relatively clear and structureless in unstained phase contrast preparations (glycogen loss) except for a slightly darker crescent shaped marginal area in the distal half which appears to be continuous with a thinner dense area proximally (fig 3C) Within the cytoplasm surrounding the paraboloid is an extremely dark body which is thickest distally (arrow fig 3C) It does not appear to separate completely the ellipsoid from the paraboloid however except at the periphery This body appears to form a dense ring between the paraboloid and the ellipsoid which continues around the paraboloid toward the proximal portion of the inner segment At times it often appears to be continuous with the external limiting membrane and at other times to continue around the base of the paraboloid Further insight into this structure requires electron microscopic studies

Owing to the great development of the paraboloid the myoid comes to represent the scant portion of the inner segment situated lateral and proximal to the paraboloid Its true morphology is not evident in Kolmer fixed phase microscopic sections

The chief component of the double cone (fig 3D) is the tallest of the cones it extends almost the entire thickness of the visual cell layer

The outer segment of the chief cone closely resembles that of the single cone in height and thickness but accounts for only about one fourth of the total length of the cone

The inner segment possesses a very prominent circular oil droplet approximately 5 μ in diameter which like the others completely fills the distal extremity of the inner segment The ellipsoid of the chief cone lies in the contour of the ellipsoid of the accessory element and consequently lies at an angle with respect to the other visual cells It is thicker distally where it houses the oil droplet and tapers proximally (at the level of the distal end of the paraboloid) where it becomes condensed into a prominent conical shaped body which gradually fades out toward the myoid

The myoid is extremely difficult to identify It appears thinner distally where it lies adjacent to the greatest diameter of the paraboloid and thicker proximally where it seems to undercut the basal portion of the paraboloid

The spatial relationship of the chief and accessory cones is not constant so that in any one section of the retina the chief cone may be observed in front behind or on either side of the accessory element As mentioned previously a better understanding of the structure of these components is obtained when they are visualized side by side or sectioned separately (fig 3C D 7) Unfortunately however double cones are more often seen as large bizarre looking cells actually representing a composite of both components (figs 2 3A 6) This appearance is produced when the double cones are sectioned at right angles to the plane in which their two components lay side by side (as in fig 3C D) The large oil droplet vacuole is that of the chief cone whereas the broad basal portion of the inner segment corresponds to the paraboloid of the accessory cone The oil droplet and ellipsoid of the accessory cone are obscured by the corresponding parts of the chief cone the myoid of the latter is obscured by the paraboloid

The examination of fresh unfixed teased preparations of the chicken retina with the light microscope reveals the presence of three differently colored oil droplets red golden yellow and yellowish green Colorless droplets are not observed The red and golden yellow droplets are spherical and of approximately the same size whereas the yellowish green are smaller and oval shaped

When viewed with phase objectives the yellowish green droplets assume a definite green shade and are seen to occupy the accessory components of the double cone Many accessory and chief cones are readily discernible in teased preparations as independent elements The chief cones however are upright not arched as shown in Kolmer fixed preparations It is assumed therefore that double cones in the

over 120 years ago[3] these droplets have been extensively investigated by many authors[4] most of whom agree as do the present investigators that only three differently-colored droplets exist in the chicken retina red yellow (golden) and yellowish green Colorless droplets have been repeatedly described but have not been identified with certainty in the present study Because of their cytological position within the cones the oil droplets are closely related to the mitochondria which form the bulk of the ellipsoid Electron microscopic studies have revealed this association in the single cones of the toad (*Bufo bufo*) (Sjostrand and Elfvin 56) in single and double cones of the turtle (Yamada 60) in certain cones of a lizard (*Lacerta muralis*) and a diurnal gecko (*Phelsuma inunguis*) (Pedler and Tansley 63) and in the cones of the frog (Takayama 60 Craig et al 63)

The color of the oil droplets are due to three stable carotenoid pigments (Wald and Zussmann 37 38 Wald 48) which in appropriate solvents closely reproduce the natural color of these droplets *in vivo* Many specific carotenoids have been implicated but only astaxanthin (red) has been adequately substantiated (Meyer et al 65)

Single cones The structure of the single cones of the chicken as perceived by earlier investigators (fig 8b c d g j,m) has corresponded to the phase microscopic findings (fig 8q) The existence of a specific color (red) in the single cone oil droplet however has not been widely accepted Schultze (1867) for example noted yellow or red droplets (fig 8b c d) whereas Hoffmann (1877) maintained that oil droplets of the single cones could assume a multitude of colors According to Dobrowolsky (1871b) red droplets are confined to cones with the longest outer segments Although the single cones are the shortest oil droplet bearing elements within the chicken retina their relatively long outer segments may be those referred to by Dobrowolsky

The red droplets of the single cones lie closer to the external limiting membrane than the other droplets and consequently form a proximal layer of red spheres

Double cones The double cones were first described by Hannover (1840) they are present in all vertebrate retinas except placental mammals Schultze (1867) examined their morphology and structure in many vertebrates and for the most part his descriptions have remained unchallenged up to the present time As the name implies double cones represent two intimately associated cones a chief and an accessory component[5] They should not be confused with twin cones however which are composed of two identical cones The significance of such multiple visual cell associations have been discussed by Kalberer and Pedler (63) The ories on the origin of double cones have been summarized by Lyall (57)

In the chicken the *chief* cones as demonstrated by phase microscopy (fig 8r) resemble closely those previously illustrated by Walls (42) and other investigators (fig 8e h k p) They are the tallest of the cones and possess the largest oil droplets The droplets are golden yellow in color and because they lie furtherest from the external limiting membrane form the most distal row of oil droplets Yellow droplets have also been observed in these elements by earlier investigators (Schultze 1867 Hoffmann 1877 Krause 1894)

The *accessory* component of the double cone is characterized by the presence of a large oval glycogen-containing paraboloid which permits its selective identification According to some authors (e g Rochon Duvigneaud 43) however the paraboloid represents an inclusion body within the myoid and this different interpretation may account for the discrepancies which exist in the literature regarding glycogen localization within the visual cells (Compare Rabinovitch et al 54 Sidman and Wislocki 54 Matsusaka 62 O'Rahilly and Meyer 63 with Yoshizawa 53 Kuwabara and Cogan 61) In

---

W lls and Judd (33) stated th t Val ntin di c e ed the oil droplets b t included no reference Many other authors considered Hannover (1840) as the d sco e er

For reviews ee Hahn (16) Walls and Judd ('33) M yer et al. (65)

The chief con deri s its name f om the trans l tion f the original German word, H uptzapfen which can also be tran lated a principal cone Far cone ha been adopted by Howard (08) Acces ory con i d rived from the German wo d N benzapfen H ward p ef rs ne r cone.

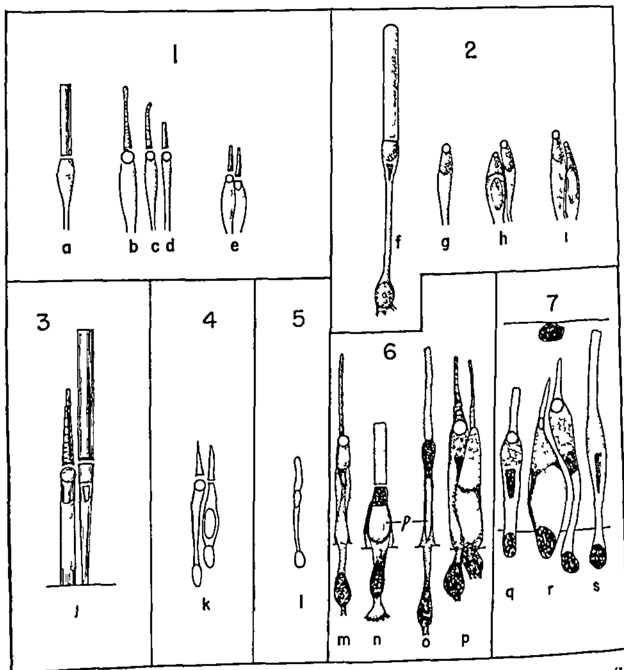


Fig 8 Visual cells of the chicken (and English sparrow) as depicted by various investigators (1) Schultze (1867) *a* rod (his fig 5a) *b c d* single cones with red or yellow oil droplets (his fig 6a) *e* double cone with yellow oil droplet in chief component and less intense yellow mass (not droplet) in accessory element (his fig 6c) (2) Hoffmann (1877) *f* rod (composite of his figs 2 and 4 with planoconvex ellipsoid and conical hyperboloid *g* single cone (his fig 33) with red or blue oil droplets *h* and *i* double cones with oval paraboloids and yellowish green droplets in the accessory components and yellow oil droplets in the chief elements (his figs 50 and 51 respectively) (3) Schultze (1872) *j* single cone with yellow oil droplet and rod with hyperboloid (his fig 324-4) (4 and 5) Detwiler (43) *k* cones (his fig 30 E) *l* rod (his fig 32 E) (6) Walls (42) *m* single peripheral cone *n* peripheral rod *o* fundal rod *p* peripheral double cone with no oil droplet in the accessory component from *Passer domesticus* (his fig 193b) Structures labeled *p* are paraboloids (7) Present investigators *q* single cone with circular red oil droplet *r* double cone with oil droplet in each component (small oval and yellowish green in accessory cone large circular and golden yellow in the chief) and large oval parabololoid in accessory cone *s* single cone with no oil droplet A conical shaped hyperboloid is present in inner segment Note that the yellow oil droplets occupy a distal row and the red droplets form a proximal layer The yellowish green droplets are intermediate in position

over 120 years ago[3] these droplets have been extensively investigated by many authors most of whom agree as do the present investigators that only three dif ferently-colored droplets exist in the chicken retina red yellow (golden) and yellowish green Colorless droplets have been repeatedly described but have not been identified with certainty in the pres ent study Because of their cytological position within the cones the oil droplets are closely related to the mitochondria which form the bulk of the ellipsoid Elec tron microscopic studies have revealed this association in the single cones of the toad (*Bufo bufo*) (Sjostrand and Elfvin 56) in single and double cones of the turtle (Yamada 60) in certain cones of a lizard (*Lacerta muralis*) and a diurnal gecko (*Phelsuma inunguis*) (Pedler and Tansley 63) and in the cones of the frog (Takayama 60 Craig et al 63)

The color of the oil droplets are due to three stable carotenoid pigments (Wald and Zussmann '37 38 Wald 48) which in appropriate solvents closely reproduce the natural color of these droplets *in vivo* Many specific carotenoids have been im plicated but only astaxanthin (red) has been adequately substantiated (Meyer et al 65)

Single cones The structure of the sin gle cones of the chicken as perceived by earlier investigators (fig 8b c d g j,m) has corresponded to the phase microscopic findings (fig 8q) The existence of a specific color (red) in the single cone oil droplet however has not been widely accepted Schultze (1867) for example noted yellow or red droplets (fig 8b c d) whereas Hoffmann (1877) maintained that oil droplets of the single cones could assume a multitude of colors According to Dobrowolsky (1871b) red droplets are confined to cones with the longest outer segments Although the single cones are the shortest oil droplet bearing elements within the chicken retina their relatively long outer segments may be those referred to by Dobrowolsky

The red droplets of the single cones lie closer to the external limiting membrane than the other droplets and consequently form a proximal layer of red spheres

Double cones The double cones were first described by Hannover (1840) they are present in all vertebrate retinas except placental mammals Schultze (1867) ex amined their morphology and structure in many vertebrates and for the most part his descriptions have remained unchal lenged up to the present time As the name implies double cones represent two intimately associated cones a chief and an accessory component[4] They should not be confused with twin cones how ever which are composed of two identical cones The significance of such multiple visual cell associations have been dis cussed by Kalberer and Pedler (63) The ories on the origin of double cones have been summarized by Lyall (57)

In the chicken the *chief* cones as dem onstrated by phase microscopy (fig 8r) resemble closely those previously illus trated by Walls (42) and other investi gators (fig 8e h k p) They are the tallest of the cones and possess the largest oil droplets The droplets are golden yel low in color and because they lie fur therest from the external limiting mem brane form the most distal row of oil droplets Yellow droplets have also been observed in these elements by earlier in vestigators (Schultze 1867 Hoffmann 1877 Krause 1894)

The *accessory* component of the double cone is characterized by the presence of a large oval glycogen-containing parabo loid which permits its selective identifica tion According to some authors (e g Rochon Duvigneaud 43) however the paraboloid represents an inclusion body within the myoid and this different inter pretation may account for the discrepan cies which exist in the literature regard ing glycogen localization within the visual cells (Compare Rabinovitch et al 54 Sidman and Wislocki 54 Matsusaka 62 O'Rahilly and Meyer 63 with Yoshi zawa 53 Kuwabara and Cogan 61) In

[3] Walls and Judd (33) st ted that Val ntin dis cov ed the oil droplet but in luded no reference Many othe uthors considered H nnover (1840) s th disc er

[4] Fo revi w see Hahn (16) Walls and Judd (33) Meyer et l (65)

Th chi f cone derives its name from the trans l tion of the original German w rd Hauptzapfen whi h can al o be transl ted a prin pal cone Far cone h s been dopted by H wa d (08) Acc ssory one is d riv d from the G rman word Nebenz pfen H ward prefers ne r c ne

routine light microscopic preparations most of the paraboloid appears structureless because of the loss of glycogen during fixation and the routine preparation of the tissue (fig 8r)

The slightly darker marginal zone around the paraboloid may be due to accumulations of ultramicroscopic tubular and vesicular elements as observed in the diurnal gecko (Pedler and Tansley 63) In the turtle paraboloid this region contains a three dimensional tight network of concentrically arranged tubules each measuring approximately 80 mμ in diameter (Yamada 60) particles approximately 35 mμ occur between these tubules At the margin of the paraboloid some of the tubules become continuous with the rough surfaced endoplasmic reticulum which surrounds this body Because of this association Yamada (60) has regarded the paraboloid tubules as part of the endoplasmic reticulum and believes that they are concerned with glycogen metabolism According to Yamada the lighter central portion of the turtle paraboloid contains a higher concentration of glycogen than the marginal zone In the electron microscope the latter consists of an accumulation of particles between 35 and 100 mμ in diameter

In the chicken paraboloid which Takayama (60) describes as being made up of an accumulation of smooth surfaced endoplasmic reticulum the fine structure of the glycogen has been shown to be influenced by the conditions of light (Yamada 63) In light adapted retinas the glycogen consists of a membrane system of a reticulum 50 to 70 A in thickness and many dense granules 190 to 400 A in size whereas in dark adapted retinas the dense granules become amorphous and the matrix increases in width Pedler and Tilly (64) report a marked difference in the fine structure of paraboloids in diurnal and nocturnal geckos

Many functions have been attributed to the paraboloid e g a reflector apparatus (Muller 26 Saxén 55) a nutrient reserve for the contractile myoid (Schmitz Moormann 27) vision (Yamada 60 Matsusaka 63)

In contrast to the majority of contemporary authorities (Walls 42 Rochon Duvigneaud 43 Detwiler 43 Prince 56 Duke Elder 58) who accept the descriptions of Schultze and therefore deny the existence of oil droplets within the accessory cones of the chicken our observations substantiate the earlier studies of Dobrowolsky (1871a), Hoffmann (1877) (fig 8h i) and Krause (1894) that such droplets do indeed exist We always find them to be yellowish green in color oval in shape smaller than the other droplets and to be a constant anatomical feature of the accessory cone (fig 8r) They also come to form an intermediate oil droplet layer within the visual cell layer of the retina because of the relative height of their carriers the accessory cones The smallness of this droplet was likewise reported by Dobrowolsky (1871a) who maintains however that its size varies with the age of the cone he also describes some double cones with similar size droplets in each component, and like Krause (1894) some accessory cones with no droplets Krause maintains that pale blue* light yellow, or colorless droplets are also present in some accessory cones Schultze (1867) denies the existence of a discrete oil droplet in the accessory cone but maintains that a conical shaped yellow mass occupies a similar location its distal surface forms the boundary toward the outer segment and its proximal parabolic surface projects into the inner segment (fig 8e) Later he refers to the latter as an ellipsoidal lentiform body which differs from the oil droplets in form and refractive power (Schultze 1872)

Verification of these data requires electron microscopic examination which unfortunately has been greatly hindered by the lack of reliable light microscopic descriptions and supporting photomicrographs Existing electron microscopic studies have failed to acknowledge oil droplets in the accessory cones of the Great Tit (*Parus major*) (Engstrom 58) and frog (*Rana pipiens*) (Nilsson 64) whereas in the turtle (species not given) Yamada (60) has presented electron micrographic evidence of its existence (see his fig 12)

---

* It is now generally agreed that the blue color observed by past authors was due to poor optical lenses and does not occur as such

The ease with which the two portions of the double cone can be separated in teased preparations has provided strong evidence that in the chicken retina at least these components are not intimately fused Electron microscopic studies of the double cones of *Bufo bufo* on the other hand indicate a more intimate union the contiguous plasma membranes being similar to those seen at retinal synaptic contacts (Sjostrand and Elfvin 56) Likewise in some fish press button like formations in the cell membrane along the whole contact surface serve to join the two components (Engstrom 63)

ACKNOWLEDGMENT

The authors gratefully acknowledge the excellent technical assistance of Mrs Celina Gernez

LITERATURE CITED

Carleton H M and R A B Drury 1958 Histological technique Third edition Oxford University Press London

Chesterman W and E H Leach 1958 A bleaching method for melanin and two staining methods Quart J Micr Sci 99 65–66

Craig E L J A Eglitis and D G McConnell 1963 Observations on the oil droplets of the principal cone cells of the frog retina Exp Eye Res 2 268–271

Detwiler S R 1943 Vertebrate photoreceptors Macmillan New York

Dobrowolsky W 1871a Die Doppelzapfen Arch f Anat Physiol und wissen Med 38 208–220

——— 1871b Zur Anatomie der Retina Arch f Anat Physiol und wissen Med 38 221–236

Duke Elder S 1958 System of ophthalmology In The Eye in Evolution Mosby St Louis

Engstrom K 1958 On the cone mosaic in the retina of Parus major Acta Zool 39 65–69

——— 1963 Structure organization and ultra structure of the visual cells in the teleost family Labridae Acta Zool 44 1–39

Feder N and R L Sidman 1958 Methods and principles of fixation by freeze substitution J Biophys Biochem Cytol 4 593–602

Hahn E 1916 Über den Farbensinn der Tagvogel und die Zapfenolkugeln Z wiss Zool 116 1–42

Hannover A 1840 Ueber die Netzhaut und ihre Gehirnsubstanz bei Wirbelthieren mit Ausnahme des Menschen Arch f Anat Physiol und wissen Med pp 320–345

Hoffmann C K 1877 Zur Anatomie der Retina III Über den Bau der Retina bei den Vogeln Niederl Arch f Zool 3 217–233

Howard A D 1908 The visual cells in vertebrates chiefly in Necturus maculosus J Morph 19 561–631

Kalberer M and C Pedler 1963 The visual cells of the alligator an electron microscopic study Vision Res 3 323–329

Krause W 1894 Die Retina V Die Retina der Vogel Internat Monatschr f Anat und Physiol 11 1–66

Kuwabara T and D G Cogan 1961 Retinal glycogen Arch Ophthalmol 66 680–688

Lyall A H 1957 Cone arrangements in teleost retinae Quart J Micr Sci 98 189–201

Matsusaka T 1962 Histochemical studies on chick retinal glycogen Jap J Ophthalmol 6 202–209

——— 1963 Electron microscopic observations on cytology and cytochemistry of the paraboloid glycogen of chick retina Jap J Ophthalmol 7 238–253

Meller K 1964 Elektronenmikroskopische Befunde zur Differenzierung der Rezeptorzellen und Bipolarzellen der Retina und ihrer synaptischen Verbindungen Z Zellforsch 64 733–750

Meller K and W Breipohl 1965 Die Feinstruktur und Differenzierung des inneren Segmentes und des Paraboloids der Photorezeptoren in der Retina von Huhnerembryonen Z Zellforsch 66 673–684

Meller K and P Glees 1965 The differentiation of neuroglia Muller cells in the retina of chick Z Zellforsch 66 321–332

Meyer D B T G Cooper and C Gernez 1965 Retinal oil droplets Second Symp Structure of the Eye J W Rohen Ed Schattauer Verlag Stuttgart pp 521–533

Muller C 1926 Das Glykogen der Retina des Frosches Z Anat Ent 81 220–238

Nilsson S E G 1964 An electron microscopic classification of the retinal receptors of the leopard frog (*Rana pipiens*) J Ultrastruct Res 10 390–416

Okuda K N Matsuo S Kitajima H Aono K Takayama A Yokoyama and S Kunimitsu 1961 Electron microscopic observations of the vertebrate retina Acta Soc Ophthal Jap 65 2126–2151

O'Rahilly R and D B Meyer 1963 Étude histologique et histochimique des cellules visuelles de la retine du poulet Ann Histochim 8 281–282

Pedler C and K Tansley 1963 The fine structure of the cone of a diurnal gecko (*Phelsuma inunguis*) Exp Eye Res 2 39–47

Pedler C and R Tilly 1964 The nature of the gecko visual cells A light and electron microscopic study Vision Res 4 499–510

Prince J H 1956 Comparative anatomy of the eye Thomas Springfield

Rabinovitch M J Mota and S Yoneda 1954 Note on the histochemical localization of glycogen and pentosepolynucleotides in the visual cells of the chick (*Gallus gallus*) Quart J Micr Sci 95 5–10

Ritter C 1891 Studien uber die Stabchenschicht der Vogel Internat Monatschr f Anat Physiol 8 241–249

Rochon Duvigneaud A 1943 Les yeux et la vision des vertebrés Masson Paris

Saxen L 1955 The glycogen inclusion of the visual cells and its hypothetical role in the

photomechanical responses Histochemical investigation during frog ontogenesis Acta Anat 25 319–330
Schmitz Moormann P 1927 Ueber den Glykogengehalt der Retina und seine Beziehungen zur Zapfenkontraktion Graefe s Arch Ophthalmol *118* 506–517
Schultze M 1866 Zur Anatomie und Physiologie der Retina Arch mikr Anat 2 175–286
——— 1867 Ueber Stabchen und Zapfen der Retina Arch mikr Anat *3* 215–245
——— 1872 The organ of vision I The retina In Stricker s Manual of Histology (trans by H C Eno) Wm Wood and Company New York
Sidman R L and G B Wislocki 1954 Histochemical observations on rods and cones in retinas of vertebrates J Histochem Cytochem 2 413–433
Sjöstrand F S and L G Elfvin 1956 Some observations on the structure of the retinal receptors of the toad eye as revealed by the electron microscope Proc Stockholm Conf on Elect Microsc pp 194–196
Takayama T 1960 Comparative anatomy of vertebrate visual cells by electron microscopy I Acta Soc Ophthalmol Jap *64* 1310–1319
Uchiyama T 1930 Beitrage zur Morphologie des Lipoidstoffwechsels III Über die Öltropfen und Glykogengebilde in den Sehzellen der Netzhaut des Haushuhns Virchow s Arch path Anat 277 631–641
Waelchli G 1883 Zur Topographie der gefärbten Kugeln der Vogelnetzhaut Graefe s Arch Ophthalmol 29 205–229
Wald G 1948 Galloxanthin a carotenoid from the chicken retina *J gen Physiol 31* 377–383
Wald G and H Zussmann 1937 Carotenoids of the chicken retina Nature *140* 197
——— 1938 Carotenoids of the chicken retina J Biol Chem *122 449–460*
Walls G L 1942 The vertebrate eye and its adaptive radiation Cranbrook Inst Science Cranbrook Michigan
Walls G L and H D Judd 1933 The intraocular filters of vertebrates Brit J Ophthalmol *17* 641–675 705–725
Wolken J J 1958 Studies of photoreceptor structures Ann *N Y Acad Sci 74* 164–181
Yamada E 1960 Observations on the fine structure of photoreceptive elements in the vertebrate eye J Electronmicroscopy *9* 1–14
Yasuzumi G *O Tezuka and* T Ikeda 1958 The submicroscopic structure of the inner segments of the rods and cones in the retina of *Uroloncha striata* Var *domestica* Flower J Ultrastruct Res *1* 295–306
Yoshizawa K *1953 Glycogen* in the retina Acta Soc Ophthalmol Jap 57 783–797

Deviations in the Sequence of Appearance of Primary Centers of Ossification in the Feet of Human Fetuses with Cleft Lip and/or Palate[1]

BERTRAM S KRAUS AND SUZANNE AHERN
Cleft Palate Research Center and School of Medicine
University of Pittsburgh Pittsburgh Pennsylvania

ABSTRACT The feet of 35 human fetuses with cleft lip and/or palate and 208 human fetuses without cleft lip or palate were cleared and stained and their conformity to the "normal" sequence of appearance of the primary centers of ossification in the 19 post tarsal bones was noted An arbitrary definition of a significant deviation from the normal sequence was established and a system of evaluating the relative severity of deviations was set up The relative number of cleft fetuses showing deviations from the accepted sequence (42 9%) was significantly higher than of non-cleft fetuses (10 6%) The cleft and non-cleft deviant fetuses were not significantly different in relative severity There was no difference between the two series in the relative frequency with which specific bones were affected In each series the fifth distal phalanx was most frequently affected In both series deviations in the order of initial ossification more frequently involved the seventh to tenth phalanges in the sequence Asymmetry was of common occurrence in deviants of both the cleft and non-cleft series There was no significant difference in the number of deviant centers per fetus in the cleft and non-cleft series

The biological mechanisms underlying the orderly and regular sequence of appearance of ossification centers in the foot are not known hence the nature of the interference with the "normal" sequence cannot be described

Chronological timetables and sequences of initial ossification of epiphyses and diaphyses of the various units of the appendicular skeleton have been established because of the apparent regularity with which these phenomena occur (Krogman 62) The initial ossification of the diaphyses of the 14 phalanges and five metatarsals of the human foot begins at about 9 ± 1 weeks and is completed at about 18 ± 1 weeks The order in which this process is initiated in the 19 bones was first described by Mall (06) and later by Frazer (46) Wood Jones (49) Noback and Robertson (51) and Kraus (61)

Mall s interpretation of the sequence of initial ossification and that of Noback and Robertson are in agreement They postulated that the sequence began with the first metatarsal and spread laterally to the fifth The next (sixth) center to appear was the first distal phalanx followed by the second third fourth and fifth in that order The proximal phalanges appeared next in the same regular sequence from 1 to 5 The intermediate phalanges from 2 to 5 completed the sequence Mall s sequence was based upon 16 cleared and stained human fetuses ranging in age from 11 to 14 weeks hence he lacked data on early and late stages of initial ossification Noback and Robertson cleared and stained 95 fetuses in the age range 9 to 18 weeks and found themselves in agreement with Mall s sequence In a study of 138 human fetuses Kraus (61) derived a different sequence Tate (61) compared the Mall sequence with the Kraus sequence and found on the basis of a rank-order statistical technique that the probability of the Kraus sequence not being the true one was less than 0 002

The sequence proposed by Kraus is illustrated in figure 1 It differs from the Mall sequence in that the first of the 19 bones to ossify is the first distal phalanx followed by the second third fourth first and fifth metatarsals in that order In addition the third distal phalanx begins to ossify before the second distal phalanx

[1] This research w s supported in p rt by grant DE01697 f om the N tional Institut of Dent l Re- arch and by th Medical Student Research Training Program grant 1SO1FR-5416-04-5

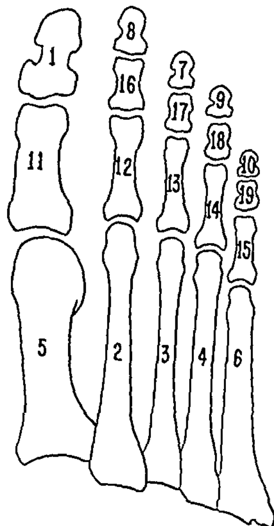


Fig 1 The sequence of appearance of primary centers of ossification of the human foot (after Kraus 61)

Otherwise the sequence is the same as that of Mall

The question posed in this paper is in fetuses of a known pathology are there significant deviations from the sequence thus established? In other words can the sequence of appearance of primary centers of ossification of the diaphyses of the foot be demonstrated to be significantly associated with a known pathologic entity? Since both the Mall and the Kraus sequences are characterized by deviant forms it would be necessary to determine if a pathologic series of fetuses produced a significantly higher number of deviant specimens than a non pathologic series

The pathologic fetal series studied in this investigation consisted of fetuses with cleft lip and/or palate Since previous studies had demonstrated that significantly greater numbers of such fetuses possessed abnormalities of external structures (Kraus Kitamura and Ooe 63) viscera (Kitamura and Kraus 64) and dental morphological features (Jordan Kraus and Neptune 65) it seemed logical to determine if the spectrum of associated malformations and defects extended to growth phenomena such as the order of development of the osseous system as expressed in the sequence of appearance of primary centers of ossification in the diaphyses of the foot This paper presents the results of this investigation

METHOD AND MATERIALS

The feet of 35 cleft palate human fetuses ranging in age from 9 to 17 weeks were cleared and stained with alizarin red S The feet of 70 non cleft fetuses were similarly treated to use as a control series For each cleft specimen two non-cleft fetuses of approximately the same age were selected Race and sex were ignored in obtaining the samples The distribution of the cleft sample according to crown rump length and fertilization age is presented in table 1

TABLE 1
Crown rump length of the cleft series (n = 35)

Crown rump length (in mm)	Number of fetuses
36–48	5
47–58	5
59–71	8
72–85	4
86–99	2
100–113	3
114–127	4
128–141	2
142–154	2

A collection of 138 non cleft fetuses previously reported (Kraus 61) was also utilized in this study The clearing and staining method has been described by Noback and Noback (44) and Kraus (61) Examination of each fetus for presence or absence of bony centers was made by means of a stereoscopic dissecting microscope at a magnification of 25 ×

A deviation was defined as follows Any specimen in which the number of ossified centers present conforms to the sequence shown in figure 1 is *normal* A fetus in

which only the center *immediately preceding* the last ossified center present is not ossified is judge a *variant* A fetus in which one (or more) unossified centers *precede the last two ossified* centers present is termed a *deviant* and is considered abnormal The reason for eliminating *variant* specimens from the abnormal classification is that if only one unossified center *immediately* precedes the last ossified center present in a given fetus then the possibility exists that had the fetus lived this center might have been the next to ossify In other words any two adjacent centers (in terms of sequential order) could conceivably be interchanged in the order of initial ossification However if a center remains unossified after the next two centers have initiated ossification this condition has been regarded as significantly deviant hence abnormal

RESULTS

The deviants found in both cleft and control series were arranged on a graph in order of the last center present in the sequence (fig 2) Among the 35 cleft fetuses 15 were found to be deviants as defined above In the two control series (n = 70 and n = 138) there were 22 deviants The percentage of deviant specimens in the cleft series was 42 9% in the control series 10 6% A Chi Square test applied to this difference gave a value of 21 76 and a probability of less than 0 001 that this difference was due to chance The non-cleft series of 70 which approximated the cleft series in age categories and hence afforded a less biased sample was compared with the cleft series according to the position of the last bony center present in the sequence regardless of whether or not earlier centers were present or absent

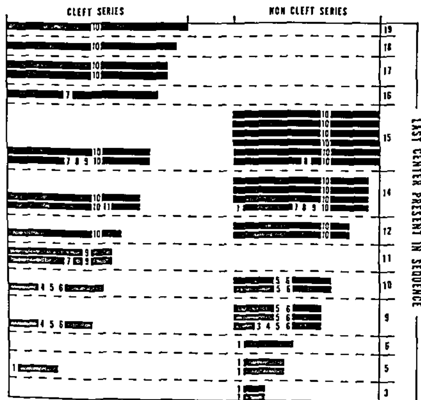


Fig 2 Centers of ossification absent in the diaphyses of the feet of cleft (n = 15) and non-cleft (n = 22) human fetuses

(table 2) The control series yielded six deviant specimens or 8 6% The difference between the cleft and non cleft series was highly significant (Chi Square = 15 1 with Yates correction factor, P < 0 001) It is therefore quite apparent that in cleft lip and/or palate fetuses the number of specimens in which the sequence of appearance of primary centers of ossification is disturbed is significantly higher than in a non cleft series of fetuses

The nature of the deviations was next investigated to determine if qualitatively there was a difference between cleft and non cleft fetuses The deviant cases in the two series are shown in histographic form in figure 2 The solid lines indicate presence of bony centers, the empty spaces, each filled with the number of the corresponding center indicate no ossification of those centers Although the biological processes involved in the regulation of sequential appearance of bony centers are unknown it is suggested that the severity of the disturbance of this process would be in direct ratio to the number of bony centers missing In addition it was thought reasonable to suppose that the earlier in the sequence these absences occurred the more certain and more severe the disturbance must have been An example of how relative degree of severity was assessed can be provided by comparing specimen no X–478 in the cleft series and no C–38 in the non-cleft series (fig 2) In each case, the last center of ossification present in the sequence is the fourteenth (the fourth proximal phalanx) In no X–478 the tenth and eleventh centers have not begun ossification in no C–38 however, the first seventh eighth ninth and tenth diaphyses are still completely cartilaginous

The maximum severity of deviation was computed by summing the consecutive positions beginning with the *next to the last bony center present* and evaluating it as zero The center immediately before zero was evaluated as 1 the center before that as 2 etc back to the first center to appear (the first distal phalanx) An example using no X–478 is the following

Evaluation	12	11	10	9	8	7	6	5	4	3	2	1	0	
Sequence	1	2	3	4	5	6	7	8	9	10	11	12	13	14

TABLE 2

Comparison of the cleft with the non-cleft fetuses matched according to the last bony center present in the sequence

Last bony center present in sequence	Cleft series		Non-cleft series	
	Total no	No of deviants	Total no	No of deviants
1	2	0	3	0
2	1	0	3	0
3	0	0	0	0
4	1	0	2	0
5	1	1	3	0
6	0	0	4	0
7	0	0	3	0
8	0	0	2	0
9	1	1	7	1
10	10	1	7	1
11	4	2	9	0
12	1	1	2	0
13	0	0	1	0
14	3	2	5	3
15	4	2	7	1
16	3	1	8	0
17	2	2	2	0
18	1	1	2	0
19	1	1	0	0
Totals	35	15	70	6

Since the last bony center present in the sequence is no 14 counting backward with no 13 as zero we obtain the following sum $0 + 1 + 2 + 3 + 4 + 5 + 6 + 7 + 8 + 9 + 10 + 11 + 12 = 78$ The maximum severity would therefore be 78 if the last ossified center present happens to be the fourteenth in the sequence In this particular case maximum severity could only be realized if all the bony centers were absent except for the thirteenth and fourteenth

The *actual* severity of deviation for no X-478 can be computed by adding the evaluations for those positions in which the bony centers are indeed absent In this case positions 10 and 11 (fifth distal phalanx and first proximal phalanx) have not begun ossification hence the actual severity is the sum of the two separate evaluations or $3 + 2 = 5$ The *relative* severity is obtained by dividing the actual severity (5) by the maximum severity (78) which is in this case 0 06 For no C-38 the relative severity rating would be $\frac{12+6+5+4+3=30}{78} = 0\ 38$ It can be justly argued that a rating of for example 0 06 (5/78) could be achieved in another way if only one center (no 8) were not ossified The question then arises is the absence of one unossified center (no 8) more or less severe than the absence of two centers (no 10 and no 11)? It might be suggested that the absence of *one* center *early* in a sequence is as severe as the absence of *two* centers *later* in the sequence There is however no way of establishing this point The advantage of this method is that it permits comparison between fetuses in different stages of ossification

Relative severity ratings for both cleft and non-cleft deviant specimens are presented in table 3 Since both actual severity ratings and maximum severity ratings are additive total relative severity ratings of 0 077 for the cleft series and 0 105 for the non-cleft series are obtained A Chi Square value of 0 58 is derived from a comparison of the two series yielding a probability of over 0 30 that the difference is due to chance This may be interpreted to mean that the degree of severity of deviation from the normal sequence is not significantly different in cleft and non-cleft fetuses

Examination of the graph presented in figure 2 reveals a number of points of interest with regard to specific centers affected The first distal phalanx which is normally the first center to commence ossification may remain unossified when even the sixth bony center is present There is one specimen (no C-38) however in which the first center was still unossified even though the fourteenth center had commenced to ossify In all 37 deviant specimens the second center (second metatarsal) to ossify was present indicating an apparent stability of this center with regard to the order of ossification All other centers up to and including the eleventh in the sequence may be affected There was no case however in which any center in the sequence after no 11 was not present when it should have been A summary of the relative number of times each bone was affected is presented in table 4 It is readily seen that in both cleft and non-cleft deviants the fifth distal phalanx (tenth in the sequence) is most frequently unossified In the cleft series out of ten deviants in which the fifth distal phalanx could have been affected nine actually showed it to be unossified Out of 12 deviants in the non cleft series in which more than ten centers were present the fifth distal phalanx was unossified in all 12 cases In the cleft series the next most common deviant units were the third and fourth distal phalanges In the non-cleft series the first distal phalanx and first and fifth metatarsals were the next most common deviant units Further examination of figure 2 seems to suggest a pattern wherein absent bony centers appear to begin ossification after the succeeding 5 or 6 centers have begun to ossify Examination of table 2 reveals that deviants in both cleft and non cleft fetuses are more apt to be found in the last half of the ossification sequence In other words the frequency of deviants in the 25 cases where ossification had not proceeded beyond the eighth center in the sequence (second distal phalanx) was 4% but in the 80 cases in which ossification had proceeded beyond this point the frequency of deviants was 25% The differ

TABLE 3

Relative severity values for cleft and non-cleft fetuses

Specimen no	No of deviant centers	Actual severity / Maximum severity	Relative severity rating
		Cleft fetuses (n = 15)	
W 307	1	(3) = 3/6	0 50
X 2466	3	(2+3+4) = 9/28	0 32
X 3079	3	(3+4+5) = 12/36	0 33
X 2462	2	(1+3) = 4/45	0 09
J 20	1	(1) = 1/45	0 02
X 2139	1	(1) = 1/55	0 02
X 158	1	(3) = 3/78	0 04
X-478	2	(2+3) = 5/78	0 06
Q-3	4	(4+5+6+7) = 22/91	0 24
X-834	1	(4) = 4/91	0 04
X 3688	1	(8) = 8/105	0 08
Q 13	1	(6) = 6/120	0 05
X 3234	1	(6) = 6/120	0 05
X 599	1	(7) = 7/136	0 05
X 193	1	(8) = 8/153	0 05
Totals	24	99/1187	0 083
		Non cleft fetuses (n = 22)	
X-400	1	(1) = 1/1	1 00
X-395	1	(1) = 1/1	1 00
X-415	1	(3) = 3/6	0 50
W 52	1	(3) = 3/6	0 50
X 503	1	(4) = 4/10	0 40
X 1919	4	(2+3+4+5) = 14/28	0 50
X 516	2	(2+3) = 5/28	0 18
X 366	2	(2+3) = 5/28	0 18
X 75	2	(3+4) = 7/36	0 19
C 136	2	(3+4) = 7/36	0 19
X 62	1	(1) = 1/55	0 02
134	1	(1) = 1/55	0 02
C 38	4	(3+4+5+6) = 18/78	0 23
47	1	(3) = 3/78	0 04
W 24	1	(3) = 3/78	0 04
39	1	(3) = 3/78	0 04
W 30	2	(4+6) = 10/91	0 11
33	1	(4) = 4/91	0 04
42	1	(4) = 4/91	0 04
81	1	(4) = 4/91	0 04
141	1	(4) = 4/91	0 04
153	1	(4) = 4/91	0 04
Totals	33	109/1148	0 095

ence was significant at the 5% level of probability The present sample however is too small to permit further investigations of this nature

Right and left asymmetry was of rather common occurrence in both cleft and non-cleft fetuses Among the deviant cleft fetuses there was a total of 24 missing bony centers of which six were unilaterally missing Among the deviant non cleft fetuses 5 out of 34 missing bony centers were unilateral A Chi Square test shows no significant difference between the two series in asymmetry When amount of asymmetry expressed in all the various centers present is computed out of 182 pairs of bony centers *missing or present* in the 15 cleft deviant specimens there were 14 cases of asymmetry or 7 7% In the 22 non cleft deviant specimens nine out of 203 pairs of centers were asymmetrical or 4 4% In the results reported above a unilateral absence of a bony center was considered to be a deviant form

TABLE 4

Relative frequencies of bones affected in deviant cleft and non-cleft fetuses

		Clefts (n = 15)		Non-clefts (n = 22)	
Sequence	Bone	Relative number of deviant specimens affected	Frequency	Relative number of deviant specimens affected	Frequency
			%		%
1	1st distal phalanx	1/15	7	6/22	27
2	2nd metatarsal	0/15	0	0/20	0
3	3rd metatarsal	0/15	0	1/20	5
4	4th metatarsal	2/15	14	1/18	6
5	1st metatarsal	2/14	14	5/17	29
6	5th metatarsal	2/14	14	5/17	29
7	3rd distal phalanx	3/14	21	1/17	6
8	2nd distal phalanx	1/13	8	2/14	14
9	4th distal phalanx	3/12	25	1/12	8
10	5th distal phalanx	9/10	90	12/12	100
11	1st proximal phalanx	1/9	11	0/10	0

even though the opposite foot showed the presence of a bony center in the corresponding unit Similarly when the fetuses were classified according to last bony center present in the sequence they were so classified whether the center was present unilaterally or bilaterally

There was no significant difference between the cleft and non-cleft deviant fetuses in the number of missing bony centers per fetus

DISCUSSION

It is becoming increasingly clear that both in its prenatal and postnatal expressions cleft lip and/or palate is not an isolated malformation Almost always in the fetus and frequently in the infant the defect is associated with diverse teratologic effects throughout the body These effects are not limited to any specific tissue derivatives nor to specific organs or structures but apparently *may occur in any combination* (Kraus Kitamura and Ooe 63 Kitamura and Kraus 64 Jordan Kraus and Neptune 65) There is no set pattern that can thus far be ascertained From a non-clinical point of view *there is no* reason for regarding the cleft itself as of special significance in the constellation of malformations and defects that affect the fetus

In the present investigation an additional parameter has been added to the range of abnormalities that are associated with cleft lip and/or palate fetuses The ordering of a growth phenomenon deviated from normal and regular sequence The departure from the usual sequence of appearance of bony centers in the foot among cleft fetuses is significantly more frequent than in non-cleft fetuses although deviations do occur in both groups A similar difference in frequency had previously been demonstrated in abnormalities of dental morphology external structural features and the various internal organs There are no *unique* abnormalities in cleft fetuses only *more of them*

These findings cannot be interpreted as yet in terms of biological processes or etiological factors

LITERATURE CITED

Frazer J 1946 The anatomy of the human skeleton 4th ed J and A Churchill Ltd London

Jordan R B Kraus and C Neptune 1965 Dental abnormalities associated with cleft lip and/or palate To appear in Cleft Palate J 1966

Kitamura H and B Kraus 1964 Visceral variations and defects associated with cleft lip and palate in human fetuses a macroscopic description Cleft Palate J *1* 99–115

Kraus B 1961 Sequence of appearance of primary centers of ossification in the human foot Am J Anat *109* 103–116

Kraus B H Kitamura and T Ooe 1963 Malformations associated with cleft lip and palate

in human embryos and fetuses Am J Obst and Gynec 86 321–328
Krogman W 1962 The human skeleton in forensic medicine 1st ed Charles C Thomas Illinois
Mall F 1906 *On ossification centers in human embryos less than one hundred days old* Am J Anat 5 433–458
Noback C and E Noback 1944 Demonstrating the osseous skeleton of human embryos and fetuses Stain Tech *19* 51–54
Noback C and G Robertson 1951 Sequenc of appearance of ossification centers in t human skeleton during the first five prena months Am J Anat *89* 1–28
Tate R 1961 *On the use of partially order observations in measuring the support for* complete order J Am Stat Assoc, 56 29 313
Wood Jones F 1949 Structure and functi as seen in the foot 2nd ed Bailliere Tind and Cox, London

Embryonic Modifications of Lacertilian Intracranial Arteries [1]

DORIS J BURDA
Department of Anatomy Stanford University School of Medicine Stanford California

ABSTRACT Intracranial arteries were studied in *Crotaphytus* adults and in a series of *Lacerta* embryos At an early embryonic period the mesencephalic artery develops posterior to the bifurcation of the cerebral carotid as the pontine flexure forms at a subsequent stage the carotid bifurcation becomes relocated further posteriorly with the result that the definitive mesencephalic artery becomes an outgrowth of the anterior encephalic artery Additional significant modifications include the progressive fusion of the two posterior encephalic arteries and the extensive branching of the middle cerebral artery along the lateral regions of the hemisphere During late stages of development the circulation to the olfactory region is gradually assumed by extracranial arteries although remnants of intracranial olfactory arteries may occasionally be retained

The lacertilian intracranial arterial system has been studied primarily in the adult condition (Corti 1847 Rathke 1857 Hofmann 00 Beddard 05 Hochstetter 06 Shindo 14 Bhatia and Dayal 33) Although references to a few *Lacerta* embryos can be found in the works of Rathke (1857) and Hochstetter (06) the only substantial ontogenetic account is that of Hafferl (20) on the gecko *Platydactylus annularis* in which emphasis is placed however on the extracranial vessels and only a minor account is given of the intracranial vasculature In the present study transformations in the intracranial pattern have been traced through successive embryonic stages of *Lacerta muralis* and particular attention has been given to concurrent changes in the development of the brain A description of the adult intracranial arteries of *Crotaphytus collaris* is also included for purposes of comparison

MATERIALS AND METHODS

The brains of three single injected adults of *Crotaphytus collaris* were removed and examined Since few of the intracranial arteries could be observed macroscopically the major portion of the vascular pattern was studied by means of a dissecting microscope at magnifications ranging from 25× to 60 ×

Serial sections of 16 *Lacerta muralis* embryos and of one *Lacerta agilis* embryo were obtained from the Minot Embryological Collection of the Harvard Medical School These embryos ranged in body length from 2 0 mm to 10 0 mm and are listed in table 1 The embryos were arbitrarily grouped into three developmental stages on the basis of the degree of brain development Studies were then made of serial sections in sagittal transverse and frontal planes at magnifications ranging from 17 5 × to 430 × Graphic reconstructions of representatives of each stage were made by tracing images projected onto transparent paper by means of a Promi projection microscope

Bilateral comparisons were made of the intracranial vasculature in each individual For the most part relatively little difference could be observed between the right and left sides thus only the right side of an individual will be described except where otherwise noted

OBSERVATIONS AND RESULTS

Adult

The pattern of intracranial arteries in the adult *Crotaphytus collaris* agrees rather closely with that found in the genera used in the works cited above The internal carotid artery travels through a canal in the floor of the basisphenoid bone and approaches the region of the pituitary

[1] A portion of a th sis pre ent d at Harvard Unive ity in partial fulfillment of requirements for th Ph.D degree

TABLE 1

Lacerta muralis and Lacerta agilis embryos from the Minot Collection The following abbreviations are used for stains listed in column 5 AC Alum cochineal BC Borax carmine E Eosine LB Lyons blue OG Orange G

Minot series number	Length	Plane	Thickness	Stain
	mm		μ	
Lacerta muralis				
907	2 0	trans	6	BC and LB
859	4 5	sag	6	BC and OG
861	4 6	trans	6	BC and LB
858	4 8	trans	6	BC and LB
726	5 0	trans	8	AC and OG
733	5 0	front	8	BC and LB
853	5 2	trans	6	BC and LB
813	6 4	trans	10	AC and OG
814	6 4	sag	10	AC and E
827	6 4	trans	8	AC and OG
812	7 4	trans	10	AC and OG
810	7 8	sag	10	AC and E
1602	9 0	trans	8	AC and OG
603	9 8	sag	10	AC and E
1603	9 9	sag	10	AC and E
1604	10 0	front	10	AC and OG
Lacerta agilis				
609	3 6	sag	8	AC and LB

fossa Just before entering the cranial cavity the carotid gives rise to a fairly large branch the nasopalatine artery (fig 1) This branch passes laterad through a foramen in the anterolateral wall of the canal and then sends branches to the floor of the orbit, the nasal region and the palate Beyond the origin of the naso palatine artery the internal carotid enters the intracranial cavity and travels antero dorsally alongside the hypophysis No post hypophyseal anastomosis could be found between the two internal carotids The intracranial portion of the internal carotid will hereafter be designated as the cerebral carotid which then divides into an anterior and a posterior encephalic artery

Anterior encephalic artery

The anterior encephalic artery proceeds dorsally and passes medial to nerve III Immediately anterior to the origin of this nerve a large mesencephalic artery is sent dorsad along the posterolateral convexity of the optic lobe The mesencephalic artery distributes numerous vessels over the lateral regions of the lobe as well as

EXPLANATION OF FIGURES

Continuous line unshaded vessels lie medially and are not visible in lateral view broken line vessels represent corresponding structures of the opposite side

Abbreviations

A Cer Anterior cerebral
A Com Anterior communicating
A Enc Anterior encephalic
A Orb Anterior orbital
Bas Basilar
C C Cerebral carotid
I Aud Internal auditory
Inf Infundibular
L Chor Lateral choroidal
M Cer Middle cerebral
M Olf Medial olfactory
Mes Mesencephalic
N Pal Nasopalatine
Oph Ophthalmic
Orb Orbital
P Cer Posterior cerebral
P Enc Posterior encephalic
Sp 1 First spinal
Trig Trigeminal
V Sp Ventral spinal

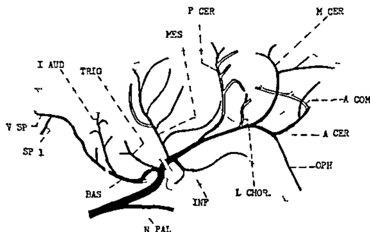


Fig 1 Lateral view of brain in *Crotaphytus collaris* adult

a few rami to the cerebellum These cerebellar rami generally pass into the fissure between the optic lobe and cerebellum and continue along the anterior concavity of the latter

Very close to the origin of the mesencephalic artery the anterior encephalic gives rise to the infundibular artery which sends small posteroventral branches to the infundibulum and which eventually ends at the base of the optic chiasma In one specimen the infundibulum was supplied by a branch which arose independently from the cerebral carotid artery

The anterior encephalic artery next sends off the large posterior cerebral artery which travels anterodorsally and somewhat parallel to the anterior encephalic At the anteroventral rim of the optic lobe the posterior cerebral turns abruptly dorsad and disappears into the fissure between the optic lobe and cerebral hemisphere The posterior cerebral passes dorsally within this fissure supplies a series of small twigs to the parietal organ and eventually ends in the choroid plexus of the third ventricle A few branches may also be sent anteriorly into the lateral choroid plexus

After giving rise to the posterior cerebral artery the anterior encephalic continues anterodorsally At the level of the optic nerve two arteries are given off quite close to each other The smaller artery the lateral choroidal passes medially under the ventral pole of the hemisphere and then turns dorsad through the foramen of Monro and into the lateral choroid plexus The larger artery is the middle cerebral which travels dorsolaterally over the lateral face of the hemisphere supplying it with a large network of vessels An anterior ramus of this artery also passes onto the lateral region of the olfactory lobe

Beyond the origin of the middle cerebral the anterior encephalic (anterior cerebral) turns slightly ventrad toward nerve II and sends off the ophthalmic artery which travels with the nerve through the optic foramen to the eye The subsequent course of the ophthalmic artery was not followed

The anterior cerebral artery travels medially along the anterior rim of the optic chiasma and gives off a fairly large lateral branch to the anterolateral surface of the hemisphere In one specimen the anterior cerebral next gave rise to a slender medial olfactory artery accompanying nerve I However since the supraorbital branch of the facialis artery sends numerous branches to this area the olfactory nerves very likely receive only small amounts of blood via intracranial olfactory arteries

The anterior cerebral continues medially and disappears into the median fissure between the cerebral hemispheres This vessel then unites with its counterpart from the other side to form the anterior communicating artery which is contained

wholly within the intercerebral fissure and which is thus not visible from a ventral view of the brain This fusion completes the circle of Willis anteriorly The anterior communicating artery then extends dorsocaudally between the hemispheres and eventually bifurcates into two vessels which end in a series of small twigs to the posteromedial face of each hemisphere

Posterior encephalic artery

The posterior encephalic extends caudad from the bifurcation of the cerebral carotid Almost immediately a trigeminal artery is sent posterodorsally toward nerve V In one of the specimens two trigeminal arteries were sent off one from the bifurcation and the other from the posterior encephalic

The posterior encephalic next turns mediad and fuses with the corresponding artery of the other side to form the basilar artery thus completing posteriorly the circle of Willis In one instance the basilar became double near the origin of nerves VII–VIII and then fused again just anterior to the foramen magnum

The basilar supplies numerous small branches to the medulla and one prominent vessel the internal auditory artery The latter sends a ramus to nerves VII–VIII and then passes dorsomedially into the choroid plexus of the fourth ventricle

The basilar artery takes a somewhat winding course along the median ventral side of the brain following the contours of the medulla as the latter bends sharply dorsad and straightens longitudinally to continue into the spinal cord At the posterior boundary of the medulla the first spinal artery joins the basilar As in other reptiles the basilar then becomes continuous with the ventral spinal artery However, the lizards apparently lack dorsal spinal arteries since no longitudinal arterial channels could be found in the dorsal regions of the spinal cord

DEVELOPMENT

Hafferl (20) describes six stages in the development of cephalic arteries in *Platydactylus* embryos ranging in body lengths from 2 5 mm to 5 0 mm headlength In the present study embryos of *Lacerta muralis* ranging in body length from 2 0 mm to 10 0 mm were used Since Hafferl was concerned primarily with the extracranial arteries his descriptions of intracranial vessels (particularly those of older embryos) are rather vague and incomplete His 2 9 mm to 5 0 mm embryos also seem older than the *Lacerta* embryos of comparable size Consequently no attempt will be made to correlate specific stages in the development of these two genera

Stage I (2 0 mm–3 6 mm)

In the 2 0 mm embryo of *Lacerta muralis* the first two aortic arches are well formed and parts of the third arch are visible The cranial flexure has occurred and each invaginated optic cup contains a rudimentary lens Otic placodes are also present

The cranial arteries are poorly developed On each side an internal carotid artery extends into the head and sends a fairly strong branch to the optic cup The rest of each internal carotid represents the anterior encephalic artery which travels anteriorly along the ventrolateral walls of the forebrain No arteries could be found in the posterior regions of the brain

In one 3 6 mm embryo of *Lacerta agilis* arches III IV V and VI are present arches I and II have disappeared Each internal carotid sends caudad a very thin posterior encephalic artery As compared with this vessel the anterior encephalic is considerably larger Consequently in the very early stages of development the anterior portions of the brain are well supplied by strong anterior encephalic arteries whereas somewhat later the posterior regions receive the smaller pair of posterior encephalics

Stage II (4 5 mm–5 0 mm)

In the 4 5 mm and 5 0 mm embroys the optic lobes are well developed the cerebral hemispheres show relatively little growth Cranial and cervical flexures are evident Outlines of future skull elements are not yet visible but vertebrae have begun to form around the notochord Since the intracranial vascular patterns of the 4 5 mm and 5 0 mm specimens are

essentially the same only the 5 0 mm embryo will be described (fig 2)

Near the posterior region of the dien cephalon the internal carotid first sends off an orbital artery which passes laterad toward the eye The internal carotid (ce rebral carotid) then divides into the an terior and posterior encephalic arteries

The anterior encephalic artery travels along the ventrolateral surface of the di encephalon and passes over the root of the optic nerve Here an ophthalmic artery is sent laterad along the nerve and appears to enter the cup Just anterior to the optic nerve another vessel the anterior orbital is sent from the anterior ence phalic artery to the eye The anterior encephalic artery then continues antero-ventrally and ends in a mass of small branches beneath the anterior rim of the hemisphere Although the right and left anterior encephalics lie quite close to each other in this region they do not fuse nor is an anastomosis formed between them

The only branch given off from the posterior encephalic is the rudimentary mesencephalic artery This vessel orig inates just anterior to the origin of the oculomotor nerve and proceeds antero-dorsally a short distance along the mes encephalon The posterior encephalic then passes medial to nerve III and continues caudally along the medulla In the 5 0 mm specimen a delicate cross-connection occurs between the two posterior ence

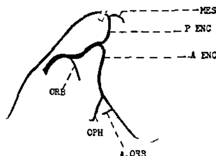


Fig 2 Reconstruction of brain in *Lacerta muralis* 4 5 mm embryo

phalic arteries at the level of nerves VII–VIII Beyond this point the two vessels remain separate and gradually disappear near the posterior boundary of the brain A ventral spinal artery could not be found in these embryos

Stage III (6 4 mm–10 0 mm)

Despite the wide range of embryos en compassed by this stage the 6 4 mm embryo already possesses at least the rudi ments of the major adult intracranial arteries and certainly in the 7 8 mm embryo the adult pattern has been well established The remaining embryos mainly show additional growth and el aboration of these vessels Although the 7 8 mm embryo has been chosen as the representative of this stage (fig 3) the following description will also include references to the earlier as well as later stage III embryos

In the 6 4 mm specimen the hemis pheres have increased in size the pontine flexure is partially developed and faint out lines of the endochondral skull bones are visible In the 7 8 mm embryo the three flexures are well formed and the expand ing hemispheres have started to grow pos teriorly over the anterior region of the diencephalon By the end of this stage the cervical flexure is greatly reduced the optic lobes and cerebral hemispheres completely cover the diencephalon and ossification of the chondrocranium is well under way

In the older embryos of this stage (9 0 mm 9 8 mm 10 0 mm) the distal end of the internal carotid is partially enclosed in a bony canal in the floor of the basis phenoid bone At the posterolateral region of the pituitary fossa the internal carotid gives rise to the nasopalatine artery which passes out through a foramen and which continues anteriorly toward the orbital and nasal regions The internal carotid then turns dorsad and enters the intra cranial cavity Although this vessel (now designated as the cerebral carotid) may send one or two small branches to the hypophysis no anastomosis could be found posterior to this structure As in the pre vious stage the cerebral carotid bifurcates into anterior and posterior rami but the location of this bifurcation has changed

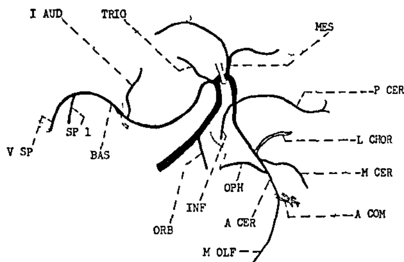


Fig 3 Reconstruction of brain in *Lacerta muralis* 7 8 mm embryo

At stage II the cerebral carotid divided near the posterior boundary of the dien cephalon In the 7 8 mm embryo of stage III the division occurs at the level of the posterior mesencephalic region As will be discussed later the modification in the bifurcation of the cerebral carotid ap parently affects the relationship of the encephalic arteries to the oculomotor nerve In the previous stage the anterior portion of the posterior encephalic artery passed medial to the root of this nerve whereas in the 7 8 mm embryo it is the posterior part of the anterior encephalic which travels medial to this nerve root

The origin of the mesencephalic artery has remained the same i e just anterior to the origin of nerve III However this vessel now takes rise from the anterior encephalic rather than from the posterior encephalic as was the case at stage II The mesencephalic now also divides into a short cranial branch along the antero ventral convexity of the midbrain and a longer caudal branch along its postero ventral convexity This caudal ramus con tinues over the anterior region of the cerebellum

In addition to its acquisition of the mesencephalic artery the anterior ence phalic gives rise to four new vessels Rudiments of three of these are already present in the 6 4 mm embryo The first artery represents the posterior cerebral which is given off at the region of the in fundibulum In the 6 4 mm specimen the posterior cerebral proceeds dorsolaterally but ends at approximately one half the distance up the side of the diencephalon In the 7 8 mm and later embryos this artery extends to the dorsal region of the diencephalon and sends off branches to the parietal organ and to the roof of the third ventricle

Very close to the origin of the posterior cerebral artery the anterior encephalic also gives rise to a small infundibular artery which passes ventromediad and supplies the region of the infundibulum and the posterior part of the optic chiasma This artery was not visible in the 6 4 mm embryo

Another small artery is the lateral cho roidal which originates in the region of the optic nerve and which in the 6 4 mm embryo passes dorsomedially toward the lateral ventricle In the 7 8 mm specimen this artery furnishes several branches to the lateral choroid plexus

The fourth new artery originates quite close to the lateral choroidal but is scarcely visible in the 6 4 mm embryo This vessel

represents the middle cerebral and is more easily found in the 7 8 mm embryo where it extends anterodorsally up the side of the hemisphere It is not until the older embryos of this stage (9 8 mm and 10 0 mm) that the middle cerebral achieves any great size or distribution of subordinate branches

Just beyond the origin of nerve II the anterior encephalic (anterior cerebral) gives off a fairly strong ophthalmic artery which travels along the anterior face of the nerve and which then bifurcates into two small branches One branch of the ophthalmic penetrates into the eye the other branch seems to end in the ventral region of the orbit The anterior orbital artery observed in stage II is possibly represented by a tiny vessel in the 6 4 mm embryos but its point of origin is ill defined This artery was not found in the 7 8 mm and older embryos

At stage II the anterior encephalic artery terminated in a network of tiny vessels at the anteroventral end of the hemisphere In the early embryo of stage III however the distal end of the anterior encephalic (anterior cerebral) turns slightly dorsad along the anterior face of the hemisphere and then passes into a capillary network near the dorsal convexity No connection between the right and left anterior cerebrals could be found In the 7 8 mm and later embryos each of these two arteries sends forth a medial olfactory vessel which extends anteroventrally along the olfactory nerve The two anterior cerebrals then turn mediodorsad within the intercerebral fissure and communicate with each other by means of one or more cross-connections

Changes in the posterior encephalic arteries involve the formation of a single basilar artery and the appearance of several new vessels for the medulla These changes are quite noticeable in the 7 8 mm embryo Close to the origin of each posterior encephalic a short trigeminal artery is sent to nerve V Each posterior encephalic then continues caudad beneath the anterior part of the medulla At the level of nerves VII–VIII a small branch is given off dorsally and probably represents the internal auditory artery of the adult Immediately posterior to this vessel the two posterior encephalics fuse to form the basilar which then continues as a single median vessel ventral to the medulla In the 9 8 mm and later embryos the fusion occurs further craniad so that the basilar is formed just posterior to the hypophysis

At the posterior region of the medulla the first pair of spinal arteries unites with the basilar The latter then continues caudad through the foramen magnum and joins the ventral spinal artery which extends along the median ventral surface of the spinal cord

Although the pattern at stage III agrees quite closely with the adult condition the following changes must eventually take place The mesencephalic artery increases its distribution of vessels to the mid brain and sends a few additional branches to the cerebellum The middle cerebral also progressively supplies a wider area of the lateral hemispheric surface Most of the circulation to the olfactory region is gradually acquired by extracranial olfactory arteries

DISCUSSION

The developmental modifications of certain lacertilian intracranial arteries are worthy of special attention These vessels include the mesencephalic cerebral carotid infundibular anterior communicating olfactory nasopalatine and ophthalmic arteries

The most drastic change occurs with respect to the origin of the mesencephalic artery This vessel appears at approximately the 4 5 mm stage and is the earliest branch given off by the posterior encephalic In the 7 8 mm embryo the mesencephalic originates from the anterior encephalic a short distance anterior to the bifurcation of the cerebral carotid and as seen in the *Crotaphytus adults* this artery is clearly an outgrowth of the anterior encephalic artery

While the mesencephalic is undergoing these changes the bifurcation of the cerebral carotid "moves" caudad Whereas the division originally occurs near the posterior region of the diencephalon its ultimate position is near the posterior boundary of the adult midbrain These modifications of the mesencephalic and cerebral carotid arteries are possibly in

terrelated and occur at a period when the pontine flexure is being formed This suggests that the latter may exert some influence on these arteries particularly since the brain ultimately shows a strong pontine flexure in the adult

During the formation of this flexure the curvature in the floor of the medulla changes from concave to convex and the diencephalon and telencephalon are brought dorsad from their previous more ventral positions Such changes would have considerable effect on the intracranial arteries particularly the posterior encephalic and the cerebral carotid While one can see that the posterior encephalic accommodates itself to the convexity in the floor of the medulla and thus acquires an S shaped appearance the subsequent sequence of events is difficult to determine since the hemodynamic adjustments apparently occur quite rapidly and are not observable in serial sections (The 6 4 mm embryo already resembles the 7 8 mm one in terms of the bifurcation and origin of the mesencephalic)

One possibility is that a small portion of the carotid stem is pushed dorsad against the proximal part of the posterior encephalic (i e that portion containing the origin of the mesencephalic artery) These two regions might then fuse so that the bifurcation of the cerebral carotid would appear to have been moved posteriorly (fig 4) This fused region of the posterior encephalic and cerebral carotid would thus constitute the new proximal portion of the anterior encephalic artery hence the mesencephalic originates from the anterior encephalic rather than from the posterior encephalic None of the embryos however shows such a radical overlapping of the posterior encephalic and cerebral carotid as depicted in figure 4C Although such a fusion might occur gradually one would nevertheless expect the origin of the mesencephalic artery to occur progressively close to the bifurcation this trend was not found in the embryos from 5 2 mm to 7 8 mm

Another possibility is that the cerebral carotid and posterior encephalic touch each other and fuse at only one point i e at the origin of the trigeminal artery and that the cerebral carotid then atrophies between

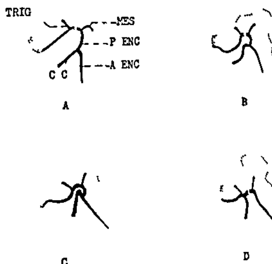


Fig 4 Hypothetical scheme no 1 for modification of the lacertilian cerebral carotid A mesencephalic originates from posterior encephalic at early stage B and C pontine flexure forms and posterior encephalic and cerebral carotid are brought into close contact (nerve III is not shown in sketch C) D overlapping portions of posterior encephalic and cerebral carotid have fused and the mesencephalic now originates from the anterior encephalic

this union and the original bifurcation (fig 5) Thus the bifurcation would occur posterior to the origin of the mesencephalic artery rather than anterior to it as in the preceding stage This connection between the posterior encephalic and cerebral carotid could not be found in any of the embryos nor were atrophied remnants of the latter vessel ever observed However it seems likely that such a union might immediately shunt the bloodstream away from the remainder of the cerebral carotid and this could then result in its rapid degeneration

Hochstetter's diagram ('06) of a 4 0 mm (headlength) *Lacerta* embryo confirms the initial posterior origin of the mesencephalic whereas in the adult *Lacerta* this artery arises from the anterior encephalic Although he does not describe the mechanism by which this change occurs he suggests that transformations of the brain and skull bones are responsible

As these modifications occur in the posterior parts of the brain the origin of the mesencephalic does not change but always remains immediately anterior to the origin of nerve III However as noted

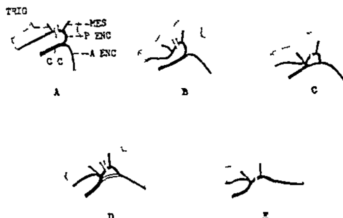


Fig 5 Hypothetical scheme no 2 for modification of lacertilian cerebral carotid A mesencephalic originates from posterior encephalic at early stage B pontine flexure forms and posterior encephalic is brought closer to cerebral carotid C posterior encephalic and cerebral carotid communicate with each other at level of trigeminal artery D blood stream is shunted directly to proximal part of posterior encephalic (the unshaded portion of the cerebral carotid indicates that segment which atrophies) E mesencephalic originates from anterior encephalic

previously there is a difference in the relationship of the encephalics to nerve III since the adult anterior encephalic also includes the proximal portion of the posterior encephalic In the early embryonic stages the oculomotor nerve crosses over the anterior part of the posterior encephalic artery in later embryos and in the adult this nerve passes over the newly formed posterior segment of the anterior encephalic

These changes also affect the origin of the trigeminal artery and would help to explain its great variability in the adult Since the bifurcation shifts to the region where this artery is given off from the posterior encephalic it is not surprising that the adult trigeminal artery might be found to arise either from the anterior or posterior encephalic or even from within the bifurcation itself

In the adult *Eumeces* (Beddard 05) the mesencephalic artery originates from the posterior encephalic artery it is obvious that in such cases the bifurcation has not been altered as greatly as in those which show an anterior encephalic origin

Rathke s description (1857) of the mesencephalic artery is somewhat confusing He refers to a large branch which arises close to the origin of the anterior encephalic artery and which extends dorsad and supplies branches to the posterior part of the hemisphere the midbrain the cerebellum and the choroid plexus of ventricles one two and three In *Crotaphytus* the distribution of this artery s branches does not include such a large area nor do any of the accounts of other genera show this to be true Although the mesencephalic may send one or two twigs into the choroid plexus of the third ventricle most of the vessels for the plexus and posterior hemispheric region originate from the anterior encephalic and lie within the fissure between the hemisphere and optic lobe Since several anterior branches from the mesencephalic also disappear into this fissure it is possible that Rathke (1857) overlooked the independent origins of the cerebral and choroidal arteries and misinterpreted these vessels as branches of the mesencephalic or that the latter actually had acquired the distal portion of these vessels

In lizards the blood supply to the infundibulum and to the chiasma is usually variable both in the adults and in the embryos References to separate infundibular and chiasmatic arteries are fairly common in the literature on the adult The infundibular artery of the *Lacerta* adult (Hochstetter 06) does not travel to the optic chiasma the latter structure instead

receives its own artery which originates from the anterior encephalic near the root of the posterior cerebral artery Corti (1847) also shows the latter condition in one of his diagrams In those cases where there is a common artery for both regions the embryonic branches of one artery have probably acquired anastomoses with those of the other whose stem has then degenerated In the three *Crotaphytus* adults used in the present study the infundibular artery generally had assumed the supply of the chiasma although in one specimen there were separate arteries for these regions

In the accounts of the adult lizard the statement is frequently made that an anterior communicating artery is lacking and hence the circle of Willis is not closed anteriorly Not only Rathke (1857) but most later authors (Hofmann 00 Beddard 05 and Hafferl 20) specifically call attention to this fact Corti (1847) describes the fusion of two arteries beneath the chiasma in *Psammosaurus* and considers this to be an anterior closure of the circle of Willis Other authors tend to ignore this feature both in their texts and in their diagrams

In the present study an anterior communicating artery was found in the *Crotaphytus* adults and rudiments of this vessel were also observed in *Lacerta* embryos at late stages of development In both the adults and embryos the anterior communicating artery is quite slender but nevertheless it does constitute an anterior closure of the circle of Willis

From the embryonic material which was available the formation of this anterior communication could not be easily followed In the 6 4 mm embryo each anterior cerebral artery turns dorsad along the anterior face of the cerebral hemisphere and terminates in a small network of capillaries As the hemispheres continue to expand anterolaterally this network comes to lie within the intercerebral fissure and cross connections form between the distal ends of the anterior cerebrals Portions of the latter structures then may fuse or else one vessel may predominate over the other to form the single anterior communicating artery of the adult

With regard to the blood supply of the olfactory regions the lateral areas are supplied by a small anterior branch of the middle cerebral Although no medial olfactory artery could be found in the 6 4 mm specimen in the 7 8 mm embryo a thin, olfactory vessel lies ventrally beneath each olfactory nerve and appears to be an outgrowth from the anterior cerebral of the corresponding side There is of course the possibility that this olfactory artery constitutes the anterior end of the anterior cerebral and that the anterior communicating artery is thus formed by medial outgrowths from the two cerebrals This is extremely doubtful, however since the latter vessels turn dorsad toward the incipient intercerebral region in early embryonic stages Moreover the absence of an olfactory artery in early embryos indicates that this vessel is probably a relatively late outgrowth and that the anterior communicating artery does represent a distal remnant of the embryonic anterior cerebral

Hochstetter (06) indicates that during later developmental stages the facialis artery joins the nasal artery which comes from the anterior cerebral and proximal portions of this nasal vessel then degenerate This would account for the fact that in the adult the extracranial arteries are the primary source of supply for the olfactory and nasal regions Since some adult lizards do retain the intracranial olfactory arteries the degree to which these vessels atrophy is probably variable

Another problem in the lizard is the relationship of the nasopalatine artery to both the intracranial and extracranial vessels Hochstetter (06) refers to an orbital artery which originates from the internal carotid of the 4 0 mm (headlength) *Lacerta* embryo He states that in his 1 8 mm embryo the orbital joins the facialis artery and that by the 5 0 mm stage the orbital artery has disappeared From this he concludes that the proximal portion of the orbital degenerates soon after acquiring a connection with the facialis

In the 1 5 mm and 5 0 mm *Lacerta* embryos of the present study there is a vessel which arises from the internal carotid quite close to the hypophyseal and infundibular regions of the brain This

branch extends craniad toward the de veloping eye and probably corresponds to the orbital artery of Hochstetter (06) Although parts of this orbital artery may be taken over by the facialis there are two other possibilities which should not be ignored namely that portions of the embryonic orbital may also be acquired by a rudimentary extracranial nasopala tine artery or else the orbital itself may develop into the nasopalatine of the adult

With regard to the first possibility one would expect to find an embryo in which the orbital artery had formed anastomo ses with a nasopalatine artery originating extracranially from the internal carotid In none of the embryos was this observed although the lack of close stages may be responsible

The second possibility is that when the chondrocranium develops the orbital ar tery may for some reason become com pletely excluded from the intracranial cavity and thus may originate from the internal carotid just before the latter en ters the brain case The orbital artery would consequently travel extracranially beneath the basisphenoid bone instead of intracranially along the floor of the hy pophyseal fossa Since the orbital artery would thus no longer be found intra cranially its presence might be easily overlooked

Hochstetter (06) believed that the naso-palatine is a special vessel found only in lizards and having no counterpart in other reptiles He mentions that this artery first appears at 5 0 mm (headlength) How ever this is the stage at which he claims that the orbital artery disappears (see above) Since the origin and course of the orbital artery in embryos of later stages correspond closely with the condi tion of the adult nasopalatine artery the latter may actually represent a somewhat modified orbital vessel which during de velopment was excluded from the brain case and which also acquired a more ex tensive extracranial area of supply Despite this relationship to the embryonic orbital it is probably best to retain the term nasopalatine for the adult artery since the greater part of it serves the nasal and palatal regions and only a small part supplies the orbit

The ophthalmic artery shows a slight amount of modification In the *Lacerta* embryos of early stages the ophthalmic artery originates from the anterior ence phalic and travels laterad along the optic stalk to the optic cup Immediately an terior to the stalk a second artery (the anterior orbital) is sent laterally from the anterior encephalic By later stages the stem of the anterior orbital has disap-peared while the ophthalmic artery shows additional branches in the anterior region of the orbit Some of these branches prob ably represent distal portions of the an terior orbital since Hochstetter (06) states that in later stages of development this artery (his "ciliary" artery) becomes incorporated into the ophthalmic

The relatively small cerebellum seems to be sufficiently supplied by means of a few branches from the posterior rami of the mesencephalic artery Corti (1847) refers to a cerebello-spinalis" artery which sends off several cerebellar rami and which corresponds in origin to the internal audi tory artery the cerebellum may therefore be supplied by branches of the internal auditory as well as rami of the mesence phalic artery

With regard to the dorsal regions of the spinal cord the absence of any noticeable dorsal spinal arteries implies that blood probably is brought to this region via the ventral spinal and its associated pairs of spinal arteries The development of these vessels has not been well studied and so it is uncertain whether or not any special condition exists in the lizards

ACKNOWLEDGMENTS

The author expresses appreciation to the Anatomy Department of the Harvard Medical School for use of the Minot Em bryological Collection Particular gratitude is extended to Professors A S Romer and L Hoadley for their suggestions and criti cisms during the course of this work This study was partially supported by USPHS pre doctoral training grant 2G–36

LITERATURE CITED

Beddard F E 1905 A contribution to the en cephalic arterial system in Sauropsida Proc Zool Soc London 2 59–70

Bhatia M L and J Dayal 1933 On the arterial system of the lizard *Hemidactylus flaviviridis* Ruppel Anat Anz 76 417–437

Corti A 1847 De systemate vasorum *Psammosauri grisei* Vindobonae 65 Pp

Hafferl A 1920 Zur Entwicklungsgeschichte der Kopfgefasse des Gecko (*Platydactylus annularis*) *Anat Hefte 59* 1–42

Hochstetter F 1906 Beitrage zur Anatomie und Entwickelung des Blutgefässsystemes der Krokodile in Voeltzkow's Reise in Ostafrika *4* 1–139

Hofmann M 1900 Zur vergleichenden Anatomie der Gehirn und Ruckenmarksarterien der Vertebraten Zeit f Morph und Anthro 2 247–322

Rathke H 1857 Untersuchungen uber die *Aortenwurzeln und die* von ihnen ausgehenden Arterien der Saurier Denk d Kais Akad Wiss Wien *13* 51–142

Shindo T 1914 Zur vergleichenden Anatomie der Arteriellen Kopfgefasse der *Reptilien Anat* Hefte 51 267–355

Growth of the Face and Jaws after Resection of the Septal Cartilage in the Rabbit [1]

BERNARD G SARNAT AND MANUEL R WEXLER
Departments of Plastic Surgery [2] and Otolaryngology [3] Division of Surgery and Research Institute Cedars-Sinai Medical Center Los Angeles California

ABSTRACT Varying amounts of the cartilaginous nasal septum were resected in 15 growing rabbits at 21 days of age Ten additional rabbits were used as unoperated on and operated on controls The postoperative survival ranged from 105 to 145 days

Within 60 to 90 days postoperatively antemortem findings were noted in the experimental animals of a shorter snout and overeruption and malocclusion of the incisors Postmortem gross findings of the dissected sectioned and x rayed skulls of the experimental animals revealed that the snout was shorter and smaller with a severe relative mandibular prognathism the nasal and premaxillary bones were smaller the nasal cavity and piriform aperture were smaller than in the control animals As a result of the shorter snout the upper incisors were lingual to the lower incisors This was the reverse of the normal findings In addition the incisors were overerupted malaligned and fractured At the posterior border of the septal defect a marked downward and forward deflection of the nasal bones was noted This was in contrast to the smoothly curved dorsum of the operated on and unoperated on control animals The extent and severity of the deformity varied approximately with the extent of the septal defect

In a previous experiment varying amounts of the septovomeral region (including cartilage vomer and premaxilla) were resected in growing rabbits (Wexler and Sarnat 61) Seventeen weeks postoperatively the gross findings showed a shorter snout (relative mandibular prognathism) with downward angulation in both the anteroposterior and lateral directions The incisors were not in occlusion and had overerupted

In a subsequent considerably less traumatic experiment the nasal septum was dislocated from the vomerine groove in young growing rabbits (Wexler and Sarnat 65) Sixteen weeks postoperatively the gross findings showed varying degrees of deformity limited to the septal and septovomeral regions No gross deformities were noted however of the snout jaws or teeth

Since resection of the septovomeral region produced a marked growth arrest of the snout and since dislocation of the septum produced no grossly visible growth arrest of the snout the present experiment was designed to determine the effect of trauma of a lesser degree than in the former experiment but of a greater degree than the latter experiment Consequently only septal cartilage was resected in growing rabbits to determine the effect upon growth of the snout

REVIEW OF THE LITERATURE

Fick in 1858 removed a portion of the nasal cartilaginous septum through a trephine opening of the nasal bones in growing dogs cats pigs and goats At autopsy the hard palate was greatly shortened anteroposteriorly and he stated that growth of the hard palate was dependent upon the growth of the nasal septum Landsberger in 1929 resected in part the anterior portion of the septum in dogs two weeks of age and killed them six months later Examination showed that the anterior part of the floor of the nasal cavity was higher than normal From this he concluded that the growing septum was an important

[1] Thi in e tigation wa support d in part by search grant HD 00179 from th N ti nal In titute of Child H lth nd Human D v l pment U S Public Health Service and a grant from the Floren B G ard Re ar h Fund

[2] Pre ent addre s 435 N R xbury Drive B verly Hill Calif rnia 90210

[3] Pre ent ddre 6360 Wilshire B ulevard Lo Angeles 48 California

ctor in pushing the floor of the nasal vity downward Selman and Sarnat 7) reported that although the fronto sal suture was a site of rapid growth extirpation in the rabbit failed to pro ce a growth arrest of the snout

RIEF DESCRIPTION OF THE OSTEOLOGY OF THE RABBIT FACE

The rabbit face is comprised in part the nasal maxillary premaxillary and ndibular bones (Craigie 48)

The nasal cavity communicates poste rly with the ventral surface of the skull the choanae which in the rabbit are completely divided Anteriorly it opens the outside by the piriform aperture ateral division is effected chiefly through median cartilaginous plate the nasal ptum This is continuous posterosupe rly as a synchondrosis with a small cres itic vertical plate of bone the perpen cular plate of the ethmoid bone and pos oinferiorly with the presphenoid Both e sites of endochondral bone formation feroposteriorly the ventral portion of the rtilaginous nasal septum is supported by vertical bony plate the vomer the dorsal argin of which is grooved to receive it is forms the septovomeral joint The mer is a median somewhat sickle aped vertical plate of bone separating the ntral portions of the nasal fossae An riorly the nasal septum bears on its ven l margin the paired enclosures of the meronasal organ which are also sup rted by the grooved surface formed in e midline by adjacent dorsal surfaces of e palatine processes of the premaxilla e septal cartilage extends anteriorly to e piriform aperture and terminates ove the basal portion of the incisors

The nasal bone is thin and elongated forms the roof of the nasal fossa and conjunction with its fellow of the op site side the dorsal boundary of the piri rm aperture The posterior border of the asal bone articulates with the anterior rder of the frontal bone The fronto asal suture is a site of growth in the oung rabbit (Selman and Sarnat 55)

The maxillae form the main portion of e upper jaw Each maxilla consists of a entral portion the body and of five proc esses — alveolar palatine orbital zygomatic and sphenorbital

The ventral portion of the maxilla with the palatine bone forms the hard palate This structure is represented chiefly by a bony palatine bridge connecting the two sides of the skull between the molars It forms the roof of the oral cavity and the floor of the nasal cavity Immediately in front of it the palatine surface is perforated by a pair of large incisive foramina which are broadly open to the nasal fossae Laterally where the palatine bones articulate with the palatine processes of the maxillae are the palatine foramina

The premaxilla or incisive bone forms the anterior part of the upper jaw It comprises a central portion the body including the alveolar portion a frontal process and a palatine process The frontal process of the premaxilla a somewhat prominent and narrow ridge extends posteriorly along the lateral surface of the nasal bone and articulates with the premaxillary process of the frontal bone

The mandible the largest element of the facial region is composed of two portions united anteriorly by the symphysis Each half comprises a horizontal portion the body of the mandible and a posterior, vertical portion the ramus The latter serves for the insertion of the muscles of mastication and for articulation with the skull The mandibular ramus forms a broad plate the lateral surface of which is occupied by the masseter muscle while the medial surface forms an area of insertion for the pterygoid muscles The surface of the ramus is greatly increased in its posteroventral portion through the expansion of the bone to form the angle The elongated articular surface is at the end of a vertical or slightly oblique condyloid process Just inferior to this on the anterior border of the ramus is the coronoid process The sigmoid notch is between these two processes The nerve and vessels of the mandible enter at the mandibular foramen on the medial surface immediately behind the last molar

The body of the mandible bears on its dorsal margin the alveoli of an incisor in front and the premolars and molars posteriorly The alveolar process of each premaxilla contains a larger labial and a

smaller lingual incisor The double set of upper incisors (both labial and lingual) distinguishes the rabbit as a lagomorph from the rodent which has only one set of upper incisors The alveolar process of each maxilla contains the premolars and molars The upper incisors and premolars and molars normally occlude with the lowers The upper incisor occludes labial to the lower one and represents a larger segment of a smaller spiral The lower incisor (although larger than the upper incisors) represents a smaller segment of a larger spiral They are worn at the incisal edges and thereby maintain occlusion A sharp bevel is present because of the harder enamel on the labial surface and the softer dentin on the lingual surface thus producing a differential in wear Whereas the basal end of the lower incisor extends to the premolar the basal end of the upper incisor is considerably anterior to the premolar The teeth in the rabbit are continuously growing and erupting

MATERIAL AND METHODS

Animals Twenty five growing rabbits were selected because of the snout and its rapid rate of growth In 15 rabbits varying amounts of the nasal cartilaginous septum were resected Six were unoperated on and four were operated on controls In the last group the same surgical procedure was followed but no nasal septum was resected They were operated upon at 21 days of age and weaned at 42 days of age

Anesthesia A solution of 1% procaine hydrochloride was injected submucosally in the sulcus between the upper incisors and lip

Surgical procedure The animals were secured on an operating board in the supine position The face and snout were cleansed with an antiseptic solution After injection of the local anesthetic agent sublabially an approximately 1 5 to 2 cm transverse incision was made through the mucosa between the upper incisors and the lip The tissues were elevated from the premaxilla entrance was gained into the nasal cavity and the septum and septovomeral joint were exposed This was performed on all operated on animals In addition in the experimental animals maximum amounts of the anterior portion and body of the cartilaginous nasal septum were resected by means of a grasping forceps The vomer was left intact No attempt was made to save mucoperichondrium The sublabial mucosal wound margins were approximated and sutured with 4–0 black silk

The postoperative survival ranged from 105 to 145 days The animals were killed by means of a lethal dose of pentobarbital sodium injected directly into the heart Immediately after death the heads were severed and a portion of the soft tissues was resected The heads were then fixed in either 70% alcohol or alcohol acetic acid formalin solution Subsequently further dissection was done

Photographs and roentgenographs Antemortem and postmortem photographs were taken of the heads in the dorsal lateral frontal and ventral views The heads were then sectioned in the left parasagittal plane with a small hack saw and photographs were taken in the parasagittal view Every effort was made to obtain comparable photographs although this was not always possible

Lateral roentgenographs were then taken of the sectioned skulls Previous to this in some instances a barium sulfate paste thick enough to adhere to the margin of the surgical defect in the septum was applied Tracings were made of selected roentgenographs

RESULTS

Antemortem observations Marked lack of forward growth of the upper face with overeruption and malocclusion of the incisors was noted in less than two months after resection of a major portion of the nasal septum (figs 1–6) Instead of the long smoothly curved tapered face seen in the operated on and unoperated on controls these animals exhibited a short rounded (irregular in the lateral view) stubby face with a pronounced indentation above the tip of the nose The appearance was suggestive of a bull dog (fig 2)

In the experimental animals the incisors were overerupted and in malocclusion a sharp bevel edge was not maintained on the labial surface (figs 4 and 11) There was difficulty ingesting food and it would become lodged between the incisors These

animals weighed less than the controls when killed At times a nasal mucopurulent discharge was noted

Postmortem observations In general, changes noted in the dissected skulls of the experimental animals were limited to the snout in the region anterior to the orbits, zygomas and molars Generally the degree of change varied directly with the amount of septum resected

The snout from above was shorter (figs 7–9) From below the palate and the incisive foramen were shorter From in front the nasal aperture was much smaller The snout when viewed from the side was tapered and shorter than the unoperated on control (figs 10–12) Whereas the snout in the normal animal was the prominent part of the anterior face and much larger than the anterior mandible this was no longer true in the experimental rabbit There was a definite anterior deflection of the snout beginning anterior to the frontonasal suture (fig 11) This was in contrast to the smoothly curved dorsum of the control animals

The nasal bones were markedly shorter less wide and less high particularly toward the incisal end than those of the control animals (figs 8 and 11) The nasal bones converged toward the premaxilla with nasal height and volume markedly reduced (figs 11 12 and 14) The premaxilla and its frontal process were also markedly shorter The end of the snout was tapered in the dorsoventral direction

Examination of the parasagittally sectioned crania revealed the extent of the nasal septum and its relation to the snout in the control animals and the relation of the extent of the septal defect to the deformity of the snout in the experimental animals (figs 10 and 11) The site of the beginning of the downward deflection of the nasal bones was correlated with the posterior border of the septal defect This was anterior to the frontonasal suture (fig 11)

The left (experimental no 14) and right (control no 13) sides of the parasagittally sectioned skulls of litter mate animals with the same survival period were approximated along the posterosuperior and occipital borders (figs 9 and 12) This dramatically demonstrated the extreme underdevelopment of the snout

In contrast to the marked changes found in the incisors none was noted in the premolars and molars except for a few instances in which the mesial surface of the upper first premolar was concave instead of convex No consistent pattern of change was seen in the incisors except for the uppers which were usually in lingual occlusion The lowers were over erupted Incisors were in marked malocclusion including fractures deviations and lack of occulsion The sharp bevel was altered

Roentgenographic observations The following additional findings were noted in the lateral roentgenographs of the parasagittally sectioned skulls in the experimental animals a smaller nasal aperture and nasal cavity with marked anterior deflection of the nasal bones a shorter palate larger pulpal cavities lesser amounts of alveolar bone supporting the incisors an increase in the proportion and amount of erupted to unerupted incisor changes in the incisal edge with frequent reversal of the bevel and concavity of the mesial surface of the upper premolar (fig 14) Tracings of the roentgenographs and superpositioning of these tracings further illustrated the differences (figs 15–17)

DISCUSSION

In a previous experiment septum septovomeral joint vomer and premaxilla were resected in growing rabbits 29 to 48 days of age (Wexler and Sarnat 61) A severe growth arrest of the snout resulted The present experiment was designed to evaluate growth of the snout after surgical removal of varying amounts of nasal septum Thus on a selective basis only the nasal septum was resected in growing rabbits 21 days of age The resulting lack of growth of the snout was as severe as in the previous group Dorsal anterior and ventral areas of the septum were removed as part of the resection The question of their role in both growth and support must be considered Also what are the roles of perichondrial and interstitial growth of the nasal cartilaginous septum?

Although the septal defect was quite large in the experimental animals it

would have been considerably larger had the nasal bones grown in the usual dorsal and anterior directions Instead the nasal bones were shorter and deflected ventrally in an anterior direction Whereas in the control animal the nasal bones and hard palate were approximately parallel in the experimental animal an anterior projection of lines from the external surface of these bones would soon intersect (figs 12 and 14) Consequently the nasal cavity was also much smaller These were appartly a direct result of the lack of the growth impetus (and support?) of the septal cartilage It would be of interest to resect the septal cartilage in adult animals to determine whether a similar deformity would result from lack of support

Although particular care was taken not to injure the septovomeral joint in these animals the effect of trauma to this and related areas and the resulting effects must be considered Consequently in two comparable groups of rabbits the surgical procedure was carried out up to the removal of septum (operated on controls) or the nasal septem was completely dislocated laterally from the vomerine groove (Wexler and Sarnat 65) No subsequent external deformity of the snout jaws or teeth was noted

With the decrease in anterior growth the snout lagged behind the mandible and a severe relative mandibular prognathism resulted The upper incisors which normally came into occlusion labial to the lowers were now frequently in a lingual malocclusion In some instances the upper and lower incisors were distorted in an attempt to maintain a semblance of occlusion The growth pattern was not that of a logarithmic spiral (Herzberg and Schour 41)

These face jaw and dental abnormalities were no doubt reflected in alterations of the anatomy and physiology of the nose temporomandibular joints and the rest of the masticatory and respiratory systems Some of these aspects will be considered in future experiments

In contrast to the severe deformities of the snout in the region of the septal resection none was consistently found posterior to the resected area in the region of the zygomas orbits and molars It is possible that these and other regions might be affected if the remaining posterior septal cartilage including the septoethmoidal and septopresphenoid sites of endochondral bone formation were resected

Primary sites of growth of bones are endochondral such as epiphyses in the long or tubular bones the costochondral junction of ribs the sphenoethmoidal and sphenooccipital synchondroses at the base of the skull the mandibular condyle and the septoethmoidal joint (Adams and Sarnat 40 Sarnat and Gans 52 Roy and Sarnat 56 Sarnat 57 Baume 61 Sarnat 63) Appositional and sutural areas of growth of bones are secondary or accommodating sites Only in the skull are all three types of bone growth found endochondral appositional (and resorptive) and sutural Local factors such as growth of the brain orbital contents and nasal septum as well as muscular tensions affect these sites (Brash McKeag and Scott 56 Sarnat and Shanedling 65) Of course systemic factors also influence the growth of bones

Surgical removal of the sphenooccipital synchondrosis in rats produced shorter skulls (DuBrul and Laskin 61) The changes in form were limited mostly to the posterior half of the neurocranium both base and vault No specific changes were noted in the face jaws or teeth

In a previous experiment in growing rabbits it was demonstrated that considerable growth of bone occurred at the frontonasal suture the nasal side contributed approximately twice the amount that the frontal side contributed (Selman and Sarnat 55) Extirpation of this suture did not affect growth of the snout (Selman and Sarnat 57) Similarly in growing monkeys the midpalatine and transpalatine sutures were extirpated and no alterations in either facial or jaw growth were noted (Sarnat 58) After extirpation of the mandibular condyle in growing monkeys however a severe deformity of the jaws and face was produced (Sarnat 57)

With less impetus from growth of the septal cartilage no doubt secondary activity at the frontonasal suture was reduced Since in this experiment the nasal bones

animals weighed less than the controls when killed At times a nasal mucopurulent discharge was noted

Postmortem observations In general changes noted in the dissected skulls of the experimental animals were limited to the snout in the region anterior to the orbits, zygomas and molars Generally the degree of change varied directly with the amount of septum resected

The snout from above was shorter (figs 7–9) From below the palate and the incisive foramen were shorter From in front, the nasal aperture was much smaller The snout when viewed from the side, was tapered and shorter than the unoperated on control (figs 10–12) Whereas the snout in the normal animal was the prominent part of the anterior face and much larger than the anterior mandible this was no longer true in the experimental rabbit There was a definite anterior deflection of the snout beginning anterior to the frontonasal suture (fig 11) This was in contrast to the smoothly curved dorsum of the control animals

The nasal bones were markedly shorter less wide and less high particularly toward the incisal end than those of the control animals (figs 8 and 11) The nasal bones converged toward the premaxilla with nasal height and volume markedly reduced (figs 11, 12 and 14) The premaxilla and its frontal process were also markedly shorter The end of the snout was tapered in the dorsoventral direction

Examination of the parasagittally sectioned crania revealed the extent of the nasal septum and its relation to the snout in the control animals and the relation of the extent of the septal defect to the deformity of the snout in the experimental animals (figs 10 and 11) The site of the beginning of the downward deflection of the nasal bones was correlated with the posterior border of the septal defect This was anterior to the frontonasal suture (fig 11)

The left (experimental no 14) and right (control no 13) sides of the parasagittally sectioned skulls of litter mate animals with the same survival period were approximated along the posterosuperior and occipital borders (figs 9 and 12) This dramatically demonstrated the extreme underdevelopment of the snout

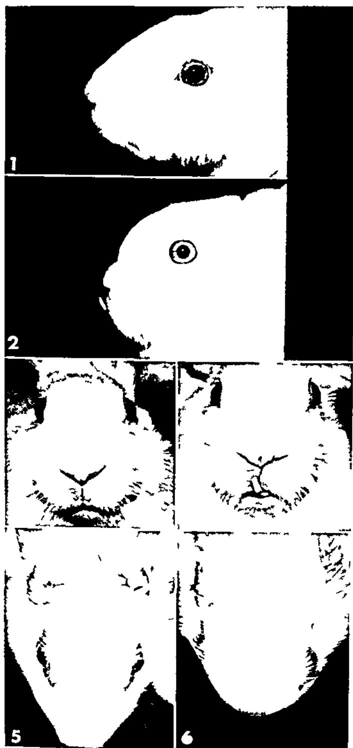
In contrast to the marked changes found in the incisors none was noted in the premolars and molars except for a few instances in which the mesial surface of the upper first premolar was concave instead of convex No consistent pattern of change was seen in the incisors except for the uppers which were usually in lingual occlusion The lowers were over erupted Incisors were in marked malocclusion including fractures deviations and lack of occulsion The sharp bevel was altered

Roentgenographic observations The following additional findings were noted in the lateral roentgenographs of the parasagittally sectioned skulls in the experimental animals a smaller nasal aperture and nasal cavity with marked anterior deflection of the nasal bones a shorter palate larger pulpal cavities lesser amounts of alveolar bone supporting the incisors an increase in the proportion and amount of erupted to unerupted incisor changes in the incisal edge with frequent reversal of the bevel and concavity of the mesial surface of the upper premolar (fig 14) Tracings of the roentgenographs and superpositioning of these tracings further illustrated the differences (figs 15–17)

DISCUSSION

In a previous experiment septum septovomeral joint vomer and premaxilla were resected in growing rabbits 29 to 48 days of age (Wexler and Sarnat 61) A severe growth arrest of the snout resulted The present experiment was designed to evaluate growth of the snout after surgical removal of varying amounts of nasal septum Thus on a selective basis only the nasal septum was resected in growing rabbits 21 days of age The resulting lack of growth of the snout was as severe as in the previous group Dorsal anterior and ventral areas of the septum were removed as part of the resection The question of their role in both growth and support must be considered Also what are the roles of perichondrial and interstitial growth of the nasal cartilaginous septum?

Although the septal defect was quite large in the experimental animals it


1
2
5
6

were found to be shorter than those of the control animals it would be of interest to study the change in activity of the fronto nasal suture by means of radiopaque implants and serial roentgenographs

LITERATURE CITED

Adams C O and B G Sarnat 1940 Effects of yellow phosphorus and arsenic trioxide on growing bones and growing teeth Arch Path *30* 1192–1202

Baume L J 1961 The postnatal growth activity of the nasal cartilage septum Helvet Odontol Acta *5* 9–13

Brash J C H McKeag and J H Scott 1956 Aetiology of Irregularity and Malocclusion of the Teeth 2nd ed Dental Board of the United Kingdom London

Craigie E H 1948 Bensley s Practical Anatomy of the Rabbit 8th ed Univ of Toronto Press Toronto

DuBrul E L and D M Laskin 1961 Preadaptive potentialities of the mammalian skull An experiment in growth and form Am J Anat *109* 117–132

Fick L 1858 Über die Ursachen der Knochenformen Neue Untersuchungen G H Wigand Gottingen

Herzberg F and I Schour 1941 The pattern of appositional growth in the incisor of the rat Anat Rec *80* 497–506

Landsberger R 1929 Die treibenden krafte zur dehnung und streckung des gesichtsschadels Zahnarztliche Rundschau 23 977–989

Roy E W and B G Sarnat 1956 Growth in length of rabbit ribs at the costochondral junction Surg Gynecol and Obst *103* 481–486

Sarnat B G 1957 Facial and neurocranial growth after removal of the mandibular condyle in the Macaca rhesus monkey Am J Surg *94* 19–30

——— 1958 Palatal and facial growth in Macaca rhesus monkeys with surgically produced palatal clefts Plast Reconstruct Surg *22* 29–41

——— 1963 Postnatal growth of the upper face Some experimental considerations Angle Orthodont *33* 139–161

Sarnat B G and B J Gans 1952 Growth of bones Methods of assessing and clinical importance Plast Reconstruct Surg *9* 140–160

Sarnat B G and P D Shanedling 1965 Postnatal growth of the orbit and upper face in rabbits Arch Ophthalm *73* 829–837

Selman A J and B G Sarnat 1955 Sutural bone growth of the rabbit snout A gross and serial roentgenographic study by means of metallic implants Am J Anat *97* 395–408

——— 1957 Growth of the rabbit snout after extirpation of the frontonasal suture A gross and serial roentgenographic study by means of metallic implants Am J Anat *101* 273–294

Wexler M R and B G Sarnat 1961 Rabbit snout growth Effect of injury to the septovomeral region Arch Otolaryng *74* 305–313

——— 1965 Rabbit snout growth after dislocation of nasal septum Arch Otolaryng *81* 68–71

PLATE 1

EXPLANATION OF FIGURES

1–6 Antemortem lateral frontal and dorsal (retouched) view photographs of rabbit no 4 (figs 1 3 and 5) which had a minor amount of the nasal septum removed and rabbit no 18 (figs 2 4 and 6) which had a major amount of the nasal septum removed at 21 days of age Note the marked contrast in facial appearance Animal no 18 has a short stubby rounded face with an indentation above the nostrils and an overerupted lower incisor (fig 2)


7

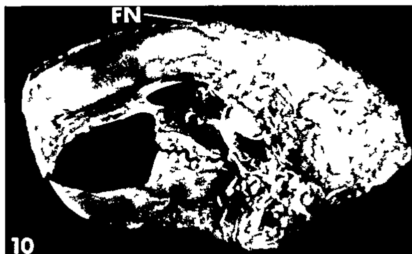

1L
8

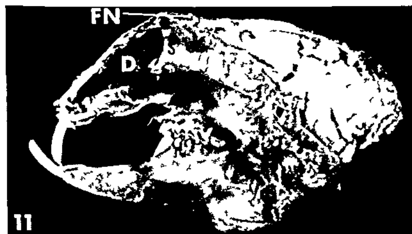

9
1L

PLATE 2

EXPLANATION OF FIGURES

7–9 Postmortem dorsal view photographs of skulls of litter mate rabbits no 13 operated on control (fig 7) and no 14 resected nasal septum (fig 8) with a postoperative survival of 110 days In no 14 note the marked lack of development of the snout In figure 9 the right side of the skull of control rabbit no 13 and the left side of the skull of experimental rabbit no 14 were approximated along the posterodorsal and occipital borders Note that the differences are limited essentially to the snout area *IL* lower incisor


FN
10

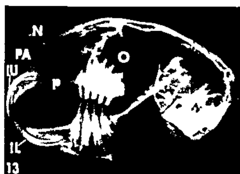

FN
D
11

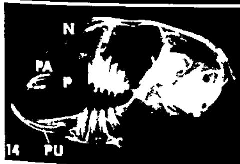

12

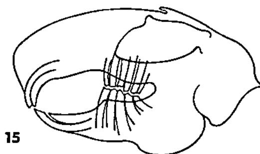
PLATE 3

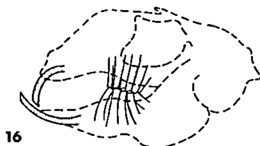
EXPLANATION OF FIGURES

10–12 Postmortem lateral view photographs of right side of left para sagittally sectioned skulls of litter mate rabbits no 13 operated on control (fig 10) and no 14 resected nasal septum (fig 11) with a postoperative survival of 110 days In rabbit no 13 (fig 10) note the length of the snout the smoothly curved dorsum the extent of the nasal cartilaginous septum and the relationship of the incisors In rabbit no 14 (fig 11) note the markedly under developed snout the septal defect the anterior downward angula tion of the nasal bones beginning at the posterior border of the septal defect the smaller nasal aperture remaining septum pos terior to the defect the frontonasal suture and the abnormal relationship of the incisors In figure 12 the right side of the skull of the operated on control rabbit no 13 and the left side of the skull of the experimental rabbit no 14 were approximated along the posterodorsal and occipital borders for contrast Note in rabbit no 14 that in an anterior direction the nasal bones con verge toward the palate *D* septal defect *FN* frontonasal suture *S* septum White dashes outline anterior part of skull of the experimental rabbit






15


16

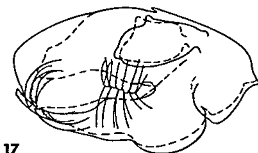
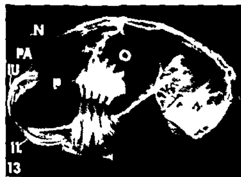
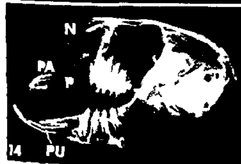

17

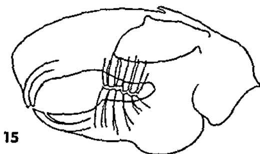
PLATE 4

EXPLANATION OF FIGURES

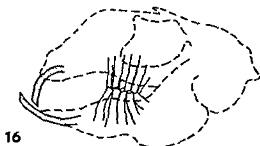
13–17 Reproduction of lateral roentgenographs (figs 13 and 14) and approximate tracings (original by Dr Herbert Muchnic figs 15–17) of lateral roentgenographs of right side of parasagittally sectioned skulls of litter mate rabbits killed at 131 days of age In figure 17 the tracings were superposed along the posterodorsal and occipital borders to contrast the differences between the control and experimental animals In control animal no 13 note the general size shape and regularity of the face jaws and incisors (figs 13 and 15) In experimental animal no 14 the nasal cartilaginous septum was resected at 21 days of age Note in animal no 14 the smaller size the different shape and the irregularity of the upper face and smaller orbit In addition note the different shape and size of the incisors and the larger pulpal cavities and the concavity of the medial surface of the upper first premolar (figs 14 and 16) *IL* lower incisor *IU* upper incisor *N* nasal bone *O* orbit *p* palate *PA* piriform aperture *PU* pulpal cavity



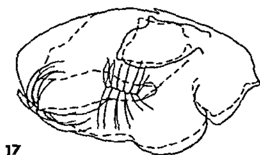




15



16



17

The Fine Structure of Rat Liver Sinusoids, Space of Disse and Associated Tissue Space [1]

WILLIAM E BURKEL [2] AND FRANK N LOW
Department of Anatomy University of North Dakota Grand Forks North Dakota

ABSTRACT Three structurally distinct zones are present in the liver sinusoid The endothelium and basement (boundary) membrane of the portal vein extend uninterruptedly into the peripheral zone The intermediate zone comprising 90% or more of the length of the sinusoid possesses a fenestrated lining and no basement membrane The short central zone has unfenestrated endothelium and a basement membrane Both are continuous with those of the central vein The space of Dissé encircles all three zones of the sinusoid It contains fat storage cells perisinusoidal cells numerous microvillae of liver cells and reticular fibers These fibers are bundles of unit collagen fibers enclosed by cytoplasm of nearby cells The space of Dissé is continuous with the tissue space at both ends of the sinusoid The liver cells lack a basement membrane whether they abut on the space of Dissé or on the tissue space proper

The unique feature of liver fine structure is the combination of fenestrations and lack of basement membranes in the intermediate zone of the sinusoid Blood plasma is thereby afforded intimate contact with the parenchymal cells and has access to the tissue space at both ends of the sinusoid This structural situation fits the known facts of liver function

The relationship of fine structure in the liver lobule to blood vascular channels is a subject of more than ordinary interest Early electron microscopic studies of the liver (Rouiller 54 56 Fawcett 55 Parks 57 Hampton 58 Novikoff and Essner 60) revealed fenestrations in the sinusoidal wall and absence of a basement membrane Hampton (60) observed "material indistinguishable from basement membrane" in the space of Disse However he hesitated to interpret this material as membranous because of the rapid transit of intravenously injected colloidal particles across the space of Disse into the parenchymal cells Wood (63) compared the sinusoids of calf and rat liver He observed a basement membrane in the calf but no fenestrations Conversely there was no basement membrane in the rat but fenestrations were present Later Hampton (64) studied liver from rat mouse dog human and newborn rabbits He observed a basement membrane only at the periphery of the liver lobule close to the interlobular tissue space containing branches of the portal vein hepatic artery and hepatic ducts His contribution is the only one that has related fine structure to its location within the liver lobule More recently Kuhn and Olivier (65) have reported that hepatic sinusoids are not fenestrated in the goat and are surrounded by basement membranes They agree with Wood (63) that the structure of the sinusoids may vary in different species

It appears that most observations of liver sinusoids have been made without realization of the highly systematic arrangement of basement membranes (boundary membranes Low 61 basal laminae Fawcett 61) throughout the body These correspond to the PAS positive membranes described in light microscopy by Gersh and Catchpole in 1949 In electron microscopy they are extracellular structures which generally define the limits of the tissue space (Low 61 64 Battig and Low 61 Low and Burkel 65) Although uninterrupted basement membranes are an integral part of tissue patterns in fine structure incompleteness of this coat does characterize certain slow flowing vascular channels (Farquhar 61 Weiss 61 Moe 63)

The diversity of observations suggested that liver tissue could be fruitfully re

[1] Supported by gr nt HE 09041 Unit d Stat s Publ c H lth S rvice Th u of n lectron mi roscope purch s d on G-16365 NSF i gratefully a knowledg d
[2] Po tdoctoral Fell w N tional In titute f Health

examined This article accordingly de scribes fine structure in the rat liver sinu soid with special emphasis on the signifi cance of basement membranes The find ings are interpreted with reference to the pattern of fine structure found elsewhere in the body, as well as with certain fea tures of liver development function and pathology

MATERIALS AND METHODS

Liver tissue from 20 healthy young adult albino rats was fixed by two methods (1) Thirteen rats were perfused through the left ventricle with 3% gluta raldehyde (Sabatini et al 63) using a technique similar to that of Palay et al (62) Small pieces of liver were subse quently excised minced washed in buffer and post fixed in 1% OsO_4 Both fixers were buffered with 0 1 M phosphate at pH 7 4 (2) Pieces of liver from seven rats were fixed by immersion in 1% OsO_4 buf fered at pH 7 4 with either veronal acetate (Palade 52) or phosphate (Millonig 61) Tissue blocks were dehydrated in a graded series of alcohols or acetone The 50% alcohol or acetone contained 1% phospho tungstic acid Tissues were left in this solution for 30 minutes to one hour in stead of the usual 10 to 15 minutes Em bedment was in either Vestopal W (Ryter and Kellenberger 58) or Epon 812 (Luft 61) followed by polymerization at 60°C for 24 hours

Thick sections (1–2 μ) were made of the face of the entire embedded tissue block These were stained with 1% toluidine blue in 1% borax for one minute The orienta tion of liver lobules was studied in these sections by light microscopy The block was subsequently trimmed and sectioned for electron microscopy The area selected always contained a portion of a portal and/or central vein so that sinusoids com municating with these structures within the plane of section could be studied Thin sections were mounted on *single hole grids* with or without formvar membrane and stained with lead citrate (Reynolds 63 Venable and Coggeshall 65)

OBSERVATIONS

The structure of the liver sinusoid dif fers in various parts of the lobule The presence or absence of basement mem branes and cellular fenestrations deter mines three distinct zones through which blood must flow as it passes from the periphery of the lobule to the central vein (fig 2) The *peripheral zone* is the first where the branches of the portal vein and hepatic artery enter the lobule The *inter mediate zone* comprises most of the length of the sinusoid At the third or *centra zone* the sinusoid enters the central vein

Peripheral zone At the periphery o the lobule the sinusoid resembles a capil lary of type A 1 α (Bennett el al 59) fo a distance of 10–50 μ (figs 3 4) It endothelium is non fenestrated and is en closed in a continuous basement mem brane without cellular investment Th perisinusoidal space of Dissé is betwee the sinusoidal wall and parenchymal cell It contains microvillae of parenchyma cells and bundles of unit collagen fiber (reticular fibers) This portion of th space of Dissé resembles the interlobula tissue space and is continuous with it

Intermediate zone The transition fro peripheral to intermediate zones is abrup often occupying only 5–10 μ (figs 3 4 5 The basement membrane disappears aft becoming spotty The lining cells becom somewhat thinner and develop fenestr tions (fig 6) *This is the sinusoid d* scribed in early electron microscopic inve tigations of the liver (Rouiller 54 5 Fawcett 55 Parks 57 Hampton 5 Novikoff and Essner 60 Wood 63) I structure corresponds to capillary type 3 α of Bennett et al (59) Here the spa of Dissé is essentially vascular No demo strable structure hinders access of t blood plasma to the numerous microvill of the parenchymal cells The intermed ate zone comprises 90% or more of t length of the sinusoid

Central zone As the central vein approached the structural situation aga changes (fig 7) The endothelium b comes continuous and a basement me brane appears This change is more abru than the transition from peripheral to i termediate zones The space of Dissé b comes typical tissue space and is contin ous with this space around the centr vein The central zone of the sinusoid the shortest of the three It is often diff

cult to demonstrate because of its extreme brevity

The basement membrane that is present at both ends of the sinusoid is continuous with the same structure surrounding the endothelium of all connecting blood vessels

Von Kupffer cells possess no basement membranes They usually have the same relation to parenchymal cells as lining cells but often span the sinusoidal lumen (fig 8) Their cytoplasm possesses more endoplasmic reticulum and mitochondria but does not always contain particulate material Positive identification is sometimes difficult

The parenchymal cells of the rat liver possess no basement membranes Their basal surfaces are characterized by microvillae which are most numerous along the sinusoids (figs 6 9) Here they extend into the perisinusoidal space of Disse Where parenchymal cells abut on the interlobular tissue space (fig 4) or surround a central vein (fig 7) microvillae are also present but are less numerous

The space of Disse itself contains microvillae reticular fibers and bits of cytoplasm The microvillae nearly fill the space in many localities (fig 9) and sometimes project into the sinusoid through fenestrations (figs 5 9) Reticular fibers traverse the space usually running in cytoplasmic gutters The cytoplasm which isolates them may be derived from the cell bodies of parenchymal cells (figs 4 5 7) or lining cells (fig 9) Unidentifiable pseudopod like processes in the space of Disse larger than microvillae also invest reticular fibers (fig 10) These may be derived from perisinusoidal cells (Wood 63 Kuhn and Olivier 65) or fat storage cells (Ito and Nemoto 52 Yamagishi 59 Nakane 63) of the sort shown in figures 10 and 11 Positive identification is difficult because the cell body usually lies out of the plane of section

DISCUSSION

It is evident that there is an orderly variation of fine structure in different parts of the rat liver lobule Figure 1 illustrates the chief regional characteristics observed in this study In the intermediate portion of the lobule the presence of fenestrations and the absence of basement membranes provide the blood plasma with unimpeded access to the liver cells This occurs in the space of Disse which is continuous not only with the sinusoidal lumen but also with the tissue space at both ends of the sinusoid An unusual relationship results involving vascular system parenchyma and tissue space (Rhodin 64) It is however best understood as a variant of similar relationships found elsewhere in the body and may be interpreted along the lines suggested below

Basement (boundary) membranes generally define the limits or boundaries of the tissue space They form a structural framework which isolates epithelium (including endothelium and mesothelium) muscle nerve and fat from the tissue space Within this space lie the formed elements of the connective tissues (Low 61 Battig and Low 61 Low and Burkel 65) As an expression of this pattern the endothelium of the blood vascular system is separated from the surrounding tissue space by its basement membrane This is especially notable in capillaries Likewise the parenchyma of organs usually epithelial is separated from the tissue space by its own basement membrane A small amount of tissue space usually persists between the basement membranes of different tissues This situation characterizes all but a few areas of the body of which the liver lobule is a notable exception

Where the common bile duct and the portal vein enter the liver they possess normal basement membrane relationships A typical epithelial basement membrane continuously encloses the bile ducts and continues to the ends of the ducts of Hering Here the basement membranes end (fig 1) The parenchymal cells themselves lack basement membranes whether they abut on the tissue space proper or on the space of Dissé The endothelium of the portal vein is likewise sheathed by a basement membrane to its smallest branches This basement membrane continues to enclose the peripheral portion of the sinusoid where it terminates The same situation in reverse applies to the hepatic veins the central veins and the central portions of the sinusoids It follows that no basement membranes are

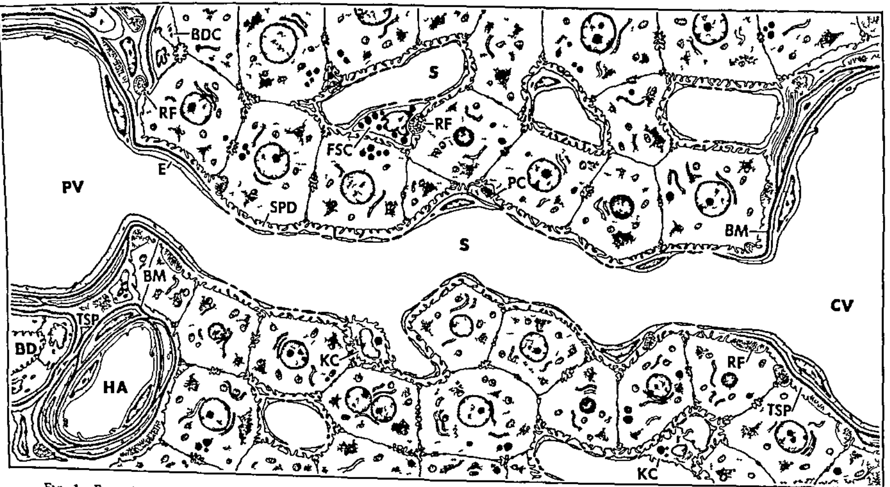


Fig 1 *Fine structure in the rat liver lobule* The periphery of the lobule is at the left where branches of portal vein (*PV*) hepatic artery (*HA*) and bile duct (*BD*) lie in the tissue space (*TSP*) Above bile duct cells (*BDC*) abut on liver cells The sinusoid (*S*) connects the portal vein with the central vein (*CV*) In the peripheral portion of the sinusoid both the endothelium (*E*) and its basement (boundary) membrane (*BM*) are continuous with those of the portal vein In the intermediate portion the lining is fenestrated and there is no basement membrane Centrally the cellular lining is continuous with the endothelium of the central vein and a basement membrane is present Reticular fibers (*RF*) are found in the tissue space and in the space of Dissé (*SPD*) which surrounds the sinusoids In places the sinusoids are lined by the cells of von Kupffer (*KC*) Perisinusoidal cells (*PC*) and fat storage cells (*FSC*) are in the space of Disse See text for interpretation

present in the intermediate portion of the lobule where the sinusoidal lining is fenestrated It is here that blood plasma has free access to the liver cells This circumstance collates well with certain features of hepatic development and pathology as well as with normal liver function

The lining cells of the liver sinusoids are derived from or closely associated with the mesenchyme (Aterman 63) These cells have accordingly been described as undifferentiated" (Wolf Heidigger 41 Maximow and Bloom 57 Hampton 64) embryonic (Altschul 54 Gasser 55) or primitive" (Ruttner et al 56 Rondez and Ruttner 60 Ham and Leeson 61) Their primitiveness is attested to by their multipotential response to stimulation They may become hemopoietic stem cells (Sorenson 60 Ham and Leeson 61) or phagocytes (Hampton 58 64 Ham and Leeson 61) In certain pathological conditions they organize to form non fenestrated endothelium and even develop basement membranes (Schaffner and Popper 63) In this condition they are in distinguishable from capillaries These changes are comparable to the normal development of the mesodermal derivatives other than the connective tissues Muscle urogenital epithelium mesothelium and most endothelium acquire basement membranes as their specialization progresses It appears then that the lack of basement membranes around the sinusoids is in accord with the primitive status of the lining cells

The parenchymal cells of the liver also possess characteristics that suggest primitiveness Their regenerative capacity is well known (Leduc 63) and their fine structure is so lacking in specialization that they have become the cellular prototype of the cytologists The absence of a basement membrane between them and the tissue space is difficult to understand if one accepts the idea of entodermal origin If as is generally held (Patten 53 Arey 54) they are entodermal extensions of the ducts of Hering then they are the only known entodermal derivatives without a basement membrane On other hand mesodermal origin for these cells (reviewed by Bloom 26) has been claimed by investigators over a span of more than half a century (Elias 55) and still finds occasional support (Wilson et al 63) Although no new embryological evidence is offered here the absence of basement membranes the unspecialized fine structure of the cell itself and the idea of mesodermal origin all fit together

The fine structural situation responsible for intimate contact between blood plasma and parenchymal cell naturally focuses attention on the space of Disse Close examination shows that this unusual space communicates freely with the vascular lumen through the fenestrations and likewise with the tissue space at the periphery and center of the lobule This provides a pathway for the seepage of blood plasma into these areas that has been suspected to account for the large volume and high protein content of hepatic lymph (Trowell 46 Bloom and Fawcett 62 Brauer 63) The bundles of unit collagen fibers (reticular fibers) in the tissue space at the margins of the lobule are in their normal" environment As they course through the space of Disse to the intermediate portion of the lobule they enter a primarily vascular zone Here they are enclosed by cytoplasmic sheaths which tend to isolate them from this unusual environment

The species variations appearing in the sinusoids of calf (Wood 63) and goat (Kuhn and Olivier 65) are not incompatible with the interpretations presented herein The presence of unfenestrated endothelium and basement membrane in these forms may be interpreted as extended development to the point reached by capillaries in most areas of the body The pathology of chronic liver disease reflects similar changes since Schaffner and Popper (63) observed essentially this process in cases of long standing cirrhosis

The unique fine structure of the liver lobule really represents an alteration of a master pattern that is found throughout the vertebrate body in general (Low 64 Low and Burkel 65) All published reports although differing in specific detail can be interpreted as variations of this pattern Normal developmental processes and certain of the abnormal changes of pathology alike bear coherent relationship to the conceptual norm This concept that of variable but patternized fine structure

provides an interesting framework for interpreting the complex and ever changing events of liver metabolism

LITERATURE CITED

Altschul R 1954 Endothelium Its Development Morphology Function and Pathology Macmillan New York

Arey L B 1954 Developmental Anatomy 6th ed W B Saunders Co Philadelphia

Aterman K 1963 The Liver Ed by Ch Rouiller Academic Press New York Vol I chap 3 61–136

Battig C G and F N Low 1961 The ultrastructure of human cardiac muscle and its associated tissue space Am J Anat 108 199–230

Bennett H S J H Luft and J C Hampton 1959 Morphological classification of vertebrate blood capillaries Am J Physiol 196 381–390

Bloom W 1926 Embryogenesis of human bile capillaries and ducts Anat Rec 36 451–465

Bloom W and D W Fawcett 1962 A Textbook of Histology 8th ed W B Saunders Co Philadelphia

Brauer R W 1963 Liver circulation and function Physiol Rev 43 115–213

Elias H 1955 Origin and early development of the liver in various vertebrates Acta Hepatol 3 1–56

Farquhar M G 1961 Fine structure and function in capillaries of the anterior pituitary gland Angiology 12 270–292

Fawcett D W 1955 Observations on the cytology and electron microscopy of hepatic cells J Nat Cancer Inst 15 1475–1502

——— 1961 The membranes of the cytoplasm Lab Invest 10 1162–1188

Gasser H 1955 Über das primare Retothelsarkom der Leber Virchow s Arch pathol Anat u Physiol 326 296–311

Gersh I and H R Catchpole 1949 The organization of ground substance and basement membrane and its significance in tissue injury disease and growth Am J Anat 85 457–521

Ham A W and T S Leeson 1961 Histology 4th ed J B Lippincott Co Philadelphia

Hampton J C 1958 An electron microscopic study of the hepatic uptake and excretion of submicroscopic particles injected into the blood stream and into the bile duct Acta Anat 32 262–291

——— 1960 A re-evaluation of the submicroscopic structure of the liver Texas Rep Biol Med, 18 602–611

——— 1964 Electron Microscopic Anatomy Ed by S M Kurtz Academic Press New York Chap 2 41–58

Ito T and M Nemoto 1952 Über die Kupfferschen Sternzellen und die Fettspeicherungszellen (fat storing cells) in der Blutkapillarenwand der menschlichen Leber Okajimas Folia Anat Japan 24 243–258

Kuhn N and M L Olivier 1965 Ultrastructure of the hepatic sinusoid of the goat Capra hircus J Cell Biol 26 977–979

Leduc, E H 1963 The liver Ed by Ch Rouiller Academic Press New York Vol II chap 14 63–89

Low F N 1961 The extracellular portion of the human blood air barrier and its relation to the tissue space Anat Rec 139 105–124

——— 1964 A boundary membrane concept of ultrastructure applicable to the total organism Proc III Europ Reg Conf on E M Prague B 115

Low F N and W F Burkel 1965 A boundary membrane concept of ultrastructural morphology Anat Rec 151 489–490

Luft J H 1961 Improvements in epoxy resin embedding methods J Biophys Biochem Cytol 9 409–414

Maximow, A A and W Bloom 1957 A textbook of Histology 7th ed W B Saunders Co Philadelphia

Millonig G 1961 Advantages of a phosphate buffer for OsO_4 solutions in fixation J Appl Physics 32 1637

Moe R E 1963 Fine structure of the reticulum and sinuses of lymph nodes Am J Anat 112 311—355

Nakane P K 1963 Ito s fat storing cell" of the mouse liver Anat Rec 145 265–266

Novikoff A and E Essner 1960 The liver cell Some new approaches to its study Am J Med 29 102–131

Palade G E 1952 A study of fixation for electron microscopy J Expl Med 95 285–298

Palay S L S M McGee Russell S Gordon and M A Grillo 1962 Fixation of neural tissue for electron microscopy by perfusion with solutions of osmium tetroxide J Cell Biol 12 385–410

Parks H 1957 The hepatic sinusoidal cell and its histological relationships Electron Microscopy Proceedings of the Stockholm Conference September 1956 Ed by F Sjostrand and J Rhodin pp 151–153 Almquist and Wiksell Stockholm

Patten B M 1953 Human Embryology 2nd ed McGraw Hill New York

Reynolds E S 1963 The use of lead citrate at high pH as an electron opaque stain in electron microscopy J Cell Biol 17 208–212

Rhodin J A G 1964 Ultrastructure and function of liver sinusoids Proc IVth Internat Symposium of R E S Kyoto Japan pp 108–124

Rondez R and J R Ruttner 1960 Die Bedeutung der Kupfferzellen bei der thioacetamidinduzierten Leberzirrhose der Ratte Med Exptl 3 189–194

Rouiller C 1954 Les canalicules biliares Étude au microscope électronique Compt Rend Soc Biol (Paris) 148 2008–2011

——— 1956 Les canalicules biliares Étude au microscope électronique Acta Anat 26 94–109

Ruttner J R H E Brunner and A P Vogel 1956 Untersuchungen uber die Kupfferschen Zellen der Rattenleber Schweiz Z allgem Pathol Bakteriol 19 738–747

Ryter A and E Kellenberger 1958 L inclusion au polyester pour l ultramicrotomie J Ultra Res 2 200–214

Sabatini D D K Bensch and R. J Barrnett 1963 Cytochemistry and electron microscopy The preservation of cellular ultrastructure and enzymatic activity by aldehyde perfusion J Cell Biol *17* 19–58

Schaffner F and H Popper 1963 Capillarization of hepatic sinusoids in man Gastroenterology *44* 239–242

Sorenson G D 1960 An electron microscopic study of hematopoiesis in the liver of the fetal rabbit Am J Anat *106* 27–40

Stenger R 1966 Hepatic sinusoids in carbon tetrachloride-induced cirrhosis Arch Path *81* 439–447

Trowell O A 1946 The experimental production of watery vacuolation of the liver J Physiol *105* 268–297

Venable J H and R Coggeshall 1965 A simplified lead citrate stain for use in electron microscopy J Cell Biol 25 407–408

Weiss L 1961 An electron microscope study of the vascular sinuses of the bone marrow of the rabbit Bull Johns Hopkins Hosp *108* 171–199

Wilson J W C S Groat and E H Leduc 1963 Histogenesis of the liver Ann New York Acad Sci *111* 8–24

Wolf Heidigger G 1941 Zur Form und Lagerung der Kupffer schen Sternzellen Z mikroskop anat Forsch 50 623–641

Wood R L 1963 Evidence of species differences in the ultrastructure of the hepatic sinusoid Zeit Zellforsch *58* 679–692

Yamagishi M 1959 Electron microscope studies on the fine structure of the sinusoidal wall and fat-storing cells of rabbit livers Arch Histol Jap *18* 223–261

Note added in proof Stenger (66) has recently reported capillarization of liver sinusoids with development of basement membranes in carbon tetrachloride poisoning This is essentially the reaction described by Schaffner and Popper (63) in long standing cirrhosis and may be similarly interpreted

provides an interesting framework for interpreting the complex and ever changing events of liver metabolism

LITERATURE CITED

Altschul R 1954 Endothelium Its Developmen Morphology Function and Pathology Macmillan New York

Arey L B 1954 Developmental Anatomy 6th ed W B Saunders Co Philadelphia

Aterman K 1963 The Liver Ed by Ch Rouiller Academic Press New York Vol I chap 3 61–136

Battig C G and F N Low 1961 The ultrastructure of human cardiac muscle and its associated tissue space Am J Anat 108 199–230

Bennett H S J H Luft and J C Hampton 1959 Morphological classification of vertebrate blood capillaries Am J Physiol 196 381–390

Bloom W 1926 Embryogenesis of human bile capillaries and ducts Anat Rec 36 451–465

Bloom W and D W Fawcett 1962 A Textbook of Histology 8th ed W B Saunders Co Philadelphia

Brauer R W 1963 Liver circulation and function Physiol Rev 43 115–213

Elias H 1955 Origin and early development of the liver in various vertebrates Acta Hepatol 3 1–56

Farquhar M G 1961 Fine structure and function in capillaries of the anterior pituitary gland Angiology 12 270–292

Fawcett D W 1955 Observations on the cytology and electron microscopy of hepatic cells J Nat Cancer Inst 15 1475–1502

——— 1961 The membranes of the cytoplasm Lab Invest 10 1162–1188

Gasser H 1955 Über das primare Retothelsarkom der Leber Virchow s Arch pathol Anat u Physiol 326 296–311

Gersh I and H R Catchpole 1949 The organization of ground substance and basem nt membrane and its significance in tissue injury disease and growth Am J Anat 85 457–521

Ham A W and T S Leeson 1961 Histology 4th ed J B Lippincott Co Philadelphia

Hampton J C 1958 An electron microscopic study of the hepatic uptake and excretion of submicroscopic particles injected into the blood stream and into the bile duct Acta Anat 32 262–291

——— 1960 A re evaluation of the submicroscopic structure of the liver Texas Rep Biol Med, 18 602–611

——— 1964 Electron Microscopic Anatomy Ed by S M Kurtz Academic Press New York Chap 2 41–58

Ito T and M Nemoto 1952 Über die Kupfferschen Sternzellen und die Fettspeicherungszellen (fat storing cells) in der Blutkapillarenwand der menschlichen Leber Okajimas Folia Anat Japan 24 243–258

Kuhn N and M L Olivier 1965 Ultrastructure of the hepatic sinusoid of the goat Capra hircus J Cell Biol 26 977–979

Leduc E H 1963 The liver Ed by Ch Rouiller Academic Press, New York Vol II chap 14 63–89

Low F N 1961 The extracellular portion of the human blood air barrier and its relation to the tissue space Anat Rec 139 10.–124

——— 1964 A boundary membrane concept of ultrastructure applicable to the total organism Proc III Europ Reg Conf on E M Prague B 115

Low F N and W E Burkel 1965 A boundary membrane concept of ultrastructural morphology Anat Rec 151 489–490

Luft J H 1961 Improvements in epoxy resin embedding methods J Biophys Biochem Cytol 9 409–414

Maximow A A and W Bloom 1957 A textbook of Histology 7th ed W B Saunders Co Philadelphia

Millonig G 1961 Advantages of a phosphate buffer for OsO_4 solutions in fixation J Appl Physics 32 1637

Moe R E 1963 Fine structure of the reticulum and sinuses of lymph nodes Am J Anat 112 311—358

Nakane P K 1963 Ito s fat storing cell of the mouse liver Anat Rec 145 265–266

Novikoff A and E Essner 1960 The liver cell Some new approaches to its study Am J Med 29 102–131

Palade G E 1952 A study of fixation for electron microscopy J Expl Med 95 285–298

Palay S L S M McGee Russell S Gordon and M A Grillo 1962 Fixation of neural tissues for electron microscopy by perfusion with solutions of osmium tetroxide J Cell Biol 12 385–410

Parks H 1957 The hepatic sinusoidal cell and its histological relationships Electron Microscopy Proceedings of the Stockholm Conference September 1956 Ed by F Sjostrand and J Rhodin, pp 151–153 Almquist and Wiksell Stockholm

Patten B M 1953 Human Embryology 2nd ed McGraw Hill New York

Reynolds E S 1963 The use of lead citrate at high pH as an electron opaque stain in electron microscopy J Cell Biol 17 208–212

Rhodin J A G 1964 Ultrastructure and function of liver sinusoids Proc IVth Internat Symposium of R E S Kyoto Japan pp 108–124

Rondez R and J R Ruttner 1960 Die Bedeutung der Kupfferzellen bei der thioacetamidinduzierten Leberzirrhose der Ratte Med Exptl 3 189–194

Rouiller C 1954 Les canalicules biliares Etude au microscope électronique Compt Rend Soc Biol (Paris) 148 2008–2011

——— 1956 Les canalicules biliares Étude au microscope électronique Acta Anat 26 94–109

Ruttner J R H E Brunner and A F Vogel 1956 Untersuchungen uber die Kupffer schen Zellen der Rattenleber Schweiz Z allgem Pathol Bakteriol 19 738–747

PLATE 1

EXPLANATION OF FIGURES

2 Low power micrograph of lobule Open vascular channels some of which contain a few residual blood cells characterize perfused liver preparations The portal vein (*PV*) connects with the central vein (*CV*) by sinusoids (*S*) which open freely into both vessels (arrows) The irregular path followed by the sinusoids prevents demonstration of their entire course in the plane of a single section The complete traverse of a sinusoid from portal to central vein is diagrammatically *represented in figure 1 which summarizes fine structure in the rat* liver lobule Glutaraldehyde OsO_4 Epon 360 ×

3 Junction of portal vein with sinusoid The portal vein (PV) is identified by nearby bile duct (*BD*) Numerous cells in the tissue space (*TSP*) also characterize the periphery of the lobule The sinusoid (*S*) is bridged over at one point by lining cells in the plane of this section but communicates freely with the portal vein The endothelium (*F*) and basement membrane (*BM*) of the portal vein continue without interruption into the peripheral zone of the sinusoid The inset illustrates the transition from the peripheral to the intermediate zones of the sinusoid Here the basement membrane ends Fenestrations appear deeper in the sinusoid (arrows) This situation is illustrated at far left above and in figure 6 Note the continuity of the tissue space and the space of Dissé (*SPD*) from the portal vein to the sinusoid Glutaraldehyde OsO_4 Epon 3 200 × (inset 8 700 ×)

PLATE 1

EXPLANATION OF FIGURES

2 Low power micrograph of lobule Open vascular channels some of which contain a few residual blood cells characterize perfused liver preparations The portal vein (*PV*) connects with the central vein (*CV*) by sinusoids (*S*) which open freely into both vessels (arrows) The irregular path followed by the sinusoids prevents demonstration of their entire course in the plane of a single section The complete traverse of a sinusoid from portal to central vein is diagrammatically represented in figure 1 which summarizes fine structure in the rat liver lobule Glutaraldehyde OsO_4 Epon 360 ×

3 Junction of portal vein with sinusoid The portal vein (*PV*) is identi fied by nearby bile duct (*BD*) Numerous cells in the tissue space (*TSP*) also characterize the periphery of the lobule The sinusoid (*S*) is bridged over at one point by lining cells in the plane of this section but communicates freely with the portal vein The endo thelium (*E*) and basement membrane (*BM*) of the portal vein con tinue without interruption into the peripheral zone of the sinusoid The inset illustrates the transition from the peripheral to the inter mediate zones of the sinusoid Here the basement membrane ends Fenestrations appear deeper in the sinusoid (arrows) This situation is illustrated at far left above and in figure 6 Note the continuity of the tissue space and the space of Dissé (*SPD*) from the portal vein to the sinusoid Glutaraldehyde OsO_4 Epon 3 200 × (inset 8 700 ×)

PLATE 2

EXPLANATION OF FIGURES

4 Peripheral sinusoid The bile duct (*BD*) and the numerous reticular fibers (*RF*) in the tissue space (*TSP*) characterize the periphery of the lobule *The left and the lower portions of the sinusoid (S) abut* on the interstitial tissue Above and to the right its relations to the parenchymal cells and the reticular fiber are typical of the peripheral sinusoidal zone Note the basement membrane (*BM*) around its entire circumference and the absence of endothelial fenestrations This sinusoid was traced well into the liver lobule in nearby sections Glutaraldehyde OsO_4 Epon 13 800 ×

5 Transition between peripheral and intermediate zones This sinusoid is deeper in the lobule than the one illustrated in figure 4 The terminal portion of the basement membrane of the peripheral sinusoidal zone is visible along the upper sinusoidal wall (arrows) Elsewhere the structure of the wall defines the zone as intermediate as illustrated in figure 6 The cytoplasmic sheath separating the reticular fiber (*RF*) from the space of Dissé (*SPD*) is typical Note the microvillus (*MV*) projecting through the fenestration Glutaraldehyde OsO_4 Epon 10 700 ×

PLATE 3

EXPLANATION OF FIGURES

6 Intermediate sinusoid The lining cells possess fenestrations (arrows) and there is no basement membrane The space of Dissé (*SPD*) is voluminous The surface of the parenchymal cells is characterized by numerous microvillae (*MV*) The blood plasma has free access to the liver cells Glutaraldehyde OsO_4 Epon 13 500 ×

7 Sinusoid entering central vein The extremely short central zone is established by the presence of the basement membrane (*BM*) note inset The reticular fiber (*RF*) at the left is surrounded by a cyto plasmic sheath typical of the space of Dissé The reticular fibers on the right are more openly located to the tissue space (*TSP*) OsO_4 Epon 11 900 × (inset 29 000 ×)

6

SPD

MV

7

RF

RF

TSP

BM

PLATE 4

EXPLANATION OF FIGURES

8 Intermediate sinusoid with von Kupffer cell The large von Kupffer cell (*KC*) spans the sinusoid (*S*) It is in intimate contact with both blood and parenchymal cells There is no basement membrane The abundant cytoplasm contains more organelles than that of the lining cell (*LC*) Glutaraldehyde OsO_4 Epon 6 500 ×

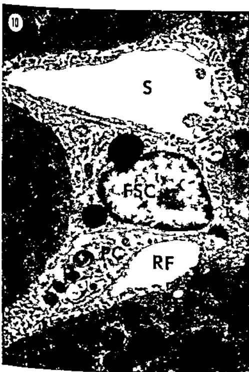
9 Sinusoidal lining cell enclosing reticular fiber The reticular fiber (*RF*) is encircled by a lining cell (*LC*) The space of *Dissé is nearly* filled with microvillae (*MV*) which occasionally project through fenestrations (arrows) OsO_4 Epon 8 000 ×

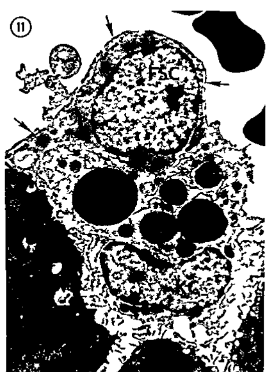
10 Contents of space of Dissé A fat storage cell (*FSC*) lies below the sinusoid (*S*) The perisinusoidal cell (*PC*) partially encloses the reticular fiber (*RF*) The remainder of the space of Dissé is largely occupied by the microvillae of surrounding parenchymal cells *Gluta* raldehyde OsO_4 Epon 9 600 ×

11 Fat storage and von Kupffer cells Lipid inclusions (*L*) in the cyto plasm and the perisinusoidal position of the upper cell (*FSC*) *identify* it as a fat storage cell It is separated from the sinusoidal lumen by the attenuated cytoplasm of a lining cell (arrows) *Although the* von Kuffer cell (*KC*) is almost completely separated from the lumen a small part of it abuts on the vascular channel on *the right* Gluta raldehyde OsO_4 Epon 6 600 ×


8
S
S
LC
KC


9
M
RF
EC


10
S
FSC
PC
RF


11
FSC
KC

Fine Structure of the Lymphatic Capillary and the Adjoining Connective Tissue Area [1]

L V LEAK AND J F BURKE

Department of Surgery Harvard Medical School and the General Surgical Services Massachusetts General Hospital Boston Massachusetts

ABSTRACT The lymphatic capillaries possess salient morphological features which differentiate them from the blood capillaries Instead of a definitive basement lamina surrounding the lymphatic wall there are numerous fine filaments (about 60 A in diameter) that are attached to the lymphatic endothelia at areas of increased el c tron density that are similar to half desmosomes The filaments extend for varying distances into the adjoining connective tissue area and seem to anchor the lymphatic vessel to the surrounding connective tissue Endothelial projections occur along both the luminal and abluminal surfaces of the cell The intercellular junctions are varied in structure along the lymphatic wall Terminal processes of adjacent endothelial cells may overlap each other interdigitate or their terminal ends may be closely apposed without overlapping At various points along the intercellular junction the apposed surface membranes are held in close apposition by adhesion devices (a) *zonula occludens* (b) *zonula adhaerens* and (c) *macula adhaerens* (desmosome) Frequently open junctions are observed along the lymphatic wall It is suggested that the areas between apposing membrane surfaces which lack attachment devices may represent specialized regions along the lymphatic wall that are easily separated and would permit the passage of excess tissue fluids and large molecules into the lumen of the lymphatic vessel The transport of colloidal carbon particles across the endothelium in vesicles of various sizes and via intercellular junctions is demonstrated

Although the endothelia of lymphatic capillaries possess structures that are simi lar to those found in blood capillaries the former possess specific characteristics that serve as criteria for differentiating them from the endothelia of blood capillaries

In an earlier light microscopic study of lymphatic capillaries Pullinger and Florey (35) suggested that collagen and reticu lum fibers were intimately associated with the lymphatic wall In a later ultrastruc tural study of lymphatic capillaries in the ear and diaphragm Casley Smith and Florey (61) described collagen fibers and fine branching irregular fibers" investing the lymphatics However an intimate as sociation or direct attachment of collagen and reticulum fibers to the lymphatic wall as suggested by the earlier studies of Pul linger and Florey (35) has not been dem onstrated with the electron microscope Therefore the present study is concerned with the ultrastructure of lymphatic capil laries and the intimate association of nu merous fine filaments with the abluminal endothelial wall in the guinea pig s ear after primary fixation in buffered formalin or glutaraldehyde followed by OsO fixa tion

MATERIALS AND METHODS

After depilating the ears of young adult albino guinea pigs with surgex (Crookes Barnes Labs Inc Wayne N J) the lym phatic capillaries were made visible for direct observation by injecting them with shellac free colloidal carbon (Biological Ink type C 11/1431a John Henschel and Co Inc New York) using a modification of Hudack and McMaster s (32) micro injection technique The carbon was di luted with ten parts of 1 N saline and fil tered before injecting the vessels

Carbon injected and non injected ani mals were anesthetized with pentobarbital sodium and the ears were quickly excised and placed in chilled buffered formalin (Pease 62) and cut into small pieces The tissue remained in the buffered for malin for two hours After pre fixation the tissue was washed and then postfixed in Millonig's OsO (61) for 30 minutes then washed dehydrated in a graded se ries of alcohols and embedded in epon Other tissue was prefixed in either 3% glutaraldehyde (pH 7 2) buffered with phosphate (Sabatini et al 63) or the tis

[1] Th w k was supp rt d by th Un t d St te Publi Health grant AI E2392

sue was prefixed in 6 5% glutaraldehyde with 2% acrolein (pH 7 2) and buffered with 0 1 M cacodylate (Sandborn et al , 64) After prefixation in glutaraldehyde the tissue was washed, postfixed in phos phate buffered OsO_4 and processed for epon embedding Sections were obtained with glass and diamond knives on a Porter Blum MT 1, stained with uranyl acetate (Watson 58) and lead citrate (Reynolds, 63) and observed in a Philips EM 200 electron microscope

OBSERVATIONS

Along the margin of the guinea pig s ear the lymphatic capillaries anastomose to form a fine plexus while near the mid zone the vessels merge into a coarser plexus In the thicker region of the ear, a fine plexus is observed just below the der mis while the coarser vessels extended near the cartilage of the ear (figs 1 and 2)

Although both the lymphatic and blood capillaries are lined by flattened endothe lial cells the lymphatic capillaries in the guinea pig s ear can be distinguished by their wider lumina the absence of a defi nitive basement lamina and the occur rence of numerous fine filaments along the abluminal endothelial surface The width of the endothelial wall varies from 0 1 μ to 6 μ (fig 3) Frequently fibroblasts are observed in the adjoining connective tissue area near the lymphatic capillary wall and occasionally smooth muscle cells and un myelinated nerves appear in the surround ing connective tissue area (figs 6 7 and 11) In the longitudinal and cross sec tions of the superficial and deep lymphatic capillaries a thin irregular basement lam ina is occasionally observed (fig 3) There are numerous fine filaments between the endothelial wall and the adjoining connec tive tissue space (figs 3 4 5 8 16 17) Many of these fine filaments appear to be directly attached to the lymphatic wall at areas of increased electron density that occur along the abluminal surface of the endothelial cell (figs 3, 5 8 9 15) These areas of increased electron density are 10 to 20 mμ in width and 500 mμ to several microns in length and are reminiscent of the half desmosomes (hemidesmosome) that are observed along the surface of the basal layer of the epidermal cells The fine filaments measure from 60 to 80 A in diameter and form a loose network between the lymphatic wall and the adjoining con nective tissue space (figs 3, 4 and 11) Many of the filaments course along the endothelial wall and continue into the con nective tissue area as long filamentous strands that surround many of the large bundles of collagen fibers in the adjoining connective tissue (figs 16 and 17)

Occasionally collagen fibers appear to be in close association with the abluminal endothelial surface, but for the most part, the collagen fibers are separated from the endothelial surface by the anchoring like filaments that occur along the endothelial cells

The intercellular junctions are varied in structure along the wall of the lymphatic capillary The distal ends of adjacent endothelial cells may overlap, interdigitate or abut each other to form intercellular junctions (figs 6 7 11 12 and 13)

At various points along the intercellular junction the apposed surface membranes of adjacent endothelial cells are held in close apposition by attachment plaques that are very similar to the junctional com plex described by Farquhar and Palade (63) and Brightman and Palay (63) The *zonula occludens* (tight junction) was observed near the lumen (fig 12) However many junctions were observed in which this tight junctional complex was absent The *macula adhaerens* (desmo somes) and the *zonula adhaerens* were encountered with some regularity between opposing membrane wall surfaces (figs 3 6 7 12 13) The *zonula occludens* (tight junction) is formed by a close ap position of the surface membranes of ad jacent endothelial cells The intercellular space contains a central membrane that is formed by the fusion of the two outer membranes of the two closely apposed unit membranes (fig 12)

The second element of the junctional complex the *zonula adherens* appears as two dense leaflets that are separated by a distance of about 200 A (figs 7 12 13)

The most common adhesion device ob served between apposing surface mem branes of the lymphatic endothelial cells is the *macula adhaerens* (desmosomes)

This tight junction is observed as areas of increased electron density in segments of adjacent plasmalemmae that are closely applied to each other (figs 6 12 13) A dense cytoplasmic plaque ranging from 250 to 350 A in width lies parallel to the dense segment (leaflet) of the plasma lemma The intercellular space between the closely applied plasmalemmae is about 225 A and contains a fuzzy material of moderate density (figs 6 13) The apposing surface membranes along the inter cellular junction of adjacent endothelial cells appear to be tightly attached in some areas i e via the *zonula occludens zonule adhaerens* and *macula adhaerens* (desmosome) while at other levels of the same junction adhesion devices are not apparent (c f fig 3 J2 and fig 14 at arrows which are semi-serial sections) Many of the attachment devices appear to be easily separated as demonstrated by the occurrence of open junctions in both carbon and non injected animals The abluminal surface of the intercellular junction is held in close contact with the surrounding connective tissue via the attached (anchoring) fine filaments (figs 9 10 15) This condition is particularly noticeable when the junctions are partially or completely open (figs 10 15) The inner segments of the intercellular junctions without the attached filaments seem to act as "swinging flaps which presumably regulate the flow of fluids and particulate materials into the lumen of the lymphatic capillary (fig 15)

Many endothelial processes extend for varying distances into the lumen of the capillary and often carbon particles appear to be trapped by these cell processes (fig 3) Numerous pinocytotic like vesicles ranging from 75 to 100 mμ in diameter appear along the luminal and abluminal surfaces and also throughout the cytoplasm (figs 4 8 18) Larger vesicles (250 to 500 mμ in diameter) with oval to irregular profiles are also observed within the cytoplasm (figs 8 18) In samples injected with colloidal carbon many of the larger vesicles contain one to several particles of carbon (figs 8 17 18) Infrequently sections are observed where invaginations in both the luminal and abluminal plasmalemmae contain carbon particles which may possibly represent either an uptake or a discharge of particles by the vesicles (fig 4) A small number of vesicles appear to contain granular or spike like projections that coat their cytoplasmic surface (figs 4 9 10 18) The vesicles are limited by a membrane about 90 A thick while the coating of these vesicles is about 200 A thick Similar vesicles were described by Wissig (62) in cells of renal tubules (See also Anderson 64 Bowers 64 Brightman and Palay 63 and Roth and Porter 62 and 64) Occasionally invaginations occurring along the luminal and abluminal surfaces contain a coating on their cytoplasmic surface and frequently carbon particles are observed in these invaginations and appear to be entering or making an exit from the cell (fig 4)

A striking feature of the cytoplasm is the occurrence of numerous filaments that in most cases appear to run parallel to the long axis of the cell (figs 16 17) Figure 18 shows an apparent accumulation of these filaments into dense regions along the periphery of the endothelial cell The cytoplasmic filaments are about 60 A in diameter and are of an undeterminable length The filaments that course along the periphery of the cell occasionally seem to be closely applied to the inner surface of the plasmalemma (figs 17 18) In cross section the cytoplasmic filaments appear as aggregates of dense granules (fig 14) The filaments that are observed throughout the cytoplasm are similar to the fine filaments that occur along the endothelial wall (figs 3 8 16 18) The endoplasmic reticulum is not very extensive in these cells and is observed as dilated cisternae with ribosomes attached to their outer surfaces (fig 16) Ribosomes also appear free in the cytoplasm The Golgi complex is located in a juxta nuclear position and occasionally stacks of the Golgi lamellae appear in the thin cytoplasmic rim of the endothelial wall (fig 18) In favorable sections paired centrioles are observed in the lymphatic endothelial cell (fig 18) Mitochondria are dispersed about the nucleus and throughout the flattened lymphatic wall The form of the nucleus varies from elongate to oval in shape and often projects into the lumen

of the capillary (fig 3) The perinuclear cisterna which surrounds the nucleus is interrupted by nuclear pores The nucleoplasm consists of dense chromatic accumulations at the periphery and a network of fine filamentous strands that occupy the central region of the nucleus

In sections fixed in glutaraldehyde numerous microtubules are observed in the cytoplasm about the nucleus and in close association with the centrioles (fig 18) These microtubules are 230 to 250 A in diameter and many can be followed for several microns from the vicinity of the centrioles into other areas of the cytoplasm Similar structures have been reported for a number of animal and plant cells by various authors (Behnke 64 De The 64 Ledbetter and Porter 63 Sandborn et al 64 Slautterback 63)

DISCUSSION

The above observations demonstrate that the lymphatic capillaries of the guinea pig s ear as do those in other regions of the body (Casley Smith 64 Casley Smith and Florey 61 Fraley and Weiss 61 French et al 60 Palay and Karlin 59a b and Papp et al 62) possess salient morphological features that differentiate them from the blood capillaries The absence of a definitive basement lamina would eliminate a selective filter between the capillary wall and the connective tissue This provides a condition in which the ground substance of the adjacent connective tissue area is in direct contact with the lymphatic wall and would allow particles and excess fluid to enter the lymphatics without being slowed down or trapped by an intervening layer From the earlier observations on the transfer of particulate materials across the basement lamina it was suggested that the basement lamina of blood vessels behaved like a filter since the passage of ferritin molecules were impeded by this dense layer that surrounded the blood vessels (Farquhar and Palade 62 Farquhar et al 61) Similar observations were noted for larger colloidal particles (Alksne 59 Farquhar and Palade 59 Majno and Palade 61 Marchesi 62) and also cells (Marchesi 61 64 Marchesi and Florey 60)

From in vivo studies on regenerating blood vessels Clark and Clark (39) suggested that there was an increase in permeability in the walls of newly formed vessels and that they were highly fragile Recent ultrastructural studies of regenerating blood vessels by Cliff (63) and Schoefl (64) demonstrate that the basement lamina is irregular and often absent from newly formed segments of blood vessels while a continuous basement lamina surrounds the somewhat older vessels Schoefl (64) observed injected particles and also cells in the loose cell junctions of newly formed vessels and suggested that particulate materials and cells could leave the bloodstream through these loose junctions

In an electron microscopic study of lymphatic capillaries Caslev-Smith and Florey (61) noted that bundles of collagen fibers and fine branching irregular fibers invested the lymphatic capillaries However no definite attachment of fine filament to the endothelial wall was demonstrated The apparent attachment of numerous filaments at points of increased electron density along the abluminal endothelial wall and the extension of these fine filaments for varying distances into the adjoining connective tissue areas suggest that the lymphatic capillary wall is anchored to the surrounding connective tissue via these fine filaments It is likely that the many endothelial projections that extend into the adjoining connective tissue area may also aid in "anchoring the lymphatic wall to the connective tissue Fraley and Weiss (61) observed similar endothelial projections in lymphatics in the penile skin of the rat and suggested that they might serve to anchor the lymphatic wall to the connective tissue area The findings in the present study provide additional morphological evidence in support of the hypothesis put forth by these workers (Fraley and Weiss 61)

Although many open junctions are observed in the control lymphatic capillaries the close association of the wall with the adjoining connective tissue is maintained as suggested by the occurrence of numerous attached filaments along the abluminal surface of the intercellular junction (c f figs 9 10 15)

It is of interest to note that the inner overlapping segments of the intercellular junction are not stabilized by the fine filaments but instead they appear to act as "swinging flaps" which would permit plasma fluids and particulate materials to flow directly into the lymphatic lumen when the junctions are partially or completely open

In a light microscopic investigation of the inflamed and edematous tissue Pullinger and Florey (35) observed that fibers of the surrounding connective tissue were attached to the lymphatic endothelial wall and suggested that "as the connective tissue fills with edema fluid and swells tension on fibers attached to the lymphatic capillaries cause their wall to be drawn apart their dilation thus being passive" The present ultrastructural observations provide morphological evidence in support of their thesis and would explain why many of the open junctions between adjacent endothelial cells appear to be pulled apart during inflammation

The occurrence of open junction in both the carbon and non-carbon injected animals suggest that the intercellular junctions are loosely bound at certain areas along the lymphatic wall (i e tight junctions may be absent from some of the intercellular junctions along the lymphatic wall) Since the lymphatic capillaries serve to remove the excess connective tissue fluid from the tissue space under normal physiological conditions the absence of tight junctions from certain points would facilitate the separation of adjacent cell surfaces along the lymphatic wall and would allow the passage of large amounts of connective tissue fluids and particulate materials into the lymphatic lumen

It is pertinent to note that the abundant cytoplasmic filaments seem to be identical to many of the filaments that are attached along the endothelial surface The accumulation of cytoplasmic filaments into dense bundles near the periphery of the endothelial cell is reminiscent of the close association of the dense fibrous content in the cortical region of the fibroblast with the extracellular fibrous material along the surface of the cell (Porter 64 Porter and Pappas 59) The morphological and biochemical studies of several investigators (Porter 64 Revel and Hay 63 Ross and Benditt 61) have demonstrated that the precursors for collagen are synthesized within the cells of fibroblasts and condrocytes also in epidermal cells (Anderson and Kollros 62 Hay 64) and transported to the cell surface in membrane bounded vesicles The recent autoradiographic studies of Hay (64) demonstrate that the Schwann cells and endothelial cells in the amphibian secrete proline rich proteins It is hoped that similar studies utilizing regenerating lymphatic vessels will provide additional information in elucidating the precise nature of the cytoplasmic filaments and those occurring along the endothelial wall

From the above observations it is evident that two distinct types of invaginations and vesicles occur in the lymphatic endothelial cells of the guinea pig s ear (a) smooth surfaced vesicles and (b) a coated vesicle The numerous pinocytotic vesicles observed in this study are similar to those described for blood capillaries by Palade (53) Moore and Ruska (57) and Wissig (58) Similar smooth surfaced vesicles have also been noted in the lymphatic endothelial cells in other parts of the body (French et al 60 Palay and Karlin 59a) The passage of materials across the cell in small vesicles was suggested by Palade (53) and Bennett (56) advanced the hypothesis that membrane flow and vesiculation may be important transport mechanisms in carrying particles and molecules including ions within into and out of the cells by way of vesicles Experimental evidence in support of Bennett s hypothesis has since been demonstrated by a number of investigators (Brandt and Pappas 60 62 Jennings et al 62 Palade 60 61 Wissig 62) Similar observations were reported by Casley Smith and Florey (61) and Casley Smith (64) for the lymphatic endothelial cell

Like the smooth surfaced pinocytotic vesicles the coated vesicles occur along both luminal and abluminal surfaces and also deep in the cytoplasm they are similar to the coated vesicles described by a number of workers (Anderson 64 Bowers 64 Brightman 62 Brightman and Palay 63 Gray 61 Roth and Porter 62 64)

The morphological investigations of both Andreson (64) and Roth and Porter (62, 64) suggest that coated vesicles are involved in the uptake of yolk protein in the oocytes of the mosquito and roach The occurrence of coated invaginations along both surfaces of the endothelial cell and coated vesicles in the deep cytoplasm suggests that their content is being transported across the endothelial cell (c f figs 4, 9 10 and 18) In connection with the transmission of materials across the endothelial cell, we are reminded of the term cytopempsis described by Moore and Ruska (57) These investigators suggested that substances were being transmitted through the cytoplasm rather than being utilized by the cell They also considered specific absorption of the plasma membrane and specific loss of components from the vesicles on their way through the cytoplasm as possible mechanisms of selection It has been suggested that the coated vesicles observed in other cell types may be involved in the selective uptake of protein from the extracellular environment (Anderson 64, Bowers, 64 Fawcett 64 Roth and Porter 62 64) Since the lymphatics also have the special function of absorbing proteins (Courtice and Simmonds 49 Courtice and Steinbeck, 51 Drinker and Field 31) the coated vesicles observed in the endothelial cells of the lymphatic vessels may represent a transport mechanism for the transmission of proteins across the endothelial cells of lymphatic capillaries The current studies utilizing labeled proteins in this system should provide additional information to determine if the coated vesicles of the lymphatic are in fact involved in the transport of protein

LITERATURE CITED

Alksne J F 1959 The passage of colloidal particles across the dermal capillary wall under the influence of histamine Quart J Exptl Physiol 44 51–56

Anderson E 1964 Oocyte differentiation and vitellogenesis in the roach *Periplaneta americana* J Cell Biol 20 131–155

Anderson E *and* J J Kollros 1962 The ultrastructure and development of balancers in *Ambystoma* embryos with special reference to the basement membrane J Ultrastruct Res 6 36–56

Behnke O 1964 A preliminary report on "Microtubules in undifferentiated and differentiated vertebrate cells J Ultrastruct Res 11 139–146

Bennett H S 1956 The concepts of membrane flow and membrane vesiculation as mechanisms for active transport and ion pumping J Biophysic Biochem Cytol 2 99–103

Bowers B 1964 Coated vesicles in the pericardial cells of the Aphid (*Myzus persicae* Sulz) *Protoplasma 59* 351–367

Brandt P W *and* G D Pappas 1960 An electron microscopic study of pinocytosis in ameba I The surface attachment phase J Biophysic and Biochem Cytol 8 675–687

——— 1962 An electron microscopic study of pinocytosis in ameba II The cytoplasmic uptake phase J Cell Biol 15 55–71

Brightman M W 1962 An electron microscopic study of ferritin uptake from the cerebral ventricles of rats Anat Rec 142 219

Brightman M W and S L Palay 1963 The fine structure of ependyma in the brain of the rat J Cell Biol 19 415–439

Casley Smith J R 1964 An electron microscopic study of injured and abnormally permeable lymphatics Ann N Y Acad Sci 116 803–830

Casley Smith J R and H W Florey 1961 The structure of normal small lymphatics Quart J Exptl Physiol 46 101–106

Clark E R and E L Clark 1939 Microscopic observations on the growth of blood capillaries in the living mammal Am J Anat 64 251–301

Cliff W J 1963 Observations on healing tissue A combined light and electron microscopic investigation Trans Roy Soc Lond Ser B 246 305–325

Courtice F C and W J Simmonds 1949 Absorption of fluids from the pleural cavities of rabbits and cats J Physiol 109 117–130

Courtice F C and A W Steinbeck 1951 The effects of lymphatic obstruction and of posture on the absorption of protein from the peritoneal cavity Aust J Exp Biol Med Sci 29 451–458

De The G 1964 Cytoplasmic microtubules in different animal cells J Cell Biol 23 265–275

Drinker C K and M E Field 1931 The protein content of mammalian lymph and the relation of lymph to tissue fluid Amer J Physiol 97 32–39

Farquhar M C and G E Palade 1959 Behavior of colloidal particles in the glomerulus Anat Rec 133 378

——— 1962 Functional evidence for the existence of a third cell type in the renal glomerulus J Cell Biol 13 55–87

——— 1963 Junctional complexes in various epithelia J Cell Biol 17 375–412

Farquhar M G S L Wissig and G E Palade 1961 Glomerular permeability I Ferritin transfer across the normal glomerular capillary wall J Exptl Med 113 47–66

Fawcett D W 1964 Local specialization of plasmalemma in micropinocytosis vesicles of erythroblasts Anat Rec *148* 370

Fraley E E and L Weiss 1961 An electron microscopic study of the lymphatic vesicles in the penile skin of the rat Am J Anat *109* 85–101

French J E H W Florey and B Morris 1960 The absorption of particles by the lymphatics of the diaphragm Quart J Exptl Physiol 45 88–103

Gray E G 1961 The granule cells mossy synapses and purkinje spin synapses of the cerebellum Light and electron microscope observations J of Anat 95 345–356

Hay E D 1964 Secretion of a connective tissue protein by developing epidermis In The Epidermis Edited by W Montagna and W C Lobitz Jr Academic Press New York p 97

Hudack S S and P D McMaster 1932 I The permeability of the wall of the lymphatic capillary J Exptl Med 56 223–238

Jennings M A V T Marchesi and H W Florey 1962 The transport of particles across the wall of small blood vessels Proc Roy Soc Lond Ser B *156* 14–19

Ledbetter M C and K. R. Porter 1963 A "microtubule in plant cell fine structure J Cell Biol *19* 239–250

Majno G and G E Palade 1961 Studies on inflammation I The effect of histamine and serotonin on vascular permeability An electron microscopic study J Biophysic and Biochem Cytol *11* 571–605

Marchesi V T 1961 The site of leucocyte emigration during inflammation Quart J Exptl Physiol. 46 115–118

——— 1962 The passage of colloidal carbon through inflamed endothelium Proc Roy Soc Lond Ser B *156* 550–552

——— 1964 Some electron microscopic observations on interactions between leukocytes platelets and endothelial cells in acute inflammation Ann N Y Acad Sc *116* 774–778

Marchesi V T and H W Florey 1960 Electron microscopic observations on the emigration of leucocytes Quart J Exptl Physiol 45 343–348

Millonig G 1961 Advantages of a phosphate buffer for OsO solutions in fixation Proc EMSA B 26 p 15 (Abstract)

Moore D H and H Ruska 1957 The fine structure of capillaries and small arteries J Biophysic and Biochem Cytol 3 457–462

Palade G E 1953 Fine structure of blood capillaries J Appl Phys 24 1424

——— 1960 Transport in quanta across the endothelium of blood capillaries Anat Rec *136* 254

——— 1961 Blood capillaries of the heart and other organs Circulation 24 368–384

Palay S L and L J Karlin 1959a An electron microscopic study of the intestinal villus I The fasting animal J Biophysic and Biochem Cytol 5 363–372

——— 1959b An electron microscopic study of the intestinal villus II The pathway of fat absorption J Biophysic and Biochem Cytol 5 373–384

Papp M P P Rohlich I Rusznak and I Toro 1962 An electron microscopic study of the central lacteal in the intestinal villus of the cat Z. Zellforsch Mikroskop Anat Abt Histochem 57 475–486

Pease D C 1962 Buffered formaldehyde as *a killing agent and primary fixative for electron* microscopy Anat Rec *142* 342

Porter K R. 1964 Cell fine structure and biosynthesis of intercellular macromolecules Biophys J 4 167–196

Porter K R and G D Pappas 1959 Collagen formation by fibroblasts of the chick embryo dermis J Biophysic Biochem Cytol 5 153–166

Pullinger B D and H W Florey 1935 Some observations on the structure and function of lymphatics Their behavior in local edema Brit J Exptl Path *16* 49–61

Reynolds E S 1963 The use of lead citrate at high pH as an electron-opaque stain in electron microscopy J Cell Biol *17* 208–212

Revel J P and E Hay 1963 An autoradiographic and electron microscopic study of collagen synthesis in differentiating cartila e Z Zellforsch Mikroskop Anat *61* 110–144

Ross R and E P Benditt 1961 Wound healing and collagen formation I Sequential changes in components of guinea pig skin wounds observed in the electron microscope J Biophysic Biochem Cytol *11* 677–700

Roth T F and K. R. Porter 1962 Specialized sites on the cell surface for protein uptake in 5th International Congress for Electron Microscopy Philadelphia (S S Breese Jr Editor) New York Academic Press Inc 2 LL-4

——— 1964 Yolk protein uptake in the oocyte of the mosquito *Aedes aegypti* L J Cell Biol 20 313–332

Sabatini D D K Bensch and R J Barrnett 1963 Cytochemistry and electron microscopy The preservation of cellular ultrastructure and enzymatic activity by aldehyde fixation J Cell Biol *17* 19–58

Sandborn E P K Koen J D McNabb and G Moore 1964 Cytoplasmic microtubules in mammalian cells J Ultrastruct Res *11* 123–138

Schoefl G I 1964 Electron microscopic observations on the regeneration of blood vessels after injury Ann N Y Acad Sci *116* 789–802

Slautterback D B 1963 Cytoplasmic microtubules I Hydra J Cell Biol *18* 367–388

Watson M L *1958 Staining of tissue sec*tions for electron microscopy with heavy metals J Biophys and Biochem Cytol 4 475–478

Wissi S L 1958 An electron microscopic study of the permeability of capillaries in muscle Anat Rec *130* 467

——— 1962 Structural differentiation in the plasmalemma and cytoplasmic vesicles of selected epithelial cells Anat Rec *142* 292

PLATE 1

EXPLANATION OF FIGURES

1 Whole mount preparation injected with colloidal carbon showing lymphatic plexus in guinea pig s ear × 115

2 Light micrograph which shows a cross section of guinea pig s ear The superficial (l_1) and deep (l_2) lymphatic capillaries are observed stained with 10% silver nitrate hematoxylin and safranin O × 460

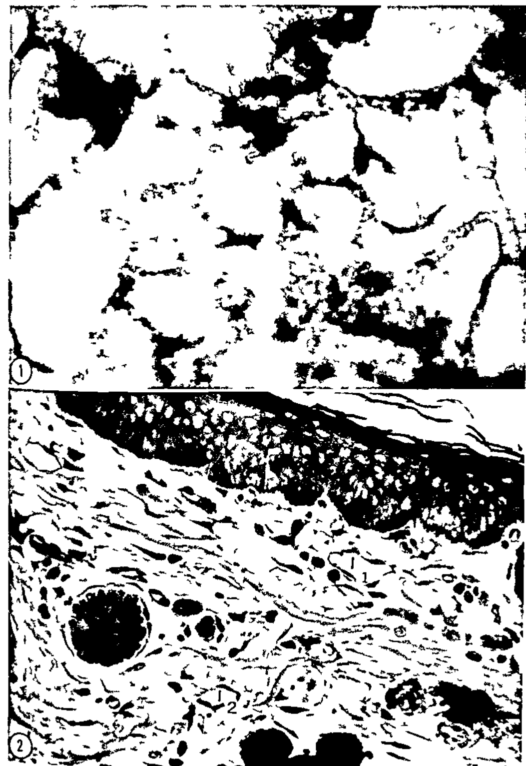

1
2
1
2

PLATE 1

EXPLANATION OF FIGURES

1 Whole mount preparation injected with colloidal carbon showing lymphatic plexus in guinea pig s ear × 115

2 Light micrograph which shows a cross section of guinea pig s ear The superficial (l_1) and deep (l_2) lymphatic capillaries are observed stained with 10% silver nitrate hematoxylin and safranin O × 460

PLATE 2

EXPLANATION OF FIGURES

3 A survey electron micrograph which shows the relationship of the lymphatic capillary to the adjoining connective tissue (*CT*) Irregular segments of the basement lamina (*bl*) are apparent at various points Fine filaments (f_1) are attached at areas of increased electron density (arrows) and extend between the collagen fibers (*CF*) Carbon particles (*c*) appear in the lumen (*L*) and in some of the intercellular junctions (*j*) Numerous cytoplasmic filaments (f_2) are apparent throughout the cytoplasm Interdigitating junctions are shown at (j_1) and (j_2) A different level of junction 2 is shown in figure 14 × 5400

4 Longitudinal sections through lymphatic capillary The fine filaments (f_1) form a loose network between lymphatic wall and connective tissue (*CT*) Smooth surface vesicles of various sizes (*v*) and coated vesicles (*cv*) appear in the cytoplasm Carbon particles (*c*) appear in the lumen (*L*) and in invaginations and vesicles × 11 800

j 1
bl
CT
f 2
L
c
f
2
j 2
3
j
j
cv
c
c
L
f
j
cv
v
4
CT

PLATE 2

EXPLANATION OF FIGURES

3 A survey electron micrograph which shows the relationship of the lymphatic capillary to the adjoining connective tissue (*CT*) Irregular segments of the basement lamina (*bl*) are apparent at various points Fine filaments (f_1) are attached at areas of increased electron density (arrows) and extend between the collagen fibers (*CF*) Carbon particles (*c*) appear in the lumen (*L*) and in some of the intercellular junctions (*j*) Numerous cytoplasmic filaments (f_2) are apparent throughout the cytoplasm Interdigitating junctions are shown at (j_1) and (j_2) A different level of junction 2 is shown in figure 14 × 5 400

4 Longitudinal sections through lymphatic capillary The fine filaments (f_1) form a loose network between lymphatic wall and connective tissue (CT) Smooth surface vesicles of various sizes (*v*) and coated vesicles (*cv*) appear in the cytoplasm Carbon particles (*c*) appear in the lumen (*L*) and in invaginations and vesicles × 11 800


L
c
*
*
*
*
5
ep
d
d
za
6
v
sm
7

PLATE 3

EXPLANATION OF FIGURES

5 A section through lymphatic capillary showing endothelial projections (*cp*) and deep clefts (*) in capillary wall Carbon particles (*c*) are scattered throughout the lumen (*L*) × 8 610

6 An interdigitating type of intercellular junction is shown in this micrograph Adjacent cells are held in close apposition with *macula adhaerens* (*d*) and *zonula adhaerens* (*za*) Part of a fibroblast is shown in upper right corner × 25 000

7 In this electron micrograph terminal endothelial processes overlap to form intercellular junction (*j*) Many small vesicles (*v*) are observed in both cell processes Part of a smooth muscle cell (*sm*) occurs near lymphatic capillary × 22 500


f1
cv
9


cv
10

PLATE 4

EXPLANATION OF FIGURES

8 Portion of lymphatic endothelial cell which shows the fine filaments (f_l) attached to dense areas along lymphatic wall (arrows) Mitochondria (*m*) numerous ribosomes (*r*) and small vesicles (*v*) are apparent Carbon particles (*c*) are observed in one of the large vesicles × 21 875

9 *This micrograph shows the anchoring filaments (f_l) attached at* dense regions (arrows) near the intercellular junction (*j*) which contains carbon particles (*c*) A coated vesicle (*cv*) occurs near luminal side × 18 750

10 The width of the intercellular junction (*j*) is quite varied (*) Filaments (f_l) are attached along the abluminal endothelial surface (arrows) A coated vesicle (*cv*) occurs in the cyotplasm × 25 000


11

PLATE 5

EXPLANATION OF FIGURE

11 A section through unmyelinated nerve fibers (*un*) and the Schwann cells (*sc*) are surrounded by a perineural cell (*pe*) that has a basement lamina (*bl*) on both surfaces An invagination with coated cytoplasmic surface (*cv*) appears at the abluminal surface (insert) Fine filaments (f_1) are attached to endothelial process in upper part of micrograph × 25 000 Insert × 90 625


bl
bl
cv
11

PLATE 6

EXPLANATION OF FIGURES

12 The terminal endothelial processes interlock to form interdigitations along the intercellular junction (*j*) A *zonula occludens* (*zo*) occurs at the luminal side while *zonula adhaerens* (*za*) and *macula adhaerens* (*d*) appear at various points along the intercellular junction Numerous vesicles (*v*) occur in the cytoplasm × 46 000 Insert shows enlargement of *zonula occludens* × 171 000

13 Terminal processes from two endothelial cells (F_1 and E_2) that interlock to form an interdigitating intercellular junction Arrows indicate sites of attachment × 60 000

PLATE 7

EXPLANATION OF FIGURES

14 Section of part of capillary shown in figure 3 from a different plane At this level the terminal processes of adjacent cells overlap (arrows) instead of interlocking as in figure 3 (junction 2) The cytoplasmic filaments (f_2) are cut in cross section and appear as dense granules × 18 000

15 Electron micrograph which shows an open intercellular junction (*j*) with attached filaments (f_1) along the abluminal endothelial surface (arrows) There are no attached filaments along the surface of the inner segments (*is*) which extend into the lumen of the capillary (*L*) × 30 600

14
f2
15
IS
L

PLATE 8

EXPLANATION OF FIGURES

16 The endoplasmic reticulum (*er*) appears as dilated vesicles with ribosomes (*r*) attached to the outer surface Numerous cytoplasmic filament (*f*) appear throughout the cell Long filamentous strands course along the wall (arrows) and extend into the connective tissue (*CT*) × 31 250

17 Large vesicles (*v*) and invaginations containing carbon particles (*c*) are shown The filamentous strands along the wall are closely applied to the dense region (arrow) and are of the same density as the filaments at the periphery of the cell × 37 500


CT
2
16
C
V
17

PLATE 9

EXPLANATION OF FIGURE

18 The nucleus (n) occupies a large portion of this cell Centrioles (Ce) mitochondria (m) microtubules (mt) Golgi complex (G) ribosomes (r) and ctyoplasmic filaments (f_2) are shown Smooth vesicles (v) and coated vesicles (cv) appear in the cytoplasm The two larger smooth vesicles contain particles of carbon (c) Note carbon particles associated with invagination (*) along the luminal surface (L) Many of the cytoplasmic filaments seem to accumulate in bundles near the periphery of the cell (arrows) Numerous fine filaments (f_1) are observed along the endothelial wall × 28 750


G
C e
r
c
f 1
c
L
c v
m t
18

Perfusion fixation of the Brain with Chrome osmium Solutions for the Rapid Golgi Method [1]

D KENT MOREST AND R R MOREST
Department of Anatomy Harvard Medical School Boston Massachusetts

ABSTRACT The characteristics of rapid Golgi impregnations of neurons in the brains of opossums rats rabbits chinchillas and cats obtained with a method employing intracardiac perfusion with osmium tetroxide-dichromate fixatives are reported Observations on all subdivisions of the brain were compared with immersion fixed Golgi preparations and formalin perfused brains prepared by Nissl or reduced silver methods Perfusion fixation yielded more uniform and extensive Golgi impregnations which were more representative of the varieties of neural structures than in immersion fixed preparations The morphological details of fine neuronal processes delicate dendritic branchlets and spines and fine elements of the axonal plexuses were more clearly and consistently demonstrable Observations with the polarizing microscope suggested that the Golgi impregnations contained silver dichromate and/or silver monochromate The procedures and the predictability nature and histological reliability of the rapid Golgi method are discussed

The Golgi methods have been choice methods for histological study of individual neurons and their processes in the central nervous system Since their introduction over 90 years ago (Golgi 1873) interest in these methods has increased for the kinds of information obtained with them facilitate the interpretation and correlation of neurological studies with a variety of newer techniques This interest has been expressed in such diverse quarters as electron microscopy (e g Hamlyn 63) pathology (Eayrs 55) microelectrode studies (e g Andersen Eccles and Voorhoeve 64) and the analysis of synaptic architecture with synapse stains and degeneration methods (e g Morest 65b)

The Golgi methods are traditionally applied to brain tissue which is first killed and then immersed in a fixative Because of the cytological distortion of central nervous tissue commonly observed with post mortem fixation both at the light and electron microscopic levels (Bodian 37 Palay McGee Russell Gordon and Grillo 62) the reliability of the classical Golgi methods may be questioned This question is especially pertinent when Golgi preparations are to be correlated with the findings of other techniques Less objectionable in this respect may be the techniques following formalin fixation of the brain (Gerota 1896) by intracardiac perfusion (e g Fox Ubeda Purkiss Ihrig and Biagioli 51) Instructive impregnations may be obtained with these techniques in adult animals (Fox and Barnard 57 personal observations) However of the many modifications of Golgi s method (for a resumé see Kallius 26 Ramon Moliner 57 58) the rapid Golgi method namely dichromate silver impregnation of tissue elements fixed by immersion in osmium tetroxide and dichromate salts has been preferentially employed by Ramon y Cajal Herrick Polyak Lorente de No and many others The anatomical record implies that the rapid Golgi method has in fact been the most generally fruitful in the study of the axonal plexuses and other neuronal elements of the central nervous system

The present report is based on a five year period of successful results with a rapid Golgi method employing intracardiac perfusion of the brain with osmium tetroxide-dichromate fixatives The results are discussed with respect to procedure the predictability and nature of the Golgi reaction and the reliability of the method as an indicator of the normal histological structure of nervous tissue

[1] This wo k w s support d in p rt by Public Health Service Research gr nt NB 06115

MATERIALS AND METHODS

The rapid Golgi method with perfusion fixation has been applied to 50 brains, including those of rabbits chinchillas and opossums ranging in age from newborn (or pouch young) to adult animals and also to adult rats and to an age graded series of cats ranging from newborn to four months of age This mtaerial was compared with a collection of several hundred immersion fixed brains prepared with the Golgi methods and studied over the past ten years The observations were made on all subdivisions of the brain from the cervical spinal cord posteriorly to the olfactory bulbs anteriorly The material has been sectioned in uninterrupted series from nearly all, or in most cases the entire brain of each animal Section thickness (40–120 μ) was always taken into account in making comparisons

The results in perfusion fixed brains were compared with those of immersion fixed littermates and animals of the same age Sometimes the perfusions were spotty i e the perfused fixative did not penetrate or blacken all parts of the brain uniformly In these cases the impregnations in successfully perfused regions were compared with those obtained with identical impregnation procedures in unblackened parts of the same brain The effects of variations in the perfusion procedure on the subsequent Golgi impregnations were determined by intraspecies comparisons between animals of comparable ages or between littermates The effects of systematic variations in the impregnation schedules and solutions were determined by comparing the results in bilaterally symmetrical parts from the same brains In addition impregnations in identical parts of the brains of littermates and of animals of the same species and similar ages were compared All comparisons were checked by reference to homonymous neuronal populations on opposite sides of the same brain and in different brains of the same species and age The criteria used to identify neuronal populations in Golgi preparations have been explained elsewhere (Morest 64 65c) The Golgi impregnations were compared with formalin perfused brains prepared by the Nissl method or by silver methods for axons (Richardson 60) and synaptic endings (Rasmussen 57) Impregnations of neuroglia and non neural elements of the brain were not evaluated

A Zeiss polarizing microscope equipped with a Bertrand lens was used to study the crystalline appearance of the Golgi impregnations in sections of neurons and on the surfaces of the tissues Such properties of birefringence as extinction angles pleochroism polarization colors and characteristics of the interference figures including apparent optic axial angle and dispersion of the optic axes were compared with the properties of crystalline samples of known compounds The crystals obtained from commercial sources or synthesized *in vitro* were recrystallized on glass slides and mounted under cover glasses in Permount (Fisher Scientific Co) or Aroclor 5460 (Monsanto Chemical Co)

Perfusion method

A *Preparation* 1 A healthy animal was deprived of food and water before the perfusion for a period depending on its age For example an adult rabbit was fasted 24–48 hours an adult opossum 72 hours a 50 day old opossum pouch young two or three hours in all cases at 20–25°C

2 Light surgical anesthesia was used just sufficient to abolish hindlimb withdrawal Young adult cats and opossums received sodium pentobarbital intraperitoneally 35 mg/kg The higher dosages usually needed for kittens were determined empirically since they varied with age size and sex Adult rats and opossum pouch young were anesthetized with chloral hydrate 350 mg/kg intraperitoneally chinchillas with sodium pentobarbital 35 mg/kg intraperitoneally Rabbits were anesthetized with sodium pentobarbital intravenously often supplemented with 40% urethane 2 0 ml/kg intraperitoneally

3 On anesthetization 30 minutes before the perfusion 1000 or 500 I U (depending on the animal s weight) of heparin sodium U S P were injected intravenously

4 Ten minutes before the perfusion 1 5 ml/kg of 50% (w/w) urea was slowly

injected intravenously One minute before perfusion 0 5 or 1 0 ml (depending on the animal s weight) of 1% sodium nitrite was injected intravenously

5 The animal was shaved and cooled with ice (after Wolfe 61) until the rectal temperature declined to 21 C where it remained until the perfusion began

B *Perfusion* The apparatus described by Palay et al (62) was satisfactory Instead of rubber tubing and heating tapes we usually have used an all glass perfusion column similar to a distillation condenser[3] the temperature of which may be controlled by a water jacket containing warm water or cold brine

1 Ligatures were placed tightly around the forelimbs across the axillae After a midventral incision over the thorax and abdomen the skin was reflected to either side The thoracic cavity was opened at the costal attachment of the diaphragm The ventral thoracic cage was raised in one flap by cutting the ribs bilaterally at the midaxillary line with bone shears The internal mammary arteries were clamped proximally and the flap of rib cage removed to expose the heart The pericardium was opened and the descending thoracic aorta clamped with a hemostat Next the right atrium was incised and the left ventricle immediately opened near the apex. With the first solution flowing a glass cannula was quickly inserted through the left ventricle into the base of the aorta where it was securely fixed with a ligature or specially shaped clamp

2 The first solution a saline solution at 38 C was perfused rapidly from a height of 120 cm above the head while the carotid sheath was gently massaged bilaterally In about 10–15 seconds the perfusate from the right side of the heart was almost free of blood At that time the fixative usually 0 25% osmium tetroxide and 3% potassium dichromate in a saline solution at pH 6 8 was introduced to the perfusion column at a temperature of 38 C As soon as fixative was detected in the perfusion fluid leaving the right atrium the temperature of the perfusion column was reduced to 4 C At the same time the rate of flow was reduced so as to require 20–30 minutes to perfuse 100–200 ml of the fixative The perfusate was continuously washed away and adequate ventilation provided for protection from the osmic acid fumes

Immersion method

The brains were removed from the skull immediately after a lethal dose of an anesthetic or under surgical anesthesia (see *Perfusion method* step A2) These animals usually stopped breathing and died 20 or 30 minutes before the brain had been removed In some cases this time was shortened to less than a minute by lowering the rectal temperature of the anesthetized animal to 21 C A number of animals were prepared according to steps A1 through A5 of the *Perfusion method* some brains were removed successively after each step Other animals were subjected to the entire *Perfusion method* including saline perfusion but no attempt was made to perfuse the fixative before removing the brain All of the brains were processed according to the *Impregnation method* below

Impregnation method

1 The brain was removed from the skull immediately at the end of the perfusion and cut into slices exactly 3 mm thick with a small brain knife on a macrotome that permits accurate control of the thickness of tissue slices (Rasmussen 31) During this time the brain was kept moist with the rapid Golgi fixative in which the slices were to be immersed

2 The entire impregnation was done at 20–25 C The slices were immersed on gauze in a volume of fixative ("first fixative") at least 50 times that of the tissue and kept in the dark for one to five days

3 The slices were rinsed briefly with 0 75% aqueous silver nitrate blotted by touching them with absorbent paper and immersed on gauze in a volume of silver nitrate solution ("first silver solution") at least 50 times that of the tissue for two to six days in the dark

4 Much of the material *underwent* double or triple impregnation In these cases the slices were removed from the first silver solution rinsed with distilled

[3] Designed by Dr R. A. Naumann, Dept. of Surgery State University of New York, Syracuse N Y

water brushed lightly and carried through the previous two steps with freshly made solutions

5 The slices were brushed free of loose surface precipitate and dehydrated in changes of 40% 70%, and 100% ethanol one hour each Dehydration was completed in a mixture of two parts ethyl ether to one part absolute ethanol (after Ramon Moliner 59) three or four changes for a total of 6–18 hours The blocks were exposed to low viscosity nitrocellulose (Hercules Powder Co, RS 1/2 sec special) in changes of 5% 10%, 20% and 30% (w/v) for one day each The solvent was two parts ether to one part ethanol After the tissue slices were embedded in 30% nitrocellulose hardened in chloroform vapor and mounted on fiber block chucks they were soaked in 70% ethanol at 4°C overnight to remove any unreduced silver from the tissue

6 The sections made on a sliding microtome were collected in serial order in 70% ethanol and passed through one change of 95% ethanol two changes of 100% 1 butanol and two changes of cedar wood oil (Oil cedar wood water white " Fritzsche Bros New York) for ten minutes in each change The sections were kept in cedar wood oil for periods up to four weeks without signs of fading They were rinsed in toluene before mounting with Permount under cover glasses

RESULTS

Impregnations

When a brain was removed after a successful perfusion (27 brains) it appeared uniformly jet black or dark gray depending on the relative proportions of white and gray matter in different regions The brain was not visibly swollen Occasionally there was a white streak in the corpus callosum Incompletely perfused brains (15 brains) had a spotty appearance often with an asymmetrical distribution of blackening on both sides of the brain After completely unsuccessful perfusions (eight brains) there was blackening only along the cerebral arteries

After successful perfusions the rapid Golgi impregnations resembled the immersion fixed specimens and the descriptions of the classical literature in that varieties of neurons with their characteristic perikarya processes, and other distinguishing morphological features were demonstrable Examples are illustrated in the photomicrographs (figs 1–12) and in drawings elsewhere (Morest 64 65a b) However the successfully perfused preparations typically differed from their immersion fixed counterparts in several ways Most striking was the uniformity of the impregnations in the perfused material Serial sections could be uniformly impregnated through an entire brain including the cervical cord This contrasted markedly with the customary patches of impregnated cells in brains fixed by immersion or by incomplete or spotty perfusions For example in every transverse section from a well perfused adult rat brain not only were the neurons and axonal plexuses well impregnated in the different cortical areas but also in *all* or *nearly all* of the neuronal populations of the diencephalon (figs 7–9) Similar results were obtained at lower levels of the brain stem in such specimens *provided* that appropriate impregnation schedules for these regions were used Only rarely did comparable impregnations occur in immersion fixed preparations and then only in certain areas usually the cortical areas

The extents of the impregnations i e the quantity of impregnated elements in equivalent volumes of tissue were nearly always greater in successfully perfused material than in comparable immersion fixed or incompletely perfused material No attempt was made to quantitate this difference since it was great enough to make a distinct qualitative difference between the pecimens Nevertheless comparisons of Golgi impregnations with Nissl or reduced silver preparations of comparable regions *indicated that only* a minority of the *neural elements could be* impregnated *in the perfusion fixed speci*mens

A significant result of successful perfusions was that the fine details of neuronal processes were more consistently preserved than in immersion fixed tissue We refer to the integrity of fine dendritic branches dendritic spines and delicate

branchlets the continuity of fine axonal plexuses and their endings and the con figuration of their terminal ramifications All these morphological features were much more frequently encountered in successfully perfused tissue Osmium stained myelin sheaths which were more abundant and more sharply delineated gave an optically crisper more coherent appearance to the tissue (fig 9) Post mortem alterations (fig 10) such as fragmentation irregular beading distor tions in shape and arrangement of cell processes and wrinkled myelin sheaths were less frequently encountered in suc cessfully perfused brains This is not to deny that such alterations were ever en countered At the same time there were isolated cells in immersion fixed prepara tions comparable to those of perfusion fixed preparations This was expected since irregularity of preservation not necessarily uniformly bad preservation is the hallmark of immersion fixed brains No evaluation of the quality of fixation in our material was made with histological techniques other than the Golgi methods

After incomplete or spotty perfusions the uniformity extent and preservation of the impregnated neurons often mir rored the distribution of the fixative in each case However the morphological preservation in such brains was not con sistently good even in apparently well blackened regions Constant features of these brains were unimpregnated tubular regions or cuffs around small blood ves sels (fig 11) Typically these cuffs sur rounded an empty vascular lumen with a disrupted endothelium Within the cuffs themselves was a dark granular material and the Golgi impregnation was completely absent The perivascular cuffs could not be attributed to an unduly elevated perfu sion pressure since they increased in fre quency in cats when the perfusion column was lowered to only 40 cm above the head — a pressure considerably below normal blood pressure However a blockage in the cerebral capillary bed might conceiv ably result in a pooling of the fixative in small arteries and lead to its extravas ation Lack of impregnation in the cuffs may have resulted from an effect of the osmium which failing to perfuse the tissue evenly might have accumulated in high concentration immediately around the vessel walls Comparable results in Golgi preparations could be produced by successful perfusion with 1% osmium tetroxide alone but not with 5% potas sium dichromate alone Other observa tions indicated that initial fixation with unusually high concentrations of osmium tetroxide (1% or higher) or prolonged initial exposures (over one week) to fixatives containing osmium tended to re duce the frequency and extent of Golgi impregnation

The immersion fixed preparations were presumably comparable to those of the classical methods which are still in gen eral use Certainly we have been able to repeat many details of the descriptions of Ramon y Cajal and Lorente de Nó in the cortex and brain stem The immersion fixed Golgi impregnations most nearly re sembling perfusion fixed preparations were obtained when the brain had been re moved in hypothermia (fig 1) Perhaps this result may be attributed to the ob servation that living neurohistological structures resist deformation by mechani cal trauma better than dead ones (Cam mermeyer 60) With hypothermia the brain could be nearly completely removed before respiration ceased No doubt all of these brains were subject to unavoid able trauma during their removal When the brain had been removed after a lethal anesthetic dose (fig 10) the preservation of the Golgi preparations was decidedly in ferior Immersion fixed brains perfused with one or another of the saline solu tions without the benefit of hypothermia exhibited the worst cellular preservation of all

Procedures

Successful application of the present method requires a mastery of the basic principles and skills of perfusion fixation of the brain These are discussed by Koenig Groat and Windle (45) and Cam mermeyer (60) The techniques of Palay et al (62) are particularly suitable for chrome-osmium perfusion We wish to ex plain certain aspects of the procedures in relation to the rapid Golgi method

Preparation Fasting and dehydrating animals not only facilitated anesthetization but also increased the extent of the im pregnations This practice has also been independently recommended for the Golgi method by Scheibel and Scheibel (64) Very young animals should not be fasted and exposed to the cold so long that they are starving shivering and in a state of shock Such animals were not promising subjects for a successful perfusion The seemingly beneficial influence of fasting perhaps resulted from the nutritional states of the animals or from metabolic effects of the increased motor activities they displayed The impregnations in new born animals were generally no more successful than those in weanlings The best results were most often obtained from animals with recently opened eyes which had begun to explore their surroundings, e g two or three week old cats and 100 day old opossums Very fine possibly un myelinated axons were readily impregnated in young adults The possible effcts of different anesthetic agents on the subse quent Golgi impregnations were not ex amined

Urea Perfusion with isotonic solutions containing dichromate salts was accom panied by grossly visible swelling of the brain Unless measures were taken to prevent this the perfusion was liable to fail, and in any case the swollen cere brum would undergo mechanical defor mation from excessive pressure in the closed skull Administration of urea counteracted this (see Clasen Cooke Pan dolfi, Carnecki and Bryar 65) If the use of urea were omitted successful perfu sions and impregnations could be obtained by raising the concentration of sodium chloride to 2 5% or by adding methyl cellulose (100 centipoise) in a concentra tion of 0 5% in the saline solutions and fixatives

Hypothermia may prevent cerebral swelling in some circumstances (Roso moff, 59) and increase the resistance of cerebral tissue to hypoxia (Rosomoff 56) Successful perfusions were possible without its use Nothing in the perfusion fixed impregnations could be attributed to its omission or inclusion Its beneficial effects for immersion fixed material have been noted It has been included in the perfusion method only as a safeguard If the perfusion were unsuccessful or incom plete the brain might then be fixed by immersion

The saline solutions used for the per fusions were a balanced salt solution buff ered at pH 7 2 (Palay et al 62) Mc Ewen s (56) saline solution buffered at pH 7 2 2 5% sodium chloride buffered at pH 7 3 with veronal acetate or unbuffered 0 9% sodium chloride initially at pH 7 2 It was not possible to attribute differences in the subsequent Golgi impregnations to use of one or another of these solutions Prolonging the saline perfusion beyond one minute often resulted in an unsuc cessful perfusion of the fixative

Fixative Satisfactory impregnations could be obtained with a solution contain ing 0 5% osmium tetroxide, 0 9% sodium chloride, and 3% potassium dichromate dihydrate) (or 3% sodium dichromate dihydrate) buffered at pH 6 8–7 0 by the addition of sodium hydroxide More extensive but less uniformly preserved impregnations could be obtained with a 0 25% osmium tetroxide concentration A concentration of 1% osmium tetroxide in our fixative or in the fixative solutions of Palade (52) Dalton (55) or Palay et al (62) allowed considerably less extensive but still useful impregnations Omission of osmium alto gether resulted in markedly inferior badly preserved preparations as might be ex pected from the findings of Baker (65) in the pancreas Successful rapid Golgi im pregnations were obtained when the fixa tive was unbuffered (initial pH 4 0) or when it was buffered with sodium hydrox ide at pH 5 8 6 8 or 7 0–7 4 The most extensive and most uniform impregnations were obtained when the fixative was acid the best preservation with a pH near neutrality

Artificial respiration was given to four animals according to Palay et al (62) This practice was discontinued when ap parently well preserved Golgi preparations were obtained in successfully perfused brains without artificial respiration In retrospect it was observed that all four perfusions with artificial respiration were entirely successful whereas the perfusions

without it did not always succeed We are inclined to favor its routine use although we have not had much experience with it

Impregnation Successfully perfused brains have been left in the skulls for periods up to five hours after the perfusion without any noticeable deterioration or improvements in the Golgi preparations If the perfusion were a failure the brain could be prepared by immersion fixation For this reason the brain was usually re moved immediately to ascertain the suc cess of the perfusion The need to prepare tissue slices exactly 3 mm thick was critical for the perfusion as well as the immersion method The total volume of the slices was less critical provided the volumes of the solutions were sufficiently large There were uniform impregnations of adult rat brain slices of 450 mm³ (a cross section of the entire cerebrum) and of young opossum brain slices of 1 600 mm³ (horizontal and parasagittal sections of the entire brain)

The most extensive impregnations oc curred when well perfused tissues were placed in a first fixative consisting of 0 25% osmium tetroxide and 3% potas sium dichromate (or 3% sodium dichro- mate dihydrate) Raising or lowering the osmium or dichromate concentrations was either deleterious or without effect Good impregnations were obtained when the initial pH was somewhere between 4 0 and 6 0 regardless of the pH of the per fused fixative It was possible to obtain rapid Golgi impregnations with the di chromate buffered at pH 7 0–7 4 but the cells were liable to be incompletely im pregnated or obscured by precipitates We have preferred raising the pH to 5 8 with sodium hydroxide Successful re sults were obtained by substituting lithium or ammonium dichromate for potassium dichromate but no particular advantage accrued and more precipitates formed The composition of the silver solutions was usually 0 75% silver nitrate One per cent or 0 25% concentrations were no more advantageous Reduction of the con centration of the third silver solution to 0 5% in cases of triple impregnation some times improved the extent of the impreg nation without increasing precipitates in the background No effects were noted from the use of 10% 20% or 30% su crose or 0 5% methyl cellulose in any or all of the impregnation solutions

Usually some tissue from each brain underwent double or triple impregnation In these samples the axonal plexuses were impregnated in preference to perikarya and dendrites which were more frequently seen after single impregnations The times in the various fluids consistent with suc cessful impregnations varied widely In several cases successfully perfused tis sues were placed directly in silver nitrate solution without immersion in a first fix ative solution Excellent uniform im pregnations were obtained but we have not had enough experience with this ma neuver to recommend its routine use The time required for a successful impregna tion varied inversely with the temperature For this reason it was desirable to keep the temperature relatively constant for routine work (e g 21 C ± 1) An aver age impregnation schedule at 21 C was three days in fixative four days in silver nitrate and when triple impregnation was used four days in third fixative five days in third silver It has not been possible to determine an optimum time schedule for all tissue samples since this varied with the age of the animal or the amount of myelin in the sample the part of the brain the pH of the perfusion fixative temperature and probably other factors It was always possible to obtain some good impregnations from a brain by pro cessing several samples simultaneously so that the times in the solutions could be systematically varied for the different samples In these cases very short times in fixatives were liable to yield incomplete impregnations i e less extensively im pregnated tissue slices and incompletely impregnated cells After very long times (more than one week) in the fixative solu tions impregnations of neural elements were almost completely lacking especially in young animals The intensity or dark ness of the impregnations was propor tional to the length of time in silver nitrate

There was no sign of fading with the dehydration and embedding schedule out lined Much longer times in mixtures

containing water, alcohol or cedar wood oil were liable to cause fading Embedding with Parlodion (purified pyroxylin) offered no advantage over the nitrocellulose the former yellowed with age, and its high viscosity made it difficult to embed the brittle tissues without cracking them If exposed to a higher temperature than 30°C at any time after osmication large pieces of tissue could become too friable to section and mount without cracking (see Ramon y Cajal, 03) None of the impregnations have faded within 5 to 10 years nor have they darkened when soaking with 70% ethanol was not omitted (Impregnation step 5)

Polarizing microscope observations

It has been implied but never verified that the Golgi impregnation contains silver chromate Since chrome silver compounds have distinctive optical properties and x ray diffraction indices (Porter and Codd '64) crystallographic analyses might identify the Golgi product within cells unaltered by extraction procedures The observations with polarized light indicated the feasibility of this approach which deserves further study

In perfusion and immersion fixed rapid Golgi preparations the impregnated material in the neurons was usually translucent, ruby red in transmitted light In relatively thin structures usually 10μ or less an anisotropy of the impregnated material was demonstrable (fig 12) It extended through the cytoplasm of the perikaryon and dendrites In several cases with axial illumination an oblique extinction angle of 30 was measured for thick dendritic segments This corresponded to the extinction angle of silver dichromate (fig 13) In such regions conoscopic examination with a Bertrand lens revealed biaxial interference figures identical to those of needle shaped sections of silver dichromate crystals There was no correspondence with silver monochromate (fig 17) potassium dichromate (fig 18) potassium chromate potassium nitrate (fig 15) silver nitrate protargol impregnated neurons (weakly anisotropic) silver (isotropic) reduced *in vitro* (fig 16), or axons impregnated by Richardson s reduced silver method Impregnated perikarya much more than 10 μ thick were often red black green black or opaque These rarely exhibited birefringence perhaps because they contained too thick and strongly colored silver dichromate — a condition reproducible *in vitro* (Chamot and Mason, 31) Thin structures dendrites and axons were usually red and birefringent when suitably transilluminated The possibility remains that the green black or red black impregnations also contained silver monochromate or chromium oxides We were unable to determine whether the crystals formed on the surfaces of the tissue slices were silver dichromate or silver monochromate (fig 14)

DISCUSSION

The most discriminating workers regarded the rapid Golgi impregnation as a form of silver chromate within the cytoplasm (see Ramón y Cajal, 1890a Liesegang 10 Kallius 26 Polyak 41) This is worth emphasizing for the rapid Golgi method which employs only strong oxidizing agents must not be identified with reduced silver methods the so-called silver methods The black reaction (la reazione nera of Golgi) does not accurately describe the rapid Golgi method since the cells often appear red in transmitted light In the original slow method without osmium tetroxide Golgi (1874) himself reported that the neural elements were colored intensely black and the connective elements including neuroglia red black In our preparations the impregnated material corresponded in color and other optical properties to silver dichromate and or silver monochromate

The present findings indicate that the extent and completeness of impregnation is governed by the length of exposure to the fixative the darkness of the impregnation, by the exposure to silver ions We are unable to support from either immersion or perfusion fixed preparations the frequently implied but rarely supported notion that the Golgi reaction when it occurs affects the entire neuron with all its processes Examples of partial impregnation of neurons were readily demonstrable Neurons with impregnation of

only the initial portions of the axons es pecially axons known to be myelinated were frequently encountered There were entire blocks of tissue even entire brains with the axonal plexuses everywhere ex tensively impregnated which contained no more than an occasional impregnated cell body However convincing examples of incompletely impregnated dendrites were seldom encountered except after spotty perfusions A careful reading of the texts of Ramón y Cajal and his con temporaries will indicate that these find ings are not a peculiarity of the present material This common attribute of rapid Golgi impregnations has not received suf ficient emphasis in the literature possibly because it might have proved misleading in the controversy and polemics surround ing the neuron doctrine It has long been known that the Golgi reaction does not or dinarily penetrate the nuclear membrane (Ramon y Cajal 1890a) The reaction also fails to impregnate intact mitochondria or the external surfaces of retinal horizontal cells (Stell 65)

The fact that the rapid Golgi method is less successful with heavily myelinated adult brains has been confirmed so often that additional examples would be super fluous It is not always clear in immer sion fixed tissue whether this should be attributed to an effect of myelin and its distribution on the diffusion of the Golgi reagents from the periphery of the tissue or to resistance of individual myelinated axons to the Golgi reaction With the per fusion method effects attributable to the diffusion rates of osmium and dichromate should have been minimized In fact neu rons and fine terminal fiber plexuses were more frequently impregnated in adult brains Even so there was no evidence that heavily myelinated axons were suc cessfully impregnated In perfusion fixed specimens it was possible to follow many gray osmium stained myelin sheaths (fig 9) Impregnations of the axons in the sheaths were rarely demonstrable and then only for a few microns in length (fig 10) A Golgi impregnation of a my elin sheath was never observed We are inclined to agree with Ramón y Cajal (1890b) who observed that the initial unmyelinated portion of cerebellar Pur kinje cell axon is precisely that which colors best by the Golgi method for generally the Golgi method very rarely im pregnates the myelinated portions of neu ral processes" Apparently the impregna tion of the axis cylinder stops abruptly where the myelin sheath begins Nor is impregnation of heavily myelinated axons usually obtained by exposing their cut ends to the Golgi reagents These observa tions imply that the development of the Golgi reaction along the axis cylinder demands that one or more of the Golgi reagents penetrate across the entire length of the axolemma If a myelin sheath is thick enough to attract a high concentra tion of osmium and/or chromium it may in some way inhibit the Golgi reaction in the adjacent axon perhaps by impeding the penetration of one of the Golgi re agents e g silver ions It should be noted that is was possible to deter the extent of the Golgi impregnation if the tissue were exposed to a high enough concentration of osmium tetroxide The possibility re mains that very thinly myelinated axons were successfully impregnated

The chemistry of the Golgi reaction has not been satisfactorily explained (see Kal lius 26) The present findings suggest that cytoplasmic substrates susceptible to the Golgi reaction are produced by initial fixation with osmium tetroxide and di chromate salts or with osmium tetroxide alone much more readily than with di chromate alone Perhaps osmium te troxide may facilitate the chromation of cytoplasmic lipid or protein molecules or the penetration of the plasmalemma by dichromate ions provided the osmium tetroxide concentration is not too high Chrome silver compounds may then form initially at chromated molecular sites perhaps exclusively on proteins as pro posed by Kallius ('26) The impregna tion may subsequently spread through the cytoplasm by a crystallization process until a lipoprotein membrane intervenes The present observations are consistent with Liesegang s (10) suggestion that Golgi impregnations may contain precipi tates of silver dichromate or a mixture of silver dichromate and monochromate The relative proportions of dichromate and monochromate formed may depend

on such factors as the hydrogen ion concentration the relative concentrations of dichromate and silver ions in the tissue at different times exposure of the impregnations to water or other reagents the use of double or triple impregnation and other factors in the chemistry of silver chromate mentioned by Liesegang (10) and Mellor (31)

From the present findings we are unable to offer a compelling explanation for the unpredictability of the rapid Golgi method or for its propensity to impregnate only a fraction of the cells However the attempt to standardize the conditions of fixation by perfusion was rewarded with more predictable results The impregnations were more uniform and provided a more representative sample of the varieties of neural structures demonstrable in each cerebral region examined Silver (42) mentioned the use of perfusion fixation for the rapid Golgi method but did not give details of his technique or an evaluation of the results The present findings indicate that the initial cytochemical events at the time of fixation must strongly influence the susceptibility of a neuron to the Golgi reaction Students of the Golgi reaction mechanism and the factors determining it in tissues should standardize and control the conditions of the initial fixation as nearly as possible Otherwise the conclusions may not have general validity This requirement necessarily limits the usefulness of immersion fixation because of its tendency for haphazard preservation of individual cells

The impregnations obtained with the perfusion method have been so exuberent that it first seemed that one of the major advantages of the Golgi method had been vitiated As Ramón y Cajal (1890a) stated it is only the method of Golgi which permits the finest axonal and dendritic processes to be traced thanks to its unique property of coloring isolated elements among the many constituting the gray matter However only those who need to use the Golgi methods to trace neural connections between remote parts of neonatal brains might find the present method frustrating thanks to an embarrassment of details But experimental methods (e g , Nauta 57) may be used to trace long neural pathways in the brain in the functionally mature brain Analyses with the Nauta method may be effectively correlated with the details observed in rapid Golgi preparations (e g Morest 65a b) One of the chief advantages of the present method is that it facilitates such correlations The perfusion method sometimes disclosed all the morphological varieties of axonal endings axodendritic or axosomatic, calycces perisomal nests baskets or boutons, etc *in a single section* of a neuronal population e g , within the medial geniculate body whereas hundreds or thousands of sections were ordinarily required to obtain as much information from immersion fixed material This does not imply that the present method avoids the necessity to study a large quantity of material before the details observed in a particular region may be considered as entirely representative

The ultimate advantage of a perfusion method which has not been fully explored is that the Golgi method may be applied to cerebral tissues in a more perfect or more uniform state of preservation than may be achieved by immersion fixation No assessment of the general quality of fixation of the present material was made with routine histological methods or electron microscopy Such an assessment would not necessarily apply to the particular elements that were successfully impregnated by the Golgi method Nevertheless in the Golgi impregnations prepared with the perfusion method the morphological details of very fine neuronal processes of the delicate dendritic branchlets and spines and the very fine elements of the axonal plexuses were more clearly and consistently demonstrable in internal portions of the brain stem as well as in cortical areas A unique advantage of the Golgi method is that it may facilitate the interpretation of synaptological studies with the electron microscope in terms of other neuroanatomical neurophysiological and neurological knowledge (e g Hamlyn 63) Moreover recent attempts to solve some cytological problems by direct electron microscopic examination of Golgi preparations have met with encouraging results (Stell 65 Blackstad 65) In any

critical attempt to correlate electron mi croscopic images with Golgi impregnated cells a question of the artifactitious aspects of the impregnation will inevitably arise To resolve such a question it is mandatory to use methods that permit correlations between Golgi impregnations of well pre served cells and equally well preserved ultrastructure The present method suit ably modified could be expected to meet this demand

LITERATURE CITED

Andersen P J C Eccles and P E Voorhoeve 1964 Postsynaptic inhibition of cerebellar Pur kinje cells J Neurophysiol 27 1138–1153

Autenrieth W 1902 Ueber einige chromsaure und dichromsaure Salze Ber Deut Chem Gesell 35 2057–2064

Baker J R 1965 The fine structure produced in cells by primary fixatives 2 Potassium dichromate Quart J Micr Sci 106 15–21

Blackstad T W 1965 Mapping of experimental axon degeneration by electron microscopy of Golgi preparations Zeit Zellforsch 67 819–834

Bodian D 1937 The structure of the verte brate synapse A study of the axon endings on Mauthner s cell and neighboring centers in the goldfish J Comp Neur 68 117–159

Cammermeyer J 1960 The post mortem origin and mechanism of neuronal hyperchromatosis and nuclear pyknosis Exp Neurol 2 379–405

Chamot E M and C W Mason 1931 Hand book of Chemical Microscopy Wiley New York Vol II 252

Clasen R A P M Cooke S Pandolfi G Car necki and G Bryar 1965 Hypertonic urea in experimental cerebral edema Arch Neurol 12 424–434

Dalton A J 1955 A chrome-osmium fixative for electron microscopy Anat Rec 121 281

Eayrs J T 1955 The cerebral cortex of normal and hypothyroid rats Acta anat 25 160–183

Fox C A and J W Barnard 1957 A quantita tive study of the Purkinje cell dendritic branch lets and their relationship to afferent fibers J Anat 91 299–313

Fox C A M Ubeda Purkiss H K Ihrig and D Biagioli 1951 Zinc chromate modification of the Golgi technic Stain Tech 26 109–114

Gerota D 1896 Contribution a l étude de for mol dans la technique anatomique Internat Monatschr Anat Physiol (Leipzig) 13 108–139

Golgi C 1873 Sulla sostanza grigia del cervello Reprinted in Golgi C Opera Omnia Hoepli Milan 1903 Vol I 91–98

——— 1874 Sulla fina anatomia del cervelletto umano Golgi C Opera Omnia Hoepli Milan Vol I 99–111

Hamlyn L H 1963 An electron microscope study of pyramidal neurons in the Ammon s Horn of the rabbit J Anat 97 189–201

Kallius E 1926 Golgische Methode In En zyklopadie der Mikroskopischen Technik 3rd Aufl Ed by R Krause Urban and Schwarzen berg Berlin Vol II 909–944

Koenig H R A Groat and W F Windle 1945 A physiological approach to perfusion fixation of tissues with formalin Stain Tech 20 13–22

Liesegang R E 1910 Untersuchungen uber die Golgi Farbung J Psychol Neurol. (Leipzig) 17 1–18

McEwen L M 1956 The effect on the isolated rabbit heart of vagal stimulation and its modi fication by cocaine hexamethonium and oua bain J Physiol 131 678–689

Mellor J W 1931 A Comprehensive Treatise on Inorganic and Theoretical Chemistry Long mans Green London Vol XI 263 340

Morest D K 1964 The neuronal architecture of the medial geniculate body of the cat J Anat 98 611–630

——— 1965a The laminar structure of the medial geniculate body of the cat J Anat 99 143–160

——— 1965b The lateral tegmental system of the midbrain and the medial geniculate body study with Golgi and Nauta methods in the cat J Anat 99 611–634

——— 1965c Identification of homologous neu rons in the posterolateral thalamus of cat and Virginia opossum Anat Rec 151 390

Nauta W J H 1957 Silver impregnation of degenerating axons In New Research Tech niques of Neuroanatomy Ed by W F Windle Thomas Springfield Chap III

Palade G E 1952 A study of fixation for elec tron microscopy J Exp Med 95 285–298

Palay S L S M McGee-Russell S Gordon and M A Grillo 1962 Fixation of neural tissues for electron microscopy by perfusion with solu tions of osmium tetroxide J Cell Biol 12 385–410

Polyak S L 1941 The Retina Univ Chicago Press Chicago Chap IV 44

Porter M W and L W Codd 1964 The Barker Index of Crystals Hoffer Cambridge Vol III Part II A 113

Ramón y Cajal S 1890a Sur l origine et les ramifications des fibres nerveuses de la moelle embryonnaire Anat Anz 5 85–95

——— 1890b Sur les fibres nerveuses de la couche granuleuse du cervelet et sur l évolution des éléments cérébelleux Internat Monatschr Anat Physiol (Leipzig) 7 12–31

——— 1903 Un consejo util para evitar los inconvenientes de la friabilidad y arrollamiento de los cortes en los preparados de Golgi y Marchi Trab Lab Invest Biol Univ Madr 2 99–100

——— 1909 Histologie du Système Nerveux de l'Homme et des Vertébrés Instituto Ramón y Cajal Madrid Vol I 70–73 (1952 reprint)

Ramon Moliner E 1957 A chlorate formalde hyde modification of the Golgi method Stain Tech 32 105–116

——— 1958 A tungstate modification of the Golgi-Cox method Stain Tech 33 19–29

——— 1959 Structure of the postcentral gyrus in cat Doctoral dissertation McGill University Montreal

Rasmussen G L 1931 Macrotome for cutting brains into blocks of uniform thickness and at any desired angle Anat Rec (Suppl) 48 61–62

——— 1957 Selective silver impregnation of synaptic endings In New Research Techniques of Neuroanatomy Ed by W F Windle Thomas Springfield Chap IV

Richardson K C 1960 Studies on the structure of autonomic nerves in the small intestine correlating the silver impregnated image in light microscopy with the permanganate fixed ultrastructure in electronmicroscopy J Anat 94 457–472

Rosomoff H L 1956 Hypothermia and cerebral vascular lesions I Experimental interruption of the middle cerebral artery during hypothermia J Neurosurg 13 332–343

——— 1959 Experimental brain injury during hypothermia Idem 16 177–187

Scheibel A and M Scheibel 1964 Personal communication

Silver M L 1942 The glial el ments of the spinal cord of the frog J Comp Neur 77 41–47

Stell W K 1965 Correlation of retinal cytoarchitecture and ultrastructure in Golgi preparations Anat Rec 153 389–398

Wolfe D E 1961 Personal communication

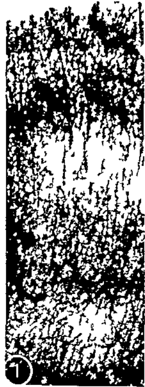
PLATE 1

EXPLANATION OF FIGURES

1 Occipital cortex parasagittal section from a 75 day old opossum pouch young (Didelphis virginiana estimated age) rapid Golgi triple impregnation The brain was removed under hypothermia and fixed by immersion in a mixture of 0 25% osmium tetroxide and 3% sodium dichromate (dihydrate) at pH 5 3 The layers of the cortex may be identified by the different quantities of fiber plexus impregnated in each The surface of the cortex is at the top of the figure × 85

2 Cerebral cortex transverse section from a 75 day old littermate of the preceding rapid Golgi double impregnation perfusion fixation at pH 7 3 followed by immersion in 0 25% osmium tetroxide and 3% sodium dichromate (dihydrate) at pH 5 3 The surface of the cortex is at the right edge of the figure The transition from the parietal area (top) to the peristriate area (bottom) is accompanied by a reduction in the thickness of the fiber plexus in layer I shown at the far right Neurons have been impregnated in every layer of the cortex The fiber plexus including the afferent axonal terminations is uniformly impregnated throughout the cortex Characteristic differences in the terminal axonal arborizations in each layer of the cortex are visible at higher magnifications The dark patches represent impregnations of neuroglial cells × 80

3 Detail from the field shown in figure 2 The apical dendrite of a small pyramidal neuron of layer II extends into the lower edge of the dense fiber plexus of layer I (top of figure) The pyramidal cell axon leaves the field directly below after giving off several collaterals Some of the fine afferent axons contacting the basal dendrites are visible at the lower right × 375


1


3

PLATE 2

EXPLANATION OF FIGURES

4 Olfactory bulb coronal section from a 100 day old opossum (estimated age) rapid Golgi triple impregnation perfusion fixation at pH 7 0 followed by immer sion in 0 25% osmium tetroxide and 3% sodium dichromate (dihydrate) at pH 5 8 From top to bottom are the fibrillar layer (*A*) of fine olfactory axons the glomerular layer (*B*) external plexiform layer (*C*) mitral cell layer (*D*) internal plexiform layer (*E*) and granular layer (*F*) Some glomeruli (*g*) are indicated which receive dendritic tufts from mitral cells (*m*) and from a tufted cell (*x*) at the far left in the external plexiform layer × 75

5 Dorsal horn of the cervical spinal cord horizontal longitudinal section from a weanling rabbit (New Zealand White) rapid Golgi triple impregnation perfu sion fixation at pH 5 8 followed by immersion in 0 25% osmium tetroxide and 3% sodium dichromate (dihydrate) at pH 5 8 Ammonium instead of potassium dichromate at pH 5 8 was used for the third impregnation The longitudinal bundle of axons in the center of the field is bordered on either side by the delicate neuropil of the substantia gelatinosa Several varieties of neurons are indicated (*a d*) × 100

6 Ventrobasal complex of thalamus transverse section from a 100 day old opossum (estimated age) rapid Golgi triple impregnation perfusion fixation at pH 7 4 followed by immersion in 0 25% osmium tetroxide and 3% sodium dichromate (dihydrate) at pH 5 8 Ammonium instead of potassium dichromate at pH 5 8 was used for the third impregnation Characteristic principal neurons are em bedded in the dense terminal afferent fiber plexus the details of which are easily resolved at higher magnifications The field fairly represents the uniformity of impregnation throughout the diencephalon in this specimen Neurons with short axons (Golgi type 2) were also frequently observed in such specimens × 120





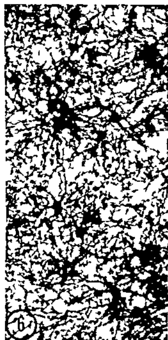


PLATE 2

EXPLANATION OF FIGURES

4 Olfactory bulb coronal section from a 100 day old opossum (estimated age) rapid Golgi triple impregnation perfusion fixation at pH 7 0 followed by immersion in 0 25% osmium tetroxide and 3% sodium dichromate (dihydrate) at pH 5 8 From top to bottom are the fibrillar layer (*A*) of fine olfactory axons the glomerular layer (*B*) external plexiform layer (*C*) mitral cell layer (*D*) internal plexiform layer (*E*) and granular layer (*F*) Some glomeruli (*g*) are indicated which receive dendritic tufts from mitral cells (*m*) and from a tufted cell (*x*) at the far left in the external plexiform layer × 75

5 Dorsal horn of the cervical spinal cord horizontal longitudinal section from a weanling rabbit (New Zealand White) rapid Golgi triple impregnation perfusion fixation at pH 5 8 followed by immersion in 0 25% osmium tetroxide and 3% sodium dichromate (dihydrate) at pH 5 8 Ammonium instead of potassium dichromate at pH 5 8 was used for the third impregnation The longitudinal bundle of axons in the center of the field is bordered on either side by the delicate neuropil of the substantia gelatinosa Several varieties of neurons are indicated (*a d*) × 100

6 Ventrobasal complex of thalamus transverse section from a 100 day old opossum (estimated age) rapid Golgi triple impregnation perfusion fixation at pH 7 4 followed by immersion in 0 25% osmium tetroxide and 3% sodium dichromate (dihydrate) at pH 5 8 Ammonium instead of potassium dichromate at pH 5 8 was used for the third impregnation Characteristic principal neurons are embedded in the dense terminal afferent fiber plexus the details of which are easily resolved at higher magnifications The field fairly represents the uniformity of impregnation throughout the diencephalon in this specimen Neurons with short axons (Golgi type 2) were also frequently observed in such specimens × 120

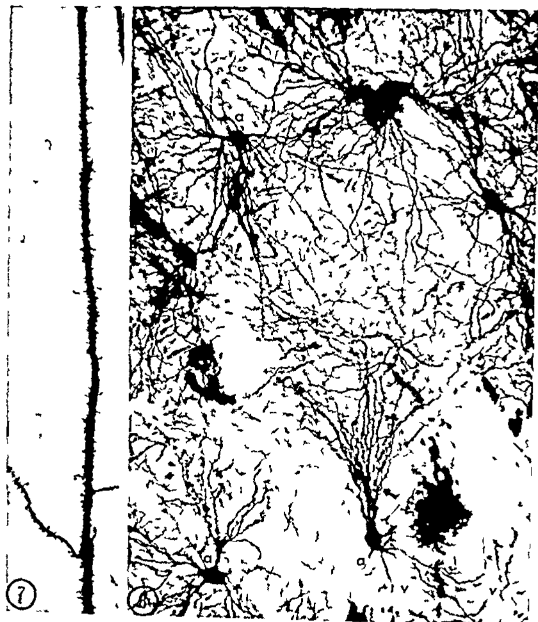

a
a
a
7
6

PLATE 3

EXPLANATION OF FIGURES

7 Sensory cortex transverse section from an adult albino rat rapid Golgi triple impregnation perfusion fixation at pH 5 8 followed by immersion in 0 25% osmium tetroxide and 3% potassium dichromate at pH 4 0 The portion of an apical dendrite shown illustrates the frequency of dendritic spines consistently observed in successfully perfused brains The terminals of some afferent axons happen to be in the plane of focus In immersion fixed brains isolated examples of spiny dendrites comparable to the one illustrated could be found However they were less consistently demonstrable The immersion fixed dendrites frequently had areas denuded of spines presumably because the spines had not been preserved or had become refractory to the Golgi reaction × 900

8 Nucleus ventralis lateralis of the thalamus transverse section from an adult albino rat rapid Golgi triple impregnation perfusion fixation at pH 5 8 followed by immersion in 0 25% osmium tetroxide and 3% potassium dichromate at pH 4 0 A number of principal neurons and their axons (*a*) have been impregnated The axon from the neuron in the lower left corner gives off a number of collateral branches before leaving the nucleus *v* empty lumina of blood vessels × 140


9


V
11

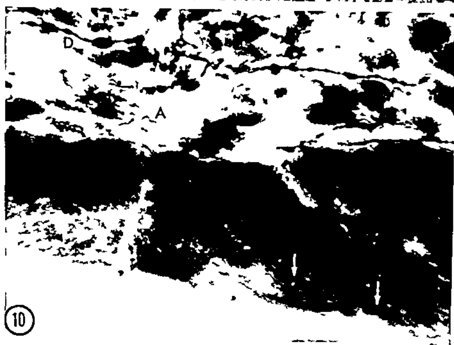

D
A
10

PLATE 4

EXPLANATION OF FIGURES

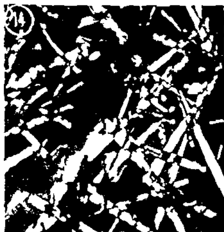
9 Putamen transverse section from an adult albino rat rapid Golgi triple impregnation perfusion fixation at pH 5 8 followed by immersion in 0 25% osmium tetroxide and 3% potassium dichromate at pH 5 8 Several neurons with thick dendrites and part of the intrinsic axonal plexus have been darkly impregnated In the background are several gray osmium stained bundles of myelin sheaths (arrows) The myelin sheaths had a smooth tubular appearance typical of well perfused brain tissue At higher magnifications there was no sign that *axis cylinders had impregnated within the tubular* profiles of the myelin sheaths Compare to figure 10 × 180

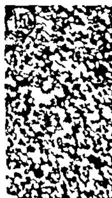
10 Cerebral peduncle transverse section from an adult albino rat rapid Golgi triple impregnation The anesthetized rat died during removal of the brain which was immersed more than 30 minutes later in 0 25% osmium tetroxide and 3% potassium dichromate at pH 5 8 The myelin sheaths of the cerebral peduncle darkly stained with osmium have been sectioned somewhat obliquely The muddly appearance of myelin and its varicose profiles are typical of immersion fixed brains A few axis cylinders in the peduncle have been impregnated by the Golgi reaction (arrows) Some of these appeared to be associated with the tubular remnants of myelin sheaths In these cases the axonal impregnation was discontinuous or fragmentary as if the Golgi reagents had penetrated the axoplasm through isolated defects or nodes of the myelin sheaths Otherwise convincing examples of Golgi impregnations of heavily myelinated axons or of myelin sheaths were not observed In the peripeduncular gray the axons (*A*) and dendrites (*D*) had a grossly beaded appearance which was not seen in this region in well perfused brains Often neurons with beaded dendrites retained one or two dendritic trees that were not beaded and that were covered with spines and branchlets The beaded dendritic trees of such neurons were denuded of spines and fine branchlets In the present study these features when absent in homologous neurons of well perfused brains were taken as evidence of incomplete histological preservation (Ramón y Cajal 09) In the lower left corner of the figure on the external surface of the peduncle is part of a cerebral vessel containing hematocytes × 250

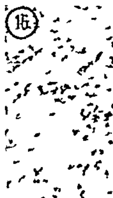
11 Dorsomedial nucleus of thalamus transverse section from a 41-day-old cat rapid Golgi double impregnation incomplete perfusion fixation at pH 5 8 followed by immersion in 0 25% osmium tetroxide and 3% potassium dichromate at pH 4 0 After the perfusion the brain was spotted with unevenly distributed patches of reduced osmium which were especially prominent along the cerebral vessels The photomicrograph shows the typical appearance of the Golgi impregnation observed in these black patches The empty lumina of small vessels (*v* e g) and capillaries were surrounded by tubular regions or cuffs containing fine gray round granules of uniform size This precipitate was presumably reduced osmium it did not at all resemble the irregular black grains of reduced silver observed in other tissues or *in vitro* (fig 16) Within these cuffs the Golgi impregnation was almost completely absent although the gray smooth profiles of apparently well preserved myelin sheaths were often observed At a distance from such vessels there was an exuberant impregnation of neurons and neuropil The dendritic fields of individual neurons appeared to be as completely impregnated as in other preparations except for those particular dendrites that ran into a vascular cuff In the latter case (arrows) the impregnation of the dendrites stopped abruptly at the margin of the cuff even though the impregnation of other dendrites pointing away from the cuff was fully developed See text (p 815) for further explanation × 135


12


13


14


15


16


17


18

PLATE 5

EXPLANATION OF FIGURES

12 Putamen transverse section adult albino rat rapid Golgi triple impregnation perfusion fixation at pH 4 0 immersion in 0 25% osmium tetroxide and 3% potassium dichromate at pH 4 0 Nitrocellulose embedding 60 μ thick section in Aroclor 5160 under cover glass A section through a neuronal perikaryon was photographed through crossed polaroids The maximum thickness of the perikaryal portion normal to the plane of section was 10 μ The dark regions were in positions of extinction the light regions in positions of brightness With axial illumination an oblique extinction angle of 30 was obtained for the dendrites at the arrows the same for silver dichromate In such regions conoscopic examination with a Bertrand lens revealed biaxial interference figures identical to those of needle shaped sections of silver dichromate crystals Nitrocellulose was birefringent only at the section s edges Identical results were obtained with unembedded impregnations mounted in Permount × 420

13 Silver dichromate crystals prepared by adding a drop of 0 75% silver nitrate to a drop of 4% potassium dichromate on a glass slide By the equation $2AgNO_3 + K_2Cr_2O_7 = 2KNO_3 + Ag_2Cr_2O_7$ there was an excess of potassium dichromate Typical crystals of potassium dichromate (fig 18) and potassium nitrate (fig 15) but not silver nitrate were also present Excessive dichromate would favor formation of silver dichromate excessive silver silver monochromate $4AgNO_3 + K_2Cr_2O_7 + H_2O = 2Ag_2CrO_4 + 2KNO_3 + 2HNO_3$ (Autenrieth 02) The crystals shown were identical in appearance and birefringence to commercially obtained silver dichromate (British Drug Houses) They were translucent ruby red weakly pleochroic and triclinic An oblique extinction angle of 30 was observed in agreement with Barker (quoted by Porter and Codd 64) The large crystals resembled those formed on tissue surfaces with the Golgi method (fig 14) The smallest crystals resembled the birefringent material often observed in Golgi impregnated neurons (fig 12) Crossed polaroids × 320

14 Typical elongated crystals formed on tissue surfaces with the Golgi method Small pinacoids also occurred Note that extinction occurred where the long crystal axes crossed at right angles The crystals were translucent red resembling silver dichromate or monochromate Crossed polaroids × 320

15 Recrystallized potassium nitrate The crystals were colorless and translucent in transmitted light strongly birefringent in polarized light Similar crystals appeared when the Golgi reagents were mixed *in vitro* They occasionally occurred in Golgi preparations where most of them would have been dissolved during dehydration Crossed polaroids × 320

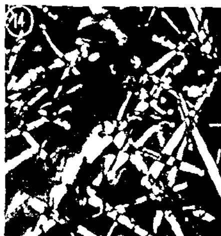
16 Isotropic silver grains reduced by formalin vapor × 320

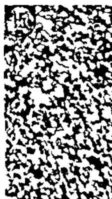
17 Silver monochromate crystals (British Drug Houses) They were red and slightly translucent strongly pleochroic monoclinic (one plane of symmetry with parallel extinction) and had an oblique extinction angle of 35 In the interference figure the optic axis was at the edge of the field Crossed polaroids × 320

18 Recrystallized potassium dichromate The triclinic crystals were isolated translucent orange tablets or plates arranged in dendritic patterns Such crystals were not detected in dehydrated Golgi preparations Crossed polaroids × 320


12

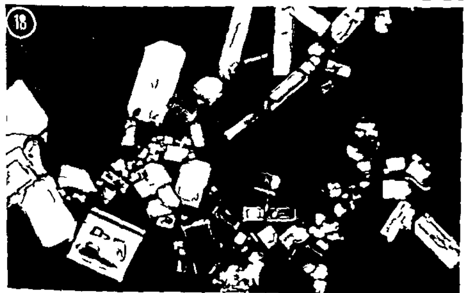

13


14




16


17


18

The Histochemistry of Mucins in Certain Primate Salivary Glands

T JOHN LEPPI AND S S SPICER

Laboratory of Experimental Pathology National Institute of Arthritis and Metabolic Diseases National Institutes of Health Public Health Service United States Department of Health Education and Welfare Bethesda Maryland

ABSTRACT Submandibular and sublingual salivary glands of squirrel and rhesus monkeys and man contain histochemically demonstrable neutral mucosubstances sialomucins and sulfomucins Judged by results obtained with a variety of staining procedures and by the effects of prior sialidase digestion periodate oxidation and certain chemical modifications on the several staining procedures differences are revealed in the types of mucosubstances within each cell type Specifically sialic acid-containing mucosaccharides are present uniformly in the mucous cells of the submandibular glands of both monkeys and in a posterior segment of the sublingual gland of the rhesus monkey Sulfomucin is the predominant secretion of the sublingual gland of the squirrel monkey and is also found in the anterior portion of the sublingual of the rhesus monkey as verified by $S^{3}O_4^{=}$ autoradiography This latter sulfomucin is admixed with a small amount of sialomucin One or the other or mixtures of these two mucins in about equal proportions are present in the mucous acini of human submandibular glands Seromucous acini in the human submandibular gland form a granular secretion with strong affinity for aldehyde fuchsin possibly attributable to a sulfated mucosubstance Other and perhaps some of the same seromucous acini in this gland produce a granular secretion containing sialic acid in probable proximity as shown by the periodate *para* diamine procedure after sialidase to a hexose or deoxy hexose A sulfomucin forms the major secretory component in the mucous acini of human sublingual glands However some mucous acini in this sublingual gland produce a mixture of sialo- and sulfomucins either in different or the same cells Seromucous demilunes or acini in the human sublingual gland produce a granular secretion rich in sialic acid like that in the submandibular gland

Although the chemical composition of the carbohydrate entities in some animal salivary mucins has been studied in detail (for reviews see Werner 53 Odin 58 Pigman and Tsuiki 59 Stary 59 Raust 62) comparatively little is known about these complex macromolecules in man and other primate species The salivary mucins as well as the blood group substances appear to consist of side-chain oligosaccharides composed of carbohydrate residues attached glycosidically to hydroxyls of amino acids in peptide chains (Gottschalk 63 Pigman and Tsuiki 59) Through exhaustive treatment with pronase and subsequent digestion with neuraminidase and further purification it has been shown that about 50% of the carbohydrate prosthetic groups in the mucin from ovine submandibular gland are linked glycosidically to the hydroxyl groups of serine and threonine (Carubelli et al 65)

Analyses for the carbohydrate components of pooled normal human salivary secretions indicate that they contain a neutral glycoprotein composed of hexosamine galactose and fucose in the carbohydrate moiety and an acid mucosubstance containing hexosamine and sialic acid in combination with a protein (Berggard and Werner 58 McCoombe et al 61)

Histochemically the sialic acid which constitutes such a significant proportion of the mucin molecule in numerous animal salivary glands is held exclusively responsible for the staining of some salivary mucins by cationic dyes such as alcian blue azure A and colloidal iron (Spicer and Warren 60 Quintarelli et al 61 Shackleford and Klapper 62) Specific digestion of sections with purified sialidase eliminates such basophilia while quantitatively releasing the sialic acid from the

tissue section or from homogenates of certain glands (Spicer and Warren 60) Mild acid hydrolysis has been used to remove similar staining reactions thought to indicate sialic acid residues located in terminal positions (Quintarelli et al 61) However it was noted that the basophilic staining of certain salivary sialomucins e g cow submandibular (Quintarelli et al 61) and rat sublingual (Spicer and Warren 60) is unaltered by sialidase digestion alone indicating variability in structure of different sialomucins Similar resistance to sialidase was noted in the sialomucins of several other ungulate salivary glands (Quintarelli et al 60 Quintarelli 63a Leppi and Spicer 65) Further differences in sialomucins as yet unexplained are apparent from the finding that brief exposure of tissue sections to 1% KOH prior to enzyme treatment and staining renders some resistant sialomucins e g that in the rat sublingual gland susceptible to sialidase digestion (Spicer and Duvenci 64) Some sialomucins differ further in showing periodate reactivity as evidenced by their staining with a periodic acid phenylhydrazine Schiff sequence and on the susceptibility of their mixed diamine staining (Spicer 65) to prior periodate oxidation Other sialomucins appeared to be periodate unreactive Evidence that the carboxyl groups of sialic acid in the submandibular gland of the rhesus monkey are masked by basic protein has been obtained from the increased alcianophilia of the mucin after treatment of tissue sections with pepsin (Quintarelli 63b) These findings suggest that although most salivary mucins contain sialic acid their structural configuration varies widely from one animal gland to another

Identification and localization of another type of acid mucin in salivary epithelia has been achieved by autoradiography after injection of $S^{35}O_4^{=}$ (Bélanger '54) Injected radioisotope is incorporated selectively in sulfated mucosubstances in the first few hours and sites of incorporation parallel exactly those showing presence of sulfomucin by specific histochemical staining methods (Spicer and Meyer 60 Spicer and Duvenci 64 Leppi and Spicer 66) Correlated $S^{35}O_4^{=}$ autoradiography and histochemical staining indicate that some salivary glands form sulfomucin exclusively, some sulfomucin together with sialomucin and others only sialomucin In some a neutral mucosubstance is demonstrable in addition to acidic mucin

The histochemical properties of the salivary glands of primates and especially man have not been investigated in detail although Shackleford and Klapper (62) and Munger (64) have studied the relationships of the serous mucous and seromucous cells of human salivary glands As yet no radioisotope incorporation studies have been performed on human salivary gland tissues to relate the known histochemical staining properties with the uptake of parenterally administered $S^{35}O_4^{=}$ Preliminary studies applying techniques employed earlier on animal tissues indicated the coexistence of sialo and sulfomucins in human submandibular and sublingual glands (Leppi and Spicer 64 Spicer and Duvenci 64 Lev and Spicer 65) The sulfomucin of human sublingual gland is unrelated to the connective tissue sulfated mucopolysaccharides as evidenced by its inertness toward testicular hyaluronidase (Leppi and Stoward 65) In other histochemical evaluations of human sublingual mucin the partial loss of basophilia following vigorous (1N HCl at 80°C for one hour) acid hydrolysis was interpreted as evidence for the presence of a sulfated component possibly similar to heparin (Quintarelli 61 Quintarelli and Robinson 61) Although definitive evidence for the presence of sialomucins in human salivary glands was not obtained in the latter studies such a component has been identified in the submandibular gland of the rhesus monkey on the basis of the elimination of basophilia by sialidase treatment (Quintarelli 63b)

The purpose of the present study is to evaluate histochemically the mucosubstances in the submandibular and sublingual salivary glands of man and two species of monkeys with a battery of methods Evidence will be presented that attests to the complexity of these mucosubstances on a histochemical basis and provides some correlation with the available chemical data

MATERIALS AND METHODS

Submandibular and sublingual salivary glands were obtained from five squirrel monkeys (*Saimiri sciureus*) and six rhesus rhesus monkeys (*Macaca mulata*) of both sexes maintained in the NIH animal colony Specimens were obtained at autopsy from eight human subjects of both sexes with illnesses unrelated to the salivary glands The gross anatomical relationships of the human and monkey glands are noted elsewhere (Leppi 66) A total of 44 salivary glands from monkeys were removed immediately and fixed 24 hours in 2% calcium acetate dissolved in 10% formalin A total of 32 salivary glands from human subjects were removed within 1–2 hours following death and fixed similarly Multiple pieces from each gland were embedded in paraffin and sectioned at 5 μ prior to staining by a battery of histochemical methods which provide some specificity in differentiating and partially characterizing mucosubstances

Table 1 outlines the histochemical methods employed for visualization of carbohydrate rich substances detailing the basis for the staining and the histochemical interpretation

Tissues were stained routinely with hematoxylin and eosin for morphology Mucosaccharides with vicinal hydroxyls were localized by the periodic acid Schiff (PAS) method (McManus 46 Hotchkiss 48 Lillie 54) following diastase digestion and polymers presumed to contain hexose or deoxyhexose by the periodic acid *para* diamine technique (Spicer and Jarrels 61) The periodic acid phenylhydrazine Schiff method was employed as a presumed means of demonstrating vicinal hydroxyls in proximity of acid groups (Spicer 61) Sections were also stained by the mixed diamine technique with and without prior periodate oxidation as a means of differentiating periodate reactive and unreactive acid mucosubstances For the same purpose selective blockage of the basophilia of periodate reactive acid mucins was demonstrated employing a sequence of routine periodate oxidation followed by a seven hour exposure to a 0 2% solution of N N dimethyl *meta* phenylenediamine (HCl), (adjusted to pH 5 0 with 0 2 M Na HPO) prior to staining with 1% alcian blue 0 02% azure A at pH 3 5 or colloidal iron (Spicer 65)

As a general basic dye method for visualization of most acid mucosaccharides staining with 1% alcian blue in 3% acetic acid at pH 2 5 was perfomed according to Mowry (56) Selective staining of sulfated mucins was accomplished with a solution of 1% alcian blue in 0 1 N HCl (pH 1 0) blotting sections dry after staining and before alcohol dehydration (Lev and Spicer 64) Azure A staining at controlled pH levels was also utilized by a 30 minute exposure of sections to a 0 02% concentration of the dye at pH 1 0 2 0 and 3 0 in extension of the Wislocki et al (47) and Dempsey et al (47) pH extinction methods employing Lillie s ('54) dilute buffered dye solutions as detailed previously (Spicer and Duvenci 64)

Staining sequences combining alcian blue (AB) at either pH 2 5 (Mowry and Winkler 56) or pH 1 0 with a PAS step were also employed Selective blockage of the carboxyl-dependent basophilia as visualized with the AB pH 2 5 PAS procedure was accomplished by a mild methylation procedure exposing sections for four hours at 37 C (Spicer 60) to methanol containing 0 1 N HCl (Fisher and Lillie 54) Restoration of basophilia was accomplished by a 15–30 minute saponification in a solution containing 1% KOH in 70% ethanol (Spicer and Lillie 59)

Further differentiation among acid mucosubstances was effected with the aldehyde fuchsin alcian blue (Spicer and Meyer 60) method for distinguishing sialomucins from sulfomucins This distinction was also made by a high iron diamine alcian blue sequence (Spicer 65) The low iron diamine alcian blue method was employed as a general basic dye sequence

Sialomucins were identified specifically by incubating sections with purified *Vibrio cholerae* sialidase (General Biochemicals Chagrin Falls Ohio Koch Light Laboratories Ltd Colnbrook Bucks England) 8–24 hours at 39 C (Spicer and Warren 60) Control sections were incubated similarly with the buffer in which the enzyme was dissolved Certain sialomucins (e g human sublingual (were rendered more susceptible to sialidase treatment by ex

TABLE 1

Histochemical methods employed for visualizing primate mucosaccharides

Method	Chemical reaction involved	Histochemical result
Radiosulfate auto radiopraphy	Injected $S^{35}O_4^{=}$ is incorporated into sulfated mucosubstances (MS) *in vivo* within 3–24 hours after injection	Localizes sulfated mucosubstances specifically
Azure A at controlled pH values	Formation of blue orthochromatic or purple metachromatic salt complexes with the extinction values indicating degree of acidity of the polymer	Strongly acid sulfated MS stain purple below pH 1 5 Weakly acid MS stain blue to purple be low pH 4 5 Sialomucins color blue to purple at pH 3 0 or above
Alcian blue at controlled pH levels	Probably formation of alcian blue complexes with carboxyls and some sulfates Extinction values indicate degree of acidity of the polyanion	At pH 2 5 sialomucins and weakly acid sulfomucins stain blue the most strongly acidic sulfomu cins stain weakly or not at all At pH 1 0 weakly and strongly acidic sulfomucins stain blue selectively
Aldehyde fuchsin alcian blue pH 2 5 sequence	Formation of salt complexes be tween cationic staining entity and sulfate and carboxyl groups Replacement through mass ac tion of first dye by second on sites where former has low affinity	Sulfated MS color purpl or blue purple sialomucins and other non sulfated acid MS color blue
Low iron diamine alcian blue pH 2 5	Formation of salt complexes be tween cationic staining entity and sulfate and carboxyl groups Replacement through mass ac tion of first dye by second on sites where former has low affinity	Sulfated MS and many sialomu cins stain black and some sialo-mucins blue
High iron diamine alcian blue pH 2 5	Formation of salt complexes be tween cationic staining entity and sulfate and carboxyl groups Replacement through mass ac tion of first dye by second on sites where former has low affinity	Sulfated MS stain black sialo-mucins stain blue
Periodic acid Schiff	Oxidation of vicinal hydroxyls to dialdehydes by periodate and formation of colored complexes with Schiff s reagent	All polysaccharides (PS) and MS containing hexoses and deoxy hexoses with *vic* glycol groups i e periodate reactive polymers color magenta to red
Periodic acid *para* diamine	Oxidation of *vic* glycols to dialde hydes and condensation of these with diamine to form brown Schiff bases	Periodate reactive PS and MS vary from colorless to different shades of brown presumably in accord ance with type of sugar present and predominance of dialde hydes after periodate
Mixed *meta* and *para* diamines at about pH 4 with and without periodate oxidation	As with *para* diamine alone except gray to yellow Schiff bases and purple salt complexes are pro duced	After oxidation periodate unreac tive acidic MS stain purple periodate reactive neutral and acidic MS stain gray or gray brown Both types of acidic MS are purple in unoxidized sec tions

TABLE 1 (*Continued*)

Histochemical methods employed for visualizing primate mucosaccharides

Method	Chemical reaction involved	Histochemical result
Periodic acid *meta* diamine basic dye sequence	Cationic *meta* diamine condensed on periodate-engendered dialdehydes neutralizes adjacent acid groups and thus blocks basophilia in polymers with *vic* glycols proximal to acid groups	Unlike periodate unreactive acid MS those with *vic*-glycols adjacent to acid groups lose basic dye staining after periodate oxidation and exposure to *meta* diamine
Periodic acid phenyl hydrazine Schiff	Phenylhydrazine selectively blocks periodate-engendered dialdehydes in neutral PS or MS leaving unblocked dialdehydes in periodate reactive and MS available to subsequent Schiff staining	Periodate reactive acidic MS stained red presumably are those in which acid groups are proximal to *vic*-glycols
Alcian blue pH 2 5-PAS	Addition of results by single methods	Neutral PS and MS color magenta alcian blue reactive periodate-unreactive acid MS stain blue Alcian blue and periodate reactive MS color purple-blue
Alcian blue pH 1 0 PAS	Addition of results by single methods	Sulfated MS stain blue or purple blue neutral and nonsulfated periodate-reactive acid MS stain red
Methylation blockage of basophilia	Esterification of caboxyl groups hydrolysis of sulfate esters	Eliminates basophilia of sialomucins after 4 hours at 37 C Basophilia of all acid MS occluded after 4 hours at 60 C
Methylation (4 hrs at 37 C) followed by saponification	Methylation blocks carboxyls Subsequent demethylation (saponification) unblocks or deesterifies carboxyls restoring their basophilia	Carboxyl groups of acid MS lose basophilia after methylation and regain it after saponification
Diastase digestion	Hydrolyzes and removes glycogen	Loss of PAS reactivity in sites containing glycogen
Sialidase digestion	Removes sialic acid from MS	Many sialomucins lose basophilia after digestion they then stain red rather than purple blue in alcian blue pH 2 5-PAS sequence i e like neutral rather than acid MS Some sialomucins stain purple gray before and red or orange brown after sialidase

PS polysaccharid MS mucosubstance

posing sections five minutes to a solution of 1% KOH in 70% ethanol (Spicer and Duvenci 64) Loss of sialic acid residues after enzymatic digestion was visualized for example by elimination of blue staining in the high iron diamine alcian blue method

In the autoradiographic study 2 mc of carrier free $Na_2S^{35}O_4$ (1 mc in 1 0 ml normal saline) from the Oak Ridge National Laboratories were injected intraperitoneally into each of two rhesus monkeys The animals were sacrificed six hours after the isotope injections and the salivary glands were removed and fixed 24 hours in calcium acetate formalin Routinely prepared paraffin sections prestained by alcian blue at either pH 2 5 or 1 0 or by the AB pH 2 5–PAS or aldehyde fuchsin alcian blue sequences were prepared for autoradiog

raphy with Kodak AR 10 stripping film by *conventional methods* Autoradiographs were developed, fixed and washed after a 7–14 day exposure at 0°C and were subsequently air dried, dehydrated, cleared and mounted

Concerning the nomenclature applied to the carbohydrate containing substances found in the primate salivary mucins of this study, we refer to discussion of a more general terminology that is probably consistent with present histochemical and *biochemical knowledge* (*Spicer et al*, 65) Briefly it has been suggested that the *mucosubstances present in epithelial sites* which are probably glycoproteins, be designated *mucins* and that where possible these may be further classified as *sialomucins* and *sulfomucins* These designations are used on the basis of histochemical tests for the presence or absence of the carboxyl groups of sialic acid and sulfate groups respectively Another type *of mucosubstance lacking demonstrable* acidic properties but rich in *vic* glycols that presumably originate from fucose and galactose residues are termed *neutral mucosubstances*

RESULTS

The major portion of the results (tables 2–4) are recorded according to visually *estimated intensity and shade* Figures in the tables indicate relative intensity of staining or labeling When two or more *colors or combinations of colors* are given for a particular site and method the first one listed is predominant and the remainder is listed in descending order of prominence Staining of mucous *acini* are described unless otherwise indicated Since *histochemical* interpretations are given (tables 2–4) for the results in the various sites only those results which require further description are described in detail

Three histologic glandular cell types varying in the carbohydrate content of their secretions may be distinguished in salivary glands In the mucous cell a finely fibrillar uniform mucous fills the cytoplasm in the seromucous cell a granular secretion is generally present with a variable amount of demonstrable carbohydrate and in the serous cell no carbohydrate is evident with histochemical methods These definitions generally follow those given by Munger (64) for the classification of salivary gland cell types

Submandibular glands Histologically there is a general predominance of seromucous demilunes and acini over the mucous secretory portions in the submandibular glands of all three primates (figs 26 34 and 39) Sections of human glands stained with hematoxylin and eosin demonstrate this feature consistently although the impression is gained that different areas in a given gland vary in the amount of mucous units relative to seromucous units with a very few areas showing mainly mucous acini and other areas almost no mucous acini This variability is particularly notable in some isolated lobules of the main submandibular gland which exhibit a predominance of mucous acini similar to that observed in portions of the sublingual gland in which mucous acini are mixed with less prominent non mucous (probably seromucous) acini A more uniform distribution of mucous acini is present throughout the submandibular glands of both monkeys and particularly in the small anterior prolongations of these glands

The variable mixed diamine reactivity of *mucous acini* in man is largely blocked by prior periodate oxidation (figs 40 and 41) while the mucins in both monkey submandibular glands are unreactive toward mixed diamine staining with or without oxidation (table 3) However the mucous acini in the glands of all three species contain periodate susceptible acid mucins as judged by the blockage of alcianophilia produced by prior periodate oxidation and exposure to the *meta* diamine reagent (figs 27 and 28)

The periodic acid *para* diamine (PAD) procedure reveals red brown staining in all of the mucous acini of both monkey glands and some of the mucous acini in human submandibular glands after sialidase digestion *This contrasts with the purple* brown color visualized in the mucous acini before digestion It is possible but not definitely proven that the mucous acini in the human glands with unaltered purple brown staining after sialidase correspond with those shown by high iron diamine reactivity to contain sulfomucins as will be described The brown coloration in the

Basophilia of mucosaccharide-containing secretion in mucous acini of certain primate salivary glands

Histologic site	Species	AB pH 2.5	AB pH 1.0	AF AB	Low iron diamine AB	High iron diamine-AB after 8-24 h buffer	High iron diamine-AB after 8-24 h sialidase	High iron diamine-AB after 5 min KOH 8-24 h sialidase	0.02% Azure A pH 1.0-2.0	0.02% Azure A pH 3.0	Azure A after dioxan-pyridine with SO_3	Histochemical interpretation
SM gland	R	1-2B	0-±B	2B	1-2B	1-?B	0-±B	0	0	0 [2]	0	Sialidase digestible sialomucin with moderate alcianophilia, masked azurophilia and no low iron diamine affinity. No sulfomucin
SM gland	S	2-3B	0	3B	3B	2-3B	0	0	0	0 [2]	—	Similar to rhesus SM except absence of sulfomucin not proven with $SO_4^=$
SM gland	M	3-4B	0-?B	4B 4BP	2-3PN	4PN 3B	4PN 3B	4PN B	0-±PB	0-PB [3]	—	Probable sialomucin (largely resistant to sialidase) in some cells. Probable sulfomucin in other cells. Masked azurophilia
SL gland anterior	R	4B	4B	4P	3PN	4PN [7]	4PN [8]	4PN [8]	1-3PB	4PB	+++	*Anterior* — Sulfomucin with strong basophilia in great majority of cells
SL gland posterior	R	1-4B	0-±B	1-4B	1-4B 3PN	1-4B	0-±B	0-±B	0	0-2PB	0	*Posterior* — Sialidase susceptible mucin with strong alcianophilia, weak azurophilia and variable low iron diamine affinity. No sulfomucin
SL gland	S	3B	4B	4P	3-4PN	4PN	4PN	4PN	1-3PB [9]	3PB	—	Probable sulfomucin with strong basophilia, metachromatic azurophilia in all cells
SL gland lesser	M	3-4B	1-3B	4P 3BP 3B	2-4PN	4PN 4B	4PN 3-4B	4PN 1-3B [1]	0-3PB [3]	2-3PB	—	*Lesser* — Probable sialomucin slightly susceptible to sialidase in minority of cells. Probable sulfomucin with strong basophilia in majority of cells
SL gland greater [9]	M	3B	0-3B	3B 3P	1-3PN	3PN 3B [11]	3PN 2-3B	3PN 1-3B [12]	0 [4]	1-2PB	—	*Greater* — Like lesser SL except more sialomucin, less metachromasia at low pH

AB, alcian blue; AF, aldehyde fuchsin; KOH treatment by a 1% solution of KOH in 70% ethanol; M, man; R, rhesus monkey; S, squirrel monkey; SL, sublingual; SM, submandibular.

Color: B, blue; N, black; P, purple.

[1] C stain intra and i terl b l r d ct c lls contain m cin staining 1 2B

[2] Some mucous acini are 1-2PB at pH 3.0 when viewed wet from staining jar. Azurophilia occurs in these same sites at pH 3.5-4.0 in dehydrated and mounted sections

[3] Occasional scattered mucous and seromucous cells ret in 2 3B staining

[4] More numerous acini are stained better than with AB at pH 1.0

[5] S rom us component c nt in purple granules such st ini g is partially reduced by a 16 hour active (60 C) methylation

[6] The majority of i l r 4PN

[7] A few acini stain 4B or 4BP with AF AB and 4B with high iron diamine-AB

[8] Widely scattered mucous acini stain 1-3B compared to 4B in buffer control

[9] t pH 2.0 rophilia is dep d

The marked variability in the staining properties of these glands permit only generalities for results with a given procedure

[11] In untreated control sections mucous acini are 1-3PN 1 2B

[12] Treatment of sections with KOH and sialidase prior to staining decreased blue staining in some but not in other SL acini and duct lumens without affecting PN staining

[13] In s m gl d rophilia is confined to altered lobule in anterior portion of gland

[14] Some mucous acini are 0-PB when viewed wet from staining jar

raphy with Kodak AR 10 stripping film by conventional methods Autoradiographs were developed fixed and washed after a 7–14 day exposure at 0°C and were subsequently air dried dehydrated, cleared and mounted

Concerning the nomenclature applied to the carbohydrate containing substances found in the primate salivary mucins of this study we refer to discussion of a more general terminology that is probably consistent with present histochemical and biochemical knowledge (Spicer et al 65) Briefly it has been suggested that the mucosubstances present in epithelial sites which are probably glycoproteins be designated *mucins* and that where possible these may be further classified as *sialomucins* and *sulfomucins* These designations are used on the basis of histochemical tests for the presence or absence of the carboxyl groups of sialic acid and sulfate groups respectively Another type of mucosubstance lacking demonstrable acidic properties but rich in *vic* glycols that presumably originate from fucose and galactose residues are termed *neutral mucosubstances*

RESULTS

The major portion of the results (tables 2–4) are recorded according to visually estimated intensity and shade Figures in the tables indicate relative intensity of staining or labeling When two or more colors or combinations of colors are given for a particular site and method the first one listed is predominant and the remainder is listed in descending order of prominence Staining of mucous acini are described unless otherwise indicated Since histochemical interpretations are given (tables 2–4) for the results in the various sites only those results which require further description are described in detail

Three histologic glandular cell types varying in the carbohydrate content of their secretions may be distinguished in salivary glands *In the mucous cell* a finely fibrillar uniform mucous fills the cytoplasm in the seromucous cell a granular secretion is generally present with a variable amount of demonstrable carbohydrate and in the serous cell no carbohydrate is evident with histochemical methods These definitions generally follow those given by Munger (64) for the classification of salivary gland cell types

Submandibular glands Histologically there is a general predominance of seromucous demilunes and acini over the mucous secretory portions in the submandibular glands of all three primates (figs 26 34 and 39) Sections of human glands stained with hematoxylin and eosin demonstrate this feature consistently although the impression is gained that different areas in a given gland vary in the amount of mucous units relative to seromucous units with a very few areas showing mainly mucous acini and other areas almost no mucous acini This variability is particularly notable in some isolated lobules of the main submandibular gland which exhibit a predominance of mucous acini similar to that observed in portions of the sublingual gland in which mucous acini are mixed with less prominent non mucous (probably seromucous) acini A more uniform distribution of mucous acini is present throughout the submandibular glands of both monkeys and particularly in the small anterior *prolongations of these glands*

The variable mixed diamine reactivity of *mucous acini* in man is largely blocked by prior periodate oxidation (figs 40 and 41) while the mucins in both monkey submandibular glands are unreactive toward mixed diamine staining with or without *oxidation (table 3) However the mucous* acini in the glands of all three species contain periodate susceptible acid mucins as judged by the blockage of alcianophilia produced by prior periodate oxidation and exposure to the *meta* diamine reagent (figs 27 and 28)

The periodic acid para diamine (PAD) procedure reveals red brown staining in all of the mucous acini of both monkey glands and some of the mucous acini in human submandibular glands after sialidase digestion This contrasts with the purple brown color visualized in the mucous acini *before digestion It is possible but not definitely proven* that the mucous acini in the human glands with unaltered purple brown staining after sialidase correspond with those shown by high iron diamine reactivity to contain sulfomucins as will be described The brown coloration in the

TABLE 4

St ining of prim te sali ary mucosubstances with comb nation basic dye ıic glycol procedures

Hist l gic ite	Species	AB pH 1 0-PAS	AB pH 2.5-PAS aft					Hi toch mical inte pretati n
			No pre-treatm nt	5 min KOH 8–24 h buffer	5 min KOH 8–24 hr sialidase	Mild MeOH	Mild MeOH 15 min KOH	
SM gland	R	4R	4RP	4RP	4R [1]	4R	4RP	Sialidase-digestible mucin in all cells These are readily esterified and de-esterified
SM gland	S	2–4R	2–4RP	2–4RP	2–4R	2–3R	2–3RP	Same as rhesus SM
SM gland	M	4BP 4R	4BP	4BP	4BP 4RP	4BP 4R	4BP	Sialomucin partially resistant to sialidase in some acini is esterifiable and deesterifiable and is non alcianophilic at pH 1 0 Sulfomucin in other acini is 4BP in all the methods
SL gland anterior	R	4BP [2]	4BP	4BP	4BP [2]	4BP [2]	4BP	*Anterior* — Sulfomucin in the great majority of cells
SL gland posterior	R	4R	4RP [1]	4RP	4R [1]	4R	4RP	*Posterior* — Sialidase susceptible mucin in all cells Their carboxyls are readily esterified and deesterified
SL gland	S	4B	4BP	4BP	4BP	4BP	4BP	Probable sulfomucin in all cells Stronger alcianophilia at pH 1 0 than at pH 2 5
SL gland lesser and greater	M	4BP 4RP 4R	4BP 4P 4RP	4BP 4P 4RP	4BP 4RP	4BP 4RP 4R	4BP	*Lesser and Greater* — Sialomucin digested by sialidase with difficulty in a few cells Probable sulfomucin in majority of cells

Abbreviation in addition to those in tables 2 and 3: Mild MeOH methylati n four h ur at 37 C
[1] A 12 hour sialidase dige ti n
[2] Some acini are 4R

TABLE 3

Reactivity of mucins in certain primate salivary glands to methods dependent on periodate oxidation of vicinal hydroxyls

Histologic site	Species	PAS after diastase	PAPS	PAD after		Metadiamine AB		Mixed diamines at pH 4 0		Histochemical interpretation
				18 hr buffer	18 hr sialidase	Without prior H_5IO_6	With prior H_5IO_6	Without prior H_5IO_6	With prior H_5IO_6	
SM gland	R	4R	0–±R	3–4PF	1–2RF	1–2B	0	0	0	Abundant *vic* glycols probably in hexose or deoxyhexose sialic acid carboxyls proximal to these groups Unexplained lack of PAPS and mixed diamine reactivity
SM gland	S	3R	1–2R	1–2PF	1–2RF	2–3B	0	0	0	Similar to rhesus SM except PAPS method *also* indicates presence of *vic* glycols proximal to acid groups
SM gland	M	4R	0–2R	2–3PF	2–3RF 2–3PF [1]	3–4B	0	3–4P	0–2P	Sialic acid carboxyls *and* sulfate esters proximal to *vic* glycols (2–3RF after sialidase presumably due to *vic* glycols of a hexose or deoxyhexose near sialic acid)
SL gland anterior	R	3R	1–2R	3CP	3CP 1–20F	4B	0	4P	1–2CP	*Anterior* — Sulfate esters and sialic acid carboxyls in proximity of *vic* glycols (1–20F in a few acini after sialidase presumably due to *vic* glycols *near* sialic acid
SL gland posterior	R	3R	0–R	1–2F	1–20F	1–4B	0	0–CP	0	*Posterior* — Sialic acid carboxyls proximal to *vic* glycols
SL gland	S	3R	1–2R	2F	2F	3B	0 [2]	3P	1–2CP	Most of sulfate esters close to *vic* glycols
SL gland lesser	M	2–4R	±R [3]	2–3PF	2–3PF 30F [4]	2–4B	0 [2]	3–4P	0 [5]	*Lesser* — Sialic acid carboxyls proximal to *vic* glycols and presumably latter account for 30F with PAD method after sialidase *Most sulfate esters are close to vic glycols* (paradoxical lack of PAPS reactivity)
SL gland greater	M	1–3R	0–±R	1–2PF	1–2PF	3B	0	2P	0	*Greater* — Like lesser gland *except for* indication that most sulfate esters are proximal to *vic* glycols

Abbreviations in addition to those in table 2 PAD periodic acid *para* diamine PAPS periodic acid phenylhydrazine-Schiff PAS periodic acid Schiff
Colors C gray F brown O orange, R, red

[1] Approximately one-half of the acini are 2–3RF many seromucous acini particularly in the accessory *portions stain* 20F after and 1–2CP before sialidase

[2] A few acini are 1–2B

[3] Seromucous demilunes are PAPS-positive

[4] The majority of acini are 2–3PF

[5] Although some mucous acini retain 1–2CP staining most mixed diamine staining is blocked after periodate *oxidation*

TABLE 4

Staining of primate salivary mucosubstances with comb nation basic d je vic gl jcol proced ires

Hist l gic ite	Species	AB, pH 1 0-PAS	AB pH 2 5-PAS ft					Histoch mic l int rp t tion
			No pre-t e tment	5 min KOH 6–24 h buff	5 min KOH 6–24 h sialida e	Mild MeOH	Mild MeOH 15 min KOH	
SM gland	R	4R	4RP	4RP	4R [1]	4R	4RP	Sialidase-digestible mucin in all cells These are readily esterified and de esterified
SM gland	S	2–4R	2–4RP	2–4RP	2–4R	2–3R	2–3RP	Same as rhesus SM
SM gland	M	4BP 4R	4BP	4BP	4BP 4RP	4BP 4R	4BP	Sialomucin partially resistant to sialidase in some acini is esterifi able and deesterifiable and is non alcianophilic at pH 1 0 Sulfo-mucin in other acini is 4BP in all the methods
SL gland anterior	R	4BP [2]	4BP	4BP	4BP [2]	1BP [2]	4BP	*Anterior* — Sulfomucin in the great majority of cells
SL gland posterior	R	4R	4RP [2]	4RP	4R [1]	4R	1RP	*Posterior* — Sialidase susceptible mu cin in all cells Their carboxyls are readily esterified and deesterified
SL gland	S	4B	4BP	4BP	4BP	4BP	4BP	Probable sulfomucin in all cells Stronger alcianophilia at pH 1 0 than at pH 2 5
SL gland lesser and greater	M	4BP 4RP 4R	4BP 4P 4RP	4BP 4P 4RP	4BP 4RP	4BP 4RP 4R	4BP	*Lesser and Greater* — Sialomucin di gested by sialidase with difficulty in a few cells Probable sulfo-mucin in majority of cells

Abbre i ti n in addition to those in table 2 nd 3 Mild MeOH methylation f ur hours at 37 C

[1] A 12 hour sialidase digestion

[2] Some acini are 4R

PAD technique may be attributed to Schiff *bases formed with the* diamine on periodate engendered aldehydes presumably in *vic* glycols of hexose or deoxyhexose (galactose or fucose) residues The change in color after sialidase is thought to reflect enhanced access of the cationic diamine to aldehydes after removal of repelling sialic acid groups

Evidence for the presence of sialomucin throughout the mucous acini of both monkey glands and in some of those of the human gland is found in the alcianophilia of the mucous acini present at pH 2 5, but none at pH 1 0 and the lack of affinity for either the high iron diamine or aldehyde fuchsin reagents and consequent blue staining when either of these is used sequentially *with alcian blue* (table 2) *In* the squirrel gland alcianophilia is present at pH 2 5 and absent at pH 1 0 in both mucous and seromucous components (figs 35 and 36) These results are indicative of sialomucin because the pK value for the carboxyl of sialic acid is approximately 2 7 and these groups would not be ionized and negatively charged in the alcian blue pH 1 0 solution At the latter pH level specific staining of sulfated mucosubstances by alcian blue has been reported (Lev and Spicer 64) The lack of azurophilia of these mucins below pH 3 0 corroborates these histochemical results Wet metachromasia is demonstrable in sections stained at pH 3 0 and alcohol resistant staining occurs only at or above pH 3 5–4 0 (table 2)

Consistent with the above evidence for presence of sialomucin is the demonstration of a loss of alcian blue reactivity in all of the mucous acini of the rhesus monkey gland and some of the mucous acini of the squirrel monkey following exposure to sialidase prior to staining This is visualized as (1) a change from red or blue purple to strong red (the residual red indicating presence of carbohydrate with *vic* glycol residues other than sialic acid) in adjacent sections stained by the alcian blue (AB) pH 2 5 PAS combination (figs *1A B*) and (2) loss of blue staining in sections stained with the high iron diamine alcian blue sequence (figs 29 30 *37 and 38*) or alcian blue alone The lack of incorporation of $S^{35}O_4^{=}$ in rhesus submandibular glands agrees with the histochemical evidence for exclusive elaboration of sialomucin by this organ (table 2) Scattered mucous and seromucous acini in the squirrel gland contain a sialidase resistant sialomucin as demonstrated by the blue staining in the high iron diamine alcian blue sequence unaltered by prior sialidase digestion

In conjunction with alcian blue staining at different pH values it was stated previously that scattered mucous acini in the *human submandibular gland lose alcianophilia* as the pH is decreased However the finding that about one half of the mucous *acini in this gland stain at pH 1 0* is thought to be evidence for the presence of a sulfomucin Accordingly most of the *acini stain blue* purple *with the AB pH* 2 5 PAS combined method but about half appear red purple with the AB pH 1 0 PAS procedure Treatment of sections with 1% KOH prior to lengthy sialidase digestion followed by AB pH 2 5 PAS staining results in a similar distribution of red purple and blue purple acini as seen in the AB pH 1 0 PAS sequence (table 4) again suggesting a mixture of sulfo and sialomucin producing acini Consistent with these results are the effects of mild methylation on the AB pH 2 5 PAS reaction in which many acini probably containing sulfomucin retain the blue purple staining whereas many presumably composed of sialomucin show red staining after methylation

These results indicating the presence of both sulfo and sialomucins in mucous acini of the human gland are confirmed by the sequential basic dye methods (table 2) Thus the high iron diamine alcian blue sequence elucidates more clearly the distribution of each type of mucosubstance such that the cells of some mucous acini are purple black (with sulfated mucosubstance) some are blue (with sialomucin) and still other acini contain both types either in different cells or the same cell of a given acinus (fig 10) The aldehyde fuchsin alcian blue combined method distinguishes blue purple acini from blue acini and these roughly correspond with acini stained purple black and blue respectively in the high iron diamine alcian blue sequence *A reduction and in some*

areas obliteration of the blue without alteration of the black or purple black in this sequence is produced by brief pretreatment of the sections with 1% KOH and a 24 hour exposure to sialidase prior to staining (table 1) Shorter exposure (8 to 16 hours) to the enzyme without saponification does not affect the alcian blue reactivity

The seromucous acini particularly of the human submandibular gland show histochemical evidence of mucosubstances Besides the mixture of blue purple and blue secretion in the mucous cells shown by the aldehyde fuchsin alcian blue sequence granules with striking purple coloration are revealed in nearly all the seromucous components of the human glands (fig 11) The aldehyde fuchsin reactivity of these granules is decreased but not eliminated following a four hour 60 C methylation but such staining is almost obliterated after similar treatment for 24 hours Paradoxically subsequent saponification following active methylation from 4 to 24 hours largely restores the aldehyde fuchsin reactivity of the granules In this regard the acid group here differs from the sulfate esters of the usual sulfomucin In some lobules these same granules are stained light gray black (with or without superimposed blue coloration) by the high iron diamine alcian blue method Although this latter method appears to be less sensitive than the aldehyde fuchsin alcian blue sequence as a means of staining these granules it does afford additional evidence suggestive of a sulfated polymer in this site

Sublingual glands of monkeys Sections of these glands stained with hematoxylin and eosin reveal predominantly mucous acini (fig 31) with a minor complement of seromucous demilunes except in the posterior portion of the rhesus sublingual gland where seromucous elements are more numerous

The anterior and posterior parts of the rhesus sublingual gland are sharply demarcated by a prominent septum of interlobar connective tissue Although the gland appears grossly as a single mass of tissue the histochemical and histological differences between the two parts show that the gland is not a single uniform entity This variability contrasts with the more uniform reactions and histology observed in the squirrel monkey sublingual gland Therefore the histochemical results on monkey sublingual glands will pertain to three sites containing distinctly different secretions the anterior and posterior portions in the rhesus and the entire gland of the squirrel monkey

The mucous acini in all three sites contain periodate reactive mucosubstances as judged by their strong diastase resistant staining with the PAS method (table 3) The periodic acid phenylhydrazine Schiff staining indicative of periodate reactive acid mucin is strong in the anterior portion of the rhesus and throughout the squirrel gland Unlike the mucosaccharides in the mucous acini in the submandibular glands of these animals the mucus in the anterior lobe of the rhesus and throughout the squirrel monkey gland displays strong purple staining with the mixed diamine method Prior periodate oxidation reduces the intensity of this staining to light gray purple indicating intermediate susceptibility of this basophilia to prior oxidation Contrastingly the scattered mucous acini in the posterior portion of the rhesus gland stain light purple without prior periodate oxidation and not at all after such treatment The mucosubstances of these primate sublingual glands display variable susceptibility of basophilia to blockage with a periodate *meta* diamine sequence as demonstrated by a loss of alcianophilia after the periodate oxidation and treatment with N N dimethyl *m* phenylenediamine This blockage of basophilia presumably involving neutralization of anionic charges in the polymer by diamine condensed on adjacent aldehydes is more complete in both portions of the sublingual gland of the rhesus monkey (figs 32 and 33) as some acini of the squirrel monkey sublingual gland remain alcianophilic after periodate *meta* diamine treatment Thus the three types of reaction which presumably evaluate proximity of vic glycols and acid groups in mucosaccharides give different results in these several sites

Other histochemical tests indicate that sulfated mucosubstance is predominantly present throughout the sublingual gland of the squirrel monkey and in the more ante

PAD technique may be attributed to Schiff bases formed with the diamine on perio date engendered aldehydes presumably in vic glycols of hexose or deoxyhexose (gal actose or fucose) residues The change in color after sialidase is thought to reflect enhanced access of the cationic diamine to aldehydes after removal of repelling sialic acid groups

Evidence for the presence of sialomucin throughout the mucous acini of both mon key glands and in some of those of the human gland is found in the alcianophilia of the mucous acini present at pH 2 5 but none at pH 1 0 and the lack of affinity for either the high iron diamine or aldehyde fuchsin reagents and consequent blue staining when either of these is used se quentially with alcian blue (table 2) In the squirrel gland alcianophilia is pres ent at pH 2 5 and absent at pH 1 0 in both mucous and seromucous components (figs 35 and 36) These results are in dicative of sialomucin because the pK value for the carboxyl of sialic acid is ap proximately 2 7 and these groups would not be ionized and negatively charged in the alcian blue pH 1 0 solution At the lat ter pH level specific staining of sulfated mucosubstances by alcian blue has been reported (Lev and Spicer 64) The lack of azurophilia of these mucins below pH 3 0 corroborates these histochemical re sults Wet metachromasia is demonstrable in sections stained at pH 3 0 and alcohol resistant staining occurs only at or above pH 3 5–4 0 (table 2)

Consistent with the above evidence for presence of sialomucin is the demonstra tion of a loss of alcian blue reactivity in all of the mucous acini of the rhesus mon key gland and some of the mucous acini of the squirrel monkey following exposure to sialidase prior to staining This is visu alized as (1) a change from red or blue purple to strong red (the residual red in dicating presence of carbohydrate with vic glycol residues other than sialic acid) in adjacent sections stained by the alcian blue (AB) pH 2 5 PAS combination (figs 1A B) and (2) loss of blue staining in sections stained with the high iron dia mine alcian blue sequence (figs 29 30 37 and 38) or alcian blue alone The lack of incorporation of $S^{35}O_4^=$ in rhesus submandibular glands agrees with the tochemical evidence for exclusive elal tion of sialomucin by this organ (tabl Scattered mucous and seromucous aci the squirrel gland contain a sial resistant sialomucin as demonstrate the blue staining in the high iron dian alcian blue sequence unaltered by sialidase digestion

In conjunction with alcian blue stai at different pH values it was stated p ously that scattered mucous acini in human submandibular gland lose alc philia as the pH is decreased How the finding that about one half of the cous acini in this gland stain at pH 1 thought to be evidence for the presenc a sulfomucin Accordingly most of acini stain blue purple with the AB 2 5 PAS combined method but about appear red purple with the AB pH 1 0 procedure Treatment of sections with KOH prior to lengthy sialidase diges followed by AB pH 2 5 PAS stainin sults in a similar distribution of red pu and blue purple acini as seen in the pH 1 0 PAS sequence (table 4) again gesting a mixture of sulfo and sialom producing acini Consistent with thes sults are the effects of mild methyla on the AB pH 2 5 PAS reaction in w many acini probably containing s mucin retain the blue purple stai whereas many presumably compose sialomucin show red staining after me lation

These results indicating the presenc both sulfo and sialomucins in muc acini of the human gland are confir by the sequential basic dye methods (t 2) Thus the high iron diamine alc blue sequence elucidates more clearly distribution of each type of mucosubst such that the cells of some mucous ac are purple black (with sulfated mucos stance) some are blue (with sialomuci and still other acini contain both ty either in different cells or the same cell a given acinus (fig 10) The aldeh fuchsin alcian blue combined method d tinguishes blue purple acini from bl acini and these roughly correspond w acini stained purple black and blue spectively in the high iron diamine alc blue sequence A reduction and in son

gland which shows no labeling of mucous acini by the isotope (fig 2) Moreover azurophilia is present in the anterior portions of the rhesus glands in the present study at pH 1 5 while such staining is observed in the posterior segment only above pH 3 0 An unidentified portion of the rhesus sublingual gland stained metachromatically below pH 2 6 with toluidine blue (Shackleford and Klapper 62)

Human sublingual glands As contrasted with the structure of the human submandibular gland the sublingual gland is composed predominantly of mucous acini (fig 42) although the amount of seromucous demilunes and acini varies considerably throughout any gland The inconstant component of the gland the greater sublingual generally contains more numerous seromucous and fewer mucous elements than the lesser or definitive gland and in this respect resembles the posterior segment of the rhesus sublingual gland

The mucous acini of human sublingual glands exhibit a considerable variation in some of the histochemical reactions for mucins The intensity of PAS staining after diastase varies somewhat in areas of the sublingual gland but generally shows a strong reaction throughout (fig 43) The periodic acid phenylhydrazine Schiff reactivity of mucous acini although quite variable in different lobules is surprisingly weak relative to the conspicuously reactive seromucous demilunes and acini as will be noted

Evidence for periodate reactive acid mucosaccharide is also found in the susceptibility of the basophilia in the mucous acini toward prior periodate oxidation and treatment with *meta* diamine as demonstrated by the blockage of alcianophilia after the periodate *meta* diamine sequence (figs 20 and 21) Loss of mixed diamine reactivity in most mucous sites after exposure to periodate prior to staining (figs 22 and 23) also points to the presence therein of periodate reactive acid mucosaccharide However some basophilia of mucous acini remained in sections treated with periodic acid prior to mixed diamine staining This persistent basophilia suggestive of the presence of a periodate unreactive acid mucosubstance in a few mucous acini appears to be localized in the same sites displaying little or no PAS reactivity (table 3)

A complicated pattern of distribution of different mucins was observed in the present study as shown for example by the irregular alcian blue reactivity at pH 1 0 in different areas of the lesser sublingual portion Similarly azurophilia at pH 1 0–2 0 varies from one group of acini or one lobule to another some acini or lobules having one or more reactive foci (fig 19) Staining appeared somewhat more prominent in the anterior segments of the lesser sublingual gland in some individuals Not more than one third of the acini in a given gland showed reactivity toward alcian blue at pH 1 0 or azure A at pH 1 0–2 0 (table 2)

Combination of alcian blue (AB) at either pH 2 5 or 1 0 with a PAS step reveals a mixture of mucins some of which stain blue others blue or red purple and others red With the AB pH 2 5-PAS method a few cells or acini stain red pointing to the presence of neutral mucosaccharide (figs 14 and 24) With the AB pH 1 0 PAS sequence there is an increased number of red acini (fig 15) probably because of the presence of sites containing sialic acid Also a general increase in red staining is present in the mucous acini of the lesser sublingual gland after KOH treatment and prolonged sialidase digestion followed by AB pH 2 5-PAS staining As with the increased red staining in AB pH 1 0 PAS compared with the AB pH 2 5 PAS method the resultant increase of red neutral mucosubstance following digestion is thought to indicate sites of sialomucin (table 4)

However the histochemical results with these combined basic dye *vic* glycol methods in conjunction with sialidase digestion or methylation require cautious interpretation since color changes in the stainable material induced by such treatment are often subtle A shift from faint gray brown or purple brown to red brown or orange brown observed in certain mucous acini with the PAD method after sialidase treatment also affords evidence for the presence of sialomucin (figs 12 and 13) The change in color is thought to reflect enhanced access of the cationic dia

rior portion of the rhesus gland Mucosaccharides containing sialic acid apparently are present with neutral mucosubstances in the posterior portion of the rhesus sublingual gland and are intermixed in small quantity with a predominant sulfomucin in the anterior part of the same gland

The mucins in all three sites are alcianophilic at pH 2 5 while only those in the squirrel and the anterior portion of the rhesus glands display similar reactivity at pH 1 0 (figs 2 and 7) The AB pH 2 5 PAS method shows blue purple mucins exclusively throughout the sublingual gland of the squirrel monkey and the anterior portion thereof in the rhesus monkey (fig 3) and reveals red purple to red mucosubstances in the posterior part of the rhesus gland (table 4) The AB pH 1 0 PAS technique shows blue sulfomucin exclusively in the squirrel monkey sublingual and blue purple sulfomucin present predominantly with infrequent intermixed red areas indicative of sialomucin in the anterior half of the rhesus gland (fig 4)

Sialidase digestion followed by staining with the AB pH 2 5 PAS technique offers further proof for the presence of sialomucin throughout the posterior part of the rhesus gland and in some areas of the anterior portion of the same gland Thus there is complete elimination of basophilia following a 12 hour digestion so that the mucin in the posterior portion stains red like neutral mucosubstance Similarly basophilia is eliminated from scattered cells in the anterior lobe by 24 hour sialidase digestion after brief pretreatment with 1% KOH Similar treatment of sections of squirrel monkey sublingual gland does not affect the AB pH 2 5 PAS staining Mild methylation of sections of rhesus sublingual gland results in the blockage of basophilia in those few scattered mucous acini in the anterior rhesus gland presumed to contain sialomucin along with uniform blockage in the posterior mucous acini Basophilia can be restored in these sites after mild methylation by removing the methyl esters from the carboxyl groups of sialic acid with a saponification step (table 4) Further evidence for a sialomucin in these two rhesus sites is found in the orange brown staining with the periodic acid para diamine (PAD) method brought about by prior sialidase digestion The brown staining of the mucous acini in the squirrel sublingual gland produced by the PAD method is unaltered following exposure to sialidase

Additional evidence for the presence of sulfo- or sialomucins exclusively or in mixtures in the different glands includes results obtained through use of combined basic dye sequences in conjunction with sialidase digestion and $S^{35}O_4^{=}$ autoradiography (table 2) Thus the mucous acini of the squirrel monkey sublingual gland are colored a uniform purple or purple black by the aldehyde fuchsin alcian blue or high iron diamine alcian blue methods respectively (figs 8 and 9) These results correlated with the uniform alcianophilia at pH 1 0 and metachromatic staining with azure A at pH 1 5 strongly indicate the presence of sulfomucin in this gland although autoradiographic data is lacking for this species

In sections of rhesus sublingual gland stained by the high iron diamine alcian blue sequence the mucin in the anterior lobes stains purple black with scattered blue sites, while that in the posterior half is uniformly blue (fig 5) Aldehyde fuchsin alcian blue staining of the same gland resulted in a distribution of purple or blue purple and blue mucous cells that is similar to the distribution of purple black and blue cells visualized by the high iron diamine alcian blue method Treatment with sialidase prior to staining with the high iron diamine alcian blue procedure did not alter the purple black staining in the anterior half of the rhesus gland but removed the alcianophilia of the posterior portion (fig 6) indicating that sulfomucin predominates in the former and sialic acid in the latter site However since some of the alcian blue reactivity remained in both anterior and posterior parts despite brief pretreatment with 1% KOH and a 24 hour sialidase digestion it appears that a sialidase resistant mucin is also present (table 2)

Autoradiography with radiosulfate confirms the histochemical evidence for sulfomucin in the anterior lobules of the rhesus sublingual gland This part of the gland reveals active incorporation of $S^{35}O_4^{=}$ as opposed to the posterior part of this same

ing of mucins in the monkey submandibular glands and in the posterior segment of the rhesus sublingual is usually absent after sialidase treatment for 8–16 hours In addition to these mucins which were readily digestible with sialidase other apparently nonsulfated mucosubstances in some of these primate salivary glands displayed a greater resistance to prolonged action of sialidase presumably because of different chemical configurations less compatible with the specificity requirements of the enzyme This was particularly true of the mucus-containing sites in the anterior segment of rhesus sublingual gland and both glands of the human where incubation with sialidase for 24 hours failed to reduce or only slightly reduced the alcian blue reactivity However brief saponification partially enhanced the sialidase digestibility of these mucins so that further diminution of alcianophilia was demonstrable

According to Gibbons (63) susceptibility to sialidase is influenced both by O acetylation of the neuraminic acid and by the position of the attachment of neuraminic acid to the adjacent sugar Although the explanation for enhanced histochemical sialidase digestibility after brief saponification remains undetermined it might involve hydrolysis of an O acetyl group since such an ester bond unlike the neuraminosidic linkage is alkali labile Sites resistant to sialidase treatment were often found to consist of an admixture of sialo- and sulfomucins either in different cells that are closely adjacent to each other or in the same cells Explanation of the striking differences in the histochemical properties of these various primate sialomucins requires more complete knowledge of the chemical structure of the neuraminic acids present the linkage between the neuraminic acids and the adjacent residues and the composition of the oligosaccharide units and the protein moiety all of which may affect the basophilia periodate reactivity and sialidase digestibility of the mucin

According to limited biochemical data the secretions of human sublingual and submandibular glands contain sialic acid (Berggard and Werner 58 McCoombe et al 61 Mandel et al 64) Except for the report of N acetylneuraminic acid in human submandibular saliva (Mandel et al 64) little biochemical information is available concerning the neuraminic acids occurring in primate salivary glands or the residues to which they are attached presumably in glycoproteins Because of the relatively slight diminution in the basophilic staining intensity of human sublingual mucin after prolonged (16 hours) acid hydrolysis at 80 C it is believed that sialic acid cannot be demonstrated histochemically in this site (Quintarelli 61 Quintarelli and Robinson 61) However the observations recorded in the present study afford histochemical evidence for the presence in both human salivary glands of relatively sialidase resistant sialomucins which can be rendered more hydrolyzable by the empirical technique of brief saponification Of particular interest is the evidence for a unique sialomucin in seromucous components of human sublingual and submandibular glands This sialomucin apparently contains a PAD reactive hexose the staining which depends on removal of proximal sialic acid groups by sialidase

Absent or weak affinity for some basic dyes especially alcian blue and azure A cannot be interpreted as proof of a neutral mucosubstance unless chemical assay autoradiography and lack of affinity for any battery of basic stains substantiate absence of sialic acid or sulfate esters This restriction is based on experience in which occasional sites known to be rich in sialic acid (e g Syrian hamster exorbital lacrimal gland) and sulfate esters (e g mouse exorbital lacrimal gland) lack alcianophilia and azurophilia but may stain with the mixed diamine iron diamine or aldehyde fuschsin methods Associated protein for example may mask affinity of acid groups in some mucins for certain of the dyes (French and Benditt 53) Quintarelli (63b) has provided evidence for such an influence by the observation that digestion with pepsin enhances alcianophilia in rhesus submandibular gland

Although there is an emerging histochemical literature on the subject there is a modicum of biochemical evidence for an epithelial or salivary mucosubstance containing sulfate residues unrelated to

ie to periodate engendered aldehydes ieighboring hexose or deoxyhexose resi s after removal of repelling sialic acid ups Acini not altered by prior sialidase estion presumably secrete either sulfo cin or sialidase resistant sialomucin ny of the seromucous demilunes and ii as will be mentioned reveal a more king shift to red or orange brown with PAD technique after the enzymatic estion

'he numerous mucous acini staining or blue purple in the AB pH 1 0 PAS cedure are presumed to contain sulfo cin Although autoradiographic proof $^{35}O_4^{=}$ incorporation in human sublin l glands is lacking other histochemical niques such as the high iron diamine an blue and aldehyde fuchsin alcian methods also are strongly indicative ie presence of sulfomucin In sections oth the lesser and greater sublingual ids purple aldehyde fuchsin reactive i correspond in location to those which purple black with the high iron dia e method (figs 16 17 and 25) If er method is combined with alcian differentiation is possible between purple or purple black areas presumed ontain sulfate and blue sites thought ontain sialomucin A 24 hour siali digestion carried out prior to staining he high iron diamine alcian blue se ice effectively reduces the alciano a of a portion of the mucous acini after pretreatment with KOH (fig 18) ing of sections of human sublingual d by the low iron diamine alcian blue ence results in a variable purple black ion with no differentiation between s of mucosubstances In this respect low iron diamine reagent reacts as a ral stain for acid mucosaccharides le 2)

ie seromucous demilunes and acini in gland particularly in the lesser por display conspicuous periodic acid ylhydrazine Schiff (PAPS) staining ative of periodate reactive acid muco haride (fig 44) These structures ob ed by the strongly stained adjacent ous acini are relatively inconspicuous iastase PAS preparations The strong S reactivity in these sites appears to espond in distribution to the orange brown staining which develops with the PAD procedure following sialidase diges tion These two observations are consist ent with the interpretation that sialomu cin, rich in residues with vicinal hydroxyls are present in the seromucous sites

DISCUSSION

Three general types of mucosubstances can be recognized in mucus producing sa livary glands by existent histochemical methods Since the carbohydrate compo nents in these mucins are incompletely characterized by histochemical or bio chemical methods they can be called in broad terms sulfomucins sialomucins or neutral mucosubstances The latter two types are known biochemically while the sulfomucin type is not It has been pointed out that glycoproteins vary through a broad spectrum in the proportion of fucose to sialic acid and that no sharp line of demarcation separates acid and neutral mucins (Hashimoto and Pigman 62) With less sensitivity histochemical results also show wide variability in intensity of basophilia of mucins Some as in the human submandibular gland stain dark blue purple with the alcian blue pH 2 5 PAS sequence reflecting high sialic acid or sulfate levels Some as for example in the submandibular gland of the squirrel monkey stain red purple reflecting either low levels or partial masking of acid groups and others red indicating complete absence or masking of acid groups Recog nizing that precise quantitative chemical information is not afforded by such a his tochemical method does not detract from the fact that it reveals otherwise unrecog nized chemical differences in various se cretions which differences generally de pend on the relative acidity of the macromolecule Presumably these differ ences are of physiologic significance

The majority of the primate mucins ex amined in this study contained at least some histochemically demonstrable sialo mucin except for the sublingual gland of the squirrel monkey These conclusions are based primarily on the complete or partial elimination of carboxyl dependent alcianophilia from sites presumed to con tain sialic acid by digestion with purified *Vibrio cholerae* sialidase Thus such stain

Draper P and P W Kent 1963 Biosynthesis of intestinal mucins 4 Utilization of [1-^{14}C] glucose by sheep colonic mucosa *in vitro* Biochem J *86* 248–254

Fisher E R and R D Lillie 1954 The effect of methylation of basophilia J Histochem Cytochem *2* 81–87

French J E and E P Benditt 1953 The histochemistry of connective tissue II The effect of proteins on the selective staining of mucopolysaccharides by basic dyes J Histochem Cytochem *1* 321–325

Gibbons R A 1963 The sensitivity of the neuraminosidic linkage in mucosubstances towards acid and towards neuraminidase Biochem J *89* 380–391

Gottschalk A 1963 The basic structure of glycoproteins and problems of their chemical and physicochemical analysis Ann N Y Acad Sci *106* 168–176

Hashimoto Y and W Pigman 1962 A comparison of the composition of mucins and blood group substances Ann N Y Acad Sci *93* 541–554

Hotchkiss R D 1948 A microchemical reaction resulting in the staining of polysaccharide structures in fixed tissue preparations Arch Biochem *16* 131–141

Kent P W and J C Marsden 1963 A sulphated sialoprotein from sheep colonic mucin Biochem J *87* 38P–39P

Leppi, T J 1966 Gross anatomical relationships between primate submandibular and sublingual salivary glands Submitted for publication

Leppi T J and S S Spicer 1964 The anatomy and histochemistry of the sublingual glands of certain primates Anat Rec *148* 384 (abstr)

——— 1965 Mucosaccharide histochemistry of bovine porcine and ovine salivary glands Anat Rec *151* 378–379 (abstr)

——— 1966 Correlative histochemical and autoradiographic studies of epithelial sulfomucins Anat Rec (abstr in press)

Leppi T J and P J Stoward 1965 On the use of testicular hyaluronidase in identifying acid mucins in tissue sections J Histochem Cytochem *13* 406–407

Lev R and S S Spicer 1964 Specific staining of sulphate groups with alcian blue at low pH J Histochem Cytochem *12* 309

——— 1965 A histochemical comparison of human epithelial mucins in normal and in hypersecretory states including pancreatic cystic fibrosis Amer J Path *46* 23–47

Levene P A 1925 Hexosamines and mucoproteins Longmans Green and Co London

Lillie R D 1954 Histopathologic Technic and Practical Histochemistry Blakiston Co New York

Mandel I D R Thompson and S A Ellison 1964 The carbohydrate components of human submaxillary saliva Arch Oral Biol *9* 601–609

McCoombe G K W Knox and H R Sullivan 1961 The carbohydrate constituents of human saliva Arch Oral Biol *3* 171–175

McManus J F A 1946 Histological demonstration of mucin after periodic acid Nature *158* 202

Mowry R W 1956 Alcian blue technics for the histochemical study of acidic carbohydrates J Histochem Cytochem *4* 407

Mowry R W and C H Winkler 1956 The coloration of acidic carbohydrates of bacteria and fungi in tissue sections with special reference to capsules of *Cryptococcus neoformans Pneumoccus* and *Staphylococcus* Amer J Path *32* 628–629

Munger B L 1964 Histochemical studies on seromucous and mucous secreting cells of human salivary glands Am J Anat *115* 411–429

Odin L 1958 Mucopolysaccharides of epithelial mucus In Chemistry and Biology of Mucopolysaccharides Ciba Foundation Symposium Ed by G E W Wolstenholme and M O Connor Little Brown Co Boston pp 234–244

Pigman W and S Tsuiki 1959 The nature of the epithelial mucins Int Dent J *9* 502–516

Quintarelli G 1961 Histochemical studies on human mucous secreting salivary glands Acta Histochem *12* 1–11

——— 1963a Histochemical identification of salivary mucins Ann N Y Acad Sci *106* 339–363

——— 1963b Masking action of basic proteins on sialic acid carboxyls in epithelial mucins Experientia *19* 230–231

Quintarelli G and L Robinson 1961 Histochemistry of human sublingual glands Nature *189* 935–936

Quintarelli G S Tsuiki Y Hashimoto and W Pigman 1960 Histochemical studies of bovine salivary gland mucins Biochem Biophys Res Comm *2* 423–426

——— 1961 Studies of sialic acid-containing mucins in bovine submaxillary and rat sublingual glands J Histochem Cytochem *9* 176–183

Raust G 1962 A review of the literature on salivary mucins J West Soc Periodont *10* 48–52

Schrager J 1964a Sulphated mucopolysaccharides of the gastric secretion Nature *201* 702–704

——— 1964b Mucopolysaccharide of the gastric secretion Nature *201* 1220–1222

Shackleford J M and and C E Klapper 1962 Structure and carbohydrate histochemistry of mammalian salivary glands Am J Anat *111* 25–47

Spicer S S 1960 A correlative study of the histochemical properties of rodent acid mucopolysaccharides J Histochem Cytochem *8* 18–34

——— 1961 The use of various cationic reagents in the histochemical differentiation of mucopolysaccharides Amer J Clin Path *36* 393–407

——— 1965 Diamine methods for differentiating mucosubstances histochemically J Histochem Cytochem *13* 211–234

those in connective tissue mucopolysaccharide Levene (25) cited several reports dealing with the isolation of substances from various epithelial sources containing so called mucoitin sulfuric acid, i e, a polysaccharide composed of hexosamine uronic acid and ester sulfate In the earlier studies cited by Levene there was some suggestion that mucoitin sulfuric acid and some of the amino sugar containing polysaccharides of connective tissues (e g the chondroitins) were similar materials Several recent biochemical studies have indicated that sulfate is present in appreciable amounts in several epithelial sites (Draper and Kent 63, Kent and Marsden, 63, Bignardi et al 64 Schrager, 64a, b) Bignardi and Kent and their respective collaborators have indicated that sulfate occurs along with sialic acid in certain tissues such as dog submandibular gland and sheep colonic mucosa These latter findings are of interest from a histochemical viewpoint because of the fact that a mixture of sialo and sulfomucins have been visualized in several epithelia

This histochemical observations of the present study support the consideration that sulfate is probably present in quantity in some salivary epithelia Thus the majority of mucous acini in the anterior segment of the rhesus sublingual displayed strong affinity for alcian blue at pH 1 0 the high iron diamine reagent and aldehyde fuchsin all of which are judged to be specific histochemical tests for sulfomucin In addition the acini were labeled heavily with $S^{35}O_4^{=}$ as judged autoradiographically Although corroborative data on isotope incorporation in human glands and the sublingual gland of the squirrel monkey is lacking mucous acini in these studies all exhibited histochemical staining properties similar to those of the anterior segment of the rhesus sublingual gland and presumably secrete sulfomucin

The loss of basophilia following periodate oxidation and exposure to *meta* diamine has been thought to imply the presence of periodate reactive vicinal hydroxyls in proximity to sulfate esters or carboxyl groups in the polysaccharides of certain mucins (Spicer 65) From this it might be expected that those mucins whose basophilia was blocked after the periodate oxidation *meta* diamine sequence should also be PAS reactive Blockage of basophilia by the periodate *meta* diamine sequence was demonstrated in each gland except in some areas of the sublingual gland of the squirrel monkey and the lesser sublingual gland of man in which some basophilia remained after such treatment These resistant mucins however, show PAS reactivity comparable to that of the ones in which basophilia is blocked Possibly in the resistant salivary mucins vicinal hydroxyls are effectively removed from the anionic groups, or alternatively these cells may secrete an acid mucosubstance lacking periodate reactive *vic* glycols as well as another neutral mucosaccharide containing such moieties On the other hand connective tissue mucopolysaccharides such as those in cartilage matrix and mast cells retain basophilia after the periodate *meta* diamine sequence and at the same time lack PAS reactivity The histochemical methods thus reveal basic differences between epithelial and connective tissues mucosubstances

ACKNOWLEDGMENTS

The authors are grateful to Mrs Jacqueline G Henson and Miss Josephine Fioravanti for their valuable technical assistance to Miss Patricia L Merriman for skilled clerical assistance and to Mr Don R Tyson for the photomicrographs

LITERATURE CITED

Bélanger L F 1954 Autoradiographic visualization of S^{35} incorporation and turnover by the mucous glands of the gastro-intestinal tract and other soft tissues of rat and hamster Anat Rec *118* 755–771

Berggard I and I Werner 1958 Carbohydrate constituents of human saliva Acta Odont Scand *16* 43–50

Bignardi C G Aureli C Balduini and A A Castellani 1964 Sulfosialopolysaccharide peptide from dog submaxillary gland Biochem Biophys Res Comm *17* 310–312

Carubelli R V P Bhavanandan and A Gottschalk 1965 Studies on glycoproteins XI The O glycosidic linkage of N acetylgalactosamine to seryl and threonyl residues in ovine submaxillary gland glycoprotein Biochem Biophys Acta *101* 67–82

Dempsey E W H Bunting M Singer and G B Wislocki 1947 The dye binding capacity and other chemo-histological properties of mammalian mucopolysaccharides Anat Rec *98* 417–429

PLATES

PLATE 1

EXPLANATION OF FIGURES

Magnifications of figures 1–25 are × 92 unless otherwise indicated

1A Submandibular gland of the rhesus monkey showing the intense staining of the widely scattered mucous acini Twelve hour exposure to the buffer of the sialidase solution followed by the alcian blue (AB) pH 2 5-periodic acid Schiff (PAS) method

1B Section adjacent to that in figure 1A Note elimination of the previously superimposed blue staining so that the mucin now stains red like neutral mucosubstance Twelve hour sialidase digestion followed by the AB (pH 2 5) PAS stain Figures 2 through 6 illu trate sublingual gland of rhesus mon key at border of anterior (lower) and pos terior (upper) lobules

2 Note the correlation of alcian blue staining at pH 1 0 of an acinus in an anterior lobule (bottom half) with the $S^{35}O$ autoradiographic label The adjacent mucous acinus in a posterior lobule is unlabeled and es en tially non alcianophilic (top half) Alcian blue (pH 1 0) stain then $S^{35}O$ autoradiograph × 645

3 The difference between more basophilic an terior (bottom) and weakly basophilic posterior (top) lobules is illustrated The pre dominantly red purple staining of the posterior lobules reflects a low level of acid groups in a PAS-reactive mucosaccharide or masking of acid groups for alcian blue AB (pH 2 5) PAS sequence

4 Note the absence of superimposed blue staining at this lower pH in some mucous cells of the anterior lobules (bottom) and in all acini of the posterior lobules Loss of alcianophilia indicated by the shift from blue or purple to red on lowering the pH is presumably due to sialic acid and corre lates with abolished alcianophilia in sec tions exposed to sialidase prior to staining with the AB (pH 2 5) PAS sequence AB (pH 1 0) PAS stain

5 Clear distinction is revealed here between the purple black sulfomucin in an anterior lobule and the blue sialomucin in a posterior lobule The blue cells scattered through the anterior lobule are not seen in this field Sixteen hour sialidase buffer then 18 hour high iron diamine alcian blue sequence

Spicer S S and J Duvenci 1964 Histochemical characteristics of mucopolysaccharides in salivary and exorbital lacrimal glands Anat Rec *149* 333–358

Spicer S S and M H Jarrels 1961 Histochemical reaction of an aromatic diamine with acid groups and periodate engendered aldehydes in mucopolysaccharides J Histochem Cytochem *9* 368–379

Spicer S S T J Leppi and P J Stoward 1965 Suggestions for a histochemical terminology of carbohydrate rich tissue components J Histochem Cytochem *13* 599–603

Spicer S S and R D Lillie 1959 Saponification as a means of selectively reversing the methylation blockade of tissue basophilia J Histochem Cytochem *7* 123–125

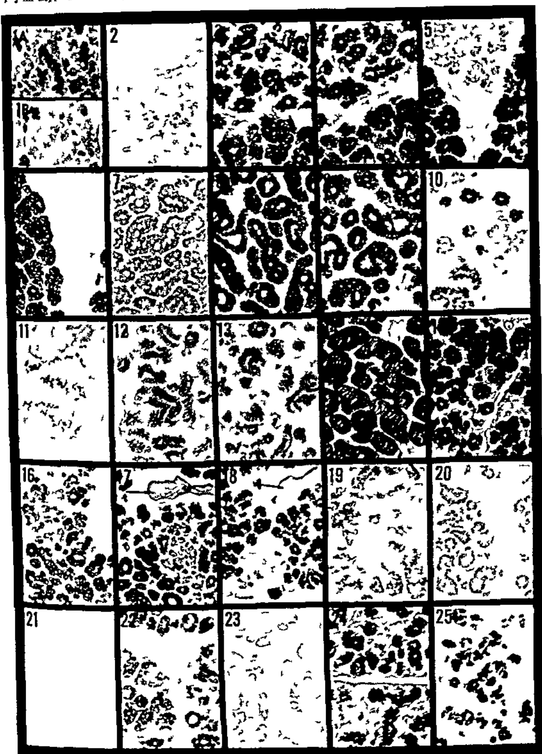
Spicer S S and D B Meyer 1960 Histochemical differentiation of acid mucopolysaccharides by mean of combined aldehyde fuchsin alcian blue staining Amer J Clin Path *33* 453–460

Spicer S S and L Warren 1960 The histochemistry of sialic acid containing mucoproteins J Histochem Cytochem *8* 135–137

Stary Z 1959 *Mucosaccharides and glycoproteins Chemistry and physiopathology* Ergebn der Physiol *50* 174–408

Werner I 1953 Studies on glycoproteins from mucous epithelium and epithelial secretions Acta Soc Med Upsal *58* 1–55

Wislocki G B H Bunting and E W Dempsey 1947 Metachromasia in mammalian tissues and its relationship to mucopolysaccharide Am J Anat *81* 1–37


1A
1B
2
5
10
11
12
13
16
19
20
21
22
23
25

6 Section adjacent to that in figure 5 demonstrating removal of alcianophilia from a posterior lobule and lack of effect of the enzyme on high iron diamine affinity in an anterior lobule Sixteen hour sialidase digestion followed by *the high iron diamine* alcian blue sequence

7–9 Figures 7 through 9 depict sublingual gland of the squirrel monkey These *three staining* characteristics of the mucous acini in this gland strongly indicate the uniform presence of sulfomucin Alcian blue (pH 1 0) method aldehyde fuchsin alcian blue sequence and the high iron diamine alcian blue sequence methods respectively

10 Submandibular gland of man showing the mixture of purple black sulfomucin and blue sialomucin in the widely *scattered* mucous acini Cf figure 17 of human sublingual gland High iron diamine alcian blue sequence

11 Section of same gland showing the blue *staining of a mucous acinus* and purple staining of granules in a seromucous acinus Aldehyde fuchsin alcian blue sequence × 645

Figures 12 through 23 show lesser sublingual gland of man

12 The brown staining of mucous acini is evident Sixteen hour sialidase buffer *periodic* acid *para* diamine method

13 *Note* increased red brown coloration of mucous acini resulting from enzymatic digestion This staining is characteristic of neutral mucosubstance presumably rich in hexose or deoxyhexose residues and the change after digestion is thought due to *en*hanced access of cationic diamine to dialdehyde after removal of sialic acid *residues* The more striking increase in many of the sublingual seromucous acini and demilunes is not seen in this field Sixteen hour sialidase digestion then periodic acid *para* diamine stain

14 The purple blue of acidic mucosubstances predominates over red purple in a few areas indicative of neutral mucosubstance or acidic mucosaccharide with masked acid groups AB (pH 2 5) PAS

15 Note the shift from blue or purple to red in some mucous acini with lowering of the pH of the alcian blue solution This change is characteristic of sialomucins Cf similar reactivity in figure 4 bottom portion AB (pH 1 0) PAS

16 The mucous acini stained purple in this section thought to secrete sialomucin correspond to those stained blue purple in figure 15 Aldehyde fuchsin alcian blue sequence

17 The mucous acini stained purple black in this section correspond in distribution to those stained blue-purple in figure 15 and purple in figure 16 Note mixture of purple black and blue stained mucus in the lumen of an intralobular duct (arrow) Eighteen hour high iron diamine alcian blue sequence

18 Section adjacent that in figure 17 showing *reduction of alcianophilia of mucous acini* and complete loss of such *staining of the* luminal mucus (arrow) without alteration of the purple black staining indicative of sulfomucin Section treated five minutes with 1% KOH followed by 24 hour sialidase digestion prior to 18 hour high iron diamine alcian blue stain

19 Demonstration of low pH bluish purple (β) metachromasia of some but not all mucous acini in a dehydrated and mounted section Azure A pH 1 0

20 Note the uniform alcianophilia of the mucous acini Treatment with *meta* diamine then periodate does not alter the alcian blue affinity Seven hour *meta* diamine periodate alcian blue (pH 2 5) sequence

21 Note complete blockage of alcianophilia in *the mucous acini with the* blue replaced by faint orange brown presumably attributable to Schiff bases formed by diamine condensed with periodate engendered aldehydes The usual weak nuclear alcianophilia remains unaltered Ten minute oxidation with 1% H_5IO_6 then seven hour exposure to *meta* diamine followed by alcian blue (pH 2 5) stain

22 The purple staining of acid mucosaccharide in the mucous acini is evident Mixed diamine pH 4 0 stain

23 Note elimination of staining as a result of the prior oxidation Ten minute oxidation with 1% H_5IO_6 followed by mixed diamine pH 4 0 stain

24 Greater sublingual gland of man showing *somewhat fewer mucous* acini and a greater proportion of seromucous cells as compared to the lesser sublingual (fig 14) AB (pH 2 5) PAS sequence

25 Section adjacent to that in figure 24 showing a mixture of sulfomucin (purple black) and sialomucin (blue) *similar to that* in the lesser gland (fig 17) Note that the mucous acini are more widely scattered than in the lesser sublingual but are still more abundant in proportion to seromucous elements than they are in the submandibular gland Eighteen hour high iron diamine alcian blue sequence

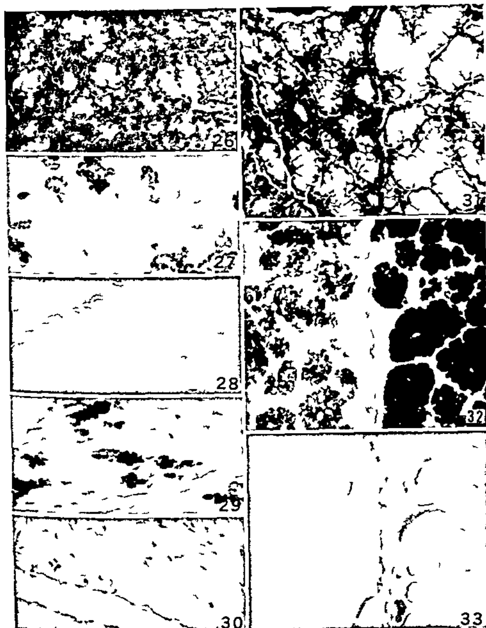

26
27
28
29
30
31
32
33

PLATE 2

EXPLANATION OF FIGURES

Magnifications for figures 26–33 are × 150

26 Submandibular gland of the rhesus monkey The scattered light *mucous acini are distributed between the darker seromucous component* Hematoxylin eosin

27 Adjacent section to that in figure 26 demonstrating the alcianophilia of mucous acini Seven hour *meta* diamine periodate alcian blue (pH 2 5) sequence

28 Section adjacent to that in figure 27 showing blockage of alcianophilia by prior periodate *meta* diamine treatment Periodate *meta* diamine alcian blue (pH 2 5) sequence

29–30 Similar adjacent sections demonstrating alcianpohilia in mucous acini of control section exposed 16 hours to buffer (fig 29) and elimination of such staining in section exposed 16 hours to sialidase solution (fig 30) Both sections were stained with the 18 hour high iron diamine alcian blue sequence

31 Sublingual gland of the rhesus monkey showing a portion of the more posterior lobules (left) with relatively abundant seromucous elements compared with anterior region of the gland (right) which is predominantly mucous in character Hematoxylin and eosin

32 Same gland as in figure 31 showing varying degrees of alcianophilia in the mucous acini of the two portions Seven hour *meta* diamine periodate alcian blue (pH 2 5) sequence

33 Section adjacent to that in figure 32 demonstrating the susceptibility of the alcianophila of the mucins in both parts of the gland to periodate *meta* diamine blockage Ten minute periodate oxidation followed by seven hour exposure to *meta* diamine and then alcian blue at pH 2 5

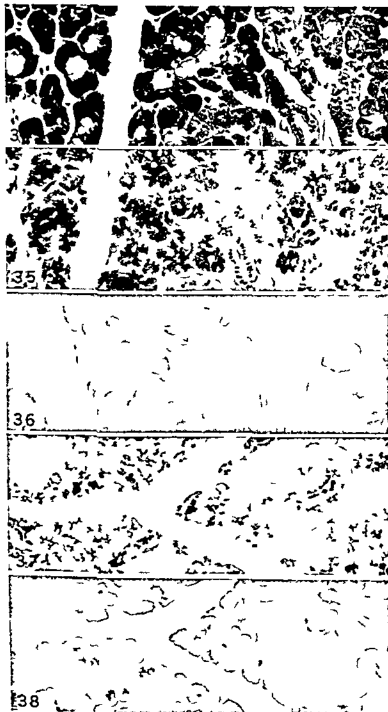

3
35
36
37
38

PLATE 3

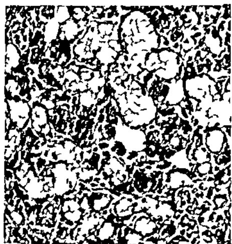
EXPLANATION OF FIGURES

Magnifications for figures 34–38 are × 150

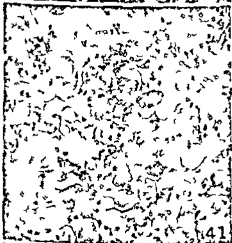
34 Submandibular gland of the squirrel monkey Mucous acini (light areas) are widely scattered between predominant seromucous acini and demilunes Hematoxylin and eosin

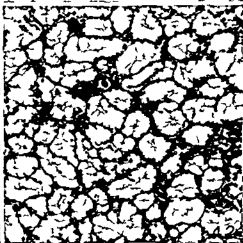
35–36 Adjacent sections of same gland showing the dark staining of the mucin and somewhat lighter staining of the seromucous elements by alcian blue at pH 2 5 (fig 35) and absence of such reactivity with alcian blue at pH 1 0 (fig 36)

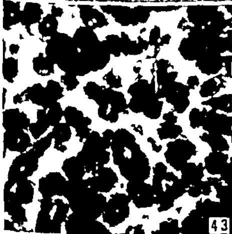
37–38 Similar adjacent sections demonstrating (blue) staining of mucous and seromucous cells in section exposed 16 hours to the buffer (fig 37) and elimination of such staining following 16 hour sialidase digestion (fig 38) Both sections exposed to 18 hour *high iron diamine alcian blue sequence*


39


40


41


42


43


44

PLATE 4

EXPLANATION OF FIGURES

Magnification for figures 39–44 are × 150

39 Submandibular gland of the human The mucous acini represented by the light gray areas vary in prevalence from the closely packed array seen here to a more widely scattered pattern Hematoxylin eosin

40 Basophilia is demonstrated in mucous acini Forty eight hour mixed diamine pH 4 0 stain

41 Basophilia of mucous acini is susceptible to prior oxidation Ten minute oxidation with 1% H_5IO_6 followed by 48 hour mixed diamine pH 4 0 stain

42 Sublingual gland of man Although the mucous acini comprise the predominant structure in this section the relative number of these secreting units varies widely throughout the gland In some areas fewer mucous acini are observed approaching in proportion to that observed in the human submandibular gland (cf fig 39) Hematoxylin eosin

43 Section of same gland showing uniform diastase resistant reactivity diastase digestion followed by PAS

44 Section adjacent to that in figure 43 showing strong periodic acid phenylhydrazine Schiff (PAPS) staining of seromucous acini and demilunes indicative of periodate reactive acid mucosubstance The *mucous acini are weakly PAPS reactive* One hour exposure at 25 C to 5% phenylhydrazine HCL interposed between periodic acid oxidation and the Schiff step

Response of the Vagina of the Spayed Guinea Pig to Low or High Doses of Estrogen

ARLO S HERMRECK AND GILBERT S GREENWALD
Departments of Obstetrics and Gynecology and Anatomy
University of Kansas Medical Center
Kansas City Kansas

ABSTRACT Spayed ginea pigs injected daily for 6 to 10 days with 10 50 150 µg of estradiol cyclopentylpropionate (ECP) developed a mucified vaginal epithelium similar to that observed during pregnancy or following treatment of ovariectomized animals with 5 mg progesterone and 1 µg of ECP

The epithelium did not mucify in spayed guinea pigs given 0 01 to 1 0 µg ECP daily for 10 or more days Vaginal cornification developed only in animals treated with 1 µg ECP but the reaction was transitory and the keratinized cells were soon replaced by a stratified squamous epithelium

Spayed and *adrenalectomized* guinea pigs injected daily with 150 µg ECP developed a stratified squamous epithelium rather than a mucified type However the vaginal epithelium was mucified in ovariectomized adrenalectomized guinea pigs receiving 150 µg ECP and corticoids or progesterone This suggests that after treatment with large doses of estrogen the adrenal of the spayed guinea pig produces progestin like hormones These progestins interacting with exogenous estrogen are responsible for vaginal mucification

On the other hand spayed rats maintained on 1 or 150 µg of ECP showed continuous vaginal cornification which indicates that there are species differences in the ability of large doses of estrogen to influence the adrenal

In preliminary experiments a distinct difference was observed in the vaginal smears of spayed guinea pigs injected with low or high doses of estradiol cyclopentyl propionate (ECP) With daily doses of 1 µg ECP cornified cells developed which were gradually replaced by nucleated epithelial cells However with large doses of the hormone (10–150 µg) cornification never occurred and the smears consisted wholly of mucous cells and leucocytes

The vaginal epithelium mucifies during pregnancy in the mouse rat hamster and guinea pig (Asdell 64) Experimental work on the rat (Silye Browne and Collip '36) and hamster (Klein 35 37) indicates that vaginal mucification can be produced in ovariectomized animals by the concerted action of estrogen and progesterone but not by either hormone alone — unless a relatively massive dose of progesterone is given (Selye 40) Deanesly (60) has similarly shown that mucification of the vaginal epithelium of the guinea pig requires both estrogen and progesterone

The histological changes of the vagina of the guinea pig during the estrous cycle and pregnancy have been described previously (Courrier 23 Selle 22 Kelly 28 Tribby 43) but the response to varying doses of estrogen has not been studied extensively The present investigation was therefore undertaken to extend our preliminary observations and to explore the possible mechanisms responsible for mucification of the vagina of the spayed guinea pig

MATERIAL AND METHODS

A total of 51 virgin guinea pigs of a mixed strain weighing 350–800 grams were bilaterally ovariectomized by the dorsal route under ether anesthesia and left untreated for 14 days Estradiol cyclopentylpropionate (ECP) deoxycorticosterone acetate (DOCA) and progesterone — all in oil — and cortisone in an aqueous vehicle were injected subcutaneously for various periods Daily vaginal smears were taken only after spontaneous rupture of the vaginal membrane At various times after administration of the hormones the animals were killed with an overdose of ether and a portion of the mid vagina was removed fixed in Bouin s fluid and embedded in

clustered in large crypts The folds of columnar epithelial cells i e the definitive basal zone had also persisted After 20 days of continuous treatment the epithelium showed no modifications from its development at day 10

Attention was next directed to the effects of higher doses of ECP on the vaginal epithelium of spayed guinea pigs Fifteen animals were given 150 µg ECP daily for 1 2 3 4 5 6 8 10 and 16 days before being killed The vaginal membrane opened in all animals after three days of treatment but cornified cells were never observed in vaginal smears One day after the injection of 150 µg ECP (i e day 1) the basal zone consisted of only two cell layers but the superficial zone had developed to a much greater extent into a series of folds protruding into the vaginal lumen (fig 5) The basic architecture of the superficial zone was that the mucoid cells were folded back on themselves with strands of stromal tissue extending into the central core In some areas a prickle cell zone separated the superficial and basal layers The development of the superficial zone was further accentuated by day 2 (fig 6) The basal zone consisted of 3 to 4 cell layers with a well developed cytoplasm By day 3 the columns of superficial cells had further proliferated and had a trabeculated interlocking appearance There were three distinct layers of cells present the mucoid superficial zone an intermediate zone of stratified cells with pycnotic nuclei and an underlying basal zone The intermediate transitional layer apparently represented an abortive attempt at cornification on the part of the squamous cells that were present at day 1 Stromal condensation was conspicuous below the epithelium invasive stromal tufts terminated in the stratified zone By day 4 the transitional zone was no longer apparent the basal layer had not increased in thickness and the prickle cells had regressed The tendency of the folds of the superficial layer to merge was further accentuated by day 4 (fig 7) By the fifth day of treatment with 150 µg ECP mucified cells of the superficial layer began to shed into the vaginal lumen which was clogged with debris Invasion of the superficial layer by leucocytes had also commenced There was a continued migration of polymorphonuclear leucocytes into the vaginal epithelium lumen on day 7 The leucocytes were clustered in pockets in the superficial layer and thus produced a vacuolated appearance of the epithelium By day 10 full blown mucification of the superficial layer was the dominant histologic feature The superficial layer consisted of nucleated epithelial cells with a foamy cytoplasm (fig 8) Leucocytes were present in only one of three specimens examined at day 10 Continued treatment with 150 µg of ECP for 16 days failed to alter the appearance of the conspicuous superficial layer

Two additional groups of spayed guinea pigs were given intermediate doses of ECP between the extremes of 1 and 150 µg of the hormone Four guinea pigs were injected daily with 10 µg ECP for ten days and killed in pairs after six and ten days of treatment In all instances the superficial layer was well developed but in addition the basal layer showed better differentiation than in animals receiving 150 µg of ECP a prickle cell zone was interposed between the superficial and basal layers Following daily treatment with 50 µg of ECP for six and ten days the vaginal epithelium still showed dominance of the superficial zone The vaginal membrane ruptured after three days of treatment in animals receiving 10 or 50 µg of ECP but cornified cells were never found in the vaginal smear

Spayed guinea pigs receiving progesterone or corticoids Two ovariectomized animals were injected daily with 5 mg progesterone the vaginal membrane never opened When killed after ten days of hormone administration the vaginal epithelium consisted of a superficial zone of mucoid cells and a basal zone of simple cuboid cells (fig 9) Four additional females were given concurrently 5 mg progesterone and 1 µg ECP for six or ten days The vaginal membrane ruptured after four days of therapy but daily smears failed to reveal the presence of cornified cells The superficial zone was the dominant layer at both six and ten days and its development did not differ essentially from animals receiving only progesterone

paraffin Sections were prepared at 10 µ and stained with hematoxylin and eosin

An additional group of 12 ovariectomized guinea pigs were pre medicated with 1/100 gr of atropine and bilaterally adrenalectomized via the dorsal approach under ether anesthesia The various aforementioned steroids were then injected daily for 6 to 10 days before the vagina was removed for histologic examination

The vaginal epithelium was described according to the classification of Tribby (43) (a) a *superficial zone* bordering the lumen (b) a *transitional zone* whose cells are partially or completely cornified (c) a *prickle cell zone* consisting of large polygonal cells (d) a *basal zone* bordering the lamina propria The four epithelial zones were not present in all situations

RESULTS

Vaginal epithelium in the ovariectomized guinea pig

Spayed guinea pig receiving no hormones Two weeks after spaying the vagina usually consisted of only two layers of cells a superficial zone of low simple columnar cells and a basal zone adjacent to the lamina propria (fig 1) The superficial cells had a mucoid appearance with the basally located nuclei oriented parallel to the long axis of the cell The basal cells had very little cytoplasm and the nuclei were almost touching each other The separation of the basal cells from the underlying stoma was not discrete a distinct basement membrane was lacking The stroma was comparatively avascular

Spayed guinea pig receiving estrogen Four animals divided into two groups were injected daily with 0 01 and 0 1 µg of ECP for ten days The vaginal membrane failed to rupture in any of the animals Histologic examination revealed that the vaginae of animals receiving 0 01 µg of ECP did not differ essentially from the bilaminar epithelium of the spayed guinea pig However after ten days of treatment with 0 1 µg ECP there was extensive development of the basal layer and proliferation of the superficial cells into a series of folds Favorably cut sections revealed that the superficial folds had a central core which was continuous with the basal layer The basal and superficial zones were separated by a transitional layer consisting of flattened cells which were 2 to 3 cells thick

An additional series of 16 spayed guinea pigs were killed (in pairs) after 1 2 3, 4, 5, 6 10 and 20 days of daily administration of 1 µg ECP The vaginal membrane opened only in animals treated for more than three days In these and subsequent experiments, the first day of injection of hormones was designated as day 0 By day 1, the basal layer had proliferated 3 to 4 cells deep and contained numerous mitotic figures the cells now had a conspicuous cytoplasm (fig 2) The basal layer was arranged in folds which invaginated the underlying stroma The stroma consisted of eosinophilic staining fibers oriented perpendicular to the vaginal epithelium The superficial layer was still present but was overshadowed by the marked hyperplasia and hypertrophy of the basal layer Nests of superficial cells were surrounded by the basal zone and in the former layer the cells had a frayed vacuolated appearance By day 2 stromal condensation was even more conspicuous and the basal layer had differentiated into two cell types a deeper columnar zone and a more superficial prickle cell zone which was three cells in thickness The original superficial zone was still present and had a streaming appearance with long finger like processes converging on the lumen By day 3 the superficial zone was completely sloughed and the vaginal lumen was full of mucoid cells and detritus The remaining epithelium — derived from the original basal zone — consisted of three discrete groups 1 The basal folds bordering on the stroma 2 An intermediate prickle cell zone of stratified squamous cells 3 Adjacent to the vaginal lumen a stratified transitional zone which was destined to cornify (fig 3) By day 4 (i e after four days of treatment with 1 0 µg ECP) the stratified cells were cornified However the cornified layer was not maintained and had almost completely desquamated by day 5 or 6 After ten days of daily treatment with 1 µg of ECP a well developed stratified squamous zone was still present the most superficial cells were flattened with leucocytes scattered among them (fig 4) In some areas leucocytes were abundant and

µg of ECP However both 10 or 50 µg of ECP still constitute a massive dose Secondly ECP is an esterified estrogen with prolonged biologic potency Hence *daily* injection of ECP may not have been necessary to elicit the modifications in the vaginal epithelium

The pattern of differentiation of the vagina of the spayed guinea pig differed in several respects from the rat In the latter species constant vaginal cornification occurred unlike the transitory episode in the guinea pig Moreover in the rat both low and high doses of estrogen elicited a similar vaginal response namely cornification The dynamics of cellular proliferation of the vaginal epithelium have been investigated with tritiated thymidine in the mouse (Perrotta 62 Husbands and Walker 63) and rat (Peckham and Kieknoffer 62) It would be of interest to apply this technique to the spayed guinea pig in view of the unique developmental fates of the superficial and basal layers

An obvious question raised by the present experiments with the guinea pig is how do high doses of estrogen induce vaginal mucification When spayed adrenalectomized guinea pigs were used daily administration of 150 µg of ECP did not develop a mucified vaginal epithelium but instead produced a high stratified type similar to that observed in spayed animals treated daily with 1 µg of ECP This indicates that under some circumstances the adrenal gland of the guinea pig is the source of a progestin as well as the corpus luteum and placenta (Deansley 60)

The specific identity of the progestational hormone of the guinea pig adrenal has not been established by the present experiments since corticoids as well as progesterone can act as progrestational compounds Robson (39) reported that daily doses of 0 1 or 0 2 mg of DOCA inhibited estrus in the intact mouse and caused vaginal mucification Courrier (42) showed that daily injection of 3 mg DOCA into spayed rats caused vaginal cornification on the third day but with a continuation of these doses leucocytes appeared in the vaginal smear and mucification was established In addition if 2 5 µg estradiol was given daily cornification failed to occur so long as the dose of DOCA was contained with cessation of the latter hormone cornification occurred in response to the estradiol Courrier (42) obtained similar results in hypophysectomized rats and in spayed guinea pigs treated with daily doses of 10 mg DOCA and 2 5 µg estradiol

In the present study spayed and adrenalectomized guinea pigs given 150 µg ECP 2 mg DOCA and 5 mg cortisone also developed vaginal mucification Hence it is possible that the administration of high doses of estrogen to spayed guinea pigs stimulated the production of endogenous adrenal corticoids and the subsequent interaction resulted in vaginal mucification

This explanation is consistent with the results of Myer and Allen (33) who found that varying doses of estrogens produced mucification of the vaginal epithelium of the guinea pig Zondek and Burstein (52) concluded that adrenal cortical function in the guinea pig appears to be related to ovarian activity and that the administration of estrogen causes an abrupt increase of urinary corticoids in both the intact and spayed female They assumed that estrogen stimulates the discharge of ACTH Allen and Bern (42) showed that oral administration of diethylstilbestrol to guinea pigs leads to definite enlargement of the adrenal cortex In both sexes stilbestrol causes vacuolation of the cortex On the other hand Clayton and Hammant (57) concluded that there is probably a direct *inhibition* of corticosteroid production by exogeneous estrogen or increased secretion of ovarian estrogens as a result of administered gonadotropins

Our studies suggest a relationship between the dose of estrogen administered and the adrenal gland output of progestins Whether this increased adrenal activity represents corticoids or progesterone per se is unknown In the current experiments the interaction of ECP with exogenous progesterone or corticoids produced identical histologic development of the vaginal epithelium We were surprised to find that the daily administration of 5 mg progesterone to the spayed guinea pig produced vaginal mucification However similar treatment of the spayed adrenalectomized animal did not modify the vagina

Two additional spayed guinea pigs were injected daily with 1 µg ECP 2 mg DOCA and 5 mg cortisone for ten days The vaginal membrane opened after seven days of treatment daily vaginal smears failed to show cornified cells Histologic examination revealed a dominant superficial zone similar to that developed by concurrent administration of ECP and progresterone

Spayed and adrenalectomized guinea pigs

Vaginal mucification presumably results from the interaction of estrogen and progesterone (for references see Introduction) In the present experiments high doses of estrogen induced vaginal mucification This raised the question whether this paradoxical effect resulted from the sole action of ECP on the epithelium or the interplay with a progestin produced by an extra gonadal source Since the adrenal cortex is an extremely versatile endocrine organ (Parkes 50), it seemed logical to remove the gland in conjunction with bilateral ovariectomy and to repeat some of the initial experiments Accordingly two weeks after spaying a series of guinea pigs were adrenalectomized and various hormones were then administered

Animals receiving estrogen and corticoids Four animals were given 150 µg ECP 5 mg cortisone and 2 mg DOCA daily for six and ten days The vaginal membrane opened after four days daily vaginal smears never contained cornified cells In all animals the vaginal epithelium consisted of a well developed superficial zone of high columnar mucified cells and a thin basal zone (fig 11) The superficial layer was infiltrated with leucocytes at day 6 but by day 10 they were no longer present

Animals receiving only estrogen Following adrenalectomy five spayed guinea pigs were maintained on 0 9% physiologic saline with lettuce provided ad libitum The animal were given 150 µg of ECP for 6 to 10 days The vaginal membrane opened after four days in all animals but cornified cells were never observed in the vaginal smears Histologic examination of the vaginae, after ten days of treatment revealed a high stratified squamous epithelium similar to that produced in ovariectomized guinea pigs treated daily with 1 µg of ECP (fig 12)

Guinea pigs receiving only progesterone Three adrenalectomized spayed animals were injected daily with 5 mg progesterone for ten days The epithelium resembled the typical castrate pattern with two layers of cells a superficial and basal group (fig 10) The histologic appearance was in marked contrast to the extensively developed superficial zone in progesterone treated animals that were spayed but which had intact adrenals

Ovariectomized rats treated with low and high doses of estrogen

This experiment was designed to determine whether the vaginal epithelium of spayed rats would react to estrogen in a similar manner to the guinea pig Four rats were bilaterally ovariectomized and left untreated for two weeks then divided into two groups and injected subcutaneously with 1 or 150 µg of ECP daily for ten days Daily vaginal smears revealed constant cornification after three days of treatment Cornification was histologically demonstrable in all animals at the conclusion of either the low or high dose of estrogen

DISCUSSION

These experiments show that the vagina of the ovariectomized guinea pig responds in markedly different ways to low or high doses of estrogen The vaginal epithelium in the untreated animal regresses to two layers a superficial columnar zone and a basal cuboidal zone Under the influence of low doses of estrogen the basal zone rapidly proliferates and the superficial layer desquamates A transient cornification then takes place and thereafter a stratified squamous epithelium is maintained On the other hand high doses of estrogen lead to dominance of the superficial zone which is transformed into a mass of high columnar mucified cells

In the present experiments two objections can possibly be raised to the use of 150 µg of ECP as the high dose of estrogen For one thing similar histologic modifications were elicited by 10 or 50 µg of the hormone In retrospect these lower doses should have been substituted for 150

PLATES

from the bilaminar arrangement of the vagina of the castrated guinea pig Thus, the adrenal of the guinea pig is capable of synthesizing and releasing estrogens as well as progestins

Our observations therefore suggest that vaginal mucification in the guinea pig results from the interaction of estrogen and a progestin but that either hormone may be secreted by the adrenal gland as well as by the ovary or placenta

This is a contribution from the Research Professorship in Human Reproduction The research was supported by grant HD 00596 03 from the N I H U S P H S and by the Ford Foundation

LITERATURE CITED

Allen B M and H Bern 1942 Influence of diethylstilbestrol upon the adrenal cortex of the guinea pig Endocrinology *31* 586–591

Asdell S A 1964 Patterns of Mammalian Reproduction Second Edition Comstock Publishing *Associates Cornell University Press*

Clayton E and J E Hammant 1957 Modification of response of adrenocorticotrophic hormone by the simultaneous administration of gonadotrophic hormones or oestrogens J Endocr *15* 225–265

Courrier R 1923 La structure de l épithelium *du vagin chez le cobaye et ses modifications* Comp Rend Assoc Anat *18* 145–151

——— 1942 L action keratinisante de la desoxycorticosterone sur le vagin et les differentes proprietes de trois substances hormonales progestatives Comp Rend Soc Biol *136* 196

Deanesly R 1960 Endocrine activity of the early placenta of the guinea pig J Endocr *21* 235–239

Husbands E Jr and B E Walker 1963 Differentiation of vaginal epithelium in mice given estrogen and thymidine H³ Anat Rec *147* 187–198

Kelly G 1929 The histological transformations in the vaginal epithelium of the guinea pig Am J Anat, *43* 247–287

Klein M 1935 Recherches sur le rôle du placenta dans l arrêt des manifestations du cycle ovarien au cours de la grossesse Comp Rend Soc Biol *119* 579–580

——— 1937 The mucification of the vaginal *epithelium in rodents Proc Roy Soc B* *124* 23–29

Meyer R K and W M Allen 1933 The production of mucified cells in the vaginal epithelium of certain rodents by oestrin and by corpus luteum extracts Anat Rec *56* 321–343

Parkes A S 1945 The adrenal gonad relationship Physio Rev *25* 203–254

Peckham B and W Kiekhofer 1962 Cellular behavior in the vaginal epithelium of estrogen treated rats Am J Ob Gyn *83* 1021–1026

Perrotta C A 1962 Initiation of cell proliferation in the vaginal and uterine epithelia of the mouse Am J Anat *111* 195–204

Robson J M 1939 Comparison of the amounts of progesterone and of deoxycorticosterone acetate needed to produce certain progesterone like actions J Physiol *96* 21P–23P

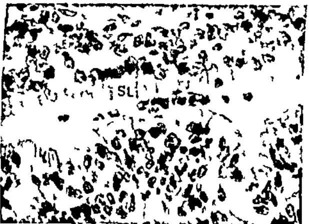
Selle R M 1922 Changes in the vaginal epithelium of the guinea pig during the oestrus cycle Am J Anat *30* 429–449

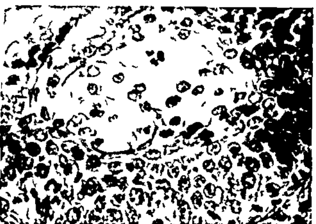
Selye H 1940 Activity of progesterone in spayed females not pretreated with estrin Proc Soc Exp Biol Med *43* 343–344

Selye H J S L Browne and J B Collip 1936 Effect of large doses of progesterone in the female rat Proc Soc Exp Biol Med *34* 472–474

Tribby, C L 1943 The intracellular lipin mucoid and glycogen of the vaginal epithelium of guinea pig Anat Rec *86* 425–451

Zondek B and S Burstein 1952 The relationship of corticoid excretion to ovarian hormones in the guinea pig Endocrinology *50* 419–428


SL




TZ
BZ


4

PLATE 1

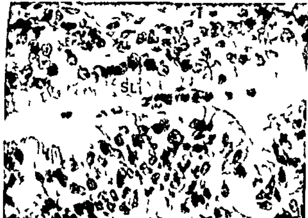
EXPLANATION OF FIGURES

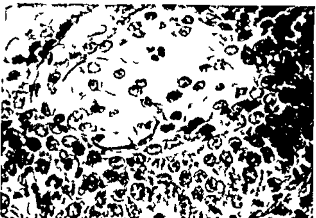
1 Vaginal epithelium of guinea pig two weeks after ovariectomy The epithelium has regressed to two layers a superficial mucoid columnar layer (*SL*) and a basal layer (*BL*) × 203

2 Vaginal epithelium of ovariectomized guinea pig killed 24 hours after the injection of 1 μg ECP Note mitotic figures (arrows) in the proliferating basal layer of the vagina Cells of the superficial layer are arranged in crypts above the basal zone × 203

3 Vaginal epithelium of ovariectomized guinea pig after three days of injection of 1 μg ECP The superficial layer has desquamated the original basal layer has differentiated into three zones basal zone (*BZ*) prickle-cell zone (*PZ*) transitional zone (*TZ*) × 203

4 Vaginal epithelium of ovarectomized guinea pig after ten days of injection of 1 μg ECP A well developed stratified squamous epithelium is present infiltrated with leucocytes (arrows) × 203


SL




TZ
PZ
BZ
3


4

PLATE 1

EXPLANATION OF FIGURES

1 Vaginal epithelium of guinea pig two weeks after ovariectomy The epithelium has regressed to two layers a superficial mucoid columnar layer (*SL*) and a basal layer (*BL*) × 203

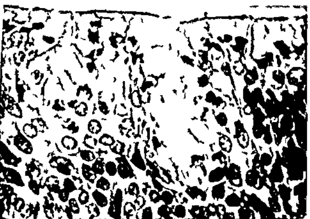
2 Vaginal epithelium of ovariectomized guinea pig killed 24 hours after the injection of 1 μg ECP Note mitotic figures (arrows) in the proliferating basal layer of the vagina Cells of the *superficial layer are arranged in crypts above the basal* zone × *203*

3 Vaginal epithelium of ovariectomized guinea pig after three days of injection of 1 μg ECP The superficial layer has desquamated the original basal layer has differentiated into three zones basal zone (*BZ*) prickle-cell zone (*PZ*) transitional zone (*TZ*) × 203

4 Vaginal epithelium of ovarectomized guinea pig after ten days of injection of 1 μg ECP A well developed stratified squam*ous epithelium is present* infiltrated with leucocytes (arrows) × 203







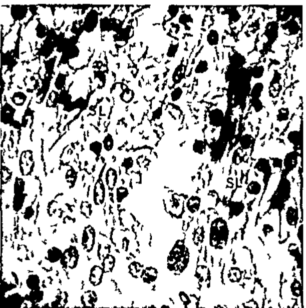

SL
SL



PLATE 2

EXPLANATION OF FIGURES

5 Vaginal epithelium of ovariectomized guinea pig after one injection of 150 μg ECP The superficial layer has proliferated more than the basal layer Compare with figure 2 $\times$ 81

6 Vaginal epithelium of ovariectomized guinea pig after daily injection of 150 μg ECP for two days Development of superficial layer is further accentuated $\times$ 81

7 Vaginal epithelium of ovariectomized guinea pig after daily injection of 150 μg ECP for four days The folds of the superficial layer (*SL*) begin to merge and have a trabeculated appearance $\times$ 203

8 Vaginal epithelium of ovariectomized guinea pig after daily injection of 150 μg ECP for ten days The superficial layer is dominant and is characterized by nucleated epithelial cells with a foamy cytoplasm $\times$ 203

An Electron Microscopic Study on the Innervation of the Intracranial Artery of the Rat

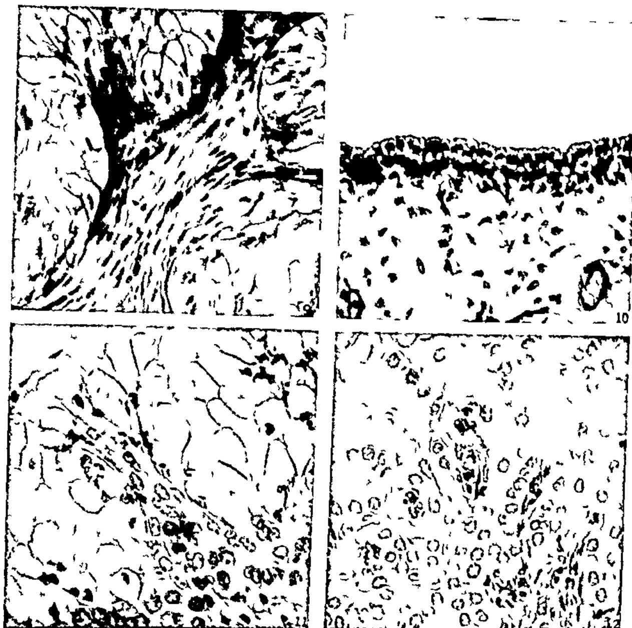
SO SATO
Department of Anatomy Tohoku University School of Medicine Sendai Japan

ABSTRACT Topographical variations in the innervation between different portions of rat intracranial artery have been studied by the aid of electron microscopy Myelinated fibers are found only around the internal carotid and the proximal portion of the basilar arteries Unmyelinated fibers are observed within the adventitia of the major intracranial arteries These fibers diminish gradually in number as getting towards the periphery and completely vanish before the disappearance of the muscular coat of the artery Most of small branch arteries have no vascular nerve around them although they show one- or two-layered arrangement of smooth muscle cells in the media Some central branches of the internal carotid and the middle cerebral arteries are accompanied by unmyelinated fibers even after they penetrate into the brain tissue The fine structures of the terminal portion of vascular nerve fibers particularly the neuromuscular relationships have also been described

While a number of light microscopic studies have established ample evidence for the presence of a nerve supply to the intracranial vessels of man and other mammals (Hassin '29 Chorobski and Penfield '32 Penfield 32 Stohr 38 Fang 61) the physiological importance of this innervation remains conflicting Molnar and Szantó (64) have suggested the possibility of a direct nervous control of the cerebral vessels in cats and rabbits whereas Carlyle and Grayson (55 56) who used the same kinds of animal in experiments drew the conclusion that the preservation of relatively constant cerebral blood flow despite changing systemic blood pressure is considered to be independent of the nervous control In man Krog (64) recognized a vasoconstrictor response from the cerebral vessels to be provoked by stimulation of the cervical sympathetics but studies of *Harmel et al (49) failed to re*veal a tonic effect exerted by the cervical sympathetics on cerebral vessels

Fine structural information concerning the innervation of intracranial vessels is also meager Pease and Molinari (60) first reported on the presence of unmyelinated fibers in the adventitia as well as on the total absence of nervous elements within the tunica media of pial blood vessels of the cat and monkey On the basis of these findings they considered the pial vessels may be exceptional by the lack of direct nervous control It has been confirmed however by later electron microscopic observations that all other blood vessels so far examined have no nervous elements within the tunica media (Parker 58 Pease and Paule 60 Lever and Esterhuizen 61 Esterhuizen and Lever 61 Brettschneider 63 64 Appenzeller 64 Altenahr 65) Samarasinghe (63) noted nerve bundles are seen in the adventitia of the basilar and the middle cerebral arteries of the rat Dahl and Nelson (64) revealed the presence of both myelinated and unmyelinated fibers within the adventitia of the superior cerebellar and the posterior inferior cerebellar arteries in man They described that efferent and presumably adrenergic nerve endings were identified in their specimens by the presence of vesicles containing an osmiophilic *center*

Further fine structural investigations are obviously worthwhile in view of the considerable current interest in the physiology of cerebral circulation and smooth muscle innervation The present study was projected to obtain by the aid of electron microscopy further anatomical information concerning the vascular nerves of the intracranial arteries Particular consideration was focused on topographical or regional variations in this innervation



EXPLANATION OF FIGURES

9 Vaginal epithelium of ovariectomized guinea pig after daily injection of 5 mg progesterone for ten days *Note marked development of superficial layer* × 69

10 Vaginal epithelium of ovariectomized and *adrenalectomized* guinea pig after daily injection of 5 mg progesterone for ten days *A bilaminar epithelium similar to the histologic picture in the castrate is present* Compare with figures 1 and 9 × 69

11 Vaginal epithelium of ovariectomized and *adrenalectomized* guinea pig after daily injection for ten days of 150 μg ECP 5 mg cortisone and 2 mg DOCA Extensive mucification results from the interaction of the hormones × 173

12 Vaginal epithelium of ovariectomized and *adrenalectomized* guinea pig after daily injection for ten days of 150 μg ECP The epithelium is stratified squamous rather than mucified Compare with figures 4 and 8 × 173

An Electron Microscopic Study on the Innervation of the Intracranial Artery of the Rat

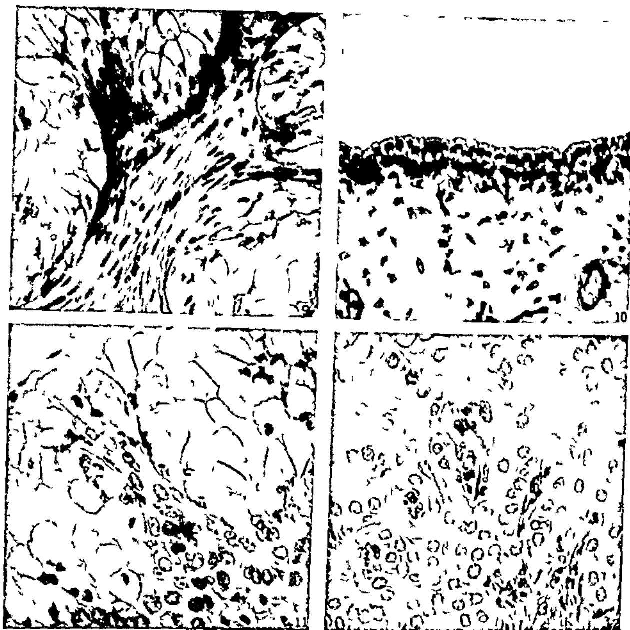
SO SATO
Department of Anatomy Tohoku University School of Medicine Sendai Japan

ABSTRACT Topographical variations in the innervation between different portions of rat intracranial artery have been studied by the aid of electron microscopy Myelinated fibers are found only around the internal carotid and the proximal portion of the basilar arteries Unmyelinated fibers are observed within the adventitia of the major intracranial arteries These fibers diminish gradually in number as getting towards the periphery and completely vanish before the disappearance of the muscular coat of the artery Most of small branch arteries have no vascular nerve around them although they show one- or two-layered arrangement of smooth muscle cells in the media Some central branches of the internal carotid and the middle cerebral arteries are accompanied by unmyelinated fibers even after they penetrate into the brain tissue The fine structures of the terminal portion of vascular nerve fibers particularly the neuromuscular relationships have also been described

While a number of light microscopic studies have established ample evidence for the presence of a nerve supply to the intracranial vessels of man and other mammals (Hassin '29 Chorobski and Penfield '32 Penfield 32 Stohr 38 Fang 61) the physiological importance of this innervation remains conflicting Molnár and Szántó (64) have suggested the possibility of a direct nervous control of the cerebral vessels in cats and rabbits whereas Carlyle and Grayson (55 56) who used the same kinds of animal in experiments drew the conclusion that the preservation of relatively constant cerebral blood flow despite changing systemic blood pressure is considered to be independent of the nervous control In man Krog (64) recognized a vasoconstrictor response from the cerebral vessels to be provoked by stimulation of the cervical sympathetics but studies of Harmel et al (49) failed to reveal a tonic effect exerted by the cervical sympathetics on cerebral vessels

Fine structural information concerning the innervation of intracranial vessels is also meager Pease and Molinari (60) first reported on the presence of unmyelinated fibers in the adventitia as well as on the total absence of nervous elements within the tunica media of pial blood vessels of the cat and monkey On the basis of these findings they considered the pial vessels may be exceptional by the lack of direct nervous control It has been confirmed however by later electron microscopic observations that all other blood vessels so far examined have no nervous elements within the tunica media (Parker 58 Pease and Paule 60 Lever and Esterhuizen 61 Esterhuizen and Lever 61 Brettschneider 63 64 Appenzeller 64 Altenahr 65) Samarasinghe (63) noted nerve bundles are seen in the adventitia of the basilar and the middle cerebral arteries of the rat Dahl and Nelson (64) revealed the presence of both myelinated and unmyelinated fibers within the adventitia of the superior cerebellar and the posterior inferior cerebellar arteries in man They described that efferent and presumably adrenergic nerve endings were identified in their specimens by the presence of vesicles containing an osmiophilic center

Further fine structural investigations are obviously worthwhile in view of the considerable current interest in the physiology of cerebral circulation and smooth muscle innervation The present study was projected to obtain by the aid of electron microscopy further anatomical information concerning the vascular nerves of the intracranial arteries Particular consideration was focused on topographical or regional variations in this innervation



EXPLANATION OF FIGURES

9 Vaginal epithelium of ovariectomized guinea pig after daily injection of 5 mg progesterone for ten days Note marked development of superficial layer × 69

10 Vaginal epithelium of ovariectomized and *adrenalectomized* guinea pig after daily injection of 5 mg progesterone for ten days A bilaminar epithelium similar to the histologic picture in the castrate is present Compare with figures 1 and 9 × 69

11 Vaginal epithelium of ovariectomized and *adrenalectomized* guinea pig after daily injection for ten days of 150 μg ECP 5 mg cortisone and 2 mg DOCA Extensive mucification results from the interaction of the hormones × 173

12 Vaginal epithelium of ovariectomized and *adrenalectomized* guinea pig after daily injection for ten days of 150 μg ECP The epithelium is stratified squamous rather than mucified Compare with figures 4 and 8 × 173

single layer in arterioles The outermost layer of the adventitia is formed by elongated fibroblasts with long processes which collectively make up an almost continuous cellular sheath around the artery (figs 7 and 10) This cellular sheath is located adjacent to the media in such a small artery as illustrated in figure 8 The extent of the adventitia is always easy to define by this characteristic feature of the outermost adventitial fibroblasts

The nerve supply to the intracranial arteries

Observations concerning the nerve supply to different segments of intracranial artery are summarized in figures 1 2 and 3 Nerve fibers and endings are always found in the territory of adventitia and none has been discovered within the media throughout the present study

The presence of myelinated fibers within the adventitia has been established in the internal carotid (I_1 I_2) and the most proximal segment of the basilar arteries (B) An example of the myelinated fibers running in the adventitia is shown in figure 10 They have a thickness ranging from 1 to 3 μ In most cases if not all the left vertebral artery of the rat is considerably thicker than its fellow of the opposite side and correspondingly all myelinated fibers around the basilar artery are traced proximally onto the left vertebral artery (V) The right vertebral artery on the other hand does not possess the myelinated fiber (V)

It is very conceivable that the myelinated fibers terminate in somewhere around the internal carotid artery in the circulus arteriosus as well as around the most proximal segment of the basilar artery since none of them reaches more peripheral segments of artery However this study has failed to clarify the termination

Unmyelinated fibers within the adventitia have been observed in many portions of intracranial artery as illustrated in figures 1 2 and 3 In general they are abundant around arteries on the inferior surface of the brain particularly around the basilar artery and the circulus arteriosus they diminish in number gradually as getting towards the periphery and completely vanish before the disappearance of

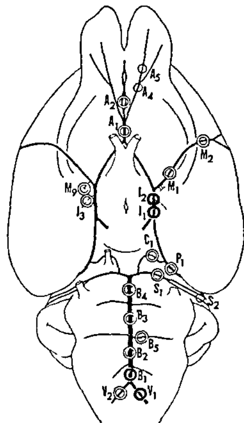


Fig 1 Diagram showing the nerve supply to the arteries on the base of the brain In figures 1–3 the single circle indicates the total absence of vascular nerve fibers the double circle indicates the presence of unmyelinated nerve fibers and the heavy circle indicates the presence of both myelinated and unmyelinated nerve fibers A_{1-5} anterior cerebral artery M_{1-2} middle cerebral artery M_3 central branch of the middle cerebral artery $I_{1,2}$ internal carotid artery I_3 small branch of I C_1 posterior communicating artery P_{1-3} posterior cerebral artery S_{1-2} superior cerebellar artery B_{1-4} basilar artery B_5 pontine branch of the basilar artery V_1 left vertebral artery V_2 right vertebral artery These symbols are also used in all figures and the text in order to indicate the position of artery

smooth muscle cells of the media Although some of the peripheral branches are thicker than 50 μ and have a two-layered arrangement of smooth muscle cells in the media still they do not receive a nerve supply at all Each segment of artery has been examined using two or three animals and no variation in the nerve distribution was noticed between different individuals

MATERIALS AND METHODS

The material for this study was obtained from 18 adult Wistar rats or both sexes Immediately after decapitation of the animal under light anesthesia with ether the skull and then the dura were opened carefully to expose the whole blood vessels on the surface of the brain untraumatized From each brain a few selected segments of the artery, about 1 or 2 mm long were removed They were fixed for two hours in ice cold 1% osmium tetroxide of Millonig (62) and after ethanol dehydration embedded in Epon 812 as described by Luft (61)

Thin sections were cut with glass knives either transversely or longitudinally to the axis of the artery and mounted on uncoated copper grids Section staining was achieved with alkaline lead (Millonig 61) or saturated solution of uranyl acetate in 50% ethanol A Hitachi HS 6 electron microscope was used for the examination Lest a nerve fiber or ending be omitted the whole circumference of the arterial wall was thoroughly examined using a large number of transverse sections

In addition sections for light microscopy were cut at 1 or 1 5 μ with glass knives and stained with 1% toluidine blue in 1% aqueous solution of borax These preparations were used mainly for a following up of myelinated fibers

OBSERVATIONS

General features of the intracranial arteries

The basilar artery in the rats has an outside diameter of about 200 μ and the internal carotid artery in the circulus arteriosus cerebri is about 150 μ thick In these large arteries the media contains five or six layers of smooth muscle cells

Figures 8 and 9 are survey micrographs of small branches approximately 20 μ in diameter which arise from the internal carotid and the middle cerebral arteries respectively The former branch is in the pia and the latter is in the brain tissue Even in such a small artery elastin appears between the endothelium and the media to form the internal elastic lamina which of course remains the more definitive layer in the larger arteries Smooth muscle cells in the media are arranged rather closely, only a narrow space being interposed among them Profiles of elastic and collagen fibers are found scattering in the space The surface of each of the smooth muscle cells is almost entirely lined with a distinct basement membrane (fig 4)

As has already been noted in the smooth musculature of various organs (Taxi 61 Dewey and Barr 62 Evans and Evans 64 Oosaki and Ishii 64 Richardson 64) close appositions of the plasma membranes are occasionally observed between neighboring muscle cells in the media (fig 6) In these areas of close apposition the plasma membrane of one cell is separated from that of a neighboring cell only by a narrow intercellular zone less than 100 A across where the basement membrane is absent

A number of rounded profiles ranging from 0 5 to 3 μ in diameter have been found within the muscle cells of the present material (fig 4) As seen in figures 4 and 5 they are enclosed by two layers of membrane one surrounds the entire circumference of the profiles and the other is a direct continuity from the plasma membrane of the muscle cells Therefore in the strict sense the profiles occupy an extracellular position outside of the very muscle cells where they are contained Since the continuity between the rounded profiles and the neighboring smooth muscle cell has been demonstrated in a few lucky sections it is likely that some if not all arise from intrusions of large cytoplasmic processes from one muscle cell into another Two membranes surrounding the rounded profile oppose each other with a narrow intervening space measuring less than 100 A across The interior of the bodies is of low density and a small amount of fragmentary membranes is scattered in the granular matrix Similar rounded bodies have also been described by many authors in the smooth muscle cells of various organs (Richardson 62 Thaemert 63 Merrillees et al 63)

The adventitia of the rat intracranial arteries consists of an abundance of collagen fibers and fibroblasts (fig 7) The fibroblasts are arranged in four or five layers in larger arteries but may be in a

single layer in arterioles The outermost layer of the adventitia is formed by elongated fibroblasts with long processes which collectively make up an almost continuous cellular sheath around the artery (figs 7 and 10) This cellular sheath is located adjacent to the media in such a small artery as illustrated in figure 8 The extent of the adventitia is always easy to define by this characteristic feature of the outer most adventitial fibroblasts

The nerve supply to the intracranial arteries

Observations concerning the nerve supply to different segments of intracranial artery are summarized in figures 1 2 and 3 Nerve fibers and endings are always found in the territory of adventitia and none has been discovered within the media throughout the present study

The presence of myelinated fibers with in the adventitia has been established in the internal carotid (I_1 I_2) and the most proximal segment of the basilar arteries (B_1) An example of the myelinated fibers running in the adventitia is shown in figure 10 They have a thickness ranging from 1 to 3 μ In most cases if not all the left vertebral artery of the rat is considerably thicker than its fellow of the opposite side and correspondingly all myelinated fibers around the basilar artery are traced proximally onto the left vertebral artery (V_1) The right vertebral artery on the other hand does not possess the myelinated fiber (V_2)

It is very conceivable that the myelinated fibers terminate in somewhere around the internal carotid artery in the circulus arteriosus as well as around the most proximal segment of the basilar artery since none of them reaches more peripheral segments of artery However this study has failed to clarify the termination

Unmyelinated fibers within the adventitia have been observed in many portions of intracranial artery as illustrated in figures 1 2 and 3 In general they are abundant around arteries on the inferior surface of the brain particularly around the basilar artery and the circulus arteriosus they diminish in number gradually as getting towards the periphery and completely vanish before the disappearance of

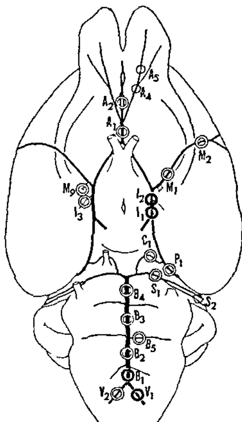


Fig 1 Diagram showing the nerve supply to the arteries on the base of the brain In figures 1–3 the single circle indicates the total absence of vascular nerve fibers the double circle indicates the presence of unmyelinated nerve fibers and the heavy circle indicates the presence of both myelinated and unmyelinated nerve fibers
A_{1-5} anterior cerebral artery M middle cerebral artery M_3 central branch of the middle cerebral artery I internal carotid artery I small branch of I C_1 posterior communicating artery P_{1-3} posterior cerebral artery S_{1-2} superior cerebellar artery B_{1-4} basilar artery B_5 pontine branch of the basilar artery V_1 left vertebral artery V_2 right vertebral artery These symbols are also used in all figures and the text in order to indicate the position of artery

smooth muscle cells of the media Although some of the peripheral branches are thicker than 50 μ and have a two-layered arrangement of smooth muscle cells in the media still they do not receive a nerve supply at all Each segment of artery has been examined using two or three animals and no variation in the nerve distribution was noticed between different individuals

MATERIALS AND METHODS

The material for this study was obtained from 18 adult Wistar rats or both sexes Immediately after decapitation of the animal under light anesthesia with ether, the skull and then the dura were opened carefully to expose the whole blood vessels on the surface of the brain untraumatized From each brain a few selected segments of the artery about 1 or 2 mm long were removed They were fixed for two hours in ice cold 1% osmium tetroxide of Millonig (62) and after ethanol dehydration embedded in Epon 812 as described by Luft (61)

Thin sections were cut with glass knives either transversely or longitudinally to the axis of the artery and mounted on uncoated copper grids Section staining was achieved with alkaline lead (Millonig 61) or saturated solution of uranyl acetate in 50% ethanol A Hitachi HS 6 electron microscope was used for the examination Lest a nerve fiber or ending be omitted the whole circumference of the arterial wall was thoroughly examined using a large number of transverse sections

In addition sections for light microscopy were cut at 1 or 1 5 μ with glass knives and stained with 1% toluidine blue in 1% aqueous solution of borax These preparations were used mainly for a following up of myelinated fibers

OBSERVATIONS

General features of the intracranial arteries

The basilar artery in the rats has an outside diameter of about 200 μ and the internal carotid artery in the circulus arteriosus cerebri is about 150 μ thick In these large arteries the media contains five or six layers of smooth muscle cells

Figures 8 and 9 are survey micrographs of small branches, approximately 20 μ in diameter, which arise from the internal carotid and the middle cerebral arteries respectively The former branch is in the pia and the latter is in the brain tissue Even in such a small artery, elastin appears between the endothelium and the media to form the internal elastic lamina which of course remains the more definitive layer in the larger arteries Smooth muscle cells in the media are arranged rather closely, only a narrow space being interposed among them Profiles of elastic and collagen fibers are found scattering in the space The surface of each of the smooth muscle cells is almost entirely lined with a distinct basement membrane (fig 4)

As has already been noted in the smooth musculature of various organs (Taxi '61 Dewey and Barr '62 Evans and Evans 64 Oosaki and Ishii, 64, Richardson 64) close appositions of the plasma membranes are occasionally observed between neighboring muscle cells in the media (fig 6) In these areas of close apposition the plasma membrane of one cell is separated from that of a neighboring cell only by a narrow intercellular zone less than 100 A across, where the basement membrane is absent

A number of rounded profiles ranging from 0 5 to 3 μ in diameter have been found within the muscle cells of the present material (fig 4) As seen in figures 4 and 5 they are enclosed by two layers of membrane, one surrounds the entire circumference of the profiles and the other is a direct continuity from the plasma membrane of the muscle cells Therefore in the strict sense the profiles occupy an extracellular position outside of the very muscle cells where they are contained Since the continuity between the rounded profiles and the neighboring smooth muscle cell has been demonstrated in a few lucky sections it is likely that some if not all arise from intrusions of large cytoplasmic processes from one muscle cell in to another Two membranes surrounding the rounded profile oppose each other with a narrow intervening space measuring less than 100 A across The interior of the bodies is of low density and a small amount of fragmentary membranes is scattered in the granular matrix Similar rounded bodies have also been described by many authors in the smooth muscle cells of various organs (Richardson 62 Thaemert 63 Merrillees et al 63)

The adventitia of the rat intracranial arteries consists of an abundance of collagen fibers and fibroblasts (fig 7) The fibroblasts are arranged in four or five layers in larger arteries but may be in a

P_2) and beyond there it loses the nerve supply (P_3) The posterior communicating artery is supplied with unmyelinated fibers (C_1) The proximal portion of the superior cerebellar artery has a supply of unmyelinated fibers (S_1) which disappear after the artery passes in front of the paraflocculus (S S_3) Distal segments of the basilar artery (B B_3 B_4) and the right vertebral artery (V_2) have adventitial unmyelinated fibers while the proximal segment of the basilar artery (B_1) and the left vertebral artery (V) have both myelinated and unmyelinated fibers in their adventitia A small number of unmyelinated fibers are also found around the roots of thicker pontine branches of the basilar artery (B_5)

The neuromuscular relationships

The nerves penetrating into the adventitia of intracranial arteries consist of bundles of unmyelinated fibers with an occasional myelinated fiber having a separate Schwann sheath (fig 10) Those unmyelinated bundles which are distant from the media comprize considerable numbers of axons submerged with the typical mesaxon in a Schwann cell cytoplasm (fig 10) The surface of the Schwann cell is lined by a basement membrane Most of these axons have a thickness ranging from 0 1 to 0 6 μ and contain prominent neurofilaments and a few mitochondria Any other formed structures are very sparse in them However some thicker axons (roughly 0 5 to 1 2 μ) are also found to be loaded with a cluster of small vesicles and mitochondria though this is rarely the case

Unmyelinated bundles close to the media comprize only a few axons invaginated in a Schwann cell process and here the cluster of small vesicles and mitochondria in the axoplasm is very prominent (figs 11–14) These small vesicles are relatively uniform in size (400 to 500 A) and have an interior of low density Their configuration is quite similar to what has been described as synaptic vesicles of the cholinergic nerve endings (De Robertis et al 63) The vesicle-containing portions of the axons are as a rule surrounded partially by the Schwann cell cytoplasm and the remaining axonal surface is separated from the tissue space by only the basement membrane which passes from the Schwann cell onto the axon Sometimes the basement membrane shows a stratification as seen in figure 11

It is often observed that the axons containing crowded vesicles and mitochondria approach the outer surface of the media to appose the smooth muscle cells with an interval as narrow as 800 A at their closest approach (figs 12–14) In these neuromuscular appositions the axons often lose their Schwann and basement membrane investments while the muscular surface is always covered with a basement membrane and does not show any structural specialization No differentiation of the axonal plasma membrane has been revealed either

DISCUSSION

The nerve supply to the intracranial arteries

Dahl and Nelson (64) have verified by the aid of electron microscopy the existence of myelinated fibers within the adventitia of the superior cerebellar and posterior inferior cerebellar arteries in man In the present material myelinated fibers are seen only around the internal carotid and the proximal portion of the basilar arteries

By light microscopic observations various types of sensory nerve ending have been found in the adventitia of the human intracranial arteries (Penfield 32 Stohr 38) Moreover Ray and Wolff ('40) elicited painful sensations by application of mechanical stimuli to the major arteries of the brain including the circulus arteriosus and the basilar artery of patients having an operation under local anesthesia So it seems probable that the myelinated fibers accompanying the rat intracranial arteries are also sensory or afferent in function although no positive *evidence for this speculation was obtained* in this study

Evidence for the intrinsic regulation of intracranial arteries has been confirmed by a number of physiological investigations while as stated elsewhere the role of neurogenic vasomotor mechanisms in this regulation is still obscure (Carlyle and Grayson 55 56 Sokoloff 59 Ganong 63 Kety 64 Molnár and Szántó 64

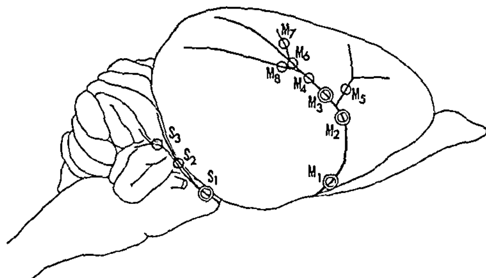


Fig 2 Diagram showing the nerve supply to the intracranial arteries Superolateral aspect

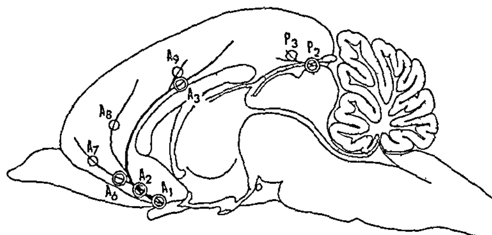


Fig 3 Diagram showing the nerve supply to the intracranial arteries Median sagittal aspect

Unmyelinated fibers around the anterior cerebral artery can be followed up until about the middle point of the upper surface of the corpus callosum (A_3) Branches emerging from this artery to the olfactory bulb as well as to the frontal and the parietal lobes have no nerve fibers around them (A_4 A_5 A_7 A_8 A_9) with the exception of the root of the main frontal branch (A_6) where a few unmyelinated fibers are still observable The middle cerebral artery loses its accompanying unmyelinated fibers in between the origin of the main frontal branch and the dividing point into the terminal branches to the parietal and the temporal lobes (M_3 M_4) These major branches of the middle cerebral artery have no adventitial nerve fibers (M_5 M_6 M_7 M_8) Relatively large central branches (thicker than 50 μ at their origin) emerging from the internal carotid and the middle cerebral arteries possess a few unmyelinated fibers around them and the fibers are observable even after the branches penetrate into the brain tissue and taper off as thin as 20 μ in diameter (I_3 M_2) Whereas smaller central branches (thinner than 20 μ at their origin) possess no nerve fiber at all

The posterior cerebral artery is accompanied by unmyelinated fibers before it reaches the level of the pineal body (P_1

P_1) and beyond there it loses the nerve supply (P_3) The posterior communicating artery is supplied with unmyelinated fibers (C_1) The proximal portion of the superior cerebellar artery has a supply of unmyeli nated fibers (S_1) which disappear after the artery passes in front of the paraflocculus (S S_3) Distal segments of the basilar artery (B_4 B_5 B) and the right vertebral artery (V_2) have adventitial unmyelinated fibers while the proximal segment of the basilar artery (B_1) and the left vertebral artery (V_1) have both myelinated and un myelinated fibers in their adventitia A small number of unmyelinated fibers are also found around the roots of thicker pontine branches of the basilar artery (B_1)

The neuromuscular relationships

The nerves penetrating into the adventi tia of intracranial arteries consist of bun dles of unmyelinated fibers with an occa sional myelinated fiber having a separate Schwann sheath (fig 10) Those unmyeli nated bundles which are distant from the media comprize considerable numbers of axons submerged with the typical mesaxon in a Schwann cell cytoplasm (fig 10) The surface of the Schwann cell is lined by a basement membrane Most of these axons have a thickness ranging from 0 1 to 0 6 μ and contain prominent neurofila ments and a few mitochondria Any other formed structures are very sparse in them However some thicker axons (roughly 0 5 to 1 2 μ) are also found to be loaded with a cluster of small vesicles and mitochon dria though this is rarely the case

Unmyelinated bundles close to the me dia comprize only a few axons invaginated in a Schwann cell process and here the cluster of small vesicles and mitochondria in the axoplasm is very prominent (figs 11–14) These small vesicles are relatively uniform in size (400 to 500 A) and have an interior of low density Their configu ration is quite similar to what has been described as synaptic vesicles of the chol inergic nerve endings (De Robertis et al 63) The vesicle-containing portions of the axons are as a rule surrounded partially by the Schwann cell cytoplasm and the remaining axonal surface is separated from the tissue space by only the basement membrane which passes from the Schwann cell onto the axon Sometimes the base ment membrane shows a stratification as seen in figure 11

It is often observed that the axons con taining crowded vesicles and mitochondria approach the outer surface of the media to appose the smooth muscle cells with an interval as narrow as 800 A at their closest approach (figs 12–14) In these neuro muscular appositions the axons often lose their Schwann and basement membrane investments while the muscular surface is always covered with a basement mem brane and does not show any structural specialization No differentiation of the axonal plasma membrane has been re vealed either

DISCUSSION

The nerve supply to the intracranial arteries

Dahl and Nelson (64) have verified by the aid of electron microscopy the ex istence of myelinated fibers within the adventitia of the superior cerebellar and posterior inferior cerebellar arteries in man In the present material myelinated fibers are seen only around the internal carotid and the proximal portion of the basilar arteries

By light microscopic observations vari ous types of sensory nerve ending have been found in the adventitia of the hu man intracranial arteries (Penfield 32 Stohr 38) Moreover Ray and Wolff ('40) elicited painful sensations by application of mechanical stimuli to the major arteries of the brain including the circulus arter iosus and the basilar artery of patients having an operation under local anes thesia So it seems probable that the mye linated fibers accompanying the rat intra cranial arteries are also sensory or afferent in function although no positive evidence for this speculation was obtained in this study

Evidence for the intrinsic regulation of intracranial arteries has been confirmed by a number of physiological investiga tions while as stated elsewhere the role of neurogenic vasomotor mechanisms in this regulation is still obscure (Carlyle and Grayson 55 56 Sokoloff 59 Ganong 63 Kety 64 Molnár and Szántó 64

Krog 64) It has been clarified by this study that although a considerable number of unmyelinated fibers can be observed around the major intracranial arteries and their larger branches the smaller branch arteries do not have vascular nerves around them and hence they are not under direct neurogenic control Since resistance to blood flow is mainly regulated through changes in the diameter of the peripheral branches rather than that of the trunk arteries the smaller branches devoid of vascular nerves may exert greater influences on the intracranial circulation If that is the case the vasomotor mechanisms would be of little if any significance for the regulation of the total intracranial blood flow

There may be some regional variations in blood flow correlating with changes in local activity in the brain Sokoloff (61) for example found that the increase in the function of the nerve cells in a localized area of the cortex is followed by an increase in local blood flow They considered the local changes in circulation to be explained by means of accumulation of metabolites in the area of increased activity whereas Krog (64) has pointed out that the neurogenic regulation may also be of significance because this delicate blood distribution can hardly be adequately taken care of without some kind of nervous involvement Perhaps the present findings give an anatomical base for Krog s consideration

In addition Pool (58) and Corday et al (63) have described that the major arteries and their larger branches of the brain in contradistinction to the smaller pial vessels are susceptible to local or limited as well as widespread vasoconstriction that may be induced by a variety of stimuli The former author pointed out on the basis of his experimental findings that intrinsic neurogenic reflex activity may play a part in this vasoconstriction Perhaps the present observations support his conclusion from an anatomical standpoint

The neuromuscular relationships

Clusters of small vesicles with a simultaneous accumulation of mitochondria are very prominent in the axoplasm near the media These vesicles have an interior of low density and their configuration is quite similar to what has been identified as synaptic vesicles of the cholinergic nerve endings (De Robertis et al 63) In addition to such clear or agranular vesicles dense cored or granular vesicles have been described in the terminal portions of vascular nerves around the arterioles of the guinea pig pancreas by Lever and Esterhuizen (61) and Esterhuizen and Lever (61) the arteries of the rat pineal gland by De Robertis and Pellegrino de Iraldi (61) as well as around the human cerebellar arteries by Dahl and Nelson (64) These investigators have considered the granular vesicles would contain catecholamine The present study however has failed to find granular vesicles and this may suggest the cholinergic endings to be predominant in the rat intracranial arteries

At the closest approach the axons crowded with agranular vesicles and mitochondria are within 800 A of the surface of smooth muscle cells (figs 12–14) The axonal surface in these regions is often denuded of both Schwann and basement membrane investments while the opposing muscular surface is always covered by a basement membrane A similar neuromuscular relationship has also been observed in many arteries (Lever and Esterhuizen 61 Esterhuizen and Lever 61 Thaemert 63 Appenzeller 64) The direct contact between naked axon and smooth muscle cell where the basement membrane is missing and the intercellular zone measures about 200 A in width has been noted in a few organs such as intrinsic muscles in the iris (Richardson 64) the muscular coat of the ductus deferens (Richardson 62 Merrillees et al 63) and the nictitating membrane (Evans and Evans 64) Such a close neuromuscular relationship has not been observed so far in the present material

ACKNOWLEDGMENT

I wish to thank Professor Toshiyuki Yamamoto M D for his encouragement and suggestions throughout all stages of this work and also Mr Masae Kato for his technical assistance in drawings

LITERATURE CITED

Altenahr E 1965 Untersuchungen uber die Feinstruktur der vegetativen Innervation der Rattenlunge Z mikr anat Forsch 72 439–518

Appenzeller O 1964 Electron microscopic study of the innervation of the auricular artery in the rat. J Anat 98 87–91

Brettschneider H 1963 Elektronenmikroskopische Studien zur vegetativen Gefassinnervation Verh Anat Ges 58 54–68

——— 1964 Die Gefassinnervation als ein Beispiel fur die feinere Morphologie der vegetativen Endformation Verh Anat Ges 59 150–171

Carlyle A and J Grayson 1955 Blood pressure and th regulation of brain blood flow J Physiol 127 15P–16P (abstract)

——— 1956 Factors involved in the control of cerebral blood flow J Physiol 133 10–30

Chorobski J and W Penfield 1932 Cerebral vasodilator nerves and their pathway from the medulla oblongata With observations on the pial and intracerebral vascular plexus Arch Neurol. and Psychiat 28 1257–1289

Corday E S F Rothenberg and D W Irving 1963 Cerebral angiospasm A cause of the cerebral stroke Am J Cardiol 11 66–71

Dahl E and E Nelson 1964 Electron microscopic observations on human intracranial arteries II Innervation Arch Neurol. 10 158–164

De Robertis E and A Pellegrino de Iraldi 1961 Plurivesicular secretory processes and nerve endings in the pineal gland of the rat J Biophys Biochem Cytol 10 361–372

De Robertis E G Rodriguez de Lores Arnaiz L Salganicoff A Pellegrino de Iraldi and L M Zieher 1963 Isolation of synaptic vesicles and structural organization of the acetylcholine system within brain nerve endings J Neurochem 10 225–235

Dewey M M and L Barr 1962 Intercellular connection between smooth muscle cells the nexus Science 137 670–672

Esterhuizen A C and J D Lever 1961 Pancreatic islet cells in the normal and $CoCl_2$-treated guinea pig A fine structural study J Endocrin 23 243–252

Evans D H L and E M Evans 1964 The membrane relationships of smooth muscles an electron microscope study J Anat 98 37–46

Fang H C H 1961 Cerebral arterial innervations in man Arch Neurol 4 651–656

Ganong W F 1963 Cerebral circulation In Review of Medical Physiology Lange Medical Publications Los Altos California 451–460

Harmel M H J H Hafkenschiel G M Austin C W Crumpton and S S Kety 1949 The effect of bilateral stellate ganglion block on the cerebral circulation in normotensive and hypertensive patients J Clin Invest 28 415–418

Hassin G B 1929 The nerve supply of the cerebral blood vessels A histologic study Arch Neurol and Psychiat 22 375–391

Kety S S 1964 The control of the cerebral circulation Circulation 30 481–483

Krog J 1964 Autonomic nervous control of the cerebral blood flow in man J Oslo City Hosp 14 25–33

Lever J D and A C Esterhuizen 1961 Fine structure of the arteriolar nerves in the guinea pig pancreas Nature 192 566–567

Luft J H 1961 Improvements in epoxy resin embedding methods J Biophys Biochem Cytol 9 409–414

Merrillees N C R G Burnstock and M E Holman 1963 Correlation of fine structure and physiology of the innervation of smooth muscle in the guinea pig vas deferens J Cell Biol 19 529–550

Millonig G 1961 A modified procedure for lead staining of thin sections J Biophys Biochem Cytol 11 736–739

——— 1962 Further observations on a phosphate buffer for osmium solutions in fixation In Fifth International Congress for Electron Microscopy ed S S Breese Jr Academic Press New York 2 P–8

Molnar L and J Szanto 1964 The effect of electrical stimulation of the bulbar vasomotor centre on the cerebral blood flow Quart J Exp Physiol 49 184–193

Oosaki T and S Ishii 1964 Junctional structure of smooth muscle cells The ultrastructure of the regions of junction between smooth muscle cells in the rat small intestine J Ultrastruc Res 10 567–577

Parker F 1958 An electron microscope study of coronary arteries Am J Anat 103 247–273

Pease D C and S Molinari 1960 Electron microscopy of muscular arteries pial vessels of the cat and monkey J Ultrastruc Res 3 447–468

Pease D C and W J Paule 1960 Electron microscopy of elastic arteries the thoracic aorta of the rat J Ultrastruc Res 3 469–483

Penfield W 1932 Intracerebral vascular nerves Arch Neurol and Psychiat. 27 30–44

Pool J L 1958 Cerebral vasospasm New Eng J Med 259 1259–1264

Ray B S and H G Wolff 1940 Experimental studies on headache Pain-sensitive structures of the head and their significance in headache Arch Surg 41 813–856

Richardson K C 1962 The fine structure of autonomic nerve endings in smooth muscle of the rat vas deferens J Anat. 96 427–442

——— 1964 The fine structure of the albino rabbit iris wtih special reference to the identification of adrenergic and cholinergic nerves and nerve endings in its intrinsic muscles Am J Anat 114 173–205

Samarasinghe D D 1963 An electron microscopic study of the arteries to the brain of the rat with special reference to the accompanying nerve fibres J Anat 97 311 (abstract)

Krog 64) It has been clarified by this study that although a considerable number of unmyelinated fibers can be observed around the major intracranial arteries and their larger branches the smaller branch arteries do not have vascular nerves around them and hence they are not under direct neurogenic control Since resistance to blood flow is mainly regulated through changes in the diameter of the peripheral branches rather than that of the trunk arteries the smaller branches devoid of vascular nerves may exert greater influences on the intracranial circulation If that is the case the vasomotor mechanisms would be of little if any significance for the regulation of the total intracranial blood flow

There may be some regional variations in blood flow correlating with changes in local activity in the brain Sokoloff (61) for example found that the increase in the function of the nerve cells in a localized area of the cortex is followed by an increase in local blood flow They considered the local changes in circulation to be explained by means of accumulation of metabolites in the area of increased activity whereas Krog (64) has pointed out that the neurogenic regulation may also be of significance because this delicate blood distribution can hardly be adequately taken care of without some kind of nervous involvement Perhaps the present findings give an anatomical base for Krog s consideration

In addition Pool (58) and Corday et al (63) have described that the major arteries and their larger branches of the brain in contradistinction to the smaller pial vessels are susceptible to local or limited as well as widespread vasoconstriction that may be induced by a variety of stimuli The former author pointed out on the basis of his experimental findings that intrinsic neurogenic reflex activity may play a part in this vasoconstriction Perhaps the present observations support his conclusion from an anatomical standpoint

The neuromuscular relationships

Clusters of small vesicles with a simultaneous accumulation of mitochondria are very prominent in the axoplasm near the media These vesicles have an interior of low density and their configuration is quite similar to what has been identified as synaptic vesicles of the cholinergic nerve endings (De Robertis et al 63) In addition to such clear or agranular vesicles dense cored or granular vesicles have been described in the terminal portions of vascular nerves around the arterioles of the guinea pig pancreas by Lever and Esterhuizen (61) and Esterhuizen and Lever (61) the arteries of the rat pineal gland by De Robertis and Pellegrino de Iraldi (61) as well as around the human cerebellar arteries by Dahl and Nelson (64) These investigators have considered the granular vesicles would contain catecholamine The present study however has failed to find granular vesicles and this may suggest the cholinergic endings to be predominant in the rat intracranial arteries

At the closest approach the axons crowded with agranular vesicles and mitochondria are within 800 A of the surface of smooth muscle cells (figs 12–14) The axonal surface in these regions is often denuded of both Schwann and basement membrane investments while the opposing muscular surface is always covered by a basement membrane A similar neuromuscular relationship has also been observed in many arteries (Lever and Esterhuizen 61 Esterhuizen and Lever 61 Thaemert 63 Appenzeller 64) The direct contact between naked axon and smooth muscle cell where the basement membrane is missing and the intercellular zone measures about 200 A in width has been noted in a few organs such as intrinsic muscles *in the iris* (Richardson 64) the muscular coat of the ductus deferens (Richardson 62 Merrillees et al 63) and the nictitating membrane (Evans and Evans 64) Such a close neuromuscular relationship has not been observed so far in the present material

ACKNOWLEDGMENT

I wish to thank Professor Toshiyuki Yamamoto M D for his encouragement and suggestions throughout all stages of this work and also Mr Masac Kato for his technical assistance in drawings


M
4
5
Sm
Sm
6
Nu
F

Sokoloff L 1959 The action of drugs on the cerebral circulation Pharmacol Rev *11* 1–85

——— 1961 Local cerebral circulation at rest and during altered cerebral activity induced by anesthesia or visual stimulation In Regional Neurochemistry Proceedings of the Fourth International Neurochemical Symposium 1960 ed S S Kety and J Elkes Pergamon Press Oxford 107–117

Stöhr Ph Jr 1938 Die mikroskopische Innervation der Blutgefasse Ergebn Anat Entwicklungsgesch 32 1–62

Taxi J 1961 Sur l innervation des fibres musculaires lisses de l intestin de Souris C R Acad Sci 252 331–333

Thaemert J C 1963 The ultrastructure and disposition of vesiculated nerve processes in smooth muscle J Cell Biol 16 361–377

PLATE 1

EXPLANATION OF FIGURES

4 A rounded profile (*R*) contained in a smooth muscle cell (*Sm*) in the media of the anterior cerebral artery (A_1) It is suggested in this figure that the rounded profile is formed by an intrusion of the cytoplasmic process into the muscle cell The area within the rectangle is enlarged in figure 5 Another smooth muscle cell with the nucleus (*N*) is seen at the lower right corner *B* basement membrane *M* mitochondria × 24 000

5 An enlargement of the outlined area of figure 4 Note the apposition of the plasma membrane of the smooth muscle cell and that of the rounded profile (arrow) × 80 000

6 A close apposition (arrow) of smooth muscle cells (*Sm*) in the media of the basilar artery (B_1) *B* basement membrane × 40 000

7 A transverse section through the adventitia of the internal carotid artery (I_2) The outermost layer (*Fo*) of the adventitial fibroblasts is shown near the upper left corner Note a bundle of unmyelinated nerve fibers (*Nu*) running in the adventitia *Cf* collagen fibers *F* fibroblasts *Sm* smooth muscle cell × 9 000

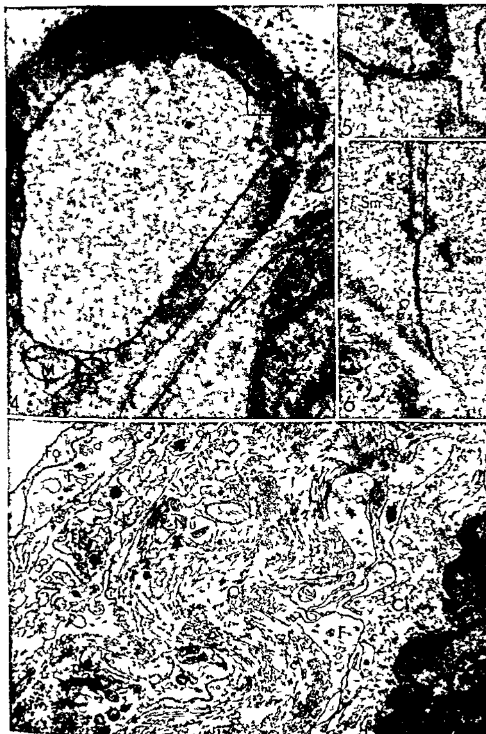

4
5
6
Sm
Sm
M
Nu
F

PLATE 2

EXPLANATION OF FIGURE

8 A cross section through a small branch (I_3) of the internal carotid artery The media consists of a single layer of smooth muscle cells (*Sm*) The extent of the adventitia is easy to define by the sheath like arrangement of the fibroblasts (*F*) A few small bundles of un myelinated fibers (*Nu*) are seen in the adventitia *El* internal elastic lamina *En* endothelium *Er* erythrocytes in the lumen × 11 000

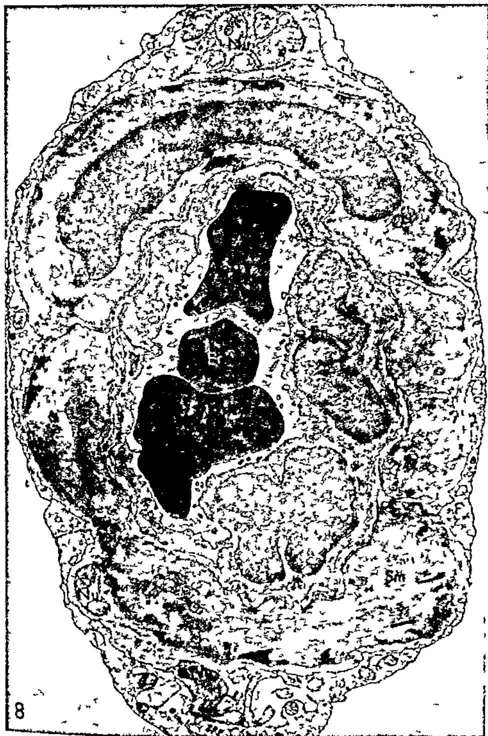

Nu
E
Sm
8

PLATE 2

EXPLANATION OF FIGURE

8 A cross section through a small branch (I_s) of the internal carotid artery The media consists of a single layer of smooth muscle cells (*Sm*) The extent of the adventitia is easy to define by the sheath like arrangement of the fibroblasts (*F*) A few small bundles of un myelinated fibers (*Nu*) are seen in the adventitia *El* internal elastic lamina *En* endothelium *Er* erythrocytes in the lumen × 11 000


Er
El
Sm
Cl
P
G

PLATE 3

EXPLANATION OF FIGURE

9 A transverse section through a central branch (M_3) of the middle cerebral artery penetrated in the brain tissue A narrow perivascular space (*P*) separates the adventitial fibroblasts (*F*) of the artery and the basement membrane (*B*) of the brain tissue Bundles of unmyelinated fibers (*Nu*) are contained in the adventitia *Cf* collagen fibers in the adventitia *El* internal elastic lamina *En* endothelium *Er* erythrocyte *G* process of an astrocyte *Sm* smooth muscle cell of the media × 12 000


Er
El
Sm
Cl
P
G

PLATE 4

EXPLANATION OF FIGURES

10 Myelinated (Nm) and unmyelinated (Nu) fibers found in the adventitia of the internal carotid artery (I_1) The outermost layer of fibroblasts (Fo) is shown at the left side of the micrograph Many axons (A) are submerged with mesaxons in a Schwann cell Cf and F collagen fibers and a process of a fibroblast of the adventitia N nucleus of the Schwann cell × 19 000

11 Unmyelinated nerve fibers found in the adventitia of the internal carotid artery (I_2) The cluster of clear vesicles (V) and mitochondria (M) is seen in the axoplasm The arrow indicates the naked surface of the axon which has no Schwann cell investment and is separated from the tissue space by only the basement membrane (B) Note the peculiar stratification of the basement membrane (St) F fibroblast × 36 000


A
A
N
A
E
Nu
A
D
Cl
R
10
S
F
F
S
M
B
11

PLATE 4

EXPLANATION OF FIGURES

10 Myelinated (*Nm*) and unmyelinated (*Nu*) fibers found in the adventitia of the internal carotid artery (I_1) The outermost layer of fibroblasts (*Fo*) is shown at the left side of the micrograph Many axons (*A*) are submerged with mesaxons in a Schwann cell *Cf* and *F* collagen fibers and a process of a fibroblast of the adventitia *N* nucleus of the Schwann cell × 19 000

11 Unmyelinated nerve fibers found in the adventitia of the internal carotid artery (I_2) The cluster of clear vesicles (*V*) and mitochondria (*M*) is seen in the axoplasm The arrow indicates the naked surface of the axon which has no Schwann cell investment and is separated from the tissue space by only the basement membrane (*B*) Note the peculiar stratification of the basement membrane (*St*) *F* fibroblast × 36 000


S
B
B
Sm
S
V
B
B
Sm
S
B
B

PLATE 5

EXPLANATION OF FIGURES

12–14 Electron micrographs illustrating the neuromuscular relationship The axonal surface is denuded of both Schwann cell (*S*) and basement membrane (*B*) investments at the closest approach (arrows) to the smooth muscle cell (*Sm*) while the opposing muscular surface is always covered by a basement membrane (*B*) Cluster of clear vesicles (*V*) and mitochondria (*M*) are prominent in the axoplasm Figures 12 and 13 × 24 000 Figure 14 × 21 000

Further Observations on the Cutaneous Branches of the Dorsal Primary Rami of the Spinal Nerves [1]

ANTHONY A PEARSON RONALD W SAUTER
AND TIMOTHY F BUCKLEY [2]
Department of Anatomy University of Oregon Medical School
Portland Oregon

ABSTRACT Recent investigators suggest that dermatomes extend as consecutive bands from the dorsal median line and question the existence of dorsal axial lines Our observations were made on serial sections of human embryos and fetuses prepared with neurofibrillar stains

Cervical nerves 1 6 7 and 8 failed to have cutaneous branches in most cases the remainder usually had cutaneous branches

With a few exceptions in T 1 all thoracic dorsal rami had cutaneous branches Usually T 1 2 and 3 became cutaneous through medial branches while T 9 through 12 did so through lateral branches However T 4 through 8 constitute a transition zone where many of these nerves became cutaneous through both medial and lateral branches Thoracic 4 5 and 6 tended to have cutaneous distribution through medial branches but T 7 and 8 through lateral branches

All lumbar dorsal rami having cutaneous distribution did so through lateral branches but independent branches became progressively less frequent below L 1 Lumbar 4 lacked direct cutaneous branches in most cases and succeeding nerves in all cases These nerves form the dorsal sacral plexus

The deficit in cutaneous distribution of lower lumbar rami was not as pronounced as in the lower cervical region A deficit is significant in relation to dorsal axial lines

Many dermatome maps of the body have been drawn based on anatomical clinical and experimental observations Each observer with his chosen method of study has tried to outline the areas of skin supplied by afferent fibers of the individual spinal nerves i e the dermatomes However there is still much to be learned about cutaneous nerves and their pattern of distribution

The sensory nerves to the dermatomes of the upper and lower extremities must pass through the brachial and lumbosacral plexuses in order to reach the limbs The course of these nerves through these plexuses is so complicated that an analysis of the distribution of the fibers in each spinal nerve is almost impossible with the usual methods of anatomical investigations

One would expect that the pattern of dermatomes on the back of the neck and trunk to be relatively simple since they are not involved in the brachial and lumbosacral plexus However there is still disagreement with regard to the dermatome maps even of this limited area In many current textbooks of anatomy gaps are shown in the sequence of cutaneous branches of the dorsal rami between the spinal nerve levels of cervical 5 through thoracic 1 and between lumbar 3 and sacral 1 The existence of these gaps has been questioned by Keegan and Garrett ('48) and they concluded that the dorsal axial lines do not exist Last ('59) has defined an axial line as that line of demarcation separating two dermatomes supplied from discontinuous spinal nerve levels The purpose of this investigation is to determine which spinal nerves possess dorsal primary rami with cutaneous branches and the significance of this information with reference to dermatome charts and especially as regards the presence of axial lines

MATERIALS AND METHODS

The approach used in this study of cutaneous nerve distribution is the same as that used in an earlier paper (Pearson

[1] This investigation was supported in part by research grant HD 00186-12 from the National Institute of Child Health and Human Development

[2] Present address Department of Neurological Surgery Radcliffe Infirmary Oxford England.

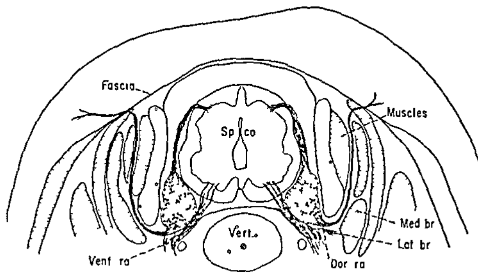


Fig 2 A composite drawing of transverse sections of a 28 mm human embryo (no 67 slides 30–32) at the level of the fifth cervical nerve Bodian method × 20

est embryo used in this series was about six weeks of age

Our observations on the cervical region (C 1 through T 1) were made on 15 embryos (i e 30 nerves were studied at each spinal level) The remaining observations were based on five embryos (i e 10 nerves at each level) The first thoracic nerve was studied with the cervical nerves because of its close relation to the dorsal axial line of the upper limb

OBSERVATIONS

Our observations on the distribution of the cutaneous branches of the dorsal rami of the spinal nerves are summarized in figure 3 This distribution was as follows cervical 1 had a cutaneous branch in only two out of the 30 nerves studied Both of these were present in one embryo In almost all of the embryos studied there were cutaneous branches of the dorsal rami of C 2 3 and 4 with but one exception at the level of C 4 In this case there was a well-developed communicating branch with C 5 Cutaneous branches at the level of C 5 were present in 22 of the 30 cases

The dorsal rami of cervical nerves 6 7 and 8 were characterized more by the absence of cutaneous branches than by their presence Cervical 6 had cutaneous branches in only two cases C 7 in only five cases and C 8 in only six cases However T 1 had cutaneous branches in 28 cases

It is usually said that the dorsal ramus of C 1 does not divide into medial and lateral branches (Cunningham 64 and others) It was interesting to note that when cutaneous branches of the dorsal rami of C 1 were present they arose from the most laterally placed bundles of this nerve The details of the course of this nerve have been described in an earlier paper (Pearson et al 63) A cutaneous branch of C 1 is shown in figure 492 in Grant s Atlas of Anatomy (62) All of the other cervical cutaneous nerves arose *from* the medial branches of the dorsal rami as did those of T 1 with but one exception

While making these observations we were able to confirm the presence of the well-documented dorsal (posterior) cervical plexus (Gray 59 and Cunningham 51) which is formed by communicating loops between cervical nerves 1 2 and 3 We also noted that a similar plexus occasionally was formed by communicating loops between cervical nerves 7 8 and thoracic 1 (see fig 11 Pearson et al 63) Some of these communications occurred deeply among the muscles and the ultimate destination of their fibers could not be determined

A second type of communication was when a branch from *each of two spinal*

Sauter and Bass 63) This study is based on human embryos and fetuses which were sectioned serially and stained by the pro targol method of Bodian (36) and the silver gelatin method of Pearson and Whit lock (49) This material included hu man specimens whose crown rump length ranged from 12 to 45 mm The distribu tion of the dorsal ramus of each spinal nerve was studied with a microscope and the pertinent data recorded In each speci men the nerves were studied on both sides Nerves lacking independent cutaneous branches were checked for branches com municating with adjacent spinal nerves No significant differences were noted be tween right and left sides

The distribution of the cutaneous branches of the dorsal rami of the spinal nerves was also studied by the dissection of a number of large human fetuses (fig 1) In the critical areas however the absence of a nerve could not be as defi nitely established by dissection as in the serial sections stained specifically for nerve fibers For this reason tabulated data on dissected material is not included

A nerve was considered to be cutaneous only when its fibers could be traced through the deep fascia and into the subcutaneous

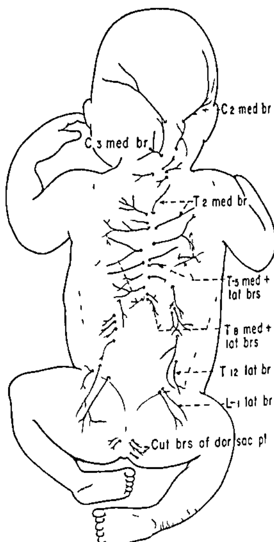


Fig 1 Dorsal view of a human fetus (175 mm C R) showing the distribution of the cutane ous branches of the dorsal primary rami Note the presence of both medial and lateral cutane ous branches from dorsal primary rami of certain thoracic nerves

tissues of the skin In the younger embryos where a layer of fascia had not yet differ entiated a nerve was considered to be cu taneous when it pierced the myotome and entered the loose mesenchyme under the skin The path of a dorsal ramus of a spinal nerve in a human embryo is shown in figure 2 According to Streeter (08) primary neurons forming peripheral nerves are well established by the end of the first month of fetal life After this period of development we consider it unlikely that peripheral nerves will establish new pat terns of distribution which involve passing through formed fascial layers The young

Abbreviations

a aorta
ant cut br anterior cutaneous branch
C cervical
Co coccygeal
cut brs of dor sac pl, cutaneous branches of dorsal sacral plexus
diaph diaphragm
dor ra dorsal ramus
e esophagus
intercost n intercostal nerve
i v c inferior veno cava
L lumbar
lat br lateral branch of dorsal primary ramus
lat cut br lateral cutaneous branch
med br medial branch of dorsal primary ramus
musc brs muscular branches
n X vagus nerve
ph n phrenic nerve
ra com rami communicantes
r at right atrium
S sacral
sp co spinal cord
symp tr g ganglion of sympathetic trunk
T thoracic
vent ra ventral primary ramus
vert vertebra
* anastomotic branch to 6th intercostal nerve

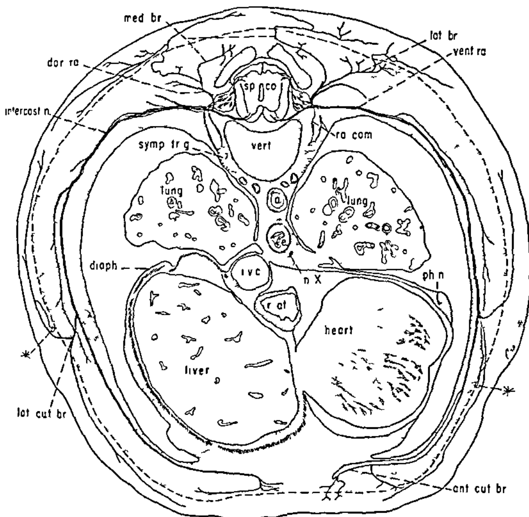


Fig 4 This is a composite drawing of transverse sections of a 32 mm human embryo (no 291 slides 63-70) showing the course of the seventh thoracic nerves Bodian method × 14

while in T 4 through T 7 (T 8) the skin is supplied more often through both the medial and lateral branches In the remaining thoracic nerves the cutaneous distribution is usually through lateral branches only The details of our observations on the individual thoracic nerves (fig 3) are described below

The cutaneous branches of T 1 are usually small and sometimes absent being absent in two cases out of 30 In one instance it became cutaneous through its lateral branch rather than its medial branch The medial branches of T 2 and T 3 had cutaneous distribution in all cases studied At T 4 a zone of transition commences and continues through T 8 This zone represents a shift from regular distribution through medial branches to regular distribution through lateral branches At T 4 and T 5 cutaneous distribution occurred through both medial and lateral branches in six out of ten cases and in the remaining four cases only the medial branches became cutaneous In eight of the ten nerves studied at the level of T 6 the cutaneous distribution was through both medial and lateral branches The re

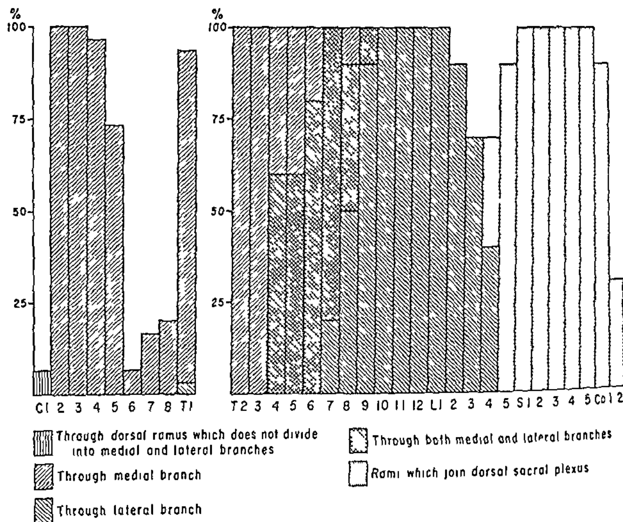


Fig 3 This table shows in percentages the occurrence of cutaneous branches from the dorsal primary rami of the spinal nerves *Note the low incidence of cutaneous branches from the dorsal primary rami at the levels of cervical nerves 6 7 and 8 and that the levels of thoracic nerves 4 through 8 are characterized by the presence of both medial and lateral cutaneous branches from their dorsal primary rami The absence of independent cutaneous branches from dorsal primary rami in the lumbar region is not as marked as in the lower cervical region*

nerves joined to form a single nerve bundle which proceeded directly into the subcutaneous tissue of the skin (see b fig 11 Pearson et al, 63) In such cases both levels were considered to have a cutaneous branch This was found once between C 7 and C 8 and four times between C 8 and T 1

Figure 4 is a composite drawing of transverse sections of a 32 mm human embryo at the level of the seventh thoracic nerve It illustrates the path of a typical spinal nerve and its cutaneous distribution It shows an intercostal nerve dividing into lateral and anterior cutaneous branches Note that the nerve on one side lacks anterior cutaneous branches and is entirely muscular in its distribution Each of the lateral cutaneous branches has an anastomotic twig which joins the next higher nerve in the subcutaneous tissue It shows the posterior primary rami dividing into medial and lateral branches On the right side both medial and lateral branches become cutaneous while on the left side only the lateral branch has cutaneous distribution

The dorsal primary rami of all the thoracic nerves have medial and lateral branches however their mode of cutaneous distribution is different in the upper middle and lower thoracic regions As a rule in T 1 through T 3 cutaneous distribution is through the medial branches only

Fig 4 This is a composite drawing of transverse sections of a 32 mm human embryo (no 291 slides 63-70) showing the course of the seventh thoracic nerves Bodian method × 14

while in T 4 through T 7 (T 8) the skin is supplied more often through both the medial and lateral branches In the remaining thoracic nerves the cutaneous distribution is usually through lateral branches only The details of our observations on the individual thoracic nerves (fig 3) are described below

The cutaneous branches of T 1 are usually small and sometimes absent being absent in two cases out of 30 In one instance it became cutaneous through its lateral branch rather than its medial branch The medial branches of T 2 and T 3 had cutaneous distribution in all cases studied At T 4 a zone of transition commences and continues through T 8 This zone represents a shift from regular distribution through medial branches to regular distribution through lateral branches At T 4 and T 5 cutaneous distribution occurred through both medial and lateral branches in six out of ten cases and in the remaining four cases only the medial branches became cutaneous In eight of the ten nerves studied at the level of T 6 the cutaneous distribution was through both medial and lateral branches The re

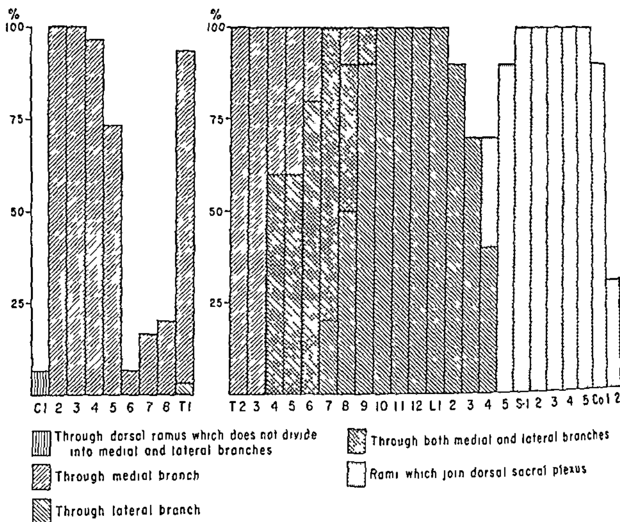


Fig 3 *This table shows in percentages the occurrence of cutaneous branches from the dorsal primary rami of the spinal nerves Note the low incidence of cutaneous branches from the dorsal primary rami at the levels of cervical nerves 6 7 and 8 and that the levels of thoracic nerves 4 through 8 are characterized by the presence of both medial and lateral cutaneous branches from their dorsal primary rami The absence of independent cutaneous branches from dorsal primary rami in the lumbar region is not as marked as in the lower cervical region*

nerves joined to form a single nerve bundle which proceeded directly into the subcutaneous tissue of the skin (see b fig 11 Pearson et al 63) In such cases both levels were considered to have a cutaneous branch This was found once between C 7 and C 8 and four times between C 8 and T 1

Figure 4 is a composite drawing of transverse sections of a 32 mm human embryo at the level of the seventh thoracic nerve It illustrates the path of a typical spinal nerve and its cutaneous distribution It shows an intercostal nerve dividing into lateral and anterior cutaneous branches Note that the nerve on one side lacks an terior cutaneous branches and is entirely muscular in its distribution Each of the lateral cutaneous branches has an anastomotic twig which joins the next higher nerve in the subcutaneous tissue It shows the posterior primary rami dividing into medial and lateral branches On the right side both medial and lateral branches become cutaneous while on the left side only the lateral branch has cutaneous distribution

The dorsal primary rami of all the thoracic nerves have medial and lateral branches however their mode of cutaneous distribution is different in the upper middle and lower thoracic regions As a rule in T 1 through T 3 cutaneous *distribution is through the medial branches only*

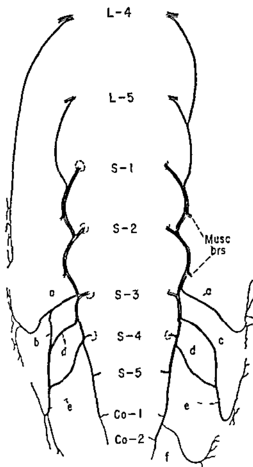


Fig 5 This is a diagram of the cutaneous branches of the dorsal sacral plexus based on the study of human embryo no 278 (45 mm C R) Bodian method See page 896 for explanation of figure

ing a series of secondary loops In some instances a branch (e) from the anterior ramus of S 5 joined the secondary loops The cutaneous branches of the secondary loops are derived from an undetermined number of the spinal nerves contributing to the dorsal sacral plexus

Any cutaneous branches below this level (S 4) arose in a random fashion from the primary loops of the lower spinal nerves (S 4 S 5 coccygeal 1 and sometimes coccygeal 2 when present) The caudal end of the primary loops supplies no muscles in man and represents the superior caudal trunk (f) of tailed animals (Cunningham '51)

DISCUSSION

The distribution of sensory nerves to the skin has been the subject of much research both experimental and clinical for more than a century Early work of an experimental nature was done on various animals and different methods were used by a number of investigators in an effort to outline the exact distribution of each sensory nerve root Likewise different regions were concentrated upon by individual workers and for many years no systematic survey of the cutaneous distribution of all the spinal nerves was done by any investigator Most early workers concentrated on unraveling the complexities of the brachial and lumbar plexuses

Eckhard (1849) wrote briefly on the cutaneous distribution of the sensory roots of the four hindmost spinal nerves of the frog and this appears to have been one of the earliest experimental inquiries in this field The frog was decapitated and all the posterior nerve roots were cut within the spinal canal except the one whose "skin field" he wished to examine The presence or absence of movement resulting from mechanical stimulation of the skin was taken as an index of residual sensibility From his observations Eckhard concluded that "the skin field to which a sensory root goes is not exactly that which overlies the muscles which are supplied by the corresponding motor root "

Peyer (1853) investigated C 5 6 7 8 and T 1 of the rabbit and he likewise divided all the nerves except the one he wished to examine However the nerve was divided outside the spinal canal and thus it was impossible to insure complete division of the dorsal root Since the motor root of that particular nerve was also severed the reflex response obtained from mechanical or thermal stimulation of the skin was somewhat impaired Peyer concluded that in the skin of the limbs of the rabbit the fields of the individual spinal nerves overlapped to a variable extent

Turck (1856 1868) did much valuable work on the dog He likewise divided the spinal nerves outside the vertebral column but differed from the previous workers in that he divided only the spinal nerve he wished to examine and he tested the skin by pinching it

maining two cases were cutaneous through medial branches only This nerve (T 6) represents the lowest level of the regular presence of medial cutaneous branches of the dorsal primary rami while T 7 is the first nerve to have cutaneous distribution in all cases through the lateral branches Eight of these ten cases at T 7 had cutaneous distribution also through their medial branches At the level of T 8 five cases had distribution through lateral branches only, while four cases became cutaneous through both medial and lateral branches Only the medial branch of the remaining case became cutaneous this appearing to be an exception At T 9 one case had distribution through both medial and lateral branches the other nine cases having only lateral cutaneous branches Thoracic 9 represents the lowest level at which a medial branch was found to be cutaneous Thoracic 10 11 and 12 became cutaneous in all cases only through their lateral branches Reference to figure 3 will help clarify the extent of the zones in the dorsal thoracic region

The lumbar nerves were also studied in five embryos (i e 10 nerves) When present, cutaneous distribution through the dorsal primary rami of the lumbar nerves is always through their lateral branches We found L 1 to be cutaneous in all cases L 2 in all but one, and L 3 in all but three cases In four cases out of ten the fourth lumbar nerve had direct branches to the skin In three cases the lateral branches of the dorsal primary rami of L 4 joined the dorsal sacral plexus through which they may have had cutaneous distribution In three cases it failed to have cutaneous branches or to join the dorsal sacral plexus

In no case did we observe an independent cutaneous branch from the dorsal primary ramus of L 5 while in nine out of ten cases it joined or communicated with the dorsal sacral plexus The remaining case had neither a cutaneous branch nor a connection with the dorsal sacral plexus

The dorsal primary rami of the sacral and coccygeal nerves were studied in the same five human embryos As expected the dorsal primary rami of the sacral and coccygeal nerves were found to be small and to diminish in size from above downward The dorsal primary rami of the first three sacral nerves divide into medial and lateral branches The medial branches are without cutaneous distribution The dorsal primary rami of the lower two sacral and the coccygeal nerves do not divide into medial and lateral branches

We have observed that the lateral branches of the dorsal primary rami of the last lumbar nerve (L 5) and the first three sacral nerves join with one another and with the dorsal primary rami of the fourth and fifth sacral and the first coccygeal nerves to form loops on the dorsal surface of the sacrum, thus confirming the presence of the dorsal sacral plexus (fig 833 Gray 59 and page 1057 Cunningham 51) In three instances a few fibers from the dorsal primary rami of the fourth lumbar nerve contributed to these loops The above loops will be referred to as primary loops From these loops branches are given to the multifidus muscle while others pierce the sacrotuberous ligament and form secondary loops deep to the gluteus maximus muscle From these secondary loops cutaneous branches arise which pierce the overlying muscle (gluteus maximus) and supply the skin and fascia over the sacrum and medial part of the gluteal region

While there is considerable variation in the pattern and arrangement of these cutaneous branches from the primary and secondary loops certain basic features were observed and are illustrated in figure 5 A large cutaneous branch (a) from the primary loops usually occurred at about the level of the third sacral foramina This cutaneous branch is thought to be formed mainly by S 1 and S 2 with possible contributions from (L 4) L 5 and S 3 through the primary nerve loops Contributions from spinal nerves lower than S 3 were considered to be less likely

A bundle of nerve fibers (b) usually ran caudally as a branch of the large nerve described above or arose directly (c) from the primary loop between S 3 and S 4 This nerve continued caudally into the coccygeal region where it gave off cutaneous branches In its course caudally it received fiber bundles (d) from the primary loops in the lower sacral region thus form

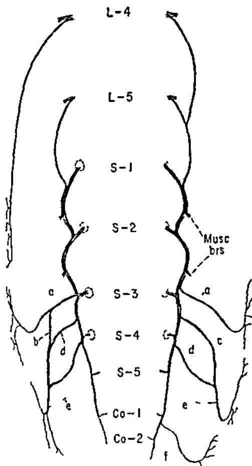


Fig 5 This is a diagram of the cutaneous branches of the dorsal sacral plexus based on the study of human embryo no 278 (45 mm C R) Bodian method See page 896 for explanation of figure

ing a series of secondary loops In some instances a branch (e) from the anterior ramus of S 5 joined the secondary loops The cutaneous branches of the secondary loops are derived from an undetermined number of the spinal nerves contributing to the dorsal sacral plexus

Any cutaneous branches below this level (S 4) arose in a random fashion from the primary loops of the lower spinal nerves (S 4 S 5 coccygeal 1 and sometimes coccygeal 2 when present) The caudal end of the primary loops supplies no muscles in man and represents the superior caudal trunk (f) of tailed animals (Cunningham 51)

DISCUSSION

The distribution of sensory nerves to the skin has been the subject of much research both experimental and clinical for more than a century Early work of an experimental nature was done on various animals and different methods were used by a number of investigators in an effort to outline the exact distribution of each sensory nerve root Likewise different regions were concentrated upon by individual workers and for many years no systematic survey of the cutaneous distribution of all the spinal nerves was done by any investigator Most early workers concentrated on unraveling the complexities of the brachial and lumbar plexuses

Eckhard (1849) wrote briefly on the cutaneous distribution of the sensory roots of the four hindmost spinal nerves of the frog and this appears to have been one of the earliest experimental inquiries in this field The frog was decapitated and all the posterior nerve roots were cut within the spinal canal except the one whose "skin field" he wished to examine The presence or absence of movement resulting from mechanical stimulation of the skin was taken as an index of residual sensibility From his observations Eckhard concluded that "the skin field to which a sensory root goes is not exactly that which overlies the muscles which are supplied by the corresponding motor root

Peyer (1853) investigated C 5 6 7 8 and T 1 of the rabbit and he likewise divided all the nerves except the one he wished to examine However the nerve was divided outside the spinal canal and thus it was impossible to insure complete division of the dorsal root Since the motor root of that particular nerve was also severed the reflex response obtained from mechanical or thermal stimulation of the skin was somewhat impaired Peyer concluded that in the skin of the limbs of the rabbit the fields of the individual spinal nerves overlapped to a variable extent

Turck (1856 1868) did much valuable work on the dog He likewise divided the spinal nerves outside the vertebral column but differed from the previous workers in that he divided only the spinal nerve he wished to examine and he tested the skin by pinching it

maining two cases were cutaneous through medial branches only This nerve (T 6) represents the lowest level of the regular presence of medial cutaneous branches of the dorsal primary rami while T 7 is the first nerve to have cutaneous distribution in all cases through the lateral branches Eight of these ten cases at T 7 had cutaneous distribution also through their medial branches At the level of T 8 five cases had distribution through lateral branches only while four cases became cutaneous through both medial and lateral branches Only the medial branch of the remaining case became cutaneous this appearing to be an exception At T 9 one case had distribution through both medial and lateral branches the other nine cases having only lateral cutaneous branches Thoracic 9 represents the lowest level at which a medial branch was found to be cutaneous Thoracic 10 11 and 12 became cutaneous in all cases only through their lateral branches Reference to figure 3 will help clarify the extent of the zones in the dorsal thoracic region

The lumbar nerves were also studied in five embryos (i e 10 nerves) When present cutaneous distribution through the dorsal primary rami of the lumbar nerves is always through their lateral branches We found L 1 to be cutaneous in all cases L 2 in all but one and L 3 in all but three cases In four cases out of ten the fourth lumbar nerve had direct branches to the skin In three cases the lateral branches of the dorsal primary rami of L 4 joined the dorsal sacral plexus through which they may have had cutaneous distribution In three cases it failed to have cutaneous branches or to join the dorsal sacral plexus

In no case did we observe an independent cutaneous branch from the dorsal primary ramus of L 5 while in nine out of ten cases it joined or communicated with the dorsal sacral plexus The remaining case had neither a cutaneous branch nor a connection with the dorsal sacral plexus

The dorsal primary rami of the sacral and coccygeal nerves were studied in the same five human embryos As expected the dorsal primary rami of the sacral and coccygeal nerves were found to be small and to diminish in size from above downward The dorsal primary rami of the first three sacral nerves divide into medial and lateral branches The medial branches are without cutaneous distribution The dorsal primary rami of the lower two sacral and the coccygeal nerves do not divide into medial and lateral branches

We have observed that the lateral branches of the dorsal primary rami of the last lumbar nerve (L 5) and the first three sacral nerves join with one another and with the dorsal primary rami of the fourth and fifth sacral and the first coccygeal nerves to form loops on the dorsal surface of the sacrum thus confirming the presence of the dorsal sacral plexus (fig 833, Gray, 59 and page 1057 Cunningham 51) In three instances a few fibers from the dorsal primary rami of the fourth lumbar nerve contributed to these loops The above loops will be referred to as primary loops From these loops branches are given to the multifidus muscle while others pierce the sacrotuberous ligament and form secondary loops deep to the gluteus maximus muscle From these secondary loops cutaneous branches arise which pierce the overlying muscle (gluteus maximus) and supply the skin and fascia over the sacrum and medial part of the gluteal region

While there is considerable variation in the pattern and arrangement of these cutaneous branches from the primary and secondary loops, certain basic features were observed and are illustrated in figure 5 A large cutaneous branch (a) from the primary loops usually occurred at about the level of the third sacral foramina This cutaneous branch is thought to be formed mainly by S 1 and S 2 with possible contributions from (L 4) L 5 and S 3 through the primary nerve loops Contributions from spinal nerves lower than S 3 were considered to be less likely

A bundle of nerve fibers (b) usually ran caudally as a branch of the large nerve described above or arose directly (c) from the primary loop between S 3 and S 4 This nerve continued caudally into the coccygeal region where it gave off cutaneous branches In its course caudally it received fiber bundles (d) from the primary loops in the lower sacral region thus form

tain of the segmental fields in the limb from mid-dorsal and mid ventral lines to be apparent rather than fundamental in character He postulated that there were complete sensory as well as motor rays and the most convincing item he found to support this theory was that furnished by the primary dorsal rami of the fifth sixth and seventh post thoracic nerves of Macacus corresponding to lumbar 4 5 and sacral 1 in man and of the eighth cervical and first thoracic nerves of Macacus These rami differed from similar rami of all the other spinal nerves in that they lacked cutaneous branches Sherrington found the cutaneous distribution of these nerves to be entirely confined to the limb i e they had no cutaneous representation from the dorsal rami along the dorsal mid line of the body He also found that when the motor roots of these particular nerves were sectioned more than half of the nerve fibers in their primary rami remained intact the remaining fibers were sensory Therefore the primary dorsal rami were partly sensory even though they had no cutaneous branches Further studies on these nerves revealed that there are sensory rays of muscular and other non-cutaneous tissues which extend from the vertebral column into the limb However the proximal portions of these sensory rays were buried beneath the skin and did not have cutaneous distribution The sensory rays in the muscular and non-cutaneous tissues extend from the muscles and ligaments of the vertebral column to the muscles and ligaments of the foot Sherrington showed that this was also true of the upper limb where the dorsal primary rami of cervical 7 8 and thoracic 1 did not possess cutaneous branches

In the limbs of the monkey Sherrington found no confirmation of Krause s statement that a nerve which supplied a muscle supplied the skin over it However he found that the pilomotor fields of the sympathetic ganglia and the cutaneous sensory fields did correspond

The "pilomotor" or "goosekin" reflex as a method of studying the cutaneous distribution of nerves in man was called to attention by Mackenzie (1893) following an earlier article by Langley and Sherrington (1891) working on cat and monkey Mackenzie found that this phenomenon could be elicited in nearly all people but it varied individually in extent of distribution and degree of excitability In some cases the skin of the trunk supplied by the ventral primary rami was selectively affected by this reflex and thus Mackenzie was able to show the extent of the distribution of these branches and could infer from this the cutaneous distribution of the dorsal rami on the back of the trunk The line of junction between the skin area of the cervical plexus and the upper thoracic nerves is illustrated in Mackenzie s paper suggesting the presence of axial lines

The foregoing is a brief summary of the early experimentations carried out to demonstrate the cutaneous distribution of spinal nerves However as observers realized that animal findings cannot necessarily be extrapolated to outline human cutaneous nerve supply interest in animal experiments waned and clinical observations gained in emphasis Early papers recording clinical and anatomical findings were published by Ross (1888) Paterson (1887 1889) Starr (1892 1894) Thorburn (1889 1893) Mackenzie (1892 1893) and Head (1893) The latter two workers were primarily interested in the reference of pain and tenderness to constant areas of the skin in cases of disease of various viscera Head sought to localize these areas of tenderness by comparing them to the areas affected in herpes zoster of the dorsal root ganglion of a single spinal nerve Subsequently in conjunction with Campbell (00) he published a detailed paper compiling his findings in a large series of cases of herpes zoster affecting dorsal root ganglia In many cases they were able to accurately locate the affected ganglion at postmortem examination From the distribution of the cutaneous vesicles in these cases of herpes zoster Head was able to draw a dermatome chart of the surface of the trunk which was the most accurate up to that time as most of the other clinical workers were attempting to outline the dermatome pattern from observations made on patients with lesions of the spinal cord itself Head and Campbell s paper has remained a valuable source of reference Their data was not complete in that there were no examples of certain

Krause (1865) investigated the nerves of the forelimb of the rabbit After sectioning the nerves he used the reflex method and followed the degeneration of nerve fibers His conclusions were at variance with those of Eckhard in that he stated (a) that a muscle is supplied with nerve fibers by the same spinal nerve that innervates the skin overlying it and (b) that each myelinated nerve fiber contained in a spinal nerve root stands in fixed relation with a definite anatomical point of the periphery

Koschewnikoff (1868) used the reflex method on the hind limb of the frog and found his results in general agreement with those of Eckhard noting that the fields of *distribution varied somewhat in different* individuals and that the skin in most regions of the hind limb is supplied by two nerve roots supporting the overlap observed by Peyer

Meyer (1869) working on frogs and using the degeneration method found that the territory of individual spinal nerves was not as sharply delimited as Krause (1865) had postulated

Herringham (1886) made studies on the human brachial plexus based on dissections He traced various nerves and their branches through the plexus to their terminal distribution in the muscles and to their areas of cutaneous distribution His generalizations include the following of two cutaneous spots in the pre axial area of a limb the lower (the more distal) was thought to be supplied by a lower nerve while of two spots in the post axial area the lower (the more distal) tends to be supplied by a higher nerve

Sherrington (1893 1898) made a careful and detailed study of the distribution of the afferent roots of the spinal nerves as a preliminary to some observations on the reflex functions of the spinal cord of the monkey He carried out experiments on the frog cat and monkey He divided the afferent roots in the spinal canal preserving the root he wished to examine after the method of Eckhard The surfaces of the limb and trunk were then explored and the points from which reflex movements could and could not be induced were located He carefully mapped the cutaneous distribution of each posterior spinal root and found that these areas composed not disjointed patches but one continuous field The field of skin belonging to each sensory spinal root he termed the sensory spinal skinfield These fields were segmentally arranged but overlapped to a certain extent with their neighbors anteriorly, posteriorly, ventrally and dorsally The shape of a sensory spinal skin field was simplest in the neck and the trunk Here it formed a band which wrapped transversely round one lateral half of the body with fairly parallel borders In the limbs these fields were distorted but it was possible to analyze them *after it had* been recognized that the cutaneous segments were seemingly dislocated from the *primitive position of attachment* to the mid dorsal and mid ventral lines of the trunk Sherrington postulated that the mid dorsal line at the level of the limb extends as a side branch almost at right angles to the rest of the mid dorsal line forming a secondary axis The mid ventral line behaves similarly in the same region The cutaneous segments of the limbs are ranged on these axes which resemble folded portions of the axial line of the trunk itself (fig 6) Sherrington also noted some overlap across these lines as well He considered the separation of cer

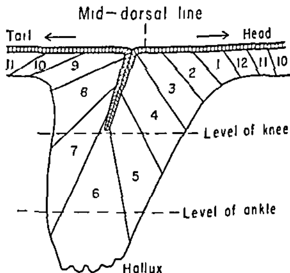


Fig 6 A diagram of the dermatomes (skin fields) of the hind limb of Macacus rhesus modified from Sherrington (1893) Included are the dermatomes of the last 3 thoracic nerves and 11 post thoracic nerves Post thoracic nerves 5 6 and 7 in Macacus correspond to lumbar 4 and 5 and sacral 1 in man

By definition a dermatome is the cutaneous area supplied by the fibers from a single dorsal root ganglion The distribution of postganglionic neurons through a single nerve root may or may not be identical with the dermatome distribution of that same nerve One would expect this to be particularly true of those nerves involved in a plexus e g the brachial plexus As one might expect stimulation of peripheral nerves with resulting vasodilatation produced patterns similar to but not necessarily identical with areas of herpetic eruption of a given nerve The dermatome areas of the upper limbs of the monkey are thought by some authors (Keegan et al 48) to be comparable to those in man and that they could be transposed without modifications Care should be taken in carrying over observations made in one animal to another as there is often a variance in patterns of dermatomes as illustrated in rabbits and man (Pearson et al 63)

The investigations of Keegan and Garrett (48) were based on clinical cases in which a herniation of the nucleus pulposus of an intervertebral disc compressed a single nerve root on cases where a single nerve root was cut in a surgical operation and in student volunteers in which single nerve roots were injected with novocaine Their work pictures the dermatomes of the limbs (C 5–T 1 and L 3–S 2) as an uninterrupted series of bands which extend from the mid-dorsal line of the trunk into the limbs They found that blocking a single spinal nerve resulted in a definite diminution of sensitivity in a dermatome They plotted areas of diminished sensitivity by the use of a light pin scratch for pain sensation Their newly defined areas of non-overlapping primary hyposensitivity were *interpreted as the "primitive dermatomes"* Failing to find gaps in the sequence of dermatomes at the levels of the upper and lower limbs in the dorsal region of the trunk these authors did not recognize the existence of the dorsal axial lines of the limbs They also challenged the concept advanced by Foerster (33) that the division of a single nerve root fails to produce a loss of sensitivity

The presence of gaps in the sequence of dermatomes in the lower cervical and lower lumbar levels on the posterior aspect of the trunk was recognized by Sherrington (1893 1898) Bolk (1898 1899) Head and Campbell (00) Johnston (09) and Haymaker and Woodhall (53 chart modified from Foerster 33) and is confirmed in our own studies

The dermatome charts of Keegan and Garrett (48) do not recognize the presence of these gaps and show a continuous distribution of each dorsal ramus on the posterior aspect of the trunk Many current textbooks of anatomy have dermatome maps illustrating both points of view recognizing that this question has not been satisfactorily answered We are unable to explain Keegan and Garrett s (48) failure to recognize these gaps nor can we account for the omission of certain sensory areas of the skin such as that supplied by the lateral cutaneous branch of the subcostal nerve (T 12) We paraphrase Keegan and Garrett when we point out that many *authors while protesting the prevailing* confusion of dermatome maps have drawn somewhat hypothetical dermatome charts which have often added to the confusion We are not in a position to evaluate Keegan and Garrett s (48) dermatome charts of the extremities However there are two fundamental questions (a) do certain dermatomes extend as a series of bands from the middle dorsal line of the trunk into the limbs and (b) are these bands (dermatomes) arranged in an uninterrupted sequence? This involves the problem of segmentation

A fundamental feature of all vertebrates is the segmentation of the paraxial mesoderm (Hamilton Boyd and Mossman 62) The somites of the body are formed from the paraxial mesoderm Each somite differentiates into a myotome from which *muscular tissues arise a dermatome* which is said to give rise to integumentary tissue and a sclerotome which is concerned with the development of the skeleton The segmentation of the paraxial mesoderm is closely related to the segmentation of the spinal cord In human embryos there are usually 4 occipital 8 cervical 12 thoracic 5 lumbar 5 sacral and 8 to 10 coccygeal pairs of somites Variations of these numbers are apt to occur A variation in the normal number is usually compensated by an addition to or

isolated nerves e g , cervical 8 and sacral 1

The dermatome charts of Bolk (1898 1899) were based on the gross dissection of a human body Johnston (09) also made painstaking dissections of individual spinal nerves in six human cadavers and traced them to their cutaneous distribution The chart shown in figure 832 in Gray s Anatomy (59) shows the cutaneous nerve distribution on the back of a body studied by Johnston In this chart medial and lateral branches of the same nerves are shown in the mid thoracic region Our study confirms this observation The gaps in the sequence of nerves on the posterior aspect of the trunk are also shown Edinger (04) and Dejerine (14) also published charts showing the dermatome patterns of the skin but the next publication that was based on painstaking clinical observations was that of Foerster ('33) In the course of his clinical work over a period of many years, he had occasion to divide many posterior roots and in many cases was able to leave one isolated nerve root intact Subsequently he accurately outlined the area of remaining sensibility in these cases and eventually succeeded in building a dermatome chart which may be compared with that of Head and Campbell Johnston and others It is of great interest that the method he used, i e the study of the cutaneous distribution of a single isolated nerve root, was the same as that originally described by Eckhard (1849) and subsequently termed the method of remaining aesthesia or residual sensibility" by Head Head (20) attributed this experimental method to Sherrington who used it on the monkey, cat and other animals although it had been used earlier by Eckhard on the frog Head wrote further and we quote

When he wanted to determine the extent of skin supplied from the fourth thoracic root he (Sherrington) destroyed several roots above and several below whilst the fourth remained intact This left a sensitive area in the centre of a zone of anesthesia every part that received its innervation however slightly from the fourth thoracic was marked out by residual sensibility

The value of this method and its universal importance has been strangely overlooked by neurologists They continue to publish reports in which the extent of the analgesia is solemnly discussed but they do not seem to recognize the importance of considernig what parts still retain their sensibility Suppose the seventh and eighth cervical and first thoracic roots have been destroyed in man certain portions of the upper extremity become insensitive to prick But when we have carefully determined the extent of the analgesia we are not justified in assuming that it represents the full supply of the divided nerve roots the area of sensory loss corresponds solely to those parts of the limb which they innervate exclusively On the other hand the upper or headward border of the loss of sensation corresponds to the lower limits of the sixth cervical root which is intact similarly the post axial limits of the analgesia mark out the upper limits of the second thoracic It is not the analgesia but the extent of the residual sensibility that is significant in such a case

The same principle applies to the loss of sensation produced by lesions of the spinal cord All the diagrams constructed to show sensory segmentation are built up on the study of analgesia in such cases the borders are carefully determined and transferred to a chart as the limits of the highest segment affected In reality the sensory condition should be looked at from the opposite point of view the upper border of the analgesia corresponds ot the caudal extension of the lowest unaffected portion of the spinal cord On the other hand the loss of sensation corresponds to those parts of the body which are exclusively supplied from below the lesion a matter of little scientific importance

This perverted outlook is responsible for much faulty diagnosis for it is more important to know what segments are still capable of exercising their functions than to determine what parts are utterly cut off from the sensory receptive centres Loss of sensation represents the negative aspect of the picture whilst residual sensibility corresponds to the functions of adjacent but intact nerve structures

The above statements of Head need to be remembered when studying dermatome patterns

Foerster (33) used several procedures in outlining dermatome patterns in man In one procedure he sectioned the dorsal roots of several spinal nerves and outlined the areas of cutaneous loss In other studies he cut nerve roots above and below the nerve in question and plotted the remaining areas of tactile and pain sensitivity The remaining tactile areas were found to be larger than those for pain and to overlap with neighboring dermatomes Foerster also used faradic stimulation of single nerve roots to outline areas of vasodilatation These areas were less extensive than for touch and pain However one should not expect the area of vasodilatation to be exactly coextensive with the dermatome distribution of a spinal nerve

Dejerine J 1914 Semiologie des Affections du Système Nerveux Masson et Cie Paris
Eckhard C 1849 Ueber Reflexbewegungen der vier letzten Nervenpaare des Frosches Zeitsch f rationelle Medizin 1st Series 7 281 Quoted from Sherrington 1893 and 1898
Edinger L 1904 Neue Darstellung der Segmentinnervation des menschlichen Korpers Zeitschrift Fur Klinische Medicin 53 52–57
Foerster O 1933 The dermatomes in man Brain 56 1–39
Grant, J C B 1962 An atlas of anatomy Fifth edition The Williams and Wilkins Co Baltimore
Gray H 1959 Anatomy of the human body 27th edition C M Goss editor Lea and Febiger Philadelphia
Hamilton W J J D Boyd and H W Mossman 1962 Human embryology Third edition The Williams and Wilkins Co Baltimore
Haymaker W and B Woodhall 1953 Peripheral nerve injuries W B Saunders Co Philadelphia and London
Head H 1893 On disturbances of sensation with especial reference to the pain of visceral disease Brain 16 1–133
——— 1920 Studies in neurology Oxford University Press London
Head H and A W Campbell 1900 The pathology of herpes zoster and its bearing on sensory localisation Brain 23 353–523
Herringham W P 1886 The minute anatomy of the brachial plexus Proceed of the Royal Society 41 423–441 Quoted from Paterson 1887
Johnston H M 1909 The cutaneous branches of the posterior primary divisions of the spinal nerves and their distribution in the skin J Anat and Physiol 43 80–92
Keegan J J and F D Garrett 1948 The segmental distribution of the cutaneous nerves in the limbs of man Anat Rec 102 409–437
Koschewnikoff A 1868 Ueber die Empfindungsnerven der hintern Extremitaten biem Frosche Archiv Fur Anatomie Physiologie und Wissenschaftliche Medicin 326–333 Quoted from Sherrington 1893
Krause W 1865 Beitrage Zur Neurologie der oberen Extremitat C F Winter Leipzig Quoted from Sherrington 1893 and 1898
Langley J N and C S Sherrington 1891 On pilo-motor nerves J of Physiol 12 278–291 Quoted from Sherrington 1898
Last R J 1959 Anatomy regional and applied Second edition Little Brown and Co Boston
Mackenzie J 1892 Sensory symptoms associated with visceral disease The Medical Chronicle 16 293 Quoted from Sherrington 1893
——— 1893 The "pilomotor" or goose-skin" reflex Brain 16 515–533
Meyer C 1869 Ueber die Nervenverbreitung in den hinteren Extremitaten Zeitschrift fur Rationelle Medizin 36 164–184 Quoted from Sherrington 1893
Paterson A M 1887 The limb plexuses of mammals J Anat and Physiol 21 611–634
——— 1889 The position of the mammalian limb regarded in the light of its innervation and development J Anat and Physiol 23 283–299
Patten B M 1953 Human embryology Second edition The Blakiston Division McGraw Hill Book Co Inc New York
Pearson A A R W Sauter and J J Bass 1963 Cutaneous branches of the dorsal (primary) rami of the cervical nerves Am J Anat 112 169–180
Pearson A A and M M Whitlock 1949 Th use of a buffer in the silver gelatin stain for nerve fibers Anat Rec 103 581–582
Peyer J 1853 Zeit f rationelle Medicin 2nd series 4 67 Quoted from Sherrington 1893
Ross J 1888 On the segmental distribution of sensory disorders Brain 10 333–361
Sherrington C S 1893 Experiments in examination of the peripheral distribution of the fibers of the posterior roots of some spinal nerves Phil Trans Roy Soc London Ser B 184 641–764
——— 1898 Experiments in examination of the peripheral distribution of the fibers of the posterior roots of some spinal nerves Part II Phil Trans Roy Soc London Ser B 190 45–186
Starr M A 1892 Local anesthesia as a guide to the diagnosis of lesions of the lower spinal cord Internat J of Med Sci Quoted from Sherrington 1893
——— 1894 Local anesthesia as a guide in the diagnosis of lesions of the upper portion of the spinal cord Brain 17 481–511
Streeter G L 1908 The peripheral nervous system in the human embryo at the end of the first month Am J Anat 8 285–301
Thorburn W 1889 A contribution to the surgery of the spinal cord Blakiston Son and Co Philadelphia
——— 1893 The sensory distribution of spinal nerves Brain 16 355–374
Turck L 1856 Ermittelung der Haut-Sensibilitatsbzi ke der Einzelnen Ruckenmarks-Nervenpaare Vorlaufige Ergebnisse von Experimental Untersuchungen Akademie der Wissen chaften 21 586 Quoted from Sherrington 1893
——— 1868 Ueber die Haut sensibilitatsbezirk der einzelnen Ruckenmarksnervenpaare Zusammengestellt von C Wedl Denkschriften der K Akademie der Wissenschaften (Wien) 29 Quoted from Sherrington 1893

a substraction from the normal somite number in an adjoining region The total number of somites in a young human embryo is about 42 to 44 The first occipital and the last 7 or 8 coccygeal somites disappear The first occipital somite is the first to appear and the others are formed in an uninterrupted craniocaudal series

The mid thoracic region is typical of somite differentiation Cells from the ventro medial portion of the somite become mesenchymal and migrate medially to fuse with similar tissue of the opposite side This portion of the somite is the sclerotome The dorso lateral portion of the somite constitutes the dermo-myotome From the ventral and dorsal edges of this dermo myotome cells proliferate which contribute embryonic muscle cells to a mass known as the myotome The lateral portion of the original dermo myotome is now called the dermatome The dermatome of the embryo is not to be confused with the area of skin supplied by a single dorsal root which constitutes the dermatome as the term is used in neurology Cells from the dermatome are usually described as spreading beneath the overlying ectoderm to which they cling and form the dermis and subcutaneous tissues

Patten (53) has pointed out that it was formerly believed that the dermis was formed from cells which came from the ventro lateral part of the somite and which was named the dermatome for this reason He considered that the term dermatome has been used so long in this way that it would be difficult to discard it but that it should be remembered that even though it does contribute some cells to the dermis the dermis is formed from mesenchymal cells which migrate from nearby mesodermal areas It is now believed that perhaps most of the cells from the ventro lateral part of the somite participate in muscle formation It should also be remembered that the dermis of the skin develops in the cephalic region where there are no somites e g areas supplied by the trigeminal nerve Arey (65) has pointed out that it is unlikely that the (embryonic) dermatomes contribute connective tissue cells far beyond the locale of the somites He further states that the assumptions (a) that all of the dermis is derived from portions of the primitive somites and (b) that each dermatome which girdles the body carries with it an afferent nerve in a manner similar to the innervation of the muscles derived from myotomes are not established and are open to question It therefore appears that the sensory innervation of the dermis of the skin is not as closely related to the segmental pattern of the body as those derived from the myotomes and sclerotomes

Our observations support those of earlier investigators (Sherrington 1898 Foerster 33 and others) who found a low incidence of cutaneous branches from the dorsal primary rami of the lower cervical nerves The absence of independent cutaneous branches from the dorsal primary rami in the lumbar regions is not as pronounced as in the lower cervical region The involvement of branches from the dorsal primary rami of the lower spinal nerves in the dorsal sacral plexus makes the analysis of the nerves in this region more difficult The presence of gaps in the sequence of the cutaneous branches of the dorsal primary rami supports the existence of dorsal axial lines

Thoracic nerves 4 through 8 constitute a zone of transition in that above these levels the cutaneous distribution from dorsal primary rami is through medial branches while below these levels cutaneous distribution is through lateral branches The transition zone (T 4–8) is characterized by the presence of both medial and lateral cutaneous branches from the dorsal primary rami

LITERATURE CITED

Arey L B 1965 Developmental anatomy Seventh edition W B Saunders Co Philadelphia

Bodian D 1936 A new method for staining nerve fibers and nerve endings in mounted paraffin sections Anat Rec 65 89–97

Bolk L 1898 1899 Die Segmentaldifferenzierung des menschlichen Rumpfes und seiner Extremitaten I Morphol Jahrb 25 465–543 II Morphol Jahrb 26 91–211 III Morphol Jahrb 27 630–711 IV Morphol Jahrb 28 105–146 Quoted from Sherrington 1898 and Keegan and Garrett 1948

Cunningham D J 1951 Cunningham s text book of anatomy Ninth edition J C Brash editor Oxford Univ Press London

——— 1964 Cunningham s textbook of anatomy Tenth edition G J Romanes editor Oxford Univ Press New York

ERRATUM

American Journal of Anatomy Volume 118 page 300

In explanation of Figure 6A the length of embryo should be 8 0 cm instead of 8 0 mm

Explanation of figures for plate 4 is reprinted below to permit correction by pasting corrected explanation over the incorrect printing

---

PLATE 4

EXPLANATION OF FIGURE

6 Photomicrographs of telencephalic choroid plexuses showing glycogen during various stages of development

A Embryo of 8 0 cm C R length (Stage II) × 120

B Embryo of 17 0 cm C-R length (Stage III) × 116

C Embryo of 28 0 cm C R length (Stage IV) × 125

D Full term newborn weighing 4,200 gm × 138

All photomicrographs are of PAS stains and are taken from areas of greatest concentration of glycogen Note gradual decrease in amount

---

Index

Index

H

I

J

K

L

M